SPATIAL VARIABILITY OF POTATO (*SOLANUM TUBEROSUM* L.) YIELD AND QUALITY ON SAND SOIL IN THE ARID REGION OF NORTHWEST CHINA

ZHANG, R. X. – ZHANG, J. F. – LI, T.* – XIONG, S. Y.

State Key Laboratory of Eco-hydraulics in Northwest Arid Region, Xi'an University of Technology, Xi'an 710048, China
(phone: +86-029-8231-2768)

**Corresponding author*
e-mail: litao@xaut.edu.cn

(Received 3rd Dec 2021; accepted 25th Feb 2022)

Abstract. The potential for significant variability in potato (*Solanum tuberosum* L.) yield and quality caused by soil properties can be employed as a foundation for site-specific soil management. The current work investigated the relationship of soil properties, including the texture, moisture, and nitrate-nitrogen, with the variability of potato yield and quality on 28 ha center-pivot irrigated fields located in northwest China, where the soil was improved in 2014 by mixing Aeolian sandy soil with feldspathic sandstone. Geostatistic and correlation analyses were utilized to extract the relationships among soil properties and potato tuber properties. K-means clustering methods were utilized to establish critical sample points and soil factors for spatial variability of potato yield and quality. The spatial dependence of the potato tuber yield and quality varied from weak to strong, and most had unstable spatial structure considering the soil temporal variability, except reducing sugar content. More than 66% of the correlation coefficients between soil sand content and tuber variables were significant. The evaluation of the K-means clustering algorithms' effectiveness showed that Θv- All, PC-All, and texture had superior prediction results for tuber yield, dry matter content, and starch, respectively. N-All and soil texture datasets exhibited the best performance for reducing sugar content. Unsatisfactory prediction results were obtained for protein and VC. The results can be utilized to realize different objectives for in-field site-specific potato management.
Keywords: *soil texture, potato quality, sand-fine mixture, geostatistics, K-means clustering*

Introduction

Potatoes (*Solanum tuberosum* L.) are considered to be the fourth most abundant food crop in China, after rice, maize, and wheat. A total of 5,815,140 ha of farmland, mostly located in the arid northwestern region of China, were used in 2016 to cultivate potatoes with an average yield of 17.04 t ha^{-1}. Potato yield and quality can change considerably within a particular field. The spatial variation of yield and quality leads to the waste of soil and water resources. Evaluating the degree and driving factors of spatial variability within-field is an important consideration to achieve site-specific management.

Potato yield temporal and spatial variability has been widely verified in the literature. Soil moisture content has been proven to be similar to the spatial distribution of crop yield or quality in many studies (Warrick et al., 1983; Wesenbeeck et al., 1988; Rockström et al., 1999; Irmak et al., 2002). Topography, soil texture, soil depth, soil organic matter, electricity conductivity and nutrients were also reported to be related to the spatial variation of potato yield (Redulla et al., 2002; Starr, 2005; Cambouris et al., 2006; Po et al., 2010; Perron et al., 2018).

According to previous reports, the coefficient of variation (CV) of potato yield ranged from 0.24 to 0.32 and the variability of potato yield was classified as moderate (Cambouris et al., 2006; Taylor et al., 2018). Geostatistical analysis was widely used in

http://www.aloki.hu ● ISSN 1589 1623 (Print) ● ISSN 1785 0037 (Online)
DOI: http://dx.doi.org/10.15666/aeer/2003_19691989

the spatial variation of potato yield. Cambouris et al. (2006) adopted that the model of the semi-variogram of potato yield was always exponential, and the proportion of the structured variance compared to all the variance was moderate and almost constant. It showed that the variation in yield attributable to spatial variability in physico-chemical properties within the field was higher than that induced by seasonal climatic variability. Similar results has reported in previous study (Perron et al., 2018). The spherical model was also used to fit the semivariograms of yield (Taylor et al., 2018). Rosenzweig et al. (2016) demonstrated that the stable model was more suitable for potato yield in the interpolation process and the proportion of the structured variance compared to all the variance was 100%. Potatoes are usually processed into French fries, starch, whole powder. Starch, reducing sugar, protein, VC and dry matter content are very important for potato industry. Although understanding the spatial variability of potato quality is important, it is rarely mentioned.

Identifying and understanding the spatial variation of potato yield and quality is currently limited by the time and resources required to do sufficient soil monitoring. To reduce the number of sampling points, root mean square error can be used to determine the number of sampling points; rational number of sampling sites was determined by geostatistical analysis (de Souza et al., 2014; Wang et al., 2015; Li et al., 2020). Many studies estimated the mean value of soil variables by looking for stable or representative points. Temporal stability analysis (TSA) has already been applied widely to reduce the number of samples needed for estimating soil water storage in a field (Vachaud et al., 1985). However, the TSA method is based solely on empirical data, the ability to recognize why certain locations are better to sample than others is limited to the sampling points used to find the rank stable locations. To solve this problem, Van Arkel et al. (2015) adopted the K-means clustering algorithm to detect critical sampling points for estimating field-scale near-surface soil moisture and compared with the TSA method. The results showed that the clustering approach on soil and topography data resulted in field-scale average moisture estimates that were as good or better than TSA, but without the need for exhaustive presampling of soil moisture. Because of the effectiveness of this method in soil moisture estimation, it is necessary to use the principle of this method to estimate the mean value of potato yield and quality.

Based on this context, the main goals of the current work are: (i) to derive the spatial variability of potato yield and quality variables (dry matter, protein, starch, reducing sugar, vitamin C) through descriptive statistics and geostatistic analysis; (ii) to evaluate the correlation between soil attributes and potato yield and quality; (iii) to verify the effectiveness of the method which finding critical sampling points using K-means clustering algorithms in the estimation of the mean value of potato yield and quality.

Materials and methods

Experimental site

The current work was performed at the commercial crop fields, located in the border of Mu Us Sandy Land, northwest China (38°09′N, 109°00′E, 1183 m a.s.l.). The experiment was accomplished on a 28.3-ha field, cropped with potato. Before soil melioration treatment, soil texture was sandy and was not suitable for planting. In order to control desertification and increase cultivated land, Chinese government had implemented a project to mix sandy soil (Aeolian sandy soil) with another local soil

http://www.aloki.hu ● ISSN 1589 1623 (Print) ● ISSN 1785 0037 (Online)
DOI: http://dx.doi.org/10.15666/aeer/2003_19691989

(feldspathic sandstone). *Figure 1* shows the location of the experimental site and photos before and after soil mixing.

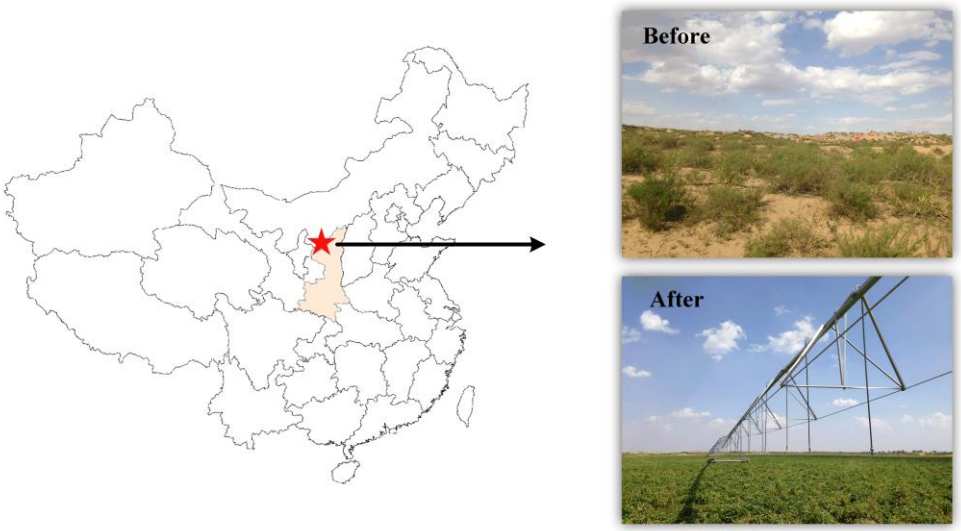

Figure 1. *Location of the experimental site in China and photos before and after soil mixing*

The physical and chemical properties of mixed soil were studied (Han et al., 2012; Zhang et al., 2021). The study fields were well mixed from a depth of 0–30 cm by Aeolian sandy soil and feldspathic sandstone in a proportion of 5 to 1 in 2014. The original aeolian sandy soil was covered with feldspathic sandstone with the mass of 850 tons per hectare. The mechanical composition of Aeolian sandy soil and feldspathic sandstone is shown in *Table 1*.

Table 1. *Composition of Aeolian sandy soil and feldspathic sandstone (%)*

Sample	Clay (＜0.002mm)	Silt (0.002-0.05mm)	Sand (0.05-2mm)	Texture
Aeolian sandy soil	0.24	4.45	95.31	Sand
Feldspathic sandstone	7.06	58.09	34.85	Silt loam

After soil improvement, potato was planted within 2015, 2016 and 2017 growing seasons. *Table 2* showed soil properties, meteorological conditions and planting management in the potato field from 2015 to 2017. In addition, the variation of initial aeolian sandy soil was also measured in 2014. The sand content of the sandy soil was more than 90% and clay content was as low as 0.24%. The coefficients of variation of soil clay, silt and sand of the sandy soil were 0.53, 0.38 and 0.05 respectively.

Meteorological conditions

The region where the experiment was installed generally has a typical semi-arid climate. In this area, the potato typically grows from May to October. *Figure 2* compares the monthly mean temperature, the rainfall, and the irrigation for all potato cropping seasons with their corresponding long-time average values (1957–2014). The rainfalls during May to October in 2016 and 2017 were 772 mm, and 634 mm, respectively, which

http://www.aloki.hu ● ISSN 1589 1623 (Print) ● ISSN 1785 0037 (Online)
DOI: http://dx.doi.org/10.15666/aeer/2003_19691989

were higher than that in 2015 (379 mm). Besides, these values were also higher than the long-term 57-year rainfall mean (423 mm). The potato growth season's average temperatures were a little greater than the long-term mean from 1957 to 2014. Moreover, the average temperature (℃) was higher in 2017 by 1.1℃, 2.3℃, and 1.6℃, than that of 2015, 2016, and 57-year period, especially within the critical stage of the onset of flowering and Tuber formation (July-August).

Table 2. *Soil properties, meteorological conditions and planting management in potato field*

Category	Property	2014	2015	2016	2017
Soil properties	Soil texture	sandy	sandy loam	sandy loam	sandy
	Clay (＜0.002mm) (soil depth:0-40cm) (%)	0.24	3.09	4.30	0.60
	Silt (0.002-0.05mm) (soil depth:0-40cm) (%)	4.45	32.01	27.24	9.40
	Sand (0.05-2mm) (soil depth:0-40cm) (%)	95.31	64.90	68.45	90.00
	Bulk dendity	\	1.42	\	1.50
	Electricity conductivity(μs/cm)	\	103.45	\	594.54
	Soil organic matter（g/kg）	0.08	1.04	1.82	1.85
	Soil nitrate-nitrogen （mg/kg）	0.012	26.69	30	27.68
	Soil available phosphorus（mg/kg）	2.68	3.15	3.25	4.28
	Soil available potassium（mg/kg）	84	73.07	89	113
Plant management	Plant area(ha)	0	28.3	28.3	28.3
	Cultivar	\	Shepody	Favorita	Shepody
	Growing season	\	5/1-9/25	5/1-9/1	5/1-9/22
	Intra-row spacing between tuber seed pieces (cm)	\	18	18	18
	Width of the ridge (cm)	\	30	30	30
	Inter-row spacing (cm)	\	90	90	90
	Irrigation amount (mm)	\	418	429	473
Meteorological conditions	Rainfall (in growing stage)	\	379	772	634
	Average temperature (℃)	\	20.0	19.9	20.8

\: no measurement was made

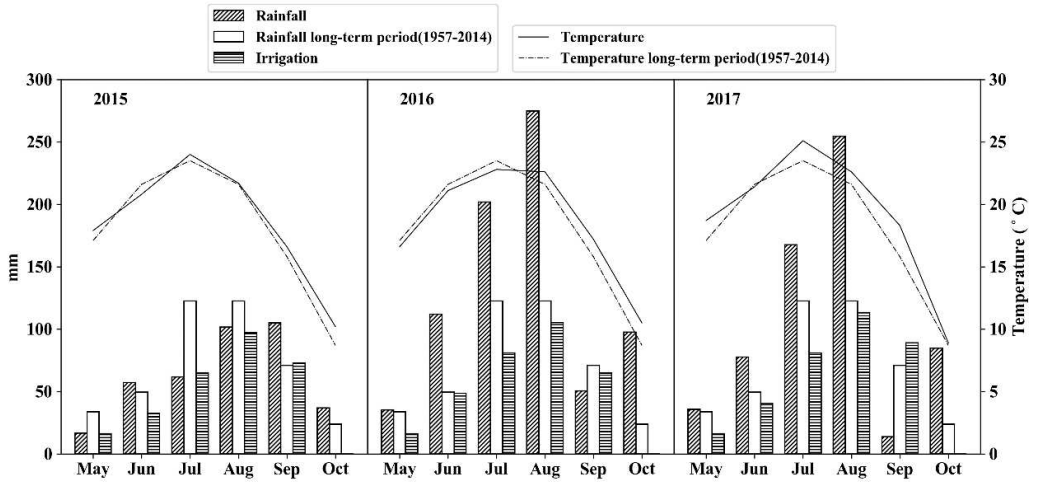

Figure 2. *The comparison between average monthly temperature, rainfall, and irrigation at the work site for all growing seasons and their corresponding long-term values (1957-2014)*

http://www.aloki.hu ● ISSN 1589 1623 (Print) ● ISSN 1785 0037 (Online)
DOI: http://dx.doi.org/10.15666/aeer/2003_19691989

Plant management

The potato cultivar 'Shepody', a widely grown cultivar processed for chip products globally, was planted in 2015 and 2017, while another potato cultivar 'Favorita', was planted in 2016. This field was a potato monoculture system with ridge tillage. The potato was sowed in early May and grown continuously under a single pass of a valley center pivot irrigation system (E2060-G, Reinke Manufacturing Company Inc. USA) equipped with Nelson sprinkler nozzles (D3000, Nelson Irrigation Corporation, USA). The irrigation amount was 11 mm for each irrigation event, and the total irrigation amount was 418 mm, 429 mm and 473 mm during the entire growing period in 2015, 2016 and 2017, respectively. The detailed irrigation schedules are shown in *Table 3*.

Table 3. *Irrigation schedules from 2015 to 2017*

Growth Stage	Irrigation quota (mm)	2015		2016		2017	
		Irrigation events	Irrigation amount (mm)	Irrigation events	Irrigation amount (mm)	Irrigation events	Irrigation amount (mm)
Germination	11	2	22	2	22	3	33
Seeding	11	5	55	6	66	6	66
Tuber formation	11	10	110	10	110	10	110
Tuber development	11	11	121	13	143	14	154
Tuber ripe	11	10	110	8	88	10	110
Whole	11	0	418	39	429	43	473

It is necessary to note that in 2015, there was no local power supply, and the sprinkler irrigation machine was powered by diesel. In order to save the cost, the irrigation frequency was lower than that in the next two years. Fertilizer application rates were adjusted using field mean nutrient amounts followed by present local agricultural authority guidelines. For each year, before planting, 4500 kg organic fertilizer, 15 kg urea, 25-30 kg diammonium phosphate and 20-25 kg potassium sulfate were applied, at the budding stage, 20 kg special fertilizer for potato were applied by center pivot irrigation system. The same plant protection traits were applied from 2015 to 2017. To avoid pests and diseases, 3 kg of 5% phoxim particles per hectare were applied before planting in each year. In order to prevent and control 28 lady beetles, 2.5% Deltamethrin and 70% Cyano (3-phenoxyphenyl) methyl 4-chloro-α-(1-methylethyl) benzeneacetate were used. Cyhalothrin and confidor were used to control aphids. In order to prevent and control the late blight, it has been prevented and treated every 7-10 days since July 15, with a total of 6 times. The drugs were Antracol, 10% Cyanostazole SC, Amesida and DuPont Yibao, Famoxate, Redomir(Gold,MZ) and Fluazinam.

Sampling points

The samplings of soil and potato were done in a grid. *Figure 3* shows sample location and the kriging map of soil sand content in 2015. One hundred and sixteen georeferenced regions were chosen from the field. The breakdown distance among the sampled regions was typically 25 m. Financial limitations and estimation precision requirements determine the whole number of samples. Soil moisture, nitrate-nitrogen (NO_3–N), and

http://www.aloki.hu ● ISSN 1589 1623 (Print) ● ISSN 1785 0037 (Online)
DOI: http://dx.doi.org/10.15666/aeer/2003_19691989

texture components were used to find critical sampling points in this study. Soil moisture and nitrogen were often used to delineate management zones because of the correlation with yield (Vrindts et al., 2005; Perron et al., 2018). The effect of soil texture on the variation of potato cannot be ignored due to its dramatic changes in time and space in the region where the experiment was installed.

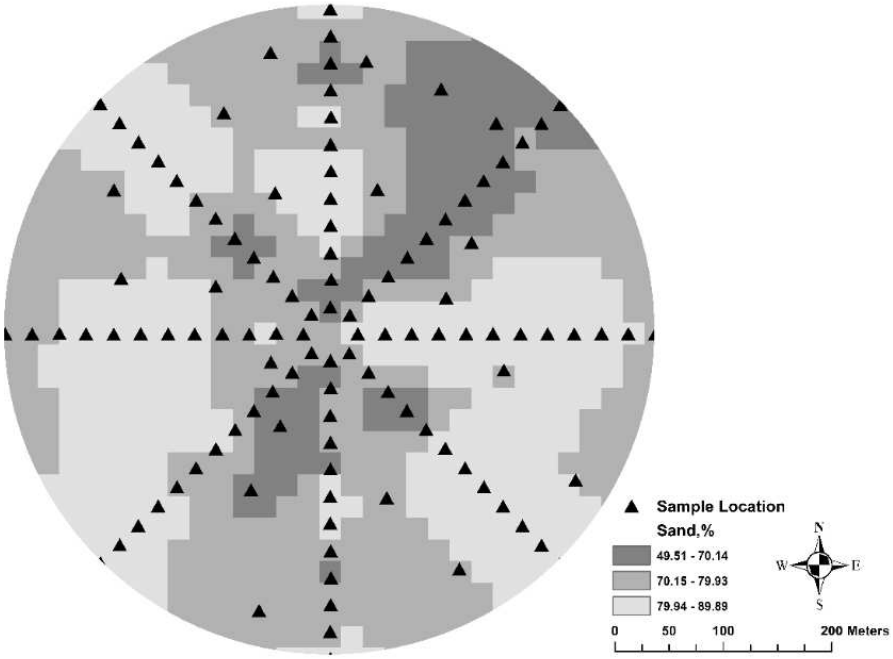

Figure 3. *Kriging map of soil sand content after mixed in 2015 and sample location*

Soil texture

At each points, soil samples were collected for soil texture measuring before planting in each growing season (2015, 2016, 2017). In order to reduce the measurement error caused by testers, testers A and B were arranged to collect soil samples independently. Three soil core samples (70 mm diameter, 52 mm height) were collected at the depth of 20 cm within a 1-m radius of each grid point by teater A and tester B, respectively. Samples were kept cool until submitted to the appropriate laboratory and air-dried, ground, and sieved through a 2 mm sieve. Soil mechanical composition of three soil core samples in each point were performed by teater A and tester B respectively using laser particle analyzer (MasterSizer 2000, Malvern Panalytical Ltd, USA). It is necessary to evaluate the reliability of measurements using the intraclass correlation coefficient (ICC). The ICC can theoretically vary between 0 and 1.0, where an ICC of 0 indicates no reliability, whereas an ICC of 1.0 indicates perfect reliability (Weir, 2005).

Table 4 showed the mean value of intraclass correlation coefficient among three years between different measurements of soil texture components. It can be seen that ICC of different measurements were higher than 0.85 indicating good reliability. The average value in each year of measurements performed by teater A and tester B were calculated and shown in *Table 4*. The USDA/FAO textural classifications systems were used to evaluate different textural classes.

http://www.aloki.hu ● ISSN 1589 1623 (Print) ● ISSN 1785 0037 (Online)
DOI: http://dx.doi.org/10.15666/aeer/2003_19691989

Table 4. *The mean value of intraclass correlation coefficient(ICC) among three years between different measurements of soil texture components*

Soil texture components	Intraclass correlation coefficient(ICC)		
	M_{A3}	M_{B3}	A*B
Clay	0.987	0.991	0.893
Silt	0.989	0.987	0.856
Sand	0.978	0.989	0.879

M_{A3}: Three measurements collected by tester A; M_{B3}: Three measurements collected by tester B; A*B:The mean value of three measurements collected by tester A and the mean value of three measurements collected by tester B

Soil nitrate-nitrogen(NO_3–N)

From each sampling location, soil composite sample was collected 3 times in June, July and August in each growing season (2015, 2016, 2017) for soil NO_3–N measuring, which was composited by three soil core samples (70 mm diameter, 52 mm height) collected at the depth of 20 cm within a 1-m radius of each grid point. NO_3–N was determined according to Cawse (1967). N_1, N_2, N_3 represented NO_3–N in June, July and August in each year.

Soil moisture

The volumetric soil water content was measured at each sampling location at depths of 0–40 cm every 4 days during the growing season using a time domain reflectometer sensor (Xi'an Bi Shui RV1, China), and the measured values of the volumetric soil water content were calibrated by a gravimetric method during the experimental period of each year. Soil moisture content was measured 35, 32 and 35 times in 2015, 2016 and 2017 respectively. Θ_{v1}, Θ_{v2}, Θ_{v3} represented the mean value of soil moisture content in June, July and August in each year.

Soil properties

Three soil core samples (70 mm diameter, 52 mm height) were collected at three random points at the depth of 20cm within a 1-m radius before planting in each growing season. One of samples was used for measuring soil bulk density determined according to cutting ring method. One of samples was used for measuring soil organic matter, available phosphorus, available potassium. Soil available potassium was extracted with ammonium acetate and determined by flame photometer (SHUMAN et al., 1990). Soil available phosphorus was extracted with sodium bicarbonate solution and determined by spectrophotometer (V-T3, Yipu Instrument Manufacturing Co., LTD, Shanghai, China) (Olsen, 1954). Soil organic matter was determined according to Yeomans et al. (1988). Another sample was used to measure soil electricity conductivity determined by conductivity meter (DDSJ-318T, Shanghai Yi Electrical Scientific Instrument Co., LTD, Shanghai, China). The average value of each year were shown in *Table 1*.

Yield and quality

Before the field's commercial harvest, a typical yield digs of 1 m-rows was carried out by hand at all sample points and weighed by an electronic scale (measuring range: 0.05-50 kg, measuring accuracy: 0.01 kg, Zhuoshangqi Co. Ltd., China). Three fresh

http://www.aloki.hu ● ISSN 1589 1623 (Print) ● ISSN 1785 0037 (Online)
DOI: http://dx.doi.org/10.15666/aeer/2003_19691989

potatoes were collected in each points and submitted to the laboratory. One fresh potato in each point was used for VC measurement and the rest were used for other quality measurement. Tuber dry matter content was determined according to oven drying method, slicing the three potatoes and mixing the processed potatoes together. Fragmented tubers were dried at 105 °C until the weight became constant. The starch content, protein, reducing sugar, vitamin C in tubers were determined according to iodine colorimetry method (McGrance et al., 1998), biuret reagent method (Yan et al., 2006), 3,5-dinitrosalicylic acid (DNS) colorimetric method (Zhao et al., 2008), moly-blue colorimetric method (Rietjens et al., 2002), respectively.

Data analyses

Statistical analysis, correlation analysis and geostatistical analysis were used to evaluate the spatial variability of potato yield and quality. ArcGIS10.3 (ESRI, Redlands, CA, USA) was adopted to construct semivariograms and kriged surface maps. The linear correlation coefficients ($P < 0.05$) were obtained through the Pearson's test by SPSS10.0 (International Business Machines Corporation, USA). The normal distribution estimation was performed on a skewness basis, i.e., for a skewness range between -1 and 1, a normal distribution was chosen for the data. If the data does not accord with normal distribution, the original data should to be log-transformed.

Semivariogram parameters, including the nugget (C_0), sill (C_1), and range (a), were utilized to define the spatial framework of all variables. Nugget describes the distance zero variance or the experimental error; sill defines the semivariance amount where the semivariogram attains the upper bound after its primary growth. It represents the maximum variance for this type of semivariogram and indicates the overall (a priori) semivariance of the selected region; the range defines the amount(x-axis) where a variable becomes spatially independent or the lag-distance where the semivariogram becomes smooth. The nugget to sill ratio determines the random part significance and estimates the spatial dependence quantitatively. Nugget/sill ratios can be divided into three categories (Cambardella et al., 1994): (i) <25%, strong spatial dependence; (ii) 25–75%, moderate spatial dependence; (iii) >75% ,spatially independent or pure nugget (i.e., when semivariograms' slopes are around zero).

Spatial variation can be described by various models (spherical, circular, etc.) fitting the semivariograms. The best-fitting model can be selected using the highest determination coefficient and confirmed through a visual inspection. The adopted lag distance was between 5 and 12, considering the variable. Cross-validation and ordinary kriging were utilized to extrapolate the amounts of unsampled field components.

K-means cluster analysis

K-means cluster algorithm aims to find categories, or clusters, containing objects with similar features. The distance measures over the different dimensions in the dataset are utilized to extract the similarity among objects. In the initial step of this algorithm, all data locations are randomly allocated to one of the k clusters. The n-dimensional centroid location, where n indicates the number of attributes in the input vector for any point, is obtained for all k clusters. The minimum Euclidean distance between the input vector and the centroid vector is derived to obtain the distance from any point to every centroid. Then, all points are reassigned to a cluster with the nearest centroid. This procedure continues iteratively until cluster membership is kept unchanged (Van Arkel et al., 2015).

http://www.aloki.hu ● ISSN 1589 1623 (Print) ● ISSN 1785 0037 (Online)
DOI: http://dx.doi.org/10.15666/aeer/2003_19691989

In order to reduce the cost of sampling, it is necessary to find optimal sampling locations with fewer soil variable types and fewer measurement times. Therefore, the data involved in clustering were divided into 8 groups. Firstly, the single measurement result of a single factor was clustered in order to analyze whether good results can be obtained at the least cost, including sand dataset, N-1 dataset, Θ_v-1dataset. Sand dataset were composed of soil sand contents in 116 sample points representing soil texture. N-1 dataset and Θ_v-1 dataset were composed of nitrogen and mean value of soil water contents in all points in August, respectively. According to the research of Tian et al. (2011), the water requirement of potato was higher from flowering stage to tuber expansion stage, and lower at seedling stage and before harvest. Secondly, multiple measurement results of single factor were clustered, including texture dataset, N-All dataset, Θ_v-All dataset. The texture dataset contains clay, silt, sand in all sampling points. N-All dataset was composed of three measurements of nitrogen, N1, N2, N3. Θv- All dataset was composed of Θv1, Θv2, Θv3, the mean value of soil moisture content in June, July and August. In addition, the principal components extracted by multi-factor were clustered. The first principal component and all principal components were clustered respectively. PC-1, as the first principal component extracted from these attributes, contains clay, silt, sand, N_1, N_2, N_3, Θ_{v1}, Θ_{v2}, Θ_{v3}. PC-All includes principal components whose eigenvalues were extracted from these attributes and are higher than 1. Eigenvectors and cumulative contribution rates of principal components in each year were shown in *Table 5*. There were 4, 3 and 4 principal components in 2015, 2016 and 2017, contained 81.58%, 82.34% and 75.65% soil information respectively.

Table 5. *Eigenvectors and cumulative contribution rates of principal components*

Principal components	2015		2016		2017	
	Eigenvectors	Cumulative contribution rates (%)	Eigenvectors	Cumulative contribution rates (%)	Eigenvectors	Cumulative contribution rates (%)
F1	3.69	40.98	3.28	36.45	2.66	29.54
F2	1.35	55.94	2.35	62.53	1.98	51.54
F3	1.28	70.12	1.78	82.34	1.15	64.32
F4	1.03	81.58	\	\	1.02	75.65

F1: the first principal component; F2: the second principal component; F3: the third principal component; F4: the fourth principal component

Then, the centroid vectors for all clusters in all datasets were determined. The input vector elements were sorted from small to large by the Euclidean distance from each cluster centroid. The smallest point was extracted as the typical sampling point for each cluster. The following weighted mean can be calculated from the typical sampling points and the number of points in the corresponding cluster to determine the estimated average of the field yield or potato quality from the sampling points detected through the clustering algorithm (*Eq.1*):

$$Y_j^{-est} = \frac{\sum_i^k Y_{BM_{ij}} * n_i}{N} \quad \text{(Eq.1)}$$

where Y_j^{-est} is the estimated mean yield or potato quality on the jth year, $Y_{BM_{ij}}$ is the yield or potato quality value on the jth year for typical sampling points of the ith cluster, where

http://www.aloki.hu ● ISSN 1589 1623 (Print) ● ISSN 1785 0037 (Online)
DOI: http://dx.doi.org/10.15666/aeer/2003_19691989

their mean is denoted by $Y_{BM_{ij}}$, n_i describes the number of sampling points in the ith cluster, N indicates the whole number of sampling points, and k denotes the number of clusters.

The sum of typical sampling points is determined by multiplying the number of clusters by the number of typical sampling points for each cluster, affecting the prediction results. In the current work, we verify the choice between two to twelve clusters, including about 10% of the observed data locations, with one to three points per cluster.

Davies-Bouldin index (DBI) and the estimation coefficient of determination (R^2) were computed to compare k-means clustering validation, and the precisions of the estimated field mean yield or potato quality from various approaches. The estimated field means are compared to the corresponding "true" field means, as the arithmetic means of the whole observations for the corresponding year.

Clustering validation, assessing clustering results' performance, is necessary to evaluate the quality of clustering algorithms. The Davies-Bouldin Index, as the most popular internal clustering validation index, attempts to maximize the intra-cluster distance and minimize the inter-cluster distances. DBI can be calculated as follows (Gao et al., 2018). For any cluster C, its similarities to the other clusters are obtained, and the maximum similarity is considered as the cluster similarity for C. The mean of these cluster similarities is considered the DBI index. The smaller DBI value means superior clustering performance. The DBI should be minimized to obtain maximum separation between clusters and attain the optimum partition.

Estimation R^2 determines to what extent the algorithm is superior to a simple employment of the field average; a positive amount demonstrates the superiority of the algorithm to the three-year field mean, whereas a negative one demonstrates its weakness comparing with the three-year field mean. Estimation R^2 can be obtained from the following sums of squared errors (*Eq.2*):

$$R^2 = 1 - \frac{\sum_j^J \left(\bar{Y}_J - Y_j^{-est}\right)^2}{\sum_j^J \left(\bar{Y}_J - \bar{Y}\right)^2} \quad \text{(Eq.2)}$$

where $\bar{Y}_J$ indicates the mathematical mean of observed yield or potato quality on the jth year across 116 sampling points, Y_j^{-est} is the estimated mean yield or potato quality on the jth year, $\bar{Y}$ is the mean of all the three-year observed yield or potato quality. By considering invalid prediction number ($R^2 < 0$) as the abscissa axis and the average value of estimation R^2 as the ordinate axis, six scatter plots of the predictive validity of different K-Means methods for selecting critical sampling points were plotted here to compare the prediction of potato yield and quality based on different K-Means methods (*Figure 5*). The dotted lines in *Figure 5* show the mean values of scatter points.

Results and discussion

Descriptive statistics

Table 6 gives the descriptive statistics in tuber yield and quality within-field for the three years. Most variables had a normal distribution. A few contrasts of both yield and quality were notable. Yield in 2015, 2016, and 2017 were 54168 kg ha^{-1}, 54487 kg ha^{-1} and 70879 kg ha^{-1}, respectively. Although the same potato cultivar 'Shepody' was planted

http://www.aloki.hu ● ISSN 1589 1623 (Print) ● ISSN 1785 0037 (Online)
DOI: http://dx.doi.org/10.15666/aeer/2003_19691989

in 2015 and 2017, the yield varied considerably. The higher rainfall within May to October was obtained in 2016 (772 mm) and 2017 (634 mm), compared with that in 2015 (379 mm). This may be due to the lower rainfall and poor irrigation management in the first year after mixing soil with Aeolian sandy soil and feldspathic sandstone. Dry matter content, protein, and starch in 2015 and 2017 were both higher than the corresponding ones in 2016. Differences in potato variety and climate can produce very different tuber yield and quality values from year to year.

Table 6. *Descriptive statistics for potato tuber yield and quality*

Year	Property	Mean	Min	Max	SD	Skewness	Kurtosis	CV	Num
2015	Yield（kg ha^{-1})	54168	19048	103001	22379	0.57	-0.47	0.41	116
	DMC(%)	25.28	15.19	34.09	3.16	0.78	-0.33	0.11	116
	Protein(%)	0.62	0.21	1.33	0.00	-0.76	0.25	0.39	116
	Starch(%)	16.37	4.88	29.64	5.84	-0.70	0.07	0.36	116
	Reducing Sugar (%)	0.15	0.09	0.25	0.00	-0.01	0.70	0.24	116
	VC(mg 100g^{-1})	29.27	11.00	48.00	10.54	-0.08	-0.20	0.36	116
2016	Yield（kg ha^{-1})	54487	29943	78411	12041	0.22	-0.71	0.22	116
	DMC(%)	21.36	14.41	28.21	3.04	0.37	0.10	0.13	116
	Protein(%)	0.54	0.25	0.90	0.15	0.43	0.48	0.32	116
	Starch(%)	11.59	2.44	22.75	4.09	0.21	0.44	0.35	116
	Reducing Sugar (%)	0.15	0.09	0.21	0.03	-0.28	-0.26	0.19	116
	VC(mg 100g^{-1})	27.12	5.00	57.50	9.02	1.29	0.13	0.33	116
2017	Yield（kg ha^{-1})	70879	43679	107448	11675	0.10	0.22	0.16	116
	DMC(%)	23.97	18.28	27.18	2.66	0.54	0.05	0.08	116
	Protein(%)	0.73	0.34	1.34	0.00	0.37	0.37	0.28	116
	Starch(%)	15.91	6.47	35.78	5.14	0.82	0.86	0.32	116
	Reducing Sugar (%)	0.10	0.04	0.27	0.00	0.87	1.39	0.32	116
	VC(mg 100g^{-1})	24.00	11.00	41.00	6.00	0.54	0.73	0.25	116

DMC, Dry matter content, VC, Vitamin C, CV: Coefficient of variation

According to the coefficient of variation (CV) as a measure of field stability with years, reducing sugar and dry matter content (DMC) were more stable than others. Spatial variation was remarkable for most variables. The CV of yield in 2015 was as high as 0.41, while the minimum yield was only 19048 kg ha^{-1}, but the highest was 103001 kg ha^{-1}. The wide yield range suggested that soil variability may significantly influence the tuber. Therefore, the mean tuber production can be considerably lower than its capability. The CV of yield tended to diminish among years, ranging from 0.41 to 0.16. In contrast, according to Cambouris studies, the potato yield variability had an approximately fixed value (from 0.24 to 0.27) in each year. Although the potato was also planted in sandy loam soil, it has a lower variation of soil sand content (CV=0.03) (Cambouris et al., 2006). A similar trend also can be seen in Protein and VC.

Descriptive statistics of soil properties are summarized in *Table 7*. Regardless of the small region of the experimental plot, the spatial and temporal variabilities of most variables were considerable. After mixed, the study fields contrast in soil texture with sandy loam to sandy among three years. Since the clay proportion remained low (lower than 5%), fluctuating from 0.6% to 4.3% through three years, soil texture was determined by silt and sand. After the first year, silt reduced moderately from 32.02% to 27.04%, then tumbled to 9.4% in the third year. In contrast to silt, sand increased slightly from

http://www.aloki.hu ● ISSN 1589 1623 (Print) ● ISSN 1785 0037 (Online)
DOI: http://dx.doi.org/10.15666/aeer/2003_19691989

64.9% to 68.45% and then raised rapidly to 90.00% through three years. This may due to instability of mixed soil and the downward migration of silt. Recent evidence suggested that continuous monoculture systems could degrade soil aggregate stability due to low organic inputs and tillage practice disturbances (Acosta-Martinez et al., 2004; Ma et al., 2016). It was reported that soil aggregate stability decreased significantly in the potato monoculture system after two years of continuous cropping. In addition, the soil was just mixed, and the soil aggregate was not stable in the process of formation. Therefore, silt may migrate downward with high-frequency irrigation and rainfall. In this study, since the rainfall in 2016 (772 mm) is higher than in 2015 (379 mm), this phenomenon was more noticeable after two cultivation years. However, soil texture in deeper than 40 cm had not been analyzed. The reasons for the drastic change of soil texture in depth of 0-40 cm need to be further studied.

Table 7. *Descriptive statistics of soil features among three years*

Year	Property	Mean	Min	Max	SD	Skewness	Kurtosis	CV	Num
2015	Clay（%）	3.09	0.24	8.28	1.48	0.76	1.68	0.48	116
	Silt（%）	32.01	7.23	59.27	12.37	0.27	-0.95	0.39	116
	Sand（%）	64.90	35.10	92.54	13.44	-0.25	-0.96	0.21	116
	Θ_{v1}（%）	11.64	6.16	19.81	3.49	-0.74	0.39	0.30	116
	Θ_{v2}（%）	9.46	5.51	17.04	2.82	-0.24	0.77	0.30	116
	Θ_{v3}（%）	11.47	4.58	19.81	4.35	-0.82	0.18	0.38	116
	N_1(mg kg^{-1})	90.49	23.59	168.54	28.17	-0.08	-0.08	0.31	116
	N_2(mg kg^{-1})	46.33	7.32	91.84	16.28	-0.25	0.06	0.35	116
	N_3(mg kg^{-1})	29.69	10.48	51.10	8.27	-0.22	0.00	0.28	116
2016	Clay（%）	3.26	0.46	7.19	1.35	0.69	-0.08	0.41	116
	Silt（%）	23.09	5.75	52.89	9.06	0.41	-0.39	0.39	116
	Sand（%）	73.65	41.16	93.53	10.17	-0.33	-0.34	0.14	116
	Θ_{v1}（%）	9.19	5.51	16.19	2.26	-0.17	0.60	0.25	116
	Θ_{v2}（%）	11.31	5.85	18.94	2.73	0.27	0.58	0.24	116
	Θ_{v3}（%）	9.09	4.96	16.71	2.60	-0.26	0.64	0.29	116
	N_1(mg kg^{-1})	88.07	54.63	131.69	15.94	-0.12	0.34	0.18	116
	N_2(mg kg^{-1})	37.83	13.75	70.20	11.36	0.63	0.44	0.30	116
	N_3(mg kg^{-1})	30.00	9.58	55.56	10.58	-0.31	0.43	0.35	116
2017	Clay（%）	2.70	0.58	8.92	1.32	0.80	1.08	0.49	116
	Silt（%）	10.38	4.28	25.83	3.82	0.08	0.25	0.37	116
	Sand（%）	86.92	65.25	95.14	5.07	0.14	-0.20	0.06	116
	Θ_{v1}（%）	10.40	6.47	14.48	3.00	0.73	1.10	0.19	116
	Θ_{v2}（%）	9.89	6.80	17.18	2.95	0.71	1.25	0.21	116
	Θ_{v3}（%）	7.68	5.15	12.15	2.51	0.34	0.98	0.16	116
	N_1(mg kg^{-1})	84.06	15.01	188.78	40.63	0.27	0.62	0.48	116
	N_2(mg kg^{-1})	40.66	4.73	79.36	16.99	-0.01	0.51	0.42	116
	N_3(mg kg^{-1})	27.68	8.76	59.43	13.24	0.17	0.85	0.48	116

CV: Coefficient of Variation. Θv_1, Θv_2, Θv_3: Mean value of soil water content in June, July and August; N_1, N_2, N_3: soil nitrate-nitrogen in June, July, August

The variation range of soil moisture content was 7.68% – 10.40% in 2017, 9.09% – 11.31% and 9.46% – 11.64% in 2015 and 2016, respectively. It can be seen that the soil moisture content in 2017 was slightly lower than that in previous two years, which was related to the change of soil texture. Soil nitrate-nitrogen declined from 90.49 mg kg^{-1}

http://www.aloki.hu ● ISSN 1589 1623 (Print) ● ISSN 1785 0037 (Online)
DOI: http://dx.doi.org/10.15666/aeer/2003_19691989

to 29.69 mg kg^{-1} within the growth period in 2015. The same trend can be seen in the next two years. Soil available nitrogen was 33 mg kg^{-1} before planting in 2015. After cultivation, soil available nitrogen in August were 29.69 mg kg^{-1}, 30 mg kg^{-1} and 27.68 mg kg^{-1} in 2015, 2016 and 2017, respectively. It can be seen that soil available nitrogen was kept approximately unchanged. The nitrogen consumption of potatoes was induced by fertilization. Meanwhile, the potato monoculture system was not conductive to nitrogen accumulation in the mixed soil.

The CV of soil sand content decreased considerably among years from 0.21 to 0.06, while the CV of clay and silt fluctuated around 0.38 and 0.48, respectively. However, according to several reported studies involving spatial variation within-field, spatial variation of soil particle distribution remained fixed year by year (Casa et al., 2008; Li et al., 2016). Meanwhile, according to the CV amounts ranging from 0.15 to 0.35, most soil chemical and physical features had moderate variability. Based on the soil survey reported by Cambouris et al. (2006), the CV of clay, silt, and sand were 0.20, 0.29, and 0.03, respectively. Similar to soil sand content, the CV of soil moisture declined during years from 0.33 to 0.16. However, for nitrogen, this was not the case. The maximum nitrogen variability was observed in 2017. In this study, fertilization was the primary source of soil nitrogen. Therefore, it is not easy to ensure the uniformity of fertilization.

Potato tuber yield and quality had between strong and weak spatial dependency, and except reducing sugar content showed non-consistent spatial variability according to soil temporal variability. This finding was compatible with Redulla's findings, demonstrating yield-driving factors variability for various fields and seasons (Redulla et al., 2002). However, the CV of yield, protein, and VC changed more dramatically among years than in previous studies. This may be due to the mixed soil's instability with the downward migration of silt.

Geostatistic analysis

The spatial variability of potato yield and quality are presented in *Figure 4*, while the best fitting model parameters are given in *Table 8*.

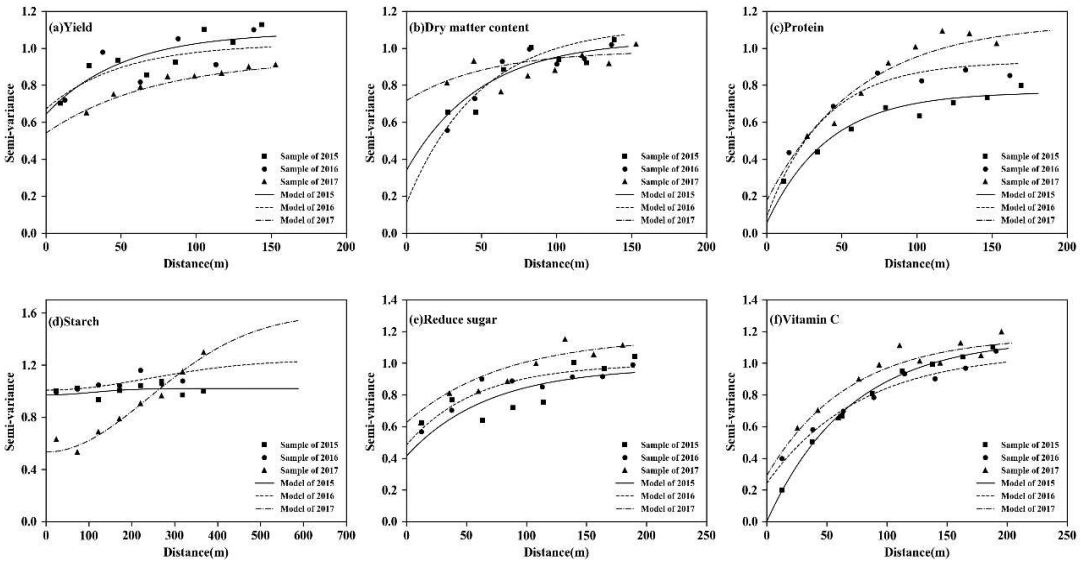

Figure 4. *Semi-variance functions of potato tuber yield and quality*

http://www.aloki.hu ● ISSN 1589 1623 (Print) ● ISSN 1785 0037 (Online)
DOI: http://dx.doi.org/10.15666/aeer/2003_19691989

Table 8. *Semi-variance function model parameters of potato tuber yield and quality*

Year	Property	Model	Nugget	Sill	Range (m)	Nugget/sill (%)	R^2	Num
2015	Yield（kg ha^{-1})	Exponential	0.80	1.14	151	70	0.86	116
	DMC(%)	Exponential	0.33	1.03	147	32	0.83	116
	Protein(%)	Exponential	0.05	0.75	122	7	0.92	116
	Starch(%)	Exponential	0.97	1.02	254	95	0.82	116
	Reducing Sugar (%)	Exponential	0.41	0.97	202	42	0.75	116
	VC(mg 100g^{-1})	Exponential	0.69	0.94	324	73	0.89	116
2016	Yield（kg ha^{-1})	Exponential	0.67	1.02	148	66	0.79	116
	DMC(%)	Exponential	0.16	1.12	145	14	0.86	116
	Protein(%)	Exponential	0	0.97	103	0	0.82	116
	Starch(%)	Exponential	1	1.22	588	82	0.86	116
	Reducing Sugar (%)	Exponential	0.48	0.99	173	48	0.79	116
	VC(mg 100g^{-1})	Exponential	0.72	1.01	321	71	0.85	116
2017	Yield（kg ha^{-1})	Exponential	0.54	0.94	216	57	0.92	116
	DMC(%)	Exponential	0.71	0.98	160	72	0.72	116
	Protein(%)	Exponential	0.17	1.13	181	15	0.80	116
	Starch(%)	Gauss	0.53	1.58	588	34	0.85	116
	Reducing Sugar (%)	Exponential	0.62	1.16	242	53	0.81	116
	VC(mg 100g^{-1})	Exponential	0.29	1.17	204	25	0.82	116

DMC, Dry matter content, VC, Vitamin C

The exponential model was the most used, that approached sill value asymptotically, while the gauss model was only utilized for starch in 2017. Tuber yield showed moderate and non-consistent spatial dependence among three years, with the nugget-to-sill ratio decreasing from 70% to 57%. It had a more significant range value (216 m) and a lower nugget-to-sill ratio (57%) in 2017 than in the previous years, indicating that the tuber yield had stronger spatial dependence in 2017. According to the above results, there was higher soil sand content in 2017. It can be concluded that potato tuber yield may have more considerable spatial dependence in sandy soil. In contrast, according to Cambouris et al. (2006), consistent and unchanged variability in tuber yield from 1998 to 2000 can be found, with the nugget-to-sill ratio around 47%. The nugget-to-sill ratio values in the current work were higher than those obtained by Cambouris et al. (2006) and derived from the relatively less uniform soil texture at the mixed-soil site.

Dry matter content exhibited two spatial patterns: moderate spatial dependence in 2015 and 2017 and strong spatial dependence in 2016. The lower nugget-to-sill ratio values for tuber dry matter content were obtained in 2015 (32%) and 2016 (14%). A similar trend can be seen in *Figure 3(b)*, whereas a more significant ratio can be observed in 2017 (72%). It can be concluded that the spatial structure of tuber dry matter content varied widely among years and was sensitive to the temporal variation of soil texture.

Tuber protein content had a strong spatial dependence with the nugget-to-sill ratio ranging from 0 and 15% and with the range value between 103m and 181m. Usually, strong spatial dependence may be due to inherent factors like soil water content and soil nutrient (Cambardella et al., 1994).

Starch in 2015 and 2016 both showed weak spatial dependence under the selected sampling procedure with the nugget-to-sill ratio between 95% and 82%, and showed moderate spatial dependence in 2017 with the nugget-to-sill ratio of 34%, indicated that

http://www.aloki.hu ● ISSN 1589 1623 (Print) ● ISSN 1785 0037 (Online)
DOI: http://dx.doi.org/10.15666/aeer/2003_19691989

a severe range value could be distinguished outside the field size, or the number of samples was not enough for the spatial dependence extrapolation. A similar variation pattern for tuber to reducing sugar content was observed among three years with similar nugget-to-sill ratio and range value, demonstrating moderate spatial dependence. It demonstrated that, even though the soil texture varied widely among years, the reducing sugar content's consistent spatial distribution could be observed. Thus, soil texture could not be considered the main factor for the structure spatial variability of the reducing sugar content.

Although tuber vitamin C showed moderate spatial dependence in three years, it had a much lower nugget-to-sill ratio (25%) in 2017 than in the previous years (73% and 71%), indicating its stronger spatial dependence in 2017. The mentioned trend was analogous to the tuber yield's spatial variability.

In conclusion, potato tuber yield and quality except reducing sugar content showed non-consistent spatial variability according to soil temporal variability. These results were compatible with previous studies. The inconsistency over time of spatial variability patterns of essential crop features like yield and protein has been demonstrated in the literature (Redulla et al., 2002; Blackmore et al., 2003; Maestrini et al., 2018).

Correlation analysis

Table 9 describes the Spearman correlation among tuber yield and quality and soil features. Although significant correlation relationships were extracted among soil features and yield, a few contrasts of the correlations can be observed between soil features and potato yield and quality in various growing seasons.

Table 9. *Spearman's correlation coefficient of potato tuber yield and quality with soil properties*

Property	Year	Clay	Silt	Sand	Θv_1	Θv_2	Θv_3	N_1	N_2	N_3
Yield	2015	NS	NS	NS	-0.31**	-0.34**	-0.43**	0.59**	-0.41**	-0.36**
	2016	NS	-0.25**	0.23*	NS	-0.27**	-0.31**	0.71**	-0.28**	-0.29**
	2017	NS	0.34*	-0.33*	NS	NS	NS	NS	NS	0.40*
DMC	2015	0.33**	0.21*	-0.24*	0.20*	NS	NS	NS	NS	-0.19*
	2016	0.27**	0.31**	-0.31**	0.36**	0.30**	0.38**	0.42**	-0.25*	-0.24*
	2017	NS	NS	NS	NS	NS	NS	NS	NS	0.38*
Protein	2015	NS	0.27**	-0.25**	NS	NS	NS	NS	NS	NS
	2016	NS	NS	NS	0.26**	NS	NS	NS	-0.23*	NS
	2017	NS	-0.33*	0.32*	-0.35*	-0.34*	-0.35*	NS	NS	-0.34*
Starch	2015	NS	0.29**	-0.28**	0.23*	0.22*	0.29**	NS	NS	NS
	2016	NS	0.23*	-0.23*	.19*	NS	NS	0.18*	NS	NS
	2017	NS	NS	NS	NS	NS	NS	NS	NS	NS
Reducing Sugar	2015	NS	-0.29**	0.28**	NS	NS	NS	NS	NS	NS
	2016	-0.21*	-0.22*	0.22*	NS	NS	NS	NS	NS	NS
	2017	NS	NS	NS	NS	NS	NS	NS	NS	NS
VC	2015	-0.20*	-0.30**	0.30**	NS	NS	NS	NS	NS	NS
	2016	NS	-0.27**	0.26**	NS	NS	NS	NS	NS	NS
	2017	-0.33*	NS	NS	-0.33*	-0.39*	NS	NS	NS	NS

DMC, Dry matter content, VC, Vitamin C, Θv_1, Θv_2, Θv_3: Mean value of soil water content in June, July and August; N_1, N_2, N_3: soil nitrate-nitrogen in June, July, August; PC-1, The First Principal Component, NS, Not Significant. *, **: Significant at the 0.05, 0.01 probability levels, respectively

http://www.aloki.hu ● ISSN 1589 1623 (Print) ● ISSN 1785 0037 (Online)
DOI: http://dx.doi.org/10.15666/aeer/2003_19691989

The yield was negatively and positively correlated to silt in 2016 and 2017, respectively. In contrast, it was positively and negatively correlated to sand in 2016 and 2017, respectively. This was compatible with earlier observations (Redulla et al., 2002), which showed that correlation coefficients among potato point yield and silt were positive in one field and negative in another with different soil textures. Although most soil moistures were negatively correlated to yield in the previous two growing seasons, this significant correlation relationship cannot be observed in 2017. In the first two years, the yield was negatively correlated with N_2 and N_3 while positively correlated with N_1. However, the yield was only positively correlated with N_3 in the last year. It can be concluded that soil texture was sandy loam in 2015 and 2016, while sandy in 2017. It also means in the sandy loam field, the more soil water content and nitrogen in August, the lower the potato yield. The opposite phenomenon can be observed in sandy soil. These results may be due to the less drainability and the lower soil moisture tension in the sandy clay loam soil than in sandy soil. The mentioned results were in good agreement with those observed in earlier studies. Saini (1976) studied the physical parameters of different soils and discovered the high correlation between the oxygen diffusion rate (ODR) and potato yield. Holder et al. (1984) extracted a remarkable relation between oxygen diffusion rate (ODR) and soil moisture tension (matric potential) at the 30 and 40 cm depths. These results indicated that irrigation might be excessive for potatoes in an andy clay loam field.

Similar to yield, dry matter content was negatively correlated with N_2 and N_3 while positively correlated with N_1 in 2016, indicating the higher nitrogen consumption in July and August (End of flowering-Onset of senescence and tuber expansion) compared with June (Onset of flowering and Tuber formation). The mentioned results were compatible with those of other works and suggested that the nitrogen absorption rate increased gradually after sowing to reach its maximum in the tuber expansion period (Wang et al., 2014). Therefore, it is necessary to fertilize nitrogen additionally in the mentioned period.

In general, more than 66% of the correlation coefficients among soil sand content and tuber variables were significant, with positive correlation coefficients ranging from 0.22 (Reducing Sugar in 2016) to 0.32 (Protein in 2017) and negative ones ranging from -0.23 (Starch in 2016) to -0.37 (DMQ in 2017). Redulla et al. (2002) reported that soil texture parts (sand, silt, clay) had a more significant effect on tuber yield than the soil chemical features (N, P, K, organic matter, pH). Spatial variation of soil texture may be the fundamental cause of the spatial variability of potato yield and quality in this mixed field.

Estimation analysis

Figure 5 shows DBI amount of clusters computed by k-means for all datasets. K-means gave higher DBI values for high-dimensional data (texture dataset, N-All dataset, Θ_v-All dataset, PC-All dataset) compared to one-dimensional data (sand dataset, Θ_v dataset, N-1 dataset, PC-1 dataset). For DBI, a lower criterion value represented the optimal cluster. In high-dimensional datasets, the smaller the Euclidean distance between clusters, the higher DBI was. According to similar results, the whole objects in a high-dimensional dataset usually were almost equidistant from each other and entirely mask the clusters (Parsons et al., 2004). However, it is also effective to determine the quality of clusters using DBI. According to the elbow principle, the optimal clustering number for K-Means on the PC-All dataset was 6, while this value was 2 for the other datasets.

Figure 6 shows six scatter plots of the predictive validity of different K-Means methods for selecting critical sampling points. For most tuber variables (except protein),

http://www.aloki.hu ● ISSN 1589 1623 (Print) ● ISSN 1785 0037 (Online)
DOI: http://dx.doi.org/10.15666/aeer/2003_19691989

points of high-dimensional datasets fall on the left of points of one-dimensional datasets, indicating that high-dimensional datasets-based yield and qualities prediction was more stable than the one-dimensional ones, suggesting that these data without temporal variation information cannot be utilized to choose critical sampling points. Prior studies have noted the importance of temporal variation for yield spatial variation (Li et al., 2016).

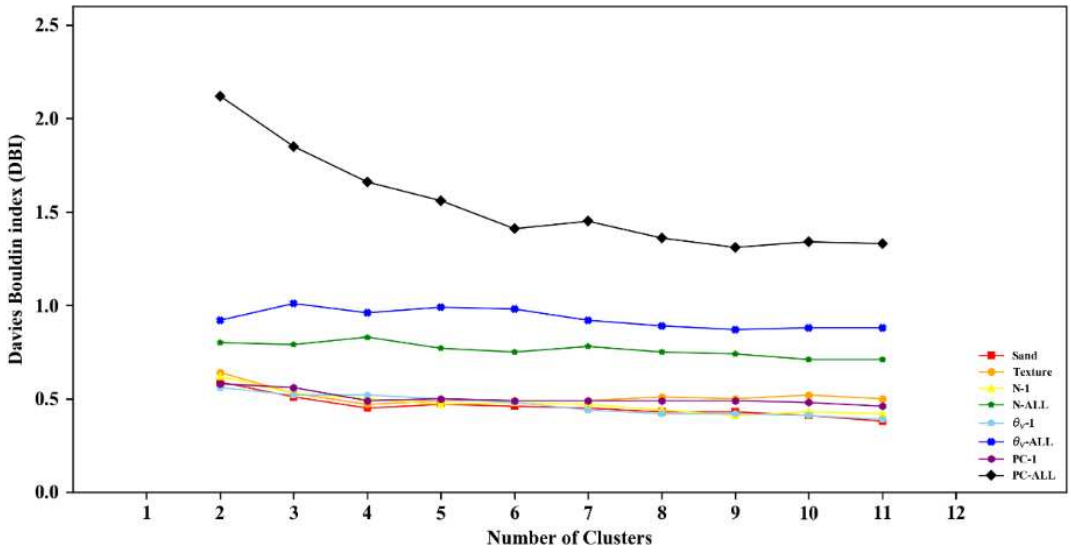

Figure 5. *DBI values of clusters*

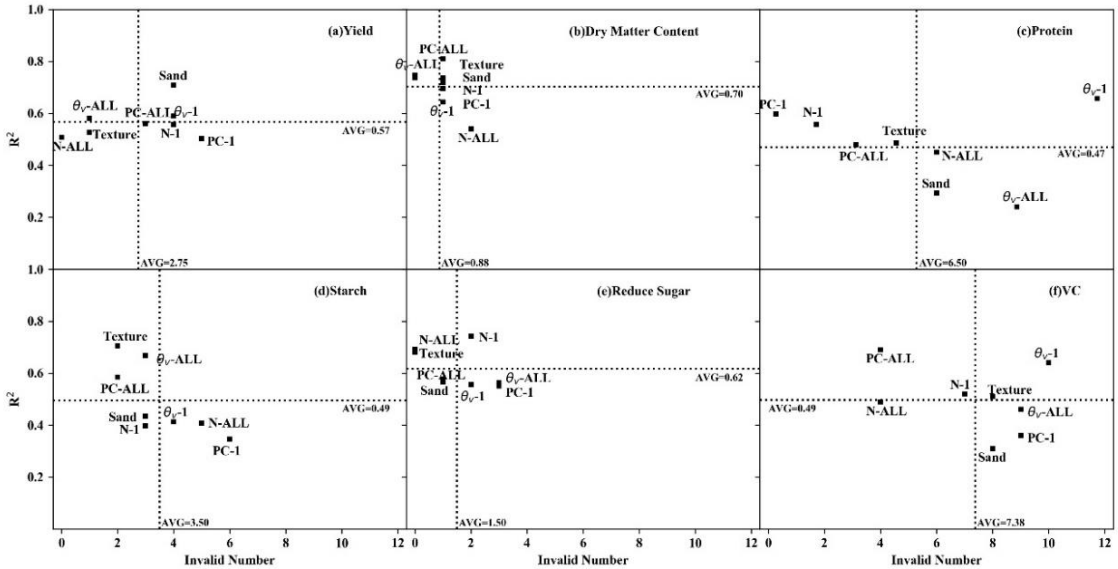

Figure 6. *Scatter plots of the predictive validity of different K-Means method*

For yield, estimation R^2 of most datasets, except sand, fluctuated moderately around the mathematical average (0.54). Although higher estimation R^2 was observed, sand dataset-based yield prediction gave inconsistent results. This result may be induced by

http://www.aloki.hu ● ISSN 1589 1623 (Print) ● ISSN 1785 0037 (Online)
DOI: http://dx.doi.org/10.15666/aeer/2003_19691989

the inconsistency of spatial variability of yield and the relationship between soil sand content and tuber yield. Θv-All had superior prediction results with the point fallen in the second quadrant (*Figure 6a*). It can thus be suggested that soil moisture was the primary constraint for spatial variability of potato yield in this site. Soil moisture content was detected as an essential factor influencing potato yields and tuber quality in several works (Van Loon, 1981; Fabeiro et al., 2001; Ahmadi et al., 2010). Fulton had reported that inadequate soil moisture could reduce the potato yield (Fulton, 1970).

Compared to yield and other potato quality, dry matter content had better prediction results, with a higher mean of estimation R^2 (0.72) and lower valid number (1) (*Figure 6b*). In the statistical sense, the lowest CV was obtained for the DMC. For DMC, the PC-All dataset gave the best performance with the estimation R^2 0.81, while the N-All dataset gave the lowest estimation R^2 (0.54), indicating that these vector data alone were not enough for the confident selection of critical sampling points.

In contrary to dry matter content, protein had unsatisfactory prediction results, with a lower mean of estimation R^2 (0.47) and higher valid number (6.5) (*Figure 6c*). For protein, both PC-1 and N-1 datasets exhibited relatively better performance. As shown in the first principal component's component matrix (Not listed in this paper), the correlation coefficients between the first principal component and soil particles were significant (correlation coefficients were about 0.77). As with the correlation results, there was a noticeable correlation between protein and soil particles across three years and a negative correlation among protein and nitrogen in August 2017.

For starch, K-means on texture dataset often provided satisfactory results, with higher estimation R^2 (0.71) than another approaches (*Figure 6d*). This finding confirmed correlation analysis results, indicating a significant correlation between soil particle distributions and potato starch. According to both analyses, the starch variation was mainly affected by soil particle distributions compared with soil moisture and nitrogen. Although the relationship between starch and soil texture has been studied in few works, some studies pointed that insufficient soil water could reduce starch yield (Jin et al., 2015). These results showed that soil texture might affect starch content in another way, requiring more depth experience and analysis.

The prediction effect of reducing sugar was only after the dry matter content (*Figure 6e*), which may be due to the consistent spatial distribution. The average values of estimation R^2 and valid number were 0.62 and 1.5, respectively. Across all metrics, the best performance belonged to N-All and soil texture datasets. Although a significant coefficient between nitrogen and reducing sugar was not observed, this finding suggested that soil particle distributions and nitrogen with temporal variation information were sufficient to select critical sampling points.

As shown in *Figure 6f*, VC had the most inconsistent results with the highest valid number (the mean value was 7.4) compared to all the potato quality and yield. These results may be due to the varied wildly spatial dependence among three years. The best performance belonged to the PC-All dataset, indicating that independent principal components extracted from soil moisture, nitrogen, and particle distribution could provide a little explanation of VC spatial variability for this site.

Taken together, K-means methods employed different soil attributes for identifying critical sampling points, which gave a more accurate estimation of the field mean of dry matter content and reducing sugar but generally performed erratically in the estimation of the field average of VC and protein. Interestingly, in all potato yield and quality variables of this study, dry matter content and reducing sugar had the lowest CV. In

http://www.aloki.hu ● ISSN 1589 1623 (Print) ● ISSN 1785 0037 (Online)
DOI: http://dx.doi.org/10.15666/aeer/2003_19691989

contrast, in the geostatistical analysis sense, VC and Protein have moderate spatial dependence, which means that there is a factor affecting their structural variations. Although correlation analysis found a significant correlation between soil attributes and VC or protein, some properties like soil moisture, nitrogen, and particle distribution could not affect VC and protein directly, not the root of variability.

Conclusions

Potato tuber yield and quality had between strong and weak spatial dependency, and except reducing sugar content showed non-consistent spatial variability according to soil temporal variability.

Correlation analysis showed that more than 66% of the correlation coefficients between soil properties and tuber variables were significant, indicating that an improvement in the temporal variation of soil texture was the most excellent chance for site-specific potato management in mixed soil.

The evaluation of K-means clustering algorithms' effectiveness showed that Θv- All, PC-All, and texture had superior prediction results for tuber yield, dry matter content, and starch, respectively. N-All and soil texture datasets exhibited the best performance for reducing sugar. Unsatisfactory prediction results were obtained for Protein and VC. These findings can be utilized to detect the possible opportunity for in-field site-specific potato management for different objectives. The method proposed by Van Arkel was effective for estimating potato quality which had stable spatial variation structure. More research is needed for potato yield and quality with large spatial-temporal variation.

Acknowledgements. This research was supported financially by the National Natural Science Foundation of China (Grant No 51609197), CAS 'Light of West China' Program (Grant No. XAB2016AW06), Programme of Introducing Talents of Discipline to Universities (No. 104-451115012), and Scientific Research Program of Education Department in Shaan Xi Province (No. 16JS084).

REFERENCES

[1] Acosta-Martinez, V., Zobeck, T. M., Allen, V. (2004): Soil microbial, chemical and physical properties in continuous cotton and integrated crop–livestock systems. – Soil Science Society of America Journal 68(6): 216-227.

[2] Ahmadi, S. H., Andersen, M. N., Plauborg, F., Poulsen, R. T., Jensen, C. R., Sepaskhah, A. R., Hansen, S. (2010): Effects of irrigation strategies and soils on field grown potatoes: Yield and water productivity. – Agricultural Water Management 97(11): 1923-1930.

[3] Blackmore, S., Godwin, R. J., Fountas, S. (2003): The analysis of spatial and temporal trends in yield map data over six years. – Biosystems Engineering 84(4): 455-466.

[4] Cambardella, C. A., Moorman, T. B., Novak, J. M., Parkin, T. B., Konopka, A. E. (1994): Field-scale variability of soil properties in central Iowa soils. – Soil Science Society of America Journal 58(5): 1501-1511.

[5] Cambouris, A. N., Nolin, M. C., Zebarth, B. J., Laverdière, M. R. (2006): Soil management zones delineated by electrical conductivity to characterize spatial and temporal variations in potato yield and in soil properties. – American Journal of Potato Research 83(5): 381-395.

[6] Casa, R., Castrignanò, A. (2008): Analysis of spatial relationships between soil and crop variables in a durum wheat field using a multivariate geostatistical approach. – European Journal of Agronomy 28(3): 331-342.

http://www.aloki.hu ● ISSN 1589 1623 (Print) ● ISSN 1785 0037 (Online)
DOI: http://dx.doi.org/10.15666/aeer/2003_19691989

[7] Cawse, P. (1967): The determination of nitrate in soil solutions by ultraviolet spectrophotometry. – Analyst 92(1094): 311-315.
[8] de Souza, Z. M., de Souza, G. S., Júnior, J. M., Pereira, G. T. (2014): Number of samples in geostatistical analysis and kriging maps of soil properties. – Ciencia Rural 44(2): 261-268.
[9] Fabeiro, C., Martın de Santa Olalla, F., De Juan, J. A. (2001): Yield and size of deficit irrigated potatoes. – Agricultural Water Management 48(3): 255-266.
[10] Fulton, J. M. (1970): Relationship of root extension to the soil moisture level required for maximum yield of potatoes, tomatoes and corn. – Canadian Journal of Soil Science 50(1): 92-94.
[11] Gao, X., Yang, M. (2018): Understanding and enhancement of internal clustering validation indexes for categorical data. – Algorithms 11(11): 177.
[12] Han, J., Xie, J., Zhang, Y. (2012): Potential role of feldspathic sandstone as a natural water retaining agent in mu us sandy land, northwest china. – Chinese Geographical Science 22(5): 550-555.
[13] Holder, C. B., Cary, J. W. (1984): Soil oxygen and moisture in relation to russet burbank potato yield and quality. – American Potato Journal 61(2): 67-75.
[14] Irmak, A., Batchelor, W. D., Jones, J. W., Irmak, S., Paz, J. O., Beck, H. W., Egeh, M. (2002): Relationship between plant avai lable soil water and yield for explaining soybean yield variability. – Applied Engineering in Agriculture 18(4): 471-484.
[15] Jin, G. H., Feng, Y. X., Liu, D. Q., Mao, R. (2015): Effect of different soil moistures on potato tuber yield and starch formation. – Journal of Northeast Agricultural University 46(10): 10-14.
[16] Li, T., Hao, X. M., Kang, S. Z. (2016): Spatial variability of grape yield and its association with soil water depletion within a vineyard of arid northwest China. – Agricultural Water Management 5: 4482-4491.
[17] Li, T., Zhang, J.-F., Xiong, S.-Y., Zhang, R.-X. (2020): The spatial variability of soil water content in a potato field before and after spray irrigation in arid northwestern China. – Water Supply 20(3): 860-870.
[18] Ma, K., Yang, Y. J., Ma, L., Wang, C. M., He, W. S. (2016): Effects of intercropping on soil microbial communities after long-term potato monoculture. – Acta Ecologica Sinica 36(10): 2987-2995.
[19] Maestrini, B., Basso, B. (2018): Predicting spatial patterns of within-field crop yield variability. – Field Crops Research 219: 106-112.
[20] McGrance, S. J., Cornell, H. J., Rix, C. J. (1998): A simple and rapid colorimetric method for the determination of amylose in starch products. – Starch-Stärke 50(4): 158-163.
[21] Olsen, S. R. (1954): Estimation of available phosphorus in soils by extraction with sodium bicarbonate. – US Department of Agriculture.
[22] Parsons, L., Haque, E., Liu, H. (2004): Subspace clustering for high dimensional data: A review. – ACM SIGKDD Explorations Newsletter 6(1): 90-105.
[23] Perron, I., Cambouris, A. N., Chokmani, K., Vargas Gutierrez, M. F., Zebarth, B. J., Moreau, G., Biswas, A., Adamchuk, V. (2018): Delineating soil management zones using a proximal soil sensing system in two commercial potato fields in New Brunswick, Canada. – Canadian Journal of Soil Science 98: 724-737.
[24] Po, E. A., Snapp, S. S., Kravchenko, A. (2010): Potato yield variability across the landscape. – Agronomy Journal 102(3): 885-894.
[25] Redulla, C. A., Davenport, J. R., Evans, R. G., Hattendorf, M. J., Alva, A. K., Boydston, R. A. (2002): Relating potato yield and quality to field scale variability in soil characteristics. – American Journal of Potato Research 79(5): 317-323.
[26] Rietjens, I. M., Boersma, M. G., de Haan, L., Spenkelink, B., Awad, H. M., Cnubben, N. H., van Zanden, J. J., van der Woude, H., Alink, G. M., Koeman, J. H. (2002): The pro-oxidant chemistry of the natural antioxidants vitamin C, vitamin E, carotenoids and flavonoids. – Environmental toxicology and pharmacology 11(3-4): 321-333.

http://www.aloki.hu ● ISSN 1589 1623 (Print) ● ISSN 1785 0037 (Online)
DOI: http://dx.doi.org/10.15666/aeer/2003_19691989

[27] Rockström, J., Barron, J., Brouwer, J., Galle, S., De Rouw, A. (1999): On-farm spatial and temporal variability of soil and water in pearl millet cultivation. – Soil Science Society of America Journal 63(5): 1308-1319.
[28] Rosenzweig, N., Steere, L., Gerondale, B., Kirk, W. (2016): A geostatistical approach to visualize the diversity of soil inhabiting bacteria and edaphic qualities in potato (Solanum tuberosum) production systems. – American Journal of Potato Research 93(5): 518-532.
[29] Saini, G. R. (1976): Relationship between potato yield and oxygen diffusion rate of subsoil. – Agronomy Journal 68(5): 823-825.
[30] Shuman, L. M., Duncan, R. R. (1990): Soil exchangeable cations and aluminum measured by ammonium-chloride, potassium-chloride, and ammonium acetate. – Commun Soil Sci Plant Anal 21(13-16): 1217-1228.
[31] Starr, G. C. (2005): Assessing temporal stability and spatial variability of soil water patterns with implications for precision water management. – Agricultural Water Management 72(3): 223-243.
[32] Taylor, J. A., Chen, H., Smallwood, M., Marshall, B. (2018): Investigations into the opportunity for spatial management of the quality and quantity of production in uk potato systems. – Field Crops Research 229: 95-102.
[33] Tian, Y., Huang, Z.-G., Yu, X.-Q. (2011): Experimental study on water requirement of potato. – Modern agricultural science and technology 8: 91-92.
[34] Vachaud, G., Passerat de Silans, A., Balabanis, P., Vauclin, M. (1985): Temporal stability of spatially measured soil water probability density function. – Soil Science Society of America Journal 49(4): 822-828.
[35] Van Arkel, Z. J., Kaleita, A. L. (2015): Identifying sampling locations for field-scale soil moisture estimation using k-means clustering. – Water Resources Research 50(8): 7050-7057.
[36] Van Loon, C. D. (1981): The effect of water stress on potato growth, development, and yield. – American Potato Journal 58(1): 51-69.
[37] Vrindts, E., Mouazen, A. M., Reyniers, M., Maertens, K., Maleki, M. R., Ramon, H., Baerdemaeker, J. D. (2005): Management zones based on correlation between soil compaction, yield and crop data. – Biosystems Engineering 92(4): 419-428.
[38] Wang, H. Y., Zhou, J. M. (2014): Root-zone fertilization: A key and necessary approach to improve fertilizer use efficiency and reduce non-point pollution from the cropland. – Soils 5: 785-790.
[39] Wang, J., Yang, R., Bai, Z. (2015): Spatial variability and sampling optimization of soil organic carbon and total nitrogen for minesoils of the loess plateau using geostatistics. – Ecological Engineering 82: 159-164.
[40] Warrick, A. W., Gardner, W. R. (1983): Crop yield as affected by spatial variations of soil and irrigation. – Water Resources Research 19(1): 181-186.
[41] Weir, J. P. (2005): Quantifying test-retest reliability using the intraclass correlation coefficient and the sem. – The Journal of Strength & Conditioning Research 19(1): 231-240.
[42] Wesenbeeck, I. J. V., Kachanoski, R. G. (1988): Spatial and temporal distribution of soil water in the tilled layer under a corn crop. – Soil Science Society of America Journal 52(2): 363-368.
[43] Yan, L., Ping, Z., Yan, N., Shukun, S., Xiuqing, Z., Hong, S. (2006): Biuret method to measure the protein content in soybean whey. – Soybean Bulletin 6.
[44] Yeomans, J. C., Bremner, J. M. (1988): A rapid and precise method for routine determination of organic carbon in soil. – Communications in Soil Science and Plant Analysis 19(13): 1467-1476.
[45] Zhang, H., Cao, T., Sun, X., Xu, Y. (2021): Temporal and spatial variation characteristics of soil mechanical composition after aeolian soil improvement by soft rock in mu us sandy land. – Bangladesh Journal of Botany: 865-872.
[46] Zhao, K., Xue, P.-J., Gu, G.-Y. (2008): Study on determination of reducing sugar content using 3, 5-dinitrosalicylic acid method. – Food Science 8: 128.

http://www.aloki.hu ● ISSN 1589 1623 (Print) ● ISSN 1785 0037 (Online)
DOI: http://dx.doi.org/10.15666/aeer/2003_19691989

LIGNIN: A DEFENSIVE SHIELD HALTING THE ENVIRONMENTAL STRESSES – A REVIEW

KHAN, P. – TONG, L. – KHAN, S. U. – ZHANG, C. – WANG, W.*

Biotechnology Research Institute, Chinese Academy of Agricultural Sciences
Beijing 100081, China

**Corresponding author*
e-mail: wangweixuan@caas.cn

(Received 10th Sep 2021; accepted 23rd Nov 2021)

Abstract. Plants are exposed to various environmental stresses, like mineral deficiency, heavy metals, high and low temperature, and drought, causing adverse effects on plant growth and productivity. Currently, various strategies are employed to generate plants that can withstand these environmental stresses. To this end, the induction of phenylpropanoid pathways are triggered by the signaling network of extracellular ATP (eATP) and dinucleotide polyphosphates (NpnN's) yielding several metabolites including lignin. Depending upon the stress, lignin plays protective, sustaining or disruptive roles in addition to its involvement in plant growth, development and defense responses. Aside from its involvement in plant development, lignin is also active in the response to numerous abiotic and biotic stress, and hence plays a significant role in plant adaptation to their environment. To differentiate it from developmental lignin, the lignin polymer generated in response to stress is referred to as 'stress lignin' or 'defense lignin.' In this review, we analyzed the role of lignin as a defensive shield under environmental stress. The physiological and molecular aspects of lignin biosynthesis were also summarized. The analysis and information presented in this review article will help in understanding and the future investigation of lignin in plants with respects to its defensive role under environmental stressed conditions.
Keywords: *abiotic stress, plant hormones, drought, minerals, toxic metals*

Introduction

Lignin is an important secondary metabolite produced by the tyrosine-phenylalanine metabolic pathway in all plants. It is the second most abundant biopolymer, accounting for 31% of the organic carbon mass in the biosphere (Fleming et al., 2002). Classically, lignin is a three-dimensional phenolic polymer formed by the oxidation of hydroxycinnamyl alcohols, namely coniferyl alcohol, p-coumaryl alcohol, and sinapyl alcohol, even though other monomers can also be integrated (Fleming et al., 2002). This class of molecules is very important in plant development as it acts as a defense barrier to both biotic and abiotic stress (Fleming et al., 2002). The hydrophobicity of lignin, for example, waterproofs xylem conducting cells, and the stiffness they give to cell walls, reinforces supporting fiber cells in xylem and phloem tissues. The chemical structure of these developmental lignins differs depending on various factors, including plant community, organ, tissue, and even cell wall layer.

Gymnosperm lignin is mostly comprised of G-units (guaicyl units resulting from coniferyl alcohol). In contrast, angiosperm lignin comprises guaicyl-syringyl lignin (G and S units, derived from coniferyl and sinapyl alcohol) (Nawawi et al., 2016). Plants use lignins to protect themselves from a variety of environmental stresses (Thompson, 1984). The lignin synthesized in this case (in response to environmental stress) is known as defense lignin (Xie et al., 2018), which differs from developmental lignin. The formation of cell walls with such material confers an impermeable barrier protecting the healthy plant tissues from dehydration and fungal infection (Lourenço and Pereira, 2018).

http://www.aloki.hu ● ISSN 1589 1623 (Print) ● ISSN 1785 0037 (Online)
DOI: http://dx.doi.org/10.15666/aeer/2003_19912015

Defense lignin formation has also been involved in plant responses to various abiotic stresses (Nicholson and Hammerschmidt, 1992). Previous studies suggest that the defense lignin is chemically different from developmental lignin (Stange et al., 2001; Cesarino, 2019). For example, defense lignin containing an abundance of p-coumaraldehyde units (H-units), contrary to developmental lignin in cucurbit that is composed of angiosperm guaiacyl-syringyl (G–S) lignin (Xie et al., 2018).

Similarly, defense lignin in almond trees and wounded poplar has G-lignin contrary to the normal G–S developmental lignin (Chezem et al., 2017). While the enzymatic reaction for both developmental and defense lignin appears to be the same but the signal transduction pathways are different. For example, phenylpropanoid ammonia lyase (PAL) and O-methyltransferase genes are differentially regulated during development against external stimuli (Gallego et al., 2018). Thus, such regulation presumably allows the plant to direct its phenolic metabolite pool to where it is needed. *Arabidopsis cinnamoyl* CoA reductase genes AtCCR1 and AtCCR2 (Xie et al., 2018) showed a differential expression pattern under pathogen attack, suggesting that the production of defense lignin is also controlled at the level of the bio-synthetic pathway.

In this respect, lignin production under biotic and abiotic stress has been demonstrated to be the outcome of a complex genetic network involving multiple enzymes that respond differentially to abiotic and biotic impacts (Hawkins and Boudet, 1996). In this context, the literature is replete with examples of plants exhibiting enhanced lignin concentration or a variation in chemical composition under stress conditions, implying complicated genetic and physiological control. It is possible that understanding how a stressor "modulates" the expression of "lignin genes" would allow us to develop study models to elucidate genetic control of lignin synthesis and its deposition in the cell wall. Here in this review, we summarize the progress in lignin for its structural features, regulatory mechanisms, and interaction with plant hormones in response to abiotic or environmental stresses.

Structure and regulation of lignin under environmental stress

Lignin polymer is produced by the phenylpropanoid pathway via oxidative coupling of three hydroxycinnamyl alcohols or monolignolos, i.e., p-coumaryl, coniferyl and sinapyl (*Fig. 1*). Their assimilation produces different units of lignin with varying degrees of methoxylation. These units are p-hydroxyphenyl (H), syringyl (S) and guaiacyl (G) units. The composition, contents, and linkage frequency of developmental lignin are different among different cell types, growth stages, and plant species. The gymnosperm and angiosperm have different compositions and units of lignin. For example, gymnosperm contains G lignin with a few H units, and angiosperm contains mostly G and S units (Logemann et al., 1995). The physical characteristics and structural features of defense lignin are different from developmental lignin (Lauvergeat et al., 2001; Bonawitz and Chapple, 2010). There is limited knowledge about stress induced lignin and its chemical nature needs to be explored. The structure of lignin polymer varies among plant species and stress. Some of the common responses regarding stress and lignin are shown in (*Fig. 2*).

Angiosperms and gymnosperms have been demonstrated to synthesize more condense lignin with a higher inter C-C bond and H units in response to several environmental stresses, including ozone exposure, high nitrogen fertilization, and mechanical stimuli (Bonawitz and Chapple, 2010; Hawkins and Boudet, 2003). Lignin observed in Norway

http://www.aloki.hu ● ISSN 1589 1623 (Print) ● ISSN 1785 0037 (Online)
DOI: http://dx.doi.org/10.15666/aeer/2003_19912015

spruce, and Jack pin shows the same features when treated with fungal elicitor (Lauvergeat et al., 2001). Compression wood has an increased amount of H units in response to gravistimulation. It was predicted that compression wood might have a higher proportion of condense linkage, but a recent report showed that compressed wood and normal wood have no statistical difference (Sato et al., 2011). Lignin induction by stress might cause the enrichment of H units that ultimately exhaust the precursors of coniferyl and sinapyl alcohol, whose incorporation in lignin monomer built a biosynthetic pathway with faster response (Lauvergeat et al., 2001). The condensation degree might be enhanced by the incorporation of H units resulting formation of C-C bonds (Sato et al., 2011; Cabané et al., 2004). In addition, it has been reported that stress always triggers monolignols comprising β-5 and β-β condensed bonds through dehydrodimerization reactions (Cabané et al., 2004). Interestingly, these structural characteristics of lignification in gymnosperm and angiosperm, in which lignin is formed in middle lamella with enriching condensed H units. The S lignin has been proven to show resistance against various microbes (Nanayakkara et al., 2011). In other studies, S lignin preferentially accumulates in infected tissues (Saito and Fukushima, 2005; Barber et al., 2000).

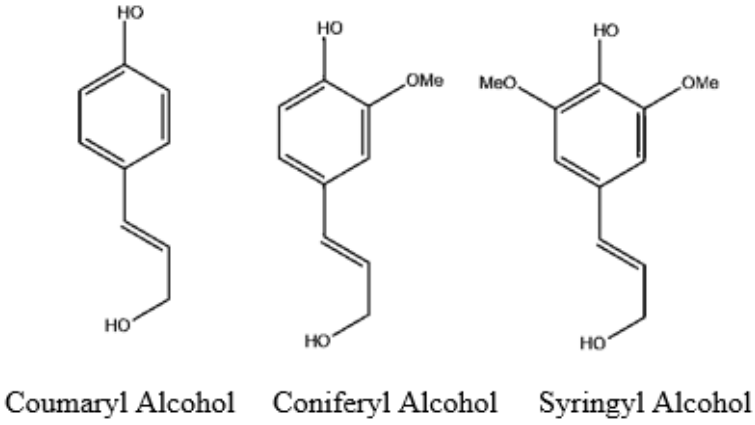

Figure 1. *Structure of lignin monomers*

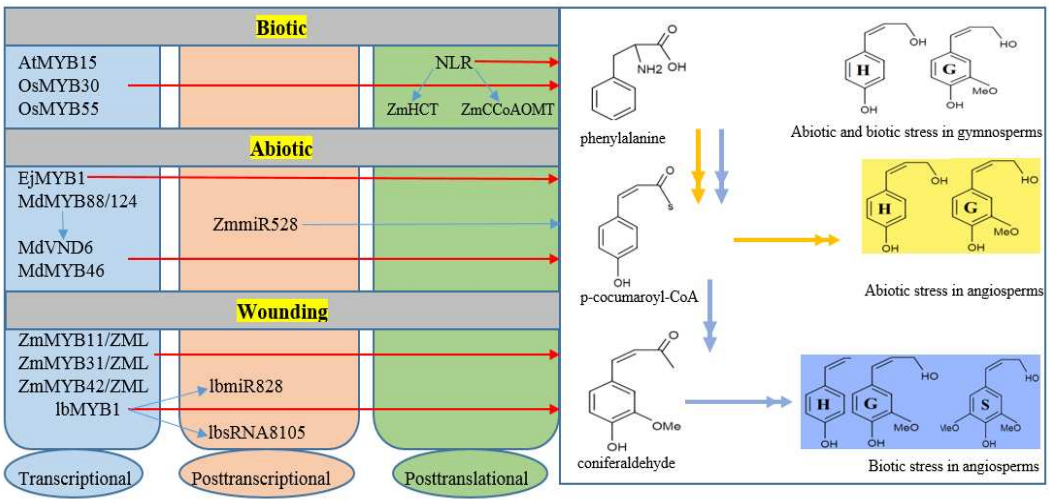

Figure 2. *Structure and regulation of lignin during stress*

http://www.aloki.hu ● ISSN 1589 1623 (Print) ● ISSN 1785 0037 (Online)
DOI: http://dx.doi.org/10.15666/aeer/2003_19912015

Moreover, it was observed that the engineered S lignin showed increased resistance against environmental stresses (Hano et al., 2006; Menden et al., 2007). The expression of monolignol genes is activated by the transcription factor AtMYB58 by binding to the AC elements in their promoter region (Eynck et al., 2012). The promoter of FERULATE 5- HYDROXYLASE (F5H) contain no AC element to synthesize S lignin (Wuyts et al., 2006); instead, (F5H) is directly regulated by SND1, but it cannot activate other lignin genes. It is a NAC master switch that activates the whole program of secondary cell wall deposition (Gallego et al., 2018; Zhou et al., 2009).

Lignin deposition under environmental dares

Lignification is an irreversible asset of energy and carbon. Developmental lignin deposition is regulated at transcriptional (Raes et al., 2003), post-transcriptional, post-translational level (Zhao et al., 2010; Cesarino, 2019). Recently, it was reported that stress related lignin is controlled at several regulatory levels, similar to that for developmental lignin. The H_2O_2 signal transduction contributes to extracellular lignin and flavonoid biosynthesis and the extracellular lignin production; on the contrary, it is severely hindered by H_2O_2 scavenging (Rao and Dixon, 2018). As a result, changes in cellular redox status caused by the accumulation of reactive oxygen species (ROS) in response to biotic and abiotic stresses are likely to be the first layer of regulation during lignin formation.

Ascorbate peroxidase stimulates the formation of the monolignol radicals in the cell wall, catalyzed by peroxidases, and detoxify hydrogen peroxide in the cytosol during monolignol formation representing a possible correlation between monolignol synthesis and detoxification of hydrogen peroxide. This enzyme exists in a diverse cellular compartment in plants, with a key function of detoxifying hydrogen peroxide produced upon abiotic stress (Gou et al., 2018).

In a monolignol pathway, coumarate 3-hydroxylase (C_3H) is the third enzyme with a secondary function associated with ROS, being caffeoyl shikimate esterase (CSE) and cinnamoyl CoA reductase (CCR). During the evolution of the monolignol pathway, the earliest land plants acquired phenylalanine ammonia-lyase (PAL) from soil bacteria through horizontal gene transfer with a primary function of defense against various environmental stresses (Gou et al., 2018; Lin et al., 2015).

The Arabidopsis lysophospholipase 2 (CSE/LPL2) binds to acyl CoA-binding protein 2 (ACBP2) through the ankyrin repeat (Laitinen et al., 2017; Caverzan et al., 2012). Hydrogen peroxide triggers the expression of lysophospholipase 2/CSE, and its loss of function and overexpression alter its sensitivity to hydrogen peroxide, in turn (Laitinen et al., 2017). Characteristics of this enzyme complex need to explore further regarding its function in monolignol formation.

The final steps in monolignol biosynthesis are sequential declines in an acyl CoA (for G units, feruloyl CoA) catalyzed via cinnamoyl CoA reductase (CCR) and cinnamyl alcohol dehydrogenase (CAD) (Weng et al., 2010). In multiple species, mathematical modeling (Gao et al., 2010) and protein interaction experiments (Miao et al., 2019) have indicated that CCR and CAD are localized in a membrane associated complex whose behavior seems dynamic. In theoretical models, the membrane cavity was previously defined as the endoplasmic reticulum (ER) outer surface (Gao et al., 2010), but it may also be the plasma membrane's inner surface. As such, previous research had demonstrated that the interaction of OsCCR2 with

http://www.aloki.hu ● ISSN 1589 1623 (Print) ● ISSN 1785 0037 (Online)
DOI: http://dx.doi.org/10.15666/aeer/2003_19912015

OsRAC1, a member of the Rac/Rop family of small membrane bound GTPases that is a positive regulator of hydrogen generation via the NADPH oxidase (N.O.X.) (Zhuo et al., 2019).

The interaction between OsRAC1 and OsCCR2 resulted in a 10-fold increase in Os-CCR2's catalyzed feruloyl CoA to coniferyl aldehyde; additionally, OsCCR2 bound to OsRAC1 primarily in the presence of GTP, which was also required for OsRAC1's activation of NOX (Zhuo et al., 2019). Stimulation of NOX induces the hydrogen peroxide needed for monolignol oxidation and polymerization via peroxidases (PX).

It is worth noting that OsCCR2 and OsRAC1 expression is directly linked to lignification through plant defense, and many plants have at least two CCR genes, each with specialized and redundant functions.

The loss of function of Arabidopsis CCR1, which is involved in the regulation of developmental lignin, results in a significant decline in reactive oxygen species (ROS) (Faraji et al., 2018). Of the several classes of enzymes that convert superoxide into hydrogen peroxide, few Cu/Zn SODs are widely distributed in the apoplast synthesizing hydrogen peroxide for lignification (Yan et al., 2019); hydrogen peroxide (H_2O_2) diffuse through membranes poorly and is mainly transported primarily through aquaporins water channels (AqP) (Kawasaki et al., 2006).

In addition, concentration gradients of hydrogen peroxide within the apoplast leading to an inward movement of H_2O_2 into the cell membrane. It is likely that this could occur even after activation of NOX (RBOH) in plant protection, even though it is less clear whether these gradients arise throughout developmental lignification (Möller et al., 2019).

Lignin in stress tolerance

Lignin and minerals

A few studies were performed to determine the effect of nitrogen fertilization on wood properties, showing lignin was increased by nitrogen due to high phenylalanine ammonia lyase (PAL) activity (Möller et al., 2019). The impact of nitrogen N seems to vary regarding plant type, degree of development, and the tissue conducted. Excess N fertilization decreased lignin in the roots but did not affect the aerial parts in pine (*P. palustris*) seedlings (*Table 1*). The nitrogen-phosphorus-potassium (NPK) fertilization in red pine (*Pinus resinosa*) decreased the lignin content of the branches (Dixon et al., 2019) but increase lignin contents in the main stem of Picea abies (Gellerstedt and Henriksson, 2008). Populus plants receiving high N (10 mM NH_4NO_3) had lowered lignin content, decreased β-O-4 binding, and increased (Möller et al., 2019) β-hydroxyphenyl unit frequency, leading affinity towards low S/G ratios. At the molecular level, pot171 gene in *Populus trichocarpa* deltoid hybrids, encoding a protein with similarity to CCoAOMT was regulated negatively in response to N (Möller et al., 2019).

The influence of calcium (Ca) on phenylpropanoid biosynthesis is not clear enough. Few studies demonstrate that the activity of guaiacol-POD and PAL increased by (Ca) (Luo et al., 2004); whereas, a decrease in phenolic compounds has also been observed (Blodgett et al., 2005). The reduction in the activity of phenylalanine ammonia-lyase (PAL) and peroxidase (POD) as well as a reduction in phenolic compound and lignin has been reported (Kostiainen et al., 2004). No significant variations in the amount of these compounds have been reported (Kolupaev et al., 2005). In *Populus tremula* and *Populus tremuloides*, wood deformation was caused by Ca deficiency (*Table 1*) (Obeso

http://www.aloki.hu ● ISSN 1589 1623 (Print) ● ISSN 1785 0037 (Online)
DOI: http://dx.doi.org/10.15666/aeer/2003_19912015

et al., 2003). Likewise, Ca is essential for lignin biosynthesis in plants. However, Ca is necessary to link certain PODs with the galacturonic pectin domains, and such a relationship exists only in the pectin chain known as Ca-pectates (Teixeira et al., 2006). Middle lamella and cell corners were reported to be the first places for lignification as they have a higher level of Ca-pectates (Tomás et al., 1997).

Table 1. *Lignin response to environmental stress (mineral stress)*

Env. Stress	Concentration	Species	Plant organs	Effect on lignin	Ref
N	High	**Maize**	**Stem**	↓	Sun et al., 2018
	High	*P. palustris*	Roots	↓	Entry et al., 1998
	High	*P. palustris*	Aerial parts	----	Entry et al., 1998
	High	Populus	Xyleum	9-10% decrease	Pitre et al., 2007
NPK	High	*P. resinosa*	Branches	↓	Blodgett et al., 2005
	High	*Picea abies*	Main stem	↑	Kostiainen et al., 2004

Lignin and toxic metal

Heavy metal toxicity may have several consequences, including blocking functional groups of important molecules (e.g., enzymes, secondary metabolites, and polynucleotides), disrupting the plant's transport mechanism for critical nutrients and ions and inactivating or triggering an excess of antioxidant enzymes by displacing essential ions from cellular sites (Lautner et al., 2007). The effects of some of the key heavy metals stress on the lignin content of plants are summarized in *Table 2*. Heavy metals like manganese (Mn), copper (Cu), cadmium (Cd), and zinc (Zn) ions are taken up by the plants through roots, where the cell wall becomes the first barrier for those ions (Penel et al., 1996). These heavy metal ions (Cu2+, Cd2+, Pb2+, etc.) trigger the pathway of phenolic compounds, resulting in increased lignin accumulation in the secondary cell wall (Carpita et al., 1993). As the polymer of lignin comprises a variety of functional groups (hydroxyl, carboxyl, and methoxyl), it can bind various heavy metal ions such as copper (Cu), cadmium (Cd), zinc (Zn), and manganese (Mn), avoiding heavy metals entry into the cytoplasm (Anwar et al., 2018). Aluminum (Al) is an important heavy metal that causes toxicity and inhibits plant growth, most commonly in root growth inhibition available in acidic soil (Wuana and Okieimen, 2011).

Root endoderm cell walls depositing sufficient lignin may prevent the entry of heavy metal into or out of vascular bundles (Anwar et al., 2018). Recently, it was reported that Al induces 4CL, CAD, C3H, and PAL gene expression in the lignin pathway (Anwar et al., 2018). In an experiment with a tea plant observed under a high concentration of Al, the activity of phenylalanine ammonia-lyase (PAL) and peroxidase (POD) in the cell wall decreased, causing reduction of lignin up to a significant level (Emamverdian et al., 2015). Similarly, Copper (Cu) caused harmful effects on plants; its higher concentration induces the expression of POD, caffeic acid, CAD, and PAL genes. The growth of soybean root was adversely affected by treating with cadmium, inducing peroxidase (POD) and Lacase (LAC) activity, accompanied by increase content of lignin (Liu et al., 2018).

Zinc (Zn) is considered vital for plants, but higher concentration leads to detrimental effects. The roots of *Thlaspi caerulescens* accumulate more Zn/Cd than Arabidopsis where Zn causes the induction of genes responsible for lignin, the reason being

http://www.aloki.hu ● ISSN 1589 1623 (Print) ● ISSN 1785 0037 (Online)
DOI: http://dx.doi.org/10.15666/aeer/2003_19912015

endodermis cell wall in the roots of *T. caerulescens* accumulate more lignin (Fang et al., 2020). These findings suggest that lignification of xylem in roots is potentially involved in the reduction of the transports of Cu, Cd, Zn and Mn to shoots, thus reduced the toxic effect of stress and stabilize ROS accumulation.

Table 2. *Lignin response to environmental stress (toxic metals)*

Env. stress	Concentration	Species	Plant organs	Effect on lignin	Ref
Ca	Low	Lemon	Seedling	↑	Castaiqeda and Perez, 1996
	High	Soybean	Roots	↓	Teixeira et al., 2006
	Low	Populus	Xyleum	↓	Lautner et al., 2007
Al	High	Maize	Roots	↑	Vardar et al., 2011
	High	Wheat	Roots	↑	Sasaki et al., 1996
	High	*Eucalyptus camaldulensis*	Root tip	↑	Tahara et al., 2005
	High	Rice	Root	↑	Ma et al., 2012
Cd	High	*Phragmites australis*	Roots	↑	Ederli et al., 2004
	High	*C. sinensis*	Callus	↑	Zagoskina et al., 2007
Zn	High	*Thlaspi caerulescens*	Roots	↑	Mortel et al., 2006
	High	*A. thaliana*	Roots	↑	
Cu	High	*Capsicum annuum*	Hypocotyls	↑	Diaz et al., 2001
	Low	*Raphanus sativus*	Roots	↑	Chen et al., 2002
	High	*Panax ginseng*	Roots	↑	Ali et al., 2006
	Low	Wheat	Leaf	↓	Robson et al., 1981
	High	Soybean	Roots	↑	Lin et al., 2005

Lignin and drought

Among various abiotic stresses, water deficit or drought is a critical environmental factor threatening the throughput and yield of various crops. It adversely affects the anti-oxidant systems, chlorophyll contents, photosynthetic activity, and stability of membrane (Ghanati et al., 2005). A key gene of the lignin pathway, Phenylalanine ammonialyase (PAL), is a key enzyme in the lignin pathway that catalyzes phenylalanine's deamination transcinnamate. In rice, drought stress caused upregulation of PAL (Yang et al., 2007). Furthermore, several adverse physiological changes have been considered because of drought stress (*Table 3*). In maize plants, the activity of anionic peroxidase is reduced by the water deficit and may reduce the synthesis of lignin (Klein et al., 2008). Lignin deposition occurred in a particular region of roots (Fahad et al., 2017; Pandey et al., 2010).

In rice plants, genes responsible for cell development and root extension were induced after exposure to 16 h water stress (Pandey et al., 2010). Similarly, water stress causes lignin deposition in *Citrullus lanatus* sp. (Pandey et al., 2010). In another study, PAL and ascorbate peroxidase activity was found to be enhanced after 28 days of exposure to water deficit in *Trifolium repens* with increased lignin biosynthesis (Alvarez et al., 2008; Fan et al., 2006). During drought stress, the yield and physiological traits were observed in *Z. mays* L. var. TWC647 by spraying amino acids

http://www.aloki.hu ● ISSN 1589 1623 (Print) ● ISSN 1785 0037 (Online)
DOI: http://dx.doi.org/10.15666/aeer/2003_19912015

leading to a significant increase in lignin contents with an increased accumulation of proline (Yoshimura et al., 2008). In another study, soybean seeds were examined under the condition of water deficit and discovered that phenol, isoflavone and lignin contents were higher in the treated seeds, and found that all these compounds play a role in biotic and abiotic stress tolerance (Lee et al., 2007).

Under drought stress, soybean significantly enhances the expression on the CCoA-OMT gene typically elongated region of roots with enhanced lignin accumulation (*Table 3*) (Komatsu et al., 2010). CAD and COMT, two key lignin genes, were upregulated under drought stress, showing a positive response in maize (Kasraie et al., 2012). Under low water stress, the Cinnamyl CoA reductase (CCR) gene upregulated significantly in maize roots (Bellaloui et al., 2012). Drought stress had a significant effect on the lignin and CCR protein expression in *Leucaena* stem development, suggesting the role played by lignin in drought stress tolerance (Yamaguchi et al., 2010).

Table 3. *Lignin response to environmental stress (drought)*

Species	Plant organs	Effect on lignin	Ref
Maize	Xylum sap	↓	Alvarez et al., 2008
Water melon	Roots	↑	Yoshimura et al., 2008
Trifolium	Leaves	↑	Bok-Rye et al., 2007
Soybean	Seeds	↑	Bellaloui et al., 2012
Soybean	Roots	↑	Al-Hakimi et al., 2006

Lignin and extreme temperature

Temperature is major abiotic stress-causing considerable damage to physiological processes and limiting plant growth and development worldwide (Bellaloui et al., 2012). High and low temperature exacerbates normal plant metabolism, including photosynthesis, nucleic acid and protein, membrane lipid peroxidation, and flower bud abortion—alteration in any of these parameters threatening agriculture by significant yield losses (Hu et al., 2009).

Likewise, other abiotic stresses, lignin, play a fundamental role in temperature (both low and high temperature) stress and improve plant growth and development (*Table 4*) (Fan et al., 2006). C3H (p-coumarate 3-hydroxylase) is a major gene involved in the lignin biosynthesis pathway. Recently, cold acclimation induced (C3H) gene expression in the Rhododendron plant leading to enhanced lignin contents in its leaves. In Rhododendron, C3H might affect the water permeability and rigidity of call wall by altering the S/G ratio during cold stress (Srivastava et al., 2015). In *Betula platyphylla*, the BpMADS12 gene regulates lignin metabolism against brassinosteroid (BR) signaling, endeavoring to elaborate the mechanisms responsible for development and wood formation (Le et al., 2015). The author reported that BpMADS12 regulates several Brassinosteroid biosynthesis genes.

Brassinosteroid (BR) is a plant steroid hormone, which is potentially involved in chilling and heat stress in a plant (Liu et al., 2018). The lignin content of the cad1 mutant was significantly lower than that of the wild type in *Medicago truncatula*; while, there was no visible growth difference between the mutant and wild types at normal temperatures. These results represented that Cinnamyl Alcohol Dehydrogenase 1 (CAD1) is involved in lignin in this MtCAD1 mutant (Liu et al., 2018).

http://www.aloki.hu ● ISSN 1589 1623 (Print) ● ISSN 1785 0037 (Online)
DOI: http://dx.doi.org/10.15666/aeer/2003_19912015

Table 4. *Lignin response to environmental stress (temperature)*

Species	Plant organs	Effect on lignin	Ref
Low temperature			
Populus tremula	Seedlings	↑	Hausman et al., 2000
Brassica napus	Seedlings	-----	Solecka et al., 1999
Glycine max	Roots	↑	Janas et al., 2000
Triticum aestivum	Leaves	----	Olenichenko and Zagoskina, 2005
High temperature			
Panicum maximum	Fifth Leaf	↑	
Setaria anceps	--------	↑	
Heteropogon contortus	Fifth Leaf	↑	
Chloris gayana	Fifth Leaf	↑	
Paspalum dilatatum	Fifth Leaf	↑	
Sorghum almum	Fifth Leaf	↑	
Cenchrus ciliaris	Fifth Leaf	↑	
Themeda australis	Fifth Leaf	↑	
Panicum coloratum	Fifth Leaf	↑	
Melinis minutiflora	Fifth Leaf	↑	
Cynodon dactylon	Fifth Leaf	↑	
Digitaria smutsii	Fifth Leaf	↑	
Astrebla lappacea	Fifth Leaf	↑	Ford et al., 1979
Triticum vulgare	Fifth Leaf	↑	
Bromus unioloides	Fifth Leaf	↑	
Festuca arundinacea	Fifth Leaf	↑	
Avena sativa		↑	
Lolium rigidum	Fifth Leaf	↑	
Dactylis glomerata	Fifth Leaf	↑	
Phleum pratense	Fifth Leaf	↑	
Phalaris tuberosa	Fifth Leaf	↑	
Danthonia caespitosa	Fifth Leaf	↑	
Hordeum leporinum	Fifth Leaf	↑	
Lolium perenne	Fifth Leaf	↑	
Panicum maximum	Fifth Leaf	↑	

Lignin and elevated CO_2

Currently, CO_2 concentrations have risen up to 400 ppm due to industrialization and are expected to double in the 2100 century (Wei et al., 2006). It is well known that an elevated level of CO_2 has profound effects on the morphology and physiology of both C3 and C4 plants. According to the previous experiments conducted in maize, elevated CO_2 causes stomatal closure and reduces its conductance but increases biomass, growth, and yield (Li et al., 2016). The growth and biomass stimulation are often concomitant

http://www.aloki.hu ● ISSN 1589 1623 (Print) ● ISSN 1785 0037 (Online)
DOI: http://dx.doi.org/10.15666/aeer/2003_19912015

with higher carbon assimilation (Zhao et al., 2013) depending on the response of the species considered. Moreover, elevated CO_2 has little effect on C4 species than herbaceous species, but trees are more responsive to CO2. Similarly, nitrogen (N) availability was found to CO_2-induced stimulation of photosynthesis. According to the source-sink balance hypothesis, it is predicted that elevated CO_2 escalates the concentration of secondary metabolites (Ainsworth and Long, 2005). The carbon availability is relatively increased by the elevated CO_2, or nutrient stress that ultimately leads to the source leaves, being rich in carbon-based secondary or structural compounds. There is a general tendency towards increasing levels of secondary compounds shown by the various authors, but the chemical nature of lignin varies depending on the species or genotype (Ainsworth and Long, 2005). There are many controversial studies about the contents of lignin and elevated CO_2. Numerous studies have shown that elevated CO_2 enhances Lignin content in tree leaves (Raven et al., 2012). However, in each case, the effect of CO_2 was shown to be highly dependent on N supply (Bidart-Bouzat and Imeh Nathaniel, 2008). Leaf lignin content was higher under the effect of elevated CO_2 in N-limited plants, whereas in plants grown with high nutrient supply, there was no change or decrease in lignin contents by elevated CO_2 (*Table 5*) (Norby et al., 2001).

Table 5. *Lignin response to environmental stress (elevated CO_2)*

Env. stress	Species	Plant organs	Effect on lignin	Ref
CO_2	Herbaceous/woody plants	Leaf liter	↑	Norby et al., 2001
	N. tabacum	Root	----	Matros et al., 2006
	N. tabacum	Leaves	-----_	Schlimme et al., 2002
	Populus tremul	**Stem**	↑	Richet et al., 2012
	Betula pendula	Leaves	↑	Oksanen et al., 2005
	Glycine max	Leaves	↑	Booker et al., 2005

The recent transcriptomic analyses show that elevated CO_2 causes stimulation of the phenylpropanoid pathway. For example, birch trees accumulated phenylpropanoid pathway transcripts during the month of august under elevated CO_2 levels cultivated for six years. In this study, the authors suggested that this stimulation would ultimately give rise to phenolic compounds (Porteaus et al., 2009). The same pattern of stimulation regarding gene expression was also observed in *Arabidopsis* grown under elevated CO_2. Among other cell wall related genes, PAL1 and LAC4 genes were upregulated.

During metabolite profiling, it was observed that elevated CO_2 affects most of the amino acids except phenylalanine, histidine, and tryptophan. In another study, genes involved in secondary metabolism, particularly phenylpropanoid pathway genes, also show increased expression in soybean grown for 40 days under elevated CO_2. However, response to elevated CO_2 was genotype dependent, as demonstrated earlier (Blaschke et al., 2002). In a study, two clones of *Populus tremuloides*, CO_2 responsive and unresponsive, were grown in long term FACE experiments. These two genotypes showed similar physiological responses, including leaf area index, photosynthesis, and stomatal conductance. It is well known that leaves are the entrance and source organs, so studies regarding the effect of elevated CO_2 on plants have been focused on leaf physiology and biochemistry. In *Populus tremuloides*, gene expression profiles of

http://www.aloki.hu ● ISSN 1589 1623 (Print) ● ISSN 1785 0037 (Online)
DOI: http://dx.doi.org/10.15666/aeer/2003_19912015

leaves and stems reflect a higher abundance of the gene in stems suggesting a higher readjustment to elevated CO_2 levels in stems (Dong et al., 2018). Most genes were found to be upregulated in leaves regarding shikimate and flavanol synthesis; whereas phenylpropanoid and lignin synthesis (C3H, COMT and CAD) genes were found to be upregulated in stems. In free air concentration enrichment (FACE) experiments, it was shown that lignin content was enhanced in the wood from coppices of both *Populus euramericana* and *Populus nigra* (Kontunen et al., 2010) and in birch as well (Cseke et al., 2009). However, other studies found contradictory results with reduced lignin (Bidart-Bouzat and Imeh Nathaniel, 2008), and no change in lignin contents was found (Druart et al., 2006).

Lignin and ozone

Among other pollutants, tropospheric ozone is well known pollutants having a detrimental effect on plants (Luo et al., 2009). The ozone concentration has been increasing since the beginning of the industrial era and is predicted to be more than double in the future (IPCC, 2007). Ozone has many adverse effects on plants' growth and yield (Mattson et al., 2005). Additionally, ozone has been shown to cause visible damage to leaves as plants respire ozone through stomata generating reactive oxygen species (ROS) after reacting with apoplast. It has also been suggested that ozone may induce plant defense reactions such as programmed cell death (Kostiainen et al., 2008). Many reports present the role of ozone in stimulating phenylpropanoid metabolism in many species both at an acute and chronic level. The PAL enzyme activity was shown to increase by ozone in *Pinus sylvestris* (Booker et al., 2009), soybean, Glycine max (Wittig et al., 2009) poplar (*Populus* spp.) and grape (Rosemann et al., 1991). There are numerous transcriptomics studies available representing that ozone control lignification through transcriptional regulation, for example, PAL, 4CL, C3H, CCoAOMT, and CCR in rice (Booker et al., 1998). COMT in beech Arabidopsis (Di Baccio et al., 2008) and CCR in birch responded to ozone treatment (Porteaus et al., 2009). Beyond the stimulation of the phenylpropanoid pathway, it was found interesting that ozone also upregulates shikimate pathway that provide substrate to phenylpropanoid pathway (Hawkins et al., 2003; Sgarbi et al., 2003).

It was found quite interesting that experiments conducted in open top chambers and natural conditions such as free air ozone fumigation facilities; plants show the same response and trend in both cases (Frei et al., 2011). Conclusively, it is obvious that the phenylpropanoid pathway is upregulated in leaves under ozone treatment so it might be involved in defense and acclimation mechanisms. However, until recently, it is not clear how does ozone affect lignin in leaves as no modifications of lignin content were observed in soybean (Wittig et al., 2009), barley (Olbrich et al., 2009), *Pinus taeda* (Janzik et al., 2005), yellow poplar (Betz et al., 2009), cotton (Plessl et al., 2005) and *Quercus ilex* (Booker et al., 1996). On the other hand, there are several contradictory reports that show an increase in Lignin contents after ozone treatments in poplar, *Trifolium* spp. (Boerner et al., 1995) sugar maple (Betz et al., 2009), *Briza maxima* (Booker et al., 2000), and rice (Booker et al., 1998).

Two possibilities are there supporting these contradictory results. The first possibility is that the ozone effect might be species dependent, so some species respond well and others not. For example, increasing contents of lignin has never been found in conifer (Wittig et al., 2009) and another possibility is the use of various techniques applied and the potential errors made in handling those techniques, i.e., Klason, LTGA, used to

http://www.aloki.hu ● ISSN 1589 1623 (Print) ● ISSN 1785 0037 (Online)
DOI: http://dx.doi.org/10.15666/aeer/2003_19912015

determine lignin contents (Baldantoni et al., 2011), especially in those cases where there are weak variations between control and experimental samples.

Extracellular ATP and uncommon nucleotide in lignin biosynthesis

Plants have established a signaling network enabling them to maintain homeostasis against external environmental stimuli. These signals are perceived by the receptors in the plasma membrane that ultimately respond to the external stimulus in the form of altered metabolism. Here, we focus on the role of extracellular ATP (eATP) and uncommon nucleotides such as mono- (pnNs) and dinucleotide polyphosphates (NpnN's) and their role as signaling molecules throughout lignin biosynthesis under abiotic stress.

Involvement of eATP in responses to abiotic stresses

Text Adenosine 5′-triphosphate (ATP), along with the other nucleotide triphosphates, has been identified as a source of energy in various cell reactions in both animal and plant species (Muntifering et al., 2006). The role of nucleotides as signaling molecules that functioned similarly in plants and animals was regarded with skepticism for decades. The discovery of a membrane receptor protein and its high affinity for extracellular nucleotides was a real breakthrough in this area (Sanz et al., 2011). In contrast, the mechanism of ATP transfer from the cytoplasm into the extracellular matrix in plants was discovered earlier (Dence, 1992). ATP can be released in a variety of ways in plants; environmental stimuli can cause the release of ATP by the exocytosis (Tripathi et al., 2018), injured cell membrane (Choi et al., 2014), and by the p-glycoprotein (PGP1) transporters (Dark et al., 2011), and plasma membrane localized nucleotide transporters (PM-ANT1) (Song et al., 2006). The interaction between eATP and receptors triggers a series of downstream physiological changes that protect the plant from environmental stresses ensuring appropriate growth and development (Kim et al., 2006). In plants, eATP, on binding to the P2K1 receptor, playing a role as an active messenger stimulating signaling pathways. Cytosolic secondary messenger, including reactive oxygen species (ROS), Ca2, and nitric oxide (NO) exist in various signaling pathways. These secondary messengers cause the phosphorylation of mitogen activated protein kinases (MAPK), and induce the expression of defense related genes (Thomas et al., 2000). Apart from eATP-triggering and signaling molecules, the classical protective hormones, namely jasmonate, ethylene, and salicylic acid, induce plant resistance to pathogens and abiotic stresses (Rieder et al., 2011).

Very few studies demonstrate the role played by eATP against different environmental stresses. Apart from mechanical stress, ATP is also generated in the presence of molecules such as L-glutamate and abscisic acid (Lim et al., 2014). Osmotic and salt stress can also cause similar reactions (Tanaka et al., 2014) and cadmium treatment (Jewell et al., 2019). Therefore, eATP accumulation induces a plant defense system against various abiotic and biotic stresses. In response to environmental stimuli, it enables rapid leaf stomatal closure (Clark et al., 2011), probably seedling viability improvement (Jeter et al., 2004) and alterations of root growth while undergoing hindrance (Hou et al., 2017).

Likewise, hypertonic salt stress disrupts the photosynthesis machinery by lowering photosystem II's maximum efficiency and depleting the photochemical quenching method (Jewell et al., 2019). Furthermore, cadmium induced abiotic stress enhances

http://www.aloki.hu ● ISSN 1589 1623 (Print) ● ISSN 1785 0037 (Online)
DOI: http://dx.doi.org/10.15666/aeer/2003_19912015

lipid peroxidation as well as antioxidant and lipoxygenase activities in *Arabidopsis thaliana* cells (Jewell et al., 2019). All of these reactions cause jasmonic acid to be synthesized, a molecule involved in a variety of stress responses (Chen et al., 2017). These reactions are linked to increased jasmonic acid synthesis, essential molecules involved in stress responses.

Cadmium is a major anthropogenic contaminant today that poses a serious threat to human health today (Kim et al., 2009). In plants, it disrupts photosynthesis and respiration, resulting in a decline in crop biomass (Tanaka et al., 2010). Cadmium, in turn, encourages oxidative stress by synthesizing reactive oxygen species (ROS) (Kim et al., 2009), alterations in gene expression (Wasternack et al., 2018; Rizwan et al., 2017) and changes in enzyme activity as well (Fargaaová et al., 2018) that ultimately lead to activating plant defense.

Uncommon nucleotides as a signaling molecule and lignin biosynthesis

Although mono and dinuceloside polyphosphates were discovered in the late twentieth century, our understanding of their biological role, especially in plants, is still limited. Mononucleoside polyphosphates (PnNs) encompass a nucleoside and oligophosphate chain, e.g., adenosine 5'tetraphosphate (p4A) and adenosine 5′-pentaphosphate (p5A). In higher plants, despite the lack of awareness about the nature and accumulation of mononucleotide polyphosphates, several enzymes have been identified that can synthesize pnNs; 4-coumarate: CoA ligase (4CL2) from *Arabidopsis thaliana* was the first plant enzyme synthesizing pnNs, and it mediates the reaction of p4A and p5A synthesis (Sarry et al., 2006). In the phenylpropanoid pathway, this enzyme contributes to flavonoids, lignin, and stilbenes biosynthesis as a branch point. Plants show responses against various environmental changes in terms of phenylpropanoid pathway activation (Herbette et al., 2006).

In *Arabidopsis thaliana*, amino acid synthetase (JAR1) is another enzyme that synthesizes p4A and triggers the function of jasmonic acid (JA) (Sanità et al., 1996). JAR1 plays a role in the action of jasmonic acid (JA) as a plant hormone, as well as catalyzing the synthesis of other JA-amido conjugates, the most important of which is jasmonic acid isoleucine. Either of the plant enzymes listed above is a member of the acyl adenylate-forming firefly luciferase superfamily (Pietrowska et al., 2003) catalyzes a two-step reaction. Firstly, ATP and acyl combine to synthesize an acyladenylate intermediate, releasing pyrophosphate simultaneously (PPi). Secondly, 4CL mediates the synthesize of uncommon mononucleoside polyphosphates, including p4A and p5A, in the absence of CoA (Herbette et al., 2006).

Only a few papers have been published so far describing the function of uncommon nucleotides in plants. Exogenous uncommon nucleotides have been shown to affect the phenylpropanoid pathway (Dixon et al., 1995). According to the most recent report, in juvenile *Arabidopsis thaliana* seedlings, diadenosine 5′,5‴ P1, P3-triphosphate (Ap3A, ApppA) and diadenosine 5′,5‴ P1, P4-tetraphosphate (Ap4A, AppppA) regulate gene expression and enzyme activity implicated in the phenylpropanoid pathway (Guranowski et al., 2007). Similarly, Ap3A and Ap4A was reported to stimulate the expression of (about 70-fold) PAL2 genes that significantly enhanced PAL activity (about 9-fold). Furthermore, it was reported that seedlings treated with Ap3A and Ap4A showed higher expression of the 4CL gene (Staswick et al., 2002). These findings also suggest that 4CL has a dual role in the plant's stress response. The activation of the phenylpropanoid pathway by NpnNs, which increases the development of various

http://www.aloki.hu ● ISSN 1589 1623 (Print) ● ISSN 1785 0037 (Online)
DOI: http://dx.doi.org/10.15666/aeer/2003_19912015

phenylpropanoid compounds, including flavonoids, lignin, anthocyanins, and salicylic acid, is recognized as one of higher plants' defensive strategies against environmental stresses (*Fig. 3*) (Pietrowska et al., 2011).

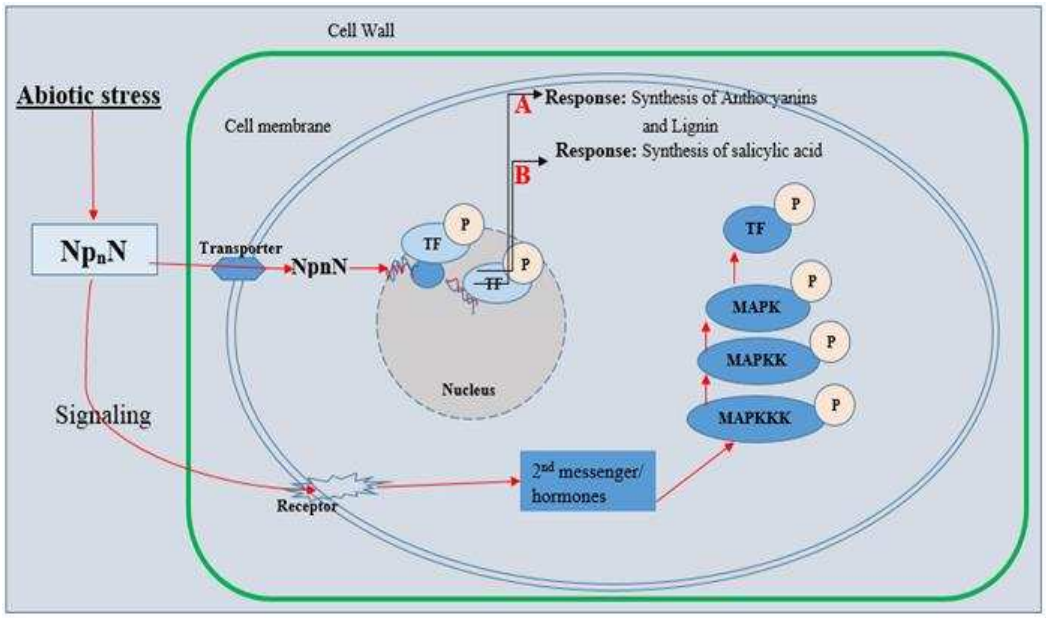

Figure 3. *Theoretical model showing NpnN signaling network of NpnN in plant cell*

Conclusion

Recently, considerable research has been done to understand the molecular and physiological mechanism of lignin to define its regulatory mechanism, signaling transduction pathway, and transcription factors involved in stress responses. Lignin is a polymer that plays a variety of roles in the plant kingdom. It is one of the most abundant renewable raw materials. Lignin biosynthesis can be influenced by various abiotic and biotic environmental influences, reducing the harmful effects as described above. Numerous studies reported various candidate genes (QTLs) and transcription factors potentially involved in lignin biosynthesis under abiotic stresses. In this review, we addressed different aspects of the lignin signaling transduction pathway to clarify how lignin induces stress tolerance and biosynthesis mechanism, but the underlying mechanism needs to be explored. For better understanding, researchers are looking into the role of the lignin-signaling pathway, hormone interactions, and crosstalk at the organ, tissue, and cell levels. Future research will explore the possibility of genetically engineering crop varieties and improving nutrient acquisition to reduce fertilizer usage.

REFERENCES

[1] Ainsworth, E. A., Long, S. P. (2005): What have we learned from 15 years of free-air CO2 enrichment (FACE)? A meta-analytic review of the responses of photosynthesis, canopy properties and plant production to rising CO2. – New Phytologist 165: 351-372. https://doi.org/10.1111/j.1469-8137.2004.01224.x.

[2] Al-Hakimi, A. M. (2006): Counteraction of drought stress on soybean plants by seed soaking in salicylic acid. – International Journal of Botany 2: 421-426.

http://www.aloki.hu ● ISSN 1589 1623 (Print) ● ISSN 1785 0037 (Online)
DOI: http://dx.doi.org/10.15666/aeer/2003_19912015

[3] Ali, M. B., Singh, N., Shohael, A. M.., Hahn, E. J., Paek, K.-J. (2006): Phenolics metabolism and lignin synthesis in root suspension cultures of *Panax ginseng* in response to copper stress. – Plant Science 171: 147-154.

[4] Alvarez, S., Marsh, E. L., Schroeder, S. G., Schachtman, D. P. (2008): Metabolomic and proteomic changes in the *xylem* sap of maize under drought. – Plant Cell and Environment 31: 325-340. https://doi.org/10.1111/j.1365-3040.2007.01770.x.

[5] Anwar, A., Liu, Y., Dong, R., Bai, L., Yu, X., Li, Y. (2018): The physiological and molecular mechanism of brassinosteroid in response to stress: a review. – Biological Research 51: 46. http://dx.doi.org/10.1186/s40659-018-0195-2.

[6] Baldantoni, D., Fagnano, M., Alfani, A. (2011): Tropospheric ozone effects on chemical composition and decomposition rate of Quercus ilex L. leaves. – Science of The Total Environment 409: 979-984. https://doi.org/10.1016/j.scitotenv.2010.11.022.

[7] Barber, M. S., McConnell, V. S., DeCaux, B. S. (2000): Antimicrobial intermediates of the general phenylpropanoid and lignin specific pathways. – Phytochemistry 54: 53-56. https://doi.org/10.1016/S0031-9422(00)00038-8.

[8] Bellaloui, N. (2012): Soybean seed phenol, lignin, and isoflavones and sugars composition are altered by Foliar Boron application in soybean under water stress. – Food and Nutrition Sciences 3: 579-590.

[9] Bellaloui, N. (2012): Soybean seed phenol, lignin, and isoflavones partitioning as affected by seed node position and genotype differences. – Food and Nutrition Sciences 3(4): 447. http://dx.doi.org/10.4236/fns.2012.34064.

[10] Betz, G. A., Knappe, C., Lapierre, C., Olbrich, M., Welzl, G., Langebartels, C., Heller, W., Sandermann, H., Ernst, D. (2009): Ozone affects shikimate pathway transcripts and monomeric lignin composition in European beech (*Fagus sylvatica* L.). – European Journal of Forest Research 128: 109-116. https://doi.org/10.1007/s10342-008-0216-8.

[11] Bidart-Bouzat, M. G., Imeh Nathaniel, A. (2008): Global change effects on plant chemical defenses against insect herbivores. – Journal of Integrative Plant Biology 50: 1339-1354. https://doi.org/10.1111/j.1744-7909.2008.00751.x.

[12] Blaschke, L., Forstreuter, M., Sheppard, L., Leith, I., Murray, M., Polle, A. (2002): Lignification in beech (*Fagus sylvatica*) grown at elevated CO2 concentrations: interaction with nutrient availability and leaf maturation. – Tree Physiology 22: 469-477. https://doi.org/10.1093/treephys/22.7.469.

Blodgett, J. T., Herms, D. A., Bonello, P. (2005): Effects of fertilization on red pine defense chemistry and resistance to *Sphaeropsis sapinea*. – Forest Ecology and Management 208: 373-382. https://doi.org/10.1016/j.foreco.2005.01.014.

[14] Boerner, R. E., Rebbeck, J. (1995): Decomposition and nitrogen release from leaves of three hardwood species grown under elevated O 3 and/or CO 2. – Plant Soil 170: 149-157. https://doi.org/10.1007/BF02183063.

[15] Bok-Rye, L., Kil-Yong, K., Woo-Jin, J., Jean-Christophe, A., Alain, O., Tae-Hwan, K. (2007): Peroxidases and lignification in relation to the intensity of water-deficit stress in white clover (*Trifolium repens* L.). – Journal of Experimental Botany 58: 1271-1277.

[16] Bonawitz, N. D., Chapple, C. (2010): The genetics of lignin biosynthesis: connecting genotype to phenotype. – Annual Review of Genetics 44: 337-363. https://doi.org/10.1146/annurev-genet-102209-163508.

[17] Booker, F. (2000): Influence of carbon dioxide enrichment, ozone and nitrogen fertilization on cotton (*Gossypium hirsutum* L.) leaf and root composition. – Plant Cell and Environment 23: 573-583. https://doi.org/10.1046/j.1365-3040.2000.00576.x.

[18] Booker, F. L., Anttonen, S., Heagle, A. S. (1996): Catechin, proanthocyanidin and lignin contents of loblolly pine (*Pinus taeda*) needles after chronic exposure to ozone. – New Phytologist 132: 483-492. https://doi.org/10.1111/j.1469-8137.1996.tb01868.x.

http://www.aloki.hu ● ISSN 1589 1623 (Print) ● ISSN 1785 0037 (Online)
DOI: http://dx.doi.org/10.15666/aeer/2003_19912015

[19] Booker, F. L., Miller, J. E. (1998): Phenylpropanoid metabolism and phenolic composition of soybean (*Glycine max* (L.) Merr.) leaves following exposure to ozone. – Journal of Experimental Botany 49: 1191-1202. https://doi.org/10.1093/jxb/49.324.1191.

[20] Booker, F. L., Prior, S. A., Torbert, H. A., Fiscus, E. L., Pursley, W. A., Hu, S. J. (2005): Decomposition of soybean grown under elevated concentrations of CO2 and O3. – Global Change Biology 11: 685-698.

[21] Booker, F., Muntifering, R., McGrath, M., Burkey, K., Decoteau, D., Fiscus, E., Manning, W., Krupa, S., Chappelka, A., Grantz, D. (2009): The ozone component of global change: potential effects on agricultural and horticultural plant yield, product quality and interactions with invasive species. – Journal of Integrative Plant Biology 51: 337-351. https://doi.org/10.1111/j.1744-7909.2008.00805.x.

[22] Cabane, M., Pireaux, J. C., Leger, E., Weber, E., Dizengremel, P., Pollet, B., Lapierre, C. (2004): Condensed lignins are synthesized in poplar leaves exposed to ozone. – Plant Physiology 134: 586-594. https://doi.org/10.1104/pp.103.031765.

[23] Carpita, N. C., Gibeaut, D. M. (1993): Structural models of primary cell walls in flowering plants: consistency of molecular structure with the physical properties of the walls during growth. – Plant Journal 3: 1-30 https://doi.org/10.1111/j.1365-313X.1993.tb00007.x.

[24] Castaiqeda, P., Perez, L. (1996): Calcium ions promote the response of citrus limon against fungal elicitors or wounding. – Phytochemistry 42: 595-598.

[25] Caverzan, A., Passaia, G., Rosa, S. B., Ribeiro, C. W., Lazzarotto, F., Margis-Pinheiro, M. (2012): Plant responses to stresses: role of ascorbate peroxidase in the antioxidant protection. – Journal of Genetics and Molecular Biology 35: 1011-1019.

[26] Cesarino, I. (2019): Structural features, and regulation of lignin deposited upon biotic and abiotic stresses. – Current Opinion in Biotechnology 56: 209-214 https://doi.org/10.1016/j.copbio.2018.12.012.

[27] Chen, E. L., Chen, Y. A., Chen, L. M., Liu, Z. H. (2002): Effect of copper on peroxidase activity and lignin content in *Raphanus sativus*. – Plant Physiology and Biochemistry 40: 439-444.

[28] Chen, D., Cao, Y., Li, H., Kim, D., Ahsan, N., Thelen, J., Stacey, G. (2017): Extracellular ATP elicits DORN1-mediated RBOHD. phosphorylation to regulate stomatal aperture. – Nature Communication 8: 2265 https://doi.org/10.1038/s41467-017-02340-3.

[29] Chezem, W. R., Memon, A., Li, F. S., Weng, J. K., Clay, N. K. (2017): SG2-type R2R3-MYB transcription factor MYB15 controls defense-induced lignification and basal immunity in Arabidopsis. – The Plant Cell 29(8): 1907-1926. https://doi.org/10.1105/tpc.16.00954.

[30] Choi, J., Tanaka, K., Cao, Y., Qi, Y., Qiu, J., Liang, Y., Lee, S. Y., Stacey, G. (2014): Identification of a plant receptor for extracellular ATP. – Science 343: 290-294 https://doi.org/10.1126/science.343.6168.290.

[31] Clark, G., Fraley, D., Steinebrunner, I., Cervantes, A., Onyirimba, J., Liu, A., Torres, J., Tang, W., Kim, J., Roux, S. J. (2011): Extracellular nucleotides and apyrases regulate stomatal aperture in Arabidopsis. – Plant Physiology 156: 1740-1753 https://doi.org/10.1104/pp.111.174466.

[32] Cseke, L. J., Tsai, C. J., Rogers, A., Nelsen, M. P., White, H. L., Karnosky, D. F., Podila, G. K. (2009): Transcriptomic comparison in the leaves of two aspen genotypes having similar carbon assimilation rates but different partitioning patterns under elevated (CO2). – New Phytologist 182: 891-911. https://doi.org/10.1111/j.1469-8137.2009.02812.x.

[33] Dark, A., Demidchik, V., Richards, S. L., Shabala, S., Davies, J. M. (2011): Release of extracellular purines from plant roots and effect on ion fluxes. – Plant Signaling & Behavior 6: 1855-1857 https://doi.org/10.4161/psb.6.11.17014.

http://www.aloki.hu ● ISSN 1589 1623 (Print) ● ISSN 1785 0037 (Online)
DOI: http://dx.doi.org/10.15666/aeer/2003_19912015

[34] de Obeso, M., Caparros-Ruiz, D., Vignols, F., Puigdomenech, P., Rigau, J. (2003): Characterisation of maize peroxidases having differential patterns of mRNA accumulation in relation to lignifying tissues. – Gene 309: 23-33. https://doi.org/10.1016/s0378-1119(03)00462-.

[35] Dence, C. W. (1992): The Determination of Lignin. – In: Lin, S.Y., Dence, C.W. (eds.) Methods in Lignin Chemistry. Springer, Berlin, pp. 33-61. https://doi.org/10.1007/978-3-642-74065-7_3.

[36] Di Baccio, D., Castagna, A., Paoletti, E., Sebastiani, L., Ranieri, A. (2008): Could the differences in O3 sensitivity between two poplar clones be related to a difference in antioxidant defense and secondary metabolic response to O3 influx? – Tree Physiology 8: 1761-1772. https://doi.org/10.1093/treephys/28.12.1761.

[37] Diaz, J., Bernal, A., Pomar, F., Merino, F. (2001): Induction of shikimate dehydrogenase and peroxidase in pepper (*Capsicum annuum* L.) seedlings in response to copper stress and its relation to lignification. – Plant Science 161: 179-188.

[38] Dixon, R. A., Barros, j. (2019): Lignin biosynthesis: old roads revisited and new roads explored. – Open Biology 9(12): 190215. https://doi.org/10.1098/rsob.190215.

[39] Dixon, R. A., Paiva, N. L. (1995): Stress-induced phenylpropanoid metabolism. – The Plant Cell 7: 1085-1097 https://www.ncbi.nlm.nih.gov/pmc/articles/PMC160915/.

[40] Dong, J., Gruda, N., Lam, S. K., Li, X., Duan, Z. (2018): Effects of elevated CO2 on nutritional quality of vegetables: a review. – Frontiers in Plant Science 9: 924 https://doi.org/10.3389/fpls.2018.00924.

[41] Druart, N., Rodriguez-Buey, M., Barron-Gafford, G., Sjodin, A., Bhalerao, R., Hurry, V. (2006): Molecular targets of elevated (CO2) in leaves and stems of Populus deltoides: implications for future tree growth and carbon sequestration. – Functional Plant Biology 33: 121-131. https://doi.org/10.1071/FP05139.

[42] Ederli, L., Reale, L., Ferranti, F., Pasqualini, S. (2004): Responses induced by high concentration of cadmium in Phragmites australis roots. – Physiologia Plantarum 121: 66-74.

[43] Emamverdian, A., Ding, Y., Mokhberdoran, F., Xie, Y. (2015): Heavy metal stress and some mechanisms of plant defense response. – Scientific World Journal 756120. https://doi.org/10.1155/2015/756120.

[44] Entry, J. A., Runion, G. B., Prior, S. A., Mitchell, R. J., Rogers, H. H. (1998): Influence of CO2 enrichment and nitrogen fertilization on tissue chemistry and carbon allocation in longleaf pine seedlings. – Plant and Soil 200: 3-11.

[45] Eynck, C., Seguin-swartz, G., Clarke, W. E., Parkin, I. A. (2012): Monolignol biosynthesis is associated with resistance to *Sclerotinia sclerotiorum* in *Camelina sativa*. – Molecular Plant Pathology 13: 887-899. https://doi.org/10.1111/j.1364-3703.2012.00798.x.

[46] Fahad, S., Bajwa, A. A.; Nazir, U., Anjum, S. A., Farooq, A., Zohaib, A., Sadia, S., Nasim, W., Adkins, S., Saud, S., et al. (2017): Crop production under drought and heat stress: plant responses and management options. – Frontiers in Plant Science 8: 1147. https://doi.org/10.3389/fpls.2017.01147.

[47] Fan, L., Linker, R., Gepstein, S., Tanimoto, E., Yamamoto, R., Neumann, P. M. (2006): Progressive inhibition by water deficit of cell wall extensibility and growth along the elongation zone of maize roots is related to increased lignin metabolism and progressive stelar accumulation of wall phenolics. – Plant Physiology 140: 603-612. https://doi.org/10.1104/pp.105.073130.

[48] Fang, K., Xie, P., Zhang, Q., Xing, Y., Cao, Q., Qin, L. (2020): Aluminum toxicity-induced pollen tube growth inhibition in apple (*Malus domestica*) is mediated by interrupting calcium dynamics and modification of cell wall components. – Environmental and Experimental Botany 171: 103928. https://doi.org/10.1016/j.envexpbot.2019.103928.

http://www.aloki.hu ● ISSN 1589 1623 (Print) ● ISSN 1785 0037 (Online)
DOI: http://dx.doi.org/10.15666/aeer/2003_19912015

[49] Faraji, M., Fonseca, L. L., Escamilla-Treviño, L., Barros-Rios, J., Engle, N., Yang, Z. K., Tschaplinski, T. J., Dixon, R. A., Voit, E. O. (2018): Mathematical models of lignin biosynthesis. – Biotechnology for Biofuels 11: 34-34 https://doi.org/10.1186/s13068-018-1028-9.

[50] Fargaaová, A., Pastierová, J., Svetková, K. J. P. S. (2018): Effect of Se-metal pair combinations (Cd, Zn, Cu, Pb) on photosynthetic pigments production and metal accumulation in Sinapis alba L. seedlings. – Plant Soil and Environment 52: 8

[51] Fleming, R. A., Barclay, H. J., Candau, J. N. (2002): Scaling-up an autoregressive time series model (of spruce budworm population dynamics) changes its qualitative behaviour. – Ecological Modelling 149(1-2): 127-142. https://doi.org/10.1016/S0304-3800(01)00519-1.

[52] Ford, C. W., Morrison, I. M.., Wilson, J. R. (1979): Temperature effects on lignin, hemicellulose and cellulose in tropical and temperate grasses. – Australian Journal of Agricultural Research 30: 621-33.

[53] Frei, M., Kohno, Y., Wissuwa, M., Makkar, H. P., Becker, K. (2011): Negative effects of tropospheric ozone on the feed value of rice straw are mitigated by an ozone tolerance QTL. – Global Change Biology 17: 2319-2329. https://doi.org/10.1111/j.1365-2486.2010.02379.x.

[54] Gallego-Giraldo, L., Posé, S., Pattathil, S., Peralta, A. G., Hahn, M. G., Ayre, B. G., Dixon, R. A. (2018): Elicitors and defense gene induction in plants with altered lignin compositions. – New Phytologist 219(4): 1235-1251. https://doi.org/10.1111/nph.15258.

[55] Gao, W., Li, H.-Y., Xiao, S., Chye, M. L. (2010): Acyl-CoA-binding protein 2 binds lysophospholipase 2 and lysoPC to promote tolerance to cadmium-induced oxidative stress in transgenic Arabidopsis. – Plant Journal 62: 989-1003 https://doi.org/10.1111/j.1365-313X.2010.04209.x.

[56] Gellerstedt, G., Henriksson, G. (2008): Chapter 9: Lignins: Major Sources, Structure and Properties. – In: Gandini, M. N., Belgacem, A. (eds.) Monomers, Polymers and Composites from Renewable Resources. Elsevier, Amsterdam, pp. 201-224. https://doi.org/10.1016/B978-0-08-045316-3.00009-0.

[57] Ghanati, F., Morita, A., Yokota, H. (2005): Deposition of suberin in roots of soybean induced by excess boron. – Plant Sciences 168: 397-405. https://doi.org/10.1016/j.plantsci.2004.09.004.

[58] Gou, M., Ran, X., Martin, D. W., Liu, C. J. (2018): The scaffold proteins of lignin biosynthetic cytochrome P450 enzymes. – Nature Plants 4: 299-310. https://doi.org/10.1038/s41477-018-0142-9.

[59] Guranowski, A., Miersch, O., Staswick, P. E., Suza, W., Wasternack, C. (2007): Substrate specificity and products of side-reactions catalyzed by jasmonate:amino acid synthetase (JAR1). – FEBS Letters 581: 815-820 https://doi.org/10.1016/j.febslet.2007.01.049.

[60] Hano, C., Addi, M., Bensaddek, L., Cronier, D., Baltora-Rosset, S., Doussot, J., Maury, S., Mesnard, F., Chabbert, B., Hawkins, S. (2006): Differential accumulation of monolignol-derived compounds in elicited flax (*Linum usitatissimum*) cell suspension cultures. – Planta 223: 975-989. https://doi.org/10.1007/s00425-005-0156-1.

[61] Hausman, J. F., Evers, D., Thiellement, H., Jouve, L. (2000): Compared responses of poplar cuttings and in vitro raised shoots to short-term chilling treatments. – Plant Cell Report 19: 954-960.

[62] Hawkins, S., Boudet, A. (1996): Wound-induced lignin and suberin deposition in a woody angiosperm (*Eucalyptus gunnii* Hook.): histochemistry of early changes in young plants. – Protoplasma 191: 96-104 https://doi.org/10.1007/BF01280829.

http://www.aloki.hu ● ISSN 1589 1623 (Print) ● ISSN 1785 0037 (Online)
DOI: http://dx.doi.org/10.15666/aeer/2003_19912015

[63] Hawkins, S., Boudet, A. (2003): Defense lignin and hydroxycinnamyl alcohol dehydrogenase activities in wounded *Eucalyptus gunnii*. – Forest Pathology 33: 91-104. https://doi.org/10.1046/j.1439-0329.2003.00308.x.

[64] Herbette, S., Taconnat, L., Hugouvieux, V., Piette, L., Magniette, M. L. M., Cuine, S., Auroy, P., Richaud, P., Forestier, C., Bourguignon, J. (2006): Genome-wide transcriptome profiling of the early cadmium response of *Arabidopsis* roots and shoots. – Biochimie 88: 1751-1765 https://doi.org/10.1016/j.biochi.2006.04.018.

[65] Hou, Q. Z., Ye, G. J., Wang, R. F., Jia, L. Y., Liang, J. Y., Feng, H. Q., Wen, J., Shi, D. I., Wang, Q. W. (2017): Changes by cadmium stress in lipid peroxidation and activities of lipoxygenase and antioxidant enzymes in Arabidopsis are associated with extracellular ATP%. – Biologia 72: 1467-1474 https://doi.org/10.1515/biolog-2017-0176.

[66] Hu, Y., Li, W. C., Xu, Y., Li, G., Liao, Y., Fu, F. L. (2009): Differential expression of candidate genes for lignin biosynthesis under drought stress in maize leaves. – Journal of Applied Genetics 50: 213-223. https://doi.org/10.1007/BF03195675.

[67] IPCC (2007): Climate Change. Synthesis Report. – International Panel on Climate Change, Geneva.

[68] Janas, K. M., Cvikrova, M., Palagiewicz, A., Eder, J. (2000): Alterations in phenylpropanoid content in soybean roots during low temperature acclimation. – Plant Physiology and Biochemistry 38: 587-593.

[69] Janzik, I., Preiskowski, S., Kneifel, H. (2005): Ozone has dramatic effects on the regulation of the prechorismate pathway in tobacco (*Nicotiana tabacum* L. cv. Bel W3). – Planta 223: 20-27.

[70] Jeter, C. R., Tang, W., Henaff, E., Butterfield, T., Roux, S. J. (2004): Evidence of a novel cell signaling role for extracellular adenosine triphosphates and diphosphates in arabidopsis. – The Plant Cell 16: 2652-2664 https://doi.org/10.1105/tpc.104.023945.

[71] Jewell, J. B., Sowders, J. M., He, R., Willis, M. A., Gang, D. R., Tanaka, K. (2019): Extracellular ATP shapes a defense-related transcriptome both independently and along with other defense signaling pathways. – Plant Physiology 179: 1144-1158 https://doi.org/10.1104/pp.18.01301.

[72] Kasraie, P., Nasri, M., Khalatbari, M. (2012): The effects of time spraying amino acid on water deficit stress on yield, yield component and some physiological characteristics of grain corn (TWC647). – Annals of Biological Research 3: 4282-4286.

[73] Kawasaki, T., Koita, H., Nakatsubo, T., Hasegawa, K., Wakabayashi, K., Takahashi, H., Umemura, K., Umezawa, T., Shimamoto, K. (2006): Cinnamoyl-CoA reductase, a key enzyme in lignin biosynthesis, is an effector of small GTPase Rac in defense signaling in rice. – Proceedings of the National Academy of Sciences 103: 230-235 https://doi.org/10.1073/pnas.0509875103.

[74] Kim, S. Y., Sivaguru, M., Stacey, G. (2006): Extracellular ATP in plants. Visualization, localization, and analysis of physiological significance in growth and signaling. – Plant Physiology 142: 984-992 https://doi.org/10.1104/pp.106.085670.

[75] Kim, S. H., Yang, S. H., Kim, T. J., Han, J. S., Suh, J. W. (2009): Hypertonic stress increased extracellular ATP levels and the expression of stress-responsive genes in *Arabidopsis thaliana* seedlings. – Bioscience Biotechnology and Biochemistry 73: 1252-1256 https://doi.org/10.1271/bbb.80660.

[76] Klein, M. A., Sekimoto, H., Milner, M. J., Kochian, L. V. (2008): Investigation of heavy metal hyperaccumulation at the cellular level: development and characterization of Thlaspi caerulescens suspension cell lines. – Plant Physiology 147: 2006-2016. https://doi.org/10.1104/pp.108.119719.

[77] Kolupaev, Y. E., Akinina, G. E., Mokrousov, A. V. (2005): Induction of heat tolerance in wheat coleoptiles by calcium ions and its relation to oxidative stress. – Russian Journal of Plant Physiology 52: 199-24.

http://www.aloki.hu ● ISSN 1589 1623 (Print) ● ISSN 1785 0037 (Online)
DOI: http://dx.doi.org/10.15666/aeer/2003_19912015

[78] Komatsu, S., Kobayashi, Y., Nishizawa, K., Nanjo, Y., Furukawa, K. (2010): Comparative proteomics analysis of differentially expressed proteins in soybean cell wall during flooding stress. – Amino Acids 39: 1435-1449. https://doi.org/10.1007/s00726-010-0608-1.

[79] Kontunen-Soppela, S., Parviainen, J., Ruhanen, H., Brosche, M., Keinanen, M., Thakur, R. C., Kolehmainen, M., Kangas-jarvi, J., Oksanen, E., Karnosky, D. F. (2010): Gene expression responses of paper birch (*Betula papyrifera*) to elevated CO2 and O3 during leaf maturation and senescence. – Environmental Pollution 158: 959-968. https://doi.org/10.1016/j.envpol.2009.10.008.

[80] Kostiainen, K., Kaakinen, S., Saranpaa, P., Sigurdsson, B. D., Linder, S., Vapaavuori, E. (2004): Effect of elevated (CO2) on stem wood properties of mature Norway spruce grown at different soil nutrient availability. – Glob. Change. Biol. 10: 1526-1538. https://doi.org/10.1111/j.1365-2486.2004.00821.x.

[81] Kostiainen, K., Kaakinen, S., Warsta, E., Kubiske, M. E., Nelson, N. D., Sober, J., Karnosky, D. F., Saranpaa, P., Vapaavuori, E. (2008): Wood properties of trembling aspen and paper birch after 5 years of exposure to elevated concentrations of CO2 and O3. – Tree Physiology 28: 805-813. https://doi.org/10.1093/treephys/28.5.805.

[82] Laitinen, T., Morreel, K., Delhomme, N., Gauthier, A., Schiffthaler, B., Nickolov, K., Brader, G., Lim, K. J., Teeri, T. H., Street, N. R. (2017): A key role for apoplastic H2O2 in Norway spruce phenolic metabolism. – Plant Physiology 174: 1449-1475 https://doi.org/10.1104/pp.17.00085.

[83] Lautner, S., Ehlting, B., Windeisen, E., Rennenberg, H., Matyssek, R., Fromm, J. (2007): Calcium nutrition has a significant influence on wood formation in poplar. – New Phytologist 173: 743-752. https://doi.org/10.1111/j.1469-8137.2007.01972.x.

[84] Lauvergeat, V., Lacomme, C., Lacombe, E., Lasserre, E., Roby, D., Grima-Pettenati, J. (2001): Two cinnamoyl-CoA reductase (CCR) genes from *Arabidopsis thaliana* are differentially expressed during development and in response to infection with pathogenic bacteria. – Phytochemistry 57: 1187-1195. https://doi.org/10.1016/S0031-9422(01)00053-X.

[85] Le Gall, H., Philippe, F., Domon, J.-M., Gillet, F., Pelloux, J., Rayon, C. (2015): Cell wall metabolism in response to abiotic stress. – Plants 4: 112-166. https://doi.org/10.3390/plants4010112.

[86] Lee, B. R., Kim, K. Y., Jung, W. J., Avice, J. C., Ourry, A., Kim, T. H. (2007): Peroxidases and lignification in relation to the intensity of water-deficit stress in white clover (*Trifolium repens* L.). – Journal of Experimental Botany 58: 1271-1279. https://doi.org/10.1093/jxb/erl280.

[87] Li, H., Yang, Y., Wang, Z., Guo, X., Liu, F., Jiang, J., Liu, G. (2016): BpMADS12 gene role in lignin biosynthesis of Betula platyphylla Suk by transcriptome analysis. – Journal of Forestry Research 27: 1111-1120. https://doi.org/10.1007/s11676-016-0229-y.

[88] Lim, M. H., Wu, J., Yao, J., Gallardo, I. F., Dugger, J. W., Webb, L. J., Huang, J., Salmi, M. L., Song, J., Clark, G. (2014): Apyrase suppression raises extracellular ATP levels and induces gene expression and cell wall changes characteristic of stress responses. – Plant Physiology 164: 2054-2067 https://doi.org/10.1104/pp.113.233429.

[89] Lin, C-C., Chen, L-M., Liu, Z-H. (2005): Rapid effect of copper on lignin biosynthesis in soybean roots. – Plant Science 168: 855-861.

[90] Lin, C. Y., Wang, J. P., Li, Q., Chen, H. C., Liu, J., Loziuk, P., Song, J., Williams, C., Muddiman, D. C., Sederoff, R. R. (2015): 4-Coumaroyl and caffeoyl shikimic acids inhibit 4-coumaric acid: coenzyme A ligases and modulate metabolic flux for 3-hydroxylation in monolignol biosynthesis of *Populus trichocarpa*. – Molecular Plant 8: 176-187. https://doi.org/10.1016/j.molp.2014.12.003.

http://www.aloki.hu ● ISSN 1589 1623 (Print) ● ISSN 1785 0037 (Online)
DOI: http://dx.doi.org/10.15666/aeer/2003_19912015

[91] Liu, Q., Luo, L., Zheng, L. (2018): Lignins: biosynthesis and biological functions in plants. – International Journal of Molecular Sciences 19: 335. https://doi.org/10.3390/ijms19020335.

[92] Logemann, E., Parniske, M., Hahlbrock, K. (1995): Modes of expression and common structural features of the complete phenylalanine ammonia-lyase gene family in parsley. – Proceeding of National Academy of Sciences 92: 5905-5909 https://doi.org/10.1073/pnas.92.13.5905.

[93] Lourenço, A., Pereira, H. (2018): Compositional Variability of Lignin in Biomass. – In: Poletto, M. (ed.) Lignin. Trends and Applications. IntechOpen, London. http://dx.doi.org/10.5772/intechopen.71208.

[94] Luo, Z. B., Langenfeld-Heyser, R., Calfapietra, C., Polle, A. (2004): Influence of free air CO2 enrichment (EUROFACE) and nitrogen fertilisation on the anatomy of juvenile wood of three poplar species after coppicing. – Trees 19: 109-118. https://doi.org/10.1007/s00468-004-0369-0.

[95] Luo, Z. B., Polle, A. (2009): Wood composition and energy content in a poplar short rotation plantation on fertilized agricultural land in a future CO2 atmosphere. – Global Change Biology 15: 38-47. https://doi.org/10.1111/j.1365-2486.2008.01768.x.

[96] Ma, B., Gao, L., Zhang, H., Cui, J., Shen, Z. (2012): Aluminum-induced oxidative stress and changes in antioxidant defenses in the roots of rice varieties differing in Al tolerance. – Plant Cell Report 31: 687-696.

[97] Matros, A., Amme, S., Kettig, B., Buck-Sorlin, G. H., Sonnewald, U., Mock, H.-P. (2006): Growth at elevated CO2 concentrations leads to modified profiles of secondary metabolites in tobacco cv. SamsunNN and to increased resistance against infection with potato virus Y. – Plant, Cell & Environment 29: 126-137.

[98] Mattson, W. J., Julkunen-Tiitto, R., Herms, D. (2005): CO2 enrichment and carbon partitioning to phenolics: do plant responses accord better with the protein competition or the growth differentiation balance models? – Oikos 111: 337-347. https://doi.org/10.1111/j.0030-1299.2005.13634.x.

[99] Menden, B., Kohlhoff, M., Moerschbacher, B. M. (2007): Wheat cells accumulate a syringyl-rich lignin during the hypersensitive resistance response. – Phytochemistry 68: 513-520. https://doi.org/10.1016/j.phytochem.2006.11.011.

[100] Miao, R., Lung, S. C., Li, X., Li, X. D., Chye, M. L. (2019): Thermodynamic insights into an interaction between ACYL-CoA-BINDING PROTEIN2 and LYSOPHOSPHOLIPASE2 in Arabidopsis. – J. Biol. Chem. 294: 6214-6226.

[101] Möller, M. N., Cuevasanta, E., Orrico, F., Lopez, A. C., Thomson, L., Denicola, A. (2019): Diffusion and transport of reactive species across cell membranes. – Advances in Experimental Medicine and Biology 1127: 3-19 https://doi.org/10.1007/978-3-030-11488-6_1.

[102] Mortel, J. E., Villanueva, L. A., Schat, H., Kwekkeboom, J., Coughlan, S., Moerland, P. D., van Themaat, E. V. L., Koornneef, M., Aarts, M. G. M. (2006): Large expression differences in genes for iron and zinc homeostasis, stress response, and lignin biosynthesis distinguish roots of *Arabidopsis thaliana* and the related metal hyperaccumulator *Thlaspi caerulescens*. – Plant Physiology 142: 1127-1147.

[103] Muntifering, R., Chappelka, A., Lin, J., Karnosky, D., Somers, G. (2006): Chemical composition and digestibility of Trifolium exposed to elevated ozone and carbon dioxide in a free-air (FACE) fumigation system. – Functional Ecology 20: 269-275. https://doi.org/10.1111/j.1365-2435.2006.01093.x.

[104] Nanayakkara, B., Manley-Harris, M., Suckling, I. D. (2011): Understanding the degree of condensation of phenolic and etherified C-9 units of in situ lignins. – Journal of Agricultural and Food Chemistry 59(23): 12514-12519. https://doi.org/10.1021/jf203285r.

http://www.aloki.hu ● ISSN 1589 1623 (Print) ● ISSN 1785 0037 (Online)
DOI: http://dx.doi.org/10.15666/aeer/2003_19912015

[105] Nawawi, D. S., Syafii, W., Akiyama, T., Matsumoto, Y. (2016): Characteristics of guaiacyl-syringyl lignin in reaction wood in the gymnosperm *Gnetum gnemon* L. – Holzforschung 70(7): 593-602.
[106] Nicholson, R. L., Hammerschmidt, R. (1992): Phenolic compounds and their role in disease resistance. – Phytopathology 30: 369-389. https://doi.org/10.1146/annurev.py.30.090192.002101.
[107] Norby, R. J., Cotrufo, M. F., Ineson, P., ONeill, E. G., Canadell, J. G. (2001): Elevated CO 2, litter chemistry, and decomposition: a synthesis. – Oecol. 127: 153-165. https://doi.org/10.1007/s004420000615.
[108] Oksanen, E., Riikonen, J., Kaakinen, S., Holopainen, T., Vapaavuori, E. (2005): Structural characteristics and chemical composition of birch (*Betula pendula*) leaves are modified by increasing CO2and ozone. – Global Change Biology 11: 732-748.
[109] Olbrich, M., Gerstner, E., Welzl, G., Winkler, J. B., Ernst, D. (2009): Transcript responses in leaves of ozone-treated beech saplings seasons at an outdoor free air model fumigation site over two growing seasons. – Plant and Soil 323: 61-74. https://doi.org/10.1007/s11104-009-0129-4.
[110] Olenichenko, N., Zagoskina, N. (2005): Response of winter wheat to cold: production of phenolic compounds and l-phenylalanine ammonia lyase activity. – Applied Biochemistry and Microbiology 41: 600-603.
[111] Pandey, A., Rajamani, U., Verma, J., Subba, P., Chakraborty, N., Datta, A., Chakraborty, S., Chakraborty, N. (2010): Identification of extracellular matrix proteins of rice (*Oryza sativa* L.) involved in dehydration-responsive network: a proteomic approach. – Journal of Proteome Research 9: 3443-3464. https://doi.org/10.1021/pr901098p.
[112] Penel, C., Greppin, H. (1996): Pectin binding proteins: characterization of the binding and comparison with heparin. – Journal of Biological Chemistry 34: 479-488.
[113] Pietrowska-Borek, M., Stuible, H. P., Kombrink, E., Guranowski, A. (2003): 4-Coumarate: coenzyme a ligase has the catalytic capacity to synthesize and reuse various (di)adenosine polyphosphates. – Plant Physiology 131: 1401-1410 https://doi.org/10.1104/pp.011684.
[114] Pietrowska-Borek, M., Nuc, K., Zielezińska, M., Guranowski, A. (2011): Diadenosine polyphosphates (Ap3A and Ap4A) behave as alarmones triggering the synthesis of enzymes of the phenylpropanoid pathway in *Arabidopsis thaliana*. – FEBS Open Biology 1: 1-6 https://doi.org/10.1016/j.fob.2011.10.002.
[115] Pitre, F. E., Pollet, B., Lafarguette, F., Cooke, J. E. K., MacKay, J. J., Lapierre, C. (2007): Effects of increased nitrogen supply on the lignification of poplar wood. – Journal of Agricultural and Food Chemistry 55: 10306-10314.
[116] Plessl, M., Heller, W., Payer, H. D., Elstner, E., Habermeyer, J., Heiser, I. (2005): Growth parameters and resistance against Drechslera teres of spring barley (*Hordeum vulgare* L. cv. Scarlett) grown at elevated ozone and carbon dioxide concentrations. – Plant Biology 7: 694-705. https://doi.org/10.1055/s-2005-873002.
[117] Porteaus, F., Hill, J., Ball, A., Pinter, P., Kimball, B., Wall, G., Adamsen, F., Hunsaker, D., LaMorte, R., Leavitt, S. (2009): Effect of free air carbon dioxide enrichment (FACE) on the chemical composition and nutritive value of wheat grain and straw. – Animal Feed Science and Technology 149: 322-332. https://doi.org/10.1016/j.anifeedsci.2008.07.003.
[118] Raes, J., Rohde, A., Christensen, J. H., Van de Peer, Y., Boerjan, W. (2003): Genome-wide characterization of the lignification toolbox in Arabidopsis. – Plant Physiology 133: 1051-1071. https://doi.org/10.1104/pp.103.026484.
[119] Rao, X., Dixon, R. A. (2018): Current models for transcriptional regulation of secondary cell wall biosynthesis in grasses. – Frontiers in Plant Science 9: 399. https://doi.org/10.3389/fpls.2018.00399.

http://www.aloki.hu ● ISSN 1589 1623 (Print) ● ISSN 1785 0037 (Online)
DOI: http://dx.doi.org/10.15666/aeer/2003_19912015

[120] Raven, J. A., Giordano, M., Beardall, J., Maberly, S. C. (2012): Algal evolution in relation to atmospheric CO2: carboxylases, carbon-concentrating mechanisms and carbon oxidation cycles. – Philosophical Transactions of the Royal Society B: Biological Sciences 367: 493-507 https://doi.org/10.1098/rstb.2011.0212.

[121] Richet, N., Afif, D., Tozo, K., Pollet, B., Maillard, P., Huber, F., Priault, P., Banvoy, J., Gross, P., Dizengremel, P., Lapierre, C., Perré, P., Cabané, M. (2012): Elevated CO2 and/or ozone modify lignification in the wood of poplars (*Populus tremula* x alba). – Journal of Experimental Botany 63: 4291-4301.

[122] Rieder, B., Neuhaus, H. E. (2011): Identification of an Arabidopsis plasma membrane–located ATP transporter important for anther development. – The Plant Cell 23: 1932-1944 https://doi.org/10.1105/tpc.111.084574.

[123] Rizwan, M., Ali, S., Adrees, M., Ibrahim, M., Tsang, D. C. W., Zia-ur-Rehman, M., Zahir, Z. A., Rinklebe, J., Tack, F. M. G., Ok, Y. S. (2017): A critical review on effects, tolerance mechanisms and management of cadmium in vegetables. – Chemosphere 182: 90-105 https://doi.org/10.1016/j.chemosphere.2017.05.013.

[124] Robson, A. D., Hartley, R. D., Jarvis, S. C. (1981): Effect of copper deficiency on phenolic and other constituents of wheat cell walls. – New Phytologist 89: 361-371.

[125] Rosemann, D., Heller, W., Sandermann, H. (1991): Biochemical plant responses to ozone: II. Induction of stilbene biosynthesis in Scots pine (*Pinus sylvestris* L.) seedlings. – Plant Physiology 97: 1280-1286. https://doi.org/10.1104/pp.97.4.1280.

[126] Saito, K., Fukushima, K. (2005): Distribution of lignin interunit bonds in the differentiating xylem of compression and normal woods of Pinus thunbergii. – Journal of Wood Science 51: 246-251. https://doi.org/10.1007/s10086-004-0644-0.

[127] Sanità di Toppi, L., Gabbrielli, R. (1999): Response to cadmium in higher plants. – Environmental and Experimental Botany 41: 105-130 https://doi.org/10.1016/S0098-8472(98)00058-6.

[128] Sanz, J., Bermejo, V., Muntifering, R., González-Fernández, I., Gimeno, B., Elvira, S., Alonso, R. (2011): Plant phenology, growth and nutritive quality of *Briza maxima*: responses induced by enhanced ozone atmospheric levels and nitrogen enrichment. – Environmental Pollution 159: 423-430. https://doi.org/10.1016/j.envpol.2010.10.026.

[129] Sarry, J. E., Kuhn, L., Ducruix, C., Lafaye, A., Junot, C., Hugouvieux, V., Jourdain, A., Bastien, O., Fievet, J. B., Vailhen, D. (2006): The early responses of *Arabidopsis thaliana* cells to cadmium exposure explored by protein and metabolite profiling analyses. – Proteomics 6: 2180-2198 https://doi.org/10.1002/pmic.200500543.

[130] Sasaki, M., Yamamoto, Y., Matsumoto, H. (1996): Lignin deposition induced by aluminum in wheat (*Triticum aestivum*) roots. – Physiologia Plantarum 96: 193-198.

[131] Sato, Y., Yajima, Y., Tokunaga, N., Whetten, R. (2011): Comparison between tracheary element lignin formation and extracellular lignin-like substance formation during the culture of isolated *Zinnia elegans* mesophyll cells. – Biologia 66: 88-95. https://doi.org/10.2478/s11756-010-0130-7.

[132] Schlimme, M., Blaschke, L., Lagrimini, M. L., Polle, A. (2002): Growth performance and lignification in tobacco with suppressed apoplastic anionic peroxidase activity under ambient and elevated co2 concentrations. – International Journal of Plant Sciences 163: 749-754.

[133] Sgarbi, E., Fornasiero, R. B., Lins, A. P., Bonatti, P. M. (2003): Phenol metabolism is differentially affected by ozone in two cell lines from grape (*Vitis vinifera* L.) leaf. – Plant Science 165: 951-957. https://doi.org/10.1016/S0168-9452(03)00219-X.

[134] Solecka, D., Boudet, A. M., Kacperska, A. (1999): Phenylpropanoid and anthocyanin changes in low temperature treated winter oilseed rape leaves. – Plant Physiology and Biochemistry 37: 491-496.

[135] Song, C. J., Steinebrunner, I., Wang, X., Stout, S. C., Roux, S. J. (2006): Extracellular ATP induces the accumulation of superoxide via NADPH oxidases in Arabidopsis. – Plant Physiology 140: 1222-1232 https://doi.org/10.1104/pp.105.073072.

http://www.aloki.hu ● ISSN 1589 1623 (Print) ● ISSN 1785 0037 (Online)
DOI: http://dx.doi.org/10.15666/aeer/2003_19912015

[136] Srivastava, S., Vishwakarma, R. K., Arafat, Y. A., Gupta, S. K., Khan, B. M. (2015): Abiotic stress induces change in Cinnamoyl CoA Reductase (CCR) protein abundance and lignin deposition in developing seedlings of Leucaena leucocephala. – Physiology and Molecular Biology of Plants 21: 197-205. https://doi.org/10.1007/s12298-015-0289-z.

[137] Stange, R. R., Ralph, J., Peng, J., Sims, J. J., Midland, S. L., McDonald, R. E. (2001): Acidolysis and hot water extraction provide new insights into the composition of the induced "lignin-like" material from squash fruit. – Phytochemistry 57: 1005-1011. https://doi.org/10.1016/S0031-9422(01)00096-6.

[138] Staswick, P. E., Tiryaki, I., Rowe, M. L. (2002): Jasmonate response locus JAR1 and several related Arabidopsis genes encode enzymes of the firefly luciferase superfamily that show activity on jasmonic, salicylic, and indole-3-acetic acids in an assay for adenylation. – The Plant Cell 14: 1405-1415 https://doi.org/10.1105/tpc.000885.

[139] Sun, Q., Liu, X., Yang, J., Liu, W., Du, Q., Wang, H., Fu, C., Li, W. X. (2018): Microrna528 affects lodging resistance of maize by regulating lignin biosynthesis under nitrogen-luxury conditions. – Molecular Plant 11(6): 806-14.

[140] Tahara, K., Norisada, M., Hogetsu, T., Kojima, K. (2005): Aluminum tolerance and aluminum-induced deposition of callose and lignin in the root tips of Melaleuca and *Eucalyptus* species. – Journal of Forestry Research 10: 325-333.

[141] Tanaka, K., Gilroy, S., Jones, A. M., Stacey, G. (2010): Extracellular ATP signaling in plants. – Trends in Cell Biology 20: 601-608 https://doi.org/10.1016/j.tcb.2010.07.005.

[142] Tanaka, K., Choi, J., Cao, Y., Stacey, G. (2014): Extracellular ATP acts as a damage-associated molecular pattern (DAMP) signal in plants. – Frontier in Plant Science 5: 446 https://doi.org/10.3389/fpls.2014.00446.

[143] Teixeira, A. F., de Bastos Andrade, A., Ferrarese-Filho, O., de Lourdes Lucio Ferrarese, M. (2006): Role of calcium on phenolic compounds and enzymes related to lignification in soybean (*Glycine max* L.) root growth. – Plant Growth Regulator 49: 69-76 https://doi.org/10.1007/s10725-006-0013-7.

[144] Thomas, C., Rajagopal, A., Windsor, B., Dudler, R., Lloyd, A., Roux, S. J. (2000): A role for ectophosphatase in xenobiotic resistance. – The Plant Cell 12: 519-533 https://doi.org/10.1105/tpc.12.4.519.

[145] Thompson, J. N. (1984): Insect Diversity and the Trophic Structure of Communities. – In: Huffaker, C. B., Rabb, R. L. (eds.) Ecological Entomology. Wiley, New York, pp. 591-606. https://ci.nii.ac.jp/naid/10028176746/.

[146] Tomas-Barberan, F. A., Gil, M. I., Castaner, M., Artes, F., Saltveit, M. E. (1997): Effect of selected browning inhibitors on phenolic metabolism in stem tissue of harvested lettuce. – Journal of Agricultural and Food Chemistry 45: 583-589. https://doi.org/10.1021/jf960478f.

[147] Tripathi, D., Tanaka, K. (2018): A crosstalk between extracellular ATP and jasmonate signaling pathways for plant defense. – Plant Signaling & Behavior 13: e1432229 https://doi.org/10.1080/15592324.2018.1432229.

[148] Vardar, F., Ismailoğlu, I., İnan, D., Ünal, M. (2011): Determination of stress responses induced by aluminum in maize (*Zea mays*). – Acta Biologica Hungarica 62: 156-170.

[149] Wasternack, C., Strnad, M. (2018): Jasmonates: news on occurrence, biosynthesis, metabolism and action of an ancient group of signaling compounds. – International Journal of Molecular Science 19: 2539. https://doi.org/10.3390/ijms19092539.

[150] Wei, H., Dhanaraj, A. L., Arora, R., Rowland, L. J., Fu, Y., Sun, L. (2006): Identification of cold acclimation-responsive Rhododendron genes for lipid metabolism, membrane transport and lignin biosynthesis: importance of moderately abundant ESTs in genomic studies. – Plant Cell Environment 29: 558-570. https://doi.org/10.1111/j.1365-3040.2005.01432.x.

[151] Weng, J. K., Chapple, C. (2010): The origin and evolution of lignin biosynthesis. – The New Phytologist 187: 273-285 https://doi.org/10.1111/j.1469-8137.2010.03327.x.

http://www.aloki.hu ● ISSN 1589 1623 (Print) ● ISSN 1785 0037 (Online)
DOI: http://dx.doi.org/10.15666/aeer/2003_19912015

[152] Wittig, V. E., Ainsworth, E. A., Naidu, S. L., Karnosky, D. F., Long, S. P. (2009): Quantifying the impact of current and future tropospheric ozone on tree biomass, growth, physiology and biochemistry: a quantitative meta-analysis. – Global Change Biology 15: 396-424. https://doi.org/10.1111/j.1365-2486.2008.01774.x.

[153] Wuana, R. A., Okieimen, F. E. (2011): Heavy metals in contaminated soils: a review of sources, chemistry, risks and best available strategies for remediation. – International Scholarly Research Notices 402647. https://doi.org/10.5402/2011/402647.

[154] Wuyts, N., Lognay, G., Swennen, R., De Waele, D. (2006): Nematode infection and reproduction in transgenic and mutant *Arabidopsis* and tobacco with an altered phenylpropanoid metabolism. – Journal of Experimental Botany 57: 2825-2835. https://doi.org/10.1093/jxb/erl044.

[155] Xie, M., Zhang, J., Tschaplinski, T. J., Tuskan, G. A., Chen, J. G., Muchero, W. (2018): Regulation of lignin biosynthesis and its role in growth-defense tradeoffs. – Frontiers in Plant Science 9: 1427. https://doi.org/10.3389/fpls.2018.01427.

[156] Yamaguchi, M., Valliyodan, B., Zhang, J., Lenoble, M. E., Yu, O., Rogers, E. E., Nguyen, H. T., Sharp, R. E. (2010): Regulation of growth response to water stress in the soybean primary root. I. Proteomic analysis reveals region-specific regulation of phenylpropanoid metabolism and control of free iron in the elongation zone. – Plant Cell Environment 33: 223-243. https://doi.org/10.1111/j.1365-3040.2009.02073.x.

[157] Yan, X., Liu, J., Kim, H., Liu, B., Huang, X., Yang, Z., Lin, Y. C. J., Chen, H., Yang, C., Wang, J. P. (2019): CAD1 and CCR2 protein complex formation in monolignol biosynthesis in *Populus trichocarpa*. – New Phytologist 222: 244-260 https://doi.org/10.1111/nph.15505.

[158] Yang, Y. J., Cheng, L. M., Liu, Z. H. (2007): Rapid effect of cadmium on lignin biosynthesis in soybean roots. – Plant Sciences 172: 632-639. https://doi.org/10.1016/j.plantsci.2006.11.018.

[159] Yoshimura, K., Masuda, A., Kuwano, M., Yokota, A., Akashi, K. (2008): Programmed proteome response for drought avoidance/tolerance in the root of a C3 xerophyte (wild watermelon) under water deficits. – Plant and Cell Physiology 49: 226-241. https://doi.org/10.1093/pcp/pcm180.

[160] Zagoskina, N., Goncharuk, E., Alyavina, A. (2007): Effect of cadmium on the phenolic compounds formation in the callus cultures derived from various organs of the tea plant. – Russian Journal of Plant Physiology 54: 237-243.

[161] Zhao, Q., Wang, H., Yin, Y., Xu, Y., Chen, F., Dixon, R. A. (2010): Syringyl lignin biosynthesis is directly regulated by a secondary cell wall master switch. – Proceedings of the National Academy of Sciences 107: 14496-14501. https://doi.org/10.1073/pnas.1009170107.

[162] Zhao, Q., Tobimatsu, Y., Zhou, R., Pattathil, S., Gallego-Giraldo, L., Fu, C., Jackson, L. A., Hahn, M. G., Kim, H., Chen, F. (2013): Loss of function of cinnamyl alcohol dehydrogenase 1 leads to unconventional lignin and a temperature-sensitive growth defect in Medicago truncatula. – Proceedings of the National Academy of Sciences 110: 13660-13665. https://doi.org/10.1073/pnas.1312234110.

[163] Zhou, J., Lee, C., Zhong, R., Ye, Z.-H. (2009): MYB58 and MYB63 are transcriptional activators of the lignin biosynthetic pathway during secondary cell wall formation in Arabidopsis. – The Plant Cell 21: 248-266. https://doi.org/10.1105/tpc.108.063321.

[164] Zhuo, C., Rao, X., Azad, R., Pandey, R., Xiao, X., Harkelroad, A., Wang, X., Chen, F., Dixon, R. A. (2019): Enzymatic basis for C-lignin monomer biosynthesis in the seed coat of *Cleome hassleriana*. – Plant Journal 99: 506-520 https://doi.org/10.1111/tpj.14340.

http://www.aloki.hu ● ISSN 1589 1623 (Print) ● ISSN 1785 0037 (Online)
DOI: http://dx.doi.org/10.15666/aeer/2003_19912015

ESTIMATION OF LEAF AREA, LEAF MASS AND SPECIFIC LEAF AREA FOR TREES OF DIFFERENT LIFE-FORMS IN A KARST FOREST BASED ON LINEAR MIXED-EFFECTS MODELS

WU, Q. C.[1] – LUO, G. L.[1] – QI, T.[2] – QI, Y. J.[1*]

[1]*College of Forestry, Guizhou University, Guiyang 550025, PR China*

[2]*College of Engineering Management, Chongqing Three Gorges University, Chongqing 404000, PR China*

**Corresponding author*
e-mail: yjqi@gzu.edu.cn; phone: +86-182-7539-9557

(Received 21st Nov 2021; accepted 15th Feb 2022)

Abstract. Leaves act as an important bridge between plants and the external environment. Many studies have been conducted to establish more accurate and efficient models for predicting values of leaf traits. However, the model based on tree species is not representative enough for tropical and subtropical forests with abundant tree species and complex structures. Additionally, ordinary models are generally insufficient to describe the spatial and temporal changes of leaves because of the variations between trees. Based on linear mixed-effects models (LMM), we estimated the leaf area (LA), leaf mass (LM), and specific leaf area (SLA) for tree species of four life forms in a karst primary forest. Our results suggested that LMM were reasonable and accurate in fitting and predicting LA and LM for different life forms in different seasons. The most accurate predictions were obtained while using the product of leaf length and leaf width. Specifically, LMM performed better (R^2 = 0.92 to 0.99 and AIC = 118.5 to 4306.76 for leaf area; R^2 = 0.88 to 0.94 and AIC = –4389.5 to –969.1 for leaf mass) than the models only considered the fixed effects (R^2 = 0.89 to 0.99 and AIC = 119.1 to 4464.79 for leaf area; R^2 = 0.79 to 0.87 and AIC = –3179.7 to –940.2 for leaf mass). The mean absolute error percent values were 0.9%–14.4% for leaf area and 1.1% to 17.1% for leaf mass for four life forms. Considering the accuracy of the models and the sampling effort, the optimal number of sample leaves for SLA estimation was about 60–80.
Keywords: *leaf structure parameters, seasonal variations, horizontal directions of canopy, random effects, non-destructive measurement*

Introduction

Leaves are important for plant growth, biomass, and nutrient conversion and form the basis for the functioning of terrestrial ecosystems (Reich et al., 1992; Kikuzawa and Lechowicz, 2011). As the important leaf morphological traits, leaf area (LA) and leaf mass (LM) estimate the leaf area index, closely relating to the plant photosynthetic efficiency, growth, and productivity (Milla and Reich, 2007; Weraduwage et al., 2015), and strongly indicate climate change and matter cycle interactions (Chen, 2017). Specific leaf area (SLA), the ratio of LM and LA, is an indicator of ecophysiological characteristics such as relative growth rate, photosynthetic capacity, and leaf longevity (Wright and Westoby, 2002; Anderson et al., 2020). Therefore, an accurate estimation of the LA, LM, and SLA can better elucidate the importance of the leaves for the efficient functioning of the forest ecosystem.

The most popular method for measuring broadleaf LA is sampling and using a scanner to scan the leaves, taking images with a fixed camera, or other such digital instruments (Peksen, 2007). Then, LA was calculated by ImageJ software (Gao et al., 2022; Yang et al., 2021), Blackspot leaf area calculator (Varma and Osuri, 2013;

http://www.aloki.hu ● ISSN 1589 1623 (Print) ● ISSN 1785 0037 (Online)
DOI: http://dx.doi.org/10.15666/aeer/2003_20172033

Basnett and Devy. 2021), or Photoshop (Kostadinov and Moteva, 2014; Liang et al., 2010). LM is usually determined by sampling the leaves, drying (in an oven), and weighing (Dwyer et al., 2014; Freschet et al., 2015). These direct methods involve destructive plant sampling, and multiple measurements on the same leaf cannot be conducted (Suárez Salazar et al., 2018). However, due to their ability to measure leaf parameters relatively accurately (Kostadinov and Moteva, 2014), they are often widely used as the basic data for modeling (Wang et al., 2019; Liu et al., 2017) and canopy structure parameters estimating, such as leaf area index (Ern et al., 2020; Liu et al., 2015). Some non-destructive alternative direct methods that can be used to measure leaf area involves using portable scanning planimeters (Lu et al., 2004), portable area meter (Santiago and Wright, 2007; Olivas et al., 2013), RGB-D sensor (Yau et al., 2021), etc. However, these tools are usually expensive and complex to conduct basic studies (Adji et al., 2021). Additionally, model methods (Pompelli et al., 2012; Serdar et al., 2006; Keramatlou et al., 2015) have been developed to estimate leaf parameters because of their merits of being non-destructive, efficient, and highly accurate. Theoretically, they estimate LA/LM by establishing mathematical models between LA/LM and one or more leaf structural parameters (e.g., length or width) (Tondjo et al., 2015; Meng et al., 2015; Cai et al., 2017). In most studies, analysis is usually performed using ordinary least squares models. However, data for modeling is usually recorded from multiple time points (i.e., longitudinal data) or multiple locations (i.e., horizontal data). There is a temporal or spatial autocorrelation in longitudinal or horizontal data (Zhang et al., 2009). For example, there are differences between plots and trees due to the geographic location, site condition, and environmental factors. In such situations, ordinary least squares methods generate certain predictive biases because they rarely consider the correlation of those data and cannot reflect individual differences (Cantoni et al., 2021). Thus, ordinary models are insufficient to describe the spatial and temporal changes in leaves (Zhang et al., 2009). Moreover, leaf traits of some species vary with seasonal changes and present significant spatial variability within canopies (Weiskittel et al., 2008; Nouvellon et al., 2010). Most of the previous studies did not consider the effects of the above two factors when constructing the models. Therefore, improving the accuracy of model estimation is an important problem that needs to be solved urgently.

Compared to traditional regression models, linear mixed-effects models contain fixed and random effects and have the advantages of incorporating diversity data, which can be a better fit and explain the potential effects of random variables that help effectively reveal the sources, such as variations in time and space (Tao, 2002). Recently, linear mixed-effects models have been widely used in forestry research. For example, Cysneiros et al. (2020) modeled the tree height-diameter relationships using linear mixed-effects models in the Atlantic Forest and confirmed the effect of the local environment on the height–diameter relationship of trees. Qi et al. (2020) applied a linear mixed model to estimate the forest biomass of Guizhou province, which solved spatial autocorrelation of the forest biomass caused by the neighborhood space regions. Zheng et al. (2021) collected tree ring growth data from 128 sites for 21 high altitude tree species and used linear mixed-effects models to quantify the best explanatory climate variables of tree growth and the spatio-temporal pattern of climate sensitivity. Besides accounting for trees as random effects, Prats et al. (2019) studied the influence of dry season on Quercus suber L. leaf traits in the Iberian Peninsula, and Liu et al. (2017) estimated the LA and LM of five deciduous broad-leaved trees in the Xiaoxing'an Mountains, both of which confirmed the validity of linear mixed-effects

http://www.aloki.hu ● ISSN 1589 1623 (Print) ● ISSN 1785 0037 (Online)
DOI: http://dx.doi.org/10.15666/aeer/2003_20172033

models. However, the applications of linear mixed-effects models for estimating leaf structure parameters are few, in general, and even fewer for estimating the parameters in karst forests of the subtropics, where tree species richness is high, and the microenvironment is heterogeneous.

This study aimed to construct linear mixed-effects models using leaf structure parameters to non-destructively and efficiently estimate LA, LM, and SLA of trees in karst primary forests. Karst primary forests have many tree species and complex structures, and hence, the model based on tree species is not representative. Life forms encompass the long-term performance in life and appearance of plants which respond and adapt to variations in environmental conditions (Jiang et al., 1999). In other words, life forms are a combination of plant structure and growth dynamics (Molles, 2000). Plants with similar life forms show convergence to adapt to the environment, which creates differences in the characteristics of the leaf structure among plants (Kenzo et al., 2016). In a karst primary forest, the stratification and life forms of tree species are obvious (Zhu, 1997). To accurately, effectively, and quickly predict the dynamic changes of LA and LM of leaves in the karst primary forest, we classified tree species based on different life forms. Therefore, taking individual trees as the random effect, we constructed linear mixed-effects models of LA and LM of four life forms using leaf size, season, and crown canopy direction as the independent variables. The aims of this study were as follows: (1) to evaluate leaf trait variations of different life forms during the growing periods and horizontal directions in the canopy (HDC); (2) to select the optimal variable and test whether growing periods and HDC have a significant effect on the development of the linear mixed-effects models for predicting LA or LM; (3) to establish linear mixed-effects models of LA and LM and evaluate the forecast accuracy of these models; (4) to determine the feasibility of predicting SLA using LA and LM prediction models.

Materials and methods

Site description

The study was conducted in the Maolan National Natural Reserve (25°09′ 20″-25°20′ 50″N, 107°52′ 10″-108°05′ 04″E) in Libo County of Guizhou, a southwest province in China. The region belongs to a central subtropical monsoon humid climate with an annual average temperature of 15.3 °C (5.2 °C in January, 23.5 °C in July), annual precipitation of 1752.5 mm, and annual relative humidity of 83%. The altitude is 430~1078.6 m with bare ground rocks and shallow soil, and the rock exposed rate is up to 90%. The vegetation is a subtropical evergreen and deciduous broad-leaved mixed forest with a stable ecosystem and an estimated 87% forest coverage. The mean annual relative humidity (RH) and precipitation are 83% and 1,320.5 mm, respectively. The reserve is rich in species and has high biodiversity.

Experimental design

We randomly selected 24 representative tree species in this area and classified them into evergreen trees, deciduous trees, evergreen shrubs, and deciduous shrubs according to their life forms. There were eight evergreen tree species with DBH (diameter at breast height) ranging from 3.4 cm to 7.9 cm, nine deciduous tree species with DBH ranging between 2.1 and 7.4 cm, six evergreen shrubs species with the DBH ranging

http://www.aloki.hu ● ISSN 1589 1623 (Print) ● ISSN 1785 0037 (Online)
DOI: http://dx.doi.org/10.15666/aeer/2003_20172033

from 1.5 to 2.1 cm, and one deciduous shrub with a DBH of 3.5 cm (*Table 1*). This dataset represented the traits of the leaves of the major tree species in the region. The trees we selected in the analysis were not inclined to larger ones. For one thing, the study area has complex terrain and high rock coverage, which is full of high risk and makes it difficult to acquire and measure leaf samples of large trees. For another thing, trees grew slowly, and small trees accounted high proportion in this study area with the harsh environment (Zhu, 1997). Based on the accuracy and sample size, the leaves of each sample tree were selected from different HDC (east, west, south, and north) and different seasons (January, April, July, and October), i.e., at least 10 sample leaves were collected in each season and each HDC, and 3460 sample leaves were obtained in total. January, April, July, and October represent the major phenological period of all broadleaf leaves, i.e., growth, lush, aging, and fall, respectively. First, we cut off the handles of the collected leaves and numbered each leaf. Then, the length and width of the leaf were measured with a ruler (with a precision of 0.1 cm). The length (L) was defined as the straight distance from the tip of the leaf to the base of the petiole, and the width (W) was the widest point perpendicular to the longitudinal axis of the leaf (Liu et al., 2017). The thickness (T) was measured by a Vernier caliper (with a precision of 0.01 mm) at the upper, middle, and lower parts of the leaf, and the final value of the thickness of each leaf was the average of three measurements. The LA was obtained by scanning the leaf using the Epson Perfection V19 image scanner (China, 300 dpi resolution). Next, we imported the images of the leaves obtained from the scanner to Photoshop 7.0 and calculated the actual area of each leaf from the proportion of the pixels of each leaf to that of the A4 paper. Finally, we dried the leaves in a 65 °C oven for 72 h and weighed each leaf to obtain the LM (precision of 0.001 g) as the actual leaf quality. The statistical characteristics of the structural parameters of the leaves are shown in *Table 1*.

Selection of the optimal independent variable

Regression models were based on linear functions of LA and power functions of LM. Specifically, leaf structure parameters such as leaf length (L), leaf width (W), leaf thickness (T), the product of leaf length and leaf width (LW), and the product of leaf length, leaf width, and leaf thickness (LWT) were used to predict LA and LM of the tree species. The statistical criteria for optimal independent variable selection were based on the lowest Akaike Information Code (AIC) value of each tree species in each life form. The two empirical models offer relatively equal support and cannot be distinguished from one another, when the AIC value difference between the first and second optimal models is less than 2.0. Then, the optimal predictive model selected is based on higher values of the coefficient of determination (R^2) (Burnham and Anderson, 2002).

Construction of linear mixed-effects models

Linear mixed-effects models of LA and LM for tree species of each life form were constructed based on the optimal independent variable selected in the previous step. Data were randomly selected (75%) from the tree species in each life form for model fitting, and 25% of the data were used for model validation. Before constructing the linear mixed-effects models, basic models were constructed as follows:

The linear model of the LA is presented in the form of *Equation 1*:

http://www.aloki.hu ● ISSN 1589 1623 (Print) ● ISSN 1785 0037 (Online)
DOI: http://dx.doi.org/10.15666/aeer/2003_20172033

$$y = bx + a \quad \text{(Eq.1)}$$

The nonlinear model of LM (power model) was (*Eq. 2*):

$$y = mx^n \quad \text{(Eq.2)}$$

To construct a linear mixed-effects model, we first transformed *Equation 2* into linear models (*Eq. 3*) as follows:

$$\ln(y) = \ln(m) + n\ln(x) \quad \text{(Eq.3)}$$

Here, y represents either the LA or the LM; b and n are coefficients; x is an independent variable (e.g., length, width); a and $\ln(m)$ are the intercept. Seasons (i.e., June, July, and September) and HDC (i.e., West, South, and North) were treated as categorical variables.

Table 1. *Basic statistical characteristics of leaf structural parameters for tree species of four life forms in a karst forest (SD: standard deviation)*

Life forms	DBH (cm)	Number of leaf samples	Mean length (cm)	Mean width (cm)	Mean thickness (mm)	Tree species
Evergreen trees n = 1256	3.4	162	2.6 (3.3)	1.2 (1.1)	0.061 (0.11)	*Boniodendron minus*
	6.8	151	9.5 (2.4)	4.1 (0.9)	0.107 (0.11)	*Cinnamomum burmanni*
	7.9	154	11.0 (2.4)	3.7 (0.9)	0.085 (0.11)	*Cyclobalanopsis glauca*
	5.4	150	10.5 (2.4)	3.0 (0.9)	0.107 (0.11)	*Machilus rehderi*
	3.7	148	10.3 (2.4)	2.4 (0.9)	0.054 (0.11)	*Euonymus dielsianus*
	3.6	176	9.9 (2.3)	3.5 (0.9)	0.088 (0.13)	*Pittosporum tenuifolium*
	4.2	164	8.7 (2.4)	3.6 (0.9)	0.072 (0.16)	*Viburnum propinquum*
	6.3	151	10.9 (2.4)	3.5 (1.0)	0.054 (0.18)	*Acer cinnamomifolium*
Deciduous trees n = 1063	3.6	131	14.1 (3.7)	8.5 (2.4)	0.092 (0.15)	*Ficus hirtavahl*
	4.9	133	8.0 (3.4)	3.3 (2.1)	0.122 (0.16)	*Platycarya longipes*
	4.7	118	8.2 (3.4)	3.7 (2.1)	0.125 (0.16)	*Carpinus kweichowensis*
	7.4	99	13.0 (3.6)	6.7 (2.3)	0.075 (0.17)	*Bridelia minutiflora*
	2.1	119	6.7 (3.2)	2.9 (2.1)	0.039 (0.17)	*Clausena dunniana*
	3.8	121	9.6 (3.4)	3.9 (2.2)	0.130 (0.18)	*Diospyros kaki*
	5.2	125	8.0 (2.8)	7.0 (2.0)	0.119 (0.19)	*Schoepfia chinensis*
	5.4	82	8.5 (2.8)	4.5 (1.7)	0.091 (0.20)	*Celtis tetrandra*
	4.7	135	8.1 (3.1)	3.3 (1.9)	0.092 (0.21)	*Sapium rotundifolium*
Evergreen shrubs n = 964	1.6	140	4.6 (2.7)	2.3 (0.8)	0.079 (0.11)	*Murraya exotica*
	1.5	150	7.4 (2.5)	3.0 (0.7)	0.075 (0.11)	*Mahonia fortunei*
	2.1	157	7.5 (2.7)	2.6 (0.8)	0.095 (0.13)	*Distylium myricoides*
	1.7	164	8.2 (2.8)	3.1 (0.8)	0.124 (0.14)	*Lindera communis*
	1.9	183	6.8 (3.2)	3.4 (0.8)	0.114 (0.14)	*Tirpitzia sinensis*
	1.8	170	11.7 (3.6)	3.7 (0.9)	0.047 (0.15)	*Mallotus philippensis*
Deciduous shrubs n = 177	3.5	177	4.8 (1.3)	2.0 (0.5)	0.079 (0.09)	*Nandina domestice*

http://www.aloki.hu ● ISSN 1589 1623 (Print) ● ISSN 1785 0037 (Online)
DOI: http://dx.doi.org/10.15666/aeer/2003_20172033

Then, linear mixed-effects models were constructed according to the theory of Littell et al. (2006) as follows:

Leaf-area linear model (*Eq. 4*):

$$y = bx + a + \theta + \varphi \quad \text{(Eq.4)}$$

Leaf-mass linear model (*Eq. 5*):

$$\ln(y) = n\ln(x) + \ln(m) + \theta + \varphi \quad \text{(Eq.5)}$$

where θ represents seasonal and canopy horizontal categorical variables; φ (as a random effect) represents tree tags to prevent potential autocorrelation among leaves of the same tree.

Therefore, taking individual trees as the random effect, we constructed linear mixed-effects models of LA and LM for four life forms using leaf size (continuous variable), season (categorical variables), and crown canopy direction (categorical variables) as the independent variables. Moreover, the conditional coefficients of determination (R_m^2) and marginal coefficients of determination (R_c^2) were used to determine how much of the variation was explained by fixed factors (season, canopy direction, and leaf size), as well as by both fixed and random factors (season, canopy direction, leaf size, and individual tree).

Validation of linear mixed-effects models

The remaining 25% of the total observed data were used to evaluate the performance of the prediction models. Then, the actual LA or LM values of the tree species of each life form were taken as a reference, and the mean absolute error (MAE) (*Eq. 6*) and the mean absolute error percent (MAE%) (*Eq. 7*) were calculated for evaluation.

$$\mathrm{MAE} = \sum_{i=1}^{n} \left| \frac{y_i - \hat{y}_i}{n} \right| \quad \text{(Eq.6)}$$

$$\mathrm{MAE\%} = \frac{1}{n} \sum_{i=1}^{n} \left| \frac{y_i - \hat{y}_i}{y_i} \right| \times 100\% \quad \text{(Eq.7)}$$

Here, y_i and $\hat{y}_i$ represent the actual SLA or LM values for the ith evaluation, and n is the number of samples.

Prediction of SLA by the regression models of LA and LM

The linear mixed-effects models of LA and LM were used to predict SLA for the tree species of each life form, and the parameters MAE and MAE% were used to assess the effectiveness of these models in predicting SLA. Additionally, to accurately and quickly predict the optimum number of leaves required for SLA per life form, all data were used to construct models, and the relationship between the difference (the mean actual SLA and the predicted SLA) and the sample size of each life form was analyzed. The formula used is as follows (*Eq. 8*):

http://www.aloki.hu ● ISSN 1589 1623 (Print) ● ISSN 1785 0037 (Online)
DOI: http://dx.doi.org/10.15666/aeer/2003_20172033

$$\text{Difference}_n\,(\%) = \left|\frac{\text{actual SLA}\bar{n} - \text{predicted SLA}\bar{n}}{\text{actual SLA}\bar{n}}\right| \times 100\% \qquad \text{(Eq.8)}$$

Here, Difference_n represents the difference between the average actual SLA and the predicted SLA when the sample size is n.

Statistical analysis

One-way analysis of variance (ANOVA) and multiple comparisons of least significant difference (LSD) were used to analyze the differences of LA or LM (at a significance level of $\alpha = 0.05$) between different seasons and different HDC. R_m^2 and AIC_m explained by fixed factors, and R_c^2 and AIC_c explained by both the fixed and random factors of the linear mixed-effects models were calculated. Models were constructed in SPSS22, and the figures were plotted in Origin2018 and Excel2010.

Results

Seasonal changes of LA and LM

The (mean) LA and (mean) LM for trees of four life forms showed significant differences across the four seasons but no significant differences across the four HDC (*Fig. 1*).

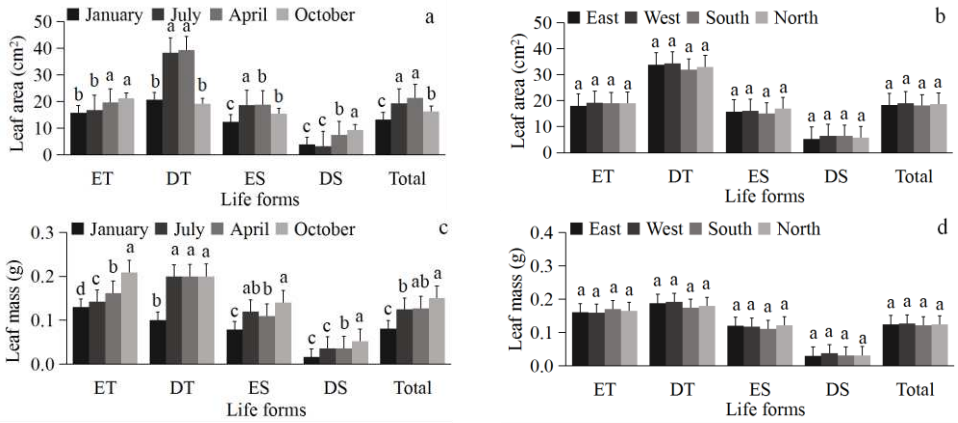

Figure 1. *The LA and LM variations in different seasons (January, April, July, and October) and HDC (east, west, south, and north) for trees of four life forms. Different lowercase letters indicate significant differences at the 0.05 significance level between LA/LM in the seasonal or canopy horizontal categories for tree species; error bars are represented by the standard errors. ER: evergreen trees, DT: deciduous trees, ES: evergreen shrubs, DS: deciduous shrubs*

Linear mixed-effects models of LA and LM

As shown in *Tables 2* and *3*, LW was the optimal dependent variable for predicting the LA and LM, based on the linear mixed-effects models. Besides, seasonal variations significantly affected the models constructed for all the tree species in the different life forms. However, the HDC had a significant effect ($P < 0.05$) in the regression model for the LA of evergreen trees and deciduous trees and did not significantly affect the LA and LM of the other life forms. The R_m^2 values of the models for LA and LM of the tree species ranged from 0.89 to 0.99 and 0.79 to 0.87, respectively. The R_c^2 values of the

http://www.aloki.hu ● ISSN 1589 1623 (Print) ● ISSN 1785 0037 (Online)
DOI: http://dx.doi.org/10.15666/aeer/2003_20172033

models for LA and LM ranged from 0.92 to 0.99 and 0.88 to 0.94, respectively. The AIC_m values of the models for LA and LM of all the tree species ranged from 119.1 to 4464.79, and –3179.7 to –940.2, respectively. The AIC_c values of the models for LA and LM ranged from 118.5 to 4306.76 and –4389.5 to –969.1, respectively. Thus, when both fixed and random factors were considered, R^2 was significantly higher and AIC was significantly lower. This indicated that the mixed-effects models could explain the variance of LA and LM of trees in the karst forest by more than 92% and 88%, respectively. Therefore, the mixed-effects models can better predict the LA and LM of trees than only considering the fixed-effects models in karst forests.

Table 2. *Linear mixed-effects model for predicting LA (cm^2) using leaf structural parameters for trees of four life forms, examined in a karst forest*

Life forms	Variable	Estimate	SE	t value	R_m^2	R_c^2	AIC_m	AIC_c
Evergreen trees n = 949	Intercept	0.6713	0.2567	2.62**	0.89	0.92	4321.9	4306.8
	Mouth (January)	0.0258	0.2448	0.11NS				
	Mouth (April)	0.6323	0.2067	3.06**				
	Mouth (July)	0.8058	0.2030	3.97***				
	Direction (east)	-0.4991	0.2142	-2.33*				
	Direction (west)	-0.1496	0.2158	-0.69NS				
	Direction (north)	-0.6350	0.2159	-2.94**				
	LW cm^2	0.6133	0.0050	122.67***				
Deciduous trees n = 800	Intercept	-1.9086	0.5353	-3.57***	0.93	0.97	4464.8	4149.5
	Mouth (January)	1.8356	0.5666	3.24**				
	Mouth (April)	1.3224	0.5295	2.50*				
	Mouth (July)	2.1084	0.5273	3.99***				
	Direction (east)	0.2325	0.3934	0.59***				
	Direction (west)	0.5967	0.3954	1.51NS				
	Direction (north)	0.3139	0.3954	0.79NS				
	LW cm^2	0.6706	0.0031	210.75***				
Evergreen shrubs n = 737	Intercept	0.3315	0.1919	1.73#	0.96	0.96	2876.0	2793.3
	Mouth (January)	-0.4491	0.2044	-2.20*				
	Mouth (April)	0.0643	0.1670	0.39NS				
	Mouth (July)	-0.2567	0.1655	-1.55NS				
	Direction (east)	0.2273	0.1748	1.30NS				
	Direction (west)	-0.0046	0.1750	-0.03NS				
	Direction (north)	0.0680	0.1765	0.39NS				
	LW cm^2	0.6519	0.0044	146.45***				
Deciduous shrubs n = 137	Intercept	0.4599	0.1935	2.38**	0.99	0.99	119.1	118.4
	Mouth (January)	-0.2683	0.1355	-1.98*				
	Mouth (April)	-0.3464	0.1449	-2.39*				
	Mouth (July)	0.1716	0.0922	1.86#				
	Direction (east)	-0.0246	0.0826	-0.30NS				
	Direction (west)	0.0848	0.0831	1.02NS				
	Direction (north)	0.1507	0.0834	1.81#				
	LW cm^2	0.5699	0.0117	48.53***				

LW is the product of length and width; L and W is the product of length and width, R_m^2 represents the variance explained by the fixed factor, and R_c^2 represents the variance explained by the fixed and random factors. AIC_m represents the Akaike information criterion of fixed effect, AIC_c represents the Akaike information criterion of fixed effect and random effect. NS represents no significant; # represents significance at the 0.1 level; * represents significance at the 0.05 level; ** represents significance at the 0.01 level and *** represents significance at the 0.001 level

http://www.aloki.hu ● ISSN 1589 1623 (Print) ● ISSN 1785 0037 (Online)
DOI: http://dx.doi.org/10.15666/aeer/2003_20172033

Table 3. *Linear mixed-effects model for predicting LM (g) using leaf structural parameters for trees of four life forms examined in a karst forest*

Life forms	Variable	Estimate	SE	t value	R_m^2	R_c^2	AIC_m	AIC_c
Evergreen trees n = 949	Intercept	0.0166	0.0047	3.51***	0.79	0.88	-3179.6	-4389.5
	Month (January)	-0.0356	0.0045	-7.87***				
	Month (April)	-0.0237	0.0038	-6.20***				
	Month (July)	-0.0229	0.0037	-6.12***				
	Direction (east)	-0.0021	0.0039	-0.55NS				
	Direction (west)	-0.0017	0.0039	-0.43NS				
	Direction (north)	-0.00518	0.0039	-1.30NS				
	$LWcm^2$	0.0057	0.0001	61.73***				
Deciduous trees n = 800	Intercept	0.0669	0.0125	5.32***	0.86	0.91	-1467.1	-1744.8
	Month (January)	-0.0718	0.0133	-5.39***				
	Month (April)	-0.0691	0.0124	-5.55***				
	Month (July)	-0.055	0.0124	-4.44***				
	Direction (east)	0.0052	0.0092	0.57NS				
	Direction (west)	0.0121	0.0093	1.31NS				
	Direction (north)	0.0023	0.0093	0.25NS				
	$LWcm^2$	0.0034	0.0001	46.67***				
Evergreen shrubs n = 737	Intercept	0.0558	0.0066	8.38***	0.87	0.93	-2017.5	-2770.1
	Month (January)	-0.0563	0.007	-7.94***				
	Month (April)	-0.0327	0.0057	-5.65***				
	Month (July)	-0.034	0.0057	-5.93***				
	Direction (east)	0.0025	0.006	0.42NS				
	Direction (west)	0.0018	0.006	0.31NS				
	Direction (north)	0.0007	0.0061	0.12NS				
	$LWcm^2$	0.0035	0.0001	23.13***				
Deciduous shrubs n = 137	Intercept	-0.0032	0.003	-1.05NS	0.87	0.94	-940.2	-969.1
	Month (January)	-0.0037	0.0021	-1.72NS				
	Month (April)	0.0035	0.0023	1.55NS				
	Month (July)	0.0036	0.0014	2.45*				
	Direction (east)	0.0014	0.0013	1.07NS				
	Direction (west)	0.0017	0.0013	1.33NS				
	Direction (north)	0.0011	0.0013	0.89NS				
	$LWcm^2$	0.0034	0.0001	18.66***				

Validation of the linear mixed-effects model

The linear mixed-effects models were used to calculate the predicted values of LA and LM, and the relationships between the predicted values and the actual values were obtained for trees of four life forms (*Fig. 2*). Significantly reliable relationships ($P < 0.01$) between the actual and predicted LA were obtained for trees of four life forms. The R^2 value ranged from 0.97 to 0.99 and from 0.84 to 0.98 for LA and LM, respectively. The mean MAE% of the LA from the linear mixed-effects models for four seasons was found to be 0.9%-14.4%, the mean MAE of LA ranged from 0.01 cm^2 to 1.45 cm^2. The mean MAE% of LM ranged from 1.1% to 17.1%, and the mean MAE of LM was between 0.01 g and 0.83 g (*Table 4*).

http://www.aloki.hu ● ISSN 1589 1623 (Print) ● ISSN 1785 0037 (Online)
DOI: http://dx.doi.org/10.15666/aeer/2003_20172033

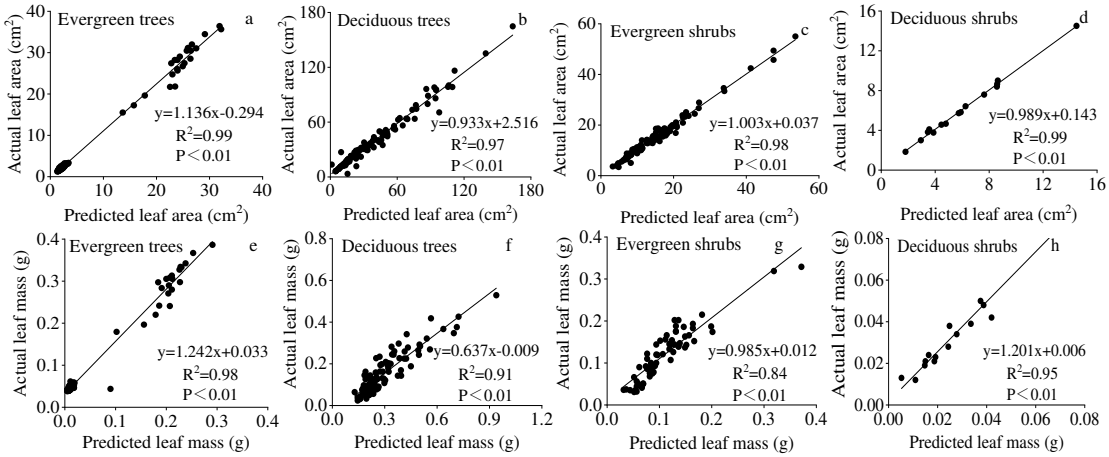

Figure 2. *The relationship between predicted and actual LA and LM from linear mixed-effects models for trees of four life forms. The datasets consisted of sample leaves (25%) for constructing models in all categories of season and HDC*

Table 4. *Validation of the linear mixed-effects models of LA (cm^2) and LM (g) for trees of four life forms, examined based on the different categories of season and HDC*

Month	Leaf traits	Evergreen trees		Deciduous trees		Evergreen shrubs		Deciduous shrubs	
		MAE	MAE%	MAE	MAE%	MAE	MAE%	MAE	MAE%
January	Leaf area	1.06	1.4	0.17	3.2	0.28	2.6	0.01	8.9
	Leaf mass	0.26	2.7	0.83	17.1	0.02	2.8	0.02	9.2
April	Leaf area	1.37	1.7	0.95	5.8	0.18	1.7	0.07	7.2
	Leaf mass	0.02	4.7	0.09	16.6	0.01	3.4	0.01	9.2
July	Leaf area	0.94	1.1	1.45	6.4	0.15	1.2	0.03	5.8
	Leaf mass	0.02	4.7	0.09	14.4	0.01	3.0	0.01	8.4
October	Leaf area	0.76	0.9	0.21	4.10	0.36	2.1	0.11	2.9
	Leaf mass	0.01	4.8	0.03	11.9	0.02	1.1	0.01	9.2

MAE: mean absolute error; MAE%: mean absolute error percent

SLA prediction

MAE% of SLA predicted from the linear mixed-effects models of LA and LM ranged from 15.6% (deciduous trees) to 19.4% (evergreen shrubs), and MAE of SLA ranged from 18.96 cm^2/g to 26.82 cm^2/g for tree species in all life forms (*Table 5*). The difference between the mean of actual and predicted SLA and the standard error (SE) of actual SLA showed a similar trend for variation (*Fig. 3*), i.e., the differences decreased with an increase in the sample size. We can see that the value of difference remained stable when the leaf sample size was 80 for evergreen trees, 60 for deciduous trees, and 70 for both evergreen shrubs and deciduous shrubs. Considering the accuracy of the models and the sampling effort, we determined that the optimum number of leaves for SLA estimation was 70 for evergreen trees (*Fig. 3a*), 60 for deciduous trees (*Fig. 3b*), 80 for evergreen shrubs (*Fig. 3c*), and 70 for deciduous shrubs (*Fig. 3d*).

http://www.aloki.hu ● ISSN 1589 1623 (Print) ● ISSN 1785 0037 (Online)
DOI: http://dx.doi.org/10.15666/aeer/2003_20172033

Table 5. *Comparison of actual SLA (cm^2/g) and predicted SLA for trees of four life forms*

Life forms (sample size)	Actual SLA	Predicted SLA	MAE	MAE%
Evergreen trees (307)	128.10	114.90	18.96	15.6
Deciduous trees (263)	211.49	198.41	22.54	17.5
Evergreen shrubs (227)	151.47	144.65	26.82	19.4
Deciduous shrub (40)	185.79	178.50	21.56	16.8

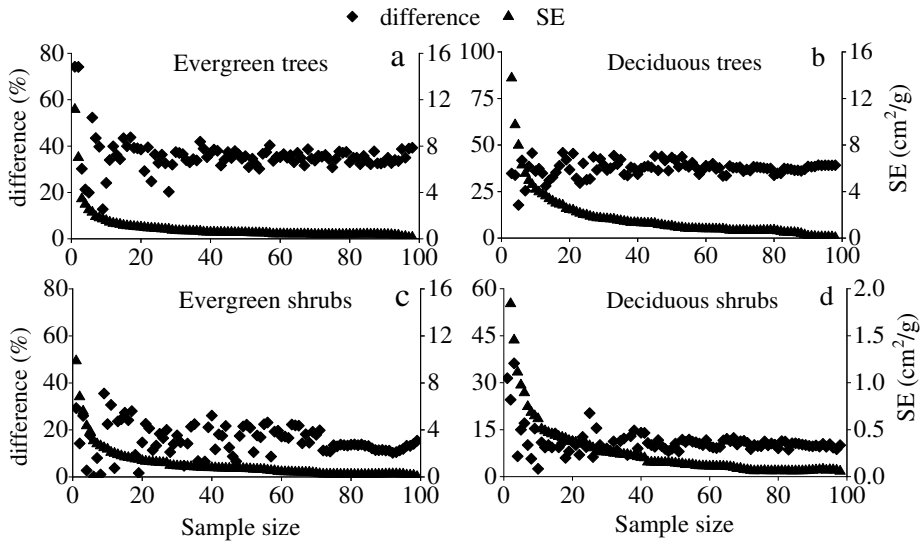

Figure 3. *Differences between the mean actual SLA and the predicted SLA as a function of sample size; SE: standard error of actual SLA*

Discussion

Optimum variable

Linear mixed-effects models were constructed in our study for estimating LA and LM in a karst primary forest. According to the results, LW was the optimal estimation variable for estimating LA when considering only the length or the width. Other studies had similar conclusions (Demirsoy et al., 2004; Pompelli et al., 2012; Montelatto et al., 2020). Especially, LW has been accepted as the optimal independent variable for predicting LA in different growing periods (Liu et al., 2017) and even in different life-history stages (Wang et al., 2019). We found similar results for different growing periods and for different life forms (*Table 3*). Moreover, LW was also the optimal estimation variable, rather than LWT or other variables in constructing the linear mixed-effects models of LM in our study. Generally, the total increase in LM is the sum of the increase in the mass due to the increase of LA and leaf thickness (Weraduwage et al., 2015), which indicates that the optimal independent variables for predicting LM are more diverse (Wang et al., 2019). Liu et al. (2017) found that for leaves with thickness greater than 0.1 mm, LWT was more suitable for linear mixed-effects models than LW, and for leaves with thickness lesser than 0.1 mm, LW was more suitable for linear mixed effects models than LWT. Similarly, Wang et al. (2019) predicted the LA and LM for broad-leaved trees of two life forms in northeastern China and found that LWT can better predict LM when L:W is greater than 1.5, and either LW or LWT can predict

http://www.aloki.hu ● ISSN 1589 1623 (Print) ● ISSN 1785 0037 (Online)
DOI: http://dx.doi.org/10.15666/aeer/2003_20172033

LM for a certain period when L:W is lesser than 1.5. These studies confirmed that LM is more sensitive to the environment than LA (Wang et al., 2019). Bell (1991) reported that the leaf size of most species results from cell multiplication in some defined meristem zones, which further influences the leaf shape. During growth, the length/width ratio of leaves remains constant (Liu et al., 2017). Thus, LM is affected by factors such as leaf length-to-width ratio (Wang et al., 2019) and leaf thickness (Liu et al., 2017). In our study, 8 of 24 tree species had average leaf thickness greater than 0.1 mm, including *Cinnamomum burmanni*, *Machilus rehderi, Carpinus kweichowensis, Bridelia minutiflora, Diospyros kaki, Schoepfia chinensis, Lindera communis* and *Tirpitzia sinensis* (*Fig. 1*). The other 16 tree species had less than 0.1 mm leaf thickness and L:W less than 1.5. The tree species with small and thin leaves comprised nearly 80% of all tree species. Therefore, leaf shape (LW) plays a significant role in predicting the LM of trees in karst primary forests.

Linear mixed-effects models

The linear mixed-effects models for estimating LA and LM for trees of four forms in karst forests were significantly better than the models that only considered the fixed effects, which illustrated that random effects caused by differences of leaves between individual/tree species should be taken into account. For karst region with abundant tree species and complex structures, modeling by different life forms considered differences between tree species and solved the problem of underrepresentation of relying only on species to build models. Actually, the linear mixed model considered fixed effects and random effects for model construction and predicted the variance of the dependent variables by establishing the design matrix of random-effects (Cantoni et al., 2021). Meanwhile, it indicated the covariance structures of the random-effects covariance matrix and the model residual covariance matrix (Tao, 2002; Littell et al., 2006), and thus, eliminated the biased estimation caused by differences among individual trees. Hence, only considering the fix effects was not the optimal parameter prediction approach.

The season has an important effect on leaf growth and is a non-negligible variable for both LA and LM model estimation. Many studies have concluded that seasonal effects on leaf growth and development (Cai et al., 2017; Liu et al., 2017; Wang et al., 2019). However, fewer reports have estimated the LM of deciduous leaves than the LA. At the beginning of leaf expansion, LA and LM are small, and most of the resources are required for photosynthesis to increase LA, which results in lower organic content and lower LM. With the increase in temperature at the beginning of the rainy season, the number of fence cells increases, and dry matter accumulates, producing an additional cell layer and increasing the leaf thickness. Finally, during the leaf shedding period, the size and dry matter accumulation of the leaves stabilizes (Lambers et al., 2008; Delagrange, 2011). Thus, the relationship between leaf length, leaf width, and leaf thickness with LA and LM differ across seasons.

Except for the LA of evergreen and deciduous trees, canopy horizontal positions showed no significant effect on the LA and LM in the linear mixed effects models (*Tables 2* and *3*). This could be related to the competition for important resources in the canopy horizontal positions. Normally, the canopy structure regulates light intensity, temperature, water, and other environmental factors in the forest by absorbing, transmitting, and scattering the photosynthetic radiation, leading to a significantly different microenvironment in the forest (Green et al., 2001; Roel et al., 2021). The

http://www.aloki.hu ● ISSN 1589 1623 (Print) ● ISSN 1785 0037 (Online)
DOI: http://dx.doi.org/10.15666/aeer/2003_20172033

microenvironment and microtopography in karst forests affect the non-uniform distribution of light at different canopy horizontal positions, which give rise to irregular differences among the trees at the same canopy horizontal position because of high heterogeneity. This is similar to the effect of the light distribution at the vertical positions of canopy layers (Liu et al., 2017), which showed that the sensibility of LA and LM to light distribution is different. We did not consider vertical positions of canopy layers because of the specificity of the study region, i.e., high rock coverage and considerable heterogeneity (Zhu, 1997), which increased the difficulty of sampling at different canopy vertical locations.

Additionally, previous studies usually constructed models of LA and LM based on tree species (Athokpam et al., 2014; Tondjo et al., 2015), and some studies have also shown that the types of empirical models for predicting LA and LM varied with species (Tondjo et al., 2015; Cai et al., 2017). However, because our study area has a high diversity of tree species, the representation of the models based on individuals from a small number of tree species was insufficient. Plants can reveal the structural characteristics of the community and the mechanism of adaptation to environmental gradients (Jiang et al., 1999; Yakimov et al., 2020). Several studies have shown that plant life forms are related to leaf traits (Wang et al., 2017; Cheng et al., 2021), although there are phylogenetic constraints on them (Grubb et al., 1975; Kenzo et al., 2016). Evergreen species may have thick and robust leaves to extend longevity in less productive habitats, such as the dark understory, whereas deciduous species may have thinner leaves with high nitrogen content and a high photosynthetic ability. These leaves might favor sun-exposed conditions, such as the canopy, to maximize carbon gain over the short periods favorable for photosynthesis (Chabot and Hicks, 1982; Niinemets et al., 2015). Karst primary forests show stratification of life forms (Zhu, 1997). Therefore, we classified the tree species into four groups based on life forms and then constructed linear mixed-effects models of these four life forms. Though few studies have constructed models for the LA and LM in plants of different life forms across growing periods, the forecast accuracy ranged from 1.9%-10.1%, 7.7%-15.1%, and 11.6%-20.6% for LA, LM, and SLA, which demonstrated that the models were effective and robust.

Moreover, our results suggested that it is feasible to predict SLA through the linear mixed-effects models of LA and LM since the predicted SLA did not significantly differ from the actual SLA. The maximum mean MAE% was 20.6% for evergreen bush, and the minimum mean MAE% was 11.6% for deciduous trees (*Table 5*). These results were similar to those obtained in other studies (Liu et al., 2017), which confirmed that the linear mixed-effects model of LA and LM is a fast and efficient method. It is also a new way to estimate SLA values of broad-leaved tree species accurately. Additionally, while considering the accuracy of the estimated model and the effort of leaf sampling, the optimum sample size of leaves from different tree species for SLA estimation was estimated to be at least 60–80 (*Fig. 3*). Compared to other studies (i.e., Liu et al., 2017), the values of the differences in *Figure 3* fluctuated considerably more with the sample size before stabilizing, and the optimal number of leaves required was greater. This might be related to the high heterogeneity in the microtopography and the microenvironment of the study area, as well as the richness in the composition of the species (Zhu, 1997; Qi et al., 2021), which simultaneously increased within-group differences and the sample size.

http://www.aloki.hu ● ISSN 1589 1623 (Print) ● ISSN 1785 0037 (Online)
DOI: http://dx.doi.org/10.15666/aeer/2003_20172033

Conclusion

In our study, linear mixed-effects performed better than the models only considered fixed effects, demonstrating they were non-destructive, fast, and reliable methods for predicting the LA and LM for trees of four life forms in a karst forest. The LW was the best predictive variable. The sampling season was an important factor affecting leaf growth and development and thus was the key variable in models' construction. The sample size for SLA estimation should be about 60–80 leaves for different life forms. In conclusion, our study provided a deep understanding of individual trees adapting to the environment in a karst primary forest and supplied a reference for the efficient and accurate determination of LA and LM for trees of different forms in species-rich forests.

Acknowledgements. The authors would like to thank the editor and anonymous reviewers for their constructive comments. This work was supported by the National Natural Science Foundation of China (32060266); the Science and Technology Planning Project of Guizhou Province of China (QKHJC[2019]1060); and the First-class Discipline Construction Project of Guizhou Province of China (GNYL[2017]007).

REFERENCES

[1] Adji, B. I., Akaffou, D. S., Kouassi, K. H., Houphouet, Y. P., Reffye, P. D., Duminil, J., Jaeger, M., Sabatier, S. (2021): Allometric models for non-destructive estimation of dry biomass and leaf area in *Khaya senegalensis* (Desr.) A. Juss., 1830 (Meliaceae), *Pterocarpus erinaceus* Poir., 1804 (Fabaceae) and *Parkia biglobosa*, Jack, R. Br. 1830 (Fabaceae). – Trees 35: 1905-1920.

[2] Anderson, C. G., Bond-Lamberty, B., Stegen, J. C. (2020): Active layer depth and soil properties impact specific leaf area variation and ecosystem productivity in a boreal forest. – PLoS One 15.

[3] Athokpam, F. D., Garkoti, S. C., Borah, N. (2014): Periodicity of leaf growth and leaf dry mass changes in the evergreen and deciduous species of Southern Assam, India. – Ecological Research 29(2): 153-165.

[4] Basnett, S., Devy, S. M. (2121): Phenology determines leaf functional traits across Rhododendron species in the Sikkim Himalaya. – Alpine Botany 131: 63-72.

[5] Bell, A. (1991): Plant Form: An Illustrated Guide to Flowering Plant Morphology. – Oxford University Press, London.

[6] Burnham, K. P., Anderson, D. R. (2002): Model Selection and Multimodel Inference: A Practical Information-theoretic Approach. – Springer-Verlag, New York.

[7] Cai, H. Y., Di, X. Y., Jin, G. Z. (2017): Allometric models for leaf area and leaf mass predictions across different growing periods of elm tree (*Ulmus japonica*). – Journal of Forestry Research 28(05): 117-124.

[8] Cantoni, E., Jacot, N., Ghisletta, P. (2021): Review and comparison of measures of explained variation and model selection in linear mixed-effects models. – Econometrics and Statistics. https://doi.org/10.1016/j.ecosta.2021.05.005.

[9] Chen, X. (2017): Spatiotemporal Processes of Plant Phenology: Simulation and Prediction. – Springer, Berlin.

[10] Cheng, X., Ping, T., Li, Z., Wang, T., Epstein, H. E. (2021): Effects of environmental factors on plant functional traits across different plant life forms in a temperate forest ecosystem. – New Forest 1-18.

[11] Chabot, B. F., Hicks, D. J. (1982): The ecology of leaf life spans. – Annual review of ecology and systematics 13: 229-259.

http://www.aloki.hu ● ISSN 1589 1623 (Print) ● ISSN 1785 0037 (Online)
DOI: http://dx.doi.org/10.15666/aeer/2003_20172033

[12] Cysneiros, V. C., Pelissari, A. L., Gaui, T. D., Luan, D. F., Machado, S. D. A. (2020): Modeling of tree height–diameter relationships in the Atlantic Forest: effect of forest type on tree allometry. – Canadian Journal of Forest Research 50(2).
[13] Delagrange, S. (2011): Light-and seasonal-induced plasticity in leaf morphology, N partitioning and photosynthetic capacity of two temperate deciduous species. – Environmental and Experimental Botany 70(1): 1-10.
[14] Demirsoy, H., Demirsoy, L., Uzun, S., Ersoy, B. (2004): Non-destructive leaf area estimation in peach. – European Journal of Horticultural Science 69(4): 144-146.
[15] Dwyer, J. M., Hobbs, R. J., Mayfield, M. M. (2014): Specific leaf area responses to environmental gradients through space and time. – Ecology 95(2): 399-410.
[16] Ern, J., Haninec, P., Pokorn, R. (2020): Leaf area index estimated by direct, semi-direct, and indirect methods in European beech and sycamore maple stands. – Journal of Forestry Research 31(3): 827-836.
[17] Freschet, G. T., Swart, E. M., Cornelissen, J. H. C. (2015): Integrated plant phenotypic responses to contrasting above-and below-ground resources: key roles of specific leaf area and root mass fraction. – The New Phytologist 206: 1247-1260.
[18] Gao, J., Wang, K., Zhang, X. (2022): Patterns and drivers of community specific leaf area in China. – Global Ecology and Conservation 33: e01971.
[19] Green, S. R., Greer, D. H., Wünsche, J. N., Caspari, H. (2001): Measurements of light interception and utilization in an apple orchard. – Acta Horticulturae 557(557): 369-376.
[20] Grubb, P. J., Grubb, E. A., Miyata, I. (1975): Leaf structure and function in evergreen trees and shrubs of Japanese warm temperate rain forest I. The structure of the lamina. – Journal of Plant Research 88(3): 197-211.
[21] Jiang, G., Tang, H., Yu, M., Ming, D., Zhang, X. (1999): Response of photosynthesis of different plant functional types to environmental changes along Northeast China Transect. – Trees 14(2): 72-82.
[22] Kenzo, T., Tanaka-Oda, A., Matsuura, Y., Hinzman, L. D. (2016): Morphological and physicochemical traits of leaves of different life-forms of various broadleaf woody plants in interior Alaska1. – Canadian Journal of Forest Research 46(12): 1475-1482.
[23] Keramatlou, I., Sharifani, M., Sabouri, H., Alizadeh, M., Kamkar, B. (2015): A simple linear model for leaf area estimation in Persian walnut (*Juglans regia* L.). – Scientia Horticulturae 184: 36-39.
[24] Kikuzawa, K., Lechowicz, M. J. (2011): Phylogenetic Variation in Leaf Longevity. Ecology of Leaf Longevity Ecological Research Monographs Series. – Springer, Tokyo.
[25] Kostadinov, G., Moteva, M. (2014): Errors of leaf area measurements by using digital camera and scanner. – Journal of Agricultural Machinery Science 5(2): 107-111.
[26] Lambers, H., Chapin, F. S., Pons, T. L. (2008): Plant Physiological Ecology. 2nd Ed. – Springer, New York.
[27] Liang, W. L., Wang, X. F., Wang, G. Y., Zhan, L., Hai, L. R. (2010): Establishing correlation between cotton field vegetation coverage and leaf area index with digital images. – Journal of Agriculture Biotechnology and Ecology 273-277.
[28] Littell, R. C., Milliken, W. W., Stroup, R. D., Wolfinger, A. (2006): SAS for Mixed Models. 2nd Ed. – SAS Press, Cary.
[29] Liu, Z., Chen, J. M., Jin, G., Qi, Y. (2015): Estimating seasonal variations of leaf area index using litterfall collection and optical methods in four mixed evergreen-deciduous forests. – Agricultural and Forest Meteorology 209-210: 36-48.
[30] Liu, Z., Zhu, Y., Li, F., Jin, G. (2017): Non-destructively predicting leaf area, leaf mass and specific leaf area based on a linear mixed-effect model for broadleaf species. – Ecological Indicators 78: 340-350.
[31] Lu, H. Y., Lu, C. T., Wei, M. L., Chan, L. F. (2004): Comparison of different models for nondestructive leaf area estimation in taro. – Agronomy Journal 96(2): 448-453.

http://www.aloki.hu ● ISSN 1589 1623 (Print) ● ISSN 1785 0037 (Online)
DOI: http://dx.doi.org/10.15666/aeer/2003_20172033

[32] Meng, F., Zhang, G., Li, X., Niklas, K. J., Sun, S. (2015): Growth synchrony between leaves and stems during twig development differs among plant functional types of subtropical rainforest woody species. – Tree Physiology 35(6): 621-631.
[33] Milla, R., Reich, P. B. (2007): The scaling of leaf area and mass: the cost of light interception increases with leaf size. – Proceedings Biological Sciences 274(1622): 2109-2114.
[34] Montelatto, M. B., Villamagua-Vergara, G. C., Castanho, F. P., Kawakami, B., Zerbinato, B., Silva, M. A., Guerra, S. P. S. (2020): Models for leaf area estimation of three forest species in a short coppice rotation. – Acta Ecologica Sinica 40(4): 263-267.
[35] Molles, M. C. (2000): Ecology: Concept and Applications. – McGraw-Hill Companies Inc., New York.
[36] Niinemets, Ü., Keenan, T. F., Hallik, L. (2015): A worldwide analysis of within-canopy variations in leaf structural, chemical and physiological traits across plant functional types. – New Phytologist 205(3): 973-993.
[37] Nouvellon, Y., Laclau, J. P., Epron, D., Kinana, A., Mabiala, A., Roupsard, O., Bonnefond, J. M., Le Maire, G., Marsden, C., Bontemps, J. D. (2010): Within-stand and seasonal variations of specific leaf area in a clonal Eucalyptus plantation in the Republic of Congo. – Forest Ecology and Management 259: 1796-1807.
[38] Olivas, P. C., Oberbauer, S. F., Clark, D. B., Clark, D. A., Ryan, M. G., O'Brien, J. J., Ordoñez, H. (2013): Comparison of direct and indirect methods for assessing leaf area index across a tropical rain forest landscape. – Agricultural and Forest Meteorology 177: 110-116.
[39] Peksen, E. (2007): Non-destructive leaf area estimation model for faba bean (*Vicia faba* L.). – Scientia Horticulturae 113: 322-328.
[40] Pompelli, M. F., Antunes, W. C., Ferreira, D. T. R. G., Cavalcante, P. G. S., Wanderley-Filho, H. C. L., Endres, L. (2012): Allometric models for non-destructive leaf area estimation of *Jatropha curcas*. – Biomass and Bioenerg 36: 77-85.
[41] Prats, K. A., Brodersen, C. R., Ashton, M. S. (2019): Influence of dry season on Quercus suber L. leaf traits in the Iberian Peninsula. – American Journal of Botany 106(5): 1-11.
[42] Qi, Y. J., Zhang, Y. C., Wang, K., Yang, T., Wu, Q. (2020): Application of spatial regression models for forest biomass estimation in Guizhou Province, Southwest China. – Applied Ecology and Environmental Research 18(5): 7215-7232.
[43] Qi, Y., Zhang, G., Luo, G., Yang, T., Wu, Q. (2021): Community-level consequences of harsh environmental constraints based on spatial patterns analysis in karst primary forest of southwest China. – Forest Ecology and Management 488(5): 119021.
[44] Reich, P. B., Walters, M. B., Ellsworth, D. S. (1992): Leaf lifespan in relation to leaf, plant and stand characteristics among diverse ecosystems. – Ecological Monographs 62: 365-392.
[45] Roel, B., Gerard, H., Thijs, P., Arnoud, B., Manuel, G., Peter, G., Santiago, C., Leng, M., Christopher, J. (2021): Paired analysis of tree ring width and carbon isotopes indicate when controls on tropical tree growth change from light to water limitations. – Tree Physiology 40: 263-267.
[46] Santiago, L. S., Wright, S. J. (2007): Leaf functional traits of tropical forest plants in relation to growth form. – Functional Ecology 21: 19-27.
[47] Serdar, U., Demirsoy, H. (2006): Non-destructive leaf area estimation in chestnut. – Scientia Horticulturae 108: 227-230.
[48] Suárez Salazar, J. C., Melgarejo, L. M., Durán Bautista, H. E., Di Rienzo, J. A., Casanoves, F. (2018): Non-destructive estimation of the leaf weight and leaf area in cacao (*Theobroma cacao* L.). – Scientia Horticulturae 229: 19-24.
[49] Tao, J. (2002): Mixed Models Analyses Using the SAS System: Course Notes. – SAS Institute, Inc., Cary, NC.

http://www.aloki.hu ● ISSN 1589 1623 (Print) ● ISSN 1785 0037 (Online)
DOI: http://dx.doi.org/10.15666/aeer/2003_20172033

[50] Tondjo, K., Brancheriau, L., Sabatier, S. A., Kokutse, A., Akossou, A., Kokou, K., Fourcaud, T. (2015): Non-destructive measurement of leaf area and dry biomass in *Tectona grandis*. – Trees 29: 1625-1631.
[51] Varma, V., Osuri, A. M. (2013): Black Spot: a platform for automated and rapid estimation of leaf area from scanned images. – Plant Ecology 214(12): 1529-1534.
[52] Wang, C., Zhou, J., Xiao, H., Liu, J., Wang, L. (2017): Variations in leaf functional traits among plant species grouped by growth and leaf types in Zhenjiang, China. – Journal of Forestry Research 28: 241-248.
[53] Wang, Y., Jin, G., Shi, B., Liu, Z. (2019): Empirical models for measuring the leaf area and leaf mass across growing periods in broadleaf species with two life histories. – Ecological Indicators 102: 289-301.
[54] Weraduwage, S. M., Chen, J., Anozie, F. C., Morales, A., Weise, S. E., Sharkey, T. D. (2015): The relationship between leaf area growth and biomass accumulation in *Arabidopsis thaliana*. – Frontiers in Plant Science 6: 167.
[55] Yau, W. K., Ng, O. A., Lee, S. B. (2021): Portable device for contactless, non-destructive and in situ outdoor individual leaf area measurement. – Computers and Electronics in Agriculture 187: 106278.
[56] Weiskittel, A. R., Temesgen, H., Wilson, D. S., Maguire, D. A. (2008): Sources of within and between-stand variability in specific leaf area of three ecologically distinct conifer species. – Annals of Forest Science 65: 14-23.
[57] Wright, I. J., Westoby, M. (2002): Leaves at low versus high rainfall: coordination of structure, lifespan and physiology. – New Phytologist 155: 403-416.
[58] Yang, K., Chen, G., Xian, J., Yu, X., Wang, L. (2021): Scaling relationship between leaf mass and leaf area: a case study using six alpine Rhododendron species in the Eastern Tibetan Plateau. – Global Ecology and Conservation 30: e01754.
[59] Yakimov, B. N., Gerasimova, A. S., Zhang, S., Ma, K., Zhang, Y. (2020): Phylogenetic α- and β-diversity elevational gradients reveal consistent patterns of temperate forest community structure. – Acta Oecologica 109: 103657.
[60] Zhang, L., Ma, Z., Guo, L. (2009): An evaluation of spatial autocorrelation and heterogeneity in the residuals of six regression models. – Forest Science 55: 533-548.
[61] Zheng, L., Shi, P., Song, M., Zhou, T., Zhang, X. (2021): Climate sensitivity of high altitude tree growth across the Hindu Kush Himalaya. – Forest Ecology and Management 486(9): 118963.
[62] Zhu, S. Q. (1997): Study on Karst Forest Ecology. II. – Guizhou Science and Technology Press, Guizhou (in Chinese).

http://www.aloki.hu ● ISSN 1589 1623 (Print) ● ISSN 1785 0037 (Online)
DOI: http://dx.doi.org/10.15666/aeer/2003_20172033

CONFLICT-INDUCED DEFORESTATION DETECTION IN AFRICAN CÔTE D'IVOIRE USING LANDSAT IMAGES AND RANDOM FOREST ALGORITHM: A CASE IN MOUNT PEKO NATIONAL PARK

KOUASSI, C. J. A.[1] – KHAN, D.[1] – ACHILLE, L. S.[1] – OMIFOLAJI, J. K.[2,3] – ESPOIRE, M. M. R. B.[4] – ZHANG, K. B.[1*] – YANG, X. H.[5*] – HORNING, N.[6]

[1]School of Soil and Water Conservation, Beijing Forestry University, Beijing, China (e-mail: anoma@bjfu.edu.cn (C. J. A. Kouassi); Dilawarafridi333@bjfu.edu.cn (D. Khan Afridi); achille@bjfu.edu.cn (L. S. Achille); ctccd@bjfu.edu.cn (K. B. Zhang))

[2]School of Ecology and Nature Conservation, Beijing Forestry University, Beijing, China (e-mail: omifolajijames@bjfu.edu.cn (J. K. Omifolaji))

[3]Department of Forestry and Wildlife Management, Federal University Dutse, Jigawa State, Nigeria

[4]School of Economics and Management, Beijing Forestry University, Beijing 100083, China (e-mail: mikimouendo@bjfu.edu.cn (M. M. R. B. Espoire))

[5]Institute of Desertification Studies, Chinese Academy of Forestry, P. O. Box 35, Yiheyuanhou, Haidian District, Beijing 100091, China (e-mail: yangxhcaf@126.com (X. H. Yang))

[6]Center for Biodiversity and Conservation, American Museum of Natural History, 200 Central Park West, New York, NY 10024-5102, USA (e-mail: nedhorning@gmail.com (N. Horning))

[*]Corresponding authors
e-mail: ctccd@126.com, yangxhcaf@126.com

(Received 2nd Jun 2021; accepted 3rd Sep 2021)

Abstract. African forests, especially in Côte d'Ivoire, have been lost during the past three decades. Worldwide, forests are being destroyed to make room for farmland. Deforestation depletes floral resources and fragments habitat. Cocoa growth threatens critical ecological zones, particularly in Côte d'Ivoire. The 2002–2007 conflict impacted Mount Peko National Park (PNMP). This issue has hastened the decline of endangered animal habitats (Colobus and Elephants). The classification approach based on Random Forest (RF) algorithm using the Mean Accuracy Decrease (MDA) has been applied for choosing a variable to select the best predictor variables in the model. A Spectral Index map and time series satellite images of the PNMP from 1985 to 2020 were used to identify land cover changes. RStudio and QGIS 3.4 software have been used to create training data. Among thirteen (13) variables studied, NIR (Near Infrared), Short-Wave Infrared 1 (SWIR 1) and SWIR bands had the increased importance of the variable for the performance of the classification prediction model. The NIR band was the greatest predictor. MDA predicted 75%. User accuracy (UA), Producer accuracy (PA), and Overall accuracy (OA) classifications were 98.75% ± 1.94, 99% ± 1.95, 97% ± 1.93. The park's dense forest remained unchanged, but nonforest was reforested and 12.22% was turned to forest. During the study period, extensive cocoa plantations were established in formerly forested regions.

Keywords: *change detection, cocoa plantation, satellite imagery, elephants, Colobus*

http://www.aloki.hu ● ISSN 1589 1623 (Print) ● ISSN1785 0037 (Online)
DOI: http://dx.doi.org/10.15666/aeer/2003_20352058

Introduction

Tropical forest ecosystems are valued for products and services all across the globe due to the resilience of these ecosystems and the sustainability of producing the products and services they offer (Malhi et al., 1999; Myers and Rocca, 2000; Pan et al., 2011; Poorter et al., 2015; Aubry-Kientz et al., 2015; Jhariya, 2017; O'Sullivan et al., 2017). Côte d'Ivoire forests provide many ecosystem services vital for maintaining the livelihoods and lifestyles of rural populations, such as firewood, fruits, fibers, medicinal plants, honey, game, and ecotourism (Aké-Assi, 1998; N'Guessan, 2004; Foley et al., 2005, 2007; Tadesse et al., 2014; O'Sullivan et al., 2017; Kassoum, 2018; Rowland et al., 2018;). According to Sangne (2009), protected areas of Côte d'Ivoire include 182 classed forests and eight national parks: the remaining remnants of the thick Ivorian forest, which covered approximately 10% of the country. Before the crisis, these woods were protected, preventing damage (Lauginie et al., 1995). The western Ivorian woods have an essential role in the protection of western chimps listed as Critically Endangered since 2016, forest elephants, and the uncommon pygmy hippopotamus (Chaléard, 1996; McGraw, 1998; Miller et al., 2007; Oates, 2011; Bitty et al., 2015). However, during the last decade, deforestation and forest degradation have become a significant issue in Africa, particularly in Côte d'Ivoire.

The Ivorian Forest massif is in decline and is now split into national parks and classified forests, reducing to less than 20% of its original size between 1960 and 1980 (Singh, 1993). Less than 10% between 1980 and 1990 (Menzies, 2000), and 7.5% between 1990 and 2000 (Chatelain et al., 2004). This makes Côte d'Ivoire the country with the highest deforestation rate in Sub-Saharan Africa, with a loss of 265,000 ha per year (Achard et al., 2002; Hansen et al., 2013) and an annual deforestation rate of 1% (Ibo and Léonard, 1994; Tutu and Akol, 2009; Ruf et al., 2015). Since 1977, Côte d'Ivoire has been the world's leading cocoa producer, accounting for more than 40% of global production and accounting for nearly 40% of total exports (Deheuvels et al., 2003; Konate et al., 2015). The changing worldwide prices of cocoa beans have pushed people to convert forest areas to cocoa plantations. This deforestation has encouraged the formation of pioneer fronts, which penetrate parks and designated forests. Cocoa farming is becoming a significant cause of deforestation and tropical forest degradation in Côte d'Ivoire (Aké-Assi, 1998; Bhagwat et al., 2008; Gnahoua et al., 2012; Konate et al., 2015). It is projected that forest clearance boosted cocoa-growing areas from 250.000 ha in 1961 to 4.000.000 ha in 2004 (Franzen and Mulder, 2007; Läderach et al., 2013; Konate et al., 2017). It is estimated that income produced by cocoa plantations following deforestation accounts for 10% of national GDP (Brou et al., 2004; Sonwa et al., 2007; Morris, 2010; Beucher and Bazin, 2012). According to the Ministry of Water and Forests of the Cote d'Ivoire land cover tree evolution was 17.000.000 ha of forests in 1960 which totaled 3.000.000 ha of forests in 2020 (http://www.eauxetforets.gouv.ci/ministere). Some authors believe that war is responsible for most of Africa's deforestation and forest degradation (Koning et al., 2007; Gorsevski et al., 2013; Nackoney et al., 2014; Ordway, 2015).

Côte d'Ivoire, like other West African nations such as Liberia and Sierra Leone, will face socio-political problems (Burgess et al., 2015).

Côte d'Ivoire suffered the most severe sociopolitical and economic turmoil in its history between 2002 and 2011. Several outbreaks of violence occurred over this lengthy period, the most significant being the breakout of an armed insurrection in 2002 and a violent post-election crisis between 2010 and 2011. Approximately 3000 individuals were

http://www.aloki.hu ● ISSN 1589 1623 (Print) ● ISSN1785 0037 (Online)
DOI: http://dx.doi.org/10.15666/aeer/2003_20352058

killed. The conflict has resulted in many displaced people and refugees, the abandonment of park and reserve protection in rebel regions, exactions and rapes on civilians, looting, and fires. These crises exacerbated the worsening of environmental conditions in the west of the country. The preceding decades' violent conflicts hastened the unlawful takeover of existing protected areas.

The socio-political conflict in Côte d'Ivoire from 2002 to 2011 resulted in the nation being divided in two, with the rebel army controlling the north and part of the west (Bouquet and d'Ivoire, 2011; Bamba et al., 2018). The consequences were catastrophic for the natural environment and protected areas (Kadet, 2015; UNEP, 2015; Kouakou et al., 2017). This conflict emphasized illicit human activities like logging, mining, and poaching (Allnutt et al., 2013; Barima et al., 2016). For example, Mount Péko National Park was not spared. Large cocoa plantations have been built inside it violating protection regulations (Bredeloup, 2003; Woods, 2003; Kouakou et al., 2015; Bamba et al., 2018; Assalé et al., 2020), resulting in massive biodiversity losses (Kouamé, 1998; N'Guessan, 2004; Yao and Yves, 2005; Matsushita et al., 2006; Lauginie, 2007; N'Da, 2007; N'Da et al., 2008; Sangne, 2009). The Ivorian Office for the Protection of Parks and Reserves (OIPR) has conducted investigations that showed the installation of settlements inside the PNMP (Kassoum, 2018). The PNMP, like other classified forests and national parks, has lost biological value due to deforestation from cocoa production (Norris et al., 2010; Tano, 2012; Bitty et al., 2015). There have been few studies in Côte d'Ivoire on the effect of the crisis on forest resources. As a result, this study aims to identify forest cover change due to the Ivorian problem's impact on forest cover. For example, the PNMP, which has been under siege by armed fighters for a long time, has been the subject of many assaults. The insurgents have set up camps and communities in public schools, official health facilities, mosques, churches, shops, and cell phone towers. Large sections of the PNMP have been turned into cocoa producing zones. Before this research, it was unclear how a 10-year armed war affects deforestation and cocoa plantation growth in Côte d'Ivoire. As a result, in this research, we used the Random Forest (RF) (Breiman, 2001) classification method for Landsat data to identify forest cover change before and during the long-term PNMP crisis. The findings will help us understand the impact of previous instability on forest cover dynamics in western Côte d'Ivoire.

Literature review

History of cocoa and impact of the armed conflict in Côte d'Ivoire

The cocoa tree was brought to Côte d'Ivoire towards the end of the nineteenth century in the east part of the country (Ruf et al., 2015). Cote d'Ivoire is an agricultural country that produces 40% of the world's cocoa bean output, which is the foundation of its economy. As a result, the sector is critical for the macroeconomic balance and social stability of the country (Darie-Rousseaux and Brown, 2016). In 2018, its production and exports accounted for almost 40% of its goods exports and 14% of its GDP (Coulibaly and Erbao, 2019). Côte d'Ivoire is the global leader, with a market share of 29% and an export value of 2 to 3 billion euro (Hausmann and Hidalgo, 2011). Agriculture exports fuel its economic success (Esso, 2009). More than one million small-scale farmers work in cocoa production, mainly in the southern half of the country, generating 500-600 kg/ha on average (Deheuvels et al., 2003, 2009; Wessel and Quist-Wessel, 2015). About 6 million people are directly supported by cocoa earnings on a social level, which have increased in recent years (Tano, 2012). At the end of the 1970s, the cocoa, coffee, and

http://www.aloki.hu ● ISSN 1589 1623 (Print) ● ISSN1785 0037 (Online)
DOI: http://dx.doi.org/10.15666/aeer/2003_20352058

wood industries accounted for 30% of GDP and 50% of Côte d'Ivoire's export profits (Ibo and Léonard, 1994). Côte d'Ivoire has been the world's top cocoa producer since 1977, accounting for more than 40% of global output. It accounts for approximately 40% of the country's exports (Ibo and Léonard, 1994; Akindès, 1994; Sanial, 2018). Côte d'Ivoire currently possesses the world's greatest crushing capacity, at 750,000 tonnes. It grinds around 20% of the world's coffee, some of which is exported. Côte d'Ivoire has implemented a policy of levying a tax on cocoa exports to maintain a level of equilibrium in the volatility of global cocoa prices (Deheuvels et al., 2003; Konate et al., 2015). Today, Côte d'Ivoire has the highest grinding capacity in the world, with 750,000 tons. It grinds about 20% of the world's beans, and a portion is exported. To increase revenues and stabilize its economy, Côte d'Ivoire has adopted a policy of imposing a tax on its cocoa exports to ensure a level of equilibrium in the fluctuation of world cocoa costs (McIntire and Varangis, 1999; Burger, 2008; Kireyev, 2010). These export tariffs provide substantial tax revenues for Côte d'Ivoire, amounting up to 10% of the state budget (Zamble, 2015). In 2010, this percentage was predicted to be 27% (Kireyev, 2010).

The changing worldwide prices of cocoa beans have pushed people to convert forest areas to cocoa plantations. This deforestation has encouraged the formation of pioneer fronts, which penetrate parks and designated forests. The decrease in cocoa prices has been directly linked to the rise in cocoa output throughout the years.

Cocoa output has increased dramatically in recent decades, mainly owing to establishing new plantations at the cost of natural forests. This trend can be attributed to the fact that some companies, such as Olam, Cargill, and Barry Callebaut, encourage farmers to establish large cocoa plantations within protected parks and classified forests (https://www.mightyearth.org), with little regard to the ecological impacts of providing cheap cocoa and authorities rarely enforce the rules governing cocoa production. Consequently, Côte d'Ivoire has become the world's biggest cocoa producer in less than 40 years, almost quadrupling its output from 550,000 tons per year in 1980 to over 2 million tons in 2018 (Fountain and HützAdams, 2018). This increase in cocoa output has depleted both natural and social capital (including child labor) in Côte d'Ivoire.

Mighty Earth, a non-governmental organization, has previously condemned the role of chocolate industry in deforestation in Côte d'Ivoire, especially in the destruction of protected regions and national parks (Wessel and Quist-Wessel, 2015). The chocolate business encourages farmers to plant illegally manufactured cocoa beans in the PNMP, promoting deforestation in Côte d'Ivoire (Climate Chance, 2018). Cocoa farming is a significant cause of deforestation and tropical forest degradation and destruction of protected areas (*Fig. 1*) in Côte d'Ivoire (Bhagwat et al., 2008; Deheuvels, 2011; Gnahoua et al., 2012).

Materials and methods

Study area

Côte d'Ivoire has a land area of 322,462 km^2 and is located between 6° and 10° north latitudes, and 2° and 10° west longitudes. Cote d'Ivoire borders Liberia and Guinea to the west, Mali and Burkina Faso to the north, Ghana to the east, and a 550-km Atlantic Ocean coastline to the south (*Fig. 2*). Topographic features run north-east to south-west. The southern plateaus have several independent topographic features grouped into five main groups: the Guinean ridge, the northern plateaus, the transition zone, the interior lowlands, and the coastal fringe. The climatic conditions are ideal for agricultural growth.

http://www.aloki.hu ● ISSN 1589 1623 (Print) ● ISSN1785 0037 (Online)
DOI: http://dx.doi.org/10.15666/aeer/2003_20352058

The forest zone of Côte d'Ivoire receives abundant rainfall, ranging from 1 600 to 2 000 mm per year. Mount Péko National Park, located in the western part of Cote d'Ivoire, has a study area of 34,000 ha. By Decree No 68-69 of 09/02/1968, this forest massif was designated as a national park to preserve the peaks of Mount Kahoué (1,125 m) (Lauginie, 2007); and Mount Péko (1,002 m). The PNMP is distinguished by its position in a zone of semi-deciduous montane woodland (Ibo, 2005). Its southern area is characterized by undulating plateaus 300 to 500 m above sea level, while the rockier northern region includes three distinct summits, including Mount Péko. The hydrographic network is mainly made up of tributaries of the Sassandra River, which runs through the park's southern boundary. Except for the inselbergs that appear in the north, the park is entirely covered with semi-deciduous rainforest. The top forest shares a border with the dry forest. Poaching has left its impact on wildlife, including big animals such as elephants and buffalo (Lauginie, 2007; Bi et al., 2013). The PNMP is rich in biodiversity, including unique species to the area and nation, and it represents a rare ecological treasure in the West African subregion (CEPF, 2000).

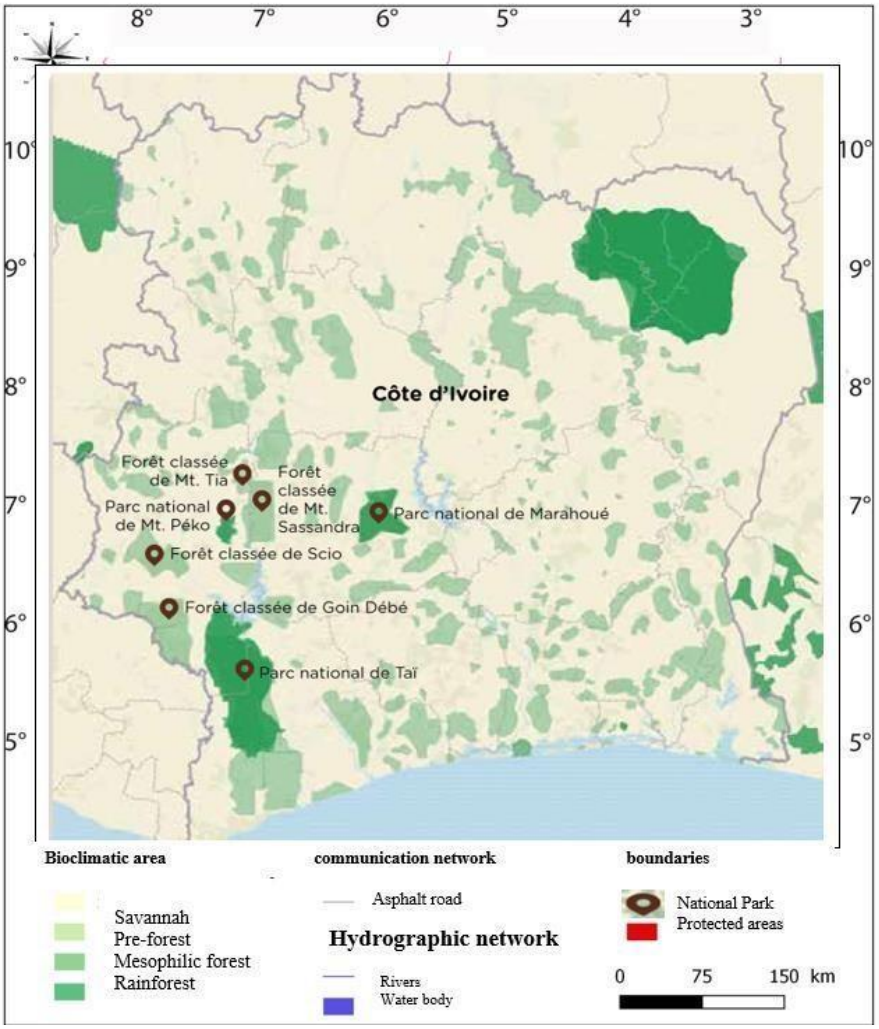

Figure 1. *Map showing the negative impacts of the crisis and development of cocoa plantations in protected areas source (https://www.protectedplanet.net/)*

http://www.aloki.hu ● ISSN 1589 1623 (Print) ● ISSN1785 0037 (Online)
DOI: http://dx.doi.org/10.15666/aeer/2003_20352058

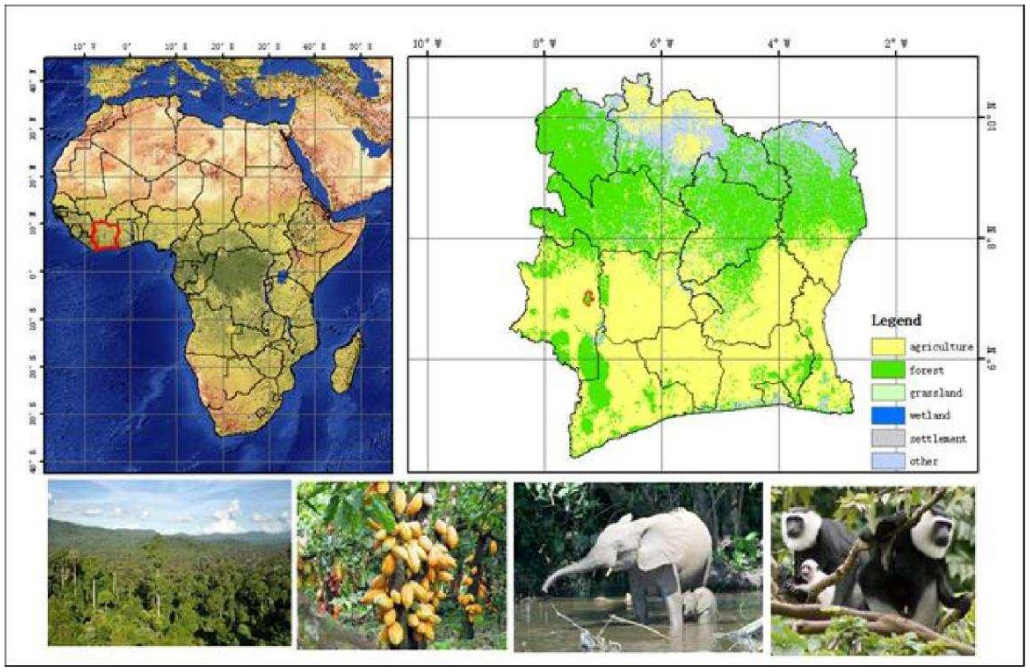

Figure 2. *Illustrated maps of the study area locations and exemplified plant and animal species. Côte d'Ivoire location (within red line) in African continent, (b) PNMP location (within red line) in Côte d'Ivoire, land cover map in background downloaded from the ESA-CCI site (http://maps.elie.ucl.ac.be/CCI/viewer/download.php). (c), (d), (e) and (f) is rainforest, cocoa plantation, elephants and colobus monkeys*

Data set

Landsat images have been downloaded from the USGS Earth Explorer website (https://earthexplorer.usgs.gov/) for this research. We chose less than 10% cloud cover. We downloaded Landsat 4-5 Thematic Mapper (TM), and Landsat 8 Operational Land Imager (OLI), and Thermal Infrared Sensor (TIRS) collection 1 level 1 image from 1985 and 2020, respectively. The images that were downloaded had previously been radiometrically and geometrically adjusted. The Landsat sensor is often utilized in land cover mapping applications in the landscape sector (Hansen and Loveland, 2012; Sharma and Joshi, 2013) and forestry mapping (Hansen and Loveland, 2012; Sharma and Joshi, 2013; Cohen and Goward, 2004; Townshend et al., 2012). The images from January-February-March-April-May-December were chosen for the study to minimize cloud cover because the rainy season in the region lasts from June to November. Image characteristics are shown in *Table 1*.

Table 1. *Characteristics of the Landsat satellite images used in this study*

No	Acquisition date	Scenes ID	Sensors	Resolution (m)	Path	Row
1	12/11/2010	LT05-L1TP-198_19850120-20170219-01-T1	Landsat 4 and 5 (TM)	30	198	55
2	05/01/2020	LC08-L1TP-198055-20200512-2020526-01-T1	Landsat 8 (OLI) and (TIRS)	30	198	55

TM = Thematic Mapper; OLI = The Operational Land Imager; TIRS = Thermal Infrared Sensor

http://www.aloki.hu ● ISSN 1589 1623 (Print) ● ISSN1785 0037 (Online)
DOI: http://dx.doi.org/10.15666/aeer/2003_20352058

Choice of the algorithm

The RF algorithm was chosen for its ability to forecast various land-use types (Gislason et al., 2006). It also discusses the significance of the factors utilized in the classification. We processed the NIR band for Landsat 4-5TM as band four (4) and the NIR band for Landsat 8OLI/TIRS as band 5. Once the changing image was acquired, it was utilized to identify the various locations on the resultant map where forest cover had grown, decreased, or stayed the same.

To produce an image with artificial colors and examine the vegetation in this color category, we layered the two multi-band images, namely date (1985) Landsat 4-5 TM (bands 1, 2, 3, 4, 5, 7) and date (2020) Landsat 8 OLI/TIRS (1, 2, 3, 4, 5, 6, 7). The color compositions were created using the near-infrared, mid-infrared, and red spectral bands from the 2020 Landsat 8 OLI/TIRS image (5/6/4) and (4/5/3) from the 1985 Landsat 4-5 TM images. We were able to see the images produced by combining false-color composite bands thanks to the categorization. We only utilized bands 12, 11, and 10 from the 2020 Landsat 8 images, corresponding to bands 6, 5, and 4. In reality, combining the two Landsat 4-5 TM and Landsat 8 OLI/TIRS images yielded 13 bands. We selected areas on the image where we knew the land use category and the change observed between 1985 and 2020 to establish training sites.

The establishment of training sites was spread across the park to identify areas with instability or no change. The training data was delineated in clusters, including gathering and defining multiple training plots in the same area. QGIS version 3.4.6 was used for processing. We used the near-infrared (NIR) band of each date to create a simple visualization of the change in Qgis. We created the training sites by generating a polygon shapefile before processing in the R program. The development of the training locations required the previous identification of places on the map where we understood the land use and the kind of change observed between 1985 and 2020. We then used and labeled the different type categories, as well as this identifying code (11: For-For), (12: For-NonFor), (21: NonFor-For), and (22: NonFor-NonFor).

The training areas were created on a computer by digitizing polygons on the multi-date (1985) and (2020) color composition for each specified spectral class (Forest to Non-Forest); (Forest to Forest); (Non-Forest to Non-Forest); and (Non-Forest to Non-Forest) (Non-Forest to Forest). Over the whole research site, 200 geometric polygons were developed, 50 for each land cover type. We assigned the value "100-100-100-500" respectively for (For-For), (For-NonFor), (NonFor-For), and (NonFor-NonFor) classes. The NonFor-NonFor class was given the number "500" since the training sites were lower in size than the other classes. These values enabled the classification algorithm to utilize the pixels in each class's formation polygons installation of the R packages "maptools", "sp", "randomForest", "raster", and "rgdal" was required prior to classification. RF classification was given to the whole collection of training areas. By combining the Landsat 4-5 TM (1985) and Landsat 8, OLI/TIRS (2020) bands utilized for the PNMP land cover categorization, thirteen (13) multi-temporal satellite imaging predictors were created. Throughout the categorization procedure, about 500 trees were mobilized to stabilize the classification.

Qgis has been used to apply the post-classification classifier majority filter (Pixel size 3×3) to the final PNMP map to improve our actual classification. This majority filter aims to remove pixel occurrences to prevent pixelated "salt and pepper" effects.

http://www.aloki.hu ● ISSN 1589 1623 (Print) ● ISSN1785 0037 (Online)
DOI: http://dx.doi.org/10.15666/aeer/2003_20352058

Statistical evaluation of classification accuracy

Calculations of accuracy: user's accuracy ($\widehat{U}$i) (*Eq. 1*), (Story and Congalton, 1986) producers' accuracy ($\widehat{P}$) (*Eq. 2*) and overall map accuracy ($\widehat{O}$) (*Eq. 3*) (Congalton and Green, 2019), allowed to estimate the accuracy of the classification. *Equations 2, 3,* and *4* are derived from Olofsson et al. (2014).

$$\widehat{Ui} = \frac{\hat{P}_{ii}}{\hat{P}_{i}} \quad \text{(Eq.1)}$$

$$\widehat{PJ} = \frac{\hat{p}_{jj}}{\hat{P}_{.j}} \quad \text{(Eq.2)}$$

$$\hat{O} = \sum_{j=1}^{n} \breve{y}_{jj} \quad \text{(Eq.3)}$$

where $\widehat{PJ}$ is the estimated proportion of area in cell, *j* of the error matrix *i* and *j* are the rows and columns of the confusion matrix.

In addition to the calculations of ($\widehat{Ui}$) and ($\widehat{PJ}$), we calculated estimates of the accuracy of final change map by combining *Equations 1* and *2* to the estimated error matrix as reported in *Table 2*. We evaluated the standard error of each class using *Equation 4:*

$$\hat{P}_{ij} = \theta_{i} \frac{n_{ij}}{n_{i.}} \quad \text{(Eq.4)}$$

where θ is the class error *''i''*, and *''j''* are the rows and columns of the confusion matrix.

The "*freq*" function in the Raster package enables us to calculate how many pixels exist in each class. It is a function that displays weighted or unweighted frequencies, including counts and proportions < NA > in the computation of pixels for area estimate. Areas were calculated by multiplying the total number of pixels by the size of each image pixel (900 m^2).

-In terms of surface area (m^2):

Each class's pixel count has been doubled by 900.

-In (ha), for the surface:

The surface area in (m^2) has been divided by 10000.

To calculate the percentage the quotient of the area in (ha) and the total area in (ha), was multiplied by 100.

$$\text{ClassArea (Ha)} = \frac{[\text{Count} \times 900]}{10000} \quad \text{(Eq.5)}$$

$$\text{ClassSurface } (m^2) = \text{Count} \times 900 \quad \text{(Eq.6)}$$

Results

Tree cover change

This descriptive study was performed on the whole territory from 1975 to 2013 (*Fig. 3*), focusing on our expanded region, the PNMP, and the Random Forest algorithm.

http://www.aloki.hu ● ISSN 1589 1623 (Print) ● ISSN1785 0037 (Online)
DOI: http://dx.doi.org/10.15666/aeer/2003_20352058

We chose to investigate the condition of the land cover prior to the time of this research in order to identify the pattern of changes that have happened. It enabled us to observe what happened before, during, and after the crisis.

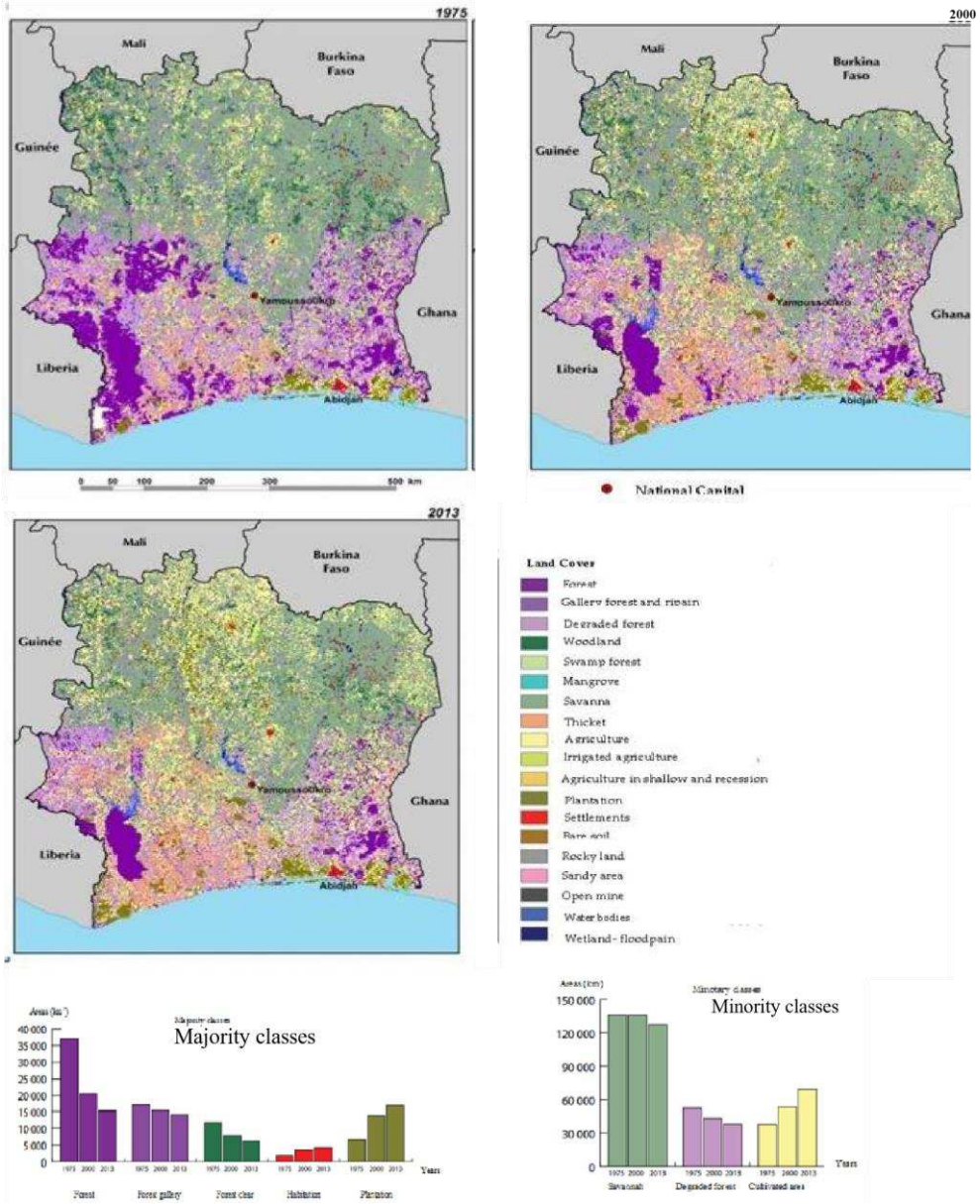

Figure 3. *Statistic Côte d'Ivoire land use and land cover class from 1975 to 2013 (CILSS, 2016)*

According to Hansen et al. (2013), the overall loss of trees is six times more than the total increase across the whole area in one year (2000). When we attempt to simulate the yearly loss from the beginning of the war in 2002 to the conclusion of the conflict in 2012, we see that the PNMP has lost a significant portion of its forest cover over these ten years (Hansen et al., 2013). The increase of cultivated land has had an impact on the woodland landscape. Indeed, deforestation caused by the expansion of agricultural land is one of the most significant and unquestionably permanent changes in Côte d'Ivoire. Historically,

http://www.aloki.hu ● ISSN 1589 1623 (Print) ● ISSN1785 0037 (Online)
DOI: http://dx.doi.org/10.15666/aeer/2003_20352058

most logging occurred inside the reserves and classed forests that surrounded about 40% of the Ivorian forest in 1975 (approximately 14,500 km^2) (CILSS, 2016). Dense forests, as well as open forests outside of protected zones, were severely damaged. Côte d'Ivoire lost almost 60% of the 37,300 km^2 of thick tropical forest in 1975 by 2013 (CILSS, 2016) (*Fig. 3*).

Similarly, the degraded forest has reduced by 28%, while open forest has dropped by 48%. Gallery forest is another significant forest type in Côte d'Ivoire. Gallery woods covered 17,100 km^2 in 1975. In 2013, this number was decreased to 14,130 km^2.

According to *Figure 4*, the park suffered its most significant loss in forest cover over the 10-year crisis period in 2012, with an estimated loss of 344590.88 Mg, which corresponds to an area of 1930.42 ha. Aside from this day, this region suffered a comparable loss in the year 2020 as it did in 2012. This is because the area was the site of violence and conflicts, and the warring parties and the people were concerned with fighting and escaping. After a few years of quiet, the warring armies entered the park to establish plantations. The park's tree loss has been a significant trend throughout the research period. The graph depicts the loss of primary forest and tree cover in the PNMP between 2001 and 2020 (https://www.globalforestwatch.org/). Over the whole time, we see a pattern of a substantial decline in tree cover across the park.

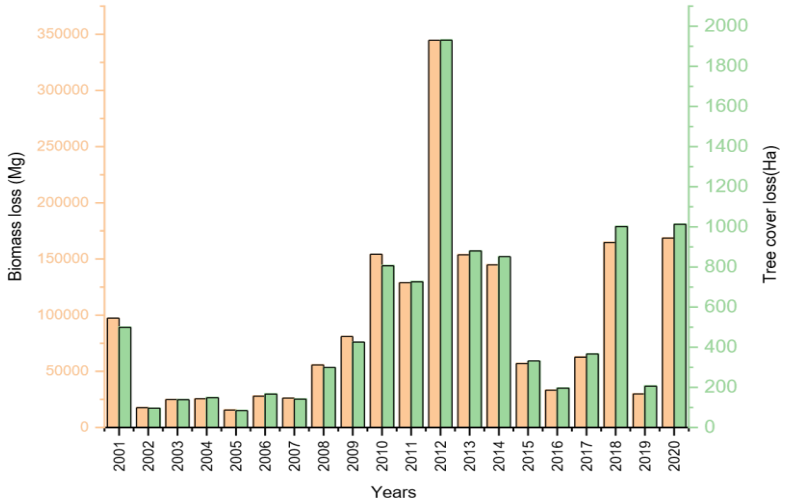

Figure 4. *PNMP Biomass and tree cover lost from 2001 to 2020*

Cocoa production increase

Figure 5 shows world cocoa prices from 1952 to 2017. The prices were high in the first ten years of the crisis, varying from 2000$ to 3000$. The world cocoa price from 2002 to 2007 increased above the trendline as the Côte d'Ivoire, the leading supplier of more than half of world production, could no longer supply the international market due to the crisis.

Vegetation index (NDVI)

Figure 6 shows the evolution of the vegetation index of the PNMP over the two periods 1985 and 2020. The figure illustrates a decrease in the NDVI pixels. The graph shows a reduction in the NDVI pixels performed in Qgis using Landsat 4-5 TM and Landsat 8

http://www.aloki.hu ● ISSN 1589 1623 (Print) ● ISSN1785 0037 (Online)
DOI: http://dx.doi.org/10.15666/aeer/2003_20352058

OLI/TIRS data. *Figure 6a* and *b* illustrate the drop in NDVI frequency values from 1400 to 1200 and in pixel values from 0.42 to -0.28 between 1985 and 2020.

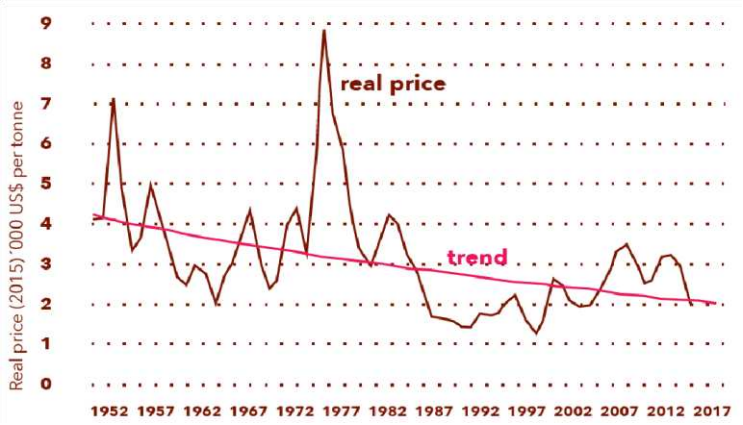

Figure 5. *Evolution of the world cocoa price trend (LMC, 2018)*

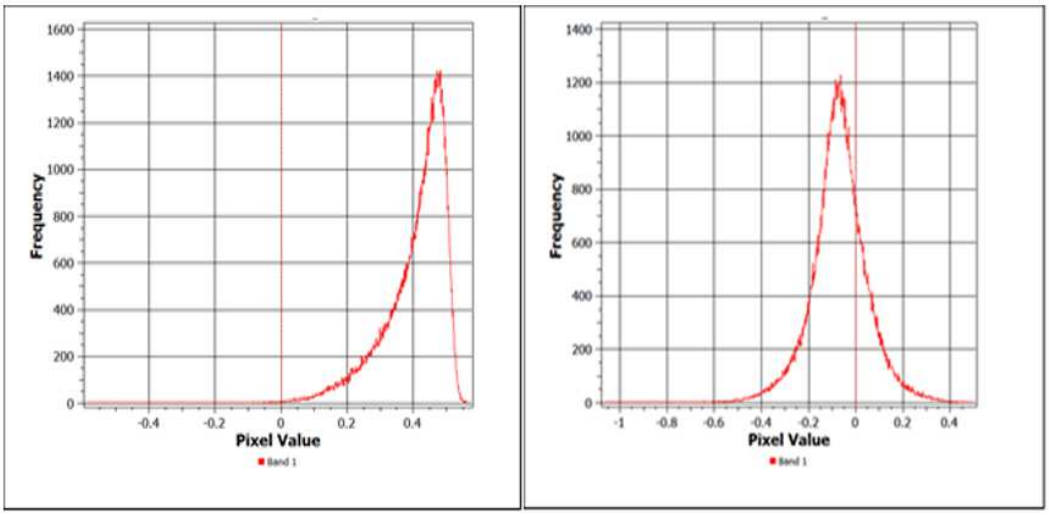

(a) 1985 (b) 2020

Figure 6. *Vegetation index NDVI (a: 1985), NDVI (b: 2020)*

As seen in *Figure 6*, there was an overall reduction in NDVI between 1985 and 2020, suggesting that the PNMP zone lost forest cover, supported by the findings (Ousmane et al., 2020).

The RF method allows to evaluate the significance of specific predictors in the model. The Random Forest model's variable importance graph (*Fig. 7*) shows the reduction in model accuracy (i.e., the percentage rise in the OOB error rate) caused by the permutation of each predictor variable. A decrease in accuracy indicates the variables increased significance for model performance.

Mean Decrease Accuracy (MDA) has been chosen because it allows quantifying the significance of variables (Genuer, 2010). MDA assesses the OOB error both before and after random permutation of the variable's values. If there is a significant reduction in OOB accuracy, the variable is deemed necessary.

http://www.aloki.hu ● ISSN 1589 1623 (Print) ● ISSN1785 0037 (Online)
DOI: http://dx.doi.org/10.15666/aeer/2003_20352058

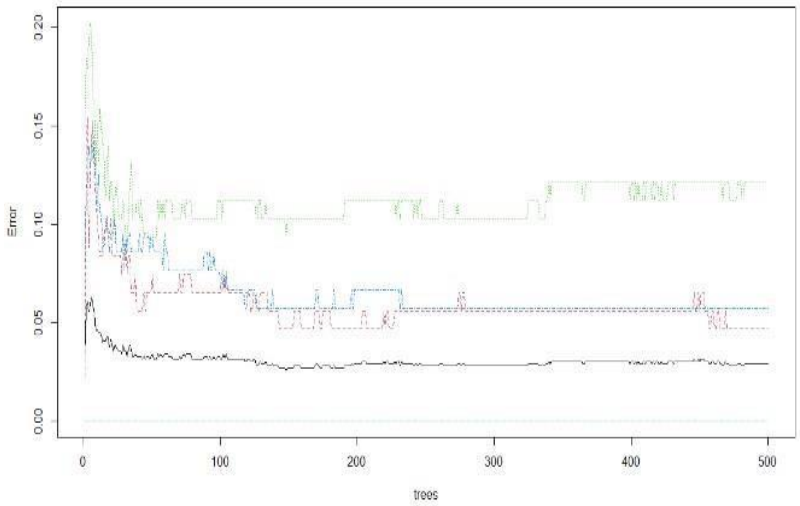

Figure 7. *Out-of-bag error rate plot. OOB error plotted against the number of trees included in the model. The error rate stabilizes after 500 trees to the point where any variations are accounted for by statistical noise*

Bands 12, 11, and 10 of the Landsat 4-5 TM and Landsat 8 OLI/TIRS image correspond to bands 6, 5, and 4 of the 2020 Landsat 8 image. We have six bands from Landsat 4-5TM image stacked on top of the 7 Landsat 8 OLI/TIRS bands. This is the same composite colour presentation as before.

This band combination combines bands from both dates to highlight changes in the shortwave infrared (SWIR) bands 13 (or the equivalent band 7 from the 2020 Landsat 8 image) and 5 (from the 1985 Landsat 4-5TM image).

The RF approach was used to assess the significance of specific variables in the classification model that was chosen. The random forest model's variable importance graph (*Fig. 8*) shows the reduction in model accuracy (i.e., the percentage rise in the OOB error rate) caused by the permutation of each predictor variable. A decrease in accuracy indicates the variables increased significance for model performance.

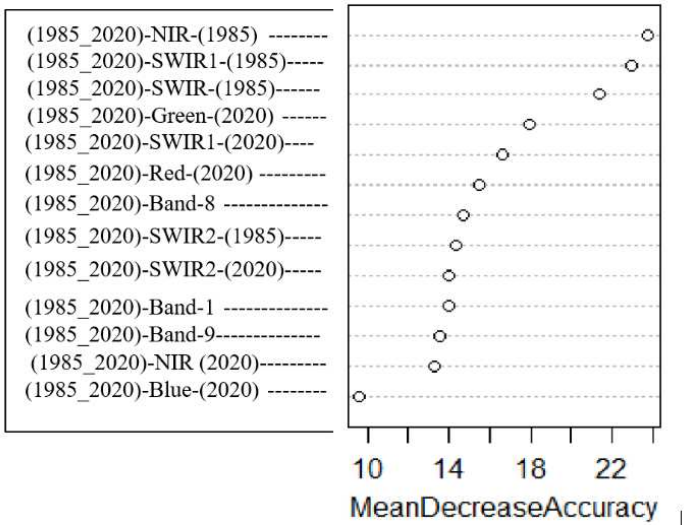

Figure 8. *Variable importance plot for random forest model, showing the mean decrease in accuracy for each predictor variable*

http://www.aloki.hu ● ISSN 1589 1623 (Print) ● ISSN1785 0037 (Online)
DOI: http://dx.doi.org/10.15666/aeer/2003_20352058

Table 2 shows the categorization findings in the form of a confusion matrix. This coefficient has a confidence interval of 0.95. The confidence interval was determined by multiplying the square root of the variance (User's accuracy ($\widehat{U}$i), Producer's accuracy ($\widehat{P}$), Overall accuracy ($\widehat{O}$), by 1.96 (Olofsson et al., 2014)).

Table 2. *The confusion matrix of the classification generated by Random Forest Landsat 4-5TM (1985) combined with Landsat 8 OLI/TIRS (2020)*

Class	For-For	For-NonFor	NonForFor	NonFor-NonFor	Total	Class.error (θ)	User's	Producer's	Overall	SE
For-For	**100**	0	2	0	102	0.0196	0.980±1.92	0.980±1.92		0.009
For-NonFor	0	**100**	0	0	100	0	1±1.96	1±1.96	0.972	0.123
NonFor-For	2	0	**100**	0	102	0.0196	0.980±1.92	0.970±1.93		0.064
NonFor-NonFor	0	0	1	**502**	503	0.0019	0.99±1.95	1±1.96		0
Total	102	100	103	502	807	0.04118	-	-		

OOB error rate estimate 0.0069%. Bold values in the diagonals indicate the number of samples (pixels) correctly classified Column totals are the total number of reference pixels in each class, and row totals are the total number of classified pixels in each class. Off diagonal numbers represent errors in the classification. SE: Standard Error

User's accuracy:

$$\widehat{Ui} = \frac{\hat{P}_{ii}}{\hat{P}_{i}} \times 100 \qquad \text{(Eq.7)}$$

Of the 102 pixels classified as (For-For), 100 were identified as For-For in the reference data; 2 NonFor-For were included in the For-For classification.

Of the 100 pixels all were identified as (For-NonFor).

Of 102 pixels classified as (NonFor-For), 100 were identified as NonFor-For in the reference data; 2 For-For were included in the (NonFor-For) classification.

Of the 503 pixels classified as (NonFor-NonFor), 502 were identified as NonFor-NonFor in the reference data, 1 NonFor-For were included in the NonFor-NonFor.

Producer's accuracy:

$$\widehat{Pj} = \frac{\hat{P}_{jj}}{\hat{P}_{.j}} \times \mathbf{100} \qquad \text{(Eq.8)}$$

Of the 102 pixels that were referenced as (For-For), 100 were correctly classified as For-For; 2 were classified as NonFor-For.

Of the 100 pixels that referenced as (For-NonFor), all were correctly classified as ForNonFor.

Of 103 pixels that referenced as (NonFor-For), 100 were correctly classified as NonFor-For; 2 were classified as For-For and 1 was classified as NonFor-NonFor. All of the 502 pixels were correctly classified as NonFor-NonFor.

Change detection analysis

Table 3 shows how much space each class takes up. The dominating class is the regular forest class (For-For) (43.16%). This class is located in the park's north-central area. The

http://www.aloki.hu ● ISSN 1589 1623 (Print) ● ISSN1785 0037 (Online)
DOI: http://dx.doi.org/10.15666/aeer/2003_20352058

map's visual analysis reveals a significant decrease in forest cover (ForNonFor) from 1985 to 2020, including the pre-and post-conflict eras. The findings indicate an alarming deforestation trend in the PNMP, with about 27.95% or 8455 ha of forest converted to nonforest. This reduction is due to cocoa farming. The For-NonFor class dominates the center area of the park. The replanting class (NonFor-For) encompasses 16.65% of the park. This type includes crops, fallow ground, and occasionally rocky outcrops that have been reforested. Finally, the regular nonforest class (NonFor-NonFor) area is 12.22% and it is located in the park's northern region.

Table 3. *National Mount Peko Park surface in 2020*

Class	Counts	Class area (m^2)	Class area (ha)	Percentage (%)
For-For	145013	1305511700	13051.17	43.16
For-NonFor	93941	84546900	8454.69	16.65
NonFor-For	5545	50350500	499.05	12.22
NonFor-NonFor	41087	36978300	3697.83	27.95

Figures 9 and *10* show the PNMP's final forest cover change map and statistic cover map. This map's visual evaluation reveals a substantial decrease in forest cover.

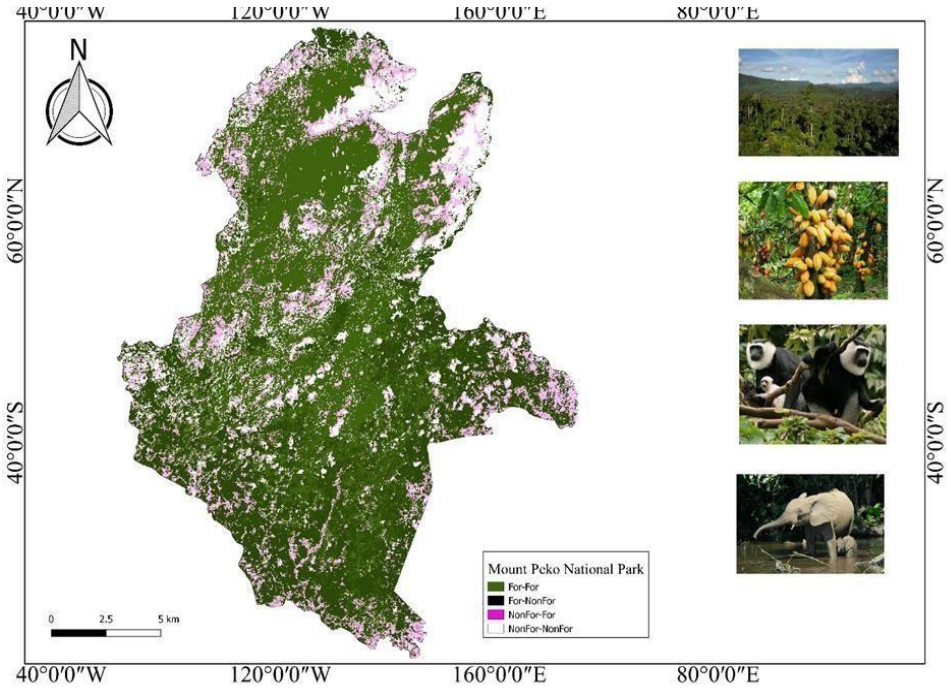

Figure 9. *represents the final forest cover change map of PNMP. Visual assessment of this map shows a significant loss of forest cover (1985-2020)*

The RF method allows to evaluate the significance of specific predictors in the model. The random forest model's variable importance graph (*Fig. 8*) shows the reduction in model accuracy (i.e., the percentage rise in the OOB error rate) caused by the permutation of each predictor variable. A decrease in accuracy indicates the variables increased significance for model performance.

http://www.aloki.hu ● ISSN 1589 1623 (Print) ● ISSN1785 0037 (Online)
DOI: http://dx.doi.org/10.15666/aeer/2003_20352058

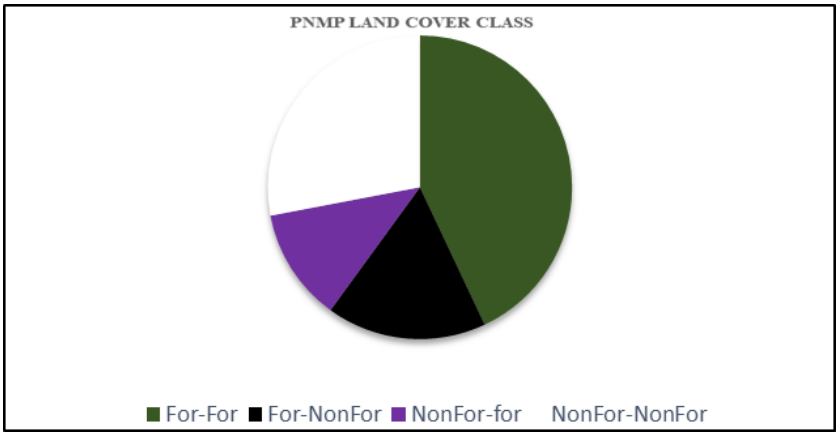

Figure 10. *Statistic land cover class (1985-2020)*

Discussion

We used a multitemporal pixel-based change detection technique tailored to the usage of multitemporal satellite pictures from various sensors. This research analyzed satellite images spanning the years 1985 to 2020. In contrast to prior research, the authors divided the forest cover change detection study into two or three time periods by distinguishing the time before, during, and after the crisis, following the suggestions of Lu and Weng, 2007, 2005; Churches et al., 2014; Lillesand et al., 2015; Wu et al., 2017; Garai and Narayana, 2018.

The RF classification approach was used to rigorously identify the changes that occurred by simple image discrimination between 1985 and 2020.

Indeed, the PNMP's land cover has altered considerably throughout the research period from 1985 until 2020. Because of the growing population and the scarcity of arable land in the region, we observe a substantial reduction in vegetated areas and an increase in cultivated land, putting further strain on the forest environment (Mather and Needle, 2000; SEP-REDD+, 2016). Much of the natural forest has been transformed into large expanses of farmed land, most of which is controlled by cocoa. Our findings are consistent with those of Sidibe et al. (2018), Ousmane et al. (2020), and Sangne et al. (2015), who found that conflicts facilitated the spread of illicit cocoa production in the PNMP and the Haut Sassandra Classified Forest. The outbreak of war in November 2002 resulted in the collapse of protection services in the PNMP and a reduction in conservation and tight protection due to severe ecological imbalances.

The armed war created an environment conducive to illicit operations such as poaching. This is supported by research conducted by Bi et al. (2012) and Bitty et al. (2013, 2015), which revealed that six elephants were murdered at Mount Péko National Park. Aside from that, there was a lack of governmental authority over protected zones in regions controlled by the armed insurrection. As a result, many protected woody species, unique flora, and animals were lost, and agricultural penetration grew.

During severe armed conflict from 2002 to 2007, cocoa bean prices rose globally as forest cover decreased. This area lost 622,000 ha of tree cover between 2001 and 2020, a 24% reduction since 2000 (https://www.globalforestwatch.org/).

These unlawful operations had become evident and noticeable, leading government officials to evict about 9,000 individuals who had established huge plantations and communities inside the PNMP (Woods, 2003). Some endangered species in the PNMP

http://www.aloki.hu ● ISSN 1589 1623 (Print) ● ISSN1785 0037 (Online)
DOI: http://dx.doi.org/10.15666/aeer/2003_20352058

were almost wiped out as a result of these clearings. For example, forest elephant populations have been devastated due to forest clearings to support cocoa production (Barnes, 1999). Human activities have pushed chimp and forest elephant species to reside beyond their native biological habitat (Short, 1981; Powell, 1997; Symstad et al., 1998; Morris, 2010; Kouakou et al., 2015).

Indeed, the loss of natural habitat boosted elephant and chimp poaching (Symstad et al., 1998; Bouché and Lungren, 2004; Graham et al., 2009; Bitty et al., 2013), mainly owing to the spread of weapons of war in the area. The armed conflict has significantly affected the Ivorian forest system, particularly the PNMP, by degrading it and converting it to cocoa production (Kone et al., 2014; Sidibe et al., 2018; Ousmane et al., 2020). These impacts have led to the reduction of animal species' ecological niches and indicate that recurrent crises are the primary causes of the deterioration of Ivorian tropical forests (Gorsevski et al., 2013; Nackoney et al., 2014; Ordway, 2015). Because the PNMP's security had been abandoned due to the conflict, the extinction of wildlife and flora had risen (McPherson and Nieswiadomy, 2000; Woods, 2003; Kouakou et al., 2015). Indeed, this tendency persists across the globe when nations conflict, as shown by studies such as Robert-Charmeteau (2015) on the landscape dynamics of A-Li forests during the Vietnam War and Rwanda's civil war (Kalpers et al., 2003; Plumptre et al., 2007).

Our findings are consistent with those of Ousmane et al. (2020), who examined the same region of the PNMP with Landsat 4-5TM and Landsat 8OLI/TIRS images in 1998, 2002, 2011, and 2016. Between 1985 and 2020, land usage and land cover in Côte d'Ivoire have changed significantly. The effects of this battle on the natural environment have been severe; the PNMP has lost a significant portion of its biological resources.

The PNMP has been occupied like the invasion of Rwandan parks and reserves during the civil war (1986-2003) and following the conflict (2003-2011), with armed rebels and refugees overexploiting forest resources (Kanyamibwa, 1998; Kalpers et al., 2003; Glew and Hudson, 2007).

Undoubtedly, the expansion of agricultural land at the cost of tropical rainforests is a major cause of tropical forest degradation in Côte d'Ivoire (Geoghegan et al., 2001; Ochoa-Gaona, 2001; Geist and Lambin, 2002; Lepers et al., 2005). Our results of reduced plant cover in the PNMP in favor of the development of large cocoa fields are consistent with the Mighty Earth team's studies in various protected areas across Côte d'Ivoire, including the PNMP. They were able to detect illicit cocoa cultivation in areas covered by woods (UNEP-WCMC, 2017). This statement is easily justified because, in 2010, Côte d'Ivoire had 13.9 million ha of natural forest or more than 43% of its surface area. In 2019, it lost 242000 ha of natural forest, accounting for approximately 56.1 Mt of CO_2 emissions (http://www.globalforestwatch.org/country/CIV).

This forest conversion was mainly caused by establishing cocoa plantations and logging, which activity was significant in the area (Myers et al., 2000; Sangne, 2009).

Cote d'Ivoire has many significant pioneer regions where cocoa is grown, with the bulk coming from the country's center-west, south-west, and west. These three major regions, which account for more than three-quarters of national output, were under the control of rebel forces, who utilized money from illicit production in the woods to fund their operations. These forces acquired foreign money by selling cocoa beans when the government officials could not meet demand on the international market due to the crisis.

The crisis has resulted in PNMP vegetation loss and the fragmentation of natural shelter niches for certain monkeys (McGraw, 1998; Grubb et al., 2003; Campbell et al., 2008). Furthermore, this dispute has resulted in a shift in harmful behavior to the

http://www.aloki.hu ● ISSN 1589 1623 (Print) ● ISSN1785 0037 (Online)
DOI: http://dx.doi.org/10.15666/aeer/2003_20352058

environment, namely selling tropical forests, unfortunately, as several authors have verified (Alvarez, 2003; Boulanger et al., 2011).

The crisis has exacerbated deforestation via mineral trafficking in the regions and massive environmental harm. As a result of the loss of a significant portion of the floral and faunal variety in the country, the Ivorian woods, in this instance, the PNMP, may have lost their essential role in development of the country (Bi et al., 2013).

Conclusion

We established the present status of the distribution of forest cover change classes inside the PNMP using Landsat 4-5 TM, and Landsat 8 OLI/TIRS time-series satellite images combined with NDVI data, with 43.16% of unaltered, intact forest. 27.95% of the forest land has been turned into nonforest (agricultural plantations, fallow, and other), 16.65% of nonforest has been converted into forest, and 12.22% nonforest areas have been converted into forest. The reduction in forest cover has benefited anthropic settings that diminish natural habitat. It is also important to note that population growth is a factor that has significantly altered the spatial structure of the natural environment. In general, the PNMP suffered a significant loss in forest cover at the start of the 2002 crisis due to abandoning the PNMP conservation (2007-2020). We were able to detect substantial deforestation throughout the research period because of satellite analysis of the PNMP. The armed conflict in Côte d'Ivoire and the conversion of forest lands to cocoa plantations were critical causes that exacerbated the PNMP's decrease in forest cover. The environmental consequences have been catastrophic. The repercussions have been twofold, with wildlife suffering as a result, including the loss of endemic species such as chimps and forest elephants, as well as other animal populations. Faced with environmental difficulties imposed by human demands, it is essential to assess existing natural resources to manage them rationally and sustainably. This research demonstrates how land cover may be monitored throughout time to give important information that can be used in the future to enhance forest management and biodiversity protection.

Recommendations

In response to this study, we would like to offer the following recommendations:

- research is needed to determine the impact of agricultural fertilizers and pesticides on soil pollution.
- research should be conducted on the impact of deforestation on soil erosion in the study area.
- assessment of the impact of population pressure on natural areas that have been designated as off-limits to development is necessary.

Acknowledgments. We are grateful to the Chinese and Cote d'Ivoire Government for the cooperation scholarship.

Funds. National Natural Science Fund Project for International and Regional Cooperation and Exchange "Sino-Argentian Cooperation Research on Temperate Grassland Degradation: Current Status Assessment and Recovery Strategies" (32061123005) and National Natural Science Fund Project "Joint Species Dsitribution Model Based Grassland Degradation Assessment and Potential Risk Projection in Hulun Buir Steppe" (41971061).

http://www.aloki.hu ● ISSN 1589 1623 (Print) ● ISSN1785 0037 (Online)
DOI: http://dx.doi.org/10.15666/aeer/2003_20352058

Conflict of interests. The authors declare that there is no conflict of interests regarding this paper.

REFERENCES

[1] Achard, F., Eva, H., Stibig, H., Mayaux, P., Gallego, J., Richards, T., Malingreau, J. (2002): Determination of deforestation rates of the world's humid tropical forests. – Science 297(5583): 999-1002.
[2] Aké-Assi, L. (1998): Impact de l'exploitation forestière et du développement agricole sur la conservation de la biodiversité biologique en Côte d'Ivoire. – Le Flamboyant 46: 2022.
[3] Allnutt, T. F., Asner, G. P., Golden, C. D., Powell, G. V. (2013): Mapping recent deforestation and forest disturbance in northeastern Madagascar. – Tropical Conservation Science 6: 1-15.
[4] Alvarez, M. D. (2003): Forests in the time of violence: conservation implications of the Colombian war. – Journal of Sustainable Forestry 16: 47-68.
[5] Assalé, A. A., Barima, Y. S., Sangne, Y. C., Bleu, D. K., Kpangui, K. B. (2020): Évaluation des services d'approvisionnement fournis par les espaces domaniaux anthropisés: cas de la forêt classée du Haut-Sassandra (Centre-Ouest de la Côte d'Ivoire). – Canadian Journal of Forest Research 50: 1002-1011.
[6] Aubry-Kientz, M., Rossi, V., Wagner, F., Hérault, B. (2015): Identifying climatic drivers of tropical forest dynamics. – Biogeosciences 12: 5583-5596.
[7] Bamba, I., Barima, Y., Sangne, Y., Andrieu, J., Assi-Kaudjhis, J. (2018): Partition du territoire et dynamique des végétations pendant la période de conflit en Côte d'Ivoire. – Tropicultura 36: 141-154.
[8] Barima, Y. S. S., Assale, A. A. Y., Vignal, M., Andrieu, J., Godron, M. (2016): Caractérisation post conflits armés des perturbations dans la forêt classée du HautSassandra en Côte d'Ivoire. – Afrique Science 12: 66-82.
[9] Barima, Y. S. S., Konan, G. D., Kouakou, A. T. M., Bogaert, J. (2020): Cocoa Production and Forest Dynamics in Ivory Coast from 1985 to 2019. – Land 9(12): 524. https://doi.org/10.3390/land9120524.
[10] Barnes, R. (1999): African Elephant Database 1998. – IUCN, Gland.
[11] Beucher, O., Bazin, F. (2012): L'agriculture en Afrique Face aux Défis du Changement Climatique. – Institut de l'énergie et de l'environnement de la Francophonie, Québec.
[12] Bhagwat, S. A., Willis, K. J., Birks, H. J. B., Whittaker, R. J. (2008): Agroforestry: a refuge for tropical biodiversity? – Trends in Ecology & Evolution 23: 261-267.
[13] Bi, S. G., Koné, I., Bitty, A. E., Koffi, J. B., Akpatou, B., Zinner, D. (2012): Distribution and conservation status of catarrhine primates in Côte d'Ivoire (West Africa). – Folia Primatologica 83: 11-23.
[14] Bi, Z. G., Kouame, D., Kone, I., Yao, C. A. (2013): Diversité végétale et valeur de conservation pour la Biodiversité du Parc National du Mont Péko, une aire protégée, menacée de disparition en Côte d'Ivoire. – Journal of Applied Biosciences 71: 5753-5762.
[15] Bitty, E. A., Gonedele'bi, S., Mcgraw, W. S. (2013): Accelerating deforestation and hunting in protected reserves jeopardize primates in southern Cote d'Ivoire. – American Journal of Physical Anthropology 150: 81-82.
[16] Bitty, E. A., Bi, S. G., Bene, J.-C. K., Kouassi, P. K., Mcgraw, W. S. (2015): Cocoa farming and primate extirpation inside Cote d'Ivoire's protected areas. – Tropical Conservation Science 8: 95-113.
[17] Bouché, P., Lungren, C. (2004): Les petites populations d'éléphants du Burkina Faso. Statut, distribution et déplacements. – Pachyderm 37: 84-91.
[18] Boulanger, A. G., Chu, A. C., Maxx, S., Waltz, D. L. (2011): Vehicle electrification: status and issues. – Proceedings of the IEEE 99: 1116-1138.
[19] Bouquet, C., D'ivoire, C. (2011): Le désespoir de Kourouma. – Armand Colin, Paris.

http://www.aloki.hu ● ISSN 1589 1623 (Print) ● ISSN1785 0037 (Online)
DOI: http://dx.doi.org/10.15666/aeer/2003_20352058

[20] Bredeloup, S. (2003): La Côte d'Ivoire ou l'étrange destin de l'étranger. – Revue Européenne des Migrations Internationales 19: 85-113.
[21] Breiman, L. (2001): Statistical modeling: the two cultures (with comments and a rejoinder by the author). – Statistical Science 16: 199-231.
[22] Brou, Y. T., Oszwald, J., Bigot, S., Servat, E. (2004): Risques de déforestation dans le domaine permanent de l'état en côte d'Ivoire: Quel avenir pour ces derniers massifs forestiers? – Télédétection 5: 105-121.
[23] Burger, K. (2008): Optimal export taxes–the case of cocoa in Côte d'Ivoire. – 107th Seminar, January 30-February 1, 2008, Sevilla, Spain, European Association of Agricultural Economists.
[24] Burgess, R., Miguel, E., Stanton, C. (2015): War and deforestation in Sierra Leone. – Environmental Research Letters 10: 095014.
[25] Burle, L. (1962): Le Cacaoyer: Tome Deuxième. – Maisonneuve et Larose, Paris.
[26] Campbell, G., Kuehl, H., Kouamé, P. N. G., Boesch, C. (2008): Alarming decline of West African chimpanzees in Côte d'Ivoire. – Current Biology 18(19): R904.
[27] CEPF (2000): Ecosysteme Forestier De Haute Guinee Dans La Zone Prioritaire De Biodiversite De Guinee (Afrique De L'ouest). – Conservation International, Arlington.
[28] Chaléard, J.-L. (1996): Les mutations de l'agriculture commerciale en Afrique de l'Ouest. – Annales de Géographie 592: 563-583.
[29] Chatelain, C., Dao, H., Gautier, L., Spichiger, R. (2004): Forest Cover Changes in Côte d'Ivoire and Upper Guinea. – In: Poorter, L., Bongers, F., Kouamé, F. N., Hawthorne, W. D. (eds.) Biodiversity of West African Forests: An Ecological Atlas of Woody Plant Species. CABI Publishing, Oxford, UK, pp. 15-32.
[30] Chauveau, J.-P. (2000): Question foncière et construction nationale en Côte d'Ivoire. – Politique Africaine 2: 94-125.
[31] Churches, C. E., Wampler, P. J., Sun, W., Smith, A. J. (2014): Evaluation of forest cover estimates for Haiti using supervised classification of Landsat data. – International Journal of Applied Earth Observation and Geoinformation 30: 203-216.
[32] Cilss (2016a): Les Paysages de l'Afrique de l'Ouest: Une Fenêtre sur un Monde en Pleine Évolution. – Geological Survey EROS, Garretson, SD.
[33] Climate Chance (2018): «L'action sectorielle» Cahier 1 Du rapport annuel de l'observatoire mondial de l'action climatique non-étatique 57. – Climate Chance, Paris.
[34] Cohen, W. B., Goward, S. N. (2004): Landsat's role in ecological applications of remote sensing. – Bioscience 54: 535-545.
[35] Congalton, R. G., Green, K. (2019): Assessing the Accuracy of Remotely Sensed Data: Principles and Practices. – CRC Press, Boca Raton, FL.
[36] Coulibaly, S. K., Erbao, C. (2019): An empirical analysis of the determinants of cocoa production in Cote d'Ivoire. – Journal of Economic Structures 8: 1-19.
[37] Darie-Rousseaux, E., Brown, K. (2016): Développement d'une gamme de services financiers diversifiés pour les producteurs de cacao en Côte d'Ivoire et dans d'autres contextes agricoles. – Techniques Financieres et Developpement 3-4: 67-79.
[38] Deheuvels, P. (2009): A multivariate Bahadur–Kiefer representation for the empirical copula process. – Zap. Nauchn. Sem. POMI 364: 120-147.
[39] Deheuvels, O. (2011): Compromis entre productivité et biodiversité sur un gradient d'intensité de gestion de systèmes agroforestiers à base de cacaoyers de Talamanca, Costa Rica. – SupAgro, Montpellier.
[40] Deheuvels, O., Assiri, A. A., Flori, A., Petithuguenin, P., Kébé, B. I. (2003): Planting and Replanting Techniques among Ivorian Cocoa Smallholders. – CIRAD, Montpellier.
[41] Esso, L. (2009): La dépendance démographique est-elle un obstacle à l'épargne et à la croissance en Côte d'Ivoire? – L'Actualité économique 85: 361-382.
[42] Foley, J. A., Defries, R., Asner, G. P., Barford, C., Bonan, G., Carpenter, S. R., Chapin, F. S., Coe, M. T., Daily, G. C., Gibbs, H. K. (2005): Global consequences of land use. – Science 309: 570-574.

http://www.aloki.hu ● ISSN 1589 1623 (Print) ● ISSN1785 0037 (Online)
DOI: http://dx.doi.org/10.15666/aeer/2003_20352058

[43] Foley, J. A., Asner, G. P., Costa, M. H., Coe, M. T., Defries, R., Gibbs, H. K., Howard, E. A., Olson, S., Patz, J., Ramankutty, N. (2007): Amazonia revealed: forest degradation and loss of ecosystem goods and services in the Amazon Basin. – Frontiers in Ecology and the Environment 5: 25-32.
[44] Fountain, A., Hütz-Adams, F. (2018): Cocoa Barometer. – Public Eye, Zurich.
[45] Franzen, M., Mulder, M. B. (2007): Ecological, economic and social perspectives on cocoa production worldwide. – Biodiversity and Conservation 16: 3835-3849.
[46] Garai, D., Narayana, A. (2018): Land use/land cover changes in the mining area of Godavari coal fields of southern India. – The Egyptian Journal of Remote Sensing and Space Science 21: 375-381.
[47] Geist, H. J., Lambin, E. F. (2002): Proximate Causes and Underlying Driving Forces of Tropical DeforestationTropical forests are disappearing as the result of many pressures, both local and regional, acting in various combinations in different geographical locations. – BioScience 52: 143-150.
[48] Genuer, R. (2010): Forêts aléatoires: aspects théoriques, sélection de variables et applications. – Université Paris Sud, Paris.
[49] Geoghegan, J., Villar, S. C., Klepeis, P., Mendoza, P. M., Ogneva-Himmelberger, Y., Chowdhury, R. R., Turner Ii, B., Vance, C. (2001): Modeling tropical deforestation in the southern Yucatan peninsula region: comparing survey and satellite data. – Agriculture, Ecosystems & Environment 85: 25-46.
[50] Gislason, P. O., Benediktsson, J. A., Sveinsson, J. R. (2006): Random forests for land cover classification. – Pattern Recognition Letters 27: 294-300.
[51] Glew, L., Hudson, M. (2007): Gorillas in the midst: the impact of armed conflict on the conservation of protected areas in sub-Saharan Africa. – Oryx 41: 140-150.
[52] Gnahoua, G., Ouallou, K., Balle, P. (2012): Les légumineuses à croissance rapide comme plantes d'ombrage dans la replantation des cacaoyers en zone de forêt semi décidue de Côte d'Ivoire. – INAFORESTA Symposium. Cocoa Based Agroforestry: Sustainability and Environment, Yaoundé, 21-22 October.
[53] Gorsevski, V., Geores, M., Kasischke, E. (2013): Human dimensions of land use and land cover change related to civil unrest in the Imatong Mountains of South Sudan. – Applied Geography 38: 64-75.
[54] Graham, M. D., Douglas-Hamilton, I., Adams, W. M., Lee, P. C. (2009): The movement of African elephants in a human-dominated land-use mosaic. – Animal Conservation 12: 445-455.
[55] Grubb, P., Butynski, T. M., Oates, J. F., Bearder, S. K., Disotell, T. R., Groves, C. P., Struhsaker, T. T. (2003): Assessment of the diversity of African primates. – International Journal of Primatology 24: 1301-1357.
[56] Hansen, M. C., Loveland, T. R. (2012): A review of large area monitoring of land cover change using Landsat data. – Remote sensing of Environment 122: 66-74.
[57] Hansen, M. C., Potapov, P. V., Moore, R., Hancher, M., Turubanova, S. A., Tyukavina, A., Thau, D., Stehman, S., Goetz, S. J., Loveland, T. R. (2013): High-resolution global maps of 21st-century forest cover change. – Science 342: 850-853.
[58] Hausmann, R., Hidalgo, C. A. (2011): The network structure of economic output. – Journal of Economic Growth 16: 309-342.
[59] Higonnet, E., Bellantonio, M., Hurowitz, G. (2017): Chocolate's Dark Secret. – Mighty Earth 24, Washington, DC.
[60] Ibo, J. (2005): Les nouvelles orientations de la gestion du patrimoine naturel en Côte d'Ivoire. Patrimoines naturels au Sud: territoires, identités et stratégies locales. – IRD Éditions, Paris.
[61] Ibo, J., Léonard, E. (1994): Appropriation et gestion de la rente forestière en Côte d'Ivoire. – Politique Africaine 53: 25-36.
[62] Jhariya, M. K. (2017): Vegetation ecology and carbon sequestration potential of shrubs in tropics of Chhattisgarh, India. – Environmental Monitoring and Assessment 189: 1-15.

http://www.aloki.hu ● ISSN 1589 1623 (Print) ● ISSN1785 0037 (Online)
DOI: http://dx.doi.org/10.15666/aeer/2003_20352058

[63] Kadet, B. G. (2015): L'ouest forestier ivoirien: enjeux et problèmes d'une zone grise. Les Cahiers d'Outre-Mer. – Revue de Géographie, Bordeaux, pp. 437-458.
[64] Kalpers, J., Williamson, E. A., Robbins, M. M., Mcneilage, A., Nzamurambaho, A., Lola, N., Mugiri, G. (2003): Gorillas in the crossfire: population dynamics of the Virunga mountain gorillas over the past three decades. – Oryx 37: 326-337.
[65] Kanyamibwa, S. (1998): Impact of war on conservation: Rwandan environment and wildlife in agony. – Biodiversity & Conservation 7: 1399-1406.
[66] Kassoum, T. (2018): Le couvert forestier en Côte d'Ivoire: une analyse critique de la situation de gestion des forêts (classées, parcs et réserves). – The International Journal of Social Sciences and Humanities Invention 5: 4387-4397.
[67] Kireyev, A. (2010): Export tax and pricing power: two hypotheses on the cocoa market in Côte d'Ivoire. – IMF Working Papers. https://doi.org/10.5089/9781455210763.001.
[68] Konate, Z., Assiri, A., Messoum, F., Sekou, A., Camara, M., Yao-Kouame, A. (2015): Antécédents culturaux et identification de quelques pratiques paysannes en replantation cacaoyère en Côte d'Ivoire. – Agronomie Africaine 27: 301-314.
[69] Konate, K. Z., Assiri, A. A., Messoum, F. G., Sekou, A., Camara, M., Albert, Y.-K. (2017): Identification de quelques contraintes paysannes en replantation cacaoyère en Côte d'Ivoire. – Sciences de la Vie, de la Terre et Agronomie 4.
[70] Kone, M., Konate, S., Yeo, K., Kouassi, P. K., Linsenmair, K. E. (2014): Effects of management intensity on ant diversity in cocoa plantation (Oume, centre west Côte d'Ivoire). – Journal of Insect Conservation 18: 701-712.
[71] Koning, R. D., Capistrano, D., Yasmi, Y., Cerutti, P. (2007): Forest-Related Conflict: Impacts, Links and Measures to Mitigate. – RECOFTC, Bangkok.
[72] Kouakou, K. A., Barima, Y. S. S., Kouakou, A., Sangne, Y., Bamba, I., Kouamé, N. (2015): Diversité végétale post-conflits armés de la Forêt Classée du Haut-Sassandra (Centre-Ouest de la Côte d'Ivoire). – J. Anim. Plant Sci 26: 4058-4071.
[73] Kouakou, A. T. M., Barima, Y. S. S., Konate, S., Bamba, I., Kouadio, J. Y., Bogaert, J. (2017): Gestion des forêts domaniales en période de conflits: cas de la forêt classée du Haut-Sassandra, Centre-Ouest de la Côte d'Ivoire. – International Journal of Biological and Chemical Sciences 11: 333-349.
[74] Kouamé, F. (1998): Influence de l'exploitation forestière sur la végétation et la flore de la forêt classée du Haut-Sassandra. – Centre-Ouest de la Côte-d'Ivoire, Daloa.
[75] Läderach, P., Martinez-Valle, A., Schroth, G., Castro, N. (2013): Predicting the future climatic suitability for cocoa farming of the world's leading producer countries, Ghana and Côte d'Ivoire. – Climatic Change 119: 841-854.
[76] Lauginie, F. (2007): Conservation de la nature et aires protégées en Côte d'Ivoire. – CEDA/NEI, Abidjan.
[77] Lauginie, F., Béligné, V., Akindes, F., Poilecot, P. (1995): Monographie des réserves naturelles de Côte d'Ivoire. – DDC/MINAGRA/WWF, Abidjan.
[78] Lepers, E., Lambin, E., Janetos, A., Defries, R., Achard, F., Ramankutty, N., Scholes, R. (2005): A synthesis of rapid land-cover change information for the 1981–2000 period. – BioScience 55: 19-26.
[79] Lillesand, T., Kiefer, R. W., Chipman, J. (2015): Remote Sensing and Image Interpretation. – John Wiley & Sons, New York.
[80] LMC (2018): Cocoa: the global market Outlook for beans, butter, liquor & powder 2018. – Brochure. LMC International, Oxford, UK.
[81] Lu, D., Weng, Q. (2005): Urban classification using full spectral information of Landsat ETM+ imagery in Marion County, Indiana. – Photogrammetric Engineering & Remote Sensing 71: 1275-1284.
[82] Lu, D., Weng, Q. (2007): Une enquête sur les méthodes de classification des images et techniques pour améliorer les performances de classification. – International Journal of Remote Sensing 28: 823-870.

http://www.aloki.hu ● ISSN 1589 1623 (Print) ● ISSN1785 0037 (Online)
DOI: http://dx.doi.org/10.15666/aeer/2003_20352058

[83] Malhi, Y., Baldocchi, D., Jarvis, P. (1999): The carbon balance of tropical, temperate and boreal forests. – Plant, Cell & Environment 22: 715-740.
[84] Mather, A., Needle, C. (2000): The relationships of population and forest trends. – Geographical Journal 166: 2-13.
[85] Matsushita, B., Xu, M., Fukushima, T. (2006): Characterizing the changes in landscape structure in the Lake Kasumigaura Basin, Japan using a high-quality GIS dataset. – Landscape and urban planning 78: 241-250.
[86] Mcgraw, W. S. (1998): Three monkeys nearing extinction in the forest reserves of eastern Cote d'lvoire. – Oryx 32: 233-236.
[87] Mcintire, J., Varangis, P. (1999): Reforming Cote d'Ivoire's cocoa marketing and pricing system. – World Bank Policy Research Working Paper. https://ssrn.com/abstract=615012.
[88] Mcpherson, M. A., Nieswiadomy, M. L. (2000): African elephants: the effect of property rights and political stability. – Contemporary Economic Policy 18: 14-26.
[89] Menzies, A. (2000): Structure et composition floristique de la forêt de la zone ouest du parc national de Taï (Côte d'Ivoire). – Diplôme, Université de Génèse.
[90] Miller, R. M., Rodríguez, J. P., Aniskowicz-Fowler, T., Bambaradeniya, C., Boles, R., Eaton, M. A., Gärdenfors, U., Keller, V., Molur, S., Walker, S. (2007): National threatened species listing based on IUCN criteria and regional guidelines: current status and future perspectives. – Conservation Biology 21: 684-696.
[91] Morris, R. J. (2010): Anthropogenic impacts on tropical forest biodiversity: a network structure and ecosystem functioning perspective. – Philosophical Transactions of the Royal Society B: Biological Sciences 365: 3709-3718.
[92] Myers, S. A., Rocca, K. A. (2000): The relationship between perceived instructor communicator style, argumentativeness, and verbal aggressiveness. – Communication Research Reports 17: 1-12.
[93] Myers, N., Mittermeier, R. A., Mittermeier, C. G., Da Fonseca, G. A., Kent, J. (2000): Biodiversity hotspots for conservation priorities. – Nature 403: 853-858.
[94] N'da, D. (2007): Étude et suivi par télédétection et système d'information géographique d'une aire protégée soumise aux pressions. – Thèse de Doctorat unique, Université de Cocody, Abidjan.
[95] N'da, H. D., N'guessan, E. K., Wajda, M. E., Affian, K. (2008): Apport de la télédétection au suivi de la déforestation dans le Parc National de la Marahoué (Côte d´ Ivoire). – Télédétection 8: 17-34.
[96] N'guessan, K. E. (2004): Utilisation des données satellitaires à haute résolution pour l'étude des ressources végétales en Côte d'Ivoire: cas des forêts classées de Badenou et du Haut Sassandra. – Thèse de Doctorat. Université Paul Sabatier, Toulouse, France.
[97] Nackoney, J., Molinario, G., Potapov, P., Turubanova, S., Hansen, M. C., Furuichi, T. (2014): Impacts of civil conflict on primary forest habitat in northern Democratic Republic of the Congo 1990–2010. – Biological Conservation 170: 321-328.
[98] Norris, K., Asase, A., Collen, B., Gockowksi, J., Mason, J., Phalan, B., Wade, A. (2010): Biodiversity in a forest-agriculture mosaic-The changing face of West African rainforests. – Biological conservation 143: 2341-2350.
[99] O'sullivan, O. S., Holt, A. R., Warren, P. H., Evans, K. L. (2017): Optimising UK urban road verge contributions to biodiversity and ecosystem services with cost-effective management. – Journal of Environmental Management 191: 162-171.
[100] Oates, J. F. (2011): Primates of West Africa: A Field Guide and Natural History. – Conservation International, Arlington.
[101] Ochoa-Gaona, S. (2001): Traditional land-use systems and patterns of forest fragmentation in the highlands of Chiapas, Mexico. – Environmental Management 27: 571-586.
[102] Olofsson, P., Foody, G. M., Herold, M., Stehman, S. V., Woodcock, C. E., Wulder, M. A. (2014): Good practices for estimating area and assessing accuracy of land change. – Remote Sensing of Environment 148: 42-57.

http://www.aloki.hu ● ISSN 1589 1623 (Print) ● ISSN1785 0037 (Online)
DOI: http://dx.doi.org/10.15666/aeer/2003_20352058

[103] Ordway, E. M. (2015): Political shifts and changing forests: effects of armed conflict on forest conservation in Rwanda. – Global Ecology and Conservation 3: 448-460.
[104] Ousmane, S., N'da Dibi, H., Kouassi, K. H., Kouassi, K. É., Ouattara, K. (2020): Crises politico-militaires et dynamique de la végétation du Parc national du Mont Péko en Côte d'Ivoire. – Bois & Forets Des Tropiques 343: 27-37.
[105] Pan, Y., Birdsey, R. A., Fang, J., Houghton, R., Kauppi, P. E., Kurz, W. A., Phillips, O. L., Shvidenko, A., Lewis, S. L., Canadell, J. G. (2011): A large and persistent carbon sink in the world's forests. – Science 333: 988-993.
[106] Plumptre, A. J., Kujirakwinja, D., Treves, A., Owiunji, I., Rainer, H. (2007): Transboundary conservation in the greater Virunga landscape: its importance for landscape species. – Biological Conservation 134: 279-287.
[107] Poorter, L., Van Der Sande, M. T., Thompson, J., Arets, E. J., Alarcón, A., Álvarez-Sánchez, J., Ascarrunz, N., Balvanera, P., Barajas-Guzmán, G., Boit, A. (2015): Diversity enhances carbon storage in tropical forests. – Global Ecology and Biogeography 24: 1314-1328.
[108] Powell, J. A. (1997): The Ecology of Forest Elephants (Loxodonta Africana Cyclotis Matschie 1900) in Banyang-Mbo and Korup Forests, Cameroon with Particular Reference to Their Role as Seed Dispersal Agents. – University of Cambridge, Cambridge.
[109] Robert-Charmeteau, A. (2015): Les impacts de la guerre du Việt Nam sur les forêts d'A Lưới. – VertigO. https://doi.org/10.4000/vertigo.16105.
[110] Rowland, J. A., Nicholson, E., Murray, N. J., Keith, D. A., Lester, R. E., Bland, L. M. (2018): Selecting and applying indicators of ecosystem collapse for risk assessments. – Conservation Biology 32: 1233-1245.
[111] Ruf, F., Schroth, G., Doffangui, K. (2015): Climate change, cocoa migrations and deforestation in West Africa: what does the past tell us about the future? – Sustainability Science 10: 101-111.
[112] Sangne, Y. (2009): Dynamique du couvert forestier d'une aire protégée soumise aux pressions anthropiques: cas de la Forêt Classée de Téné dans le Département d'Oumé (Centre-ouest de la Côte d'Ivoire). – Université de Cocody, Abidjan.
[113] Sangne, C., Barima, Y., Bamba, I., N'doumé, C.-T. (2015): Dynamique forestière postconflits armés de la Forêt classée du Haut-Sassandra (Côte d'Ivoire). – VertigO. https://doi.org/10.4000/vertigo.16784.
[114] Sep-Redd+ (2016): Données Forestières De Base Pour La REDD+ En Côte D'ivoire Inventaire De La Biomasse Forestière Pour L'estimation Des Facteurs D'émission. – FAO, Rome.
[115] Sharma, R., Joshi, P. (2013): Monitoring urban landscape dynamics over Delhi (India) using remote sensing (1998–2011) inputs. – Journal of the Indian Society of Remote Sensing 41: 641-650.
[116] Short, J. (1981): Diet and feeding behaviour of the forest elephant. – Mammalia 45: 177-185.
[117] Sidibe, O., Henri, K. K., Armand, Z. D., Djaha, K., Traore, K. (2018): Dynamics of human pressures on the Mont Péko National Park (West-Côte d'Ivoire). – European Scientific Journal ESJ 14: 109.
[118] Singh, K. (1993): L'évaluation des ressources forestières tropicales. – Unasylva 44: 1020.
[119] Sonwa, D. J., Nkongmeneck, B. A., Weise, S. F., Tchatat, M., Adesina, A. A., Janssens, M. J. (2007): Diversity of plants in cocoa agroforests in the humid forest zone of Southern Cameroon. – Biodiversity and Conservation 16: 2385-2400.
[120] Story, M., Congalton, R. G. (1986): Accuracy assessment: a user's perspective. – Photogrammetric Engineering and Remote Sensing 52: 397-399.
[121] Symstad, A. J., Tilman, D., Willson, J., Knops, J. M. (1998): Species loss and ecosystem functioning: effects of species identity and community composition. – Oikos 81: 389-397.

http://www.aloki.hu ● ISSN 1589 1623 (Print) ● ISSN1785 0037 (Online)
DOI: http://dx.doi.org/10.15666/aeer/2003_20352058

[122] Tadesse, G., Zavaleta, E., Shennan, C., Fitzsimmons, M. (2014): Prospects for forestbased ecosystem services in forest-coffee mosaics as forest loss continues in southwestern Ethiopia. – Applied Geography 50: 144-151.
[123] Tano, A. M. (2012): Crise cacaoyère et stratégies des producteurs de la sous-préfecture de Méadji au Sud-Ouest ivoirien. – Toulouse 2.
[124] Townshend, J. R., Masek, J. G., Huang, C., Vermote, E. F., Gao, F., Channan, S., Sexton, J. O., Feng, M., Narasimhan, R., Kim, D. (2012): Global characterization and monitoring of forest cover using Landsat data: opportunities and challenges. – International Journal of Digital Earth 5: 373-397.
[125] Tutu, K., Akol, C. (2009): Reversing Africa's Deforestation for Sustainable Development. – Yanful, E. K. (ed.) Appropriate Technologies for Environmental Protection in the Developing World. Springer, Dordrecht.
[126] UNEP (2015): Évaluation environnementale post-conflit Côte d'Ivoire. – UNEP, Nairobi, Kenya.
[127] UNEP-WCMC (2017): Protected Area Profile for Côte D'Ivoire from the World Database of Protected Areas. – UNEP-WCMC, Cambridge, UK.
[128] Wessel, M., Quist-Wessel, P. F. (2015): Cocoa production in West Africa, a review and analysis of recent developments. – NJAS-Wageningen Journal of Life Sciences 74: 1-7.
[129] Woods, D. (2003): The tragedy of the cocoa pod: rent-seeking, land and ethnic conflict in Ivory Coast. – Journal of Modern African Studies 41(4): 641-655.
[130] Wu, C., Du, B., Cui, X., Zhang, L. (2017): A post-classification change detection method based on iterative slow feature analysis and Bayesian soft fusion. – Remote Sensing of Environment 199: 241-255.
[131] Yao, A., Yves, C. (2005): Pratiques paysannes et dynamique de la biodiversité dans la forêt classée de Monogaga (Côte d'Ivoire). – Muséum National d'Histoire Naturelle, Paris.

http://www.aloki.hu ● ISSN 1589 1623 (Print) ● ISSN1785 0037 (Online)
DOI: http://dx.doi.org/10.15666/aeer/2003_20352058

EFFECT OF VARIOUS CULTURE CONDITIONS ON THE ANTIMICROBIAL ACTIVITY BY BACTERIA FROM PASSU GLACIER, PAKISTAN

RABBANI, I.[1] – AHMAD, T.[1] – MAQSOOD-UR-REHMAN, M.[1] – RAFIQ, M.[2] – NAWAZ, S.[1] – IRFAN, M.[3] – SHAH, A. A.[1] – HASAN, F.[1*]

[1]*Department of Microbiology, Quaid-i-Azam University, Islamabad, Pakistan*

[2]*Department of Microbiology, Balochistan University of Information Technology and Management Sciences, Quetta, Pakistan*

[3]*Department of Oral Biology, College of Dentistry, University of Florida, Gainesville, FL, United States*

[*]*Corresponding author*
e-mail: farihahasan@yahoo.com; phone: +92-519-064-3065

(Received 15th Feb 2021; accepted 10th June 2021)

Abstract. Microorganisms inhabiting cold environments have an incredible potential to produce secondary metabolites including antibacterial, antifungal and antiviral compounds. The aim of the study was to evaluate the possibility of using cold adapted bacteria isolated from Passu glacier for the production of antimicrobial metabolites. Agar well diffusion assay was used to select four best antimicrobial compound producers coded as HTP12, HTP13, HTP36 and LTP10. These strains were identified as *Alcaligenes faecalis*, *Pseudochrobactrum saccharolyticum*, *Alcaligenes pakistanensis* and *Alcaligenes pakistanensis*, respectively, by their phylogenetic analysis. The media, temperature, incubation time and pH were optimized for antimicrobial compound production. The effect of nitrogen sources, carbon sources and salts on antibiotic production was also determined. *Alcaligenes pakistanensis* (LTP10) showed the best antimicrobial activity in Luria Bertani broth, at 25°C, pH 7 and incubation time of 96 hrs against various bacterial ATCC strains and clinical isolates. Yeast extract increased antibiotic activity of *Alcaligenes pakistanensis* (LTP10) while glucose, starch, tryptophan, threonine, L-leucine, arginine, NaCl and KCl decreased the activity. This study concludes that the psychrophilic bacteria are abundant, undiscovered, and good producers of antimicrobial metabolites under optimum conditions. This will lead to the discovery of potent and novel metabolites which could be of medical and industrial importance.
Keywords: *psychrophilic bacteria, Alcaligenes pakistanensis, agar well diffusion assay, antimicrobial metabolites, antibiotic production optimization*

Introduction

The environment which is not suitable and is considered severe for the survival of human beings is referred to as extreme environment and most of the world's extreme environments are low temperature environments. These low temperature environments provide harsh conditions for the survival and growth of organisms but still harbour a large persistent community of microbes. These persistent microbes have adaptations to cope with the challenges of low temperature environments for their survival and successful colonization (Margesin et al., 2002; Furhan, 2020). There are a lot of microorganisms reported that have the ability to adapt and even show best growth and survival in harsh conditions like low or absent oxygen, high salt concentration, less nutrient availability and oxidative stress which occurs due to low temperature environments (D'Amico et al., 2006; Yarzábal, 2016). Cold-loving microbes have adapted several different mechanisms such as production of high amounts of fatty acids, proteins and non-polar carotenoids for excess fluidity of membrane, possess cold adapted enzymes and containing cold acclimation proteins (caps), antifreeze

http://www.aloki.hu ● ISSN 1589 1623 (Print) ● ISSN 1785 0037 (Online)
DOI: http://dx.doi.org/10.15666/aeer/2003_20592076

proteins and cryoprotectants that enable them to surmount the adverse effects of low temperature (Morgan-Kiss et al., 2006; Collins and Margesin, 2019). In cold environment low availability of nutrients stimulate the microorganisms to release antimicrobial compounds which empower them to decrease the inter-species competition for nutrients (Yogabaanu et al., 2017; Artini et al., 2019). Such extraordinary characteristics of cold-adapted microorganisms have increased the possibility of using these as a novel source of industrially important antimicrobial compounds (Paun et al., 2021). This attracts the consideration of most scientists because these environments are not extensively explored and there is a maximum chance of novel species with capability of new antibiotics production (Bruntner et al., 2005; Núñez-Montero et al., 2019). A number of reports confirm antimicrobial compounds from cold environment but are mostly restricted to Polar Regions only (Rampelotto et al., 2016). As antibiotic resistance is becoming a worldwide problem, exploring extreme environments like glaciers for antibiotic producing bacteria is really significant.

Antimicrobial metabolites production by microorganisms depends upon availability of specific cultural conditions such as temperature, pH, incubation time, medium composition, carbon sources, nitrogen sources, salts etc. The primary objective of this research was to study the effect of different cultural conditions for maximum production of antimicrobial compounds from bacterial isolates of Passu glacier. There is limited information available concerning the antimicrobial metabolites from microorganisms inhabiting glaciers and rarely from Karakoram mountain range. Thus, in this study, bacterial strains isolated from Passu glacier, were evaluated for antimicrobial compounds production. To investigate such kind of unexplored habitat, for the microorganisms with the ability to produce novel antimicrobial metabolites, is an important need of the time.

Materials and methods

Test organisms

ATCC strains such as *Escherichia coli* (ATCC 25922), *Salmonella enterica* (ATCC 14028), *Bacillus subtilis* (ATCC 6633), *Staphylococcus aureus* (ATCC 25923), *Pseudomonas aeruginosa* (ATCC 27853), and *Staphylococcus epidermidis* (ATCC 12228) were used as test organisms in the current study. Similarly, clinical isolates of *Escherichia coli, Psuedomonas aeruginosa, Staphylococcus aureus, Salmonella enterica, Candida albicans* and *Candida krusei* (collected from Pakistan Institute of Medical Sciences hospital) were also used as test organisms.

Screening of isolates for antimicrobial activity

A total of 28 bacterial isolates from Passu glacier with antibiotic activity were available at Applied Environmental and Geomicrobiology Lab, Quaid-i-Azam University, Islamabad. Out of these, 11 isolates (HTP9, HTP12, HTP13, HTP14, HTP19, HTP27, HTP36, HTP37, HTP38, LTP8 and LTP10) were selected on basis of their high antimicrobial activity. Spot-on-lawn and agar well diffusion assays were used for the confirmation of their antimicrobial potential.

Spot-on-lawn method

This method was used for screening of antibacterial compound producing bacterial isolates against ATCC bacterial strains. Sterile normal saline was used for the preparation of

http://www.aloki.hu ● ISSN 1589 1623 (Print) ● ISSN 1785 0037 (Online)
DOI: http://dx.doi.org/10.15666/aeer/2003_20592076

inoculum of test strains using 0.5 McFarland standards. Bacterial cells suspensions in normal saline was dipped by sterile cotton swab and streaked uniformly over the plate surface containing Mueller-Hinton agar (MHA) to pledge uniform circulation of the inoculum. The plates were left undisturbed for one hour in the laminar flow hood and the bacterial cultures were spotted on MHA plates inoculated with test microorganisms. The plates were kept at 15°C for 3 days and then at 37°C for 24 hours. The appearance of clear zone of inhibition around spots of isolated strains verified the antibacterial activity.

Agar well diffusion assay

Isolates HTP12, HTP13, HTP36 and LTP10 were selected on the basis of their best antimicrobial activity as shown by spot-on-lawn method. These isolates were inoculated in Luria-Bertani broth and incubated at 15ºC for 7 days. After every 24 hrs, samples were taken from the broth and subjected to centrifugation. The agar well diffusion assay was used for analysis of the cell free supernatant, so obtained (Hwanhlem et al., 2017).

Identification of isolates

DNA extraction

The DNA of isolated strains was extracted chemically by phenol-chloroform method (Wright et al., 2017). Gel electrophoresis confirmed the extraction of DNA.

Polymerase chain reaction

The samples of isolated DNA were then amplified by polymerase chain reaction using 16SrRNA primer. Primary denaturation temperature was 96°C for 5 minutes followed by 32 cycles of denaturation, annealing and extension. The temperatures for denaturation, annealing and extension were 94°C for 2 minutes, 55°C for 1 minute and 72°C for 1.5 minutes respectively. The final extension was carried out at 72°C for 10 minutes.

Phylogenetic analysis

ClustalW program executed in MEGA 4.0 was used to study Phylogenetic analysis of isolates (Mahtab et al., 2019). The phylogenetic analysis revealed the sequences of DNA and the analogous sequences were downloaded from National Center for Biotechnology Information (NCBI). After aligning all the sequences, Neighbor Joining method in MEGA4.0 was used for creating phylogenetic tree. The significance of the created tree was studied by Bootstrap analysis (1000 replicate).

Optimum growth conditions of isolates

Effect of incubation period on growth

The isolated strains were incubated in Luria-Bertani broth at 15°C for 6 days to determine their optimum incubation period by taking their absorbance (OD) at 600 nm after every 24 hours using UV/Visible spectrophotometer.

Effect of temperature on growth

The isolated strains were grown at different temperatures in Luria-Bertani broth (i.e., 5, 15, 25 and 35°C) to determine their optimum growth temperature by taking their absorbance (OD) after every 24 hours using UV/Visible spectrophotometer.

http://www.aloki.hu ● ISSN 1589 1623 (Print) ● ISSN 1785 0037 (Online)
DOI: http://dx.doi.org/10.15666/aeer/2003_20592076

Effect of pH on growth

The isolated strains were incubated at different pH (i.e., pH 5.0, 7.0 and 9.0) to determine their optimum growth pH by taking their absorbance (OD) at 600 nm after every 24 hours using UV/Visible spectrophotometer.

Optimization of antimicrobial activity

Luria-Bertani broth was used for preparation of inoculum and incubated at 15ºC. After every 24 hrs, samples were taken from the broth for a total of 120 hours. The production of antimicrobial compounds in culture medium was determined by agar well diffusion assay (Hwanhlem et al., 2017). The antimicrobial activity of the four isolates were determined in three parallel experiments.

Incubation time

The incubation time effect on antimicrobial compound production was confirmed by taking samples after every 24 hours for 120 hours.

Incubation temperature

The optimum antibiotic production by selected isolates was studied at different temperatures i.e. 5, 15, 25 and 35ºC.

Incubation pH

The antibiotic activity of the selected isolates was determined at different pH values i.e., 4.0, 5.0 and 9.0.

Medium selection

To determine the optimum production of antibacterial compounds by selected isolates, Nutrient broth (NB), Tryptic soya broth (TSB) and Luria Bertani (LB) broth were used as culture media.

Effect of carbon sources

To evaluate the carbon source effect on the production of antimicrobial metabolites, the selected isolates were grown in Luria-Bertani media containing additional glucose and starch in 1 and 2% concentration.

Effect of nitrogen sources

Luria-Bertani broth containing additional tryptophan, threonine, L-leucine, arginine and yeast extract in 1% concentration was used to evaluate the effect of nitrogen sources on the production of antimicrobial metabolites.

Effect of salts

To determine the effect of salts on the production of antimicrobial compounds, the selected isolates were inoculated in Luria-Bertani media containing additional NaCl (2 and 3%) and KCl (1 and 2%).

http://www.aloki.hu ● ISSN 1589 1623 (Print) ● ISSN 1785 0037 (Online)
DOI: http://dx.doi.org/10.15666/aeer/2003_20592076

Antibacterial and antifungal activity against clinical isolates

Alcaligenes pakistanensis (LTP10) was found to be the best antimicrobial compounds producer and was inoculated in Luria-bertani broth and incubated at 25ºC at pH 7 for 96 hours. After 96 hours, the antibacterial and antifungal activity of cell free supernatant of *Alcaligenes pakistanensis* (LTP10) was evaluated against clinical isolates of *Staphylococcus aureus, Escherichia coli, Pseudomonas aeruginosa, Salmonella enterica, Candida albicans* and *Candida krusei,* that were collected from Pakistan Institute of Medical Sciences hospital (PIMS), by agar well diffusion technique.

Antibiotic sensitivity test of isolates

Antibiotics sensitivity of selected isolates *Alcaligenes faecalis* (HTP12)*, Pseudochrobactrum saccharolyticum* (HTP13)*, Alcaligenes pakistanensis* (HTP36) and *Alcaligenes pakistanensis* (LTP10) against various available antibiotics discs in the market was analyzed by Kirby-Bauer disc diffusion method according to the guidelines of the CLSI (clinical and laboratory standards institute) 2013. The plates were transferred to incubator kept at 15°C for 72 hrs. Zone of inhibition was observed and noted after 24 hours of incubation.

Statistical analysis

The difference in activity at different culture conditions was analyzed statistically by measuring their standard deviation and p-value. The p-value was calculated using T.Test in Microsoft Excel 365 to determine the statistical significance of the differences in zone of inhibition under different culture conditions.

Results

In the present study, a total of eleven bacterial isolates coded as HTP12, HTP13, HTP14, HTP19, HTP27, HTP36, HTP37, HTP38, LTP8 and LTP10 from Passu glacier were selected. On the basis of their antimicrobial activity, it was found that LTP10 showed better activity.

Screening of bacterial isolates for antimicrobial activity

The selected strains were screened for antagonistic activity by using spot-on-lawn and agar well diffusion assay against ATCC test strains. After 72 hrs of incubation, the antimicrobial activity was confirmed by the zone of inhibition around the spots of isolates as shown in *Table 1*.

Out of eleven isolated strains, four isolates HTP12, HTP13, HTP36 and LTP10 showed maximum zone of inhibition against test strains. These 4 strains were again evaluated by agar well diffusion assay and their zone of inhibition was measured in mm as shown in *Fig. 1*.

Identification of isolates by phylogenetic analysis

The result of BLAST of total 4 strains show that there are 3 different strains having 90% or more than 90% identity with their respective specie. The isolated strains were identified as *Alcaligenes faecalis* (KF641844), *Pseudochrobactrum saccharolyticum* (KX977558) and *Alcaligenes pakistanensis* (AB968096) as shown in *Table 2 and Fig. 2*.

http://www.aloki.hu ● ISSN 1589 1623 (Print) ● ISSN 1785 0037 (Online)
DOI: http://dx.doi.org/10.15666/aeer/2003_20592076

Table 1. *Antimicrobial activity of isolates against ATCC bacterial strains by spot-on-lawn assay*

Isolates	*Staphylococcus aureus*	*Bacillus subtilis*	*Staphylococcus epidermidis*	*Escherichia coli*	*Pseudomonas aeruginosa*	*Salmonella enterica*
HTP9	+	-	-	+	-	-
HTP12	+++	++	+	++	++	+
HTP13	++	++	+	+	+	-
HTP14	++	++	+	+++	++	+
HTP19	++	-	+	+++	++	-
HTP27	-	++	-	-	-	+
HTP36	++	++	+	++	+++	-
HTP37	+	-	+	+	-	-
HTP38	+	-	-	++	-	+
LTP8	++	+++	++	++	+++	-
LTP10	+++	+++	++	++	++	++

Inhibition zone: +++ = strong (> 15 mm), ++ = moderate (10-15 mm), + = low (5-9 mm), - = no activity

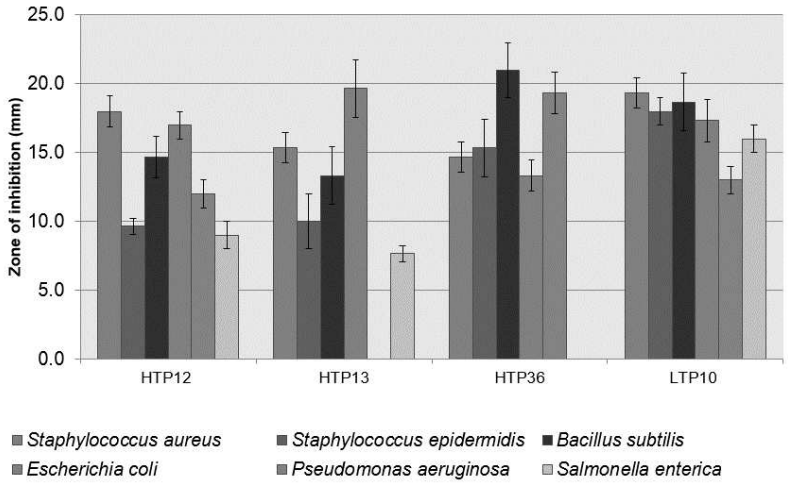

Figure 1. *Zone of inhibition (mm) of isolates against ATCC test strains by agar well diffusion assay after 72 hours. Error bars represent standard deviation (SD) of triplicate measurements of zone of inhibition (mm)*

Table 2. *Identification of isolates by their phylogenetic analysis*

Isolates	Homologous species	Groups	Identity %age
HTP 12	*Alcaligenes faecalis* (KF641844)	Proteobacteria Betaproteobacteria Burkholderiales Alcaligenaceae	99.80
HTP13	*Pseudochrobactrum saccharolyticum* (KX977558)	Proteobacteria Alpha Proteobacteria Rhizobiales Brucellaceae Pseudochrobactrum	99.02
HTP36	*Alcaligenes pakistanensis* (AB968096)	Proteobacteria Betaproteobacteria Burkholderiales Alcaligenaceae	100.00
LTP 10	*Alcaligenes pakistanensis* (AB968096)	Proteobacteria Betaproteobacteria Burkholderiales Alcaligenaceae	99.68

http://www.aloki.hu ● ISSN 1589 1623 (Print) ● ISSN 1785 0037 (Online)
DOI: http://dx.doi.org/10.15666/aeer/2003_20592076

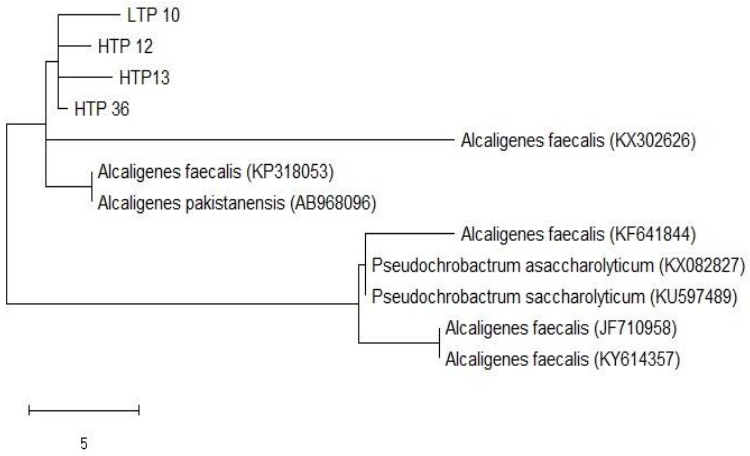

Figure 2. *Phylogenetic relation of study samples with other similar strains downloaded from NCBI*

Optimum growth conditions of isolates

The optimum incubation period for growth shown by selected isolates *Alcaligenes faecalis* (HTP12), *Pseudochrobactrum saccharolyticum* (HTP13), *Alcaligenes pakistanensis* (HTP36) and *Alcaligenes pakistanensis* (LTP10) was found to be 72 hours. The three isolates *Alcaligenes faecalis* (HTP12), *Pseudochrobactrum saccharolyticum* (HTP13), *Alcaligenes pakistanensis* (HTP36) revealed maximum growth at temperature of 25ºC and pH 7.0 while isolate *Alcaligenes pakistanensis* (LTP10) has shown maximum growth at 15 ºC and pH 7.0 as shown in *Figs. 3, 4, 5*.

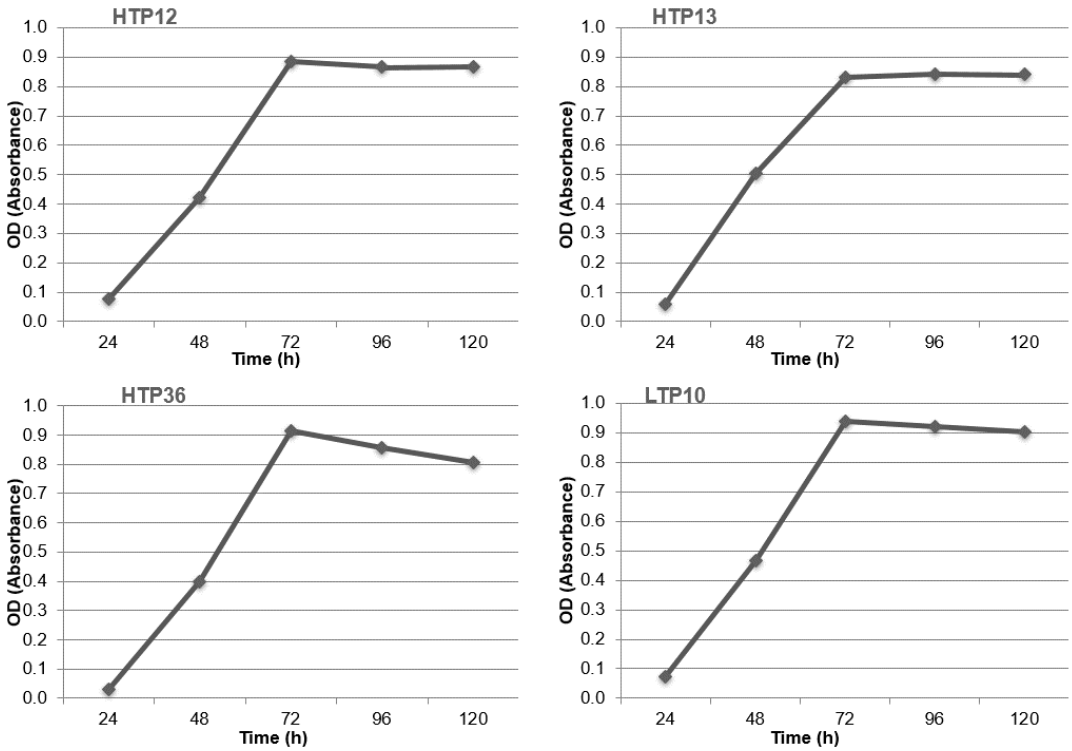

Figure 3. *Effect of incubation period on growth of isolates*

http://www.aloki.hu ● ISSN 1589 1623 (Print) ● ISSN 1785 0037 (Online)
DOI: http://dx.doi.org/10.15666/aeer/2003_20592076

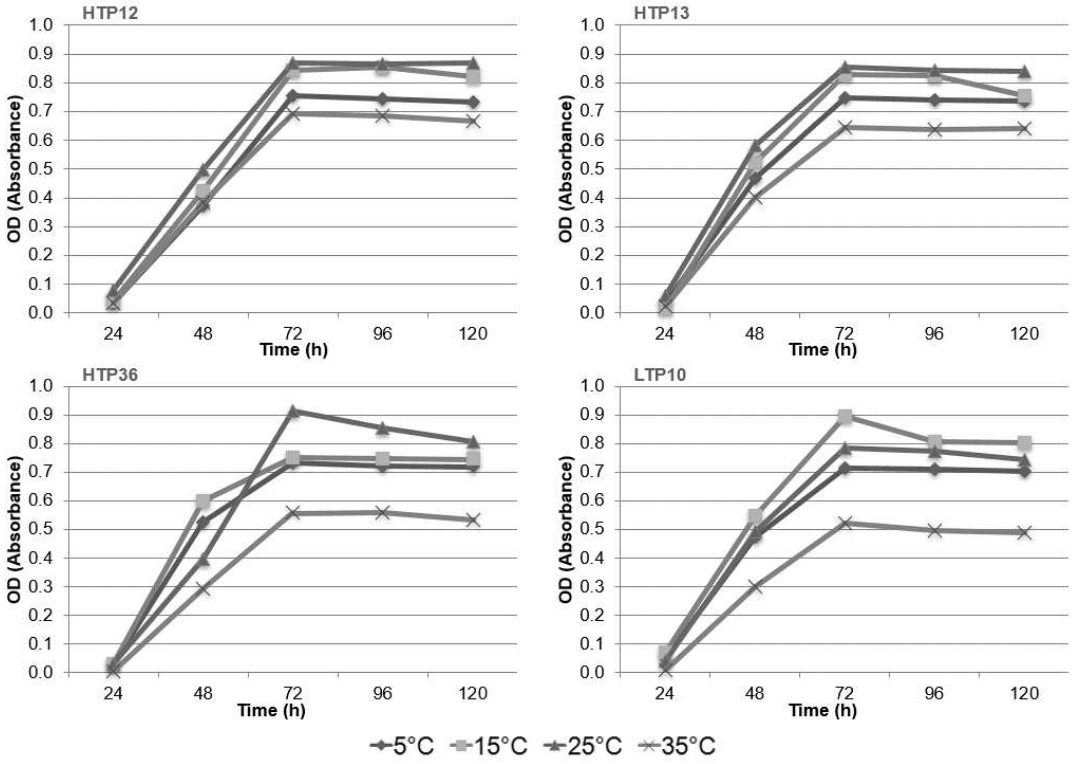

Figure 4. *Effect of temperature on growth of isolates*

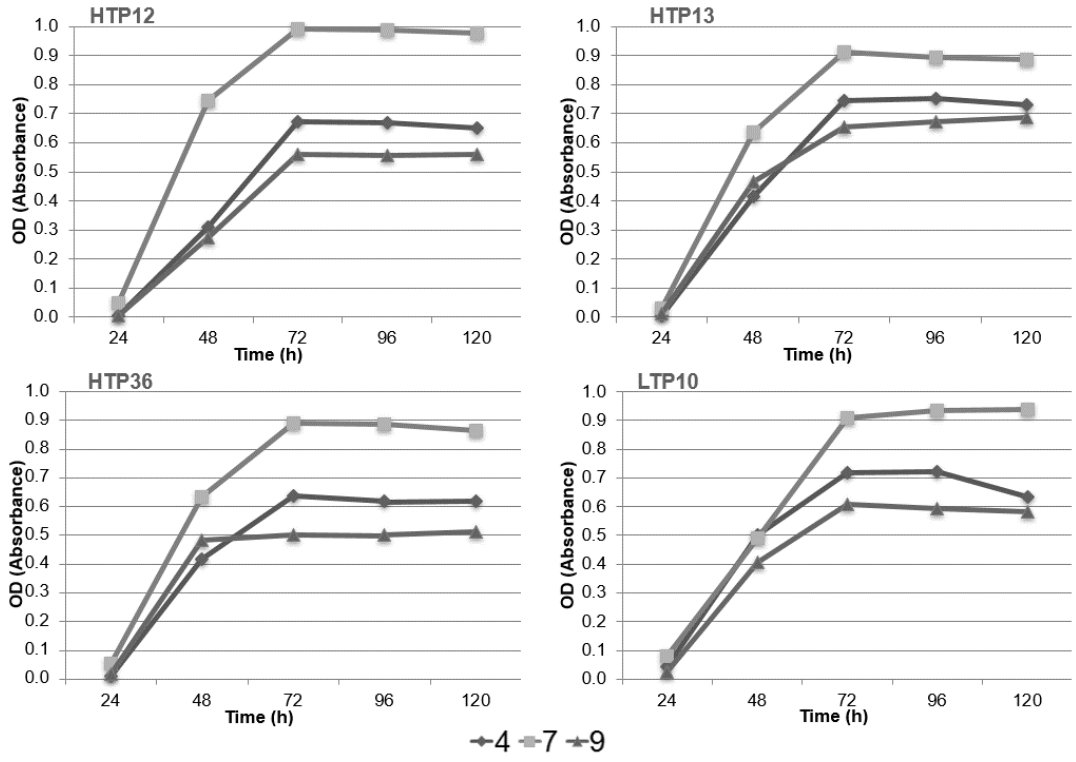

Figure 5. *Effect of pH on growth of isolates*

http://www.aloki.hu ● ISSN 1589 1623 (Print) ● ISSN 1785 0037 (Online)
DOI: http://dx.doi.org/10.15666/aeer/2003_20592076

Optimization of antimicrobial compound production

The production of antibacterial compounds by the isolated strains was confirmed by agar well diffusion assay. The best activity was shown by *Alcaligenes pakistanensis* (LTP10). Different cultural conditions like selection of growth media, incubation time, temperature, pH and addition of carbon sources, nitrogen sources and salts were considered.

Effect of time of incubation

All the four isolates have demonstrated maximum antimicrobial activity after 96 hours of incubation. The difference in antimicrobial activity at different incubation time was significant statistically ($P < 0.05$). The maximum antimicrobial activity of *Alcaligenes pakistanensis* (LTP10) and *Alcaligenes pakistanensis* (HTP36) was found against *Escherichia coli* (ATCC 25922) and *Bacillus subtilis* (ATCC 6633) respectively with 20±1 mm zone of inhibition as shown in *Fig. 6*.

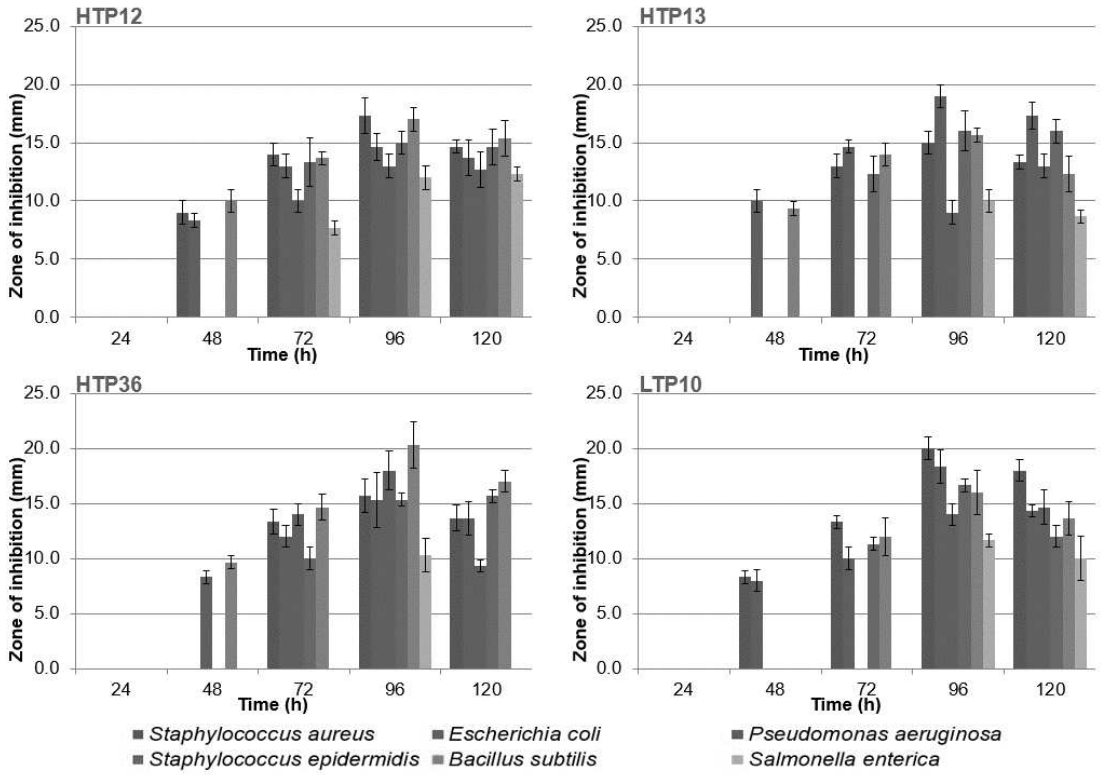

Figure 6. *Zone of inhibition (mm) of isolates against test strains at various incubation periods. Error bars represent standard deviation (SD) of triplicate measurements of zone of inhibition (mm). $P < 0.05$*

Effect of culture medium

Nutrient broth (NB), tryptic soya broth (TSB) and Luria-Bertani (LB) broth were used to evaluate maximum antimicrobial activity of selected isolates. The difference in antimicrobial activity of all the four isolates in different culture media was significant statistically ($P < 0.05$). The cell free supernatants of all the four isolates from Luria-

http://www.aloki.hu ● ISSN 1589 1623 (Print) ● ISSN 1785 0037 (Online)
DOI: http://dx.doi.org/10.15666/aeer/2003_20592076

bertani broth have confirmed maximum activity against test organisms. The best activity was shown by *Alcaligenes pakistanensis* (LTP10) against *Staphylococcus aureus* (ATCC 25923) and *Escherichia coli* (ATCC 25922) with zone of inhibition of 20.7±1.5 mm and 21±1 mm respectively as shown in *Fig. 7*.

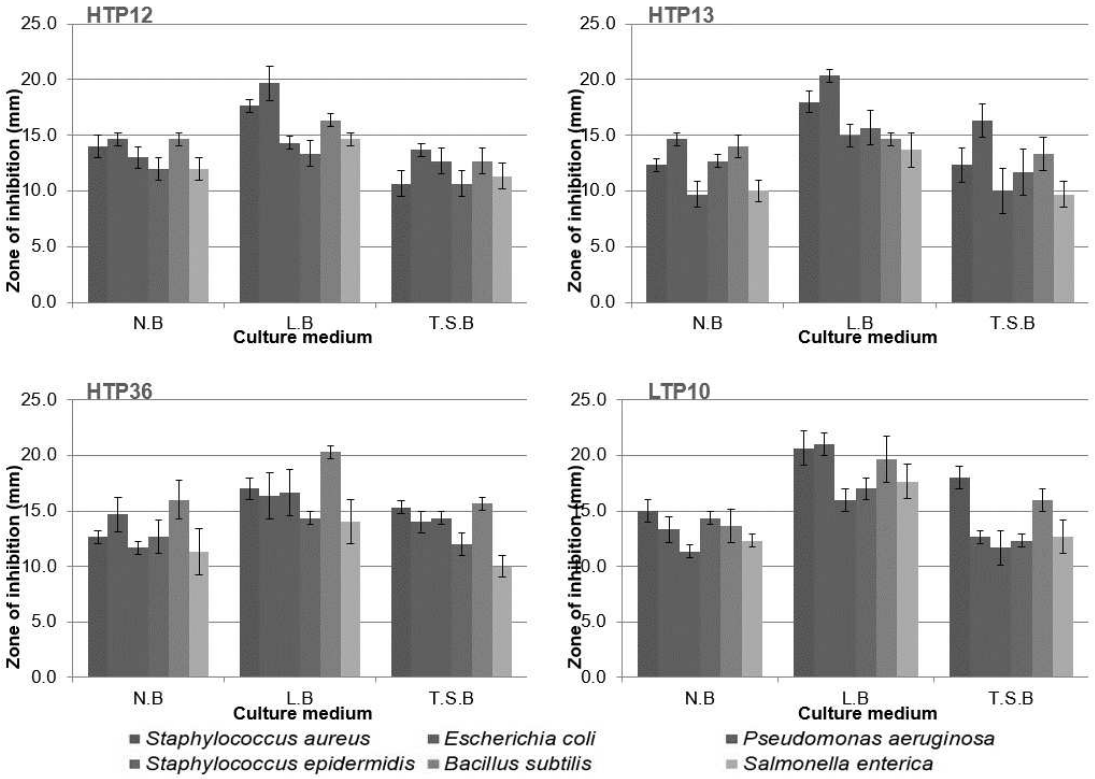

Figure 7. *Zone of inhibition (mm) of isolates against test strains in different culture media. Error bars represent standard deviation (SD) of triplicate measurements of zone of inhibition (mm). $P < 0.05$*

Effect of temperature

The difference in antimicrobial activity of all the four isolates at different temperature was significant statistically ($P < 0.05$). The isolated strains have shown maximum antimicrobial activity at 25°C after 96 hours of incubation in Luria-Bertani broth. The maximum zone of inhibition of 20.3±2.1 mm was shown by *Alcaligenes pakistanensis* (LTP10) against *Staphylococcus aureus* (ATCC 25923) as shown in *Fig. 8*.

Effect of pH

The difference in antimicrobial activity at different pH was significant statistically ($P < 0.05$). All the four isolates have confirmed maximum antimicrobial activity at pH 7. The maximum antimicrobial activity was shown by *Alcaligenes pakistanensis* (LTP10) against *Staphylococcus aureus* (ATCC 25923) with 23.3±0.6 mm zone of inhibition (*Fig. 9*).

http://www.aloki.hu ● ISSN 1589 1623 (Print) ● ISSN 1785 0037 (Online)
DOI: http://dx.doi.org/10.15666/aeer/2003_20592076

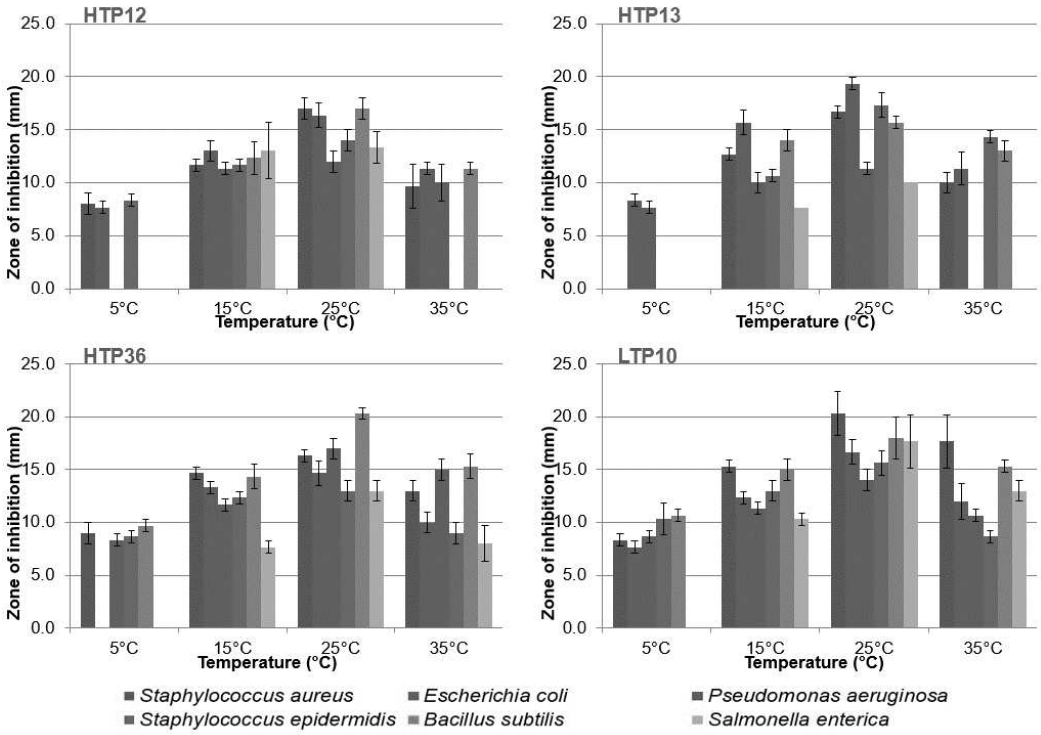

Figure 8. *Zone of inhibition (mm) of isolates against test strains at different temperatures. Error bars represent standard deviation (SD) of triplicate measurements of zone of inhibition (mm). $P < 0.05$*

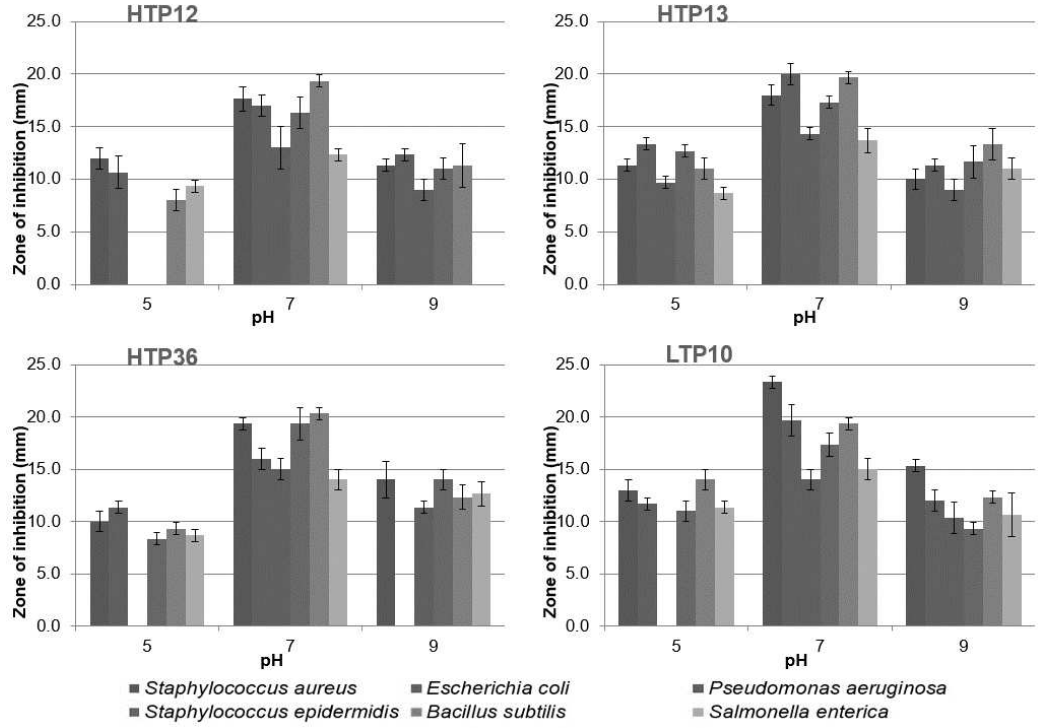

Figure 9. *Zone of inhibition (mm) of isolates against test strains at different pH. Error bars represent standard deviation (SD) of triplicate measurements of zone of inhibition (mm). $P < 0.05$*

http://www.aloki.hu ● ISSN 1589 1623 (Print) ● ISSN 1785 0037 (Online)
DOI: http://dx.doi.org/10.15666/aeer/2003_20592076

Effect of carbon sources

The addition of carbon sources to culture media found to have negative effect on the antimicrobial activity of isolated strains. The antibacterial activity in terms of zones of inhibition was decreased by 2 to 8 mm against *Staphylococcus aureus* (ATCC 25923) and *Escherichia coli* (ATCC 25922) by addition of glucose and starch in 1% and 2% concentrations as given *Table 3*.

Table 3. *Effect of carbon sources on antibiotic activity of isolates*

Isolates	Zone of inhibition (Mean value in mm ± SD) of isolates in against *S. aureus* & *E. Coli*									
	Staphylococcus aureus					*Escherichia coli*				
	*Control	Glucose (1%)	Glucose (2%)	Starch (1%)	Starch (2%)	*Control	Glucose (1%)	Glucose (2%)	Starch (1%)	Starch (2%)
HTP12	15 ± 1.5	13 ± 1.3	10 ± 1.2	14 ± 0.6	13 ± 0.7	18 ± 1.5	13 ± 1.2	15 ± 0.5	15 ± 0.5	14 ± 1.0
HTP13	17 ± 2.0	14 ± 0.7	11 ± 1.5	15 ± 1.7	14 ± 1.8	20 ± 1.3	15 ± 2.0	16 ± 1.4	17 ± 0.3	16 ± 1.2
HTP36	16 ± 1.0	14 ± 0.6	12 ± 0.5	13 ± 1.3	13 ± 2.0	14 ± 0.5	12 ± 0.5	10 ± 1.5	14 ± 0.6	12 ± 0.8
LTP10	21 ± 1.3	16 ± 1.0	15 ± 0.3	15 ± 1.2	16 ± 1.0	21 ± 0.3	17 ± 0.8	16 ± 0.3	18 ± 0.4	13 ± 0.6

*Control = Isolate culture in Luria-Bertani broth

Effect of nitrogen sources

The addition of different nitrogen sources such as amino acids and yeast extract have varying effects on antimicrobial production of isolated strains. Tryptophan, threonine, L-leucine and arginine have decreased the antimicrobial activity of isolates while yeast extract has increased the activity. *Alcaligenes pakistanensis* (LTP10) has shown an increase of 3 mm against *Escherichia coli* (ATCC 25922) with addition of 1% yeast extract. Similarly, antimicrobial activity of *Alcaligenes pakistanensis* (HTP36) against *Staphylococcus aureus* (ATCC 25923) was increased by 2 mm after addition of 1% yeast extract as given in *Table 4*.

Table 4. *Effect of nitrogen sources on antibiotic activity of isolates*

Isolates	Zone of inhibition (Mean value in mm ± SD) of isolates in against *S. aureus* & *E. Coli*					
	Staphylococcus aureus					
	**Control	*Trp	*Thr	*Leu	*Arg	*Y.E.
HTP12	16 ± 0.5	12 ± 1.5	--	11 ± 1.2	13 ± 0.7	16 ± 2.0
HTP13	17 ± 1.2	14 ± 0.5	13 ± 1.5	15 ± 0.6	--	16 ± 1.2
HTP36	18 ± 0.6	13 ± 0.6	14 ± 0.5	12 ± 0.8	10 ± 0.3	20 ± 0.3
LTP10	20 ± 0.3	14 ± 1.2	--	13 ± 1.1	16 ± 1.2	21 ± 0.6
	Escherichia coli					
HTP12	17 ± 1.2	--	15 ± 1.5	14 ± 0.5	10 ± 0.6	15 ± 1.3
HTP13	19 ± 0.5	16 ± 1.0	14 ± 1.5	--	--	21 ± 1.5
HTP36	15 ± 1.7	10 ± 0.5	--	13 ± 1.0	12 ± 0.3	16 ± 1.0
LTP10	19 ± 0.5	--	12 ± 0.5	--	16 ± 0.5	22 ± 1.7

*Trp = Tryptophan, Thr = threonine, Leu = L-leucine, Arg = Arginine, Y.E. = Yeast extract, **Control = Isolate culture in Luria-Bertani broth

http://www.aloki.hu ● ISSN 1589 1623 (Print) ● ISSN 1785 0037 (Online)
DOI: http://dx.doi.org/10.15666/aeer/2003_20592076

Effect of salts

Sodium chloride (2% and 3%) and potassium chloride (1% and 2%) were added to culture media separately. High concentration of salts in culture media resulted in lowering or diminishing the antimicrobial activity of isolates as given in *Table 5*.

Table 5. *Effect of salts on antibiotic activity of isolates*

Isolates	Zone of inhibition of isolates in (Mean value in mm ± SD) against *S. aureus* & *E. Coli*					
	Staphylococcus aureus			*Escherichia coli*		
	*Control	NaCl (2%)	NaCl (3%)	Control	KCl (1%)	KCl (2%)
HTP12	17 ± 0.4	13 ± 0.5	10 ± 0.6	15 ± 0.6	10 ± 0.7	--
HTP13	16 ± 0.3	12 ± 0.8	--	16 ± 1.3	12 ± 1.3	9 ± 0.3
HTP36	19 ± 1.3	12 ± 1.0	--	15 ± 0.5	11 ± 0.5	8 ± 0.6
LTP10	21 ± 1.6	15 ± 1.2	10 ± 1.3	20 ± 0.5	14 ± 1.7	--

*Control = Isolate culture in Luria-Bertani broth containing 1 % NaCl (w/v)

Antibacterial and antifungal activity of Alcaligenes pakistanensis against clinical isolates

The best antibiotic producer strain *Alcaligenes pakistanensis* (LTP10) was evaluated for its antimicrobial activity against clinical bacterial and fungal isolates. It was found that the cell free supernatant of culture medium of *Alcaligenes pakistanensis* (LTP10) after 96 hours of incubation at the optimized conditions has shown good activity against clinical isolates of *Staphylococcus aureus, Escherichia coli*, *Psuedomonas aeruginosa, Salmonella enterica* and *Candida albicans* while no activity was confirmed against *Candida krusei* as shown in *Fig. 10*.

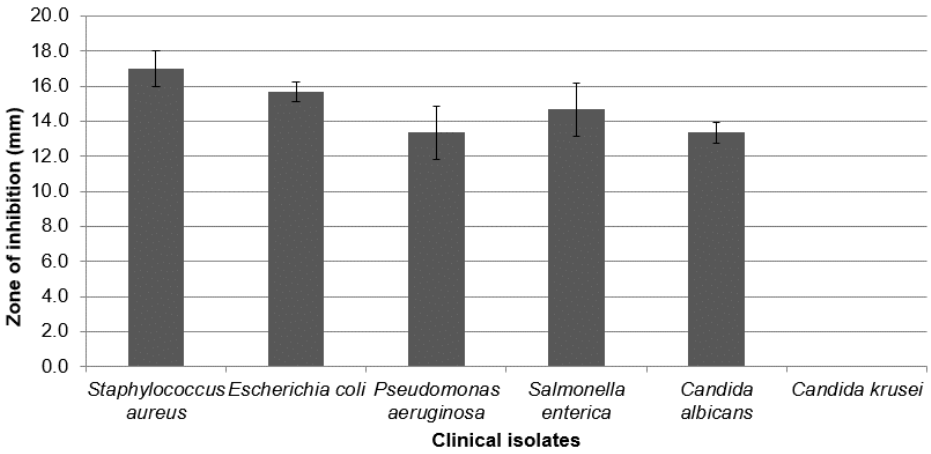

Figure 10. *Zone of inhibition (mm) of CFS of Alcaligenes pakistanensis (LTP10) against clinical isolates. The bars represent standard deviation (SD) of triplicate measurements of zone of inhibition (mm)*

Antibiotic sensitivity test of isolates

Antibiotic discs were used for testing sensitivity of isolated strains. The isolate *Alcaligenes pakistanensis* (LTP10) was resistant to penicillin, monobactams, cephalosporins, quinolones, metronidazole, carbapenem, macrolide, oxazolidinone and

http://www.aloki.hu ● ISSN 1589 1623 (Print) ● ISSN 1785 0037 (Online)
DOI: http://dx.doi.org/10.15666/aeer/2003_20592076

glycopeptide while sensitive to ceftaroline, imipenem, cefepime, meropenem, and ticarcillin as given in *Table 6*.

Table 6. *Sensitivity of selected isolates against antibiotic discs*

Isolated strains	Resistant to antibiotics	Sensitive to antibiotics
Alcaligenes faecalis HTP12	Penicillin G Cephalosporin Quinolones Monobactams Carbapenem Ertapenem	Ticarcillin Nalidixic acid Meropenem Piperacillin
Pseudochrobactrum saccharolyticum HTP13	Penicillin Macrolide Cephalosporins Quinolones Oxazolidinone Glycopeptide	Ceftaroline Imipenem Nalidixic acid Ertapenem Piperacillin
Alcaligenes pakistanensis HTP36	Penicillin Monobactams Cephalosporins Quinolones Metronidazole Macrolide Oxazolidinone Glycopeptide	Ceftaroline Imipenem Cefepime Meropenem Ticarcillin Carbapenem
Alcaligenes pakistanensis LTP10	Penicillin Monobactams Cephalosporins Quinolones Metronidazole Carbapenem Macrolide Oxazolidinone Glycopeptide	Ceftaroline Imipenem Cefepime Meropenem Ticarcillin

Discussion

Microbial secondary metabolites are the source of vital bioactive compounds which can be used for the cure of microbial diseases. However, main threat to clinical settings and hospitals is the emergence of multidrug resistant microorganisms (Dantas et al., 2008). That's why researcher and scientists have an increasing curiosity to discover novel antimicrobial compounds from unexplored area which can solve problem of drug resistance up to certain limit (Selvameenal et al., 2009). According to Sanchez et al. (2009) psychrophilic microorganisms are known as a possible source of novel antimicrobial metabolites.

http://www.aloki.hu ● ISSN 1589 1623 (Print) ● ISSN 1785 0037 (Online)
DOI: http://dx.doi.org/10.15666/aeer/2003_20592076

In the present work, the bacterial strains, having the ability to produce secondary metabolites isolated from Passu glaciers were monitored to produce antimicrobial metabolites by using agar well diffusion assay (Wefky et al., 2009; Abd-Elnaby et al., 2016). The reason for selecting isolates from Passu glacier was to find out antimicrobial metabolites producing microorganisms in that unexplored area. The temperature of that region is less than 0°C, and at such a low temperature, the microorganisms that are present are psychrophiles and psychrotrophs and suffer some harsh conditions such as nutrient deficiency, oxidative stress, high salt concentration, competition and stressful environment, which stimulate the genes responsible for the production of antimicrobial metabolites. Bruntner et al. (2005) reported a novel antibiotic Frigocyclinone produced by a *Streptomyces griseus* strain isolated from Antarctica. These antmicrobial metabolites help the producer organisms to compete and survive in such environment (Oyedele and Ogunbanwo, 2014).

A total of four bacterial isolates were selected among antibiotic producing isolates from Passu glacier. These isolates were coded as HTP12, HTP13, HTP36 and LTP10 and were identified as *Alcaligenes faecalis*, *Pseudochrobactrum saccharolyticum, Alcaligenes pakistanensis* and *Alcaligenes pakistanensis* respectively, through phylogenetic analysis. Among these bacterial strains, *Alcaligenes pakistanensis* (LTP10) showed greater activity and maximum zone of inhibition. *Alcaligenes faecalis* (HTP6) was found to be active against selected ATCC strains [*Staphylococcus aureus* (ATCC 25923) and *Pseudomonas aeruginosa* (ATCC 27853)] and various clinical isolates (*S. aureus*, *E. faecalis*, *Candida albicans* and *Aspergillus fumigatus*) (Rafiq et al., 2016). Fandi et al. (2014) reported antimicrobial activities in terms of zones of inhibition (mm) of some thermophiles, isolated from Jordan hot springs, against *Staphylococcus aureus*, *Bacillus subtilis, Escherichia coli* and fungal pathogenic strains.

The isolated strains were incubated at various pH, temperature and incubation periods in different culture media to determine optimum pH, temperature and incubation period for their growth. The selected strains were found to grow at low temperature of 5°C up to maximum of 35°C with maximum growth at 15-25°C in Luria-Bertani broth. These were grouped as psychrotrophs which are cold-loving organisms, having an optimal temperature for growth at above 15°C (Yuan et al., 2017). Margesin et al. (1994) reported that psychrophilic bacteria have shown best growth at around 15°C after 3 days of incubation. The isolates showed maximum growth at neutral pH 7 after 72 hours of incubation period. Heather and Vanderzant (1957) reported that psychrophiles showed maximum growth at environment having neutral pH and temperature around 15°C.

The production of secondary metabolites by microbes is dependent on different physical factors. In the current research work, the effect of different parameters such as pH, temperature, time of incubation and culture media were also considered for production of active metabolites. The maximum antibiotic production by isolates was noted at 25°C and pH 7 after 96 hours of incubation. There was decline in antimicrobials production as temperature increases and pH increases or decreases. Awais et al. (2007) and Gebreel et al. (2008) confirmed that bacitracin was produced by *Bacillus* sp. at temperature range of 25°C to 30°C and pH 7. Oyedele and Ogunbanwo (2014) reported that *Bacillus subtilis* showed maximum antagonistic activity after 96 hrs of incubation.

An important factor in designing of successful laboratory experiments is medium formulation. The components of culture media must contain the elements required for the growth and secondary metabolites production (Abd-Elnaby et al., 2016). The isolated strains were inoculated in LB broth along with extra sources of carbon such as glucose

http://www.aloki.hu ● ISSN 1589 1623 (Print) ● ISSN 1785 0037 (Online)
DOI: http://dx.doi.org/10.15666/aeer/2003_20592076

(1% and 2%) and starch (1% and 2%) separately and incubated for 96 hours at 25°C and pH 7. The cell free supernatant from culture broth of *Alcaligenes pakistanensis* (LTP10) with 1-2% glucose and starch has shown a decrease in zone of inhibition by 2-5 mm against *Staphylococcus aureus* and *Escherichia coli*. The effect of nitrogen sources was also studied on the antibiotic production of isolates. Nitrogen sources such as tryptophan, threonine, L-leucine, arginine and yeast extract were added separately to LB broth which was inoculated with isolates and incubated for 96 hours at 25°C and pH 7. The activity of *Alcaligenes pakistanensis* (LTP10) incubated in LB broth with 1 % yeast extract was increased by 3 mm against *Escherichia coli* while that of *Alcaligenes pakistanensis* HTP36 increased by 2 mm against *Staphylococcus aureus*. Rinker and Kelly (2000) reported the effects of different sources of carbon and nitrogen on the growth and production of antimicrobial metabolites by *Thermococcus* sp.

The isolates used in this study have shown resistance to a number of antibiotic classes. *Alcaligenes pakistanensis* (LTP10) was resistant to greater number of antibiotics. To protect themselves from their own antibiotics, antibiotic producing bacteria restrain different complicated mechanisms. The major mechanisms of self-defense in antibiotic producing microorganisms include antibiotic modification, antibiotic target modification, antibiotic efflux, antibiotic target bypass, antibiotic target protection and antibiotic sequestration by special proteins (Peterson and Kaur, 2018). An interesting fact is that the genes responsible for self-resistance are nearly all the time crowded together with the genes for biosynthesis of antibiotics, and their expression is co-regulated (Mak et al., 2014). Thus resistance to a number of antibiotics by *Alcaligenes pakistanensis* (LTP10) ensures its greater potential of antibiotic production.

Conclusion

This research work was designed to search for microorganisms from Passu glacier capable of producing antimicrobial metabolites and optimizing conditions for maximum antimicrobial compound production by isolates. The findings of this study recommends that the antimicrobial compounds produced by the isolates of Passu glaciers should be characterized and identified by analytical techniques like HPLC, LCMS and NMR in order to find their nature. It is also recommended that extreme environments like glaciers, deep seas, oceans, deserts, hot springs, marine environments etc should be explored to find out microorganisms having the ability to produce novel antimicrobial compounds.

REFERENCES

[1] Abd-Elnaby, H., Abo-elala, G., Abdel-raouf, U., Abd-elwahab, A., Hamed, M. (2016): Antibacterial and anticancer activity of marine *Streptomyces parvus*: optimization and application. – Biotechnology & Biotechnological Equipment 30: 180-191.

[2] Artini, M., Papa, R., Vrenna, R., Lauro, C., Ricciardelli, A., Casillo, A., Corsaro, M. M., Tutino, M. L., Parrilli, E., Selan, L. (2019): Cold-adapted bacterial extracts as a source of anti-infective and antimicrobial compounds against *Staphylococcus aureus*. – Future Microbiology 14(16): 1369-1382.

[3] Awais, M., Shah, A. A., Hameed, A., Hasan, F. (2007): Isolation, identification and optimization of bacitracin produced by *Bacillus* sp. – Pakistan Journal of Botany 39(4): 1303.

http://www.aloki.hu ● ISSN 1589 1623 (Print) ● ISSN 1785 0037 (Online)
DOI: http://dx.doi.org/10.15666/aeer/2003_20592076

[4] Bruntner, C., Binder, T., Pathom-Aree, W. (2005): Frigocyclinone, a novel angucyclinone antibiotic produced by a *Streptomyces griseus* strain from Antarctica. – Journal of Antibiotics 58: 346-349.
[5] Collins, T., Margesin, R. (2019): Psychrophilic lifestyles: mechanisms of adaptation and biotechnological tools. – Applied Microbiology and Biotechnology 103: 2857-2871.
[6] D'Amico, S., Collins, T., Marx, J. C., Feller, G., Gerday, C. (2006): Psychrophilic microorganisms: challenges for life. – EMBO Reports 7: 385-389.
[7] Dantas, G., Sommer, M. O., Oluwasegun, R. D., Church, G. M. (2008): Bacteria subsisting on antibiotics. – Science 320: 100-103.
[8] Fandi, K., Al-Muaikel, N., Al-momani, F. (2014): Antimicrobial activities of some thermophiles isolated from Jordan hot springs. – International Journal of Chemical, Environmental and Biological Sciences 2(1): 57-60.
[9] Furhan, J. (2020): Adaptation, production, and biotechnological potential of cold-adapted proteases from psychrophiles and psychrotrophs: recent overview. – Journal of Genetic Engineering and Biotechnology 18: 36.
[10] Gebreel, H. M., El-Mehalawy, A. A., El-Kholy, I. M., Rifaat, H. M., Humid, A. A. (2008): Antimicrobial activities of certain bacteria isolated from Egyptian soil against pathogenic fungi. – Research Journal of Agriculture and Biological Sciences 4(4): 331-339.
[11] Heather, C., Vanderzant, C. (1957): Effects of temperature and time of incubating and pH of plating medium on enumerating heat-treated psychrophilic bacteria. – Journal of Dairy Science 40: 1079-1086.
[12] Hwanhlem, N., Ivanova, T., Haertlé, T., Jaffrès, E., Dousset, X. (2017): Inhibition of food-spoilage and foodborne pathogenic bacteria by a nisin Z-producing Lactococcus lactis subsp. lactis KT2W2L. – LWT - Food Science and Technology 82: 170-175.
[13] Mahtab, M., Khan, F., Azama, M., Rizvi, M., Sultana, A., Shuklaa, I., Almatroudi, A. (2019): Molecular characterization and phylogenetic analysis of human pathogenic Leptospira species circulating in a tertiary care hospital of Western Uttar Pradesh in India. – Pathogens and Global Health 113(6): 275-281.
[14] Mak, S., Xu, Y., Nodwell, J. R. (2014): The expression of antibiotic resistance genes in antibiotic-producing bacteria. – Molecular Microbiology 93: 391-402.
[15] Margesin, R., Schinner, F. (1994): Properties of cold-adapted microorganisms and their potential role in biotechnology. – Journal of Biotechnology 33: 1-14.
[16] Margesin, R., Feller, G., Gerday, C., Russell, N. J. (2002): Cold-adapted microorganisms: adaptation strategies and biotechnological potential. – Encyclopedia of Environmental Microbiology 2: 871-885.
[17] Morgan-Kiss, R. M., Priscu, J. C., Pocock, T., Gudynaite-Savitch, L., Huner, N. P. (2006): Adaptation and acclimation of photosynthetic microorganisms to permanently cold environments. – Microbiology and Molecular Biology Reviews 70: 222-252.
[18] Núñez-Montero, K., Lamilla, C., Abanto, M., Maruyama, F., Jorquera, M. A., Santos, A., Martinez-Urtaza, J., Barrientos, L. (2019): Antarctic *Streptomyces fildesensis* So13.3 strain as a promising source for antimicrobials discovery. – Scientific Reports 9: 7488.
[19] Oyedele, A. O., Ogunbanwo, T. S. (2014): Antifungal activities of bacillus subtilis isolated from some condiments and soil. – African Journal of Microbiology Research 8: 1841-1849.
[20] Paun, V. I., Lavin, P., Chifiriuc, M. C., Purcarea, C. (2021): First report on antibiotic resistance and antimicrobial activity of bacterial isolates from 13,000-year old cave ice core. – Scientific Reports 11: 514.
[21] Peterson, E., Kaur, P. (2018): Antibiotic Resistance Mechanisms in Bacteria: Relationships Between Resistance Determinants of Antibiotic Producers, Environmental Bacteria, and Clinical Pathogens. – Frontiers in Microbiology 9: 1-21.
[22] Rafiq, M., Hayat, M., Hassan, N., Ibrar, M., Haleem, A., Rehman, M., Ahmad, F., Shah, A. A., Hasan, F. (2016): Characterization of antibacterial compounds produced by psychrotrophic *Alcaligenes faecalis* HTP6 isolated from Passu Glacier, Pakistan. – International Journal of Biosciences 8: 122-35.

http://www.aloki.hu ● ISSN 1589 1623 (Print) ● ISSN 1785 0037 (Online)
DOI: http://dx.doi.org/10.15666/aeer/2003_20592076

[23] Rampelotto, P. H. (2016): Biotechnology of extremophiles. – Springer, Brazil.
[24] Rinker, K. D., Kelly, R. M. (2000): Effect of carbon and nitrogen sources on growth dynamics and exopolysaccharide production for the hyperthermophilic archaeon *Thermococcus litoralis* and bacterium *Thermotoga maritima*. – Biotechnology and Bioengineering 69: 537-547.
[25] Sanchez, L. A., Gómez, F. F., Delgado, O. D. (2009): Cold-adapted microorganisms as a source of new antimicrobials. – Extremophiles 13: 111-120.
[26] Selvameenal, L., Radhakrishnan, M., Balagurunathan, R. (2009): Antibiotic pigment from desert soil actinomycetes; biological activity, purification and chemical screening. – Indian Journal of Pharmaceutical Sciences 71: 499.
[27] Wefky, S. H., Abou-Elela, G. M., El-Bestawy, E. (2009): Optimization of fermentation conditions for bioactive compounds production by marine bacterium *Enterococcus faecium*. – Journal of Applied Sciences Research 5(10): 1445-1454.
[28] Wright, M. H., Adelskov, J., Greene, A. C. (2017): Bacterial DNA Extraction Using Individual Enzymes and Phenol/Chloroform Separation. – Journal of Microbiology & Biology Education 18(2): 48.
[29] Yarzábal, L. A. (2016): Antarctic Psychrophilic Microorganisms and Biotechnology: History, Current Trends, Applications, and Challenges. – In: Castro-Sowinski, S. (ed.) Microbial Models: From Environmental to Industrial Sustainability. Microorganisms for Sustainability 1. Springer, Singapore.
[30] Yogabaanu, U., Weber, J. F., Convey, P., Rizman-Idid, M., Alias, S. A. (2017): Antimicrobial properties and the influence of temperature on secondary metabolite production in cold environment soil fungi. – Polar Science 14: 60-67.
[31] Yuan, L., Sadiq, F. A., Liu, T., Flint, S., Chen, J., Yang, H., Gu, J., Zhang, G., He, G. (2017): Psychrotrophic bacterial populations in Chinese raw dairy milk. – LWT 84: 409-418.

http://www.aloki.hu ● ISSN 1589 1623 (Print) ● ISSN 1785 0037 (Online)
DOI: http://dx.doi.org/10.15666/aeer/2003_20592076

TREE MORPHOLOGY, YIELD EFFICIENCY AND FRUIT QUALITY OF KINNOW MANDARIN (*CITRUS NOBILIS* LOUREIRO × *CITRUS DELICIOSA* TENORA) BUDDED ON DIFFERENT ROOTSTOCKS IN THE NORTH-WESTERN REGION OF INDIA

PANDEY, K.[1*] – RATTANPAL, H. S.[2] – SIDHU, G. S.[3] – SINGH, J.[2]

[1]*Division of Fruits & Horticultural Technology, ICAR-Indian Agricultural Research Institute, New Delhi, India*

[2]*Department of Fruit Science, Punjab Agricultural University, Ludhiana, India*

[3]*School of Agricultural Biotechnology, Punjab Agricultural University, Ludhiana, India*

[*]*Corresponding author*
e-mail: pandeykuldeephort@gmail.com

(Received 28th Feb 2021; accepted 14th May 2021)

Abstract. This experiment aimed to evaluate the horticultural performance viz, tree morphology, yield efficiency and fruit quality of Kinnow mandarin budded on ten rootstocks in the north-western region of India. Results revealed, rootstocks had a significant effect on several variables. Differences among the rootstock girth were recorded during the sixth year after planting (YAP) where the significantly highest values were found in Rough lemon and NRCC-6 however, the lowest value was present in NRCC-5. In the seventh year after planting, trees of Kinnow mandarin on all rootstocks produced similar yield efficiency. Trees on Carrizo citrange showed the highest fruit yield whereas, minimum fruit yield was observed on NRCC-4 during the sixth YAP. During seventh YAP, maximum influence on total soluble solids (TSS) content of Kinnow mandarin was recorded from the fruits obtained from trees on NRCC-1 and CRH-12, whereas fruits from trees on NRCC-3 had minimum soluble solids content. In both seasons, the maximum ascorbic acid content was recorded in fruits on CRH-12, whereas the minimum was observed from the fruits harvested from Carrizo citrange.
Keywords: *fruit yield, ascorbic acid, total soluble solids (TSS), Carrizo*

Introduction

Citrus is one of the most important fruit crops, grown throughout the tropical and sub-tropical regions of the world. India ranks fifth in global citrus production with an annual production of more than 13.2 million mt, which contributes 8.72% of the world's citrus production. In India, citrus cultivation is dominated by mandarins (*Citrus reticulata* Blanco), which contribute 40.76% of total citrus production. A North-western state of India, Punjab is the largest mandarin growing region, with a total production of 13.98 million tonnes from 1.1 million ha area (Anonymous, 2019). Kinnow mandarin (*C. nobilis* Lourerio × *C. deliciosa* Tenora) is the ruling citrus cultivar of Punjab and because of its better adaptability and high returns, Kinnow has replaced most of sweet oranges (Mosambi, Jaffa and Blood Red). With the popularization of Kinnow cultivation, it has now acquired the status of an independent citrus industry in Punjab (Aulakh et al., 2016).

Rough lemon (*C. jambhiri* Lush) rootstock has been commercially used for Kinnow mandarin in north-western region of India. Kinnow budded onto Rough lemon is generally vigorous in growth, produce higher yield, and having large fruit size with

http://www.aloki.hu ● ISSN 1589 1623 (Print) ● ISSN1785 0037 (Online)
DOI: http://dx.doi.org/10.15666/aeer/2003_20772093

thicker peel and poor fruit quality (Nasir et al., 2011). However, it is susceptible to *Phytophthora* (Lacey, 2012) and salinity (Dubey and Sharma, 2016), which has decreased the productive age of the orchards and is not suitable for wet and poorly drained soils. These drawbacks of Rough lemon are proving to be a limiting factor in preventing the progress of citrus industry of the region. The choice of rootstock is an important and permanent part of orchard, however soil and local climatic conditions are important factors in the selection of rootstocks too. Although any citrus variety can be used as rootstock but some of them are better suited to particular conditions than others (Davies and Albirgo, 1994). Rootstocks have ability to manipulate tree performance and longevity, since they typically regulate the level of tolerance to diseases like Tristeza and gummosis, roots penetration, adoption to soil pH, high salinity and alkalinity, excess soil moisture, nutrient uptake, tree stature, fruit yield, fruit quality and maturity (Soost and Cameron, 1975; Wutscher, 1979). Many researchers have reported that rootstocks impart more than twenty horticultural characteristics including leaf nutrient status, vigour and size, depth of rooting, low temperature tolerance, adoption to adverse soil conditions, disease resistance and fruit quality (Castel, 1987; Josan and Thatai, 2008; Singh et al., 2019). Although it has already been understood that stock and scion have a mutual effect upon one another, for the healthy development of a composite plant, there has to be a congenial relationship between them.

No rootstock is found suitable in all circumstances (Saini et al., 2020). There is a growing need to found a suitable rootstock for Kinnow mandarin to replace the Rough lemon. However, only limited information is available about concerned rootstocks effects on Kinnow mandarin performance. Therefore, this study aimed to evaluate the performance of Kinnow mandarin budded onto ten rootstocks in the north-western Indian region, in terms of tree characters, productivity and fruit characteristics.

Materials and Methods

Experimental site and planting material

The experiment was carried out in College Orchard of Department of Fruit Science, Punjab Agricultural University (PAU), Ludhiana, India (latitude 30° 53' N, longitude 75° 48' E; elevation 244 m). The soil was well drained and deep alluvial. Ludhiana features a humid subtropical under the Köppen climate classification, with average maximum and minimum temperatures of 35.8 °C and 2.7 °C, respectively, and an average annual rainfall of 630 mm and out of which 90% was received during rainy season (July to September) (Singh et al., 2020). The monthly mean temperature and, mean precipitation and mean relative humidity are presented from 2015 to 2017 period in *Fig. 1*.

Ten rootstocks *i.e*., Rough lemon (*C. jambhiri* Lush.), Carrizo citrange, CRH-12 [*C. sinensis* (L.) Osbeck × *Poncirus trifoliata* (L.) Raf], Volkamer lemon (*C. volkameriana* L.) NRCC-1, NRCC-2, NRCC-5 {*C. jambhiri* Lush × [*C. sinensis* (L.) Osbeck × *P. trifoliata* (L.) Raf]} and NRCC-3, NRCC-4, NRCC-6 [*C. jambhiri* Lush × *P. trifoliata* (L.) Raf] were evaluated when budded with Kinnow mandarin (*Fig. 2*).

The seeds of the rootstocks were sown (during September 2009) in polybags of size 7" × 12". To fill the polybags, potting material used was composed of one part of healthy soil, one-part sand, one-part cow dung manure and one-part coco peat. When the seedling attained pencil thickness, spring budding was performed during

http://www.aloki.hu ● ISSN 1589 1623 (Print) ● ISSN1785 0037 (Online)
DOI: http://dx.doi.org/10.15666/aeer/2003_20772093

February-March. Budded Kinnow plants were transplanted in field during September 2010 in rectangular system of planting spaced at 3 m × 6 m, following a randomized block design with three replications *i.e.*, tree on each rootstock. The plants were fertilized with 440-770 g nitrogen, 220-385 g phosphorus, and 40-80 kg farm yard manure per plant, as per package and practices of PAU, Ludhiana. Entire FYM was applied during the month of December, while nitrogen was applied in two split doses *i.e.*, February/March (before flowering) and April/May (after fruit set). However, phosphorus was applied along with first dose of nitrogen. Weed, pest and disease management were performed as per standard commercial practices. Other cultural operations were undertaken routinely. The study was carried out in two consecutive years *i.e.*, 2016-17 (sixth year after planting) and 2017-18 (seventh year after planting). All the recommended practices for Kinnow mandarin cultivation were given as per PAU recommendations.

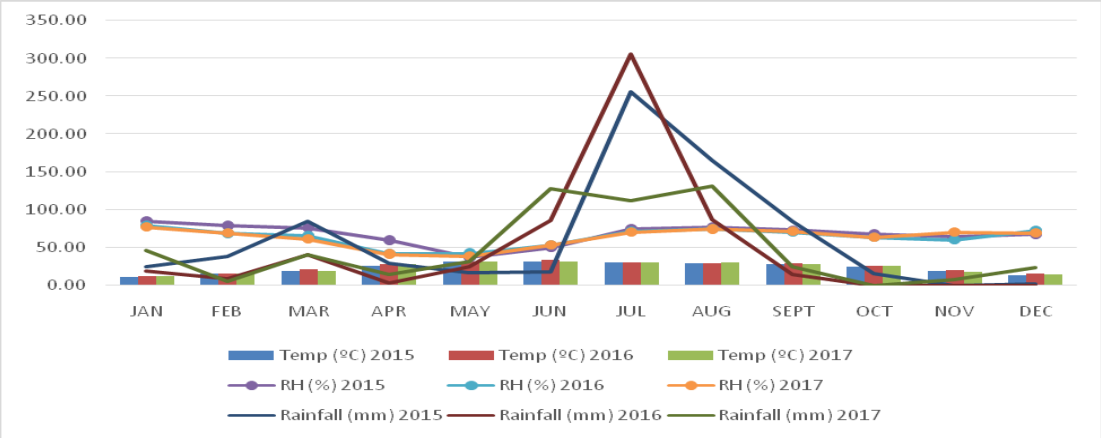

Figure 1. *Monthly mean temperature (°C), relative humidity (%) and precipitation (mm) of experimental site during 2015-2017*

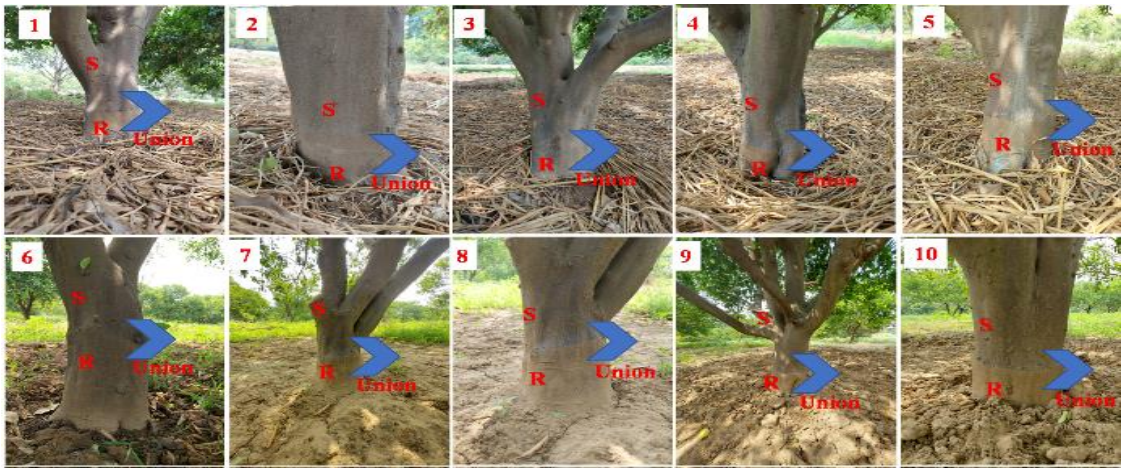

Figure 2. *S: Scion (Kinnow mandarin, R: Rootstock 1: Rough lemon, 2: Carrizo citrange, 3: CRH-12, 4: Volkamer lemon, 5: NRCC-1, 6: NRCC-2, 7: NRCC-5, 8: NRCC-3, 9: NRCC-4, 10: NRCC-6*

http://www.aloki.hu ● ISSN 1589 1623 (Print) ● ISSN1785 0037 (Online)
DOI: http://dx.doi.org/10.15666/aeer/2003_20772093

Growth parameters

All the growth factors were recoded once per year before flowering began. The circumference of scion and rootstock (10 cm above/below the bud union) was measured annually with the help of digital Vernier's Callipers (Mitutoyo Inc. Japan). Tree shape was assumed to be one - half of the prolate spheroid and the tree volume was calculated by following (Morse and Robertson, 1987) *Equation 1*:

$$\text{Tree Volume} = 0.524 \times \text{height} \times \text{width}^2 \quad \text{(Eq.1)}$$

Weight of harvested fruits per tree was recorded at harvest time and yield efficiency was calculated by the ratio of yield to tree volume.

Fruit quality parameters

Ten representative fruits per replication were randomly selected from all the directions for determining the vegetative physio-chemical characteristics. Fruits were harvested from 10th to 20th January 2016-17 at the same time for same rootstock. Average fruit weight (g) of 20 mature fruits was determined by individual fruit weight. The fruit yield was determined by multiplying the average weight of the fruit to number of fruits per plant. Fruit height (cm), width (cm), rind thickness (mm) and pedicel thickness (mm) were measured with the help of digital Vernier's Callipers (Mitutoyo Inc. Japan). Fruit rind and flesh colour was assessed by using Color Flex meter (Hunter Lab Color Flex, Hunter Associates Inc., Reston, VA, USA) (Hunter and Harold, 1987) for estimation of 'L' 'a' 'b' values and results were expressed as a citrus color index using *Equation 2*:

$$\text{Citrus color index (CCI= a}\times 1000/\text{L}\times\text{b)} \quad \text{(Eq.2)}$$

where a* indicates chromaticity on a green (−) to red (+) axis and b* indicates chromaticity on a blue (−) to yellow (+) axis; this index is widely used in the citrus industry as a maturation index (DOGV, 2006). CCI gives four types of values: negative value means dark green color, value around zero means green-yellow color, small positive value means yellow color and high positive value means red-orange color. The juice was extracted by rotatory extractor and the juice, peel and pulp were weighed and expressed as a percentage of the total fruit weight. The total soluble solid content (TSS) was measured using a digital refractometer (Hanna Instruments, Woonsocket, Rohde Island, USA) and expressed as °Brix. The titratable acidity was estimated by titrating 2.0 ml of fruit juice against N/10 sodium hydroxide (NaOH) solution using phenolphthalein as an indicator and then TSS/acid ratio was estimated. Ascorbic acid was determined by 2, 6-dichlorophenol indophenol method (AOAC, 2000) and results were expressed as mg ascorbic acid per 100 ml juice.

Statistical analysis

The data rootstock girth, scion girth, tree height, spread of the tree, tree volume, number of fruits per tree, fruit yield, yield efficiency, fruit weight, fruit length, fruit width, pedicel thickness, rind thickness, juice %, rind %, pulp %, total soluble solids, titratable acidity, TSS: acid ratio, ascorbic acid, rind Citrus Colour Index and flesh Citrus Colour Index were analyzed statistically with three replications via two-way

http://www.aloki.hu ● ISSN 1589 1623 (Print) ● ISSN1785 0037 (Online)
DOI: http://dx.doi.org/10.15666/aeer/2003_20772093

analysis of variance (ANOVA) using the SAS software (version 9.3 SAS institute Inc., Cary, NC USA) and differences among the means assessed by LSD test with a P value 0.05. Furthermore, the standardized traits mean values were pooled and used to investigate correlation.

Results and Discussions

Rootstock girth

Differences among the rootstock trunk girth are evident from *Table 1*, that in the sixth year after planting (YAP) Rough lemon (38.3 cm) and NRCC-6 (38.3 cm) were significantly the highest, while NRCC-5 (25.3 cm) was the lowest one. Carrizo citrange (36.3 cm) and CRH-12 (33.5 cm) were statistically at par. In the seventh YAP, maximum stock trunk girth was achieved by Carrizo citrange (41.7 cm) which was statistically at par with Volkamer lemon (41.4 cm), Rough lemon (41.3 cm) and NRCC-6 (41.1 cm) while minimum was recorded in NRCC-1 (31.5 cm). Similar findings have also been found on Marisol mandarin, where rootstock girth was maximum in Carrizo citrange and minimum in Cleoptara mandarin after fifth year of planting. Whereas, during sixth YAP all studied rootstocks were statistically at par, showing no significant differences among them (Bassal, 2009). Also, Chahal and Gill (2015) while evaluating six exotic sweet orange varieties, found that plants on Volkameriana rootstock yielded significantly higher stock girth than C-35 and Benton.

Table 1. *Effect of different rootstocks on tree growth parameters of Kinnow mandarin*

Rootstocks	Rootstock (cm)		Scion (cm)		Tree height (m)		Spread of the tree (m)		Canopy volume (m^3)	
	6th YAP	7th YAP	6th YAP	7th YAP	6th YAP	7th YAP	6th YAP	7th YAP	6th YAP	7th YAP
Carrizo	36.3^{abc}	41.7^{a}	30.9^{abc}	35.0^{a}	3.0^{a}	3.2^{bc}	2.9^{ab}	3.1^{abc}	11.8^{ab}	16.1^{ab}
CRH-12	33.5^{abc}	33.5^{bc}	28.1^{dbc}	28.1^{cd}	2.7^{a}	3.0^{bc}	2.6^{b}	2.9^{cd}	9.9^{b}	13.2^{bc}
NRCC-1	27.1^{de}	31.5^{c}	24.5^{d}	26.6^{d}	2.1^{b}	2.4^{d}	2.3^{c}	2.6^{e}	5.9^{c}	8.5^{d}
NRCC-2	31.8^{cd}	40.5^{a}	25.9^{cd}	34.7^{ab}	2.8^{a}	2.9^{bc}	2.9^{ab}	3.1^{abc}	12.5^{a}	14.6^{ab}
NRCC-3	31.7^{cd}	38.9^{ab}	25.2^{d}	32.1^{abc}	2.8^{a}	2.9^{bc}	2.8^{ab}	3.2^{ab}	11.6^{ab}	14.9^{ab}
NRCC-4	33.1^{bc}	38.9^{ab}	25.1^{d}	32.1^{abc}	3.0^{a}	3.0^{bc}	2.9^{ab}	3.1^{abc}	13.0^{a}	15.1^{ab}
NRCC-5	25.3^{e}	35.2^{abc}	19.3^{e}	30.0^{bcd}	2.7^{a}	2.7^{bc}	2.6^{b}	2.8^{de}	9.7^{b}	11.1^{cd}
NRCC-6	38.3^{a}	41.1^{a}	34.0^{a}	35.4^{a}	2.9^{a}	3.1^{bc}	2.9^{ab}	3.2^{ab}	12.4^{a}	16.6^{a}
Rough lemon	38.3^{a}	41.3^{a}	33.8^{a}	33.9^{ab}	2.8^{a}	2.9^{bc}	2.8^{ab}	3.3^{a}	11.4^{ab}	16.5^{a}
Volkamer lemon	37.3^{ab}	41.4^{a}	32.5^{ab}	33.5^{ab}	2.8^{a}	3.5^{a}	3.0^{a}	3.0^{bcd}	12.6^{a}	16.5^{a}
LSD (P≤ 0.05)	5.16	6.81	5.18	4.78	0.46	0.48	0.27	0.21	2.37	2.94

Note: In small letters the superscript shows significant difference at P<0.0

Scion girth

A significant variation in scion trunk girth was observed among different rootstocks (*Table 1*). In sixth YAP, maximum scion trunk girth was recorded on NRCC-6 (34.0 cm) rootstock followed by those on Rough lemon (33.8 cm) and it was minimum on NRCC-5 (19.3 cm). In the seventh YAP, trees budded on NRCC-6 (35.4 cm) and Carrizo (35.0 cm) had significant, maximum scion girth while trees on NRCC-1 (26.6 cm) showed minimum in this respect. Similar results were also obtained by De

http://www.aloki.hu ● ISSN 1589 1623 (Print) ● ISSN1785 0037 (Online)
DOI: http://dx.doi.org/10.15666/aeer/2003_20772093

Assis Alves Mourao Filho et al. (2007) who found that scion girth of Fallglo mandarin trees on Cleopatra mandarin was wider than that of trees on Swingle citrumelo. Contrarily, Chahal and Gill (2015) revealed that scion trunk girth of sweet oranges was not affected by rootstocks.

Tree height

Rootstocks had a significant effect on tree height, tree spread and canopy volume (*Table 1*). During sixth YAP, trees on NRCC-1 (2.1 m) had minimum height whereas, trees on NRCC-4 (3.0 m), Carrizo citrange (3.0 m), Rough lemon (2.8 m), NRCC-2 (2.8 m), NRCC-6 (2.8 m) Volkamer lemon (2.8 m), CRH-12 (2.7) and NRCC-5 (2.7 m) were statistically at par with each other. In the seventh YAP, trees budded on Volkamer lemon (3.5 m) and NRCC-1 (2.4 m) had maximum and minimum tree heights respectively. However, those budded on to Carrizo (3.2 m), NRCC-6 (3.1 m), CRH-12 (3.0 m), NRCC-4 (3.0 m), Rough lemon (2.9 m), NRCC-2 (2.9 m), NRCC-3 (2.9 m) were statistically similar to each other. According to studies of Georgiou (2000) trees budded on Estes rough lemon had lowest value of plant height whereas, highest canopy height was induced by Rough lemon although it was not significantly different from those induced by *C. taiwanica*, Swingle citrumelo, Yuma citrange and Carrizzo citrange. Furthermore, Tahiti lime budded on Catania 2 Volkamer lemon, Orlando tangelo, Morton citrange and Swingle citrumelo rootstock had maximum plant height in both experiments (irrigated & non-irrigated condition) (Espinoza-Nunez et al., 2011). Similar outcomes have been found in some of the earlier experiments (Hearn and Hutchison, 1997; Figueiredo et al., 2001; Stenzel et al., 2003; Garcia-Sanchez et al., 2006; de Assis Alves Mourao Filho et al., 2007). On the other hand, Sau et al. (2018) while working on Nagpur mandarin, disclosed that plant height was not affected by the different rootstocks.

Spread of the tree

In the sixth YAP, the trees budded onto Volkamer lemon (3.0 m) showed the highest values of spread of the tree, whereas, lowest value was recorded on NRCC-1 (2.3). Trees of Kinnow mandarin budded on Rough lemon (3.3 m) were significantly higher than those on NRCC-3 (3.2 m), Carrizo citrange (3.1), NRCC-2 (3.1 m) and NRCC-4 (3.1 m) whereas, trees on NRCC-1 (2.6 m) showed lowest value of spread of the tree during seventh YAP (*Table 1*). In similar studies, of Nova mandarin (Georgiou, 2000) and Clementine mandarin (Georgiou, 2002), was found that trees on Sour orange showed highest values of tree spread.

Canopy volume

The trees budded onto NRCC-4 (13.0 m^3), Volkamer lemon (12.6 m^3), NRCC-2 (12.5 m^3) and NRCC-6 (12.4 m^3) had the highest tree volume and did not significantly differ from each other whereas, trees on NRCC-1(5.9 m^3) had the lowest in this respect during the 6th YAP (*Table 1*). In the 7th YAP, highest canopy volume was recorded on NRCC-6 (16.6 m^3) and it was not significantly different from those budded on Rough lemon (16.5 m^3) and Volkamer lemon (16.5 m^3), while lowest tree volume was found on NRCC-1 (8.5 m^3) (*Table 1*).

In this aspect, Forner-Giner et al. (2003) disclosed that, canopy volume of Navelina orange trees was maximum on the 03017rootstock selection, without any substantial

http://www.aloki.hu ● ISSN 1589 1623 (Print) ● ISSN1785 0037 (Online)
DOI: http://dx.doi.org/10.15666/aeer/2003_20772093

differences especially in comparison to the Volkamer lemon, 030123 and 030146. In addition, Okitsu Satsuma mandarin on Sunki mandarin and Swingle citumelo rootstock produced maximum tree size and canopy volume (Tazima et al., 2013). While, smallest canopy of Valencia orange was measured on Cleopatra mandarin than other rootstocks (Zekri, 2000).

Number of fruits per tree

Number of fruits per tree were significantly affected by rootstocks (*Table 2*). Trees on NRCC-6, NRCC-4, Carrizo, NRCC-2, Rough lemon and Volkamer lemon had statistically similar number of fruits (496.1, 489.9, 489.3, 457.8, 455.3 and 405.8, respectively). However, lowest numbers were recorded on NRCC-5 (278.9) and CRH-12 (245.7) during first year of experiment. In the 7th YAP, highest numbers of fruits per tree were recorded on NRCC-6 (491.8), Carrizo citrange (491.6) and Rough lemon (483.4) whereas trees on NRCC-4 (211.3) had lowest number of fruits (*Table 2*). Results have similarity with the experiments of Sharma et al. (2000a) who reported that cumulative yield (number of fruits per tree) of seven seasons of Kinnow mandarin was found maximum on Jatti Khatti, followed by Karun Jamir and Estes rough lemon while, it was minimum on Cleopatra mandrain. Similar findings were also reported by Aulakh (1999) and Sharma et al. (2002a).

Table 2. *Effect of different rootstocks on fruit trait yield parameters of Kinnow mandarin*

Rootstocks	Number of fruits per tree		Fruit yield (kg/tree)		Yield efficiency (kg/m^3)		Fruit weight (g)		Fruit height (cm)		Fruit width (cm)	
	6th YAP	7th YAP	6th YAP	7th YAP	6th YAP	7th YAP	6th YAP	7th YAP	6th YAP	7th YAP	6th YAP	7th YAP
Carrizo	489.3^{a}	491.6^{a}	103.53^{a}	104.34^{a}	8.94^{a}	6.44^{a}	212.3^{abc}	211.1^{ab}	6.04^{bc}	6.00^{b}	7.40^{b}	7.33^{bc}
CRH-12	245.7^{c}	375.7^{cd}	53.56^{c}	80.67^{abc}	5.51^{e}	6.19^{a}	216.0^{ab}	217.0^{a}	6.13^{b}	6.09^{b}	7.25^{b}	7.21^{bc}
NRCC-1	293.5^{bc}	293.5^{de}	52.67^{c}	59.57^{cd}	8.87^{a}	7.15^{a}	179.2^{d}	202.2^{ab}	7.28^{a}	7.36^{a}	8.01^{a}	7.99^{a}
NRCC-2	457.8^{a}	477.4^{ab}	85.17^{ab}	83.57^{abc}	6.83^{cd}	5.77^{a}	185.8^{cd}	176.9^{c}	6.00^{bc}	5.96^{b}	7.20^{b}	7.26^{bc}
NRCC-3	390.8^{ab}	390.8^{bc}	83.83^{ab}	78.52^{abc}	7.30^{bcd}	5.30^{ab}	214.0^{ab}	201.2^{ab}	6.27^{b}	6.27^{b}	7.11^{b}	7.14^{bc}
NRCC-4	489.9^{a}	211.3^{e}	100.57^{a}	45.14^{d}	7.82^{bc}	3.09^{b}	206.5^{abc}	211.3^{ab}	5.87^{bc}	5.89^{b}	7.20^{b}	7.16^{bc}
NRCC-5	278.9^{c}	377.2^{cd}	63.68^{bc}	74.47^{bc}	6.69^{d}	6.8^{a}	229.8^{a}	196.4^{b}	5.15^{d}	6.08^{b}	7.24^{b}	7.33^{bc}
NRCC-6	496.1^{a}	491.8^{a}	103.25^{a}	98.55^{ab}	8.27^{ab}	6.04^{a}	206.8^{abc}	201.6^{ab}	5.61^{cd}	5.67^{b}	7.50^{b}	7.41^{b}
Rough lemon	455.3^{a}	483.4^{a}	90.69^{a}	96.96^{ab}	8.16^{ab}	5.94^{a}	201.3^{bcd}	198.6^{b}	5.95^{bc}	5.90^{b}	7.21^{b}	7.26^{bc}
Volkamer lemon	405.8^{a}	431.3^{abc}	83.11^{ab}	91.21^{ab}	6.63^{d}	5.56^{ab}	206.5^{abc}	210.2^{ab}	5.63^{cd}	5.67^{b}	7.10^{b}	7.05^{c}
LSD (P≤ 0.05)	108.27	91.75	23.66	28.60	1.04	2.54	27.23	16.89	0.49	0.64	0.50	0.33

Note: In small letters the superscript shows significant difference at P<0.

Fruit yield

Data in *Table 2* shows that rootstocks had significant effect on fruit yield (kg/tree) in both seasons, although trees on Carrizo citrange (103.53 kg) had maximum average fruit yield followed by NRCC-6 (103.25 kg), NRCC-4 (100.57 kg) and Rough lemon (90.69 kg) which were statistically at par with each other. Whereas, minimum fruit yield was recorded on NRCC-1 (52.67 kg) during the sixth YAP. On Carrizo citrange (104.34 kg), similar to the previous year, maximum fruit yield was produced in the

http://www.aloki.hu ● ISSN 1589 1623 (Print) ● ISSN1785 0037 (Online)
DOI: http://dx.doi.org/10.15666/aeer/2003_20772093

seventh YAP, and NRCC-4 (45.14 kg) reported minimum. The trees on NRCC-2 (83.57 kg), CRH-12 (80.67 kg) and NRCC-3 (78.52 kg) had similar yield and were in between. Present results show similarities where, common clementine trees on Carrizo citrange were most productive (Hussain et al., 2013).

Furthermore, Citrange rootstocks were found to have significant effect on fruit yield (Georgiou, 2000, 2002; Stenzel et al., 2003). On the contrary, fruit yield of Fallglo and Sunburst mandarin were not significantly affected by different rootstocks, from 2000 through 2006 (de Assis Alves Mourao Filho et al., 2007).

Yield efficiency

In the sixth YAP, yield efficiency was affected by different rootstocks (*Table 2*). Trees on Carrizo citrange (8.94 kg/m^3) produced highest yield efficiency followed by NRCC-1 (8.87 kg/m^3) which was significantly different from trees budded on NRCC-6 (8.27 kg/m^3) and Rough lemon (8.16 kg/m^3), whereas, lowest was produced on CRH-12 (5.51 kg/m^3) in this respect. In the seventh YAP, trees of Kinnow mandarin on all rootstocks produced similar yield efficiency, where the highest was produced on NRCC-1 (7.15 kg/m^3) while the lowest was on NRCC-4 (3.09 kg/m^3) (*Table 2*). Similar kind of findings reported by several researchers, worked on different mandarin varieties and reported that yield of these varieties was significantly affected by rootstocks (Georgiou, 2002; de Assis Alves Mourao Filho et al., 2007; Cantuarias-Aviles et al., 2010). In addition, Forner-Giner et al. (2003) reported that trees of Navelina orange on Cleoptara mandarin and Carrizo citrange had similar yield efficiency. In contrast, Georgiou and Gregoriou (1999) revealed that rootstocks did not bring significant variation in yield efficiency.

Fruit weight

During both the years of study, fruit weight was significantly affected by rootstocks (*Table 2*). Trees budded on NRCC-5 (229.8 gm) gave fruits with highest weight followed by CRH-12 (216.0 gm) and NRCC-3 (214.0 gm), which were significantly different from NRCC-1 (179.2 gm) that produced fruits with lowest weight during sixth YAP. In the seventh YAP, Kinnow fruit with maximum weight of 217.0 gm were produced on CRH-12, which was significantly higher than those on NRCC-4 (211.3 gm), Carrizo citrange (211.1 gm), Volkamer lemon (210.2 gm), NRCC-6 (201.6 gm) and NRCC-3 (201.2 gm). Lowest fruit weight was obtained from the fruits on NRCC-2 (176.9 gm). Sharma et al. (2002b) found that fruit weight of Campabell Valencia was significantly affected by rootstocks, where average fruit weight was maximum on Troyer closely followed by Carrizo citrange while the minimum was recorded on Jatti Khatti. Besides, heaviest fruits of Nagpur mandarin were harvested on Rough lemon rootstock (Sau et al., 2018). In contrast to this, fruits of Fallglo mandarin produced similar fruit weight on different rootstocks (de Assis Alves Mourao Filho et al., 2007).

Fruit height

Fruits of Kinnow mandarin produced on NRCC-1 (7.28 cm) rootstock, had significantly highest fruit height and fruits from the Carrizo citrange (6.04 cm), NRCC-2 (6.00 cm), Rough lemon (5.95 cm) and NRCC-4 (5.87 cm) were significantly at par. Fruits produced on NRCC-5 (5.15 cm) had lowest fruit height during first season

http://www.aloki.hu ● ISSN 1589 1623 (Print) ● ISSN1785 0037 (Online)
DOI: http://dx.doi.org/10.15666/aeer/2003_20772093

(*Table 2*). In the second season, rootstocks had no significant effect on the fruit height of Kinnow mandarin except on NRCC-1 rootstock.

Fruit width

In the 6th YAP, fruit width was not affected by rootstocks, whereas trees on NRCC-1 (8.01 cm) produced fruits with maximum fruit width. During second season, fruits of Kinnow mandarin with maximum fruit width were produced on NRCC-1 (7.99 cm) while, minimum fruit width (7.05 cm) was found on Volakmer lemon (*Table 2*). The above findings are in agreement with those recorded by Continella et al. (2018) who observed that Tarocco Scire sweet orange on Carpenter, Furr and F6P12 had largest fruit width and lowest was recorded on Swingle Citrumelo. Bassal (2009) reported that there was no significant effect of rootstocks on fruit width of Marisol clementine during both the season.

Pedicel thickness

The Kinnow fruits from the trees budded on different rootstocks showed significant variation with respect to pedicel thickness (*Table 3*). Fruits from the trees budded on NRCC-6 (3.75 mm) and NRCC-2 (3.69 mm) had highest pedicel thickness, whereas, fruits from the Volkamer lemon rootstock had lowest pedicel thickness, in both seasons.

Table 3. *Effect of different rootstocks on quality parameters of Kinnow mandarin*

Rootstocks	Pedicel thickness (mm)		Rind thickness (mm)		Juice (%)		Peel (%)		Pulp (%)	
	6th YAP	7th YAP	6th YAP	7th YAP	6th YAP	7th YAP	6th YAP	7th YAP	6th YAP	7th YAP
Carrizo	3.14^{cd}	3.20^{bcd}	3.14^{d}	3.28^{cd}	57.75^{a}	57.69^{a}	22.82^{d}	22.75^{f}	15.98^{bcd}	16.13^{bc}
CRH-12	3.45^{abc}	3.39^{abc}	3.39^{bcd}	3.48^{bcd}	48.45^{d}	48.31^{e}	24.03^{bc}	24.19^{ef}	15.01^{cde}	14.85^{cde}
NRCC-1	3.25^{bcd}	3.18^{bc}	3.61^{ab}	3.59^{abcd}	54.38^{ab}	54.78^{ab}	25.28^{bcd}	25.36	14.19^{efg}	14.34^{def}
NRCC-2	3.67^{a}	3.54^{a}	3.85^{a}	3.91^{a}	54.12^{abc}	54.04^{bc}	29.00^{a}	28.78^{a}	16.00^{bc}	15.91^{bc}
NRCC-3	3.13^{cd}	3.26^{abc}	3.34^{bcd}	3.40^{bcd}	54.49^{ab}	54.51^{ab}	24.95^{bcd}	25.00^{cde}	14.69^{def}	14.78^{cde}
NRCC-4	3.55^{ab}	3.47^{ab}	3.58^{abc}	3.62^{abc}	50.65^{bcd}	50.70^{cde}	26.51^{abc}	26.42^{bc}	13.58^{fg}	13.47^{ef}
NRCC-5	3.48^{abc}	3.35^{abc}	3.19^{cd}	3.27^{d}	52.69^{bcd}	52.54^{bcd}	25.69^{bcd}	25.79^{cde}	15.89^{bcd}	15.67^{bcd}
NRCC-6	3.75^{a}	3.52^{a}	3.75^{ab}	3.68^{ab}	53.00^{bc}	52.71^{bcd}	26.27^{abc}	26.19^{bcd}	13.11^{g}	13.06^{f}
Rough lemon	3.24^{bcd}	3.17^{dc}	3.66^{ab}	3.59^{abcd}	50.02^{cd}	49.37^{de}	27.79^{ab}	27.64^{ab}	17.45^{a}	17.97^{a}
Volkamer lemon	3.00^{d}	2.96^{d}	3.54^{abcd}	3.47^{bcd}	51.98^{bcd}	52.04^{bcd}	25.01^{bcd}	24.69^{de}	16.90^{ab}	16.83^{ab}
LSD (P≤ 0.05)	0.39	0.29	0.41	0.34	4.26	3.53	3.13	1.61	1.30	1.49

Note: In small letters the superscript shows significant difference at P<0.0

Rind thickness

It is an important factor responsible for the freshness of citrus fruits. Fruits with thick rind are low in juice whereas thin rind fruits are not suitable for storage and shipping Sharma et al. (2016). Data revealed that the rind thickness was significantly affected by the rootstocks (*Table 3*). Fruits obtained from the tree budded on NRCC-2 had highest rind thickness in both years, whereas, in 6th YAP, it was lowest on Carrizo citrange (3.14 mm). During next season, lowest rind thickness was recorded on NRCC-5 (3.27 mm) while, fruits on CRH-12 (3.48 mm), Volakamer lemon (3.47 mm) and

http://www.aloki.hu ● ISSN 1589 1623 (Print) ● ISSN1785 0037 (Online)
DOI: http://dx.doi.org/10.15666/aeer/2003_20772093

NRCC-3 (3.40 mm) were significantly to each other. Similarly, fruits of Allen Eureka showed the highest rind thickness on Macrophylla, Volkamer lemon and Rough lemon whereas, lowest rind thickness was observed on Cleoptara, Amblycarpa, Sour orange and Taiwanica rootstocks (Al-Jaleel et al., 2005). Rind thickness of Valencia and Navel orange, on Tawanica, Macrophylla and Rough lemon was recorded highest while, fruits with thinnest rind were collected from Cleoptara, Amblycarpa and sour orange rootstock (Zekri and Al-Jaleel, 2004). Likewise, Sharma et al. (2002c) found that fruits of Kinnow mandarin were thick peeled on Jatti Khatti (4.9 mm) and Karna Khatta (4.9 mm) rootstocks whereas, those on Troyer and Carrizo ctrange were thin peeled (4.6 mm).

Juice, peel and pulp content

Rootstocks significantly affect juice, rind and pulp content in the fruits (*Table 3*). Juice content varied from 57.75% to 48.45%. Fruits from trees on Carrizo citrange had maximum juice content whereas it was lowest from trees on CRH-12. Same trend was observed in both the years. Juice content of Tarocco Scire pigmented sweet orange was recorded maximum (52 %) on Bitters rootstock while it was recorded minimum (46%) on F6P12 (Continella et al., 2018). In another similar experiment, Folha Murcha mandarin budded on Cravo Limeira, FCAV trifoliate and Sunki mandarin had highest juice content whereas, it was lowest on Flying Dragon rootstock (Cantuarias-Aviles et al., 2010). In this context, Georgiou (2002) reported that fruits of Clementine mandarin on Swingle citrumelo rootstock, had significantly higher juice content and it significantly reduced on Volkamer lemon and Palestine sweet lime.

Regarding peel content, Kinnow mandarin fruits on Carrizo citrange (22.82% & 22.75%) had minimum peel percentage compared to those on Rough lemon (27.79% & 27.64%), NRCC-6 (26.27% & 26.19%) and NRCC-4 (26.51% & 26.42%). Fruits with maximum peel percentage were obtained from trees on NRCC-2 (29.00% & 28.78%) in both the years. Results showed concordance with a study conducted by Romero et al. (2006) who found that fruits of Clemenules mandarin on Cleoptara mandarin had lower peel percentage. Inverse to this, Bassal (2009) reported no significant differences in peel percentage due to rootstocks. Pulp content was recorded minimum in Kinnow fruits on NRCC-6 (13.11% & 13.06) and maximum content was recorded on Rough lemon (17.45% & 17.97%) rootstock in both seasons.

Total soluble solids

A perusal of the data in the *Table 4* reveals that TSS was significantly affected by different rootstocks. Kinnow fruits from trees on NRCC-1 (11.29) rootstock showed maximum soluble solids content, and it significantly differed from CRH-12 (11.21), NRCC-5 (10.88), Carrizo citrange (10.58) and NRCC-3 (9.58) and NRCC-6 (9.28) which showed the minimum value in the sixth YAP. Similarly, during seventh YAP, maximum soluble solid content was recorded from the fruits obtained from trees on NRCC-1 (11.30) and CRH-12 (10.93) whereas fruits from trees on NRCC-3 (9.07) had minimum total soluble solids content. AA118 Trifoliate orange and Holansis Trifoliate orange rootstocks induced high TSS in Clementine fruits whereas, Gou Tou sour orange and Da Hong Pao mandarin induced low TSS (Hussain et al., 2013). Likewise, fruits of Kinnow mandarin on Troyer citrange had maximum TSS while it was minimum on Jatti Khatti (Sharma et al., 2002c). Fruits of ‘Fremont’ tangerine and ‘Washington Navel’

http://www.aloki.hu ● ISSN 1589 1623 (Print) ● ISSN1785 0037 (Online)
DOI: http://dx.doi.org/10.15666/aeer/2003_20772093

recorded highest TSS on Carrizo citrange rootstock reported by Ali (2002) and Tuzcu et al. (2004), respectively.

Table 4. *Effect of different rootstocks on quality parameters of Kinnow mandarin*

Rootstocks	Total soluble solids (°Brix)		Titratable Acidity (%)		TSS: acid ratio		Ascorbic acid (mg/100ml juice)		Rind CCI (Citrus Color Index)		Flesh CCI (Citrus Color Index)	
	6th YAP	7th YAP	6th YAP	7th YAP	6th YAP	7th YAP	6th YAP	7th YAP	6th YAP	7th YAP	6th YAP	7th YAP
Carrizo	10.58^{abcd}	10.13^{bc}	0.98^{a}	0.91^{b}	10.80^{e}	11.46^{e}	20.85^{e}	20.64^{d}	10.38^{ab}	7.94^{ab}	5.08^{abc}	5.65^{a}
CRH-12	11.21^{ab}	10.93^{a}	1.00^{a}	1.09^{a}	11.23^{e}	9.96^{f}	25.01^{a}	24.86^{a}	8.83^{b}	8.38^{a}	5.95^{abc}	5.26^{a}
NRCC-1	11.29^{a}	11.30^{a}	1.01^{a}	0.92^{b}	11.17^{e}	12.38^{de}	20.88^{e}	20.64^{d}	9.10^{b}	8.01^{ab}	6.46^{abc}	5.92^{a}
NRCC-2	10.26^{cde}	10.07^{bc}	0.81^{b}	0.74^{cd}	12.68^{d}	13.29^{cd}	22.44^{bcde}	22.12^{bcd}	11.09^{a}	7.65^{abc}	5.87^{abc}	4.89^{a}
NRCC-3	9.58^{ef}	9.07^{d}	0.66^{c}	0.61^{e}	14.51^{ab}	14.97^{ab}	21.41^{de}	21.50^{cd}	10.04^{ab}	7.65^{abc}	5.74^{abc}	5.63^{a}
NRCC-4	10.29^{cde}	9.60^{cd}	0.79^{b}	0.78^{c}	13.02^{cd}	12.25^{e}	21.09^{e}	21.34^{cd}	10.07^{ab}	7.77^{abc}	5.65^{abc}	5.21^{a}
NRCC-5	10.88^{abc}	10.60^{ab}	0.79^{b}	0.75^{c}	13.78^{bc}	14.20^{bc}	23.69^{abc}	23.55^{ab}	10.64^{ab}	8.01^{ab}	4.32^{bc}	5.00^{a}
NRCC-6	9.28^{f}	9.67^{cd}	0.68^{c}	0.67^{de}	13.62^{c}	14.39^{b}	21.99^{dce}	22.09^{bcd}	9.85^{ab}	7.20^{bc}	4.11^{c}	4.59^{a}
Rough lemon	10.48^{bcd}	10.03^{bc}	0.71^{c}	0.67^{de}	14.76^{a}	15.07^{ab}	23.02^{bcd}	22.20^{bc}	9.76^{ab}	6.72^{c}	7.11^{a}	5.01^{a}
Volkamer lemon	10.02^{def}	9.73^{cd}	0.66^{c}	0.62^{e}	15.19^{a}	15.63^{a}	24.00^{ab}	23.78^{a}	9.30^{ab}	7.79^{abc}	5.22^{abc}	5.67^{a}
LSD (P≤ 0.05)	0.77	0.76	0.05	0.69	0.87	1.02	1.83	1.53	1.83	1.18	2.27	1.88

Note: In small letters the superscript shows significant difference at P<0.0

Titratable acidity

Titratable acidity (TA) of mandarins plays an important role in determining maturity and juice attributes. In this experiment, the accumulation of TA in fruits was significantly affected by rootstocks. In the first season, juice of fruits from tress on NRCC-1 (1.01), CRH-12 (1.00) and Carrizo citrange (0.98) had the highest TA and it was significantly different from those on NRCC-2 (0.81), Rough lemon (0.71), NRCC-3 (0.66) and Volkamer lemon (0.66). Acidity of the fruit juice from Kinnow trees on NRCC-3 (0.61) and Volkamer lemon (0.62) were significantly lower than those on NRCC-6 (0.67), Rough lemon (0.67) and NRCC-2 (0.74). The highest juice acidity was recorded for Kinnow fruits budded on CRH-12 (1.09) in the second season (*Table 4*). Continella et al. (2018) also found that fruits of Tarocco Scire pigmented sweet orange on Citrumelo produced highest titratable acidity. Fruits of Common clementine on Holansis Trifoliate orange and AA18 Trifoliate orange were more acidic whereas, on Carrizo citrange were comparatively less acidic (Hussain et al., 2013). Likewise, titratable acidity of Oneco mandarin was maximum on Flying Dragon Trifoliate orange while it was minimum on Volkamer lemon rootstock (Gonzatto et al., 2011).

TSS: acid ratio

TSS: acid ratio was significantly affected by rootstocks. Kinnow fruits produced from the trees on Volkamer lemon (15.19) and Rough lemon (14.76) gave highest value of TSS: acid ratio whereas it was recorded lowest on Carrizo citrange (10.80), CRH-12 (11.23) and NRCC-1 (11.17) during first year. In the second year, highest TSS: acid ratio was recorded from fruits which were obtained from trees on Volkamer lemon

http://www.aloki.hu ● ISSN 1589 1623 (Print) ● ISSN1785 0037 (Online)
DOI: http://dx.doi.org/10.15666/aeer/2003_20772093

(15.63) and it was significantly higher than those on Rough lemon (15.07), NRCC-3 (14.97), NRCC-6 (14.39) and NRCC-5 (14.20). However, fruits from trees on CRH-12 (9.96) gave the lowest value of TSS: acid ratio (*Table 4*). An analogous trend was observed by Georgiou (2002) where maximum TSS: acid ratio was recorded on sour orange rootstock and minimum TSS: acid ratio was on Palestine sweet lime. Similarly, Marisol clementine trees on sour orange produced fruits with low TSS: acid ratio whereas, the highest TSS: acid ratio was on Carrizo citrange (Bassal, 2009). One of the leading cause of variations in the quality attributes of most citrus fruits may be due to the unequal aggregation of TSS that may be a result of disparity of plant-water interactions for inherent differences in rootstock (Barry et al., 2004).

Ascorbic acid content and citrus colour index (CCI)

Data presented in *Table 4* shows significant variations in content of fruit ascorbic acid on different rootstocks. Maximum ascorbic acid content was recorded on CRH-12 (25.01 & 24.86), whereas fruits on Carrizo citrange (20.85 & 20.64) had lowest ascorbic acid content, in both seasons (*Table 4*). In this regard, Sau et al. (2018) on Nagpur mandarin and Demirkeser et al. (2005) on Rohde Red Valencia orange reported that the effects of rootstocks on ascorbic acid were not statistically significant. Color of the fruit is a deciding external factor for its quality and consumer acceptance. Kinnow trees budded onto NRCC-2 produced fruits with deepest orange peel colour during first year of experiment while fruits from CRH-12 rootstock produced orange color in second year. On the other hand, Rough lemon induced deepest orange colour in flesh whereas, in second year no significant variation was found among all the rootstocks. The above findings are in agreement with those obtained by Legua et al. (2011) on Lane Late navel orange, where they found out fruits on *C. macrophylla* and *C. volkameriana* had richest external colour and poorest on Gou Tou. In addition, Forner-Griner et al. (2003) also observed that Cleopatra mandarin induced lower colour index in Navelina oranges. Rootstock FA 418 had induced lower index of fruit color than other rootstocks (Forner-Giner et al., 2014).

Correlation coefficient

Simple coefficient correlation between tree and fruit morphology and biochemical factors of Kinnow mandarin were calculated and are presented in *Table 5*. Fruit weight showed significant negative correlation with the rind percent (r = -0.70) and rind thickness (r = -0.77). Fruit width showed positive correlation with fruit height (0.77) and yield efficiency (0.76), however, it was found negatively correlated with spread of the tree (r = -0.74) and tree volume (r = -0.75). The fruit height showed high positive correlation with flesh citrus colour index (r = - 0.68) and had negative correlation with spread of the tree (r = -0.69), tree volume (r = -0.75) and tree height (r = -0.79). Spread of the tree showed strong positive correlation with tree volume (r = 0.96) tree height (r = 0.82), rootstock girth (r = 0.86), scion girth (r = 0.75), number of fruits per tree, (r = 0.77) and fruit yield (r = 0.78) while negatively correlated with TSS (r = -0.66) and titratable acidity (r = -0.85). The tree volume was found positively correlated with tree height (r = 0.93), rootstock girth (r = 0.91), scion girth (r = 0.80), number of fruits per tree, (r = 0.76) and fruit yield (r = 0.81) whereas, it was negatively correlated with TSS (r = -0.79). Tree height showed high significant positive correlation with rootstock girth (r = 0.82), scion girth (r = 0.71) and fruit yield (r = 0.0.73).

http://www.aloki.hu ● ISSN 1589 1623 (Print) ● ISSN1785 0037 (Online)
DOI: http://dx.doi.org/10.15666/aeer/2003_20772093

Table 5. *Correlation coefficient between tree and fruit morphology and biochemical factors of Kinnow mandarin*

	Fwt	**Fd**	**Fl**	**Sot**	**Tvol**	**Tht**	**RoG**	**ScG**	**ToF**	**Tss**	**TA**	**T:A**	**Asa**	**Yeff**	**Fyi**	**Pup**	**Rip**	**Jup**	**Rit**	**Pet**	**Rcci**	**Fcci**
Fwt	1.00																					
Fd	-0.39	1.00																				
Fl	-0.41	0.77**	1.00																			
Sot	0.03	-0.74*	-0.69*	1.00																		
Tvol	0.17	-0.75*	-0.75*	0.96**	1.00																	
Tht	0.42	-0.78**	-0.79**	0.82**	0.93**	1.00																
RoG	0.05	-0.49	-0.56	0.86**	0.91**	0.82**	1.00															
ScG	-0.02	-0.30	-0.46	0.75*	0.80**	0.71*	0.96**	1.00														
ToF	-0.21	-0.29	-0.47	0.77**	0.76*	0.61	0.86**	0.88**	1.00													
Tss	-0.04	0.54	0.51	-0.85**	-0.79**	-0.62	-0.67*	-0.57	-0.60	1.00												
TA	0.09	0.48	0.50	-0.66*	-0.56	-0.35	-0.47	-0.40	-0.45	0.81**	1.00											
T:A	-0.07	-0.41	-0.43	0.49	0.39	0.22	0.36	0.31	0.32	-0.63*	-0.95**	1.00										
Asa	0.36	-0.45	-0.45	-0.00	0.04	0.20	-0.05	-0.05	-0.22	0.21	0.01	0.12	1.00									
Yeff	-0.28	0.76**	0.47	-0.40	-0.41	-0.46	-0.10	0.08	0.20	0.30	0.22	-0.15	-0.47	1.00								
Fyi	0.05	-0.36	-0.56	0.78**	0.81**	0.73*	0.90**	0.90**	0.95**	-0.63	-0.42	0.30	-0.16	0.17	1.00							
Pup	-0.06	-0.36	-0.22	0.18	0.18	0.19	0.27	0.26	0.29	0.13	-0.16	0.32	0.33	0.07	0.27	1.00						
Rip	-0.70*	-0.09	-0.14	0.30	0.14	-0.12	0.09	0.07	0.22	-0.18	-0.44	0.40	-0.00	-0.19	-0.00	0.10	1.00					
Jup	-0.25	0.33	0.26	-0.06	-0.07	-0.10	-0.00	0.03	0.32	-0.13	0.03	-0.11	-0.68*	0.59	0.29	-0.05	-0.28	1.00				
Rit	-0.77**	0.12	0.07	0.24	0.15	-0.07	0.22	0.28	0.26	-0.18	-0.22	0.14	-0.09	-0.12	0.03	-0.16	0.79**	-0.23	1.00			
Pet	-0.22	0.03	-0.23	0.12	0.06	-0.02	-0.10	-0.09	0.05	-0.06	0.07	-0.24	0.00	-0.22	-0.04	-0.56	0.50	-0.18	0.47	1.00		
Rcci	-0.07	-0.17	-0.19	-0.00	-0.02	0.04	-0.28	-0.37	0.00	0.02	0.11	-0.23	-0.14	-0.11	-0.04	-0.02	0.03	0.49	-0.23	0.33	1.00	
Fcci	-0.29	0.20	0.68*	-0.27	-0.31	-0.37	-0.15	-0.15	-0.28	0.36	0.28	-0.16	-0.18	0.09	-0.34	0.33	-0.00	-0.09	0.08	-0.54	-0.38	1.00

Abbreviation of Fwt- Fruit weight, Fd- Fruit width, Fl- Fruit length, Sot- Spread of the tree, Tvol- Tree Volume, Tht- Tree height, RoG- Rootstock girth, ScG- Scion girth, ToF- Number of fruits per tree, Tss- Total soluble solids, TA- Titratable acidity, T: A- TSS: acid ratio, Asa- Ascorbic acid, Yeff- Yield efficiency, Fyi- Fruit yield, Pup- Pulp %, Rip- Rind %, Jup- Juice %, Rit- Rind thickness, Pet- Pedicel thickness, Rcci- Rind Citrus Colour Index, Fcci- Flesh Citrus Colour Index. *Correlation is significant at the 0.05 level (2-tailed). ** Correlation is significant at the 0.01 level (2-tailed)

http://www.aloki.hu ● ISSN 1589 1623 (Print) ● ISSN1785 0037 (Online)
DOI: http://dx.doi.org/10.15666/aeer/2003_20772093

Rootstock girth was positively correlated with scion girth (r = 0.96), number of fruits per tree (r = 0.86) and fruit yield (r = 0.90) but had a negative correlation with TSS (r = - 0.67). Scion girth had significant positive correlation with number of fruits per tree (r = 0.88) and fruit yield (r = 0.90). TSS showed significant positive correlation with titratable acidity (r = -0.81) and negative correlation with TSS: acid ratio (r = -0.63). Titratable acidity and ascorbic acid were found to have negative correlation with TSS: acid ratio (r = -0.95) and juice % (r = -0.68), respectively. Number of fruits per tree and rind % had a significant positive correlation with fruit yield (r = 0.95) and rind thickness (r = 0.79), respectively. All other biochemical and morphological parameters were found non-significantly correlated for the rootstocks under investigation.

Conclusion

The study highlighted the effect of different rootstocks in determining different qualitative aspects of Kinnow mandarin and suggest that pedological condition can be a limiting factor in the choice of alternative rootstocks of Rough lemon, at least in the considered experimental area. It can be inferred from the current findings that rootstocks bring considerable number of alterations that influence fruit quality, yield and plant growth of Kinnow mandarin. Fruit yield, yield efficiency and juice content on Carrizo citrange was highest while, peel content and peel thickness were the lowest. Fruit quality attributes, like TSS was maximum on NRCC-1, ascorbic acid was maximum on CRH-12 whereas, minimum titratable acidity was observed on Volkamer lemon and NRCC-3 but it was not significantly lower than NRCC-6 and Rough lemon in the first year and Volkamer lemon in second year. The fruit weight was recorded highest on CRH-12 but the maximum fruit height and fruit width was recorded on NRCC-12. Scion girth was maximum on NRCC-6 but it was statistically similar to Rough lemon in the first year and to Carrizo citrange in the second year of the experiment. Lowest tree height, tree spread and tree volume were recorded on NRCC-1. In nutshell, the profitability of citrus production is limited by the rootstock and the findings of this experiment we can say Carrizo citrange will be helpful in future for Kinnow mandarin on the basis of yield efficiency and will provide a better production over rough lemon in north-western India.

Acknowledgements. The authors are grateful to the Head, Department of Fruit Science, PAU Ludhiana, India for providing the requisite research funding and facilities.

REFERENCES

[1] Al-Jaleel, A., Zekri, M., Hammam, Y. (2005): Yield, fruit quality, and tree health of ‘Allen Eureka’ lemon on seven rootstocks in Saudi Arabia. – Sci. Hortic. 1058: 457-465.

[2] Ali, G. M. (2002): Effects of four citrus rootstocks on fruit quality and storability of ‘Fremont’ tangerine. – Tanta Univ. J. Agric. Res. 28: 312-326.

[3] Anonymous (2019): National Horticulture Board, Ministry of Agriculture Government of India. 3rd Advance Estimate. – Available at http://www.nhb.gov.in/.

[4] De Assis Alves Mourao Filho, F., Espinoza-Nunez, E., Stuchi, E. S., Ortega, E. M. M. (2007): Plant growth, yield, and fruit quality of ‘Fallglo’ and ‘Sunburst’ mandarins on four rootstocks. – Sci. Hortic. 14: 45-49.

http://www.aloki.hu ● ISSN 1589 1623 (Print) ● ISSN1785 0037 (Online)
DOI: http://dx.doi.org/10.15666/aeer/2003_20772093

[5] Association of Official Analytical Chemists (AOAC) (2000): Official Methods of Analysis, 17th ed. – AOAC International, Gaithersburg, MD.
[6] Aulakh, P. S. (1999): Evaluation of rootstocks for Kinnow mandarin under rainfed condition in the lower Shivaliks of Punjab. – In Proceedings of International Symposium on Citriculture, held at NRC for Citrus, Nagpur, pp. 476-78.
[7] Aulakh, P. S., Thind, S. K., Arora, P. K. (2016): Kinnow. – Published by Additional Director of Communication for Punjab Agricultural University.
[8] Barry, G. H., Castle, W. S., Davies, F. S. (2004): Soluble Solids Accumulation in 'Valencia' sweet orange as related to rootstock selection and fruit size. – J. of the Am. Soci. for Hortic. Sci. 129: 594-598.
[9] Bassal, M. A. (2009): Growth, yield and fruit quality of 'Marisol' clementine grown on four rootstocks in Egypt. – Sci. Horti. 119: 132-137.
[10] Cantuarias-Aviles, T., de Assis Alves Mourao Filho, F., Stuchi, E. S., Silva, S. R., Espinoza-Nunez, E. (2010): Tree performance and fruit yield and quality of 'Okitsu' Satsuma mandarin grafted on 12 rootstocks. – Sci. Hortic. 123: 318-322.
[11] Castle, W. S. (1987): Citrus rootstocks. – Rootstocks for fruit crops.
[12] Chahal, T. S., Gill, P. P. S. (2015): Performance of exotic sweet orange (*Citrus sinensis* Osbeck) cultivars on different rootstocks under north western India. – Ind. J. of Sci. and Tech. 8: 1-8.
[13] Continella, A., Pannitteri, C., La Malfa, S., Legua, P., Distefano, G., Nicolosi, E., Gentile, A. (2018): Influence of different rootstocks on yield precocity and fruit quality of 'Tarocco Scire' pigmented sweet orange. – Sci. Hortic. 230: 62-67.
[14] Davies, F. S., Albrigo, L. G. (1994): Rootstocks. – In: Atherton, J., Rees, A. (eds.) Citrus. CAB, Wallingford, UK, pp. 83-107.
[15] Demirkeser, T. H., Kaplankiran, M., Yildiz, E. (2005): The effects of some citrus rootstocks on fruit yield and quality for 'Rohde Red Valencia' orange during the period of the juvenility in Dortyol (Hatay-Turkey) conditions. – In: 7th International Society of Citrus Nurserymen Congress. Cairo, Egypt, September 17-21. (Abst. No. 28).
[16] DOGV (2006): Diari Oficial de la Comunitat Valenciana. – Espana, Vol. 5346: 30321-30328.
[17] Dubey, A. K., Sharma, R. (2016): Effect of rootstocks on tree growth, yield, quality and leaf mineral composition of lemon (*Citrus limon* (L.) Burm.). – Sci. Hortic. 200: 131-136.
[18] Espinoza-Nunez, E., de Assis Alves Mourao Filho, F., Stuchi, E. S., Cantuarias-Aviles, T., dos Santos Dias, C. T. (2011): Performance of 'Tahiti' lime on twelve rootstocks under irrigated and non-irrigated conditions. – Sci. Hortic. 129(2): 227-231.
[19] Figueiredo, J. O., Pio, R. S., Teofilo Sobrinho, J., Laranjeira, F. F., Salibe, A. A. (2001): Comportamento de quinze porta-enxertos para o tangor 'Murcott' na regiao de Porto Feliz, SP. – Fitotecnia, Revi. Bra. de Fruti 23: 147-151.
[20] Forner-Giner, M. A., Alcaide, A., Primo-Millo, E., Forner, J. B. (2003): Performance of 'Navelina' orange on 14 rootstocks in Northern Valencia (Spain). – Sci. Hortic. 98: 223-232.
[21] Forner-Giner, M. A., Rodriguez-Gamir, J., Martinez-Alcantara, B., Quinones, A., Iglesias, D. J., Primo-Millo, E., Forner, J. (2014): Performance of Navel orange trees grafted onto two new dwarfing rootstocks (Forner-Alcaide 517 and Forner-Alcaide 418). – Sci. Hortic. 179: 376-387.
[22] Garcia–Sanchez, F., Perez-Perez, J. G., Botia, P., Martınez, V. (2006): The response of young mandarin trees grown under saline conditions depends on the rootstock. – Eur. J. Agro. 24: 129-139.
[23] Georgiou, A. (2000): Performance of 'Nova' mandarin on eleven rootstocks in Cyprus. – Sci. Hortic. 84: 115-126.
[24] Georgiou, A. (2002): Evaluation of rootstocks for 'Clementine' mandarin in Cyprus. – Sci. Hortic. 93: 29-38.

http://www.aloki.hu ● ISSN 1589 1623 (Print) ● ISSN1785 0037 (Online)
DOI: http://dx.doi.org/10.15666/aeer/2003_20772093

[25] Georgiou, A., Gregoriou, C. (1999): Growth, yield and fruit quality of 'Shamouti' orange on fourteen rootstocks in Cyprus. – Sci. Hortic. 80: 113-121.
[26] Gonzatto, M. P., Kovaleski, A. P., Brugnara, E. C., Weiler, R. L., Sartori, I. A., Lima, J. G. D., Bender, R. J., Schwarz, S. F. (2011): Performance of 'Oneco' mandarin on six rootstocks in South Brazil. – Pes. Agro. Bras. 46: 406-411.
[27] Hearn, C. J., Hutchison, D. J. (1977): The performance of 'Robinson' and 'Page' citrus hybrids on 10 rootstocks. – Proc. Fla. State Hort. Soc. 90: 44-47.
[28] Hunter, R. S., Harold, R. W. (1987): The measurement of appearance. – John Wiley & Sons, pp. 304-305.
[29] Hussain, S., Curk, F., Anjum, M. A., Pailly, O., Tison, G. (2013): Performance evaluation of common clementine on various citrus rootstocks. – Sci. Hortic. 150: 278-282.
[30] Josan, J. S., Thatai, S. K. (2008): Studies on the evaluation of rootstocks for 'Kinnow' mandarin under north Indian conditions. – Indian J. Hort. 65: 3323-3334.
[31] Lacey, K. (2012): Citrus rootstocks for WA. – Farm Note. Department of Agriculture and Food, Government of Western Australia.
[32] Legua, P., Bellver, R., Forner, J. B., Forner-Giner, M. A. (2011): Trifoliate hybrids rootstocks for 'Lane Late' navel orange in Spain. – Sci Agric. 68: 548-553.
[33] Morse, J. G., Robertson, C. A. (1987): Calculating canopy area of citrus trees and surface area of fruits. – The Florida Entomologist 70: 68-171.
[34] Nasir, M. A., Makon, M. N. K., Khan, A. U. R., Ahmad, S., Ishfaq, M. (2011): Effect of different rootstocks on vegetative growth and canopy of 'Kinnow' Mandarin plants. – J. Agric. Res. 49: 65-71.
[35] Romero, P., Navarro, J. M., Perez-Perez, J., García-Sanchez, F., Gomez-Gomez, A., Porras, I., Martinez, V., Botia, P. (2006): Deficit irrigation and rootstock: their effects on water relations, vegetative development, yield, fruit quality and mineral nutrition of 'Clemenules' mandarin. – Tree Physi. 26: 1537-1548.
[36] Saini, A. K., Singh, H., Jawandha, S. K., Gill, K. S. (2020): Influence of Prunus rootstocks and spacing on performance of Japanese plum grown under sub–tropical conditions. – Sci. Hortic. 268: 109380.
[37] Sau, S., Ghosh, S. N., Sarkar, S., Gantait, S. (2018): Effect of rootstocks on growth, yield, quality, and leaf mineral composition of 'Nagpur' mandarin (*Citrus reticulata* Blanco.), grown in red lateritic soil of West Bengal, India. – Sci. Hortic. 237: 142-147.
[38] Sharma, J. N., Jason, J. S., Thatai, S. K. (2002a): Performance of Kinnow mandarin on different rootstocks under arid-irrigated region of Punjab. – Ind. J. Hort. 59(3): 266-69.
[39] Sharma, J. N., Jason, J. S., Thatai, S. K. (2002b): Effect of rootstocks on tree health, yield and quality of Kinnow mandarin under arid-irrigated region of Punjab. – Ind. J. Hort. 59: 373-77.
[40] Sharma, J. N., Thatai, S. K., Jason, J. S. (2002c): Effect of different rootstock on tree vigour, yield and fruit quality of 'Campabell Valencia' sweet orange. – Ind. J. Hort. 59: 135-39.
[41] Sharma, R. M., Dubey, A. K., Awasthi, O. P., Kaur, C. (2016): Growth, yield, fruit quality and leaf nutrient status of grapefruit (*Citrus paradisi* Macf.): Variation from rootstocks. – Sci. Hortic. 210: 41-48.
[42] Singh, S., Singh, J., Mirza, A. (2019): Evaluation of Mandarin Cultivars on Different Root Stocks-A Review. – Int. J. of Curr. Micro. Appl. Sci. 8: 1213-1222.
[43] Singh, G., Rattanpal, H. S., Gupta, M., Sidhu, G. S. (2020): Standardization of stage wise water requirement in drip irrigated Kinnow mandarin orchards under sub-tropical conditions. – J. Agromet 22(3): 305-312.
[44] Soost, R. K., Cameron, J. W. (1975): Citrus. – In: Janick, J., Moore, J. N. (eds.) Advances in fruit breeding. Purdue University Press, West Lafayette, pp. 507-540.
[45] Stenzel, N. M. C., Neves, C. S. V. J., Gomes, J. C., Medina, C. C. (2003): Performance of 'Ponkan' mandarin on seven rootstocks in Southern Brazil. – Hort Sci. 38: 176-178.

http://www.aloki.hu ● ISSN 1589 1623 (Print) ● ISSN1785 0037 (Online)
DOI: http://dx.doi.org/10.15666/aeer/2003_20772093

[46] Tazima, Z. H., Neves, C. S. V. J., Yada, I. F. U., Leite Jr, R. P. (2013): Performance of 'Okitsu' Satsuma Mandarin on nine rootstocks. – Sci. Agri. 70: 422-427.
[47] Tuzcu, O., Yildirim, B., Yesiloglu, T. (2004): Effect of different rootstocks and sectors on fruit yield and its distribution depending to the tree canopy. – In: 10th International Society of Citriculture Congress. Agadir, Morocco, February 15-20. (Abst. No. 239).
[48] Wutscher, H. K. (1979): Citrus rootstocks. – Hortic. Rev. 1: 237-269.
[49] Zekri, M. (2000): Evaluation of orange trees budded on several rootstocks and planted at high density on flatwoods soil. – Proc. Fla. State Hort. Soc. 113: 119-123.
[50] Zekri, M., Al-Jaleel, A. (2004): Evaluation of rootstocks for 'Valencia' and 'Navel' orange trees in Saudi Arabia. – Fruits 59: 91-100.

http://www.aloki.hu ● ISSN 1589 1623 (Print) ● ISSN1785 0037 (Online)
DOI: http://dx.doi.org/10.15666/aeer/2003_20772093

RICE GRAIN QUALITY, AFFECTED BY A COMBINED FOLIAR SPRAY OF DIFFERENT BIOSTIMULATED COMPONENTS UNDER DIFFERENT LEVELS OF WATER STRESS

ABDEL MEGEED, T. M.[1*] – ELSHAMEY, E. A.[1] – GHARIB, H. S.[2] – HAFEZ, E. M.[2] – EL-SAYED, A.[2]

[1]*Rice Research and Training Center, Field Crops Research Institute, Agricultural Research Center, Kafrelsheikh, Egypt*

[2]*Agronomy Department, Faculty of Agriculture, Kafrelsheikh University, Kafrelsheikh, Egypt*

**Corresponding author*
e-mail: taher.mohamed2018@gmail.com; phone: +20-100-405-5681

(Received 20th Jun 2021; accepted 21st Mar 2022)

Abstract. A field experiment was conducted to find out the effect of some plant biostimulants and plant growth regulating substances on a Sakha108 rice cultivar grown under different irrigation intervals by determining the grain quality characteristics as well as the nutritional value after milling in the 2018 and 2019 growing seasons at the farm of Agricultural Research Station, Sakha, Kafrelsheikh, Egypt. The Experiment was conducted using Randomized Complete Block Design with Strip plot arrangements. Main plots consisted of the four irrigation intervals while sub plots contained the different plant biostimulants and plant growth regulators at different concentrations. Physical (husking yield, milling recovery, and head rice ratio), chemical (amylose and protein contents) and cooking parameters (gelatinous temperature, kernel elongation, amylose content, protein content, carbohydrate content, lipids content, ash, phosphorus and potassium) of the harvested grains were determined in the laboratory. The main results indicated that spraying plant substances during this study increased all studied characteristics as compared to control treatment. Spraying with Crop plus surpassed Cytokinin treatments and provided the highest value for all the studied characteristics. Spraying Crop plus under irrigation every 12 days for plants afflicted by water stress, relieves the harmful effects of stress and improves all grain quality characteristics and the nutritional value as compared with control. These results benefit for farmers who suffer from shortage of irrigation water in their rice field.
Keywords: *Crop plus, Cytokinin (CK), abscisic acid (ABA), plant biostimulants, milled grain quality*

Introduction

Rice (*Oryza sativa* L.) is considered to be one of the most important stable food crops in Egypt. It plays a critical role in Egyptian food security. Drought is a significant limiting factor that has a negative impact on rice production. Due to limited water supplies and a variety of biotic and abiotic difficulties, there is a high demand for sustainable rice production systems. During the summer season, rice occupies around 22% of Egypt's entire growing area and consumes roughly 20% of the country's total water resources. Because Egypt's water resources are restricted, in addition to the country's growing population, the overall water requirements for the rice crop are a severe challenge due to the river Nile's limited irrigation water supply. Some rice-growing areas, particularly those near the terminal irrigation canals in the northern part of the Nile Delta, have irrigation water shortages at various phases of growth, which is considered one of Egypt's most significant constraints to rice production (Abd Allah et al., 2009). Abdel-Megeed et al. (2017) also found that sprayed rice cultivar by Cytokinin prolonged the irrigation interval from 4 days up to 8 days that led to save reasonable amount of irrigation water. Rice is mostly considered a starchy food, but

http://www.aloki.hu ● ISSN 1589 1623 (Print) ● ISSN 1785 0037 (Online)
DOI: http://dx.doi.org/10.15666/aeer/2003_20952112

since animal products can be scarce or expensive in Egypt, it is often the most important source of protein in Egyptians diet as well. The Egyptian rice varieties vary in grain quality characteristics as well as nutritional value after milling (Metwally et al., 2016). Those characteristics are not important only to the consumers but, they are important to the marketer and miller. Although rice is consumed worldwide, there is no universal rice quality attribute (Vidal et al., 2007). Nevertheless, rice appearance and cooked rice texture are the characters considered as main quality attributes by consumers (Okabe, 1979; Rousset et al., 1999). Thus, measuring and understanding factors that influence appearance and texture properties are a great challenge for industries and breeders in meeting consumer preferences. Water is a major constituent of plant tissue as reagent for chemical reactions and solvent for translocation of metabolites and minerals as well as an essential component for cell enlargement through increasing turgor pressure (Cruscio et al., 2008). The occurrence of soil moisture stress affects many of the physiological processes such as photosynthesis and transpiration resulting in reduced growth and poor grain filling (Samonte et al., 2001). Mohapatra and Bal (2006) studied the cooking quality and instrumental textural attributes of cooked rice for different milling fractions of three rice varieties. They found that cooking qualities as well as textural attributes were found to be varied among the varieties. Frei and Becker (2005) reported that rice protein quality is determined by the amino acid composition and its digestibility. Rice protein quality is very high when compared to other crops. Rice has favorable amino acid compositions, a high amount of lysine and a high protein digestibility which makes it a fairly good source of protein in diets where animal protein is limited.

Several researchers have reported that the use of stimulating substances is one of the effective means of improving rice grain quality and enhancing the milled rice nutritional value. Pan et al. (2013) indicated that foliar application plant growth regulators (gibberellic acid, paclobutrazol, 6-Benzylaminopurine) enhanced yield, grain quality characteristics and antioxidant enzyme activities in super hybrid rice. Kamboj and Mathpal (2019) found that foliar application of plant growth regulators, i.e., gibberellic acid cytokinin enhanced the translocation of zinc from vegetative parts to the grains of the rice. They also reported a favorable effect of plant growth regulators on protein content in milled grains due to the translocation of synthesized proteins towards grain by increasing longevity of leaves thus resulted in higher grain protein content. Therefore, soil moisture stress appears to be a major factor for the gap in producing enough quantity of rice as well as grain quality (Tomlins et al., 2005). However, drought effect on crop is depending on soil nutrient content (Gandah et al., 2003) as well as climate and cultivar (Cooper et al., 1987).

Various studies show that water stress negatively affects plants including rice and reduce yields in crops. Application of hormones and growth regulators on the other hand, improves growth parameters in the plants under drought stress. Therefore, the present study aimed to investigate the effect of foliar different plant growth regulator and biostimulants on Sakha108 rice variety production and grain quality under different levels of drought stress under Egyptian conditions. Also, determine the most beneficial combined foliar spray for a rice cultivar grown in Egypt under water stress conditions, in order to aid farmers in their efforts to produce crops with the best possible quality characteristics as well as nutritional value.

http://www.aloki.hu ● ISSN 1589 1623 (Print) ● ISSN 1785 0037 (Online)
DOI: http://dx.doi.org/10.15666/aeer/2003_20952112

Materials and methods

A field experiment was carried out in the farm of Agricultural Research Station, Sakha, Kafrelsheikh, Egypt, the latitude and longitude of the field experiment (31°05′17″N, 30°56′44″E) and the experimental conditions of the study have been described in *Table 1* during 2018 and 2019 in rice growing seasons to identify the impact of foliar application of bio-stimulants by different levels of seaweed extracts named commercially [Crop plus at rates 0.5, 1.00 and 1.5 ml/1 l water]. Biozyme Crop plus is a commercial formulation of seaweed extract (*Ascophyllum nodosum*), enzymes and hydrolyzed proteins whereas, spic cytozyme contain gibberellic acid, auxins, Cytokinins, seaweed extract (*Ascophyllum nodoum*), hydrolysed proteins and trace elements and plant growth regulator named i.e. [Cytokinin (CK) and Abscisic acid with concentration of 15, 20, 25 ppm] and Trafos-K (Trafos-K is a registered trademark of products Trade crop nutri-performance, Co., in Spain, it has been obtained from Perfect-Egypt Company, Al-Sadat City. The chemical composition of Trafos-K is Phosphorus "P2O5" 42% (w/v) and Potassium "K2O" 28% (w/v), in the form potassium phosphite at rates 1, 1.5 and 2 ml/l l water) to improve the vegetative and reproductive growth of Sakha108 rice cultivar under different irrigation intervals, i.e., irrigation every 3 days (I1), irrigation every 6 days (I2), irrigation every 9 days (I3) and irrigation every 12 days (I4) (water stress). From the previous studies Sahaka 108 rice variety consume about 5800 m^3 water following the normal way of irrigation (continuous flooding) under transplanting method but I did not use water meter to determine water consumption of Sakha 108 rice variety with different irrigation intervals during this study. The field experiments were laid out in a strip design with four replications. The irrigation treatments were applied in the main plots, while the plant growth biostimulating growth regulating substances (PGRs) and Trafos-K as shown in *Table 2* were placed in the sub- plots. Rice variety was sprayed with plant bio-stimulated, growth regulators (PGRs) and Trafos-K four time after 15, 30, 45 and 60 days after transplanting (DAT). Pre-germinated seeds of rice cultivar at the rate of 120 kg/ha, were broadcasted manually in the nursery on 10th of May in 2018 and 2019 seasons.

Nitrogen (Urea 46% N) was added according to the treatments in two splits. Two thirds added as basal and incorporated in dry soil before flooding (transplanting). The other 1/3 was applied as top-dress just before panicle initiation (about 30 days after transplanting). Phosphorus as a single super phosphate 15% at the rate of 36.89 kg P2O5/ha was added to the soil before tillage and zinc (ZnSO4) was applied as recommended at the rate of 24 kg ZnSO4/ha. Seedlings were manually pulled and transferred to the permanent field and transplanted in 20 × 20 cm between rows and hills. The sub plot size was 12 m^2. The number of seedling/hill was 2-3 seedling. Seven days after transplanting, the herbicide Saturn 50% at the rate of 4.8 l ha^{-1} was mixed with enough amount of sand to make it easy for homogenous distribution to control the weeds.

At harvest, the central area of 10 m^2 (2.5 m × 4 m)/plot was manually harvested then, dried for about five days, then mechanically threshed and the yield at the 14% moisture content was recorded and converted into (ton/ha). Grain quality characteristics: milling recovery, gelatinization temperature, kernel elongation and amylose content was estimated according to Cruz and Khush (2000): 150 (g) cleaned rough rice at 14% moisture content was dehulled using an Experimental Huller Machine (Satake - Japan). The brown rice was separated and weighed then the hulling percentage was calculated. The brown rice was milled using MC GILL Rice Miller No.2. (S.K. Appliances –

http://www.aloki.hu ● ISSN 1589 1623 (Print) ● ISSN 1785 0037 (Online)
DOI: http://dx.doi.org/10.15666/aeer/2003_20952112

India). The total milled rice was weighed and milled rice percentage was calculated. Whole milled grains were separated from the total milled rice using a rice sizing device SKU: 61-220-50 (Seedburo – USA). The percentage of head rice was calculated.

Table 1. *Means of climate parameters of the experimental site during 2018 and 2019 seasons*

Years	Climatic condition	May	June	July	August
2018	Air temp (°C)	27.5	28.95	29.8	29.55
	RH (%)	59.75	61.75	66.8	66.9
2019	Air temp (°C)	28.65	30.5	30.95	31.55
	RH (%)	57.15	65.75	69.8	72.65

Table 2. *Plant bio stimulants and the amount of this components during period of rice plant growing*

No	Growth biostimulants	Dose	No	Growth biostimulants	Dose
1	Crop Plus (T_1)	0.5 ml/1 l water	8	ABA (T_8)	20 ppm
2	Crop Plus (T_2)	1.0 ml/1 l water	9	ABA (T_9)	25 ppm
3	Crop Plus (T_3)	1.5 ml/1 l water	10	Trafos K (T_{10})	1 ml/1 l water
4	Cytokinin (T_4)	15 ppm	11	Trafos K (T_{11})	1.5 ml/1 l water
5	Cytokinin (T_5)	20 ppm	12	Trafos K (T_{12})	2 ml/1 l water
6	Cytokinin (T_6)	25 ppm	13	Tap water (T_{13})	-----
7	ABA (T_7)	15 ppm			

Six grains of whole milled rice were placed in boxes containing 1.7% KOH and arranged so that the kernels do not touch each. The boxes were covered and incubated for 23 h at 30° C. The appearance and disintegration of endosperm were graded visually according to the numerical scale of the gelatinization temperature. Kernel elongation was measured using the Micrometer, the length of five milled grains was measured (mm) and their average was determined for each treatment (before cooking). Grains were left in a test tube filled with 30 ml of distilled water for 30 min, then for another 10 min in 98° C a water tub. After that, the tubes were placed in cold water until reaching room temperature. Grains were lifted from the distilled water, dried (by filter paper), and measured again by graph papers (after cooking). Kernel elongation percentage was calculated as the percentage of grain expanding before and after cooking.

Amylose content was determined by weighing accurately 100 mg of sample into 100 ml volumetric flask then carefully adding 1 ml of 95% ethanol and 9 ml 1 N Na OH. The mixture was heated for 10 min in a boiling water bath to gelatinize the starch; then cooled, and the content made up to volume 100 ml with water. Pipette 5 ml portion of the gelatinization starch solution, 1 ml of 1N acetic acid, and 2 ml of iodine solution were added and made up to a volume of 100 ml with distilled water. The content was shaken and stands for 20 min before reading the transmission at 620 nm by Spectronic 1201 Spectrophotometer (Milton Roy, USA)**.**

http://www.aloki.hu ● ISSN 1589 1623 (Print) ● ISSN 1785 0037 (Online)
DOI: http://dx.doi.org/10.15666/aeer/2003_20952112

Protein, carbohydrate, lipids, ash, phosphorus and potassium determination in rice grain: Plant samples were taken from the grain after milling (50 grams of milled rice). All plant samples were placed in paper bags and oven-dry at 70° C for 48 h. Grain samples were ground to powder and digested according to the method of Chapman and Pratt (1961) before chemical analysis as follows: the nitrogen content of milled grains was determined by using the Microkieldahl method (Jackson, 1967) to calculate protein content. Total carbohydrate was calculated by difference as mentioned by (Fraser and Holmes, 1959). Lipids was determined according to A.O.A.C. (2000). The phosphorus content of milled grain was determined using Spectronic 1201 Spectrophotometer (Milton Roy, USA) following the procedures of Watanabe and Olsen (1965). The Potassium content of grain was determined using Elico CL378 Flame Photometer (RHYS international LTD, India) according to Peterpurgski (1968) method. The energy composition was calculated according to A.O.A.C. (2000) and Singh and Singh (2019). Representative soil samples were taken from the experimental sites at (0-30 cm) depth from soil Surface. Chemical analysis were done and the results are presented in *Table 3* according to Black et al. (1965).

Table 3. *Soil mechanical and chemical properties of the experimental site*

Seasons of study	Soil texture (%)	pH	EC dS/m	Organic matter (%)	Available N (mg kg^{-1})	Available P (mg kg^{-1})	Available K (mg kg^{-1})
2018	Clayed	7.9	1.8	1.65	22.5	14.45	346
2019	Clayed	8.1	1.45	1.68	24.4	14.12	357

Statistical analysis: The collected data were subjected to statistical analysis and were tested at 5% level of significance to interpret the differences among the treatments, which adapted by Waller and Duncan (1969). All the collected data were subjected to statistical analysis according to procedure described by Gomez and Gomez (1984).

Results and discussion

Data present in *Tables 4* and *5* showed that hulling, milling and head rice percentage as affected by different water intervals and plant growth regulators (PGRs) in both 2018 and 2019 seasons. These characters are considered as the most important traits that affect rice quality and consumer demand.

Application of different plant growth regulators (PGRs) with different material and concentration at different growth stages of rice under different water irrigation significantly effect in hulling, milling and head rice %. Data indicated that rice plant which treated and irrigated every 3-days gave the highest hulling %, milling % and heading rice % more irrigated every 6-days. While the lowest value was obtained rice plant irrigated every 12-days. Using plant growth regulator at different growth of rice variety improving and gave the greatest hulling %, milling % and heading rice %, where rice variety treated by 1.5 cm concentration of Crop plus recorded the highest value of hulling %, milling % and heading rice % followed by when rice variety treated by 1.5 and 0.5 cm concentration of Crop plus, respectively. While the lowest value was obtained from T_{13} (Tap Water only). There results were hold true in the two studied seasons. Such findings had also been pointed out by Abdel-Megeed et al. (2017, 2020) and Zheng (2020).

http://www.aloki.hu ● ISSN 1589 1623 (Print) ● ISSN 1785 0037 (Online)
DOI: http://dx.doi.org/10.15666/aeer/2003_20952112

Table 4. *Hulling %, milling % and head rice % of Sakha108 rice cultivars as affected by different irrigation intervals and growth regulators during 2018 and 2019 season*

Treatments	2018			2019		
	Hulling %	**Milling %**	**Heading %**	**Hulling %**	**Milling %**	**Heading %**
Irrigation interval (A):						
(I_1)	80.662a	71.646a	65.646a	79.144a	70.692a	67.56a
(I_2)	79.638b	71.077b	64.454b	78.592b	69.592b	66.65b
(I_3)	79.131c	70.338c	62.223c	78.015c	69.069c	65.22c
(I_4)	78.388d	69.738d	60.254d	77.236d	68.308d	63.98d
F Test	**	**	**	**	**	**
Growth regulates treatment (B):						
(T_1)	81.500c	72.650c	67.750c	80.025c	71.375c	68.30c
(T_2)	82.063b	73.075b	68.400b	80.925b	71.900b	69.00b
(T_3)	83.350a	74.075a	70.300a	81.600a	72.550a	69.50a
(T_4)	79.325f	71.400e	64.600f	78.900e	69.950e	66.58f
(T_5)	80.175e	71.550e	65.750e	79.350d	70.475d	67.15e
(T_6)	80.875d	71.900d	66.800d	79.425d	71.225c	67.60d
(T_7)	78.700g	69.850h	61.475i	77.950g	68.975f	65.13h
(T_8)	78.825g	70.325g	62.050h	78.142fg	69.175f	65.18h
(T_9)	79.250f	70.875f	63.075g	78.193f	69.750e	65.95g
(T_{10})	77.025j	68.000k	57.750l	75.775j	66.500i	62.43k
(T_{11})	77.500i	68.875j	58.025k	76.125i	67.600h	63.38j
(T_{12})	78.000h	69.375i	58.700j	76.600h	68.450g	63.93i
(T_{13})	76.325k	67.150l	56.200m	74.200k	64.475j	62.00l
F Test	**	**	*			**
Interaction: AXB	**	**	**	**	**	**

I1: irrigation every3-days, I2: irrigation every 6-days, I3: irrigation every 9-days, I4: irrigation every 12-days, T_1: 0.5 ml Crop plus, T_2: 1.00 ml Crop plus, T_3: 1.5 ml Crop plus, T_4: 15 ppm Cytokinin, T_5: 20 ppm Cytokinin, T_6: 25 ppm Cytokinin, T_7: 15 ppm ABA, T_8: 20 ppm ABA, T_9: 25 ppm ABA, T_{10}: 1 ml Trafos K, T_{11}: 1.5 ml Trafos K, T_{12}: 2 ml Trafos K, T_{13}: Tap water

The interaction between different irrigation intervals and different PGRs had a significant influence on hulling %, milling % and heading rice %. From the results presented in *Table 5*, it could be concluded that plants which treated by Crop plus produced the highest hulling %, milling % and heading rice % respectively, in the table under different water irrigation every 3, 6, 9 and 12 days, followed by treated by Cytokinin and ABA, while treated by Trafos K come in the last rank of plant growth regulator. While the lowest hulling %, milling % and heading rice % were obtained when rice plant treated by Tap water treated under irrigation every 12 days. These results are in harmony with that recorded by Anjum et al. (2007), Cuevas et al. (2016), Gharieb et al. (2016), Singh (2011) and Zhao (2018).

Data in the same table showed also, that rice plants which irrigated every 3-days and treated with different dose of Crop plus and 25 ppm of Cytokinin recoded the same of panicle length. Nearly of the same values of panicle length were recorded when rice plants irrigated every 8 days and treated even planted sprayed with 1.5, 1.0 and 0.5 ppm of Crop plus and 25 ppm Cytokinin without any significant difference between them. It means that tested rice sprayed by Crop plus led to extend the irrigation interval from 3-days up to every 9 days consequently save reasonable amount of irrigation water without significant reduction in the sink capacity (No. of panicle). While the lowest

http://www.aloki.hu ● ISSN 1589 1623 (Print) ● ISSN 1785 0037 (Online)
DOI: http://dx.doi.org/10.15666/aeer/2003_20952112

value of hulling %, milling % and heading rice % were found with irrigation every 12 days under control treatment (without any spray). These results are in coincidence with that reported by Akita (1989), Canady (2012), Anonymous (2013), Bhattacharya (2019) and Abdel-Megeed et al. (2020).

Table 5. *Hulling %, milling % and head rice % of Sakha108 rice cultivars as affected by the interaction between different irrigation intervals and growth regulators in 2018 and 2019 seasons*

	Irrigation intervals							
	I1	**I2**	**I3**	**I4**	**I1**	**I2**	**I3**	**I4**
	2018				**2019**			
	Hulling %							
(T_1)	84.100a	81.100uv	80.800uv	80.000vw	80.60ef	80.300fg	80.100gh	79.100k-m
(T_2)	84.300a	82.300d-f	81.600efg	80.050g-k	81.50bc	81.200cd	80.800de	80.200fg
(T_3)	84.600a	84.500bc	82.800cd	81.500g-k	82.10a	81.800ab	81.500bc	81.000de
(T_4)	79.800h-l	79.500a	79.100b	78.900de	79.90ghi	78.900l-n	78.800m-o	78.000rs
(T_5)	81.800cd	80.100j-n	79.600l-o	79.200m-p	80.00ghi	79.500i-k	79.400j-l	78.500n-r
(T_6)	82.800b	80.600g-j	80.500j-n	79.600k-o	80.00ghi	79.600h-j	79.100k-m	79.000k-n
(T_7)	79.700b	78.600f-h	78.400f-i	78.100j-n	78.700m-p	78.200r-s	78.100q-s	76.800vw
(T_8)	79.700i-m	78.800o-q	78.600o-r	78.200p-s	78.767m-o	78.300o-r	78.200p-s	77.300tu
(T_9)	79.700i-m	79.500n-p	78.900o-q	78.900p-s	78.800m-o	78.600m-q	78.300o-r	77.070uv
(T_{10})	77.800i-m	77.400j-n	76.500m-p	76.400m-p	77.000uv	76.100xy	75.200z	74.800z
(T_{11})	78.500q-t	78.100s-u	77.600vw	75.800vw	77.700st	76.400wx	75.200z	75.200z
(T_{12})	79.100o-q	78.100p-s	77.800rst	77.000wx	78.000rs	78.000rs	75.200z	75.200z
(T_{13})	76.700l-o	76.700p-s	76.500q-t	75.400tuv	75.800y	74.800z	74.300z	71.900z
	Milling %							
(T_1)	74.000c	73.300d	72.200ef	71.100ik	73.500b	71.300ef	70.700ghi	70.000jk
(T_2)	74.600b	74.100c	72.300ef	71.300h-j	73.800ab	71.900d	71.000fgh	70.900f-h
(T_3)	75.900a	74.200bc	73.500d	72.700e	74.000a	72.600c	72.500c	71.100f-h
(T_4)	72.500e	71.700gh	70.700k-m	70.700k-m	70.800f-h	70.000jk	69.700kl	69.300l-o
(T_5)	72.600e	72.000fg	70.700k-m	70.900j-l	71.700de	70.700ghi	69.900jk	69.600k-m
(T_6)	72.700e	72.300ef	71.500hi	71.100i-k	73.500b	71.200fg	70.300ij	69.900jk
(T_7)	70.400l-n	69.900o-q	69.700p-r	69.400r-t	69.500k-n	69.000n-q	68.900o-q	68.500qr
(T_8)	70.600k-m	70.500lm	70.300m-o	69.900o-q	69.800j-l	69.300l-o	69.000n-q	68.600p-r
(T_9)	71.700gh	71.500hi	70.300m-o	70.000n-p	70.600hi	69.800j-l	69.500k-n	69.100m-p
(T_{10})	69.000s-u	68.200xy	68.000y	66.800z	67.800st	66.900vw	66.600w	64.700y
(T_{11})	69.400r-t	68.900tuv	68.800u-w	68.400w-y	68.200rs	67.600t	67.500tu	67.100uv
(T_{12})	69.500q-s	69.400r-t	69.300r-t	69.300r-t	68.900o-q	68.400r	68.300r	68.200rs
(T_{13})	68.500v-x	68.000y	67.100z	65.000z	66.900vw	66.000x	64.000z	61.000z
	Head rice %							
(T_1)	68.700cd	68.100e	67.300gh	66.900hi	70.20c	69.20d	68.00g	65.80jk
(T_2)	69.100bc	68.700cd	67.900ef	67.900ef	71.00b	69.90c	69.00de	66.10ij
(T_3)	71.900a	71.500a	69.500b	68.300de	71.70a	70.10c	69.90c	66.30i
(T_4)	66.800i	65.300lm	63.300pq	63.000q	68.50f	67.90g	65.20mn	64.70o-q
(T_5)	66.900hi	66.300j	65.300lm	64.500o	69.70c	68.70ef	65.30l-n	64.90n-p
(T_6)	67.600fg	67.500fg	65.900jk	66.200j	70.00c	68.90def	66.00ij	65.50k-m
(T_7)	65.000mn	62.100r	60.200t	58.600v	66.80h	65.70jkl	64.70o-q	63.30t
(T_8)	65.600kl	63.700p	60.300t	58.600v	66.80h	65.70jkl	64.70o-q	63.50st
(T_9)	66.000jk	64.700no	62.000r	59.600u	67.80g	67.20h	64.60o-q	64.20qr
(T_{10})	61.200s	61.100s	57.600w	51.100z	63.80rs	62.80u-w	62.20x	60.90y
(T_{11})	62.200r	60.200t	57.500w	52.200y	64.30q	63.50st	63.00t-v	62.70vw
(T_{12})	62.200r	60.200t	56.000x	56.400x	65.00no	64.40pq	63.20tu	63.10tuv
(T_{13})	60.200t	58.500v	56.100x	50.000z	62.70vw	62.50wx	62.10x	60.70y

I1: irrigation every3-days, I2: irrigation every 6-days, I3: irrigation every 9-days, I4: irrigation every 12-days, T_1: 0.5 ml Crop plus, T_2: 1.00 ml Crop plus, T_3: 1.5 ml Crop plus, T_4: 15 ppm Cytokinin, T_5: 20 ppm Cytokinin, T_6: 25 ppm Cytokinin, T_7: 15 ppm ABA, T_8: 20 ppm ABA, T_9: 25 ppm ABA, T_{10}: 1 ml Trafos K, T_{11}: 1.5 ml Trafos K, T_{12}: 2 ml Trafos K, T_{13}: Tap water

http://www.aloki.hu ● ISSN 1589 1623 (Print) ● ISSN 1785 0037 (Online)
DOI: http://dx.doi.org/10.15666/aeer/2003_20952112

The Gelatinous temperature, kernel elongation and amylose content were varied the irrigation intervals by different stimulating compounds application (*Tables 6* and *7*). Irrigation every 3-days recorded the highest values of gelatinous temperature, kernel elongation and amylose content. While irrigation every 12-days come the last rank recorded the lowest value of gelatinous temperature, kernel elongation and amylose content. Starch is the main component of milled rice grain. It is made up of two starchy fractions: amylose and amylopectin. After cooking, rice grains with high amylose content are dry, fluffy, separate and hard, while those with low amylose content are glossy, soft and sticky. So, Amylose content is considered to be one of the most important predictors of the eating quality of cooked rice. Milled rice cultivars may be generally classified based on their apparent amylose content into waxy (1-2%), very low (2-12%), low (12-20%), intermediate (20-25%) or high (>25%) (Bao, 2012). Based on the results, the studied genotypes under the current study belong to low amylose content rice types that meet the Egyptian consumers' preferences. The significant variation in amylose content among the studied genotypes could be attributed to the genetic background of those varieties. These results are in harmony with that recorded by Okabe (1979), Rousset (1999), Samonte (2001), Anjum et al. (2007), Singh (2011), Cuevas et al. (2016), Gharieb et al. (2016) and Zhao (2018).

Table 6. *Gelatinous temperature, kernel elongation and amylose % of Sakha108 rice cultivars as affected by different irrigation intervals and growth regulators during 2018 and 2019 season*

Treatments	2018			2019		
	Gelatinous temperature	Kernel elongation	Amylose %	Gelatinous temperature	Kernel elongation	Amylose %
Irrigation interval (A):						
(I_1)	6.662a	57.95a	18.38a	6.17a	57.94a	18.27a
(I_2)	6.383b	56.67b	17.10b	5.89b	56.66b	16.99b
(I_3)	6.194c	56.46c	16.92c	5.70c	56.47c	16.80b
(I_4)	5.873d	56.24d	16.67d	5.38d	56.23d	16.56c
F Test	**	**	**	**	**	**
Growth regulates treatment (B):						
(T_1)	6.763ab	57.19c	17.69b	6.13b	56.79d	17.61a-c
(T_2)	6.963a	57.56b	17.76ab	6.24b	57.69b	17.69ab
(T_3)	7.063a	57.86a	17.84a	6.41a	57.89a	17.78a
(T_4)	6.303c	56.98e	17.27de	5.77c	56.70de	17.20d-f
(T_5)	6.403bc	56.98e	17.36cd	5.80c	56.79d	17.31c-e
(T_6)	6.483bc	57.08d	17.45c	5.83c	57.55c	17.39b-d
(T_7)	5.823d	56.44gh	17.15f	6.44a	56.55f	16.95f-i
(T_8)	6.113cd	56.46gh	17.15f	5.63d	56.56f	17.04e-h
(T_9)	6.253c	56.65f	17.22ef	5.63d	56.65ef	17.13d-g
(T_{10})	5.798d	56.31i	16.89h	5.29f	56.32g	16.62i
(T_{11})	6.108cd	56.42h	16.92h	5.41e	56.35g	16.70hi
(T_{12})	6.108cd	56.54g	17.03g	5.41e	56.42g	16.83ghi
(T_{13})	5.438e	56.32i	16.69i	5.21f	56.42g	16.75hi
F Test	**	**	**	**	**	**
Interaction: AXB	*	*	**	*	*	**

I1: irrigation every3-days, I2: irrigation every 6-days, I3: irrigation every 9-days, I4: irrigation every 12-days, T_1: 0.5 ml Crop plus, T_2: 1.00 ml Crop plus, T_3: 1.5 ml Crop plus, T_4: 15 ppm Cytokinin, T_5: 20 ppm Cytokinin, T_6: 25 ppm Cytokinin, T_7: 15 ppm ABA, T_8: 20 ppm ABA, T_9: 25 ppm ABA, T_{10}: 1 ml Trafos K, T_{11}: 1.5 ml Trafos K, T_{12}: 2 ml Trafos K, T_{13}: Tap water

http://www.aloki.hu ● ISSN 1589 1623 (Print) ● ISSN 1785 0037 (Online)
DOI: http://dx.doi.org/10.15666/aeer/2003_20952112

Table 7. *Gelatinous temperature, kernel elongation and amylose % of Sakha108 rice cultivars as affected by the interaction between different irrigation intervals and growth regulators in 2018 and 2019 seasons*

	Irrigation intervals							
	I1	**I2**	**I3**	**I4**	**I1**	**I2**	**I3**	**I4**
	2018				**2019**			
	Gelatinous temperature							
(T_1)	7.02b-d	6.80d-g	6.52h-l	6.71e-i	6.39c-f	6.17f-j	5.89k-n	6.08g-k
(T_2)	7.22ab	7.00b-d	6.72e-h	6.91cde	6.50b-d	6.28d-g	6.00h-m	6.19f-i
(T_3)	7.32a	7.10a-c	6.82d-g	7.01bcd	6.67ab	6.45d-e	6.17f-j	6.36c-f
(T_4)	6.70e-i	6.42j-m	6.27l-n	5.82q-s	6.17f-j	5.89k-n	5.74m-p	5.29rs
(T_5)	6.80d-g	6.52h-l	6.37k-m	5.92p-r	6.20e-i	5.92j-n	5.77l-p	5.32rs
(T_6)	6.88c-f	6.60g-k	6.45i-m	6.00o-r	6.23e-i	5.95i-n	5.80l-o	5.35qrs
(T_7)	6.22mno	5.94p-r	5.79rs	5.34u	6.84a	6.56bc	6.41c-f	5.96i-n
(T_8)	6.51h-l	6.23m-o	6.08n-p	5.63st	6.03gl	5.75m-p	5.60o-q	5.15s
(T_9)	6.65f-j	6.37k-l	6.22m-o	5.77rs	6.03g-l	5.75m-p	5.60o-q	5.15s
(T_{10})	6.23mno	5.92p-r	5.75rs	5.29u	5.72n-p	5.41q-s	5.24s	4.78t
(T_{11})	6.54h-k	6.23m-o	6.06n-q	5.60st	5.84k-o	5.53 p-r	5.36q-s	4.90t
(T_{12})	6.54h-k	6.23m-o	6.06n--q	5.60st	5.84k-o	5.53p-r	5.36q-s	4.90t
(T_{13})	5.97o-r	5.62st	5.41tu	4.75v	5.74m-p	5.39q-s	5.18s	4.52u
	Kernel elongation							
(T_1)	58.33c	57.11k-m	56.30r-u	57.02l-n	57.80c-e	56.58lm	56.30n-s	56.49l-p
(T_2)	58.53b	57.31i-k	57.20j-l	57.22j-l	58.70b	57.48g-i	57.20j	57.39h-j
(T_3)	58.86a	57.64d-f	57.40g-j	57.55e-h	58.90a	57.68d-g	57.40h-j	57.59e-h
(T_4)	58.13c	56.85n-p	56.70p-q	56.25s-u	57.85cd	56.57lm	56.42n-r	55.97w-z
(T_5)	58.13c	56.85n-p	56.70p-q	56.25s-u	57.94c	56.66kl	56.51l-o	56.06t-y
(T_6)	58.23c	56.95m-o	56.80op	56.35r-u	58.70b	57.42hi	57.27ij	56.82k
(T_7)	57.11d-g	56.31r-u	56.16t-v	55.71x-z	57.70d-g	56.42m-r	56.27p-u	55.82z
(T_8)	57.31d-g	56.33r-u	56.18s-v	55.73x-z	57.71d-f	56.43m-q	56.28o-u	55.83z
(T_9)	57.64d	56.52qr	56.37r-t	55.92wx	57.80c-e	56.52l-n	56.37m-r	55.92xy
(T_{10})	56.85f-i	56.18s-v	56.01vw	55.55z	57.50f-h	56.19r-w	56.02v-z	55.56z
(T_{11})	56.85d-g	56.29s-v	56.12u-w	55.66yz	57.53f-h	56.22q-v	56.05u-z	55.59z
(T_{12})	56.95de	56.41rs	56.24s-u	55.78xy	57.60e-h	56.29n-t	56.12s-x	55.66z
(T_{13})	57.35h-j	56.00vw	55.79xy	56.13u-w	57.45hi	56.10s-y	55.89yz	56.23q-v
	Amylose %							
(T_1)	18.70a-c	17.48j-m	17.20n-r	17.39k-n	18.62ab	17.40g-n	17.12j-s	17.31h-o
(T_2)	18.77ab	17.55i-k	17.27m-p	17.46j-m	18.70ab	17.48f-m	17.20i-r	17.39g-n
(T_3)	18.85a	17.63ij	17.35k-o	17.54i-l	18.79a	17.57e-l	17.29h-p	17.48f-m
(T_4)	18.42d-f	17.14o-s	16.99r-u	16.54x-z	18.35a-d	17.07j-t	16.92l-u	16.47r-x
(T_5)	18.51c-e	17.23n-q	17.08p-t	16.63w-y	18.46a-d	17.18i-r	17.03k-t	16.58o-x
(T_6)	18.60b-d	17.32l-o	17.17n-r	16.72v-x	18.54a-c	17.26i-q	17.11j-s	16.66n-w
(T_7)	18.30e-g	17.02q-t	16.87t-v	16.42yz	18.10a-g	16.82l-v	16.67n-w	16.22u-x
(T_8)	18.30e-g	17.02q-t	16.87t-v	16.42yz	18.19a-f	16.91l-u	16.76m-v	16.31t-x
(T_9)	18.37ef	17.09p-t	16.94s-v	16.49yz	18.28a-e	17.00l-t	16.85l-u	16.40s-x
(T_{10})	18.07h	16.76v-x	16.59w-y	16.13z	17.80d-j	16.49q-x	16.32t-x	15.86x
(T_{11})	18.10gh	16.79u-w	16.62w-y	16.16z	17.88c-i	16.57o-x	16.40s-x	15.94wx
(T_{12})	18.21f-h	16.90t-v	16.73v-x	16.27z	18.01b-h	16.70n-w	16.53p-x	16.07v-x
(T_{13})	17.71i	16.36z	16.22z	16.49yz	17.78d-k	16.43r-x	16.22u-x	16.56o-x

I1: irrigation every3-days, I2: irrigation every 6-days, I3: irrigation every 9-days, I4: irrigation every 12-days, T_1: 0.5 ml Crop plus, T_2: 1.00 ml Crop plus, T_3: 1.5 ml Crop plus, T_4: 15 ppm Cytokinin, T_5: 20 ppm Cytokinin, T_6: 25 ppm Cytokinin, T_7: 15 ppm ABA, T_8: 20 ppm ABA, T_9: 25 ppm ABA, T_{10}: 1 ml Trafos K, T_{11}: 1.5 ml Trafos K, T_{12}: 2 ml Trafos K, T_{13}: Tap water

http://www.aloki.hu ● ISSN 1589 1623 (Print) ● ISSN 1785 0037 (Online)
DOI: http://dx.doi.org/10.15666/aeer/2003_20952112

Foliar spray of different stimulating compounds increased significantly gelatinous temperature, kernel elongation and amylose content. The highest values of gelatinous temperature, kernel elongation and amylose content were observed when rice plant treated with crop plus followed by cytokinin, ABA and Trafos K which come in the last rank and recorded the lowest value of gelatinous temperature, kernel elongation and amylose content. Data in the same table revealed that Plant growth regulators caused an increase in gelatinous temperature, kernel elongation and amylose content as compared with control. The highest gelatinous temperature, kernel elongation and amylose content were found when rice plants sprayed with Crop plus at 1.5 ml/1 l followed sprayer at concentration 1 ml/1 l while sprayer by crop plus by 0.5 ml/1 l water and Cytokinin with 25 and 20 ppm recorded nearly the same value followed by ABA which came in the third rank gave nearly the same value under different concentration of ABA in this aspect. Similar results were observed in the two seasons of study. These results are in line with that obtained by Pospíšilová (1999), Ramya et al. (2011) and Abdel-Megeed et al. (2020).

The interaction between different irrigation intervals and different PGRs had a significant influence on gelatinous temperature, kernel elongation and amylose content. From the results presented in *Table 7,* it could be concluded that plants which treated by Crop plus produced the highest gelatinous temperature, kernel elongation and amylose content under different water irrigation every 3, 6, 9 and 12 days, followed by treated by Cytokinin and ABA, while treated by Trafos K come in the last rank of plant growth regulator. While the lowest number of tillers were obtained when rice plant treated by Tap water treated under irrigation every 12 days. Data in *Table 7* show that foliar application of Crop plus by 1.5 or 1 ml/1 l under either the irrigation every 3-days or 6-days recorded nearly the highest values of gelatinous temperature, kernel elongation and amylose content in the two studied seasons.

It can be easily observed that there was any significant difference between the irrigation every 3-days and 6-days intervals in gelatinous temperature, kernel elongation and amylose content when treated rice by 1.5 or 1.00 ml/1 l of crop plus. It might be due to the role of these substances to help the plant for keeping the water inside the cell more time consequently extend the period of irrigation intervals that led to save reasonable amount of irrigation water. These results are in coincidence with that reported by Akita (1989), Singh (2011), Canady (2012), Anonymous (2013), Gharieb et al. (2016), Zhao (2018), Bhattacharya (2019) and Abdel-Megeed et al. (2020).

Data in *Tables 8* and *9* revealed significant differences among different water intervals, foliar spray stimulating compound and the interaction for protein, carbohydrate and lipids content percentage in both seasons. Within irrigation intervals, data in *Table 8* clarified that irrigation every 3 days produced the greatest contents of protein in 2018 season while in 2019 season irrigation every 6 and 9-days come in the first rank and recorded the highest value of protein content followed by irrigation every 3-days. Carbohydrates and lipids gave the highest value when irrigated every 3-days followed by irrigation every 6 days while irrigation every 12 days gave the least because of the injury of water stress under this treatment. The results showed that the protein, carbohydrate and lipids content percentage decreased under lower soil moisture level but the degree of reduction in different genotypes did not indicate the tolerance level of the genotypes. Decreased carbohydrate and lipids content percentage under lower soil moisture levels might be due to inhibition of translocation of assimilate to the grains due to moisture stress. Such findings had also been pointed out by Abdel-Megeed et al. (2017, 2020) and Zheng (2020).

http://www.aloki.hu ● ISSN 1589 1623 (Print) ● ISSN 1785 0037 (Online)
DOI: http://dx.doi.org/10.15666/aeer/2003_20952112

Table 8. *Protein, carbohydrate and lipids content % of Sakha108 rice cultivars as affected by different irrigation intervals and growth regulators during 2018 and 2019 season*

Treatments	2018			2019		
	Protein	**Carbohydrate**	**Lipids content %**	**Protein**	**Carbohydrate**	**Lipids content %**
Irrigation interval (A):						
(I_1)	8.99a	76.41a	0.5718a	7.828c	77.88a	0.5396a
(I_2)	8.72b	75.13b	0.5428b	8.291a	76.60b	0.5118b
(I_3)	8.53b	74.94c	0.5234bc	8.147b	76.41c	0.4928bc
(I_4)	8.28c	74.70d	0.5046c	7.116d	76.17d	0.4685c
F. Test	*	**	*	*	**	*
Growth regulates treatment (B):						
(T_1)	9.57b	75.93b	0.57a-c	8.023d	77.04c	0.54ab
(T_2)	9.99a	76.03b	0.58ab	8.543b	77.12b	0.55ab
(T_3)	10.16a	76.18a	0.59a	9.183a	77.21a	0.57a
(T_4)	8.54de	75.43d	0.54c-f	7.836ef	76.87d	0.50cde
(T_5)	8.69d	75.70c	0.54d-e	8.163c	77.03c	0.50cd
(T_6)	9.11c	75.74c	0.55a-d	8.423b	77.04c	0.52bc
(T_7)	8.22ef	74.84e	0.52d-f	7.618g	76.67g	0.48cde
(T_8)	8.32ef	74.93e	0.52d-f	7.718fg	76.75f	0.49cde
(T_9)	8.51de	75.69c	0.53d-f	7.898de	76.81e	0.49cde
(T_{10})	7.62h	74.49h	0.49f	6.998j	76.28i	0.47e
(T_{11})	7.84gh	74.64fg	0.50ef	7.323i	76.29i	0.47de
(T_{12})	8.07fg	74.71f	0.51def	7.468h	76.53h	0.47de
(T_{13})	7.54h	74.53gh	0.50ef	6.804k	76.27i	0.47de
F. Test	**	**	*	**	**	*
Interaction: AXB	*	*	NS	*	*	NS

I1: irrigation every3-days, I2: irrigation every 6-days, I3: irrigation every 9-days, I4: irrigation every 12-days, T_1: 0.5 ml Crop plus, T_2: 1.00 ml Crop plus, T_3: 1.5 ml Crop plus, T_4: 15 ppm Cytokinin, T_5: 20 ppm Cytokinin, T_6: 25 ppm Cytokinin, T_7: 15 ppm ABA, T_8: 20 ppm ABA, T_9: 25 ppm ABA, T_{10}: 1 ml Trafos K, T_{11}: 1.5 ml Trafos K, T_{12}: 2 ml Trafos K, T_{13}: Tap water

Data presented in *Table 8* assert that significant differences were found among the tested PGRs and biostimulated on protein, carbohydrate and lipids content percentage in both seasons of study. Within various PGRs and biostimulated application, plants which spraying with 1.5 ml/1 l Crop gave the highest value of protein, carbohydrate and lipids content percentage followed by spraying also with 1 ml/1 l of Crop plus while spraying with 25 ppm Cytokinin come in next rank without significant when plants spraying with 0.5 ml/1 l of Crop plus in the two seasons under study. The lowest protein, carbohydrate and lipids content percentage was obtained when rice did not receive any of PGR (control). These results are in line with that obtained by Pospíšilová (1999), Ramya et al. (2011) and Abdel-Megeed et al. (2020).

For the interaction of protein, carbohydrate and lipids content percentage clarified in *Table 9* that application of Crop plus under irrigation every 3-days produced the highest value of number of filled grains followed by irrigation every 9 days and surpassed both Cytokinin and ABA which perform the same trend. It can be also, noticed that the application of any of PGR to the tested cultivar caused an increase in protein, carbohydrate and lipids content percentage as compared with control. The application of different stimulating compounds increased significantly the contents of protein and

http://www.aloki.hu ● ISSN 1589 1623 (Print) ● ISSN 1785 0037 (Online)
DOI: http://dx.doi.org/10.15666/aeer/2003_20952112

lipids over control treatment. Foliar application of crop plus recorded the highest values of protein content, carbohydrate and lipids content. There are highly significant differences in protein, carbohydrate and lipids content percentage with respect to different irrigation intervals × stimulating compound interaction suggesting that all irrigation intervals treatments responded differently to stimulating compound application. Khan et al. (2016) found that application of plant growth regulators (gibberellic acid, indole acetic acid and kinetin) significant increase in soluble protein contents of two rice cultivars. These results are in coincidence with that reported by Akita (1989), Canady (2012), Anonymous (2013), Abdel-Megeed et al. (2017, 2020), Gharieb et al. (2016), Bhattacharya (2019) and Metwally et al. (2020).

Table 9. *Protein, carbohydrate and lipids content % of Sakha108 rice cultivars as affected by the interaction between different irrigation intervals and growth regulators in 2018 and 2019 seasons*

	Irrigation intervals							
	I1	**I2**	**I3**	**I4**	**I1**	**I2**	**I3**	**I4**
	2018				**2019**			
	Protein							
(T_1)	9.83a-d	9.61b-f	9.33c-h	9.52b-g	8.28h-l	8.06k-n	7.78n-p	7.97m-o
(T_2)	10.25ab	10.03a-c	9.75a-e	9.94a-d	8.80c-e	8.58e-h	8.30h-l	8.49f-i
(T_3)	10.42a	10.20ab	9.92a-d	10.11ab	9.44a	9.22ab	8.94b-d	9.13b
(T_4)	8.94f-k	8.66h-m	8.51i-n	8.06l-s	7.88m-o	8.31h-l	8.16j-m	7.00u-x
(T_5)	9.09e-j	8.81g-l	8.66h-m	8.21k-r	8.03k-n	8.81c-e	8.66d-f	7.15s-w
(T_6)	9.51b-g	9.23d-i	9.08e-j	8.63h-m	8.13j-m	9.23ab	9.08b-c	7.25r-v
(T_7)	8.62h-m	8.34j-p	8.19k-r	7.74o-u	7.41q-t	8.34g-k	8.19i-m	6.53yz
(T_8)	8.72h-m	8.44j-o	8.29i-q	7.84n-u	7.51p-r	8.44f-j	8.29h-l	6.63yz
(T_9)	8.91f-k	8.63h-m	8.48i-o	8.03m-s	7.68o-q	8.63e-g	8.48f-i	6.80xy
(T_{10})	8.05l-s	7.74o-u	7.57q-u	7.11u	7.12t-w	7.43q-s	7.26r-v	6.18z
(T_{11})	8.27k-q	7.96m-t	7.79n-u	7.33s-u	7.24r-v	7.96m-o	7.79n-p	6.30z
(T_{12})	8.50i-o	8.19k-r	8.02m-s	7.56q-u	7.30r-u	8.19j-m	8.02l-n	6.36z
(T_{13})	7.82n-u	7.47r-u	7.26tu	7.60p-u	6.94wx	6.59yz	6.97v-x	6.72xy
	Carbohydrate							
(T_1)	76.94ab	75.72e-k	75.44j-m	75.63g-k	78.05cd	76.83lm	76.55q-t	76.74no
(T_2)	77.04ab	75.82d-i	75.54i-l	75.73e-t	78.13bc	76.91l	76.63p-q	76.82l-n
(T_3)	77.19a	75.97d-f	75.69e-k	75.88d-h	78.22a	77.00k	76.72o	76.91l
(T_4)	76.58c	75.30lm	75.15mn	74.70p-r	78.02de	76.74no	76.59q-s	76.14y
(T_5)	76.85bc	75.57h-l	75.42j-m	74.97n-p	78.18ab	76.90l	76.75m-o	76.30w
(T_6)	76.89b	75.61g-l	75.46j-l	75.01no	78.19ab	76.91l	76.76m-o	76.31vw
(T_7)	75.99de	74.71p-r	74.56q-t	74.11u-w	77.82g	76.54r-t	76.39uv	75.94z
(T_8)	76.08d	74.80o-q	74.65q-s	74.20uv	77.90fg	76.62p-r	76.47tu	76.02z
(T_9)	76.84bc	75.56i-l	75.41k-m	74.96n-p	77.96ef	76.68op	76.53st	76.08yz
(T_{10})	75.67f-k	74.36s-u	74.19uv	73.73x	77.46i	76.15xy	75.98z	75.52z
(T_{11})	75.82d-i	74.51q-t	74.34tu	73.88wx	77.47i	76.16xy	75.99z	75.53z
(T_{12})	75.89d-g	74.58q-t	74.41r-u	73.95vwx	77.71h	76.40u	76.23wx	75.77z
(T_{13})	75.56i-l	74.21uv	74.00v-x	74.34tu	77.30j	75.95z	75.74z	76.08yz

The ash, phosphorus and potassium contents in milled rice grains differed significantly among genotypes and stimulating compounds, with a significant interaction (*Tables 10* and *11*). Ash, phosphorus and potassium contents was higher when rice plant irrigated every 3-days followed by irrigation every 6-days and 9-days

http://www.aloki.hu ● ISSN 1589 1623 (Print) ● ISSN 1785 0037 (Online)
DOI: http://dx.doi.org/10.15666/aeer/2003_20952112

without any significant between them, while irrigation every 12-days come in the last ranks and recorded the lowest ash, phosphorus and potassium contents. Stimulating compounds foliar application spray increased the content of ash, phosphorus and potassium in milled rice grains compared to control. Data indicated that Crop plus treatments of plant growth biostimulated at all tested growth stages with different concentration recorded the nearly the same value of ash, phosphorus and potassium contents and came in the first rank followed by when rice planted treated by Cytokinin which came in the second rank in the two seasons of study without any significant differences among them. The lowest value of ash, phosphorus and potassium contents recorded when rice plant not treated by any of plant growth regulator (Tap water only). These results are in coincidence with that reported by Akita (1989), Gemici (1993), Gemici et al. (1998), Canady (2012), Anonymous (2013), European Bio-stimulants Industry Council (2013), Bhattacharya (2019) and Abdel-Megeed et al. (2020).

Table 10. *Ash, phosphorus and potassium content % of Sakha108 rice cultivars as affected by different irrigation intervals and growth regulators during 2018 and 2019 season*

Treatments	2018			2019		
	Ash content %	Phosphorus content %	Potassium content %	Ash content %	Phosphorus content %	Potassium content %
Irrigation interval (A):						
(I_1)	0.64a	0.25a	0.23a	0.61a	0.26a	0.25a
(I_2)	0.61b	0.22b	0.20b	0.58b	0.23b	0.23b
(I_3)	0.59b	0.20b	0.18b	0.57b	0.21b	0.21b
(I_4)	0.57c	0.18c	0.16c	0.54c	0.19c	0.18c
F Test	**	**	**	**	**	**
Growth regulates treatment (B):						
(T_1)	0.67bc	0.26a	0.23a-c	0.64bc	0.26a-c	0.25a-c
(T_2)	0.69ab	0.26a	0.23ab	0.66ab	0.27ab	0.26ab
(T_3)	0.72a	0.26a	0.24a	0.68a	0.27a	0.26a
(T_4)	0.61ef	0.22bc	0.19d-f	0.58ef	0.22de	0.21de
(T_5)	0.62de	0.22bc	0.20c-e	0.60de	0.23cde	0.22c-e
(T_6)	0.65cd	0.23ab	0.20bcd	0.62cd	0.24bcd	0.23b-d
(T_7)	0.57g	0.20bcd	0.16ef	0.54g	0.20e	0.19e
(T_8)	0.58fg	0.20bcd	0.17d-f	0.56fg	0.21de	0.21de
(T_9)	0.60efg	0.21bcd	0.18d-f	0.57efg	0.21de	0.21de
(T_{10})	0.51h	0.18d	0.17d-f	0.51h	0.19e	0.20de
(T_{11})	0.52h	0.19cd	0.17d-f	0.51h	0.20e	0.21de
(T_{12})	0.54h	0.19cd	0.18d-f	0.51h	0.21de	0.21de
(T_{13})	0.51h	0.19cd	0.16f	0.50h	0.20e	0.18e
F Test	**	*	*	**	*	*
Interaction: AXB	*	*	*	*	*	*

I1: irrigation every3-days, I2: irrigation every 6-days, I3: irrigation every 9-days, I4: irrigation every 12-days, T_1: 0.5 ml Crop plus, T_2: 1.00 ml Crop plus, T_3: 1.5 ml Crop plus, T_4: 15 ppm Cytokinin, T_5: 20 ppm Cytokinin, T_6: 25 ppm Cytokinin, T_7: 15 ppm ABA, T_8: 20 ppm ABA, T_9: 25 ppm ABA, T_{10}: 1 ml Trafos K, T_{11}: 1.5 ml Trafos K, T_{12}: 2 ml Trafos K, T_{13}: Tap water

Regarding the interaction effect data in *Table 11* revealed that statistical differences were found in ash, phosphorus and potassium contents due to the interaction between different irrigation intervals and various plant growth regulators in both seasons.

http://www.aloki.hu ● ISSN 1589 1623 (Print) ● ISSN 1785 0037 (Online)
DOI: http://dx.doi.org/10.15666/aeer/2003_20952112

Table 11. *Ash, phosphorus and potassium content % of Sakha108 rice cultivars as affected by the interaction between different irrigation intervals and growth regulators in 2018 and 2019 seasons*

	Irrigation intervals							
	I1	**I2**	**I3**	**I4**	**I1**	**I2**	**I3**	**I4**
	2018				**2019**			
	Ash content %							
(T_1)	0.70a-d	0.68a-f	0.65c-i	0.67b-g	0.67a-e	0.65a-g	0.62b-j	0.64a-h
(T_2)	0.72a-c	0.69a-d	0.67b-g	0.69a-e	0.69ab	0.67a-f	0.64a-h	0.66a-f
(T_3)	0.75a	0.73ab	0.70a-d	0.72a-c	0.71a	0.69a-c	0.66a-f	0.68a-d
(T_4)	0.65c-i	0.62e-m	0.61f-o	0.56l-u	0.62b-j	0.59f-n	0.58g-p	0.53l-s
(T_5)	0.66b-h	0.63d-l	0.62e-m	0.57j-t	0.64a-h	0.61c-k	0.60e-m	0.55j-r
(T_6)	0.69a-e	0.66b-h	0.65c-j	0.60f-p	0.66a-f	0.63b-i	0.62b-j	0.57g-q
(T_7)	0.61f-n	0.58i-s	0.57k-t	0.52q-x	0.58g-o	0.55j-r	0.54k-s	0.49r-t
(T_8)	0.62e-m	0.59h-r	0.58i-t	0.53o-w	0.60e-l	0.57g-q	0.56i-r	0.51o-t
(T_9)	0.64d-k	0.61f-n	0.59g-q	0.55m-v	0.61d-k	0.58g-o	0.57h-r	0.52m-t
(T_{10})	0.55m-v	0.52r-x	0.50t-x	0.46x	0.55j-s	0.52n-t	0.50p-t	0.46t 0.46t
(T_{11})	0.56l-v	0.53p-x	0.51s-x	0.47wx	0.55j-s	0.52n-t	0.50p-t	0.46t
(T_{12})	0.58i-s	0.55m-v	0.53o-w	0.49u-x	0.55j-s	0.52n-t	0.50p-t	0.51o-t
(T_{13})	0.54n-w	0.51s-x	0.48v-x	0.52r-x	0.53l-t	0.49q-t	0.47st	
	Phosphorus content %							
(T_1)	0.28ab	0.26a-e	0.23a-k	0.25a-g	0.29ab	0.26a-f	0.24a-l	0.25a-g
(T_2)	0.28ab	0.26a-e	0.23a-k	0.25a-g	0.29a	0.27a-f	0.24a-j	0.26a-g
(T_3)	0.29a	0.27a-d	0.24a-i	0.26a-e	0.30a	0.28a-d	0.25a-i	0.27a-f
(T_4)	0.26a-f	0.23a-k	0.21a-m	0.17h-n	0.26a-f	0.24a-l	0.22a-n	0.18h-n
(T_5)	0.26a-e	0.23a-j	0.22a-l	0.17g-n	0.27a-e	0.24a-j	0.23a-m	0.18g-n
(T_6)	0.27a-c	0.25a-g	0.23a-k	0.19e-n	0.28a-c	0.25a-i	0.24a-l	0.19f-n
(T_7)	0.24a-h	0.21a-l	0.20c-n	0.15k-n	0.24a-j	0.21b-n	0.20d-n	0.15mn
(T_8)	0.24a-h	0.21a-l	0.20c-n	0.15k-n	0.25a-i	0.22a-n	0.21c-n	0.16k-n
(T_9)	0.25a-g	0.22a-k	0.21b-m	0.16i-n	0.25a-h	0.23a-m	0.21b-n	0.17j-n
(T_{10})	0.22a-k	0.19d-n	0.17g-n	0.13n	0.24a-k	0.21b-n	0.19f-n	0.14n
(T_{11})	0.23a-k	0.20c-n	0.18e-n	0.14mn	0.24a-j	0.21f-n	0.19e-n	0.15n
(T_{12})	0.24a-j	0.20b-m	0.19e-n	0.14l-n	0.25a-i	0.22e-n	0.20c-n	0.16l-n
(T_{13})	0.21a-l	0.18f-n	0.16j-n	0.19d-n	0.23a-l	0.20c-n	0.17i-n	0.21b-n
	Potassium content %							
(T_1)	0.25a-c	0.23a-h	0.20a-m	0.22a-i	0.28a-c	0.25a-e	0.23a-i	0.24a-g
(T_2)	0.26ab	0.24a-f	0.21a-k	0.23a-h	0.28ab	0.26a-d	0.23a-i	0.25a-e
(T_3)	0.27a	0.25a-d	0.22a-j	0.24a-f	0.29a	0.27abc	0.24a-h	0.26a-d
(T_4)	0.23a-h	0.20a-m	0.19b-p	0.14j-p	0.25a-e	0.22a-i	0.21b-j	0.16h-j
(T_5)	0.24a-g	0.21a-l	0.19a-o	0.15i-p	0.26a-d	0.23a-i	0.22a-j	0.17f-j
(T_6)	0.24a-e	0.22a-j	0.20a-n	0.16h-p	0.27a-c	0.24a-h	0.23a-i	0.18d-j
(T_7)	0.20a-m	0.17d-p	0.16g-p	0.11p	0.23a-i	0.20d-j	0.19d-j	0.14j
(T_8)	0.21a-k	0.18b-p	0.17e-p	0.12n-p	0.25a-f	0.22b-j	0.20b-j	0.16ij
(T_9)	0.22a-j	0.19a-o	0.18c-p	0.13k-p	0.25a-e	0.23b-j	0.21b-j	0.17g-j
(T_{10})	0.22a-j	0.18b-p	0.17e-p	0.12op	0.25a-f	0.22c-j	0.20c-j	0.15ij
(T_{11})	0.22a-j	0.19b-p	0.17d-p	0.12m-p	0.25a-e	0.22b-j	0.20b-j	0.16ij
(T_{12})	0.22a-i	0.19a-o	0.17c-p	0.13m-p	0.25a-e	0.22b-j	0.21b-j	0.16ij
(T_{13})	0.19b-p	0.15i-p	0.13l-p	0.16f-p	0.21b-j	0.18ij	0.15ij	0.19d-j

I1: irrigation every3-days, I2: irrigation every 6-days, I3: irrigation every 9-days, I4: irrigation every 12-days, T_1: 0.5 ml Crop plus, T_2: 1.00 ml Crop plus, T_3: 1.5 ml Crop plus, T_4: 15 ppm Cytokinin, T_5: 20 ppm Cytokinin, T_6: 25 ppm Cytokinin, T_7: 15 ppm ABA, T_8: 20 ppm ABA, T_9: 25 ppm ABA, T_{10}: 1 ml Trafos K, T_{11}: 1.5 ml Trafos K, T_{12}: 2 ml Trafos K, T_{13}: Tap water

http://www.aloki.hu ● ISSN 1589 1623 (Print) ● ISSN 1785 0037 (Online)
DOI: http://dx.doi.org/10.15666/aeer/2003_20952112

Spraying Crop plus with different concentration even 1.5, 1.00 and 0.5 ml/1 l water gave the highest ash content under irrigation every 3, 6, 9 and 12-days and recorded nearly the same value without any significant difference between them. For phosphorus and potassium contents data showed that crop plus and cytokinin spraying with different concentration recorded nearly the same value of phosphorus and potassium contents under different irrigation intervals 3, 6 and 9-days while under irrigation every 12-days crop plus come in the first rank and recorded the highest value of phosphorus and potassium contents. Pan et al. (2013) reported that foliar application of different stimulating compounds could enhance the lodging resistance and increase root biomass and root activity to improve phosphorus and potassium accumulation in milled grains. These results are in harmony with that recorded by Anjum et al. (2007), Singh (2011), Cuevas et al. (2016), Gharieb et al. (2016), Metwally et al. (2016, 2020) and Zhao (2018).

Conclusion

The low availability of water during this work had less effect on the yields. This might be due to its late occurrence during the rice plants life cycles. Similar results were found by Boonjung and Fukai (1996). Husking yield gave an idea of the total amount of edible grains after husking. Results showed that this trait was very slightly affected by the occurrence of drought at ripening stage. Therefore, the occurrence of drought during grain ripening stage could be considered as a useful factor that might help to reduce broken grain in milled rice with high level of head whole. Several factors are generally recognized as probable cause of breakage of rice during milling.

The study clearly showed physico-chemical variation in rice grain when moisture stress occurs during grain maturity stage. There were significant differences among both the stressed and the check samples. Late drought that occurs during ripening stage appears to decrease the main characteristics defining rice grain quality including total milling rate, head rice ratio, and protein content. Since the criteria of choice of a given variety depend on each consumer, it might not be well advised to conclude that the occurrence of water deficit during ripening stage necessarily or not enhance rice grain quality. However, the reproducibility of this trial is possible only in the case where weather conditions remain similar throughout consecutive years. The progressive higher carbon dioxide concentration due to climate change might be a limiting factor since the biosynthesis of protein and amylose which are the key elements of grains component is significantly influenced by atmospheric conditions especially after heading stage. More investigations should be done on water stress at rice plant reproductive stage to better understand the physiological phenomenon that happened when this constrain occurs

Irrigation every 3 days gave the highest grain quality without any significant differences with irrigation every 6 days followed by 9 days while irrigation every 12 days recorded the lowest grain quality. According to the previous results, it can be concluded that sprayed Sakha 108 rice cultivar by Crop plus and Cytokinin under water stress increase the rice grain quality. Also, Sakha 108 rice cultivar responded to Crop plus application compared to other regulator growth under water stress. Crop plus prolonged the irrigation interval from 3 days up to 9 days without any significant difference in grain quality. These results are very important for the farmers whose have shortage of water in rice fields without any negative effective on grain quality.

http://www.aloki.hu ● ISSN 1589 1623 (Print) ● ISSN 1785 0037 (Online)
DOI: http://dx.doi.org/10.15666/aeer/2003_20952112

Finally, this study needed to more study to reach the best results about using different growth regulators under different water stress with more studies for determine the amount of irrigation intervals.

REFERENCES

[1] A. O. A. C. (2000): Official and Tentative Methods of Analysis. 2nd Ed. – American Oil Chemists Society, Chicago, IL.
[2] Abd Allah, A. A., Mohamed, A. A. A., Gab-Allah, M. M. (2009): Genetic studies of some physiological and shoot characters in relation to drought tolerance in rice. – J. Agric. Res. Kafrelsheikh Univ. 35(4).
[3] Abdel-Megeed, T. M., El-Habet Howida, B. I., Hashem, I. M., Badawy, S. A. (2017): Impact of some plant growth regulating substances on the yield and its components of Giza179 and Giza177 rice cultivars under different irrigation interval treatments. – J. Plant Production, Mansoura Univ. 8(3): 369-379.
[4] Abdel-Megeed, T. M., Gharib, H. S., Hafez, E. M., El-Sayed, A. (2020): Effect of some plant growth regulators and biostimulants on the productivity of Sakha108 rice plant (*Oryza sativa* L.) under different water stress conditions. – Applied Ecology and Environmental Research 19(4): 2859-2878.
[5] Akita, S. (1989): Field Evaluation of Cytozyme Crop Plus on Grain Yield of Rice. (Preliminary Results). Worldwide Research on Cytozyme Products. Abstract. – Cytozyme Laboratories Inc., U.S.A.
[6] Anjum, F. M., Pasha, I., Bugti, M. A., Butt, M. S. (2007): Mineral composition of different rice varieties and their milling fractions. – Pakistan Journal of Agricultural Sciences 44(2): 332-336.
[7] Anonymous (2013): Bio-Stimulants market - By Active Ingredients, Application, Crop Types & Geography-Global Trends & Forecasts to 2018. – www.marketsandmarkets.com.
[8] Bao, J. S. (2012): Toward understanding the genetic and molecular bases of the eating and cooking qualities of rice. – Cereal Foods World 57: 148-156.
[9] Bhattacharya, A. (2019): Effect of High-Temperature Stress on the Metabolism of Plant Growth Regulators. Chap. 6. – Indian Institute of Pulses Research, Kanpur, India, pp. 485-591.
[10] Black, C.A., Evans, D. D., Ensminger, L. E., Clark, F. E. (1965): Methods of Soil Analysis. Part 2. Chemical and Microbiological Properties. – American Soc. of Agronomy, Inc., Madison, WI.
[11] Boonjung, H., Fukai, S (1996): Effects of soil water deficit at different growth stages on rice growth and yield under upland conditions. – Phenol. Biomass Prod. Yield 48: 47-55.
[12] Canady, M. (2012): Effect of Crop plus on physiological response related to photosynthesis in citrus. – Technical Data Reports, Cytozyme Laboratories, Inc. 10(1).
[13] Cruscio, C. A. C., Arf, O., Soratto, R. P., Mateus, G. P. (2008): Grain quality of upland rice cultivars in response to cropping systems in the Brazilian tropical savanna. – Sci. Agric. (Piracicaba, Braz.) 65(5): 468-473.
[14] Chapman, H. D., Pratt, P. F. (1961): Method of Analysis for Soils Plant and Water. - California Citrus Experiment Station, Univ. of California, Division of Agricultural Sciences, USA.
[15] Cooper, P. J. M., Gregory, P. J., Keating, J. D. H., Brown, S. C. (1987): Effect of fertilizer, variety and location on barley production under rainfed conditions in northern Syria. 2. Soil water dynamics and crop water use. – Field Crops Res. 16: 67-84.
[16] Craigie, J. S. (2011): Seaweed extract stimuli plant science and agriculture. – J. Appl. Phycol. 23: 371-393.

http://www.aloki.hu ● ISSN 1589 1623 (Print) ● ISSN 1785 0037 (Online)
DOI: http://dx.doi.org/10.15666/aeer/2003_20952112

[17] Cruz, N. D., Khush, G. S. (2000): Rice Grain Quality Evaluation Procedures. – In: Singh, R. K. et al. (eds.) Aromatic Rices. Oxford & IBH Publishing, New Delhi, pp.15-28.
[18] Cuevas, R. P., Pede, V. O., McKinley, J., Velarde, O., Demont, M. (2016): Rice grain quality and consumer preferences: a case study of two rural towns in the Philippines. – PLoS ONE 11(3): e0150345. https://doi.org/10.1371/journal.pone.0150345.
[19] Duncan, B. (1955): Multiple range and multiple F. test. – Biometrics 11: 1-42.
[20] European Bio-stimulants Industry Council (2013): Economic Overview of the Bio-stimulants Sector in Europe. – https://biostimulants.eu/.
[21] Fraser, J. R., Holmes, D. C. (1959): Proximate analysis of wheat flour carbohydrates. IV Analysis of whole meal flour and some of its fractions. – Journal of the Science of Food and Agriculture 10(9): 506-512.
[22] Frei, M., Becker, K. (2005): On Rice, Biodiversity & Nutrients. – University of Hohenheim, Stuttgart. http://www. greenpeaceweb. org/gmo/nutrients. pdf.
[23] Gandah, M., Bouma, J., Brown, J., Hiernaux, P., Van-Duivenbooden, N. (2003): Strategies to optimize allocation of limited nutrients to sandy soils of the Sahel: a case study from Niger, West Africa. – Agric. Ecosyst. Environ. 94: 311-319.
[24] Gemici, M. (1993): Effect of Cytozyme Crop plus on Triticum durum (Wheat). – Doga-Tr. J. of Botany. 17. 133-139.
[25] Gemici, M., Güven, A., Katmerm, P. (1998): Effects of Cytozyme Crop Plus on Lycopersicum esculentum Mill. – Plant Yield. Tr. J. of Botany 22: 7-11.
[26] Gharieb, A. S., Metwally, T. F., Abou-Khadrah, S. H., Glela, A. A., El Sabagh, A. (2016): Quality of rice grain is influenced by organic and inorganic sources of nutrients and antioxidant application. – Cercetari Agronomice in Moldova (Agronomic Research in Moldavia) (4168): 57-68.
[27] Gomez, K. A., Gomez, A. A. (1984): Statistical Procedures of Agricultural Research. 2nd Ed. – John Wiley and Sons, New York.
[28] Hare, P. D., Cress, W. A., Van Staden, J. (1997): The involvement of cytokinins in plant responses to environmental stress. – Plant Growth Regul. 23: 79-103.
[29] Jackson, M. L. (1967): Soil Chemical Analysis. – Prentice Hall of India, New Delhi, pp. 144-197.
[30] Kamboj, S., Mathpal, B. (2019): Improving rice grain quality by foliar application of plant growth regulators under various mode of Zn application. – Plant Archives 19(2): 2181-2184.
[31] Khan, S. U., Gurmani, A. R., Qayyum, A., Abbasi, K. S., Liaquat, M., Zahoor, A. (2016): Exogenously applied gibberellic acid, indole acetic acid and kinetin as potential regulators of source-sink relationship, physiological and yield attributes in rice (*Oryza sativa*) genotypes under water deficit conditions. – International Journal of Agriculture and Biology 18(1): 139-145.
[32] Metwally, T. F., El-Zun, H. M., Abdelfattah, N. A. H. (2016): Performance of some rice genotypes sown on different dates in yield, quality traits and infestation by lesser grain borer. – Journal of Plant Production, Mansoura University, Egypt 7(9): 973-982.
[33] Metwally, T. F., Mohamed, A. A. E., Sorour, S. G. R., Elsayed, G. A. (2020): Stimulating compounds affect the grain quality characteristics and the nutritional value of rice (Oryza sativa). – Applied Ecology and Environmental Research 18(5):6829-6840.
[34] Mohapatra, D., Bal, S. (2006): Cooking quality and instrumental textural attributes of cooked rice for different milling fractions. – Journal of Food Engineering 73(3): 253-254.
[35] Okabe, M. (1979): Texture measurement of cooked rice and its relationship to the eating quality. J. Texture Stud. 10: 131-152.
[36] Pan, S., Rasul, F., Li, W., Tian, H., Mo, Z., Duan, M., Tang, X. (2013): Roles of plant growth regulators on yield, grain qualities and antioxidant enzyme activities in super hybrid rice (*Oryza sativa* L.) – Rice 6(1): 1-10.

http://www.aloki.hu ● ISSN 1589 1623 (Print) ● ISSN 1785 0037 (Online)
DOI: http://dx.doi.org/10.15666/aeer/2003_20952112

[37] Peterpurgski, A. V. (1968): Handbook of Agronomic Chemistry. – Kolos Publishing House, Moscow, pp. 29-86 (in Russian).
[38] Pospíšilová, J., Rulcová, J. (1999): Can synthetic cytokinins alleviate water stress in Phaseolus vulgaris leaves? – Biol. Plant. 42(Suppl.): S77.
[39] Pospíšilová, J., Synková, H., Rulcová, J. (2000): Cytokinins and water stress. – Biologia Plantarum 43(3): 321-328.
[40] Ramya, S. S., Nagaraj, S., Vijayanand, N. (2011): Influence of seaweed liquid extracts on growth, biochemical and yield characteristics of Cyamopsis tetragonolaba (L.) Taub. – Journal of Phytology 3(9): 37-41.
[41] Rousset, S., Pons, B., Martin, J. M. (1999): Identifying objective characteristics that product clusters produced by sensory attributes in cooked rice. – J. Texture Stud. 30: 50-532.
[42] Samonte, S., Wilson, L. T., McClung, A. M., Tarpley, L. (2001): Seasonal dynamics of non-structural carbohydrate in 15 diverse rice genotypes. – Crop Sci. 41: 902-909.
[43] Singh, N., Pala, N., Mahajan, G., Singh, S., Shevkani, K. (2011): Rice grain and starch properties: effects of nitrogen fertilizer application. – Carbohydrate Polymers 86(1): 219-225.
[44] Singh, N., Singh, D. (2019): The nutritional composition of local rice varieties in Guyana. – Greener Journal of Agricultural Sciences 9(2): 138-145.
[45] Tomlins, K. I., Manful, J. T., Larwer, P., Hammond, L. (2005): Urban consumer preference and sensory evaluation of locally produced and imported rice in West Africa. – Food Qual. Preference 16: 79-89.
[46] Vidal, V., Pons, B., Brunnschweiler, J., Handschin, S., Rouau, X., Mestres, C. (2007): Cooking behavior of rice in relation to kernel physicochemical properties. – J. Agric. Food Chem. 55: 336-346.
[47] Waller, R. A., Ducan, D. B. (1969): Bayes rule for the Symmetric Malliple Comason problem. – J. Am. Stat. Assoc. 64: 1484-1499.
[48] Watanabe, F. S., Olsen, S. R. (1965): Test of an ascorbic acid method for determining phosphorus in water and NaHCO3 extracts from soils. – Soil Science Society of America Journal S29(6): 677-678.
[49] Zhao, D. S., Li, Q. F., Zhang, C. Q., Zhang, C., Yang, Q. Q., Pan, L. X., Ren, X. Y., Lu, J., Gu, M. H., Liu, Q. Q. (2018): GS9 acts as a transcriptional activator to regulate rice grain shape and appearance quality. – Nature Communications 9(1): 1-14.
[50] Zheng, C., Zhang, Z., Hao, S., Chen, W., Pan, Y., Wang, Z. (2020): Agronomic growth performance of super rice under water-saving irrigation methods with different water-controlled thresholds in different growth stages. – Agronomy 10: 239.

http://www.aloki.hu ● ISSN 1589 1623 (Print) ● ISSN 1785 0037 (Online)
DOI: http://dx.doi.org/10.15666/aeer/2003_20952112

EFFECTS OF ANTHOCYANINS ON FUNCTIONS OF PHOTOSYNTHESIS SYSTEM IN THREE SYRINGA LEAVES UNDER LOW LIGHT CONDITIONS

CAI, Y.[1#] – QI, Y.[2#] – ZHU, S.[1] – NIAN, H.[1] – LIU, X.[1*] – AN, B.[1*]

[1]*College of Horticulture, Jilin Agricultural University, Changchun 130118, China*

[2]*Jilin Economic Management Cadre Institute, Changchun 130118, China*

[#]*These authors contributed equally to this work*

*****Corresponding authors*
e-mail: jlndbya2020@126.com (An, B.); 112345818@qq.com (Liu, X.)

(Received 28th Jul 2021; accepted 26th Jan 2022)

Abstract. In this study, taking *Syringa oblata Iandl* (SI), *Syringa oblata var. affinis Lingelsh* (SL) and *Syringa chinensis* (SC) as the test material, the functional role of anthocyanins in photosynthetic apparatus in leaves of three varieties under different light conditions were investigated. In the low light, P_n, G_s and T_r values of *Syringa* leaves decreased. Meanwhile, minimal fluorescence (F_o), maximum fluorescence (F_m) and absorption flux per reaction center (*ABS*/*RC*) in young leaves of SI was lower than those of SL and SC, which indicated that anthocyanins could reduce the absorption of light in *Syringa* leaves. Furthermore, the parameters of PSII photochemical efficiency (F_v/F_m), PSII potential activities (F_v/F_o), electron transport rate (*ETR*) and actual photochemical efficiency (Φ_{PSII}) of SI was higher than that of SL and SC in low light, respectively. The number of PSII reactive center, *ABS*/*RC*, maximal trapped energy flux per reaction center (TR_o/RC), electron transport flux per reaction center (ET_o/RC) and dissipated energy flux per reaction center (DI_o/RC) of SL and SC were significantly higher those of SI in low light, while the proportion of inactivation of reactive center in SL and SC were higher than others in low light.
Keywords: *Syringa, anthocyanin, PSII, chlorophyll fluorescence, OJIP*

Introduction

Anthocyanin is an important water-soluble compound, which drives from glycosylation derives of anthocyanidin through combining different monosaccharides with glucosidic bond. The chemical species play functions as osmotic adjustment substances in abiotic stresses such as high light, low temperature and strong UV-light. Most salient among the flavonoids were the anthocyanins-universal plant colorants presented the red, purple, and blue hues apparent in many fruits, vegetables, cereal grains, and flowers. Some plant species show red leaves, this is mainly due to the accumulation of anthocyanins that covered the green chlorophyll reflectance, although accumulation was usually transient (Gould et al., 1995). Leaf anthocyanins have positive effects on various damages caused by photooxidation (Gould et al., 2002), UV-B radiation (Lindoo and Caldwell, 1978; Mendez et al., 1999), and pests and diseases (Hamilton et al., 2001; Karageorgou and Manetas, 2006). Particularly anthocyanins can protect photosynthetic apparatus against high light and alleviate photoinhibition. The Anthocyanin has a strong absorption in the visible spectrum between 400 nm and 600 nm. Similar as photosynthetic pigments, anthocyanins in vegetative tissues preferentially absorb green and ultraviolet light and present lower absorbance of blue light, while little absorbance of red light. The absorption characteristics of anthocyanins has potential roles in consumption of excess light captured by leaf chlorophyll. The

http://www.aloki.hu ● ISSN 1589 1623 (Print) ● ISSN 1785 0037 (Online)
DOI: http://dx.doi.org/10.15666/aeer/2003_21132128

accumulation of anthocyanins disturbs efficiency of leaf absorption to light energy, and the distribution of light energy in the photosynthetic apparatus. In recent years, light regulation on anthocyanin synthesis during photomorphogenesis have been widely studied by molecular and Chlorophyll fluorescence tools (Burger and Edwards, 1996; Dodd et al., 1998). Anthocyanin, the PSI and the PSII synthesis were regulated by the phytochrome–mediated activation of their respective signal transduction pathways. Synthesis of anthocyanins and lack of chlorophyll have significant impacts on leaf photosynthesis of many plant species in seedling period, which seedlings are susceptible to light-induced stress. Pietrini and Massacci (1998) found that anthocyanins in red leaves reduced the photosynthetically active radiation reaching the chloroplasts by 40%. Anthocyanin accumulation in leaves also protected the mesophyll cells (Chalker-Scott, 1999), reduced photoinhibition (Hughes and Smith, 2007) and photo-oxidative damage (Steyn et al., 2002) through filtering or attenuating high-power blue-violet with excess solar energy. Short-term cold spells or long-term seasonal low temperature can also induce anthocyanin synthesis. Anthocyanin synthesis is coincided with recovery of photosynthetic activity in cold environments. An increasing accumulation of anthocyanin might be an adaptive response of plants to low temperature. Low temperature has an even greater effect on carbohydrate metabolism by limiting assimilate utilization. Anthocyanin accumulation probably protected the plant tissues exposed to low temperature/light combined stress against photoinhibition.

Syringa has a tree shape, elegant flower color, dense inflorescence, red fruit in early autumn, with high ornamental value, and *Syringa* has a strong cold resistance, *Syringa oblata Iandl* (SI), *Syringa oblata var. affinis Lingelsh* (SL) and *Syringa chinensis* (SC) can be cultivated in the northern of China. Especially *Syringa oblata Iandl* (SI) having purple-red leaves due to anthocyanin accumulation, are important ornamental plants both for flower and foliage (Liu et al., 2010; Xie et al., 2006). However, *Syringa oblata var. affinis Lingelsh* (SL) and *Syringa chinensis* (SC) has green leaves, with very little anthocyanin content in leaves. In the present study, we studied chlorophyll fluorescence parameters of of three *Syringa* species by using the chlorophyll fluorescence technique, and analyzed the effects of anthocyanin accumulation on light absorption, distribution, conversion and electron transfer in photosynthesis processes in natural light and low light. The aim of this study was to reveal the function of anthocyanin in photosynthesis.

Materials and methods

Plant material and growth conditions

The seedlings of *Syringa oblata var. affinis Lingelsh* (SL), *Syringa oblata Iandl* (SI) and *Syringa chinensis* (SC) were provided by Jilin Agricultural University in August 2019. The leaves of *Syringa oblata Iandl* (SI) rich in Ant were purple-red, but the leaves of S*yringa oblata var. affinis Lingelsh* (SL) and *Syringa chinensis* (SC) were all green growing under natural light. The three *Syringa* species were all triennial and 1.5 m height. There were not shaded by shrubs.

Three *Syringa* species were collected for measurement of photosynthetic parameters: Five cuttings of each species were cultivated indoors under an artificial lamp (Microwave sulfur lamp-N1, Suzhou, China) with a lighting intensity of 100 $\mu mol \cdot m^{-2} \cdot s^{-1}$. The other seedlings remained under an outdoor natural. The diurnal variation of photosynthetic active radiation (PAR) and temperature were shown in *Figure 1*. The PAR and temperature were lower in the morning, in particular atmospheric temperature had been

http://www.aloki.hu ● ISSN 1589 1623 (Print) ● ISSN 1785 0037 (Online)
DOI: http://dx.doi.org/10.15666/aeer/2003_21132128

below 10 ℃, which was made a significant effect on photosynthetic apparatus in plant leaves. But at noon, temperature and PAR was still very strong, especially the PAR reached 1800 μmol·m^{-2}·s^{-1}, while the lower the temperature of the environment in the autumn, so light intensity could easily lead to photoinhibition of leaves. Plants under low light or natural light were watered in the same manner, and fertilizers were not applied.

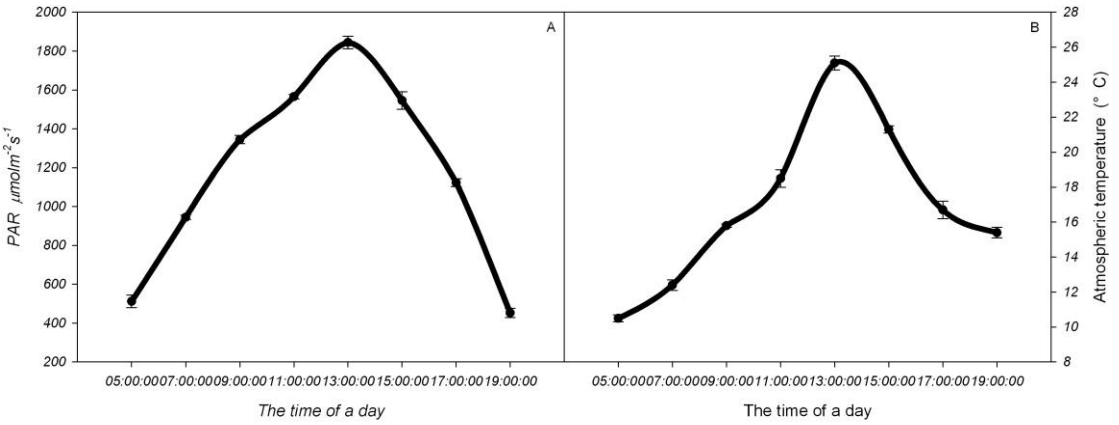

Figure 1. *Diurnal change of PAR and temperature in Jilin Agricultural University in August 2019. Data in the figure are mean ± SD*

Determination of photosynthetic gas exchange parameters

The net photosynthetic rate (P_n), stomatal conductance (G_s), transpiration rate (T_r) and intercellular CO_2 concentration (C_i) of the second fully expanded functional leaf of *Syringa* were measured at 9:00-11:00 a.m. by using Li-6400 photosynthetic measurement system (Licor company, USA). The PFD was provided by the instrument's light source at 1200 μmol·m^{-2}·s^{-1}, and CO_2 concentration was fixed at 400 μmol·m^{-2}·s^{-1} using CO_2 cylinder. The process was repeated 5 times.

Chlorophyll and anthocyanin contents

Contents of Chlorophyll, Chlorophyll 'a' and 'b' were determined by the method of Inskeep and Bloom (1985). Anthocyanin content was measured by the method of Pirie and Mullins (1976).

Chlorophyll fluorescence measurements

We measured the chlorophyll fluorescence parameters (F_m, F_o, F_v/F_m, and F_v/F_o) of the natural light and low light leaves by using a portable pulse amplitude modulation fluorometer (PAM-2000, Walz, Effeltrich, Germany) according to the method of Hu et al. (2007). Apparent electron transport rate (*ETR*) and actual photochemical efficiency (Φ_{PSII}) of the leaves were determined at nature light (about 1200 μmol·m^{-2}·s^{-1}). We also measured light absorption and characteristic parameters of PSII reaction center by the method of Hendrickson (2008) and Zhou (2007), including quantum yield of photochemistry (Φ_{PSII}); quantum yield of trans-thylakoid pH gradient and xanthophyll-regulated thermal energy dissipation (Φ_{NPQ}); quantum efficiency of fluorescence and constitutive thermal dissipation ($\Phi_{f,D}$); and quantum yield of thermal dissipation associated with the presence of non-functional PSII(Φ_{NF}).

http://www.aloki.hu ● ISSN 1589 1623 (Print) ● ISSN 1785 0037 (Online)
DOI: http://dx.doi.org/10.15666/aeer/2003_21132128

A fluorescence induction transient (OJIP) of the low light leaves and natural light leaves were determined by the mini hansatech fluorescence monitoring system (FluorPen FP 100max, Chech). It can get absorption flux per reaction center (*ABS/RC*), rapped energy flux per reaction center (TR_o/RC), electron transport flux per reaction center (ET_o/RC), and dissipated energy flux per reaction center (DI_o/RC). All the above measurements were performed during 9:00 am – 11:00 am, with five replications (Hendrickson et al., 2004).

Determination of OJIP curve

The leaves of different treatments were dark adapted for 0.5 h, then the leaves on the new shoots were selected to fully expand. The OJIP curve was measured by mini modulation palmtop chlorophyll fluorescence meter (fluoropen FP 100 max, Czech Republic), and the fluorescence intensity ft of each time point on the OJIP curve was used to draw the curve.

Statistical analysis

Excel and SPSS software (Version. 22) were used to conduct statistical analyses on the measured data. The data in the figure was denoted as mean ± standard deviation (SD). One way ANOVA and least significant difference (LSD) were used to compare the differences among different data groups.

Results and analysis

Photosynthetic characteristics

The photosynthetic gas exchange parameters of *Syringa* leaves were significantly affected by low light. In the low light, P_n, G_s and T_r values of *Syringa* leaves decreased (*Fig. 2*). The P_n, G_s and T_r descent range of *Syringa oblata var. affinis Lingelsh* (SL) and *Syringa chinensis* (SC) than *Syringa oblata Iandl* (SI).

Chlorophyll and anthocyanin content

The contents of total Chlorophyll, Chla and Chlb in natural light were significantly lower than that in low light for all the three varieties (*Fig. 3A-C*). Ant content of leaves in the low light were higher than that in natural light leaves for *Syringa oblata Iandl* (SI). However, Ant content in leaves of *Syringa oblata Iandl* (SI) showed no significant differences among three varieties of *Syringa* in the low light ($p < 0.05$). Ant content in leaves of *Syringa oblata Iandl* (SI) was significantly increased by 65.3% and 66.1% than that of *Syringa oblata var. affinis Lingelsh* (SL) and *Syringa chinensis* (SC) in the natural light, respectively.

Standardized OJIP curves

According to this standardization of OJIP curve (*Fig. 4A*), compared with the natural light, the relative variable fluorescence V_t of three *Syringa* leaves in low light increased significantly, and the relative variable fluorescence V_I of point I increased significantly more than that of point J (*Fig. 4B-C*). The results showed that the V_J and V_I of *Syringa oblata var. affinis Lingelsh* (SL) and *Syringa chinensis* (SC) under natural light were significantly higher than those of *Syringa oblata Iandl* (SI) ($P<0.05$).

http://www.aloki.hu ● ISSN 1589 1623 (Print) ● ISSN 1785 0037 (Online)
DOI: http://dx.doi.org/10.15666/aeer/2003_21132128

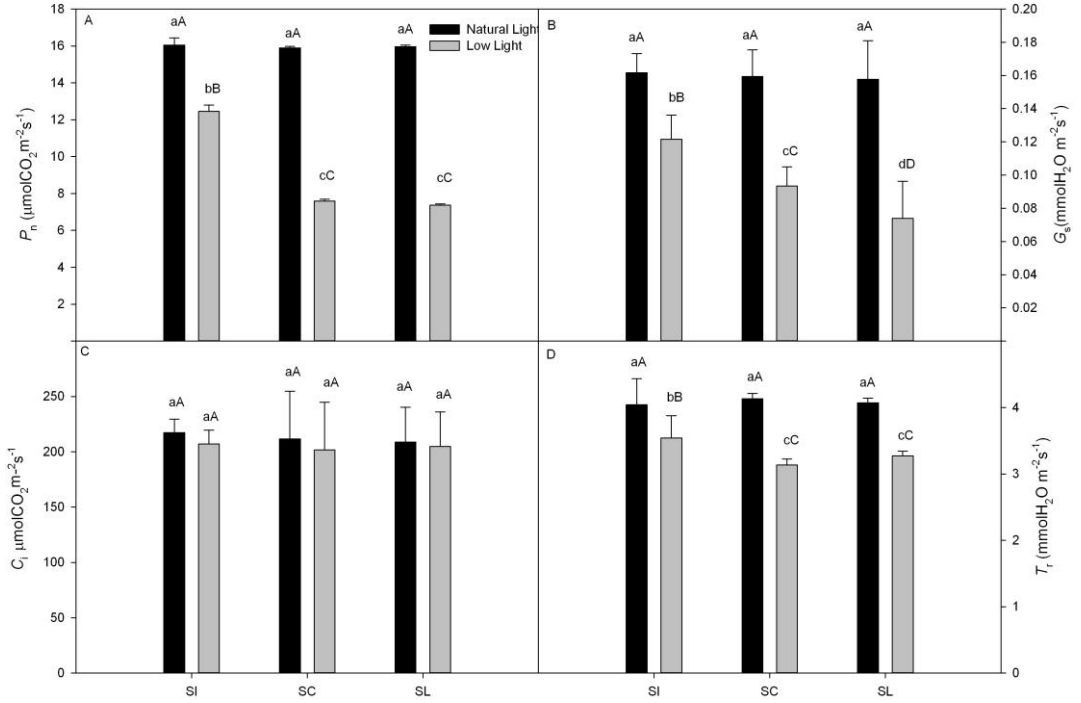

Figure 2. *Photosynthetic characteristics among three varieties of Syringa. Data in the figure are mean ± SD, values followed by different small letters mean significant difference ($p < 0.05$), values followed by different capital letters mean very significant difference ($p < 0.01$). SI: Syringa oblata Iandl; SC: Syringa chinensis; SL: Syringa oblata var. affinis Lingelsh*

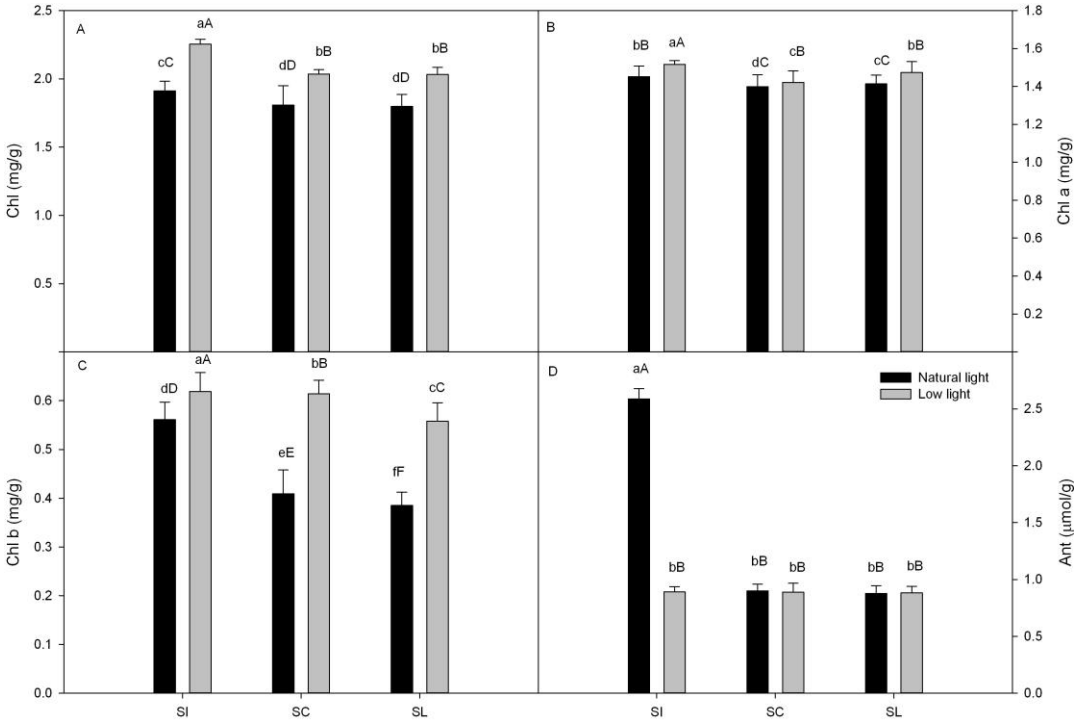

Figure 3. *Chlorophyll and anthocyanin content in leaves among three varieties of Syringa. Data in the figure are mean ± SD, values followed by different small letters mean significant difference ($p < 0.05$), values followed by different capital letters mean very significant difference ($p < 0.01$). SI: Syringa oblata Iandl; SC: Syringa chinensis; SL: Syringa oblata var. affinis Lingelsh*

http://www.aloki.hu ● ISSN 1589 1623 (Print) ● ISSN 1785 0037 (Online)
DOI: http://dx.doi.org/10.15666/aeer/2003_21132128

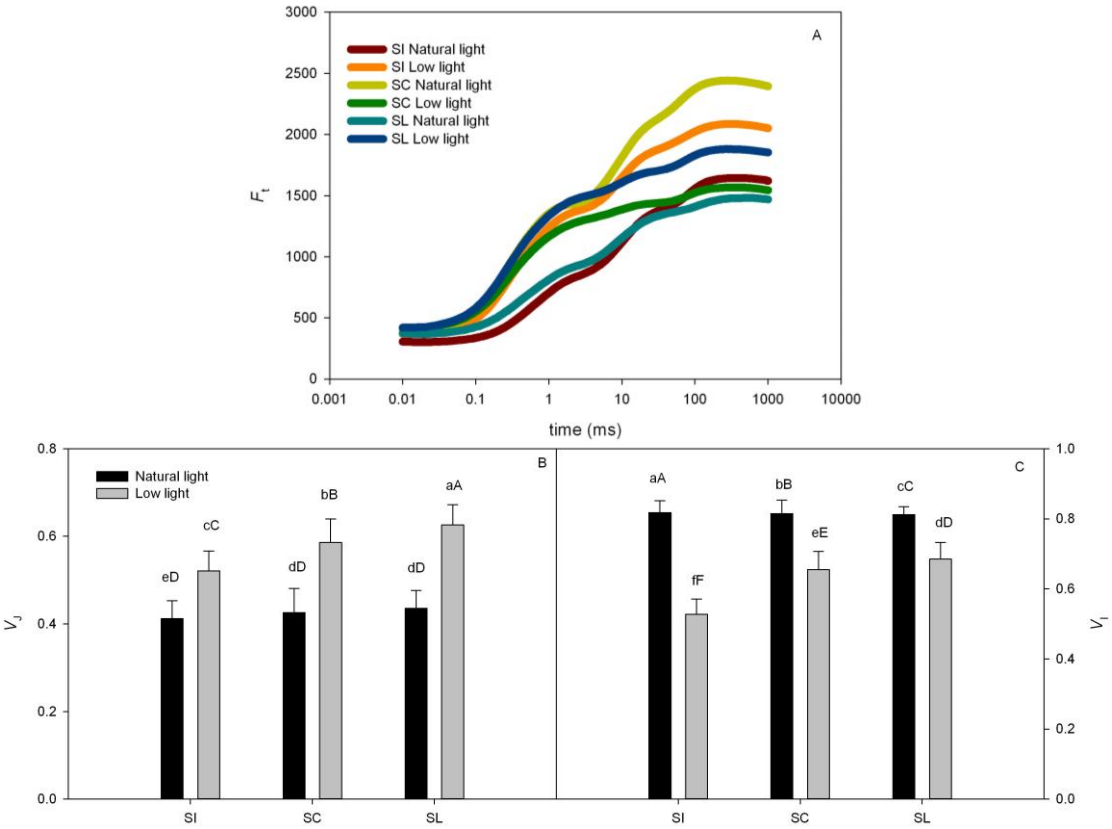

Figure 4. *The rise kinetics of relative variable fluorescence $V_t = (F_t\text{-}F_o)/(F_m\text{-}F_o)$ and difference of V_J and V_I in leaves of 3 cultivars Syringa under different light conditions. Data in the figure are mean ± SD, values followed by different small letters mean significant difference ($p < 0.05$), values followed by different capital letters mean very significant difference ($p < 0.01$). SI: Syringa oblata Iandl; SC: Syringa chinensis; SL: Syringa oblata var. affinis Lingelsh*

Minimal fluorescence (F_o) and maximum fluorescence (F_m)

The F_o of leaves in the natural light were lower than that in the low light leaves for *Syringa oblata Iandl* (SI) significantly ($P<0.01$), but the F_o was lower than *Syringa oblata var. affinis Lingelsh* (SL) and *Syringa chinensis* (SC) (*Fig. 5A*). In *Syringa oblata var. affinis Lingelsh* (SL) and *Syringa chinensis* (SC), F_m of the leaves in the low light were also lower than that in the natural light leaves ($P<0.01$), in the natural light leaves of three *Syringa* at F_o and F_m had no significant difference ($P>0.05$).

PSII photochemical efficiency

F_v/F_m of leaves in the low light was significantly lower than that in the natural light for the three *Syringa* species. F_v/F_o of leaves in the low light were lower than the natural light by 18.89% ($p<0.01$) for *Syringa oblata var. affinis Lingelsh* (SL) and 23.74% ($p<0.01$) for *Syringa chinensis* (SC) (*Fig. 6A-B*). There were no significant difference in F_v/F_o ($p>0.05$) between in the low light and in the natural light leaves of *Syringa oblata Iandl* (SI).

There were no obvious differences in *ETR* and Φ_{PSII} of leaves in the natural light between the three species. However, *ETR* and Φ_{PSII} of leaves in the low light were

http://www.aloki.hu ● ISSN 1589 1623 (Print) ● ISSN 1785 0037 (Online)
DOI: http://dx.doi.org/10.15666/aeer/2003_21132128

significantly lower in *Syringa oblata var. affinis Lingelsh* (SL) than *Syringa oblata Iandl* (SI) by 18.50% and 12.14%, respectively, and *Syringa chinensis* (SC) by 19.38% and 12.30%, respectively. ($p>0.05$) (*Fig. 6C-D*).

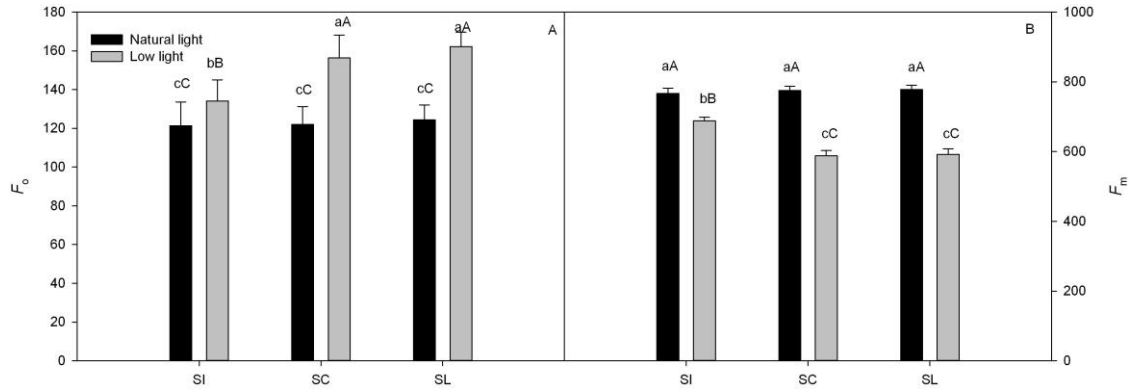

Figure 5. *Minimal fluorescence (F_o) and maximum fluorescence (F_m) in leaves of three Syringa. Data in the figure are mean ± SD, values followed by different small letters mean significant difference ($p < 0.05$), values followed by different capital letters mean very significant difference ($p < 0.01$). SI: Syringa oblata Iandl; SC: Syringa chinensis; SL: Syringa oblata var. affinis Lingelsh*

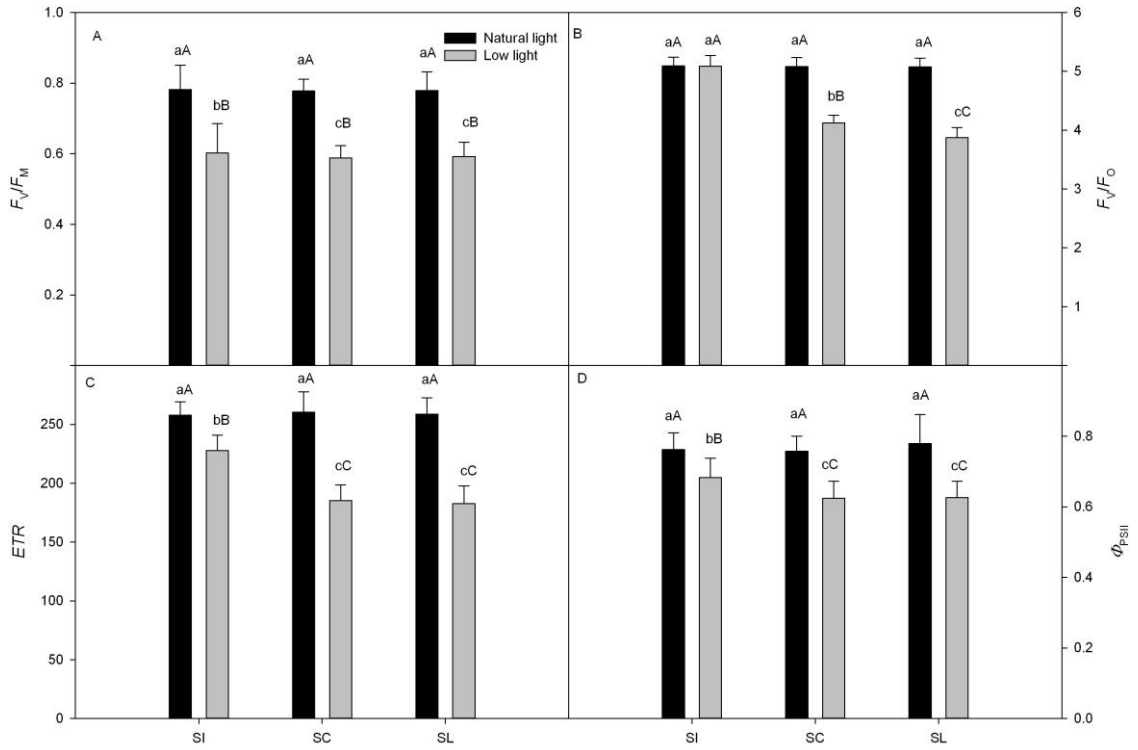

Figure 6. *PSII photochemical efficiency (F_v/F_m), actual photochemical efficiency (Φ_{PSII}), the electron transport rate (ETR) and potential activities (F_o/F_m) in leaves of three Syringa. Data in the figure are mean ± SD, values followed by different small letters mean significant difference ($p < 0.05$), values followed by different capital letters mean very significant difference ($p < 0.01$). SI: Syringa oblata Iandl; SC: Syringa chinensis; SL: Syringa oblata var. affinis Lingelsh*

http://www.aloki.hu ● ISSN 1589 1623 (Print) ● ISSN 1785 0037 (Online)
DOI: http://dx.doi.org/10.15666/aeer/2003_21132128

Specific activity coefficient of PSII reaction center in leaves of Syringa

ABS/*RC*, TR_o/*RC*, ET_o/*RC* and DI_o/*RC* had no significant differences in the natural light for the three *Syringa* (*Fig. 7A-D*). These parameters were significantly higher in the low light than in the natural light ($p < 0.01$) for *Syringa oblata var. affinis Lingelsh* (SL) and *Syringa chinensis* (SC). The values of DI_o/*RC* and ET_o/*RC* of the leaves in the low light were no significant differences between in the natural light and in the low light for *Syringa oblata Iandl* (SI) ($p < 0.05$).

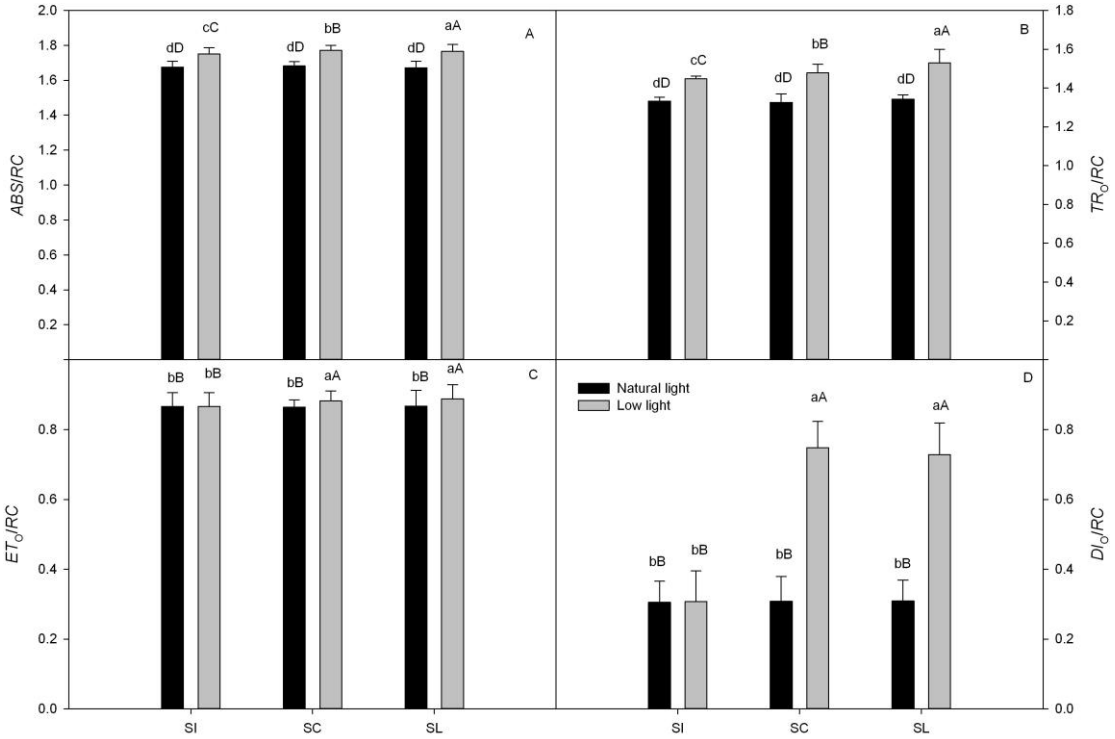

Figure 7. *The values of ABS/RC, TRo/RC, ETo/RC and DIo/RC leaves. Data in the figure are mean ± SD, values followed by different small letters mean significant difference ($p < 0.05$), values followed by different capital letters mean very significant difference ($p < 0.01$). SI: Syringa oblata Iandl; SC: Syringa chinensis; SL: Syringa oblata var. affinis Lingelsh*

PSII energy allocation pathways in leaves of Syringa

The Φ_{NF} in the low light was higher than that in the natural light for all the three *Syringa*, but the Φ_{NPQ} showed opposite trends (*Fig. 8*). The Φ_{PSII} in the low light were much lower than the natural light leaves for *Syringa oblata var. affinis Lingelsh* (SL). The Φ_{PSII} in the low light of *Syringa oblata Iandl* (SI) was higher than the *Syringa oblata var. affinis Lingelsh* (SL) and *Syringa chinensis* (SC). The Φ_{NF} values were listed in a decreasing order: *Syringa oblata var. affinis Lingelsh* (SL) > *Syringa chinensis* (SC) > *Syringa oblata Iandl* (SI).

Chl a fluorescence kinetics the selected JIP-test parameters

According the JIP-test parameters, we found that PI_{ABS}, F_J, F_I, F_m, Ψ_o and φE_o in the leaves of three *Syringa* were significantly lower than under natural light (*Fig. 9*). All parameters showed a declining trend. However, the φD_o of *Syringa oblata var. affinis*

http://www.aloki.hu ● ISSN 1589 1623 (Print) ● ISSN 1785 0037 (Online)
DOI: http://dx.doi.org/10.15666/aeer/2003_21132128

Lingelsh (SL) and *Syringa chinensis* (SC) were higher than *Syringa oblata Iandl* (SI) under the low light.

Discussion

In the present study, the Chl, Chla and Chlb of leaves in the natural light were lower than in the low light for all the three cultivars. The contents of Chl, Chla and Chlb in the low light of *Syringa oblata var. affinis Lingelsh* (SL) and *Syringa chinensis* (SC) were significantly lower than that of *Syringa oblata Iandl* (SI). It indicates a low efficiency of light absorption and utilization for the low light due to low contents of the photosynthetic pigments. Anthocyanins have the potential roles in relieving damage of excessive light energy to photosynthetic apparatus. In this study, we found the high content of anthocyanins in the low light may be a protection mechanism for the leaves.

In this experiment, under the low light, P_n, G_s and T_r in leaves of *Syringa* decreased. The stomatal limitation of *Syringa* leaves was significantly improved by the low light. This indicated that the low light impacts the photosynthetic mechanism of *Syringa* leaves, which is related to the reduction of CO_2 utilization capacity, even when the stomatal conductance is reduced. In a word, inoculation with anthocyanins can improve photosynthetic capacity by increasing the stomatal opening and tolerance of photosynthetic apparatus to the low light and other non-stomatal factors. According to Farquhar et al. (1982), it can be concluded that the reduction of photosynthetic capacity of *Syringa* leaves caused by the low light is due to the limitation of both stomatal and non-stomatal factors.

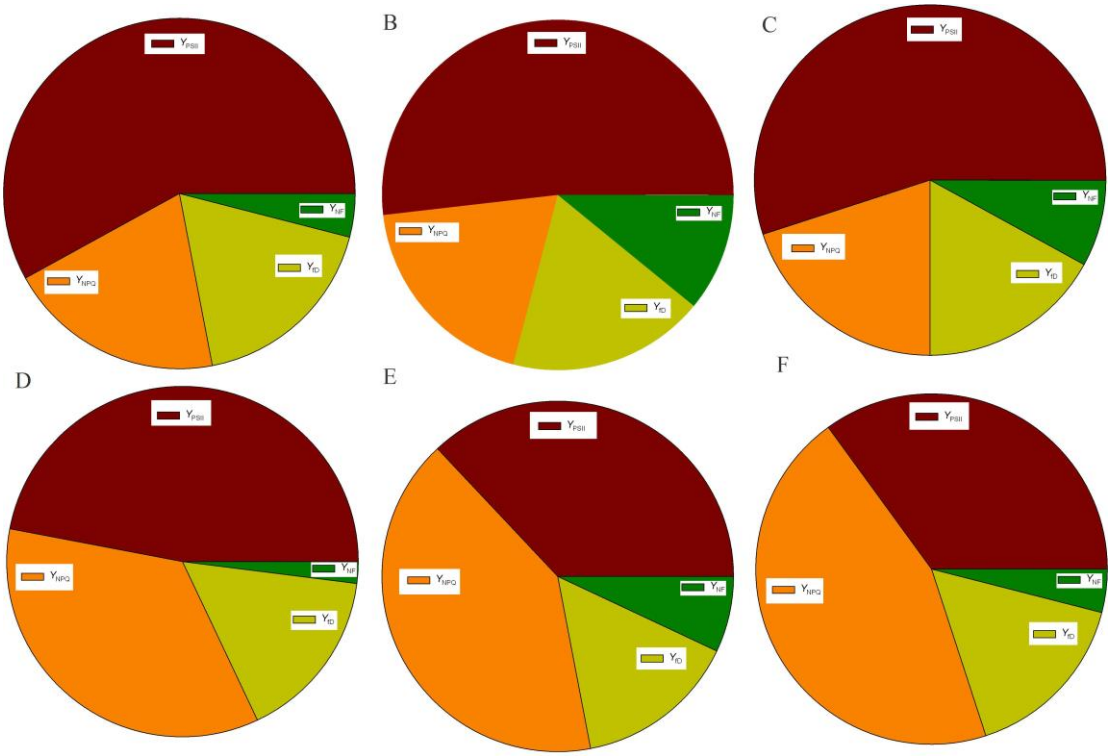

Figure 8. *PSII energy allocation pathways in natural light leaves of Syringa oblata Iandl (A), Syringa chinensis (B) and Syringa oblata var. affinis Lingelsh (C) and in low light leaves of Syringa oblata Iandl (D), Syringa chinensis (E) and Syringa oblata var. affinis Lingelsh (F)*

http://www.aloki.hu ● ISSN 1589 1623 (Print) ● ISSN 1785 0037 (Online)
DOI: http://dx.doi.org/10.15666/aeer/2003_21132128

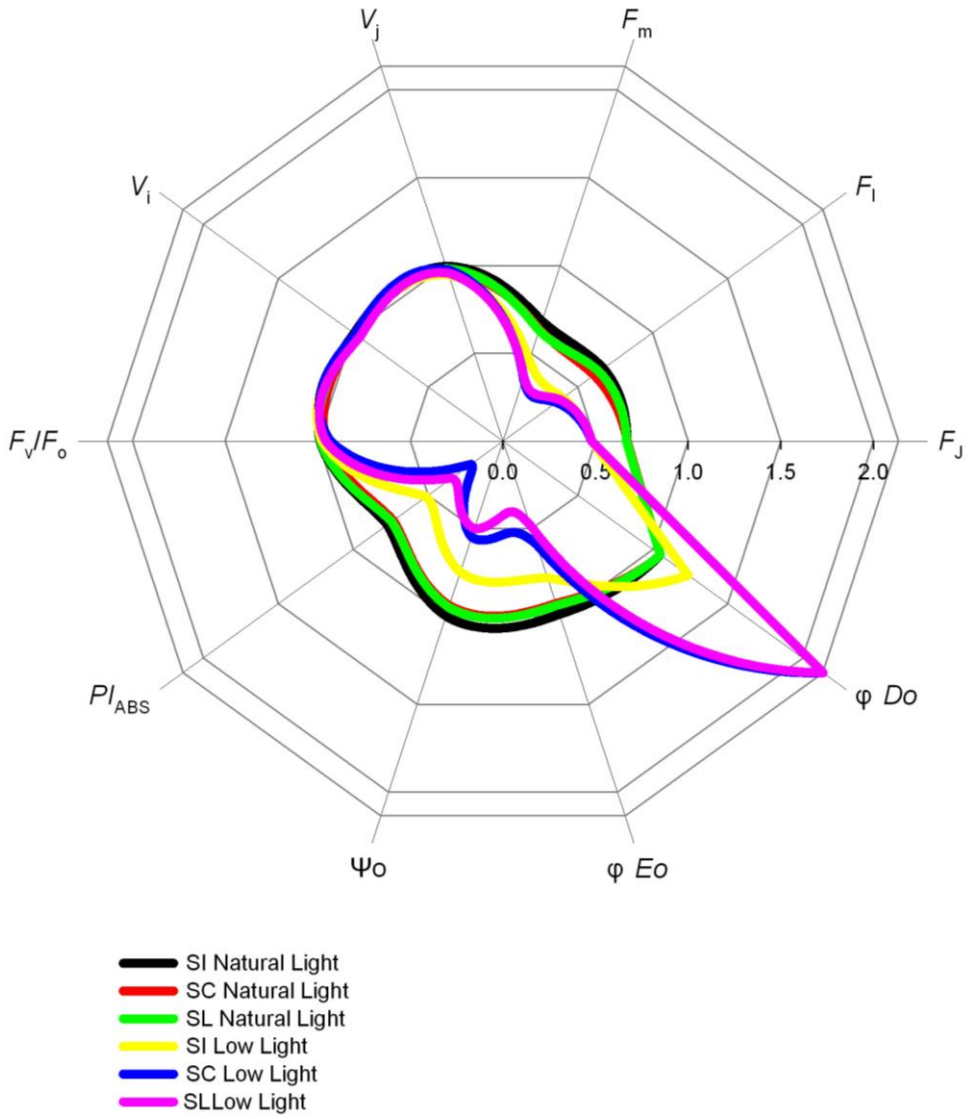

Figure 9. *Radar-plot of parameters derived from the JIP-Test of three Syringa. SI: Syringa oblata Iandl; SC: Syringa chinensis; SL: Syringa oblata var. affinis Lingelsh*

Among the leading functional hypotheses for the presence of anthocyanins in leaves is that of photoprotection of chloroplasts; under saturated light, anthocyanins potentially mitigate photoinhibitory and photo-oxidative damage by absorbing a proportion of the photons surplus to the requirements of the light reactions of photosynthesis (Kevin et al., 2011). The chlorophyll in plant leaves can absorb light energy, so does the Ant (Jiang et al., 2005). In addition, coloration of variety coleus plants major impact of the interaction of Chl and Ant contents (Zhang et al., 2010). In present study, the content of Ant in the low light leaves of *Syringa oblata Iandl* (SI) was higher than *Syringa oblata var. affinis Lingelsh* (SL) and *Syringa chinensis* (SC). However, this effect of Ant existence on photosynthetic pigments was expected in view of earlier studies that showed the role of filtration (Chalker-Scott et al., 1999), attenuation (Gould, 2004) and reflection light (Lee et al., 1979). Anthocyanins were synthesized to alleviate oxidative stress resulting from low water potentials, either through acting as an antioxidant or through light-attenuation. As a result, the absorbing light capacity of the low light

http://www.aloki.hu ● ISSN 1589 1623 (Print) ● ISSN 1785 0037 (Online)
DOI: http://dx.doi.org/10.15666/aeer/2003_21132128

leaves in *Syringa oblata Iandl* (SI) was lower than *Syringa oblata var. affinis Lingelsh* (SL) and *Syringa chinensis* (SC). In other words, reduced the proportion of PS II absorb the light energy in the low light leaves of *Syringa oblata Iandl* (SI) due to Ant could avoid potential hazard by the excess light energy of PSII. By contrast, those parameters were remarkably similar between red and green leaves. Red leaves are evidently better equipped to deal with surplus incident photons, elevating their photochemical performance to that of green leaves (Kevin et al., 2011).

The relative fluorescence intensity F_t of each point on the OJIP curve of *Syringa oblata Iandl* (SI) leaves is significantly lower than that of *Syringa oblata var. affinis Lingelsh* (SL) and *Syringa chinensis* (SC), which may be due to the fact that there are a lot of anthocyanins in SI leaves, which attenuates part of the action light intensity. However, under low light, the synthesis of anthocyanin in *Syringa oblata Iandl* (SI) leaves was inhibited, which led to the increase of the relative fluorescence intensity F_t of each point on the OJIP curve, which further indicated that the existence of anthocyanin could reduce the fluorescence quenching in plant leaves to a certain extent, which may suggest that anthocyanin has a certain defense mechanism of light damage (Chen et al., 2017). In our experiment, the increase of V_I in three *Syringa* leaves under low light intensity was significantly larger than that in V_J, that is to say, the main reason for the obstruction of electron transfer on the electron acceptor side of PS II in three kinds of *Syringa* leaves was that the low light intensity led to the increase of V_J and V_I, and the increase of V_J and V_I could reflect the accumulation of Q_A^-, It is related to the ability reduction of Q_B and PQ to accept electronic, and the reduction of PQ library capacity is the main speed limit step (Zhang et al., 2012; Tariq et al., 2017).

Correlation analysis showed a high correlation between pigment content and chlorophyll fluorescence parameters in low light leaves of the three *Syringa* species (*Table 1*). The *Syringa oblata Iandl* (SI) due to abound with Ant that attenuated energy which used for photosynthesis organization. Therefore, the F_o and F_m of the *Syringa oblata Iandl* (SI) was lower than that of the *Syringa oblata var. affinis Lingelsh* (SL) and *Syringa chinensis* (SC) which had lower Ant pigment. Scilicet, no matter the reaction center was all opened or closed, the yield for Chlorophyll fluorescence were all relatively low. It indicates that light absorption of the two *Syringa* was obviously decreased due to the existence of Ant. In this study, the experiment was conducted in late August in the autumn of Harbin, with the conditions of declining temperature and high light intensity. The combined effects of low temperature and high light often led to leaf photoinhibition or even light damage (Feng et al., 2009; Zhang et al., 2011a). The experimental results showed that all the values of F_v/F_m, F_v/F_o, *ETR* and Φ_{PSII} of leaves in the low light were all higher in *Syringa oblata Iandl* (SI) than in the *Syringa oblata var. affinis Lingelsh* (SL) and *Syringa chinensis* (SC). It indicates that the protective effects of the Ant in the *Syringa oblata var. affinis Lingelsh* (SL) and *Syringa chinensis* (SC) were weaker. The reduction of the PSII reaction center activity and the open level of reaction center blocked the electron transport of leaves and inhibited primary reaction of photosynthesis, all the factors led to the reduction of light quantum reaching PSII reaction center (Zhang et al., 2012; Tariq et al., 2017; Liu et al., 2019). So the proportion of light energy for photochemical reaction was reduced. However, the activity of PSII reaction center was inhibited significantly for the leaves with higher Ant content.

http://www.aloki.hu ● ISSN 1589 1623 (Print) ● ISSN 1785 0037 (Online)
DOI: http://dx.doi.org/10.15666/aeer/2003_21132128

Table 1. *Correlation coefficients between pigment content and chlorophyll fluorescence parameters in low light leaves of three Syringa*

	Chl	**Chla**	**Chlb**	**Ant**
$\mathbf{F_o}$	0.99**	0.99**	0.98**	-0.97**
$\mathbf{F_m}$	0.97**	0.98**	0.96**	-0.95*
$\mathbf{F_v/F_m}$	-0.85*	-0.84*	-0.90*	0.89*
$\mathbf{F_v/F_o}$	-0.79	-0.76	-0.85	0.83
$\mathbf{\Phi_{PSII}}$	-0.99**	-0.99**	-0.99**	0.99**
ETR	-0.99**	-0.99**	-0.98**	0.98**
ABS/RC	0.99**	0.99**	0.99**	-0.99**
$\mathbf{TR_o/RC}$	0.99**	0.99**	0.99**	-0.99**
$\mathbf{ET_o/RC}$	0.99**	0.98**	0.99**	-0.99**
$\mathbf{DI_o/RC}$	0.99**	0.99**	0.98**	-0.97**

*, ** indicate statistical significance at a = 0.05 or a = 0.01, respectively

Variation parameters of the reaction center unit specific activity were not only attenuated light absorption and utilization, but also reflect the important indicators of the number of the active reaction center and the activity of the reaction center under stress (Havaux and Tardy, et al., 1997; Strasser et al., 1995; Zhang et al., 2011b; Li et al., 2019). In the present study, the *ABS/RC, TR_o/RC*, *ET_o/RC* and *DI_o/RC* in *Syringa oblata Iandl* (SI), which were rich in Ant, were both striking lower than the low light leaves of *Syringa oblata var. affinis Lingelsh*. It implies that the number of reaction center in the low light leaves of the *Syringa oblata var. affinis Lingelsh* (SL) and *Syringa chinensis* (SC) was decreased under low temperature and high light stress in the autumn. This force had a surplus of the active reaction center rising on the function, which showed an augmentation at the parameter of the reaction center unit specific activity. However, the low light leaves with a high content of Ant led to reduction of light absorption, which potentially reduced the high light damage to PSII reaction center.

Based on the theory of Luke Hendrickson, excitation energy captured by leaf pigments is distributed to the following four parts: Φ_{NF}, Φ_{PSII}, Φ_{NPQ}, $\Phi_{f,D}$. It was an important part for researching the photosynthesis of plants that could research the trace of leaves absorption of light eventually. We have earlier reported whereabouts of light energy was more directly to actual photochemical efficiency (Φ_{PSII}) and Non-photochemical quenching (NPQ) to represent (Genty et al., 1898; Bilger et al., 1995; Hendrickson et al., 2004, 2005; Cai et al., 2019;), however, the increase in NPQ value was just due to an establishment of trans-thylakoid pH gradient and xanthophyll cycle in the higher plant (Lavaud and Kroth, 2006; Yin et al., 2019; Yang et al., 2020). But NPQ could not represent all processes of non- photochemical quenching, for this reason we need to redefine the photosynthesis of excitation energy distribution. Excitation energy are distributed into four parts (Φ_{NF}, Φ_{PSII}, Φ_{NPQ} and $\Phi_{f,D}$) based on the theory of Luke Hendrickson (Hendrickson et al., 2005; Guo et al., 2017). In the present study, light absorption of PSII reaction center in the low light leaves of *Syringa* due to the content of Ant has distribution again. Φ_{PSII} values of the low light leaves of *Syringa oblata Iandl* (SI) was higher than that of *Syringa oblata var. affinis Lingelsh* (SL) and *Syringa chinensis* (SC), however their Φ_{NF} values were significantly lower than *Syringa oblata var. affinis Lingelsh* (SL) and *Syringa*

http://www.aloki.hu ● ISSN 1589 1623 (Print) ● ISSN 1785 0037 (Online)
DOI: http://dx.doi.org/10.15666/aeer/2003_21132128

chinensis (SC). It implies that PSII reaction center in the low light leaves of *Syringa oblata Iandl* (SI). *Syringa oblata var. affinis Lingelsh* (SL) and *Syringa chinensis* (SC) could maintain the normal transmission of electron and reduce the number of leaves deactivation reaction center under the low temperature and high light stress in the autumn. The low light leaves with a low content of Ant absorbed more light energy, this led to light excess and light damage to PSII reaction center in the autumn. In contrast, the deactivation reaction center had the capability of the non-radiant energy dissipation which was an important role for the restitution of the reaction center of PSII and maintenance of the function of active reaction center (Lee et al., 2011; Yin et al., 2019; Yang et al., 2020). Therefore, the low light leaves of the *Syringa oblata var. affinis Lingelsh* (SL) and *Syringa chinensis* (SC) maintained normal physiologic function of photosystems through reducing the activity and the number of the PSII reaction center. Where difference with the *Syringa oblata var. affinis Lingelsh* (SL) and *Syringa chinensis* (SC), the low light leaves of the *Syringa oblata Iandl* (SI) due to the existence of Ant reached a balance between light energy absorption and utilization under the low temperature and high light in the autumn, which could ensure the normal physiologic function of the photosynthesis mechanism in the low light leaves.

Conclusions

The existence of the Ant was testified that could have obvious effect on the characteristics of chlorophyll fluorescence and distribution parameter of the light in the low light leaves of the *Syringa* under the low temperature and high light stress in the autumn. The photochemical activity of the low light leaves in the *Syringa oblata Iandl* (SI) which were rich in the Ant were much higher than the *Syringa oblata var. affinis Lingelsh* (SL) and *Syringa chinensis* (SC) due to the lower content of the Ant. The Ant in the low light leaves can maintain the activity and quantity of PSII reaction center under low temperature and high light stress in the autumn. It can also keep photosynthetic physiological function in the low light leaves through changing the light distribution parameter of PSII reaction center that alleviate the photoinhibition of the low light leaves in the *Syringa oblata Iandl* (SI). Our results provide the basis for different light utilization schemes for *Syringa* In order to further explain the decline of photosynthetic mechanism capacity and especially chlorophyll fluorescence, induced by low light, but this needs further study.

REFERENCES

[1] Bilger, W., Schreiber, U., Bock, M. (1995): Determination of the quantum efficiency of PS II and of non-photochemical quenching of chlorophyll fluorescence in the field. – Oecologia 102: 425-432.

[2] Burger, J., Edwards, G. E. (1996): Photosynthetic efficiency and photodamage by UV and visible radiation, in red versus green leaf *coleus* varieties. – Plant Cell Physiol 37: 395-399.

[3] Cai, Y. T., Zhang, H., Qi, Y. P., Ye, X., Huang, Z. S., Guo, J. X., Chen, L. S., Yang, L. T. (2019): Responses of reactive oxygen species and methylglyoxal metabolisms to magnesium-deficiency differ greatly among the roots, upper and lower leaves of Citrus sinensis. – BMC Plant Biology 19(1): 76.

http://www.aloki.hu ● ISSN 1589 1623 (Print) ● ISSN 1785 0037 (Online)
DOI: http://dx.doi.org/10.15666/aeer/2003_21132128

[4] Chalker-Scott, L. (1999): Environmental significance of anthocyanins in plant stress responses. – Photoche. Photobiol 70: 1-9.
[5] Chen, Y. E., Zhang, C. M., Su, Y. Q., Ma, J., Zhang, Z. W., Yuan, M., Zhang, H. Y., Yuan, S. (2017): Responses of photosystem II and antioxidative systems to high light and high temperature co-stress in wheat. – Environ. & Exp. Bot.135: 45-55.
[6] Dodd, I. C., Critchley, C., Woodall, G. S., Stewart, G. R. (1998): Photoinhibition in differently coloured juvenile leaves of species. – J. Exp. Bot 49: 1437-1445.
[7] Farquhar, G. D., Sharkey, T. D. (1982): Stomatal conductance and photosynthesis. – Annual Review of Plant Physiology 33(33): 317-345.
[8] Feng, C. S., Yan, X. J., Lu, X. S. (2009): Comparative study on photosynthetic pigments of different fall dormancy types of alfalfa in Beijing. – Prat. Tur. Sci 26(5): 95-98.
[9] Genty, B., Briantais, J. M., Baker, N. R. (1989): The relationship between quantum yield of photosynthetic electron transport and quenching of chlorophyll fluorescence. – Bio. Bioph. Acta 990: 87-92.
[10] Gould, K. S. (2004): Nature's Swiss army knife: the diverse protective roles of anthocyanins in leaves. – J. Bio. Biotech. 5: 314-320.
[11] Gould, K. S., Kuhn, D. N., Lee, D. W., Oberbauer, S. F. (1995): Why leaves are sometimes red. – Nature 378: 241-242.
[12] Gould, K. S., McKelvie, J., Markham, K. R. (2002): Do anthocyanins function as antioxidants in leaves? Imaging of H_2O_2 in red and green leaves after mechanical injury. – Plant. Cell. Environ 25: 1261-1269.
[13] Guo, P., Li, Q., Qi, Y. P., Yang, L. T., Ye, X., Chen, H. H., Chen, L. S. (2017): Sulfur mediated alleviation of aluminum toxicity in Citrus grandis seedlings. International Journal of Molecular Sciences – 18(12): 2570.
[14] Hamilton, W. D., Brown, S. P. (2001): Autumn tree colours as a handicap signal. Proceedings of the Royal Society of London. – Biol. Sci 268: 1489-1493.
[15] Havaux, M., Tardy. F. (1997): Thermostability and photostability of photosystem II in leaves of the Chlorina-F2 barley mutant deficient in light-harvesting chlorophyll a/b protein complexes. – Plant. Physiol 113: 913-923.
[16] Hendrickson, L., Furbank, F. T., Chow, W. S. (2004): A simple alternative approach to assessing the fate of absorbed light energy using chlorophyll fluorescence. – Photosyn. Res. 82: 73-81.
[17] Hendrickson, L., Britta, F., Pogsonm, B. J., Wah, S. C. (2005): A simple chlorophyll fluorescence parameter that correlates with the rate coefficient of photoinactivation of Photosystem II. – Photosyn. Res 84: 43-4.
[18] Hu, Y. B., Sun, G. Y., Wang, X. C. (2007): Induction characteristics and response of photosynthetic quantum conversion to changes in irradiance in mulberry plants. – J. Plant. Physiol 164: 959-968.
[19] Hughes, N.M., Smith, W. K. 2007. Attenuation of incident light in *Galax urceolata* (Diapensiaceae): concerted influence of adaxial and abaxial anthocyanic layers on photoprotection. – Americ. J. Bot. 94: 784-790.
[20] Inskeep, W. P., Bloom. P. R. (1985): Extinction coefficients of chlorophyll a and b in N, N-Dimethylformamide and 80% acetone. – Plant. Physiol 77(2): 483-485.
[21] Jiang, W. B., Zhuang, M., Han, H. Z., Dai, M. S., Hua, G. P. (2005): Progress on color emerging mechanism and photosynthetic characteristics of colored-leaf plants. – Acta. Horticul. Sin 2(2): 352-358.
[22] Karageorgou, P., Manetas, Y. (2006): The importance of being red when young: anthocyanins and the protection of young leaves of Quercus coccifera from insect herbivory and excess light. – Tree. Physiol 26: 613-621.
[23] Kevin, S., Gould, A., Dana, S., Dudle, Howard, Neufeld. (2011): Why some stems are red: cauline anthocyanins shield photosystem II against high light stress. – J. Exp. Bot. 61(10): 2707-2717.

http://www.aloki.hu ● ISSN 1589 1623 (Print) ● ISSN 1785 0037 (Online)
DOI: http://dx.doi.org/10.15666/aeer/2003_21132128

[24] Lavaud, J., Kroth. P. G. (2006): In diatoms, the transthylakoid proton gradient regulates the photoprotective non-photochemical fluorescence quenching beyond its control on the xanthophyll cycle. – Plant. Cell. Physiol 47: 1010-1016.
[25] Lee, D. W., Lowry, J. B., Stone, B. C. (1979): Abaxial anthocyanin layer in leaves of tropical rainforest plants: enhancer of light capture in deep shade. – Biotropica.11: 70-77.
[26] Lee, H. Y., Hong, Y. N., Chow, W. S. (2001): Photoinactivation of photosystem II complexes and photoprotection by nonfunctional neighbours in *Capsicum annuum* L. leaves. – Planta 212: 332-342.
[27] Li, Q., Chen, H. H., Qi, Y. P., Ye. X, Yang, L. T., Huang, R. Z., Chen, L. S. (2019): Excess copper effects on growth, uptake of water and nutrients, carbohydrates, and PSII photochemistry revealed by OJIP transients in citrus seedlings. – Environmental Science and Pollution Research International 26(29): 30188-30205.
[28] Lindoo, S. J., Caldwell, M.M (1978): Ultraviolet-B radiation-induced inhibition of leaf expansion and promotion of anthocyanin production. – Plant Physiol. 61: 278-282.
[29] Liu, H. M., Che, Y. S., Che, D. D., Yan, Y. Q., Wu, F. Z. (2010): Effects of drought stress on photosynthesis capability of *Syringa fritschiana* and *Syringa bunmalba Goldmound*. – Chi. J. Appl. Ecol 21(8): 2004-2009.
[30] Liu, X. J., Xu, N., Wu, Y. N., Li, J. B., Zhong, H. X., Zhang, H. H. (2019): Photosynthesis, chilling acclimation and the response of antioxidant enzymes to chilling stress in mulberry seedlings. – Journal of Forest Research 30(6): 2021-2029.
[31] Mendez, M., Jones, D. G., Manetas, Y. (1999): Enhanced UV-B radiation under field conditions increases anthocyanin and reduces the risk of photoinhibition but does not affect growth in the carnivorous plant *Pinguicula vulgaris*. – New. Phytol 144: 275-282.
[32] Pietrini, F., Massacci, A. (1998): Leaf anthocyanin content changes in Zea mays L. grown at low temperature: significance for the relationship between the quantum yield of PS II and the apparent quantum yield of CO_2 assimilation. – Photo. Res. 53(3): 213-219.
[33] Pirie, A., Mullins, M.G (1976): Changes in anthocyanin and phenolics content of grapevine leaf and fruit tissues treated with sucrose, nitrate, and abscisic acid. – Plant Physiol 58: 468-472.
[34] Steyn, W. J., Wand, S. J. E., Holcroft, D. M., Jacobs, G. (2002): Anthocyanins in vegetative tissues: a proposed unified function in photoprotection. – New. Phytol. 155: 349-361.
[35] Strasser. R. J., Srivastava, A., Govindjee (1995): Polyphasic chlorophyll a fluorescence transient in plants and cyanobacteria. – Photoche. Photobiol 61: 32-42.
[36] Tariq, A., Pan, K., Olatunji, O. A., Graciano, C., Li, Z. L., Sun,F., Sun, X. M., Song, D. G., Chen, W. K., Zhang, A. P., Wu, X. G., Zhang, L., Mingrui, D., Xiong, Q. L., Liu, C. G. (2017): Phosphorous application improves drought tolerance of Phoebe zhennan. – Front. Plant Sci. 8: 1561.
[37] Xie, H. H., Yang, L. L., Bao, Z. Y. (2006): Resources of the Syringas and their application to landscaping. – Sci. Sil. Simic 42(7): 104-112.
[38] Yang, X., Henry, H. A. L., Zhong, S., Meng, B., Sun, W. (2020): Towards a mechanistic understanding of soil nitrogen availability responses to summer vs. winter drought in a semiarid grassland. – Science Total Environment 741: 140272.
[39] Yin, L., Xu, H., Dong, S., Chu, J., Dai, X., and He, M. (2019): Optimised nitrogen allocation favours improvement in canopy photosynthetic nitrogen-use efficiency: Evidence from late-sown winter wheat. – Environmental and Experimental Botany 159: 75-86.
[40] Zhang, B. B., Jiang, W. B., Weng, M. L., Han, J. (2010): Effects of shading on photosynthetic characteristics of red-leaf peach. – Acta. Horticul. Sin 37(8): 1287-1294.
[41] Zhang, H. H., Bao, Z., Xu, N., Wang, P., Yin, P. D., Sun, G. Y. (2011a): Promoting effect of calcium on photosynthesis of tobacco seedlings under chilling and high Light acclimation. – J. Nucl. Agri. Sci. 25(3): 582-587.

http://www.aloki.hu ● ISSN 1589 1623 (Print) ● ISSN 1785 0037 (Online)
DOI: http://dx.doi.org/10.15666/aeer/2003_21132128

[42] Zhang, H. H., Zhang, X. L., Xu, N., He, G. Q., Jin, W. W., Yue, B. B., Li, X., Sun, G. Y. (2011b): Effects of exogenous $CaCl_2$ on the functions of flue-cured tobacco seedlings leaf photosystem II under drought stress. – Chi. J. Appl. Ecol 22(5): 1195-1200.
[43] Zhang, Z. S., Li, G., Gao, H. Y., Zhang, L. T., Yang, C., Liu, P., Meng, Q. W. (2012): Characterization of photosynthetic performance during senescence in stay-green and quick-leaf-senescence, *Zea mays* L. Inbred Lines. – Plos One 7(8): e42936.
[44] Zhou, Y. H., Lam, H. M., Zhang, J. H. (2007): Inhibition of photosynthesis and energy dissipation induced by water and high light stresses in rice. – J. Exp. Bot 5(58): 1207-1217.

http://www.aloki.hu ● ISSN 1589 1623 (Print) ● ISSN 1785 0037 (Online)
DOI: http://dx.doi.org/10.15666/aeer/2003_21132128

CHARACTERIZATION OF SOIL ORGANIC CARBON FUNCTIONAL GROUPS AS INFLUENCED BY CONTINUOUS FERTILIZATION AND CROPPING OF FINGER MILLET (*ELEUSINE CORACANA)* – MAIZE *(ZEA MAYS* L.) CROPPING SEQUENCE USING FT-IR SPECTROSCOPY

JAYANTHI, D. – GOKILA, B.*

Department of Soil Science & Agricultural Chemistry, Tamil Nadu Agricultural University, Coimbatore 641003, India

**Corresponding author*
e-mail: gokilasingh@gmail.com

(Received 29th Jul 2021; accepted 23rd Nov 2021)

Abstract. Soil organic carbon (SOC) is a factor for soil quality changes and continuous intensive cropping may change the soil organic matter (SOM) over the years. Characterization of SOC and its functional groups show the evidence of recalcitrant nature of SOM without oxidation under long run fertilization and manuring in sandy clay loam soil. Infrared Fourier transform spectroscopy (FT-IR) measures the absorbance of infrared radiation (4000 - 400 cm^{-1}) by bonds expressing dipole moments (e.g., C-O, C = O, C = C, C-H, N-H) in functional groups that constitute SOM. Irrespective of the treatments, 100% NPK + FYM has recorded the highest transmittance intensity of hydrophilic bond of carboxyl (C = O;1698 - 1701 cm^{-1}) carbonyl (3500 - 3200 cm^{-1} and 1400 cm^{-1}), aromatic benzenes (C = C;1650 cm^{-1}), alkenes (C-H; 2922 - 2926 cm^{-1}), S-S (500 - 400 cm^{-1}), and P = S (800 - 580 cm^{-1}) bonds. Addition of manures and mineral fertilizers have increased the SOC stock, SOC sequestration, Humic acid (HA), Fulvic acid (FA), welt ratio of HA and FA, soil microbial biomass carbon (SMBN) and soil microbial biomass nitrogen (SMBN) in the long run. The continuous application of mineral fertilizer as well as FYM over four decades have increased the more stable soil organic carbon compared to control.
Keywords: *humic acid, fulvic acid, soil reactive phases, Fourier transform, microbial biomass*

Introduction

The continuous cropping system, high yielding varieties, irrigation and high analysis fertilizer naturally enhance the mining of nutrients from the soil other than externally supplied by application of fertilizers and manures. Large amount of nutrient has to be applied to soil in chemical form that might have impact on soil properties and soil productivity in the long-run intensive cultivation of crops. The long-term fertilizer experiments indicate the extent to which yield, and related parameters and the quality of ecosystem can be predicted. These are also capable of serving as an early warning system to detect problems that threaten future productivity (Berzsenyi et al., 2000).

Important soil functions depend on content and composition of clay minerals and soil organic matter (SOM). SOM is an important part in the global carbon cycle. Approximately 81% of the organic carbon that is active in the terrestrial carbon cycle is stored in soils (Paustian et al., 2000; Wattel-Koekkoek et al., 2001). SOM functional groups strongly affect sorption characteristics such as the cation exchange capacity (Gressel et al., 1995) and in turn it is reflected in soil fertility.

For characterization of SOM composition and their functional groups in cultivated soil (Kögel-Knabner, 2000), the soil needs secondary reactions and wet chemical extraction procedures for elucidating the humus formation (Grover and Baldock, 2010; Schmidt et al.,

http://www.aloki.hu ● ISSN 1589 1623 (Print) ● ISSN 1785 0037 (Online)
DOI: http://dx.doi.org/10.15666/aeer/2003_21292141

2011) and decomposition in soil. Also avoiding the tedious chemical digestion process spectroscopic techniques such as Fourier transform infrared (FTIR) spectroscopy has been used for characterization of SOM composition. For an example, by using FTIR spectroscopy, SOM functional groups such as carboxyl (C = O) groups that are responsible for cation exchange (Celi et al., 1997) or alkyl (C–H) groups that account for wettability (Capriel et al., 1995) can be analyzed. FTIR spectra of plant and less-decomposed bog samples, which indicate a change in the molecular structure of the alkyl groups and possibly reflects a transformation of OM from simpler (plant) to more resistant aliphatic compounds in decomposed bog and fen samples (Zaccone et al., 2007).

Several infrared absorption bands are characteristic for the molecular structure. The absorption intensity reflects the proportional amounts of functional groups. Infrared spectra of humic acids from peat, coal, lignite, lignin from straw, black earth soils, podzol and Chernozem soils are relatively parallel (Van der Marel and Beutelspacher, 1976). However, there are differences in the absorption intensity and the wave number of absorption caused by slight differences in SOM composition. Heller et al. (2015) observed the second C–H band with a maximum absorption intensity at 2860 cm^{-1} and also an increase in the decomposition of more labile carbohydrates in contrast to less-decomposed bog and plant samples (Mudgil et al., 2012). Differences in crop yields might be explained by variations in the hydrophilic character of the SOM. The hydrophilic character of organic substances depends on the composition (type and amount) of functional groups, mainly carboxyl and hydroxyl-groups (Autorenkollektiv, 1984) and may affect the soil water storage capacity of the plough horizon.

Water repellent substances in SOM include aliphatic constituents (Capriel, 1997) and waxes (Franco et al., 2000). The amount of hydrophilic C = O groups (i.e., O and N containing hydroxyl and carboxyl groups) relative to that of hydrophobic C-H groups determines the hydrophobic character of SOM (Morrison and Boyd, 1983). The spatial arrangement of the hydrophobic components within the soil affects water affinity that influences the resistance to microbial degradation, the rate of wetting, and the adsorption processes. These properties play an essential role in the dynamics of SOM.

The weaker influence of field effects on bands as compared with C, N, and P fractions and its lower sensitivity to non-SOC field effects indicates functional group composition is more strongly associated with SOC among different fields than C, N, and P fractions (Margenot et al., 2015). The aliphatic C-H bands have positively correlated with SOC particularly labile organic C fractions (POXC, EOC, PMN and EON) and labile SOM fractions under organic management that increase SOM content (Marriott and Wander, 2006).

Measured fractions reflect processes such as mineralization (e.g., POXC, PMN) or are biomass-based measures (e.g., MBC, MBN), which is likely why these fractions are sensitive to field specific differences like nutrient management (Culman et al., 2012; Kallenbach and Grandy, 2011). Fractions like POXC and MBC are considered labile and are strongly associated (DuPont et al., 2010); yet showed different associations with bands, suggesting differences in functional group chemistry may underlie in the case of similarly labile fractions.

Long-term experiments have shown that organic matter management can increase labile C in the short-term and total soil C in the longer-term (Stevenson, 1982). The objectives of this study were to characterize Soil Organic Matter functional group with FT-IR spectroscopy under continuous cropping of finger millet (*Eleusine coracana)* - maize *(Zea mays* L.) cropping sequence.

http://www.aloki.hu ● ISSN 1589 1623 (Print) ● ISSN 1785 0037 (Online)
DOI: http://dx.doi.org/10.15666/aeer/2003_21292141

Materials and methods

Site description

Indian Council of Agricultural Research (ICAR) has initiated the first long-term field experiment at Kanpur, India in 1905 subsequently long-term experiments were initiated at Pusa and Coimbatore in 1908 and 1909, respectively. Tamil Nadu Agricultural University initiated All India Coordinated Research Project on Long Term Fertilizer Experiment (LTFE) in 1972 at Coimbatore under irrigated conditions. Since inception, this LTFE center followed finger millet-maize-cowpea cropping sequence. From the year 2000 onwards finger millet - maize cropping system is being followed.

The present study was carried out on continuous experimentation with finger millet-maize cropping sequence over 49 years and 111 crops were raised so far. The soils of the experimental site belonged to Periyanaickenpalayam soil series and according to USDA soil taxonomy it has classified as sandy clay loam in texture and taxonomically grouped under *Vertic Ustropept.*

The experiment had ten set of treatments *viz.,* 50% NPK (T_1), 100% NPK (T_2), 150% NPK (T_3), 100% NPK + HW (T_4), 100% NPK + Zn (T_5), 100% NP (T_6), 100% N (T_7), 100% NPK + FYM (T_8), 100% NPK (-S free) (T_9) and absolute control (T_{10}) with four replications. Out of ten treatments, four treatments were selected to study the functional group of SOM from the experiment which are absolute control, 100% recommended NPK, 100% recommended NPK + FYM @ 10 t ha^{-1} and 100% NP alone. These four treatments showed the impact of mineral fertilizer alone including effects of sulphur (SSP as a P source), exclusion of K, mineral fertilizer along with manure 10 t ha^{-1} of FYM and absolute control. In this cropping sequence, usually maize and finger millet crops were raised between January to May (summer period) and June-September (Monsoon period) respectively. SOC characterization was done by using the post-harvest samples of 110th Finger millet crop, which has harvested on 28.09.2020.

Experimental details

Raised bed nursery was prepared and finger millet (CO 13) was sown, and the seedlings were transplanted with 30 cm X 10 cm spacing in main field. As per the treatment structure, twenty days before the transplanting of crop farmyard manure @ 10 t ha^{-1} was applied uniformly over the main field. Hundred percent-recommended doses of N, P_2O_5 and K_2O @ 90:45:17.5 kg ha^{-1} respectively was applied basally in the main field.

Soil sampling

Core sampler was used to collect the undisturbed soil core from 0-15 cm depth from four treatments with five replications for bulk samples. Bulk samples were mixed thoroughly and sub sampling (standard soil sampling method – quartering) was adopted for SOC functional group analysis through FTIR. For soil biochemical properties, humic acid and fulvic acid analysis the soils were collected from all the ten treatments along with four replications. The collected soil samples were air dried in room temperature and the clods were broken by wooden mallets and sieved with 2 mm mesh so that samples were free of roots or plant debris.

http://www.aloki.hu ● ISSN 1589 1623 (Print) ● ISSN 1785 0037 (Online)
DOI: http://dx.doi.org/10.15666/aeer/2003_21292141

Functional groups of SOM by Fourier Transform Infrared Spectroscopy (FT-IR)

FTIR spectrometers are mostly used for measurements in the mid and near IR regions. For the mid-IR region, 2-25 µm (5000-400 cm^{-1}), the most common source is a silicon carbide element heated to about 1200 K. The output is similar to a blackbody. Shorter wavelengths of the near-IR, 1-2.5 µm (10000-4000 cm^{-1}), require a higher temperature source, typically a tungsten-halogen lamp. The long wavelength output of these is limited to about 5 µm (2000 cm^{-1}) by the absorption of the quartz envelope. For the far-IR, especially at wavelengths beyond 50 µm (200 cm^{-1}) a mercury discharge lamp gives higher output than a thermal source.

The air-dried soil samples were ground and sieved through a 2 mm sieve for further analysis. For FTIR analysis, the sample (300 mg) was mixed with 900 mg KBr (FTIR grade 99%) and ground in an agate mortar. The homogenous mixture was transferred into a diffuse reflectance cup without any pressure and leveled with a microscope glass slide. The FTIR spectra of the samples were measured on FTIR spectrometer. Soil microbial biomass C (SMB-C) and N (SMB-N) was estimated by chloroform-fumigation-extraction methods (Vance et al., 1987; Jenkinson, 1988) and SOC was estimated by Walkley and Black (1934) through chromic acid wet digestion.

The SOC stock was calculated by using the following formulae in terms of Mg C ha^{-1}:

$$\text{SOC stock (Mg C ha}^{-1}) = (D \times \frac{BD}{100} \times OC \times 10^4\ m^{-2}\ ha^{-1}) / 100 \qquad \text{(Eq.1)}$$

where D is the Depth of soil (cm) layer; B is the Bulk density (g cm^{-3}); OC is the organic carbon in g kg^{-1}; SOC sequestration (kg ha^{-1}) = SOC stock in last year – SOC stock in initial year.

Fractionation of humic acid and fulvic acid

For analysis of humic substance, 10 g of air-dried soil was taken in a 200 ml propylene flask and 100 ml of 0.1 N NaOH solution was added to soil and kept for shaking at 24 h with room temperature. Then the sample was undergone centrifuging at 10,000 rpm for 10 min to separate the dark colored supernatant solution from the soil and again 50 ml of distilled water was added to the residual soil for collecting supernatant and this process was repeated until the supernatants obtained were clear or uncolored.

The alkaline extract was acidified by washing with 2N HCl (pH 2) then it was allowed to stand for 24 h at room temperature then the soluble material (fulvic acid) was separated from the coagulates (Humic Acid) by centrifugation. Both fractions were dried by rotary evaporator at about 40 °C.

Welt ratio (E4/E6 value of HA and FA)

To know the degree of humification, the alkali soluble fraction of humic acid and fraction was determined by using the ratio of optical absorbance at 465 and 665 nm. Each sample of 10 mg HA and FA samples were dried at 60 °C and dissolved by 25 ml of 0.05 N $NaHCO_3$ (Mangrich et al., 2000) and the absorbance of HA and FA were measured at 465 nm and 665 nm.

$$\text{E4 / E6 ratio} = \frac{Optical\ absorbance\ at\ 465\ nm}{Optical\ absorbance\ at\ 665\ nm} \qquad \text{(Eq.2)}$$

http://www.aloki.hu ● ISSN 1589 1623 (Print) ● ISSN 1785 0037 (Online)
DOI: http://dx.doi.org/10.15666/aeer/2003_21292141

Statistical analysis

The experimental design was randomized block design and to compare the differences in measured soil attribute between treatments and replications one way ANOVA was used and the significant differences between the treatments were tested by using Duncan's multiple-range test (DMRT) for comparison of means at $P < 0.05$ significance level. The normalized FTIR spectral data are used to derive the spectral images by using Origin Pro 8.5 software packages.

Results

FT-IR transmittance spectra

The FTIR spectra of the soil samples in different treatments under long term fertilizer experiment are given in *Table 1*. The band wavelength of 1081 cm^{-1} shows C-O vibration of C–O-C group of cellulose (Grube et al., 2006) and 1400 cm^{-1} for carboxylic and carbonylic groups (Parker, 1971). Similarly, 1540 cm^{-1} is due to C = C (Cocozza et al., 2003) and 1600 -1613 cm^{-1} for C-C conjugated with C = O or COO^- (Niemeyer et al., 1992; Cocozza et al., 2003) and 1698 - 1701 cm^{-1} stands for C = O (carboxylic, cyclic and acyclic aldehydes and ketones) (Gondar et al., 2005). Aliphatic C-H (methyl and methylene) groups were resulted from the 2922 - 2926 cm^{-1} wave band (Niemeyer et al., 1992; Cocozza et al., 2003) and O-H group (including alcohols (R-OH), Phenols, water molecules (strong stretching) are from 3500 - 3200 cm^{-1} waveband (Cocozza et al., 2003) (*Fig. 1*).

Table 1. *Soil organic carbon functional groups in various fertilizer management practices under finger millet–maize cropping sequence*

Control	100% NP	100% NPK	100% NPK + FYM
OH group (including alcohols (R-OH), phenols, water molecules (low conc)	OH group (including alcohols (R-OH), phenols, water molecules (high conc)	OH group (including alcohols (R-OH), phenols, water molecules (medium stretching)	OH group (including alcohols (R-OH), phenols, water molecules (strong stretching)
Carbonyl (RCOR), carboxylic (RCOOH)	Carbonyl (RCOR), carboxylic (RCOOH)	Carbonyl (RCOR), carboxylic (RCOOH)	C = O (carboxylic acids), amide ($RCONR_2$)
C-H aromatic (meta disubstituted benzenes - weak), vinyl (Cis substituted alkenes)	C-H aromatic (meta disubstituted benzenes), vinyl (Cis substituted alkenes)	P-O (phosphorus oxide)	C = O (carboxylates salts), amino acid, zwitterions
Alkyl halogen (C –Br, C-F, C-I, Si-Cl)	S - S (disulphide bond)	C-H aromatic (meta disubstituted benzenes), vinyl (monosubstituted alkenes)	C = O (aliphatic amines)
Peroxides (R-O-O-R)	P-O-P	P = S (P-S-S-P)	C-H (cis disubstituted alkenes)
	Peroxides (R-O-O-R)	Halogens (C-Cl, C-F, CF)	C-H (aromatic – meta disubstituted benzenes) strong
	P = S (phosphorothioate)		P = S (phosphorothioate)
			S – S (disulphide bond)
			Halogen (C-Cl, RCF_3)

Control

Transmittance spectra of control treatment showed the presence of OH group (including alcohols (R-OH), Phenols, water molecules (Low Conc), Carbonyl (RCOR),

http://www.aloki.hu ● ISSN 1589 1623 (Print) ● ISSN 1785 0037 (Online)
DOI: http://dx.doi.org/10.15666/aeer/2003_21292141

Carboxylic (RCOOH), C-H aromatic (meta disubstituted benzenes - Weak), Vinyl (Cis substituted alkenes), Alkyl Halogen (C –Br, C-F, C-I, Si- Cl) and Peroxides (R-O-O-R) functional groups in soil.

100% NPK

The transmittance spectrum for the soils with 100% NPK treatment showed the presence of OH group (including alcohols (R-OH), Phenols, water molecules (medium stretching), Carbonyl (RCOR), Carboxylic (RCOOH), P-O (Phosphorus Oxide), C-H aromatic (meta disubstituted benzenes), Vinyl (monosubstituted alkenes), Halogens (C-Cl, C-F, CF) and P = S (P-S-S-P) (Phosphorothioate).

100%NPK + FYM

Over the years, application of mineral fertilizer along with FYM treatment contained strong stretching OH groups (including alcohols (R-OH), Phenols, water molecules, C = O (Carboxylic Acids), Amide ($RCONR_2$), C = O (Carboxylates (salts), amino acid, Zwitterions, C = O (Aliphatic Amines), C-H (Cis disubstituted alkenes), C-H (Aromatic - meta disubstituted Benzenes) strong P = S (Phosphorothioate), S - S (Disulphide Bond) and Halogen (C-Cl, RCF_3) functional groups.

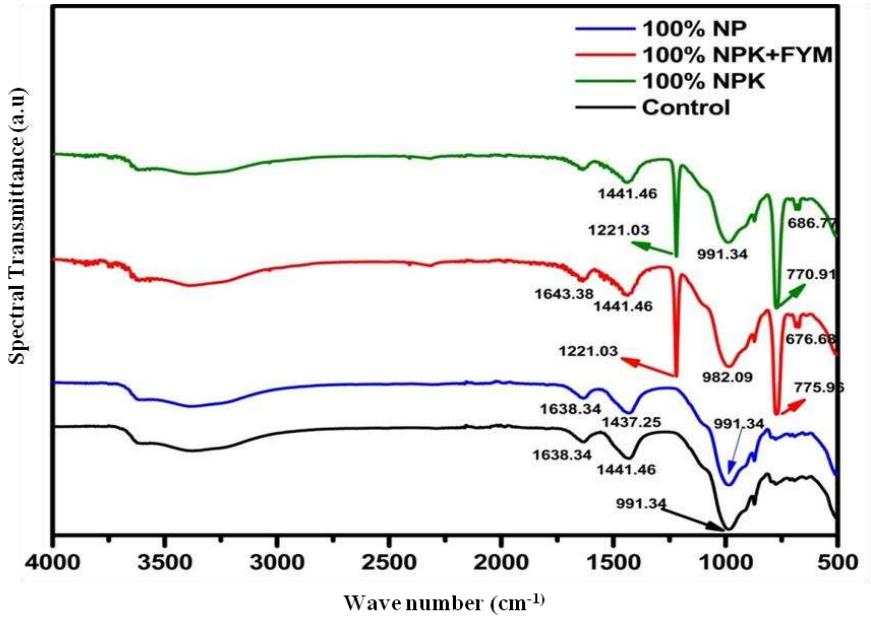

Figure 1. *Spectral transmittance pattern of different treatments by using FT-IR spectroscopy*

100%NP

Omission of K and application of NP mineral fertilizer showed the presence of OH group (including alcohols (R-OH), Phenols, water molecules (High Conc), Carbonyl (RCOR), Carboxylic (RCOOH), C-H aromatic (meta disubstituted benzenes), Vinyl (Cis substituted alkenes), S - S (Disulphide Bond), P-O-P and Peroxides (R-O-O-R) and P = S (Phosphorothioate).

http://www.aloki.hu ● ISSN 1589 1623 (Print) ● ISSN 1785 0037 (Online)
DOI: http://dx.doi.org/10.15666/aeer/2003_21292141

SOC stock and carbon sequestration/depletion

Over the four decades, application of inorganic and organic nutrients showed significant buildup of SOC stock and carbon sequestration except in control. The highest net carbon sequestration was recorded in greater extent under INM over 47 years (6342 kg ha^{-1}) followed by application of 150%NPK (5550 kg ha^{-1}) and also the SOC stock was registered as high in INM (133.3 Mg C ha^{-1}) followed by 150% NPK (108.2 Mg C ha^{-1}) (*Fig. 2*).

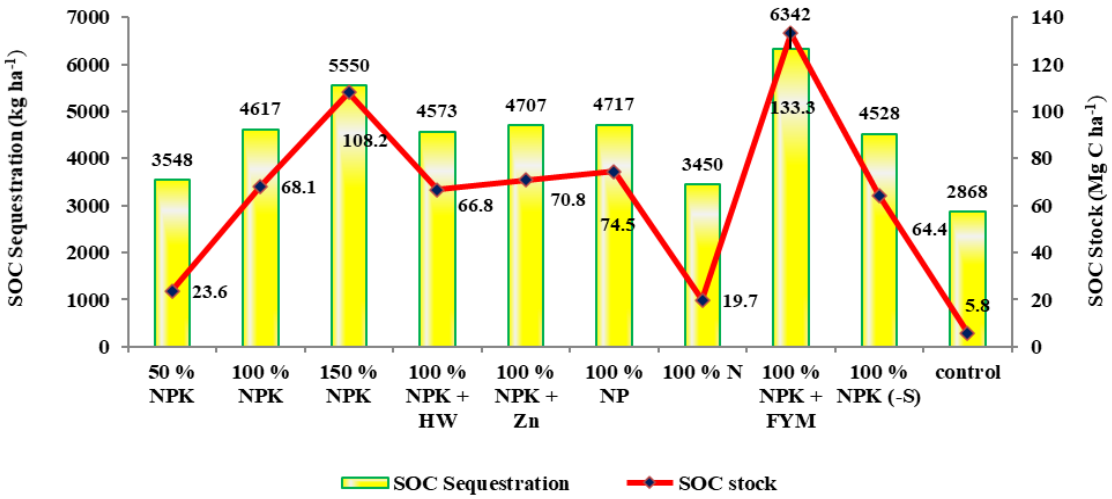

Figure 2. *Soil organic carbon (SOC) sequestration (kg ha^{-1}) and SOC stock (Mg C ha^{-1})*

Changes of biochemical properties (SOC, SMBC and SMBN)

Biochemical changes are one of the nutrient transformations in soil and a pool of nutrients for crop growth. Continuous application of manure along with fertilizers (INM or T_8) led to increase in ($P < 0.05$) SOC (%), SMBC and SMBN compared to control which was ranged from 0.490 – 0.749%, 195 – 319 and 19.90 – 47.16 mg kg^{-1} respectively in finger millet (*Table 2*).

Humic acid (HA) and fulvic acid (FA) fractions

SOC stability in soil was characterized by quantification of humic acid (HA) and fulvic acid (FA) properties further the spectroscopic studies has been performed in fraction of HA and FA fractions with the optical absorbance of 465 and 665 nm (E_4/E_6 or Welt ratio) (*Table 3*).

Humic and fulvic acid fractions were significantly higher in the treatment of FYM @10 t ha^{-1} along with 100% NPK followed by 150% NPK and the lowest values were found in control treatment. Application of FYM @10 t ha^{-1} was recorded the highest HA of 0.79 and FA of 3.93% in 100% NPK + FYM 10 t ha^{-1} and the lowest HA of 0.10 and FA of 0.78% in control treatment in continuous addition of manures and fertilizers with intensive cropping.

Welt ratio (E_4/E_6) significantly implied by addition of manures and fertilizers and the lowest E_4/E_6 values of 3.85 and 6.54 and the highest value of 4.73 and 7.93 was observed in humic and fulvic acid respectively.

http://www.aloki.hu ● ISSN 1589 1623 (Print) ● ISSN 1785 0037 (Online)
DOI: http://dx.doi.org/10.15666/aeer/2003_21292141

Table 2. *Soil biochemical changes by continuous fertilization and intensive cropping under finger millet–maize cropping sequence*

Treatments	Soil organic carbon (%)	Soil biomass carbon (mg kg^{-1})	Soil biomass nitrogen (mg kg^{-1})
50% NPK	0.559	281	30.76
100% NPK	0.59	300	42.29
150% NPK	0.652	317	43.82
100% NPK + HW	0.61	294	34.23
100% NPK + Zn	0.61	293	38.63
100% NP	0.588	284	28.93
100% N	0.571	188	22.16
100% NPK + FYM	0.74	319	47.16
100% NPK (-S)	0.613	295	37.15
Control	0.49	195	19.9
SEd	0.013	5.92	0.939
CD (p = 0.05)	0.028	10.08	1.59

Table 3. *Soil organic fraction (SOC) by continuous fertilization and intensive cropping under finger millet–maize cropping sequence*

Treatments	HA (%)	FA (%)	E4/E6 (HA)	E4/E6 (FA)
50% NPK	0.30 *g*	2.78 *d*	4.30 *c*	7.75 *b*
100% NPK	0.67 *bc*	3.35 *b*	4.10 *de*	6.98 *de*
150% NPK	0.70 *b*	3.42 *b*	4.05 *e*	6.80 *f*
100% NPK + HW	0.63 *cd*	3.36 *b*	4.16 *d*	7.03 *cd*
100% NPK + Zn	0.66 *bc*	3.40 *b*	4.28 *c*	6.84 *ef*
100% NP	0.43 *f*	3.00 *c*	4.51 *b*	7.71 *b*
100% N	0.52 *e*	2.41 *e*	4.59 *b*	7.82 *ab*
100% NPK + FYM	0.79 *a*	3.93 *a*	3.85 *f*	6.54 *g*
100% NPK (-S)	0.61 *d*	3.30 *b*	4.14 *de*	7.16 *c*
Control	0.10 *h*	0.78 *f*	4.73 *a*	7.93 *a*
SEd	0.01	0.05	0.04	0.07
CD (p = 0.05)	0.02	0.11	0.10	0.15

Discussion

Characterization of soil organic matter functional groups by FTIR spectroscopy

Control

Continuous cropping and omission of mineral fertilizer and organic manure could have reduced the organic carbon and carbon sequestration (*Fig. 1*). In control treatment it was maintained with no mineral fertilizer and manure, the contribution of root biomass may be the reason for the presence of weak C-H aromatic and peroxide functional groups. Sometimes presence of peroxide functional groups acts as catalyst in the decomposition of organic matter, which might have resulted in the lower organic carbon content (0.49%),

http://www.aloki.hu ● ISSN 1589 1623 (Print) ● ISSN 1785 0037 (Online)
DOI: http://dx.doi.org/10.15666/aeer/2003_21292141

and carbon sequestration (2868 kg ha^{-1}). Positive correlation (which is modest) is between the proportions of soil C in aromatics and carbonyls functional groups in cultivated, non-cultivated, grass cultivated and forest whole soils (Mahieu et al., 1999). Similarly, Rumpel et al. (2006) who reported that in soil of tropics, OM accumulation in the soil is low as high temperatures and moist conditions cause high litter decomposition and mineralization rates, resulting in low levels of OM accumulating in the soil. Similarly, Heller et al. (2015) who suggested that more aerobic conditions in topsoil peats resulted in larger rates of mineralization and causes a considerable loss of C under long-term arable farming.

100% NPK

As compared to the control treatment, it contained phosphate and aromatic carbon functional groups excluding peroxides. This might have attributed to the presence of higher humic acid (0.67%) and fulvic acid (3.35%) coupled with higher organic carbon (0.59%) and total carbon stock (4617 kg ha^{-1}). This was in line with the findings of Jasmund and Lagaly (1993) who revealed that, the CEC active part of SOM is able to interact with clay mineral particles building up organo mineral complexes using polyvalent cation as a bridge. This stabilization is the cause that fertilization needs a longer time to affect SOM composition in soil. SOC functional groups identification, the C–H and C = O absorption bands, which are specific for organic matter in soil (Heller et al., 2015). The increasing ratio of C to O functional group (Margenot et al., 2015) is thought to be associated with greater recalcitrance of SOM (Ding et al., 2002).

100% NPK + FYM

Application of 100% NPK along with FYM was found favorable for increased content of humic acid (0.77%) and fulvic acid (3.93%) which might have contributed to the presence of amide (Margenota et al., 2015) and functional groups containing sulphur as compared to other treatments. Continuous additions of FYM have resulted in higher organic carbon content (0.74%) and carbon stock (6342 kg ha^{-1}) and humic acid. Humic substances coated on clay mineral have many types of reactive functional groups present as a reactive surface. Sulfur nucleophiles can react with some of those functional sites, incorporating sulfur into humic substances. Thus, sulfhydryl (thiol) and polysulfide functionalities are from the reactions involving hydrogen sulfide (HS^-) and polysulfide ions, respectively. Thiol groups can react in a variety of ways. When a thiol group is added across an unsaturated bond, an organic sulfide bond has to be formed.

Adding a thiol group to an unsaturated bond represents a diagenetic mechanism for introducing a sulfide bond in humic substances. However, compounds containing sulfide bonds are common in organisms (for example, the amino acid methionine), and therefore, the sulfide bond also could be of biological origin (Vairavamurthy et al., 1987). This was supported by the findings of Wattel-Koekkoek et al. (2001) who found that the higher stability of OM from the smectitic soil is caused by its interaction to cation bridges, and its content of aromatic components. Also supported by Autorenkollektiv (1984) who stated that, hydrophilic character organic substances depends on the composition (type and amount) of functional groups, mainly carboxyl and hydroxyl-groups and may affect the soil water storage capacity, CEC and stability of SOM in the plough horizon. Persson and Axe (2005) and Heller et al. (2015) reported that the large C-H/C = O ratio might

http://www.aloki.hu ● ISSN 1589 1623 (Print) ● ISSN 1785 0037 (Online)
DOI: http://dx.doi.org/10.15666/aeer/2003_21292141

have protected the C-H containing SOM against microbial decomposition because of the adsorption of heavy metal especially Fe.

100% NP

Absence of potassium application would have resulted in the less stable organo-metal complex containing peroxide functional groups. When comparing the treatments, control and omission of K plots observed the peroxide functional groups and absence of carboxylates. This may be because of the less stable aggregates by weak interaction of cation bridges with clay organo-metal complexes leading to easily soluble OM. This was in association with the findings of Wattel-Koekkoek et al. (2001) who argued that higher stability of OM from smectite is caused by interaction to cation bridges and its content of aromatic components also Kaiser and Ellerbrock (2005) stated that the solubility of SOM is related to a certain degree to the stability of SOM components.

Biochemical changes in continuous addition of chemical fertilizers and organic amendments on soil

Combined application of mineral fertilizer along with organic amendments would help to increase the plant biomass yield and increases the carbon input to soil which is a main factor for higher SOC (0.74%). Also, addition of FYM with mineral fertilizer produces the cationic bridges with the functional groups, which leads to reduced SOM solubilization or oxidation. These SOM provide a better soil environment for proliferation of soil microbial population which would increase the SMBC (319 mg kg^{-1}) and SMBN (47.16 mg kg^{-1}). Even though, mineral fertilizer alone also gave higher plant biomass that could increase the SOC (0.652%), SMBC (317 mg kg^{-1}) and SMBN (43.82 mg kg^{-1}) but when compared the manure with mineral fertilizer, these mineral fertilizer treatments (50% NPK, 100% NPK and 150% NPK) decreased the SOM and other microbial biomass like SMBC and SMBN (Li et al., 2008). Because application of mineral fertilizers alone did not improve soil physical properties like aggregate stability and low bulk density, which may directly have influenced the soil biological as well as physico-chemical properties. Though application of organic amendments, provide some extents of major and micronutrients and carbon inputs to soil. This was in agreement with the findings of Jiang et al. (2014) who stated that greater SOM was observed by the application of organics + fertilizers treatments than either organics or fertilizers alone, which may also be attributed to increased root growth associated with additional C inputs from roots (Luo et al., 2015).

Humic acid and fulvic acid fractions

By using FYM @10 t ha^{-1} has added quantum of nutrients as well as organic matter to the soil since, observed the highest HA (0.79) and FA (3.93%) in 100% NPK + FYM 10 t ha^{-1} (Marinari et al., 2007) and the lowest was in (HA of 0.10 and FA of 0.78%) control treatment.

Spectroscopic analysis of humic fractions of HA and FA, the lowest welt ratio of 3.85 and 6.54 and the highest value of 4.73 and 7.93 was observed in humic and fulvic acid respectively. Here, the welt ratio was less than 5 showing the high degree of humification (Freppaz et al., 2002) and well decomposed organic matter with high molecular weight aromatic molecules in their structure (Duval, 1993) and low molecular weight have high welt ratio (Chen et al., 1977) of fulvic acid. In addition, Peat soil showed selective

http://www.aloki.hu ● ISSN 1589 1623 (Print) ● ISSN 1785 0037 (Online)
DOI: http://dx.doi.org/10.15666/aeer/2003_21292141

enrichment of more recalcitrant compounds that could be traced by their alkyl-C groups with NMR spectroscopy (Leifeld et al., 2012).

Conclusion

The results of this investigation indicated that differences in fertilizer applications viz., mineral fertilizers alone and along with FYM in finger millet – maize cropping sequence over a long period (over 48 years) lead to differences in the amount and functional composition of SOM in swell shrink soil (*Vertic Ustropept)*. Among the different treatments such as 100% NPK, 100% NPK + FYM, 100% NP and control, INM treatment (100% NPK + FYM) observed the P = S (Phosphorothioate), S-S (Disulphide Bond), aromatic C- H functional group were present. This may be due to high carbon stability by the way of high degree of humification and high weight aromatic molecules and formation of clay metal ion complexes through cationic bridges of polyvalent cations. Control and 100% NP treatments observed the peroxide and strong stretching of hydroxyl functional group. It showed the easily soluble and oxidizable OM which lead to less carbon stock. The results suggest that application of mineral fertilizers along with FYM increases the carbon stock and sequestration by the presence of more recalcitrant SOM, CEC and nutrient availability over the years of cropping in smectitic clay. According to the present studies, it is strongly recommended for future studies to identify and quantify the SOC functional groups by practicing various nutrient management in the long run.

Acknowledgements. The author has acknowledged Indian Council of Agriculture Research and Tamil Nadu Agricultural University for financial support during the course of study.

REFERENCES

[1] Autorenkollektiv (1984): Organikum. – VEB Deutscher Verlag der Wissenschaften, Berlin.
[2] Berzsenyi, Z., Gyorffyand, B., Lap, D. Q. (2000): Effect of crop rotation and fertilisation on maize and wheat yields and yield stability in a long-term experiment. – Eur. J. Agron. 13(2-3): 225-244.
[3] Capriel, P., Beck, T., Borchert, H., Gronholz, J., Zachmann, G. (1995): Hydrophobicity of the organic matter in arable soils. – Soil Biology and Biochemistry 27(11): 1453-1458.
[4] Celi, L., Schnitzer, M., Nègre, M. (1997): Analysis of carboxyl groups in soil humic acids by a wet chemical method, Fourier-transform infrared spectrophotometry, and solution-state carbon-13 nuclear magnetic resonance. A comparative study. – Soil Science 162(3): 189-197.
[5] Chen, Y., Senesi, N., Schnitzer, M. (1977): Information provided on humic substances by E4/E6 ratios. – Soil Science Society of America journal 41(2): 352-358.
[6] Cocozza, C., D'orazio, V., Miano, T. M., Shotyk, W. (2003): Characterization of solid and aqueous phases of a peat bog profile using molecular fluorescence spectroscopy, ESR and FT-IR, and comparison with physical properties. – Organic Geochemistry 34(1): 49-60.
[7] Culman, S. W., Snapp, S. S., Freeman, M. A., Schipanski, M. E., Beniston, J., Lal, R., Wander, M. M. (2012): Permanganate oxidizable carbon reflects a processed soil fraction that is sensitive to management. – Soil Science Society of America Journal 76(2): 494-504.
[8] Ding, G., Novak, J. M., Amarasiriwardena, D., Hunt, P. G., Xing, B. (2002): Soil organic matter characteristics as affected by tillage management. – Soil Sci. Soc. Am. J. 66: 421-429.

http://www.aloki.hu ● ISSN 1589 1623 (Print) ● ISSN 1785 0037 (Online)
DOI: http://dx.doi.org/10.15666/aeer/2003_21292141

[9] Franco, C. M. M., Clarke, P. J., Tate, M. E., Oades, J. M. (2000): Hydrophobic properties and chemical characterization of natural water repellent materials in Australian sands. – Journal of Hydrology 231: 47-58.
[10] Freppaz, D., Minciardi, R., Robba, M., Sacile, R., Taramasso, A. (2002): Renewable energy: a decision support system for forest biomass exploitation. – International Congress on Environmental Modelling and Software. Integrated Assessment and Decision Support, Lugano, Switzerland, June 24-27.
[11] Gondar, D., Lopez, R., Fiol, S., Antelo, J. M., Arce, F. (2005): Characterization and acid–base properties of fulvic and humic acids isolated from two horizons of an ombrotrophic peat bog. – Geoderma 126(3-4): 367-374.
[12] Gressel, N., McColl, J. G., McGrath, A. E., Powers, R. F. (1995): Spectroscopy of aqueous extracts of forest litter. II: Effects of management practices. – Soil Science Society of America Journal 59(6): 1723-1731.
[13] Grover, S., Baldock, J. (2010): Carbon decomposition processes in a peat from the Australian Alps. – European Journal of Soil Science 61(2): 217-230.
[14] Grube, M., Lin, J. G., Lee, P. H., Kokorevicha, S. (2006): Evaluation of sewage sludge-based compost by FT-IR spectroscopy. – Geoderma 130(3-4): 324-333.
[15] Heller, C., Ellerbrock, R. H., Roßkopf, N., Klingenfuß, C., Zeitz, J. (2015): Soil organic matter characterization of temperate peatland soil with FTIR-spectroscopy: effects of mire type and drainage intensity. – European Journal of Soil Science 66(5): 847-858.
[16] Jasmund, K., Lagaly, G. (1993): Clay Mineral and Clays. – Steinkopff Verlag, Darmstadt.
[17] Jenkinson, D. (1988): Determination of Microbial Biomass Carbon and Nitrogen in Soil. – In: Wilson, J. R. (ed.) Advances in Nitrogen Cycling in Agricultural Systems. CABI, Wallingford, pp. 368-386.
[18] Jiang, G., Xu, M., He, X., Zhang, W., Huang, S., Yang, X., Murphy, D. V. (2014): Soil organic carbon sequestration in upland soils of northern China under variable fertilizer management and climate change scenarios. – Global Biogeochemical Cycles 28(3): 319-333.
[19] Kaiser, M., Ellerbrock, R. (2005): Functional characterization of soil organic matter fractions different in solubility originating from a long-term field experiment. – Geoderma 127(3-4): 196-206.
[20] Kallenbach, C., Grandy, A. S. (2011): Controls over soil microbial biomass responses to carbon amendments in agricultural systems: a meta-analysis. – Agric. Ecosyst. Environ. 144: 241-252.
[21] Kögel-Knabner, I. (2000): Analytical approaches for characterizing soil organic matter. – Organic Geochemistry 31(7-8): 609-625.
[22] Leifeld, J., Steffens, M., Galego-Sala, A. (2012): Sensitivity of peatland carbon loss to organic matter quality. – Geophysical Research Letters 39(14).
[23] Li, W. Q., Xiao-Jing, L., Khan, M. A., Gul, B. (2008): Relationship between soil characteristics and halophytic vegetation in coastal region of North China. – Pak J Bot 40(3): 1081-90.
[24] Luo, Z., Wang, E., Smith, C. (2015): Fresh carbon input differentially impacts soil carbon decomposition across natural and managed systems. – Ecology 96(10): 2806-2813.
[25] Mahieu, N., Powlson, N. D., Randall, E. W. (1999): Statistical analysis of published carbon-13 CPMAS NMR spectra of soil organic matter. – Soil Science Society of America Journal 63(2): 307-319.
[26] Mangrich, A. S., Lobo, M. A., Tanck, C. B., Wypych, F., Toledo, E., Guimarães, E. (2000): Criterious preparation and characterization of earthworm-composts in view of animal waste recycling. Part I. Correlation between chemical, thermal and FTIR spectroscopic analyses of four humic acids from earthworm-composted animal manure. – Journal of the Brazilian Chemical Society 11: 164-169.
[27] Margenot, A. J., Calderón, F. J., Bowles, T. M., Parikh, S. J., Jackson, L. E. (2015): Soil organic matter functional group composition in relation to organic carbon, nitrogen, and

http://www.aloki.hu ● ISSN 1589 1623 (Print) ● ISSN 1785 0037 (Online)
DOI: http://dx.doi.org/10.15666/aeer/2003_21292141

phosphorus fractions in organically managed tomato fields. – Soil Science Society of America Journal 79(3): 772-782.

[28] Marinari, S., Liburdi, K., Masciandaro, G., Ceccanti, B., Grego, S. (2007): Humification-mineralization pyrolytic indices and carbon fractions of soil under organic and conventional management in central Italy. – Soil and Tillage Research 92(1-2): 10-17.

[29] Marriott, E. E., Wander, M. M. (2006): Total and labile soil organic matter in organic and conventional farming systems. – Soil Science Society of America Journal 70(3): 950-959.

[30] Morrison, R. T., Boyd, R. N. (1983): Textbook of Organic Chemistry. – Verlag Chemie, Weinheim (in German).

[31] Mudgil, D., Barak, S., Khatkar, B. S. (2012): X-ray diffraction, IR spectroscopy and thermal characterization of partially hydrolyzed guar gum. – International Journal of Biological Macromolecules 50(4): 1035-1039.

[32] Niemeyer, J., Chen, Y., Bollag, J. M. (1992): Characterization of humic acids, composts, and peat by diffuse reflectance Fourier-transform infrared spectroscopy. – Soil Science Society of America Journal 56(1): 135-140.

[33] Paustian, K., Six, J., Elliott, E. T., Hunt, H. W. (2000): Management options for reducing CO_2 emissions from agricultural soils. – Biogeochemistry 48(1): 147-163.

[34] Persson, P., Axe, K. (2005): Adsorption of oxalate and malonate at the water-goethite interface: molecular surface speciation from IR spectroscopy. – Geochimica et Cosmochimica Acta 69(3): 541-552.

[35] Rumpel, C., Alexis, M., Chabbi, A., Chaplot, V., Rasse, D. P., Valentin, C., Mariotti, A. (2006): Black carbon contribution to soil organic matter composition in tropical sloping land under slash and burn agriculture. – Geoderma 130(1-2): 35-46.

[36] Schmidt, M. W., Torn, M. S., Abiven, S., Dittmar, T., Guggenberger, G., Janssens, I. A., Trumbore, S. E. (2011): Persistence of soil organic matter as an ecosystem property. – Nature 478: 49-56.

[37] Stevenson, F. J. (1994): Humus Chemistry: Genesis, Composition, Reactions. – John Wiley & Sons, Hoboken, NJ.

[38] Vairavamurthy, A., Mopper, K. (1987): Geochemical formation of organosulphur compounds (thiols) by addition of H_2S to sedimentary organic matter. – Nature 329: 623-625.

[39] Van der Marel, H. W., Beutelspacher, H. (1976): Atlas of Infrared Spectroscopy of Clay Minerals and Their Admixtures. – Elsevier Publishing Company, Amsterdam.

[40] Vance, E. D., Brookes, P. C., Jenkinson, D. S. (1987): An extraction method for measuring soil microbial biomass C. – Soil biology and Biochemistry 19(6): 703-707.

[41] Walkley, A., Black, I. A. (1934): An examination of the Degtjareff method for determining soil organic matter, and a proposed modification of the chromic acid titration method. – Soil Science 37(1): 29-38.

[42] Wattel-Koekkoek, E. J. W., Van Genuchten, P. P. L., Buurman, P., Van Lagen, B. (2001): Amount and composition of clay-associated soil organic matter in a range of kaolinitic and smectitic soils. – Geoderma 99(1-2): 27-49.

[43] Zaccone, C., Miano, T. M., Shotyk, W. (2007): Qualitative comparison between raw peat and related humic acids in an ombrotrophic bog profile. – Organic Geochemistry 38(1): 151-160.

http://www.aloki.hu ● ISSN 1589 1623 (Print) ● ISSN 1785 0037 (Online)
DOI: http://dx.doi.org/10.15666/aeer/2003_21292141

SPATIOTEMPORAL AND BIOLOGICAL VARIABILITY OF RED TIDE IN TIANJIN COASTAL WATERS DURING THE PAST 15 YEARS

QIAO, Y. L.[1,2*] – LUO, Y.[3,4] – YIN, X. Y.[5] – NOMAN, M. A.[6] – SUN, J.[6]

[1]*School of Environmental Science and Engineering, Tianjin University, 135 Yaguan Road, 300350 Tianjin, P. R. China*
(phone/fax: +86-22-8312-7822)

[2]*Tianjin Natural Resources Ecological Restoration and Renovation Center, 29 Hubei Road, 300040 Tianjin, P. R. China*

[3]*Third Institute of Oceanography, Minister of Natural Resources, 178 Daxue Road, 361005 Xiamen, P. R. China*

[4]*College of Environmental Science and Engineering, Ocean University of China, 238 Songling Road, Qingdao, Shangdong 266100, P. R. China*

[5]*Tianjin Fisheries Research Institute, 442 South Jiefang Road, 300221 Tianjin, P. R. China*

[6]*College of Marine Science and Technology, China University of Geosciences (Wuhan), 388 Rumo Road, Wuhan 430074, P. R. China*

[*]*Corresponding author*
e-mail: tjsmarine@163.com; phone/fax: +86-22-8312-7822

(Received 10th Aug 2021; accepted 23rd Nov 2021)

Abstract. Red tide is a major marine ecological disaster in the coastal area which indicates the change of ecological environment. Bohai Bay is an important platform for the Beijing-Tianjin-Hebei area for regional economic integration, which is an important channel for the marine biology in the Yellow Sea and Bohai Sea. Therefore, in this work, the red tide data from 2002 to 2017 were analyzed to study the spatiotemporal distribution and the changing characteristics of biological groups in this area. In the past 15 years, the occurrence of red tide has been limited from the month of June to August. Spatially, the red tide occurrence was less common in the south than north, and the most frequent red tide event recorded from Tianjin Port channel to the northern area of Jianhe kou. The main red tide biota were *dinoflagellates*, *diatoms* and *Chrysophytae* and the dominant red tide species were *Noctiluca scintillans*, *Skeletonema costatum*, *Phaeocystis globosa* and *Karenia mikimotoi.* Besides, the red tide caused by toxic algae was increasing year by year. However, the high seawater temperature in summer, flood, anthropogenic nutrient influx, and favorable southwest and southeast monsoon wind positively influenced the red tide events.
Keywords: *red tide, spatial-temporal, biological group, coastal waters, Tianjin*

Introduction

The frequency of algal blooms in the marine ecosystem, including Harmful Algal Blooms (HABs), is expanding around the world (Glibert et al., 2005; Guy, 2014; Borowitzka, 2018). HABs are often referred to as 'red tide', when it changes the color of the sea to red or almost brown (Zohdi and Abbaspour, 2019). Generally, red tide occurs when the algae like protists and dinoflagellates proliferate extensively in the coastal or marine environment, and within few weeks each cell produces one million daughter cells (Guy, 2014). It is one of the three major coastal pollution types in the world and has

http://www.aloki.hu ● ISSN 1589 1623 (Print) ● ISSN1785 0037 (Online)
DOI: http://dx.doi.org/10.15666/aeer/2003_21432155

deleterious effect on the natural resources, coastal and marine life, as well as the human health (Guy, 2014). However, red tide can be harmful or harmless based on the species involved and their physiological and biological features (Zohdi and Abbaspour, 2019). Most of those are non-toxic, but some of the species contributing to the red tide are highly toxic (Guy, 2014). Fish accumulate toxins from the toxic-containing algal cells through the food chain which ultimately come to human contact by consuming those fishes (Borowitzka, 2018). Due to increasing severity on human health, red tide has become the matter of concern all over the world including China (Zhao et al., 2004). Besides, red tide is an important indicator to reflect the change of ecological environment in coastal waters (Cong et al., 2008).

The coastal area is a coupling area of various ecosystems, rich in marine biodiversity, relatively active in material circulation and energy conversion, and plays an important role in maintaining the structural stability and general functioning of the marine ecosystem (Costanza et al., 1997). Bohai Bay, one of the three semi enclosed bays in Bohai Sea, is the spawning ground, fattening ground, feeding ground and important migration channel for marine organisms (Qiao et al., 2018). At the same time, it also carries the regional economic development of Beijing, Tianjin and Hebei. It is one of the most obvious sea areas affected by the coastal man-made disturbance. With the development of coastal urbanization, the pollution of Tianjin coastal waters in Bohai Bay is increasing, and the exchange capacity of semi enclosed bay water is weak. Consequently, the eutrophication of the water body is increasing, and the frequency, area and harm of red tide are increasing year by year. Therefore, the study of red tide in this area is of great significance. Bohai Bay is an early area of red tide research in China (Kang et al., 1982; Zou et al., 1983). In the initial studies, field survey was used to calculate and obtain the data of nutrients and organisms, to evaluate the eutrophication status of water body, and to study the changes of time, space and groups of red tide in combination with the biological and ecological characteristics. This method has been used up to now though the disadvantage of limited space coverage (Li and Lin, 1999; Wei et al., 2004; Huang et al., 2018). With the development of monitoring methods and research technologies, the frequency of red tide monitoring station layout and comprehensive investigation is increasing, and new technologies such as remote sensing and sensors are being applied to red tide analysis (Tan and Shi, 2006; Shi and Wang, 2012). The determination method of red tide also extended the knowledge of the relationship between the distribution characteristics in the sea area and the biological species (Sun et al., 2001; Shi et al., 2012) Plenty of research have been done worldwide to deepen the understanding of the occurrence characteristics and laws of red tide phenomena by new technologies (Song et al., 2016).

However, there are very few researches carried out based on the longer time scale of red tide in Tianjin coastal area of Bohai Bay. In this paper, 15 years long time series (from 2005 to 2017) red tide monitoring data were collected to study the temporal and spatial characteristics of red tide, variability of biological groups, and factors influencing the red tide events and biological groups, which may provide substantial information about the change of biological groups and the mechanism of red tide occurrence in Tianjin coastal area of Bohai Bay.

http://www.aloki.hu ● ISSN 1589 1623 (Print) ● ISSN1785 0037 (Online)
DOI: http://dx.doi.org/10.15666/aeer/2003_21432155

Materials and Methods

Study area

Tianjin city is located in the west of the arc shaped coastline of Bohai Bay (*Figure 1*). The total length of this coastline is about 153.67 km and the sea area is about 3000 km^2, including 335.99 km^2 intertidal zone. The sediment of this coast is typical silty sand and muddy. Haihe River system flows through the Beijing, Tianjin and Hebei area of the North China Plain, carrying a large amount of nutrient rich coastal water from the Tianjin into the Bohai Bay (Qiao et al., 2018). As a result of marine development activities and land-based pollution, up to 2017, 34 occasions of red tide experienced in Tianjin sea area of Bohai Bay (*Table 1*). All of these red tides have occurred in coastal waters, and the time was relatively short, particularly from June to August (Qiao et al., 2019).

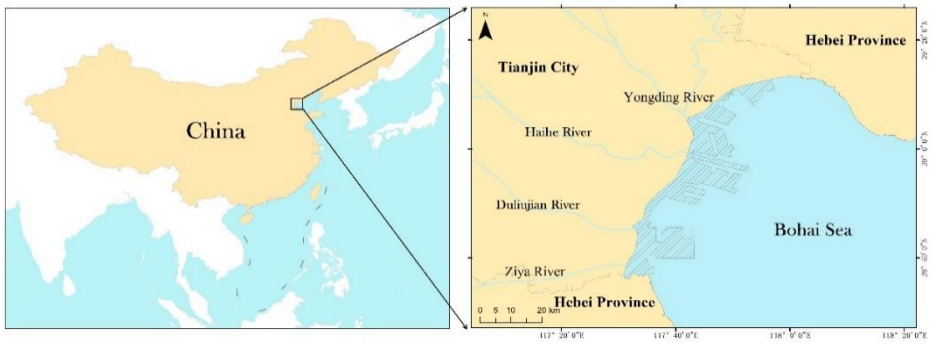

Figure 1. *Location map of Tianjin*

Data acquisition and interpretation

The occurrence time, frequency, area, species of red tide and other relevant information were collected from Tianjin marine environmental quality bulletin (Tianjin Oceanic Administration 2002-2017). The raw dataset of red tide in Tianjin coastal waters from 2002 to 2017 were analyzed by basic statistical method. The frequency of red tide events, causative species, area covering and the annual frequency of algal species were analyzed.

Results and discussion

Spatial variation of red tide

In total 34 red tide were recorded during 2002-2017 in Tianjin coastal waters (*Figure 2*, *Table 1*), with an average of 2.3 events annually. Among them, maximum frequency (six events) of red tide event was found during 2017. In 2002, 2003, 2005, 2008, 2014 and 2015, there was only one red tide event recorded every year. During the recent past five years, the frequency of red tide occurrence increased significantly. Particularly from 2012 to 2017, 17 red tide events recoded in this area which accounted 50% of the total number of red tides recorded during the whole study period. However, this trend was also recorded in the Bohai sea area previously (Song et al., 2016). There were only 3 HAB recorder from the whole Bohai sea area from 1952 to 1989, which has been increased significantly during 2000 to 2014 by occurring 148 HAB events (Song et al., 2016).

http://www.aloki.hu ● ISSN 1589 1623 (Print) ● ISSN1785 0037 (Online)
DOI: http://dx.doi.org/10.15666/aeer/2003_21432155

Table 1. *Red tide events in Tianjin coastal area during 2002-2017*

year	Date: Month(occur +,no-)									Frequency of red tide number	Main Species	Distribution Area
	Mar	Apr	May	Jun	Jul	Aug	Sep	Oct	Nov			
2002	-	-	-	-	+	-	-	-	-	1	*Gymnodinium aerucyinosum Stein*	Tianjin harbor basin
2003	-	-	-	-	+	+	-	-	-	1	*Noctiluca scintillans*	East of Dagu anchorage、Tianjin Port
2004	-	-	-	-	-	+	-	-	-	2	*Karenia mikimotoi*	Tianjin coastal waters
2005	-	-	-	+	-	-	-	-	-	1	*Chattonella marina*	Tianjin coastal waters
2006	-	-	-	+	-	+	-	+	-	3	*Phaeocystis globosa*、*Heterosigma akashiwo*、*Noctiluca scintillans*	Tianjin red tide monitoring area and its adjacent waters
2007	-	-	-	+	+	+	-	+	+	3	*Skeletonema costatum*、*Phaeocystis globosa*、*Eucampia zodiacus*	Tianjin red tide monitoring area and its adjacent waters
2008	-	-	-	+	+	+	-	-	-	1	*Ceratium furca*、*Nitzschia closterium f.minutissima*	Tianjin red tide monitoring area and its adjacent waters
2009	-	-	-	-	+	+	+	-	-	3	*Skeletonema costatum*、*Noctiluca scintillans*	North of the main channel of Tianjin port to Hangu sea area and caijiapu sea area
2010	-	-	+	+	+	-	+	+	+	2	*Noctiluca scintillans*、*Coscinodiscus wailesii*、*Nitzschia pungens*	North of the main channel of Tianjin port to Hangu sea area
2011	-	-	-	-	-	-	-	-	-	-	-	
2012	-	-	-	+	+	+	-	-	-	2	*Leptocylindrus danicus*、*Pseudonitzschia delicatissima*、*Eucampiazoodiacus*、*Thalassiosira nordenskioeldi*、*Chaetoceros curvisetus*、*Skeletonema costatum*	Sea area near Hangu, Hangu to Tanggu offshore
2013	-	-	-	+	+	+	+	-	-	3	*Noctiluca scintillans*、*Pseudo-nitzschia pungens*、*Mesodinium rubrum*、*Skeletonema costatum*、*Thalassiosira nordenskioeldi*、*Chaetoceros affinis*、*P.delicatissima*	East Sea area of Tianjin Port Channel, East of Tianjin Port Economic Zone
2014	-	-	-	-	+	+	+	-	-	1	*Karenia mikimotoi*、*Cochlodinium polykrikoides Margalef*、*Ceratium furca*、*Prorocentrum micans*、*Thalassiosiraezcentrica*	Sea area near Zhongxin ecological city in Binhai New Area

http://www.aloki.hu ● ISSN 1589 1623 (Print) ● ISSN1785 0037 (Online)
DOI: http://dx.doi.org/10.15666/aeer/2003_21432155

Date										Frequency of red tide number	Main Species	Distribution Area
year	Month(occur +,no-)											
	Mar	Apr	May	Jun	Jul	Aug	Sep	Oct	Nov			
2015	-	-	-	-	-	+	+	-	-	1	*Cochlodium polykrikoides* *Thalassiosira pacifica*、*Alexandrium catenella*、*Gymnodinium catenatum*、*Cochlodinium polykrikoides Margalef*、*Ceratium furca*、*Gymnodinium impudicum*、*Akashiwo sanguinea*、*Scrippsiella trochoidea*、*Eucampia zodiacus*、*Thalassiosira rotula* *Thalassiosira pacifica*、*Rhizosolenia delicatula*、*Eucampia cornuta*、*Mosodinium rubrum*、*Thalassiosira rotula* 、*Ceratium furca*、*Leptocylindrus*、*Nitzschia pungens*、*Lauderia annulata*、*Gymnodinium impudicum*	South Sea area of Tianjin Port
2016	-	-	-	+	+	+	-	-	-	4		Tianjin red tide monitoring area and its adjacent waters
2017	+	-	-	+	+	+	-	-	-	6		North of Tianjin Port channel to Hangu sea area、Sea area near Hangu

http://www.aloki.hu ● ISSN 1589 1623 (Print) ● ISSN1785 0037 (Online)
DOI: http://dx.doi.org/10.15666/aeer/2003_21432155

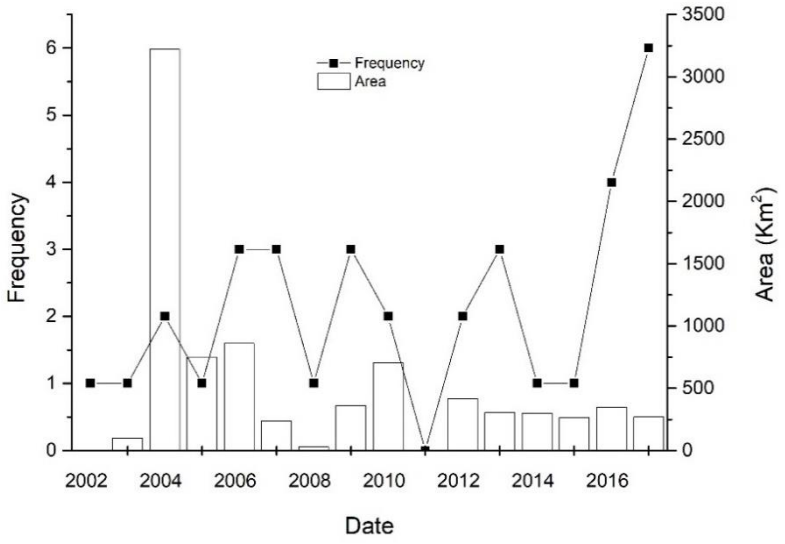

Figure 2. *Statistics of red tide area (histogram) and frequency (line chart) in Tianjin Coastal Area during 2002-2017*

During the study period, red tide covered the overall area of 8168.05 km^2 in Tianjin coastal waters, whereas annually it covered an average area of 544.54 km^2. In 2004, the largest expansion of red tide occurred in tian jin coastal, 3220.00 km^2, followed by 860.00 km^2 in 2006, and the least expansion 0.50 km^2 recorded in 2008. According to previous report, in the whole Bohai sea, areas with the highest concentrations of HAB found in the Bohai Bay, and tend to move from coastal waters to offshore Bohai sea (Song et al., 2016).

Temporal variation of red tide

During 2002-2017, the occurrence period of red tide in Tianjin coastal area was between June and August (*Fig. 3*), which is same as Hebei Province (Mo, 2010; An et al., 2015). In the month of August, the most number of red tide events recorded, which accounting for 27.3% of the total events (*Fig. 3*), July and June followed by comprising 25% and 20% of the total events. Similar kind of results also reported in the whole Bohai sea area where most HAB outbreaks reported in the month of June followed by July and August (Song et al., 2016). Which depicts that the summer season is advantageous for the extensive growth of algal cells and bloom formation. During this time, the Haihe River system intrude largest amount of freshwater into the sea (Zhang et al., 2020). Besides, the land-based domestic sewage, industrial waste water and agricultural non-point source pollution flow into the Bohai Bay. In summer, the prevailing southeast wind transports the nutrients from the lower layer of the coast to the surface of the sea through vertical mixing (Kan et al., 2016). Due to the poor water capacity of Bohai Bay, during the high tide period the content of COD, inorganic nitrogen (IN) and inorganic phosphorius (IP) in the coastal water is higher than that in the normal and low water period (Wu et al., 2007). Therefore, the red tide organisms propagate rapidly, and the seawater surface is seriously eutrophicated (Sun et al., 2004). On the other hand, within a suitable temperature range, the occurrence of red tide is positively correlated with the surface temperature of seawater (Dou et al., 2015). In summer, the variation range of sea water temperature is between 25℃ and 30℃, the surface water temperature is relatively stable,

http://www.aloki.hu ● ISSN 1589 1623 (Print) ● ISSN1785 0037 (Online)
DOI: http://dx.doi.org/10.15666/aeer/2003_21432155

and the daily variation of temperature difference is less than 1°C (Wu et al., 2007; Yin et al., 2015). Therefore, the proximal water temperature might assist in the red tide outbreak. In addition, in recent 15 years, the time cycle of red tide event in Tianjin coastal waters has been extended. Particularly, the red tide recorded in March 2017 shows the instance that the duration of red tide is ahead of schedule. Similarly, the red tide recorded in October 2007 and November 2010 revealed the occurrence time of red tide also has a trend of postponements.

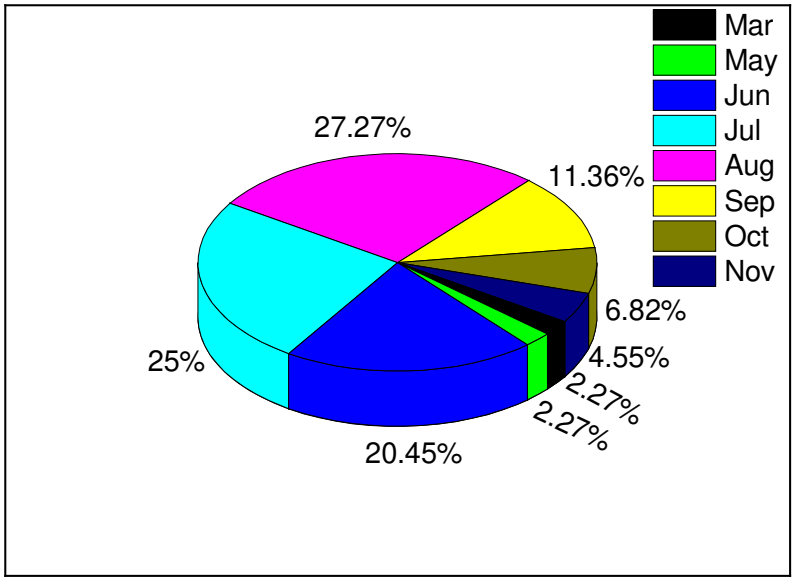

Figure 3. *Temporal variation of Red tide events in the Tianjin coastal area*

Variability of red tide biota

The main red tide causing species are characterized by high carbon content and play a key role in the stability and balance of marine ecosystem (Sun et al., 1999). There are 90 red tide species recorded in the sea area of China and about 30 species in the Bohai Sea area. The main biological groups of red tide in the Bohai Sea include dinoflagellates, diatoms, chromoflagellates, brown flagellates and protozoa. Among them, dinoflagellates, diatoms and chromoflagellates are the dominant red tide causing groups accounting for 75.20% of the total number of red tide in the Bohai Sea and 73.70% of the total area (Guo et al., 2015). It was reported that the dominant red tide species *Noctiluca* and *Chlorella*, accounting for 37.60% and 43.50% of the total red tide events. Before 1990s, the dominant species of red tide in the Bohai Sea mainly included *Noctiluca scientillans* and *Prorocentrum dentatum* (Song et al., 2016). The number of species of red tide biota is increasing year by year, from a single species before 2002 to 10 species in 2017 (*Fig. 4*). After entering into the 21st century, the dominance of red tide species has increased, and the species that can produce toxins, such as *Phaeocystis globosa*, *Gymnodinium catenatum*, *Prorocentrum dentatum*, *Alexandrium catenella*, *Karenia mikimotoi*, and *Skeletonema costatum* were recorded (Lin et al., 2008; Guo et al., 2015). Some species such as *Phaeocystis globosa*, *Karenia mikimotoi* and *Chattonella marina* never caused HAB before 2000 (Song et al., 2016). This change in red tide species composition might be mostly because of dispersal of species through anthropogenic interventions, such as ballast water discharge by worldwide transportation (Richardson, 1997) or by wind from

http://www.aloki.hu ● ISSN 1589 1623 (Print) ● ISSN1785 0037 (Online)
DOI: http://dx.doi.org/10.15666/aeer/2003_21432155

seaward open ocean, and in part to the eutrophication around there (Anderson et al., 2008). Besides, the seasonal and annual changes of red tide community also can be the process of species succession (Sun et al., 2002). However, the dominant *N.a scientillans* was responsible for maximum red tide events in this area causing five red tide events (*Fig. 4*). Not only during our study period, but also before 2000 it was reported that most of the HAB events caused by *N. scientillans* (Song et al., 2016). Even the first report of HAB in the Bohai sea during 1952 was caused by *N.a scientillans* (Fei, 1952). Another study reported that, from 1952 to 2014, a total of 57 HAB outbreaks caused by *N.a scientillans* (Song et al., 2016). Besides, *Skeletonema costatum*, *Phaeocystis globosa* and *Karenia mikimotoi* causes 4,3 and 3 red tide events respectively (*Fig. 4*). The first occurrence of the toxic red tide algae *K. mikimotoi* and *P. globosa* reported in 2006 and 2007, respectively (*Fig. 4*). Later on, the toxic red tide organisms gradually evolved into the dominant species of red tide, and the red tide caused by the toxic algae in the coastal waters showed an increasing trend (*Fig. 4*).

	Gymnodinium aeruginosum	*Noctiluca scintillans*	*Karenia mikimotoi*	*Chattonella marina*	*Phaeocystis globosa*	*Heterosigma akashiwo*	*Skeletonema costatum*	*Eucampia zodiacus*	*Ceratium furca*	*Nitzschia closterium*	*Coscinodiscus wailesii*	*Nitzschia pungens*	*Leptocylindrus danicus*	*Pseudonitzschia delicatissima*	*Thalassiosira nordenskioeldi*	*Chaetoceros curvisetus*	*Pseudo-nitzschia pungens*	*Mesodinium rubrum*	*Chaetoceros affinis*	*Cochlodinium polykrikoides*	*Prorocentrum micans*	*Thalassiosira eccentrica*	*Thalassiosira pacifica*	*Alexandrium catenella*	*Gymnodinium catenatum*	*Gymnodinium impudicum*	*Akashiwo sanguinea*	*Scrippsiella trochoidea*	*Thalassiosira rotula*	*Rhizosolenia delicatula*	*Eucampia cornuta*	*Lauderia annulata*
2017									*			*	*						*					*					*	*	*	*
2016								*	*												*			*	*	*	*	*	*	*			
2015																				*												
2014			*						*											*	*	*										
2013		*					*						*	*	*		*	*	*													
2012							*	*					*	*	*	*																
2011																																
2010		*									*	*																				
2009		*					*																									
2008									*	*																						
2007					*		*	*																								
2006		*			*	*																										
2005				*																												
2004			*																													
2003		*																														
2002	*																															

Figure 4. *Annual variation of red tide species in Tianjin coastal waters from 2002 to 2017*

The statistical analysis of the past 15 years red tide events shows that the red tide biota has obvious seasonality. With the increase of sea water temperature, the composition and proportion of nitrogen and phosphorus in the coastal water become imbalanced (Liu and Yuan, 2008). As a result, the red tide breaks out and the species and community structure of the red tide biota change. Consequently, the changing red tide biota led to the change of the nutrient concentration and structure of the water body, showing a dynamic relationship of interaction (Liu and Yuan, 2008). Among them, *N. scientillans* is a heterotrophic Dinoflagellata, widely distributed in the coastal areas of China, and able to tolerate high temperature and salinity (Guo et al., 2015). It begins to proliferate in March

http://www.aloki.hu ● ISSN 1589 1623 (Print) ● ISSN1785 0037 (Online)
DOI: http://dx.doi.org/10.15666/aeer/2003_21432155

every year and enters into the outbreak period during April to October (Yin et al., 2013). Red tide causing by *N. scientillans* is easy to break out in Tianjin estuary and areas with poor hydrodynamic conditions in the north. It occurred in 2003, 2006, 2009 and 2010 for a short duration (June and August) resulting in changes of physical and chemical factors of water body and impact on water ecological environment. *S. costatum*, a diatom species having a wide range of temperature and salinity tolerance, which is distributed near the shore, a good indicator of pollution. The growth of *S. costatum* cells is limited by nitrogen element. In spring, summer and autumn, red tide can be formed by explosive reproduction of this species (Wang et al., 2006). In 2007, 2009, 2012 and 2013, it happened in the coastal waters during July to September. Besides, in 2004 and 2014, red tide broke out by toxic *K. mikimotoi* in Tianjin coastal waters. *K. mikimotoi* is active on the surface of the water body especially within 2 meters of water depth (Chen et al., 2015). It has obvious diel vertical movement, and its growth has obvious correlation with rainfall, light and trace elements (Chen et al., 2015). However, in 2006 the first occurrence of red tide cause by *P. globosa* observed in Tianjin sea area which evolved into dominant species over time (*Fig. 4*). is a typical toxic and harmful red tide alga, generally in the South Sea area and widely distributed in high water temperature (Qi et al., 2001).

Causative factors of red tide

The cause and mechanism of red tide are different due to the biological groups and species, and closely related to the hydrological and meteorological conditions (Lin et al., 2008; Zou et al., 2015). The natural and geographical environment of the coastal area determines the basic conditions for the outbreak of red tide, such as hydrology, temperature, salinity and nutrients. Therefore, similar red tide biota also shows different bio-ecological characteristics in different sea areas (Zhao et al., 2003).

The temporal and spatial variation of red tide in Tianjin coastal waters is related to the flux of land-based sources into the sea, the pollutants entering into the sea, the surface temperature and the rapid eutrophication of estuarine water. COD, IN, concentration of IP pollutant discharge into the sea is related to the occurrence of red tide, which indicates that the red tide in Tianjin coastal area of Bohai Bay may be greatly affected by land-based emission, which is consistent with the research of Liu Hanlin and Shi Haiming (Shi et al., 2010; Liu et al., 2019). Direct input of land runoff and sewage outfall, the atmospheric deposition flux is also an important source of nitrogen in the marine waters (Ma et al., 2012). Because of the anthropogenic influence, during the last six decades, the concentration of IN increased 7-fold (Xin et al., 2019). Consequently, the phytoplankton biomass increased several folds in recent past and phytoplankton community shifted from diatom dominance to dinoflagellates. Red tide was a rare phenomenon before 1980s but occurring very frequently after 1990s, which changed the Bohai sea area from N-limited to P-limited ecosystem (Xin et al., 2019).

Marine sediment exchange flux is the main source of surface nutrients (Zhang et al., 2009). Tianjin shallow sea beach is a typical accumulation type plain coast. Under the joint action of current and tide, the content of suspended particulate matter in the sediment of the sea area is very high and one of the highest in the world (Mu, 2015). During the past 15 years, human disturbance such as marine exploitation and channel dredging in Tianjin coastal area has increased. Therefore, the concentration of suspended solids has been increased, and the transparency of sea water has been significantly reduced, which directly or indirectly affects the red tide biota (Dou et al., 2015; Guo et al., 2015; Huang et al., 2018).

http://www.aloki.hu ● ISSN 1589 1623 (Print) ● ISSN1785 0037 (Online)
DOI: http://dx.doi.org/10.15666/aeer/2003_21432155

In Bohai Bay, most of the red tide broke out in summer season especially from June to August. Summer flood carries tremendous amount of land-based nutrients and pollutants, and the temperature rises from June to August. After reaching at the peak in August, the surface temperature of the sea began to decrease, and the land-based pollutants continued to reduce. Besides, Tianjin has obvious monsoon characteristics. In summer, the coastal wind speed of Tianjin is relatively lower, and the southerly wind prevails in this area (Xu et al., 2018). Analyzed that during the red tide, the wind speed force 3 and 4, and the wind direction was mainly southeast and southwest wind (Zhang et al., 2020). This condition is suitable to raise nutrients from the deep layer of sea water to the surface. Therefore, in summer the surface sea water is under the conditions of high temperature, sufficient light and nutrient rich so as to speed up the growth rate of red tide organisms (Zhang et al., 2020). In addition, low wind speed and waves are conducive to the aggregation of red tide organisms and promote the occurrence of red tide in the coastal waters (Zhang et al., 2020).

However, red tide organisms are a kind of media living in the water body, which has weak or no ability of movement (Mu, 2015). The hydrodynamic condition is closely related to the biomass of red tide organism. Their life cycle, movement and nutrition supply depend on the water current. Therefore, the spatiotemporal and biological changes of red tide contain a series of complex oceanographic and ecological processes, and the research of related fields needs to be further expanded.

Conclusion

Based on the red tide monitoring data of Tianjin marine environmental quality bulletin (2002 to 2017), this paper studies the temporal and spatial changes of red tide in Tianjin coastal area of Bohai Bay. Following are the summary of the red tide event in recent 15 years.

(1) During the past 15 years from 2002 to 2017, 34 red tides were recorded, with an accumulated area of about 8168.05 km^2. The annual average occurrence of red tides was 2.3 events, with an area of 544.54 km^2. The occurrence frequency of red tide increased but the occurrence area of red tide decreased and tends to be stable as a whole, which shows that the prevention and control of land-based water pollution have played an obvious role in the control of pollutants since the 11^{th} five-year plan of China, and the effect of environmental quality improvement in Tianjin coastal waters is obvious.

(2) The occurrence time of the red tide in the coastal waters was mostly in June to August every year, which has obvious seasonal variations. The occurrence of the red tide is sometimes advanced or delayed, which results in the prolongation of the period of the generation and dissipation of the red tide. The spatial distribution of red tide is characterized by less in the south, more in the north, and more in the sea area from the anchorage of Tianjin port to Hangu sea area, showing the change rule of diffusion from the near shore estuary and shoal to the north and east sea areas.

(3) The red tide biota in the coastal area includes Dinoflagellatae, Bacillariophyceae, Chrysophyta, etc. The species of red tide biota increased from 1 to 10. The dominant species of red tide organisms are *Noctiluca scintillans*, *Skeletonema costatum*, *Phaeocystis globosa* and *Karenia mikimotoi*. The number of toxic red tide organisms increased significantly, and harmful red tide in coastal waters showed an increasing trend.

(4) Land source pollutants, sea surface temperature, wind speed and wind direction have an impact on the occurrence of red tide. Land source pollutant flux has a relatively

http://www.aloki.hu ● ISSN 1589 1623 (Print) ● ISSN1785 0037 (Online)
DOI: http://dx.doi.org/10.15666/aeer/2003_21432155

large impact on runoff, indicating that the red tide organisms in Tianjin coastal waters may be greatly affected by the input of land source nutrients. In this paper, the analysis of factors affecting the growth of red tide organisms is not comprehensive enough. Other environmental variables such as suspended solids, atmospheric deposition and hydrodynamic forces may also affect the changes of red tide organisms' time and biota. The research work in related fields needs to be further expanded.

Acknowledgements. This study is supported by the National Marine Public Welfare Research Project [Nos. 201505027 and 201505018], National Key R&D Program of China [2019YFD0901105], National Science Foundation of Fujian Province, China [2018J01062] and Marine ecological early warning monitoring project (2019), Marine early warning and monitoring division, MNR.

REFERENCES

[1] An, X. L., Li, X. M., Li, Z. X. (2015): Study on the Hazard Grading, Spatial-Temporal Distribution and Changes of Dominant Causative Organisms for Alleviating Harmful Algae Blooms in Hebei Coastal Sea Areas. – China Ocean Technology 34(1): 69-75.

[2] Anderson, D. M., Burkholder, J. M., Cochlan, W. P., Glibert, P. M., Gobler, C. J., Heil, C. A., Kudela, R. M., Parsons, M. L., Rensel, J. E. J., Townsend, D. W., Trainer, V. L., Vargo, G. A. (2008): Harmful algal blooms and eutrophication: examining linkages from selected coastal regions of the United States. – Harmful Algae 8(1): 39-53.

[3] Borowitzka, M. A. (2018): Chapter 3-Biology of Microalgae. – In: Levine, I. A., Fleurence, J. (eds.) Microalgae in Health and Disease Prevention. Academic Press, pp. 23-72.

[4] Chen, B. H., Xie, E. Y., Gao, Y. H., Dong, J. W., Zhou, Q. L. (2015): Toxic effects of red tide caused by Karenia on marine organisms. – Journal of Fujian Fisheries 37(3): 241-249.

[5] Cong, P. F., Zhang, F. S., Qu, L. M. (2008): Overview on monitoring and forecast of red tide hazard. – Journal of Catastrophology 23(2): 127-130.

[6] Costanza, R., d'Arge, R., de Groot, R., Farber, S., Grasso, M., Hannon, B., Limburg, K., Naeem, S., O'Neill, R. V., Paruelo, J., Raskin, R. G., Sutton, P., van den Belt, M. (1997): The value of the world's ecosystem services and natural capital. – Nature 387: 253-260.

[7] Dou, Y., Gao, J. W., Shi, X. T., Chen, R. N., Zhou, W. L. (2015): Outbreak Frequency and Factors Influencing Red Tides in Nearshore Waters of the South China Sea from 2000 to 2013. – Journal of Hydroecology 36(3): 31-37.

[8] Fei, H. N. (1952): The cause of red tides. – SciArt 22: 1-3.

[9] Glibert, P. M., Anderson, D. M., Gentien, P., Graneli, E., Sellner, K. G. (2005): The global, complex phenomena of harmful algal blooms. – Oceanography 18(2): 136-147.

[10] Guo, H., Ding, D. W., Lin, F. G., Guan, C. J. (2015): Characteristics and Patterns of Red Tide in China Coastal Waters During the Last 20a. – Advances in Marine Science 33(4): 547-558.

[11] Guy, R. C. (2014): Red Tide. – In: Wexler, P. (ed.) Encyclopedia of Toxicology (Third Edition). Academic Press, pp. 65-66.

[12] Huang, H., Yi, Y., Lu, Y., Zuo, G., Rong, Z. (2018): Study on dynamics of net-phytoplankton in Bohai Bay ecological monitoring area in summer from 2004 to 2015. – Acta Oceanologica Sinica 40(1): 115-128.

[13] Kan, W. J., Fan, D. J., Zhang, Q. F., Tu, J. B. (2016): Seasonal Variation and Assessment of Water Quality in Bohai bay in Tianjin Shore Sea Areas. – Transaction of Oceanology and Limnology 1: 25-29.

[14] Kang, Y. D., Lv, P. D., Zhang, K. C. (1982): The determination of phytoplankton photosynthesis in the Bohai Bay. – Transactions of Oceanology and Limnology 4: 47-51.

[15] Li, B. H., Lin, F. Q. (1999): The report of red tide monitoring in Bohai Bay (Tianjin sea area) in 1998. – Tianjin Fishery 3: 43-44.

http://www.aloki.hu ● ISSN 1589 1623 (Print) ● ISSN1785 0037 (Online)
DOI: http://dx.doi.org/10.15666/aeer/2003_21432155

[16] Lin, F. G., Lu, X. W., Luo, H., Ma, M. H. (2008): History, status and characteristics of red tide in Bohai Sea. – Marine Environmental Science 27(S2): 1-5.
[17] Liu, X. H., Yuan, Y. L. (2008): Recent ecological degradation in coastal areas of Bohai Sea. – Marine Environmental Science 5: 531-536.
[18] Liu, H. L., Nie, H. T., Wang, Y. L. (2019): Estimation method of pollutant load into sea using statistical data Tianjin city. – Marine Environmental Science 38(6): 968-976.
[19] Ma, S., Yang, X. F., Li, Z. W. (2012): An approach of estimating the atmospheric deposition of nitrogen to the coastal water using GOME-2 satellite data. – Marine Environmental Science 31(2): 272-276.
[20] Mo, Q., Li, Z. X., Li, X. M. (2010): A survey of red tide organisms in the coastal areas of Hebei Province. – Hebei Fisheries 6: 46-47.
[21] Mu, D. (2015): The Influence of Nutrients on the Dynamics of the Plankton of Bohai Bay. – Tianjin University (In Chinese).
[22] Qi, Y. Z., Shen, P. P., Wang, Y. (2001): Taxonomy and lifecycle of genus Phaeocystis (Prymnesiophyceae). – Journal of Tropical and Subtropical Botany 9(2): 174-184.
[23] Qiao, Y. L., Yin, X. Y., Sun, Y., Yu, H., Wang, W. F. (2018): The Construction of Marine Ecological Civilization in Tianjin. – Ocean Development and Management 35(6): 71-75.
[24] Qiao, Y. L., Yin, X. Y., Yu, H., Wang, W. F. (2019): The Ecosystem Based Marine Environment Management in Tianjin. – Ocean Development and Management 36(4): 13-16.
[25] Richardson, K. (1997): Harmful or exceptional phytoplankton blooms in the marine ecosystem. – Advances in marine biology 31: 301-385.
[26] Shi, H. M., Yin, C. L., Zhang, Q. F., Xu, Y. S., Wang, B. (2010): Analysis of variations and structure characteristic of nutrients in Red-tide Monitoring Area of Bohai Bay. – Marine Environmental Science 29(2): 246-249.
[27] Shi, W., Wang, M. H. (2012): Satellite views of the Bohai Sea, Yellow Sea, and East China Sea. – Progress in Oceanography 104: 30-45.
[28] Song, N. Q., Wang, N., Lu, Y., Zhang, J. R. (2016): Temporal and spatial characteristics of harmful algal blooms in the Bohai Sea during 1952–2014. – Continental Shelf Research 122(1): 77-84.
[29] Sun, J., Liu, D. Y., Qian, S. B. (1999): Study on phytoplankton biomass I. Phytoplankton measurement biomass from cell volume or plasma volume. – Acta Oceanologica Sinica 21(2): 75-85.
[30] Sun, J., Liu, D. Y., Qian, S. B. (2001): Preliminary study on the seasonal succession and development pathway of phytoplankton community in the Bohai Sea. – Acta Oceanologica Sinica 20(2): 251-253.
[31] Sun, J., Liu, D. Y., Yang, S. M., Guo, J., Qian, S. (2002): The preliminary study on phytoplankton community structure in the central Bohai sea and the Bohai strait and its adjacent area. – Oceanologia et Limnologia Sinica 33(5): 461-471.
[32] Sun, T., Tao, J. H. (2004): The study of pollutant transport on the action of waves in the near-shore area of Bohai Bay. – Oceanologia et Limnologia Sinica 35(2): 110-119.
[33] Tan, S. C., Shi, G. Y. (2006): Remote sensing for ocean primary productivity and its spatio-temporal variability in the China Seas. – Acta Geographica Sinica 61(11): 1189-1199.
[34] Tianjin Oceanic Administration (2002-2017): Bulletin of marine environmental status of Tianjin. – Tianjin: Tianjin Oceanic Administration (in Chinese).
[35] Wang, Z. L., Li, R. X., Zhu, M. Y. (2006): Study on Population Growth Processes and Interspecific Competition of Prorocentrum donghaiense and Skeletonema costatum in Semi-Continuous Dilution Experiments. – Advances in Marine Science 24(4): 495-503.
[36] Wei, H., Sun, J., Moll, A., Zhao, L. (2004): Phytoplankton dynamics in the Bohai Sea observations and modelling. – Journal of Marine Systems 44(3/4): 233-251.
[37] Wu, G. H., Li, W. Q., Zheng, H. Q. (2007): Water pollution characteristics in Tianjin sea area of the Chinese Bohai Bay. – Acta Oceanologica Sinica 29(2): 144-149.

http://www.aloki.hu ● ISSN 1589 1623 (Print) ● ISSN1785 0037 (Online)
DOI: http://dx.doi.org/10.15666/aeer/2003_21432155

[38] Xin, M., Wang, B., Xie, L., Sun, X., Chen, K. (2019): Long-term changes in nutrient regimes and their ecological effects in the Bohai Sea, China. – Mar Pollut Bull 146: 562-573.
[39] Xu, L. Z., Bu, Q. J., Xu, C. Y. (2018): Climatic Characteristics and Disastrous Weather Effects in Tianjin Coastal Area. – Tianjin Science & Technology 45(9): 109-113.
[40] Yin, C. L., Zhang, Q. F., Zou, T., Zhang, C. P., Cui, J., Sun, J. W. (2013): Analysis for *Noctiluca scintilans* red tide in Bohai bay. – Transaction of Oceanology and Limnology 2: 99-104.
[41] Yin, C. L., Zhang, Q. F., Kan, W. J., Zhang, Y. N. (2015): Nutrient Variation and Eutrophication Assessment of Bohai Bay in Tianjin. – Journal of Tianjin University of Science & Technology 30(1): 56-61.
[42] Zhang, J. F., Li, Q. X., Tao, J. H. (2009): Exchange flux and effect factors of nutrients between bottom sediment and water in Bohai Bay. – Marine Environmental Science 28(5): 492-496.
[43] Zhang, Q., Sun, J. W., Feng, Y. Z., Li, X. B., Wang, L. N., Cui, J. (2020): Research on the basic characteristics of red tide in Tianjin coastal area. – Marine Forecasts 37(1): 62-66.
[44] Zhao, D. Z., Zhao, L., Zhang, F. S. (2003): Type of formation, distribution and temporal trend of red tides occurred in the china sea. – Marine Environmental Science 3: 7-11.
[45] Zhao, D. Z., Zhao, L., Zhang, F. S., Zhang, X. Y. (2004): Temporal occurrence and spatial distribution of red tide events in China's coastal waters. – Human and Ecological Risk Assessment 10(5): 945-957.
[46] Zohdi, E., Abbaspour, M. (2019): Harmful algal blooms (red tide): a review of causes, impacts and approaches to monitoring and prediction. – International Journal of Environmental Science and Technology 16(3): 1789-1806.
[47] Zou, J. Z., Dong, L. P., Qin, B. P. (1983): Preliminary study on the eutrophication and HABs in the Bohai Bay. – Marine Environmental Science 2(2): 41-54.
[48] Zou, T., Ye, F. J., Liu, X. M. (2015): Analysis of the environmental conditions for the occurrence of red tide in Tianjin coastal waters. – Marine Forecasts 37(3): 241-249.

http://www.aloki.hu ● ISSN 1589 1623 (Print) ● ISSN1785 0037 (Online)
DOI: http://dx.doi.org/10.15666/aeer/2003_21432155

RESPONSE OF THE PS II FUNCTION OF *MORUS ALBA* VAR. 'QIUYU' SEEDLING LEAVES TO DIFFERENT NITROGEN FORMS

XU, N.[1,2*] – YU, S. P.[1,2*] – DING, J. N.[1,2] – SHI, C. Q.[1,2]

[1]*Harbin University, Harbin 150086, China*

[2]*Key Laboratory of Heilongjiang Province for Cold-Regions Wetlands Ecology and Environment Research, Harbin University, Harbin 150086, China*

[*]*Corresponding author*
e-mail:wetlands1972@126.com; xunan0451@126.com

(Received 26th Aug 2021; accepted 3rd Dec 2021)

Abstract. In order to gain insights into the effect of different nitrogen forms on the photosynthetic ability of *Morus alba,* we studied chlorophyll fluorescence characteristics of one-year-old *M. alba* leaves treated with nitrate-nitrogen (NO_3^--N), ammonium-nitrogen (NH_4^+-N) and ammonium nitrate (NH_4NO_3). We found that the PSII photochemical activity, electron transport rate and light energy usage of the *M. alba* leaves were significantly lower in plants treated with NH_4^+-N compared to those treated with NO_3^--N and NH_4NO_3. We did not observe a significant difference in photosynthetic parameters between the NO_3^--N and NH_4NO_3 treatments. There was an increase in the relative variable fluorescence values at the J step (V_J) and I step (V_I) of *M. alba* leaves under the NH_4^+-N treatment compared to the NO_3^--N and NH_4NO_3 treatments. In addition, the values of V_k and V_L in *M. alba* leaves in plants treated with NH_4^+-N were significantly lower than the NO_3^--N and NH_4NO_3 treatments, suggesting that the inhibition of the oxygen-evolving complex (OEC) activity and the declined stability of the thylakoid membrane structure in *M. alba* leaves contributed to the decline of the photochemical activity in the PSII reaction center under the treatment of NH_4^+-N.
Keywords: *Morus alba, Chlorophyll fluorescence, nitrogen, photosynthetic, OJIP curves*

Introduction

Nitrogen is one of the most important elements for plants. Over half of the nitrogen in plants mainly exists within chloroplasts in the form of enzymes, participating in the photosynthetic metabolic processes (Shangguan et al., 2000) and playing an important role in their growth and development (Wang and Baerenklau, 2014). Except for a small amount of amino acids absorbed by plants, nitrogen is mainly absorbed by the roots in the form of nitrate-nitrogen (NO_3^--N), ammonium-nitrogen (NH_4^+-N) and, organic nitrogen (Chapin et al., 1993; Kuelland, 1994). NO_3^--N or NH_4^+-N constitutes the major form of absorption (Lin and Lin, 2011). Different plants have unique preferences for the type of nitrogen that the roots absorb. For example, *Picea glauca* (Kim et al., 2002), *Pinus sylvestris* (Nordin et al., 2001) and *Oryza sativa* L. (Matsudo et al., 2009) prefer NH_4^+-N, while excessive NH_4^+-N can be toxic to the NO_3^--N-preferring plants like *Haematococcus pluvialis* (Choi et al., 2003) and *Neochloris oleoabundans* (Li et al., 2008; Pruvost et al., 2009). A relatively high concentration of NO_3^--N can significantly improve the stress resistance of *Indian mustard* (Nathawat et al., 2007) and *Spirulina platensis* (Danesi et al., 2002), while the application of NH_4^+-N was proven to be more beneficial for *Hordeum vulgare* L. under salt stress (Ali et al., 2001). Many researches have also been conducted studying the absorption volume, absorption rate, and absorption proportion of NH_4^+-N and NO_3^--N in crops such as rice, wheat and

http://www.aloki.hu ● ISSN 1589 1623 (Print) ● ISSN1785 0037 (Online)
DOI: http://dx.doi.org/10.15666/aeer/2003_21572170

vegetables such as cabbage, lettuce, and spinach (Ambus et al., 2011; Sutton et al., 2012; Gruffman et al., 2012).

Morus alba L. is the most widely cultivated and utilized plant in China., *M. alba* can be classified depending on its applications as *M. alba* for silkworm, consumption, fruit, feed, or virescence and so on (Wang et al., 2004; Liu et al., 2019). *M. alba* leaves are highly nutritious, with protein content similar to alfalfa, which is 80%~100% higher than that of forage grass of the grass family, and 40%~50% higher than that of legume forage (Wang et al., 2004; Liu et al., 2019). *M. alba* leaves are rich in amino acids with appropriate proportions, especially rich in glutamic acid, making the *M. alba* leaves an excellent source of protein, and feed combined with *M. alba* leaves can have an enhanced nutritional value (Xu et al., 2012; Liu et al., 2019). With the development of the "South-north" relocation policy which is aimed to encourage planting *M. alba* trees in the Northern part of China, *M. alba* is being cultivated at an increasing rate. *M. alba* trees are resistant to salinity and drought (Hu et al., 2007; Zhang et al., 2012; Pang et al., 2014), therefore the cultivation acreage of *M. alba* in the saline-alkali soil area of the stock breeding grassland region of Song Nen Plain is relatively large, to help rehabilitate the degraded grassland and increase the forage capacity. However, the cultivation of *M. alba* in the saline-alkali regions of Northwestern Heilongjiang Province has resulted in slow growth before July, likely caused by the low temperature and less rainfall in the spring. In order to speed up the growth of *M. alba* at the early stages, a previous study has found that increasing nitrogen fertilization could promote the growth of *M. alba* (Zhang et al., 2012; Pang et al., 2014) and the appropriate amount of nitrogen application was determined as well.

The strong stress resistance ability of *M. alba* makes it an excellent tree species for vegetation restoration in degraded ecosystems (Sun et al., 2003; Chen et al., 2006; Liu et al., 2019). However, the lack of nitrogen in the soil of these degraded ecosystems limits plant growth, affecting vegetation recovery (Britto et al., 2001; Jan et al., 2013; Guo et al., 2017; Mu et al., 2021). Careful application of nitrogen fertilizer is one of the important measures that can be adopted to speed up the recovery of degraded ecosystems. In our previous study, we found that *M. alba* preferred NO_3^--N. Application of NO_3^--N to *M. alba* increased photosynthetic ability and electron transport rate of the leaves compared to plants that were treated with NH_4^+-N (Nathawat et al., 2007). In addition to increased photosynthesis, the salt tolerance of *M. alba* also improved with the application of NO_3^--N (Zhang et al., 2013). However, it remains unclear what causes the high electron transport rate and photosynthetic capacity of *M. alba* under the treatment of NO_3^--N. In this study, chlorophyll fluorescence technology and fast chlorophyll fluorescence kinetics (OJIP) method were used to study the physiological responses of the leaves of *M. alba* seedlings, such as PS II photochemical reactivity, oxygen-evolving complex (OEC) function at the electron donor side, electron transport ability at the electron receptor side, electron storage capacity, thylakoid membrane structure state and light allocation parameters under different nitrogen forms; the reasons for the higher photosynthetic capacities under NO_3^--N treatment compared to NH_4^+-N treatment. In order to provide theoretical basis for the rational allocation of tree species in the process of vegetation restoration in the degraded ecological nitrogen deficient area, and provide some basic data and provide some basic data for rational fertilization for *M. alba*.

http://www.aloki.hu ● ISSN 1589 1623 (Print) ● ISSN1785 0037 (Online)
DOI: http://dx.doi.org/10.15666/aeer/2003_21572170

Materials and methods

Materials

Seeds of Mulberry 'Qiuyu' were received from the Heilongjiang Academy of Agricultural Sciences, China. Uniform mulberry seeds with orange color were selected for surface disinfection with 3.0% NaCl solution for 20 min, then washed with sterile water, soaked in sterilized saturated $CaSO_4$ solution for 6 h, and placed in an incubator at 37°C to accelerate germination. After blanking, the seeds were sown to the culture medium for seedling growth. The medium was fully mixed with fully mixed peatsoil and vermiculite in a ratio of 1:1(V/V). The medium was high-temperature sterilized, and the temperature was 25/23°C (light/dark), the light intensity was 400 $\mu mol \cdot m^{-2} \cdot s^{-1}$, the photoperiod was 12/12 h(light/dark). Cultured in an artificial climate box with relative humidity of about 75%, and managed the seedling stage for about 25 days. When the main radicle of seed germination grew to about 3 cm, seedlings with relatively consistent growth were selected to pull out from the culture substrate, carefully washed the culture substrate on the root surface, and then moved into the culture substrate (length 50 cm; width 40 cm; high 30 cm). The culture medium was Hogland nutrient solution, and the pH value of the medium was 6.0± 0.1. In order to prevent the roots from seeing light, the hydroponic box was wrapped with black light-proof paper, and the electric air pump was used for continuous ventilation. After one week of culture, the seedlings germinated white new roots and began to be treated with nitrogen fertilizer. The molar ratios of (NH_4^+-N) (NO_3^--N) in each treatment were 100:0, 50:50, 0:100, respectively. The concentration of other nutrient elements is completely the same, and the solution formula of each treatment is shown in *Table 1*. The culture medium was replaced every 3 days. The two upper fully expanded attached leaves of six to eight weeks old plants were used for experiments.

Table 1. *Nutrition composition of the hydroponics solution with different percentage of ammonium and nitrate nitrogen*

Nutrition Composition	NH_4^+:NO_3^-		
	100:0	**50:50**	**0:100**
$Ca(NO_3)_2$ (mmol·L^{-1})	1.50	0.50	0.00
KNO_3 (mmol·L^{-1})	2.00	1.50	0.00
$(NH_4)_2SO_4$ (mmol·L^{-1})	0.00	1.25	0.25
K_2SO_4 (mmol·L^{-1})	0.00	0.25	1.00
$CaSO_4$ (mmol·L^{-1})	0.00	0.50	1.00
$CaCl_2$ (mmol·L^{-1})	0.00	0.50	0.50
KH_2PO_4 (mmol·L^{-1})	1.00	1.00	1.00
$MgSO_4$ (mmol·L^{-1})	1.00	1.00	1.00
NaCl (mmol·L^{-1})	0.50	0.50	0.50

Experimental design

The experiment was conducted using a simple randomized block design. There were three treatments of the experiment, with different percentage of ammonium and nitrate nitrogen (NO_3^-N : NH_4^+-N) which were 100:0, 50:0 and 0:100 (*Table 1*). There were 3 seedlings in each treatment and 3 replicates in each treatment. The growth parameters and

http://www.aloki.hu ● ISSN 1589 1623 (Print) ● ISSN1785 0037 (Online)
DOI: http://dx.doi.org/10.15666/aeer/2003_21572170

photosynthetic parameters were measured after the seedlings were cultured in different nitrogen nutrient solution for 2 weeks.

Growth parameters determination

Select the processing relative consistent growth in mulberry branch contact with the ground diameter, the record for the ground diameter, each treatment for the plant, respectively will be filming for the root and aboveground 105℃ for 30 min, 60℃ after drying to constant weight according to its weight, or get the underground biomass and biomass on the ground, and calculate the total biomass (the sum of underground biomass and the ground biomass), root-shoot ratio = underground biomass/biomass on the ground.

Measurement of chlorophyll fluorescence

PSII Chl fluorescence measurements were done using an FMS-2 portable pulse modulated fluorometer (*Hansatch*, UK). The maximum PSII quantum yield (F_v/F_m) was determined in dark adapted (15 min) samples. After a short log phase, the fluorescence transient was induced by continuous actinic white light (1200 μmol m^{-2} s^{-1}) for 2 h, provided by Fluorimeter light source. Maximum quantum yield of PSII (F_v/F_m), photochemical quenching coefficient (q_p), and the actual PSII efficiency under irradiance (Φ_{PSII}) were calculated according to Genty et al. (1989), Chlorophyll a fluorescence transient was measured with a Handy-PEA fluorometer (*Hansatch*, UK). Having been dark adapted for 1 h before heat treatment, all the leaves were immediately exposed to a saturating light pulse (3000 μmol·m^{-2}·s^{-1} PFD) for 2 s after heat treatment in the dark at different times. Each transient obtained from the dark-adapted samples was analyzed according to the JIP-test (Strasser et al., 1995) by utilizing the following original data: (1) the fluorescence intensity at 20 ms (F_o, when all RCs of PSII are open); (2) the maximum fluorescence intensity (F_m, when all RCs of PSII are closed) and (3) the fluorescence intensities at 300 ms (K-step), 2 ms (J-step) and 30 ms (I-step). The maximum quantum yield of PSII photochemistry (F_v/F_m) was calculated as: $F_v/F_m = (F_m–F_o) / F_m$, in this study, $F_m = F_P$. The relative variable fluorescence intensity at J-step (V_J) and I-step (V_I) were calculated as: $V_t = (F_t–F_o)/(F_m–F_o)$. V_K and V_L were the relative variable fluorescence on the V_{O-J} and V_{O-K} point at 0.3 and 0.15 ms.

According to the JIP-test (Strasser et al., 1995; Zhang et al., 2018a) could obtain such as that maximum quantum yield of PSII photochemistry (F_v/F_m), Performance index on absorption basis (PI_{ABS}), Probability that a trapped exciton moves an electron into the electron transport chain beyond Q_A^- (at t=0) (Ψ_o), Quantum yield for electron transport (at t=0) (φE_o), quantum yield of absorption flux to dissipated energy (φD_o), Absorption flux per RC (*ABS*/*RC*), Trapped energy flux per RC (at t=0) (TR_o/RC), Electron transport flux per RC (at t=0) (ET_o/RC) and Dissipated energy flux per RC (at t=0) (DI_o/RC).

Statistical analysis

Excel and SPSS software (Version. 22) were used to conduct statistical analyses on the measured data. The data in the figure was denoted as mean ± standard deviation (SD). One-way ANOVA and least significant difference (LSD) were used to compare the differences among different data groups (n=3).

http://www.aloki.hu ● ISSN 1589 1623 (Print) ● ISSN1785 0037 (Online)
DOI: http://dx.doi.org/10.15666/aeer/2003_21572170

Results and analysis

The effect of different nitrogen forms on chlorophyll fluorescence parameters in the leaves of mulberry

When NH^{4+}-N:NO^{3-}-N is 50:50, the above ground biomass and underground biomass of mulberry seedlings reach the highest respectively (2.85 g/ plant and 0.993 g/ plant), and the total biomass from high to low is 50:50, 100:0, 0:100, the difference is very significant (*Table 2*) (P<0.05). The root-shoot ratio of the seedlings was the largest when NH^{4+}-N:NO^{3-}-N was 100:0, but the difference was not significant when it was 0:100, and the difference was the smallest when it was 50:50, which was 27.3% and 27.2% lower than the former two, respectively, and the difference was significant (P<0.05). The ground diameter is the largest when NH^{4+}-N:NO^{3-}-N is 50:50, which is about 1.5 times of that of 100:0 and 0:100, and the difference is extremely significant.

Table 2. *Biomass on leaves of mulberry seedlings to different nitrogen forms*

$NH4^+$-N:$NO3^-$-N	Above ground biomass (g)	Underground biomass (g)	Total biomass (g)	Root-shoot ratio (%)	Ground diameter(mm)
100:0	1.21±0.02b	0.308±0.04b	1.519±3.11b	3.98±0.51a	0.31±0.14b
50:50	2.85±0.0.06a	0.993±0.10a	3.840±3.90a	2.89±0.37b	0.54±0.15a
0:100	1.21±0.06b	0.35±0.03bc	1.563±3.66b	3.97±0.19a	0.32±0.15b

The effect of different nitrogen forms on F_v/F_m, $\Phi_{PS\ II}$, q_p and NPQ in the leaves of mulberry

To characterize the effect of NO_3^-N, NH_4^+-N, NH_4NO_3 treatment on mulberry leaf photosynthesis parameters, we measured the values of F_v/F_m, $\Phi_{PS\ II}$ and q_p of the *M. alba* leaves under various treatments. We observed a significant decrease in F_v/F_m, $\Phi_{PS\ II}$ and q_p in plants treated with NH_4^+-N compared to NO_3^--N and NH_4NO_3 (*Fig. 1*). Specifically, we observed a decrease of 9.13% (P<0.01), 55.53% (P<0.01) and 26.27% (P<0.01) for F_v/F_m, $\Phi_{PS\ II}$ and q_p, respectively, when compared to NO_3^--N, and 10.65% (P<0.01), 55.36% (P<0.01) and 38.87% (P <0.01) when compared to the NH_4NO_3 treatment respectively. All differences were highly significant. Under NH_4^+-N treatment, the NPQ value of mulberry leaves was significantly higher than those treated with NO_3^--N and NH_4NO_3. The differences of the chlorophyll fluorescence parameters of mulberry leaves under the treatments of NO_3^--N and NH_4NO_3 were insignificant.

Responses of $\Phi_{PS\ II}$ and ETR of mulberry seedling leaves to illumination intensity under the treatment of different nitrogen forms

We next tested the values of $\Phi_{PS\ II}$ and ETR of mulberry seedling leaves treated by different nitrogen forms under different illumination intensity conditions. In general, we observed that increasing the illumination intensity resulted in a decrease in $\Phi_{PS\ II}$ of mulberry seedling leaves (*Fig. 2*). ETR values first increased and then declined upon increased illumination, suggesting that there was light saturation. However, we observed significant differences between the different nitrogen treatments. Plants treated with NO_3^--N and NH_4NO_3 did not show difference in $\Phi_{PS\ II}$ and ETR at different illumination intensities. However, in plants treated with NH_4^+-N, the $\Phi_{PS\ II}$ was significantly lower at different illumination intensities (P<0.01). There was no difference in ETR of plants

http://www.aloki.hu ● ISSN 1589 1623 (Print) ● ISSN1785 0037 (Online)
DOI: http://dx.doi.org/10.15666/aeer/2003_21572170

illuminated with 100 and 200 μmol·m^{-2}·s^{-1}, but when the illumination intensity exceeded 200 μmol·m^{-2}·s^{-1}, the ETR under NH_4^+-N treatment was significantly lower than those under the treatment of NO_3^--N and NH_4NO_3 (P<0.01). Lastly, the light saturation point was above 1,000 μmol·m^{-2}·s^{-1} for NO_3^--N and NH_4NO_3 treatments, and around 600 μmol·m^{-2} s^{-1} for the NH_4^+-N treatment.

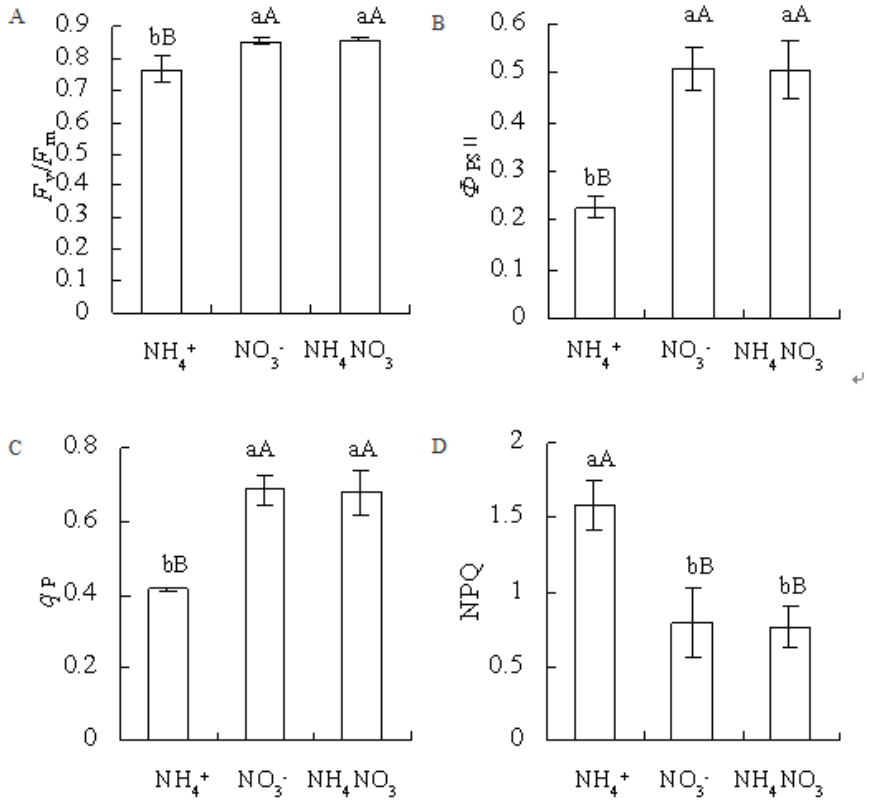

Figure 1. *Responses of chlorophyll fluorescence parameters F_v/F_m, $\Phi_{PS\,II}$, q_p and NPQ in the leaves of mulberry seedlings to different nitrogen forms. Means ± SD of three replicates are presented. Values followed by different small letters mean significant difference (p<0.05), values followed by different capital letters mean very significant difference (p<0.01). n=3*

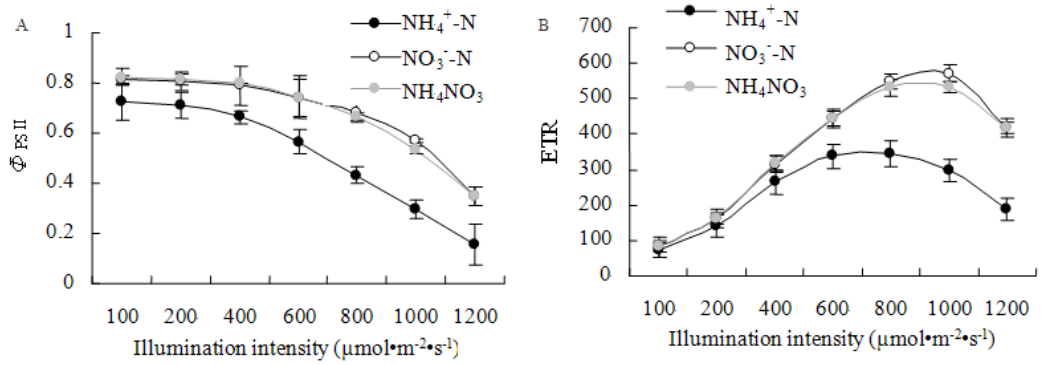

Figure 2. *Responses of chlorophyll fluorescence parameters of mulberry seedling leaves to illumination intensity under the treatment of different nitrogen fertilizer treatments. Means ± SD of three replicates are presented. n=3*

http://www.aloki.hu ● ISSN 1589 1623 (Print) ● ISSN1785 0037 (Online)
DOI: http://dx.doi.org/10.15666/aeer/2003_21572170

Responses of OJIP curves in leaves of mulberry seedlings to different nitrogen forms

Fig. 3-A shows that there were significant differences in terms of the OJIP curves of mulberry leaves under the treatments of different nitrogen forms. We did not observe a difference in the relative fluorescent intensities at the O and J step on the OJIP curve in plants treated with NO_3^--N and NH_4NO_3. With the extension of time, the relative fluorescent intensities of mulberry leaves at the I and P step under the treatment of NH_4NO_3 gradually became lower than those treated with NO_3^--N. Under the NH_4^+-N treatment, the relative fluorescent intensities of mulberry leaves at the O and J step were significantly higher than those treated with NO_3^--N and NH_4NO_3, but at the P step, the relative fluorescence intensity was lower than those under the treatments of NO_3^--N and NH_4NO_3.

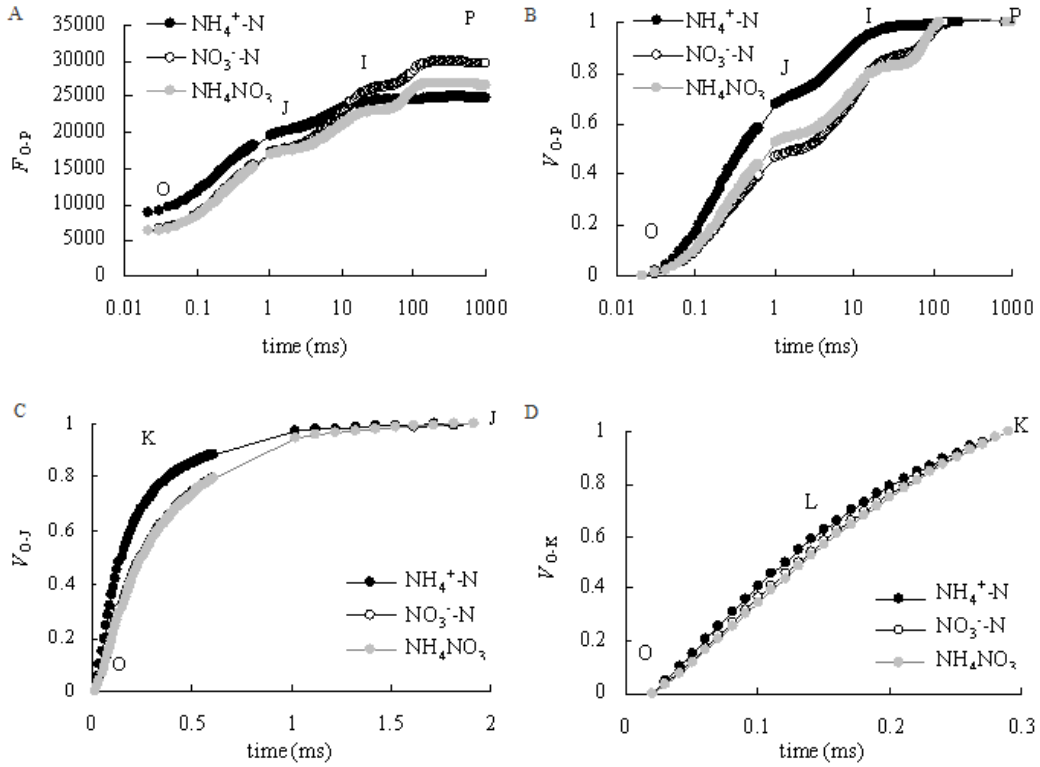

Figure 3. *Responses of OJIP curve and the standardized O-P, O-J and O-K curves in leaves of mulberry seedlings to different nitrogen forms. Chlorophyll a fluorescence transients were analyzed with the JIP-test*

After standardization of the OJIP curve according to O-P, O-J and O-K, we observed that under the NH_4^+-N treatment, the relative variable fluorescences of the *M. alba* leaves at the J step (2 ms) and the I step (30 ms) were significantly increased compared to the NO_3^--N and NH_4NO_3 treatments. Under the NH_4NO_3 treatment, the relative variable fluorescence of the mulberry leaves at the J step was slightly higher compared to the NO_3^--N treatment, but there was no significant difference between the two treatments at the I step (*Fig. 3-B*). The relative variable fluorescence of the mulberry leaves at the K step (0.3 ms) was significantly higher in the NH_4^+-N treatment compared to NO_3^--N and NH_4 NO_3 treatments, while there was no significant difference between the NO_3^--N and

http://www.aloki.hu ● ISSN 1589 1623 (Print) ● ISSN1785 0037 (Online)
DOI: http://dx.doi.org/10.15666/aeer/2003_21572170

NH_4NO_3 treatments (*Fig. 3-C*). There were no major differences in the standardized O-K curves between the different treatments, however, the relative variable fluorescence of the mulberry leaves at the L step (0.15 ms) was higher in the NH_4^+-N treatment compared to the NO_3^--N and NH_4NO_3 treatments (*Fig. 3-D*).

The effect of nitrogen forms on the variable fluorescence in the OJIP curve in mulberry seedling leaves

We next conducted a quantitative analysis of the differences in the relative variable fluorescence at each point, and found that the relative variable fluorescence of V_L, V_K, V_J, and V_I of *M. alba* leaves at the L, K, J and I step were all significantly higher in the NH_4^+-N treatment compared to the NO_3^--N and NH_4NO_3 treatments. The increases were 7.19% (P>0.05), 29.97% (P<0.01), 46.39% (P<0.01) and 15.02% (P<0.01), respectively, when compared to NO_3^--N treatment, and 10.38% (P>0.05), 31.43% (P<0.01), 31.38% (P<0.01) and 19.83% (P<0.01) when compared to the NH_4NO_3 treatment (*Fig. 4*). All variables except for V_L showed highly significant differences. The differences of the relative variable fluorescence between the NO_3^--N and NH_4NO_3 treatments were relatively small. One notable difference was the 4.13% (P<0.05) increase of V_I in the NO_3^--N treatment compared to the NH_4NO_3 treatment.

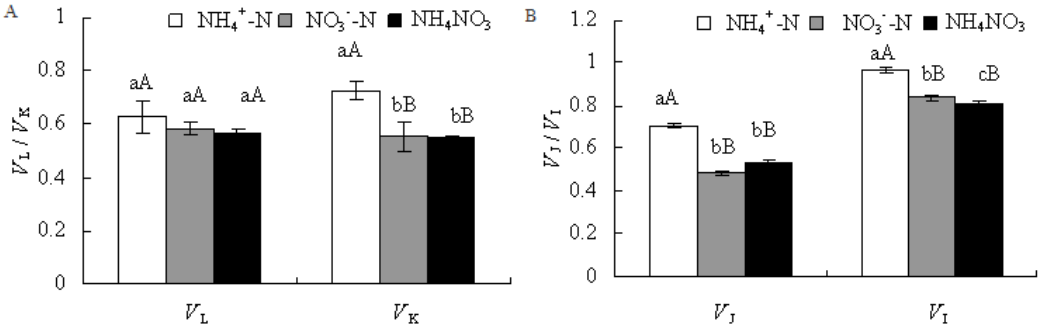

Figure 4. *Responses of V_L, V_K, V_J and V_I in leaves of mulberry seedlings to different nitrogen forms. Means ± SD of three replicates are presented. values followed by different small letters mean significant difference ($p<0.05$), values followed by different capital letters mean very significant difference ($p<0.01$). n=3*

Responses of S_m, N, φE_o and φD_o in leaves of mulberry seedlings to different nitrogen forms

We observed significantly higher S_m and N in mulberry leaves in plants treated with NH_4^+-N compared to the NO_3^--N and NH_4NO_3 treatments. The S_m and N were, slightly lower under the NH_4NO_3 treatment compared to the NO_3^--N treatment, but the difference was not significant (*Fig. 5*). Under the NH_4^+-N treatment, the φE_o of mulberry leaves were 54.27% (P<0.01) lower compared to the NO_3^-N treatment, and 47.27% (P<0.01) lower compared to the NH_4NO_3 treatment. The φE_o of mulberry leaves was 15.30% (P>0.05) higher under NO_3^--N treatment compared to the NH_4NO_3 treatment. Under NH_4^+-N treatment, the φD_o of mulberry leaves were 68.64% (P<0.01) lower compared to the NO_3^--N treatment, and 54.11% (P<0.01) lower compared to the NH_4NO_3 treatment. There was no significant difference in φD_o between the NO_3^--N and NH_4NO_3 treatments.

http://www.aloki.hu ● ISSN 1589 1623 (Print) ● ISSN1785 0037 (Online)
DOI: http://dx.doi.org/10.15666/aeer/2003_21572170

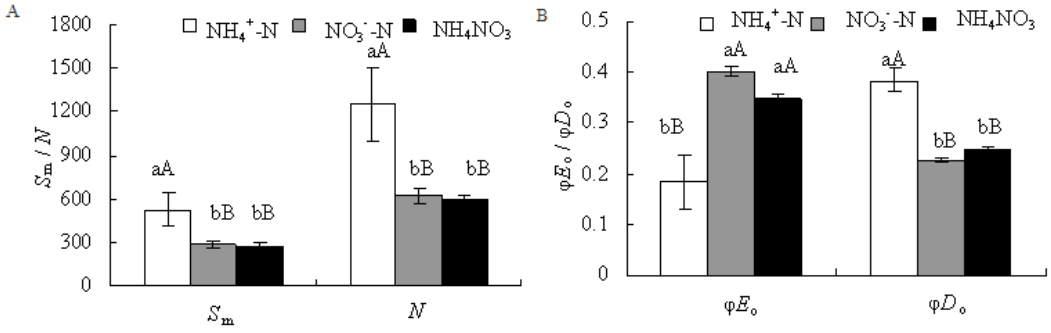

Figure 5. *Responses of S_m, N, φE_o and φD_o in leaves of mulberry seedlings to different nitrogen forms. Means ± SD of three replicates are presented. values followed by different small letters mean significant difference ($p<0.05$), values followed by different capital letters mean very significant difference ($p<0.01$). n=3*

Discussion

In our study, compared with the single nitrogen nutrition, the proper NH^{4+}-N:NO^{3-}-N ratio can promote mulberry growth. There are great differences in the uptake and utilization of nitrogen forms in plants, and the uptake of nitrogen is different in different plants or in different growth stages of the same plant. The pure supply of NH^{4+}-N will inhibit the absorption of K^+ and Ca^{2+}, and bring ammonia toxicity, limiting the growth of plants (Gruffman et al., 2012; Liu et al., 2019; Khan et al., 2020). However, the pure supply of NO^{3-}-N tends to increase the pH of rhizosphere, which is not conducive to the absorption and utilization of mineral nutrients (Ipperisiel et al., 1989; Guo et al., 2017; Cai et al., 2019). Combined with the results of previous studies and our study, the reasons for the highest growth of mulberry when the ratio of NH^{4+}-N and NO^{3-}-N was 50:50 were as follows: on the one hand, it was conducive to root growth, increased the absorption and transformation of soil nutrients, and reduced ammonia poisoning (Omara, 1989; Zhang et al., 2019; Yang et al., 2020); On the other hand, under the condition of solution culture, ammonium nitrogen will not be quickly converted to nitrate nitrogen, which not only avoids the reduction of cation absorption under the condition of single ammonium nitrogen supply, but also avoids the low nitrogen utilization rate caused by the easy leaching of NO^{3-}-N in soil culture, which can save more energy and increase the absorption of phosphorus than single nitrate nitrogen. Therefore, mulberry grows best when NH^{4+}-N and NO^{3-}-N are properly proportioning.

Chlorophyll fluorescence analysis is important in understanding the absorption and utilization of light energy by plants, and the function of the photosynthesis system. The effects of different nitrogen forms on a plant's photosynthesis system can be different. For example, the study by Chen et al. showed that rice plants under water-stress had less inhibitory effect on the photosynthetic capability when treated with NH_4^+-N compared to the plant treated with NO_3^--N, and the content of Rubisco in the leaves was higher (Sun et al., 2003; Chen et al., 2006; Guo et al., 2017; Yang et al., 2020). Here, we found that treating *M. alba* with NH_4^+-N resulted in significantly decreases in F_v/F_m, $\Phi_{PS\ II}$ and q_p in the leaves compared to the NO_3^--N treatment. From the illumination response curves of the chlorophyll fluorescence parameters, we also observed that mulberry leaves under different light intensities result in significantly lower $\Phi_{PS\ II}$ and ETR in the NH_4^+-N treatment compared to NO_3^--N. Under the treatment of NH_4^+-N, the ETR light saturation point was significantly lower than those under the treatment of NO_3^--N. This suggests that

http://www.aloki.hu ● ISSN 1589 1623 (Print) ● ISSN1785 0037 (Online)
DOI: http://dx.doi.org/10.15666/aeer/2003_21572170

treating mulberry with NH_4^+-N reduces the PS II photochemical activity and solar energy utilization capacity of the *M. alba* leaves compared to NO_3^--N treatment. Interestingly, we observed significantly higher NPQ in *M. alba* leaves treated with NH_4^+-N, indicating that the leaves of *M. alba* treated with NH_4^+-N depended on the non-radiative energy dissipation mechanism of the xanthophyll cycle to reduce the excess excitation energy in leaves. However, this would also reduce the proportion of light energy used in photochemical reactions under NH_4^+-N treatment, thus directly leading to a reduced supply of the assimilatory power such as ATP and NADPH, and further inhibiting the photosynthetic carbon assimilation ability, thereby reducing the amount of photosynthate accumulation. This is consistent with the results obtained by a large number of studies showing that application of NH_4^+-N alone can have a toxic effect on plants (Britto et al., 2001; Cai et al., 2017; Mu et al., 2021).

In addition, rational application of NH_4^+-N and NO_3^--N can significantly mitigate ammonium salt poisoning in plants. The study by Jan et al. showed that, compared to the application of NO3$^-$-N alone, a mixed application of NH_4^+-N and NO_3^--N can significantly increase dry matter accumulation and protein content in plants (Jan et al., 2013; Mu et al., 2021). However, the study by Nathawat et al. found that a mixed application of NH_4^+-N and NO_3^--N, the yield of *Brassica juncea* L. seeds showed no difference compared to single application of NO_3^--N, but was significantly higher than a single application of NH_4^+-N (Nathawat et al., 2007; Yang et al., 2019). A mixed application of NH_4^+-N and NO_3^--N can also benefit the growth of *Citrus reticulata* (Nathawat et al., 2007; Cai et al., 2017). In this study, we found that chlorophyll fluorescence parameters of mulberry leaves were significantly higher in NH_4NO_3 treated plants compared to NH_4^+-N, but showed no significant difference compared to NO_3^--N treatment. The treatment of NH_4NO_3, which is equivalent to a treatment with 1 : 1 ratio mix of NH_4^+-N and NO_3^--N, can significantly relieved ammonium salt poisoning in *M. alba*, and achieve an equimolar treatment level as NO_3^--N.

The fast chlorophyll fluorescence kinetics technologies can qualitatively and quantitatively measure the functions of different sections of the photosynthesis process, and it is very important for the in-depth study on the photosynthetic function of plants. In this study, we observed significant differences in the OJIP curves between the different nitrogen treatments. Under the NH_4^+-N treatment, the relative fluorescence intensities of the mulberry leaves at the O and J step were significantly higher compared to NO_3^--N and NH_4NO_3, but at the P step, the relative fluorescence intensities were lower than those under the treatments of NO_3^-N and NH_4NO_3. Therefore, the NH_4^+-N treatment resulted in a less pronounced OJIP curve, which suggests that the PSII reaction center was less active. However, OJIP curve can be strongly influenced by environmental factors, and OJIP curves offend require standardization. In this study, we standardized the OJIP curve as O-P, O-J and O-K respectively, and under the NH_4^+-N treatment, the relative variable fluorescences V_J and V_I at the J step (2 ms) and I step (30 ms) were significantly increased compared the NO_3^-N and NH_4NO_3 treatments. Under the NH_4NO_3 treatment, the relative variable fluorescence of the mulberry leaves at the J step was slightly higher than those under the treatment of NO_3^--N, while there was no significant difference between the two treatments at the I step. V_I reflects the situation of electron transfer from Q_A to Q_B at the receptor side of the PSII reaction center. Increased relative variable fluorescence at the I step caused by the inhibition of the transport process from Q_A to Q_B (Zhang et al., 2018a,b). Therefore, the results from this experiment showed that treating mulberry with NH_4^+-N reduced the capacity of electron transport from Q_A to Q_B at the receptor side of

http://www.aloki.hu ● ISSN 1589 1623 (Print) ● ISSN1785 0037 (Online)
DOI: http://dx.doi.org/10.15666/aeer/2003_21572170

the PSII reaction center compared to treatments of NO_3^--N and NH_4NO_3. However, under the treatment of NH_4^+-N, the S_m and N of mulberry leaves were significantly higher, indicating that the PQ pool at the receptor side of the PS II reaction center was larger, and Q_A^- was reduced more often. These also indicate that the low Q_A to Q_B transport capacity under the treatment of NH_4^+-N results from decreased electron acceptability of Q_B in the mulberry leaves, and not because of a reduced capacity to accept electrons by the PQ pool downstream of the electron transport. The relative instability of the Q_B function of mulberry leaves has been shown in previous experiments (Xu et al., 2012; Liu et al., 2019).

Under NH_4^+-N treatment, the relative variable fluorescence V_K of the mulberry leaves at the K step (0.3 ms) was significantly higher than those under the treatments of NO_3^-N and NH_4NO_3, and there was no significant difference between the NO_3^-N and NH_4NO_3 treatments. This suggests that under the NO_3^--N and NH_4NO_3 treatments, the oxygen-evolving complex (OEC) activities of mulberry leaves were significantly higher than the NH_4^+-N treatment. High OEC activity facilitates the water splitting function at the donor side and provides sufficient electron supply for the photosynthetic electron transport chain. Low OEC activity in mulberry leaves under the NH_4^+-N treatment can lead to incomplete water splitting, resulting in the production of active oxygen molecules such as H_2O_2, thus undermining the normal function of the photosynthetic system. The decrease in the capacity of accepting electrons by Q_B at the electron transport receptor side may be caused by the attack by active oxygen molecules. NH_4^+-N treatment can change the ultrastructure of *Lycopersicon esculentum* leaf cells, and cause chloroplast swelling, fuzzy or even broken layers, and significant accumulation of osmiophilic granules. In contrast, treatment of NH_4NO_3 can significantly improve this situation (Zhang et al., 2012a, 2018a,b). The osmiophilic granule is an important sign of the dissociation of the thylakoid membrane (Zhang et al., 2012b, 2018; Penella et al., 2014). We found that the differences of the standardized O-K curves under different treatments were relatively small, but under the NH_4^+-N treatment, the relative variable fluorescence V_L at the L step (0.15 ms) was higher than those under the NO_3^--N and NH_4NO_3 treatments. These results suggest that NH_4^+-N treatment alone results in lower structural stability of the thylakoid membrane of the mulberry leaf compare to NO_3^--N and NH_4NO_3 treatments. However, the variation ranges of V_L under different treatments were all significantly smaller than those of V_K, V_J and V_I, indicating that the stability of the thylakoid structure of mulberry leaves is less vulnerable to damage under the treatments of different nitrogen comparing to the OEC activity and the electron transfer function at the receptor side of the PSII reaction center.

Conclusions

The PSII photochemical activity of the mulberry leaves was significantly higher in the NO_3^--N treatment compared to NH_4^+-N, and applying NH_4^+-N alone was toxic to mulberry. It not only reduced the PSII photochemical activity and the electron transport capacity in the leaves, but also inhibited the oxygen evolving complex function. The light energy absorbed by leaves was mainly dissipated in the form of invalid heat energy. The proportion of the light energy used in photochemical reaction was decreased, and even the thylakoid structure was altered in the NH_4^+-N treatment. However, under the treatments of NO_3^-N and NH_4NO_3, the photosynthetic capacity of mulberry leaves was significantly higher than the NH_4^+-N treatment. There was no significant difference between the NO_3^-N and NH_4NO_3 treatments; and the treatment of NO_3^--N could

http://www.aloki.hu ● ISSN 1589 1623 (Print) ● ISSN1785 0037 (Online)
DOI: http://dx.doi.org/10.15666/aeer/2003_21572170

significantly relieve the ammonium toxicity in mulberry caused by applying NH_4^+-N alone. Our results provide the basis for the development of new nitrogen fertilizer utilization schemes for *M. alba.* In order to further explain the decline of photosynthetic mechanism capacity, especially chlorophyll fluorescence, the enzymatic induced by sole nitrogen forms, but this needs further study.

Funding. This study was financially supported by China-Norway International Collaboration Project (Grant No.CHN-17/0019); The project of Heilongjiang Province Key Laboratory of Cold Region Wetland Ecology and Environment Research (No.201910) of the Harbin University; Young Doctoral Research Foundation of Harbin University (No.2020106); Harbin University of Dr Youth "Internet + double gen start-up fund project" (HUSC202108).

REFERENCES

[1] Ali, A., Tucker, T. C., Thompson, T. L., Salim, M. (2001): Effects of salinity and mixed ammonium and nitrate nutrition on the growth and nitrogen utilization of barley. – Journal of Agronomy and Crop Science 186: 223-228.

[2] Ambus, P., Skiba, U., Butterbach-Bahl, K., Sutton, M. A. (2011): Reactive nitrogen and greenhouse gas flux interactions in terrestrial ecosystems. – Plant and Soil 343(1): 1-3.

[3] Britto, D. T., Siddiqi, M. Y., Glass, A. D. M., Kronzucker, H. J. (2001): Futile transmembrane NH_4^+ cycling: A cellular hypothesis to explain ammonium toxicity in plants. – Proceedings of the National Academy of Sciences of the United States of America 98: 4255-4258.

[4] Cai, Y. T., Zhang, H., Qi, Y. P., Ye, X., Huang, Z. S., Guo, J. X., Chen, L. S., Yang, L. T. (2019): Responses of reactive oxygen species and methylglyoxal metabolisms to magnesium-deficiency differ greatly among the roots, upper and lower leaves of Citrus sinensis. – BMC Plant Biology 19(1): 76.

[5] Chapin, F. S., Autumn, K., Pugnaire, F. (1993): Evolution of Suites of Traits in Response to Environmental Stress. – The American Naturalist 142: 78-92.

[6] Chen, G., Zhou, Y., Guo, S. W., Shen, Q. (2006): Effects of Different Nitrogen Forms on Rice Seedlings Growth with Partial Roots Exposed to Water Stress. – Chinese Journal of Rice Science 20(6): 638-644.

[7] Choi, S. L., Suh, I. S., Lee, C. G. (2003): Lumostatic operation of bubble column photobioreactors for *Haematococcus pluvialis* cultures using a specific light uptake rate as a control parameter. – Enzyme Microb. Technol 33: 403-409.

[8] Danesi, E. D. G., Rangel-Yagui, C. O., Carvalho, J. C. M., Sato, S. (2002): An investigation of effect of replacing nitrate by urea in the growth and production of chlorophyll by Spirulina platensis. – Biomass Bioenerg 23: 261-269.

[9] Genty, B., Briantais, J. M., Baker, N. R. (1989): The relationship between quantum yield of photosynthetic electron transport and quenching of chlorophyll fluorescence. – Biochim Biophys Acta 990: 87-92.

[10] Gruffman, L., Ishida, T., Nordin, A., Nasholm, T. (2012): Cultivation of Norway spruce and Scots pine on organic nitrogen improves seedling morphology and field performance. – Forest Ecology and Management 276(15): 118-124.

[11] Guo, P., Li, Q., Qi, Y. P., Yang, L. T., Ye, X., Chen, H. H., Chen, L. S. (2017): Sulfur mediated alleviation of aluminum toxicity in Citrus grandis seedlings. – International Journal of Molecular Sciences 18(12): 2570.

[12] Hu, Y. B., Sun, G. Y., Wang, X. C. (2007): Induction characteristics and response of photosynthetic quantum conversion to changes in irradiance in mulberry plants. – Journal of Plant Physiology 164: 959-968.

http://www.aloki.hu ● ISSN 1589 1623 (Print) ● ISSN1785 0037 (Online)
DOI: http://dx.doi.org/10.15666/aeer/2003_21572170

[13] Ipperisiel, D., Alli, I., Machenze, A. F., Mehuys, G. R. (1989): Nitrogen distribution, yield, and quality of silage corn after four nitrogen fertilization. – Agron. J 81: 783-789.
[14] Jan, A., Osman, M. B., Amanullah (2013): Response of chickpea to nitrogen sources under salinity stress. – Journal of Plant Nutrition 36: 1373-1382.
[15] Khan, A., Wang, Z., Xu, K., Li, L., He, L., Hu, H., Li, L. Y., Zhu, X. G. (2020): Validation of an Enzyme-Driven Model Explaining Photosynthetic Rate Responses to Limited Nitrogen in Crop Plants. – Frontiers and Plant Science 11: 533341.
[16] Kim, T., Mills, H. A., Wetzstein, H. Y. (2002): Studies on effects of nitrogen form on growth, development, and nutrient uptake in pecan. – Journal of Plant Nutrition 25(3): 497-508.
[17] Kuelland, K. (1994): Amino Acid Absorption by Arctic Plants: Implications for Plant Nutrition and Nitrogen Cycling. – Ecology 75: 2373-2383.
[18] Li, Y., Horsman, M., Wang, B., Wu, N., Lan, C. Q. (2008): Effects of nitrogen sources on cell growth and lipid accumulation of green alga *Neochloris oleoabundans*. – Appl. Microbiol. Biotechnol 81: 629-636.
[19] Li, Q., Chen, H. H., Qi, Y. P., Ye, X., Yang, L. T., Huang, R. Z., Chen, L. S. (2019): Excess copper effects on growth, uptake of water and nutrients, carbohydrates, and PSII photochemistry revealed by OJIP transients in citrus seedlings. – Environmental Science and Pollution Research International 26(29): 30188-30205.
[20] Lin, Q., Lin, J. D. (2011): Effects of nitrogen source and concentration on biomass and oil production of a *Scenedesmus rubescens* like microalga. – Bioresource Technology 102(2): 1615-21.
[21] Liu, X. J., Xu, N., Wu, Y. N., Li, J. B., Zhong, H. X., Zhang, H. H. (2019): Photosynthesis, chilling acclimation and the response of antioxidant enzymes to chilling stress in mulberry seedlings. – Journal of Forest Research 30(6): 2021-2029.
[22] Matsudo, M. C., Bezerra, R. P., Sato, S., Perego, P., Converti, A., Carvalho, J. C. M. (2009): Repeated fed-batch cultivation of Arthrospira (Spirulina) platensis using urea as nitrogen source. – Biochem. Eng. J. 43: 52-57.
[23] Mu, X., Chen, Y. (2021): The physiological response of photosynthesis to nitrogen deficiency. – Plant Physiology and Biochemistry 158: 76-82.
[24] Nathawat, N. S., Kuhad, M. S., Goswami, C. L., Patel, A. L., Kumar, R. (2007): Interactive effect of N source on salinity on growth indices and ion content of Indian mustard. – Journal of Plant Nutrition 30: 569-98.
[25] Nordin, A., Uggla, C., Näsholm, T. (2001): Nitrogen forms in bark, wood and foliage of nitrogen-fertilized *Pinus sylvestris*. – Tree Physiology 21(1): 59-64.
[26] Omara, H. A. (1989): The effect of spacing, nitrogen and phosphorus application on growth and yield of maize (*Zea mays* L.). – M.Sc. Thesis, Univ. of Khartoum, Faculty of Agric.
[27] Pang, H. S., Zhang, H. H., Tian, Y., Ao, H., Sun, G. Y. (2014): Effects of NO_3^--N on growth and photosynthetic characteristics of mulberry seedlings under Na_2CO_3 stress. – Pratacultural Science 31(8): 1515-1522.
[28] Penella, C., Nebauer, S. G., Bautista, A. S., Lópezgalarza, S., Calatayud, A. (2014): Rootstock alleviates PEG-induced water stress in grafted pepper seedlings: physiological responses. – J Plant Physiol. 171(10): 842-51.
[29] Pruvost, J., van Vooren, G., Cogne, G., Legrand, J. (2009): Investigation of biomass and lipids production with *Neochloris oleoabundans* in photobioreactor. – Bioresour. Technol. 100: 5988-5995.
[30] Shangguan, Z. P., Shao, M. A., Dyckmans, J. (2000): Effect of nitrogen nutrition and water deficit on net photosynthetic rate and chlorophyll fluorescence in winter wheat. – Journal of Plant Physiology 156(1): 46-51.
[31] Strasser, R. J., Srivastava, A., Govindjee, A. (1995): Polyphasic chlorophyll a fluorescence transient in plants and cyanobacteria. – Photochemistry and Photobiology 61(1): 32-42.

http://www.aloki.hu ● ISSN 1589 1623 (Print) ● ISSN1785 0037 (Online)
DOI: http://dx.doi.org/10.15666/aeer/2003_21572170

[32] Sun, G. H., Zeng, X. P., Zhao, P., Peng, S. L. (2003): Comparison of photosynthetic parameters in leaves of Citrus grands grown under different forms of nitrogen source during photosynthetic acclimation to elevated CO_2. – Acta Ecologica Sinica 23(1): 14-21.
[33] Sutton, M. A., Reis, S., Billen, G., Cellier, P., Erisman, J. W., Mosier, A. R., Nemitz, E., Sprent, J., Grinsven, H. V., Voss, M. (2012): Nitrogen and Global Change. – Biogeosciences 9(1): 1691-1693.
[34] Wang, C. H., Xing, X. R., Han, X. G. (2004): Advances in study of factors affecting soil N mineralization in grassland ecosystems. – Chinese Journal of Applied Ecology 15(11): 2184-2188.
[35] Wang, J., Baerenklau, K. A. (2014): Crop response functions integrating water, nitrogen, and salinity. – Agricultural Water Management 139: 17-30.
[36] Xu, N., Zhang, H. H., Zhu, W. X., Li, X., Yue, B. B., Jin, W. W., Wang, L. Z., Sun, G. Y. (2012): Effects of nitrogen form on seeding growth and its photosynthetic characteristics of forage mulberry. – Pratacultural Science 29(10): 1568-1572.
[37] Xu, C., Fisher, R., Wullschleger, S. D., Wilson, C. J., Cai, M., McDowell, N. G. (2012): Toward a mechanistic modeling of nitrogen limitation on vegetation dynamics. – PLoS One 7: e37914.
[38] Yang, X., Henry, H. A. L., Zhong, S., Meng, B., Sun, W. (2020): Towards a mechanistic understanding of soil nitrogen availability responses to summer vs. winter drought in a semiarid grassland. – Science Total Environment 741: 140272.
[39] Yin, L., Xu, H., Dong, S., Chu, J., Dai, X., He, M. (2019): Optimised nitrogen allocation favours improvement in canopy photosynthetic nitrogen-use efficiency: Evidence from late-sown winter wheat. – Environmental and Experimental Botany 159: 75-86.
[40] Zhang, H. H., Zhang, X. L., Hu, Y. B., Li, X., Xu, N., Tian, Y., Zhang, T., Sun, G. Y. (2012a): Growth characteristics and photosystem II functions of *Sorghum bicolor* × *S. sundanense* seedlings under drought stress. – Acta Agrestia Sinica 20(5): 881-887.
[41] Zhang, Z. S., Li, G., Gao, H. Y., Zhang, L. T., Yang, C., Liu, P. (2012b): Characterization of photosynthetic performance during senescence in stay-green and quick-leaf-senescence *Zea mays* L. inbred lines. – Plos One 7(8): e42936.
[42] Zhang, H. H., Zhang, X. L., Li, X., Xu, N., Sun, G. Y. (2013): Role of D1 Protein Turnover and Xanthophylls Cycle in Protecting of Photosystem II Functions in Leaves of *Morus alba* under NaCl Stress. – Scientia Silvae Sinicae 49(1): 99-106.
[43] Zhang, H. H., Feng, P., Yang, W., Sui, X., Li, X., Gu, S. Y., Xu, N. (2018a): Effects of flooding stress on the photosynthetic apparatus of leaves of two Physocarpus cultivars. – Journal of Forest Research 29(4): 1049-1059.
[44] Zhang, H. H., Xu, N., Sui, X., Zhong, H. X., Yin, Z. P., Li, X., Sun, G. Y. (2018b): Photosystem II function response to drought stress in leaves of two alfalfa (*Medicago sativa*) varieties. – International Journal of Agriculture and Biology 20(5): 1012-1020.
[45] Zhang, K., Wu, Y., Hang, H. (2019): Differential contributions of NO3-/NH4+ to nitrogen use in response to a variable inorganic nitrogen supply in plantlets of two Brassicaceae species in vitro. – Plant Methods 15: 86.

http://www.aloki.hu ● ISSN 1589 1623 (Print) ● ISSN1785 0037 (Online)
DOI: http://dx.doi.org/10.15666/aeer/2003_21572170

QUANTITATIVE RESEARCH ON ECOLOGICAL COMPENSATION IN COASTAL AREAS BASED ON ECOLOGICAL FOOTPRINT

YANG, B. Q.[1] – LIU, Y.[2*]

[1]*Department of Economic Management, College of Information Engineering, Fuyang Normal University, Fuyang 236041, China*

[2]*Department of Design Art, College of Information Engineering, Fuyang Normal University, Fuyang 236041, China*

[*]*Corresponding author*
e-mail: daisy861206@163.com

(Received 27th Aug 2021; accepted 23rd Nov 2021)

Abstract. Environmental degradation has severely restricted the economic development of coastal beach areas. Quantitative analysis of ecological compensation in coastal beach areas will help to understand the current situation of local resources and environment. Therefore, this paper proposes a quantitative analysis method for coastal beach ecological compensation based on changes in ecological footprint. According to the ecological red line regional ecological compensation theory, the subject and object of ecological compensation are clarified, and the ecological footprint calculation model and ecological compensation sharing model are constructed. From the ecosystem service value, ecological footprint calculation, ecological carrying capacity and ecological footprint efficiency, direct income loss compensation, static from the perspectives of evaluation compensation and dynamic evaluation compensation, the quantitative analysis of ecological compensation in coastal beach areas has been realized. In this paper, a certain place is selected as the experimental area, and the principal component analysis method is used to evaluate the effect of local ecological compensation. The results show that the level of ecological surplus in 2020 has significantly increased compared to that of 2010; The ecological capacity per capita in the study area is lower than the national average; The ecological compensation effect after normalization treatment is obviously better than that before normalization.
Keywords: *changes in human ecological footprint, coastal areas, ecological compensation, Principal Component Analysis, ecological carrying capacity, evaluation*

Introduction

The ecological environment supports the survival and development of human society by providing ecological products and services to humans, but the value and characteristics of the ecological environment have not yet been fully reflected in social and economic activities. The external effects of use are significant, and protection and benefit are out of touch (Kosev and Vasileva, 2019). With the rapid development of society and economy, the destruction and pollution of the ecological environment are becoming more and more serious. As one of the effective ways to solve the problems of the ecological environment, ecological compensation has been paid more and more attention by people. In recent years, the ecological compensation mechanism has become a research hotspot in the academic circle. Scholars at home and abroad have conducted in-depth and extensive research on the scope of ecological compensation, compensation standards, compensation basis, compensation methods, etc. One such study involves the determination of ecological compensation standards. This is the focus and difficulty of whether the practice can be carried out (Itsukushima, 2019).

http://www.aloki.hu ● ISSN 1589 1623 (Print) ● ISSN1785 0037 (Online)
DOI: http://dx.doi.org/10.15666/aeer/2003_21712185

In reference to the study by Wang et al. (2019), taking Changsha City, Hunan Province, China as an example, proposed a quantitative analysis method for ecological compensation based on the value of ecological services, using Swedish carbon tax law, industrial oxygen production cost method, and alternative cost method. Fully consider the beneficial value of the ecological services of cultivated land resources and the cost of environmental pollution control, construct and establish an accounting system for the ecological service value of cultivated land, and quantify the amount of ecological compensation. The results show that the value of ecological service benefits provided by cultivated land resources in Changsha city from 2011 to 2017 increased from 1.6867×10~(9)US dollars to 1.7447×10~(9)US dollars in 2017, while the cost of environmental pollution control increased from 9.7281×10~(8)US dollars reduced to 9.1891×10~(8) US dollars, the value of the ecological service benefits of cultivated land resources is far greater than the cost of environmental pollution control; the average value of ecological compensation for cultivated land in Changsha from 2011 to 2017 was 6.8688×10~(8) US dollars, and the ecological compensation amount of various districts and counties is quite different. Reference (Wang et al., 2020) takes Hubei province as an example, proposes research on ecological compensation methods from the perspective of the main function zone. From the perspective of the main function zone, on the basis of measuring the value of the ecosystem services in Hubei Province, define the ecological compensation and compensation payment subjects, to determine the level and order of ecological compensation and compensation payment. The results show that: (1) the spatial distribution of total value, market value and non-market value of ecosystem services in Hubei province is similar, showing a pattern of "high in the west, low in the east". High value areas are mostly concentrated in key ecological function areas and main agricultural product producing areas, while low value areas are mostly concentrated in key development areas; (2) The ecological compensation level of the 30 key ecological function areas can be divided into five levels, showing a spatial distribution pattern of "high in the west and low in the east"; (3) The ecological compensation priority of 29 main agricultural product producing areas is divided into five levels; (4) The compensation payment level of the 30 key development zones is divided into five levels, showing a spatial distribution pattern of "east first, west later". In the practice of ecological compensation payment, the national level key development zones should be prior to the provincial level key development zones. Reference (Nie and Cheng, 2019) proposed a regional horizontal forest ecological compensation method based on the marginal effect theory. Based on the marginal effect theory, taking 2016 as the time section, the marginal benefit of forest ecological construction was calculated, and the critical value of horizontal compensation was obtained. Combined with the unbalanced coordinated development of the region, the forest ecological compensation value was obtained according to the expert weighting method. The results show that in theory, Beijing should provide 814675375 US dollars / year to 1996419312.5 US dollars / year for forest ecological compensation in Zhangcheng area. In fact, in fact, the amount of ecological compensation for Zhangcheng covered areas in Beijing during the 13th Five Year Plan period is only 111250000 US dollars / year. Therefore, Beijing should increase the compensation for forest ecology in Zhangcheng area of Hebei province on the basis of existing compensation.

Based on the above research results, in order to further improve the effect of ecological compensation analysis, this paper proposes a quantitative research method of

http://www.aloki.hu ● ISSN 1589 1623 (Print) ● ISSN1785 0037 (Online)
DOI: http://dx.doi.org/10.15666/aeer/2003_21712185

ecological compensation in coastal beach area based on the change of ecological footprint.

Materials and methods

Quantitative analysis method of ecological compensation in beach areas based on changes in ecological footprint

Ecological compensation is a kind of public system which aims at protecting the ecological environment and promoting the harmonious development between human and nature. According to the value of ecosystem services, the cost of ecological protection and the cost of development opportunity, the government and the market are used to regulate the interest relationship among the stakeholders of ecological protection. The following is a quantitative analysis of ecological compensation in coastal beach areas from the aspects of ecological compensation theory, subject and object of ecological compensation, ecological footprint calculation model and ecological compensation sharing model (Salemi et al., 2019).

Theoretical basis of ecological compensation in the ecological red line area

The ecological red line was first applied in the process of urbanization, aiming to standardize the development space of the city, and then gradually extended to the ecological environment protection. The proposal of the ecological red line is based on the country's ecological security and sustainable economic and social development, and is to maintain the boundary line of the land and space through the implementation of the strictest control system. The "ecological red line" cannot be simply understood as a regional boundary. It is a hierarchical system that includes many ecological protections point sets, line clusters and locations (Smee, 2019). In short, point set is the layer of ecological red line area, on which there are many ecological value protection targets; Line cluster, with the connotation of dynamic change, mainly refers to the cluster close to sensitive protection point source in the belt area formed by rivers, lakes and swamps in the ecological red line area (Dong and Liu, 2020); Location, from the macro level, refers to those vulnerable areas with important or special ecological value or high ecological sensitivity.

According to the theory of ecological red line, the ecological compensation standard of coastal beach area is set:

Assuming that the ecological spillover value in year i is E_i ($i = 1, 2, ..., k$), and the construction period of the tidal flat area are N years, then the ecological spillover value before the tidal flat area is E_0, the ecological spillover value of the tidal flat area after reclamation, that is, the ecological spillover value at the end of year N is E_N. This article defines the ecological spillover value increment S_n in year n as follows:

$$S_n = E_0 - E_n \quad \text{(Eq.1)}$$

It can be seen from formula (*Eq.1*) that the increment of ecological spillover value in year n is relative to the initial value E_0, and the final value is subtracted from the initial

http://www.aloki.hu ● ISSN 1589 1623 (Print) ● ISSN1785 0037 (Online)
DOI: http://dx.doi.org/10.15666/aeer/2003_21712185

value. The purpose is to make it non-negative under normal circumstances (Yang et al., 2019). The increment of ecological spillover value before and after reclamation is taken as the theoretical standard of ecological compensation, which is essentially based on the value of ecological damage as the basis for compensation.

Determination of the subject and object of ecological compensation

Definition of the subject of ecological compensation

The so-called subject of ecological compensation refers to "who will bear the responsibility of ecological compensation". The main body of ecological compensation in coastal wetland areas should include two parts: one is "who benefits, who compensates". The beneficiaries of wetland protection, including the international community, governments, enterprises and individuals, should give back to coastal wetland protectors; The second is "whoever destroys it, who is responsible." Any government, enterprise and individual that destroys the ecological environment of the wetland should pay economic compensation or even legal liability for the loss of the value of the ecological environment (Su et al., 2020).

Definition of the object of ecological compensation

The object of ecological compensation refers to "who will receive ecological compensation". The object of ecological compensation in beach areas should also include two parts: one is to protect the coastal wetland resources, and the local residents whose income is damaged, and the employees of the wetland nature reserve who contribute to the protection of the wetland (Ferro-Azcona et al., 2019); Second, groups or individuals whose living environment is threatened and their economic income is damaged due to the destruction of the wetland ecological environment.

Ecological footprint calculation model

The calculation of the ecological footprint is based on the following two basic facts: one is that humans can determine most of the resources they consume and the amount of waste they produce; the other is that these resources and wastes can be converted into the corresponding ecologically productive land area. Assume that all types of material consumption, energy consumption and wastewater treatment require a certain amount of land area and water area (Stone et al., 2019). The calculation formula of ecological footprint is as follows:

$$EL = \sum_{j=1}^{n}\sum_{i=1}^{n}\beta_j\varphi_i\left(Z_j\right) + \sum_{s=1}^{n}a_{s,i}(t) \qquad \text{(Eq.2)}$$

In the formula, i represents the type of consumption item; φ_i represents the per capita consumption of the i-th consumption item; represents the equilibrium factor; $a_{s,u}$ represents the ecologically productive land area converted by the i-th consumer product; Z_j represents the ecological footprint per capita; t represents the ecological footprint of the total population.

The calculation of ecological footprint mainly includes the consumption of biological resources and energy consumption. The consumption of biological resources mainly

http://www.aloki.hu ● ISSN 1589 1623 (Print) ● ISSN1785 0037 (Online)
DOI: http://dx.doi.org/10.15666/aeer/2003_21712185

includes agricultural products, animal products, wood, aquatic products, etc. in the energy consumption part, the footprint of raw coal, coke, natural gas, crude oil, gasoline, kerosene, diesel oil, fuel oil, heat, electricity, etc. can be calculated according to the data (Boutahar et al., 2019). The calculation method of ecological footprint is to add up the area of land per capita ecological demand of biological resources and energy resources calculated above, and then allocate appropriate weight, namely, equilibrium factor, to obtain the ecological footprint of coastal beach area.

Construction of ecological compensation sharing model

This study combines the upstream and downstream water consumption and economic affordability of coastal beach areas to establish a regional and central ecological compensation cost allocation model, in order to provide scientific suggestions for the implementation of ecological compensation in coastal beach areas. The specific model is as follows:

$$W(x,y)=\frac{P(x\cap y)}{\min\left(P(x),P(y)\right)} \quad \text{(Eq.3)}$$

In the formula, $P(x)$ represents the amount of ecological compensation along the beach; $P(y)$ represents the amount of ecological compensation cost apportionment.

Considering that the value of model parameters is easily affected by the external environment, and has uncertainty. In this paper, Crystal Ball software is used to analyze the sensitivity of model parameters. Firstly, Monte Carlo simulation method is used to sample the probability distribution function of model parameters, and establish the distribution function of ecological compensation, so as to obtain important mathematical features in the model, such as mathematical expectation, variance, interval estimation, etc. (Park et al., 2019). On this basis, variance analysis is used to analyze the parameters, and the sensitivity of the parameters is determined according to the proportion of the normalized square of the rank correlation coefficient between the input and the output of ecological compensation. The specific formula is as follows:

$$P(x)=\log\frac{P_g(x,y)}{P_c(x,y)}\times 100\% \quad \text{(Eq.4)}$$

$$P(y)=\frac{P_g(x,y)}{P_c(x,y)P_g(x,y)}dxdy \quad \text{(Eq.5)}$$

In the formula, $P_g(x,y)$ represents the variance contribution rate of the parameter variable; $P_c(x,y)$ represents the correlation coefficient of the ecological compensation amount.

http://www.aloki.hu ● ISSN 1589 1623 (Print) ● ISSN1785 0037 (Online)
DOI: http://dx.doi.org/10.15666/aeer/2003_21712185

Quantitative analysis of ecological compensation based on ecological footprint

The determination of ecological compensation standards is generally based on three aspects: determination based on the standard of ecosystem service value evaluation; determination based on the standard of protection cost; determination based on the standard of protection loss (Sun and Wang, 2018). Domestic and foreign studies generally use service value evaluation as the basis for determining compensation standards. Based on the existing theoretical methods, this paper analyzes the dynamic changes of ecological footprints along beaches, and finally quantitatively analyzes the ecological compensation standards according to the efficiency of ecological footprints. The calculation steps are as follows:

(1) Ecosystem service value

In this paper, emergy analysis method is applied to the evaluation of ecosystem service function in coastal beach area. The environmental energy input of ecosystem is mainly considered. The renewable resource input includes solar energy, wind energy, rain energy, tidal energy and evapotranspiration energy, which are converted into solar energy through the corresponding emergy conversion rate, on this basis, the natural production value of different types of ecosystems was calculated (Zeng et al., 2020). In order to make the calculation of renewable resources input scientific and reasonable, emergy experts put forward different calculation methods from the aspects of completeness of calculation, avoiding repeated calculation and consistency with reality. In this paper, using evapotranspiration as renewable resources input can not only improve the estimation accuracy of renewable resources input, but also avoid the impact of time scale on renewable resources input to a large extent. According to the principle of emergy analysis, the emergy of environmental input and the calculation formula of each index are as follows:

$$\begin{aligned} EL_1 &= K_{TV1} \times u_1 \\ EL_2 &= K_{TV2} \times u_2 \times u_1 \\ EL_3 &= K_{TV3} \times u_3 \times u_2 \times u_1 \\ EL_4 &= K_{TV4} \times u_4 \times u_3 \times u_2 \times u_1 \\ EL_5 &= K_{TV5} \times u_5 \times u_4 \times u_3 \times u_2 \times u_1 \\ EL_6 &= K_{TV6} \times u_6 \times u_5 \times u_4 \times u_3 \times u_2 \times u_1 \end{aligned} \quad \text{(Eq.6)}$$

$$EL_{total} = \sum_{i=6}^{n} \left(EL_1 + EL_2 + EL_3 + EL_4 + EL_5 + EL_6 \right) \quad \text{(Eq.7)}$$

In the formula, EL_1, EL_2, EL_3, EL_4, EL_5 and EL_6 respectively represent solar energy, surface wind energy, rainwater chemical energy, tidal energy, evapotranspiration energy and soil organic matter loss energy.

(2) Calculate ecological footprint, ecological carrying capacity and ecological footprint efficiency. Among them, the ecological footprint efficiency refers to the output of a unit of ecological footprint, which is a method for quantitative analysis and comparison of resource utilization efficiency and capacity differences in different regions (Yang et al., 2019). Because the ecological compensation of nature reserves is

http://www.aloki.hu ● ISSN 1589 1623 (Print) ● ISSN1785 0037 (Online)
DOI: http://dx.doi.org/10.15666/aeer/2003_21712185

mostly aimed at the farmers in the surrounding communities, the efficiency analysis of agricultural ecological footprint can also be used. Calculation method is:

$$ED = \sigma_i(t) - \frac{\alpha_i - \alpha_i^*}{EL_{total}} \quad \text{(Eq.8)}$$

In the formula, $\sigma_i(t)$ represents the ecological footprint efficiency; α_i represents the total ecological footprint; α_i^* represents the agricultural ecological footprint efficiency.

(3) Compensation for direct income loss caused by returning farmland to forests and lakes: compensation for direct income loss caused by returning farmland to forests, returning farmland to lakes and banning fishing in lakes is based on compensation for loss of cultivated land and lake surface, and is the lowest compensation standard to protect residents' rights and interests. Calculation method is:

$$EU = M_q\left(N_g \times N_q \times N_t\right) \quad \text{(Eq.9)}$$

In the formula, M_q represents the minimum ecological compensation value; N_g the area of returning farmland to forests and lakes; N_q represents the adjustment coefficient of cultivated land compensation, which can be determined according to the level of regional social and economic development.

(4) Static evaluation and compensation based on ecological carrying capacity: compare the ecological carrying capacity of the protected area and the area in the same year, and take the difference as the basis for compensation, which objectively increases the resettlement subsidy for the value of ecosystem services. Calculation method is:

$$EA = \frac{1}{2}\sum_{i=1}^{n}\left\|a^i - a^l\right\|^2 + a^d \times a^z \quad \text{(Eq.10)}$$

In the formula, a^i represents the static evaluation compensation value; a^l represents the total ecological carrying capacity of the beach area; a^d represents the area of the beach area; a^z represents the static ecological compensation adjustment coefficient, which can be adjusted according to the relevant regulations and the level of regional social and economic development. The value of a^z is 1.

(5) Dynamic evaluation and compensation based on ecological carrying capacity: comparing the changes of ecological carrying capacity of coastal beach areas in different years, and taking the difference as the basis of compensation, it is the evaluation of the degree of residents' cooperation with the ecological construction of the reserve and the work efficiency of the management department of coastal beach areas, as well as the ecological compensation and subsidies for the work and the work of the management department of coastal beach areas. Calculation method is:

http://www.aloki.hu ● ISSN 1589 1623 (Print) ● ISSN1785 0037 (Online)
DOI: http://dx.doi.org/10.15666/aeer/2003_21712185

$$ER = \sum_{i=1}^{n} \left[d_i(n) \times h_i(n) \times f_i(n) \right] \quad \text{(Eq.11)}$$

In the formula, $d_i(n)$ represents the dynamic evaluation compensation value; $h_i(n)$ represents the total ecological carrying capacity of the beach area in different years; $f_i(n)$ represents the dynamic ecological compensation adjustment coefficient, which can be adjusted according to the relevant regulations and the level of regional social and economic development (Yang et al., 2019). The value of $f_i(n)$ is 1 in this article.

Results and discussion

Select the experimental area, and use the quantitative analysis method of ecological compensation for coastal beach areas designed in this paper based on the ecological footprint changes to quantitatively analyze the area.

Overview of the study area

The experimental research area is located in Taizhou City, Zhejiang Province, China, on the southern edge of the northern subtropical zone. It has a maritime monsoon climate with four distinct seasons. The total area of reclamation is 25 374 hm^2, which is located in the geometric center of the metropolis and the geographical position is superior. The annual sunshine duration is 2048.4 hours, the total annual solar radiation is 468 608 J/cm^2, the average temperature is 16°C, and the frost-free period is 244 days. The annual precipitation is 1272.8 mm, and the average annual runoff is 5.122×108 m^3. East to southeast wind prevails in summer and northwest to north wind prevails in winter. The east wind prevails throughout the year. The average wind speed is 3 m/s and the annual windy day is 9.6 days. The planning and construction period of the new area is from 2010 to 2030. Before the start of development in 2010, there is a vast tidal flat with an average tidal range of 2.1 m over the years. The construction of the area will be completed in 2030. The topographic map is shown in the figure (*Fig. 1*) below:

Figure 1. *The topography of the study area*

http://www.aloki.hu ● ISSN 1589 1623 (Print) ● ISSN1785 0037 (Online)
DOI: http://dx.doi.org/10.15666/aeer/2003_21712185

Data sources

Data sources: (*Eq.1*) the results of the Eighth National Forest Inventory (*Eq.2*) According to the first-hand data obtained from the interview, investigation and field investigation of the Landscaping Bureau, bureau of statistics, forest construction ecological zone, public welfare forest protection zone and relevant forestry experts in the study area, the current situation of ecological compensation in the study area is obtained according to the above data sources, as shown in *Table 1*.

Table 1. *Current status of ecological compensation in the study area*

Project	Current status of ecological compensation
Total forest area	258.37 million hm^2
Forest conservation investment	An average of 9.35 US dollars/hm^2, most of the investment is national investment, a small part is provincial public welfare forest investment
Natural forest	754,100 hm^2, with an investment of 15.40 million US dollars
Forest land not listed as public welfare forest	132.59hm^2
Other inputs	3.86 million US dollars

According to the forest resource inventory data released by the State Forestry Administration, the forest area of the study area is 2,583,700 hm^2, including 1,984,400 hm^2 collective forests and 597,700 hm^2 state-owned forests.

According to formula (*Eq.6*) and formula (*Eq.7*), the value of the ecosystem service function of the study area is obtained, as shown in *Table 2*.

Table 2. *The value of ecosystem services in the study area*

Energy category	Quantity/J	Emergy conversion rate	Emergy
Tidal energy	1.08×10^{18}	1093	1.08×10^{20}
Surface wind energy	1.35×10^{18}	3964	2.03×10^{17}
Solar energy	1.67×10^{14}	54128	1.94×10^{20}
Surface wind energy	4.59×10^{17}	3654	7.24×10^{19}
Rainwater chemical energy	3.21×10^{14}	7892	4.17×10^{18}
Evapotranspiration	1.09×10^{17}	11258	1.53×10^{18}
Organic matter loss energy	8.52×10^{15}	2648	2.57×10^{20}

Evaluation of the effectiveness of ecological compensation in beach areas

In the quantitative analysis of the effectiveness of ecological compensation system at the county (District) level, the first thing to do is to choose the analysis method. The appropriate analysis method will often achieve twice the result with half the effort. At present, there are many methods to evaluate the effect in academic circles, such as factor analysis, analytic hierarchy process, principal component analysis, fuzzy comprehensive evaluation, regression analysis, etc. Ecological compensation system is a system involving multiple interest groups such as government, social organizations and farmers. It is an important part of ecological protection mechanism with ecological resources, environment and economic benefits as the main content, relevance among

http://www.aloki.hu ● ISSN 1589 1623 (Print) ● ISSN1785 0037 (Online)
DOI: http://dx.doi.org/10.15666/aeer/2003_21712185

interest groups as the link, and complex index system as the evaluation scale. In order to evaluate the effect of ecological compensation, it is necessary to clarify the contribution value of each index of ecological compensation system to ecological protection. In order to facilitate in-depth study, this paper uses the principal component analysis method to analyze the effect of ecological compensation in coastal beach area.

If there are A samples and select B indicators ($B<a$), each indicator can be understood as a variable, that is, b indicators. In fact, there are b variables in the evaluation model, and the set of variables can be expressed as $B=\{b_1,b_2,...,b_n\}$, the principal component analysis method is to combine b indicators into a linear distribution to generate a new evaluation indicator system, denoted as $F=\{f_1,f_2,..,f_n\}$. This newly generated indicator system can retain most of the original information, and the indicators are independent of each other. The specific steps for evaluating the effect of ecological compensation in beach areas are as follows:

(1) Simplify the initial data according to standardization requirements. The purpose is to eliminate the dimensional problem, which can be expressed by formula (*Eq.12*):

$$m_i=\sum_{i=1}^{n} r_i\eta_i \tag{Eq.12}$$

In the formula, m_i represents the standardized value; r_i represents the initial data; η_i represents the average value of the sample.

(2) Using the correlation system matrix κ of the standardized data to find the eigenvectors and eigenvalues, the eigenvectors and eigenvalues can be obtained from equation $\left(\kappa-m_i\right)^2=0$.

(3) Determine the number of principal components to be evaluated, and then obtain the variance contribution rate and the cumulative contribution rate.

If the t-th component is V_t, its variance contribution rate is the ratio of its variance to the variance of all components. It can be seen that the greater the contribution value, the greater the amount of information. The cumulative contribution rate refers to the ratio of the variance of the first t principal components to the variance of the principal components, and its calculation formula is:

$$T_Q=\frac{\sum_{i=1}^{n} t_{ci}}{\sum_{i=1}^{n} g_i} \tag{Eq.13}$$

The formula (*Eq.13*) expresses the size of the amount of information contained in the first t principal components. Under normal circumstances, the number of principal components is determined based on the amount of information of the first t principal components. In actual calculations, the evaluation basis is the cumulative contribution rate of the first t principal components. This formula can be understood as the first t

http://www.aloki.hu ● ISSN 1589 1623 (Print) ● ISSN1785 0037 (Online)
DOI: http://dx.doi.org/10.15666/aeer/2003_21712185

principal components only occupy a part of the amount of information. The first t principal components can be determined by formula (*Eq.14*):

$$\eta_t = a \times h \times P + b \times C + c \times B \quad \text{(Eq.14)}$$

It can be concluded that the cumulative evaluation index is:

$$T_{zi} = \sum_{i=1}^{n} t_{zi}(\eta_t) \quad \text{(Eq.15)}$$

(4) After the weighted average of t principal components is processed, the comprehensive evaluation score can be obtained. In order to make the score more intuitive, the comprehensive evaluation data can be normalized.

Quantitative analysis of ecological compensation in beach areas

Based on the evaluation process of the effect of ecological compensation in the coastal area, a quantitative analysis of the effect of ecological compensation in the coastal area is carried out. The specific results are as follows.

(1) Ecological footprint status of coastal areas

According to the above calculation formulas of ecological footprint and ecological carrying capacity and the evaluation process of ecological compensation effect in beach areas, and using the data sources in section 3.2 to calculate the ecological footprint of the study area from 2010 to 2020, the results are shown in *Table 3*.

Table 3. *Ecological footprint of coastal areas*

Years	Ecological footprint per capita hm^2/person	Per capita ecological carrying capacity hm^2/person	Ecological surplus	Amount to GDP ratio/%
2010	752.3	4.01	-2017.2	0.19
2011	683.1	3.95	-1954.3	0.23
2012	701.5	4.13	-954.5	0.24
2013	699.3	3.69	-1028.7	0.21
2014	671.5	4.28	-1596.3	0.18
2015	652.8	3.71	-1254.3	0.15
2016	720.8	3.64	-947.2	0.17
2017	741.8	3.32	-984.0	0.20
2018	690.5	4.15	-856.9	0.19
2019	715.0	3.67	-847.1	0.19
2020	726.3	4.08	-1010.8	0.17

According to *Table 3*, the ecological footprint per capita in the study area in 2010 is 752.3 hm^2, the per capita ecological capacity is 4.01 hm^2, and the per capita ecological surplus is -2017.2. From the horizontal comparison, the per capita ecological footprint

http://www.aloki.hu ● ISSN 1589 1623 (Print) ● ISSN1785 0037 (Online)
DOI: http://dx.doi.org/10.15666/aeer/2003_21712185

and ecological surplus level are higher than the average level of the western provinces in China, while the per capita ecological footprint is lower than that of the western provinces in China; From the vertical comparison, the level of ecological surplus in 2020 is significantly increased compared with that of 2010.

(2) The ecological carrying capacity of the study area

Fig. 2 shows the ecological carrying capacity of the study area from 2010 to 2020.

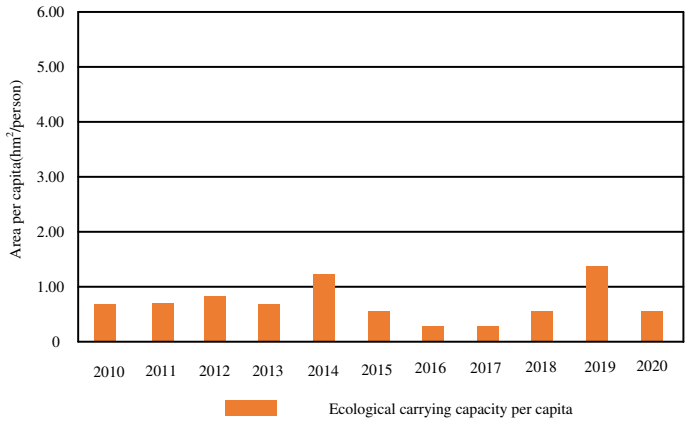

Figure 2. *The ecological carrying capacity of the study area from 2010 to 2020*

It can be seen from *Fig. 2* that the per capita ecological carrying capacity of the study area is lower than the national average, which shows that the region needs to rely on the ecological carrying capacity of economically underdeveloped regions to support the local consumption load.

(3) Comprehensive evaluation of the effect of ecological compensation in the study area

The comprehensive score of the actual effect of ecological compensation in the study area from 2010 to 2020 can be calculated by using the evaluation method of ecological compensation effect in coastal beach area. See *Table 4* for specific data. In order to facilitate comparison, we should normalize the data, and convert all the comprehensive scores into the values between 0-1. The closer the score is to 0, the worse the ecological compensation effect is, and the closer to 1, the better the ecological compensation effect is.

Table 4. *Comprehensive evaluation of ecological compensation effect in the study area*

Years	Before normalization	After normalization
2010	0.23	0.78
2011	0.31	0.80
2012	0.35	0.83
2013	0.38	0.85
2014	0.40	0.86
2015	0.41	0.86
2016	0.43	0.91
2017	0.43	0.94
2018	0.49	0.95
2019	0.51	0.96
2020	0.53	1.00

http://www.aloki.hu ● ISSN 1589 1623 (Print) ● ISSN1785 0037 (Online)
DOI: http://dx.doi.org/10.15666/aeer/2003_21712185

The results show that the effect of ecological compensation after normalization is better than that before normalization. It is worth mentioning that this score is relative, not absolute. The above analysis of the actual effect of ecological compensation in the study area also reflects the effect of the implementation of ecological compensation policy in the study area since 2010 to a certain extent. According to the scores in *Table 4*, the development track of ecological compensation effect can also be predicted, and the results are shown in *Fig. 3*.

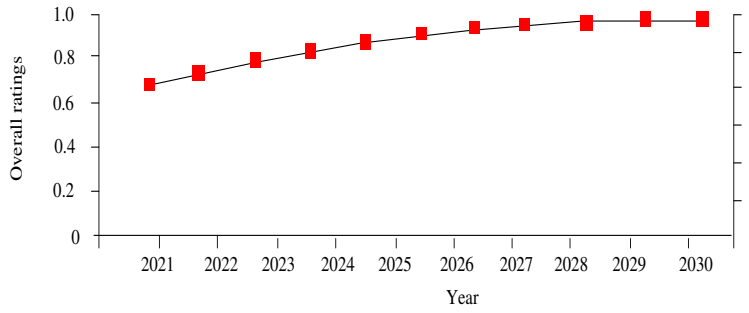

Figure 3. *Forecast of ecological compensation effect*

(4) Calculation results of ecological footprint per capita

Fig. 4 shows the calculation results of the ecological footprint per capita in the study area.

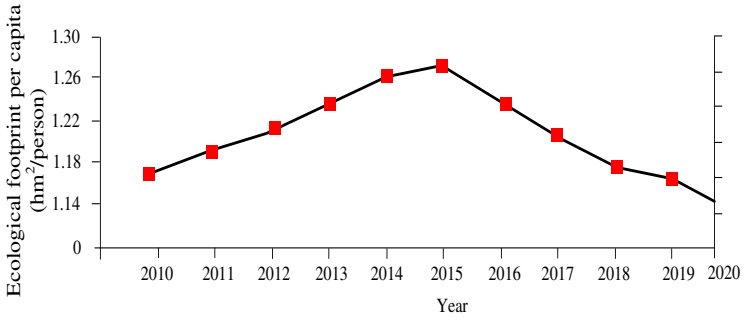

Figure 4. *Ecological footprint per capita in the study area*

According to *Fig. 4*, the per capita ecological footprint of the study area showed an upward trend from 2011 to 2015, and a downward trend from 2016 to 2018. On the one hand, over the past five years, with the development of social economy, people's production and life style and consumption structure are changing. The demand of residents in the study area for meat, aquatic products and milk is gradually increasing. The demand for pork increases from 32 Kg per capita to 35.7 Kg per year, and the demand for aquatic products increases from 5.4 Kg to 7.1 Kg per year. The demand for food crops has changed little, and the demand for other consumer goods has also changed to varying degrees, resulting in changes in the ecological footprint. On the other hand, since 2016, the government has strengthened the protection of resources and environment, people's awareness of resource conservation has gradually improved, some consumer goods have been intensively used, and the per capita consumption has

http://www.aloki.hu ● ISSN 1589 1623 (Print) ● ISSN1785 0037 (Online)
DOI: http://dx.doi.org/10.15666/aeer/2003_21712185

decreased. The most obvious performance is the demand for raw coal, which has decreased from 1.39Kg per capita to 1.09 Kg per year, leading to a significant decline in per capita ecological footprint.

Conclusion

On the basis of absorbing the existing research results, this paper proposes a quantitative analysis method of ecological compensation in coastal beach areas based on changes in ecological footprint. The research results show that this method has the characteristics of strong practical pertinence. This paper takes the ecological red line layout along the beach area as a breakthrough point in the research, upholds the concept of environmental sustainable development, and aims to improve the ecological compensation mechanism to evaluate the effectiveness of the ecological red line regional ecological compensation in the study area. The results show that the ecological surplus in the study area in 2020 has a substantial increase compared with the per capita ecological surplus in the study area in 2010; the per capita ecological carrying capacity of the study area is lower than the national average; the effect of ecological compensation after normalization is obviously better the effect of ecological compensation before normalization. It shows that this method can realize the accurate analysis of the study area and provide a reference for the ecological development path of the area. Although the evaluation method in this article can realize the evaluation of the local human ecological footprint, it has not yet considered the impact of the development of industrial manufacturing on the data. This aspect will be studied in the future and a more accurate evaluation model will be proposed.

Acknowledgement. Key Projects of Humanities and Social Sciences Research in the Anhui Higher Education Institutions of China in 2016 - Study on Regional Landscape Construction Model in Northern Anhui Province in the process of urbanization (No. SK2016A0708); Key Projects of Humanities and Social Sciences Research in the Anhui Higher Education Institutions of China in 2018 - Research on the correlation between Financial flexibility and Corporate value from the Perspective of property right Nature - Taking listed companies in Anhui Province as an Example (No. SK2018A0728).

REFERENCES

[1] Boutahar, L., Maanan, M., Bououarour, O., Richir, J., Pouzet, P., Gobert, S., Maanan, M., Zourarah, B., Benhoussa, A., Bazairi, H. (2019): Biomonitoring environmental status in semi-enclosed coastal ecosystems using Zostera noltei meadows. – Ecological Indicators 104(9): 776-793.

[2] Dong, Q., Liu, X. (2020): The Legal Norms of Ecological Compensation in Coastal Cities under Regional Cooperation. – Journal of Coastal Research 103(1): 552.

[3] Ferro-Azcona, H., Espinoza-Tenorio, A., Calderon-Contrera, R., Ramenzoni, V. C., de las Mercedes Gómez Pais, M., Mesa-Jurado, M. A. (2019): Adaptive capacity and social-ecological resilience of coastal areas: A systematic review. – Ocean & coastal management 173(5): 36-51.

[4] Itsukushima, R. (2019): Study of aquatic ecological regions using fish fauna and geographic archipelago factors. – Ecological indicators 961(1): 69-80.

[5] Kosev, V., Vasileva, V. (2019): Ecological sustainability and stability of quantitative signs in vetch (Vicia villosa) varieties. – Indian Journal of Agricultural Sciences 89(7): 1108-1114.

http://www.aloki.hu ● ISSN 1589 1623 (Print) ● ISSN1785 0037 (Online)
DOI: http://dx.doi.org/10.15666/aeer/2003_21712185

[6] Li, Y. (2019): The reform of the ecological compensation mechanism in the basin based on the community of life - Taking the Minjiang basin as an example. – Chinese Administration 3: 95-100.
[7] Nie, C. J., Cheng, M. L. (2019): Research on Regional Lateral Forest Ecological Compensation Based on the Theory of Marginal Effect. – Forestry Economics 41(01): 25-32+41.
[8] Park, J. C., Redwine, J. R., Hill, T. D., Kotun, K. (2019): Water resource and ecotone transformation in coastal ecosystems. – Ecological Modelling 405: 69-85.
[9] Salemi, M., Jozi, S. A., Malmasi, S., Rezaian, S. A. (2019): New Model of Ecological Carrying Capacity for Developing Ecotourism in the Protected Area of the North Karkheh, Iran. – Journal of the Indian Society of Remote Sensing 47(11): 1937-1947.
[10] Smee, D. L. (2019): Coastal Ecology: Living Shorelines Reduce Coastal Erosion. – Current Biology 29(11): 411-413.
[11] Stone, R., Callaway, R., Bull, J. C. (2019): Are biodiversity offsetting targets of ecological equivalence feasible for biogenic reef habitats? – Ocean & Coastal Management 177(7): 97-111.
[12] Su, K., Sun, X., Guo, H., Long, Q., Yue, D. (2020): The Establishment of a cross-regional differentiated ecological compensation scheme based on the benefit areas and benefit levels of sand-stabilization ecosystem service. – Journal of Cleaner Production 270(27): 122490.
[13] Sun, H. R., Wang, H. (2018): Urban Green Space Landscape Ecological Balance Optimal Design Simulation. – Computer Simulation 35(01): 214-217.
[14] Wang, X., Yang, J., Li, T. (2019): Study on ecological compensation based on ecological service value: a case study of Changsha City. – Jiangsu Journal of Agricultural Sciences 35: 219-226.
[15] Wang, W. W., Ye, J., Zhang, L. G., Wei, C., Zhang, H. W., Liu, H. H. (2020): Research on ecological compensation from the perspective of main functional areas: a case study of Hubei Province. – Acta Ecological Sinical 40: 269-278.
[16] Yang, R., Zhang, Y., Li, X. (2019): Innovating the ecological compensation mechanism of the Yongding River Basin to promote the coordinated development of Beijing-Tianjin-Hebei. – Ecological Economy 35(12): 138-142.
[17] Yang, X., Zhang, F., Luo, C., Zhang, A. (2019): Farmland Ecological Compensation Zoning and Horizontal Fiscal Payment Mechanism in Wuhan Agglomeration, China, From the Perspective of Ecological Footprint. – Sustainability 11: 2326.
[18] Zeng, Z., Ye, Y., Guo, W., Li, S. (2020): Research on the ecological compensation mechanism based on the management idea of ecological protection red line - Taking Guangming District of Shenzhen as an example. – Journal of Ecological Environment 29(09): 93-101.

http://www.aloki.hu ● ISSN 1589 1623 (Print) ● ISSN1785 0037 (Online)
DOI: http://dx.doi.org/10.15666/aeer/2003_21712185

PLANT GROWTH PROMOTING BACTERIA (PGPB) ENHANCE GROWTH AND YIELD OF STRAWBERRY CULTIVARS

BADAR, M. A.[1*] – MEHMOOD, K.[1] – HASSAN, I.[1] – AHMED, M.[2] – AHMAD, I.[3*] – AHMAD, N.[3] – HASAN, M. U.[3]

[1]*Department of Horticulture, PMAS Arid Agriculture University, Rawalpindi 46300, Pakistan*

[2]*Department of Agronomy, PMAS Arid Agriculture University, Rawalpindi 46300, Pakistan*

[3]*Institute of Horticultural Sciences, University of Agriculture, Faisalabad 38040, Pakistan*

**Corresponding author*
e-mail: adnanbadar.uaf@gmail.com, iftikharahmadhashmi@gmail.com

(Received 25th Sep 2021; accepted 21st Mar 2022)

Abstract. A study was conducted to evaluate the effect of various plant growth promoting bacteria (PGPB) on growth, yield and physicochemical quality attributes of strawberry cultivars. Runners of three commercial strawberry cultivars, viz. 'Chandler', 'Tuft's' and 'Camarosa' were acquired from a certified runner supplier in Swat, KPK, Pakistan and were planted in 10 cm plastic pots. Three plant growth promoting bacterial isolates, viz. *Pseudomonas fluorescens* (T_1), *Bacillus subtilis* (T_2) and *Pseudomonas aeruginosa* (T_3) were applied after two weeks of runners planting with no PGPB application as control (T_0). Results revealed that plants supplied with *Bacillus subtilis* (T_2) had highest number of leaves per plant (38.33), leaf area index (41.69 cm^2), crown diameter (1.36 cm), number of runners (5.42), fruit set (86.11%), average yield (226.97 g), soluble solid contents (SSC) (8.43 ^{0}Brix), ascorbic acid (49.98 mg 100 mL^{-1}), total sugars (5.72%) and Anthocyanin contents (37.55 mg 100 mL^{-1}), while minimum plant growth and physicochemical characteristics were recorded for plants with no PGPB (control). Among cultivars, 'Chandler' responded better to PGPB application compared to two other cultivars. Therefore, use of PGPB, particularly *Bacillus subtilis,* has the potential to affect growth, yield and physicochemical quality characteristics of strawberry cultivars and may be used by strawberry growers for lowering fertilizer cost by alternating with organic PGPB to enhance the growth and yield of strawberry.
Keywords: *bacterial isolates, biochemical attributes, biofertilizer, minor fruit production*

Introduction

Strawberry (*Fragaria ananassa* Duch.) is a valuable minor fruit crop grown worldwide for its delicious fruit having excellent aroma, sweetness and attractive color (Ali et al., 2021). It is a rich source of antioxidants including anthocyanins, phenolic compounds, vitamins and sugars and can be consumed as fresh, juice and as raw material for processing industry to make jam, jelly and syrup (Ayub et al., 2010; Hanif and Budiyati, 2011). Agroclimatic conditions of Pakistan are quite suitable for strawberry cultivation (Aslam and Rasool, 2012) and it is primarily grown in Charsadda, Mansehra, Mardan, Haripur, Swat, Islamabad, Gujrat, Lahore and Karachi. Strawberry cultivars and variable use of chemical fertilizers are the major sources of variability, which affect its yield and quality. There are approximately 500 commercial strawberry cultivars worldwide, however, very few are available in Pakistan, which also need to be evaluated in various agro-climatic conditions for their adaptability in local agro-climatic zones. For successful strawberry cultivation, selection of well adapted and high yielding cultivars is of paramount importance (Galletta and Maas, 1990).

Inadequate application of chemical fertilizers is a serious threat to climate, soils and human health. Therefore, bio-fertilizers are used to protect soils from degradation and

http://www.aloki.hu ● ISSN 1589 1623 (Print) ● ISSN 1785 0037 (Online)
DOI: http://dx.doi.org/10.15666/aeer/2003_21872203

food contamination. Organic nutrients can increase soil enzyme activity, availability of nitrates, access to total organic carbon and soil fertility quotients (Okwuagwu et al., 2003). Improved plant nutrition by PGPB is mostly due to increased phosphorous absorption through inorganic phosphate solubilization or organic phosphate mineralization. They often release organic acids that contribute to the availability of nutrients and result in increased plant growth by taking water and mineral nutrients (Biswas et al., 2000). PGPB specifically activate growth regulators such as auxin, gibberellins, cytokinin, inorganic phosphorus solubilization and nutrient mineralization along with symbiotic N-fixation (Glick, 1995; Zahir et al., 2004). Application of PGPB improves plant growth, yield, enhances fruit shelf life, texture, and quality (Gupta and Kaushal, 2017).

PGPB have the potential to enhance the yield of important field crops. Generally, PGPB enhance plant growth and yield by synthesizing particular compounds for the plants. They facilitate the uptake of certain nutrients from the soil and protect the plants from diseases (Saravanakumar et al., 2008). Enhanced crop yield was recorded in maize, chickpea, soybean, rice, peanut, sugarcane and wheat as PGPB are able to increase agronomic efficiency by reducing production costs. They are also helpful to reduce environmental pollution, once the use of chemical fertilizers is reduced or eliminated if the inoculants are efficient (De Souza et al., 2015). Vegetable production and quality could be enhanced with supplementation of PGPB by enhancing nutrient uptake and indirect inhibition of pathogen attack during production cycle (Mekonnen et al., 2021). Tomato seedlings provided with 1% liquid PGPB significantly increased biomass, yield and helped in mitigating water deficit irrigation or enhanced water use efficiency (Le et al., 2018). Likewise, the application of PGPB combined with aqueous vermicompost extract markedly increased retaining and uptake of nutrients from the substrate employed for tomato production (Ruiz and Sanjuan, 2022). Recent study revealed that exogenous application of PGPB (*A. brasilense* DSM 2298) combined with variable doses of nitrogen (30 or 60 Kg ha^{-1}) significantly increased yield of lettuce with enhanced total phenolic concentration, ascorbic acid content, chlorophyll, soluble solid contents and total sugars (Consentino et al., 2022).

Considering the research gap, the effect of three PGPB was analyzed on three commercial cultivars grown in Pakistani climatic conditions. Therefore, present study was carried out to evaluate the effect of PGPB on growth, yield and physicochemical quality characteristics of ‘Chandler’, ‘Tuft’s’ and ‘Camarosa’ strawberry cultivars.

Methods

Experiment layout and treatments

The study was conducted at Horticulture Research Area, PMAS-Arid Agriculture University, Rawalpindi, during 2016-17. Prior to the trial, soil samples were taken and different soil physicochemical properties (pH, EC, NPK, bulk density) were estimated (*Table 1*). The runners of three strawberry cultivars, viz. ‘Chandler’, ‘Tuft’s’ and ‘Camarosa’ were sourced from a certified strawberry runner supplier from Swat, KPK, Pakistan, and planted in 10 cm plastic pots. Plants were maintained in a greenhouse set at 25 ± 3°C, no additional fertilizer was applied to the plants except PGPB and were irrigated according to weather conditions and plant requirement based on plant growth stage. Three Plant Growth Promoting Bacterial isolates, viz. *Pseudomonas fluorescens* (T_1), *Bacillus subtilis* (T_2) and *Pseudomonas aeruginosa* (T_3) were applied at 10^6

http://www.aloki.hu ● ISSN 1589 1623 (Print) ● ISSN 1785 0037 (Online)
DOI: http://dx.doi.org/10.15666/aeer/2003_21872203

$CFU \cdot mL^{-1}$ after two weeks of runners planting. 5 mL of the bacterial suspensions were used to inoculate each treated plant after 15 days of transplanting. Plants receiving no PGPB were considered as control (T_0) and same amount of buffer was provided to uninoculated plants.

Table 1. *Physicochemical characteristics, viz. pH, EC, NPK, and bulk density of soil samples in study area. Means are averages of three samples*

Treatments	pH	EC (dS m^{-1})	N	P	K	Bulk density
Control (no PGPB) (T_0)	6.3 a[a]	0.96 a	4.36 b	2.36 b	89.23 c	0.94 a
Pseudomonas fluorescens (T_1)	5.9 b	0.88 a	5.80 a	2.33 b	105.33 b	1.01 a
Bacillus subtilis (T_2)	5.9 b	0.48 b	4.16 b	3.23 a	138.26 a	0.64 b
Pseudomonas aeruginosa (T_3)	5.0 b	0.54 b	4.13 b	3.86 a	112.4 b	0.73 b
Mean	5.77	0.71	4.61	2.94	111.30	0.83

[a]Means within a column followed by the same letter are not significant at $P \leq 0.05$

Physical parameters

Plant physical parameters, viz. number of leaves per plant, leaf area index (cm^2), crown diameter (cm), number of runners per plant, plant biomass (g) measured by taking recording both fresh and dry weight, number of flowers per truss, number of trusses per plant, number of flowers per plant, flower diameter (cm), days to flower induction, fruit set (%), number of fruits per plant, fruit weight (g), fruit yield per plant (g) were measured by multiplying average fruit weight and number of fruits per plant. Biomass was measured by taking strawberry plants fresh and dry weights. Plant biomass was measured at the end of harvesting season.

Leaf area index was measured by ADC area AM-100 in which 10 leaves per plant were taken for average estimation and average was recorded from each replication for data analysis. Leaf area index was performed after harvesting the fruits. Formula for calculation of leaf area index is as under;

$$\text{Leaf area index} = \text{Leaf area } (m^2) \,/\, \text{Ground area } (m^2)$$

Biochemical analysis of fruit

Soluble solid contents (SSC) of fruit juice was determined by handheld Refractometer (ATAGO, RS-5000 Atago, Japan). Titrable acidity (TA) of the juice was calculated by taking 10 mL of juice in 100 mL conical flask, which was diluted up to 50 mL with distilled water and titrated against 0.1 N NaOH using 2 to 3 drops of phenolphthalein as an indicator till pink color end point was achieved and TA was expressed as percentage (%). Ascorbic acid contents of fruit juice were determined by the method described by Ruck (1969). Strawberry juice @ 10 mL was added to 0.4% oxalic acid solution in 100 mL volumetric flask. Then 5 mL of diluted and filtrated aliquot was titrated against 2, 6–dichlorophenolindophenol dye, to light pink color end point. Juice was extracted by squeezing the fruits using muslin cloth manually. Sugars in juice (extracted through squeezing) were estimated following the method of Hortwitz (1960) in which 10 mL juice was taken in 250 mL volumetric flask and diluted with 100 mL water, 25 mL 25% lead acetate solution and 10 mL 20% potassium oxalate.

http://www.aloki.hu ● ISSN 1589 1623 (Print) ● ISSN 1785 0037 (Online)
DOI: http://dx.doi.org/10.15666/aeer/2003_21872203

Then the volume was made with distilled water. The filtrate was used for the estimation of different forms of sugars. Sugars were expressed as percentage.

Anthocyanin content

Anthocyanin concentration (mg pf-3-GLE/100 g FW) from fruit juice was measured by the pH differential method (Giusti and Wrolstad, 2001) in spectrophotometer Plasma spectrophotometer Inductively Couple (Perkin-Elmer, Optima 2100 DV, ICP/OES, Shelton, CT, USA) with distilled water and determining λ max (510 nm and 700 nm), two dilutions (A) and (B) of the extracts were prepared with different buffers. One (A) was prepared by adding 0.4 mol of extract and 3.6 mol of potassium chloride buffer 0.025 M, (pH 1.0 to 4.0) mol cuvettes. The second dilution (B) was prepared in the same way with the addition of sodium acetate buffer (0.4 M, pH 4.5). The dilutions were allowed to equilibrate for 20 min and measurements immediately followed. The reading of distilled water was found to have no difference in relation to buffer. The absorbance of each diluted sample was measured at 510 nm and 700 nm.

Statistical analysis

The experimental layout was completely randomized design with factorial arrangement of treatments replicated three times. Data were analyzed using analysis of variance (ANOVA) and general linear models procedures of SAS (version 9.3, SAS Inst., Inc., Cary, NC, USA) and Fisher's LSD at $P \leq 0.05$ was used to separate means (Steel et al., 1997).

Results and discussion

Leaf NPK contents (%)

Highest NPK was recorded in 'Chandler' (4.93 ± 0.09, 0.57 ± 0.09, 2.37 ± 0.19) followed by 'Tuft' (4.53 ± 0.27) when treated with *Bacillus subtilis* (T_2) (*Fig. 1*). Improved NPK status in 'Chandler' leaves was might be due to more nitrogen fixation, phosphate Solubilization and potassium availability which was facilitated by PGPB. Leaf NPK uptake in strawberry is supported by earlier findings of Consentino et al. (2022), which reported that more nutrient uptake was noted in lettuce which were treated with *A. brasilense* DSM 2298.

Number of leaves per plant and leaf area index (cm²)

Results revealed that PGPB inoculation enhanced number of leaves per plant. Maximum number of leaves (38.33 ± 0.88) were observed in 'Chandler' followed by 'Camarosa' (36.00 ± 0.58) and 'Tuft' (33.00 ± 1.15), when supplied with *Bacillus subtilis* (T_2) (*Fig. 2*). Increased number of leaves were observed in maize, wheat and pigeon pea by Tilak and Reddy (2006). For leaf area index of strawberry, results depicted significant results in which *Bacillus subtilis* (T_2) produced greatest leaf area index (41.69 ± 0.89) following *Pseudomonas aeruginosa* (T_3) (39.48 ± 0.47) and *Pseudomonas fluorescens* (T_1) (32.85 ± 0.81). Similar findings were observed in earlier reports that PGPB application increased plant growth for lettuce (Consentino et al., 2022), *Agave americana* (La-Torre-Ruiz et al., 2016) and strawberry (Esitken et al., 2010).

http://www.aloki.hu ● ISSN 1589 1623 (Print) ● ISSN 1785 0037 (Online)
DOI: http://dx.doi.org/10.15666/aeer/2003_21872203

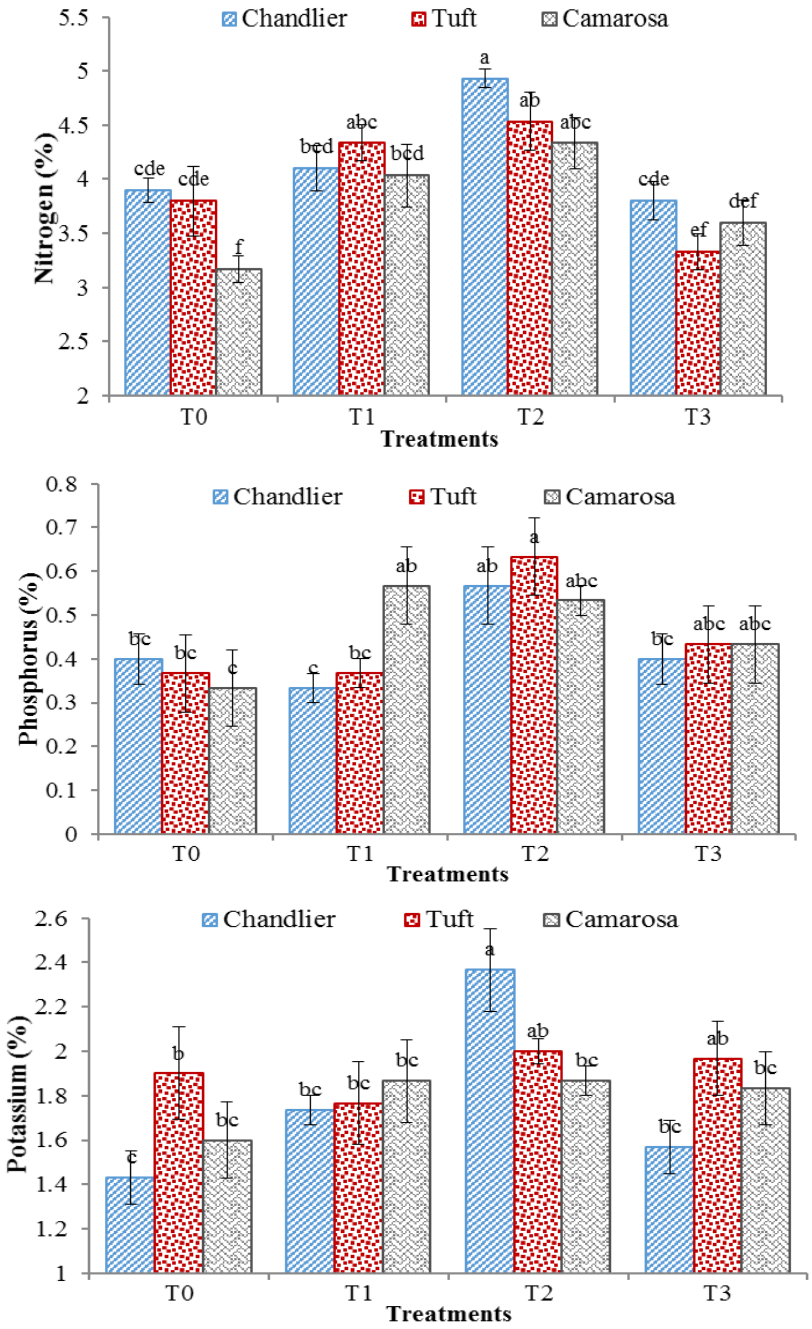

Figure 1. *Effect of various plant growth promoting bacteria (PGPB) on leaf NPK contents of strawberry cvs. Chandler, Tufts and Camarosa. Vertical bars indicate means ± SE. n = 3*

Crown diameter (cm), number of runners and plant biomass (g)

Data regarding crown diameter exhibited greatest crown diameter (1.36 ± 0.10) in 'Chandler' followed by 'Tuft' (1.32 ± 0.05) and 'Camarosa' (1.09 ± 0.04). However, plants subjected with T_2 (*Bacillus subtilis*) produced maximum crown diameter (1.54 ± 0.08) followed by *Pseudomonas aeruginosa* (T_3) (1.31 ± 0.05) and *Pseudomonas fluorescens* (T_1) (1.20 ± 0.05) (*Fig. 3*). Patten and Glick (2002) reported

http://www.aloki.hu ● ISSN 1589 1623 (Print) ● ISSN 1785 0037 (Online)
DOI: http://dx.doi.org/10.15666/aeer/2003_21872203

that various PGPRs that produce GA, IAA, cytokinin and other plant hormones, play an important role in production of plant material, stimulate plant cell elongation and cell break. In addition, highest number of runners (5.42 ± 0.0.57) were produced in 'Chandler' following 'Tuft' (4.00 ± 0.56) and 'Camarosa' (3.67 ± 0.68). Plants supplied with *Bacillus subtilis* (T_2) yielded greatest number of runners (7.22 ± 0.40) followed by *Pseudomonas aeruginosa* (T_3) (4.56 ± 0.50) and *Pseudomonas fluorescens* (T_1) (3.00 ± 0.41). Lowest number of runners were recorded in control (T_0) (2.67 ± 0.33). Plants supplied with *Bacillus subtilis* (T_2) demonstrated highest plant biomass (120.78 ± 1.74) followed by *Pseudomonas aeruginosa* (T_3) (117.33 ± 0.78) and Control (T_0) (116.00 ± 1.48). 'Chandler' weighed greatest plant biomass (127.00 ± 1.73) followed by 'Tuft' (118.33 ± 1.20) and 'Camarosa' (117.00 ± 1.53) when supplied with *Bacillus subtilis* (T_2) (*Fig. 3*). This is due to P solubilization which was enhanced by *Bacillus* spp. (Egamberdiyeva, 2005).

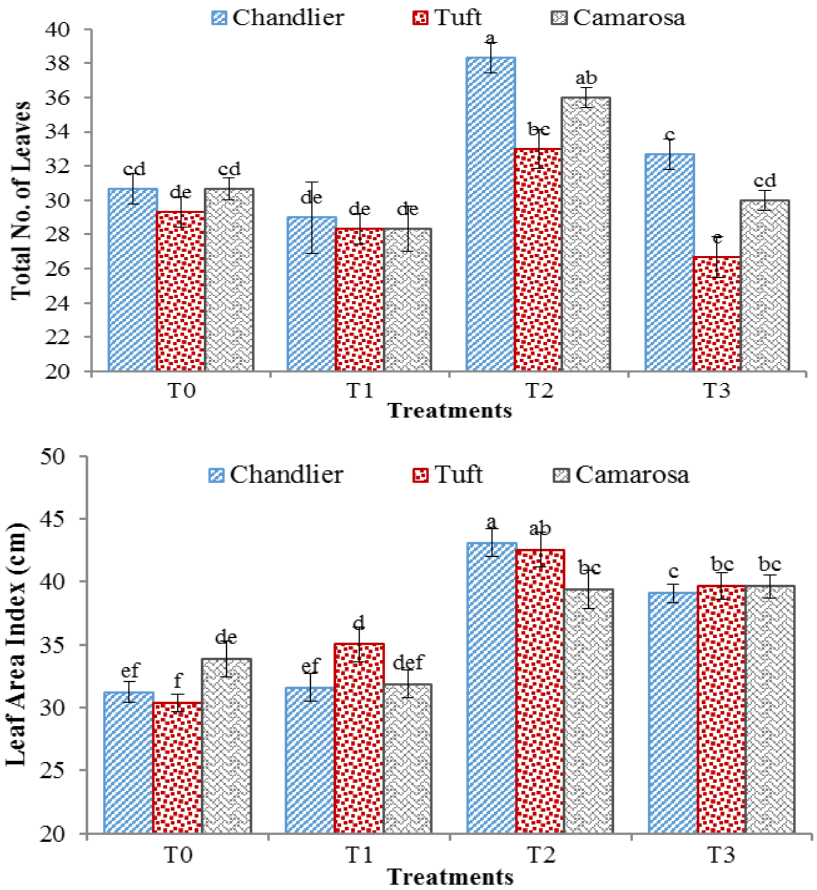

Figure 2. *Total number of leaves and leaf area index of strawberry cvs. Chandler, Tufts and Camarosa treated with various plant growth promoting bacteria (PGPB). Vertical bars indicate means ± SE. n = 30*

Days to flower induction and number of flowers per truss

Strawberry plants grown with *Pseudomonas aeruginosa* (T_3) initiated flowers in least time (99.33 ± 0.83 days) followed by *Bacillus subtilis* (T_2) (99.67 ± 1.24) and *Pseudomonas fluorescens* (T_1) (101.22 ± 0.89), which were statically at par (*Fig. 4*).

http://www.aloki.hu ● ISSN 1589 1623 (Print) ● ISSN 1785 0037 (Online)
DOI: http://dx.doi.org/10.15666/aeer/2003_21872203

Among cultivars, 'Chandler' flowered earlier after 95.33 ± 0.88 days of planting followed by 'Tuft' (101.00 ± 1.15) and 'Camarosa' (102.67 ± 1.20) with *Bacillus subtilis* (T_2). However, longest time (107.33 ± 0.67 days) were taken by 'Camarosa' and 105.67 ± 1.20 days by 'Tuft' for flower induction. Similar results were also reported by Kurokura et al. (2017). Maximum number of flowers (4.00 ± 0.62) per truss were recorded in 'Chandler' following 'Tuft' (3.42 ± 0.43) and 'Camarosa' (3.08 ± 0.42). Plants supplied with *Bacillus subtilis* (T_2) had highest number of flowers (5.44 ± 0.53) per truss followed by *Pseudomonas aeruginosa* (T_3) (3.56 ± 0.41) and control (T_0) (2.67 ± 0.37). Least number of flowers per truss were recorded in plants supplied with *Pseudomonas fluorescens* (T_1) (2.33 ± 0.33). Among cultivars, 'Chandler' had highest number of flowers (7.00 ± 0.58) per truss following 'Tuft' (5.00 ± 0.58) and 'Camarosa' (4.33 ± 0.88) when grown with *Bacillus subtilis* (T_2). 'Camarosa' had least number of flowers (2.00 ± 0.58) per truss as compared to 'Tuft' (2.33 ± 0.88) and 'Chandler' (2.67 ± 0.33) when supplied with *Pseudomonas fluorescens* (T_1).

Total number of flowers, flower diameter (cm) and number of trusses per plant

Highest number of flowers (33.08 ± 2.25) were recorded in 'Chandler' followed by 'Tuft' (28.67 ± 2.05) and 'Camarosa' (28.00 ± 2.39). Plants grown with *Bacillus subtilis* (T_2) had highest number of flowers (37.56 ± 1.31) followed by *Pseudomonas aeruginosa* (T_3) (36.22 ± 0.68) and *Pseudomonas fluorescens* (T_1) (24.33 ± 1.52) (*Fig. 5*). Rahman and Islam (2019) stated that PGPB applied to strawberry improved total number of flowers. Maximum flower diameter (1.88 ± 0.14) was recorded in 'Chandler' followed by 'Camarosa' (1.73 ± 0.07) and 'Tuft' (1.65 ± 0.10). Plants supplied with *Bacillus subtilis* (T_2) produced maximum flower diameter (2.12 ± 0.14) followed by *Pseudomonas aeruginosa* (T_3) (1.78 ± 0.08) and *Pseudomonas fluorescens* (T_1) (1.66 ± 0.09). Minimum flower diameter was recorded in plants without PGPB application (Control) (1.45 ± 0.06) (*Fig. 5*). Among cultivars, 'Chandler' produced maximum flower diameter (2.61 ± 0.08) followed by 'Tuft' (1.96 ± 0.11) and 'Camarosa' (1.80 ± 0.21) when supplied with *Bacillus subtilis* (T_2). Highest number of trusses (6.75 ± 0.35) were recorded in 'Chandler' followed by 'Tuft' (5.08 ± 0.34) and 'Camarosa' (4.50 ± 0.36). 'Chandler' showed maximum number of trusses (8.00 ± 0.58) followed by 'Tuft' (6.00 ± 0.58) and 'Camarosa' (3.33 ± 0.33) when supplied with *Pseudomonas fluorescens* (T_1) (*Fig. 5*). 'Camarosa' had minimum number of trusses (3.33 ± 0.33) compared to 'Tuft' (6.00 ± 0.58) and 'Chandler' (8.00 ± 0.58) when grown with *Bacillus subtilis* (T_2). Among PGPB, *Pseudomonas fluorescens* proved a best performing treatment in respect to emergence of flowers and fruit trusses. Bhattacharyya and Jha (2012) reported that PGPB application can increase flower trusses and root growth.

Fruit parameters

Fruit set (%) and average number of fruits per plant

Application of *Bacillus subtilis* (T_2) exhibited highest fruit set percentage (86.11 ± 0.87) followed by *Pseudomonas aeruginosa* (T_3) (85.87 ± 0.25) and *Pseudomonas fluorescens* (T_1) (85.78 ± 0.72), which were statistically at par (*Fig. 6*). Minimum fruit set percentage was recorded in plants which were grown without any PGPB application (control) (71.37 ± 2.49). Among cultivars, 'Chandler' had highest fruit set percentage (88.50 ± 1.19) followed by 'Tuft' (85.20 ± 1.10) and 'Camarosa' (84.63 ± 1.43), when supplied with *Bacillus subtilis* (T_2). Mena-Violente and Olade-

http://www.aloki.hu ● ISSN 1589 1623 (Print) ● ISSN 1785 0037 (Online)
DOI: http://dx.doi.org/10.15666/aeer/2003_21872203

Portugal (2007) obtained similar results and found that the addition of *Bacillus subtilis* improved tomato yield. Maximum average number of fruits (27.25 ± 2.7) were also recorded in 'Chandler' followed by 'Tuft' (23.83 ± 2.15) and 'Camarosa' (23.25 ± 2.23). Bacterial isolate *Bacillus subtilis* (T_2) produced maximum average number of fruits (32.89 ± 1.51) followed by *Pseudomonas aeruginosa* (T_3) (31.22 ± 0.68) and *Pseudomonas fluorescens* (T_1) (19.67 ± 1.39) (*Fig. 6*).

Fruit weight (g) and average yield (g)

Maximum fruit weight (9.70 ± 0.51) was recorded in 'Camarosa' followed by 'Tuft' (9.25 ± 0.66), while 'Chandler' had lowest fruit weight (8.77 ± 0.90). Among PGPB, *Bacillus subtilis* (T_2) had greatest fruit weight (11.18 ± 0.82) followed by *Pseudomonas aeruginosa* (T_3) (9.64 ± 0.45) and *Pseudomonas fluorescens* (T_1) (9.31 ± 0.77) (*Fig. 7*). Raspberry using *Bacillus* M3 and *Bacillus* OSU-142 produced maximum fruit weight, yield and fruit mineral contents. Mena-Violente and Olade-Portugal (2007) found that the introduction of *Bacillus subtilis* improved the weight of tomatoes. Maximum average yield (263.19 ± 49.74) recorded in 'Chandler' followed by 'Camarosa' (226.97 ± 25.07) and 'Tuft' (226.74 ± 31.18). Among PGPBs, *Bacillus subtilis* (T_2) produced greatest average yield (376.86 ± 41.16) followed by *Pseudomonas aeruginosa* (T_3) (299.76 ± 15.10) and *Pseudomonas fluorescens* (T_1) (174.10 ± 6.25) (*Fig. 7*). Lowest average yield was recorded in plants with no PGPB (control) (104.15 ± 6.25).

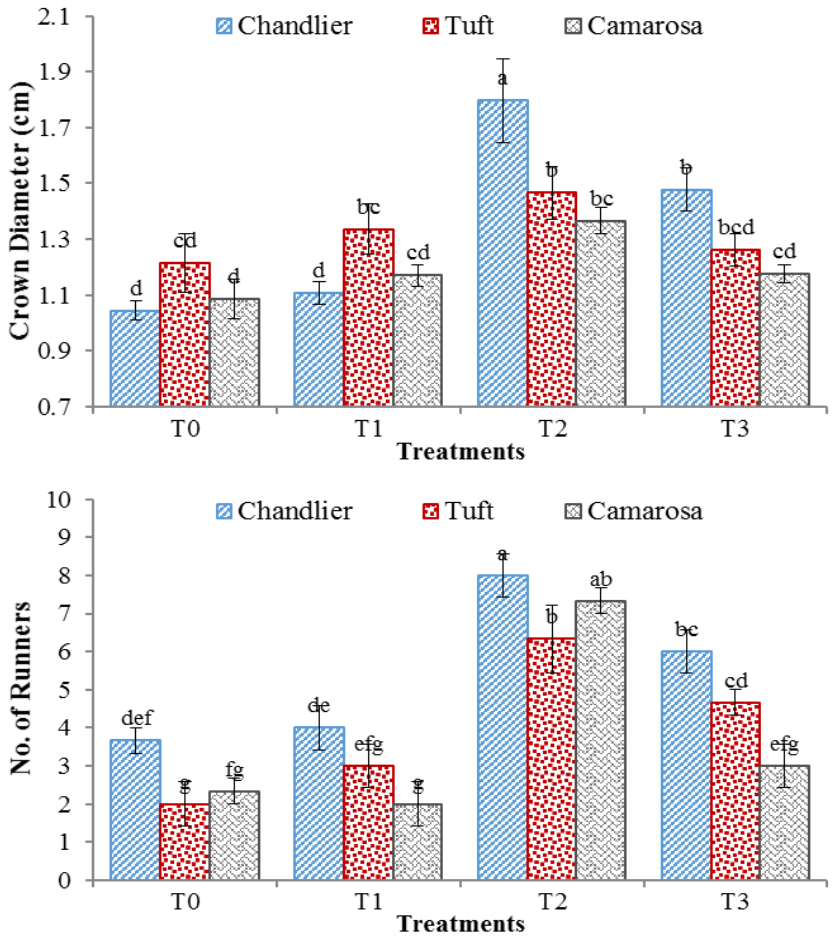

http://www.aloki.hu ● ISSN 1589 1623 (Print) ● ISSN 1785 0037 (Online)
DOI: http://dx.doi.org/10.15666/aeer/2003_21872203

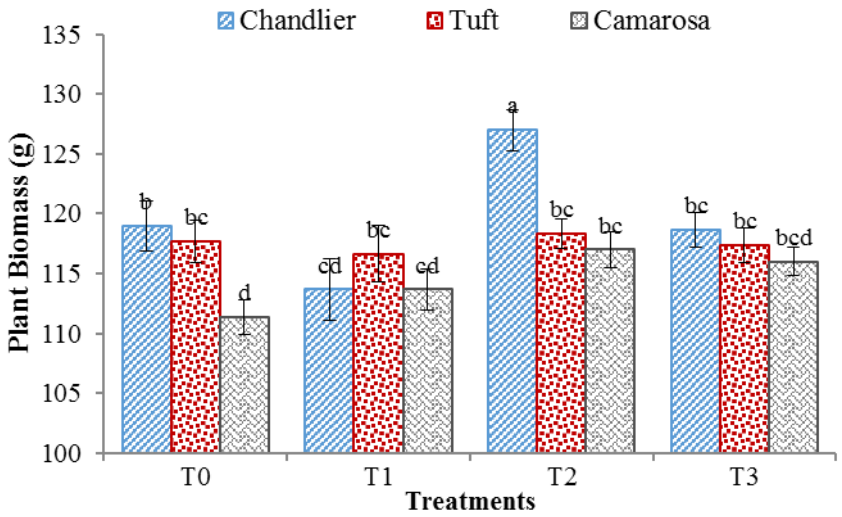

Figure 3. *Crown diameter, number of runners and plant biomass data of strawberry cvs. Chandler, Tufts and Camarosa treated with various plant growth promoting bacteria (PGPB). Vertical bars indicate means ± SE. n = 30*

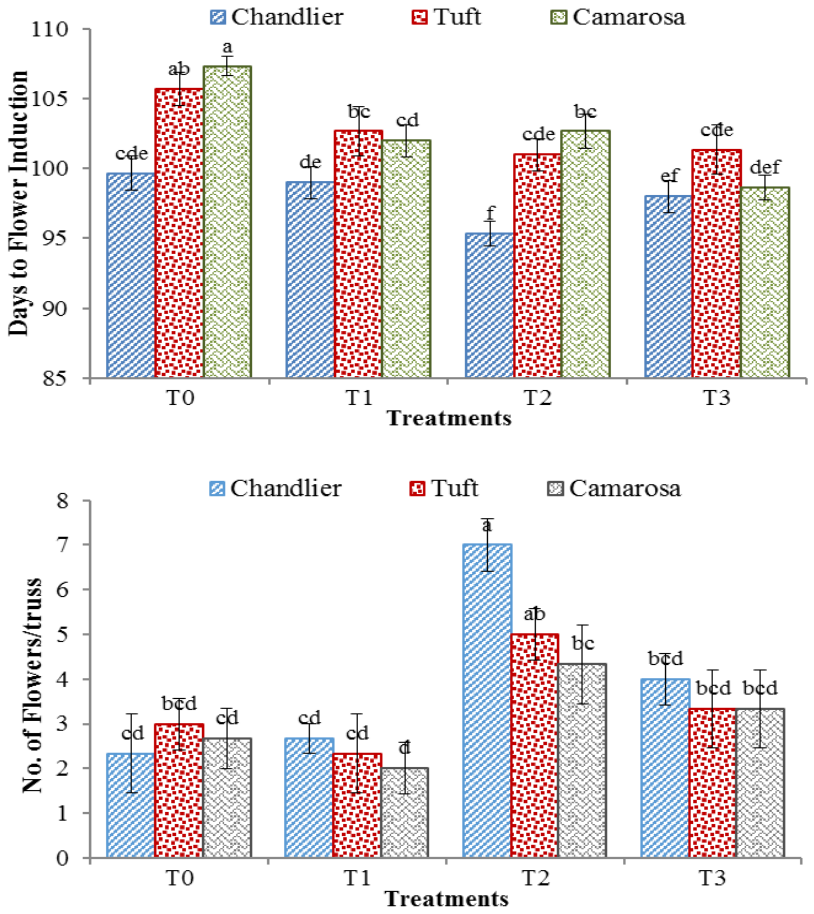

Figure 4. *Days to flower induction and number of flower per truss data of strawberry cvs. Chandler, Tufts and Camarosa treated with various plant growth promoting bacteria (PGPB). Vertical bars indicate means ± SE. n = 30*

http://www.aloki.hu ● ISSN 1589 1623 (Print) ● ISSN 1785 0037 (Online)
DOI: http://dx.doi.org/10.15666/aeer/2003_21872203

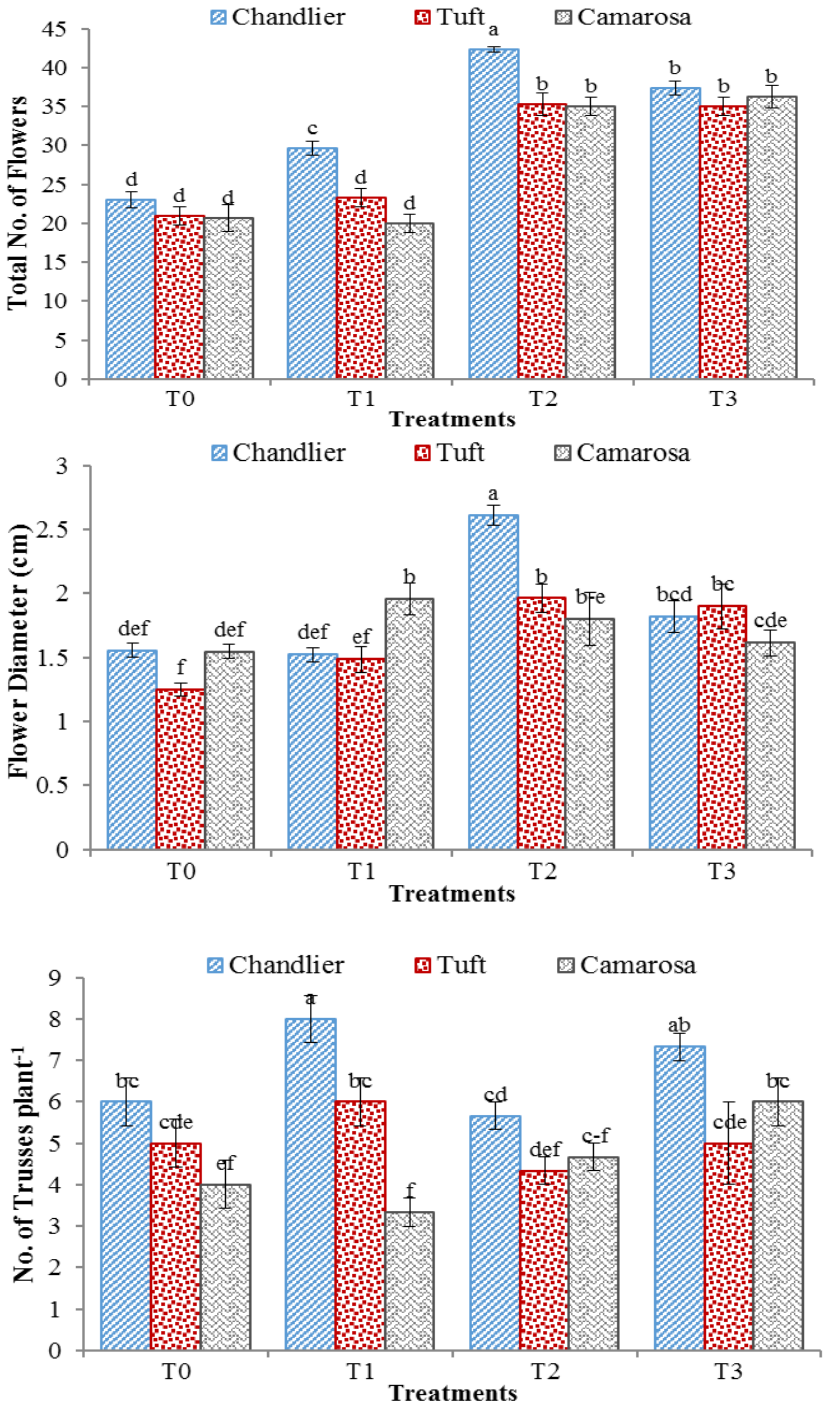

Figure 5. *Total number of flowers, flower diameter (cm) and number of trusses plant^{-1} data of strawberry cvs. Chandler, Tufts and Camarosa treated with plant growth promoting bacteria (PGPB). Vertical bars indicate ± SE of means. n = 3 replicates*

Biochemical analysis of fruit

Soluble solid contents (°Brix)

Maximum total soluble solid contents (8.43 ± 0.45) were recorded in fruit of 'Chandler' followed by 'Tuft' (8.38 ± 0.45) and 'Camarosa' (7.64 ± 0.28). Among

http://www.aloki.hu ● ISSN 1589 1623 (Print) ● ISSN 1785 0037 (Online)
DOI: http://dx.doi.org/10.15666/aeer/2003_21872203

PGPB, *Bacillus subtilis* (T_2) had highest soluble solid contents (9.35 ± 0.34) followed by *Pseudomonas fluorescens* (T_1) (8.35 ± 0.49) and *Pseudomonas aeruginosa* (T_3) (8.20 ± 0.30) (*Fig. 8*). Consentino et al. (2022) reported that PGPB application markedly increased total soluble solids (TSS) and total sugars in lettuce which is in-line with our finding in strawberry fruits.

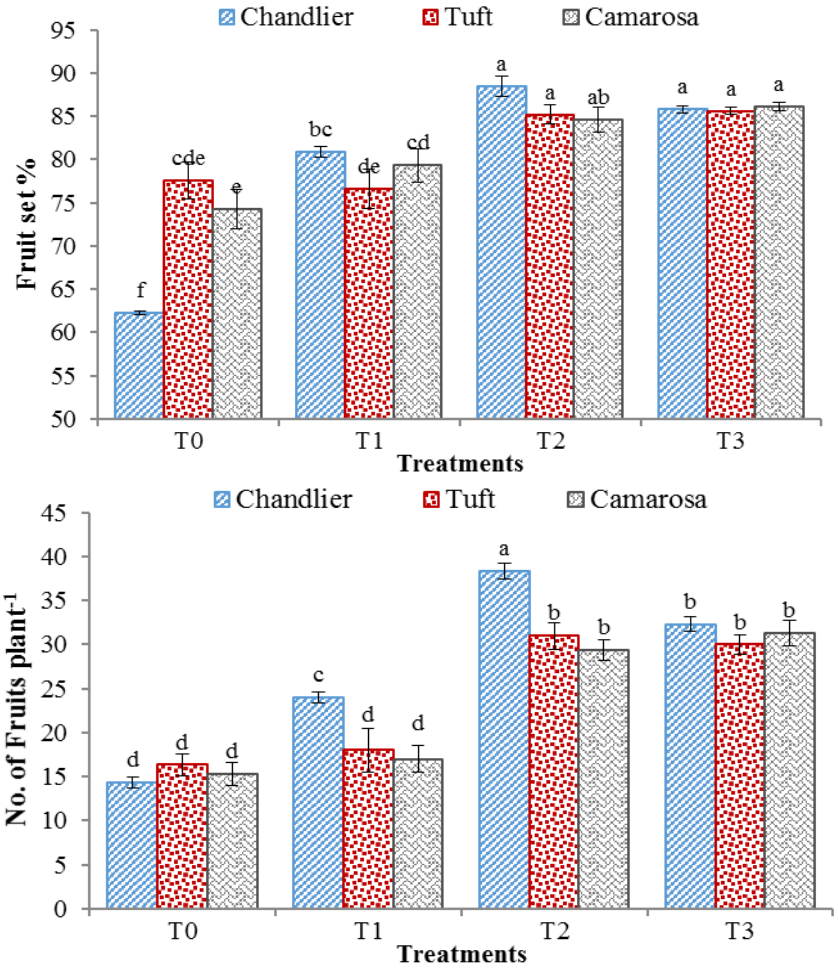

Figure 6. *Fruit set (%) and number of fruits plant^{-1} data of strawberry cvs. Chandler, Tufts and Camarosa treated with plant growth promoting bacteria (PGPB). Vertical bars indicate ± SE of means. n = 3 replicates*

Titrable acidity (%)

Plants supplied with *Pseudomonas fluorescens* (T_1) produced fruits with lowest titrable acidity as compared to other PGPB supplied plants. Among cultivars, 'Chandler' fruit had lowest titrable acidity (0.72 ± 0.06) as compared to 'Camarosa' (0.72 ± 0.07) and 'Tuft' (0.76 ± 0.0.04) (*Fig. 8*).

TA/TSS ratio

Minimum TA/TSS ratio (9.48 ± 0.24) was recorded in 'Camarosa' fruit followed by 'Chandler' (10.21 ± 0.56) and 'Tuft' (10.56 ± 0.45). Fruits of strawberry cultivars which were grown without any PGPB had lowest TA/TSS ratio (8.47 ± 0.27) followed by

http://www.aloki.hu ● ISSN 1589 1623 (Print) ● ISSN 1785 0037 (Online)
DOI: http://dx.doi.org/10.15666/aeer/2003_21872203

Pseudomonas aeruginosa (T_3) (10.06 ± 0.48) and *Bacillus subtilis* (T_2) (10.68 ± 0.48). Among cultivars, 'Chandler' fruit had highest TA/TSS ratio (12.22 ± 0.71) followed by 'Tuft' (9.93 ± 0.49) and 'Camarosa' (9.89 ± 0.50) when supplied with *Bacillus subtilis* (T_2) (*Fig. 8*).

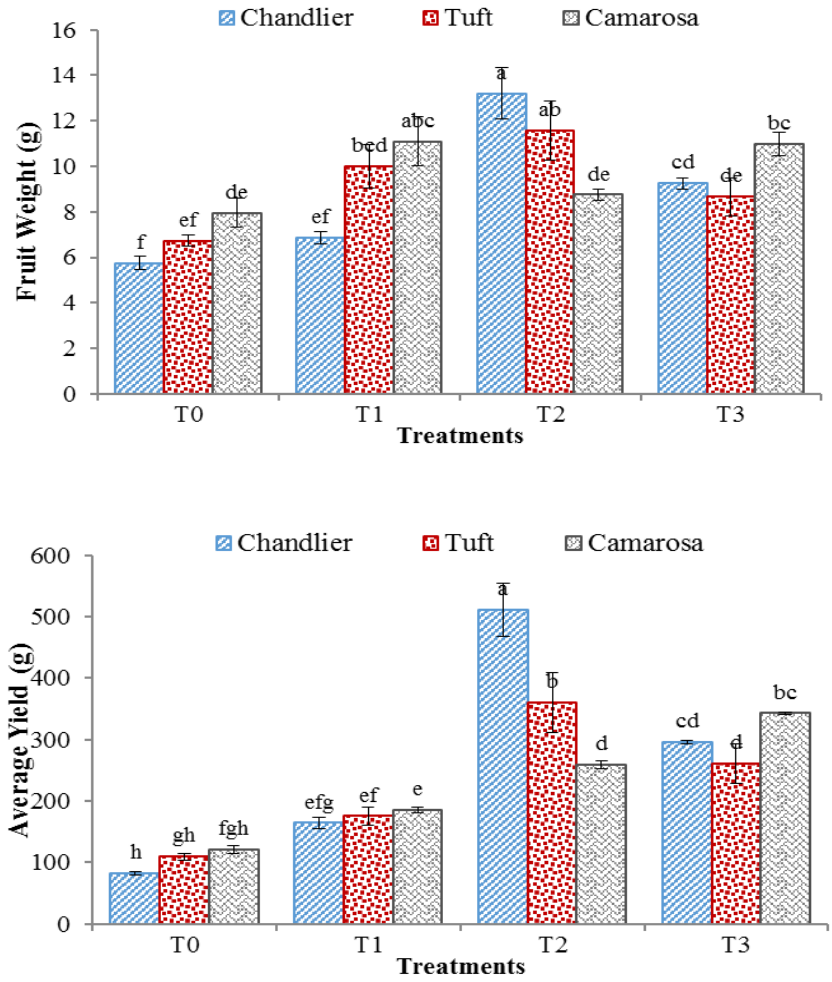

Figure 7. *Fruit weight (g) and average yield (g) data of strawberry cvs. Chandler, Tufts and Camarosa treated with plant growth promoting bacteria (PGPB). Vertical bars indicate ± SE of means. n = 3 replicates*

Ascorbic acid (mg 100 mL^{-1})

Plants grown with application of *Bacillus subtilis* (T_2) had highest ascorbic acid (57.41 ± 1.21) followed by *Pseudomonas fluorescens* (T_1) (53.32 ± 1.17) and *Pseudomonas aeruginosa* (T_3) (51.75 ± 0.62) (*Fig. 9*). Among cultivars, 'Chandler' fruit had lowest ascorbic acid (49.98 ± 1.30) compared to 'Tuft' (52.83 ± 0.64) and 'Camarosa' (56.82 ± 1.64). Ascorbic acid is known as one of the bioactive compounds also stated as non-enzymatic antioxidant which has imperative position in fruits (Hasan et al., 2021). Our results of higher ascorbic acid contents in strawberry fruits harvested from PGPB treated plants are also supported by finding of Consentino et al. (2022) in lettuce grown under application of PGPB with varying doses of nitrogen exhibited higher ascorbic acid content as compared to control.

http://www.aloki.hu ● ISSN 1589 1623 (Print) ● ISSN 1785 0037 (Online)
DOI: http://dx.doi.org/10.15666/aeer/2003_21872203

Total sugars (%)

Highest total sugars (5.72 ± 0.13) were recorded in 'Chandler' fruit followed by 'Camarosa' (5.57 ± 0.11) and 'Tuft' (5.54 ± 0.12) (*Fig. 9*). Among bacterial isolates, *Bacillus subtilis* (T_2) resulted in highest total sugars (5.93 ± 0.15) followed by *Pseudomonas aeruginosa* (T_3) (5.78 ± 0.11) and no PGPB (Control) (5.44 ± 0.11).

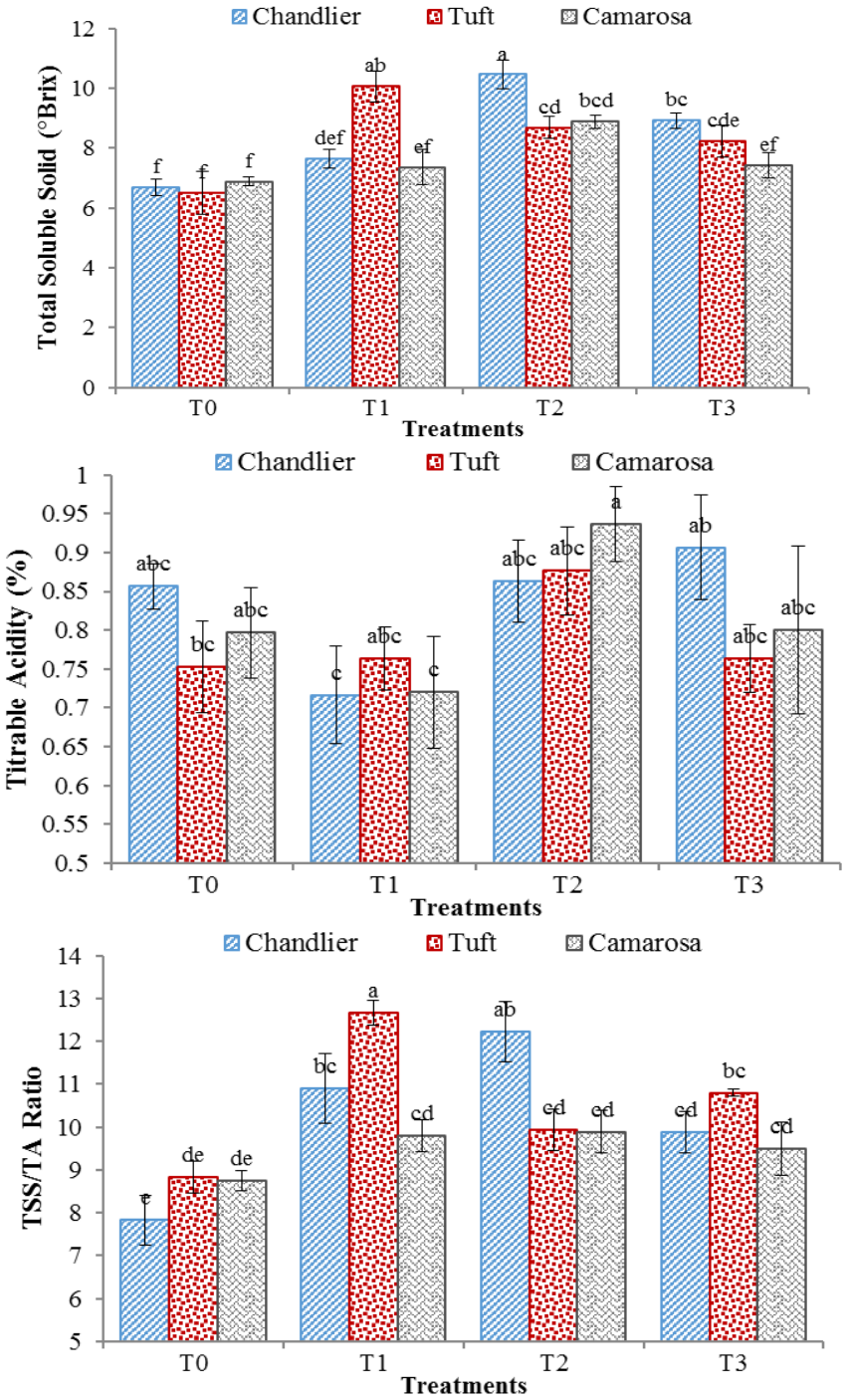

Figure 8. *Biochemical Analysis (TSS, TA, TSS/TA ratio) of fruits strawberry cvs. Chandler, Tufts and Camarosa treated with plant growth promoting bacteria (PGPB). Vertical bars indicate ± SE of means. n = 3 replicates*

http://www.aloki.hu ● ISSN 1589 1623 (Print) ● ISSN 1785 0037 (Online)
DOI: http://dx.doi.org/10.15666/aeer/2003_21872203

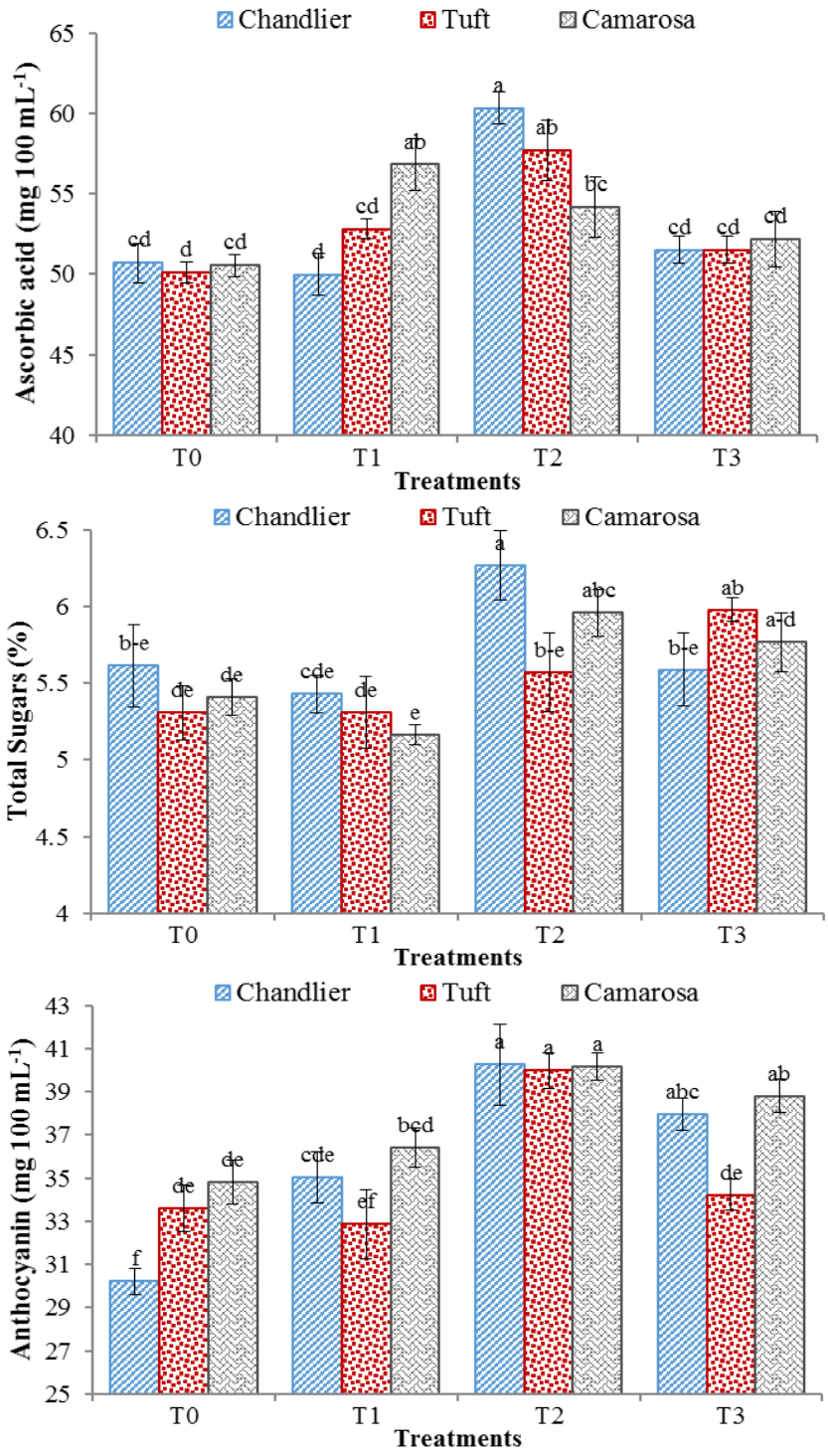

Figure 9. *Biochemical Analysis (ascorbic acid, total sugars, anthocyanin) of fruits strawberry cvs. Chandler, Tufts and Camarosa treated with plant growth promoting bacteria (PGPB). Vertical bars indicate ± SE of means. n = 3 replicates*

Anthocyanin contents (mg 100 mL^{-1})

Highest anthocyanin contents (37.55 ± 0.72) were recorded in 'Camarosa' fruit followed by 'Chandler' (35.88 ± 1.24) and 'Tuft' (35.16 ± 0.98). While, among

http://www.aloki.hu ● ISSN 1589 1623 (Print) ● ISSN 1785 0037 (Online)
DOI: http://dx.doi.org/10.15666/aeer/2003_21872203

bacterial isolates, plants supplied with *Bacillus subtilis* (T_2) had highest anthocyanin contents (40.14 ± 0.62) followed by (*Pseudomonas aeruginosa* (T_3) (37.00 ± 0.80) and *Pseudomonas fluorescens* (T_1) (34.77 ± 0.82) (*Fig. 9*). Minimum anthocyanin contents were recorded in plants with no PGPB application (control) (32.87 ± 0.83). Red colored berries contains more anthocyanin contents which might be affected in different production and postharvest conditions (Ali et al., 2016). PGPB treated strawberry cultivars enhanced anthocyanin contents in addition to the increased production, and has been found similar as earlier revealed by Lingua et al. (2013) who stated that arbuscular mycorrhizal (AM) fungi in combination with *Pseudomonas* strains displayed enhanced anthocyanin contents in strawberry fruits.

Conclusion

In summary, PGPB significantly improved growth and resulted in better performance of strawberry cultivars. Among tested PGPBs, *Bacillus subtilis* proved best for enhancing performance of strawberry, while among cultivars, 'Chandler' is best one having higher yield of quality fruit. Therefore, PGPBs may be used for commercial production of 'Chandler' strawberry for lowering its fertilizer requirements and improving yield and quality.

REFERENCES

[1] Ali, S., Khan, A. S., Malik, A. U., Shahid, M. (2016): Effect of controlled atmosphere storage on pericarp browning, bioactive compounds and antioxidant enzymes of litchi fruits. – Food Chemistry 206: 18-29.

[2] Ali, M. M., Anwar, R., Malik, A. U., Khan, A. S., Ahmad, S., Hussain, Z., Hasan, M. U., Nasir, M., Chen. F. (2021): Plant growth and fruit quality response of strawberry is improved after exogenous application of 24-Epibrassinolide. – Journal of Plant Growth Regulation. https://doi.org/10.1007/s00344-021-10422-2.

[3] Aslam, M., Rasool, S. (2012): Potential of strawberry's export from Pakistan. – Pakistan Journal of Food Science 22(4): 206-207.

[4] Ayub, M., Ullah. J., Muhammad, A., Zeb, A. (2010): Evaluation of strawberry juice preserved with chemical preservatives at refrigeration temperature. – International Journal of Nutrition and Metabolism Research 2(2): 027-032.

[5] Bashan, Y., Harrison, S. K., Whitmoyer, R. E. (1990): Enhanced growth of wheat and soybean plants inoculated with *Azospirillum brasilense* is not necessarily due to general enhancement of mineral uptake. – Applied and Environmental Microbiology 56(3): 769-775.

[6] Bhattacharyya, P. N., Jha, D. K. (2012): Plant growth-promoting rhizobacteria (PGPR): emergence in agriculture. – World Journal of Microbiology Biotechnology 28(4): 1327-1350.

[7] Biswas, J. C., Ladha, J. K., Dazzo, F. B. (2000): Rhizobia inoculation improves nutrient uptake and growth of lowland rice. – Soil Science Society of America Journal 64: 1644.

[8] Çakmakçı, R., Dönmez, F., Aydın, A., Fiahin, F. (2006): Growth promotion of plants by plant growth-promoting rhizobacteria under greenhouse and two different field soil conditions. – Soil Biology & Biochemistry 38: 1482-1487.

[9] Consentino, B. B., Aprile, S., Rouphael, Y., Ntatsi, G., De Pasquale, C., Iapichino, G., Alibrandi, P., Sabatino, L. (2022): Application of PGPB combined with variable N doses affects growth, yield-related traits, N-fertilizer efficiency and nutritional status of lettuce grown under controlled condition. – Agronomy 12(2): 236.

http://www.aloki.hu ● ISSN 1589 1623 (Print) ● ISSN 1785 0037 (Online)
DOI: http://dx.doi.org/10.15666/aeer/2003_21872203

[10] De Souza, R., Ambrosini, A., Passaglia, L. M. P. (2015): Plant growth-promoting bacteria as inoculants in agricultural soils. – Genetics and Molecular Biology 38: 401-419.
[11] Egamberdiyeva, D. (2005): Plant-growth-promoting rhizobacteria isolated from a Calcisol in a semi-arid region of Uzbekistan: biochemical characterization and effectiveness. – Journal of Plant Nutrition and Soil Science 168(1): 94-99.
[12] Esitken, A., Yildiz, H. E., Ercisli, S., Donmez, M. F., Turan, M., Gunes, A. (2010): Effects of plant growth promoting bacteria (PGPB) on yield, growth and nutrient contents of organically grown strawberry. – Scientia Horticulturae 124(1): 62-66.
[13] Galletta, G. J., Maas, J. L. (1990): Strawberry genetics. – HortScience 25(8): 871-879.
[14] Gholami, A., Shahsavani, S., and Nezarat, S. (2009): The effect of plant growth promoting rhizobacteria (PGPR) on germination, seedling growth and yield of maize. – World Academy of Science, Engineering and Technology 49: 19-24.
[15] Giusti, M. M., Wrolstad, R. E. (2001): Characterization and measurement of anthocyanins by UV-Visible spectroscopy. – Current Protocols in Food Analytical Chemistry 00(1): F1.2.1-F1.2.13.
[16] Glick, B. R. (1995): The enhancement of plant growth by free-living bacteria. – Canadian Journal of Microbiology 41(2): 109-117.
[17] Gupta, S., Kaushal, R. (2017): Plant growth promoting Rhizobacteria: bioresouce for enhanced productivity of Solanaceous vegetable crops. – Acta Scientific Agriculture 1(3): 10-15.
[18] Hanif, Z., Budiyati, E. (2011): Diversity technology strawberry cultivation in different regional production center. – Proceedings of Natural Resource Climate and Food Security in Developing Countries, pp. 614-624.
[19] Hasan, M. U., Riaz, R., Malik, A. U., Khan, A. S., Anwar, R., Rehman, R. N. U., Ali, S. (2021): Potential of *Aloe vera* gel coating for storage life extension and quality conservation of fruits and vegetables: an overview. – Journal of Food Biochemistry 45(4): e13640.
[20] Helaly, A. A. E., Ibrahim, F. R. (2019): Influence of iron, zinc and tyrosine acid on growth, yield components and chemical constituents of *Hibiscus sabdariffa* L. plant. – Chemia Analityczna 44: 21-30.
[21] Hortwitz, W. (1960): Official and Tentative Methods of Analysis. – Association of the Official Agriculture Chemist, Washington, DC.
[22] Kurokura, T., Hiraide, S., Shimamura, Y., Yamane, K. (2017): PGPR improves yield of strawberry species under less-fertilized conditions. – Environmental Control in Biology 55(3): 121-128.
[23] La-Torre-Ruiz, D., Ruiz-Valdiviezo, V. M., Rincón-Molina, C. I., Rodríguez-Mendiola, M., Arias-Castro, C., Gutiérrez-Miceli, F. A., Palomeque-Dominguez, H., Rincón-Rosales, R. (2016): Effect of plant growth-promoting bacteria on the growth and fructan production of *Agave americana* L. – Brazilian Journal of Microbiology 47: 587-596.
[24] Le, T., Pék, Z., Takács, S., Neményi, A., Helyes, L. (2018): The effect of plant growth-promoting rhizobacteria on yield, water use efficiency and brix degree of processing tomato. – Plant, Soil and Environment 64(11): 523-529.
[25] Lingua, G., Bona, E., Manassero, P., Marsano, F., Todeschini, V., Cantamessa, S., Copetta, A., D'Agostino, G., Gamalero, E., Berta, G. (2013): *Arbuscular mycorrhizal* fungi and plant growth-promoting *Pseudomonads* increases anthocyanin concentration in strawberry fruits (*Fragaria* x *ananassa* var. Selva) in conditions of reduced fertilization. – International Journal of Molecular Sciences 14(8): 16207-16225.
[26] Mekonnen, H., Kibret, M. (2021): The roles of plant growth promoting rhizobacteria in sustainable vegetable production in Ethiopia. – Chemical and Biological Technologies in Agriculture 8(1): 1-11.
[27] Patten, C. L., Glick, B. R. (2002): Role of *Pseudomonas putida* indole acetic acid in development of the host plant root system. – Applied and Environmental Microbiology 68: 3795-3801.

http://www.aloki.hu ● ISSN 1589 1623 (Print) ● ISSN 1785 0037 (Online)
DOI: http://dx.doi.org/10.15666/aeer/2003_21872203

[28] Pesakovic, M., Karaklajić-Stajić, Ž., Milenković, S., Olga, M. (2013): Bio-fertilizer affecting yield related characteristics of strawberry (*Fragaria×ananassa* Duch.) and soil micro-organisms. – Scientia Horticulture 150: 238-243.
[29] Pırlak, L., Köse, M. (2009): Effects of plant growth promoting rhizobacteria on yield and some fruit properties of strawberry. – Journal of Plant Nutrition 32(7): 1173-1184.
[30] Rahman, M., Islam, M. A. (2019): Concentrations and health risk assessment of trace elements in cereals, fruits, and vegetables of Bangladesh. – Biological Trace Element Research 191(1): 243-253.
[31] Ruck, J. A. (1969): Chemical methods for analysis of fruit and vegetable products. – SP 50, Summerland Research Station, Department of Agriculture, Canada.
[32] Ruiz, J. L., Sanjuan, S. M. D. C. (2022): The use of plant growth promoting bacteria for biofertigation; effects on concentrations of nutrients in inoculated aqueous vermicompost extract and on the yield and quality of tomatoes. – Biological Agriculture & Horticulture 1-17. https://doi.org/10.1080/01448765.2021.2010596.
[33] Saravanakumar, D., Ciavorella, A., Spadaro, D., Garibaldi, A., Gullino, M. L. (2008): *Metschnikowia pulcherrima* strain MACH1 outcompetes *Botrytis cinerea*, *Alternaria alternata* and *Penicillium expansum* in apples through iron depletion. – Postharvest Biology and Technology 49: 121-128.
[34] Seema, K., Mehta, K., Singh, N. (2018): Studies on the effect of plant growth promoting rhizobacteria (PGPR) on growth, physiological parameters, yield and fruit quality of strawberry cv. 'Chandler'. – Journal of Pharmacognosy and Phytochemistry 7(2): 383-387.
[35] Steel, R. G. D., Torrie, J. H., Dicky, D. A. (1997): Principles and Procedures of Statistics: A Biometrical Approach. – McGraw Hill Book Co., New York.
[36] Tilak, K. V. B. R., Reddy, B. S. (2006): *Bacillus cereus* and *B. Circulans*-novel inoculants for crops. – Current Science 90(5): 642-644.
[37] Zahir, Z. A., Arshad, M., Frankenberger, W. T. (2004): Plant growth promoting rhizobacteria: applications and perspectives in agriculture. – Advances in Agronomy 81(1): 98-169.

http://www.aloki.hu ● ISSN 1589 1623 (Print) ● ISSN 1785 0037 (Online)
DOI: http://dx.doi.org/10.15666/aeer/2003_21872203

GREEN SYNTHESIS OF SILVER AND COPPER NANOPARTICLES FROM LEAVES OF *EUCALYPTUS GLOBULUS* AND ASSESSMENT OF ITS ANTIBACTERIAL POTENTIAL TOWARDS *XANTHOMONAS CITRI* PV. *CITRI* CAUSING CITRUS CANKER

ATIQ, M.[1*] – MAZHAR, H. M. R.[1] – RAJPUT, N. A.[1] – AHMAD, U.[1*] – HAMEED, A.[2] – LODHI, A. M.[3] – USMAN, M.[1] – NAWAZ, A.[1] – AMMAR, M.[1] – KHALID, M.[1]

[1]*Department of Plant Pathology, University of Agriculture, Faisalabad, Pakistan*

[2]*Institute of Plant Protection, MNS-Agriculture University, Multan, Pakistan*

[3]*Department of Plant Protection, Faculty of Crop Protection, Sindh Agriculture University, Tandojam, Pakistan*

**Corresponding authors*
e-mail/phone: dratiqpp@gmail.com/+92-33-3439-6981 (M. Atiq);
usamasono@gmail.com (U. Ahmad)

(Received 7th Oct 2021; accepted 17th Mar 2022)

Abstract. Green synthesis of nanoparticles has ushered in a new research field known as green or phyto-nanotechnology. Plant based nanotechnology has emerged as an imperative tool for the management of plant diseases. In comparison to other conventional techniques, green synthesis of various nanoparticles was found to be non-toxic, low-cost, and profitable, resulting in more stable synthesized materials. Plant-extract based methods for synthesizing nanoparticles are far more efficient and cost-effective to manage plant diseases. For the management of citrus canker, silver and copper nanoparticles were evaluated under lab conditions. The highest inhibition zone was produced under silver + copper nanoparticles (21.06 mm) follow by silver (18.26 mm) and copper nanoparticles (15.27 mm) respectively. In field, maximum disease incidence was exhibited by copper nanoparticles (41.24%), and minimum disease incidence (35.23%) was observed when silver and copper nanoparticles were used in combination as compared to the control. Minimum disease severity (23.23%) was observed when of silver and copper nanoparticles were applied in combination followed by silver nanoparticles (28.31%) and copper nanoparticles (35.23%) as compared to control under field conditions. Complete Randomized Design (CRD) was used for the laboratory and greenhouse experiments while Randomized Complete Block Design (RCBD) was used for the field experiment.
Keywords: *nanotechnology, canker, AgNPs, Xanthomonas citri pv. citri*

Introduction

Citrus (*Citrus latifolia*) is an important fruit crop of the world. It is a member of the *Rutaceae* family. The extracted pulp and juices of citrus fruit are used for medicinal purposes, as well as for the preparation of various dishes (Alamgir, 2018). In 2020 its production worldwide was 194.4 million tons from an area of 13.9 million ha and in Pakistan citrus production was estimated as 2.29 million tons from an area of 206.6 thousand ha, the worldwide juice industry is utilized to achieve 2.2 million tons (FAOSTAT, 2020). The assessment of production losses has not been fully evaluated. The presence of canker lesions, however, makes the fruit unacceptable for the fresh market. Among all diseases, citrus canker (CC) is the main constraint to the productions of citrus crops in Pakistan as well as the repose of the world (Ware, 2015). Typical symptoms of citrus bacterial canker disease are necrotic lesions on twigs, leaf, stem,

http://www.aloki.hu ● ISSN 1589 1623 (Print) ● ISSN 1785 0037 (Online)
DOI: http://dx.doi.org/10.15666/aeer/2003_22052213

fruit, leaves and fruit become corky with a yellow halo and a watery border after a particular time interval tree decline and defoliation (Dewdney and Graham, 2016). In the years 2015-2016, the European Union rejected 144 consignments of Pakistani citrus due to *Xanthomonas citri* pv *citri* (*Xcc*) disease (Pervaiz, 2015). *Xcc* is an obligatory gram-negative rod-shaped bacterium with a single polar flagellum (1.5-2.0 x 0.5-0.75). For successful infection, it needs a temperature of 28-30 °C and its colony color is yellow due to the formation of "*xanthomonadin*" pigment (Afroz et al., 2013).

Different management strategies have been used to control citrus canker like, chemical, biological, cultural control and use of resistant varieties. To stop the disease from spreading pruning of infected trees, copper-based chemicals (Antibiotics and plant extracts) are strongly recommended to reduce the risk of disease (Ullah et al., 2019). The most economical, ecofriendly, and effective management of canker is the use of resistant source but under conducive environmental conditions, resistant varieties become susceptible, and disease appeared in epidemic form. Nanoparticles biosynthesis using different plant parts (i.e. leaves, stem, flower, roots) introduced developing research area referred as phyto-nanotechnology or green nanotechnology. Plant based nanotechnology opens up new door in agricultural field. In this miserable condition farmers have no option except the use of chemicals but due to their health hazard effects and environmental pollution issue, use of nanoparticles is the best option, as they are ecofriendly and have least effect on human health. That is why, in current study, (AgNPs) and (CuNPs) were evaluated against citrus canker (Dipankar and Murugan, 2012). Use of green synthesis of nanoparticles is the most appropriate ecofriendly and with least health hazard effect. Biosynthesis of Nanoparticles using different plant parts (i.e. leaves, stem, flower, roots) introduced developing research area referred as phyto-nanotechnology or green nanotechnology. Plant based nanotechnology opens up new door in agricultural field. Green synthesis of various nanoparticles using this technique found to be non-toxic, low-cost, and profitable which marks as more stable synthesized materials in comparison to other traditional techniques (Parveen et al*.,* 2016). Among other methods the most frequently used approach is the green synthesis of NPs using plant extract. These have some distinctive advantages like less biohazardous, being easily assessable and serve as a source of active constituents (Baker et al., 2013). Copper nanoparticles (CuNPs) can be biologically synthesized using a variety of plant extracts. Copper has great potential in a wide variety of catalytic, biological, and sensor applications and is more commonly used in the form of nanoparticles, leading to the development of different techniques for the formulation of copper nanoparticles. Copper nanoparticles (CuNPs) are important because of their high conductivity, as compared to other metallic nanoparticles such as silver nanoparticles (Kasana et al*.,* 2017). Silver (AgNPs) and copper nanoparticles (CuNPs) are the comprehensively researched nanomaterial, that fascinate scientists because of their broad-spectrum antimicrobial efficacy (Nedelcu et al., 2014). So in current study silver and copper nanoparticles were developed from eucalyptus leaves and were evaluated against *Xcc* causing citrus canker.

Evaluation of nanoparticles in lab for the management of citrus canker

Preparation of nanoparticles

Eucalyptus leaves were collected from the Botanical Garden of UAF. Then, these leaves were washed with distilled water and dried for 10-14 days under shade and then oven dry at 65 °C for 4 hours and then grind to get a fine powder of the leaves. Then

http://www.aloki.hu ● ISSN 1589 1623 (Print) ● ISSN 1785 0037 (Online)
DOI: http://dx.doi.org/10.15666/aeer/2003_22052213

20 g of eucalyptus powder was mixed with 100 mL of methanol in a beaker that was covered with aluminum foil. For 24 h, solution was kept in a dark room. After that, the solution was stirred for 15 min. at the temperature of 70 °C. Then whatman's filter paper no.41 was used to filter the solution. The extraction was mixed with 0.5 M silver nitrate (17g) and 15.0 g of copper sulfate in a beaker separately. Then the solution was stirred for 5-10 min with the help of a magnetic stirrer. After stirring, kept the beakers in an ultrasonic cleaner (YJ 5120-1) for heating for 60 min and then kept the samples in the furnace oven (Memmert oven 100-800). After 60 min. samples were grinded with the help of pestle and mortar and save them in test tubes for further use and then 0.25, 0.5 and 0.75% concentrations were prepared by adding 0.25 g, 0.55 g and 0.75 g silver and copper nanoparticles in 100 mL bottle separately (*Fig. 1*).

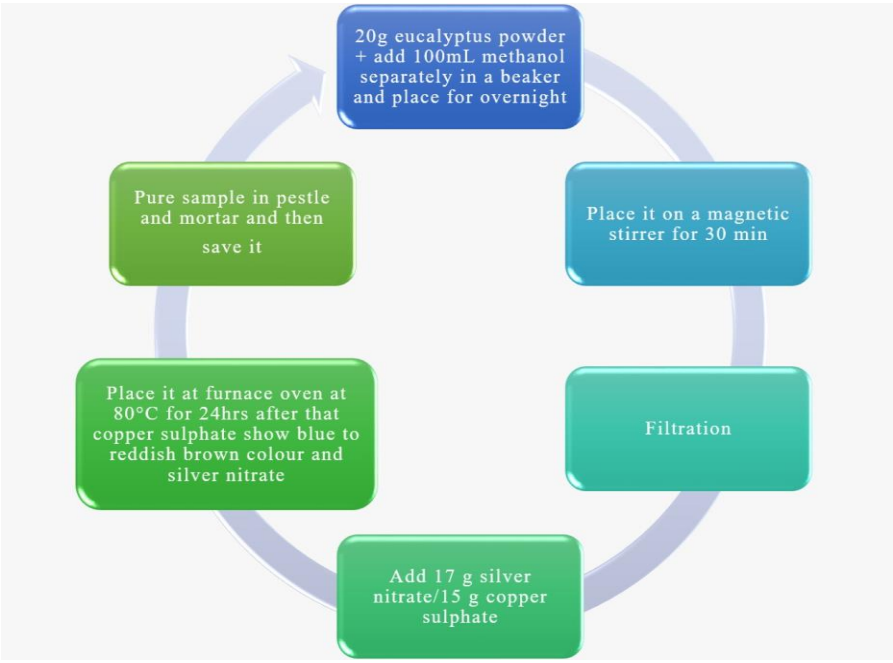

Figure 1. *Summary for preparation of nanoparticles*

Evaluation of (AgNPs) and (CuNPs) nanoparticles in lab condition

Nutrient agar (NA) media was prepared in the molecular Phyto-bacteriology laboratory, Department of plant pathology, University of Agriculture, Faisalabad (UAF). 1 Cm circular pieces of filter paper were cut and autoclaved at 121 °C for 15 Psi for 15 min and placed in NA containing Petri plates. A sterilized cotton swab was used to disperse bacterial culture in the Petri plate (9 cm) in a laminar airflow chamber (RTVL-1312, Robus United Kingdom). Then pieces of sterilized filter paper were dipped into different concentrations of filtered Nanoparticles (0.25, 0.5 and 0.75%) and placed them in the center of the NA plates with *Xcc* culture. These plates were wrapped and incubated at 28 ± 2 °C. The trial was designed by using Completely Randomized Design (CRD) with three replications per treatment. The control plates were treated with distilled water and inhibition zones were measured with the help of a digital Vernier caliper (500-196, Mitutoyo) after 24, 48 and 72 h. Fisher's Least Significant Difference Test (LSD) at 5% probability was used to examine data from inhibition zones (Steel et al., 1997).

http://www.aloki.hu ● ISSN 1589 1623 (Print) ● ISSN 1785 0037 (Online)
DOI: http://dx.doi.org/10.15666/aeer/2003_22052213

Evaluation of silver and copper nanoparticles in the field for the management of citrus canker

One year old Grapefruit plants were obtained from a nursery, Institute of Horticultural Sciences (IHS), University of Agriculture Faisalabad (UAF) and transplanted in the Research Area, Department of Plant Pathology, University of Agriculture, Faisalabad, using P×P = 1.0 m and R×R = 1.5 m distance in a field trial. These plants were treated with distilled water before being put in the field. Aqueous suspension of the bacteria was prepared from 48-h-old actively growing culture and bacterial concentration was measured with the help of a spectrophotometer @ 1×10^8 CFU/mL (Hitachi U-2001, model 121003UV/Vis). The bacterial suspension was inoculated early in the morning in the plants with the help of a syringe method. Bacterial suspension was injected into the midrib of the leaf as well as veins of the lower surface of the plant leaves. After three days Ag and Cu nanoparticles were assessed under field conditions @ 0.25, 0.5 and 0.75% concentrations while in control treatment only distilled water was sprayed on citrus plants under Randomized Completely Randomized design (RCRD) by maintaining three replications of each treatment. Data regarding canker was recorded after 7, 14 and 21 days intervals.

Analysis of data

Complete Randomized Design (CRD) was used for laboratory and Randomized Complete Block Design (RCBD) was used for field experiment. Least significant difference (LSD) was used with the probability level of 0.05% to observe the difference in treatments impact against *Xcc*.

Results

Maximum inhibition zone was produced by (silver + copper) nanoparticles (21.06) follow by silver (18.26) and copper nanoparticles (15.27) mm respectively as compared to control (*Fig. 2*). Interaction between treatments and concentrations (T×C) showed that maximum inhibition zone (21.50) mm was produced by silver + copper nanoparticles @ 0.75% (21.31 mm) , 0.5% and (20.37) 0.25% respectively while copper nanoparticles exhibited minimum inhibition zones (14.22, 15.13, 16.45) mm @ 0.25, 0.5 and 0.75% concentrations respectively as compared to the control. Treatments and duration of time expressed that copper exhibited minimum inhibition zones (14.07, 15.24, and 16.48) mm followed by silver nanoparticles (17.96, 18.65, and 18.17) mm and silver + copper nanoparticles (20.21, 21.08, and 21.88) respectively (*Fig. 3*). Maximum disease incidence was expressed by copper nanoparticles (41.24) %, and minimum disease incidence (35.23) was observed when silver nanoparticles + copper nanoparticles were applied in combination as compared to control (*Fig. 4*). Treatments and concentration interaction (T×C) of copper nanoparticles showed maximum disease severity 45.450, 42.478 and 35.811% while minimum disease severity was showed by the combination of both silver nanoparticles + copper nanoparticles (42.67, 34.15 and 28.86%) @ 3, 5 and 7% concentrations respectively as compared to control (*Fig. 5*). Treatments and days interaction (T×D) exhibited that copper nanoparticles expressed 42.75, 42.00 and 38.97% disease severity while silver nanoparticles showed (35.46, 35.21 and 35.01) % and silver nanoparticles + copper nanoparticles exhibited (23.25, 22.21 and 21.45) % disease severity when applied @ 3, 5 and 7% after 7, 14 and 21 days respectively as compared to the control (*Fig. 5*).

http://www.aloki.hu ● ISSN 1589 1623 (Print) ● ISSN 1785 0037 (Online)
DOI: http://dx.doi.org/10.15666/aeer/2003_22052213

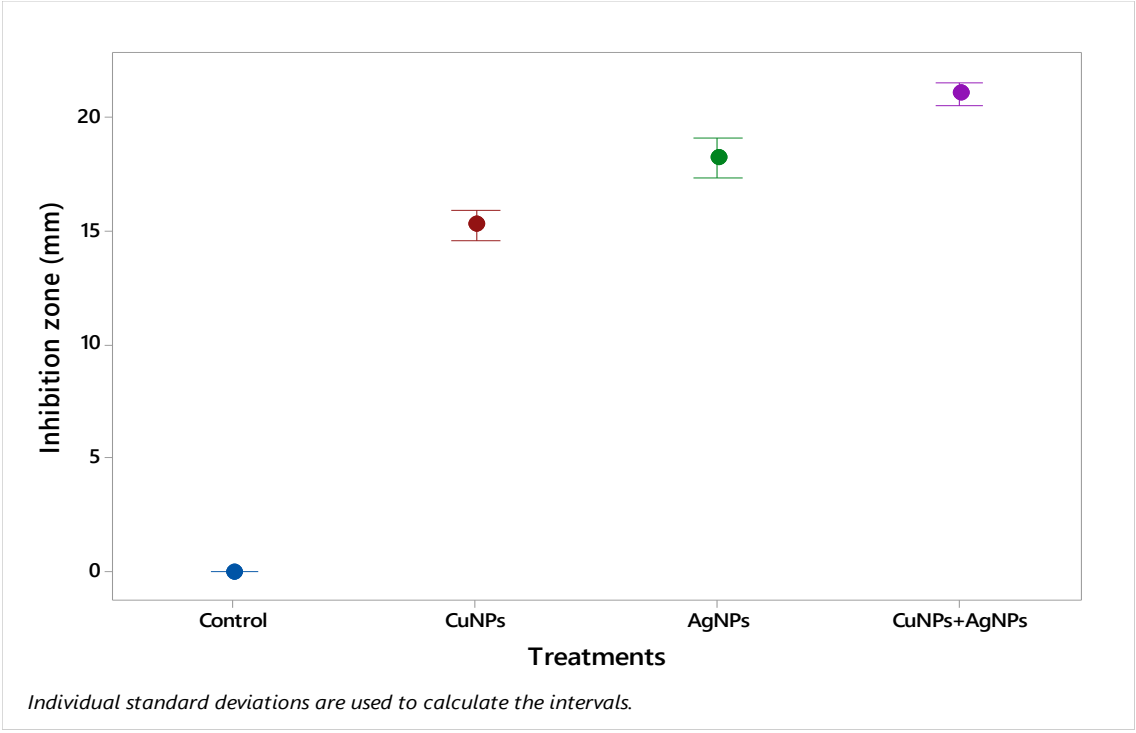

Figure 2. *Evaluation of silver and copper nanoparticles alone and in combination under lab. conditions*

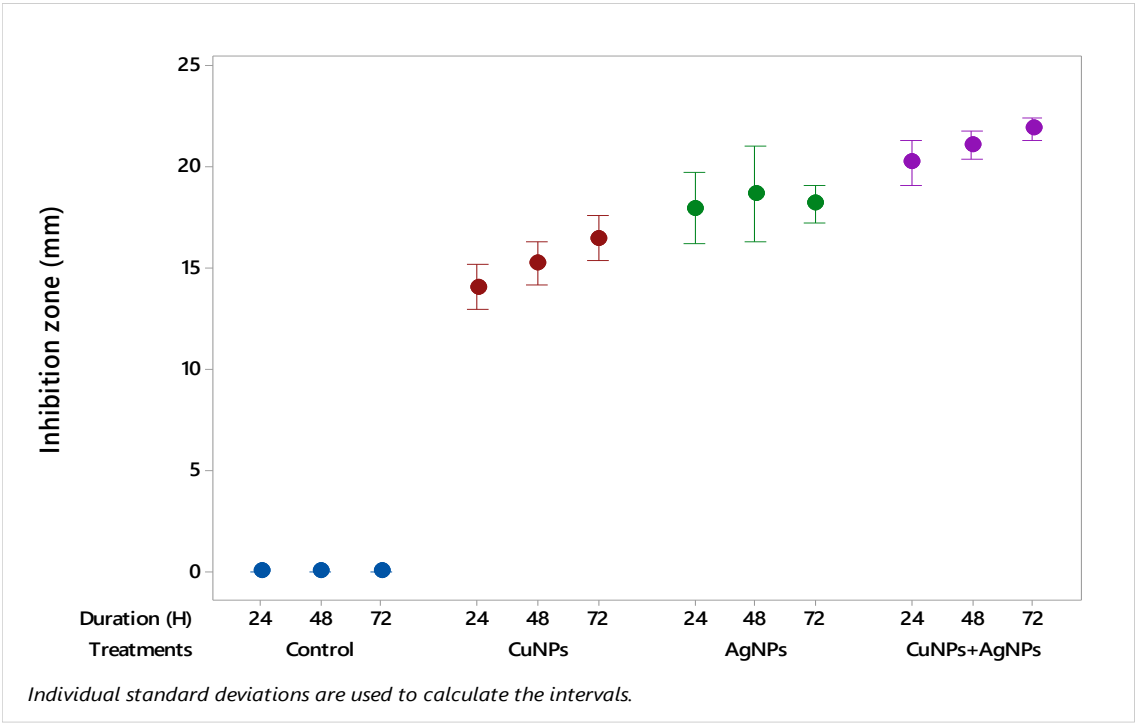

Figure 3. *Impact of interaction b/w treatments and duration of time on growth of Xanthomonas citri pv. citri under lab. conditions*

http://www.aloki.hu ● ISSN 1589 1623 (Print) ● ISSN 1785 0037 (Online)
DOI: http://dx.doi.org/10.15666/aeer/2003_22052213

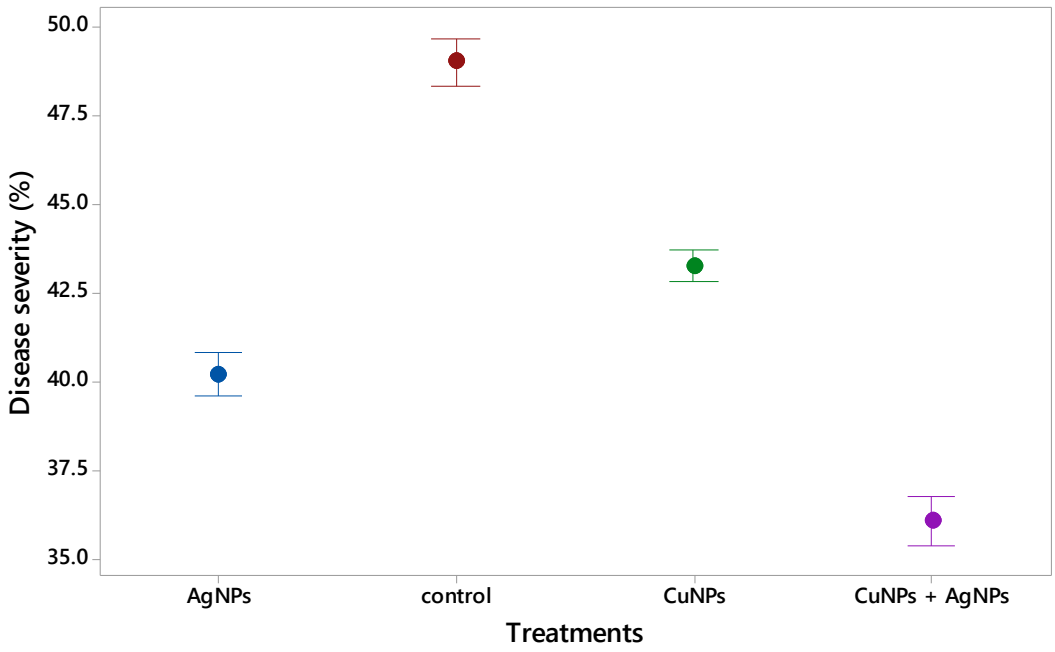

Figure 4. *Evaluation of silver and copper nanoparticles alone and in combination under field conditions*

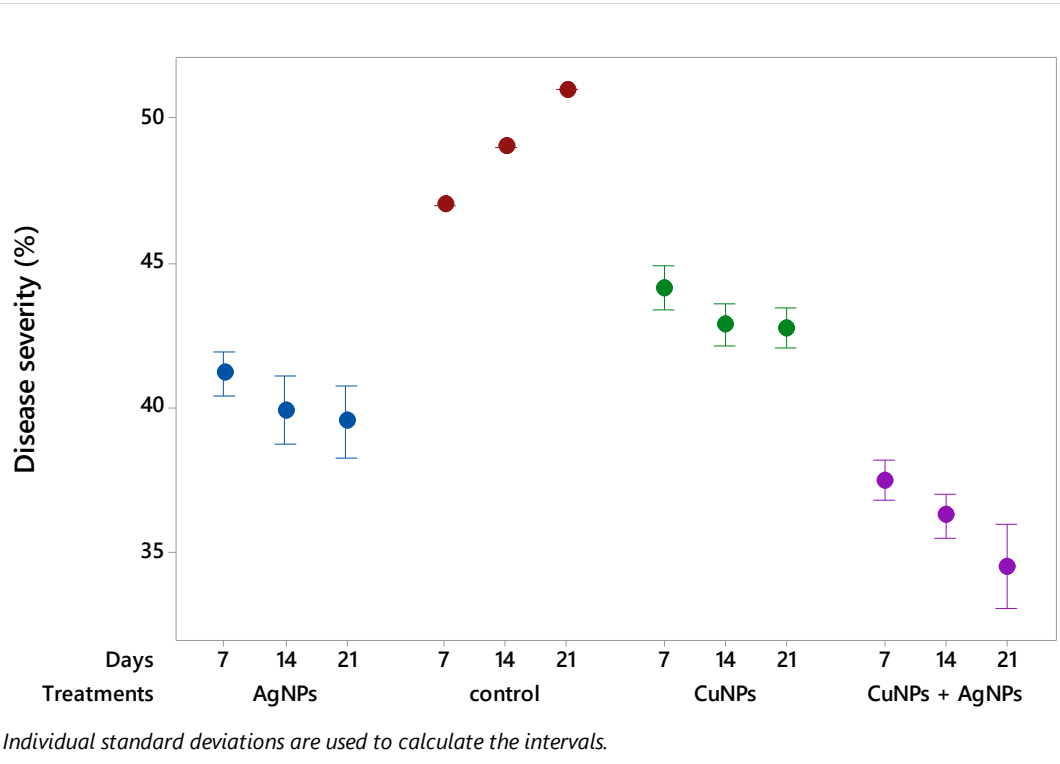

Figure 5. *Impact of interaction b/w treatments and days on the development of citrus canker under field conditions*

http://www.aloki.hu ● ISSN 1589 1623 (Print) ● ISSN 1785 0037 (Online)
DOI: http://dx.doi.org/10.15666/aeer/2003_22052213

Discussion

Among various control measures, scientist and researchers are striving for environment friendly management of plant diseases. Currently, green nanotechnology draws the attention of scientists to work on nanoparticles for the management of plant diseases. These nanoparticles are of various types including silver, gold, zinc, copper nanoparticles etc. Green nanotechnology offers nano-tools for biosystems transformation to nanomaterial synthesis through green approaches, by inhibiting any chemicals toxicity (Nasrollahzadeh et al., 2019). Green synthesis is well defined as use of environment friendly tools for plant and other microorganism for the biosynthesis of nanoparticles. These efficient green methodologies are free of imperfections related with conventional artificial approaches because nanoparticles are environment friendly. Bio-formulation of plant derived aqueous extracts introduced various benefits which include fast synthesis and more essentially, devoid of expensive processing for nanoparticles formulation (Das et al., 2014). Green synthesis of nanoparticles using plant extracts, provides a broad-scale formation of effective nanoparticles. Phyto-nanotechnology provides targeted distribution to specific sites in a controlled manner, minimizing the use of various plant-protection chemicals, reducing nutrient losses by the use of nano-fertilizers and increasing yield by using proper nutrients (Das et al., 2014). In the contemporary study, eucalyptus based (silver and copper) nanoparticles were evaluated in the lab conditions towards *Xcc* causing citrus canker. Among nanoparticles, silver nanoparticles showed maximum inhibition zone while under greenhouse and field conditions, combination of Ag + CuNPs expressed minimum disease severity. Results of the current study are supported by the finding of Wang et al. (2017), who studied and described that antibacterial efficacy of AgNPs of *Eucalyptus globulus* has inhibitory effect against citrus canker. AgNPs of *E. globulus* plant has great antibacterial properties against citrus canker. Outcomes of the present study were also supported by Vadlapudi and Amanchy (2017) who evaluated silver nanoparticles derived from *Myriostacha wightiana* leaf extract which showed antibacterial activity against *R. solanacearum* On weekly basis, the disease incidence of citrus canker was measured in response to various concentrations of green synthesis of CuNPs and AgNPs at 0.25%, 0.5% and 0.75%. In comparison to other nanoparticles, AgNPs @ 0.75% showed less disease incidence against canker after one week. In an attempt to determine the effect of green synthesized AgNPs in Kinnow, similar results were obtained by Hussain et al. (2018). Same results were also reported by Agnihotri et al. (2014) who tested AgNPs against *Staphylococcus aureus, Vibrio cholera and Pseudomonas aeruginosa* and found effective . Similarly AgNPs were used against citrus canker and observed reduction in disease incidence under green house and field conditions. Because of easy availability and non-toxic nature of plants as well as the stability and antibacterial potential of biosynthesized nanoparticles, green synthesis method of nanoparticle is very simple, speedy, cost-effective and ecofriendly**.** In the field of agriculture, Ag nanoparticles are cost-effective and effective antibacterial agent for large-scale production for the management of plant diseases.

Conclusion

In lab experiments, combination of silver and copper nanoparticles showed best results in reducing microbial growth followed by silver nanoparticles and copper nanoparticles. While in field experiments, maximum disease incidence was expressed by copper nanoparticles while minimum disease incidence was observed when silver

http://www.aloki.hu ● ISSN 1589 1623 (Print) ● ISSN 1785 0037 (Online)
DOI: http://dx.doi.org/10.15666/aeer/2003_22052213

and copper nanoparticles were used in combination. It was concluded that the combination of silver and copper nanoparticles can be used in future for the management of citrus canker.

Acknowledgements. We are highly thankful to scientists of Molecular Citrus Pathology laboratory, Department of Plant Pathology, University of Agriculture, Faisalabad for providing research facilities under project NRPU-HEC# 6373.

REFERENCES

[1] Afroz, A., Zahur, M., Zeeshan, N., Komatsu, N. (2013): Plant-bacterium interactions analyzed by proteomics. – Frontiers in Plant Science 4: 1-18.
[2] Agnihotri, S., Mukherji, S., Mukherji, S. (2014): Size-controlled silver nanoparticles synthesized over the range 5–100 nm using the same protocol and their antibacterial efficacy. – Rsc Advances 4(8): 3974-3983.
[3] Alamgir, A. N. M. (2018): Therapeutic Use of Medicinal Plants and Their Extracts. – Springer International, New York.
[4] Baker, S., Rakshith, D., Kavitha, K. S., Santosh, P., Kavitha, H. U., Rao, Y., Satish, S. (2013): Plants: emerging as nano factories towards facile route in synthesis of nanoparticles. – BioImpacts: BI. 3: 111.
[5] Das, V. L., Thomas, R., Varghese, R. T., Soniya, E. V., Mathew, J., Radhakrishnan, E. K. (2014): Extracellular synthesis of silver nanoparticles by the Bacillus strain CS 11 isolated from industrialized area. – Biotechnology 4: 121-126.
[6] Dewdney, M. M., Graham, J. H., Rogers, M. E. (2016): Citrus canker. – Florida Citrus Pest Management Guide. SP-43: 93-96.
[7] Dipankar, C., Murugan, S. (2012): The green synthesis, characterization and evaluation of the biological activities of silver nanoparticles synthesized from *Iresine herbstii* leaf aqueous extracts. – Colloids and Surfaces B: Biointerfaces 98: 112-119.
[8] FAOSTAT 2020. Food and Agriculture Organization Statistical Database. – FAO, Rome.
[9] Hussain, M., Raja, N. I., Mashwani, Z. R. (2018): Green synthesis and characterization of silver nanoparticles and their effects on antimicrobial efficacy and biochemical profiling in *Citrus reticulate*. – IET Nanobiotechnology 12: 514-519.
[10] Kasana, R. C., Panwar, N. R., Kaul, R. K., Kumar, P. (2017): Biosynthesis and effects of copper nanoparticles on plants. – Environ. Chemistry Letters 15: 233-240.
[11] Nasrollahzadeh, M., Sajjadi, M., Sajadi, S. M., Issaabadi, Z. (2019): Green nanotechnology. – Interface Science and Technology 28: 145-198.
[12] Nedelcu, I. A., Ficai, A., Sonmez, M., Ficai, D., Oprea, O., Andronescu, E. (2014): Silver based materials for biomedical applications. – Current Organic Chemistry 18: 173-184.
[13] Parveen, K., Banse, V., Ledwani, L. (2016): Green synthesis of nanoparticles: their advantages and disadvantages. – AIP Conference Proceedings 1724(1): 20-48.
[14] Pervaiz, S. (2015): Fruit, vegetable fail to enter European Union. A report. – http://the dailystar.net/business.
[15] Steel, R. G. D., Torrie, J. H. (1997): Principles and Procedures of Statistics: A Biometrical Approach. – McGraw-Hill Co. Inc, New York.
[16] Ullah, M. I., Riaz, M., Arshad, M., Khan, A. H., Afzal, M., Khalid, S., Riaz, M. (2019): Application of organic fertilizers affect the citrus leafminer, *Phyllocnistis citrella* Lepidoptera: Gracillariidae infestation and citrus canker disease in nursery plantations. – International Journal of Insect Science 11: 1179543319858634.
[17] Vadlapudi, V., Amanchy, R. (2017): Synthesis, characterization, and antibacterial activity of Silver Nanoparticles from Red Algae, *Hypnea musciformis.* – Advances in Biological Research 11(5): 242-249.

http://www.aloki.hu ● ISSN 1589 1623 (Print) ● ISSN 1785 0037 (Online)
DOI: http://dx.doi.org/10.15666/aeer/2003_22052213

[18] Wang, C., Zhao, M., Li, J., Yu, J., Sun, S., Ge, S., Guo, Z. (2017): Silver nanoparticles/graphene oxide decorated carbon fiber synergistic reinforcement in epoxy-based composites. – Polymer 131: 263-271.
[19] Ware, M. (2015): Oranges: health benefits, nutritional information. – https://www.medicalnewstoday.com/articles/272782.

http://www.aloki.hu ● ISSN 1589 1623 (Print) ● ISSN 1785 0037 (Online)
DOI: http://dx.doi.org/10.15666/aeer/2003_22052213

AMINO ACID CONTENTS OF SOME LEGUME PLANTS GROWING IN WADI SUDR, SOUTH-WEST SINAI, EGYPT

EL-ABSY, K. M.

Eco-physiology Unit, Plant Ecology and Ranges Department, Desert Research Center
P.O. Box 11753, Cairo, Egypt
(e-mail: karima.mohamed77@yahoo.com; phone: +966-55-239-4864)

(Received 13th Oct 2021; accepted 25th Feb 2022)

Abstract. The identification of soil properties and phytochemical compounds including the amino acid profile is at the base of this study, which investigates the adaptive behavior of three legumes plants *Acacia tortilis* (Forssk.), *Alhagi graecorum* Boiss. and *Retama raetam* (Forsk.) collected from Wadi Sudr, South-West Sinai, Egypt. The ANOVA displayed that most mechanical and chemical properties of the soil associated with the three plant species were significantly affected by plants and depths and their interaction ($p<0.01$). Also, water content was significantly affected by plants, seasons, depths and their interaction ($p<0.01$). As for plant analysis, the plants, seasons and their interaction was significant ($p<0.05$ or $p<0.01$) for most amino acid profiles, photosynthetic pigment contents and chemical compositions of three legumes species in Wadi Sudr region. The amount of most chemical properties was higher in the soil associated with *R. raetam* compared to the soil of the other plants. Most amino acids, photosynthetic pigments, Na^+, K^+ and SO_4^{2-} concentrations of the three studied plants in the dry season were higher than in the wet season. According to PCA, the PCA1 and PCA2 extracted had eigenvalue >1 and mainly distinguished the soil and plant variables in different groups across the three studied plants. According to biplot and based on the plants studied, PCA1 and PCA2 with the highest variability showed positive or negative correlation to soil and plant variables, but, they differed in their degree of significance/insignificance and consistency in quantity. The PCA revealed high positive correlations among some soil variables as well as among some amino acid profile and other plant variables under the plants studied. Some soil variables were positively correlated with some amino acids such as leucine, phenylalanine, valine, lysine, aspartic, arginine, serine and isoleucine as well as some photosynthetic pigments and other plant chemical concentrations.
Keywords: *amino acids, chemical composition, legume plants, PCA*

Introduction

The Sinai Peninsula occupies a portion of the foreland shelf of the Arabo-Nubian massif that dips gradually northward toward the Mediterranean Sea (Said, 1962). South Sinai is characterized by arid climatological conditions and a diversity of plant species. Wadi Sudr region is located in the southern section of the western coast of Sinai, which represents one of the largest and most developed wadis (Morsy et al., 2015; Mohamed et al., 2018). Wadi Sudr is characterized by diverse communities and species as well as the wide areas covered by well-developed plant communities, due to the abundance of extensive water resources, the channel broadness, the fragile nature of the sediments, the variation in the thickness of the surface sediments and the presence of local stone silos (Girgis and Ahmed, 1985; Morsy et al., 2015). Wadi Sudr is exposed to several environmental variables, which have impacted the ecosystem particularly the vegetation (Mohamed et al., 2018).

Climate change is the central issue of our time, with it is posing a major and increasing threat to global food security and affecting every country on every habitable continent (El-Hashash and El-Absy, 2019). Given the physical parameters (temperature, rainfall patterns, carbon dioxide fertilization) and changes in agro-ecosystems as well as the adaptive responses of human systems it is extremely difficult to predict the exact future

http://www.aloki.hu ● ISSN 1589 1623 (Print) ● ISSN1785 0037 (Online)
DOI: http://dx.doi.org/10.15666/aeer/2003_22152233

effects of climate change on plant productivity (FAO, 2016). Salinity, drought and environmental stresses are major constraints to plant growth worldwide, especially Egypt. Stress conditions induce the accumulation of numerous reactive oxygen species and osmolytes such as proline, soluble proteins, soluble sugars, and betaine, that will play a critical role during stress acclimation in plants (Pradhan et al., 2020; Salama et al., 2021).

The Legumes family (also called Leguminosae or Fabaceae) constitutes the third-largest family of flowering plants in the world after Asteraceae and Orchidaceae families (Pua and Davey, 2007). Legumes plants comprise of more than 19,000 different described species (Bennetau-Pelissero, 2019). Some legume species are annual herbs, some are vines, and some are bushes and trees distributed around the world in many different environments. In this study, three species of the legumes family (*Acacia tortilis* Forssk, *Alhagi graecorum* Bioss and *Retama raetam* Forssk) growing in Wadi Sudr region, Southwest Sinai, Egypt were chosen.

Acacia tortilis (Forssk.) Hayne ssp. raddiana (*A. tortilis*) plants are distinguished for growing in the desert due to their ability to tolerate the drought, salinity and alkalinity, drifting sand, grazing and repeated cutting as well as climatic changes in temperature (Derbel et al., 2007; Malakootian et al., 2018). It is native to arid and semi-arid areas of Africa and the Middle-East (Orwa et al., 2009). It is grown in the Sinai region, Egypt and *A. tortilis* seeds are used for animal fodder (Embaby and Rayan, 2016). It has also been used commercially and medicinally as it is considered beneficial for treating many different diseases such as skin allergy, cough and inflammatory reaction (Yadav et al., 2013). *A. tortilis* eventually has proved to be the most promising species for desert rehabilitation and greening (Gill and Al-Shankiti, 2015).

Alhagi graecorum Boiss. (*A. graecorum*) is grown naturally in xeric, halic and mesic habitats (Hassanein and Mazen, 2001) as well as found in deep moist, dry, rocky, or saline soils, and occasionally in cultivated fields (Boulos, 2009). It is native to North Africa, the Middle East, southeastern Europe and Russia (Awmack and Lock, 2002). It is widely distributed in Egypt and seems to have wide ecological amplitude, it has been recorded in various bioclimatic regions like Nile region, oasis, Mediterranean region, Eastern and Western Deserts, Red Sea coast and Sinai (Boulos, 2009). It is palatable and grazed by camels and camels in the deserts (Boulos, 2009), also the dried plants are used to treat bilharziasis, rheumatic pains, constipation, and worms (Boulos and El-Hadidi, 1984).

Retama raetam (Forsk.) Webb & Berthel (*R. raetam*) is usually found in the Egyptian Sinai Peninsula, Tunisia, Libya, Saudi Arabia and Northeastern Mediterranean region (Nasser et al., 2013). *R. raetam* used as a major source of fodder for livestock species such as sheep, goats and camels as well as in traditional medicine for the treatment of hypertension, diabetes, rheumatism, fever, inflammation, eczema, and microbial infections (Al-Onazi et al., 2021).

The growth of legumes plants and nitrogen fixation are affected by chemical compounds in the soil. Soil pH also affects the physical, chemical and biological properties of the soil as well as plant growth (Al-Mujahidy et al., 2013). Chemical properties in soil have been correlated with legumes plants, therefore, the details of soil property can be easily interpreted and allow rapid improvement of chemical properties in the soil during nitrogen fixation and root biomass (Yuvaraj et al., 2020).

In order for a plant to complete its life cycle, a plant needs relatively large amounts (>0.1% of dry mass) of essential macronutrients such as Ca^{2+}, Mg^{2+}, N, P, K^{+} and S (Maathuis et al., 2009). Pyankov et al. (2001) stated that the concentrations of main chemical components as nitrogen, organic acids, and mineral substances recorded lower

http://www.aloki.hu ● ISSN 1589 1623 (Print) ● ISSN1785 0037 (Online)
DOI: http://dx.doi.org/10.15666/aeer/2003_22152233

values in stress-tolerant and higher values in ruderal species. Kamel and El-Absy (2020) explained that most of the chemical compounds in the plant were significantly affected by seasonal changes and different locations. This may reflect seasonal changes in physiological needs and effort, rather than availability in plant content (Estevez et al., 2010).

Proteins are a large set of organic molecules that are essential to the structure and functioning of cells in all living things (Aremu et al., 2017). Amino acids are the building blocks of proteins and are categorized into essential and non-essential amino acids based on their building in humans. Essential amino acids are synthesized only by plant species, whilst non-essential amino acids are synthesized by both plant species and people (Kumar et al., 2019). Plants are a rich source of amino acids, and glutamic and aspartic acids are the most abundant amino acids in plants (Kumar et al., 2017).

It was found that the interrelationships between different plant communities and environmental factors are very complex, which reflects simultaneous changes in factors like depth of groundwater, soil moisture and stability as well as salinity content (Zhang et al., 2005). The principal component analysis (PCA) method was extensively used to study the relationship between soil properties and vegetation have been conducted by several researchers for example Juhos et al. (2015); Ferraz et al. (2019) and Metwally et al. (2019). Also, the PCA has also been used to identify the differences between amino acids in different plant species (Zhu et al., 2017; Kaur et al., 2018; Kumar et al., 2019).

The aim of the current work is to study the adaptive behavior of some wild plants of the legumes family collected from Wadi Sudr through 1) determining and analysing the content of soil properties and phytochemical compounds including the amino acid profile 2) assessing the correlation between the environmental factors and plant properties using principal component analysis under dry and wet seasons.

Materials and methods

Study site

This study was carried out at Wadi Sudr in Ras Sudr, South Sinai, Egypt between August 2019 (dry) and January 2020 (wet). It was located at latitudes: 29°36′54″-29°51′54″ N, longitudes: 32°41′30″-33°09′ 07″ E (*Fig. 1*). From the North, Wadi Sudr borders Gebel El Raha (about 600 m), and from the South, Sinn Bishr (about 618 m). The Wadi Sudr originates from the hill slope of the EL-Tih plateau. The main trunk of the Wadi Sudr extends roughly in a northeast-southwest direction for about 55 km and flows into the Gulf of Suez at Ras Sudr town (about 55 km south of the El Shatt) (Girgis and Ahmed, 1985; Mohamed et al., 2018).

Collection and preparation of plant material

Three plants were used in this study, namely, *A. tortilis*, *A. graecorum* and *R. raetam* (*Fig. 2*). Three samples from the aerial parts in each species were collected at random from Wadi Sudr during the dry and wet seasons of 2019 and 2020, respectively. Drying of collected plant materials was done in the oven at 70°C to a constant weight after which dried samples were milled to a fine powder and stored in brown bags at room temperature until chemical analyses.

http://www.aloki.hu ● ISSN 1589 1623 (Print) ● ISSN1785 0037 (Online)
DOI: http://dx.doi.org/10.15666/aeer/2003_22152233

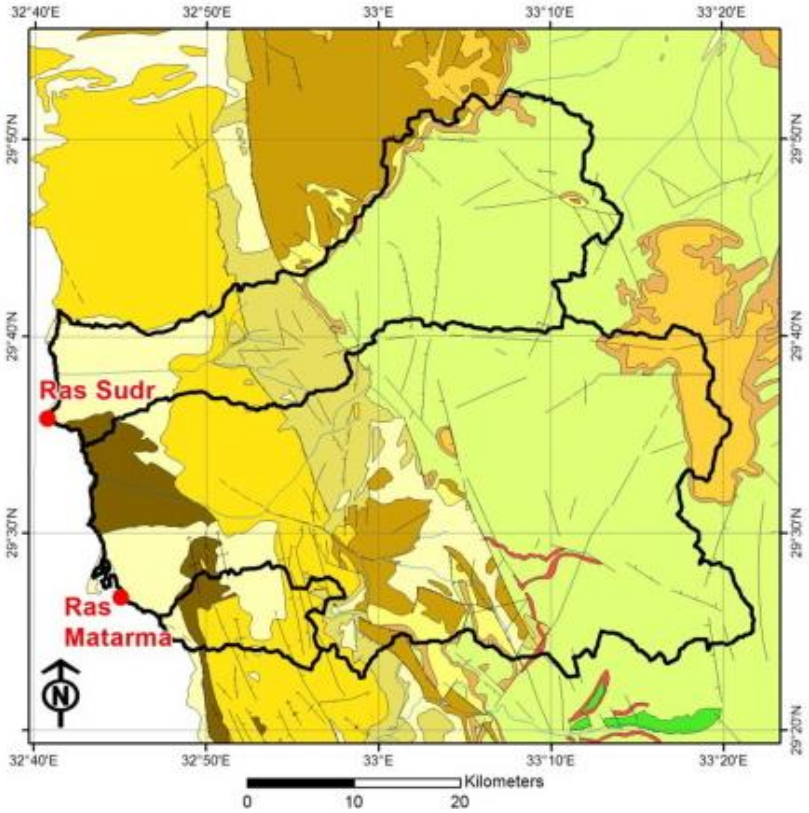

Figure 1. *Location map of Wadi Sudr, South-West Sinai, Egypt (Gabr and El Bastawesy, 2015)*

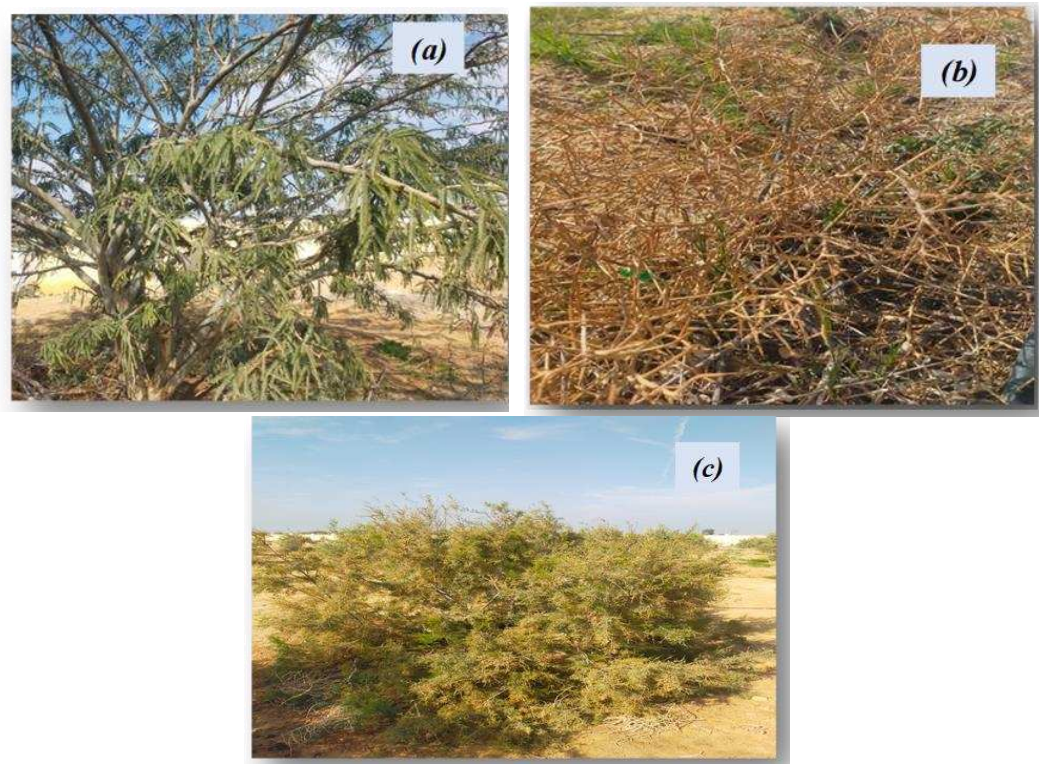

Figure 2. *The species studied from Wadi Sudr, (a) A. tortilis, (b) A. graecorum and (c) R. raetam*

http://www.aloki.hu ● ISSN 1589 1623 (Print) ● ISSN1785 0037 (Online)
DOI: http://dx.doi.org/10.15666/aeer/2003_22152233

Soil analysis

Soil samples were collected from the soil associated with the three studied plants carefully made from three random points at two depths (0-20 cm and 20-40 cm) at the Wadi Sudr. Three replicates were taken from each sample and carried to the laboratory in closed tins to be used for soil analyses. Soil samples were air-dried, sieved and used for mechanical analysis of soil particles as suggested by Jackson (1967) and Rowell (1994) for soil texture. The soil moisture content and sulphate concentration were calculated according to the method described by Rowell (1994). Electrical conductivity (EC) and pH value for each sample were carried out using soil-water paste, according to Jackson (1962), EC was expressed as mohms/cm. The mineral contents of soil including Cl^-, Ca^{2+}, Mg^{2+}, Na^+ and K^+ were determined using a saturation paste that described by Tuzuner (1990).

Plant analysis

The concentrations of Sodium (Na^+), potassium (K^+) and calcium (Ca^{2+}), magnesium (Mg^{2+}), and sulphate (SO_4^{2-}) were determined by atomic absorption spectrophotometry (GBC Avanta E, Victoria, Australia) (Chapman, 1965). Total nitrogen (N) content was determined using the micro-Kjeldahl method (Bremner, 1965). Photosynthetic pigment parameters were quantified spectrophotometrically, using the wavelengths of 663, 645 and 470 nm, chlorophyll a, chlorophyll b and total carotenoids were calculated by equations of Lichtenthaler (1987), respectively. Crude protein % was determined by multiplying the total nitrogen by 6.25 according to Allen (1989). The plant water content was obtained following the equation described by Jin et al. (2017). All amino acid contents were analyzed at the Central Laboratories, Faculty of Agriculture, Al-Azhar University, Cairo, Egypt, using the Clait Amino Acid Analyzer SW (Pellet and Young, 1980)

Statistical analysis

Data values are expressed as Mean±standard deviation (SD). Analysis of Variance (two-way ANOVA) was performed to determine the effect of plant species (P), season (S) and P × S interaction using SPSS software package (version 20). The test of significance of the means was determined by the Least Significance Difference (LSD) when the ANOVA suggested a significant difference at $P \leq 0.05$ and $P \leq 0.01$. The Principal Components Analysis (PCA) was used to correlate the plant analysis with the soil variables studied using the computer program STATGRAPHICS Centurion 19.

Results and discussions

Soil analysis

The texture is one of the most important physical properties of soil. *Table 1* lists the means and ANOVA of mechanical properties for the soil adjoined of three species from the two depths across Wadi Sudr region. All mechanical properties (%) were highly significant ($p<0.01$) affected by the three plant species, the two depths and their interaction, except the two studied factors for very coarse sand had insignificant difference. Similarly, many authors, for example Mohammed et al. (2016), Abdedaiem et al. (2020) and Kamel and El-Absy (2020) have also reported that soil mechanical properties were significantly different between plants studied under different habitat

http://www.aloki.hu ● ISSN 1589 1623 (Print) ● ISSN1785 0037 (Online)
DOI: http://dx.doi.org/10.15666/aeer/2003_22152233

conditions. In contrast to these results, Desta et al. (2018) mentioned that soil physical properties measured were not statistically different ($p < 0.05$) under *A. tortilis*. The highest percentage of fine sand was found in the root-associated soil of the three plant species in two depths, followed by medium sand and coarse sand. The fine sand % was significantly higher in the soil associated of *A. tortilis* than other species at the two depths, also in the 20-40 depth than in the 0-20 depth across the three plant species. Thus, the adjoining soil of the studied plants and collected from 0-20 and 20-40 depths in the Wadi Sudr area are sandy in texture. This result is in line with earlier studies reported by El-Lamey (2020). Lal (2012) reported that, the leguminous plants enhance the soil physical properties by being a soil conditioner and enhancing physical residences.

Table 1. *Mechanical properties of the adjoining soil samples of the studied plants from different depths at Wadi Sudr*

Plants (P)	Depths (D)	Very Coarse Sand	Coarse Sand	Medium Sand	Fine Sand	Very Fine Sand	Clay and Silt	Soil Texture Class
R. raetam	0 – 20	0.78±0.01	9.33±0.01	26.41±0.18	58.38±0.23	2.64±0.02	2.46±0.13	Sandy
	20 – 40	1.32±0.00	3.96±0.08	5.46±0.00	86.7±0.31	1.70±0.09	0.86±0.01	Sandy
A. graecorum	0 – 20	0.73±0.03	6.21±0.11	12.35±0.04	76.13±0.28	3.85±0.03	0.73±0.11	Sandy
	20 – 40	1.61±0.06	2.92±0.09	5.04±0.09	86.81±0.15	2.82±0.04	0.8±0.09	Sandy
A. tortilis	0 – 20	2.51±0.03	6.68±0.10	4.38±0.11	84.02±0.21	1.46±0.07	0.95±0.12	Sandy
	20 – 40	0.73±0.01	5.34±0.07	2.11±0.08	90.17±0.19	0.92±0.10	0.73±0.08	Sandy
LSD for	P	NS	**	**	**	**	**	
	D	NS	**	**	**	**	**	
	P x D	**	**	**	**	**	**	

The results represent the values of mean ± standard deviation. Statistically significant differences at *$p < 0.05$ and **$p < 0.01$

The water content % showed significant differences ($P < 0.01$) between the plant species, seasons and depths as well as first and second-order interactions (*Fig. 3*). Likewise, significant differences of water content % in soil associated with the plants have been reported by Desta et al. (2018), El-Lamey (2020) and Liu et al. (2020). Higher values of soil water content were recorded in the case of *R. raetam* at the two seasons and depths than other plant species. Also, significant increases were found in the wet season and at 20-40 depth than in others season and depth for the soil water content of the three studied plants, due to rainfall, which leads to normal plant growth under Wadi Sudr drought conditions. The results of this study were in accordance with those of Singh (2004), Do et al. (2008) and El-Lamey (2020) who also observed higher value of water content % in the wet season than in the dry season.

The means and ANOVA of soil chemical properties associated with different plants at 0-20 and 20-40 depths were summarized in *Table 2*. According to the two-way ANOVA, all soil chemical analyses supporting the three plant species exhibited highly significant differences ($P < 0.01$) between the species, the depths and their interaction, except pH (between the studied factors) and SO_4^{2-} (interaction) which showed no significant differences. This is consistent with the previous studies by Desta et al. (2018) in *A. tortilis*, El-Lamey (2020) in *R. raetam* and Salama et al. (2021) in *A. graecorum*, Chemical properties of soil, such as electrical conductivity (EC), Na^+, Ca^{2+}, Mg^{2+}, SO_4^{2-} and Cl^-

http://www.aloki.hu ● ISSN 1589 1623 (Print) ● ISSN1785 0037 (Online)
DOI: http://dx.doi.org/10.15666/aeer/2003_22152233

were significantly higher across the two depths in *R. raetam* than in the two plants *A. graecorum* and *A. tortilis*. While, the values of K^+ have increased significantly during the two depths in *A. tortilis* compared with their values in *R. raetam* and *A. graecorum*. In soil of plant species, the maximum amount of Na^+, K^+, Mg^{2+}, SO_4^{2-} and Cl^- were found in 0-20 depth and less in 20-40 depth, whilst Ec and Ca^{2+} were higher in the 20-40 depth than in the 0-20 depth. Soil pH associated with the three studied plants in Wadi Sudr tended to be somewhat alkaline, and there was no significant difference between the plant species and depths. The result of pH corroborates the result obtained by Salama et al. (2021), who also mentioned that alkalinity may be due to the increase in total soluble salts in soil of *A. graecorum*. Comole et al. (2021) mentioned that plants can adapt and thrive in locations with different soil properties.

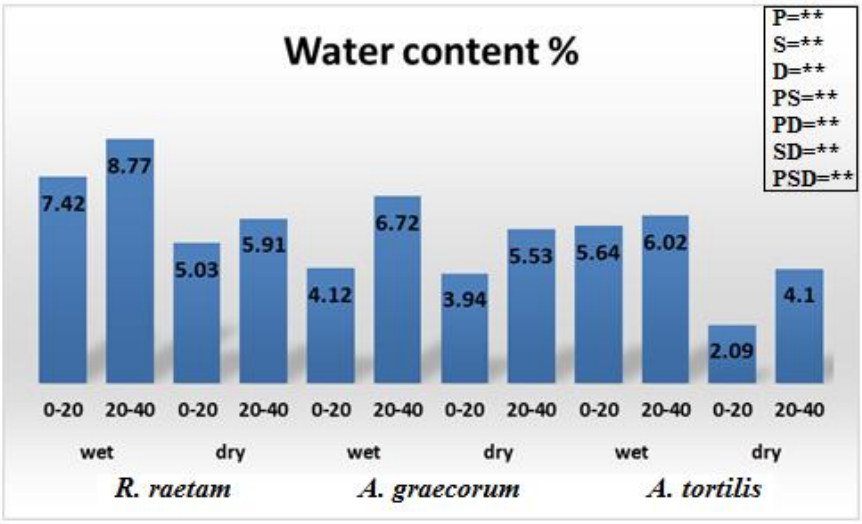

Figure 3. *Water content % at the soil associated with three plant species at two depths and the two seasons during Wadi Sudr. According to three-way ANOVA test followed by LSD, water content % between the species (P), seasons (S), depths(D) and their interactions are significantly different (P < 0.01)*

Table 2. *Soil chemical properties associated with the studied plants from different depths at Wadi Sudr*

Plants (P)	Depths (D)	Soil Chemical Properties							
		Ec	pH	Na^+	K^+	Ca^{2+}	Mg^{2+}	SO_4^{2-}	Cl^-
R. raetam	0 – 20	27.87±0.09	7.41±0.09	40.40±0.14	10.50±0.07	19.80±0.08	49.85±0.08	11.72±0.13	37.70±0.12
	20 – 40	125.80±0.12	7.74±0.07	4.78±0.09	2.10±0.02	148.02±0.13	10.80±0.02	3.70±0.00	9.23±0.10
A. graecorum	0 – 20	21.97±0.10	7.09±0.01	21.32±0.12	11.20±0.08	9.49±0.03	31.71±0.10	8.57±0.07	12.90±0.08
	20 – 40	80.07±0.07	7.30±0.04	2.10±0.08	4.52±0.01	16.53±0.09	8.90±0.04	2.40±0.08	4.14±0.07
A. tortilis	0 – 20	17.77±0.02	7.27±0.08	10.49±0.11	20.20±0.09	5.94±0.09	15.11±0.05	7.43±0.11	7.20±0.05
	20 – 40	39.87±0.13	7.59±0.02	1.12±0.01	8.33±0.11	11.10±0.07	7.40±0.01	2.10±0.08	1.24±0.01
LSD for	P	**	NS	**	**	**	**	**	**
	D	**	NS	**	**	**	**	**	**
	P x D	**	NS	**	**	**	**	NS	**

The results represent the values of mean ± standard deviation. EC: Electrical Conductivity; Na^+: Sodium; K^+: Potassium; Ca^{2+}: Calcium; Mg^{2+}: Magnesium; SO_4^{2-}: Sulfate; Cl-: Chloride. Statistically significant differences at *p < 0.05 and **p < 0.01

http://www.aloki.hu ● ISSN 1589 1623 (Print) ● ISSN1785 0037 (Online)
DOI: http://dx.doi.org/10.15666/aeer/2003_22152233

Plant analysis

Photosynthetic pigment contents

Table 3 shows the photosynthetic pigment contents in the three plants under wet and dry seasons at Wadi Sudr area. Statistically significant differences ($p<0.01$) in chlorophyll a (Chl a), chlorophyll b (Chl b), total carotenoids, Chl a+b and total pigment were noticed among the three plants, seasons and their interaction, using two-way ANOVA. Chl a/b between the two seasons was significantly different ($p<0.01$), however, was not found to be statistically significant among the three plant species and plants x seasons interaction. These results similar to those described by Kebbas et al. (2015) in *A. tortilis*, Nasir Khan et al. (2016) in *R. raetam* and Salama et al. (2021) in *A. graecorum*.

Table 3. *Photosynthetic pigment contents of three legumes species during wet and dry seasons at Wadi Sudr*

Plants (P)	Seasons (S)	Chlorophyll a (Chl a)	Chlorophyll b (Chl b)	Total Carotenoids	Chl a+b	Chl a/b	Total pigment
R. raetam	Wet	15.54±0.28	9.63±0.08	159.79±0.38	25.17±0.09	1.63±0.01	184.96±0.31
	Dry	21.95±0.15	14.46±0.07	273.01±0.53	36.41±0.05	1.53±0.05	309.42±0.25
A. graecorum	Wet	5.27±0.09	3.36±0.11	895.31±0.62	8.63±0.12	1.73±0.12	903.94±0.19
	Dry	21.01±0.21	15.28±0.00	516.76±0.41	36.29±0.00	1.38±0.10	553.05±0.41
A. tortilis	Wet	16.79±0.09	9.74±0.03	649.73±0.75	26.53±0.07	1.74±0.09	676.26±0.22
	Dry	19.65±0.13	31.25±0.10	119.87±0.21	50.9±0.09	0.63±0.00	170.77±0.57
LSD for	P	**	**	**	**	NS	**
	S	**	**	**	**	*	**
	P x S	**	**	**	**	NS	**

The results represent the values of mean ± standard deviation. Statistically significant differences at *$p < 0.05$ and **$p < 0.01$

During the dry season, the maximum values were found for Chl a in *R. raetam* and for Chl b and Chl a+b in *A. tortilis*. As for the wet season, total carotenoids and total pigment in *A. graecorum* as well as Chl a/b in *A. tortilis* recorded the highest values. Generally, the concentrations of Chl a, Chl b and Chl a+b in the three plants as well as total carotenoids and total pigment in *R. raetam* were higher values in the dry season than in the wet season. While the maximum values of Chl a/b in the studied plants as well as total carotenoids and total pigment at *A. graecorum* and *A. tortilis* were registered in the wet season compared with their values in the dry season. Salama et al. (2021) reported the highest concentration of chlorophyll a and b in the summer season while their ratio in *A. graecorum* in the winter season were found to modify enabling the plants to adapt to light condition changes. Furthermore, for *A. tortilis*, Singh and Khajuria (1991) and Kebbas et al. (2015) found higher contents of total chlorophyll and carotenoids in the stressed plants, however, the Chl a/b ratio was not affected by the drought. Ait Said et al. (2013) hypothesized that a decrease in Chl a can be considered as a protective adaptive mechanism that prevents increased photon absorption. The Chl a/b ratio was higher due to higher Chl a content than Chl b content (Huang et al., 2021).

http://www.aloki.hu ● ISSN 1589 1623 (Print) ● ISSN1785 0037 (Online)
DOI: http://dx.doi.org/10.15666/aeer/2003_22152233

Mineral contents

Mineral contents of the plant species at the wet and dry seasons in Wadi Sudr area are presented in *Table 4*. Statistically significant differences ($p<0.01$) were noted in studied chemical compositions (Na^+, K^+, Ca^{2+}, Mg^{2+} and SO_4^{2-}) among the different studied plants, seasons, and their interactions. As for nitrogen content (N), significant differences showed among the three studied plants ($p<0.01$) and seasons ($p<0.05$), but insignificant for plants x seasons interaction. These outcomes are generally consistent with El-Lamey (2020), Al-Onazi et al. (2021) and Salama et al. (2021).

Table 4. *Chemical compositions of three legumes species during the wet and dry seasons at Wadi Sudr*

Plants (P)	Seasons (S)	Na^+	K^+	Ca^{2+}	Mg^{2+}	SO_4^{2-}	N
R. raetam	Wet	40.11±0.35	99.41±0.21	135.00±0.37	100.21±0.42	1.91±0.18	3.94±0.19
	Dry	54.31±0.22	150.00±0.64	133.10±0.83	94.50±0.34	2.12±0.21	3.84±0.20
A. graecorum	Wet	39.14±0.34	61.10±0.71	195.00±0.62	129.90±0.81	2.11±0.15	5.81±0.16
	Dry	47.21±0.43	62.50±0.62	82.21±0.41	124.50±0.51	3.41±0.12	3.61±0.15
A. tortilis	Wet	9.42±0.19	40.21±0.51	75.00±0.47	37.90±0.24	0.91±0.09	2.88±0.09
	Dry	10.94±0.25	82.51±0.34	69.20±0.29	35.50±0.31	1.49±0.20	1.99±0.08
LSD for	P	**	**	**	**	**	**
	S	**	**	**	**	**	*
	P x S	**	**	**	**	**	NS

The results represent the values of mean ± standard deviation. Na^+: Sodium; K^+: Potassium; Ca^{2+}: Calcium; Mg^{2+}: Magnesium; SO_4^{2-}: Sulfate; N: Nitrogen, Statistically significant differences at *$p < 0.05$ and **$p < 0.01$

During the three plant species, the dry season had higher values of Na^+, K^+ and SO_4^{2-} than those reported in the wet season. On the other hand, the values of Ca^{2+}, Mg^{2+} and N were higher in the wet season than in the dry season in the studied plants. Na^+ and K^+ contents at the two seasons recorded the highest values of *R. raetam*, followed by *A. graecorum* and *A. tortilis*. Further, the maximum Mg^{2+}, SO_4^{2-} and N contents were observed in *A. graecorum*, followed by *R. raetam* and *A. tortilis* during the two seasons. A higher Ca^{2+} content was found in *A. graecorum* at the wet season as compared to other species in the seasons, but lower in *A. tortilis* at the dry season. The anions and cations accumulation in *A. graecorum* were significantly increased during winter season (Salama et al., 2021), while total K^+ in *A. graecorum* (Salama et al., 2021) as well as potassium, Sodium, calcium and magnesium contents in *R. raetam* at Wadi Sudr (El-Lamey, 2020) showed the opposite response at the summer season. Rubanza et al. (2007) reported that *A. tortilis* had moderate to high levels of mineral contents.

Osuagwu et al. (2012) reported that plant species differ in content of the minerals as well as the reactions under adverse conditions in the same region. Na^+ is often stored in the vacuoles resulting in increased osmotic pressure (Wyn Jones, 1981) and avoid Na^+ toxicity (Salama et al., 2021), K^+ ions are essential for reducing the uptake of Na^+. Concentrations of Na^+ and K^+ as well as ion balance play important roles in plant salt tolerance (Zheng et al., 2015). To drought tolerance mechanisms, accumulated K^+ in *A. graecorum* may be employed during the dry seasons (Prajapati and Modi, 2012). Salama et al. (2015) stated that the absorption and removal of inorganic osmoregulatory

http://www.aloki.hu ● ISSN 1589 1623 (Print) ● ISSN1785 0037 (Online)
DOI: http://dx.doi.org/10.15666/aeer/2003_22152233

ions like K^+, Na^+, Ca^{+2} and Mg^{+2} are useful means of osmotic gradient re-adjustment in stressed plants. An increased concentration of Ca^{2+} and Mg^{2+} without reaching toxic levels counteracts the inhibitory effect of Na^+ and may contribute to its physiological salt tolerance mechanisms (Gul and Khan, 2006; Grigore et al., 2012).

Water content % and crude protein

Based on two-way ANOVA, statistically significant differences ($P < 0.01$) determined with respect to water content % and crude protein between the plants, seasons and their interaction (*Fig. 4*). Similar results were recorded in the study of Mabeza et al. (2014), Al-Qahtani et al. (2020), El-Lamey (2020) and Kamel and El-Absy (2020). Water content % and crude protein were significantly higher at the wet season than at the dry season in the three plant species. *R. raetam* recorded the greater value of water content % at the wet season, followed by *A. graecorum* and *A. tortilis*. Crude protein at the wet season had the highest value in *A. graecorum*, followed by *R. raetam* and *A. tortilis*. A similar result in *R. raetam* at Wadi Sudr was reported by El-Lamey (2020). As for *A. tortilis* it is well adapted to dry environments (Kebabs et al., 2015).

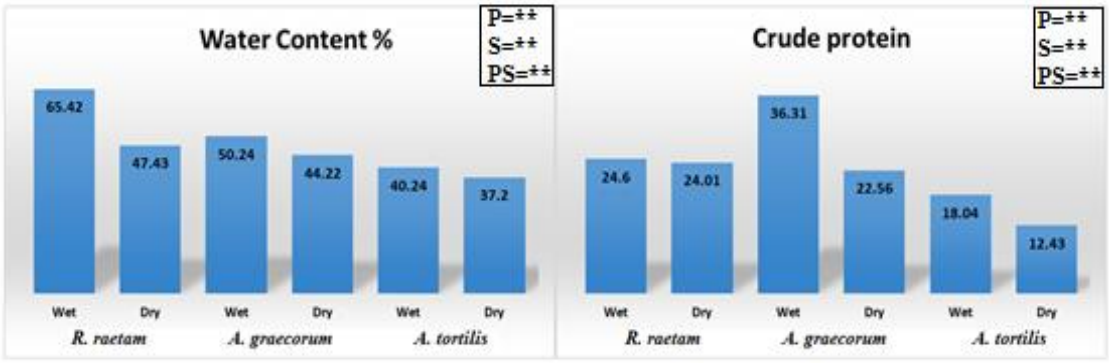

Figure 4. *Water content % and crude protein of three plant species from Wadi Sudr during the wet and dry seasons. According to two-way ANOVA test followed by LSD, the parameters between the species, seasons and their interaction are significantly different ($P < 0.01$)*

Amino acid composition

Table 5 outlines a detailed amino acid profile performed on three legumes plant species under the wet and dry seasons in Wadi Sudr area. Two-way ANOVA exhibited statistically significant differences between the three studied plants for all amino acids except glutamic acid, histidine, glycine and threonine. While, serine, glycine, arginine, alanine, phenylalanine, tryptophan and proline were statistically significant differences between seasons. As for plants x seasons interaction, the observed differences were not statistically significant for all amino acids, except serine and tyrosine. Similar results were obtained in the investigations conducted by Grela et al. (2017), El-Lamey (2020) and Salama et al. (2021).

The highest concentrations of aspartic acid, proline, leucine and arginine, and the lowest concentrations of cysteine and methionine were recorded in the three studied plants under the wet and dry seasons. Based on data of the two season, all amino acid concentrations of the three studied plants were higher in the dry season than in the wet season, except for isoleucine and lysine in *R. raetam*, cysteine in *A. graecorum* and

http://www.aloki.hu ● ISSN 1589 1623 (Print) ● ISSN1785 0037 (Online)
DOI: http://dx.doi.org/10.15666/aeer/2003_22152233

histidine in *A. tortilis*. The concentrations of aspartic acid, arginine, valine, phenylalanine, leucine and lysine were higher in *R. raetam* than in other plants. On the other hand, the maximum values of serine, glycine, tyrosine, cysteine and isoleucine were registered in *A. graecorum*. As for the other amino acids, they were greater in *A. tortilis* than in *R. raetam* and *A. graecorum* plants. The highest accumulation of proline had in *A. tortilis*, followed by *R. raetam* and *A. graecorum* during the wet and dry seasons at Wadi Sudr region. The levels of some amino acids were significantly reduced in *R. raetam* during summer season at Wadi Sudr (El-Lamey, 2020), while total free amino acids were increased in *A. graecorum* during winter season (Salama et al., 2021). As for *A. tortilis*, lower levels of isoleucine, lysine, and threonine were found (Embaby and Rayan, 2016). Osmotic modification may be accompanied by protein accumulation to improve drought tolerance of plant species (Salama et al., 2021). Also, the amino acids can play the same role during some mechanisms: acting as compatible osmolytes, regulating pH, acting as nitrogen or carbon reservoir (Ali et al., 2020), precursors for energy-associated metabolites, ROS scavengers, and potential regulatory and signaling molecules (Hildebrandt et al., 2015). Therefore, the synthesis of protein types rich in certain amino acids could be the key to survival for the species (Kasim et al., 2008). Proline accumulates under stress conditions and have more intimate association with survival adaptability of plants, considered to act as a compatible osmolyte (Verslues and Sharma, 2010) and stimulate root elongation at low water potentials (Yamada et al., 2005). Leucine, isoleucine and valine also play an important role in plant drought tolerance as an alternative source of respiratory substrates (Pires et al., 2016).

Table 5. *The amino acids profile (mg/g) of three different species from Wadi Sudr during wet and dry seasons*

Plants (P)	***R. raetam***		***A. graecorum***		***A. tortilis***		**LSD for**		
Seasons (S) / **Amino acids**	**Wet**	**Dry**	**Wet**	**Dry**	**Wet**	**Dry**	**P**	**S**	**PxS**
Aspartic acid	16.33±0.01	17.53±0.09	13.66±0.10	14.35±0.08	12.23±0.11	12.91±0.10	**	NS	NS
Glutamic acid	5.94±0.06	6.81±0.10	6.86±0.08	8.01±0.11	7.72±0.00	7.04±0.09	NS	NS	NS
Serine	2.20±0.03	3.31±0.07	2.43±0.05	3.45±0.02	2.44±0.09	1.98±0.03	*	*	*
Histidine	1.44±0.05	1.32±0.08	1.22±0.09	1.13±0.07	1.62±0.08	1.54±0.01	NS	NS	NS
Glycine	3.26±0.00	4.32±0.03	3.85±0.05	4.98±0.06	3.88±0.10	4.65±0.07	NS	**	NS
Threonine	2.11±0.05	3.32±0.06	2.50±0.01	2.98±0.00	2.97±0.11	3.09±0.04	NS	NS	NS
Arginine	10.09±0.04	9.16±0.07	8.77±0.09	8.24±0.04	7.88±0.04	6.97±0.01	**	*	NS
Alanine	2.88±0.06	3.15±0.07	3.10±0.03	3.65±0.10	4.65±06	4.89±0.04	**	*	NS
Tyrosine	3.66±0.00	2.97±0.03	4.19±0.05	5.31±0.07	3.11±0.03	3.67±0.07	**	NS	*
Cysteine	0.52±0.06	0.50±0.08	0.70±0.09	0.670.01	0.56±0.07	0.54±0.02	*	NS	NS
Valine	6.43±0.03	6.23±0.04	4.26±0.04	3.96±0.00	3.33±0.04	3.84±0.07	**	NS	NS
Methionine	0.40±0.01	0.53±0.07	0.61±0.06	0.690.02	0.80±0.01	0.89±0.01	**	NS	NS
Phenylalanine	5.54±0.04	6.32±0.05	4.12±0.11	4.89±0.01	4.92±0.00	5.61±0.05	**	*	NS
Isoleucine	7.90±0.08	7.65±0.00	8.44±0.08	8.06±0.08	7.12±0.04	6.98±0.08	**	NS	NS
Leucine	9.44±0.07	9.89±0.04	7.10±0.06	7.27±0.10	8.70±0.08	8.98±0.06	**	NS	NS
Lysine	4.60±0.05	4.52±0.11	4.12±0.09	4.01±0.05	3.66±0.10	3.99±0.03	*	NS	NS
Tryptophan	1.230.00	1.65±0.01	1.88±0.00	2.08±0.11	2.44±0.00	2.97±0.01	**	*	NS
Proline	13.70±0.08	14.87±0.10	10.76±0.07	11.64±0.07	16.40±0.11	17.82±0.09	**	*	NS

The results represent the values of mean ± standard deviation. Statistically significant differences at *$p < 0.05$ and **$p < 0.01$

http://www.aloki.hu ● ISSN 1589 1623 (Print) ● ISSN1785 0037 (Online)
DOI: http://dx.doi.org/10.15666/aeer/2003_22152233

Principal component analysis

Principal component analysis (PCA) is a multivariate statistical technique. The PCA has been used to estimate the similarities and dissimilarities among the soil and plant chemical variables in the three studied plant species. The results are graphically displayed in a biplot of the first two PCAs (PCA1 and PCA2). Out of the PCAs, the PCA1 and PCA2 extracted had eigenvalues larger than one (Eigenvalue >1) (*Fig. 5*). While the rest PCAs had eigenvalues less than one (Eigenvalue < 1). Therefore, the PCA1 was kept for the final analysis, in which, the PCA1 and PCA2 explains variance more than an individual attribute (Sharma, 1996) and it expresses more variability and support to select the variable with a positive loading factor. The contributions of PCA1 to the total variance were higher than that of the other components, with PCA1 describing only about <60% of the measured data total variability in the original variables at the three studied plants. This result indicates that the first two PCAs may be used to summarize the original variables in any further analysis of the data, as well as to explain the total variation and the grouping of the PCAs. The PCA1 and PCA2 had mainly distinguished the soil and plant analysis across the three studied species in different groups. Thus, the PCA1 and PCA2 were employed to draw a biplot, and to explain relationships of soil and plant analysis across the plant species studied. The eigenvalue of the first four PCAs (Kumar et al., 2019; Liu et al., 2020) and the two first PCA components (Gil et al., 2014; Abdedaiem et al., 2020) are greater than 1, and they also explained the largest part of the total variance in soil properties, amino acids and environmental conditions at different plant species.

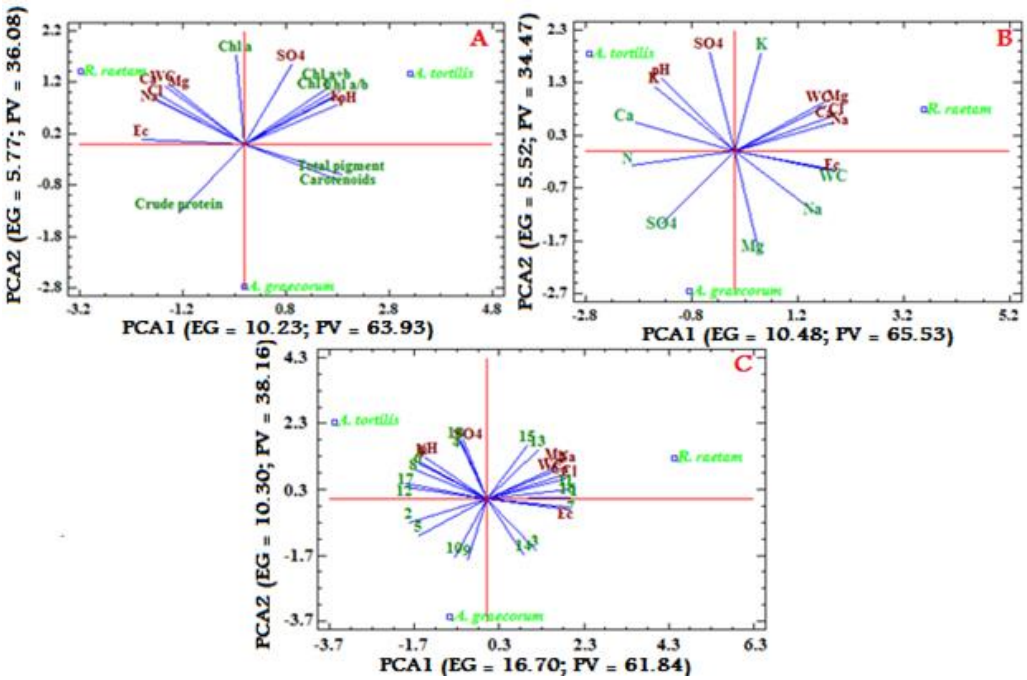

Figure 5. *Biplot diagram based on first two PCs axes of soil chemical variables (brown points) with (A) Photosynthetic pigments and crude protein, (B) Mineral compositions and water content as well as with (C) amino acids contents in plants studied (green points). Symbols: EG: Eigenvalue; EV: Explained variance; EC: Electrical Conductivity; Cl-: Chloride; Na^+: Sodium; K^+: Potassium; Ca^{2+}: Calcium; Mg^{2+}: Magnesium; SO_4^{2-}: Sulfate; WC: Water content; 1: Aspartic; 2: Glutamic; 3: Serine; 4: Histidine; 5: Glycine; 6: Threonine; 7: Arginine; 8: Alanine; 9: Tyrosine; 10: Cysteine; 11: Valine; 12: Methionine; 13: Phenylalanine; 14: Isoleucine; 15: Leucine; 16: Lysine; 17: Tryptophan; 18: Proline*

http://www.aloki.hu ● ISSN 1589 1623 (Print) ● ISSN1785 0037 (Online)
DOI: http://dx.doi.org/10.15666/aeer/2003_22152233

During the three plant species, the soil variables were divided into two groups. The first group consisted of pH, K^+ and SO_4^{2-}. While, the second group comprised of other soil variables (*Fig. 5*). The soil variables inside each group were significantly positively or negatively associated with each other. Abdedaiem et al. (2020) showed that correlation between pH and EC of *R. raetam* was significant. Significant correlations among several soil chemical properties were observed by Liu et al. (2020). As for the plant chemical variables, positive or negative correlations were noticed among Chl b, Chl a+b, Chl a/b, between carotenoids and total pigment (*Fig. 5A*), among WC, Na^+ and Mg^{2+}, between N and SO_4^{2-} (*Fig. 5B*), among aspartic, arginine, valine, lysine, among threonine, alanine, tryptophan and methionine, among tyrosine, cysteine, glutamic and glycine, between serine and isoleucine, between phenylalanine and leucine as well as between histidine and proline (*Fig. 5C*) in the studied plants. Kaspary et al. (2020) mentioned that the importance of the relationship between Chl a and Chl b is due to assessing the ability of plants to capture light during shade. Positive correlations were found among mineral contents (Yinping et al., 2021). The most amino acids were significantly positively associated with each other (Kumara et al., 2019). No negative correlations were observed among the amino acids in plants studied by Kumar et al. (2017).

In the *Fig. 5A*, the soil variables i.e., pH, K^+ and SO_4^{2-} had a positive correlation with plant variables i.e., Chl b, carotenoids, Chl a+b, Chl a/b, total pigment, and that occupied the first and fourth quadrants of the diagram of *A. tortilis*, and also strongly correlated with PCA1. While, the rest soil and plant variables were positively associated with PCA2 and occurred in the second and third quarters with *R. raetam*. The EC, Na^+, Ca^{2+}, Mg^{2+}, Cl^- and WC variables in soil were positively correlated with K^+, WC, Na^+ and Mg^{2+} (*Fig. 5B*), leucine, phenylalanine, valine, lysine, aspartic, arginine, serine, and isoleucine (*Fig. 5C*) in plants. These soil and plant variables were strongly correlated with PCA1, which were located in first and fourth quarters of the diagram of *R. raetam*. On the other hand, the other soil and plant variables were located in second (*A. tortilis*) and third (*A. graecorum*) quarters, and that were strongly correlated with PCA2. These results indicated that the first two PCAs were affected by most soil and plant chemical variables across the three plant species studied. Also, the chemical variables of the soil associated with *R. raetam*, *A. graecorum* and *A. tortilis* during the winter and summer seasons show better soil chemical characteristics, which influence the distribution of legumes plants growing in Wadi Sudr, South-West Sinai.

The PCA1 had a high positive correlation with soil variables (Cl^-, Na^+, Ca^{2+}, Mg^{2+} and K^+/Na^+ ratios) and plant variables (water content, proline, and glycine betaine) and related to water stress and to salt stress (Gil et al., 2014). PCA1 included aspartic acid, glutamine, glycine, histidine, isoleucine, and serine, while, PCA2 consisted of cysteine and methionine, phenylalanine, and tyrosine (Kumara et al., 2019). Gil et al. (2014) reported that proline content had correlated with soil variables as Cl^-, Na^+ (positively) and soil moisture (negatively). Concerning chlorophyll, the contributions of soil and climate variables to the total variance were very low, while interspecific variation was the main factor affecting chlorophyll content (Li et al., 2018). Proline levels in the plants exhibited significant correlation with the variables associated with environmental stress (Gil et al., 2014), which indicate a functional role of proline in the stress tolerance mechanisms of plant species (Grigore et al., 2011).

http://www.aloki.hu ● ISSN 1589 1623 (Print) ● ISSN1785 0037 (Online)
DOI: http://dx.doi.org/10.15666/aeer/2003_22152233

Conclusions

Significant divergences for most soil mechanical and chemical properties between plants, depths and their interaction as well as for most amino acids, photosynthetic pigments contents and chemical compositions between plants, seasons and their interaction were observed by ANOVA. The highest contents of most soil chemical properties were recorded at *R. raetam*. The concentrations of most amino acids, photosynthetic pigments, Na^+, K^+ and SO_4^{2-} were higher in the dry season than in the wet season across the three studied plants. Based on the variation in the plants studied, the first two principal component analysis (PCA1 and PCA2) were strong enough to separate soil and plant variables. PCA1 and PCA2 formed different groups from soil and plant variables, which are closely related with each other, especially with some amino acids. The results of PCA from our study could be useful in future studies and may lead to the maintenance of cellular osmotic balance to protect the plant during different stress conditions.

Acknowledgements. This research received no specific grant from any funding agency in the public, commercial, or not-for-profit sectors.

REFERENCES

[1] Abdedaiem, R., Rejili, M., Mahdhi, M., de Lajudie, P., Mars, M. (2020): Soil properties shape species diversity and community composition of native arbuscular mycorrhizal fungi in Retama raetam roots growing on arid ecosystems of Tunisia. – International Journal of Agriculture & Biology 23: 438-446. DOI:10.17957/IJAB/15.1307.

[2] Ait Said, S., Torre, F., Derridi, A., Gauquelin, T., Mevy, J. P. (2013): Gender, Mediterranean drought, and seasonality: photosystem II photochemistry in Pistacia lentiscus. – Photosynthetica 51: 552-564. DOI: 10.1007/s11099-013-0055-9.

[3] Ali, S., Rizwan, M., Arif, M. S., Ahmad, R., Hasanuzzaman, M., Ali, B., Hussain, A. (2020): Approaches in enhancing thermotolerance in plants: An updated review. – Journal of Plant Growth Regulation 39: 456-480. https://doi.org/10.1007/s00344-019-09994-x.

[4] Allen, S. E. (1989): Chemical analysis of ecological materials. – Blackwell Scientific Publications, Oxford, London Edinburgh, 368p.

[5] Al-Mujahidy, S. M. J., Hassan, M. M., Rahman, M. M., Mamun-or-Rashid, A. (2013): Study on measurement and statistical analysis of adherent soil chemical compositions of leguminous plants and their impact on nitrogen fixation. – International Journal of Biosciences 3: 112-119. http://dx.doi.org/10.12692/ijb/3.6.112-119.

[6] Al-Onazi, W., Al-Mohaimeed, A. M., Amina, M., El-Tohamy, M. F. (2021): Identification of chemical composition and metal determination of Retama raetam (forssk) stem constituents using ICP-MS, GC-MS-MS, and DART-MS. – Journal of Analytical Methods in Chemistry 9: 6667238. https://doi.org/10.1155/2021/6667238.

[7] Al-Qahtani, H., Alfarhan, A. H., Al-Othman, Z. M. (2020): Changes in chemical composition of Zilla spinosa Forssk. medicinal plants grown in Saudi Arabia in response to spatial and seasonal variations. – Saudi Journal of Biological Sciences 27(10): 2756-2769. https://doi.org/10.1016/j.sjbs.2020.06.035.

[8] Aremu, M. O., Audu, S. S., Gav, B. L. (2017): Comparative review of crude protein and amino acids of leguminous seeds grown in Nigeria. – International Journal of Sciences 6(8): 88-97. https://doi.org/10.18483/ijSci.1390.

[9] Awmack, C. S., Lock, J. M. (2002): The genus Alhagi (Leguminosae: Papilionoideae) in the Middle East. – Kew Bulletin 57: 435-445. https://doi.org/10.2307/4111121.

http://www.aloki.hu ● ISSN 1589 1623 (Print) ● ISSN1785 0037 (Online)
DOI: http://dx.doi.org/10.15666/aeer/2003_22152233

[10] Bennetau-Pelissero, C. (2019): Plant Proteins from Legumes. – In: Mérillon, J. M., Ramawat, K. (eds.) Bioactive Molecules in Food. Reference Series in Phytochemistry. Springer, Cham. https://doi.org/10.1007/978-3-319-78030-6_3.
[11] Boulos, L. (2009): Flora of Egypt Checklist. – Al Hadara Publishing, Cairo, Egypt, 410p.
[12] Boulos, L., El-Hadidi, M. (1984): The Weed Flora of Egypt. – American Univ. Cairo Press, Cairo.
[13] Bremner, J. M. (1965): Total nitrogen and inorganic forms of nitrogen. – In: Black, C. A. (ed.) Methods of Soil Analyses. American Society of Agronomy, Madison, Wisconsin, pp. 1149-1237.
[14] Chapman, H. (1965): Cation-exchange capacity. – In: Methods of Soil Analysis: Part 2 Chemical and Microbiological Properties 9: 891-901. John Wiley & Sons: Hoboken, NJ, USA.
[15] Comole, A. A., Malan, P. W., Tiawoun, M. A. P. (2021): Effects of Prosopis velutina invasion on soil characteristics along the riverine system of the Molopo river in north-west province, South Africa. – International Journal of Ecology 2021: 6681577. https://doi.org/10.1155/2021/6681577.
[16] Derbel, S., Noumi, Z., Werner, A. K. (2007): Life cycle of the coleopter Bruchidius raddianae and the seed predation of the Acacia tortilis Subsp. raddiana in Tunisia. – Comptes Rendus Biologies 330: 49-54.
[17] Desta, K. N., Lisanenwork, N., Muktar, M. (2018): Physico-chemical properties of soil under the canopies of Faidherbia albida (Delile) A. Chev and Acacia tortilis (Forssk.) Hayen in park land agroforestry system in Central Rift Valley, Ethiopia. – Journal of Horticulture and Forestry 10(1): 1-8. https://doi.org/10.5897/JHF2016.0491.
[18] Do, F. C., Rocheteau, A., Diagne, A. L., Goudiaby, V., Granier, A., Lhomme, J. P. (2008): Stable annual pattern of water use by Acacia tortilis in Sahelian Africa. – Tree Physiology 28(1): 95-104. https://doi.org/10.1093/treephys/28.1.95.
[19] El-Hashash, E. F., El-Absy, K. M. (2019): Barley (*Hordeum vulgare* L.) Breeding. – In: Al-Khayri, J., Jain, S., Johnson, D. (eds.) Advances in Plant Breeding Strategies: Cereals. Springer, Cham. https://doi.org/10.1007/978-3-030-23108-8_1.
[20] El-Lamey, T. M. (2020): Changes in some chemical compounds of Retama raetam (Forssk.) Webb & Berthel. in response to different environmental conditions. – Journal of Biodiversity and Environmental Sciences 16(2): 78-91.
[21] Embaby, H. E., Rayan, A. M. (2016): Chemical composition and nutritional evaluation of the seeds of Acacia tortilis (Forssk.) Hayne ssp. raddiana. – Food Chemistry 200: 2-68. https://doi.org/10.1016/j.foodchem.2016.01.019.
[22] Estevez, J. A., Landete-Castillejos, T., García, A. J., Ceacero, F., Martínez, A., Gaspar-López, E., Calatayud, A., Gallego, L. (2010): Seasonal variations in plant mineral content and free-choice minerals consumed by deer. – Animal Production Science 50: 177-185. https://doi.org/10.1071/AN09012.
[23] FAO (2016): The state of food and agriculture: climate change, agriculture and food security. – Available from: https://www.fao.org/3/a-i6030e.pdf.
[24] Ferraz, G. A. S., Pferra, P. F. P., Martins, F. B., Silva, F. M., Damasceno, F. A., Barbari, M. (2019): Principal components in the study of soil and plant properties in precision coffee farming. – Agronomy Research 17(2): 418-429. https://doi.org/10.15159/AR.19.114.
[25] Gabr, S., El Bastawesy, M. (2015): Estimating the flash flood quantitative parameters affecting the oil-fields infrastructures in Ras Sudr, Sinai, Egypt, during the January 2010 event. – The Egyptian Journal of Remote Sensing and Space Science 18(2): 37-149. https://doi.org/10.1016/j.ejrs.2015.06.001.
[26] Gil, R., Bautista, I., Boscaiu, M., Lidon, A., Wankhade, S., Sánchez, H., Llinares, J., Vicente, O. (2014): Responses of five Mediterranean halophytes to seasonal changes in environmental conditions. – AoB PLANTS 6: plu049. https://doi.org/10.1093/aobpla/plu049.

http://www.aloki.hu ● ISSN 1589 1623 (Print) ● ISSN1785 0037 (Online)
DOI: http://dx.doi.org/10.15666/aeer/2003_22152233

[27] Gill, S., Al-Shankiti, A. (2015): Priming of *Prosopis cineraria* (L.) druce and Acacia tortilis (forssk) seeds with fulvic acid extracted from compost to improve germination and seedling vigor. – Global Journal of Environmental Science and Management 1(3): 225-232. https://doi.org/10.7508/GJESM.2015.03.005.

[28] Girgis, W. A., Ahmed, A. M. (1985): An ecological study of Wadis of South West Sinai, Egypt. – Bulletin Desert Institute 35(1): 265-308.

[29] Grela, E. R., Kiczorowska, B., Samolińska, W., Matras, J., Kiczorowski, P., Rybiński, W., Hanczakowska, E. (2017): Chemical composition of leguminous seeds: part I-content of basic nutrients, amino acids, phytochemical compounds, and antioxidant activity. – European Food Research and Technology 243: 1385-1395. https://doi.org/10.1007/s00217-017-2849-7.

[30] Grigore, M. N., Boscaiu, M., Vicente, O. (2011): Assessment of the relevance of osmolyte biosynthesis for salt tolerance of halophytes under natural conditions. – The European Journal of Plant Science and Biotechnology 5: 12-19. https://doi.org/10.1016/j.copbio.2011.05.457.

[31] Grigore, M. N., Boscaiu, M., Llinares, J., Vicente, O. (2012): Mitigation of salt stress-induced inhibition of Plantago crassifolia reproductive development by supplemental calcium or magnesium. – Notulae Botanicae Horti Agrobotanici Cluj-Napoca 40: 58-66. https://doi.org/10.15835/nbha4028246.

[32] Gul, B., Khan, M. A. (2006): Role Of Calcium In Alleviating Salinity Effects In Coastal Halophytes. – In: Khan, M. A., Weber, D. J. (eds.) Ecophysiology of High Salinity Tolerant Plants. Tasks for Vegetation Science vol 40, Springer, Dordrecht. https://doi.org/10.1007/1-4020-4018-0_6.

[33] Hassanein, A. M., Mazen, A. M. A. (2001): Adventitious bud formation in Alhagi graecorum. – Plant Cell, Tissue and Organ Culture 65: 31-35. https://doi.org/10.1023/A:1010637407780.

[34] Hildebrandt, T. M., Nunes Nesi, A., Araújo, W. L., Braun, H. P. (2015): Amino acid catabolism in plants. – Mol Plant 8(11): 1563-79. doi: 10.1016/j.molp.2015.09.005. PMID: 26384576.

[35] Huang, Z., Liu, Q., An, B., Wu, X., Sun, L., Wu, P., Liu, B., Ma, X. (2021): Effects of planting density on morphological and photosynthetic characteristics of leaves in different positions on Cunninghamia lanceolata saplings. – Forests 12: 853. https://doi.org/10.3390/f12070853.

[36] Jackson, M. L. (1962): Soil chemical analysis. – Constable and Co. Ltd. London.

[37] Jackson, M. L. (1967): Soil chemical analysis. – Pritice Hall of India Private, New Delhi, India.

[38] Jin, X., Shi, C., Yu, C. Y., Yamada, T., Sacks, E. J. (2017): Determination of leaf water content by visible and near-infrared spectrometry and multivariate calibration in Miscanthus. – Frontiers Plant Science 8: 7 21. https://doi.org/10.3389/fpls.2017.00721.

[39] Juhos, K., Szabó, S., Ladányi, M. (2015): Influence of soil properties on crop yield: a multivariate statistical approach. – International Agrophysics 29: 433-440. https://doi.org/10.1515/intag-2015-0049.

[40] Kamel, A. M., El-Absy, K. M. (2020): Seasonal variations in protein patterns and mineral contents of Lycium showii under different habitat conditions. – Asian Plant Research Journal 6(4): 91-103. https://doi.org/10.9734/aprj/2020/v6i430141.

[41] Kasim, W. A., El-Shourbagy, M. N., Ahmed, A. M., El-Absy, K. M. (2008): Physiological adjustment of Arthrocnemum macrostachyum and Nitraria retusa to Saline Habitats in Sinai, Egypt. – Australian Journal of Basic and Applied Sciences 2(3): 418-428. Corpus ID: 56351907.

[42] Kaspary, T. E., Cutti, L., Bellé, C., Casarotto, G., Ramos, R. F. (2020): Nondestructive analysis of photosynthetic pigments in forage radish and vetch. – Crop Production Rev. Ceres 67(6): 424-431. https://doi.org/10.1590/0034-737X202067060001.

http://www.aloki.hu ● ISSN 1589 1623 (Print) ● ISSN1785 0037 (Online)
DOI: http://dx.doi.org/10.15666/aeer/2003_22152233

[43] Kaur, R., Kaur, R., Sharma, A., Kumar, V., Sharma, M., Bhardwaj, R., Thukral, A. K. (2018): Microbial production of dicar-boxylicacids from edible plants and milk using GC-MS. – Journal of Analytical Science and Technology 9(1): 21. http://dx.doi.org/10.1186/s40543-018-0154-0.

[44] Kebbas, S., Lutts, S., Aid, F. (2015): Effect of drought stress on the photosynthesis of Acacia tortilis subsp. raddiana at the young seedling stage. – Photosynthetica 53: 288-298. https://doi.org/10.1007/s11099-015-0113-6.

[45] Kumar, V., Sharma, A., Kaur, R., Thukral, A. K., Bhardeaj, R., Ahmed, P. (2017): Differential distribution of amino acids in plants. – Amino Acids 49: 821-869. https://doi.org/10.1007/s00726-017-2401-x.

[46] Kumar, V., Sharma, A., Kohli, S. K., Yadav, P., Bali, S., Bakshi, P., Parihar, R. D., Yuan, H., Yan, D., He, Y., Wang, J., Yang, Y., Bhardwaj, R., Thukral, A. K., Zheng, B. (2019): Amino acids distribution in economical important plants: a review. – Biotechnology Research and Innovation 3(2): 197-207. https://doi.org/10.1016/j.biori.2019.06.004.

[47] Lal, R. (2012): Climate change and soil degradation mitigation by sustainable management of soils and other natural resources. – Agricultural Research 1: 199-212. https://doi.org/10.1007/s40003-012-0031-9.

[48] Li, Y., He, N., Hou, J., Xu, L., Liu, C., Zhang, J., Wang, Q., Zhang, X., Wu, X. (2018): Factors influencing leaf chlorophyll content in natural forests at the biome scale. – Frontiers Ecology and Evolution 6: 64. https://doi.org/10.3389/fevo.2018.00064.

[49] Lichtenthaler, H. K. (1987): Chlorophylls and carotenoids: pigments of photosynthetic biomembranes. – In: Packer, L., Douce, R. (ed.) Methods in enzymology, London: Academic Press 148: 350-382. https://doi.org/10.1016/0076-6879(87)48036-1.

[50] Liu, R., Pan, Y., Bao, H., Liang, S., Jiang, Y., Tu, H., Nong, J., Huang, W. (2020): Variations in soil physico-chemical properties along slope position gradient in secondary vegetation of the Hilly region, Guilin, Southwest China. – Sustainability 12(4): 1303. https://doi.org/10.3390/su12041303.

[51] Maathuis, F. J. M. (2009): Physiological functions of mineral macronutrients. – Current Opinion in Plant Biology 12(3): 250-258. https://doi.org/10.1016/j.pbi.2009.04.003.

[52] Mabeza, G., Irvine, D., Mpofu, T., Masama, E. (2014): Potential of Acacia tortilis as protein concentrate for goats. – Journal of Renewable Agriculture 2(4): 49-52. https://doi.org/10.12966/jra.12.01.2014.

[53] Malakootian, M., Mahvi, A. H., Mansoorian, H. J., Khanjani, N. (2018): Agrowaste based ecofriendly bio-adsorbent for the removal of phenol: Adsorption and kinetic study by Acacia tortilis pod shell. – Chiang Mai Journal of Science 45(1): 55-368.

[54] Metwally, M. S., Shaddad, S. M., Liu, M., Yao, R. J., Abdo, A. I., Li, P., Jiao, J., Chen, X. (2019): Soil properties spatial variability and delineation of site-specific management zones based on soil fertility using fuzzy clustering in a hilly field in Jianyang, Sichuan, China. – Sustainability 11(24): 7084. https://doi.org/10.3390/su11247084.

[55] Mohamed, S., Khattab, H., Morsy, A. (2018): Assessment of environmental fluctuations in phytochemical constituents of some xerophytes inhabiting Wadi Sudr and their antimicrobial bioactivity. – Egyptian Journal of Botany 58(3): 515-527. https://doi.org/10.21608/ejbo.2018.3690.1174.

[56] Mohammed, M., Abule, E., Lisanework, N. (2016): Impact of woody plants species on soil physico-chemical properties along grazing gradients in rangelands of eastern Ethiopia. – Tropical and Subtropical Agroecosystems 19: 343-355.

[57] Morsy, A., Khatab, H. K., Sherbiny, E. A., Eldemirdash, J. E. (2015): Floristic diversity and vegetation analysis of Wadi Sudr, south-west Sinai peninsula. – Taeckholmia 35: 99-119. https://doi.org/10.21608/TAEC.2015.12223.

[58] Nasir Khan, M., Mobin, M., Abbas, Z. K., Al-Mutairi, K. A. (2016): Impact of varying elevations on growth and activities of antioxidant enzymes of some medicinal plants of Saudi Arabia. – Acta Ecologica Sinica 36(3): 141-148. https://doi.org/10.1016/j.chnaes.2015.12.009.

http://www.aloki.hu ● ISSN 1589 1623 (Print) ● ISSN1785 0037 (Online)
DOI: http://dx.doi.org/10.15666/aeer/2003_22152233

[59] Nasser, A., Barakat, M., Laudadio, V., Cazzato, E., Tufarelli, V. (2013): Potential contribution of Retama raetam (Forssk.) Webb & Berthel as a forage shrub in Sinai, Egypt. – Arid Land Research and Management 27(3): 257-271. https://doi.org/10.1080/15324982.2012.756561.

[60] Orwa, C., Mutua, A., Kindt, R., Jamnadass, R., Anthony, S. (2009): Agroforestree Database: a tree reference and selection guide version 4.0. – World Agroforestry Centre, Kenya.

[61] Osuagwu, G. G. E., Edeoga, H. O. (2012): The influence of water stress (drought) on the mineral and vitamin contnt of leaves of Gongronema latifolium (Benth). – International Journal of Medicinal and Aromatic Plants 2: 301-309.

[62] Pellet, P. I., Young, V. R. (1980): Nutritional Evaluation of Protein Foods. – The United Nation's University Hunger Programme. Food and Nutrition Bulletin, Suppl. 4, The United University, Tokyo.

[63] Pires, M. V., Pereira Júnior, A. A., Medeiros, D. B., Daloso, D. M., Pham, P. A., Barros, K. A., Engqvist, M. K., Florian, A., Krahnert, I., Maurino, V. G., Araújo, W. L., Fernie, A. R. (2016): The influence of alternative pathways of respiration that utilize branched-chain amino acids following water shortage in Arabidopsis. – Plant Cell Environment 9(6): 1304-19. doi: 10.1111/pce.12682.

[64] Pradhan, A. K., Rehman, M., Saikia, D., Jyoti, S. Y., Poudel, J., Tanti, B. (2020): Biochemical and mlecular mechanism of abiotic stress tolerance in plants. – Plant ecophysiology and adaptation under climate change: Mechanisms and Perspectives I. Springer, pp. 825-853. https://doi.org/10.1007/978-981-15-2156-0.

[65] Prajapati, K., Modi, H. (2012): The importance of potassium in plant growth-a review. – Indian Journal Plant Physiology 1(02): 177-186.

[66] Pua, E. C., Davey, M. (2007): Tropical Tree Legumes. – In: Pua, E. C., Davey, M. (eds.) Transgenic Crops V. Biotechnology in Agriculture and Forestry vol 60. Springer, Berlin, Heidelberg. https://doi.org/10.1007/978-3-540-49161-3_17.

[67] Pyankov, V. I., Ivanov, L. A., Lambers, H. (2001): Chemical composition of the leaves of plants with different ecological strategies from the boreal zone. – Russian Journal of Ecology 32: 221-229. https://doi.org/10.1023/A:1011354019319.

[68] Rowell, D. L. (1994): Soil science methods and applications. – Longman Publishers, Singapors, 229p.

[69] Rubanza, C. D., Shem, M. N., Bakengesa, S. S., Ichinohe, T., Fujihara, T. (2007): The content of protein, fibre and minerals of leaves of selected Acacia species indigenous to north-western Tanzania. – Archives of Animal Nutrition 61(2): 151-156. doi: 10.1080/17450390701203907.

[70] Said, R. (1962): The Geology of Egypt. – Elsevier, Amsterdam, 377p. https://doi.org/10.1126/science.140.3562.41-a.

[71] Salama, F., Sayed, S., Abd El-Gelil, A. (2015): Ecophysiological responses of Calligonum polygonoides and Artemisia judaica plants to severe desert aridity. – Turk Journal Botany 39(2): 253-266. DOI:10.3906/BOT-1404-15. Corpus ID: 73551642.

[72] Salama, F. M., Abd El-Ghani, M. M., Gaafar, A. E., Hasanin, D. M., Abd El-Wahab, D. A. (2021): Adaptive eco-physiological mechanisms of Alhagi graecorum in response to severe aridity in the Western desert of Egypt. – Plant Biosystems - An International Journal Dealing with all Aspects of Plant Biology. https://doi.org/10.1080/11263504.2021.1887957.

[73] Sharma, S. (1996): Applied Multivariate Techniques. – Wiley: New York, NY, USA.

[74] Singh, C., Khajuria, H. N. (1991): Evaluation of acacias-chlorophyll content. – Advances in Plant Sciences 4(2): 252-255.

[75] Singh, G. (2004): Growth, biomass production, and soil water dynamics in Acacia tortilis plantation in relation to microhabitat and surface vegetation in the hot arid region of Indian desert. – Arid Land Research and Management 18(2): 153-169. https://doi.org/10.1080/15324980490280816.

http://www.aloki.hu ● ISSN 1589 1623 (Print) ● ISSN1785 0037 (Online)
DOI: http://dx.doi.org/10.15666/aeer/2003_22152233

[76] Tuzuner, A. (1990): Soil and water laboratory analysis guide. – Ankara: General Directorate of Rural Services Publications.
[77] Verslues, P. E., Sharma, S. (2010): Proline metabolism and its implications for plantenvironment interaction. – Arabidopsis Book 8: e0140. https://doi.org/10.1199/tab.0140.
[78] Wyn Jones, R. (1981): Salt tolerance. – Physiology Processes Limiting Plant Productivity.
[79] Yadav, P. K. R., Kothiyal, P. (2013): A review on Acacia tortilis. – International Journal of Pharmaceutical and Phytopharmacological Research 3(2): 93-96.
[80] Yamada, M., Morishita, H., Urano, K., Shiozaki, N., Kazuko, Y., Shinozaki, K., Yoshiba, Y. (2005): Effects of free proline accumulation in petunias under drought stress. – Journal of Experimental Botany 56(417): 1975-1981. https://doi.org/10.1093/jxb/eri195.
[81] Yinping, L., Tian, H., He, Q., Geng, Z., Yan, S., Tuniyazi, G., Bai, X. (2021): Investigation of the geographical environment impact on the chemical components of *Peganum harmala* L. Through a Combined Analytical Method. – ACS Omega 6(39): 25497-25505. https://doi.org/10.1021/acsomega.1c03420.
[82] Yuvaraj, M., Pandiyan, M., Gayathri, P. (2020): Role of legumes in improving soil fertility status. – In: Hasanuzzamanm, M. (ed.) Legume crops - prospects, production and uses. IntechOpen, http://dx.doi.org/10.5772/intechopen.93247.
[83] Zhang, Y. M., Chen, Y. N., Pan, B. R. (2005): Distribution and floristics of desert plant communities in the lower reaches of Tarim River, southern Xinjiang, People's Republic of China. – Journal of Arid Environments 63(4): 772-784. https://doi.org/10.1016/j.jaridenv.2005.03.023.
[84] Zheng, H., Zhao, H., Liu, H., Wang, J., Detang Zou, D. (2015): QTL analysis of Na+ and K+ concentrations in shoots and roots under NaCl stress based on linkage and association analysis in japonica rice. – Euphytica 201: 109-121. https://doi.org/10.1007/s10681-014-1192-3.
[85] Zhu, S., Guo, S., Duan, J. A., Qian, D., Yan, H., Sha, X., Zhu, Z. (2017): UHPLC-TQ-MS coupled with multivariate statistical analysis to characterize nucleosides, nucleobases and amino acids in Angelicae sinensis radix obtained by different drying methods. – Molecules (Basel, Switzerland) 22(6): 918. https://doi.org/10.3390/molecules22060918.

http://www.aloki.hu ● ISSN 1589 1623 (Print) ● ISSN1785 0037 (Online)
DOI: http://dx.doi.org/10.15666/aeer/2003_22152233

VOLATILE OIL COMPOSITION OF *TEUCRIUM* SPECIES OF NATURAL AND CULTIVATED ORIGIN IN THE LAKE DISTRICT OF TURKEY

DÖNMEZ, İ. E.

Department of Forest Products Engineering, Faculty of Forestry, Isparta University of Applied Sciences, 32100 Isparta, Turkey
e-mail: emrahdonmez@isparta.edu.tr; phone: +90-246-214-6521; fax: +90-246-214-6599

(Received 21st Oct 2021; accepted 17th Mar 2022)

Abstract. The genus *Teucrium* belongs to the *Lamiaceae* family. *Lamiaceae* is one of the important plant groups because most members of this group are used as medicinal and aromatic plants. In this study, the leaves and flowers of *Teucrium chamaedrys subsp. chamaedrys* and *Teucrium polium*, which were taken from both their natural habitat and cultivars, were analysed by SPME and GC-MS in two vegetation periods. The amount and the composition of volatile oil of cultivated plants were compared with plants from natural areas. Caryophyllene (12.20-23.74%) was the most abundant component in all samples of *Teucrium chamaedrys* except in samples from natural habitats of the first vegetation period. Moreover, 2-hexen-1-al (12.79-13.98%), germacrene-D (11.99-19.60%) and α-pinene (3.80-11.68%) were the dominant components of the *T. chamaedrys,* while in *Teucrium polium* samples, β-myrcene (19.52-25.28%) was the common component in both sampling area of the first vegetation period, limonene (30.87-31.79%) had the highest amount in the second vegetation period. Besides, α-thujone (3.13-18.87%), α-pinene (0.94-17.93%) and germacrene-D (4.31-15.63%) were detected as major components in samples from both natural habitats and cultivars of *T. polium*.
Keywords: *Lamiaceae, SPME, GC-MS, Myrcene, Pinene, Germacrene*

Introduction

Volatile oils can be obtained from plants or herbal drugs, and they have distinctive odor, taste besides color, appearance and have volatile compounds at room temperature. It is known that volatile oil contains a large amount of terpenes and a small amount of alcohols, aldehydes, esters and phenolics (Edris, 2007). There are many ways to reveal the volatile oil components of plants. Although distillation and extraction are quite well-known methods, Solid Phase Micro Extraction (SPME) is used as it is new and easily applicable. It is suitable for both combining the sample preparation, extraction and concentration sections in a single step and for providing significant gains in processing time and cost. To identify volatile organic compounds in the samples SPME can be combined with Gas Chromatography-Flame Ionization Detector (GC-FID) or Gas Chromatography-Mass Spectrometry (GC-MS) (Vas and Vekey, 2004). There are many studies about volatile oils (Tumen et al., 2010; Fakir et al., 2014; Dönmez and Salman, 2017), chemical composition of bush, shrubs or especially medicinal and aromatic plants are gaining interest because of the extension of the area of usage (Bahramikia and Yazdanparast, 2012; Özcan et al., 2013).

Volatile oils can be used in many areas and volatile oil of medicinal and aromatic plants has gained an important role from the aspect of science and economics. Using plants as a treatment of some illness is common all over the world since ancient times. Moreover, volatile oils are used to prepare primitive medicine and drugs by folk. In recent years, the use of volatile oils has also increased with the increase of interest in aromatherapy and phytotherapy, which is a branch of alternative medicine (Rangahau, 2001).

http://www.aloki.hu ● ISSN 1589 1623 (Print) ● ISSN 1785 0037 (Online)
DOI: http://dx.doi.org/10.15666/aeer/2003_22352245

The *Lamiaceae* family grows almost everywhere in the Mediterranean climate regardless of the plant type and height. *Lamiaceae* family has 400 genus and 3200 species around the world, and it is represented by 45 genus and more than 546 species in Turkey. Most of the members of the *Lamiaceae* family *Lavandula sp., Mellissa sp., Mentha sp., Origanum sp., Thymus sp., Salvia sp.*), due to their ornamental leaves and flowers, are rich in volatile oils. It has a great importance in some industries such as landscape, medicine, pharmacy, food, cosmetics and perfumery and there are many studies on these plants (Başer, 2008; Kargıoglu et al., 2008; Kahraman et al., 2009; Dönmez, 2016; Wesolowska and Jadczak, 2019; Alsaraf et al., 2021; Virchea et al., 2021). *Teucrium chamaedrys* subsp. *chamaedrys* and *Teucrium polium* are species which belong to the *Lamiaceae* family. Although there are studies on the medicinal and aromatic properties of these species (Katayoun et al. 2005; Bağcı et al., 2010; Belmakki et al., 2013; Özcan et al., 2013; Raei et al., 2013), the changes in the composition and amount of volatile oil after cultivation studies are not known. For this reason, these two taxa were evaluated in the study.

The genus *Teucrium* consists of about 100 species and it can be seen in temperate regions of Asia, Europe and North Africa (Mabberley, 1997; Bukhari et al., 2015). The species belonging to this genus have been used for the treatment of various diseases since ancient times, due to the various active substances they contain. It is known that some species of this genus, which are among the medicinal and aromatic plants, are used in the treatment of diabetes in different countries (Baytop, 1991; Dönmez, 2019; Dönmez and Önal, 2019).

Teucrium chamaedrys L. subsp. *chamaedrys* L. can be found up to 1800 m. from sea level in the European-Siberian region. It can also be seen in the western part of the Mediterranean, Agean, Marmara and Central Anatolian part of Turkey in forest clearings, steep cliffs, slopes and barren pastures (Tekin, 2007). It is a perennial woody plant which has 20-30 cm diameter and 15-30 cm length. Leaves have 1.4 × 1.8 cm in rectangle aspect, flowerbeds are 0.5 × 1.2 cm and they have pink color. Virgo flowers are 12-20 cm long and the flowering period is 2 months (June-July). It is also known that the vegetation period is 6 months (March-September).

Teucrium polium is widely distributed in the Mediterranean countries and in the Middle East. It grows naturally in all regions in Turkey up to 2050 m from sea level and can be found in bushes and maquies, steppes, fields, rocks and arid slopes (Davis, 1982; Tekin, 2007), *Teucrium polium* has 8-15 cm length and 10-40 cm diameter. Moreover, the leaves are 0.15 × 0.75 cm and rectangular, the flowers are 0.4 × 0.7 cm and whitish, Virgo flowers are 5-12 cm long. The structure of leaves and body are more effective in the visual characteristics of the plant compared to its flower. The vegetation duration is 6 months (March-August) and the flowering period is 4 months (April-July). (Elmasri et al., 2016).

In this study, it was aimed to determine the composition and the amount of volatile oil and the yield of the same plant species in both natural habitat and their cultivars after the cultivation of *Teucrium chamaedrys* subsp. *chamaedrys* and *Teucrium polium*.

Materials and methods

Materials

Teucrium chamaedrys subsp. *chamaedrys* and *Teucrium polium*, belonging to *Lamiaceae* family, were used for determining volatile oil yield and composition. In the

http://www.aloki.hu ● ISSN 1589 1623 (Print) ● ISSN 1785 0037 (Online)
DOI: http://dx.doi.org/10.15666/aeer/2003_22352245

vegetation period of 2015, field studies were carried out and the areas where the plants grow naturally were determined. *Teucrium chamaedrys* subsp. *chamaedrys* was taken from Aziziye, Burdur and *Teucrium polium* was removed from another region of Aziziye, Burdur. During the flowering period (July), the plants were collected with their roots and planted in Isparta Süleyman Demirel University (SDU) Botanical Garden, named as cultivation area. Environmental characteristics of both areas can be seen in *Table 1*. Experimental plots in the cultivation area were established in SDU Botanical Garden in accordance with the "Randomized Complete Block Design" with 3 replications and 25 plants for each replication at a depth of 30 cm with a distance of 20 cm between plants (*Fig. 1*). The plants were irrigated every other day between June and August. Survival rate of *Teucrium chamaedrys* subsp. *chamaedrys* and *Teucrium polium* was 96% and 72%, respectively, at the end of the 2016 and 2017 vegetation period. In 2016 and 2017, during the flowering period (July) of the plants, approximately 10 samples were taken simultaneously from both the natural and cultivation area and stored at -24 °C until volatile oil analysis.

Table 1. *Details and environmental characteristics of sampling areas*

		Longitude (E)	Latitude (N)	Altitude (m)	Relative humidity (%)	Min. temp. (°C)	Max. temp. (°C)	Average annual temp. (°C)	Average annual rainfall (mm)
N.H.	T. c.	30° 15' 25"	37° 25' 30"	1600	55	-15.0	41.0	13.3	429
	T. p.	30° 14' 31"	37° 24' 40	1200					
C.A.		30°31' 39	37°50' 46"	1025	61	-21.0	38.7	12.3	508.3

N.H.: Natural Habitat (Burdur-Aziziye), C.A.: Cultivation area (Isparta-SDU Botanical Garden), T.c.: *Teucrium chamaedrys* subsp. *chamaedrys,* T.p.: *Teucrium polium*

Figure 1. *A view of T. chamaedrys subsp. chamaedrys and (a) and T. Polium (b)*

Volatile oil yield

In order to determine volatile oil yield, hydrodistillation with Clevenger apparatus (European type Clevenger apparatus, Ildam Cam Ltd. Ankara-Turkey) was used. The material is directly immersed in water, and it had direct contact with hot water and heat. For determining volatile oil yield of each species, 100 g ground samples were submitted to hydrodistillation for 5 h using a Clevenger apparatus. Sampling and hydrodistillation with Clevenger apparatus can be seen in *Figure* 2. Volatile oil yield was calculated as ml/100 g samples (Tümen et al., 2010).

http://www.aloki.hu ● ISSN 1589 1623 (Print) ● ISSN 1785 0037 (Online)
DOI: http://dx.doi.org/10.15666/aeer/2003_22352245


Figure 2. *Sampling and hydrodistillation*

SPME and GC-MS analyses

The leaves and flower samples that were collected from both natural habitat and cultivars were put into paper packages and transferred to the laboratory in the same day to avoid exposure to sunlight and samples were subjected to solid phase microextraction (SPME). 2 g of samples were placed into a 10 ml vial. After incubation for 30 min at 60 °C, SPME fibre was pushed through the headspace of a sample vial to absorb the volatiles and then inserted directly into the injection port of the GC-MS (Shimadzu 2010 Plus GC-MS with the capillary column, Restek Rxi®-5Sil MS 30 m × 0.25 mm, 0.25 µm) at a temperature of 250 °C for desorption (5 min) of the adsorbed volatile compounds. The constituents were identified using retention times of standard substances by aligning mass spectra with the data given in the Wiley, NIST Tutor, FFNSC library.

Results and discussion

Analyses for getting volatile oil and determining volatile oil yield of both *Teucrium* species was performed in two vegetation periods (2016 and 2017) on the samples gathered from their natural habitat and cultivars at the same time.

Volatile oil yield of both *Teucrium* species was calculated after hydrodistillation (*Table 2*). It was found that volatile oil yield of *Teucrium chamaedrys* subsp. *chamaedrys* was found very close in both samples during two vegetation periods. It was determined as 0.20 ml/100 g in natural habitat plants and 0.30 ml/100 g in cultivars in the first vegetation period (2016). It was 0.20 and 0.35 ml/100 g, respectively, in the second vegetation period (2017).

Table 2. *Volatile oil yield of natural habitat and cultivars of Teucrium species*

Volatile oil yield (ml/100 g)	First vegetation period		Second vegetation period	
	Natural habitat	Cultivar	Natural habitat	Cultivar
Teucrium chamaedrys	0.20	0.30	0.20	0.35
Teucrium polium	0.80	0.90	0.85	0.90

Volatile oil yield of *Teucrium polium* was determined higher than that of the *T. chamaedrys*. In the first vegetation period, it was found 0.80 ml/100 g in natural habitat plants and 0.90 ml/100 g in cultivars for *T. polium*. It had also similar results for the

http://www.aloki.hu ● ISSN 1589 1623 (Print) ● ISSN 1785 0037 (Online)
DOI: http://dx.doi.org/10.15666/aeer/2003_22352245

second vegetation period. Natural habitat plants had 0.85 ml/100 g and cultivars had 0.90 ml/100 g volatile oil yield in the second vegetation period for *Teucrium polium*.

The volatile components in the leaves and flowers of *Teucrium* species collected from the sampling plots were identified through gas chromatography mass spectroscopy (GC-MS) after solid phase micro extraction (SPME). The amount and the composition of volatile oil of *Teucrium chamaedrys* L. subsp. *chamaedrys* L. can be seen in *Table 3*. 41 components in the samples from both natural habitat and cultivars of the first vegetation period were determined. However, 44 and 39 components, respectively, were identified in the second vegetation period. Although limonene (13.49%) and 2-hexen-1-al (12.79%) were determined as the dominant components in the samples from natural habitat, caryophyllene (19.82%) and germacrene-D (14.49%) had the highest concentration in the samples from cultivars of the first vegetation period. In addition, caryophyllene, the most abundant component, was found as the major component in the samples from both natural habitat (23.03%) and cultivars (23.74%) in the second vegetation period, like in the samples collected in Corsica and Sardinia studied by Muselli et al. (2009). Germacrene-D was the other component having the highest amount in both samples in the second vegetation period as 18.14% and 19.60% respectively. In the studies by Bağcı et al. (2010), Katayoun et al. (2005) and Maccioni et al. (2021) that germacrene-D was found the dominant component. It was previously reported that germacrene-D was also the most abundant component in some *Lamiaceae* species (Dönmez, 2019).

Table 3. *The amount and the composition of T. chamaedrys subsp. chamaedrys volatile compounds (%)*

Compounds	1st vegetation period		2nd vegetation period	
	Amount (%)		Amount (%)	
	Natural habitat	Cultivars	Natural habitat	Cultivars
Acetaldehyde	0.16	-	-	-
Ethanol	-	0.20	0.02	0.08
2-Butenal	0.16	0.30	-	-
3-Methylbutanal	0.28	0.23	-	-
2- Methylbutanal	-	0.23	-	-
2-Propanone	-	-	0.14	0.20
2-Pentanone	0.67	-	-	-
2-ethyl-Furan	0.64	0.42	-	-
cis-3-Methylcyclohexanol	-	-	0.37	-
n-Hexanal	1.00	1.49	0.61	-
2-Hexen-1-al	12.79	13.98	0.13	0.17
3-Hexene-1-ol	1.91	0.66	0.09	0.10
2-Hexen-1-ol	0.30	0.28	-	-
n-Hexanol	0.83	0.74	-	-
2,4-Hexadienal	0.65	0.70	-	-
α-Thujene	-	-	0.09	0.10
α-pinene	7.68	3.80	10.42	11.68
Benzaldehyde	0.50	0.87	0.54	-
Sabinene	0.16	-	0.21	0.24
β-pinene	4.04	-	-	-
1-Octen-3-one	0.32	-	-	-

http://www.aloki.hu ● ISSN 1589 1623 (Print) ● ISSN 1785 0037 (Online)
DOI: http://dx.doi.org/10.15666/aeer/2003_22352245

Bicycloheptane	-	2.25	5.52	6.34
1-Octen-3-ol	8.74	6.57	0.31	0.36
β-Myrcene	6.98	5.53	0.64	-
Myrcene	-	-	1.21	1.66
2,4-Heptadienal	0.99	0.86	-	-
Ethyl-hexanol	0.32	0.23	-	-
3-Octanone	-	-	0.13	0.26
p-cymene	-	0.19	-	-
Me-Cymol	-	-	0.51	0.73
Limonene	13.49	6.77	16.81	17.72
Benzene acetaldehyde	0.17	0.28	-	-
Benzene	0.16	-	-	-
Benzoic acid	2.29	2.11	-	-
Ocimene	-	0.30	-	-
β- ocimene	0.25	-	0.13	0.26
1,4-Cyclohexadiene	-	-	0.10	0.12
α-terpinolene	0.19	-	-	-
1,6-Octadien-3-ol	0.83	0.61	0.09	0.10
Nonanal	0.16	0.21	-	-
2,4-Octadienal	-	0.24	-	-
l-linalool	-	-	0.19	0.14
α-copaene	0.37	1.08	0.58	0.63
α-Cubebene	0.19	1.04	0.19	0.24
β-bourbonene	2.89	2.51	3.89	4.31
Bicycloelemene	-	-	0.01	0.09
α-Bergamotene	-	-	1.01	0.68
β-cubebene	0.34	1.49	1.64	0.96
α-panasinsen	-	-	1.01	1.37
Caryophyllene	12.20	19.82	23.03	23.74
Caryophyllene oxide	0.82	0.31	0.24	0.30
Germacrene-D	11.99	14.49	18.14	19.60
bicyclogermacrene	0.87	1.12	1.96	1.39
β-Farnesene	-	-	1.32	1.65
Farnesene	-	-	0.09	0.13
Epi-bicyclosesquiphellandrene	0.56	0.30	0.42	0.33
β-Sesquiphellandrene	-	-	0.93	0.07
Cadina-1,4-diene	-	-	0.68	-
γ-Cadinene	0.69	1.33	0.81	0.64
δ-cadinene	-	1.28	-	-
β-selinene	-	-	0.61	0.09
α-Muurolene	0.34	0.37	0.41	0.35
β-Bisabolene	-	0.25	0.26	0.12
α-humulene	1.74	4.24	2.41	2.82
Alloaromadendrene	0.33	0.34	-	-
Camphene	-	-	0.13	0.08
Geranyl nitrile	-	-	0.09	0.07

http://www.aloki.hu ● ISSN 1589 1623 (Print) ● ISSN 1785 0037 (Online)
DOI: http://dx.doi.org/10.15666/aeer/2003_22352245

Volatile components determined by SPME and GC-MS of *Tecrium polium* can be seen in *Table 4*. While 48 components were determined in the natural habitat of *T. polium*, the amount and the composition of the 46 components from cultivars of *T. polium* were identified in the first vegetation period. β-myrcene was found as the highest component in both natural habitat (19.52%) and cultivars (25.28%). α-thujene and Germacrene-D can also be evaluated as major components of *T. polium*. α-thujene was determined as 18.87% in the samples from natural habitat and Germacrene-D was 15.63% in the samples from cultivars of first vegetation period. In the second vegetation period, 53 components in the samples from natural habitat and 45 components from cultivars of *T. polium* were detected. Limonene was the most abundant component of the second vegetation period and it was determined as 30.87% in the samples from natural habitat and 31.79% in the samples from cultivars. In addition, α-pinene was also dominant component of the second vegetation period with 15.68% in the samples from natural habitat and 17.93% in the samples from cultivars of *T. polium*. In most of the studies on the amount and composition of *T. polium*, β-myrcene, Germacrene-D and α-pinene were found as the components with the highest concentration (Belmakki et al., 2013; Özcan et al., 2013; Raei et al., 2013) like in the present study, however, α-thujone and limonene can also be considered as the significant components. On the contrary, the study of Saleh et al. (2020), 6-epi-shyobunol, t-muurolol, germacrene-D, Delta-cadinene and aromadendrene were found as dominant components in the samples collected from Egypt.

Table 4. *The amount and the composition of T. polium volatile compounds (%)*

Compounds	1st vegetation period		2nd vegetation period	
	Amount (%)		Amount (%)	
	Natural habitat	Cultivars	Natural habitat	Cultivars
Acetaldehyde	-	0.15	-	-
1,1-Ethylacetate	-	-	0.12	0.17
2-methylfuran	-	-	0.01	0.04
Allylbromide	-	-	0.11	0.08
Ethanol	0.25	0.80	-	-
2-Butenal	0.90	0.76	-	-
2-ethyl-Furan	0.26	-	-	-
Valeraldehyde	-	0.17	-	-
cis-3-Methylcyclohexanol	-	0.20	-	-
n-Hexanal	0.44	0.51	0.35	-
2-Hexen-1-al	5.62	4.88	0.2	0.24
3-Hexene-1-ol	0.39	0.56	0.1	0.11
n-Hexanol	0.25	0.26	-	-
2,4-Hexadienal	0.22	-	0.61	-
α-Thujene	18.87	11.43	3.13	3.80
α-pinene	0.94	-	15.68	17.93
2,6,6-Trimethylbicyclohept-2-ene	0.28	0.54	0.11	0.15
Bicyclohex-2-ene,	-	0.16	0.09	0.11
Camphene	-	-	0.2	0.21
Benzaldehyde	0.40	0.81	-	-
Sabinene	9.89	5.68	1.79	2.09
1-Octen-3-one	-	-	0.31	0.43

http://www.aloki.hu ● ISSN 1589 1623 (Print) ● ISSN 1785 0037 (Online)
DOI: http://dx.doi.org/10.15666/aeer/2003_22352245

Bicycloheptane,	1.16	0.65	4.98	5.87
1-Octen-3-ol	1.17	2.27	0.64	0.33
β-Myrcene	19.52	25.28	3.87	4.58
2,4-Heptadienal,	0.18	0.39	-	-
3-Octanol	0.24	-	-	-
l-Phellandrene	0.17	-	-	-
ethyl-Hexanol	-	0.71	-	-
2,4-Heptadienal,	0.29	0.55	-	-
α-terpinene	1.00	-	0.11	017
p-cymene	2.30	-	-	-
Cyclopentanecarboxyaldehyde	-	1.83	-	-
Cymol	-	-	3.04	2.92
Me-cymol	-	2.65	-	-
Limonene	3.18	4.48	30.87	31.79
Trans-Limonene oxide	-	-	0.42	0.14
Verbenol	-	-	0.21	0.27
4-terpineol	-	-	0.09	0.12
p-allylanisole	-	-	0.4	0.41
Berbenone	-	-	0.22	0.27
Eucalyptol	-	-	0.13	0.19
Ocimene	0.76	0.63	0.08	0.11
β- ocimene	3.52	3.84	0.71	0.73
Cyclopropane	0.18	-	-	-
Spirohexan-5-on	-	0.25	-	-
1,4-Cyclohexadiene	1.07	0.64	0.75	0.81
α-terpinolene	0.33	0.31	-	-
1,6-Octadien-3-ol	-	-	0.42	0.29
Benzene	0.42	-	-	0.55
Tridecane	-	-	0.51	0.24
l-linalool	0.17	-	0.40	0.43
α-thujone	-	-	0.18	0.16
p-Mentha-1,5,8-triene	0.53	0.49	0.96	-
2,4,6-octatriene	0.59	-	0.81	-
3-Cyclohexen-1-ol	0.48	-	0.23	-
α-copaene	0.88	-	0.15	-
Benzoic acid	-	0.65	-	-
α-Cubebene	-	0.20	-	-
β-bourbonene	0.31	1.22	0.61	0.72
β-elemene	0.30	-	0.18	0.22
Germacrene-B	1.81	-	1.19	1.21
α-Bergamotene	0.35	-	0.14	0.17
β-cubebene	-	0.21	-	-
Germacrene-D	4.31	15.63	10.87	11.33
α-gurjunene	-	-	0.09	0.11
1-Cyclopentacyclopropan benzene	-	0.42	-	-
β-Farnesene	9.23	1.98	4.94	5.26

http://www.aloki.hu ● ISSN 1589 1623 (Print) ● ISSN 1785 0037 (Online)
DOI: http://dx.doi.org/10.15666/aeer/2003_22352245

Epi-bicyclosesquiphellandrene	0.36	0.51	0.28	0.32
Naphthalene	-	0.66	-	0.19
Cadina-1,4-diene	0.29	-	0.87	-
β-selinene	-	0.17	0.15	-
α-cubebene	-	0.72	-	-
bicyclogermacrene	0.54	2.13	1.29	1.39
α-bisabolene	0.60	-	0.55	-
α-muurolene	-	0.37	0.11	0.17
β-Bisabolene	1.29	0.30	-	-
γ-Cadinene	3.14	0.97	0.81	0.91
δ-cadinene	0.19	1.47	0.51	0.63
α-humulene	0.42	-	0.69	-
β-eudesmol	-	0.51	-	-

Conclusions

T. chamaedrys subsp. chamaedrys and *T. polium* were cultivated in 2015. The amount and the composition of the volatile components were identified in 2016 and 2017 by using leaves and flowers of these plant species from both natural habitat and cultivars. It was found that they contained the same components and the amount of components were close to each other in both sampling areas. As a result of the study, it is understood that both *Teucrium* taxa can adapt to the culture area without changing their biochemical properties. This is a particularly important result for these two plant species belonging to the *Lamiaceae* family, which are known to be used as medicinal and aromatic plants. In this direction, it is thought that these plants can be evaluated in industrial scale and can also be used in different industries such as pharmaceuticals and cosmetics due to their chemical composition. While it is evaluated in industrial uses, it will be possible to grow these plants instead of collecting them from nature. Therefore, the biodiversity in the natural habitat will be protected and it will be possible to provide the required plant material sufficiently.

Acknowledgements. This work is a part of a project supported by The Scientific and Technological Research Council of Turkey (TUBITAK) with the project number 114O345. The author would like to thank Doc. Dr. Şirin Dönmez for providing samples.

REFERENCES

[1] Alsaraf, S., Hadi, Z., Akhtar, M. J., Khan, S. A. (2021): Chemical profiling, cytotoxic and antioxidant activity of volatile oil isolated from the mint (*Mentha spicata* L.,) grown in Oman. – Biocatalysis and Agricultural Biotechnology 34: 102034.

[2] Bagci, E., Yazgın, A., Hayta, S., Cakıloglu, U. (2010): Composition of the essential oil of Teucrium chamaedrys L. (Lamiaceae) from Turkey. – Journal of Medicinal Plants Research 4(23): 2587-2589.

[3] Bahramikia, S., Yazdanparast, R. (2012): Phytochemistry and medicinal properties of Teucrium polium L. (Lamiaceae). – Phytotherapy Research 26(11): 93.

[4] Başer, K. H. C. 2008: Biological and phamacological activities of carvacrol and carvacrol bearing essential oils. – Current Pharmaceutical Design 14(29): 3106-3120.

http://www.aloki.hu ● ISSN 1589 1623 (Print) ● ISSN 1785 0037 (Online)
DOI: http://dx.doi.org/10.15666/aeer/2003_22352245

[5] Baytop, T. (1991): Pharmaceutical Botany Textbook (Farmasotik Botanik Ders Kitabı). – Istanbul University Press, Istanbul (in Turkish).
[6] Belmakki, N., Bendimerad, N., Bekhechi, C., Fernandez, X. (2013): Chemical analysis and antimicrobial activity of Teucrium polium L. essential oil from Western Algeria. – Journal of Medicinal Plants Research 7(14): 897-902.
[7] Bukhari, N. A., Al-Otaibi, R. A., Ibrahim, M. M. (2015): Biodiversity characteristics of teucrium polium species in Saudi Arabia. – Saudi Journal of Biological Sciences 22(2): 181-185.
[8] Davis, P. H. (1982): Flora of Turkey and The East Aegean Islands. Vol. 7. – Edinburg University Press, Edinburgh.
[9] Dönmez, Ş. (2016): Uses of some medicinal and aromatic plants in the landscape architecture grown in the Lakes District. – International Journal of Advanced Research 4(8): 30-36.
[10] Dönmez, Ş. (2019): Volatile oil composition of *ajuga* species of natural and cultivated origin in the Lake District of Turkey. – Applied Ecology and Environmental Research 17(2): 3859-3866.
[11] Dönmez, Ş., Önal, F. (2019): Germination ability and biochemical properties of *Ajuga chamaepitys* subsp. *chia* var. chia and *Ajuga orientalis* cultivated in climatic conditions in Lake District, Turkey. – Applied Ecology and Environmental Research 17(2): 3837-3848.
[12] Dönmez, İ. E., Salman, H. (2017): Volatile compounds of myrtle (*Myrtus communis* L.) leaves and berries. – Turkish Journal of Forestry 18: 328-332.
[13] Edris, A. E. (2007): Pharmaceutical and therapeutic potentials of essential oils and their individual volatile constituents: a review. – Phytotherapy Research: An International Journal Devoted to Pharmacological and Toxicological Evaluation of Natural Product Derivatives 21(4): 308-323.
[14] Elmasri, W. A., Hegazy, M. F., Mechef, Y., Paré, W. P. (2016): Structure-antioxidant and antitumor activity of *Teucrium polium* phytochemicals. – Phytochemistry Letters 15: 81-87.
[15] Fakir, H., Erbaş, S., Özen, M., Dönmez, İ. E. (2014): The effects of different harvest dates on essential oil content and composition in chaste tree (Vitex agnus-castus L.) (Hayıt (*Vitex agnus-castus* L.) (da Farklı Toplama Zamanlarının Uçucu Yağ Oranı ve Bileşenleri Üzerine Etkisi. – European Journal of Science and Technology 1: 25-28 (in Turkish).
[16] Kahraman, A., Celep, F., Doğan, M. (2009): Morphology, anatomy and palynology of *Salvia indica* L. (Labiatae). – World Applied Sciences Journal 6(2): 289-296.
[17] Kargıoğlu, M., Cenkci, S., Serteser, A., Evliyaoğlu, N. (2008): An ethnobotanical survey of Inner-West Anatolia Turkey. – Human Ecology 36: 763-777.
[18] Katayoun, M., Akbarzadeh, M., Rostami, B. (2005): The essential oil composition of *Teucrium chamaedrys* L. from Iran. – Flavour and France Journal 20(5): 544-546.
[19] Mabberley, D. J. (1997): The Plant Book. A Portable Dictionary of the Vascular Plants. – Cambridge University Press, Cambridge.
[20] Mehrabani, D., Rezaee, A., Azarpira, N., Fattahi, M. R., Amini, M., Tanideh, N., Panjehshahin, M. R., Saberi-Firoizi, M. (2009): The healing effects of *Teucrium polium* in the repair of indomethacin-induced gastric ulcer in rats. – Saudi Medical Journal 30(4): 494-499.
[21] Maccioni, A., Falconieri, D., Sanna, C., Porcedda, S., Piras, A., Maxia, A. (2021): Characterization of essential oils from different taxa belonging to the genus *Teucrium* in Sardinia Island, Italy. – Plants 10(7): 1359.
[22] Muselli, A., Desjobert, J. M., Paolini, J., Bernardini, A. F., Costa, J., Rosa, A., Dessi, M. A. (2009): Chemical composition of the essential oils of *Teucrium chamaedrys* L. from Corsica and Sardinia – Journal of Essential Oil Research 21: 138-143.
[23] Özcan, S., Yılar, M., Belgüzar, S., Önen, H. (2013): Chemical composition, antifungal and herbicidal effects of essential oil isolated from *Teucrium polium* L. (*Teucrium polium*

http://www.aloki.hu ● ISSN 1589 1623 (Print) ● ISSN 1785 0037 (Online)
DOI: http://dx.doi.org/10.15666/aeer/2003_22352245

L.) (Uçucu Yağının Herbisidal ve Antifungal Etkileri ile Kimyasal İçeriğinin Belirlenmesi). – Gaziosmanpaşa Journal of Scientific Research 5: 94-103 (in Turkish).

[24] Raei, F., Ashoori, N., Eftekhar, F., Yousefzadi, M. (2013): Chemical composition and antibacterial activity of *Teucrium polium* essential oil against urinary isolates of *Klebsiella Pneumoniae*. – Journal of Essential Oil Research 26(1): 65-69.

[25] Rangahau, M. K. (2001): Essential oils and their production. –Crop and Food Research 39: October.

[26] Saleh, I., Abd-ElGawad, A., El Gendy, A. E. N., Abd El Aty, A., Mohamed, T., Kassem, H., Aldosri, F., Elshamy, A., Hegazy, M. E. F. (2020): Phytotoxic and antimicrobial activities of *Teucrium polium* and *Thymus decussatus* essential oils extracted using hydrodistillation and microwave-assisted techniques. – Plants 9(6): 716.

[27] Tekin, E. (2007): The Best Wild Flowers of Turkey (Türkiye'nin En Güzel Yabani Çiçekleri). – Turkish Isbank Publications, Ankara (in Turkish).

[28] Tümen, İ., Hafızoğlu, H., Kılıç, P. A., Dönmez, İ. E., Sivrikaya, H., Reunanen, M. (2010): Yields and constituents of essential oil from cones of *Pinaceae* spp natively grown in Turkey. – Molecules 15: 5797-5806.

[29] Vas, G., Vekey, K. (2004): Solid-phase microextraction: a powerful sample preparation tool prior to mass spectrometric analysis. –Journal of Mass Spectrometry 39:233-254.

[30] Virchea, L. I., Gligor, F. G., Frum, A., Mironescu, M., Myachikova, N. I., Georgescu, C. (2021): Phytochemical analysis and antioxidant assay of *Melissa officinalis* L. (lemon balm). – In BIO Web of Conferences 40: 02004.

[31] Wesolowska, A., Jadczak, D. (2019): Comparison of the chemical composition of essential oils isolated from two thyme (*Thymus vulgaris* L.) cultivars. – Notulae Botanicae Horti Agrobotanici Cluj-Napoca 47(3): 829-835.

http://www.aloki.hu ● ISSN 1589 1623 (Print) ● ISSN 1785 0037 (Online)
DOI: http://dx.doi.org/10.15666/aeer/2003_22352245

INFLUENCE OF PLANT GEOMETRY AND INTERCROPPING ON SOIL FERTILITY AND NUTRIENT BUDGETING UNDER SUSTAINABLE SUGARCANE INITIATIVE PLANTING OF SUGARCANE (*SACCHARUM OFFICINARUM* L.) IN INDIA

SARANRAJ, T.[1*] – NAGESWARI, R.[2] – CHANDRASEKARAN, R.[3] – TAYADE, A. S.[4]

[1]*ICAR-KVK, TNAU, Vellore, Tamil Nadu, India*

[2]*TNAU, Tapioca and Castor Research Station, Salem, Tamil Nadu, India*

[3]*AC & RI, Kudumiyanmalai, TNAU, Tamil Nadu, India*

[4]*ICAR-Sugarcane Breeding Institute, Coimbatore, Tamil Nadu, India*

**Corresponding author*
e-mail: tsaranrajagronomy@gmail.com

(Received 27th Oct 2021; accepted 25th Feb 2022)

Abstract. Field experiments were conducted at Sugarcane Research Station, Tamil Nadu Agricultural University, Tamil Nadu during 2016-17 and 2017-18. The experiments were laid out the strip plot design with three replications. Among the different crop geometries, sugarcane double planting at 150 cm registered significantly higher available N, P and K in the post harvest soil which was closely followed by those at 150 cm in single row. With respect to different intercropping systems, higher available NPK was recorded under sugarcane + sunn hemp intercropping. The treatment combination of 150 cm double row planting with sunn hemp as intercrop recorded higher soil available P. The result of nutrient balance studies revealed sugarcane planting in double row at 150 cm crop geometry along sunn hemp as a planting system more favorable for the restoration of soil fertility where in higher net available N and P was observed. The results of the experiments revealed that double row planting of sugarcane at 150 cm spacing with *in-situ* incorporation of sunn hemp on 45th DAS increased the nutrient availability and maintained soil fertility of plant- ratoon sugarcane agroecosystem under tropical Indian conditions.
Keywords: *sustainable sugarcane initiative (SSI), plant geometry, intercropping, soil fertility and nutrient budgeting*

Introduction

Seed material, water and fertilizers are the important inputs for sugarcane production. Sustainable Sugarcane Initiative (SSI) is a method of sugarcane production which involves use of less seed materials, water and optimum fertilizers to achieve higher yields. Among the various irrigation methods, surface drip irrigation is the most efficient method for enhancing the input use efficiency of both water and nutrients. SSI under surface drip fertigation system can improve the water and nutrient use efficiency. Maintaining optimum plant population with suitable crop geometry is an important factor for sustained cane production and introduction of mechanization.

Significant differences in the uptake of N, P and K due to influence of various row spacing's and intercrops were observed by More (2003). The uptake of nutrients also differed significantly and it was higher in paired row planting (150 cm) than single row planting (270 cm) of sugarcane. Patel et al. (2014) observed that the planting geometries had significant influence on nutrient content in sugarcane plant and nutrient status of soil after harvest, while, uptake of nutrients by sugarcane were higher under 60-120-

http://www.aloki.hu ● ISSN 1589 1623 (Print) ● ISSN 1785 0037 (Online)
DOI: http://dx.doi.org/10.15666/aeer/2003_22472259

60 cm paired row planting compared to normal 90 cm and 120 cm twin row planting geometries. In the context of sugarcane mechanization, the SSI method of sugarcane planting is gaining more significance under tropical Indian sugarcane farming; however, the information on suitable crop geometries benefitting for the intercrop to restore the depleting soil health of plant-ratoon sugarcane agroecosystem is lacking.

With this background, the present field experiment was conducted to assess the nutrient budgeting and soil fertility status under different plant geometry and intercropping under sustainable sugarcane initiative.

Materials and methods

Field experiments were laid out during *special* seasons of 2016-17 and 2017-18 at Sugarcane Research Station, Tamil Nadu Agricultural University (TNAU), Sirugamani, located at Cauvery delta zone of Tamil Nadu. The geographical location of the experiment site is 10° 56'N latitude and 78° 26'E longitude with an altitude of 78.12 m above the MSL. The farm receives an average rainfall of 730.3 mm. The soil of the experimental site was well drained clay loam in texture with low in available nitrogen, medium in available phosphorus and high in available potassium. The initial soil status showed 234, 15.8 and 467 kg/ha of $KMnO_4$-N, Olsen P and NH_4OAc-K, respectively. The soil EC (0.29 dsm^{-1}) pH (8.58) and organic carbon (0.58%) indicated fairly suitable soil for the growth sugarcane crop. The experiments were laid out in strip plot design (SPD) with four treatments in main plot and four treatments in sub plot replicated thrice. The net plot size adopted was 27.0 m^2 (9.0 m × 3.0 m). Short duration pulses of green gram (ADT 3), black gram (VBN5) and sunn hemp (CO1) maturing in 60-75 days were used for the study. The main plot treatments comprised of crop geometry *viz.,* M_1- 150 × 60 cm Single row planting, M_2-150 × 60 cm Double row planting, M_3- 180 × 60 cm Single row planting and M_4-180 × 60 cm Double row planting (*Table 1*). The subplot treatments were S_1-Sole crop of Sugarcane, S_2-Sugarcane + Green gram, S_3-Sugarcane + Black gram and S_4-Sugarcane + Sunn hemp. The intercrops were raised in additive series *viz*., 3 rows under a row spacing of 150 cm in sugarcane and 4 rows under 180 cm (*Fig. 1*). The recommended schedule of drip fertigation for SSI was followed under surface drip irrigation system. The recommended dose followed was 300:100:200 kg/NPK/ha^{-1}. No additional fertilizers were applied to the intercrops.

Table 1. *Number of bud chip settling used per hectare in different crop geometries*

Different crop geometries adopted for SSI planting method			
Single row planting		**Double row planting**	
150 cm × 60 cm	180 cm × 60 cm	150 cm × 60 cm	180 cm × 60 cm
11,111	9,260	22,222	18,520

Post-harvest soil samples after the harvest of plant crop and ratoon crop were collected plot wise from a depth of 0-20 cm. The soil samples collected by using screw augur were air dried, powdered and passed through a 2 mm sieve and stored in clean polythene bags. The samples thus collected and processed were used for the determination of available nitrogen, phosphorus and potassium (kg ha^{-1}).

http://www.aloki.hu ● ISSN 1589 1623 (Print) ● ISSN 1785 0037 (Online)
DOI: http://dx.doi.org/10.15666/aeer/2003_22472259

The net gain in available nitrogen, phosphorus and potassium (kg ha^{-1}) was calculated using the corresponding available nutrient status at the beginning and at the end of the specific period (Sadanandan and Mahapatra, 1973).

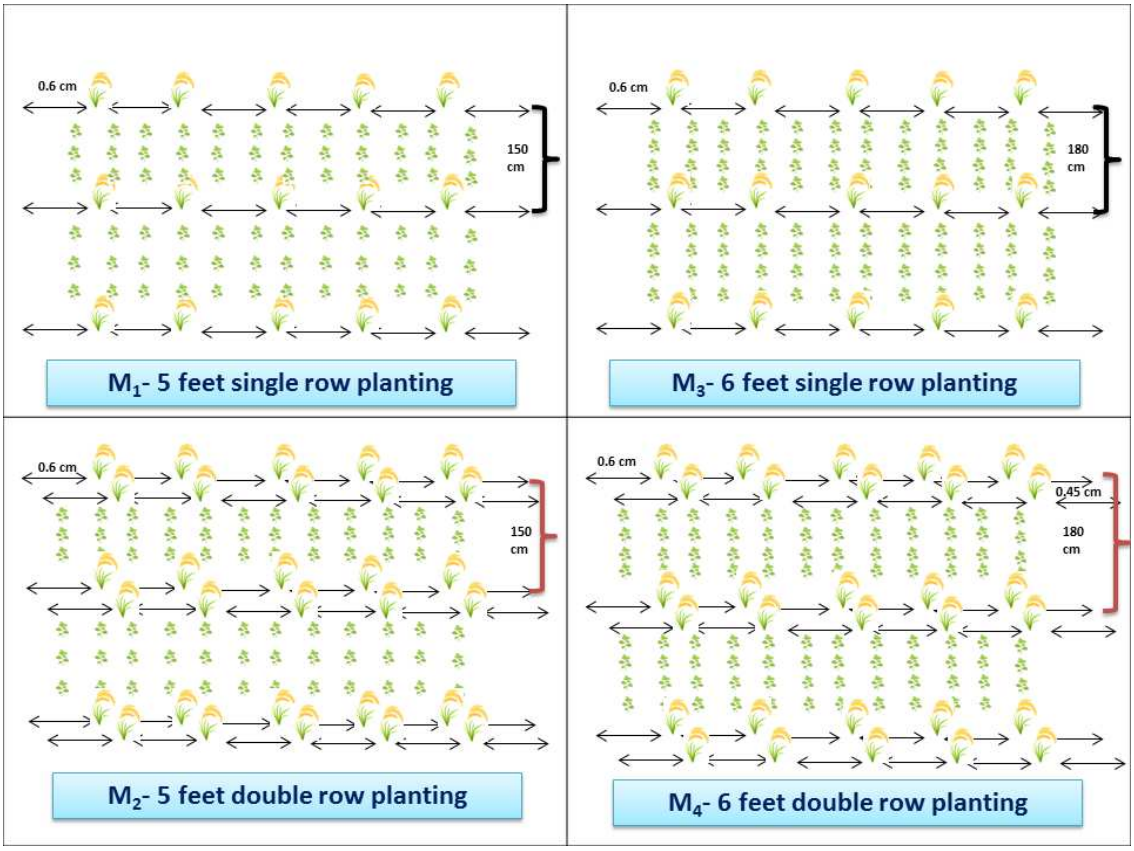

Figure 1. *Diagram for plant geometry (single and double row planting)*

Results

Influence of spacing and row arrangement and intercropping systems on soil available nitrogen of sugarcane

In plant crop (2016-17), among the planting rows, even though 180 cm double row planting (M_4) recorded higher available nitrogen 193.9 kg/ha, the difference between the treatments did not reach the level of significance (*Table 2*). With regard to intercropping systems, sugarcane with sunn hemp (S_4) recorded significantly higher nitrogen than other intercropping systems which were comparable among themselves. The interaction between crop geometries and intercropping systems under SSI planting method on available nitrogen was not significant during the plant crop.

In ratoon crop, among the crop geometries rows, even though 180 cm single row planting (M_3) recorded higher available nitrogen, the difference between the treatments did not reach the level of significance. With regard to intercropping systems, sugarcane with sunn hemp (S_4) recorded significantly higher nitrogen than the other intercropping systems which were comparable among themselves. The interaction between crop geometries and intercropping systems under SSI practices on available nitrogen was not significant in the ratoon crop.

http://www.aloki.hu ● ISSN 1589 1623 (Print) ● ISSN 1785 0037 (Online)
DOI: http://dx.doi.org/10.15666/aeer/2003_22472259

Table 2. *Influence of spacing and row arrangement and intercropping systems on soil available nitrogen (kg/ha) of sugarcane*

Treatment	Plant crop (2016-17)					Ratoon crop (2017-18)				
	M_1	**M_2**	**M_3**	**M_4**	**Mean**	**M_1**	**M_2**	**M_3**	**M_4**	**Mean**
S_1	173.0	170.0	180.0	175.8	**174.7**	184.9	180.2	190.9	185.9	**185.4**
S_2	170.0	168.0	170.0	173.0	**170.2**	180.7	178.2	185.7	181.9	**181.6**
S_3	168.0	165.0	160.0	170.0	**165.7**	179.8	177.9	183.8	180.8	**180.6**
S_4	250.8	250.0	258.0	257.0	**253.9**	280.0	280.0	290.7	289.9	**285.1**
Mean	**190.4**	**188.2**	**192.0**	**193.9**		**206.3**	**204.1**	**212.8**	**209.6**	
	M	**S**	**M at S**	**S at M**		**M**	**S**	**M at S**	**S at M**	
SEd	2.7	3.9	7.9	8.4		3.1	6.9	8.9	10.9	
CD (P = 0.05)	NS	9.5	NS	NS		NS	17.1	NS	NS	

Main plot	Spacing and row arrangement	Sub plot	Intercropping systems
M_1	150 × 60 cm Single row planting	S_1	Sole crop of sugarcane
M_2	150 × 60 cm Double row planting	S_2	Sugarcane + Green gram
M_3	180 × 60 cm Single row planting	S_3	Sugarcane + Black gram
M_4	180 × 60 cm Double row planting	S_4	Sugarcane + Sunn hemp

Influence of spacing and row arrangement and intercropping systems on soil available phosphorus of sugarcane

In plant crop, among the planting rows, 180 cm single row planting recorded significantly higher phosphorus 34.36 kg/ha followed by 180 cm double rows. Planting at 150 cm in double rows recorded the lower phosphorus (*Table 3*). With regard to intercropping systems, sugarcane with sunn hemp (S_4) recorded higher available phosphorus followed by the other systems which were comparable among themselves. The interaction effects were significant wherein, the treatment combinations, sugarcane planted at 180 cm in single row with sunn hemp (M_3S_4) recorded higher available phosphorus. All the treatment combinations involving planting at 150 cm in single row (M_2S_3) recorded lower available phosphorus. Similar trends were also observed in ratoon crop also.

Influence of spacing and row arrangement and intercropping systems on soil available potassium of sugarcane

Marginally higher available potassium was recorded among the crop geometries i.e. planting at 180 cm single row (M_3) (587.8 kg/ha) and 180 cm double row (M_4) than 150 cm in double row (M_2) during 2016-17 in plant sugarcane crop (*Table 4*). With regard to intercropping systems, sugarcane with sunn hemp (S_4) recorded significantly higher (623.5 kg ha^{-1}) available potassium which was closely followed by sole crop of sugarcane (S_1) whereas; other systems were found comparable to sugarcane with sunn hemp.

In ratoon crop, planting at 180 cm single row planting (M_3) recorded higher potassium over the rest of crop geometries. With regard to intercropping systems, sugarcane with sunn hemp (S_4) recorded higher available potassium followed by the

http://www.aloki.hu ● ISSN 1589 1623 (Print) ● ISSN 1785 0037 (Online)
DOI: http://dx.doi.org/10.15666/aeer/2003_22472259

other systems which were comparable among themselves. Lower potassium recorded at sugarcane with black gram (S_3). The interaction effects were absent during plant and ratoon crop.

Table 3. *Influence of spacing and row arrangement and intercropping systems on soil available phosphorus (kg/ha) of sugarcane*

Treatment	Plant crop (2016-17)					Ratoon crop (2017-18)				
	M_1	**M_2**	**M_3**	**M_4**	**Mean**	**M_1**	**M_2**	**M_3**	**M_4**	**Mean**
S_1	27.90	23.10	32.80	30.72	**28.63**	25.00	20.99	33.00	29.00	**27.00**
S_2	26.90	21.10	31.81	29.91	**27.43**	23.90	20.15	31.72	27.71	**25.87**
S_3	24.51	19.88	30.71	28.00	**25.78**	22.81	18.23	30.83	26.88	**24.69**
S_4	47.53	45.88	50.50	48.80	**48.18**	62.82	60.00	65.10	64.00	**62.98**
Mean	**31.71**	**27.49**	**36.46**	**34.36**		**33.63**	**29.84**	**40.16**	**36.90**	
	M	**S**	**M at S**	**S at M**		**M**	**S**	**M at S**	**S at M**	
SEd	0.84	0.44	1.19	0.95		0.65	0.59	1.29	1.26	
CD (P = 0.05)	2.05	1.08	2.70	2.07		1.60	1.45	2.82	2.74	

Main plot	Spacing and row arrangement	Sub plot	Intercropping systems
M_1	150 × 60 cm Single row planting	**S_1**	Sole crop of sugarcane
M_2	150 × 60 cm Double row planting	**S_2**	Sugarcane + Green gram
M_3	180 × 60 cm Single row planting	**S_3**	Sugarcane + Black gram
M_4	180 × 60 cm Double row planting	**S_4**	Sugarcane + Sunn hemp

Table 4. *Influence of spacing and row arrangement and intercropping systems on soil available Potassium (kg/ha) of sugarcane*

Treatment	Plant crop (2016-17)					Ratoon crop (2017-18)				
	M_1	**M_2**	**M_3**	**M_4**	**Mean**	**M_1**	**M_2**	**M_3**	**M_4**	**Mean**
S_1	568.9	565.9	575.8	573.9	**571.1**	542.8	538.8	555.8	548.2	**546.4**
S_2	565.8	563.8	572.8	572.8	**568.8**	541.9	535.2	553.9	547.8	**544.7**
S_3	564.8	561.8	573.7	570.2	**567.6**	540.8	533.2	551.8	546.7	**543.1**
S_4	620.8	618.8	628.9	625.7	**623.5**	665.1	650.1	660.2	658.4	**658.5**
Mean	**580.0**	**577.6**	**587.8**	**585.6**		**572.6**	**564.3**	**580.4**	**575.3**	
	M	**S**	**M at S**	**S at M**		**M**	**S**	**M at S**	**S at M**	
SEd	18.6	9.1	26.8	21.3		3.1	9.0	18.3	20.2	
CD (P = 0.05)	NS	22.2	NS	NS		7.7	22.1	NS	NS	

Main plot	Spacing and row arrangement	Sub plot	Intercropping systems
M_1	150 × 60 cm Single row planting	S_1	Sole crop of sugarcane
M_2	150 × 60 cm Double row planting	S_2	Sugarcane + Green gram
M_3	180 × 60 cm Single row planting	S_3	Sugarcane + Black gram
M_4	180 × 60 cm Double row planting	S_4	Sugarcane + Sunn hemp

Influence of spacing and row arrangement and intercropping systems on soil available N balance of sugarcane

Inplant crop (2016-17), the net gain in soil available N was higher with 180 cm single row intercropped with sunn hemp (M_3S_4) which was followed by 180 cm double

http://www.aloki.hu ● ISSN 1589 1623 (Print) ● ISSN 1785 0037 (Online)
DOI: http://dx.doi.org/10.15666/aeer/2003_22472259

rows with sunn hemp (M_4S_4). A net loss of 39 kg ha^{-1} of soil available N was observed with 180 cm single row planting with black gram (M_3S_3). This was followed by 150 cm double rows with black gram (M_2S_3) (*Tables 5* and *6*). The similar trends with respect to available soil N balance were also recorded in ratoon crop.

Influence of spacing and row arrangement and intercropping systems on soil available P balance of sugarcane

In most of the treatment combinations, both positive as well the negative soil available P trend was observed during plant crop, The net gain in respect of soil available P was higher with 180 cm single row intercropped with sunn hemp (M_3S_4) which was closely followed by 180 cm double rows with sunn hemp (M_4S_4). A net loss of 24 kg ha^{-1} of soil available P was observed under sugarcane planted at 150 cm in double rows with black gram (M_2S_3) which was followed by 150 cm double rows with green gram (M_2S_2) (*Tables 7* and *8*). Similar trends were also registered in ratoon crop during second year of experimentation.

Table 5. *Influence of spacing and row arrangement and intercropping systems on soil available N balance of sugarcane plant crop (2016-17)*

Treatment	Initial soil N (kg/ha) A	Total N applied (kg/ha) B	Plant uptake (kg/ha) C	Expected balance D = (a + b)-c	Post harvest soil N (kg/ha) E	Computed balance (kg/ha)	Net gain or loss (kg/ha)
M_1S_1	199	300	399	100	173	-99	-26
M_1S_2	199	300	402	97	170	-102	-29
M_1S_3	199	300	414	85	168	-114	-31
M_1S_4	199	300	421	78	251	-121	52
M_2S_1	199	300	427	72	170	-127	-29
M_2S_2	199	300	433	66	168	-133	-31
M_2S_3	199	300	466	33	165	-166	-34
M_2S_4	199	300	491	8	250	-191	51
M_3S_1	199	300	364	135	180	-64	-19
M_3S_2	199	300	363	136	170	-63	-29
M_3S_3	199	300	376	123	160	-76	-39
M_3S_4	199	300	390	109	258	-90	59
M_4S_1	199	300	382	117	176	-82	-23
M_4S_2	199	300	390	109	173	-90	-26
M_4S_3	199	300	405	94	170	-105	-29
M_4S_4	199	300	373	126	257	-73	58

			SEd	CD	SEd	CD	SEd	CD	SEd	CD	SEd	CD
M	Standard value	Standard value	7.0	17.1	2.36	5.70	2.7	NS	1.31	3.21	0.91	2.22
S			4.4	10.8	1.64	4.03	3.9	9.5	1.80	4.41	0.85	2.09
M at S			11.4	25.6	3.65	8.26	7.9	NS	3.80	8.14	1.44	3.23
S at M			10.1	21.9	3.26	7.15	8.4	NS	3.99	8.68	1.40	3.14

http://www.aloki.hu ● ISSN 1589 1623 (Print) ● ISSN 1785 0037 (Online)
DOI: http://dx.doi.org/10.15666/aeer/2003_22472259

Table 6. *Influence of spacing and row arrangement and intercropping systems on soil available N balance of sugarcane Ratoon crop (2017-18)*

Treatment	Initial soil N (kg/ha) A	Total N applied (kg/ha) B	Plant uptake (kg/ha) C	Expected balance D = (a + b)-c	Post harvest soil N (kg/ha) E	Computed balance (kg/ha)	Net gain or loss (kg/ha)
M_1S_1	173	325	399	99	185	-74	12
M_1S_2	170	325	409	86	181	-84	11
M_1S_3	168	325	420	73	180	-95	12
M_1S_4	251	325	432	144	280	-107	29
M_2S_1	170	325	443	52	180	-118	10
M_2S_2	168	325	466	27	178	-141	10
M_2S_3	165	325	486	4	178	-161	13
M_2S_4	250	325	547	28	280	-222	30
M_3S_1	180	325	349	156	191	-24	11
M_3S_2	170	325	349	146	186	-24	16
M_3S_3	160	325	354	131	184	-29	24
M_3S_4	258	325	380	203	291	-55	33
M_4S_1	176	325	382	119	186	-57	10
M_4S_2	173	325	387	111	182	-62	9
M_4S_3	170	325	398	97	181	-73	11
M_4S_4	257	325	415	167	290	-90	33

	SEd	CD		SEd	CD	SEd	CD	SEd	CD	SEd	CD	SEd	CD
M	2.7	NS	Standard value	**8.9**	**22.0**	1.57	3.84	3.1	NS	2.29	5.62	0.37	0.91
S	3.9	9.5		5.3	12.9	2.38	5.83	6.9	17.09	1.35	3.31	0.73	1.79
M at S	7.9	NS		14.6	32.5	3.24	7.05	8.9	NS	3.86	8.59	0.82	1.78
S at M	8.4	NS		12.6	27.3	3.69	8.30	10.9	NS	3.39	7.32	1.03	2.35

Influence of spacing and row arrangement and intercropping systems on soil available K balance of sugarcane

In plant crop, lower K loss was observed under single row planting of sugarcane + sunn hemp at crop geometry of 180 cm (M_2S_4) which was followed by 180 cm double row intercropped with sunn hemp (M_2S_4). Higher K loss (-111 kg ha^{-1}) was recorded under the treatment combination of sugarcane planted at 150 cm in double rows (M_2S_3) (*Tables 9* and *10*).

In ratoon crop (2017-18), the net gain in respect of soil available K was higher with 150 cm single row intercropped with sunn hemp (M_1S_4) which was closely followed by 180 cm double rows with sunn hemp (M_4S_4). A net loss of (-29 kg ha^{-1}) of soil available K was observed in 180 cm double rows with black gram (M_2S_3) which was followed by 180 cm double rows with green gram (M_2S_2).

Discussion

Post-harvest soil available nutrients NPK

Soil fertility was quantified with available N, P and K in soil. Adequate supply of nutrients would satisfy nutrient demand of crop besides improving the soil fertility. In

http://www.aloki.hu ● ISSN 1589 1623 (Print) ● ISSN 1785 0037 (Online)
DOI: http://dx.doi.org/10.15666/aeer/2003_22472259

2016-17 and 2017-18 plant crop and ratoon crop among the planting rows, 180 cm double row planting (M_4) recorded higher concentration of available NPK which was closely followed by 180 cm double row planting (M_3).

Table 7. *Influence of spacing and row arrangement and intercropping systems on soil available P balance of sugarcane plant crop (2016-17)*

Treatment	Initial soil P (kg/ha) A	Total P applied (kg/ha) B	Plant uptake (kg/ha) C	Expected balance D = (a + b)-c	Post harvest soil P (kg/ha) E	Computed balance (kg/ha)	Net gain or loss (kg/ha)
M_1S_1	44	100	75	69	28	26	-16
M_1S_2	44	100	75	69	27	25	-17
M_1S_3	44	100	76	68	25	24	-19
M_1S_4	44	100	79	65	48	21	4
M_2S_1	44	100	83	61	23	17	-21
M_2S_2	44	100	85	60	21	16	-23
M_2S_3	44	100	85	59	20	15	-24
M_2S_4	44	100	96	48	46	4	2
M_3S_1	44	100	68	76	33	32	-11
M_3S_2	44	100	70	74	32	30	-12
M_3S_3	44	100	70	74	31	30	-13
M_3S_4	44	100	73	71	51	27	7
M_4S_1	44	100	74	71	31	27	-13
M_4S_2	44	100	75	69	30	25	-14
M_4S_3	44	100	75	69	28	25	-16
M_4S_4	44	100	77	67	49	23	5

			SEd	CD	SEd	CD	SEd	CD	SEd	CD	SEd	CD
M	Standard value	Standard value	1.52	3.72	1.35	3.31	0.84	2.05	0.44	1.09	0.14	0.34
S			1.17	2.86	1.36	3.35	0.44	1.08	0.33	0.81	0.17	0.43
M at S			1.94	4.49	2.95	6.42	1.19	2.70	0.70	1.58	0.44	0.95
S at M			1.68	3.81	2.96	6.44	0.95	2.07	0.64	1.40	0.45	0.98

The intercropping systems, sugarcane with sunn hemp (S_4) recorded significantly higher NPK than the other intercropping system of sugarcane with black gram. Sunn hemp plant was succulent enough and easily decomposable, which accumulated 133 kg N ha^{-1} as reported by Sanya siraju (1952). The increase in soil available nutrients with result of daincha incorporation was very well documented by Swarup (1991) who reported that green manuring with daincha improved the available N in soil throughout the profile compared to initial status. The author was also of the opinion that the P availability improved due to greater mobilization of native soil P compounds by vigorous daincha root system and added biomass. Similar findings were made out by Yadav (1984), Jadhav (1996) and Nasir Ahmed (1999). Two rows of daincha incorporated on 45 DAP registered higher post-harvest soil nutrients followed by other systems as per the findings reported by Guru (1997).

The sugarcane with sunn hemp (S_4) recorded significantly higher available nitrogen, phosphorus and potassium which were followed by sole crop of sugarcane (S_1),

http://www.aloki.hu ● ISSN 1589 1623 (Print) ● ISSN 1785 0037 (Online)
DOI: http://dx.doi.org/10.15666/aeer/2003_22472259

sugarcane + green gram and sugarcane + black gram intercropping. This may be attributed to incorporation of green manure sunn hemp in sugarcane on 45th day which lead to significant higher available NPK.

Growing of green manures in the inter row spacing and incorporation at appropriate time not only fulfill crop nutrient requirement but also maintain soil fertility. Since, sugarcane produces heavy biomass during its ontogeny and it requires high amount of Nitrogen. To meet the increasing nitrogen demand of sugarcane crop, the practice of green manuring coupled with nitrogen application found highly beneficial (Guru, 1997). Improved available soil nitrogen status due to growing of Sesbania *aculeata* and its *in situ* soil incorporation was also reported by Venkatakrishnan (1980).

Results of experimental findings of Shankaraiah et al. (1999) on intercropping and incorporation of legume have established the beneficial effect of increased NUE in sugarcane. Similarly, sunn hemp intercropping and its in *situ* soil incorporation on 45thdays after planting of sugarcane also increased availability plant nutrients like NPK and organic carbon content (Jayapaul et al. 2000).

Talashiltar and Patil (1979) and Ghosh et al. (1981) reported the production of phenolic and aliphatic acids during decomposition of organic matter and thereby solubilized appreciable amount of phosphates resulting in increased P availability in soil. *Sesbania aculeate* increased the microbial population of soil and thus enhanced mineralization of soil and other essential nutrients Khind and Maskina (1986).

Table 8. *Influence of spacing and row arrangement and intercropping systems on soil available P balance of sugarcane Ratoon crop (2017-18)*

Treatment	Initial soil P (kg/ha) A		Total P applied (kg/ha) B	Plant uptake (kg/ha) C		Expected balance D = (a + b)-c		Post harvest soil P (kg/ha) E		Computed balance (kg/ha)		Net gain or loss (kg/ha)	
M_1S_1	28		100	71		57		25		29		-3	
M_1S_2	27		100	71		56		24		29		-3	
M_1S_3	25		100	71		54		23		29		-2	
M_1S_4	48		100	74		74		63		26		15	
M_2S_1	23		100	76		47		21		24		-2	
M_2S_2	21		100	76		45		20		24		-1	
M_2S_3	20		100	77		43		18		23		-2	
M_2S_4	46		100	90		56		60		10		14	
M_3S_1	33		100	64		69		33		36		0	
M_3S_2	32		100	64		68		32		36		0	
M_3S_3	31		100	65		66		31		35		0	
M_3S_4	51		100	70		81		65		31		15	
M_4S_1	31		100	67		64		29		33		-2	
M_4S_2	30		100	67		63		28		33		-2	
M_4S_3	28		100	68		60		27		32		-1	
M_4S_4	49		100	72		77		64		28		15	
	SEd	**CD**		**SEd**	**CD**	**SEd**	**CD**	**SEd**	**CD**	**SEd**	**CD**	**SEd**	**CD**
M	0.84	2.05	Standard value	1.24	3.04	1.37	3.37	0.65	1.60	0.48	1.19	0.18	0.44
S	0.44	1.08		1.19	2.90	0.64	1.58	0/59	1.45	0.52	1.28	0.24	0.59
M at S	1.19	2.70		1.92	4.31	2.22	4.97	1.29	2.82	0.98	2.14	0.38	0.84
S at M	0.95	2.07		1.89	4.22	1.86	3.98	1.26	2.74	1.0	2.20	0.42	0.93

http://www.aloki.hu ● ISSN 1589 1623 (Print) ● ISSN 1785 0037 (Online)
DOI: http://dx.doi.org/10.15666/aeer/2003_22472259

Table 9. *Influence of spacing and row arrangement and intercropping systems on soil available K balance of sugarcane plant crop (2016-17)*

Treatment	Initial soil K (kg/ha) A	Total K applied (kg/ha) B	Plant uptake (kg/ha) C	Expected balance D = (a + b)-c	Post harvest soil K (kg/ha) E	Computed balance (kg/ha)	Net gain or loss (kg/ha)
M_1S_1	676	200	488	388	569	-288	-107
M_1S_2	676	200	489	387	566	-289	-110
M_1S_3	676	200	490	386	565	-290	-111
M_1S_4	676	200	530	346	621	-330	-55
M_2S_1	676	200	519	357	566	-319	-110
M_2S_2	676	200	520	356	564	-320	-112
M_2S_3	676	200	520	356	562	-320	-114
M_2S_4	676	200	598	278	619	-398	-57
M_3S_1	676	200	469	407	576	-269	-100
M_3S_2	676	200	470	406	573	-270	-103
M_3S_3	676	200	470	406	574	-270	-102
M_3S_4	676	200	490	386	629	-290	-47
M_4S_1	676	200	486	390	574	-286	-102
M_4S_2	676	200	487	389	573	-287	-103
M_4S_3	676	200	490	386	570	-290	-106
M_4S_4	676	200	520	356	626	-320	-50

			SEd	CD	SEd	CD	SEd	CD	SEd	CD	SEd	CD
M	Standard value	Standard value	7.4	18.2	6.85	16.76	18.6	NS	3.87	9.47	2.18	5.35
S			2.7	6.6	7.10	17.39	9.1	22.2	7.15	17.51	2.34	5.74
M at S			10.8	24.4	15.83	34.29	26.8	NS	10.50	22.57	3.35	7.53
S at M			8.2	17.6	15.94	34.60	21.3	NS	12.11	26.90	3.45	7.81

Suitability of Prickly sesban or local daincha *(Sesbania aculeata* L.), African daincha *(Sesbania rostrata* L.), indigo *(Indigofera tintoria* L.) and sunn hemp *(Crotolaria juncea* L.) as a green manuring crops due to their fast growth habits was reported by Alam et al. (1997). The total N and availability of P and K of soil also increased slightly after use of green manures. Kormilitsyn (1995) reported that the green manure had the greatest effect on crop productivity. However, the increase in yield depends upon the quantity of organic matter and N, soil ploughed in the results of the above scientists lead support to the present findings.

Soil available nutrient balance NPK

Different crop geometries and legume-based intercropping in sugarcane increased soil available nutrient balance during the sugarcane plant and ratoon crop cycle of our experimentations. The post- harvest soil nutrient balance was found positive and indicated a net gain due to legume-based intercropping in sugarcane. Further, the mineralization of green manures and release pattern of nutrients into soil solution differs largely and accordingly, the final balance of soil organic carbon and available NPK reflected source-wise.

http://www.aloki.hu ● ISSN 1589 1623 (Print) ● ISSN 1785 0037 (Online)
DOI: http://dx.doi.org/10.15666/aeer/2003_22472259

Table 10. *Influence of spacing and row arrangement and intercropping systems on soil available K balance of sugarcane Ratoon crop (2017-18)*

Treatment	Initial soil K (kg/ha) A		Total K applied (kg/ha) B	Plant uptake (kg/ha) C		Expected balance D = (a + b)– c		Post harvest soil K (kg/ha) E		Computed balance (kg/ha)		Net gain or loss (kg/ha)	
M_1S_1	569		200	519		250		543		-319		-26	
M_1S_2	566		200	519		247		542		-319		-24	
M_1S_3	565		200	520		245		541		-320		-24	
M_1S_4	621		200	530		291		665		-330		44	
M_2S_1	566		200	525		241		539		-325		-27	
M_2S_2	564		200	525		239		535		-325		-29	
M_2S_3	562		200	525		237		533		-325		-29	
M_2S_4	619		200	600		219		650		-400		31	
M_3S_1	576		200	468		308		556		-268		-20	
M_3S_2	573		200	469		304		554		-269		-19	
M_3S_3	574		200	470		304		552		-270		-22	
M_3S_4	629		200	485		344		660		-285		31	
M_4S_1	574		200	517		257		548		-317		-26	
M_4S_2	573		200	518		255		548		-318		-25	
M_4S_3	570		200	519		251		547		-319		-23	
M_4S_4	626		200	528		298		658		-328		33	
	SEd	**CD**		**SEd**	**CD**	**SEd**	**CD**	**SEd**	**CD**	**SEd**	**CD**	**SEd**	**CD**
M	18.6	NS	Standard value	5.7	13.9	6.69	16.38	3.1	7.7	5.48	13.41	0.35	0.87
S	9.1	22.2		5.0	12.3	4.11	10.06	9.0	22.1	5.25	12.86	0.39	0.96
M at S	26.8	NS		12.4	27.1	12.57	27.65	18.3	NS	13.79	29.72	0.68	1.50
S at M	21.3	NS		12.1	26.3	11.41	24.45	20.2	NS	13.70	29.48	0.70	1.55

At the end of the plant –ratoon crop cycle, there was no appreciable net gain of nitrogen under different crop geometries with sole crop of sugarcane, which again proved that sugarcane is an exhaustive crop wherein absorption of nutrient depleted the native soil nutrient pool increasingly and moreover the weed competition accelerated the nutrient depletion to greater extent by sole sugarcane. Whereas, double row planting of sugarcane with sunn hemp intercrop showed positive balance of nitrogen, indicating the overall net gain. The increased nutrient indices under sunn hemp intercropping were due to increased availability of plant nutrients owing to sunn hemp incorporation on 45 DAP and this is in conformity with findings of Swarup (1991) and Guru (1997). Neelima and Bhanu murthy (2009) reported that soil nitrogen balance was positive under incorporation of total plant (16 kg N/ha) or shoot (11 kg N/ha) of sunn hemp green manure and also with the application of 120 (1 kg N/ha) and 180 kg (19 kg N/ha).

Net gain of available P was realized under different crop geometries and intercropping systems during both plant and ratoon crops (2016 to 2017).

The negative and positive potassium (K) balance was noticed under the treatment combination of various crop geometries and intercropping systems. Lesser negative balance was observed in crop geometries with sunn hemp during the first plant crop, net gain K also observed under sugarcane with sunn hemp during the ratoon crop.

http://www.aloki.hu ● ISSN 1589 1623 (Print) ● ISSN 1785 0037 (Online)
DOI: http://dx.doi.org/10.15666/aeer/2003_22472259

Conclusion

From the results of the experiments, it could be concluded that double row planting of sugarcane at 150 cm spacing with *in-situ* incorporation of sunn hemp on45th DAS increased the nutrient availability and maintained soil fertility of plant- ratoon sugarcane agroecosystem under tropical Indian condition. Intercropping studies based different planting methods under sub surface drip fertigation. Intercropping studies on root systems stabilization in sugarcane by using subsurface drip fertigation methods.

Acknowledgements. We have boundless pleasure in placing on record my deep sense of gratitude to Dr. M. Mohamed Amanullah, Professor (Agronomy), Maize Research Station, TNAU, Vaagarai for his guidance, valuable advice, constant encouragement, useful suggestions, kind and timely help to carry out the study.

REFERENCES

[1] Alam, F., Majid, M. A., Islam, M. J. (1997): Effect of biomanures on sugarcane. – Indian Journal of Agriculture Science 67(10): 450-455.
[2] Ghosh, S. C., Omanwar, P. K., Sachan, R. S., Sharma, R. B. (1981): Reserves of organic and total phosphorus in cultivated and forested mouisols. – Indian Journal of Soil Science 29: 332-336.
[3] Guru, G. (1997): Influence of population and stage of incorporation of intercropping of intercropped green manure (Daincha) and nitrogen levels on sugarcane. – M.Sc. (Agri.) Thesis, Tamil Nadu Agricultural University, Madurai.
[4] Jadhav, S. B. (1996): Effect of incorporation of sugarcane trash on cane productivity and soil fertility. – In: Proceedings of 22nd Congress of the ISSTC held at Cartagena, Colombia, pp. 104-108.
[5] Jayapaul, G. P., Duraisingh, R., Senthilvel, T., Joseph, M. (2000): Influence of population and stage of incorporation of intercropped green manure (daincha) and nitrogen levels on yield and quality of sugarcane. – Indian Sugar 51(2): 989-991.
[6] Khind, C. S., Maskina, M. S. (1986): Effect of sesbania green manure on water management and yield of lowland rice. – International Rice Research Notes11(5): 45.
[7] Kormilitsyn, V. F. (1995): Agro-chemistry of green manuring in irrigated agriculture in the Volga region. Part 2. Agrochemical and Agro-ecological aspects of using sowings of annual legumes as green manure. – Agrokhimiya 77-93.
[8] More, S. M. (2003): Study on effect of row spacing, planting system and intercropping on growth, yield and economics of *suru* sugarcane (Co 86032) and its ratoon under drip irrigation. – Ph. D. Thesis, MPKV, Rahuri.
[9] Nasir Ahmed, S. (1999): Influence of sunn hemp intercropping in sugarcane. – Sugar Journal 24: 51-54.
[10] Neelima, T. L., Bhanumurthy, V. B. (2009): Growth and yield attributes of rice as influenced by N fertilizer and differential incorporation of sunn hemp green manure. – Journal of Rice Research 2(1): 45-50.
[11] Patel, D., Raj, V. C., Tandel, B. (2014): Study the influence of planting distance and variety on growth of sugarcane. – Journal of International Academic Research 2: 1092.
[12] Sadanandan, N., Mahapatra, I. C. (1973): Studies on multiple cropping –balance of total and available phosphorus in various cropping pattern. – Indian Journal of Agronomy 18: 459-463.
[13] Sanya Siraju, B. K. (1952): Companion cropping with autumn planted sugarcane. – Annual Report: Indian Institute Sugarcane Research, Lucknow, pp. 20-21.

http://www.aloki.hu ● ISSN 1589 1623 (Print) ● ISSN 1785 0037 (Online)
DOI: http://dx.doi.org/10.15666/aeer/2003_22472259

[14] Shankaraiah, C., Nagaraju, M. S., Usha Ravindra. (1999): Ways and means to improve fertilizer use efficiency in sugarcane. – Co-operative Sugar 30(10): 965-969.
[15] Swarup, A. (1991): Long term effect of green manuring (*Sesbania aculeate*) on soil properties and sustainability of rice and wheat yield on sodic soil. – Indian Society Soil Science 27: 201-202.
[16] Talashiltar, F. C., Patil, S. (1979): Effect of organic manures on the availability of phosphorus from single superphosphate and rock-phosphate. – Indian Journal of Soil Science 27: 201-202.
[17] Venkatakrishnan, S. (1980): Mineralization of green manure (*Sesbania aculeate*), nitrogen in sodic and reclaimed soils under flooded conditions. – Plant and Soil 54: 149-152.
[18] Yadav, R. L. (1984): Soil fertility in relation to crop yields of sugarcane based cropping systems in North Central India. – Journal Agronomy and Crop Science153(5): 328-333.

http://www.aloki.hu ● ISSN 1589 1623 (Print) ● ISSN 1785 0037 (Online)
DOI: http://dx.doi.org/10.15666/aeer/2003_22472259

EFFECTS OF HUMUS AND HUMIC ACID ON PLANT GROWTH AND NUTRITIONAL UPTAKE OF LETTUCE (*LACTUCA SATIVA* L.)

EKBIÇ, E.[1*] – KÖSE, M. A.[2]

[1]*Department of Horticulture, Agricultural Faculty, Ordu University, 52200 Ordu, Turkey*

[2]*Republic of Turkey Ministry of Agriculture and Forestry, Giresun Directorate of Provincial Agriculture and Forestry, Giresun, Turkey*

**Corresponding author*
e-mail: ercanekbic@gmail.com; phone: +90-452-226-5200 ext.: 6238; fax: +90-452-234-6632

(Received 27th Oct 2021; accepted 4th Feb 2022)

Abstract. This study was carried out to determine the effects of humus and humic acid application on the morphological properties and plant nutritional contents of lettuce. Experiment was established in completely randomized design with 3 replicates including 0, 250, 500 and 1000 kg/ha humus and 0, 15 and 30 l/ha humic acid applications. The results showed that effects of humus and humic acid applications on leaf number, leaf width, leaf length, plant weight, dry matter ratio, N, P, K, Ca and Mg contents of lettuce were statistically significant. The highest mean plant weight values were obtained from the plots under 1000 kg/ha humus and 30 l/ha humic acid application at 245.68 g and 238.69 g respectively. The highest average dry matter ratio values were also obtained from the 1000 kg/ha humus and 30 l/ha humic acid applied plots as 5.93% and 5.87%, respectively. The highest average N content values were obtained in 500 and 1000 kg/ha humus applied plots at 4.28% as well as 15 l/ha and 30 l/ha gave the higher values 4.25% and 4.27% respectively. Based on the results of this study, 1000 kg/ha humus and 30 l/ha humic acid doses recommended in terms of plant growth and plant nutrient contents in lettuce.
Keywords: *Lactuca sativa L. var. crispa, biological application, plant nutrition, plant growth*

Introduction

Lettuce (*Lactuca sativa* L.) is a winter crop in the salad group, which has an important place in human nutrition due to its fibrous structure and rich mineral content (Kim et al., 2016). 94% of Turkey's agricultural lands has been reported to be poor in terms of organic matter (Ay, 2015). In greenhouse lettuce cultivation chemical products are used excessively and in large quantities because of the cultivation of high-yielding varieties in the same place every year, providing a suitable environment for diseases and pests due to poor acclimatization of greenhouse, excessive content of nutrients in the soil and increased nutrient requirement due to the use of high-yielding varieties (Tüzel and Gül, 2008). As a result of the use of excessive inorganic fertilizers, depending on the environmental conditions, nitrogen does not decompose in the plant, causing an increase in the amount of nitrite and nitrate in the plant. Özgen et al. (2011) reported that inorganic fertilization caused three times more nitrate accumulation in lettuce and salad than organic fertilization. In addition, excessive, intense and unconscious use of chemical products in agricultural production causes the accumulation of nitrate and nitrite in the plant, as well as the accumulation of toxic and dangerous chemical substances in the environment. These pollute soil and groundwater (Li et al., 2021), threatening human health and natural life. Those practices, which cause environmental pollution, disrupt the soil structure, increase harmful chemicals in the plant and threaten human health in order to obtain high yields, have increased the demand for healthy

http://www.aloki.hu ● ISSN 1589 1623 (Print) ● ISSN 1785 0037 (Online)
DOI: http://dx.doi.org/10.15666/aeer/2003_22612269

agricultural production in recent years and have created a consumer pressure on the producer. In this respect, organic and good agricultural practices, which include effective and efficient use of soil, water and plant resources, protection of the environment, food safety in terms of public health, and at the end, leaving a more livable nature to future generations, have become the most important agenda of the world. In today's agricultural production, plant nutrition and fertilization are regulated, implemented and monitored not only as processes that provide high yields, but also for high quality and healthy agricultural production, protecting the environment and natural resources and observing food safety. In order to increase the quality and productivity along with sustainability in agriculture, the techniques of using biological applications instead of excessive and intensive use of chemicals have gained importance (Montalvo et al., 2020; Chianese et al., 2020). Different plant wastes, farm manure, chicken manure, garbage compost and organic industrial wastes can be used to eliminate the lack of biological source in the soil. Those materials improve the physical, chemical and biological properties of the soils and provide nutrients to the soil, thus positively affecting the yield and quality in plant production (Noroozisharaf and Kaviani, 2018; Kaya et al., 2018; Popescu and Popescu, 2018). It is stated that humic compounds constitute the most important part of coal and occur as a result of chemical change of vegetable and woody parts (Ay, 2015; Miao et al., 2018). Humic substances are a reserve for microorganisms, through elements such as C, N, S and P in their structure. Because of this feature, they enrich the microflora of the soil (Yılmaz and Alagöz, 2001; Larcher, 2003). Humic acid is one of the most important humic substances. Humic and fulvic acids are humus structures that dissolve in alkaline environment (Ay, 2015). Humic substances increase the yield in plants and sugar accumulation in fruits and vegetables by increasing the amount of organic matter and water holding capacity in the soil, improving the physical properties of the soil such as drainage and aeration and increasing the usefulness of nutrients in the soil (Kunç, 2002). The positive effect of organic fertilizers is due to the organic compounds released through the decomposition by microorganisms in the soil and the humus formed by humic and fulvic acids in their structure. Humic and fulvic acids improve soil structure by increasing aggregate formation in the soil due to their colloidal properties. It is also known that due to the ion exchange capacity of the reactive side groups of humic compounds, they interact with pesticides and herbicides to form stable structures and render them harmless to plants and groundwater (Hellal et al., 2006). It has also been reported that humic compounds provide resistance against different stress conditions in plants (Nardi et al., 2002). Furthermore, humic acid application is resulted in cadmium concentration in lettuce (Horuz et al., 2015). Humic acid also accelerate the N metabolism by increasing nitrate reductase activity (Haghighi et al., 2012).

Alternative organic matter sources should be used in the light of scientific data in agricultural lands where organic matter reserves are rapidly decreasing and problems are occurring in terms of the availability of nutrients. These practices such as humus-rich compost application (Solaiman et al., 2019) ensure the sustainability of soil fertility by keeping the risk of environmental pollution at a minimum level, as well as obtaining maximum productivity and quality in plant production. Studies on the interactive relationships between organic matter application and plant nutrients are still insufficient, and up-to-date scientific data are needed on the basis of different soil and product groups, especially in terms of plant growth and product quality. In this paper we

http://www.aloki.hu ● ISSN 1589 1623 (Print) ● ISSN 1785 0037 (Online)
DOI: http://dx.doi.org/10.15666/aeer/2003_22612269

experimented effects of different humus and humic acid doses on plant growth and mineral nutrient content of lettuce.

Materials and methods

The study was carried out in Eastern Blacksea region of Turkey (Bulancak-Giresun (Latitude: 40.874° (North), Longitude: 38.266° (East), Altitude: 421 m) in unheated plastic house. The soil properties of experimental area as follow; clay loam texture, water holding capacity 59%, $CaCO_3$ 0.48%, pH 6.88, organic matter content 4%, and without saline problem. Plant material was *Lactuca sativa* var. *crispa* cv. Olenka. Before the seedlings were planted in the experimental area, 150 kg/ha N, 100 kg/ha P and 150 kg/ha K fertilizers were applied to the all plots (Eşiyok, 2012). The experiment was established completely randomized plot design with 3 replicates. Seedlings were planted as 30 cm x 20 cm between and within the rows (plot size 2.4 m^2). Four doses (0, 250, 500, and 1000 kg/ha) of leonardite sourced Delta Super Humus (Delta Agricultural Chemicals Industry and Trade Co. Inc., Turkey) and 3 doses (0, 15 and 30 l/ha) of humic acid Delta Humate 12 (Delta Agricultural Chemicals Industry and Trade Co. Inc., Turkey) were applied to the soil before planting. Plants were harvested at 60 days after transplanting. The yellowed and carious outer leaves were removed after harvest and completely excluded from the analysis. Leaf number per plant (Ln), leaf length (Ll) and width (Lw), plant weight (Pw) and dry matter ratio (Dmr) (Dmr = (Fw/Dw)*100, where Fw: fresh weight, Dw: dry weight) properties of the lettuce were measured. The leaves were dried in the oven at 72 °C till constant weight was ensured. Plant nutrient content of lettuce leaf were measured using ICP-OES (Vista-Pro Axial, Agilent Tech., Mulgrave, AUSTRALIA) (Kacar, 2014). Prior to the measurement, 0.2 g of dry leaf sample was digested in a closed microwave digestion system (Marsexpress Cem Corp., Matthews, NC, USA) in the presence of 5 ml of concentrated nitric acid (HNO_3) and 2 ml of hydrogen peroxide (H_2O_2). Deionized water (H_2O) was used to top-up the volume of the samples to 20 ml. The analytical data was compared to the certified values of a standard reference material (SRM 1573a Tomato Leaf, National Institute of Standards and Technology, Gaithersburg, MD, USA). The variance analysis were applied to data in JMP v.10.0 (SAS inc. USA) statistical program. Means were compared using Tukey HSD post-hoc test (Tukey Honest Significant Difference).

Results

Effect of humus and humic acid on morphological features

Humus, humic acid and humus x humic acid interactions were also found to be significant ($P < 0.05$) with regard to those parameters such as leaf number, leaf length, leaf width, and plant weight, dry matter ratio (*Table 1*). The highest leaf number value was obtained in the plot that the highest humus and humic acid doses were applied (27.0) while the lowest value (13.7) was measured in control plot (no humus and humic acid applied). The average values showed that the highest leaf number values were obtained from 1000 kg/ha humus and 30 l/ha humic acid application as 23.2 and 21.0 respectively. This study showed that the number of leaves in lettuce also increased with the increase in humus and humic acid doses. Similarly the highest leaf length (28.20 cm) and leaf width (22.14 cm) values were obtained in 1000 kg/ha humus and

http://www.aloki.hu ● ISSN 1589 1623 (Print) ● ISSN 1785 0037 (Online)
DOI: http://dx.doi.org/10.15666/aeer/2003_22612269

30 l/ha humic acid applied plots. As increasing doses of humus and humic acid increased significantly the leaf length and leaf width mean values. Plant weight values changed between 106.40 g and 321.97 g while dry matter ratio values between 5.19 g and 6.60 g. The highest mean plant weight values were obtained from the plots 1000 kg/ha humus and 30 l/ha humic acid applied plots 245.68 g and 238.69 g respectively. Dry matter content values changed between 5.17% and 6.60%. Similar to the above parameters the highest dry matter content value was also obtained from the 1000 kg/ha humus + 30 l/ha humic acid applied plot as 6.60%. The highest average dry matter ratio values were also obtained from the 1000 kg/ha humus and 30 l/ha humic acid applied plots as 5.93% and 5.87% respectively.

Table 1. *The effects of humus and humic acid applications on leaf number, leaf length, leaf width, plant weight and dry matter ratio of lettuce*

Humus (kg/ha)	Humic acid (l/ha)	Ln	Ll (cm)	Lw (cm)	Pw (g)	Dmr (%)
0		15.6 C	18.57 C	15.41 C	130.68 D	5.23 C
250		18.0 B	21.53 B	17.42 B	166.92 C	5.33 C
500		19.1 B	22.38 B	18.24 B	200.87 B	5.66 B
1000		23.2 A	25.16 A	19.75 A	245.68 A	5.93 A
	0	17.2 C	20.17 C	16.29 C	124.34 C	5.37 B
	15	18.8 B	22.11 B	17.72 B	195.23 B	5.38 B
	30	21.0 A	23.44 A	19.11 A	238.69 A	5.87 A
0	0	13.7 d	16.89 f	14.02 f	106.40 g	5.19 d
0	15	15.6 cd	18.78 ef	16.26 def	125.70 f	5.17 d
0	30	17.5 bcd	20.04 de	15.97 ef	160.50 e	5.34 cd
250	0	15.7 cd	19.31 de	15.46 ef	110.80 g	5.29 cd
250	15	19.0 bc	22.77 bc	18.48 bcd	181.00 d	5.22 d
250	30	19.2 bc	22.51 bc	18.33 bcd	208.97 c	5.49 cd
500	0	17.8 bcd	21.12 cd	16.98 cde	126.90 f	5.46 cd
500	15	19.3 bc	22.98 bc	17.75 b-e	212.40 c	5.46 cd
500	30	20.2 b	23.02 bc	19.99 ab	263.30 b	6.06 b
1000	0	21.5 b	23.36 bc	18.71 bc	153.27 e	5.53 cd
1000	15	21.1 b	23.90 b	18.39 bcd	261.80 b	5.67 bc
1000	30	27.0 a	28.20 a	22.14 a	321.97 a	6.60 a

Ln: leaf number per plant, Ll: leaf length, Lw: leaf width, Pw: plant weight, Dmr: dry matter ratio The differences between mean values indicated by different letters are significant according to the Tukey HSD test ($P<0.05$)

Effects of humus and humic acid on leaf nutrient contents

Results related to plant nutrient content of the lettuce were given in *Table 2*. Humus and humic acid application significantly ($P < 0.5$) increased leaf N content. The highest average N content values were obtained in 500 and 1000 kg/ha humus applied plots as 4.28% as well as 15 l/ha and 30 l/ha gave the higher values 4.25% and 4.27% respectively. The highest average N content values were obtained in 500 and 1000 kg/ha humus applied plots as 4.28%, similarly 15 l/ha and 30 l/ha humic acid applications gave also high values 4.25% and 4.27% respectively. Humus and humic acid interaction was found to be significant in respect to the leaf P, K, Ca and Mg

http://www.aloki.hu ● ISSN 1589 1623 (Print) ● ISSN 1785 0037 (Online)
DOI: http://dx.doi.org/10.15666/aeer/2003_22612269

contents. The highest P and Ca values were obtained from the 500 kg/ha humus and 30 l/ha humic acid applied plots while 1000 kg/ha humus and 30 l/ha humic acid applied plots gave the highest K content. In respect to the Mg content the values were changed according to the humus and humic acid dose interaction. Based on the statistical processing the highest Mg content value (0.29%) obtained from the 250 kg/ha humus + 0 humic acid and 1000 kg/ha humus + 30 l/ha humic acid treatments which differed only from the 0 humus + 0 humic acid treatment. With increasing humic acid does, the average P, K, Ca and Mg values increased as well as N. Similarly, while increasing humus doses increased the mean P and K contents, the mean Ca and Mg content values were not statistically significant.

Table 2. *The effects of humus and humic acid applications on N, P, K, Ca, and Mg contents of lettuce*

Humus (kg/ha)	Humic acid (l/ha)	N (%)	P (%)	K (%)	Ca (%)	Mg (%)
0		4.15 B	0.64 B	8.61 C	1.09	0.25
250		4.18 B	0.64 B	9.24 B	1.20	0.27
500		4.28 A	0.69 A	9.44 B	1.16	0.25
1000		4.28 A	0.71 A	10.17 A	1.14	0.26
	0	4.16 B	0.61 C	8.84 C	1.08 B	0.25
	15	4.25 A	0.64 B	9.30 B	1.12 B	0.26
	30	4.27 A	0.74 A	9.96 A	1.25 A	0.27
0	0	4.11	0.58 e	8.12 d	1.00 c	0.20 b
0	15	4.20	0.67 cd	8.83 cd	1.06 bc	0.28 ab
0	30	4.15	0.66 cde	8.88 cd	1.23 abc	0.27 ab
250	0	4.10	0.59 de	9.23 bc	1.11 abc	0.29 a
250	15	4.17	0.61 de	9.32 bc	1.29 ab	0.25 ab
250	30	4.27	0.71 bc	9.18 bc	1.19 abc	0.26 ab
500	0	4.20	0.60 de	9.14 bc	1.00 c	0.22 ab
500	15	4.31	0.66 cde	9.30 bc	1.14 abc	0.27 ab
500	30	4.34	0.82 a	9.87 b	1.34 a	0.26 ab
1000	0	4.23	0.66 cde	8.85 cd	1.23 abc	0.28 ab
1000	15	4.30	0.67 cd	9.74 b	0.97 c	0.22 ab
1000	30	4.31	0.79 ab	11.91 a	1.23 abc	0.29 a

N: Nitrogen, P: Phosphorus, K: Potassium, Ca: Calcium, Mg: Magnesium. The differences between mean values indicated by different letters are significant according to the Tukey HSD test ($P<0.05$)

Discussion

Application of humic substance such as humus and humic acid contributed plant growth in lettuce. Bozkurt et al. (2004) and Tüfenkçi et al. (2006) reported that humic acid application had been increased the leaf number in lettuce. In addition, Çivit (2010) reported that organic matter sourced leonardit application also increased the lettuce leaf number. Aksu (2017) reported that humic acid application increased the leaf length and width as in our study. Application of plant wastes such as hazel nut husk and tea waste composts also contributed positively to plant growth in lettuce (Çağlar, 2014). The researcher reported that leaf length and leaf width values increased significantly by application of those plant waste compost. Furthermore Horuz et al. (2015), Mirdad

http://www.aloki.hu ● ISSN 1589 1623 (Print) ● ISSN 1785 0037 (Online)
DOI: http://dx.doi.org/10.15666/aeer/2003_22612269

(2016) and Rodrigues et al. (2018) reported that humic acid application increased dry matter content of lettuce. Other than humus and humic acid organic fertilizer such as Ko-Humax also increased plant dry matter in lettuce (Demir et al., 2003). Humic substances such as humus and humic acid contribute to plant growth positively by stimulating the root growth (Canellas et al., 2002; Busato et al., 2010; Zandonadi et al., 2010; Martinez-Balmori et al., 2014; Maji et al., 2017). Humic acid also increased plant biomass by stimulating cell respiration and increasing photosynthetic activity rate in the plant (Fan et al., 2014; Olivares et al., 2015). In addition, humus together with shading contributes seedling emergence in lettuce (Pallaoro et al., 2020). Humus-rich compost application to the soil increase nutrient uptake by stimulating mycorrhizal colonization and ensure sustainability of soil fertility (Solaiman et al., 2019). On the other hand, Roosta et al. (2017) reported that containing humic substance nano-fertile fertilizer might be effective positively on plant nutrient uptake in also hydroponic system.

Conclusion

Today, organic and sustainable agricultural practices continue to increase. In order to realize quality productions with environment-friendly production techniques, farmers have been using many different techniques and applications to complete the deficient organic matter in the soil. The addition of different organic sourced matters such as plant wastes or humus and humic acids to the soil is the most practical of these applications. It is known that there has been a significant increase in the use of organic materials such as humus and humic acid in recent years. Application of organic materials such as humus and humic acid to the soil increases the availability of macro and micro nutrients. Furthermore, due to the regulation of the soil structure, it is thought that it will significantly increase plant growth in lettuce production, and prevent the use of excessive fertilizers. In this study, it was determined that with the increase of humus and humic acid doses applied to the soil, plant growth and the amount of plant nutrients in the leaves increased. The highest humus and humic acid doses gave the highest values in both plant growth parameters and plant nutrient content values. In addition to the use of biological applications such as humus and humic acid applied in this study, it is also recommended to research the effect of different plant waste composts.

Acknowledgements. The study was financially supported by Ordu University Scientific Research Projects Coordination Unit (Project code: TF-1329).

REFERENCES

[1] Aksu, G. (2017): Effects of humic acid applications on lettuce growth and on some properties of soil contaminated by cadmium. – VIII International Scientific Agriculture Symposium, “Agrosym 2017”, Jahorina, Bosnia and Herzegovina, October 2017. Book of Proceedings, pp. 800-804.

[2] Ay, F. (2015): Geological and economical importance of humic acid and humic acid sources [Hümik Asit ve Hümik Asit Kaynaklarinin Jeolojik ve Ekonomik Önemi]. – Cumhuriyet Üniversitesi Fen Fakültesi Fen Bilimleri Dergisi (CFD) 36(1): 28-51.

[3] Bozkurt, M. A., Turkmen, O., Yıldız, M., Cimrin, K. M. (2004): The influence of humic acid application in high nitrogen levels on the yield, nitrate and nutrient contents in lettuce. – Paper presented at the International Soil Congress, Erzurum.

http://www.aloki.hu ● ISSN 1589 1623 (Print) ● ISSN 1785 0037 (Online)
DOI: http://dx.doi.org/10.15666/aeer/2003_22612269

[4] Busato, J. G., Zandonadi, D. B., Dobbss, L. B., Façanha, A. R., Canellas, L. P. (2010): Humic substances isolated from residues of sugar cane industry as root growth promoter. – Sci Agric 67: 206-212.
[5] Çağlar, S. (2014): Effects of hazelnut husk and tea waste compost on the yield and quality of lettuce (*Lactuca sativa* L. var. *crispa*) [Fındık zuruf kompostu ve çay kompostu karışımlarının kıvırcık marulda (*Lactuca sativa* L. var. *crispa*) verim ve kaliteye etkisi]. – Yüksek lisans tezi, Ordu Üniversitesi Fen Bilimleri Enstitüsü Bahçe Bitkileri anabilim dalı, Ordu.
[6] Canellas, L. P., Okorokova-Façanha, A., Olivares, F. L., Façanha, A. R. (2002): Humic acids isolated from earthworm compost enhance root elongation, lateral root emergence, and plasma membrane H+-ATPase activity in maize roots. – Plant Physiol 130: 1951-1957.
[7] Chianese, S., Fenti, A., Lovino, P., Musmarra., D., Salvestrini, S. (2020): Sorption of organic pollutants by humic acids: a review. – Molecules 24(4): 918.
[8] Çivit, B. (2010): Effect of some natural substances (Gidya, Zeolite and Leonardite) on the yield and growth of lettuce (*Lactuca sativa* L. var. *longifolia*) [Bazı doğal maddelerin (Gidya, Zeolit ve Leonardit) marulda (*Lactuca sativa* L. var. *longifolia*) verim ve büyüme üzerine etkisi]. – Kahramanmaraş Sütcü İmam Üniversitesi, Fen Bilimleri Enstitüsü, Yüksek Lisans Tezi.
[9] Demir, H., Gölükçü, M., Topuz, A., Özdemir, F., Polat, E., Şahin, H. (2003): The effect of different organic fertilizers on the mineral contents of yedikule and iceberg lettuce typies grown in organic farming [Yedikule ve iceberg tipi marul çeşitlerinin mineral madde içeriği üzerine ekolojik üretimde farklı organik gübre uygulamalarının etkisi]. – Mediterranean Agricultural Sciences 16(1): 79-85.
[10] Eşiyok, D. (2012): Summer and Winter Crop Vegetable Cultivation. [Kışlık ve yazlık sebze yetiştiriciliği]. – Meta Basım Matbaacılık Hizmetleri, İzmir, Turkey.
[11] Fan, H., Wang, X., Suna, X., Lia, Y., Sun, X., Zheng, C. (2014): Effects of humic acid derived from sediments on growth, photosynthesis and chloroplast ultrastructure in chrysanthemum. – Sci. Hortic. 177: 118-123.
[12] Haghighi, M., Kafi, M., Fang, P. (2012): Photosynthetic activity and N metabolism of lettuce as affected by humic acid. – International Journal of Vegetable Science 18: 182-189.
[13] Hellal, A. A., Imam, D. M., Khalifa, S. M., Aly, H. F. (2006): Interaction of pesticides with humic compounds and their metal complexes. – Radiochemistry 48: 419.
[14] Horuz, A., Karaman, M. R., Güllüce, M. (2015): Effect of humic acid application on the reduction of cadmium concentration in lettuce (*Lactuca sativa* L.). – Fresenius Environmental Bulletin 24(10): 3141-3147.
[15] Kacar, B. (2014): Plant, Soil and Fertilizer Analysis 2: Easily Applicable Plant Analysis [Bitki, Toprak ve Gübre Analizleri 2, Kolay Uygulanabilir Bitki Analizleri]. – Nobel Akademik Yayıncılık, Yayın (910).
[16] Kaya, C., Akram, N. A., Ashraf, M., Sonmez, O. (2018): Exogenous application of humic acid mitigates salinity stress in maize (*Zea mays* L.) plants by improving some key physico-biochemical attributes. – Cereal Research Communications 46: 67-78.
[17] Kim, M. J., Moon, Y., Tou, J. C., Mou, B., Waterland, N. L. (2016): Nutritional value, bioactive compoundsand health benefits of lettuce (*Lactuca sativa* L.). – Journal of Food Composition and Analysis 49: 19-34.
[18] Kunç, Ş. (2002): Use of humic acids in agriculture [Humik asitlerin tarımda kullanımı]. – Hasad Dergisi 7: 46-58.
[19] Larcher, W. (2003): Physiological Plant Ecology: Ecophysiology and Stress Physiology of Functional Groups. – Springer Science & Business Media, Berlin.
[20] Li, Y., Bi, Y., Mi, W., Xie, S., Ji, L. (2021): Land-use change caused by anthropogenic activities increase fluoride and arsenic pollution in groundwater and human health risk. – Journal of Hazardous Materials 406: 124337.

http://www.aloki.hu ● ISSN 1589 1623 (Print) ● ISSN 1785 0037 (Online)
DOI: http://dx.doi.org/10.15666/aeer/2003_22612269

[21] Maji, D., Misra, P., Singh, S., Kalra, A. (2017): Humic acid rich vermicompost promotes plant growth by improving microbial community structure of soil as well as root nodulation and mycorrhizal colonization in the roots of Pisum sativum. – Appl. Soil Ecol. 110: 97-108.
[22] Martinez-Balmori, D., Spaccini, R., Aguiar, N. O., Novotny, E. H., Olivares, F. L., Canellas, L. P. (2014): Molecular characteristics of humic acids isolated from vermicomposts and their relationship to bioactivity. – J. Agric. Food Chem. 62: 11412-11419.
[23] Miao, Z. H., Li, K., Liu, P. Y., Li, Z., Yang, H., Zhao, Q., Chang, M., Yang, Q., Zhen, L., Xu., C. Y. (2018): Natural humic-acid-based phototheranostic agent. – Advanced Healthcare Materials 7(7): 1701202.
[24] Mirdad, Z. M. (2016): Effect of N fertigation rates and humic acid on the productivity of crisphead lettuce (*Lactuca sativa* L.) grown in sandy soil. – Journal of Agricultural Science. 8(8): 149-157.
[25] Montalvo, S., Huilinir, C., Borja, R., Sanchez, E., Herrmann, C. (2020): Application of zeolites for biological treatment processes of solid wastes and wastewaters. A review. – Bioresource Technology 301: 122808.
[26] Nardi, S., Pizzeghello, D., Muscolo, A., Vianello, A. (2002): Physiological effects of humic substances on higher plants. – Soil Biol. and Biochem. 34: 1527-1536.
[27] Noroizisharaf, A., Kaviani, M. (2018): Effect of soil application of humic acid on nutrients uptake, essential oil and chemical compositions of garden thyme (*Thymus vulgaris* L.) under greenhouse conditions. – Physiology and Molecular Biology of Plants 24: 423-431.
[28] Olivares, F. L., Aguiar, N. O., Rosa, R. C. C., Canellas, L. P. (2015): Substrate biofortification in combination with foliar sprays of plant growth promoting bacteria and humic substances boosts production of organic tomatoes. – Sci. Hortic. 183: 100-108.
[29] Özgen, S., Şekerci, S., Karabıyık, T. (2011): The effect of organic and inorganic fertilization on nitrate accumulation of lettuce and salad [Organik ve inorganik gübrelemenin marul ve salataların nitrat birikimi üzerine etkisi]. – VI. Türkiye Ulusal Bahçe Bitkileri Kongresi 4-8 Ekim 2011, Şanlıurfa.
[30] Pallaoro, D. S., Rodrigues de Aquino Arantes, C., Ribeiro Correa, A., Clarete Camili, E., Barbosa Coelho, M. F. (2020): Effects of humus and shading levels in the production of *Lactuca canadensis* L. seedlings. –Acta Agronómica 60(1): 32-37.
[31] Popescu, G. C., Popescu, M. (2018): Yield, berry quality and physiological response of grapevine to foliar humic acid application. – Crop Production and Management 27(2): 273-282.
[32] Rodrigues, L. U., Silva, R. R. da., Freitas, G. A. de., Santos, A. C. M. dos., Tavares, R. de C. (2018): Ácidos húmicos no desenvolvimento inicial de alface. – Pesquisa Aplicada & Agrotecnologia, Guarapuava-PR 11(2): 101-109.
[33] Roosta, H. R., Safarizadeh, M., Hamidpour, M. (2017): Effect of humic acid contained nano-fertile fertilizer spray on concentration of some nutrient elements in two lettuce cultivars in hydroponic system. –Journal of Science and Technology of Greenhouse Culture 7(28): 51-59.
[34] Solaiman, Z. M., Yang HongJun, Archdeacon, D., Tippett, O., Tibi, M., Whiteley, A. S. (2019): Humus-rich compost increases lettuce growth, nutrient uptake, mycorrhizal colonisation, and soil fertility. –Pedosphere 29(2): 170-179.
[35] Tüfenkçi, S., Türkmen, O., Sönmez, F., Erdinç, C., Sensoy, S. (2006): Effects of humic acid doses and application times on the plant growth, nutrient and heavy metal contents of lettuce grown on sewage sludge-applied soils. – Fresenius Environmental Bulletin 15(4): 295-300.
[36] Tüzel, Y., Gül, A. (2008): Good Agricultural Practices in Greenhouse [Seralarda iyi tarım uygulamaları]. –Tibyan Yayınları, İzmir.

http://www.aloki.hu ● ISSN 1589 1623 (Print) ● ISSN 1785 0037 (Online)
DOI: http://dx.doi.org/10.15666/aeer/2003_22612269

[37] Yılmaz, E., Alagöz, Z. (2001): Effects of humic acid application on aggregate formation and durability in soils [Humik asit uygulamasının topraklarda agregat oluşum ve dayanıklılığı üzerine etkileri]. Türkiye 2. Ekolojik Tarım Sempozyumu. – 14-16 Kasım 2001, Antalya, pp. 134-143.
[38] Zandonadi, D. B., Santos, M. P., Dobbss, L. B., Olivares, F. L., Canellas, L. P., Binzel, M. L., Okorokova-Façanha, A. L., Façanha, A. R. (2010): Nitric oxide mediates humic acids-induced root development and plasma membrane H+-ATPase activation. – Planta 231: 1025-1036.

http://www.aloki.hu ● ISSN 1589 1623 (Print) ● ISSN 1785 0037 (Online)
DOI: http://dx.doi.org/10.15666/aeer/2003_22612269

EFFECTS OF LONG-TERM CROPPING OF TIBETAN BARLEY (*KUNLUN 14*) ON SOIL MICROBIAL DIVERSITY, ENZYMATIC ACTIVITIES, AND CROP PHENOTYPIC QUALITY

ZHAO, Y.[1,2#] – YAO, Y. H.[1,3,4,5#] – YAO, X. H.[1,3,4,5] – WU, K. L.[1,3,4,5*]

[1]*Qinghai University, Xining 810016, China*

[2]*College of Eco-Environmental Engineering, Qinghai University, Xining 810016, China*

[3]*Qinghai Academy of Agricultural and Forestry Science, No. 253 Ningda Road, Xining 810016, China*

[4]*Qinghai Key Laboratory of Hulless Barley Genetics and Breeding, Xining 810016, China*

[5]*Qinghai Subcenter of National Hulless Barley Improvement, Xining 810016, China*

[#]*Equal first authors*

**Corresponding author*
e-mail: wklqaaf@sina.com, kunlunwu@yahoo.com

(Received 8th Nov 2021; accepted 23rd Dec 2021)

Abstract. There is limited information presenting the effect of long-term continuous cropping of Tibetan barley. The current study applied integrated high throughput sequencing and bioinformatics to determine the effect of long-term continuous cropping of Tibetan barley on the soil microbial, enzymatic characteristics and the plant agronomic traits. Results indicated that *Arthrobacter*, *Sphingomonas, Gaiella, Bacillus, Massilia, Knoellia, Mycobacterium* and *Pedobacter* were the dominant genera. The significant increase of these genera under increased cropping years was an indication of the constant depleted quality of the soil, promoting the survival of these bacterial genera generally associated with bioremediation of degraded soils. The microbial carbon and nitrogen biomass were significantly altered between the difference cropping years. There were statistically significant differences in the enzymatic activities among the cropping years ($P < 0.05$). Both the soil acid phosphatase enzymatic activity (10 μmol/day/gram) and sucrase enzymatic activity (80 μg/day/gram) were both highest after ten years of continuous cropping. The soil urease enzymatic activity was highest (750 μg/day/gram) at five years of continuous cropping while the soil polyphenol oxidase enzymatic activity was highest (440 μg/day/gram) at the control treatment. Moreover, there was a steady decline in all the agronomic traits (tillering number, number of kernels per ear, grain weight per plant, weight of a thousand seeds per plant, number of per plant and main ear length per plant) with increase in continuous cropping years, indicating the detrimental impact of long-term continuous cropping on highland barley phenotypic characteristics and yield quantity.
Keywords: *continuous cropping, crop quality, microbial community, nutrient deficiency, soil microbiology*

Introduction

Continuous cropping is an agricultural practice involving long-term cultivation of the same or allied plant species in the same soil or piece of land over a long period of continuous planting seasons (Krupenikov et al., 2011). Over the years, the common harmful effects of continuous cropping include nutrient deficiency in soil, emergence of plant diseases and insect pests and reduced organic matter contents. Measures such as crop rotation, application of organic fertilizers or use of microbial technologies have been recommended as potential solutions to these impacts (Rigon and Calonego, 2020). This has prompted most farmers to undertake rotational farming as a means of improving soil

http://www.aloki.hu ● ISSN 1589 1623 (Print) ● ISSN 1785 0037 (Online)
DOI: http://dx.doi.org/10.15666/aeer/2003_22712283

quality and yield. Moreover, several related diseases may become aggravated with declined yield and quality under such continuous cultivation and management conditions (Gao et al., 2006). As an alternative, several studies have recommended the change of physicochemical properties of the soil, soil nutrient content, soil microbial community structure, soil enzyme activity, plant agronomic traits and physiological and biochemical indexes through rotational farming (Monaci et al., 2017). In some circumstances, continuous cropping systems under no-till (NT) systems has also been recognized as an important alternative to crop-fallow system. Intensified cropping systems have shown greater benefits than the crop-fallow systems with such benefits ranging from soil and water conservation, improved soil properties, increased soil organic carbon concentration (SOC) concentration and improved crop production (Tang et al., 2014). On the other hand, diverse crop rotations and continuous cropping systems has been confirmed to return more above- and below-ground biomass to soil than the continuous cropping systems with extended fallow periods. Additionally, annual return of crop residues under the NT systems has shown high potential in protecting the soil surface from water and wind erosion, reduce water evaporation, increase soil macro-aggregation, and enhance accumulation of carbon (Tang et al., 2014).

Recently, studies have pointed out that continuous cropping can be sustained for decades but requires careful management for good soil nutrient conditions and microbial ecology. Indeed, the changes in bacterial community diversity under continuous cropping of different vegetables have been shown to lead to the disorder of the functions of bacterial community, resulting to disrupted ecological balance in the soil and consequently lowering the crop quality (Lyu et al., 2020). For example, breaking continuous potato cropping with legumes improves the soil microbial communities, enzyme activities and tuber yield through phytoremediation. Indeed, phytoremediation of organic contaminants in the soil has majorly been related to the action of multiple enzymes in the plant rhizosphere soil (Liu et al., 2015). Despite all these underlying effects of continuous cropping on both the soil and quality of yield parameters, there is no sufficient information on the effects of long term (up to ten years) continuous cropping of Tibetan barley on the soil microbial and enzymatic dynamics as well as the crop phenotypic characteristic. Therefore, the goal of this study was to experimentally determine the effects of long-term continuous cropping of the Tibetan barley on soil microbial and enzymatic properties and the plant's phenotypic traits. The study was undertaken through integrated high throughput sequencing and bioinformatics as well as soil enzymatic activities and yield quantities measurements.

Materials and methods

Site description

The study was undertaken on an experimental field in Qinghai province, China located at 37°21' N and 101°43' E, within an altitude of 2,987 m. It has Qinghai-Tibet plateau climatic features with a cold, warm, and humid climate with annual sunshine hours range of between 2260 and 2740 h. The annual average temperature is 8.0 °C with a daily temperature range of 11.6–17.5 °C. The annual rainfall is between 530 and 560 mm, annual evaporation of between 1130 and 1340 mm (Zhang et al., 2000). The regional soil type is Kastanozems based on the FAO classification (Yan et al., 2018).

http://www.aloki.hu ● ISSN 1589 1623 (Print) ● ISSN 1785 0037 (Online)
DOI: http://dx.doi.org/10.15666/aeer/2003_22712283

Experimental design and sample collection

The experiment was set up in the experimental field in Qinghai province from August 10th the year 2020. The experimental farmland was a fallow plot covered with green grass for period of more than 5 years prior to the start of each experimental treatment and control. The treatments and control (Non cropping soil) were designed in quadruplicate measuring 5 m by 5 m, and marked as indicated in *Table 1*. The study involved one genotype of Tibetan barley (*Kunlun 14*). Each treatment field was subjected to conventional management and the soil and plant sampling was done during the flowering period of the Tibetan barley at Zadoks growth scale of 69. The conventional management involved planting at 15 cm by 15 cm for row spacing, periodic mechanical weeding and irrigation whenever it was necessary, and application of diammonium phosphate fertilizer at a rate of 7.5 kg per acre annually, which continued for the entire experimental period.

Table 1. *Experimental arrangement design*

Treatments	**Plots per treatment**			
Control	CK-1	CK-2	CK-3	CK-4
2 years treatment	CC2-1	CC2-2	CC2-3	CC2-4
5 years treatment	CC5-1	CC5-2	CC5-3	CC5-4
10 years treatment	CC10-1	CC10-2	CC10-3	CC10-4

The soil was sampled in triplicate from the root area at 22.5 cm depth where the root zone was evenly distributed, and five plants were randomly sampled from each quadruplicate plots, giving a total of 80 plant samples. The soil was fully mixed, loaded into a self-sealed bag, put into the ice box, quickly brought back to the laboratory under -80 °C refrigerator and ferried to the laboratory for further analysis.

DNA extraction and PCR amplification and bio-information analysis process

The isolation of DNA followed the protocol presented in Han et al. (2017). The paired end (PE) reads obtained by Miseq sequencing were first stitched according to the overlap relationship, and the sequence quality was controlled and filtered. The samples were distinguished and OTU clustering and species taxonomy analysis carried out. These included the Diversity Index Analysis, based on the OTU clustering results. The detection of sequencing depth, based on taxonomic information was carried out at various classification levels of the statistical division of the community structure analysis. On the basis of the above analysis, a series of in-depth statistical and visual analysis was undertaken on the multi-sample community composition and system development information, such as multi-analysis and difference differentiation test.

Taxonomic analysis and species composition and variance analysis

The OTU Taxonomics Comprehensive Information Table, which combines the OTU analysis results with the taxonomic information, and the rank-abundance curve was used to analyze the abundance and uniformity of species OTU. This involved Pan/Core Species Analysis, Alpha Diversity Analysis and Dilution curve analysis as described in Willis (2019) and Costa et al. (2020). To study the diversity of microorganisms in the

http://www.aloki.hu ● ISSN 1589 1623 (Print) ● ISSN 1785 0037 (Online)
DOI: http://dx.doi.org/10.15666/aeer/2003_22712283

environment, the richness and diversity of the microbiome was calculated using the diversity within the individual samples. This was achieved through the species Venn chart analysis and community composition analysis as described in Lam et al. (2016). The Circos sample and species diagrams with visual circles were used to provide description on the correspondence between samples and species, to reflect the proportion of the dominant species composition of each (or group) sample, and the different samples of each dominant species were used to determine the relationship between samples and species (Krzywinski et al., 2009). Species variance analysis was applied to detect differences in abundance between different groups (or samples) of the microbiome through determination of the difference significant test between groups and through LEfSe multi-level species differential analysis.

Sample comparison and functional predictive analysis

The alpha diversity of the microbial communities present in the soil samples under different treatments was determined through the use of Ace, Chao, Shannon and Simpson indices as described in Chernov et al. (2015). Beta Diversity Analysis and Sample grouping analyses were accomplished as described in Legendre and Condit (2019). The beta diversity analysis was undertaken through sample hierarchical clustering. The Hierarchical clustering of distance matrices was done to determine how close the sample branches were. This was undertaken through the Partial least square's discriminant analysis (PLS-DA). Using the COG libraries, the functional predictive analysis was undertaken through PICRUSt to show the effect of the 16S marker gene in the genome of the species using. The cluster of orthologous groups (COG) was determined as described in Tatusov et al. (2000) and were constructed by applying the criterion of consistency of genome-specific best hits to the results of an exhaustive comparison of all protein sequences from these genomes.

Soil enzymatic activity and agronomic traits

The level of soil acid phosphatase (S-ACP), soil urease (S-UE), soil sucrase (S-SC) and soil polyphenol oxidase (S-PPO) enzymatic activities were determined in this study as these are the major enzymes having been strongly associated with continuous cropping and soil quality (Liu et al., 2015). The analysis for the soil enzymatic activities were conducted in quadruplicate for all the soil sample. Determination of agronomic traits involved the measurement of the Tilling number, number of kernels per ear, grain weight per plant, thousand seed weight per plant, number of spikelets per plant and main ear length per plant. The soil microbial biomass carbon and soil microbial biomass nitrogen were determined under each treatment following the procedures outlined in Makarov et al. (2016) on substrate-induced respiration method. Briefly, Moist soil containing 10 ± 40 g oven-dry soil, were amended with a series of glucose concentrations (0.5, 1, 2, 4, 6 and 10 mg gÿ1 o.d. soil) in solution (to adjust soil moisture to 120% WHC). The soils were then incubated at 258 °C with shaking at 150 rev min per minute after adding liquid glucose, and CO_2 evolution was determined over after the addition of glucose.

Statistical data analysis

Data was analyzed using SPSS, QIIME and R software. Mean differences were calculated at a p value of 0.05. Significant differences among the means were

http://www.aloki.hu ● ISSN 1589 1623 (Print) ● ISSN 1785 0037 (Online)
DOI: http://dx.doi.org/10.15666/aeer/2003_22712283

determined using the LSD test. T-tests and Metastats (http://metastats.cbcb.umd.edu/) in Mothur were used to compare the differences, and all p-values were adjusted with the false discovery rate (FDR) using the Benjamini-Hochberg (BH) method with the mt.rawp2adjp function in R.

Results

Classification and taxonomic status identification

More than 400 000 valid reads were generated with an average mean length of 400 bp after MiSeq Illumina sequencing. The sequences were distributed among 24,417 OTU and 97% identity applied as the cutoff. Taxonomic composition analysis of the OTU's were generated and an abundance distribution compiled through community bar plot analysis for the top 10 taxonomies for each treatment. Based on that, the top 10 dominant phyla were Actinobacteria, Proteobacteria, Acidobacteria, Chloroflexi, Bacteriodetes, Gemmatimonadetes, Firmicutes, Verrucomicrobia, Nitrospira, and Planctomycetes (*Fig. 1a*). The dominant genera representatives from the dominant phyla were; *Arthrobacter* (phylum actinobacteriota), *Sphingomonas* (phylum proteobacteria), *Gaiella* (phylum actinobacteriota), *Bacillus* (phylum firmicutes), *Massilia* (phylum Proteobacteria), *Knoellia* (phylum actinobacteriota), *Mycobacterium* (phylum actinobacteriota) and *Pedobacter* (phymum bacteroidota). The dominance of these genera had significant difference across the cropping years ($P < 0.050$), and their numbers increased with increase in the cropping years. Through Kruskal-Wallis H test for genus variation between cropping years, there was significant statistical difference ($p < 0.05$). Through Venn analysis, the highest number of species (1311) occurred at five years of continuous cropping, followed by 1304 at ten years of continuous cropping. The similarity was highest in species between five and ten years of continuous cropping and both had biggest difference with species under the control (CK) treatment (*Fig. 1b*), indicating the uniqueness and shift in the soil microbial characteristics across the cropping years.

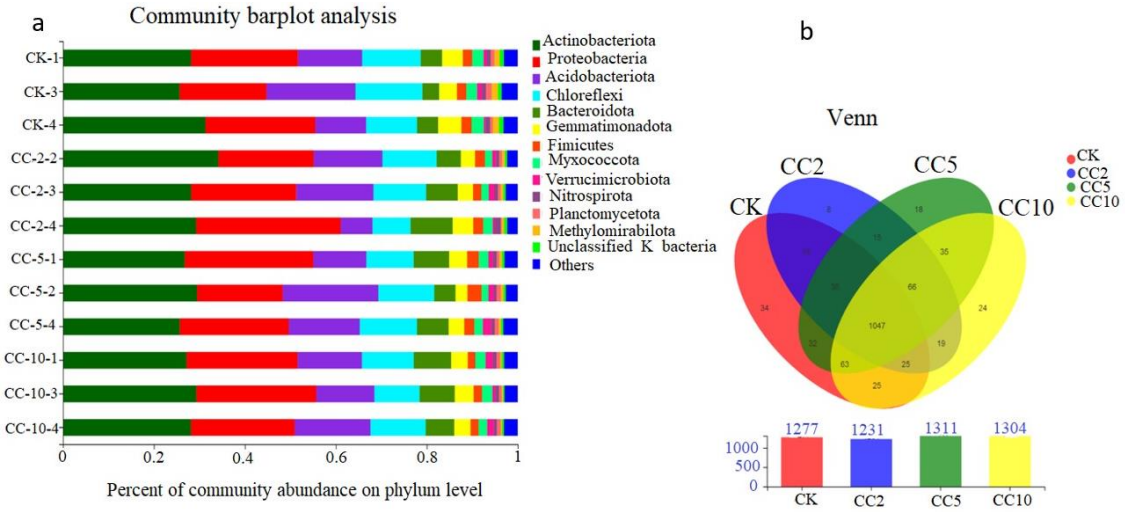

Figure 1. *Species distribution and relationship through community bar plot (a) and Venn analyses (b)*

http://www.aloki.hu ● ISSN 1589 1623 (Print) ● ISSN 1785 0037 (Online)
DOI: http://dx.doi.org/10.15666/aeer/2003_22712283

Microbial taxonomic composition

Based on the alpha diversity analysis through the use of Ace, Chao, Shannon and Simpson indices, there was statical differences in species abundance across the treatment years $P < 0.05$) (*Fig. 2*). This also indicated possible uniqueness and difference in microbial characteristics across the cropping years.

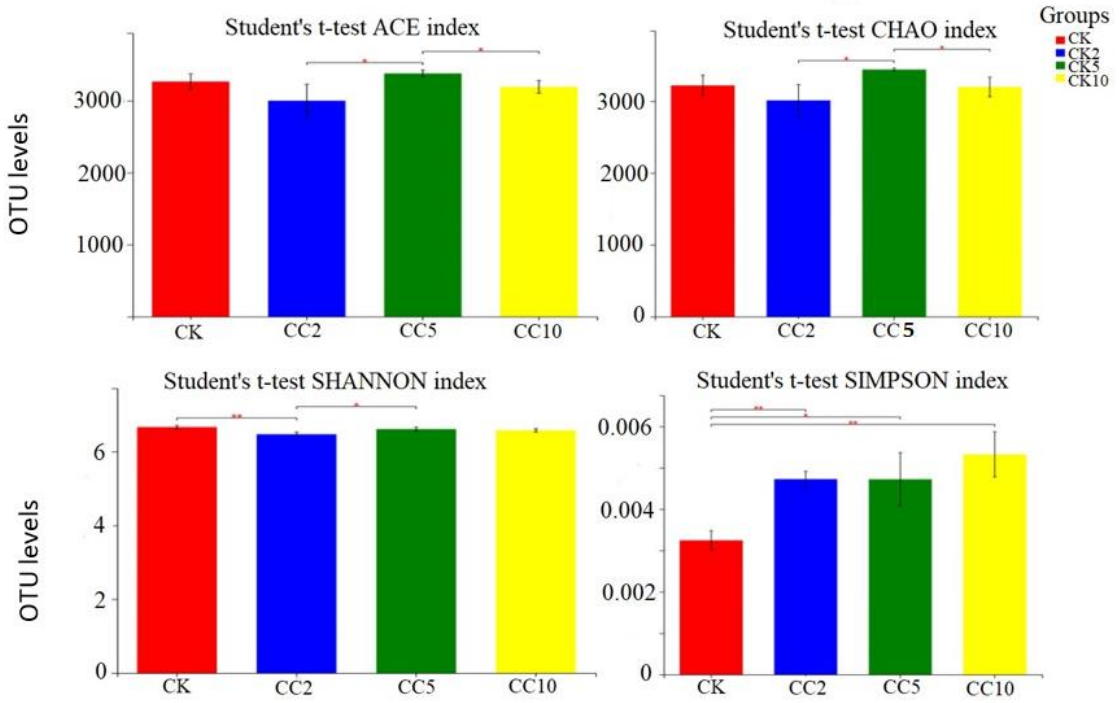

Figure 2. *Microbial community diversity between treatments based on Ace, Chao, Shannon and Simpson indices. Error bars indicate standard error of the means and asterisks indicates bars with no statistical differences*

Sample similarities and function classification

The species relationship between treatment groups through Partial Least Square Discriminant Analysis (PLS-DA) is provided in *Figure 3*. Through PLS-DA analysis at species level, it was noted that the control treatment had the least co-relation with the other treatments. This equally indicated possible uniqueness and differences in microbial characteristics between the non-cropped and continuously cropped soils. The Clusters of Orthologous Groups (COG) classification is provided in *Figure 4* and indicated that the functional characteristics of communities across the treatments were majorly on energy production and conversion, amino acid transport and metabolism, general function prediction and signal transduction mechanism.

Microbial biomass content, enzyme activities and agronomic traits within and across the cropping systems

There was statistically significant difference in the microbial biomass carbon content between the control, two years continuous cropping and the five years continuous

http://www.aloki.hu ● ISSN 1589 1623 (Print) ● ISSN 1785 0037 (Online)
DOI: http://dx.doi.org/10.15666/aeer/2003_22712283

cropping. However, there was no statistically significant difference in the microbial biomass carbon content between the control and the ten years continuous cropping. In contrary, there was statistically significant difference in the microbial biomass nitrogen content between the control and the two years continuous cropping, but no statistically significant difference in the microbial biomass nitrogen content between the control, five years and ten years continuous cropping (*Fig. 5*). Additionally, results on soil enzymatic activities indicated a steady increase in both the soil acid phosphatase enzymatic activity (S-ACP) and soil sucrase enzymatic activity (S-SC) with the increase in continuous cropping years (CK to CC10). Furthermore, the highest value of soil urease enzymatic activity (S-UE) was at the five years continuous cropping, while the soil polyphenol oxidase enzymatic activity (S-PPO) was highest at the control treatment. All the values for the reported enzymatic activities had statistically significant difference between the treatments (*Fig. 6*). Moreover, there was a steady decline in all the agronomic traits (Tillering number, number of kennels per ear, grain weight per plant, thousand seed weight, number of spikelets and the main ear length with increase in continuous cropping years. All the agronomic traits had general decline with increase in continuous cropping years of the Tibetan barley (*Fig. 7*).

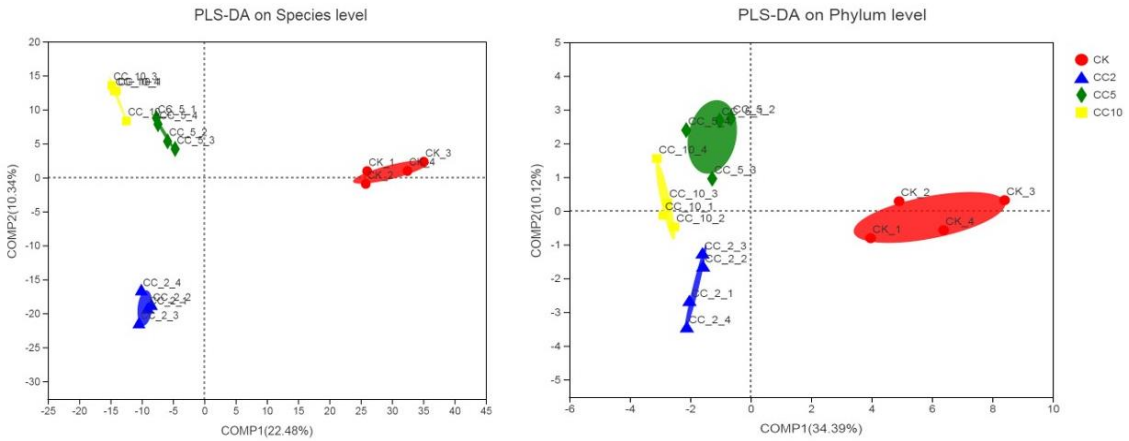

Figure 3. *Relationship in species between treatment groups through Partial Least Square Discriminant Analysis*

Discussion

Continuous cropping remains one of the most debatable farming practices in regards to its impact on soil and plant quality (Wienhold et al., 2006). From the top ten phyla, Actinobacteria, Proteobacteria, Acidobacteria and Chloroflexi were the most dominant. Indeed, previous studies have shown that actinobacteria majorly occurs in the soil and plays significant role in the decomposition of the organic matter of dead organisms so that the molecules can be taken up anew by plants. The proteobacteria include a wide variety of pathogens, while others are free-living, and include many of the bacteria responsible for nitrogen fixation (Yang, et al., 2020).

From previous studies, most of the dominant genera; *Sphingomonas, Gaiella, Bacillus, Massilia, Knoellia, Mycobacterium* and *Pedobacter* from the top 10 dominant phylum have been found to enhance the process of nitrogen fixation while others like the *Sphingomonas* are specifically common in degraded soils (Walsh et al., 2019). *Bacillus* spp. Have been recorded to serve multiple ecological functions in soil

http://www.aloki.hu ● ISSN 1589 1623 (Print) ● ISSN 1785 0037 (Online)
DOI: http://dx.doi.org/10.15666/aeer/2003_22712283

ecosystem from nutrient cycling to conferring stress tolerance to plants. Members of the genus *Bacillus* are known to have multiple beneficial traits which help the plants directly or indirectly through acquisition of nutrients, overall improvement in growth by production of phytohormones, protection from pathogens and other abiotic stressors. Studies have also shown that *Massilia* colonized and proliferated on the seed coat, radicle, roots, and also on hyphae of phytopathogenic *Pythium aphanidermatum* infecting crops (Ofek et al., 2012). Moreover, *Mycobacterium* has been associated with acidic soils (Walsh et al., 2019). Members of the *Sphingomonas* and *Pedobacter* genera are often isolated from contaminated soils due to their unique abilities to support in situ bioremediation (Zhou et al., 2016).

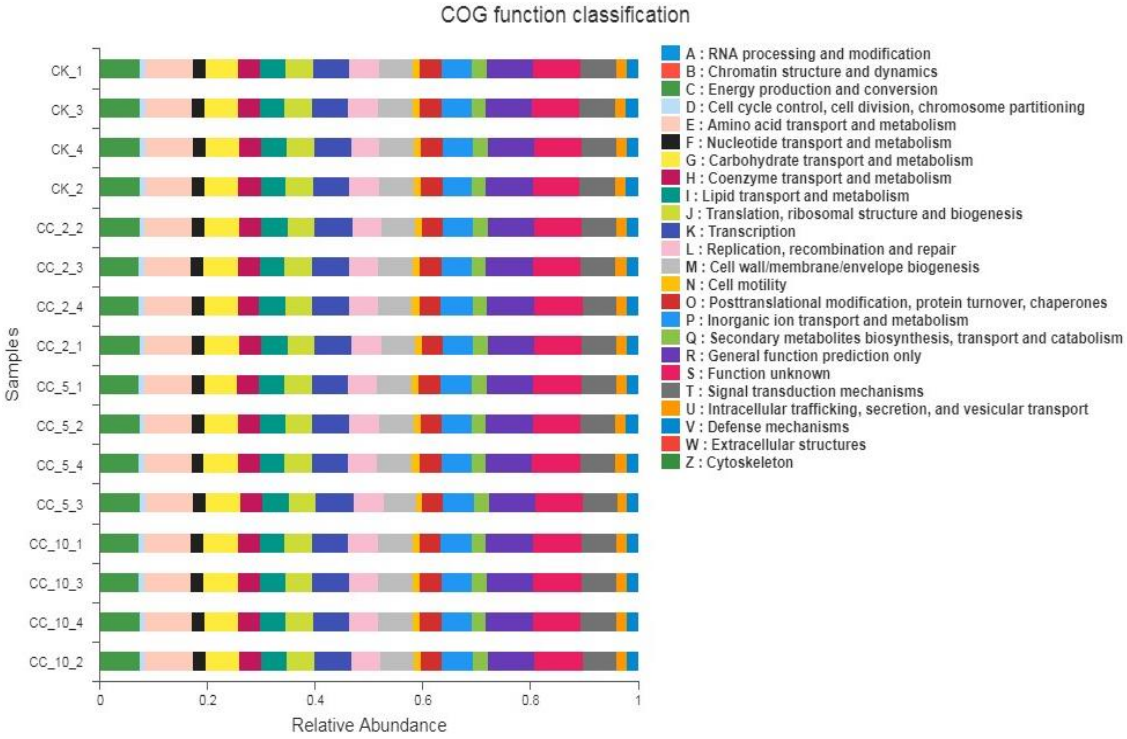

Figure 4. *Clusters of Orthologous Groups (COG) classification*

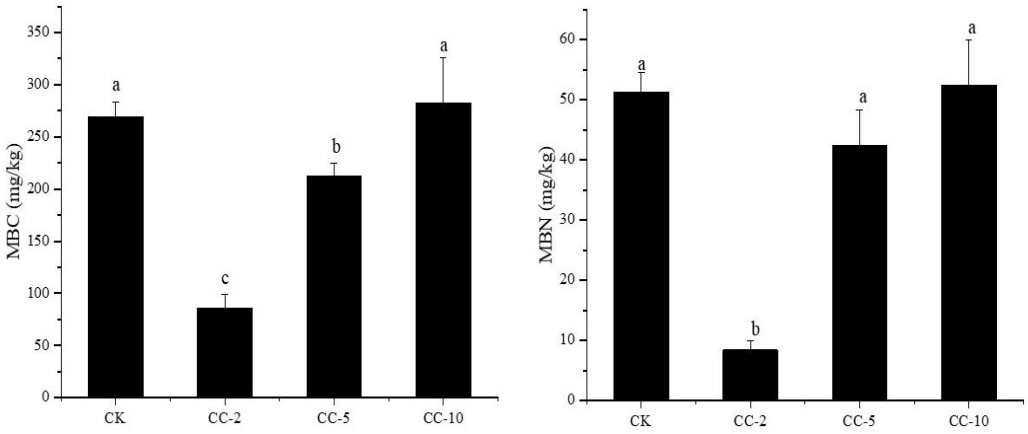

Figure 5. *Microbial biomass carbon (MBC) and microbial biomass nitrogen (MBN).. (Bars with the different letters at the top under the same treatment are statistically different)*

http://www.aloki.hu ● ISSN 1589 1623 (Print) ● ISSN 1785 0037 (Online)
DOI: http://dx.doi.org/10.15666/aeer/2003_22712283

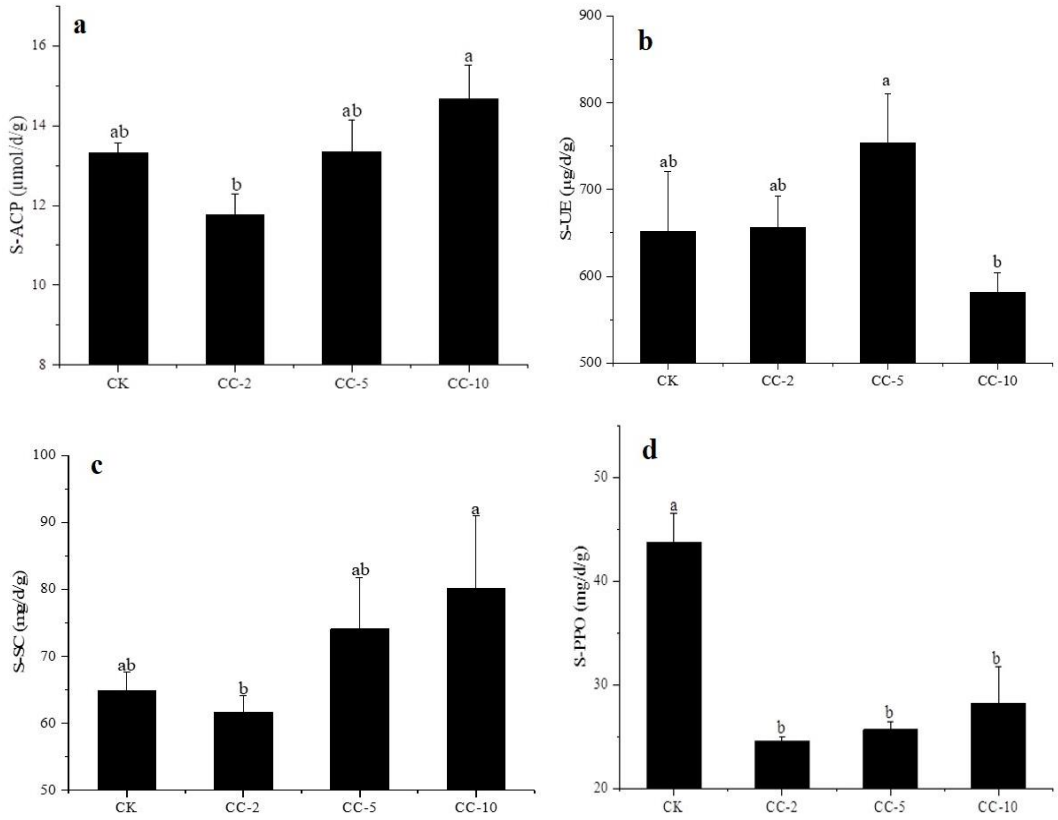

Figure 6. *(a) Soil Acid phosphatase enzymatic activity (S-ACP), (b) Soil urease enzymatic activity (S-UE), (c) Soil sucrase enzymatic activity (S-SC), (d) Soil polyphenol oxidase enzymatic activity (S-PPO). (Bars with the different letters at the top under the same treatment are statistically different)*

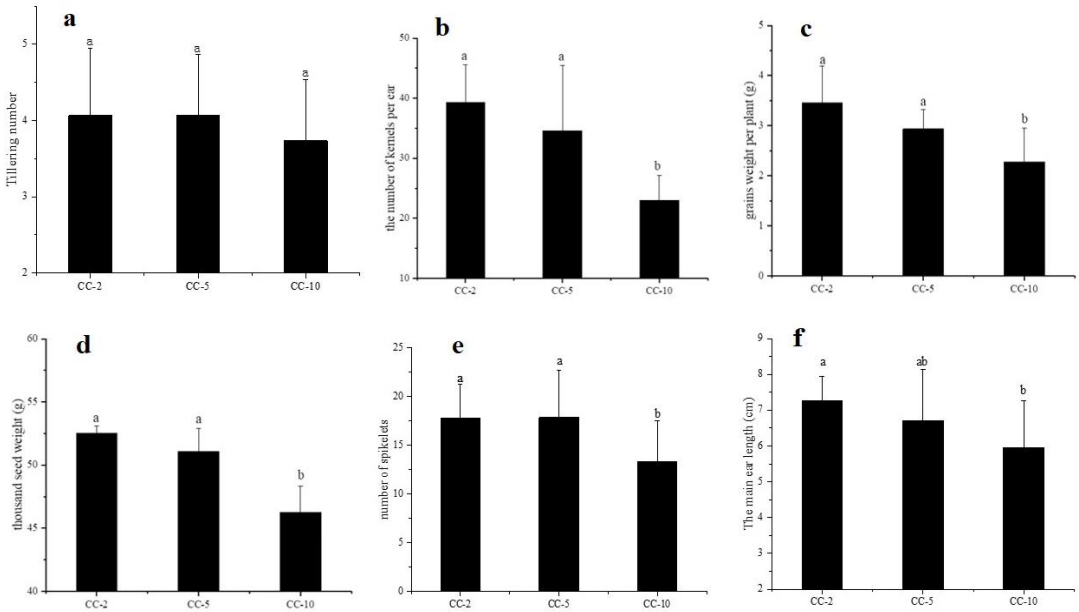

Figure 7. *Tilling number (a), number of kennels per ear (b), grain weight per plant (c), weight of a thousand seed per plant (d), number of spikelet (e), main ear length (f). (Bars with the different letters at the top under the same treatment are statistically different)*

http://www.aloki.hu ● ISSN 1589 1623 (Print) ● ISSN 1785 0037 (Online)
DOI: http://dx.doi.org/10.15666/aeer/2003_22712283

Through Venn analysis, it was shown that the highest number of bacterial species occurred at five years continuous cropping and there was highest relationship in species between five years continuous cropping and ten years continuous cropping treatments, supporting the contribution of continuous cropping on the emergence of the noted bacterial communities. Furthermore, based on the Ace, Chao, Shannon and Simpson diversity indices, it was shown that the microbial diversity had significant statistical variation between the treatment group, with Simpson clearly pointing out the increase in diversity with increase in cropping years. Indeed, through PLS-DA, it was noted that the control treatment had the least co-relation with the other treatment years, and the functional characteristics of communities across the treatment years were majorly on energy production and conversion, amino acid transport and metabolism, general function prediction and signal transduction mechanism. These findings showed the temporal variation in microbial community structure and associated functional characteristics under long term continuous cultivation of highland barley as had earlier been report by Nemadodzi et al. (2020). Moreover, the COG classification indicated that the functional characteristics of communities across the treatments were majorly on energy production and conversion, amino acid transport and metabolism, general function prediction and signal transduction mechanism, indicating the most needed microbial functions with increase in cropping years which result to the degradation in the quality of the soil.

Soil microbial biomass is the main driving force in the decomposition of organic materials and is frequently used as an early indicator of changes in soil properties that result from soil management and environment stresses in agricultural ecosystems. Furthermore, microbial interaction within the soil elevates the spatial heterogeneity of both the soil microbial biomass Carbon and Nitrogen (Richter et al., 2018). The microbial carbon and nitrogen biomass were both lower within the two years of continuous cropping treatment than the other treatments. This could be based on the clearance of the available carbon and nitrogen at the early stages of the continuous cropping before the replenishment take over in the following years of continuous cropping, due to the emergence in the identified microbial genera (Mooshammer et al., 2017).

Acid phosphatase is an enzyme widely found in soil that frees the attached phosphate group from other molecules and is used by microorganisms to access organically-bound phosphate (Bacmaga et al., 2015). Sucrose plays an important role in biological systems by influencing the osmoregulation, tolerance to temperature and desiccation, cell signaling and carbon transport and storage (Gu et al., 2019). The enzymatic hydrolysis of sucrose by the enzyme sucrase results in the formation of its two monosaccharide components. According to the present study, continuous cropping promoted the occurrence of these two classes of soil enzymatic activities. However, there was reduction in the occurrence of Soil urase enzymatic activity (S-UE) and the Soil polyphenol oxidase enzymatic activity (S-PPO) with increase in continuous cropping. Soil urease is majorly considered to be of microbial in origin, and its activity in soils is due to accumulated urease. This enzyme is remarkably stable in organo-mineral complexes found in soil (Dharmakeerthi et al., 1996). The enzyme urease plays numerous roles in the survival of most plants. It is mainly involved in the nitrogen metabolism, where urea is primarily used as a source of nitrogen necessary for growth. It also catalyzes the hydrolysis of urea to ammonium and carbamate ions, which decompose to carbon dioxide and ammonia. Urease activity is widely distributed in the

http://www.aloki.hu ● ISSN 1589 1623 (Print) ● ISSN 1785 0037 (Online)
DOI: http://dx.doi.org/10.15666/aeer/2003_22712283

soil where it also plays essential role in nitrogen metabolism (Kumar, 2015). Studies have shown that phenolic compounds exuded by roots are significant in the allelopathic interactions among plants and root enzymes that destroy phenolics and may protect plants against allelopathic inhibition and thus aid in invasiveness. Phenolic-degrading enzymes are mostly found in aboveground plant parts, but have also been previously reported in root tissues (Sinsabaugh, 2010). Furthermore, the decline in all the agronomic traits (Tilling number, number of kennels per ear, grain weight per plant, thousand seed weight, number of spikelets and the main ear length) with increase in continuous cropping years was an indication of the effect of continuous cropping on the Tibetan barley phenotypic traits. Indeed, studies have shown that that continuous cropping greatly affect the yield of most highland crops which may be for this case include the Tibetan barley (Li et al., 2020).

Conclusion and recommendation

The highest number of species occurred at five years of continuous cropping. The species similarity was highest between five and ten years of continuous cropping and both had biggest difference with species under the control, indicating the uniqueness and shift in the soil microbial characteristics across the cropping years. Indeed, through the different indices, there was statical differences in species abundance. The Clusters of Orthologous Groups (COG) classification indicated that the functional characteristics of communities across the treatments were majorly on energy production and conversion, amino acid transport and metabolism, general function prediction and signal transduction mechanism. All the values for the reported enzymatic activities had statistically significant difference between the treatments and the agronomic traits had general decline with increase in continuous cropping years of the Tibetan barley. Therefore, a long-term study on the correlation between the changes in specific soil properties and the soil microbial community structure, enzymatic characteristics and the plant agronomic traits is recommended.

Acknowledgements. This work was supported by the National Key R&D Program of China (Grant no. 2019YFD1001700), the National Science Foundation of China (Grant no. 32060447), and the China Agriculture Research System (Grant no. CARS-05).

REFERENCES

[1] Baćmaga, M., Kucharski, J., Wyszkowska, J. (2015): Microbial and enzymatic activity of soil contaminated with azoxystrobin. – Environmental Monitoring and Assessment 187(10): 615. https://doi.org/10.1007/s10661-015-4827-5.

[2] Chernov, T. I., Tkhakakhova, A. K., Kutovaya, O. V. (2015): Assessment of diversity indices for the characterization of the soil prokaryotic community by metagenomic analysis. – Eurasian Soil Sc. 48: 410-415. https://doi.org/10.1134/S1064229315040031.

[3] Costa, S. S., Guimarães, L. C., Silva, A., Soares, S. C., Baraúna, R. A. (2020): First steps in the analysis of prokaryotic pan-genomes. – Bioinformatics and Biology Insights 14: 1-9. https://doi.org/10.1177/1177932220938064.

[4] Dharmakeerthi, R., Thenabadu, M. (1996): Urease activity in soils: a review. – Journal of the National Science Foundation of Sri Lanka 24(3): 159-195. DOI: http://doi.org/10.4038/jnsfsr.v24i3.5548.

http://www.aloki.hu ● ISSN 1589 1623 (Print) ● ISSN 1785 0037 (Online)
DOI: http://dx.doi.org/10.15666/aeer/2003_22712283

[5] Gao, Q., Meng, X. Z., Yu, H. F. (2006): Reason analysis and control methods ofsuccession cropping obstacle. – Shandong Agricultural Sciences 3: 60-63 (in Chinese with English abstract).
[6] Gu, C., Zhang, S., Han, P., Hu, X., Xie, L., Li, Y., Brooks, M., Liao, X., Qin, L. (2019): Soil enzyme activity in soils subjected to flooding and the effect on nitrogen and phosphorus uptake by oilseed rape. – Frontiers in Plant Science 10: 368. https://doi.org/10.3389/fpls.2019.00368.
[7] Tang, H-M., Xiao, X-P., Tang, W-G., Lin, Y-C., Wang, K., Yang, G-L. (2014): Effects of winter cover crops residue returning on soil enzyme activities and soil microbial community in double-cropping rice fields. – PloS ONE 9(6): e100443. https://doi.org/10.1371/journal.pone.0100443.
[8] Han, G., Lan, J., Chen, Q., Yu, C., Bie, S. (2017): Response of soil microbial community to application of biochar in cotton soils with different continuous cropping years. – Scientific Reports 7(1): 10184. https://doi.org/10.1038/s41598-017-10427-6.
[9] Krupenikov, I. A., Boincean, B. P., Dent, D. (2011): Farming and Soil Health. – In: The Black Earth. International Year of Planet Earth. Springer, Dordrecht. https://doi.org/10.1007/978-94-007-0159-5_17.
[10] Krzywinski, M., Schein, J., Birol, I., Connors, J., Gascoyne, R., Horsman, D., Jones, S. J., Marra, M. A. (2009): Circos: an information aesthetic for comparative genomics. – Genome research 19(9): 1639-1645. https://doi.org/10.1101/gr.092759.109.
[11] Kumar, S. (2015): Plant Ureases: physiological significance, role in agriculture and industrial applications. A review South Asian J. – Food Technol. Environ. 1(2): 105-115.
[12] Lam, F., Lalansingh, C. M., Babaran, H. E., Wang, Z., Prokopec, S. D., Fox, N. S., Boutros, P. C. (2016): VennDiagramWeb: a web application for the generation of highly customizable Venn and Euler diagrams. – BMC Bioinformatics 17: 401. https://doi.org/10.1186/s12859-016-1281-5.
[13] Legendre, P., Condit, R. (2019): Spatial and temporal analysis of beta diversity in the Barro Colorado Island forest dynamics plot, Panama. – For. Ecosyst. 6: 7. https://doi.org/10.1186/s40663-019-0164-4.
[14] Li, M., Yang, F., Wu, X., Yan, H., Liu, Y. (2020): Effects of continuous cropping of sugar beet (Beta vulgaris L.) on its endophytic and soil bacterial community by high-throughput sequencing. – Ann Microbiol 70(39). https://doi.org/10.1186/s13213-020-01583-8.
[15] Liu, R., Dai, Y., Sun, L. (2015): Effect of rhizosphere enzymes on phytoremediation in PAH-contaminated soil using five plant species. – PloS one 10(3): e0120369. https://doi.org/10.1371/journal.pone.0120369.
[16] Lyu, J., Jin, L., Jin, N., Xie, J., Xiao, X., Hu, L., Tang, Z., Wu, Y., Niu, L., Yu, J. (2020): Effects of different vegetable rotations on fungal community structure in continuous tomato cropping matrix in greenhouse. – Front Microbiol. 11: 829. https://doi.org/10.3389/fmicb.2020.00829.
[17] Makarov, M. I., Malysheva, T. I., Maslov, M. N., Kuznetsova, E. Y., Menyailo, O. V. (2016): Determination of carbon and nitrogen in microbial biomass of southern-Taiga soils by different methods. – Eurasian Soil Sc. 49: 685-695. https://doi.org/10.1134/S1064229316060053.
[18] Monaci, E., Polverigiani, S., Neri, D., Bianchelli, M., Santilocchi, R., Toderi, M., D'Ottavio, P., Vischetti, C. (2017): Effect of contrasting crop rotation systems on soil chemical and biochemical properties and plant root growth in organic farming: first results. – Italian Journal of Agronomy 12(4). https://doi.org/10.4081/ija.2017.831.
[19] Mooshammer, M., Hofhansl, F., Frank, A. H., Wanek, W., Hämmerle, L., Leitner, S., Schnecker, J., Wild, B., Watzka, M., Keiblinger, K. M., Zechmeister-Boltenstern, S., Richter, A. (2017): Decoupling of microbial carbon, nitrogen, and phosphorus cycling in response to extreme temperature events. – Science Advance 3: e1602781. http://advances.sciencemag.org.

http://www.aloki.hu ● ISSN 1589 1623 (Print) ● ISSN 1785 0037 (Online)
DOI: http://dx.doi.org/10.15666/aeer/2003_22712283

[20] Nemadodzi, L. E., Vervoort, J., Prinsloo, G. (2020): NMR-based metabolomic analysis and microbial composition of soil supporting Burkea africana growth. – Metabolites 10(10): 402. https://doi.org/10.3390/metabo10100402.
[21] Ofek, M., Hadar, Y., Minz, D. (2012) Ecology of root colonizing Massilia (Oxalobacteraceae). – PLoS ONE 7(7): e40117. https://doi.org/10.1371/journal.pone.0040117.
[22] Richter, A., Huallacháin, D. O., Doyle, E., Clipson, N., Van Leeuwen, J. P., Heuvelink, J. B., Creamer, R. E. (2018): Linking diagnostic features to soil microbial biomass and respiration in agricultural grassland soil: a large-scale study in Ireland. – European Journal of Soil Science 68(3): 414-428. https://doi.org/10.1111/ejss.12551.
[23] Rigon, J. P. G., Calonego, J. C. (2020): Soil carbon fluxes and balances of crop rotations under long-term no-till. – Carbon Balance Manage 15: 19. https://doi.org/10.1186/s13021-020-00154-3.
[24] Sinsabaugh, R. L. (2010): Phenol oxidase, peroxidase and organic matter dynamics of soil. – Soil Biology and Biochemistry 42(3). 391-404. https://doi.org/10.1016/j.soilbio.2009.10.014.
[25] Tatusov, R. L., Galperin, M. Y., Natale, D. A., Koonin, E. V. (2000): The COG database: a tool for genome-scale analysis of protein functions and evolution. – Nucleic Acids Research 28(1): 33-36. https://doi.org/10.1093/nar/28.1.33.
[26] Walsh, C. M., Gebert, M. J., Delgado-Baquerizo, M., Maestre, F. T., Fierer, N. 2019. A global survey of mycobacterial diversity in soil. – Appl Environ Microbiol 85: e01180-19. doi: 10.1128/AEM.01180-19.
[27] Wienhold, B., Pikul, J., Liebig, M., Mikha, M., Varvel, G., Doran, J., Andrews, S. (2006): Cropping system effects on soil quality in the Great Plains: synthesis from a regional project. – Renewable Agriculture and Food Systems 21(1): 49-59. https://doi.org/10.1079/RAF2005125.
[28] Willis, A. D. (2019): Rarefaction, alpha diversity, and statistics. – Front. Microbiol. 10: 2407. https://doi.org/10.3389/fmicb.2019.02407.
[29] Yang, T., Siddique, K. H. M., Liu, K. (2020): Cropping systems in agriculture and their impact on soil health. A review. – Global Ecology and Conservation 23: e01118. https://doi.org/10.1016/j.gecco.2020.e01118.
[30] Zhou, L., Li, H., Zhang, Y., Han, S., Xu, H. (2016): Sphingomonas from petroleum-contaminated soils in Shenfu, China and their PAHs degradation abilities. – Brazilian Journal of Microbiology 47(2): 271-278. https://doi.org/10.1016/j.bjm.2016.01.001.

http://www.aloki.hu ● ISSN 1589 1623 (Print) ● ISSN 1785 0037 (Online)
DOI: http://dx.doi.org/10.15666/aeer/2003_22712283

THE EFFECT OF IMMOBILIZED *BACILLUS AMYLOLIQUEFACIENS* JF-1 MODULATE DYNAMICS ON SOIL MICROBIAL COMMUNITIES AND DISEASE SUPPRESSION CAUSED BY *FUSARIUM GRAMINEARUM*

LIU, H. L.[1] – QI, Y. Q.[1] – WANG, J. H.[1*] – JIANG, Y.[1] – GENG, M. X.[1] – LIU, Y. X.[2]

[1]*College of Resources and Environment, Jilin Agricultural University, Changchun, China (phone: +86-187-3245-8429)*

[2]*Shuangqiao Zone, Chengde City, Hebei Province, China (phone: +86-159-3009-2008)*

**Corresponding author e-mail: wjh489@126.com; phone: +86-152-4314-9594*

(Received 1st Nov 2021; accepted 25th Mar 2022)

Abstract. Stalk rot in maize, which is mainly caused by *Fusarium graminearum*, is a common soilborne disease in maize-producing areas of the world. Here we show the potential of *Bacillus amyloliquefaciens* JF-1 as a biological control against *Fusarium graminearum*. The inhibition rate of *F. graminearum* mycelial growth by JF-1 was 83.95%. Scanning electron microscopy revealed that mycelia treated with JF-1 had swelling and deformation. Moreover, the antagonistic mechanism of JF-1 crude extract decreased the intracellular ATP content of pathogens and led to significant nucleic acid leak. To evaluate the potential use of JF-1 in agriculture, a pot experiment revealed that the control efficiency of JF-1 cells immobilized with maize straw biochar against maize stalk rot at seedling stage reached 65.36%. The immobilized microorganisms of maize biochar improved the physical and chemical properties and soil fertility, as well as the microbial community structure, increased the relative abundance of *Proteobacteria*, *Actinobacteria*, *Mortierellomycota* and *Glomeromycota*, and reduced the relative abundance of *Ascomycota*, which includes *F. graminearum*, with pathogenic potential, transforming the soil microbial community from 'pathological' to 'healthy'. This discovery confirms that JF-1 can be used as a biological control agent to effectively reduce the incidence of maize disease.

Keywords: *agricultural wastes, soil nutrients, maize disease, soil remediation, biological control*

Introduction

Maize (*Zea mays* L.) is not only an important food and forage crop but also a major industrial raw material and energy source (Deutsch et al., 2018; Savary et al., 2019). With an increase in the degree of intensive crop planting, continuous cropping obstacles, such as deterioration of maize growth and decline in yield and quality, have been observed. The occurrence of soil-borne diseases is an important factor causing continuous cropping obstacles (Ren et al., 2008). Stalk rot, a soil-borne disease caused by *Fusarium graminearum*, is widely distributed in many maize growing areas of the world. *F. graminearum* is a soil-borne fungus, which mainly infects maize roots and can cause damage throughout the growth period of the plant. *F. graminearum* is considered as a species complex that can produce not only deoxynivalenol in the form of 3-acetyldeoxynivalenol (3ADON chemotype) or 15-acetyldeoxynivalenol (15ADON chemotype) but NIV and acetylated derivatives (NIV chemotype) (Chen et al., 2022). It can also inhibit the synthesis and transformation of proteins in animal cells, leading to apoptosis of animal cells; it thus threatens the health of humans and

http://www.aloki.hu ● ISSN 1589 1623 (Print) ● ISSN 1785 0037 (Online)
DOI: http://dx.doi.org/10.15666/aeer/2003_22852302

animals in addition to that of infected crops (Pestka, 2010; Rocha et al., 2005). In recent years, due to reasons, such as straw carrying pathogenic fungi returned to the soil and long-term continuous cropping, the continuous accumulation of pathogenic fungi in soil has become an important cause of maize stalk rot infection, posing a serious threat to the soil microecological environment and agricultural economy.

As a plant disease control technology with broad application potential, biological control can control soil-borne diseases through antagonism of microorganisms toward pathogenic fungi, improvement of the physical and chemical properties of soil, and induction of plant resistance gene expression. Recently, biological control of plant diseases has been achieved in many crops (Qi et al., 2020; Liu et al., 2021). Studies have shown that the genera *Bacillus* and *Pseudomonas* play a key role in the control of various plant pathogenic fungi, such as *Eutypa lata*, *Gaeumannomyces graminis*, and *Magnaporthe oryzae* (Wakelin et al., 2002; Shan et al., 2013; Abo-Elyousr et al., 2009). *Paenibacillus polymyxa* can inhibit pathogenic fungi by secreting chitinase, cellulase, protease, and other enzymes that can destroy the cell wall structure of pathogenic fungi (Jensen et al., 2002). *Pseudomonas monteilli* not only enhances the ability of plant roots to absorb nutrients but also enhances the resistance of plants to pesticides and heavy metal pollution stress (Ramesh et al., 2009; Rani et al., 2009). Jain et al. (2019) reported that the encapsulation of pea seeds by biocontrol bacteria can induce systemic resistance to *Sclerotinia sclerotiorum* and improve the activities of catalase and guaiacol.

Many researchers have isolated antagonistic bacteria with a broad spectrum of antifungal properties from soil and plants; however, few reports exist on the improvement of the soil microbial community and soil remediation by microbial agents prepared using microorganisms and crop residues. We selected *Bacillus amyloliquefaciens* JF-1 (GenBank accession number: MW578378), which was preserved in our lab that isolated through disease soil, with efficiently inhibition on *F. graminearum* and investigated its inhibitory effect on the growth of pathogenic fungus of maize stalk rot. Additionally, the effects on bacterial and fungal communities in soil were explored. The study findings can have profound implications for agricultural production, food safety, and soil ecology.

Materials and methods

Inhibitory effects of JF-1 on pathogenic fungal hyphae

After the activation of *B. amyloliquefaciens* JF-1 strain, it was inoculated in Luria Bertani (LB) medium (10.0 g peptone, 5.0 g yeast extract, 10.0 g NaCl, 20.0 g agar, 1000 mL distilled water, pH = 7.0). The sterile filtrate of JF-1 was prepared as follows: (1) JF-1 was inoculated in 100 mL LB liquid medium; (2) It was then incubated in a constant-temperature oscillator (Thermostatic HZQ-X300C, Shanghai Yiheng Science Instrument Co. Ltd., China) with constant shaking at 150 rpm and 30 °C for 24 h. JF-1 bacterial liquid was centrifuged in a cryogenic high-speed centrifuge LC-LX-HLR300D (Shanghai Lichen Technology Bangxi Instrument Technology Co. Ltd., China) at 7,104 g for 10 min. After centrifugation, the supernatant was filtered through a sterile filter membrane (0.22 μm), and the sterile filtrate was mixed with potato dextrose agar (PDA) medium at volume percentages of 5%, 10%, 20%, and 40%. The pathogenic fungus causing maize stalk rot (*F. graminearum*, GenBank accession number BGC0001600) was inoculated at the center

http://www.aloki.hu ● ISSN 1589 1623 (Print) ● ISSN 1785 0037 (Online)
DOI: http://dx.doi.org/10.15666/aeer/2003_22852302

of solid PDA medium, and the PDA plate without sterile filtrate was used as the blank control. The fungus was cultured in an incubator at 30 ℃ for 7 days. The fungal inhibition rate was calculated according to the following formula:

$$\text{Fungal inhibition rate} = [(A1 - A2) / A1] \times 100\% \quad \text{(Eq.1)}$$

where A_1 is the colony diameter without any sterile filtrate addition (blank control) and A_2 is the colony diameter treated with sterile filtrate.

JF-1 inhibition mechanisms on F. graminearum in maize

Determination of fungal cell wall degrading enzymes and plant auxin ability of JF-1

The ability of JF-1 to secrete protease, cellulase, chitinase, and indole-3-acetic acid (IAA) was quantitatively determined using an ELISA kit, as previously described (Jiang et al., 2020).

Preparation of JF-1 crude extract fungal inhibition

The implementation method referred to previous study (Du et al., 2017), $(NH_4)_2SO_4$ was added to the sterile filtrate of JF-1 LB culture until 60% saturation, rested at 4 ℃ for 2 h. The sterile filtrate of JF-1 LB culture was centrifuged at 7,104 g for 10 min, and then removed the supernatant, placed in a dialysis bag with the molecular weight cutoff of 8,000–14,000 DA; the dialysis bag was placed in 0.1 mol/L PBS buffer (pH 7. 0) overnight for dialysis. Finally, the solution in the dialysis bag was centrifuged for 10 min at 7,104 g and the supernatant was remained.

Determining the effect of JF-1 crude extract on ATP content of pathogenic fungal cells

Referring to the methods of research by Bajpai et al. (2015), 10 mL JF-1 crude extract was mixed with 100 mL fungal suspension (prepared by 0.1 mol/L PBS buffer) and inoculated in the oscillator at 28 ℃ and 150 rpm, 2 mL of the mixture at 0, 2, 4, 6, 8 and 10 h were took out and centrifuged at 7,104 g for 10 min and the supernatant was removed. The ATP content was measured with ATP assay kit (JianCheng, China), and 10 mL aseptic water was added as blank control. Each treatment was repeated thrice.

Determining the effect of JF-1 crude extract on nucleic acid leakage of pathogenic fungal cells

The nucleic acid contents were referring to a method of Souza et al. (2010), the change of cell membrane integrity was predicted by measuring the change of absorbance value of supernatant at 260 nm (Teethaisong et al., 2014). 10 mL JF-1 crude extract was mixed with 100 mL fungal suspension (prepared by 0.1 mol/L PBS buffer, the fungus was cultured by shaking in liquid PDA medium at 25 ℃ for 3~4 d and centrifuged at 7,104 g for 10 min and the supernatant was removed) and inoculated in the oscillator at 28 ℃ and 150 × g, respectively, 2 mL of the mixture at 0, 2, 4, 6, 8 and 10 h were took out and centrifuged at 7,104 g for 10 min, the absorbance value of the supernatant was determined by a UV-Vis spectrophotometer (Shimadzu UV-2600 spectrophotometer, Japan) at 260 nm, and 10 mL aseptic water was added as blank control. Each treatment was repeated thrice.

http://www.aloki.hu ● ISSN 1589 1623 (Print) ● ISSN 1785 0037 (Online)
DOI: http://dx.doi.org/10.15666/aeer/2003_22852302

Pot experiment of JF-1 on soil remediation of maize disease

Soil samples were taken from a patch of black soil (0-20 cm) with a high incidence of maize stalk rot and continuous cultivation for years, located in Jingyue District, Changchun City, Jilin Province, China, and belonging to the continental subhumid monsoon climate type of North temperate zone. Following this, 5 g each of sterilized distilled water, sterilized straw, and sterilized straw biochar were added into an equal volume of JF-1 bacterial suspension with a concentration of 1×10^8 CFU/mL at a ratio of 1: 40 (m/V), and the culture was centrifuged at 30 ℃ and 150 rpm for 12 h. Following this, the culture was centrifuged at 7,104 g for 10 min. The supernatant was removed to obtain a single JF-1 microbial agent, maize straw combined with JF-1 microbial agent, and maize straw biochar combined with JF-1 microbial agent, and they were stored in a refrigerator at 4 ℃ for subsequent use. The pot experiment was divided into three treatment groups, namely (1) T1 treatment: 10 g of single JF-1 microbial agent; (2) T2 treatment: maize straw combined with 10 g JF-1 microbial agent; and (3) T3 treatment: maize straw biochar combined with 10 g JF-1 microbial agent, and a CK blank control with no addition of substances. (Biochar preparation: An appropriate amount of maize stalk powder was placed into a crucible, sealed with aluminum foil paper, and placed into a muffle furnace. The pyrolysis temperatures were controlled at 400 ℃, using a heating rate of 10 ℃/min and a residence time of 1 h. The biochar samples were obtained through pyrolysis at the corresponding temperature for 1 h). Ten grams each of different microbial agents were evenly mixed with 500 g soil and they were added into small PVC pots. Each treatment was repeated thrice. The soil samples were inoculated with a highly pathogenic *F. graminearum* spores suspension with a concentration of 1×10^8 CFU·mL^{-1} at a ratio of 1:50 (spore suspension: soil, V/m). The soil moisture content was adjusted to 70% of the field moisture content, and the temperature was maintained at 30 ℃ during the day and 20 ℃ at night. After 90 days of culture, 100 g soil of each pot were collected and stored for future experiments and three maize seeds were planted in each pot, when the seedlings at the four-leaf stage, the plant height, fresh weight and root length (the length of the longest root was measured by avernier caliper) were measured and the disease index and control efficiency were calculated. The disease index and control efficiency were assayed as described by Wu et al. (2015); malondialdehyde (MDA) content in maize roots was measured by the thiobarbituric acid-reactive substances assay.

Determination of the physicochemical properties and enzyme activities of soil

The physicochemical properties of soil, including pH value, organic matter content, alkali-hydrolysable nitrogen, available phosphorus, available potassium, and cation exchange capacity, were measured according to previous studies (Qi et al., 2021; Wang et al., 2020). Soil enzymes include invertase, urease, catalase, and phosphatase, and the measurement method was based on previous studies (Chang et al., 2019).

Extraction and PCR amplification of microbial DNA from soil samples

Extraction of microbial DNA from soil samples

DNA was extracted from soil samples using an E.Z.N.A Mag-Bind Soil DNA Kit (Omega Corporation of America) according to manufacturer's instructions. Genomic

http://www.aloki.hu ● ISSN 1589 1623 (Print) ● ISSN 1785 0037 (Online)
DOI: http://dx.doi.org/10.15666/aeer/2003_22852302

DNA was accurately quantified using the Qubit 2.0 DNA test kit to determine the amount of DNA added in the PCR reaction mixture.

PCR amplification

Taking the total microbial DNA of soil samples as the template, PCR amplification was performed using the bacterial V3-V4 region-specific primer (338F 5'-ACTCCTACGGGAGCAG-3'; 806R 5'-GGACTACHVGGGTWTCTAAT-3') and fungal ITS specific primers (ITS1F 5'-CTTGGTCATTAGAGGAAGTAA-3'; ITS2 5'-TGCGTTCTTCATCGATGC-3'). PCR amplification was divided into the following steps: (1) 50 μL PCR amplification reaction contained 15 μL 2 × Taq master Mix, 1 μL of 10 μM Bar-primer F, 1 μL of 10 μM Bar-primer R, and 10-20 ng genomic DNA template filled with water; (2) Illumina bridge PCR compatible primers were introduced in the 50 μL amplification system, and the reaction contained 15 μL 2 × Taq master Mix, 1 μL of 10 μM primer F, 1 μL of 10 μM primer R, and 20 ng PCR product generated from the first step filled with water. The PCR products were determined using 1% agarose gel electrophoresis, and the DNA was purified and recovered. Beijing Auwigene Gene Technology Co., Ltd was commissioned to complete high-throughput sequencing.

Statistical analysis

The raw data were first screened to remove sequences < 200 bp in length and chimeras to obtain good quality sequences as clean-tags. Program vsearch 2.7.1 was used to perform OTU (Operational Taxonomic Units) classification on the processed sequences, and OTUs at 97% similarity level were clustered. Bioinformatic analysis was performed based on the results of OTUs clustering analysis. Venn diagrams were plotted by R to count the number of common and unique OTUs to multiple samples (Fouts et, al. 2012). Origin 2019 (OriginLab, USA) was used for statistical analysis. The average value for each treatment was calculated, and differences between the groups were calculated via one-way analysis of variance using the least significant differences test at 5% ($P < 0.05$) probability level. Chao1, Shannon, and Simpson indices were calculated by the following equations (Sun et al., 2022).

$$\boldsymbol{Chao}1 = \boldsymbol{S_{obs}} + \frac{n\,(n1\text{-}1)}{2\,(\boldsymbol{n}2 + 1)} \quad \text{(Eq.2)}$$

where Chao1 means the evaluated OTU number; Sobs means the observed OTU number; n1 means the OTU number with singletons; n2 means the OTU number with doubletons.

$$\text{Shannon} = -\sum_{i=1}^{S_{obs}} \frac{n_i}{N} \ln \frac{n_i}{N} \quad \text{(Eq.3)}$$

$$\text{Simpson} = 1 - \frac{\sum_{i=1}^{S_{obs}} n_i\,(n_i\text{-}1)}{N\,(N\text{-}1)} \quad \text{(Eq.4)}$$

where Sobs means the measured OTU number; ni means the OTU number with sequence of i; N means the number of all sequences.

http://www.aloki.hu ● ISSN 1589 1623 (Print) ● ISSN 1785 0037 (Online)
DOI: http://dx.doi.org/10.15666/aeer/2003_22852302

Results

Inhibitory effect of JF-1 on pathogenic fungus hyphae

According to the results in *Table 1,* the inhibition ability of JF-1 on the mycelia of pathogenic fungi increased with the increase in the concentration of the JF-1 sterile filtrate. When the concentration of the sterile filtrate reached 40%, the inhibition rate of mycelia was the highest (83.95%). As revealed in *Figure 1,* It was found by scanning electron microscopy that the mycelia of pathogenic fungi were enlarged and deformed, while the surface of the blank control group was smooth, full, and without any mycelial deformation. The results showed that the JF-1 sterile filtrate could inhibit *F. graminearum* by destroying its mycelia.

Table 1. *Inhibitory effect of JF-1 on hyphae of pathogenic fungi*

JF-1 concentration (%)	***F. graminearum***	
	CD (mm)	**FIR (%)**
Blank control	81 ± 3 a	-
5	52 ± 5 b	35.80 d
10	43 ± 6 c	46.91 c
20	25 ± 4 d	69.14 b
40	13 ± 5 e	83.95 a

All the presented values are means of three replicates. Means were subjected to analysis of variance and were separated by LSD test. Letters represent the significant difference among the mean values and ± are standard error values of the means. CD is colony diameter, FIR is fungal inhibition rate

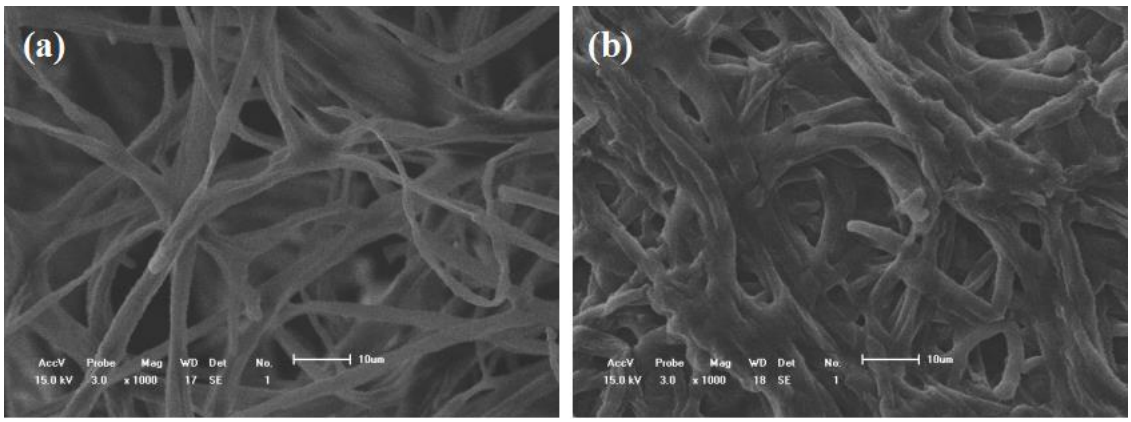

Figure 1. *Inhibitory effect of JF-1 on pathogenic fungus hyphae. Morphology of pathogenic fungus hyphae observed by scanning electron microscope (×1000), (a) is blank control and (b) is pathogenic fungus hyphae treated with JF-1*

JF-1 inhibition mechanisms on F. graminearum in maize

JF-1 produces fungal cell wall degrading enzymes and plant auxin

JF-1 bacterial liquid possessed a high content of main fungal cell wall hydrolases (*Table 2*). Among them, 18.79 pg mL^{-1} protease, 76.35 pg mL^{-1} cellulase enzyme, and 65.57 pg mL^{-1} chitinase facilitated plant growth and IAA production, and the level of

http://www.aloki.hu ● ISSN 1589 1623 (Print) ● ISSN 1785 0037 (Online)
DOI: http://dx.doi.org/10.15666/aeer/2003_22852302

the JF-1 strain reached 4.29 pmol L^{-1}, which were significantly higher than that of the blank control ($P < 0.05$).

Table 2. *Determination of fungal cell wall degrading enzymes and plant auxin ability of JF-1*

Metabolites	JF-1	Blank control
Pro (pg mL-1)	18.79 ± 0.07 a	3.74 ± 0.04 b
Cel (pg mL-1)	76.35 ± 0.38 a	6.73 ± 0.49 b
Chi (pg mL-1)	65.57 ± 0.87 a	5.53 ± 0.72 b
IAA (pmol L-1)	4.29 ± 0.03 a	0.48 ± 0.07 b

All the presented values are means of three replicates. Means were subjected to analysis of variance and were separated by LSD test. Letters represent the significant difference among the mean values and ± are standard error values of the means. Pro is Protease activity, Cel is Cellulase activity, Chi is Chitinase activity, IAA is indole-3-acetic acid.3.2.2 JF-1 decreased the ATP content of pathogenic fungal cells

JF-1 decreased the ATP content of pathogenic fungal cells

As illustrated in *Figure 2,* the ATP content of fungal cells treated with JF-1 crude extract decreased sharply (0.18 μmol/g) when compared with the blank control at 2 h. The decrease in ATP content reached a maximum value of 0.22 μmol/g after 8 h. The ATP content in fungal cells of the blank control was maintained at a stable level, whereas the ATP content of fungus treated with JF-1 crude extract was significantly lower than the blank control for the period of 0-10 h ($P < 0.05$). This may be due to the influence of JF-1 crude extract on the ability of *F. graminearum* to generate ATP, or due to the destruction of the cell membrane structure of *F. graminearum*, resulting in ATP leakage.

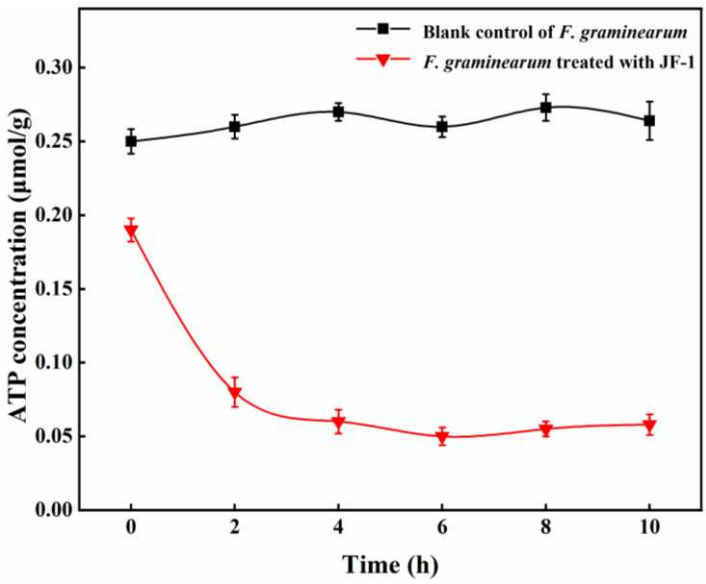

Figure 2. *JF-1 decreased the ATP content of pathogenic fungal cells. All the presented values are means of three replicates. Mean values were calculated and statistical analysis was performed using Origin 2019. All the mean values were subjected to analysis of variance, and means were separated at 5% probability. Error bars represent the standard error values of the means*

http://www.aloki.hu ● ISSN 1589 1623 (Print) ● ISSN 1785 0037 (Online)
DOI: http://dx.doi.org/10.15666/aeer/2003_22852302

JF-1 increased nucleic acid leakage of pathogenic fungal cells

Extracellular nucleic acid results from the leakage of nucleic acid from damaged cells and its content can be used as an indicator of the degree of cell damage and the formation of cell membrane holes. As shown in *Figure 3* in the period of 0–10 h, the absorbance of the supernatant of blank control at OD_{260nm} was always maintained at approximately 0.2. The absorption value of the supernatant treated with JF-1 crude extract reached 1.17 at 2 h. In the range of 0–10 h, the absorbance of the supernatant treated with JF-1 crude extract was always higher than that of blank control, indicating that the membrane permeability of *F. graminearum* cells had been changed by the JF-1 crude extract, resulting in nucleic acid leakage. However, at 6 h and 10 h, the fluctuation in the trend of absorption value may be due to the reuse of extracellular nucleic acid by *F. graminearum* cells as nutrients.

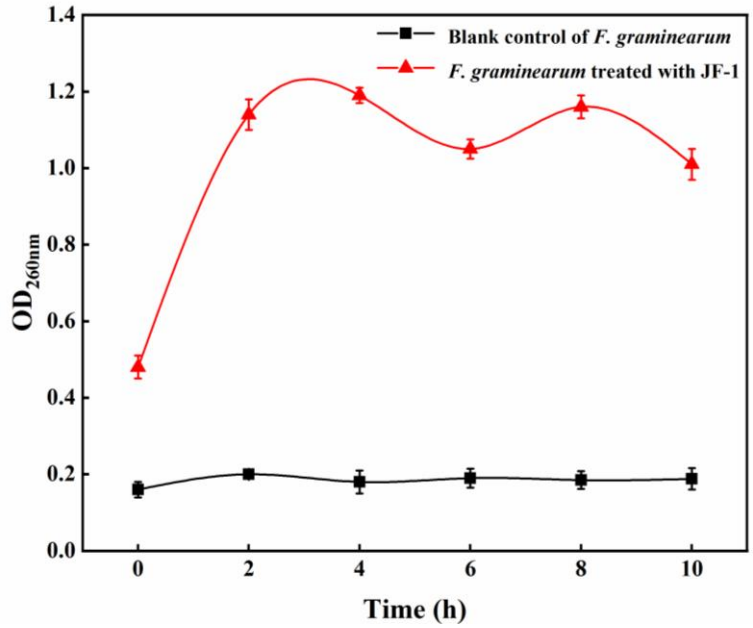

Figure 3. *Determining the effect of JF-1 on nucleic acid leakage of pathogenic fungal cells. All the presented values are means of three replicates. Mean values were calculated and statistical analysis was performed using Origin 2019. All the mean values were subjected to analysis of variance, and means were separated at 5% probability. Error bars represent the standard error values of the means*

Determination of the efficacy of JF-1 in reducing stalk rot in maize

Maize seedling experiment was carried out on the soil treated with T1, T2 and T3, all of which had a visible promotive effect on the growth of maize at the seedling stage, as shown in *Figure 4*. Notably, compared with blank control, T3 treatment increased the height, root length, and fresh weight of maize most significantly, increasing them by 19.71%, 9.04%, and 26.92%, respectively ($P < 0.05$). Simultaneously, compared with blank control, the control efficiency of T1, T2, and T3 treatments on stalk rot of maize seedlings reached 61.64%, 49.72%, and 65.36%, respectively, and the content of MDA in the root of maize seedlings decreased by 50.17%, 32.75%, and 67.60%, respectively.

http://www.aloki.hu ● ISSN 1589 1623 (Print) ● ISSN 1785 0037 (Online)
DOI: http://dx.doi.org/10.15666/aeer/2003_22852302

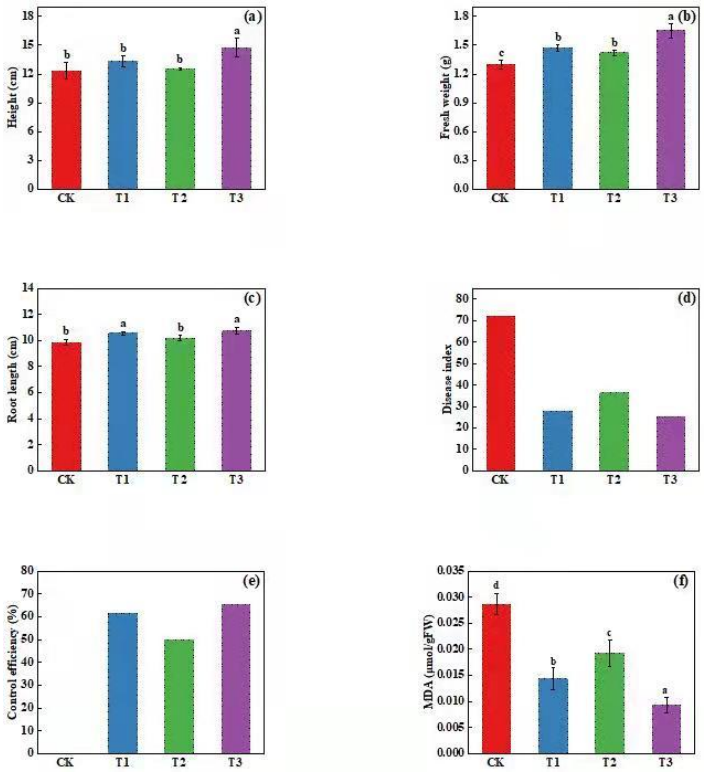

Figure 4. *The efficacy of JF-1 in reducing stalk rot in maize. All the presented values are means of three replicates. Means were subjected to analysis of variance and were separated by LSD test. Letters represent the significant difference among the mean values and ± are standard error values of the means. (a) is plant height; (b) is fresh weight; (c) is root length; (d) is disease index; (e) is control efficiency and (f) is MDA content. CK is blank control, T1 is single JF-1 microbial agent; T2 is maize straw combined with JF-1 microbial agent; T3 is maize straw biochar combined with JF-1 microbial agent*

Determination of the physicochemical properties and enzyme activities of soil

Maize straw combined with JF-1 and maize straw biochar combined with JF-1 significantly changed the physical and chemical properties and enzyme activities of soil ($P < 0.05$; *Table 3*). The soil pH values and cation exchange capacities of the T2 and T3 groups significantly increased ($P < 0.05$) compared to those of CK blank control group. The pH value increased by 3.37% and 5.86% and cation exchange capacity increased by 3.09% and 5.35% in T2 and T3 groups, respectively. After treatments with the three different JF-1 microbial agents, both the activities of soil nutrients and enzymes changed, and the effect of the T3 treatment were more obvious, compared with the CK blank control group, the organic matter, available N, available P, and available K content increased by 39.81%, 28.07%, 14.10%, and 4.91%, respectively. Thus, urease, invertase, phosphatase, and catalase increased by 94.51%, 43.40%, 52.78%, and 85.93%, respectively.

Results of soil microbial sequencing and differences in soil microbial community diversity

The DNA sequencing results of bacteria and fungi in the soil samples are shown in *Tables 4* and *5,* respectively. The sequencing coverage rate of all samples reached over

http://www.aloki.hu ● ISSN 1589 1623 (Print) ● ISSN 1785 0037 (Online)
DOI: http://dx.doi.org/10.15666/aeer/2003_22852302

98%, indicating that the sequencing depth of samples was sufficient to meet the requirements of subsequent numerical analysis. Alpha diversity is usually measured using the Chao1, Shannon, and Simpson indices. Among these, the Chao1 index reflects the richness of species, while the Shannon and Simpson indices reflect the diversity of species.

Table 3. *Effects of different treatments on soil physicochemical properties and enzyme activities*

Treatment	CK	T1	T2	T3
pH	5.63 ± 0.05 cd	5.68 ± 0.02 c	5.97 ± 0.03 b	6.15 ± 0.08 a
CEC (cmol kg^{-1})	20.73 ± 0.34 cd	20.85 ± 0.40 c	21.37 ± 0.93 b	21.84 ± 0.81 a
OM (g kg^{-1})	20.65 ± 0.73 d	21.88 ± 0.84 c	25.39 ± 0.61 b	28.87 ± 0.55 a
AN (mg kg^{-1})	96.84 ± 6.71 d	104.32 ± 5.16 c	115.37 ± 7.98 b	124.02 ± 6.34 a
AP (mg kg^{-1})	23.47 ± 0.26 cd	23.51 ± 0.19 c	26.73 ± 0.31 ab	26.78 ± 0.33 a
AK (mg kg^{-1})	214.83 ± 0.45 cd	215.47 ± 0.86 c	225.93 ± 0.59 a	225.38 ± 0.45 ab
URE (mg/g·d^{-1})	3.46 ± 0.25 d	3.87 ± 0.31 c	4.92 ± 0.18 b	6.73 ± 0.27 a
INV (mL/g·d^{-1})	8.25 ± 0.39 d	8.74 ± 0.26 c	10.69 ± 0.41 b	11.83 ± 0.33 a
PHO (μg/g·d^{-1})	0.36 ± 0.03 cd	0.39 ± 0.05 c	0.54 ± 0.01 ab	0.55 ± 0.02 a
CAT (mL/g·d^{-1})	3.34 ± 0.06 d	5.46 ± 0.11 c	5.78 ± 0.07 b	6.21 ± 0.09 a

All the presented values are means of three replicates. Means were subjected to analysis of variance and were separated by LSD test. Letters represent the significant difference among the mean values and ± are standard error values of the means. CK is blank control, T1 is single JF-1 microbial agent; T2 is maize straw combined with JF-1 microbial agent; T3 is maize straw biochar combined with JF-1 microbial agent. CEC is cation exchange capacity, OM is organic matter, AN is available nitrogen, AP is available phosphorus, AK is available potassium, URE is urease activity; INV is invertase activity; PHO is phosphatase activity; CAT is catalase activity

Table 4. *Effects of different treatments on the α diversity of bacterial community*

Sample	Number	Chao1	Coverage	OTUs	PD whole tree	Shannon	Simpson
CK	10682 ± 1983 d	5837.32 ± 142.89d	0.99	2868 ± 168 d	187 ± 18d	8.23 ± 0.56 cd	0.98
T1	12391 ± 1734 bc	6382.16 ± 127.67a	0.98	3128 ± 192 b	212 ± 21b	8.56 ± 0.41 c	0.98
T2	13095 ± 1802 a	6192.78 ± 138.24b	0.99	3207 ± 181 a	223 ± 15a	9.26 ± 0.53 a	0.99
T3	12893 ± 1879 b	6012.2 ± 165.43c	0.98	2949 ± 207 c	201 ± 19c	8.97 ± 0.62 b	0.99

All the presented values are means of three replicates. Means were subjected to analysis of variance and were separated by LSD test. Letters represent the significant difference among the mean values and ± are standard error values of the means. CK is blank control, T1 is single JF-1 microbial agent; T2 is maize straw combined with JF-1 microbial agent; T3 is maize straw biochar combined with JF-1 microbial agent

Table 5. *Effects of different treatments on the α diversity of fungal community*

Sample	Number	Chao1	Coverage	OTUs	PD whole tree	Shannon	Simpson
CK	10689 ± 1637 ab	1298.34 ± 128.13 b	0.99	1623 ± 119 a	182 ± 13 a	7.21 ± 0.51 a	0.94
T1	98201 ± 1702 c	1223.98 ± 102.32 c	0.99	1512 ± 103 c	163 ± 16 c	6.87 ± 0.67 b	0.98
T2	10735 ± 1629 a	1382.92 ± 138.27 a	0.98	1587 ± 138 b	175 ± 17 b	7.03 ± 0.46 ab	0.95
T3	95839 ± 1826 cd	1104.23 ± 129.74 d	0.99	1489 ± 121 cd	141 ± 11 d	5.83 ± 0.59 c	0.96

All the presented values are means of three replicates. Means were subjected to analysis of variance and were separated by LSD test. Letters represent the significant difference among the mean values and ± are standard error values of the means. CK is blank control, T1 is single JF-1 microbial agent; T2 is maize straw combined with JF-1 microbial agent; T3 is maize straw biochar combined with JF-1 microbial agent

Four soil samples were analyzed, the total operational taxonomic units (OTUs) of bacteria of the T1, T2, and T3 treatments increased by 9.07%, 11.82%, and 2.82%,

http://www.aloki.hu ● ISSN 1589 1623 (Print) ● ISSN 1785 0037 (Online)
DOI: http://dx.doi.org/10.15666/aeer/2003_22852302

respectively compared to those of CK blank control group. The Chao1 and Shannon indices of T1 treatment increased by 9.34% and 4.00%, respectively, those of T2 treatment increased by 6.09% and 12.52%, respectively, and those of T3 increased by 2.96% and 9.00%, respectively. The application of a single JF-1 microbial agent, maize straw combined with JF-1 microbial agent, and maize straw biochar combined with JF-1 microbial agent significantly increased the richness and diversity of the soil bacterial community ($P < 0.05$), and maize straw combined with JF-1 microbial agent showed the most significant increase ($P < 0.05$). As shown in *Figure 5a*, in the four treatments, the number of the same bacterial OTUs was 1,202. After T1, T2, T3, and CK blank control treatments, the OTU counts of unique bacteria in the soil samples were 577, 766, 368, and 457, respectively. Maize straw combined with a JF-1 microbial agent most significantly ($P < 0.05$) improved the abundance of unique bacteria in soil, by 67.61% as compared to that in the CK blank control group.

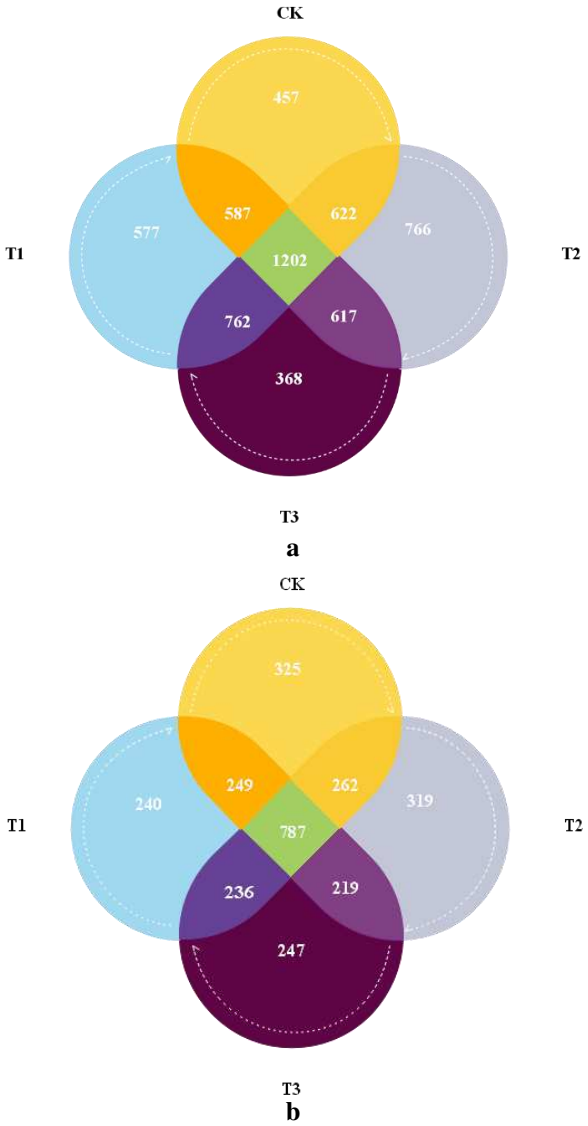

Figure 5. *OTUs number of bacterial and fungal communities in different treatments. The Venn diagrams showing the numbers of bacterial (a) and fungal (b) OTUs in different soil samples. CK is blank control, T1 is single JF-1 microbial agent; T2 is maize straw combined with JF-1 microbial agent; T3 is maize straw biochar combined with JF-1 microbial agent*

http://www.aloki.hu ● ISSN 1589 1623 (Print) ● ISSN 1785 0037 (Online)
DOI: http://dx.doi.org/10.15666/aeer/2003_22852302

The total OTUs of fungi in groups treated with T1, T2, and T3 decreased by 6.84%, 2.22%, and 8.26%, respectively, as compared to those in the CK blank control group. The Chao1 and Shannon indices of the T1 treatment decreased by 5.73% and 4.72%, respectively, as compared to those of CK blank control group. The Chao1 index of the T2 treatment increased by 6.51% and the Shannon index decreased by 2.50%. The Chao1 index of T3 treatment decreased by 14.95% and the Shannon index decreased by 19.14% as compared to those of CK blank control group. In conclusion, a single JF-1 microbial agent and maize straw biochar combined with JF-1 microbial agent significantly reduced the community richness and diversity of soil fungi ($P < 0.05$), and the effect of maize straw biochar combined with JF-1 microbial agent was more significant. However, maize straw combined with JF-1 microbial agent increased the richness of soil fungal community but decreased the diversity of soil fungal community. As shown in *Figure 5b*, among the four treatments, the number of the same fungi OTUs was 787 after T1, T2, T3, and CK blank control group treatments, and the OTU counts of unique fungi in the soil samples were 240, 319, 247, and 325, respectively, indicating that a single JF-1 microbial agent and maize straw biochar combined with a JF-1 microbial agent significantly reduced the abundances of unique soil fungi ($P < 0.05$) by 26.15% and 24.00%, respectively, as compared to the abundance in the CK blank control group.

Analysis of the differences in bacterial and fungal diversities at the phylum level between different treatments

The differences in bacterial community composition were analyzed at the phylum level (*Fig. 6a*). In the four soil samples, 41 phyla, 121 classes, 267 orders, 402 families, and 685 genera were detected. After T1, T2 and T3 treatments, the relative abundances of *Proteobacteria*, *Actinobacteria*, and *Gemmatimonadetes* were significantly higher ($P < 0.05$) than those in the CK blank control group, the relative abundance of *Acidobacteria* and *Chloroflexi* were significantly lower than that of CK blank control group ($P < 0.05$). After the single JF-1 microbial agent treatment, maize stalk combined with JF-1 microbial agent treatment, and maize stalk biochar combined with JF-1 microbial agent treatment, the relative abundances of *Proteobacteria*, which accounted for 23.42% in the CK blank control group, were increased by 10.04%, 6.37%, and 12.02%, respectively. The relative abundance of the second-most dominant bacteria, *Acidobacteria*, which accounted for 14.14% in the CK blank control group, decreased by 4.24%, 7.27%, and 10.56% in the T1, T2, and T3 groups, respectively, and it became the third dominant phylum in all three treatments groups. In contrast, the relative abundance of *Actinobacteria*, the third dominant bacteria accounting for 13.30% in CK blank control group, increased by 3.76%, 5.77%, and 9.16% in T1, T2, and T3 treatments, respectively, becoming the second dominant phylum in all three groups.

Differences in fungal community composition were analyzed at the phylum level (*Fig. 6b*). 13 phyla, 27 classes, 63 orders, 122 families, and 237 genera were detected in the four groups of soil samples. After T1, T2 and T3 treatments, the relative abundances of *Mortierellomycota* and *Basidiomycota* were significantly increased ($P < 0.05$) as compared to those of CK blank control group, the relative abundance of *Ascomycota* was significantly lower than that in the CK blank control group ($P < 0.05$). The relative abundance of *Ascomycota*, which accounted for 52.63% in CK blank control group, decreased by 5.99%, 12.45%, and 18.35% after a single JF-1 microbial agent treatment, maize stalk combined with JF-1 microbial agent treatment, and maize stalk biochar

http://www.aloki.hu ● ISSN 1589 1623 (Print) ● ISSN 1785 0037 (Online)
DOI: http://dx.doi.org/10.15666/aeer/2003_22852302

combined with JF-1 microbial agent treatment, respectively. The abundance of the second dominant phylum *Basidiomycota*, which accounted for 16.25% in the CK blank control group, increased by 5.04%, 6.02%, and 9.04% in T1, T2, and T3 groups, respectively, making it the third most dominant phylum in the three groups. The abundance of another dominant phylum, *Mortierellomycota*, which accounted for 14.37% in the CK blank control group, increased by 6.99%, 9.29%, and 12.64% after T1, T2, and T3 treatments, respectively, making it the second-most dominant phylum in all three treatment groups.

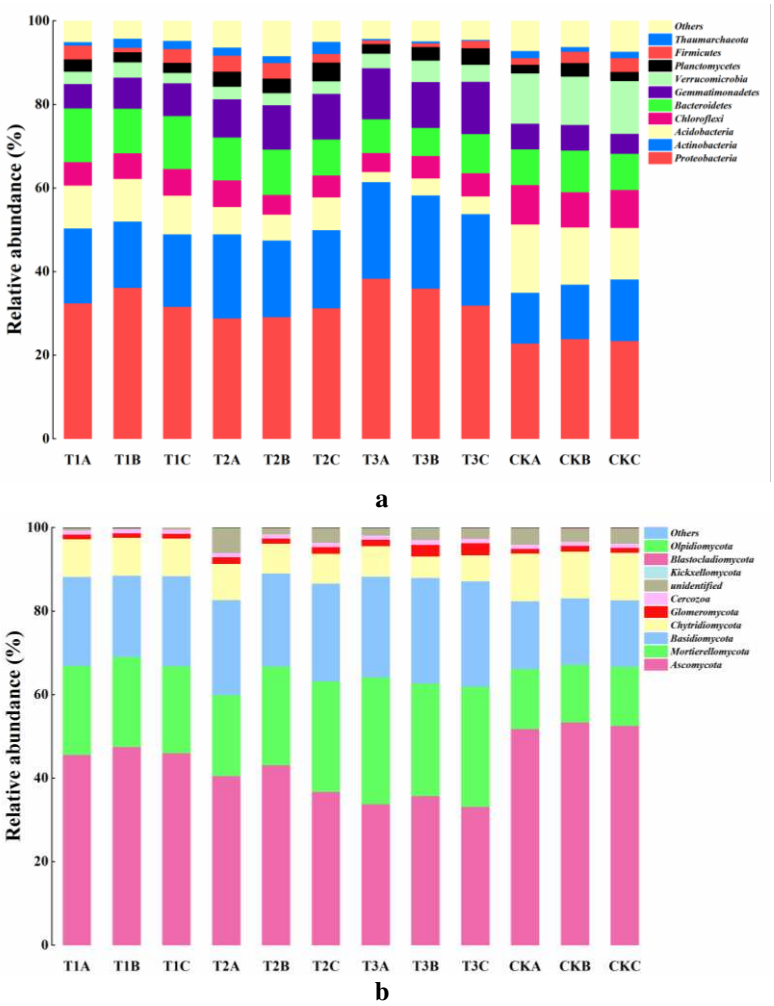

Figure 6. *Analysis of relative abundance of bacterial and fungal communities at phylum level. Bacterial diversity (a) and fungal diversity (b) in different soil samples at phylum level. CK is blank control, T1 is single JF-1 microbial agent; T2 is maize straw combined with JF-1 microbial agent; T3 is maize straw biochar combined with JF-1 microbial agent*

Discussion

Researchers have analyzed the inhibitory effect of antagonistic bacteria against plant diseases from different perspectives (Zhao et al., 2014; Leclère et al., 2005). In this study, the inhibition rates of the sterile fermentation filtrate of *B. amyloliquefaciens* JF-1 was 83.95% for *F. graminearum* mycelial growth; chitinase, cellulase, and protease, with high activities, were obtained from the JF-1 fermentation broth. Treatment of

http://www.aloki.hu ● ISSN 1589 1623 (Print) ● ISSN 1785 0037 (Online)
DOI: http://dx.doi.org/10.15666/aeer/2003_22852302

pathogenic fungi with JF-1 crude extract resulted in a decreased intracellular ATP content and nucleic acid leakage. The decrease in intracellular ATP content is a result of damage to the cell membrane, which affects its normal physiological activities (Olanya et al., 2015). Nucleic acid macromolecular substances penetrate the entire cell membrane and cytoplasm; the release of nucleic acid indicates that the integrity of the cell membrane has been destroyed (Kohanski et al., 2010). Additionally, JF-1 has the ability to secrete IAA. IAA can promote the growth of plant roots and facilitate the absorption of soil nutrients by plants (Mano and Morisaki, 2008). Therefore, it was inferred that JF-1 could promote the growth of plant roots.

The early infection of maize seedling roots with *F. graminearum* posed a serious hidden danger for a maize stalk rot outbreak. JF-1 immobilized with maize straw biochar had a 65.36% control effect on *F. graminearum* infection at the root of maize seedlings. The content of malondialdehyde (MDA) in the roots of maize seedlings decreased by 67.60%. The increase in MDA content in maize plants indicates that the damage to the maize cell membrane is aggravated (AbdElgawad et al., 2021). Therefore, JF-1 effectively protected maize seedlings from *F. graminearum.*

The ability of a microbial community to regulate the soil ecosystem depends on the stability of the soil structure and soil physical and chemical properties (Bissett et al., 2013). In this study, JF-1 microbial agents improved the physicochemical properties of maize disease soil. Among them, maize straw biochar combined with JF-1 microbial agent showed the most significant increase ($P < 0.05$), and the pH value, organic matter, and cation exchange capacity increased by 5.86%, 39.81%, and 5.35%, respectively. Many studies have shown that the genus *Bacillus* can activate the insoluble substances in soil for plant use and increase the content of available phosphorus and potassium in soil (Ogut et al., 2016; Ku et al., 2018; Lucio et al., 2018); The metal cation and ash contents in the biochar and straw can improve the cation exchange capacity of soil (Tan et al., 2017). Some metal ions in the soil participate in the life activities of microorganisms and play a key role in the expression of certain proteins and genes (Zhang et al., 2019). The activities of urease, invertase, phosphatase, and catalase increased using JF-1, which may be due to the colonization effect of JF-1 in soil. Compared to JF-1 application alone, straw and biochar combined with JF-1 increased the soil enzymes more significantly ($P < 0.05$), possibly because straw and biochar directly returned to the field, thus, affecting soil microorganisms and enzyme activities (Chen et al., 2014; Ji et al., 2014). To our knowledge, the environment was repaired by JF-1 microbial agents for the beneficial microorganisms in soil and growth of crops.

The soil microbial community is often called the “second genome of plants” (Berendsen et al., 2012). This study showed that after remediation with three treatments of JF-1 microbial agents, the microbial biomass of bacteria in maize disease black soil significantly increased ($P < 0.05$) and the richness and diversity of bacterial community improved. After different JF-1 microbial agent treatments, *Proteobacteria* and *Actinobacteria* in the soil samples were increased while *Acidobacteria* was decreased to a certain extent. This trend was most obvious in the soil samples treated with maize straw biochar combined with JF-1. *Actinobacteria* protects plant roots from infection by pathogenic fungi, and some species of *Actinobacteria* promote plant growth (Khamna et al., 2009). Studies have found that *Proteobacteria* and *Actinobacteria* are associated with the suppression of plant diseases (Mendes et al., 2011), and the increased relative abundance of *Proteobacteria* and *Actinobacteria* decreases the risk of soil diseases (Li

http://www.aloki.hu ● ISSN 1589 1623 (Print) ● ISSN 1785 0037 (Online)
DOI: http://dx.doi.org/10.15666/aeer/2003_22852302

and Xu, 2020). *Acidobacteria*, an acidophilic bacteria, mostly lives in soil with poor nutrition, and its abundance is often negatively correlated with soil pH (Jones et al., 2009). The decrease of *Acidobacteria* may be caused due to an increase in soil pH value after the application of microbial agents. Additionally, similar to *Acidobacteria*, *Chloroflexi* is also suitable for growing in oligotrophic environments (Fierer et al., 2007). After restoration with microbial agents, the increased nutrients in the soil may be an important reason for the decline in the abundance of *Acidobacteria* and *Chloroflexi*.

According to the analysis of fungal sequencing results at the phylum level, *Ascomycota*, *Mortierellomycota*, and *Basidomycota* were the three dominant phyla of maize disease black soil. After treatment with three groups of different JF-1 microbial agents, *Ascomycota* in soil samples showed a significant decrease ($P < 0.05$). This change was most significant in the soil treated with maize stalk biochar combined with JF-1 ($P < 0.05$); *Mortierellomycota* and *Basidomycota* showed different degrees of increase in each treatment, which may be because *F. graminearum* belongs to *Ascomycota*. The inhibition of *F. graminearum* using JF-1 led to a decrease in the relative abundance of *Ascomycota* in the soil. *Basidomycota*, an important decomposer in soil, plays an important role in the nutrient cycle (Yelle et al., 2008), and nutrients in microbial agents may promote its growth and reproduction. It has been reported that *Ascomycota* is closely related to the occurrence of soil diseases (Tedersoo et al., 2014). Yuan et al. (2020) showed that the relative abundance of *Ascomycota* is higher in soils with a high incidence of plant diseases, while the relative abundance of *Mortierellomycota* is higher in healthy soils, which was consistent with the results of this study. Interestingly, *Glomeromycota* (relative abundance > 1%) is a fungus that can form a complex with the roots of most plants to improve plant nutrient absorption and disease resistance (Liu et al., 2015; Caroline et al., 2017). The relative abundance of *Glomeromycota* was obviously increased in the soil treated with maize straw combined with JF-1 and maize straw biochar combined with JF-1; however, this change was not observed in the disease soil treated with a single JF-1 microbial agent. Therefore, the combination of straw biochar with JF-1 microbial agent had a good repairing effect on the chemical and microecological environment of maize disease soil, and it improves soil ecology and inhibits maize disease.

Conclusion

The bacterial biological control strain JF-1 can inhibit the mycelial growth of *F. graminearum* by secreting chitinase, protease, and other fungal cell wall-degrading enzymes. Maize straw biochar combined with JF-1 microbial agents can repair the physicochemical properties, soil enzyme activities, and microbial community structure of maize disease soil. The biological control bacterium JF-1 can be used as an efficient and cheap microbial agent; thus, JF-1 has a good development potential and application prospect for the prevention and control of maize stalk rot. In addition, the composite application of multiple functional microorganisms and the optimization of carriers are the directions of future research.

Conflict of interests. All authors declare that there is no conflict of interests in this study.

Funding details. The work was supported by Major Science and Technology Projects in Jilin Province under Grant number 20200402002NC.

http://www.aloki.hu ● ISSN 1589 1623 (Print) ● ISSN 1785 0037 (Online)
DOI: http://dx.doi.org/10.15666/aeer/2003_22852302

REFERENCES

[1] AbdElgawad, H., Zinta, G., Abuelsoud, W., Hassan, Y. M., Alkhalifah, D. H. M., Hozzein, W. N., Zrieq, R., Beemster, G. T. S., Schoenaers, S. (2021): An actinomycete strain of *Nocardiopsis lucentensis* reduces arsenic toxicity in barley and maize. – Journal of Hazardous Materials 417(5): 126055.

[2] Abo-Elyousr, K. A. M., Mohamed, H. M. (2009): Note biological control of *fusarium* wilt in tomato by plant growth-promoting yeasts and rhizobacteria. – Plant Pathology Journal 25(2): 199-204.

[3] Bajpai, V. K., Sharma, A., Baek, K. H. (2015): Antibacterial mode of action of Ginkgo biloba leaf essential oil: effect on morphology and membrane permeability. – Bangladesh Journal of Pharmacology 10(2): 337-350.

[4] Berendsen, R. L., Pieterse, C., Bakker, P. (2012): The rhizosphere microbiome and plant health. – Trends in Plant Science 17(8): 478-486.

[5] Bissett, A., Brown, M. V., Siciliano, S. D., Thrall, P. H. (2013): Microbial community responses to anthropogenically induced environmental change: towards a systems approach. – Ecology Letters 16: 128.

[6] Caroline, Gutjahr, Martin, Parniske. (2017): Cell biology: control of partner lifetime in a plant–fungus relationship. – Current Biology 27(11): R420–R423.

[7] Chang, H., Wang, T., Huang, Z., Bai, Y., Wang, C., Liu, S. (2019): Effects of straw degrading bacteria on straw degradation rate, soil physicochemical properties and enzyme activities. – Acta Agriculturae Boreali-Sinica 34: 161-167.

[8] Chen, L., Zhang, J., Zhao, B., Yan, P., Zhou, G., Xin, X. (2014): Effects of straw amendment and moisture on microbial communities in Chinese fluvo-aquic soil. – Journal of Soils & Sediments 14(11): 1829-1840.

[9] Deutsch, C. A., Tewksbury, J., Tigchelaar, M., Battisti, D. S., Merrill, S. C., Huey, R. B., Naylor, Rosamond. L. (2018): Increase in crop losses to insect pests in a warming climate. – Science 361(6405): 916-919.

[10] Du, B., Li, N., Li, Y. (2017): Study on antifungal activity and stability of endogenic 445 fungus Y-6 in pepper. – Henan Agricultural Sciences 46(6): 67-73.

[11] Fierer, N., Bradford, M. A., Jackson, R. B. (2007): Toward an ecological classification of soil bacteria. – Ecology 88(6): 1354-1364.

[12] Fouts, D. E., Szpakowski, S., Purushe, J., Torralba, M., Waterman, R. C., MacNeil, M. D., Alexander, L. J., Nelson, K. E., Kolokotronis, S. O. (2012) Next generation sequencing to define prokaryotic and fungal diversity in the bovine rumen. – PLoS ONE 7(11): e48289.

[13] Jain, S., H. B. (2015): Biological management of *sclerotinia sclerotiorum* in pea using plant growth promoting microbial consortium. – Journal of Basic Microbiology 55(8): 961-972. http://doi. org/10.1002/jobm.201400628.

[14] Jensen, P. (2002): *Paenibacillus polymyxa* produces fusaricidin-type antifungal antibiotics active against *leptosphaeria maculans*, the causative agent of blackleg disease of canola. – Canadian Journal of Microbiology 48(2): 159-169.

[15] Ji, B., Hu, H., Zhao, Y., Mu, X., Liu, K., Li, C. (2014): Effects of deep tillage and straw returning on soil microorganism and enzyme activities. – The Scientific World Journal. https://doi.org/10.1155/2014/451493.

[16] Jiang, N., Song, L. S., Jiang, S. Y., Feng, S. X., Chen, Q. P., Zhang, Z. J., Huang, X. Y. (2020) Prevention and control effects of medicinal plant endophyte *Bacillus methylotrophicus* on *Siraitia grosvenorii* leaf blight. – J Zhejiang Univ Sci B 33: 77-84.

[17] Jones, R. T., Robeson, M. S., Lauber, C. L., Hamady, M., Knight, R., Fierer, N. (2009): A comprehensive survey of soil acidobacterial diversity using pyrosequencing and clone library analyses. – Isme Journal 3(4): 442.

[18] Khamna, S., Yokota, A., Lumyong, S. (2009): *Actinomycetes* isolated from medicinal plant rhizosphere soils: diversity and screening of antifungal compounds, indole-3-acetic

http://www.aloki.hu ● ISSN 1589 1623 (Print) ● ISSN 1785 0037 (Online)
DOI: http://dx.doi.org/10.15666/aeer/2003_22852302

acid and siderophore production. – World Journal of Microbiology & Biotechnology 25(4): 649-655.
[19] Kohanski, M. A., Dwyer, D. J., Collins, J. J. (2010): How antibiotics kill bacteria: from targets to networks. – Nature Reviews Microbiology 8(6): 423-435.
[20] Ku, Y., Xu, G., Wang, F., Liu, H., Yang, X. (2018): Root colonization and growth promotion of soybean, wheat and Chinese cabbage by *Bacillus cereus* yl6. – Plos One 13(11): e0200181.
[21] Leclere, V., Bechet, M., Adam, A., Guez, J. S., Wathelet, B., Ongena, M., Thonart, P., Gancel, F., Chollet-Imbert, M., Jacques, P. (2005): Mycosubtilin overproduction by *Bacillus subtilis* bbg100 enhances the organism's antagonistic and biocontrol activities. – Applied & Environmental Microbiology 71(8): 4577.
[22] Li, J., Xu, Y. (2020): Effects of continuous cropping years of lily on soil microbial diversities under greenhouse cultivation. – Chinese Journal of Soil Science 51(2): 343-351.
[23] Liu, Y., Johnson, N. C., Lin, Mao, L., Shi, G., Jiang, S., Ma, X., Du, G., An, L., Feng, H. (2015): Phylogenetic structure of arbuscular mycorrhizal community shifts in response to increasing soil fertility. – Soil Biology & Biochemistry 89: 196-205.
[24] Liu, H., Qi, Y., Wang, J., Jiang, Y., Geng, M. (2021) Synergistic effects of crop residue and microbial inoculant on soil properties and soil disease resistance in a Chinese Mollisol. – Scientific Reports 11: 24225.
[25] Lucio, V., Liliana, I., Adriana, F. (2018): Growth promotion of rapeseed (brassica napus) associated with the inoculation of phosphate solubilizing bacteria. – Applied Soil Ecology S0929139318300489.
[26] Mano, H., Morisaki, H. (2008): Endophytic bacteria in the rice plant. – Microbes & Environments 23(2): 109. http://doi. org/10.1264/jsme2.23.109.
[27] Mendes, R., Kruijt, M., Bruijn, I. D., Dekkers, E., Voort, M., Schneider, J., Piceno, Y. M., Desantis, T. Z., Andersen, G. L., Bakker, P. A. H. M. (2011): Deciphering the rhizosphere microbiome for disease-suppressive bacteria. – Science 332(6033): 1097-100. http://doi. org/10.1126/science.1203980.
[28] Ogut, M., Er, F. (2016): Mineral composition of field grown winter wheat inoculated with *phosphorus solubilizing* bacteria at different plant growth stages. – Journal of Plant Nutrition 00-00. http://doi. org/10.1080/01904167.2015.1047518.
[29] Olanya, O. M., Ukuku, D. O., Niemira, B. A. (2013): Effects of temperatures and storage time on resting populations of Escherichia coli O157: H7 and *Pseudomonas fluorescens* in vitro. – Food Control 39(1): 128-134.
[30] Pestka, J. J. (2010): Deoxynivalenol-induced proinflammatory gene expression: mechanisms and pathological sequelae. – Toxins 2(6): 1300-1317.
[31] Qi, Y., Wang, J. (2021): Antagonistic effect of *frankia* f1 on ginseng crops soil-borne diseases and microbial community soil structure. – Biocontrol Science and Technology 1: 1-16.
[32] Qi, Y., Li, X., Wang, J., Wang, C., Zhao, S. (2020): Efficacy of plant growth-promoting bacteria *Streptomyces werraensis* F3 for chemical modifications of diseased soil of ginseng. – Biocontrol Science and Technology 31(1): 1-15.
[33] Ramesh, P., Panwar, N. R., Singh, A. B., Ramana, S. (2009): Effect of organic nutrient management practices on the production potential, nutrient uptake, soil quality, input-use efficiency and economics of mustard (Brassica juncea). – Indian Journal of Agricultural Science 79(1): 40-44.
[34] Rani, A., Souche, Y. S., Goel, R. (2009): Comparative assessment of in situ bioremediation potential of cadmium resistant acidophilic *Pseudomonas putida* 62bn and alkalophilic *Pseudomonas monteilli* 97an strains on soybean. – International Biodeterioration & Biodegradation 63(1): 62-66.

http://www.aloki.hu ● ISSN 1589 1623 (Print) ● ISSN 1785 0037 (Online)
DOI: http://dx.doi.org/10.15666/aeer/2003_22852302

[35] Ren, L., Su, S., Yang, X., Xu, Y., Huang, Q., Shen, Q. (2008): Intercropping with aerobic rice suppressed fusarium wilt in watermelon. – Soil Biology & Biochemistry 40(3): 834-844.
[36] Rocha, O., Ansari, K., Doohan, F. M. (2005): Effects of trichothecene mycotoxins on eukaryotic cells: a review. – Food Additives Contaminants 22(4): 369-378.
[37] Savary, S., Willocquet, L., Pethybridge, S. J., Esker, P., McRoberts, N., Nelson, A. (2019): The global burden of pathogens and pests on major food crops. – Nat Ecol Evol 3: 430-439.
[38] Shan, H., Zhao, M., Chen, D., Cheng, J., Jing, L., Feng, Z., Ma, Z., An, D. (2013): Biocontrol of rice blast by the phenaminomethylacetic acid producer of *Bacillus methylotrophicus* strain bc79. – Crop Protection 44: 29-37.
[39] Souza, E. L., Barros, J. C., Oliveira, C. E., Maria, L. C. (2010): Influence of Origanum vulgare L. essential oil on enterotoxin production, membrane permeability and surface characteristics of *Staphylococcus aureus*. – International Journal of Food Microbiol 137(2): 308-311.
[40] Sun, Z. C., Lin, M., Du, C. H., Hao, Y. W., Zhang, Y. H., Wang, Z. M. (2022): The use of manure shifts the response of α-diversity and network while not β-diversity of soil microbes to altered irrigation regimes. – Applied Soil Ecology 174: 104423.
[41] Tan, Z., Lin, C. S. K., Ji, X., Rainey, T. J. (2017): Returning biochar to fields: a review. – Applied Soil Ecology 116: 1-11.
[42] Tedersoo, L., Bahram, M., Polme, S., Koljalg, U., Yorou, N. S., Al, E. (2014): Global diversity and geography of soil fungi. – Science 346(6213): 1078-1078.
[43] Teethaisong, Y., Autarkool, N., Sirichaiwetchakoon, K., Krubphachaya, P., Kupittayanant, S., Eumkeb, G. (2014): Synergistic activity and mechanism of action of stephania suberosa forman extract and ampicillin combination against ampicillin-resistant staphylococcus aureus. – Journal of Biomedical Science 21(1): 90.
[44] Wakelin, S. A. (2002): Biological control of *aphanomyces euteiches* root rot of pea with spore-forming bacteria. – Australasian Plant Pathology 31(4): 401-407.
[45] Wang, Y., Huang. J., Liu, K., Han, T., Du, J., Ma, X., Hao, X., Zhou, B., Liu, C., Zhang, H., Jiang, X. (2020): Evaluation and spatial variability of paddy soil fertility in typical county of northeast China. – Journal of Plant Nutrition and Fertilizers 26(2): 256-266.
[46] Wu, X., Chen, S., Yang, Y., Wang, Y., Liu, Y., Chen, J. (2015): Application of *Trichoderma* granules to control corn stem rot. – Journal of Plant Protection 42(06): 1030-1035. https://doi.org/10.13802/j.cnki.zwbhxb.2015.06.026.
[47] Yelle, D. J., Ralph, J., Lu., F., Hammel, K. E. (2010): Evidence for cleavage of lignin by a brown rot Basidiomycete. – Environmental Microbiology 10(7): 1844-1849.
[48] Yuan, J., Wen, T., Zhang, H., Zhao, M., Shen, Q. (2020): Predicting disease occurrence with high accuracy based on soil macroecological patterns of *fusarium* wilt. – The ISME Journal.
[49] Zhang, J., Xu, Y., Liang, S., Ma, X., Sun, F. (2019): Synergistic effect of *Klebsiella* sp. fh-1 and *Arthrobacter* sp. nj-1 on the growth of the microbiota in the black soil of northeast China. – Ecotoxicology and Environmental Safety 190: 110079.
[50] Zhao, P., Quan, C., Wang, Y., Wang, J., Fan, S. (2014): *Bacillus amyloliquefaciens* q-426 as a potential biocontrol agent against fusarium oxysporum f. sp. spinaciae. – Journal of Basic Microbiology 54(5): 448-456.

http://www.aloki.hu ● ISSN 1589 1623 (Print) ● ISSN 1785 0037 (Online)
DOI: http://dx.doi.org/10.15666/aeer/2003_22852302

PRECIPITATION AND UNDERSTORY VEGETATION DIVERSITY DRIVE VARIATIONS IN SOIL ORGANIC CARBON DENSITY: RESULTS FROM FIELD SURVEYS AND SATELLITE DATA OF TWO DIFFERENT PERIODS IN THE GREATER KHINGAN MOUNTAINS OF NORTHEAST CHINA

LI, F. Z.[1] – LIU, Y.[1,2] – ZHANG, C.[1] – SA, R. L.[1,2] – TIE, N.[1,3*]

[1]*Forestry College, Inner Mongolia Agricultural University, Hohhot 010019, Inner Mongolia, China*
(e-mail:fengzili@emails.imau.edu.cn, phone:+86-153-2607-5875;ly9810@163.com; zc51study@163.com; sarula213@163.com)

[2]*National Field Scientific Observation and Research Station of Forest Ecosystem in Greater Khingan Mountains, Inner Mongolia, Genhe 022350, China*

[3]*Inner Mongolia Academy of Forestry Sciences, Hohhot 010010, Inner Mongolia, China*
(e-mail: wangtieniu@126.com)

[*]*Corresponding author*
e-mail: wangtieniu@126.com

(Received 2nd Nov 2021; accepted 26th Jan 2022)

Abstract. The forest ecosystem in Greater Khingan Mountains (GKM) is the largest primary forest in northern China. Accurate assessment of the regional carbon (C) pool of soils and analysis of the control factors are essential for setting appropriate forest management policies. Our study was designed to prove the hypothesis that forest soil acts as a C sink owing to continuous C accumulation, which results from constant biomass production within the GKM forests. We investigated topsoil (0-20 cm) C dynamics and diving force in GKM forests (both the Inner Mongolia and Heilongjiang sectors) based on field data from 2000 to 2019. The mean soil organic C density (SOCD) in the topsoil was 10.64 ± 0.83 kg C m^{-2} across the GKM, and the increase rate was 0.15±0.05 kg C m^{-2} y^{-1}. Our results also demonstrated the critical role of precipitation and under vegetation diversity in shaping soil organic C dynamics across the GKM, suggesting that the relationship between the soil C cycle and temperature is unstable in northern ecosystems. Our results provided a new reference range for estimating surface soil C pools in GKM forests ecosystems based on field measurements.
Keywords:*carbon sequestration,spatial variations, carbon–climate feedback,boreal forests, soil inventory*

Abbreviations:GKM: Greater Khingan Mountains; C: Carbon; SOC: Soil organic carbon; SOCD: Soil organic carbon density; SCS: Soil carbon storage; CO_2: Carbon dioxide; N_2O: Nitrous oxide; MAT: Mean annual temperature; MAP: Mean annual precipitation; MGT: Mean growing temperature; MGP: Mean growing precipitation; NDVI: Normalized difference vegetation index; DBF: Deciduous broadleaved forests; DNF: Deciduous needleleaf forests; BNMF: Broadleaved and needleleaf mixed forests; Alt: Altitude; Soil. D: Soil depth; Liiter. D: Litter depth; NH_4^+-N: Ammonium nitrogen concentration; AP: Available phosphorous; AK: Available potassium; Age. Forest: the age of the forests at the individual sampling site

Introduction

Although forests represent just 30% of the land cover, they account for 45% of terrestrial ecosystem C stocks and nearly 50% of terrestrial net primary production (Bonan, 2008). Researchers currently agree that enhancing forest soil C stocks is an effective and environmentally friendly way to absorb carbon dioxide (CO_2) from

http://www.aloki.hu ● ISSN 1589 1623 (Print) ● ISSN 1785 0037 (Online)
DOI: http://dx.doi.org/10.15666/aeer/2003_23032328

anthropogenic emissions (Tharammal et al., 2019; Bossio et al., 2020). Sustainable forest management has been carried out by the Chinese government to protect forest resources, resulting in a significant increase in forest areas from 13.9% (1990s) to 21.0% (2010s) (Tang et al., 2018). Many studies based on field surveys and modeling have assessed the C stocks in forest ecosystems in response to this increase in forest area. The forest topsoil C stock increased significantly from the 1980s to the 2000s, at a rate of increase ranging from 14.1 to 25.5 g C m^{-2} y^{-1} (mean rate of 20.0 g C m^{-2} y^{-1}, 95% confidence) (Yang et al., 2014b). Similar studies found that the forest C stock plays a sink role in China (Yang et al., 2011; Pan et al., 2011; Tharammal et al., 2019). However, soil carbon sink largely depends on the interaction between soil and climate (Crowther et al., 2019). If the soil carbon emission caused by warming exceeds the soil carbon input caused by vegetation growth, the soil ecosystem may become the source of atmospheric carbon dioxide(Schimel et al., 1994; Davidson and Janssens, 2006). It is, therefore, important to obtain an objective understanding of the role played by the forests C balance, to limit global climate warming and to adjust forests management policies (Hopkins et al., 2012).

Environmental factors such as climate and plant diversity, which are directly associated with latitude, limit the distribution power of forest biomass (He, 2012). Interactions and mechanisms among multiple factors (such as climate, site, soil physical and chemical properties, and land use patterns) will affect the distribution of vegetation and soil C storage. The rate of C input and output of the soil is governed by temperature, soil nutrient conditions and atmospheric CO_2 concentrations in the short term (Tian et al., 2011). Decomposition of soil organic matter, the main way in which organic C enters the soil, is frequently affected by ambient temperatures (Davidson and Janssens, 2006). On a national scale, the average annual temperature rise in China was significantly higher thanthe change in global average from 1982 to 2011, exceeding 1°C on average (Fang et al., 2017). These changes will, in turn, feed back into the forest ecosystem in terms of species community (Chen et al., 2018), stoichiometric ratio (Yang et al., 2014a) and ecosystem function in the long term (Crowther et al., 2019). Climate factors are therefore expected to influence the dynamics of soil organic C at large scales.

The area covered by forest in China is vast, at approximately 156 M ha, and it occupies more than one climate zone (Guo et al., 2013). The Greater Khingan Mountains (GKM) forests are mainly distributed in northeastern China and include eastern Inner Mongolia Autonomous Region and northern Heilongjiang Province (Meng et al., 2014; Zhao et al., 2014). These forests are one of the most sensitive ecosystems to global warming (Fu et al., 2018), and forests of the dominant species – *Larixgmelinii* Rupr. (Jiang et al., 2002) - cover more than 57% of the GKM (Bull and Nilsson, 2004; DFPRC, 2014). *Betula platyphylla* Suk. and *Populusdavidiana* are mainly distributed on eastfacing ridges, and *Pinus sylvestris* var. *mongolica* and *Quercus mongolica* form the remaining forest (Bull and Nilsson, 2004; DFPRC, 2014). Like in most high altitude ecosystems, soil stores a huge amount of C due to the long cold season and relatively humid environment in GKM, which provides a better area for analyzing the feedback between soil C and climate change. Two studies of forest C storage in GKM (including both Inner Mongolia and Heilongjiang Province in northeastern China) have suggested that the forest C stock acts as a C sink (Meng et al., 2014; Zhao et al., 2014). In contrast, a recent study based on the InVEST model showed that the soil stock is stable while ecosystem C stock has experienced a slight decrease in northeastern China (Mao et al., 2019). However, due to the limited data and difficult large-scale field survey in GKM area, there is little research

http://www.aloki.hu ● ISSN 1589 1623 (Print) ● ISSN 1785 0037 (Online)
DOI: http://dx.doi.org/10.15666/aeer/2003_23032328

on the historical dynamics of SOC in GKM. How the soil C pool of the GKM responds to increased climate change remains uncertain.

In order to detect the change of soil carbon storage in GKM, 204 soil profiles were obtained from 68 sites of GKM. We compared our 68 field surveys obtained in 2017 (representing data from the 2010s) with 107 field surveys published in 2000-2010 (representing data from the 2000s) (Xu et al., 2018a). Since plant production is the main C input of soil in terrestrial ecosystems, satellite data sets which can reflect vegetation growth have been general used to evaluate aboveground biomass(Shen et al., 2015; Zhang et al., 2016). And many studies have shown that the satellite data set can be combined with ground observation data to estimate regional SOC reserves (Yang et al., 2008, 2009; Ding et al., 2016). Therefore, based on the satellite-based SOC estimation method, we analyzed the historical changes of SOC in GKM forests by comparing the data of current measurements (2010s) and historical literature published (2000s). The specific objectives of this research were as follows: (1) based on field survey and satellite data set, to verify the hypothesis that soils of GKM forests can function as C sinks in the regional C cycle because of the underlying C accumulation in vegetation biomass in the 2000s and 2010s (Pan et al., 2011; Fang et al., 2012; Yang et al., 2014b); and (2) analyze the factors influencing SOCD both in spatial distribution and long term scale. Application of our results is expected to improve C sequestration budgets, and thus contribute to sustainable forest management.

Materials and Methods

Data sources

The 2010s soil sampling was conducted between June and August 2017 in GKM, China (geographical range is 119°36′-125°19′E, and 47°3′-53°20′N) (Liu et al., 2020). We defined "forests" as an area of land > 0.067 ha that is dominated by trees and with a canopy density of > 0.2 (Tang et al., 2018). According to the system sampling method, 56 sampling points were set in a 0.5° × 0.5° (~60×60 km) grid. Temporary standard plots were visually uniform, well populated stands of > 1 ha; at least 100 m from any openings to minimize the impact of edge effects; and round, with a radius of 17.5 m (or 500.34 m^2). To allow analysis of the soil properties, five pits were dug along an "s" route in each temporary standard plot to collect topsoil (0-20 cm) samples, so that sampling points were more representative (Zhu et al., 2020). The soil samples were manually selected to remove fine roots of plants for properties analysis, passed through a 2 mm sieve, and then divided into three parts. One sample was dried at a constant temperature of 105°C for measuring bulk density. The other sample stored at 4°C was extracted with 1 M KCl solution, and then analyzed using a flow injection analyzer (Autoanalyzer 3 SEAL, Bran and Luebbe) for NH_4^+-N concentrations. The third sample Air-dried were extracted with 0.03 M NH_4F and 0.025 M HCl, and analyzed colorimetrically to determine available P concentrations using vanado-molybdate method (Bray and Kurtz, 1945).Soil pH was determined in a 1:5 soil to deionized water suspension using a pH probe (PB-10, Sartorius).Additionally, the average rock content (> 2 mm) of each soil type was replaced by the same soil type (Zhu, 1996). In 2019 we supplemented our 2017 work with samples taken from 12 points in the central GKM, using the same plot setting and soil survey methods. This gave us a total of 68 soil samples were used as soil data for 2010s (*Fig. 1, Table A1*). The age of the forest at the individual sampling site was obtained from the satellite images that developed a top-down method to downscale the provincial statistics

http://www.aloki.hu ● ISSN 1589 1623 (Print) ● ISSN 1785 0037 (Online)
DOI: http://dx.doi.org/10.15666/aeer/2003_23032328

of national forest inventory data into 1km stand age map using climate data and Light Detection And Ranging (LiDAR) derived forest height (Zhang et al., 2017).

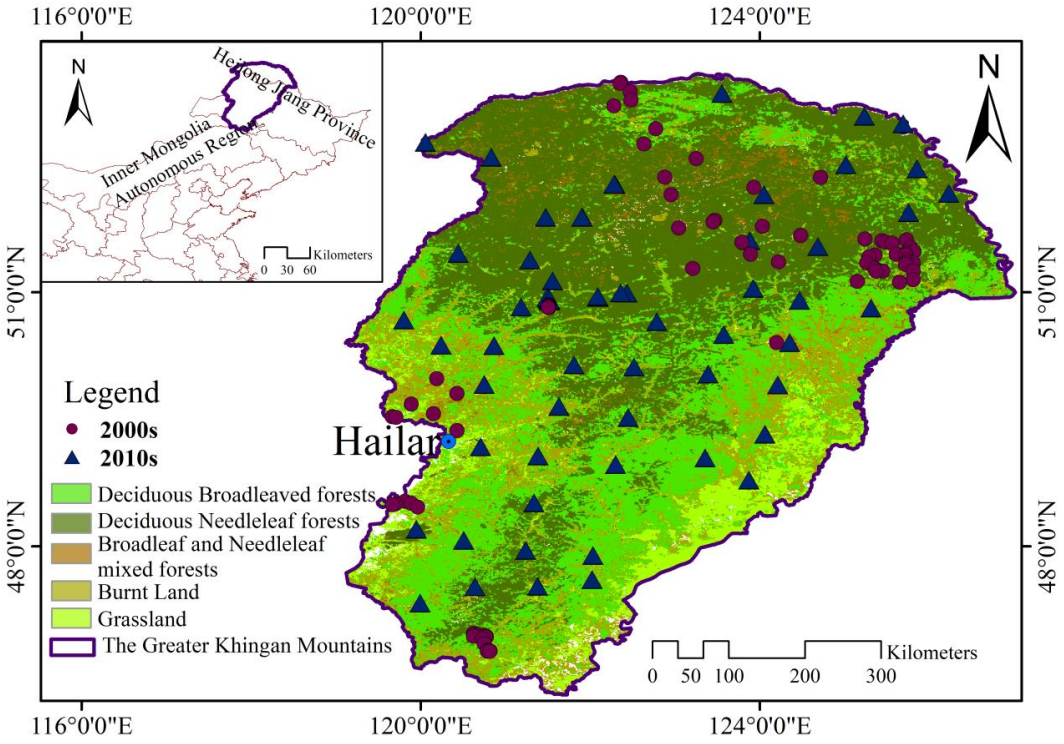

Figure 1. *Locations of the sampling sites of the two periods (2000s and 2010s) in the Greater Khingan Mountains, northeastern China. Solid purple dot, 2000s; solid blue triangle, 2010s*

The SOCD of 2000s soil was selected from the "2010s China Land Ecosystem Carbon Density Dataset" (Xu et al., 2018a), which lists SOCD from field surveys in 2004-2012. Selection of the soil data was based on (1) experiments conducted in 2000-2009 with no restriction on publication year; and (2) experimental sites in the forest ecosystem of the GKM (according to latitude and longitude coordinates) and soil depths of 0-20 cm. We used a total of 107 observations of soil samples to represent the 2000s.

Environmental factors have traditionally been used to represent the changes in the soil C cycle across landscapes (Crowther et al., 2019). We used the annual variations in temperature and precipitation to analysis the climate change trend at regional level in the GKM during 1981 to 2019. Mean annual temperature (MAT, °C), mean annual precipitation (MAP, mm), mean growing temperature (MGT, °C) and mean growing precipitation (MGP, mm) for each sites were calculated using CRU_ts4_pre and CRU_ts4_tmp datasets, CRU TS provides 0.5° resolution monthly data covering the global land surface from 1901 to 2020, provided by the National Centre for Atmospheric Science (NCAS) in the United Kingdom (https://crudata.uea.ac.uk/cru/data/hrg/).

Annual variation in the remotely sensed normalized difference vegetation index (NDVI) was used to explore the vegetation growth trend at regional level in the GKM. The NDVI data set was obtained from the GIMMS NDVI3g dataset with the spatial resolution of 8 km from 1982 to 2015 (https://ecocast.arc.nasa.gov/data/pub/gimms/), and Moderate Resolution Imaging Spectroradiometer (MODIS) through the United States Geological Survey (USGS; http://modis.gsfc.nasa.gov), with a spatial resolution of 250 m

http://www.aloki.hu ● ISSN 1589 1623 (Print) ● ISSN 1785 0037 (Online)
DOI: http://dx.doi.org/10.15666/aeer/2003_23032328

for every 16 day interval over the 2000-2019 (MOD13Q1) (Tucker et al., 2004, 2005). Monthly composites were obtained by application of the maximum value composition (MVC) method (Holben, 1986). The NDVI data were selected from GIMMS NDVI3g dataset from 1982 to 1999 and MOD13Q1 from 2000 to 2019.

Data processing

Soil C is mainly distributed at depths of 0-100 cm; is concentrated at depths of 0-20 cm; and decreases as soil depth increases (Crowther et al., 2019). The soil organic C density (SOCD) and soil C storage (SCS) in the top 20 cm were calculated by *Eq.1*and *Eq.2*:

$$SOCD = \sum_{i=1}^{n} SOCi \times BDi \times Ti \times (1 - Ci)/100 \quad \text{(Eq.1)}$$

where *SOCD*, *SOCi*, *BDi*, *Ti* and *Ci* represent soil organic C density (kg C cm^{-2}), soil organic C (g kg^{-1}), bulk density (g cm^{-3}), layer thickness (cm) and percentage of the fraction > 2 mm, respectively; and:

$$SCS = SOCDi \times Ai \quad \text{(Eq.2)}$$

where *SCS*, *SOCDi* and *Ai* represent soil C storage (Pg C), soil organic C density (kg C cm^{-2}) and area (m^2), respectively.

Forest types in 2010s field survey were distinguish according to the principles and bases of Chinese vegetation regionalization, which defined the: deciduous broadleaved forests (DBF, deciduous broadleaved species stock accounts for more than 80% of stand stock), deciduous needleleaf forests (DNF, deciduous needleleaf species stock accounts for more than 80% of stand stock) and broadleaf and needleleaf mixed forests (BNMF, Coniferous or broad-leaved trees account for 20% to 80% of stand stock)(Chinese Academy of Sciences, 2001; Ministry of ecology and environment of the people' s Republic of China, 2021).Forest types in 2000s dataset were distinguish according the global land cover data (GlobalLandCover30, second-class product data, with a spatial resolution of 1 km) (http://www.globallandcover.com).Different forest types area using the raster statistical function of ArcGis (ArcGis 10.2.2, ESRI).

To examine understory vegetation diversity, we selected four indices of *αlpha* diversity. These focus on measuring the number of biological species in the community and reflect the coexistence results of species through competition for resources in the community (Wu, 2015). The calculation formulae(Chen and Zhang, 1999) are*Eq.3-Eq.6*:

$$\text{Shannon–Wiener indices: } H = -\sum_{i=1}^{S} P_i ln\, P_i \quad \text{(Eq.3)}$$

$$\text{Simpson diversity indices: } P = 1 - \sum_{i=1}^{S} P_i^2 \quad \text{(Eq.4)}$$

$$\text{Pielou evenness indices: } E = H' / ln\, S \quad \text{(Eq.5)}$$

$$\text{Margalef indices: } D = \frac{S-1}{ln\, N} \quad \text{(Eq.6)}$$

http://www.aloki.hu ● ISSN 1589 1623 (Print) ● ISSN 1785 0037 (Online)
DOI: http://dx.doi.org/10.15666/aeer/2003_23032328

where S is the total number of species for each sample, N is the sum of all important values for S species; and P_i is the important value of the first species. Creation of an understory vegetation diversity indices was performed in R (4.0.3) using the "vegan" package.

Statistical analyses

Sen + Mann-Kendall trend analyses were used to analyze changes in NDVI over the past 20 years (2000-2019)(Liu, 2017). A method for longtime series trend analysis can be created by combining the trend degree in the Sen slope estimator method with the trend degree test in the Mann-Kendal method, and the latter has become an important method to judge the trend of longtime series data(Gocic and Trajkovic, 2013).

The time series length of this study was 10 year (2000-2009, 2010-2019), so the Mann-Kendall Z trend test (Z_{MK} test) was used to test statistics. The Z_{MK} test trend criterion was based on *Table 1*(Seenu and Jayakumar, 2021). We performed the Sen + Mann-Kendall trend analyses using MATLAB (2016).Take into account the influence of grassland and farmland distribution, We extracted forest areas from Sen+Man-Kendall results of NDVI according to the satellite images on a 1:1 million vegetation map of China (Hou, 2019)(http://data.tpdc.ac.cn). Then recalculated the area and proportion of different types.

Table 1. *Normalized difference vegetation index (NDVI) trend analysis results of the Sen + Mann-Kendall method with a confidence interval of 95%*

NDVI Trend	Rating	2000s		2010s		Change in NDVI	
		Area (10^4 m^2)	Percent %	Area (10^4 m^2)	Percent %	Area (10^4 m^2)	Percent %
$\beta < 0$, $\|Z\| > 1.96$	Decreased obviously	0.03	0.14	0.01	0.05	-0.02	-0.09
$\beta < 0$, $\|Z\| \leq 1.96$	Decreased slightly	4.78	25.34	0.40	2.12	-4.38	-23.21
$\beta > 0$, $\|Z\| \leq 1.96$	Increased slightly	12.61	66.80	6.35	33.66	-6.25	-33.14
$\beta > 0$, $\|Z\| > 1.96$	Increased obviously	1.45	7.71	12.10	64.16	10.65	56.45

In order to analyze the SOCD dynamics, we compared the SOCD changes in the two periods both in field survey and satellite estimation. SOCD based on field survey is calculated by *Eq. 1* and *Eq. 2*. Single factor analysis of Variance (ANOVA) was conducted to determine whether SOCD derived from field survey differed significantly during the 2000s and 2010s in different forest types. The effect of two periods (2000s and 2010s) was considered significant if $P < 0.05$. ANOVA was carried out using the "vegan" package in R version 4.0.3.

SOCD based on satellite estimation is estimated by obtaining the polynomial regression relationship between NDVI and SOCD. Polynomial regression model is a kind of linear regression model, in which the regression function is linear about the regression coefficient(Schmidt et al., 2013; Zhang et al., 2014).Vegetation indices commonly used in terrestrial ecosystem research include normalized difference, enhancement, soil adjustment and modified soil adjustment vegetation indices(Zhang et al., 2016). NDVI has been widely used in inversion of terrestrial vegetation and terrestrial ecosystem carbon dynamics(Yang et al., 2008, 2009; Ding et al., 2016).We use the polynomial regression relationship between SOCD and the corresponding NDVI data to obtain the SOCD spatial distribution maps of the two periods (2000s and 2010s). Then the paired t-test was used to compare the changes of SOCD in the two periods from the grid level. Finally, the SOCD difference of each grid in the two periods is calculated, and the

http://www.aloki.hu ● ISSN 1589 1623 (Print) ● ISSN 1785 0037 (Online)
DOI: http://dx.doi.org/10.15666/aeer/2003_23032328

distribution map of SOCD changes from 2000s to 2010s is obtained. The NDVI data details of this part could be found in the "data source" above in this paper. In addition, reduce the influence of bare soil, water and construction land grid on the simulation results, the grid units with annual NDVI < 0.1 in 20 years were removed for analysis(Piao et al., 2006). In order to verify the reliability of SOCD based on NDVI estimation, we randomly selected 75 % of the soil samples to establish the relationship between SOCD density and NDVI, and then the remaining 25 % were verified. Polynomial regression and the paired t-test were performed in ~~in~~ R version 4.0.3, paired t-test was carried out using the "dplyr" package.

We used redundancy analysis (RDA) to decompose the spatial variation in SOCD into variation related to environmental variables (Alt (m); MAP (mm); MAT (°C); Soil depth (cm); Litter depth (cm); Age. Forest (year); $NH4^+$-N (mg g^{-1}); AP (mg g^{-1}); AK (mg g^{-1}); under vegetation diversity: Margalef, Shannon-Wiener, Simpson diversity and Pielou indices). Further the multiple regression was performed to assess the relative importance of each environmental variable in different forests types based on standardized regression coefficients. Multiple linear regression analysis was used to simulate the relationship between SOCD and climate (MAP (mm); MAT (°C)) at grid level during the 2000s and 2010s. The SOCD map based on NDVI estimation was resample so that the same resolution as climate data. RDA was carried out using the "vegan" package in R version 4.0.3. Multiple linear regression analysis was performed in R version 4.0.3.

Results

Climate change and NDVI trend analysis from 1981to 2019

Climate change in 1981 to 2019

From 1982 to 2019, the annual average NDVI showed a significant increase trend with fluctuated between 0.33 and 0.40 (P <0.05). From 1981 to 2019, MAT has a significant increase overall, with an annual average temperature of -3.67 °C to -1.31 °C (P < 0.05). MAP showed a slight downward trend with an annual average precipitation of 330.12 mm to 571.85 mm, but did not reach a significant level (P > 0.05) (*Fig. 2*).

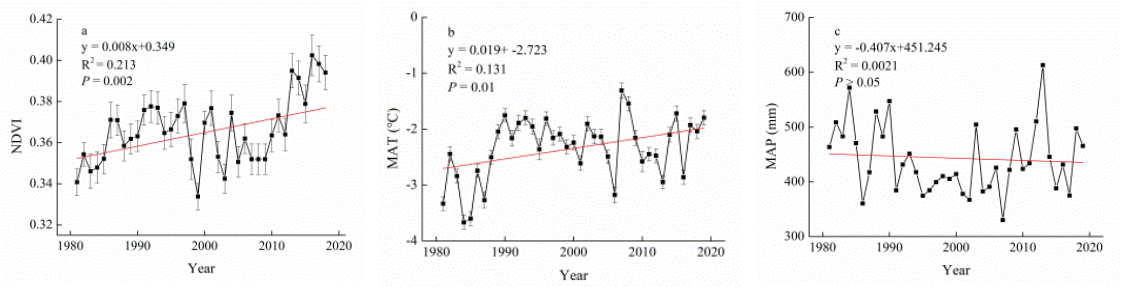

Figure 2. *Annual trends of NDVI, precipitation and temperature in 1981-2019*

From 1982 to 2019, the NDVI in growing season showed a significant increase trend with fluctuated between 0.42 and 0.53 (P < 0.05). From 1981 to 2019, MGT increased significantly, with an average temperature of 9.67 °C to 11.98 °C (P < 0.05). MGP showed a slight downward trend with an average precipitation of 285.68 mm to 558.62 mm, but did not reach a significant level (P > 0.05) (*Fig.3*).

http://www.aloki.hu ● ISSN 1589 1623 (Print) ● ISSN 1785 0037 (Online)
DOI: http://dx.doi.org/10.15666/aeer/2003_23032328

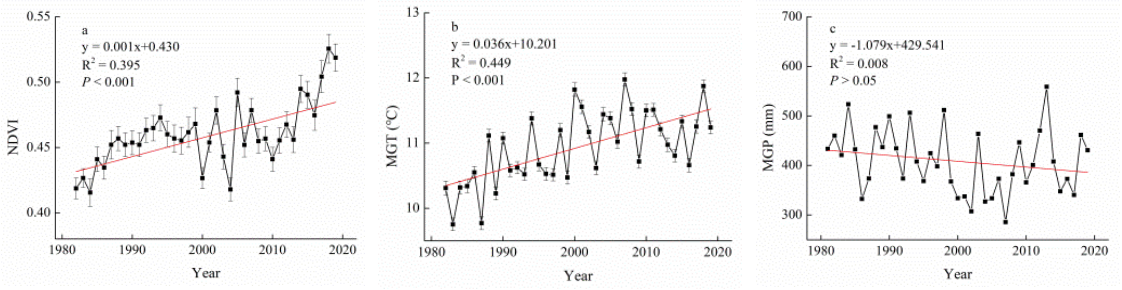

Figure 3. *Trends of NDVI, precipitation (mm) and temperature (°C) in growing season in 1981-2019*

NDVI trend analysis

The spatial distribution characteristics of forest vegetation change trend in the GKM, based on the Sen + Mann-Kendall tests (implemented as shown in *Table 1*), were obtained for the 2000s (2000-2009) and 2010s (2010-2019) (*Fig.4*). From 2000 to 2009 the vegetation change trend in the GKM increased overall, and the area of vegetation change with an upward trend reached 74.51%. The NDVI increased in the north, east and south of the GKM, and decreased in the west and southeast (*Fig. 4*). From 2010 to 2019, the trend in vegetation change of GKM increased overall, and the area showing a rising trend reached 97.82%. There was a large increase in the central and western parts of the GKM, and a downward trend in the eastern part (*Fig.4*).

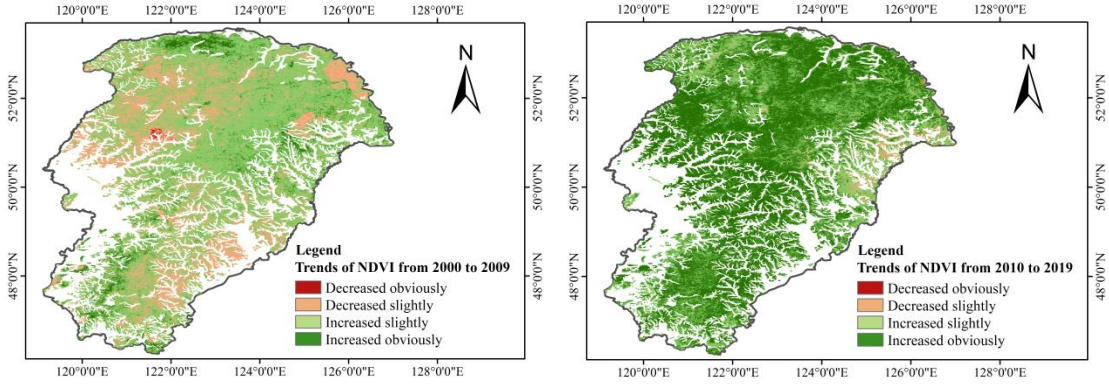

Figure 4. *Trends of inter-annual normalized difference vegetation index (NDVI) from 2000 to 2009 and 2010 to 2019*

Table 1 shows the Z value level based on the Sen + Mann-Kendall test, and the NDVI change trend and area of the two periods (2000s: 2000-2009; 2010s: 2010-2019). From 2000 to 2009, 7.71% of the vegetation of the area significantly improved, 66.80% of the area slightly improved, 25.34% of the area degraded slightly and 0.14% of the area was clearly degraded, indicating that the vegetation trend increased during 2000-2009. From 2010 to 2019, 64.16% had a significant improvement in vegetation, 33.66% had a slight improvement, 2.12% had a slight degradation and 0.05% of the GKM showed significant degradation, indicating that the vegetation trend increased during 2010-2019. Overall, the NDVI increased significantly by 56.45% between the 2000s and 2010s (*Table 1*).

http://www.aloki.hu ● ISSN 1589 1623 (Print) ● ISSN 1785 0037 (Online)
DOI: http://dx.doi.org/10.15666/aeer/2003_23032328

Dynamics of SOCD across the GKM in the 2000s and 2010s

Dynamics of SOCD based on field survey

Based on the dataset of 2000s (Xu et al., 2018a)and 2010s (this study), the average SOCD at 0-20 cm depth in the 2000s and 2010s was 9.15 ± 0.36 kg C m^{-2}(Xu et al., 2018a)and 10.64 ± 0.83 kg C m^{-2}(this study), respectively. The SCS (soil C storage) in the surface layer (0-20 cm) of GKM in the 2000s and 2010s was 2.91±1.14 Pg C (Xu et al., 2018a)(Pg = 10^{15}g) and 3.38 ± 2.63 Pg C (this study), respectively (*Table A2*). The surface SOCD in GKM increased significantly from the 2000s to the 2010s, and the mean increase rate was 0.15 ± 0.05 kg C m^{-2} y^{-1} ($P < 0.05$). In DBF the average increase was 0.34 ± 0.12 kg C m^{-2} y^{-1} ($P < 0.05$). The increase in BNMF and DNF did not reach a significant level, and the increase rates were 0.26 ± 0.15 kg C m^{-2} y^{-1} ($P > 0.05$) and 0.03 ± 0.009 kg C m^{-2} y^{-1} ($P > 0.05$), respectively (*Fig. 5*).

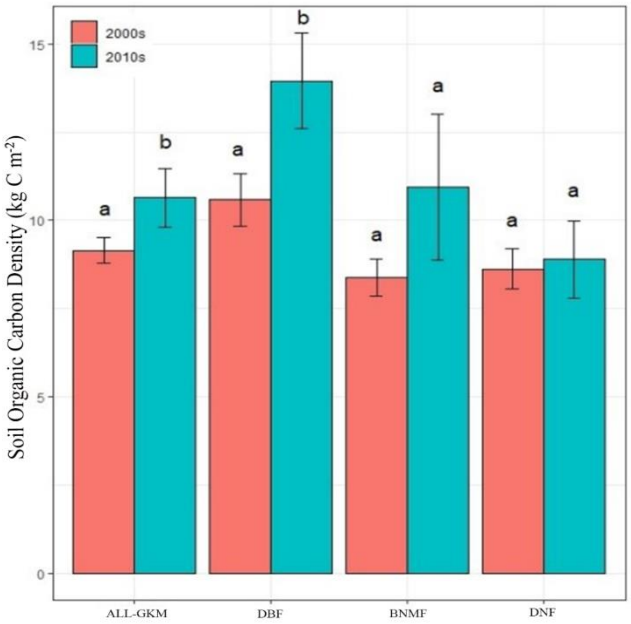

Figure 5. *Soil organic carbon density (kg C m^{-2}) of different periods and forests types at a confidence interval of 95%. The same letter indicates that the statistical test is not significant ($P > 0.05$). Vertical bars represent the standard error of the mean*

Dynamics of SOCD based on NDVI estimation

*Table 2*shows the parameters of SOCD estimated by polynomial regression based on NDVI, where Adj.R> 0.5 and $P < 0.001$, indicating that the polynomial regression relationship based on NDVI can better invert SOCD (*Fig. A1*).

Table 2. *Polynomial regression results of soil organic carbon density (SOCD, kg C m^{-2}) and normalized difference vegetation index (NDVI)*

	Summary					ANOVA		
	Intercept/SE	**B1/SE**	**B2/SE**	**Adj.R^2**	**RMSE**	**n**	**F**	**P**
2000s	-10.20/3.32	73.06/18.36	-48.74/24.48	0.68	2.13	107	115.19	***
2010s	-13.90/6.33	96.65/37.30	-66.15/52.46	0.53	4.70	50	27.55	***

***: P<0.001, at a 95% confidence interval

http://www.aloki.hu ● ISSN 1589 1623 (Print) ● ISSN 1785 0037 (Online)
DOI: http://dx.doi.org/10.15666/aeer/2003_23032328

The results showed that there was a significant correlation between the simulated SOCD and the measured SOCD (Adj.R^2 = 0.81, Adj.R^2 = 0.71, P < 0.001, *Fig. 6*). Therefore, based on NDVI, we choose polynomial regression method to develop SOCD of GKM.

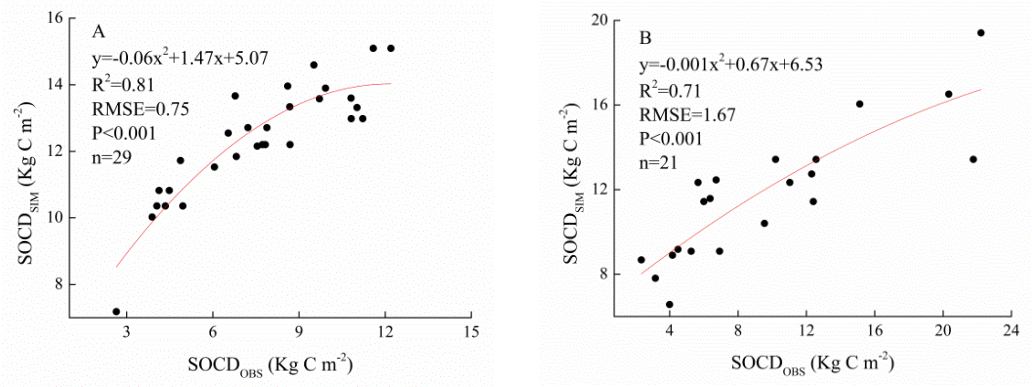

Figure 6. *Correlation between simulated and measured soil organic carbon density ($SOCD_{SIM}$; $SOCD_{OBS}$; kg C m^{-2}) in the Greater Khingan Mountains for the period of 2000s (A) and 2010s (B), derived from polynomial regression*

Based on NDVI estimation, the spatial distribution of SOCD varies greatly in two periods, and the SOCD change shows large spatial heterogeneity (*Fig. A2*). According to the paired t-test results (*Table 3*), SOCD increased by 0.32± 0.001 g C m^{-2} yr^{-1} on average from 2000s to 2010s (P < 0.001).

Table 3. *The paired t-test results of Soil organic carbon density (SOCD, kg C m^{-2}) difference comparison between 2000s and 2010s*

	Summary				
	change in SOCD	**Conf. int**	**t**	**df**	**P**
2000s-2010s	-3.21	-3.21, -3.20	-993.74	991437	***

Conf. int: at a 95% confidence interval; ***: P<0.001

Due to the limitation of data resolution and the large range of study area, SOCD changes are not analyzed at different forests types. According to different forests regions of GKM, SOCD change was compared. It can be seen that from 2000s to 2010s, the increase of SOCD was mainly concentrated in the northeastern and northern forest regions, while the eastern and southern forest regions showed a flat state of increase and decrease (*Fig. 7*). The above results show that the SOCD storage increase in the south of GKM is lower than that in the north of GKM from 2000s to 2010s.

Impact factors of SOCD

The SOCD of the in the GKM forests showed a great change in spatial distribution, ranging from 1.22 to 28.22 kg C m^{-2} (*Fig. A3*). The average SOCD was 10.64 ± 0.83 kg C m^{-2}. Among the three forests types (*Fig. 8A*), DBF (13.95 ± 1.35 kg C m^{-2}) had the highest SOCD, followed by BNMF (10.94 ± 2.05 kg C m^{-2}), DNF (8.89 ± 1.10 kg C m^{-2}) had the lowest SOCD. Across the GKM forests area (*Fig. 8B*), the SOCD

http://www.aloki.hu ● ISSN 1589 1623 (Print) ● ISSN 1785 0037 (Online)
DOI: http://dx.doi.org/10.15666/aeer/2003_23032328

of southern (13.83 ± 1.96 kg C m^{-2}) and eastern (13.11 ± 1.55 kg C m^{-2}) areas were the highest, and the central forest area (3.80 ± 0.69 kg C m^{-2}) was the lowest.

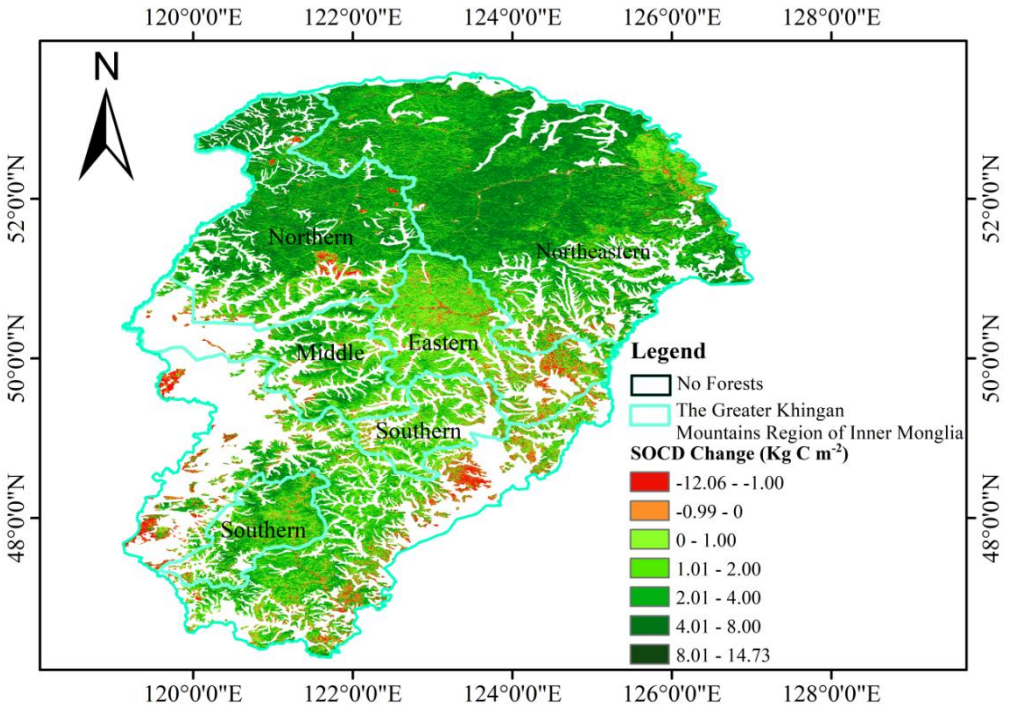

Figure 7. *Soil organic carbon density (kg C m^{-2}) changes in the Greater Khingan Mountains between 2000s and 2010s*

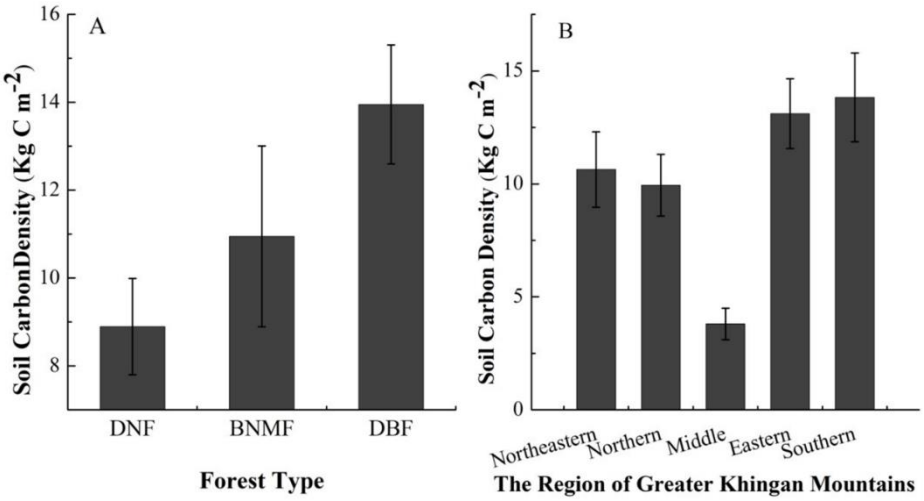

Figure 8. *Soil organic carbon density (kg C m^{-2}) of different forests types and regions*

We used RDA to investigate the relationship between topsoil SOCD and environmental and under vegetation diversity (*Fig. 9*). RDA1 and RDA2 explained 15.82% and 4.91% of the total variation, respectively. The length of arrows indicated that soil depth, Shannon-Wiener indices, Simpson indices, MAT and MGT were the most

http://www.aloki.hu ● ISSN 1589 1623 (Print) ● ISSN 1785 0037 (Online)
DOI: http://dx.doi.org/10.15666/aeer/2003_23032328

important environmental factors affecting SOCD. In contrast, the slope and Soil depth had no significant effect on SOCD. Altitude and slope were nearly vertical in orientation, indicating that they affected SOCD independently, and the influence of these two factors was more reflected in DNF. The angle between SOCD and pH or MAP was acute, indicating that the SOCD was closely positively correlated with these two factors.

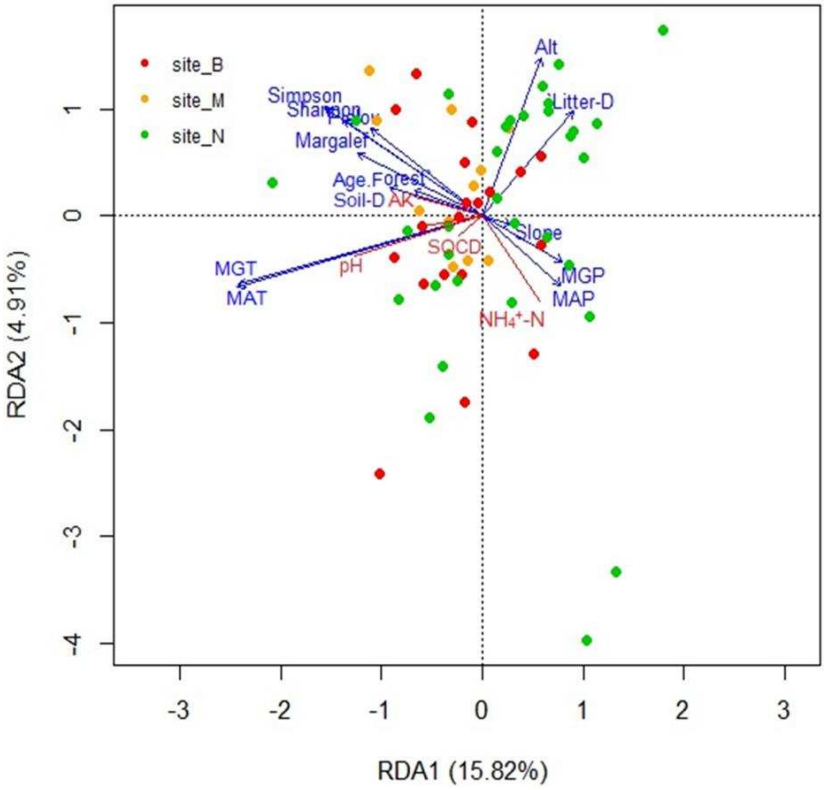

Figure 9. *Redundancy analysis (RDA) of soil organic carbon density (SOCD, kg C m^{-2}) indicators and environmental factors. site_B, deciduousbroadleavedforest; site_M, broadleaf and needleleaf mixed forest; site_N, deciduousneedleleafforest*

Multiple regression was used to quantitatively analyze the relative importance of site, soil nutrients, climate and under vegetation diversity on SOCD in different forests types. The results showed that the SOCD of DNF and DBF was affected by both biotic and abiotic factors, but that the SOCD of BNMF was mainly affected by abiotic factors (*Fig. 10*). Multiple regression models explained 31.8%, 98.8% and 52.5% of SOCD variation in DNF, DBF and BNMF, respectively. We found, using the standardized regression coefficient and its P value, that the slope and Pielou indices had a considerable negative effect on SOCD in DNF ($P < 0.05$). Other variables with large (but not significant) effects included the Simpson indices (positive effect), Shannon indices (negative effect), MAP (positive effect) and MGP (negative effect) ($P > 0.05$). The pielou indices, Shannon indices and MGP significantly promoted changes in SOCD in DBF ($P < 0.05$); while the Simpson indices, Margalef indices, and MAP, had significant negative effects ($P < 0.05$). Abiotic factors had a great influence on soil nutrients in BNMF. Of these, litter depth had a considerable negative effect on SOCD ($P < 0.05$), while NH_4^+-N and AP had relatively small but significant effects ($P < 0.05$).

http://www.aloki.hu ● ISSN 1589 1623 (Print) ● ISSN 1785 0037 (Online)
DOI: http://dx.doi.org/10.15666/aeer/2003_23032328

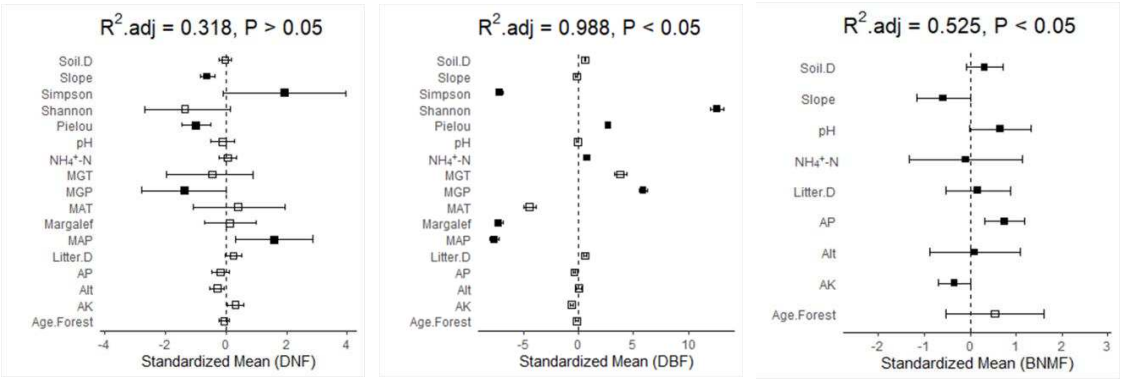

Figure 10. *Multiple regression of abiotic and biotic factors affecting soil organic carbon density (SOCD, kg C m^{-2}) in three different forests types. The points in the figure represent the mean of the standardized regression coefficient, the error bars represent the standard error and the solid points indicate variables that have significant effects on soil organic carbon density (P < 0.05)*

Correlation analysis between SOCD and MAP and MAT in two periods based on NDVI estimation. Multiple linear regression shows, the SOCD dynamics showed a positive correlation with MAP both in 2000s and 2010s, but a negative relationship in 2000s and weak relationship in 2010s with MAT (*Fig. 11*). The results showed that due to the increase of temperature in recent years, the limiting effect of precipitation on SOCD was enhanced(*Table A3.* $Estimate_{MAP2000S}$=0.29, P<0.01; $Estimate_{MAP2010S}$=0.56, P < 0.001), and the effect of MAT was weakened(*Table A3.* $Estimate_{MAT2000S}$=-0.24, P <0.01; $Estimate_{MAT2010S}$=-0.001, P>0.05).

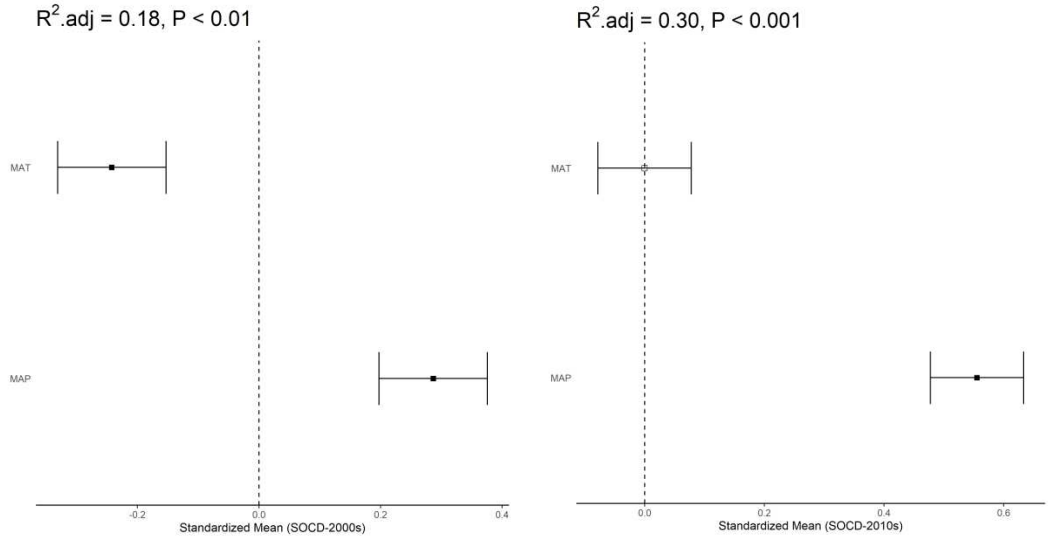

Figure 11. *Correlation analysis between SOCD and MAP and MAT in two periods based on normalized difference vegetation indexestimation, derived from multiple linear regression. The points in the figure represent the mean of the standardized regression coefficient, the error bars represent the standard error and the solid points indicate variables that have significant effects on soil organic carbon density (P < 0.05)*

http://www.aloki.hu ● ISSN 1589 1623 (Print) ● ISSN 1785 0037 (Online)
DOI: http://dx.doi.org/10.15666/aeer/2003_23032328

Discussion

Dynamics of SOCD

Accurate estimation of the soil C pool size is crucial for assessing the function of soil in the global C cycle, particularly in cold temperate forest where approximately 48% of C is stored in the top 30 cm of soil(Yang et al., 2007). The average SOCD in the surface soil (0-20 cm) in the GKM was 10.64 ± 0.83 kg C m^{-2} (*Table A2*), which was close to the whole China forests mean SOCD (11.53 ± 2.24 kg C m^{-2}) reported by Xu et al.(2018b). Our result was lower than the whole China forests mean SOCD (16.38 ± 8.4 kg C m^{-2}) reported by Tang et al.(2018), and this may have been because of the extensive area of young forests and frequent disturbance activities leading to a lower biomass in GKM (Fang et al., 2007). The mean SOCD in different forests types changed from 9.15 ± 0.36 to 10.64 ± 0.83 kg C m^{-2} over the 2000s to the 2010s, and the mean rate of increase was 0.15 ± 0.05 kg C m^{-2} y^{-1} ($P < 0.05$, *Table A2*). This trend of increase was also observed in DBF ($P < 0.05$), but not obvious in BNMF ($P > 0.05$) and DNF ($P > 0.05$, *Table A2*).

The results based on field survey showed that, in GKM, SOCD increased significantly in the period 2000s-2010s (*Fig. 5*, $P < 0.001$). Our results showed that the gross regional scale change in topsoil SOCD ranged from 0.03 ± 0.009 to 0.34 ± 0.12 kg C m^{-2} y^{-1}. Furthermore, the change in rate of SCS in the topsoil ranged from 0.04 to 0.48 Tg C y^{-1} (Tg = 10^{12} g) from the 2000s to the 2010s. The paired t - test results showed that, SOCD based on NDVI estimation increased significantly in the period 2000s-2010s in GKM (*Table 3*; $P < 0.001$), with a mean increased rate of 0.32±0.0001 kg C m^{-2} y^{-1} (mean SOCD of 11.60±0.0001 kg C m^{-2} in 2000s and 14.17±0.0001 kg C m^{-2} in 2010s, *Table A4.*). And the SOCD change difference results show that (*Fig. 7*), SOCD mainly increases in the north of GKM more than in the south, which may be due to the wide distribution of the old forests in the north of GKM, less human disturbance, which is conducive to the accumulation of SOCD(Mao et al., 2019).In the south of GKM, human activities are frequent, especially a large number of plantation activities. The establishment and management of plantations often involve serious human disturbances, such as deforestation and intense land preparation, which may lead to rapid and substantial soil organic carbon losses and affect longterm soil organic carbon recovery(Yang et al., 2019).

The C store in GKM forests topsoil may be ascribed to its natural accumulation in mineral soil during forest development. The increased NDVI we observed in this study could be interpreted as demonstrating this hypothesis (*Fig. 4*). From the 2000s to the 2010s, NDVI increased by 52.57% (*Table 1*). This may partly have been because China's national conservation policies have led to a substantial increase in forest area, enhancing their ability to capture more atmospheric C, directly promoting C sequestration capacity(Tang et al., 2018). The SOCD of an old forests ecosystem increased at an average rate of 0.61 kg C m^{-2} y^{-1} between 1979 and 2003 in southern China, indicating that old forests can remove C from the atmosphere(Zhou et al., 2006). A comprehensive global flux experiment also affirmed that old forests is an important C sink in terrestrial ecosystems, and has a rate of increase of 1.3 Pg C y^{-1}(Luyssaert et al., 2008). It is clear that surface soil C in the GKM region played a significant role as a C sink from 2000 to 2019, and that this may have partly been a result of the accumulation of natural C resulting from China's national conservation policies.

Another factor affecting the ability of forest to act as C sinks is the effect of climate change. The variations of temperature in growing season and inter annual in GKM have

http://www.aloki.hu ● ISSN 1589 1623 (Print) ● ISSN 1785 0037 (Online)
DOI: http://dx.doi.org/10.15666/aeer/2003_23032328

shown a significant increase trend from 2000 to 2019 ($P < 0.05$), whereas variations of precipitation decreased from 2000 to 2019 ($P > 0.05$, *Fig. 3*, *Fig. 4*). Climate warming has been accelerated as atmospheric CO_2 and soil nitrous oxide (N_2O) concentrations have risen, these changes may exacerbate global warming, which could enhance both vegetation growth and litter fall into soils, subsequently result in a soil C sink(Davidson and Janssens, 2006). Atmospheric CO_2 concentrations increased at a rate of 1.43 ppm y^{-1} in China (ppm = mg) from 1961 to 2005(Tian et al., 2011). Application of the process-based global vegetation model (DyN-LPJ) indicated that the decadal average N_2Oemissions in the 20thcentury ranged from 8.2 to 9.5 Tg N y^{-1}(Xu-Ri et al., 2012). GKM has been found to be very sensitive to climate change, as it has a short, warm summer and a long, cold winter that lasts for 9 months (Xu, 1998). Simultaneous heat and precipitation in summer are beneficial to vegetation growth under conditions of climate warming. The long cold season is beneficial to the input of external C which offsets the C lost by soil respiration, and thus the function of a C sink is established.

Uncertain analysis

The SOCD estimated based on NDVI (11.60 ±0.0001Kg C m^{-2}, 2000s; 14.17±0.0001 Kg C m^{-2}, 2010s) was higher than that based on field survey (9.15±0.36 Kg C m^{-2}(Xu et al., 2018a), 2000s; 10.64±0.83 Kg C m^{-2}, 2010s) in the two periods. It is generally believed that satellite-based estimation of SOCD can effectively reduce uncertainties caused by soil spatial heterogeneity. The difference of estimation in this paper may be due to the uneven spatial distribution of sampling points in the two periods. In 2010s, the sampling points were set according to the system sampling method through the geographical grid of 0.5°×0.5°, and the distribution was relatively uniform. However, due to the limitation of historical published data, the location distribution of sampling points in 2000s is not uniform. The regression relationship used to generate SOCD may cause potential uncertainty.

In order to overcome this difference, buffer analysis was carried out based on the sample location of 2000s to minimize the error caused by terrain inconsistency caused by different sampling locations. The ANOVA results showed that when r= 0.5°, 0.8° and 1°, the average SOCD of 2010s is significantly higher than 2000s ($P < 0.05$, *Table A4*). Therefore, we believe that the difference between the positions of different same points is within the allowable range of error, that is, the change of the two periods is due to the increase of forest vegetation area and the recovery of above-ground vegetation in the past 20 years. In addition, due to the widespread low temperature season and the distribution of large permafrost in GKM region, the soil properties are relatively stable (Baumann et al., 2009).

Impact factors of SOCD

Many field data were used to compare the effects of biotic and abiotic factors on SOCD spatial distribution in different forests types in GKM. Consistent with general theories and empirical experiments, RDA analysis showed that both biotic and abiotic factors affected the spatial pattern of SOCD in the surface soil of GKM (*Fig. 9*). Of these, climate (MAT, MAP), under vegetation diversity indices (Shannon-Wiener indices, Simpson indices) and site (Alt) had a significant influence ($P < 0.05$). The effects of biotic and abiotic factors on SOCD varied greatly in different types of forest. Multiple regression analysis clearly showed the influence of climate and the under vegetation diversity indices on SOCD spatial distribution in DNF and DBF, and climate (MAP, MGP) was higher

http://www.aloki.hu ● ISSN 1589 1623 (Print) ● ISSN 1785 0037 (Online)
DOI: http://dx.doi.org/10.15666/aeer/2003_23032328

than under vegetation diversity indices (*Fig. 10*). This is consistent with studies showing that the large scale spatial distribution pattern of SOCD is mainly regulated by climate (Post et al., 1982; Yang et al., 2007). However, the explanatory ability of temperature on SOCD was lower than that of precipitation in DNF and DBF (*Fig. 10*), and the dominant advantage of precipitation was more significant in DBF ($P < 0.05$). This is contrary to the traditional theory that the pattern of spatial distribution of forest SOCD is mainly controlled by C loss resulting from soil microbial heterorespiration under conditions of global warming(Valentini et al., 2000). Recent studies also show that the C density of *Piceaasperata* Mast. and *Abiesfabri* Mast. is mainly controlled by temperature on the Tibetan Plateau(Jia et al., 2021). In our results, high precipitation had a greater ability to explain SOCD (*Fig. 10*). MAP had a positive effect on SOCD, indicating that precipitation promotes the input of C into soil by vegetation and litter in DNF, thereby increasing SOCD. MAP had a negative effect on SOCD, and this may have been because soil rock fragment content is higher in DBF than in DNF; the SOC may have been washed away following high precipitation, leading to leaching in DBF(Lin et al., 2016).

Multiple regression analysis showed that the under vegetation diversity indices had a greater ability to explain the SOCD spatial pattern in DBF than in DNF ($P < 0.05$, *Fig. 10*). The consistently positive effects found in the current study were corroborated by our investigation, which showed that higher under vegetation diversity increases soil C inputs such as aboveground net primary productivity and belowground biomass(Liang et al., 2016; Liu et al., 2021), and promotes soil microbial community diversity and activity. The increased SOCD may originate from suppressed C loss from microbial decomposition (Rasse et al., 2005; Chen et al., 2018).

High soil pH had a negative effect on SOCD in all three forests types in GKM, and was significant in BNMF ($P < 0.05$, *Fig. 10*). The effect of high soil pH on SOCD may impact soil C input by regulating the diversity and productivity of aboveground vegetation (Chen et al., 2018). High soil acidity enhanced SOCD by limiting soil microbial vitality and expediting the movement of dissolved organic C eluviate into the deep layer (Funakawa et al., 2014). High levels of nitrogen deposition will also lead to soil acidification, but C retention caused by nitrogen deposition may be offset by the balance of greenhouse gases (CO_2 and N_2O etc.), resulting in a heating effect on the climate (Qu et al., 2020).

In contrast to the traditional view, we investigated the long term effects of climate factors on SOCD from 2000 to 2019 at the grid level, and found the influence of MAP was higher than MAT on SOCD (*Fig. 11*). A simulation study has shown that climate warming significantly enhanced ecosystem C sinks in spring during 1980 to 1989, but it was clear that this occurrence was reduced at the beginning of the 2000s (Piao et al., 2017). Giardina and Ryan (2000)showed that soil microbial activity did not change significantly under experimental conditions of temperature limitation, and decomposition did not change significantly when only temperature was increased. In this study, MAP was found to have a strong effect on SOCD in GKM forests (*Fig. 11*). Decomposition may be controlled by precipitation rather than by low temperatures, because of the long cold season, and by the large area of permafrost in the GKM(Baumann et al., 2009). GKM is located on the 400 mm precipitation line in China. The east side of the ridge is affected by the southeastern monsoon and experiences more than 400 mm precipitation annually. The west side of the ridge is affected by the Mongolia Siberia airflow, and so is drier and cooler than the east side(Xu, 1998). Soil moisture restricts microbial activities more than soil temperature in an arid soil environment, thus controlling soil C dynamics (Lin et al.,

http://www.aloki.hu ● ISSN 1589 1623 (Print) ● ISSN 1785 0037 (Online)
DOI: http://dx.doi.org/10.15666/aeer/2003_23032328

2016; Přívětivý and Šamonil, 2021). Therefore, using MAP as a key factor in the development of large scale models will be of significance in assessing C dynamics in GKM in the future.

Conclusions

The SOCD estimated based on NDVI (11.60 ±0.0001Kg C m^{-2}, 2000s; 14.17±0.00001 Kg C m^{-2}, 2010s) was significantly higher than that based on field survey (9.15 ± 0.36 Kg C m^{-2}(Xu et al., 2018a), 2000s; 10.64±0.83 Kg C m^{-2}, 2010s), illustrating a rate of increase of 0.15 ±0.05 kg C m^{-2} y^{-1} from 2000 to 2019. These data provided a benchmark for exploration of the dynamic effects of climate warming on the soil C of a boreal forest ecosystem in the northeastern cold temperate zone. The SOCD exhibited a strong correlation with under vegetation diversity in terms of spatial distribution, and this indicated that conservation of biodiversity promotes regional forest C sequestration. This study validated the plant diversity-soil C storage hypothesis on a broad spatial scale. Our results also demonstrated the critical role of MAP in shaping SOCD dynamics across the GKM from 2000 to 2019, suggesting that the linkage between soil C uptake and temperature is unstable in northern ecosystems. Data on SOCD were limited, however, and it was unclear whether the significant inter-annual correlation between SOCD and precipitation reflected inter-decadal changes, and whether long term changes have taken place in the ecological response to climate warming in boreal forest ecosystems. Further research is needed into longer term observations, using more focused analysis of soil C dynamics, to simulate C-climate feedback in regions of major soil organic C storage.

Acknowledgements. We would like to thank the members of the field investigators, and Drs. Bing Wang, Zhunxia Zhang, Fangjian Yang and Chao Zhang for their assistance in the soil sample collection and laboratory. This research was funded by Inner Mongolia Autonomous Region Science and Technology Plan Project: Research and Demonstration on Key Technologies of Ecological Restoration of Betula platyphylla Secondary Forest in Greater Khingan Mountains, grant number 2020GG0067, and the Inner Mongolia Autonomous Region Graduate Education Innovation Program (Graduate Research Innovation Funding Project, 2020): Dynamics of Soil Carbon Density and its Influencing Factors in the Greater Khingan Mountains of Northeast China, grant number BZ2020049.

Conflicts of Interests. The authors have no conflicts of interests to disclose.

REFERENCES

[1] Baumann, F., He, J.S., Schmidt, K., Kühn, P., Scholten, T. (2009): Pedogenesis, permafrost, and soil moisture as controlling factors for soil nitrogen and carbon contents across the Tibetan Plateau. – Global Change Biology 15 (12): 3001-3017. https://doi.org/10.1111/j.1365-2486.2009.01953.x.

[2] Bonan, G. B. (2008): Forests and climate change: forcings, feedbacks, and the climate benefits of forests. – Science 320: 1444-1449. https://doi.org/10.1126/science.1155121.

[3] Bossio, D.A., Cook-Patton, S.C., Ellis, P.W. (2020): The role of soil carbon in natural climate solutions. – Nat Sustain3: 391-398. https://doi.org/10.1038/s41893-020-0491-z.

[4] Bray, R. H., Kurtz, L. T. (1945): Determination of total, organic, and available forms of phosphorus in soils. – Soil Science59(1): 39-46.https://doi.org/10.1097/00010 694-194501000-00006.

[5] Bull, G.Q., Nilsson, S. (2004): An Assessment of China's Forest Resources. – International Forestry Review 6(3): 210-220. https://doi.org/10.1505/ifor.6.3.210.59979.

http://www.aloki.hu ● ISSN 1589 1623 (Print) ● ISSN 1785 0037 (Online)
DOI: http://dx.doi.org/10.15666/aeer/2003_23032328

[6] Chen, T., Zang, J. (1999): A comparation of fifteen species diversity indices. – HeNan Science 17: 56-57.
[7] Chen, L., Liang, J., Qin, S., Liu, L., Fang, K., Xu, Y., Ding, J., Li, F., Luo, Y., Yang, Y. (2016): Determinants of carbon release from the active layer and permafrost deposits on the Tibetan Plateau. – Nature Communications 7: 1-12. https://doi.org/10.1038/ncomms13046.
[8] Chen, S., Wang, W., Xu, W., Wang, Y., Wan, H., Chen, D., Tang, Z., Tang, X., Zhou, G., Xie, Z., Zhou, D., Shangguan, Z., Huang, J., He, J.S., Wang, Y., Sheng, J., Tang, L., Li, X., Dong, M., Wu, Y., Wang, Q., Wang, Z., Wu, J., Chapin III, F.S., Bai, Y. (2018): Plant diversity enhances productivity and soilcarbon storage. – PNAS 115(16): 4027-4032. https://doi.org/10.1073/pnas.1700298114.
[9] Chinese Academy of Sciences. (2001): Vegetation Atlas of China. – SciencePress, Beijing.
[10] Crowther, T.W., van den Hoogen, J., Wan, J., Mayes, M.A., Keiser, A.D., Mo, L., Averill, C., Maynard, D.S. (2019): The global soil community and its influence on biogeochemistry. – Science 365(6455). https://doi.org/10.1126/science.aav0550.
[11] Davidson, E.A., Janssens, I.A. (2006): Temperature sensitivity of soil carbon decomposition and feedbacks to climate change. – Nature 440(7081): 165-173. https://doi.org/10.1038/nature04514.
[12] DFPRC (2014): Statistics of China's Forest Resources (2009-13). – Department of Forestry of PR China, Beijing, China 25-31. https://doi.org/10.1016/S0378-1127(02)00299-2.
[13] Ding, J.Z., Li, F., Yang, G.B., Chen, L.Y., Zhang, B.B., Liu, L., Fang, K., Qin, S.Q., Chen, Y.L., Peng, Y.F., Ji, C.J., He, H.L., Smith, P., Yang, Y.H. (2016): The permafrost carbon inventory on the Tibetan Plateau: a new evaluation using deep sediment cores. – Global Change Biology 22(8): 2688-2701. https://doi.org/10.1111/gcb.13257.
[14] Fang, J., Guo, Z., Piao, S., Chen, A. (2007): Terrestrial vegetation carbon sinks in China, 1981–2000. – Science in China Series D: Earth Sciences 50(9): 1341-1350. https://doi.org/10.1007/s11430-007-0049-1.
[15] Fang, J., Shen, Z., Tang, Z., Wang, X., Wang, Z., Feng, J., Liu, Y., Qiao, X., Wu, X., Zheng, C. (2012): Forest community survey and the structural characteristics of forests in China. – Ecography 35(12): 1059-1071. 1059-1071. https://doi.org/10.2307/23409648.
[16] Fang, Y., Michalak, A.M., Schwalm, C.R., Huntzinger, D.N., Berry, J.A., Ciais, P., Piao, S., Poulter, B., Fisher, J.B., Cook, R.B., Hayes, D., Huang, M., Ito, A., Jain, A., Lei, H., Lu, C., Mao, J., Parazoo, N.C., Peng, S., Ricciuto, D.M., Shi, X., Tao, B., Tian, H., Wang, W., Wei, Y., Yang, J. (2017): Global land carbon sink response to temperature and precipitation varies with ENSO phase. – Environmental Research Letters 12(6): 064007. https://doi.org/10.1088/1748-9326/aa6e8e.
[17] Fu, Y., He, H.S., Zhao, J., Larsen, D.R., Zhang, H., Sunde, M.G., Duan, S. (2018): Climate and Spring Phenology Effects on Autumn Phenology in the Greater Khingan Mountains, Northeastern China. – Remote Sensing of Environment 10(3): 449. https://doi.org/10.3390/rs10030449.
[18] Funakawa, S., Fujii, K., Kadono, A., Watanabe, T., Kosaki, T. (2014): Could Soil Acidity Enhance Sequestration of Organic Carbon in Soils? – In: Hartemink, A., McSweeney, K. (eds.) Soil Carbon - Progress in Soil Science. Springer, Cham. https://doi.org/10.1007/978-3-319-04084-4_22.
[19] Giardina, C., Ryan, M. (2000): Evidence that decomposition rates of organic carbon in mineral soil do not vary with temperature. – Nature 404: 858-861.https://doi.org/10.1038/35009076.
[20] Gocic, M., Trajkovic, S. (2013): Analysis of changes in meteorological variables using Mann-Kendall and Sen's slope estimator statistical tests in Serbia. – Global and planetary change 100:172-182. https://doi.org/10.1016/j.gloplacha.2012.10.014.
[21] Guo, Z., Hu, H., Li, P., Li, N., Fang, J. (2013): Spatio-temporal changes in biomass carbon sinks in China's forests from 1977 to 2008. – Sci China Life Sci 56(7): 661-671. https://doi.org/10.1007/s11427-013-4492-2.

http://www.aloki.hu ● ISSN 1589 1623 (Print) ● ISSN 1785 0037 (Online)
DOI: http://dx.doi.org/10.15666/aeer/2003_23032328

[22] He, J.S. (2012): Carbon cycling of Chinese forests: from carbon storage, dynamics to models. – Science China Life Sciences 55: 188-190. https://doi.org/10.1007/s11427-012-4285-z.
[23] Holben, B.N. (1986): Characteristics ofmaximum-value composite images from temporal AVHRR data. – InternationalJournal of Remote Sensing 7(11): 1417-1434. https://doi.org/10.1080/01431168608948945.
[24] Hopkins, F.M., Torn, M.S., Trumbore, S.E. (2012): Warming accelerates decomposition of decades-old carbon in forest soils. – Proceedingsof the National Academy of Sciences of the United States of America 109(26): 1753-1761. https://doi.org/10.1073/pnas.1120603109.
[25] Hou, X. (2019): 1:1 million vegetation map of China. – National Tibetan Plateau Data Center. http://data.tpdc.ac.cn.
[26] Jia, L., Wang, G., Lou, J. (2021): Carbon storage of the forest and its spatial pattern in Tibet, China. – Journal of Mountain Science 18(7): 1748-1761. https://doi.org/10.1007/s11629-020-6520-6.
[27] Jiang, H., Apps, M., Peng, C., Zhang, Y., Liu, J. (2002): Modelling the influence of harvesting on Chinese boreal forest carbon dynamics. – For Ecol Manage 169: 65-82. https://doi.org/10.1016/S0378-1127(02)00299-2.
[28] Liang, J., Crowther, T.W., Picard, N., Wiser, S., Zhou, M. (2016): Positive biodiversity-productivity relationship predominant in global forests. – Science 354(6309): 196-200. https://doi.org/10.1126/science.aaf8957.
[29] Lin, L., Zhu, B., Chen, C., Zhang, Z., Wang, Q.-B., He, J.-S. (2016): Precipitation overrides warming in mediating soil nitrogen pools in an alpine grassland ecosystem on the Tibetan Plateau. – Scientific Report 6: 1-9. https://doi.org/10.1038/srep31438.
[30] Liu, Z. (2017): Variation characteristics and trend of precipitation over the Shangsha river basin. – Anhui Agricultural Science Bulletin.
[31] Liu, Y., Yue, C., Wei, X., Blanco, J.A., Trancoso, R. (2020): Tree profile equations are significantly improved when adding tree age and stocking degree: an example for Larixgmelinii in the Greater Khingan Mountains of Inner Mongolia, northeast China. – European Journal of Forest Research 139(3): 443-458. https://doi.org/10.1007/s10342-020-01261-z.
[32] Liu, Y., Shangguan, Z., Deng, L. (2021): Vegetation Type and Soil Moisture Drive Variations in Leaf Litter Decomposition Following Secondary Forest Succession. – Forests 12(9): 1195. https://doi.org/10.3390/f12091195.
[33] Luyssaert, S., Schulze, E., Börner, A. (2008): Old-growth forests as global carbon sinks. – Nature 455: 213-215. https://doi.org/10.1038/nature07276.
[34] Mao, D., He, X., Wang, Z., Tian, Y., Xiang, H., Yu, H., Man, W., Jia, M., Ren, C., Zheng, H. (2019): Diverse policies leading to contrasting impacts on land cover and ecosystem services in Northeast China. – Journal of Cleaner Production 240: 1-11. https://doi.org/10.1016/j.jclepro.2019.117961.
[35] Meng, X., Liu, Q., Tao, L., Deng, L., Li, W., Wen, Z. (2014): Carbon storage of young and middle age forest in south and north Daxing'anling mountains. – Journal of Central South University of Forestry & Technology 34(6): 37-43. https://doi.org/1673-923X(2014)06-0037-07.
[36] Ministry of ecology and environment of the people' s Republic of China. (2021): Technical specification for investigation and assessment of national ecological status - Field observation of forest ecosystem.
[37] Pan, Y., Birdsey, R.A., Fang, J., Houghton, R. (2011): A Large and Persistent Carbon Sink in the World's Forests. – Science 333(6045): 988-993. https://doi.org/10.1111/j.1469-8137.2011.03645.x.
[38] Piao, S., Fang, J., Zhou, L., Ciais, P., Zhu, B. (2006): Variations in satellite-derived phenology in China's temperate vegetation. – GlobalChange Biology 12: 672-685. https://doi.org/10.1111/j.1365-2486.2006.01123.x.

http://www.aloki.hu ● ISSN 1589 1623 (Print) ● ISSN 1785 0037 (Online)
DOI: http://dx.doi.org/10.15666/aeer/2003_23032328

[39] Piao, S., Liu, Z., Wang, T., Peng, S., Ciais, P., Huang, M., Ahlstrom, A., Burkhart, J.F., Chevallier, F., Janssens, I.A., Jeong, S.-J., Lin, X., Mao, J., Miller, J., Mohammat, A., Myneni, R.B., Peñuelas, J., Shi, X., Stohl, A., Yao, Y., Zhu, Z., Tans, P.P. (2017): Weakening temperature control on the interannual variations of spring carbon uptake across northern lands. – Nature Climate Change 7(5): 359-363. https://doi.org/10.1038/nclimate3277.

[40] Post, W.M., Emanuel, W.R., Zinket, P.J., Stangenberger, A.G. (1982): Soil carbon pools and world life zones. – Nature 298: 156-159. https://doi.org/10.1038/298156a0.

[41] Přívětivý, T., Šamonil, P. (2021): Variation in Downed Deadwood Density, Biomass, and Moisture during Decomposition in a Natural Temperate Forest. – Forests 12(10): 1352. https://doi.org/10.3390/f12101352.

[42] Qu, S., Xu-Ri, Yu, J., Li, F., Wei, D., Borjigidai, A. (2020): Nitrogen deposition accelerates greenhouse gas emissions at an alpine steppe site on the Tibetan Plateau. – Science of the Total Environment 765(1): 144277. https://doi.org/10.1016/j.scitotenv.2020.144277.

[43] Rasse, D.P., Rumpel, C., Dignac, M.-F. (2005): Is soil carbon mostly root carbon? Mechanisms for a specific stabilisation. – Plant and Soil 269: 341-356. https://doi.org/10.1007/s11104-004-0907-y.

[44] Schimel, D. S., Braswell, B.H., Holland, E.A., McKeown, R., Ojima, D.S., Painter, T., Parton, W.J., Townsend, A.R. (1994): Climatic, edaphic, and biotic controls over storage and turnover of carbon in soils. – Global Biogeochemical Cycles 8: 279-293. https://doi.org/10.1029/94GB00993.

[45] Schmidt, C. O., Ittermann, T., Schulz, A., Grabe, H. J., Baumeister, S. E. (2013): Linear, nonlinear or categorical: how to treat complex associations in regression analyses? polynomial transformations and fractional polynomials. – International Journal of Public Health58(1): 157-160. https://10.1007/s00038-012-0363-z.

[46] Seenu, P. Z., Jayakumar, K. V. (2021): Comparative study of innovative trend analysis technique with Mann-Kendall tests for extreme rainfall. – Arabian Journal of Geosciences 14(7): 536. https://doi.org/10.1007/s12517-021-06906-w.

[47] Shen, M.G., Piao, S.L., Jeong, S.J., Zhou, L.M., Zeng, Z.Z., Ciais, P., Chen, D.L., Huang, M.T., Jin, C.S., Li, L.Z., Li, Y., Myneni, R.B., Yang, K., Zhang, G.X., Zhang, Y.J., Yao, T.D. (2015): Evaporative cooling over the Tibetan Plateau induced by vegetation growth. – Proceedings of the NationalAcademy of Sciences of the United States of America 112: 9299-9304. https://doi.org/10.1073/pnas.1504418112.

[48] Tang, X., Zhao, X., Bai, Y., Tang, Z., Wang, W., Zhao, Y., Wan, H., Xie, Z., Shi, X., Wu, B., Wang, G., Yan, J., Ma, K., Du, S., Li, S., Han, S., Ma, Y., Hu, H., He, N., Yang, Y., Han, W., He, H., Yu, G., Fang, J., Zhou, G. (2018): Carbon pools in China's terrestrial ecosystems: New estimates based on an intensive field survey. – PNAS 115(16): 4021-4026. https://doi.org/10.1073/pnas.1700291115.

[49] Tharammal, T., Bala, G., Devaraju, N., Nemani, R. (2019): A review of the major drivers of the terrestrial carbon uptake: model-based assessments, consensus, and uncertainties. – Environmental Research Letters 14(9): 093005. https://doi.org/10.1088/1748-9326/ab3012.

[50] Tian, H., Melillo, J., Lu, C., Kicklighter, D., Liu, M., Ren, W., Xu, X., Chen, G., Zhang, C., Pan, S., Liu, J., Running, S. (2011): China's terrestrial carbon balance: Contributions from multiple global change factors. – Global Biogeochemical Cycles 25(1): 1-16. https://doi.org/10.1029/2010GB003838.

[51] Tucker, C.J., Pinzon, J.E., Brown, M. E. (2004): Global Inventory Modeling and Mapping Studies. – Global Land Cover Facility, University of Maryland.

[52] Tucker, C.J., Pinzon, J.E., Brown, M. E., Slayback, D., Pak, E. W., Mahoney, R., Vermote, E., El Saleous, N. (2005): An Extended AVHRR 8-km NDVI Data Set Compatible with MODIS and SPOT Vegetation NDVI Data. – International Journal of Remote Sensing 26: 4485-4498.

http://www.aloki.hu ● ISSN 1589 1623 (Print) ● ISSN 1785 0037 (Online)
DOI: http://dx.doi.org/10.15666/aeer/2003_23032328

[53] Valentini, R., Matteucci, G., Dolman, A.J., Schulze, E.-D., Rebmann, C., Moors, E.J. (2000): Respiration as themain determinant of carbonbalance in European forests. – Nature 404: 861-865. https://doi.org/10.1038/35009084.

[54] Wu, H. (2015): Comparative study of species diversity indices of different type communities. – Journal of Central South University of Forestry & Technology 35(5): 84-89.

[55] Xu, H. (1998): Forests in Greater Khingan Mountains, China. – Science PressBeijing, China, pp. 3-6.

[56] Xu, L., He, N., Yu, G. (2018a): 2010s China Land Ecosystem Carbon Density Dataset. – Science Data Bank 4(1). https://doi.org/10.11922/csdata.2018.0026.zh; Data DOI: https://doi.org/10.11922/sciencedb.603.

[57] Xu, L., Yu, G., He, N., Wang, Q., Gao, Y., Wen, D., Li, S., Niu, S., Ge, J. (2018b): Carbon storage in China's terrestrial ecosystems: A synthesis. – Scientific Reports 8(2806): 1-13. https://doi.org/10.1038/s41598-018-20764-9.

[58] Xu-Ri, Prentice, I.C., Spahni, R., Niu, H.S. (2012); Modelling terrestrial nitrous oxide emissions and implications for climate feedback. – New Phytologist 196(2): 472-488. https://doi.org/10.1111/j.1469-8137.2012.04269.x.

[59] Yang, Y., Mohammat, A., Feng, J., Zhou, R., Fang, J. (2007): Storage, patterns and environmental controls of soil organic carbon in China. – Biogeochemistry 84: 131-141. https://doi.org/10.1007/s10533-007-9109-z.

[60] Yang, Y., Fang, J., Tang, Y., Ji, C., Zheng, C., He, J., Zhu, B. (2008): Storage, patterns and controls of soil organic carbon in the Tibetan grasslands. – GlobalChange Biology 14(7): 1592-1599. https://doi.org/10.1111/j.1365-2486.2008.01591.x.

[61] Yang, Y., Fang, J., Smith, P., Tang, Y., Chen, A., Ji, C., Hu, H., Rao, S., Tan, K., He, J.-S. (2009): Changes in topsoil carbon stock in the Tibetan grasslands between the 1980s and 2004. – Global Change Biology 15(11): 2723-2729. https://doi.org/10.1111/j.1365-2486.2009.01924.x.

[62] Yang, Y.H., Luo, Y.Q., Finzi, A.C. (2011): Carbon and nitrogen dynamics during forest stand development: a global synthesis. – New Phytologist 190(4): 977-989. https://doi.org/10.1111/j.1469-8137.2011.03645.x.

[63] Yang, Y., Wang, G., Shen, H., Yang, Y., Cui, H., Liu, Q. (2014a): Dynamics of carbon and nitrogen accumulation and C:N stoichiometry in a deciduous broadleaf forest of deglaciated terrain in the eastern Tibetan Plateau. – Forest Ecologyand Management 312: 10-18. https://doi.org/10.1016/j.foreco.2013.10.028.

[64] Yang, Y.H., Li, P., Ding, J.Z., Zhao, X., Ma, W.H., Ji, C.J., Fang, J.Y. (2014b): Increased topsoil carbon stock across China's forests. – Global Change Biology 20(8): 2687-2696. https://doi.org/10.1111/gcb.12536.

[65] Yang, Z., Chen, S., Liu, X., Xiong, D., Xu, C., Arthur, M.A., McCulley, R.L., Shi, S., Yang, Y. (2019): Loss of soil organic carbon following natural forest conversion to Chinese fir plantation. – Forest Ecology and Management 449: 117476. https://doi.org/10.1016/j.foreco.2019.117476.

[66] Zhang, T., Zhang, Q., Wang, Q. (2014): Model detection for functional polynomial regression. – Computational Statistics & Data Analysis70: 183-197. https://doi.org/10.1016/j.csda.2013.09.007.

[67] Zhang, C., Lu, D., Chen, X., Zhang, Y., Maisupova, B., Tao, Y. (2016): The spatiotemporal patterns of vegetation coverage and biomass of the temperate deserts in Central Asia and their relationships with climate controls. – Remote Sensing of Environment 175: 271-281. https://doi.org/10.1016/j.rse.2016.01.002.

[68] Zhang, Y., Yao, Y., Wang, X., Liu, Y., Piao, S. (2017): Mapping spatial distribution of forest age in China. – Earth and Space Science4(3): 108-116. https://doi.org/10.1002/2016EA000177.

http://www.aloki.hu ● ISSN 1589 1623 (Print) ● ISSN 1785 0037 (Online)
DOI: http://dx.doi.org/10.15666/aeer/2003_23032328

[69] Zhao, W., Li, F., Zhuang, C., Wang, S. (2014): Spatial Distribution of Carbon Density for Larch Forest in Daxing'an Mountain. – Journal of Northeast Forestry University 42(6): 1-5. https://doi.org/10.13759/j.cnki.dlxb.20140523.027.
[70] Zhou, G., Liu, S., Li, Z. (2006): Old-growth forests can accumulate carbon in soils. – Science 314: 1417. https://doi.org/10.1126/science.1130168.
[71] Zhu, K. (1996): China soil species description. – National Soil Survey Office, China Agriculture Press, Beijing, China. ISBN: 9787109040014. (in Chinese).
[72] Zhu, J., Wang, C., Zhou, Z., Zhou, G., Hu, X., Jiang, L., Li, Y., Liu, G., Ji, C., Zhao, S., Li, P., Zhu, J., Tang, Z., Zheng, C., Birdsey, R.A., Pan, Y., Fang, J. (2020): Increasing soil carbon stocks in eight permanent forest plots in China. – Biogeosciences 17(3): 715-726. https://doi.org/10.5194/bg-17-715-2020.

http://www.aloki.hu ● ISSN 1589 1623 (Print) ● ISSN 1785 0037 (Online)
DOI: http://dx.doi.org/10.15666/aeer/2003_23032328

APPENDIX

Table A1. *Information of the sampling points*

Sample sites	Longitude (°E)	Latitude (°N)	Altitude (m)	Slope (°)	aspect
1	123.5555	53.3491	384.5	11	NE
2	125.2366	53.0775	241.9	4	S
3	125.6913	52.9904	233.4	2	NE
4	125.0161	52.5054	368.3	7	NS
5	125.8554	52.4578	370.6	2	NS
6	126.2322	52.1672	365.9	2	N
7	120.0591	52.7695	451.3	14	N
8	120.8355	52.5942	464.7	24	SE
9	123.2463	52.2147	637.9	3	SW
10	125.7564	51.9425	359.8	3	NE
11	122.2076	51.7776	838.3	11	SW
12	123.8825	51.6108	721.0	3	NW
13	124.6865	51.5411	560.5	3	NE
14	121.5112	50.9352	589.7	10	SW
15	121.2882	51.3818	1009.8	12	E
16	123.9258	51.0470	563.8	3	NW
17	124.4692	50.9044	548.7	2	NW
18	125.3149	50.8160	435.8	5	NW
19	119.8033	50.6746	635.8	15	NW
20	121.1850	50.8286	791.8	18	S
21	122.7866	50.6547	606.4	2	NS
22	123.5743	50.5033	453.1	3	NE
23	124.3528	50.4060	437.1	20	NS
24	122.0220	47.6090	467.9	22	E
25	120.2438	50.3773	707.2	10	N
26	120.8675	50.3724	660.7	6	SW
27	121.8085	50.1454	908.7	20	SE
28	122.5167	50.1199	572.6	1	S
29	123.3901	50.0371	439.7	15	S
30	124.2128	49.9079	334.6	6	NE
31	121.3788	47.5316	610.8	18	NE
32	120.6427	47.5263	1087.7	12	NE
33	119.9947	47.3310	945.8	26	N
34	120.7520	49.9117	839.1	8	N
35	121.6310	49.6524	758.6	13	S
36	122.4485	49.5209	590.8	2	SE
37	124.0619	49.3260	392.1	5	NW
38	121.2396	47.9531	755.6	11	N
39	120.5106	48.0737	919.3	6	NE
40	119.9517	48.2030	822.7	9	NW
41	120.7081	49.1771	764.0	25	NE

http://www.aloki.hu ● ISSN 1589 1623 (Print) ● ISSN 1785 0037 (Online)
DOI: http://dx.doi.org/10.15666/aeer/2003_23032328

Sample sites	Longitude (°E)	Latitude (°N)	Altitude (m)	Slope (°)	aspect
42	121.3836	49.0670	773.4	26	N
43	122.2989	48.9663	261.2	9	N
44	123.3565	49.0451	372.5	3	SE
45	123.8718	48.7824	291.2	8	S
46	121.3363	48.5146	997.0	10	W
47	122.0335	47.8940	533.0	6	NE
48	121.5556	51.1339	850.2	12	S
49	122.4342	50.9908	741.5	22	S
50	122.4336	50.9903	498.5	8	S
51	122.4331	50.9903	855.5	23	E
52	122.0917	50.9439	436.3	3	NE
53	122.0936	50.9419	972.8	4	NE
54	122.0903	50.9461	855.5	23	E
55	122.0875	50.9511	502.0	7	SE
56	122.3608	50.9931	403.8	15	NW
57	121.5053	50.9397	822.5	9	SE
58	121.5056	50.9233	829.4	6	S
59	121.4922	50.9397	483.2	6	NW
60	121.5214	50.8976	742.2	11	SE
61	121.5207	50.9118	571.5	6	SW
62	121.5224	50.9135	590.4	23	SE
63	122.2867	52.2862	907.0	5	SE
64	122.2881	52.2754	819.7	7	S
65	122.2865	52.2868	898.0	8	NE
66	121.9091	51.8886	676.0	7	S
67	121.9034	51.8751	797.8	10	S
68	121.9042	51.8765	843.5	12	S

Table A2. *Changes in soil organic carbon density (SOCD, kg C m^{-2}) and soil carbon storage (SCS,Tg C) at 0-20 cm depth (at a 95% confidence interval) from the 2000s to the 2010s across the Greater Khingan Mountains*

	Area (10^4 m^2)	Mean SOCD/SE (Kg C m^{-2})		Change in SOCD /SE		Change in SCS
		2000s	2010s	(g C m^{-2} yr^{-1})	% yr^{-1}	(Tg C yr^{-1})
ALL-GKM	31.79	9.15/0.36	10.64/0.83	0.15/0.05*	0.16	0.48
DBF	11.78	10.59/0.74	13.95/1.35	0.34/0.12*	0.32	0.40
BNMF	1.55	8.38/0.53	10.94/2.05	0.26/0.15	0.31	0.04
DNF	18.46	8.63/0.56	8.89/1.10	0.03/0.009	0.03	0.06

ALL-GKM, all of the Greater Khingan Mountains; DBF, deciduous broadleaved forests; BNMF, broadleaf and needleleaf mixed forests; DNF, deciduous needleleaf forests. "*" represent the statistical test is significant ($P < 0.05$)

http://www.aloki.hu ● ISSN 1589 1623 (Print) ● ISSN 1785 0037 (Online)
DOI: http://dx.doi.org/10.15666/aeer/2003_23032328

Table A3. *multiple linear regression between soil organic carbon density and MAP and MAT in two periods, based on normalized difference vegetation index estimation.(MAP, mean annual precipitation (mm); MAT, mean annual temperature (°C))*

	Intercept/SE	Estimate/SE		n
		MAP	MAT	
2000s	1.20E-15/0.08	0.29/0.01**	-0.24/0.01**	129
2010s	-3.23E-16/0.07	0.56/0.08***	-0.001/0.08	129

***, P < 0.001; **, 0.001< P <0.01, at a 95% confidence interval

Table A4. *Changes in soil organic carbon density (SOCD, kg C m^{-2}) based on normalized difference vegetation index (NDVI) estimation at 0-20 cm depth from the 2000s to the 2010s across the Greater Khingan Mountains*

SOCD	Min	Max	Mean/SE
2000s	2.46	17.18	11.60/0.0001
2010s	2.78	21.33	14.17/0.0001

Table A5. *Results of variance analysis of SOCD in different buffers*

Buffers	Period	SOCD (Kg C m^{-2})						ANOVA	
		N	Mean/SE	Conf. int		Min	Max	F	P
	2000s	107	9.10/0.49	8.14	10.07	0.77	39.09		
R1=0.5°	2010s	20	11.26/1.63	7.83	14.69	2.46	24.30	2.640	0.026*
R2=0.8°	2010s	39	11.39/1.07	9.25	13.56	2.34	28.22	4.906	0.018*
R3=1°	2010s	49	11.67/0.99	9.66	13.71	2.34	28.22	6.694	0.011*

Conf. int: at a 95% confidence interval; *: P<0.05

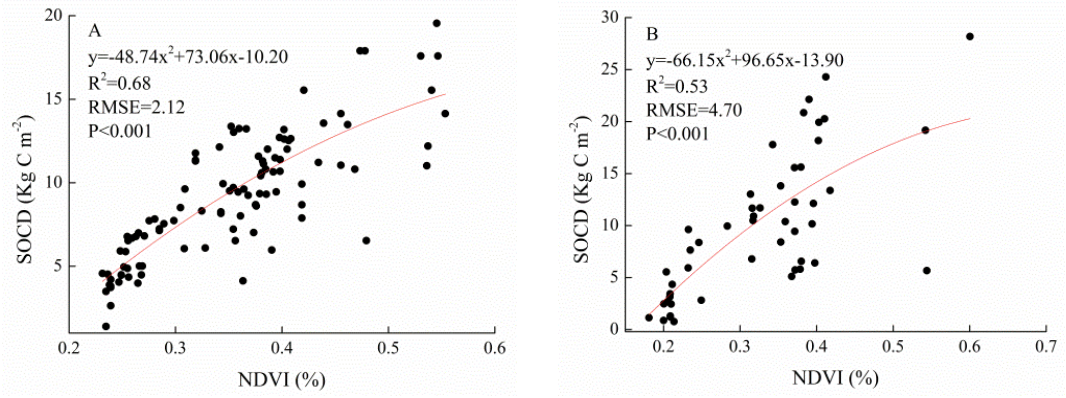

Figure A1.*Correlation between normalized difference vegetation index(NDVI) and soil organic carbon density (SOCD,kg C m^{-2}) in theGreaterKhinganMountainsforthe period of 2000s (A) and 2010s (B), derived from polynomial regression*

http://www.aloki.hu ● ISSN 1589 1623 (Print) ● ISSN 1785 0037 (Online)
DOI: http://dx.doi.org/10.15666/aeer/2003_23032328

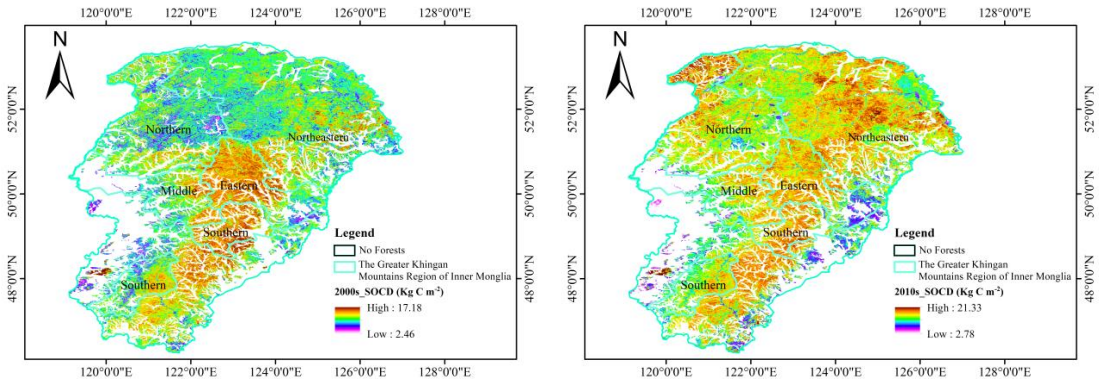

Figure A2. *Spatial distribution of soil organic carbon density (SOCD, kg C m^{-2}) based on normalized difference vegetation index (NDVI) estimation at 0-20 cm depth from the 2000s to the 2010s across the Greater Khingan Mountains*

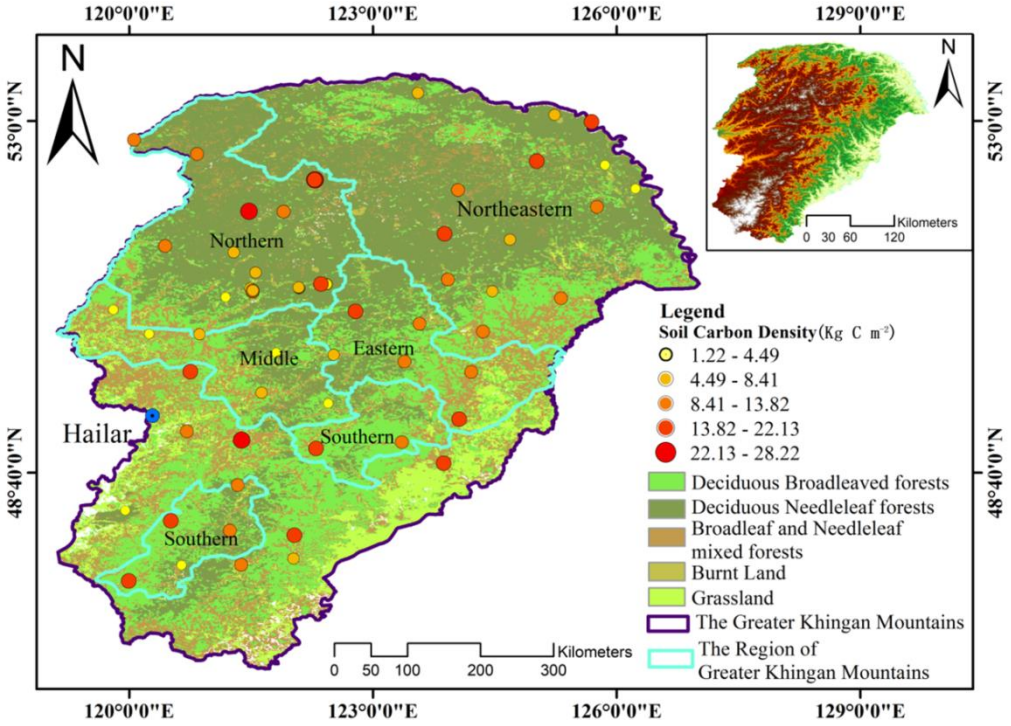

Figure A3. *Spatial distribution of soil organic carbon density (kg C m^{-2}) in the Greater Khingan Mountains*

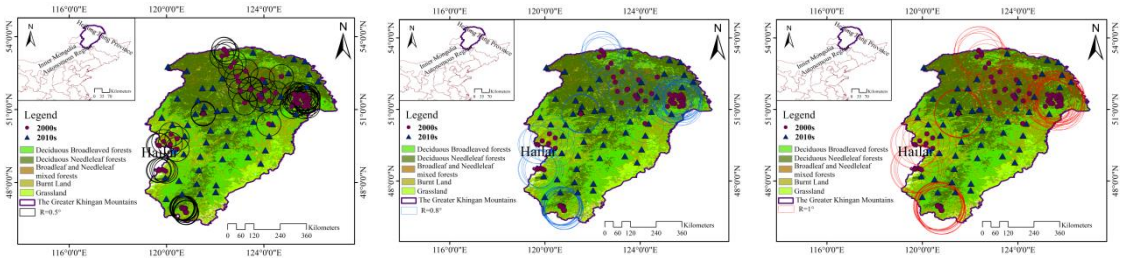

Figure A4. *Buffer overlap diagram of 2010S sample point and 2000s sample point (r = 0.5°, r = 0.8°, r = 1°)*

APPLIED ECOLOGY AND ENVIRONMENTAL RESEARCH 20(3):2303-2328.
http://www.aloki.hu ● ISSN 1589 1623 (Print) ● ISSN 1785 0037 (Online)
DOI: http://dx.doi.org/10.15666/aeer/2003_23032328

INSECTICIDAL ACTIVITY OF ETHANOL AND AQUEOUS EXTRACTS OF MEDICINAL PLANTS AGAINST GREEN PEACH APHID (*MYZUS PERSICAE)*

HYDER, M.* – LI, Y. – WANG, M. – MAO, J. – ZHANG, L.*

Key Laboratory of Integrated Pest Management in Crops, Ministry of Agriculture, Institute of Plant Protection, Chinese Academy of Agricultural Sciences, Beijing 100193, P. R. China

**Corresponding authors*
e-mail: sahito.2k10pt192@hotmail.com, zhanglisheng@caas.cn; phone: +86-010-8210-9581

(Received 12th Nov 2021; accepted 21st Mar 2022)

Abstract. The green peach aphid *Myzus persicae* (Homoptera: Aphididae) is one of the most common and harmful pests. Plant extracts contain many active compounds for defense against pests, and an extensive search for effective and ecological pest control alternatives, particularly those derived from botanicals, is currently underway. This study evaluated the effectiveness of five botanicals from *Citrullus colocynthis*, *Nicotiana tobaccum* L.*,* and seeds of *Trachyspermum ammi, Azadirachta indica,* and *Withania coagulans* against *Myzus persicae*. Botanical oils were extracted using ethanol oil extraction (EOE) from powder and extraction through boiling (ETB) of powder and tested for insecticidal efficacy in a laboratory and a greenhouse. The highest mortality (81.7%) was caused by *T. ammi*, followed by *C. colocynthis* (76.5%), *N. tobaccum* (63.0%), *A. indica* (56.5%), and *W. cagulans* (50.0%). EOE resulted in a higher mortality at 48-h intervals, and fumigation resulted in the highest mortality at 24-h intervals, with the EOE extracts effectively reducing female aphid fecundity. EOE also was more effective against aphids in cucumber than ETB in greenhouse. Taken together, the EOE extracts were more effective than ETB, and all plant extracts possessed significant insecticidal properties, with potential as botanical insecticides for use in integrated pest management programs.
Keywords: *essential oils, mortality, contact toxicity, repellency, fecundity*

Introduction

The green peach aphid *Myzus persicae* (Hemiptera: Aphididae) is one of the most prominent and destructive pests. Green peach aphids feed on over 800 species of plants, including ornamental plants (Van Driesche et al., 2008), vegetables (Hofsvang and Hågvar, 1979; Freuler et al., 2003), fruits (Kim and Kim, 2004), and weeds, but have also been found to attack barley, rye, and winter wheat, as well as on potatoes in northern climates (Davis and Radcliffe, 2008). This aphid is extremely polyphagous and transmits more than 100 plant viruses. It has a wide range of genetic variations in color, life cycle, host-plant relationships, and methods of resisting insecticides (Blackman and Eastop, 2007; Davis and Radcliffe, 2008). Because of its high reproductive rate and short generation time, the green peach aphid is able to adapt to insecticides and develop resistance to active compounds rapidly (Machial, 2010).

Insecticides, such as organophosphates, pyrethroids, and modern chemical insecticides, have been shown to be effective in controlling insects (Umrao et al., 2013). However, due to the widespread use of these insecticides, many pests have developed insecticide resistance (Ahmad and Arif, 2009; Jan et al., 2015). Conventional insecticides have long been used to manage insect pests. Although the dangers and drawbacks of synthetic insecticides were not anticipated when they were first introduced, their use has led to disruptions in the natural balance via their effects on natural enemies, pollinators and other wild life, as well as the evolution of tolerance and the reappearance of treated

http://www.aloki.hu ● ISSN 1589 1623 (Print) ● ISSN1785 0037 (Online)
DOI: http://dx.doi.org/10.15666/aeer/2003_23292342

populations (Vitousek et al., 1997). According to the World Health Organization, pesticide contamination kills 200,000 people globally each year. Insecticidal toxicity, a high risk for disease, residual toxicity, biomagnifications, use limits, and poor environmental impacts have led to a rise in the use of botanical insecticides (Feng and Zheng, 2007; Khater, 2012; Tomé et al., 2013). In addition to biological regulation, pheromones, and plant-derived chemicals, new pest management techniques are urgently needed. Despite the fact that pesticide resistance is widespread, certain mechanisms of insecticide resistance have been identified. The first report of pesticide resistance in *M. persicae* species dates back to 1955 (Anthon, 1955). Resistance to a key class of pesticides includes organophosphates, carbamates, cyclodienes, pyrethroids, and neonicotinoids has now made this species the most significant and robustly resistant species on aphid have been found (Bass et al., 2014).

Controlling harmful pests with synthetic chemical insecticides is crucial for new farming practices, improving crop yield as a result. However, the indiscriminate use of synthetic pesticides for agricultural production and safety has been a source of carcinogenesis, reproductive issues, and mutagenesis in humans via contamination through touch, inhalation, and dietary exposure (Kazem and Shereif, 2010; Lu et al., 2018). These circumstances have prompted a search for efficient and environmentally friendly pest control alternatives, especially those extracted from natural plant resources (Fetoh and Asiry, 2012). Many insecticides originating from botanical sources are readily available, inexpensive, open to farmers, safer for humans, with negligible residual effects, as well as being target-specific and less harmful to vertebrates, pollinators (Batta, 2004; Isman, 2006; Koul et al., 2008).

Due to these challenges, researchers and farmers have been exploring alternative insect control options under the integrated pest management program (IPM). IPM integrates all available resources to control insect species that inflict economic damage. Mechanical control, cultural traditions, biological agents, and botanical extract practices are also part of IPM. In terms of the severity and nature of insect attacks, these are optional. Alkaloids, terpenoids, flavonoids, phenols, glycosides, sitosterols, and tannins are only some of the secondary metabolites present in plants (Gulzar et al., 2019). While plant compounds may be hazardous to variety of insect species when consumed, antifeeding action disrupting (molt inhibitory or anti-molting) (Ulrichs et al., 2008). Plant extracts and botanical pesticides have become increasingly popular in agricultural fields in recent years because of their low cost, lack of residual effects, environmentally friendly nature, and toxic effects on important pests, including aphids, jassids, whiteflies, trips, and mites (Stumpf and Nauen, 2001). Since they are safe for beneficial species, target-specific, and compatible with biological control agents, neem oils and extracts are considered the best choice for insect pest management in vegetables (Tang et al., 2002). Tobacco, sweetsop, and garlic extracts, in particular, have been found to be effective biopesticides for controlling cowpea insect pests (Ahmed et al., 2009). *Citrullus colocynthis*, a botanical insecticide, has also attracted the interest of researchers, and the efficacy of its extracts and isolated compounds has been tested against commercially significant insect pests. Several pests were found to be repelled by this plant's antifeedant, deterrent, and infertility effects (Seenivasan et al., 2004). Studies on the effects of *Citrullus colocynthis* fruit, leaf, stem, and root extracts of *Rhopalosiphum padi* L. found that the stem extract was more effective against this pest than the other component extracts (Khalid, 2015). The antimicrobial effects of *Withania coagulans* and *Withania munifera* leaves, roots, and fleshy buds were also tested, and were found to have an inhibitory effect on bacterial

http://www.aloki.hu ● ISSN 1589 1623 (Print) ● ISSN1785 0037 (Online)
DOI: http://dx.doi.org/10.15666/aeer/2003_23292342

and *Fusarium* wilt, as well as being effective against bacterial Fusarium wilt in tomatoes (Najeeb et al., 2019; Khan et al., 2019). *Anopheles stephensi* larvae are repelled by *Trachyspermum ammi* shoots and leaves from the Blue Mint Bush (*Ziziphora clinopodioides*). Previous studies have also used ajwain oil at various concentrations and exposure periods to fumigate adult *Oryzaephilus surinamensis*, *Rhyzopertha dominica*, and *Tribolium confusum* (Habashi et al., 2011; Torabi et al., 2017). In the present study, the insecticidal effects of different botanicals were evaluated to identify safe alternatives for the management of insect pests. Botanical oils were extracted using EOE and ETB and tested for insecticidal efficacy under both laboratory and greenhouse conditions.

Material and methods

Preparation of plant extracts

The five botanicals used were *Azadirachta indica*, *Withania coagulans Trachyspermum ammi*, and leaves of *Nicotiana tobaccum* L. *Citrullus colocynthis*. Botanical oil was extracted using two methods: ethanol oil extraction from EOE and ETB. Either the seeds or leaves of each botanical plant were washed before being dried in an oven at 45°C for 48 h. The dried material was then ground and pushed through a sieve with a 40-mm mesh. The EOE (ethanol oil extraction from powder), the powder was separated with 95 percent ethanol (1 g of powder in 5 ml of ethanol), and the mixture was stored in bottles at room temperature (20–25°C) for 7 days. To ensure the proper mixing and dissolution of the powder in ethanol, the bottles were shaken twice daily. After filtering the mixture with filter paper, the residuals were dissolved using the same method solution with a ratio. In a rotary evaporator, the first and second solvents were mixed and dried until all of the liquid was evaporated. The oil was collected in a brown collection bottle and stored at 4°C. Then, 0.3 mL of dimethyl sulfoxide (DMSO) with 1% Tween-20 was added to 5 mL of the crude extract solution. The ETB dried powder content was boiled separately for 30–40 min in 2 liters of water, and then sieved through muslin cloth. Each mixture was stored in its own bottle at 4°C. For the control solution, 0.3 mL of DMSO, 1%Tween-20, and 5 mL of double-distilled water were mixed together. The essential oil was extracted using the technique reported by Su et al. (2009).

Laboratory conditions

The aim of the laboratory experiment was to validate the efficacy of various plant extracts and their effects on aphid mortality. The experiments were performed at Langfang Research station laboratory of Institute of Plant Protection, Chinese Academy of Agricultural Sciences, Beijing, China. The toxicity of each treatment was investigated through fumigation, contact, and fecundity experiments. Complete randomized design CRD with five replications was used for the laboratory experiments.

Test 1: Fumigant toxicity

For this experiment, 0.5 ml of each essential oil in solution was applied onto 9-cm-diameter filter paper using a micropipette after being soaked separately. Thereafter, the dried filter paper was kept on the underside of the petri dishes. Thirty aphids (2^{nd} and 3^{rd} instar) were placed in 9-cm petri dishes, which were sealed with polythene strips. The petri dishes were incubated at 25 ± 2°C, 50% RH, and a photoperiod of 10:14 h L:D. Throughout the bioassay test, the petri dishes were examined at 2, 6, 12, and 24 h to assess

http://www.aloki.hu ● ISSN 1589 1623 (Print) ● ISSN1785 0037 (Online)
DOI: http://dx.doi.org/10.15666/aeer/2003_23292342

fumigant toxicity against each extract aphid, observed in terms of the percentage of mortality.

Test 2: Contact toxicity and fecundity

Contact toxicity tests were performed to confirm the effectiveness of the different extracts. During this test, both types of extractions were applied using CRD with five replications. In each petri dish, twenty-five field-collected aphids (2^{nd} and 3^{rd} instar) were separated using cabbage leaves that were soaked with each extraction solution (10 ml/100 ml water). Once they had settled, botanical extracts were applied using a fine hand sprayer (Flip & Spray^{TM} Bottles; Thomas Scientific, USA), using two spray applications to completely cover the Petri dish area. Excess solution was removed using a tissue paper. A lid with four holes drilled was used to cover the petri dishes while allowing for ventilation. Lastly, the petri dishes were incubated at 25 ± 2°C, 50% RH, and a photoperiod of 10:14 h L: D. The petri dishes were examined consecutively at 6, 12, 24, and 48 h starting from extract application.

To determine the fecundity of *Myzus persicae*, the extracts were subjected to the same process described above. In each petri dish (9-cm diameter) ten adult aphids were placed on cabbage leaves after 24 h. Surviving adults were transferred into new petri dishes with fresh food to assess the fecundity of the mature aphids. Data on fecundity were recorded from each treatment on a daily basis for five days.

Greenhouse study

The glasshouse experiment was carried out to assess the effectiveness of several essential oils against green peach aphid on cucumber cultivated in net houses. Cucumber seedlings were cultivated in germination trays and transplanted during the last week of April 2019, keeping a row to row and plant to plant spacing of 60 cm x 30 cm. The seedlings were placed in raised beds 30 cm by following recommended cultural and management practices. The cucumber was cultivated using a randomized complete block design (RCBD) with six treatments and two methods (EOE, ETB) for each treatment performed in triplicate. Each sub-plot size measured as 10 × 10 m. The treatments were as follows: T1 (*Citrullus colocynthis*), T2 (*Trachyspermum ammi*), T3 (*Nicotiana tobaccum* L), T4 (*Azadirachta indica*), T5 (*Withania cagulans*), and T6 (control). The extracts were sprayed using a Knapsack sprayer. After each treatment, the sprayer was rinsed twice to prevent contamination. The aphid population was counted on 10 randomly selected plants from each subplot. Aphid populations were randomly examined on 10 randomly selected plants from a sub-plot, and each selected plant was examined. Pre-treatment observations were recorded 24 h prior to application, and post-treatment aphid counting was conducted at 1-, 2-, 4-, and 7-day intervals. The environmental conditions inside greenhouses followed seasonal trends (April: 24 ± 0.4 °C, 40.2 ± 1.9% RH; May: 25.3 ± 0.4 °C, 45.6 ± 1.6% RH; June: 26.2 ± 0.4 °C, 48.5 ± 1.9% RH; July: 26.5 ± 0.5 °C, 50.8 ± 1.5% RH).

Data analysis

The materials and techniques were evaluated based on the mortality, reduction, and fecundity percentage and corrected using Abbott's formula (*Eq.1*) (Abbott, 1925).

$$Corrected\ \%\ mortality\ =\ \frac{(1-n\ in\ T\ after\ treatment\ )}{n\ in\ Co\ after\ treatment} \times\ 100 \qquad \text{(Eq.1)}$$

http://www.aloki.hu ● ISSN 1589 1623 (Print) ● ISSN1785 0037 (Online)
DOI: http://dx.doi.org/10.15666/aeer/2003_23292342

where *n* is the insect population, *T* is "treated", and *Co* is the control. The mortality, reduction, and fecundity data were subjected to factorial analysis of variance (ANOVA) using Minitab 16.1 software. To analyze the influence of treatments on mortality, reduction, and fecundity of the treated green peach aphid *M. persicae*, the means were compared using Tukey's HSD test at a 5% level of significance.

Results

Effect of botanicals on the mortality rate of green peach aphid through fumigation toxicity

The effectiveness of fumigation of each treatment was determined by counting the mortality of *Myzus persicae* after treatment with each extract. Each botanical extract had adverse effects on the pest. Mortality was found to increase with the exposure period. Mortality data are presented in *Table 1*, with significant differences at 2 h (F=69.1; df=4; $P < 0.000$), 6 h (F=27.4; df=4; $P < 0.001$), 12 h (F=24.9; df=4; $P < 0.000$), and 24 h (F=2.7 ; df=4; $P < 0.012$). The highest mortality was reported after 24 h of exposure. The interval wise mortality caused by *Trachyspermum ammi* was 81.7% and 65.20% (EOE) and 75.45% and 57.92% (ETB= after 24 h and 12 h of exposure, respectively, followed by *Citrullus colocynthis* (76.5% and 60.0% (EOE) and 67.73% and 45.0% (ETB)), *Nicotiana tobaccum* L. (63.0% and 51.60% (EOE) and 60.0% and 36.25% (ETB)), *Azadirachta indica* (56.5% and 32.20% (EOE) and 49.09% and 31.67% (ETB)), and *Withania cagulans* (50.0% and 30.40% (EOE) and 46.36% and 28.33% (ETB)) after 24 h and 12 h of exposure. Extracts obtained using the EOE method resulted in a higher mortality than those obtained via the ETB method.

Table 1. *Fumigant toxicity effect of botanicals extracts against aphid M. persicae in laboratory*

Treatments	Method	Pre-treatment	Post-treatment population and mortality percentage (%)[a]			
			2 h	6 h	12 h	24 h
Citrullus colocynthis	**EOE**	30	21.5 (28.33) f	15.2 (43.70) fg	10 (60.0) cd	5.4 (76.5) c
	ETB	30	24.2 (19.33) d	18.7 (25.20) e	13.2 (45.0) c	7.1 (67.73) c
Trachyspermum ammi	**EOE**	30	18.4 (38.67) g	13.3 (50.74) g	8.7 (65.20) d	4.2 (81.7) cd
	ETB	30	23.4 (22.00) e	16.1 (35.60) f	10.1 (57.92) cd	5.4 (75.45) c
Nicotiana tobaccum L	**EOE**	30	20.1 (33.00) b	15.7 (41.85) f	12.1 (51.60) c	8.5 (63.0) c
	ETB	30	26.1 (13.00) c	20.3 (18.80) d	15.3 (36.25) bc	8.8 (60.00) c
Azadirachta indica	**EOE**	30	25.4 (15.33) cd	21.1 (21.85) d	16.2 (35.20) b	10 (56.5) b
	ETB	30	27.4 (8.67) b	22.3 (10.80) cd	16.4 (31.67) b	11.2 (49.09) b
Withania coagulans	**EOE**	30	26.2 (12.67) c	22.4 (17.04) cd	17.4 (30.40) b	11.5 (50.0) b
	ETB	30	28 (6.67) b	22.8 (8.80) c	17.2 (28.33) b	11.8 (46.36) b
Control	**EOE**	30	30 a	27 a	25 a	23 a
	ETB	30	30 a	25 b	24 a	22 a
Significance level	**-**		F=69.1, df 4 P < 0.000	F=27.4, df 4 P < 0.001	F=24.9, df 4 P < 0.000	F=2.7, df 4 P < 0.012

EOE, ethanol oil extraction from powder; ETB, extraction through boiling of powder. **(%)** Percentage reduction due to the post application of treatments at a particular time mentioned in parentheses. [a]Means followed by same letters withen colum are non-significantly different from each other, (LSD; P=0.05)

http://www.aloki.hu ● ISSN 1589 1623 (Print) ● ISSN1785 0037 (Online)
DOI: http://dx.doi.org/10.15666/aeer/2003_23292342

Effect of botanicals on mortality rate of green peach aphid through fumigation toxicity contact toxicity

Table 2 shows the mortality (percentage) of *Myzus persicae* due to contact toxicity. The maximum mortality was recorded after 24 h. According to the results, the highest mortality was 71.19% and 85.71% (EOE) and 67.54% and 75% (ETB), caused by the crude extract of *Trachyspermum ammi* at 24 h and 48 h, respectively, followed by *Citrullus colocynthis* with 65.25% and 71.43% (EOE) and 48.25% and 58.33% (ETB) at 24 h and 48 h, respectively, *Nicotiana tobaccum* L. with 52.54% and 66.33% (EOE) and 45.61% and 54.76% (ETB) at 24 h and 48 h, and *Azadirachta indica* with 25.0% and 32.28% (EOE) and 18.0% and 26.85% (ETB) at 6 h and 12 h. The same trend of mortality was observed for *Withania cagulans* at 6 h to 48 h of exposure, with 19.0%, 25.71%, 38.14%, and 46.94% (EOE), and 12.0%, 21.30%, 28.95, and 32.14% (ETB), respectively. The EOE and ETB extracts were found to be effective compared to the control, and the highest mortality in the aphid population was observed up to 24 h after exposure. The extracts obtained through ETB did not perform as well as the extracts obtained through ETB.

Table 2. *Contact toxicity effect of botanicals extracts against aphid M. persicae on cabbage leaves in laboratory*

Treatments	Method	Pre-treatment	Post-treatment population and mortality percentage (%)			
			6 h	12 h	24 h	48 h
Citrullus colocynthis	**EOE**	25	15.25 (39.00) e	13.75 (47.62) c	10.25 (65.25) de	7 (71.43) de
	ETB	25	18.25 (27.00) d	16.5 (38.89) bc	14.75 (48.25) d	8.75 (58.33) d
Trachyspermum ammi	**EOE**	25	14.5 (41.7) e	12.3 (54.29) c	8.5 (71.19) e	3.5 (85.71) g
	ETB	25	16.75(33.00)de	13.75 (49.07) c	9.25 (67.54) e	5.25 (75.00) f
Nicotiana tobaccum L	**EOE**	25	19.5 (22.00) d	16.25(38.10)bc	14 (52.54) d	8.25 (66.33) d
	ETB	25	20.75 (18.00) c	18.75(30.56)bc	15.5 (45.61) cd	9.5 (54.76) d
Azadirachta indica	**EOE**	25	18.75 (25.00) d	17.75(32.28)bc	16.5 (44.07) c	11.5 (53.06) d
	ETB	25	20.5 (18.00) c	19.75 (26.85) b	18.75 (34.21) bc	11.75 (44.05) d
Withania coagulans	**EOE**	25	20.25 (19.00) c	19.5 (25.71) b	18.25 (38.14) bc	13 (46.94) c
	ETB	25	22 (12.00) b	21.25 (21.30) b	20.25 (28.95) b	14.25 (32.14) c
Control	**EOE**	25	25 a	26.25 a	29.5 a	24.5 a
	ETB	25	25 a	27 a	28.5 a	21 b
Significance level	-	-	F=4.49, df 4 P < 0.010	F=2.44, df 4 P < 0.084	F=33.05, df 4 P < 0.000	F=6.14, df 4 P < 0.002

EOE, ethanol oil extraction from powder; *ETB,* extraction through boiling of powder. **(%)** Percentage reduction due to the post application of treatments at a particular time mentioned in parentheses. [a]Means followed by same letters withen colum are non-significantly different from each other, (LSD; P=0.05)

Effect of botanicals on fecundity rate of the green peach aphid

The impact of botanical extracts on fecundity revealed that *Withania coagulans* was the least effective. Aphid gave birth to a non-significant number of offspring (21.6 and 35 EOE and 22.3 and 32 ETB nymphs per female) in *W. coagulans*-treated petri dishes and the control (*Fig. 1*). During the same time period, green peach aphids treated with *Nicotiana tobaccum* L. and *Azadirachta indica* extract also gave birth to offspring (19.6 and 17.3 EOE and 18.6 and 18 ETB nymphs per female). The *Citrullus colocynthis* EOE and ETB extract had the lowest fecundity, with females producing only 9.3 and 13.3

http://www.aloki.hu ● ISSN 1589 1623 (Print) ● ISSN1785 0037 (Online)
DOI: http://dx.doi.org/10.15666/aeer/2003_23292342

nymphs in 5 days. Similarly, during the same incubation period, adult aphids were treated with *Trachyspermum ammi* EOE, and the ETB botanicals were ranked the second lowest. In terms of fecundity, these females produced 12.6 and 16.6 offspring, respectively. Significant differences in fecundity were observed between all botanical extracts (F=2.10; df=4; P < 0.123). The results revealed that *C. colocynthis* performed well in reducing the fecundity of *M. persicae*.

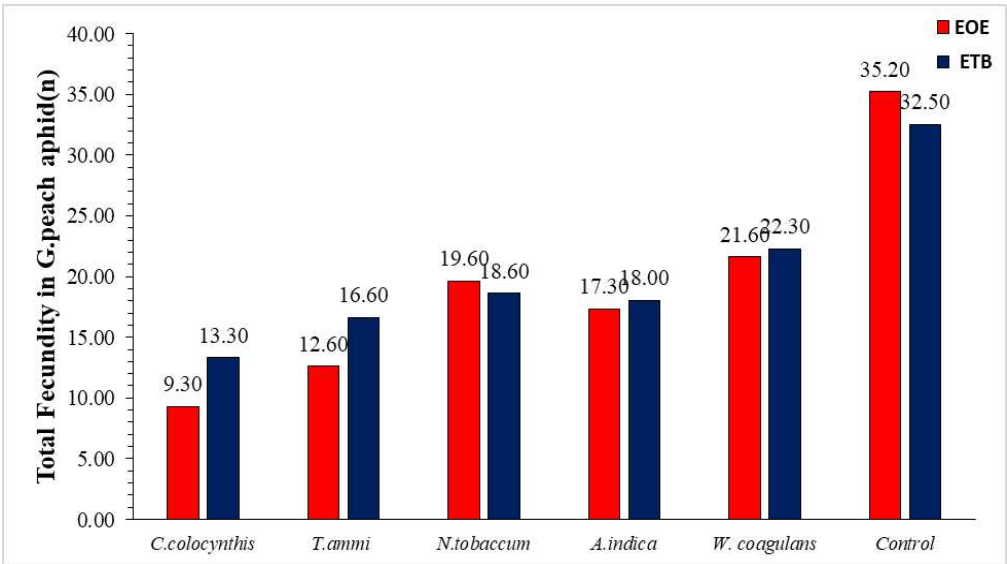

Figure 1. *Total fecundity (nymphs produced) in green peach aphids treated with EOE and ETB botanical extracts*

Population reduction of M. persicae in greenhouse

All treatments were effective under greenhouse conditions. The aphid populations were clearly affected by both extraction methods. The efficacy at 24 h post-treatment (*Table 3*) revealed that *Citrullus colocynthis* showed a maximum reduction in the *Myzus persicae* population of 50.48% (EOE) and 41.05% (ETB), followed by *Trachyspermum ammi* with 41.23% (EOE) and 31.20%, (ETB), Tobacco Desi with 41.23% (EOE) and 31.20% (ETB), neem seed with 35.05% (EOE) and 22.53% (ETB), and *Withania coagulans* with 24.23% (EOE) and 15.49% (ETB). *Citrullus colocynthis* performed well at 3-day intervals after treatment and resulted in a maximum of 70.9% (EOE) and 63.30% (ETB) in the aphid population, followed by *Trachyspermum ammi* with an efficacy of 62.30% (EOE) and 49.48% (ETB), *Nicotiana tobaccum* L. with 63.30% (EOE) and 50.79% (ETB), neem seed with 48.4% (EOE) and 40.29% (ETB), and *Withania coagulans* with 45.56% (EOE) and 34.93% (ETB). After seven days of treatment, *Citrullus colocynthis* was consistently the most effective in reducing the populations of aphids, with a reduction of 79.42% (EOE) and 68.50% (ETB), followed by *Trachyspermum ammi* with 73.91% (EOE) and 60.19% (ETB), Tobacco Desi with 67.38% (EOE) and 57.9% (ETB), *Azadirachta indica* with 53.77% (EOE) and 46.89% (ETB), and *Withania coagulans* with 50.0% (EOE) and 42.78% (ETB). According to the average output of all biopesticides (Fig. 1), the *Citrullus colocynthis* extract was the most successful against aphids, followed by *Trachyspermum ammi*, *Nicotiana tobaccum* L., *Azadirachta indica*, and *Withania coagulans*.

http://www.aloki.hu ● ISSN 1589 1623 (Print) ● ISSN1785 0037 (Online)
DOI: http://dx.doi.org/10.15666/aeer/2003_23292342

Table 3. *Effect of foliar application of botanicals extracts against aphid M. persicae on cucumber plants in greenhouse*

Treatments	Method	Pre-treatment	Post-treatment population and reduction percentage (%)			
			24 h	48 h	96 h	168 h
Citrullus colocynthis	EOE	60	38.3 (50.48) fg	32.2 (61.41) g	25.7 (70.99) f	19.5 (79.42) h
	ETB	73.43	45.6 (41.05) e	39.34 (52.86) ef	32.52 (63.30) e	29.85 (68.50) f
Trachyspermum ammi	EOE	52.7	45.46 (41.23) e	41.35 (50.45) e	33.4 (62.30) e	24.72 (73.91)g
	ETB	68.9	53.22 (31.20) cd	48.53 (41.85) d	44.76 (49.48) d	37.72 (60.19) e
Nicotiana tobaccum L	EOE	66.4	43.7 (43.50) f	37.83 (54.67) f	32.52 (63.30) e	30.91 (67.38) f
	ETB	63.35	54.27 (29.84) c	46.9 (43.80) d	43.6 (50.79) d	39.8 (57.99) e
Azadirachta indica	EOE	70.6	50.24 (35.05) d	47.3 (43.32) d	45.65 (48.48) d	43.8 (53.77) d
	ETB	83.6	59.92 (22.53) b	54.1 (35.17) c	52.9 (40.29) c	50.32 (46.89)b
Withania coagulans	EOE	81.5	58.37 (24.54) bc	53.45 (35.95) c	48.23 (45.56) d	47.35 (50.03) c
	ETB	75.5	65.37 (15.49) b	61.72 (26.04) b	57.65 (34.93) b	54.22 (42.78)b
Control		63.2	77.35 a	83.45 a	88.6 a	94.75 a
Significance level			F=15.27, df 4 P < 0.000	F=3.94, df 4 P < 0.018	F=12.47, df 4 P < 0.003	F=29.66, df 4 P < 0.035

EOE, ethanol oil extraction from powder; *ETB*, extraction through boiling of powder. [(%)] Percentage reduction due to the post application of treatments at a particular time mentioned in parentheses. [a]Means followed by same letters withen colum are non-significantly different from each other, (LSD; P=0.05)

Discussion

Due to the problems associated with the use of synthetic chemicals for pest control, there is an urgent need to incorporate natural products, primarily those derived from plant sources, for use in pesticides against insects. This is especially true for *Myzus persicae*, which is increasingly causing damage in vegetable and fruit-growing regions around the world. Because of their strong efficacy against various insect pests, plant extracts and essential oils are widely used for pest control. The plants chosen in this study, namely *Citrullus colocynthis, Trachyspermum ammi, Nicotiana tobaccum* L.*, Azadirachta indica*, and *Withania coagulans*, are to some degree natural insect repellents and promising resources to combat infestations by the green peach aphid. In this study, the phytochemical constituents of the extracts of the above-mentioned plants were identified, and their insecticidal activity was assessed using residual and contact toxicity methods. Essential oils or bio-pesticide extraction from plant parts is dependent on the plant material and solvent used. In our results, ethanol was used to obtain a high polarity and extract yields during solvent extraction, as previously reported (Awang et al., 2017). Ethanol was found to yield more from *Melastoma malabathricum* leaves compared to other solvents. Furthermore, using ethanol as an extraction solvent, a relatively high extract yield from *C. colocynthis* and *C. sativa* has been previously reported (Maqsood et al., 2020).

The fumigant activity of plant volatiles can be exploited as a control of the phytophagous insects of greenhouse crops. However, due to the volatile and unstable nature of these compounds, this idea has yet to gain commercial ground. The essential oils of anise and cumin have been reported to be toxic against cotton aphids (*Aphis gossypii* Glover) (Hemiptera: Aphididae) (Isman, 2000). In the present study, the mortality of *Myzus persicae* was determined using EOE and ETB from different plants under laboratory conditions by fumigation toxicity. All of the botanical extracts were

http://www.aloki.hu ● ISSN 1589 1623 (Print) ● ISSN1785 0037 (Online)
DOI: http://dx.doi.org/10.15666/aeer/2003_23292342

found to be effective and resulted in mortality at 2 h against aphids and increased with the exposure period. The present study is in line with previous studies. In a laboratory, the bioassay inside small air-tight dishes, vapors of anise essential oil (EO), or its major compound (E)-anethole, were effective against the bird cherry-oat aphid *Rhopalosiphum padi* L. (Pascual et al., 2017). In the red flour beetle adults, *Tribolium castaneum*, (E)-anethole in combination with 1,8-cineole provided the best results in terms of fumigant toxicity (Koul et al., 2007). Various concentrations and exposure times of ajwain (*Trachyspermum ammi*) oil have been found to have fumigant activity against adults of *Oryzaephilus surinamensis*, *Rhyzopertha dominica*, and *Tribolium confusum* (Habashi et al., 2011).

In the present study, the results of contact toxicity under laboratory conditions further revealed that treatment with *Trachyspermum ammi* had the highest mortality and was the most effective against aphids, followed by *C. colocynthis*, *Nicotiana tobaccum* L., *Azadirachta indica*, and *Withania coagulans*. Additionally, extracts obtained by extraction via the ETB of the leaves and seeds of various plants were found to perform less well than extracts obtained by the EOE method. Similarly, Maqsood et al. (2020) found that, after 48 h of exposure, treatment with *Brevicoryne brassicae* resulted in the highest mortality rate (83.33 ± 1.29%), followed by *Citrullus colocynthis* and *C. indica*, with mortality rates of 81.67 ± 3.41% and 81.67% ± 1.67%, respectively. With regards to the essential oil of *Myristica fragrans* extracted using ethanol, the maximum concentration (10 mg/mL) was found to result in a high mortality in the nymphs of whiteflies (72.50 ± 4.23%), while the lowest concentration resulted in the lowest nymph mortality (Wagan et al., 2017). The Trifolio company's neem oil, which contained 0.04% azadirachtin and an equivalent amount of 3-tigloyl-azadirachtol, caused approximately 90% mortality of *Schistocerca gregaria* within 2 days (Zia, 2009). The ethanol-essential oil of *Gardenia jasminoides* and its components were tested in a contact toxicity procedure against the nymphal stage of the whitefly (Wagan et al., 2018). The action of aqueous extracts of tobacco, tagetes, and tephrosia of *Callosobruchus spp.* were also evaluated against insect pests (Kawuki et al., 2005). Similarly, in laboratory conditions, Vekaria and Patel (2000) tested tobacco leaf extracts against aphids.

Fecundity is an important aspect of insect populations, which can be influenced by plant extracts, resulting in reduced fecundity. In the present study, differences in fecundity were observed after *Myzus persicae* was exposed to a range of extracts. Aphids treated with the extracts were found to reproduce at a slower rate than untreated aphids; treatment with *Citrullus colocynthis* extract resulted in the lowest fecundity, while treatment with *Trachyspermum ammi* botanicals resulted in the second lowest fecundity during the same incubation period. In a previous study, the longevity and fecundity of cotton aphids were both found to be harmed by treatment with neem and eucalyptus extracts (Bayhan et al., 2006). Similarly, Pavela et al. (2004) observed the lowest fecundity in cabbage aphids after exposure to systemic neem extract. The combination of entomopathogenic fungi and botanical extracts was also found to have a negative impact on fecundity. In a similar study, when aphids were treated with a binary mixture of *Beauveria bassiana* and eucalyptus extract, the lowest fecundity (7 nymphs per female) was observed (Ali et al., 2017). In another study, aphids exposed to neem seed extracts and citrus aphids yielded a smaller number of nymphs. The negative effects of the fungal infections of *Beauveria bassiana* and *Metarhizium anisopliae* on the fecundity, fertility, and egg-laying of Russian wheat aphids have also been previously explored (Wang and Knudsen, 1993; Tang et al., 2002).

http://www.aloki.hu ● ISSN 1589 1623 (Print) ● ISSN1785 0037 (Online)
DOI: http://dx.doi.org/10.15666/aeer/2003_23292342

Research has demonstrated that *Cassia sophera* and *Ageratum conyzoides* extracts induced mortality in *B. brassicae* comparable to the synthetic insecticide emamectin benzoate (Amoabeng et al., 2013). *Elettaria cardamomum,* another medicinal plant, was found to be effective against this pest (Jahan et al., 2016). According to reports, *B. brassicae* is sensitive to 1,8-cineole, a chemical compound found in *Laurus nobilis* caused a 52% reduction in reproduction (Kahan et al., 2008). In the present study, compared to the average output of all biopesticides, *Citrullus colocynthis* extract was the most successful against aphids, followed by *Trachyspermum ammi, Nicotiana tobaccum* L., *Azadirachta indica*, and *Withania coagulans*. In line with the present study, leaf extracts were found to exert the greatest pesticide action against *B. brassicae*; however, extracts from the leaves and fruits of *C. colocynthis* have also been found to be repellant against *Aphis craccivora* (Farghaly et al., 2009). Cucurbitacin E glycosides isolated from *C. colocynthis* extract have previously shown effective insecticidal activity against *Aphis craccivora* (Farghaly et al., 2009). Moreover, *Nicotiana tabacum* L. was found to be highly effective against insect pests of cabbage, wheat, peas, grammes, and other crops (Lal and Verma, 2006). The efficacy and control level of tobacco (variety IT86D-719) against insect pests of cowpea and their effects on yield were determined by Ahmed et al. (2009). These extracts have potential for use in novel eco-friendly sprays that are commercially available for use by small farmers. In fact, some have already been introduced by farmers in several regions, adding to the urgency of their evaluation. The use of natural bio-insecticides has been shown to be both efficient and environmentally beneficial, resulting in a reduction of the pesticide load on biodiversity. Furthermore, essential oils extracted from natural plants are widely believed to be healthy for humans and the environment, making them a potential source of new botanical insecticides.

Conclusion

In conclusion, the results presented in this study indicate that the EOE method of extraction was more effective against aphids than the ETB method. The highest activity in the fumigant toxicity, contact toxicity, fecundity, and greenhouse experiments were associated with extracts obtained using this method for the maximum duration. However, further studies are needed to fractionate and isolate the active compounds responsible for aphid mortality, as well as to examine their risks and compatibility, to improve aphid eco-friendly management.

Acknowledgements. This research was financed by the National Key R&D Program of China (2019YFD1002103), the Projects of Guizhou Tobacco Corporation (201941), the Major Projects of China National Tobacco Corporation (110202001032 (LS-01)), and the Agricultural Science and Technology Innovation Program (CAAS-ZDRW202108).

REFERENCES

[1] Abbott, W. S. (1925): A method of computing the effectiveness of an insecticide. – Journal of Economic Entomology 18: 265-267.

[2] Ahmad, M., Arif, M. I. (2009): Resistance of Pakistani field populations of spotted bollworm Earias vittella (Lepidoptera: Noctuidae) to pyrethroid, organophosphorus and new chemical insecticides. – Pest Management Science 4: 433-439.

http://www.aloki.hu ● ISSN 1589 1623 (Print) ● ISSN1785 0037 (Online)
DOI: http://dx.doi.org/10.15666/aeer/2003_23292342

[3] Ahmed, B. I., Onu, I., Mudi, L. (2009): Field bio efficacy of plant extracts for the control of post flowering insect pests of cowpea (*Vigna unguiculata* (L.) Walp.) in Nigeria. – Journal of Biopesticides 1: 37-43.
[4] Ahmed, M. M., Ji, M., Qin, P. U. Z., Liu, Y., Sikandar, A., Iqbal, M. F., Javeed, A. (2019): Phytochemical screening, total phenolics and flavonoids content and antioxidant activities of *Citrullus colocynthis* L. and *Cannabis sativa* L. – Applied Ecology and Environmental Research 17(3): 6961-6979. https://doi.org/10.15666/aeer/1703_69616979.
[5] Ali, S., Ullah, M. I., Arshad, M., Iftikhar, Y., Saqib, M., Afzal, M. (2017): Effect of botanicals and synthetic insecticides on *Pieris brassicae* (L., 1758) (Lepidoptera: Pieridae). – Turkish Journal of Entomology 41(3): 275-284. https://doi.org/10.16970/entoted.308941.
[6] Amoabeng, B. W., Gurr, G. M., Gitau, C. W., Nicol, H. I., Munyakazi, L., Stevenson, P. C. (2013): Tri-Trophic Insecticidal Effects of African Plants against Cabbage Pests. – PLOS ONE 8(11): 10.1371. https://doi.org/10.1371/annotation/f0351003-b6f8-4249-ace5-bcd84dead916.
[7] Anthon, E. W. (1995): Evidence for green peach aphid resistance to organophosphorus insecticides. – J. Econ. Entomol. 48: 56-57.
[8] Awang, M. A., Aziz, R., Sarmidi, M. R., Abdullah, L. C., Yong, P. K., Musa, N. F. (2017): Comparison of different solvents on the extraction of *Melastoma malabathricum* leaves using soxhlet extraction method. – Der Pharmacia Lettre 8: 153-157.
[9] Bass, C., Puinean, A. M., Zimmer, C. T., Denholm, I., Field, L. M., Foster, S. P., Gutbrod, O., Nauen, R., Slater, R., Williamson, M. S. (2014): The evolution of insecticide resistance in the peach potato aphid, *Myzus persicae*. – Insect Biochem. Mol. Biol. 51: 41-51.
[10] Batta, Y. (2004): Control of rice weevil (*Sitophilus oryzae* L., Coleoptera: Curculionidae) with various formulations of *Metarhizium anisopliae*. – Crop Protection 23: 103-108. https://doi.org/10.1016/j.cropro.2003.07.001.
[11] Bayhan, S. O., Bayhan, E., Ulusoy, M. R. (2006): Impact of neem and extracts of some plants on development and fecundity of *Aphis Gossypii* Glover (Homoptera: Aphididae). – Bulgarian Journal of Agricultural Science 12: 781-787.
[12] Blackman, R. L., Eastop, V. E. (2007): Taxonomic issues. – In: Van Emden, H. F., Harrington, R. (ed.) Aphids as crop pests. Cromwell Press, UK (electronic version).
[13] Davis, J. A., Radcliffe, E. B. (2008): Reproduction and feeding behavior of Myzus persicae on four cereals. – J. Econ. Entomol. 101: 9-16.
[14] Farghaly, S., Torkey, H., Abou-Yousef, H. (2009): Natural extracts and their chemical constituents in relation to toxicity against whitefly (*Bemisia tabaci*) and aphid (*Aphis craccivora*). – Australian Journal of Basic and Applied Sciences 3: 3217-3223.
[15] Feng, W., Zheng, X. (2007): Essential oils to control Alternaria alternate *in vitro* and *in vivo*. – Food Control 9: 1126-1130. https://doi.org/10.1016/j.foodcont.2006.05.017.
[16] Fetoh, B. E.-S. A., Asiry, K.A. (2012): Toxicological and larvicidal activities of Alzanzalakhet, Melia azedarach against cucurbit fly, *Dacus ciliatus* at Hail Province in Saudi Arabia. – Toxicological and Environmental Chemistry 94: 1350-1356. https://doi.org/10.1080/02772248.2012.705466.
[17] Freuler, J., Fischer, S., Mittaz, C., Terrettaz, C. (2003): The role of banker plants in the enhancement of the action of *Diaeretiella rapae* (M'Intosh) (Hymenoptera, Aphidiinae) the primary parasitoid of the cabbage aphid *Brevicoryne brassicae* (L.). – IOBC/WPRS Bull. 26: 277-299.
[18] Gulzar, A., Ali, M. M., Tariq, M., Bodlah, I., Tariq, K., Ali, A. (2019): Lethal and sublethal effects of *Azadirachtin indica* seed extract on the development of spotted Bollworm Earias vittella (Fab.). – Gesunde Pflanzen 71(1): 19-24. https://doi.org/10.1007/s10343-018-0437-9.
[19] Habashi, A. S., Safaralizadeh, M. H., Safavi, S. A. (2011): Fumigant toxicity of *Carum copticum* L. oil against *Tribolium confusum* du val, *Rhyzopertha dominica* F. and *Oryzaephilus surinamensis*. – Munis Entomology & Zoology 6(1): 282-289.

http://www.aloki.hu ● ISSN 1589 1623 (Print) ● ISSN1785 0037 (Online)
DOI: http://dx.doi.org/10.15666/aeer/2003_23292342

[20] Hofsvang, T., Hågvar, E. B. (1979): Different introduction methods of *Ephedrus cerasicola* starý to control *Myzus persicae* (Sulzer) in small paprika glasshouses. – Z. Angew. Entomol. 88: 16-23.
[21] Isman, M. B. (2000): Plant essential oils for pest and disease management. – Crop Protection 19: 603-608. https://doi.org/10.1016/S0261-2194(00)00079-X.
[22] Isman, M. B. (2006): Botanical insecticides, deterrents, and repellents in modern agriculture and an increasingly regulated world. – Annual Review of Entomology 51: 45-66. https://doi.org/10.1146/annurev.ento.51.110104.151146.
[23] Jahan, F., Abbasipour, H., Hasanshahi, G. (2016): Fumigant toxicity and nymph production deterrence effect of five essential oils on adults of the cabbage aphid, *Brevicoryne brassicae* L. (Hemiptera: Aphididae). – Journal of Essential Oil Bearing Plants 19: 140-147. https://doi.org/10.1080/0972060X.2014.935032.
[24] Jan, M. T., Abbas, N., Shad, S. A., Rafiq, M., Saleem, M. A. (2015): Baseline susceptibility and resistance stability of Earias vittella Fabricius (Lepidoptera: Noctuidae) to cypermethrin, deltamethrin and spinosad. – Phytoparasitica 43(4): 577-582. https://doi.org/10.1007/s12600-015-0477-y.
[25] Kahan, A., Padín, S., Ricci, M., Ringuelet, J., Cerimele, E., Ré, S., Henning, C., Basso, I. (2008): Toxic activity of laurel essential oil and cineole on *Brevicoryne brassicae* L. over cabbage. – Revista de la Facultad de Ciencias Agrarias 40: 41-48.
[26] Kawuki, R. S., Agona, A., Nampala, P., Adipala, E. (2005): A comparison of effectiveness of plant-based and synthetic insecticides in the field management of pod and storage pests of cowpea. – Crop Protection 24(5): 473-478. https://doi.org/10.1016/j.cropro.2004.09.017.
[27] Kazem, M. G., El-Shereif, S. (2010): Toxic effect of capsicum and garlic xylene extracts in toxicity of boiled linseed oil formulations against some piercing sucking cotton pests. – American-Eurasian Journal of Agricultural and Environmental Science 8: 390-396.
[28] Khalid, A. (2015): Aphidicidal activity of different aqueous extracts of bitter apple *Citrullus colocynthis* (L.) against the bird cherry-oat aphid, *Rhopalosiphum padi* (L.) (Homoptera: Aphididae) under laboratory conditions. – Journal of Animal and Plant Sciences 25: 456-462.
[29] Khan, R. A. A., Ahmad, B., Ahmad, M., Ali, A., Naz, I., Fahim, M. (2019): Management of *Ralstonia solanacearum* (Smith) Yabuuchi wilt in tomato (*Solanum Lycopersicum* L.) with dried powder of the medicinal plant *Withania somnifera* (L.) Dunal. – Pakistan Journal of Botany. https://doi.org//10.30848/PJB2019-1(8).
[30] Khater, H. F. (2012): Prospects of botanical biopesticides in insect pest management. – Pharmacologia 3(12): 641-656. https://doi.org/10.5567/pharmacologia.2012.641.656.
[31] Kim, Y., Kim, J. (2004): Biological control of Aphis gossypii using barley banker plants in greenhouse grown oriental melon. – In: California Conference on Biological Control IV (Berkeley, CA: Center for Biological Control, College of Natural Resources, University of California), pp. 124-126.
[32] Koul, O., Singh, G., Singh, R., Singh, J. (2007): Mortality and reproductive performance of *Tribolium castaneum* exposed to anethole vapours at high temperature. – Biopesticides International 3: 126-137.
[33] Koul, O., Walia, S., Dhaliwal, G. (2008): Essential oils as green pesticides: potential and constraints. – Biopesticides International 4: 63-84.
[34] Lal, C., Verma, L. R. (2006): Use of certain bio-products for insect-pest control. – Indian Journal of Traditional Knowledge 1: 79-82.
[35] Lu, C., Chang, C.-H., Palmer, C., Zhao, M., Zhang, Q. (2018): Neonicotinoid residues in fruits and vegetables: An integrated dietary exposure assessment approach. – Environmental Science and Technology 52: 3175-3184. https://doi.org/10.1021/acs.est.7b05596.

http://www.aloki.hu ● ISSN 1589 1623 (Print) ● ISSN1785 0037 (Online)
DOI: http://dx.doi.org/10.15666/aeer/2003_23292342

[36] Machial, C. M. (2010): Efficacy of plant essential oils and detoxification mechanisms In: *Christoneura rosaceana*, *Trichopusia in*, *Dysaphis plantagainea*, and *Myzus persicae*. – Ph.D. Thesis, University of British Columbia, Vancouver, Canada.

[37] Maqsood, A., Qin, P., Zumin, G., Yuyang, L., Aatika, S., Dilbar, H., Ansar, J., Jamil, S., Mazher, F. I., Ran, A., Hongxia, G., Ying, D., Weijing, W., Yumeng, Z., Mingshan, J. (2020): Insecticidal activity and biochemical composition of *Citrullus colocynthis*, *Cannabis indica* and *Artemisia argyi* extracts against cabbage aphid (*Brevicoryne brassicae* L.). – Scientific Reports. https://doi.org/10.1038/s41598-019-57092-5.

[38] Najeeb, S., Ahmad, M., Khan, R., Naz, I., Ali, A., Alam, S. (2019): Management of bacterial wilt in tomato using dried powder of *Withania coagulans* (L.) Dunal. – Australasian Plant Pathology 48: 183-192. https://doi.org/10.1007/s13313-019-0618-8.

[39] Pascual-Villalobos, M. J., Cantó-Tejero, M., Vallejo, R., Guirao, P., Rodríguez-Rojo, S., Cocero, M. J. (2017): Use of nanoemulsions of plant essential oils as aphid repellents. – Industrial Crops and Products 110: 45-57. https://doi.org/10.1016/j.indcrop.2017.05.019.

[40] Pavela, R., Barnet, M., Kocourek, F. (2004): Effect of Azadirachtin applied systemically through roots of plants on the mortality, development and fecundity of the cabbage aphid (*Brevicoryne brassicae*). – Phytoparasitica 32(3): 286-294.

[41] Seenivasan, S., Jayakumar, M., Raja, N., Ignacimuthu, S. (2004): Effect of bitter apple, *Citrullus colocynthis* (L.) Schrad seed extracts against pulse beetle, Callosobruchus maculatus Fab. (Coleoptera: Bruchidae). – Entomon-Trivandrum 29: 81-84.

[42] Stumpf, N., Nauen, R. (2001): Cross-resistance, inheritance, and biochemistry of mitochondrial electron transport inhibitor-acaricide resistance in *Tetranychus urticae* (Acari: Tetranychidae). – Journal of Economic Entomology 94(6): 1577-1583. https://doi.org/10.1603/0022-0493-94.6.1577.

[43] Su, Y. P., Yang, C. J., Hua, H. X., Cai, W. L., Lin, Y. J. (2009): Bioactivities of ethanol extractsfrom thirteen plants against *Nilaparvata lugens* (Stal). – Chinese Agricultural Science Bulletin 25: 198-202.

[44] Tang, Y. Q., Weathersbee, A. A., Mayer, R. T. (2002): Effect of neem seed extract on the brown citrus aphid (Homoptera: Aphididae) and its parasitoid *Lysiphlebus testaceipes* (Hymenoptera: Aphidiidae). – Environmental Entomology 31(1): 172-176. https://doi.org/10.1603/0046-225X-31.1.172.

[45] Tomé, H. V. V., Martins, J. C., Corrêa, A. S., Galdino, T. V. S., Picanço, M. C., Guedes, R. N. C. (2013): Azadirachtin avoidance by larvae and adult females of the tomato leafminer *Tuta absoluta*. – Crop Protection 46: 63-69. https://doi.org/10.1016/j.cropro.2012.12.021.

[46] Torabi-Pour, H., Shayeghi, M., Vatandoost, H., Abai, M. R. (2017): Larvicidal effects and phytochemical evaluation of essential oils of *Trachyspermum ammi* and *Ziziphora clinopodioides* against larvae *Anopheles stephensi*. – Journal of Herbmed Pharmacology 6(4): 185-190.

[47] Ulrichs, C. H., Mews, I., Adhikart, S., Bhattacharya, A., Goswami, A. (2008): Antifeedant Activity and Toxicity of Leaf Extracts from Portesia coarctata Takeoka and Their Effects on the Physiology of Spodoptera littoralis (F.). – Journal of Pest Science 18: 79-84. https://doi.org/10.1007/s10340-007-0187-4.

[48] Umrao, R. S., Singh, S., Kumar, J., Singh, D., Singh, D. (2013): Efficacy of novel insecticides against shoot and fruit borer (*Earias vittella* Fabr.) in okra crop. – HortFlora Research Spectrum 2(3): 251-254.

[49] Van Driesche, R., Hoddle, M., Center, T. (2008): Control of Pests and Weeds by Natural Enemies: An Introduction to Biological Control. – Blackwell, Malden, MA, USA. 473p.

[50] Vekaria, M. V., Patel, G. M. (2000): Bioefficacy of botanicals and certain chemical insecticides and their combinations against the mustard aphid, *Lipaphis erysimi*. – Indian Journal of Entomology 62(2): 150-158.

[51] Vitousek, P. M., Mooney, H. A., Lubchenco, J., Melillo, J. M. (1997): Human domination of Earth's ecosystems. – Science 277: 494-499.

http://www.aloki.hu ● ISSN 1589 1623 (Print) ● ISSN1785 0037 (Online)
DOI: http://dx.doi.org/10.15666/aeer/2003_23292342

[52] Wagan, T. A., Wang, W., Hua, H., Cai, W. (2017): Chemical constituents and toxic, repellent, and oviposition-deterrent effects of ethanol-extracted *Myristica fragrans (Myristicaceae)* oil on *Bemisia tabaci (Hemiptera: Aleyrodidae).* – Florida Entomologist 100(3): 594-601. https://doi.org/10.1653/024.100.0317.

[53] Wagan, T. A., Cai, W., Hua, H. (2018): Repellency, toxicity, and anti-oviposition of essential oil of *Gardenia jasminoides* and its four major chemical components against whiteflies and mites. – Scientific Reports 8: 9375. https://doi.org/10.1038/s41598-018-27366-5.

[54] Wang, Z. G., Knudsen, G. R. (1993): Effect of *Beauveria bassiana* (Fungi: Hyphomycetes) on fecundity of the Russian wheat aphid (Homoptera: Aphididae). – Environmental Entomology 22(4): 874-878. https://doi.org/10.1093/ee/22.4.874.

[55] Zia, F. (2009): Effect of different neem products on the mortality and fitness of adult *Schistocerca gregaria* (Forskål). – Journal of King Abdulaziz University: Science 21: 299-315. https://doi.org/10.4197/Sci.21-2.8.

http://www.aloki.hu ● ISSN 1589 1623 (Print) ● ISSN1785 0037 (Online)
DOI: http://dx.doi.org/10.15666/aeer/2003_23292342

A REVIEW OF RESEARCH ON THE DEVELOPMENT AND EVOLUTION OF SCRUB DUNES

BA, Z. D. – DU, H. S.* – WANG, S. H.

Key Lab. of Remote Sensing of Ecological Environment in Jilin Province, Jilin Normal Univ., Siping 136000, China

**Corresponding author*
e-mail: duhs@jlnu.edu.cn; phone: +86-151-4466-1359

(Received 16th Nov 2021; accepted 25th Mar 2022)

Abstract. Scrub dunes are an important part of the landscape in arid and semi-arid regions, and their occurrence is a sign of land degradation and desertification. The fertile island effect is of great significance to curb the degradation of ecological functions and biodiversity conservation in arid and semi-arid regions. In recent decades, with the continuous development of desert science, a lot of research work has been carried out on the spatial distribution, morphological characteristics, formation conditions, dynamic processes; development patterns and evolution of scrub dunes, and fruitful results have been achieved. In future research, the spatial and temporal scope of the study should be further expanded to achieve a multi-angle, multi-scale and multi-dimensional comprehensive studies, so as to provide a scientific basis for the regional sand prevention and control method.
Keywords: *scrub dune, morphology pattern, dune formation, airflow pattern, dune evolution*

Introduction

Scrub dunes are a type of wind-deposited bio morphology formed by the accumulation of sandy material in and around scrub due to wind and sand flows are blocked by scrubs (Tengberg and Chen, 1998; Khalaf and Al-Awadhi, 2012), and a product of the proximal movement of sandy material under wind action (Khalaf et al., 1995; Langford, 2000). In addition to wind conditions (Bristow and Hill, 2020), sand sources and vegetation, the development of scrub dunes is also influenced by topography, precipitation and groundwater (Wang et al., 2010; Wang, 2003; Tengberg and Chen, 1998). Therefore, scrub dunes contain a wealth of information on regional environmental change. In most regions, scrub dunes with high vegetation cover (e.g., >14%) show little surface erosion even during the season of highest wind-sand activities (Kuriyama et al., 2005; Wiggs et al., 1995; Pye and Tsoar, 1990). Their internal deposition is relatively continuous from embryonic to mature development (Wang et al., 2006, 2008, 2010), and their unique developmental and sedimentary characteristics make it an ideal vehicle for studying wind-sand activities (Chen et al., 2019; Tsoar and Møller, 2020), Dry-Wet conditions, hydrological characteristics, and ecological environments and their evolution in arid and semi-arid regions. In addition, because of the close relationship with the dynamics of the Gobi, dry rivers and dry lake basins, the development process of scrub dune formation in arid and semi-arid regions also records the history of regional geomorphological evolution. In grassland reclamation areas, scrub dunes are the product of wind erosion of agricultural soils (Li et al., 2021), and their occurrence is a main characteristics of the occurrence of regional soil wind erosion and desertification (Li et al., 2014; Quets et al., 2013), and their development process is also related to the grassland reclamation process, which is one of the direct indicators of the degree of land desertification (Tengberg, 1995). Therefore, the study of the

http://www.aloki.hu ● ISSN 1589 1623 (Print) ● ISSN 1785 0037 (Online)
DOI: http://dx.doi.org/10.15666/aeer/2003_23432363

development of scrub dune formation and its relationship with environmental changes not only helps to improve the theory of aeolian geomorphology (Goudie, 2020; Cong et al., 2020) and desertification science, but also has important significance to enrich the research in the field of global change (Hermas et al., 2019).

Distribution and morphological characteristics of scrub dunes

Distribution of scrub dunes

Scrub dunes are widely developed in most arid semi-arid and sub-humid regions of the world along the leading edge of alluvial fans (dive level depth 1-3 m) (King et al., 2006; Wang et al., 2006; Parsons et al., 2003), degraded grasslands and agricultural lands, desert oasis transition regionals, agro-pastoral interface regions, desert margins and river banks that penetrate into the desert. It is also found in alluvial plains, lake basin depressions, dry deltas, along dry riverbeds (dive level depth 2-5 m) and some sandy coastal regions (Wu et al., 2006a, 2008; Qong et al., 2002; Dong, 2001), it is also found in alpine valleys, plateau basins and other alpine desert areas at altitudes of 4,000 to 5,000 m above sea level (Wu, 2003; Zhu, 1999), and even some arid and semi-arid desert areas where the negative effects of human activities (e.g. over-cultivation, overgrazing) are severe the only wind-deposited landscapes. These areas not only have good moisture and plant growth conditions (Wu et al., 2006a; Dong, 2020), but also have a large amount of erodible material, which provides favorable conditions for scrub dune development (Xia et al., 2005; Khalaf et al., 1995; Hesp, 1981). Scrub dunes are found in the southwestern United States (Seifert et al., 2009; Parsons et al., 2003; Langford, 2000; Rango et al., 2000), Africa (Dougill and Thomas, 2002; Tengberg and Chen, 1998; Tengberg, 1995; Nickling and Wolfe, 1994) and the Middle East (El-Bana et al., 2003; Khalaf et al., 1995; Warren, 1982), all of which are present on a large scale and cover approximately 5% of the global land area (*Fig. 1*) (Thomas et al., 2005).

Figure 1. *The top view of shrub dunes in Songnen Sandy Land, Jilin Province, China*

http://www.aloki.hu ● ISSN 1589 1623 (Print) ● ISSN 1785 0037 (Online)
DOI: http://dx.doi.org/10.15666/aeer/2003_23432363

Morphological characteristics of scrub dunes

Scrub dunes can be isolated and scattered, or clustered in groups, probably related to the type of scrub, for example, *Tamarisk chinensi* is more isolated (Kang et al., 2019; Du et al., 2007), while Nitraria retusa is mostly clustered in groups (Zhang et al., 2018). The typical form of scrub dune is a raised sandbag with a rounded top and gentle slope (Yeh et al., 2020; Cowling et al., 2019), which can be broadly classified into conical, hemispherical and dome-shaped except for the early shield-shaped and late irregular forms. The draped, less branched and densely planted thickets often form taller cone-like dunes, while the prostrate, less branched and less densely planted ones often form relatively short hemispherical or dome-like dunes (Hesp, 1981). For example, on the southern coast of South Africa, Gazania rigens and Arctotheca populifolia form conical and hemispherical scrub dunes respectively (Hesp and Mclachlan, 2000); on the northern coast of Kuwait, Scrub dunes such as Nitraria retusa and Suaeda vermiculata are commonly dome shaped morphologically (Khalaf et al., 2014, 1995); in the Tarim Basin, Tamarisk chinensis scrub dunes are hemispherical in morphology, while reed and camel thorn scrub dunes are semi-ellipsoidal (Wu et al., 2008). In addition, scrub dunes have different morphologies at different developmental stages. For example, Zhu Zhenda and Chen Guangting (1994) showed that under a single wind direction, the morphology of scrub dunes undergoes four stages: Straight sand bars — isosceles triangular sand spout — the profile is a streamlined, ovoid mound of sand — nearly circular or oval mound of sand. The height of scrub dunes is mainly influenced by the evolutionary stage, vegetation type, sand source abundance and water supply and demand balance (Wang et al., 2010; Tengberg and Chen, 1998; Rhodes and Pownall, 1994), such as 0.4-1.8 m for scrub dunes formed by Caragana microphylla, 0.13-4.5 m for those formed by Nitraria retusa, and Tamarisk chinensis forms 1 to 15 m (Du et al., 2010; Hermas et al., 2019), mainly related to its clump canopy height (*Fig. 2*) (Khalaf et al., 1995).

Figure 2. *Nitraria shrub dunes*

http://www.aloki.hu ● ISSN 1589 1623 (Print) ● ISSN 1785 0037 (Online)
DOI: http://dx.doi.org/10.15666/aeer/2003_23432363

Conditions and dynamical processes in the formation of scrub dunes

Conditions for the formation of scrub dunes

Vegetation, wind conditions and sand sources are key factors in the development and morphological evolution of scrub dunes (Taminskas et al., 2020; Molina et al., 2020), scrub vegetation is the primary condition for their formation, the presence of upwind sand sources is the physical condition for their formation, and strong winds are the dynamic condition for their formation (Hesp, 1981; Zhao et al., 2020). However, it should be noted that if wind strength and frequency are both sufficient (Fitoka, 2020; Li, 2009), the area of scrub dune formation must have both good moisture conditions for scrub development and a dry surface to ensure the supply of sand (Feng et al., 2021),which obviously constitute a contradiction between these two conditions, resulting in many areas of vigorous scrub growth not being able to form scrub dunes due to lack of sand sources, while areas with sufficient sand sources cannot grow scrub due to moisture limitation (Hilgendorf et al., 2021; Pan et al., 2019). The ability of a region to form scrub dunes depends on the dynamic balance between moisture conditions and sand source availability in the region (Dougill and Thomas, 2002; Hesp and Smyth, 2017). Therefore, scrub dunes in semi-arid areas only form in areas where moisture conditions and sand supply can easily reach a dynamic equilibrium (Li et al., 2020), such as desert oasis transition regions, desert margins, river banks, floodplains, Lake Basin depressions, dry riverbed shores, and degraded grasslands. In addition, a variety of scrubs in arid and semi-arid areas can trap sand material to form scrub dunes, such as Caragana microphylla (Ding et al., 2019), Nitraria retusa, Tamarisk chinensis, Artemisia ordosica and Achnatherum splendens, etc. However, there are significant differences in their height, canopy morphology and scale, and these factors also play a key role in controlling the development of scrub dunes formed around them (Yao et al., 2021), and the morphology of dunes varies among different scrubs (Ma and Lu, 2019). The flexibility and density of scrub branches are closely related to the morphology of scrub dunes (Zhao et al., 2019), for example, scrub with upright branches and high branch density tends to form conical dunes, while scrub with soft branches and low density tends to form hemispherical dunes (Gunn, 2021; Wu et al., 2009).

Dynamical processes of scrub dune formation

Regional wind-sand activities are the driving force behind the formation of scrub dunes. On the one hand, wind-sand activities enable material to be transported and deposited on the surface of scrub dunes; on the other hand, under the influence of micro-geomorphology, the near-surface air flow accelerates, the ability of air flow to carry sand material increases, and the surface erosion intensifies. It causes local activation of scrub dunes (Acosta et al., 2021; Wang et al., 2021). A combination of domestic and international wind tunnel and field experiments (Pakari and Ghani, 2019; Zhong et al., 2021), the dynamics mechanism of scrub dune formation can be briefly described as follows: after the development of scrub in the field, the wind speed is still high in a certain range in front and on both sides of it (Miri et al., 2021; Pei and Pang, 2020), although it is a deceleration regional of airflow, which shows slight wind erosion, and a certain range above it is an acceleration regional of airflow, and a certain range behind it is a weak vortex regional and an obvious deceleration regional of airflow (Gillies et al., 2014; Cornelis and Gabriels, 2005); the wind-sand flow over and through the scrub rapidly shifts from unsaturated to saturated, and sand material begins

http://www.aloki.hu ● ISSN 1589 1623 (Print) ● ISSN 1785 0037 (Online)
DOI: http://dx.doi.org/10.15666/aeer/2003_23432363

to be deposited, gradually forming a fledgling wind-shadowed dune trailing a long tail; as the amount of sand material deposited increases, the fully permeable scrub changes to a lower impermeable scrub dune (Zhang et al., 2013; Abbate et al., 2019; Gong et al., 2021), and the scrub increases the roughness of the dune surface (Wang et al., 2020). The top of the exposed dune eliminates the area of strong wind erosion that is common on top of the dune, and its dense bottom and sparse top structure also reduces the extent of the airflow deceleration zone on the leeward slope and significantly decelerates the airflow on the windward slope and sides, resulting in a shortening of the length of the dune in the windward direction and an increase in height and width on both sides, which eventually evolves into a vertical projection with an elliptical or sub-circular shape (*Table 1*) (Zhang et al., 2013; Marzialetti et al., 2019).

Table 1. *Morphology, soil and vegetation status of the scrub dunes at different stages of development*

Developmental stage	Morphology	Soil	Vegetation status
Increases	Conical or hemispherical, with good correlation of morphological parameters	The surface is predominantly fluvial, with no crust or a small distribution	Higher vegetation cover and better growth on scrub dunes, less scrub dieback on dunes; lower vegetation cover and poorer growth on interdune sites
Stabilise	Conical or hemispherical, with good correlation of morphological parameters	The surface is predominantly clean skinned, without or with a small distribution of fluvial sand	High vegetation cover and good growth on both scrub dunes and interdunes, with less scrub dieback on dunes
Degeneration	Hemispherical or with wind erosion collapse, morphological parameters poorly correlated	The surface is predominantly fluvial, with no crust or a small distribution	Low vegetation cover and poor growth on both scrub dunes and interdunes, with more dead scrub on the dunes

Patterns of scrub dune development and succession processes

Patterns of scrub development

Under dry and windy conditions, the sand flow is blocked by shrubs and sand material is deposited in the shrubs and scrub downwind (Yang et al., 2019), forming sand bars, and with continued wind action and continued deposition of sandy material, the length of the sand bars shortens and the tails merge, forming a dawn scrub dune, or wind shadow dune (Xia et al., 2004a). When the height of dune increases, low scrub is formed downwind and around the dune, which increases the vegetation cover and is more conducive to reducing wind erosion and intercepting wind and sand flow. When the dune height increases excessively, the scrub roots die because they cannot reach the water table (Miao et al., 2022; Mahmoud et al., 2020; Wang et al., 2010), the plant stems break due to wind action, the root system loses adhesion, the dune starts to activate, the windward slope blows and the leeward slope piles up, and with the continuous action of wind, the scrub dune all blows and turns into drifting sand land, and the scrub dune dies out (Qong et al., 2002; Du et al., 2007). Therefore, scholars

http://www.aloki.hu ● ISSN 1589 1623 (Print) ● ISSN 1785 0037 (Online)
DOI: http://dx.doi.org/10.15666/aeer/2003_23432363

mostly summarize the process into three stages: growth, stabilization and decline. In addition, scrub dunes can also be in a stable state when the wind is weakened and dust cannot be raised, but scrub dunes in a stable state may grow again after changes in sand sources and wind (Conery et al., 2020; Wang et al., 2015); when sand sources are reduced or even depleted, the water table drops or the scrub dies, scrub dunes suffer strong erosion, the height gradually decreases, the horizontal scale continues to increase, and the whole dune gradually tends to die out (Wang et al., 2010; Molina et al., 2020). The process of scrub dune erosion is a kind of ecological geomorphological process, and its various aspects are intertwined with a series of ecological processes of plant growth, death and dune morph dynamic processes, as well as the dynamic response and feedback between them (Tang et al., 2008).

Scrub succession process

Arid and semi-arid scrub is divided into primary scrub and secondary scrub. Primary scrub has developed a complete mechanism to adapt to local habitats during long-term evolution (Huang et al., 2010), it is mainly distributed in typical grassland and mixed agro-pastoral areas with low water table and relatively poor moisture conditions, and in arid desert areas with high water table and relatively good moisture conditions (Provoost and Declerck, 2020). There are two opposite processes of succession in secondary scrub. The first is due to deterioration of regional moisture conditions, where herbaceous growth is stunted while shrubs win in competition due to deeper root systems, called grassland scrubification (Harte et al., 2015; Sulub-Tun et al., 2020), and is a common phenomenon in arid and semi-arid grasslands. The process involves scrub developing mainly in degraded areas of grasslands with low water tables and relatively poor moisture conditions, and will decline when moisture conditions deteriorate to the point where the minimum requirements needed for shrub growth cannot be met. The second is that in some severely degraded vegetation areas, when moisture conditions improve, scrub develops before herbaceous plants due to better adaptation (Zhao et al., 2009a). In this process, scrub is mainly located in regionals with high water table and relatively good moisture conditions. When moisture conditions continue to improve, herbaceous plants recover and scrub declines due to competition with herbaceous plants (*Fig. 3*) (Zhao et al., 2009b; Rafi et al., 2019).

Construction of the scrub dune chronological sequence and dating of formation

Construction of a chronological sequence of scrub dunes

The chronological sequence of scrub dunes can be determined from the chronology of their vertical profiles (Yang et al., 2019), which is a prerequisite for revealing the developmental process of their formation. Currently, the chronology of scrub dunes is mainly based on grain layer counting (Zhao et al., 2011; Xia et al., 2004b), Accelerator Mass Spectrometric (AMS).14C (Weems and Monger, 2012) and Optically Stimulated Luminescence (OSL). Stimulated Luminescence (OSL) (Forman and Pierson, 2003), dating methods, with varying applicability and advantages and disadvantages (*Table 1*). Although scrub dunes are of relatively short age (1-3 years), the use of OSL dating can enable the establishment of chronological sequences under certain conditions (Ballarini et al., 2003; Bailey et al., 2001). OSL dating is inevitably inaccurate in some areas because scrub dune sediments originate mainly from adjacent areas, are transported over short

http://www.aloki.hu ● ISSN 1589 1623 (Print) ● ISSN 1785 0037 (Online)
DOI: http://dx.doi.org/10.15666/aeer/2003_23432363

distances (Khalaf et al., 1995; Farrell and Connolly, 2021), do not necessarily receive sufficient light recession, and quartz brightness varies from place to place (Hanson et al., 2009; Rhodes and Pownall, 1994). However, for most scrub dunes, the buried annual leaf litter within the sediment provides excellent material for AMS14C dating, and the chronological sequences thus established are relatively accurate (Weems and Monger, 2012; Wang et al., 2008, 2010). However, on some occasions, due to factors such as species differences or poor preservation, material ideal for AMS14C dating does not exist in some dunes (Sun et al., 2019, 2020). Therefore, a more appropriate dating method, or a combination of different methods, should be used to establish a credible chronological sequence, depending on regional realities (*Table 2*) (Barsanti et al., 2020).

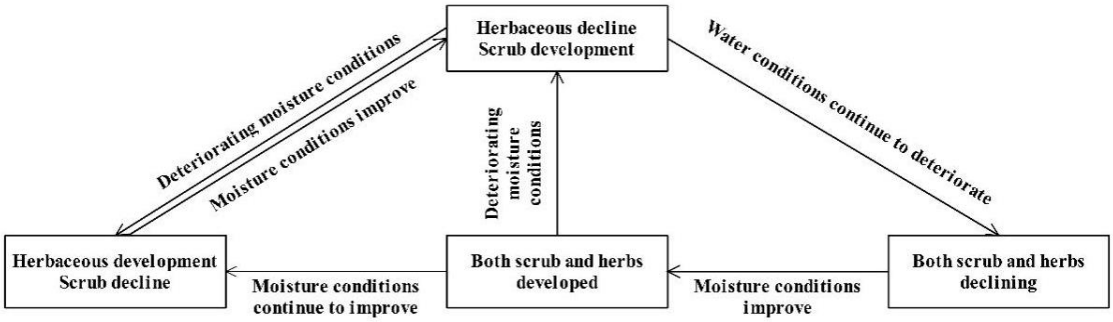

Figure 3. *Scrub succession in arid and semi-arid zones*

Table 2. *Comparison of different dating methods for scrub dunes*

Evaluation	Method		
	Layer count	**AMS^{14}C**	**OSL**
Strengths	Simple and relatively accurate dating method	Smaller error, suitable for short timescale dating	Applicable to the dating of wind-formed deposits
Deficiencies	Blurred boundaries or missing layers affect the dating accuracy, and layers are rare	Organic residue burial has limitations	Large errors in some samples and relatively low dating accuracy

In the scrub dunes, wind-generated sand accumulates in spring and dead leaves in autumn, and there is a theoretical wind-generated sand-dead leaves interaction layer in the dunes with an accuracy of up to years (Chojnacki et al., 2020). These clear chronological layers are similar to tree chronologies, lake sediment layers, etc., allowing chronological sequences to be accurate to the year (Wu et al., 2019; Kiani et al., 2021). However, the presence of striated layers has only been found in tamarisk scrub sands in the Taklamakan Desert and Lop nor in China (Wang et al., 2015; Xia et al., 2005; Jiang and Yang, 2019), and has not been reported in other regions of the world or in other types of scrub sands. The exact conditions for the existence of this layer need further study.

Dating the formation of scrub dunes

In addition to dating methods such as grain layer counts, AMS^{14}C and OSL, recent studies have found that in polar, alpine and desert areas lacking tree distribution, some shrub species and even perennial herbs have recognizable annual rings and formation

http://www.aloki.hu ● ISSN 1589 1623 (Print) ● ISSN 1785 0037 (Online)
DOI: http://dx.doi.org/10.15666/aeer/2003_23432363

patterns that can be used to determine population age structure and reconstruct regional high-resolution climate and environmental evolution histories (Lan et al., 2021; Xiao et al., 2014; Liang and Eckstein, 2009; Yeh et al., 2020). The age of scrub dune formation varies considerably between regions (*Table 2*), which may be due to the different sensitivity of environmental evolution to global climate change in different regions on the one hand, and to regional factors influencing environmental evolution on the other. It was found that several red willow scrub dunes in the Lop Nor region in the growth phase were formed more than 100 years ago (Zhao et al., 2011; Xia et al., 2005, 2004b), However, the two tamarisk scrub dunes on the Alashan Plateau (Hu et al., 2019; Xie and Steinberger, 2005), which are in a growth phase and 800 m apart, are about 200 years apart in age (Wang et al., 2010, 2008), and the relict scrub dunes in the south-central United States are 2400-700 years old (Gillies et al., 2014; Seifert et al., 2009), suggesting that clusters of scrub dunes in the same area may have formed simultaneously or slowly and gradually (*Table 3*).

Table 3. *Age and environment of scrub sand dune formation in arid and semi-arid zones*

Study area	Formative era	Method of fixing the year	Forming the environment	Number of sand dunes	References
South Central USA	2400-700 years	OSL	Climate drought	4	Gillies et al., 2014; Seifert et al., 2009
Chihuahuan Desert, USA	About 1100 years ago	AMSC	Climate drought	1	Weems and Monger, 2012
Southern Taklamakan Desert	200 to 450 years	AMSC	—	3	Zhao et al., 2016
Lop Nor on the south-eastern edge of the Mongolian Plateau	700 to 60 years	OSL	Deteriorating water conditions	4	Wang et al., 2006
	About 100 years ago	layer count	—	1	Xia et al., 2004a, 2005
Mopti region West Africa	—	—	Farming, grazing, Climate drought	—	Nickling and Wolfe, 1994
Western Sahel region	About 50 years ago	Satellite images, field surveys	Climate drought	—	Tengberg, 1995

Environmental significance of sediment indications from scrub dunes

Environmental significance of sediment grain size characteristics indications

Some progress has been made in research on the particle size characteristics of sediments from scrub dunes (*Table 3*). A number of studies have indicated that particle size variations effectively document the evolution of regional physical sources and/or the wind-sand environment. For example, in the northern foothills of the Yinshan Mountains, changes in the content of particle size fractions larger than 500 μm reveal the evolutionary history of the regional wind and sand environment (Wang et al., 2006). On the Alashan Plateau, when the scrub dunes develop to a certain height, the particle size fraction of the material source stabilises and the change in particle size reveals the evolution of the regional surface from arable land and dry riverbed to the Gobi (Wang et al., 2008; Qin et

http://www.aloki.hu ● ISSN 1589 1623 (Print) ● ISSN 1785 0037 (Online)
DOI: http://dx.doi.org/10.15666/aeer/2003_23432363

al., 2015). In general, changes in the content of the fine-grained fraction (<10 μm) of the sediment record changes in the source, while changes in the content of the coarse-grained fraction (>100 μm) are indicative of changes in the intensity of regional wind and sand activity (Wang et al., 2010; Liu et al., 2009). In the Lop nor region, given the similarity of sediment grain size frequency curves and probabilistic accumulation curves between sediment layers within the dunes, some scholars have suggested that there is relative consistency in the regional depositional environment over time, but that changes in coarse sand content and median grain size reflect changes in the strength of depositional dynamics (Zhao et al., 2009a; Zhang et al., 2011). In the south-central USA, the grain size characteristics of sediment from different orientations of scrub dunes are indicative of regional palaeowind changes (Seifert et al., 2009; Zhang et al., 2008). Grain size is sometimes used as a secondary indicator in characterizing regional climatic dry or wet variability, and chalky clay layers in wind-deposited profiles rich in organic residues of tamarisk in the Lobos' region can help to reveal relatively wet regional climatic conditions during the Little Ice Age (*Table 4*) (Liu et al., 2011).

Table 4. *Indication of grain size and δ13C of organic residues in sediments from different areas of scrub dunes*

Research area	Particle size targets	Indicative meaning	$\delta^{13}C$ Indicator Signification	Country
Tarim Basin[a] (Xia et al., 2005)	—	—	Atmospheric CO_2 concentration and changes in climate cold/warm, dry/wet	China, Xinjiang Uygur Autonomous Region
Tarim Basin[a] (Zhao et al., 2009)	Coarser sand content and median grain size	Variation in the strength of sedimentation dynamics	—	China, Xinjiang Uygur Autonomous Region
Tarim Basin[a] (Liu et al., 2011)	Silt layer clay layer	Combining $\delta^{13}C$ indicators of climate change	Changes in dry/wet climate	China, Xinjiang Uygur Autonomous Region
Alaska Plateau[a] (Wang et al., 2008)	Content of fine particles less than 16 μm and coarse particles greater than 200 μm	Wind power changes	—	USA, State of Alaska
Alaska Plateau[a] (Wang et al., 2008)	Less than 10 μm fine particles Greater than 100 μm coarse particle fraction content	Variation in physical sources and intensity of wind and sand activity	Changes in regional moisture conditions	USA, State of Alaska
Yinshan Mountains[b] (Wang et al., 2008)	Content of particle fractions larger than 500 μm	Wind power changes	—	China, Inner Mongolia Autonomous Region
Arkansas, USA[c] (Seifert et al., 2009)	Greater than 63 μm less than 2000 μm sand fraction content	Ancient wind direction change	—	USA, Arkansas

[a]*Tamarix chinesis*
[b]*Caragana microphylla*
[c]Indeterminate scrub dune

http://www.aloki.hu ● ISSN 1589 1623 (Print) ● ISSN 1785 0037 (Online)
DOI: http://dx.doi.org/10.15666/aeer/2003_23432363

In general, grain size characteristics are a valid proxy in the use of scrub dune sediments as indicators of environmental change, but also in the context of the regional environment and the specific evolution of the dunes. For example, during the development of the dunes, there is some change in the physical source during wind and sand activity as well as environmental changes (e.g. changes in water table and vegetation cover), and this should be fully taken into account in inversion studies of regional environmental evolution. In addition, as scrub dunes continue to develop and increase in height, the ability of coarse-grained fractions to be transported to the top of the dunes by leapfrogging, etc., gradually decreases (Dong et al., 2005; Lancaster, 1995; Anderson, 1991; White et al., 1976; Bagnold, 1941), which leads to a decrease in the amount of coarse-grained fraction transported to the top of the dunes from the This has resulted in a gradual reduction in sediment grain size from the early stages of formation to the mature stages of development, although regional wind and sand activity has not diminished, or even intensified.

Environmental significance of sediment total organic carbon content, total nitrogen content and carbon to nitrogen ratio value indications

The plant communities in arid and semi-arid zones are relatively simple and have low productivity, while the vegetation that builds scrub dunes and their well-developed root systems provide good conditions for organic matter and Nitrogen (N) storage (Zhang et al., 2011; Cakan and Cigdem, 2006; Day and Ludeke, 1993) and can be used to reflect regional vegetation development history through changes in Total Organic Carbon (TOC) and Total Nitrogen (TN) content in wind-sand accumulations (Zuo et al., 2010; Li et al., 2008). For example, in the northern Sinai Peninsula (Zuo et al., 2010; Li et al., 2008), the TOC and TN contents of the wind and sand accumulation can be used to invert the vegetation development history of the region. For example, in the northern Sinai Peninsula (Egypt), the high organic matter content in the wind-sand layer reflects good regional vegetation development, favorable moisture conditions and low temperatures (El-Bana et al., 2003; Zhang, 2019). In the northern foothills of the Yin Mountains, a comparison of TOC, TN, P_2O_5 and K_2O contents in scrub dune sediments, undisturbed soils and cultivated land was used to invert the history of regional land degradation and scrub dune development (Wang et al., 2006; Liu et al., 2008). In the northern Negev Desert (Israel), the nitrogen content of the surface 0-10 cm sediment of different scrub dunes reveals changes in soil moisture conditions (Zhang et al., 2015), while dissolved organic carbon reveals changes in temperature and shows that the total organic matter content of the scrub dune sediment is relatively stable under different temperature and moisture conditions (Xie and Steinberger, 2005; Foth, 1990). Some scholars have also pointed out that changes in TOC content, TN content and Carbon to nitrogen ratio (C/N) values of tamarisk scrub dunes in the Lop nor region are mainly controlled by changes in atmospheric CO_2 concentration, but also reflect regional climate changes in cold/warm, dry/wet (Zhao et al., 2011; Xia et al., 2005). In fact, although the Chrono sequence of the scrub dunes in this region is relatively accurate, changes in TOC content, TN content and C/N values are not in good agreement with the instrumental temperature and precipitation measured by neighboring weather stations (Zhao et al., 2016). For example, changes in TOC content and temperature are opposite to each other, and changes in TN content and precipitation are opposite to each other, which have not been adequately and reasonably explained. Therefore, the

http://www.aloki.hu ● ISSN 1589 1623 (Print) ● ISSN 1785 0037 (Online)
DOI: http://dx.doi.org/10.15666/aeer/2003_23432363

environmental significance of the TOC content, TN content and C/N values of the scrub dunes needs to be further explored.

The interrelation of influencing factors of shrub dune development

Reciprocal feedbacks of scrub dunes and vegetation

The interaction between wind-sand activities and vegetation is mainly reflected in two aspects: firstly, the modification and control of near-surface wind-sand activities by vegetation, which is manifested in the construction of landscape formation and the control of its morphological evolution in plant-based wind and sand landscape types (Telfer et al., 2020); secondly, the response process of vegetation to wind-sand activities, which is mainly manifested in the distribution pattern of vegetation and the response of vegetation succession to it (Wu et al., 2006a, b). The sand-blocking ability of plants is the result of the joint action of the above-ground part of plants (height, canopy, stems and leaves, etc.) and the below-ground part (root system), which can increase the surface roughness and change the structure of the near-ground airflow field, thus playing a key role in the sand-blocking of plants (Gao et al., 2015); the below-ground part of plants keeps water and soil, accumulates nutrients, and changes soil physical and chemical properties through the long-term interaction with soil and soil microorganisms, which contributes to plant growth and evolution (Zhang et al, 2021). The subsurface part of plants, through long-term interaction with soil and soil microorganisms, retains water and soil, accumulates nutrients, and changes soil physical and chemical properties (Doniger et al., 2020), providing good conditions for plant growth and succession and sand retention (Zhang, 2019; Lopez et al., 2020), while the improvement of soil properties in sand dunes also affects plant growth and distribution patterns (Tengberg, 1995; Leenders et al., 2007). Under certain environmental conditions, sand material continues to be deposited with the developmental succession of vegetation, and wind shadow dunes gradually evolve into scrub dunes (Conery et al., 2020). Dune morphology and depositional structure are influenced by vegetation type and morphology, while wind speed, blowing time, plant height and crown width, and sidelight area also influence the dune development process (Zuo et al., 2018; Zhao et al., 2021).

Reciprocal feedbacks of scrub dunes with vegetation and soils

There is a positive feedback between shrubs and soil heterogeneity (He et al., 2021; Hou et al., 2019), which is related to shrubs changing soil physicochemical properties through their own physiological activities, decomposition of decaying dead branches and leaves, and root activities (Wang et al., 2020); scrub canopy width is positively correlated with fine, very fine, and chalky sand in the soil, but canopy height has little effect on the percent content of sand grain size; the soil particle composition of scrub dunes is dominated by fine sand content, and The trend of soil water content changes in different parts was consistent; the nutrient content of the scrub soil was significantly higher than that of the inter dune site, thus verifying that scrub affects soil water, redistribution of nutrients and enhances soil heterogeneity (Wang et al., 2015). On the other hand, changes in soil properties of sand dunes also affect the survival, growth and distribution patterns of vegetation (El-Bana et al., 2003). Therefore, scrub dune is a dynamic bio morphology that changes over time, and the plant growth, soil

http://www.aloki.hu ● ISSN 1589 1623 (Print) ● ISSN 1785 0037 (Online)
DOI: http://dx.doi.org/10.15666/aeer/2003_23432363

physicochemical properties and biodiversity of scrub dune and inter dune sites change accordingly with their formation (He and Zhao, 2004), development and decline processes, and when extended to the regional spatial scale, the regional landscape and ecosystem change with the development and morphological evolution of scrub dune (Marrero-Rodríguez et al., 2020).

The role of scrub dune development on the ecology

Scrub is divided into primary scrub and secondary scrub. Primary scrub has developed a well-developed mechanism to adapt to local habitats over a long period of evolution, and it is mainly distributed in typical grassland and agro-pastoral areas where the water table is low and moisture conditions are relatively poor (El-Sheikn et al., 2010). Secondary scrub, on the other hand, is mainly distributed in arid desert areas where the water table is high and moisture conditions are relatively good (Qiu et al., 2015; Tyler et al., 2021). There are two opposing processes of succession in secondary scrub with important ecological impacts (Yan et al., 2019). The first is caused by the deterioration of regional moisture conditions, where herbaceous growth is stunted while shrubs win in competition due to deeper root systems, and is called grassland scrubbing, and a common phenomenon in arid and semi-arid grasslands (Cai et al., 2020). In this process, scrub mainly develops in degraded grassland areas with low water table and relatively poor moisture conditions, and will decline when moisture conditions deteriorate to the point where the minimum requirements for shrub growth cannot be met; the second is in some severely degraded vegetation areas, and when moisture conditions improve, scrub develops before herbaceous plants because it is more adaptable. In this process, scrub is mainly located in areas with high water tables and relatively good moisture conditions, and when moisture conditions continue to improve, herbaceous plants recover and scrub declines due to competition with herbaceous plants (Jia and Li, 2008; Kinast et al., 2013). In any case, when the dominance of scrub declines, herbaceous plants increase species diversity (Sperandii et al., 2019), especially during the decline of scrub, herbaceous plants lack shelter and community diversity declines, and scrub communities tend to decline; soils show an increase in the average particle size of sediment, a trend of decreasing clay and powder particles, an increase and then decrease in the specific gravity of fine sand, and a continuous increase in the content of coarse sand particles; soil capacity increases, water content, soil respiration decreases The organic matter, total N, and pH increased and then decreased (Bo and Zheng, 2015). In general, due to the large amount of wind and sand materials stored in the cluster scrub dunes, they play a protective role for the stability of the surface they are on, especially for the oasis on the downwind side from drifting sand invasion, and are of great importance for the protection of deserts and oases and the enhancement of desert ecosystem services (Mou, 2019).

Conclusion

The development or retention of well-adapted scrub in arid and semi-arid areas is the primary condition for the formation of scrub dunes, the presence of upwind sand sources is the physical condition for their formation, and strong wind is the dynamic condition for their formation, where the role of wind is to connect the sand sources to the scrub.

http://www.aloki.hu ● ISSN 1589 1623 (Print) ● ISSN 1785 0037 (Online)
DOI: http://dx.doi.org/10.15666/aeer/2003_23432363

When regional moisture conditions deteriorate, herbaceous plants decline and scrub develops, and when moisture conditions deteriorate to a certain extent, regional moisture conditions and sand supply reach a dynamic equilibrium, and wind strength and frequency are sufficient, scrub dunes gradually form. In the early stage of scrub development, when the regional moisture conditions and sand supply are in dynamic equilibrium, scrub and scrub dunes may appear simultaneously, and if they are not in dynamic equilibrium, the time of scrub dune development depends on the time of formation of this dynamic equilibrium.

At present, scholars mostly focus on static research on scrub dunes, but in fact scrub dunes are dynamic bio morphological features that change with time. The plant growth, soil physical and chemical properties and biodiversity of scrub dunes change with the process of their formation, development and decline, and when extended to the regional spatial scale, the regional landscape and ecosystem change with the development and morphological evolution of scrub dunes. Therefore, there is an urgent need for a multidisciplinary and comprehensive study to reveal the mechanism of the geomorphological process of scrub dune development.

Acknowledgments. This study was supported by National Natural Science Foundation of China (No. 41871022).

REFERENCES

[1] Abbate, A., Campbell, J. W., Kimmel, C. B., Kern, W. H. (2019): Urban development decreases bee abundance and diversity within coastal dune systems. – Global Ecology and Conservation 20: e00711.

[2] Acosta, A. T. R. (2021): Coastal dune vegetation zonation in Italy: squeezed between environmental drivers and threats. – Tools for Landscape-Scale Geobotany and Conservation 315-326.

[3] Anderson, R. S. (1991): Wind modification and bed response during saltation of sand in air. – ActaMechanica l: 21-51.

[4] Bagnold, R. A. (1941): The Physics of Blown Sand and Desert Dunes. – Methuen, London.

[5] Bailey, S. D., Wintle, A. G., Duller, G. A. T., Bristow, C. S. (2001): Sand deposition during the last millennium at Aberffraw, Anglesey, North Wales as determined by OSL dating of quartz. – Quaternary Science Reviews 20(5-9): 701-704.

[6] Ballarini, M., Wallinga, J., Murray, A. S., Heteren, V., Oost, A. P., Bos, A. J. J., Eijk, C. W. E. V. (2003): Optical dating of young coastal dunes on a decadal time scale. – Quaternary Science Reviews 22(10): 1011-1017.

[7] Barsanti, M., Garcia-Tenorio, R., Schirone, A., Barsanti, M., Garcia-Tenorio, R., Schirone, A., Rozmaric, M., Ruiz-Fernández, A. C., Sanchez-Cabeza, J. A., Delbono, I., Conte, F., De Oliveira Godoy, J. M., Heijnis, H., Eriksson, M., Hatje, V., Laissaoui, A., Nguyen, H. Q., Okuku, E., Al-Rousan, Saber, A., Uddin, S., Yii, M. W., Osvath, I. (2020): Challenges and limitations of the 210Pb sediment dating method: results from an IAEA modelling interlaboratory comparison exercise. – Quaternary Geochronology 59: 101093.

[8] Bo, T. L., Zheng, X. J. (2015): A new expression describing the migration of aeolian dunes. – Catena 118(7): 1-8.

[9] Bristow, C. S., Hill, N. (2020): Dune Morphology and Palaeowinds from Aeolian Sandstones in the Miocene Shuwaihat Formation, Abudhabi, United Arab Emirates. – In:

http://www.aloki.hu ● ISSN 1589 1623 (Print) ● ISSN 1785 0037 (Online)
DOI: http://dx.doi.org/10.15666/aeer/2003_23432363

Alsharahan, A. S. et al. (eds.) Quaternary Deserts and Climatic Change. CRC Press, Boca Raton, FL, pp. 553-564.

[10] Cai, Y., Yan, Y., Xu, D., Xu, X., Wang, C., Wang, X., Chen, J., Xin, X. P., Eldridge, D. J. (2020): The fertile island effect collapses under extreme overgrazing: evidence from shrub-encroached grassland. – Plant and Soil 448: 201-212.

[11] Cakan, H., Cigdem, K. (2006): Interactions between mycorrhizal colonization and plant life forms along the successional gradient of coastal sand dunes in the eastern Mediterranean, Turkey. – Ecological Research 21(2): 301-310.

[12] Chen, F. H., Fu, B. J., Xia, J., Wu, D., Wu, S. H., Zhang, Y. L., Sun, H., Liu, Y., Fang, X. M., Qin, B. Q. (2019): Important progress and prospects of basic research on physical geography and living environment in China in the past 70 years. – Scientia Sinica (Terrae) 49(11): 1659-1696.

[13] Chojnacki, M., Fenton, L. K., Weintraub, A. R., Edgar, L. A., Jodhpurkar, M. J., Edwards, C. S. (2020): Ancient Martian aeolian sand dune deposits recorded in the stratigraphy of Valles Marineris and implications for past climates. – Journal of Geophysical Research: Planets 125(9): e2020JE006510.

[14] Conery, I., Brodie, K., Spore, N., Walsh, J. (2020): Terrestrial LiDAR monitoring of coastal foredune evolution in managed and unmanaged systems. – Earth Surface Processes and Landforms 45(4): 877-892.

[15] Cornelis, W. M., Gabriels, D. (2005): Optimal windbreak design for wind-erosion control. – Journal of Arid Environments 61(2): 315-332.

[16] Cowling, R. M., Logie, C., Brady, J., Middleton, M., Grobler, B. (2019): Taxonomic, biological and geographical traits of species in a coastal dune flora in the southeastern cape floristic region: regional and global comparisons. – PeerJ 7: e7336.

[17] Day, A. D., Ludeke, K. L. (1993): Plant Nutrients in Desert Environments. – Springer, Berlin.

[18] Ding, X. F., Hao, G., Dong, K., Wang, Y. K., Gao, S. B., Chen, L., He, X. D., Zhao, N. X., Gao, Y. B. (2019): Effects of flat stubble treatment on the spatial pattern of plant communities in Caraganamicrophylla scrub neighbors. – ActaEcologicaSinica 9(11).

[19] Dong, Y. X. (2001): Research on the formation and evolution of coastal dunes in foreign countries. – Marine Geology and Quaternary Geology 21: 93-98.

[20] Dong, Z. B., Lu, P. (2019): Wind and sand geomorphology in the era of deep space exploration. – Advances in Earth Science 34(10): 1001-1014.

[21] Dong, Z., Huang, N., Liu, X. (2005): Simulation of the probability of midair interparticle collisions in an aeolian saltating cloud. – Journal of Geophysical Research 110(D24): 1064-1067.

[22] Dong, X., Hao, Y. G., Xin, X. M., Duan, R. B., Zhang, R. H., Ma, Y., Liu, F., Xue, D., Yu, G. H., Zhi, M. X. (2020): Comparative study on sand-fixing capability of three typical shrubs in otindag sandy land. – Forest Research 33(1): 76-83.

[23] Doniger, T., Adams, J. M., Marais, E., Maggs-Kolling, G., Sherman, C., Kerfahi, D., Yang, Y., Steinberger, Y. (2020): The 'fertile island effect' of Welwitschia plants on soil microbiota is influenced by plant gender. – FEMS Microbiology Ecology 96(11): fiaa186.

[24] Dougill, A. J., Thomas, A. D. (2002): Nebkha dunes in the Molopo Basin, South Africa and Botswana: formation controls and their validity as indicators of soil. – Journal of Arid Environments 50(3): 413-428.

[25] Du, J. H., Yan, P., E, Y. H. (2007): Distribution patterns and characteristics of white thorn scrub dunes in different evolutionary stages in Minqin, Gansu. – Journal of Ecology 26(8): 1165-1170.

[26] Du, J. H., Yan, P., Dong, Y. X. (2010): The progress and prospects of nebkhas in arid areas. – Journal of Geographical Sciences 20: 712-728.

http://www.aloki.hu ● ISSN 1589 1623 (Print) ● ISSN 1785 0037 (Online)
DOI: http://dx.doi.org/10.15666/aeer/2003_23432363

[27] El-bana, M. I., NIJS, Khedr, A. A. (2003): The importance of phytogenic mounds (nebkhas) for restoration of arid degraded rangelands in Northern Sinai. – Restoration Ecology 11: 317-324.
[28] El-Sheikh, M., Abbadi, G. A., Bianco, P. M. (2010): Vegetation ecology of phytogenic hillock (Nabkhas) in coastal habitats of JalAz-Zor National Park, Kuwait: role of patches and edaphic factors. – Flora 205(12): 832-840.
[29] Farrell, E., Connolly, N. (2021): Historic and contemporary dune inventories to assess dune vulnerability to climate change impacts. – Irish Geography 52(1): 38.
[30] Feng, T. J., Zhang, Z. Q., Zhang, L. X., Xu, W., He, J. S. (2021): Progress in the study of factors influencing water condensation in arid and semi-arid ecosystems and its role. – Acta Ecologica Sinica 41(02): 456-468.
[31] Fitoka, E., Tompoulidou, M., Hatziiordanou, L., Apostolakis, A., Hofer, R., Weise, K., Ververis, C. (2020): Water-related ecosystems' mapping and assessment based on remote sensing techniques and geospatial analysis: the SWOS national service case of the Greek Ramsar sites and their catchments. – Remote Sensing of Environment 245: 111795.
[32] Forman, S. L., Pierson, J. (2003): Formation of linear and parabolic dunes on the eastern Snake River Plain, Idaho in the nineteenth century. – Geomorphology 56(1): 189-200.
[33] Foth, H. D. (l990): Fundamentals of Soil Science. – John Wiley and Sons, New Jersey.
[34] Gao, Y., Dang, X. H., Yu, Y., Wang, J., Wang, S., Yuan, W. J., Zhang, X. W. (2015): Morphological characteristics and sand-fixing capacity of Artemisia sphaerocphala scrub dunes at the Southeastern margin of the Ulaanbaatar Desert. – China Desert 35(1): 0001-0007.
[35] Gillies, J. A., Nield, J. M., Nickling, W. G. (2014): Wind speed and sediment transport recovery in the lee of a vegetated and denuded nebkha within a nebkha dune field. – Aeolian Research 12: l35-141.
[36] Gong, X. W., Guo, J. J., Jiang, D. M. (2020): Contrasts in xylem hydraulics and water use underlie the sorting of different sand-fixing shrub species to early and late stages of dune stabilization. – Forest Ecology and Management 457: 117705.
[37] Gong, X. W., Guo, J. J., Fang, L. D., Bucci, S. J., Goldstein, G., Hao, G. Y. (2021): Hydraulic dysfunction due to root-exposure-initiated water stress is responsible for the mortality of Salix gordejevii shrubs on the windward slopes of active sand dunes. – Plant and Soil 459(1): 185-201.
[38] Goudie, A. S. (2020): Themes in Desert Geomorphology. – In: Pitty, A. (ed.) Themes in Geomorphology. Routledge, London, pp. 122-140.
[39] Gunn, A. L. (2021): Scale-dependent coupling between aeolian form and flow. – University of Pennsylvania.
[40] Hanson, P. R., Joeckel, R. M., Young, A. R., Horn, J. (2009): Late Holocene dune activity in the Eastern Platte River Valley, Nebraska. – Geomorphology 103(4): 555-561.
[41] Harte, J., Saleska, S. R., Levy, C. (2015): Convergent ecosystem responses to 23-year ambient and manipulated warming link advancing snowmelt and shrub encroachment to transient and long-term climate-soil carbon feedback. – Global Change Biology 21(6): 2349-2356.
[42] He, Z. B., Zhao, W. Z. (2004): Spatial patterns of two dominant plant populations in the transition zone of the Heihe River Basin desert oasis. – Journal of Applied Ecology 15(6): 947-952.
[43] He, J., Yan, Y. J., Yi, X. S., Wang, Y., Dai, Q. H. (2021): Soil heterogeneity and its interaction with plants in karst areas. – Chinese Journal of Applied Ecology 32(06): 2249-2258.
[44] Hermas, E., Alharbi, O., Alqurashi, A., Niang, A. J., Al-Ghamdi, K., Al-Mutiry, M., Farghaly, A. (2019): Characterisation of sand accumulations in Wadi Fatmah and Wadi Ash Shumaysi, KSA, using multi-source remote sensing imagery. – Remote Sensing 11(23): 2824.

http://www.aloki.hu ● ISSN 1589 1623 (Print) ● ISSN 1785 0037 (Online)
DOI: http://dx.doi.org/10.15666/aeer/2003_23432363

[45] Hesp, P. A. (1981): The formation of shadow dunes. – Journal of Sedimentary Petrology 51: 101-112.
[46] Hesp, P. A., Mclachlan, A. (2000): Morphology, dynamics, ecology and fauna of Arctotheca populifolia and Gazania rigens nabkha dunes. – Journal of Arid Environment 44(2): 155-172.
[47] Hesp, P. A., Smyth, T. A. G. (2017): Nebkha flow dynamics and shadow dune formation. – Geomorphology 282: 27-38.
[48] Hilgendorf, Z., Marvin, M. C., Turner, C. M., Walker, I. J. (2021): Assessing geomorphic change in restored coastal dune ecosystems using a multi-platform aerial approach. – Remote Sensing 13(3): 354.
[49] Hou, J., Yang, J., Tan, J. (2019): A new method for revealing spatial relationships between shrubs and soil resources in arid regions. – Catena 183: 104187.
[50] Hu, F., Yang, X., Li, H. (2019): Origin and morphology of barchan and linear clay dunes in the Shuhongtu Basin, Alashan Plateau, China. – Geomorphology 339: 114-126.
[51] Huang, H. X., Wang, G., Chen, N. L. (2010): Advances in the adaptation of desert shrubs to adversity. – Deserts of China 30(5): 1060-1067.
[52] Jia, X. H., Li, X. R. (2008): Spatial distribution patterns of white thorn scrub dunes in different habitats at the southeastern edge of Tengger Desert. – Environmental Science 29(7): 2046-2054.
[53] Jiang, Q., Yang, X. (2019): Sedimentological and geochemical composition of aeolian sediments in the Taklamakan Desert: implications for provenance and sediment supply mechanisms. – Journal of Geophysical Research: Earth Surface 124(5): 1217-1237.
[54] Kang, J. P., Ma, Y. Y., Ma, S. Q., Xue, Z. W., Yang, L. L., Han, L., Liu, W. Y. (2019): Population structure and spatial pattern dynamics of tamarisk in the transition zone of a desert oasis. – Acta Ecologica Sinica 39(1): 265-276.
[55] Khalaf, F. I., Al-awadhi, J. M. (2012): Sedimentological and morphological characteristics of gypseous coastal nabkhas on Bubiyan Island, Kuwait, Arabian Gulf. – Journal of Arid Environments 82: 31-43.
[56] Khalaf, F. I., Misak, R., Al-dousari, A. (1995): Sedimentological and morphological characteristics of some nabkha deposits in the northern coastal plain of Kuwait, Arabia. – Journal of Arid Environments 29(3): 267-292.
[57] Khalaf, F. I., Al-hurban, A. E., AL-Awadhi, J. (2014): Morphology of protected and non-protected Nitraria retusa coastal nabkha in Kuwait, Arabian Gulf: a comparative study. – Comparative study. Catena 115: 115-122.
[58] Kiani, M., Raave, H., Simojoki, A., Tammeorg, O., Tammeorg, P. (2021): Recycling lake sediment to agriculture: effects on plant growth, nutrient availability, and leaching. – Science of the Total Environment 753: 141984.
[59] Kinast, S., Meron, E., Yizhaq, H., Ashkenazy, Y. (2013): Biogenic crust dynamics on sand dunes. – Physical Review E 87(2).
[60] King, J., Nickling, W. G., Gillies, J. A. (2006): Aeolian shear stress ratio measurements within mesquite-dominated landscapes of the Chihuahuan Desert, New Mexico, USA. – Geomorphology 82: 229-244.
[61] Kuriyama, Y., Mochizuki, N., Nakashima, T. (2005): Influence of vegetation on aeolian sand transport rate from a backshore to a foredune at Hasaki, Japan. – Sedimentology 52(5): 1123-1132.
[62] Lan, Z., Zhao, Y., Zhang, J., Jiao, R., Khan, M. N., Sial, T. A., Si, B. (2021): Long-term vegetation restoration increases deep soil carbon storage in the Northern Loess Plateau. – Scientific Reports.
[63] Lancaster, N. (1995): The Geomorphology of Desert Dunes. – Routledge, Oxon.
[64] Langford, R. P. (2000): Nabkha (coppice dune) fields of south-central New Mexico, U.S.A. – Journal of Arid Environments 46: 25-41.

http://www.aloki.hu ● ISSN 1589 1623 (Print) ● ISSN 1785 0037 (Online)
DOI: http://dx.doi.org/10.15666/aeer/2003_23432363

[65] Leenders, J. K., Van, B. J. H., Sterk, G. (2007): The effect of single vegetation elements on wind speed and sediment transport in the Sahelian regional of Burkina Faso. – Earth Surface Processes and Landforms 32(10): 1454-1474.
[66] Li, W. J. (2009): Preliminary study on the characteristics of tamarisk sandpiles around Lake Aibi in Xinjiang. – Xinjiang Normal University, Urumqi.
[67] Li, P. X., Wang, N., He, W. M., Bertil, O., Krusi., Gao, S. Q., Zhang, S. M., Yu, F. H., Dong, M. (2008): Fertile islands under Artemisia ordosica in inland dunes of northern China: effects of habitats and plant developmental stages. – Journal of Arid Environments 72(6): 953-963.
[68] Li, J. C., Gao, J., Zou, X. Y., Kang, X. Y. (2014): The relationship between nebkha formation and development and desert environmental changes. – Acta Ecologica Sinica 34: 266-270.
[69] Li, J., Wang, Y., Yao, Q. (2020): Nebkhas origination in arid and semi-arid regions: an overview. – Acta Ecologica Sinica 40(6): 500-505.
[70] Li, J. J., Jiao, J. Y., Cao, X., Bai, L. C., Chen, T. D., Yan, X. Q., Qi, H. K. (2021): The spatial differentiation of dune movement in Qaidam Basin and its response to morphological parameters. – Transactions of the Chinese Society of Agricultural Engineering 37(07): 309-314.
[71] Liang, E. Y., Eckstein, D. (2009): Dendrochronological potential of the alpine shrub Rhododendron nivale on the south-eastern Tibetan Plateau. – Ann Bot-London 104(4): 665-670.
[72] Liu, B., Zhao, W. Z., Yang, R. (2008): Characteristics and spatial heterogeneity of Tamarix ramosissima nebkhas at desert-oasis ecotone. – Acta Ecologica Sinica 28(4): 1446-1455.
[73] Liu, J. W., Li, Z. Z., Wu, S. L., Li, W. J., Wang, S. P., Cao, X. D., Ling, Z. Y. (2009): Spatial heterogeneity of morphological characteristics of the white thorn sand mounds around Lake Aibi in Xinjiang. – Deserts of China 29(4): 628-635.
[74] Liu, W., Liu, Z., An, Z., Wang, X., Chang, H. (2011): Wet climate during the 'Little Ice Age' in the arid Tarim Basin, northwestern China. – The Holocene 21(3): 409-416.
[75] Lopez, O. M., Hegy, M. C., Missimer, T. M. (2020): Statistical comparisons of grain size characteristics, hydraulic conductivity, and porosity of barchan desert dunes to coastal dunes. – Aeolian Research 43(4): 100576.
[76] Ma, F., Lu, P. (2019): Characteristics of wind conditions in areas where crescentic dunes and linear dunes coexist. – Journal of Desert Research 39(3): 98.
[77] Mahmoud, A. M. A., Novellino, A., Hussain, E., Marsh, S., Psimoulis, P., Smith, Martin. (2020): The use of SAR offset tracking for detecting sand dune movement in Sudan. – Remote Sensing 12(20): 3410.
[78] Marrero-Rodríguez, N., García-Romero, L., Sánchez-García, M. J., Hernandez-Calvento, L., Espino, E. P. C. (2020): An historical ecological assessment of land-use evolution and observed landscape change in an arid aeolian sedimentary system. – Science of the Total Environment 716: 137087.
[79] Marzialetti, F., Giulio, S., Malavasi, M., Sperandii, M. G., Acosta, A. T. R., Carranza, M. L. (2019): Capturing coastal dune natural vegetation types using a phenology-based mapping approach: the potential of Sentinel-2. – Remote Sensing 11(12): 1506.
[80] Miao, R., Liu, Y., Wu, L., Wang, D., Liu, Y., Miao, Y., Ma, J. (2022): Effects of long-term grazing exclusion on plant and soil properties vary with position in dune systems in the Horqin Sandy Land. – Catena 209.
[81] Miri, A., Dragovich, D., Dong, Z. (2021): Wind flow and sediment flux profiles for vegetated surfaces in a wind tunnel and field-scale windbreak. – Catena 196: 104836.
[82] Molina, R., Manno, G., Lo, Re. C., Anfuso, G. (2020): Dune systems' characterization and evolution in the Andalusia Mediterranean coast (Spain). – Water 12(8): 2094.

http://www.aloki.hu ● ISSN 1589 1623 (Print) ● ISSN 1785 0037 (Online)
DOI: http://dx.doi.org/10.15666/aeer/2003_23432363

[83] Mou, R. (2019): Exploratory application of low-coverage sand control and combined engineering and biological sand control models in desertification control. – Journal of Temperate Forestry Research 2(1): 59-62.
[84] Nickling, W. G., Wolfe, S. A. (1994): The morphology and origin of nabkhas, region of Mopti, Mali, West Africa. – Journal of Arid Environments 28(1): 13-30.
[85] Pakari, A., Ghani, S. (2019): Airflow assessment in a naturally ventilated greenhouse equipped with wind towers: numerical simulation and wind tunnel experiments. – Energy and Buildings 199: 1-11.
[86] Pan, K. J., Zhang, Z. C., Dong, Z. B., Zhang, C. X., Li, X. C. (2019): Physico-chemical properties of surface sediments from crescent-shaped sand dunes in the Hexi Corridor. – Journal of Desert Research 39(1): 44.
[87] Parsons, A. J., Wainwright, J., Schlesinger, W. H., Abrahams, A. D. (2003): The role of overland flow in sediment and nitrogen budgets of mesquite dune fields, southern New Mexico. – Journal of Arid Environments 53: 61-71.
[88] Pei, Y. Z., Pang, G. H. (2020): Wind tunnel simulations of sand piles in Salix scrub under net and sand-bearing winds. – The Farmers Consultant 6: 164.
[89] Provoost, S., Declerck, L. (2020): Early scrub development in De Westhoek coastal dunes (Belgium). – Folia Geobotanica 55(4): 315-332.
[90] Pye, K., Tsoar, H. (1990): Aeolian Sand and Sand Dunes. – Unwin Hyman, Boston.
[91] Qin, J., Wu, T., Zhong, D. Y. (2015): Spectral behavior of gravel dunes. – Geomorphology 231(2): 331-342.
[92] Qiu, G. Y., Li, C., Yan, C. H. (2015): Characteristics of soil evaporation, plant transpiration and water budget of Nitraria dune in the arid Northwest China. – Agricultural and Forest Meteorology 203: 107-117.
[93] Qong, M., Takamura, H., Hudaberdi, M. (2002): Formation and internal structure of tamarix cones in the Taklimakan Desert. – Journal of Arid Environments 50: 81-97.
[94] Quets, J. J., Temmerman, S., El-bana, M. I., Al-Rowaily, L. S., Assaeed, A. M., Nijsa, I. (2013): Unraveling landscapes with phytogenic mounds (nebkhas): an exploration of spatial pattern. – ActaOecol 49: 53-63.
[95] Rafi, Z. N., Kazemi, F., Tehranifar, A. (2019): Effects of various irrigation regimes on water use efficiency and visual quality of some ornamental herbaceous plants in the field. – Agricultural Water Management 212: 78-87.
[96] Rango, A., Chopping, M., Ritchie, J., Havstad, K., Kustas, W., Schmugge, T. (2000): Morphological characteristics of shrub coppice dunes in desert grasslands of southern New Mexico derived from scanning LIDAR. – Remote Sensing of Environment 74: 26-44.
[97] Rhodes, E. J., Pownall, L. (1994): Zeroing of the OSL signal in quartz from young glaciofluvial sediments. – Radiation Measurements 23(2): 581-585.
[98] Seifert, C. L., Cox, R. T., Forman, S. L., Foti, T. L., Wasklewice, T. A., McColgan, A. T. l. (2009): Relict nebkhas (pimple mounds) record prolonged late Holocene drought in the forested region of south-central United States. – Quaternary Research 71: 329-339.
[99] Sperandii, M. G., Bazzichetto, M., Acosta, A. T. R., Barták, V., Malavasi, M. (2019): Multiple drivers of plant diversity in coastal dunes: a Mediterranean experience. – Science of the Total Environment 652: 1435-1444.
[100] Sulub-Tun, R. A., Rodríguez-García, C. M., Peraza-Echeverría, L., Torres-Tapia, L. W., Peraza-Sanchez, S. R., Perez-Brito, D., Vera-Ku, B. M. (2020): Antifungal activity of wild and nursery Diospyros cuneata, a native species of dune scrub. – South African Journal of Botany 131: 484-493.
[101] Sun, Q., Wang, H., Zamanian, K. (2019): Radiocarbon age discrepancies between the carbonate cement and the root relics of rhizoliths from the BadainJ aran and the Tengeri deserts, Northwest China. – Catena 180: 263-270.

http://www.aloki.hu ● ISSN 1589 1623 (Print) ● ISSN 1785 0037 (Online)
DOI: http://dx.doi.org/10.15666/aeer/2003_23432363

[102] Sun, Q., Zamanian, K., Huguet, A., Huguet, A., Fa, K. Y., Wang, H. (2020): Characterization and formation of the pristine rhizoliths around Artemisia roots in dune soils of Tengeri Desert, NW China. – Catena 193: 104633.
[103] Taminskas, J., Šimanauskienė, R., Linkevičienė, R., Volungevicius, J., Slavinskiene, G., Povilanskas, R., Satkunas, J. (2020): Impact of hydro-climatic changes on coastal dunes landscape according to normalized difference vegetation index (the case study of Curonian spit). – Water 12(11): 3234.
[104] Tang, Y., Liu, L. Y., Haas, Wang, Z., Sun, B. Y., Du, J. H. (2008): Comparative study on the morphology and sand-blocking capacity of three species of scrub and grass at the southern edge of the Mauwusu Sands. – Soil and Water Conservation Research 15(2): 44-48.
[105] Telfer, M. W., Gholami, H., Hesse, P. P., Fisher, A., Hartley, R. (2020): Testing models of linear dune formation by provenance analysis with composite sediment fingerprints. – Geomorphology 364: 107208.
[106] Tengberg, A. (1995): Nebkha dunes as indicators of wind erosion and land degradation in the Sahel regional of Burkina Faso. – Journal of Arid Environments 30(3): 265-282.
[107] Tengberg, A., Chen, D. L. (1998): A comparative analysis of nebkhas in central Tunisia and northern Burkina Faso. – Geomorphology 22(2): 181-192.
[108] Thomas, D. S. G., Knight, M., Wiggs, G. F. S. (2005): Remobilization of southern Africa desert dune systems by twenty-first century global warming. – Nature 435: 1218-1221.
[109] Tsoar, H., Møller, J. T. (2020): The Role of Vegetation in the Formation of Linear Sand Dunes. – In: Nickling, G. W. (ed.) Aeolian Geomorphology. – Routledge, London, pp. 75-96.
[110] Tyler, R. G., Chris, H. H., Thomas, E. B. (2021): Re-evaluation of large Martian ripples in Gale Crater: granulometric evidence for an impact mechanism and terrestrial analogues. – Jgr Planets 126(12).
[111] Wang, T. (2003): Deserts and Desertification in China. – Hebei Science and Technology Press, Shijiazhuang.
[112] Wang, X. M., Wang, T., Dong, Z. B., Liu, X., Qian, G. (2006): Nebkha development and its significance to wind erosion and land degradation in semi-arid northern China. – Journal of Arid Environments 65: 129-141.
[113] Wang, X. M., Xiao, H. L., Li, J. C., Qiang, M. R., Su, Z. Z. (2008): Nebkha development and its relationship to environmental change in the Alaxa Plateau, China. – Environmental Geology 56(2): 359-365.
[114] Wang, X. M., Zhang, C. X., Zhang, J. W., Hua, T., Zhang, X., Wang, L. (2010): Nebkha formation: implications for reconstructing environmental changes over the past several centuries in the Ala Shan Plateau, China. – Paleoclimatology 297(3-4): 697-706.
[115] Wang, Y., Li, C., Li, A. D., Yang, Z. H., Zhang, Q. T., Liang, X. J., Qiu, G. Y. (2015): Relationship between degradation of white thorn sand pile and soil moisture. – Journal of Ecology 35(5): 1407-1421.
[116] Wang, F., Guo, S. J., Zhang, W. X., Wang, F. L., Han, F. G., Li, J. H. (2020): Soil grain size characteristics of white thorn scrub dunes at different successional stages in arid desert areas. – Journal of Northwest Forestry Academy 35(1): 15-20.
[117] Wang, Z. Y., Niu, G. H., Liu, B. L. (2021): Comparison and applicability of three indicators for estimating the intensity of wind and sand activity. – Journal of Desert Research 41(3): 118.
[118] Warren, J. K. (l982): The hydrological setting, occurrence and significance of gypsum in late Quaternary salt lakes in South Australia. – Sedimentology 29: 609-637.
[119] Weems, S. L., Monger, H. C. (2012): Banded vegetation-dune development during the Medieval Warm Period and 20th century, Chihuahuan Desert, New Mexico, USA. – Ecological Society of America 3(3): 1-16.
[120] White, B. R., Greeley, R., Iversen, J. D., Pollack, J. B. (1976): Estimated grain saltation in a Martian atmosphere. – Journal of Geophysical Research 81(32): 5643-5650.

http://www.aloki.hu ● ISSN 1589 1623 (Print) ● ISSN 1785 0037 (Online)
DOI: http://dx.doi.org/10.15666/aeer/2003_23432363

[121] Wiggs, G. F. S., Thomas, D. S. G., Bullard, J. E., Livingstone, L. (1995): Dune mobility and vegetation cover in the southwest Kalahari Desert. – Earth Surface Processes and Landforms 20(6): 515-529.
[122] Wu, Z. (2003): Wind and Sand Landforms and Sand Control Engineering. – Science Press, Beijing.
[123] Wu, S. L., Li, Z. Z., Hui, J. (2006a): Experimental study of surface pressure distribution characteristics of scrub dunes. – Geography of Arid Regions 290(6): 790-796.
[124] Wu, S. L., Li, Z. Z., Xiao, C. X., Sun, Q. M., Liu, L. M. (2006b): Research progress and significance of scrub sandpiles. – Deserts of China 26(5): 734-738.
[125] Wu, S. L., Li, J., Chen, S. J., Liu, Q., Zhao, F., Lu, X. (2009): The shape character and development stage of nebkha. – High Technology Letters 15: 440-445.
[126] Wu, Z., Wang, S., Jin, N. (2019): Phosphorus (P) release risk in lake sediment evaluated by DIFS model and sediment properties: a new sediment P release risk index (SPRRI). – Environmental Pollution 255: 113279.
[127] Xia, X. C., Zhao, Y. J., Wang, F. B., Cao, Q. Y., Mu, G. J., Zhao, J. F. (2004a): Stratification features of Tamarix cone and its possible age significance. – Chinese Science Bulletin 49(14): 1539-1540.
[128] Xia, X. C., Zhao, Y. J., Wang, F. B. (2004b): Stratigraphic features of red willow sandbags and their possible chronological significance. – Science Bulletin 49(13): 1337-1338.
[129] Xia, X. C., Zhao, Y. J., Wang, F. B., Cao, Q. Y. (2005): Environmental significance exploration to Tamarix Cone age layer in Lop Nur Lake region. – Chinese Science Bulletin, Chinese Science Bulletin 50(20): 2395-2397.
[130] Xiao, S. C., Xiao, H. L., Peng, X. M., Tian, Q. Y. (2014): Intra-annual stem diameter growth of Tamarix ramosissima and association with hydroclimatic factors in the lower reaches of China's Heihe River. – Journal of Arid Land 6(4): 498-510.
[131] Xie, G., Steinberger, Y. (2005): Nitrogen and carbon dynamics under the canopy of sand dune shrubs in a desert ecosystem. – Arid Land Research and Management 19(2): 147-160.
[132] Yan, B. L., Lu, S. J., Wang, Z. W., Han, G. D. (2019): Progress in the study of the causes of grassland scrubbing and its impact on ecosystems. – Chinese Journal of Grassland 41(2): 95-1012.
[133] Yang, Y. Y., Liu, L. Y., Shi, P. J., Zhao, M. D., Dai, J. D., Lu, Y. L., Zhang, G. M., Zuo, X. Y., Jia, Q. P., Liu, Y., Liu, Y. (2019): Converging effects of shrubs on shadow dune formation and sand trapping. – Journal of Geophysical Research: Earth Surface 124(7): 1835-1853.
[134] Yao, X. L., Yang, G. J., Wu, B., Jiang, L. N., Wang, F. (2021): Biomass estimation models for six shrub species in Hunshandake sandy land in Inner Mongolia, Northern China. – Forests 12(2): 167.
[135] Yeh, T. F., Chu, J. H., Liu, L. Y. (2020): Differential gene profiling of the heartwood formation process in Taiwania cryptomerioides Hayata xylem tissues. – International Journal of Molecular Sciences 21(3): 960.
[136] Zhang, X. G. (2019): A preliminary study on the theory of low-coverage sand management and its application in arid and semi-arid areas. – Forestry Science and Technology Information 51(04): 28-29.
[137] Zhang, P. Z., Cheng, H., Edwards, R. L., Chen, F. H., Wang, Y. J., Yang, X. L., Liu, J., Tan, M., Wang, X. F., Liu, J. H. (2008): A test of climate, sun, and culture relationships from an18l0-year Chinese cave record. – Science 322(5903): 940-942.
[138] Zhang, P. J., Yang, J., Zhao, L. Q., Bao, S., Song. B. (2011): Effect of Caragana tibetica nebkhas on sand entrapment and fertile islands in steppe-desert ecotones on the Inner Mongolia Plateau, China. – Plant and Soil 347(1): 79-90.

http://www.aloki.hu ● ISSN 1589 1623 (Print) ● ISSN 1785 0037 (Online)
DOI: http://dx.doi.org/10.15666/aeer/2003_23432363

[139] Zhang, P., Haas, Wu, X., Yang, Y., Du, H. S. (2013): Field observational study on the airflow structure of a single Artemisia oleifera scrub sandpile. – Journal of Applied Basic and Engineering Sciences 21(5): 881-889.
[140] Zhang, P., Haas, Yang, I., Wu, X. (2015): Response of small-leaved brome (Caragana microphylla) scrub dune morphology to sand supply forms and abundance. – China Desert 35(6): 1453-1460.
[141] Zhang, Z. C., Dong, Z. B., Qian, G. Q., Li, J. Y., Luo, W. Y. (2018): Formation and development of dunes in the northern Qarhan Desert, central Qaidam Basin, China. – Geological Journal 53(3): 1123-1134.
[142] Zhang, Z. G., Dong, X., Xin, Z. M. (2021): Distribution and prediction of the biomass of sandbags in scrubs of the genus White Spurge. – Pratacultural Science 38(6): 1069-1077.
[143] Zhao, Y. J., Song, Y., Xia, X. C., Wang, X. Y., Li, X. F. (2009a): Particle size characteristics of sand material in the sedimentary grain layer of the Lop nor red willow sandbags over the last 150 years. – Arid Zone Resources and Environment 23(12): 103-107.
[144] Zhao, Y. J., Xia, X. C., Wang, F. B., Cao, Q. Y., Gao, W. M., Wei, L. T. (2009b): Characteristics and environmental indications of sand graininess in the red willow sand pack layer of the Lop nor region. – Arid Zone Geography 30(6): 791-796.
[145] Zhao, Y. J., Li, X. F., Xia, X. C., Wang, X. Y. (2011): Carbon and nitrogen content of organic matter and climate change in the Lop nor red willow sandbag sediment layer. – Resources and Environment of Arid Regions 25(4): 149-154.
[146] Zhao, Y. J., Che, G. H., Liu, H., Zeng, J., Xia, X. C. (2016): Carbon and nitrogen content of organic matter and climatic and environmental changes in the red willow sand packs at the southern edge of the Taklimakan Desert. – Arid Zone Geography 39(3): 461-467.
[147] Zhao, Y. C., Gao, X., Lei, J. Q., Li, S. H., Cai, D. X., Song, S., Zhao, Y., Gao, X., Lei, J. (2019): Effects of wind velocity and nebkha geometry on shadow dune formation. – Journal of Geophysical Research: Earth Surface 124(11): 2579-2601.
[148] Zhao, Y. C., Gao, X., Lei, J. Q., Li, S. Y. (2020): Nebkha alignments and their implications for shadow dune elongation under unimodal wind regime. – Geomorphology 365: 27-38.
[149] Zhao, X., Xia, H., Pan, L., Song, H., Niu, W., Wang, R., Qin, Y. (2021): Drought monitoring over Yellow River Basin from 2003–2019 using reconstructed MODIS land surface temperature in google earth engine. – Remote Sensing (Basel, Switzerland) 13(18): 3748.
[150] Zhong, H. Y., Lin, C., Sun, Y., Kikumoto, H., Jimenez-Bescos, C., Zhong, H. Y., Lin, C., Sun, Y. (2021): Boundary layer wind tunnel modeling experiments on pumping ventilation through a three-story reduce-scaled building with two openings. – Building and Environment 108043.
[151] Zhu, Z. D. (1999): Deserts, Desertification and Desertification in China and Measures to Control Them. – China Environmental Science Press, Beijing.
[152] Zhu, Z. D., Chen, G. T. (1994): Sandy Desertification. – Science Press, Beijing.
[153] Zuo, X. A., Zhao, H. L., Zhao, X. Y., Zhang, T. H., Guo, Y. R., Wang, S. K., Drake, S., Zuo, X., Zhao, H., Zhao, X. (2010): Spatial pattern and heterogeneity of soil properties in sand dunes under grazing and restoration in Horqin Sandy Land, Northern China. – Soil and Tillage Research 99(2): 202-212.
[154] Zuo, H. J., Yang, Y., Zhang, H. F., Yao, L. Q., Yan, X. D., Wu, X. G., Liu, B. H., Yam, M. (2018): Study on morphological characteristics of white thorn scrub sandpile in Alashan Gobi region. – Soil and Water Conservation Research 25(1): 263-269.

http://www.aloki.hu ● ISSN 1589 1623 (Print) ● ISSN 1785 0037 (Online)
DOI: http://dx.doi.org/10.15666/aeer/2003_23432363

SOIL QUALITY AND GROWTH PERFORMANCE OF CROPS OF AGROECOSYSTEMS IN THE VICINITY OF FLUORITE MINING

KHAN, I.[1] – CHANDIO, T. A.[2] – GUL, S.[1,3*] – SHAHEEN, U.[4] – REHMAN, G. B.[1] – JAN, S.[5]

[1]*Department of Botany, University of Balochistan, Quetta, Pakistan*

[2]*Geological Survey of Pakistan, Saryab Road, Quetta, Pakistan*

[3]*Department of Natural Resource Sciences, McGill University, Montreal, QC, Canada*

[4]*Department of Zoology, University of Balochistan, Quetta, Pakistan*

[5]*Department of Microbiology, Faculty of Biological Sciences, Quaid-i-Azam University, Islamabad, Pakistan*

[*]*Corresponding author*
e-mail: shamim.gul@mail.mcgill.ca

(Received 18th Nov 2021; accepted 25th Mar 2022)

Abstract. This study investigated the influence of fluoride on the number of macrofauna species on the soil surface and in the upper soil layer (0-10 cm depth) and crop growth performance on agricultural lands in the vicinity of fluorite mining activities in District Loralai, Balochistan, Pakistan. Results demonstrated that ants were sensitive to the fluoride above the concentration of 55 mg kg^{-1} soil; whereas, grasshoppers, crickets, spiders and toothed earwigs were tolerant to high fluoride concentrations (e.g. 74 mg kg^{-1} soil). The concentration of fluoride in soil was positively correlated with the concentration of fluoride in vegetables (R^2 = 0.75; $P \leq 0.05$ for leaves, R^2 = 0.48 $P \leq 0.05$ for fruits, R^2 = 0.81 $P \leq 0.05$ for stems and R^2 = 0.61 $P \leq 0.05$ for roots). Crop growth performance parameters such as yield and nutrient efficiency ratios concerning nitrogen and phosphorus had no obvious relationships with the concentrations of soil organic matter or fluoride in soil. These results conclude that concentration of fluoride in soil might have had negative influence on soil fauna and crop growth performance as no relationship was found between these parameters with the soil quality indicator i.e. soil organic matter.
Keywords: *farming systems, nitrogen use efficiency, phosphorus use efficiency, soil fauna, soil organic matter*

Introduction

Mine tailings from mining activities, negatively influence surrounding ecosystems, by contaminating air, water and soil, through dispersion of metal(oids) (Gil-Loaiza et al., 2016). Moreover, mine tailings as abandoned dumping sites, generally possess acidic pH, which is threatening to the surrounding vegetation including agricultural lands (Mendez et al., 2014; Zhang et al., 2014) and further increases the bioavailability of heavy metals in soil (Takac et al., 2010). Empirical evidences suggest that mining activity causes contamination of agricultural soils from high distances (Djebbi et al., 2017; Gao et al., 2017). For example, findings of Limei et al. (2008) showed that the rice-cultivated agricultural lands in Chenzhou City, China, which were at 23 km to 63 km distances from mining activities, had concentration of cadmium, that exceeded many times its critical concentration in rice, soil and vegetables. Fluorite mining also adversely affects soil quality of agroecosystems through irrigation, which contains fluoride contamination (Davies, 1994).

http://www.aloki.hu ● ISSN 1589 1623 (Print) ● ISSN1785 0037 (Online)
DOI: http://dx.doi.org/10.15666/aeer/2003_23652379

Balochistan province of Pakistan is famous for deposits of coal, chromite, copper, gypsum, fluorite, celestite, iron, barite, limestone, marbles etc. (Malkani, 2011). Loralai has approximately 50000 tons of fluorite deposits and the fluorite mining in this region is in progress (Malkani et al., 2017). Fluorite has been excavated from three sites in Loralai; whereas, local people of this region rely on livestock and agriculture. Extensive fluorite mining can have influence on crops and soils of agricultural lands of this region. The objectives of this study are to assess 1) concentration of fluoride in agricultural soils and crops and 2) soil quality and crop growth performance of agricultural lands. The hypotheses of this study are; 1) soils of agricultural lands of this region have contamination of fluoride and the concentration of fluoride in crops has a positive relation with the concentration of fluoride in soil, 2) fluoride contamination of soils of agricultural lands has disturbed vegetation-soil ecosystem relationship as growth performance of crops has no positive relationship with soil quality indicators (e.g. organic matter).

Materials and methods

Study area

Loralai district is the part of Zhob division, which is located in the northeast of Baluchistan province, Pakistan. This area is also called as Bori and occupies an area of 8155 square kilo meters. It lies between the latitudes of 67°41'18"- 69°44'22"East and 29°54'50"- 30°41'28" North. This region has Mediterranean type arid climate, with summer temperature of 40 to 45 °C and winter temperature of 3 to 10 ^{o}C. Rainfall mostly occurs in winter to spring, occasionally summer season also receives rainfall. Snowfall also occurs in winter. The yearly mean temperature is 28.1 ^{0}C. January is the coldest month, and July is the warmest month in the year. Dargai, Baharvala and Mahiwal are the fluorite mining sites of Loralai.

Sampling procedure

Two sets of samples were collected. First set of samples involved sampling of vegetables and soils from agricultural lands at various distances from mining sites (*Figure 1*). This sampling was carried out to measure the concentration of fluoride in soil and vegetables. The second set of samples involved sampling of vegetables and soils from the agricultural lands that are close to mining sites (*Figure 2*). The second set of sampling was carried out to measure aboveground vegetable biomass, nitrogen (N), phosphorus (P) and nitrogen and phosphorus efficiency ratios of tested vegetables, macrofauna of surface soil and upper soil layer (0-10 cm depth) and physico-chemical properties of soils.

For the first set of samples, at each selected site (cropland), 5 spots were selected randomly at various distances within a given cropland, crops were cut down above the soil surface. The soil samples were collected from the same spot, from 0-15 cm depth, using 5 cm diameter and 10 cm height soil corer. Samples of vegetables and soil were taken during the field visit in June 2– 2019 to March 17 2020. A control for soil and vegetables was chosen from five fields from the city Duki, which is located 63 km away from Loralai. The coordinates of vegetable and soil samples of data set 1 and 2 are given in supplementary *Table A1* and in the maps as *Figure 1* for data set 1 and *Figure 2* for data set 2. For the second set of samples, 17 croplands were selected (*Figure 3*). At each selected site (cropland), five spots were selected randomly at various distances. At each spot, 0.5 x 0.5 m plots were marked with colored rope, within that square area, crops were

http://www.aloki.hu ● ISSN 1589 1623 (Print) ● ISSN1785 0037 (Online)
DOI: http://dx.doi.org/10.15666/aeer/2003_23652379

cut down above the soil surface and were collected in zip-lock plastic bags. The soil samples were collected from the center of each plot after harvest of vegetation, from 0-10 cm depth, with the same procedure as described above. Soil samples were collected in zip-lock plastic bags and were stored in refrigerator at 4ºC until used for chemical analysis.

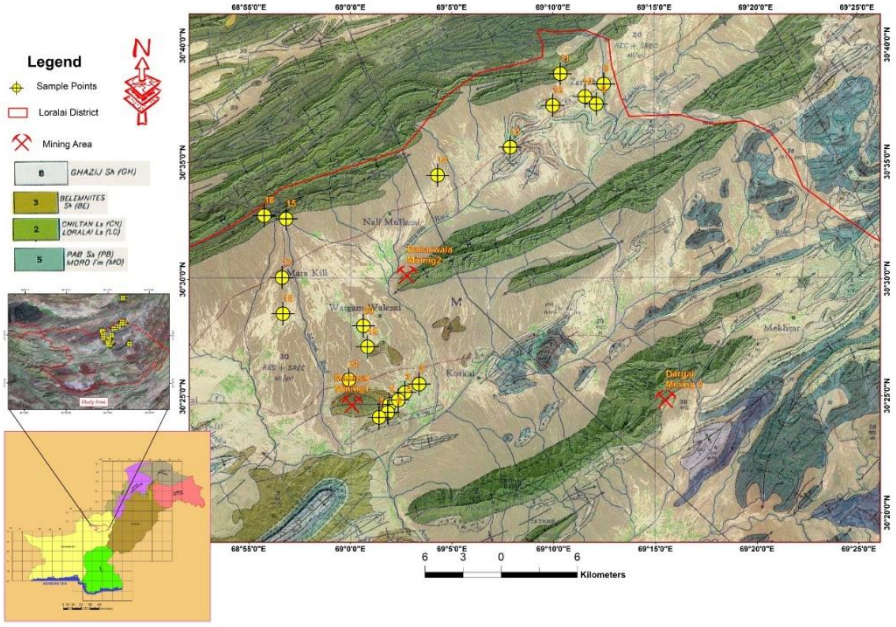

Figure 1. *The names of villages as sampling sites, mentioned in yellow circle are as follows; 1) Tor Thana, 2) Terrag, 3) Kotakai, 4) Chamaza, 5) Saper Chamaza, 6) Chijan Wa, 7) Sagri, 8) Shabozai, 9) Mahiwal, 10) Cheena Alizai, 11) Nali Walizai, 12) Agberg, 13) Tangi Sar, 14) Zarra, 15) Kochan, 16) Zara Kalam, 17) Darai, 18) Marra Tangi, 19) Juma Killi, 20) Manzaki*

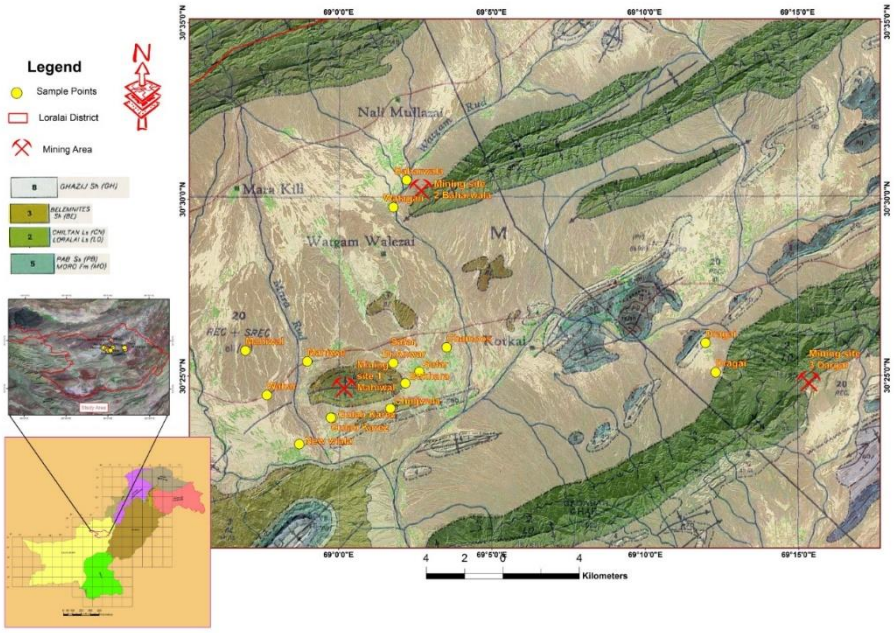

Figure 2. *Coordinates of data set 1 and data set 2*

http://www.aloki.hu ● ISSN 1589 1623 (Print) ● ISSN1785 0037 (Online)
DOI: http://dx.doi.org/10.15666/aeer/2003_23652379

Table 1. *Mean ± SD water soluble fluoride in soil (mg kg^{-1} in 0-15 cm depth soil), leaf, fruits, stem and root tissues (mg kg^{-1})*

Sampling sites (villages with their names)	Fluoride in soil	pH of soil	Vegetable	Fluoride in leaf	Fluoride in fruit	Fluoride in shoot	Fluoride in root
Cheena Alizai	23.3±0.96^{a}	6.24	Spinach	17.47±0.67^{a}	--	11.7±0.57^{a}	8.53±0.54^{a}
Tor Thana	14.19±0.54^{b}	6.65	Potato	13.42±0.55^{b}	4.77±0.12^{a}	4.52±0.12^{b}	8.11±0.12^{b}
Kachi Alizai	13.52±0.34^{c}	6.96	Onion	3.55±2.90^{d}	3.20±0.15^{c}	2.09±0.09^{e}	5.78±0.09^{c}
Aghberg	8.6±0.35^{g}	6.63	Cabbage	2.90±0.09^{e}	2.51±0.16^{d}	1.33±0.09^{f}	3.09±0.07^{f}
Mahiwal	11.0±0.36^{e}	6.91	Garlic	5.09±0.10^{c}	1.77±0.10^{f}	2.02±0.04^{e}	3.62±0.22^{e}
			Wheat	1.71±0.13^{g}	1.22±0.12^{h}	2.14±0.12^{e}	3.52±0.09^{e}
Sagri	12.78±0.26^{d}	--	Carrot	3.60±0.08^{d}	3.45±0.08^{b}	3.88±0.07^{c}	5.27±0.11^{d}
Shabozai	9.23±0.18^{f}	6.97	Pea	2.85±0.07^{e}	1.20±0.05^{h}	2.92±0.05^{d}	3.03±0.04^{f}
Nali Walizai	7.42±0.44^{h}	6.95	Cauliflower	2.45±0.04^{f}	1.50±0.06^{g}	1.45±0.06^{f}	5.53±0.06^{cd}
			Mustard	1.51±0.11^{g}	1.95±0.10^{e}	2.96±0.11^{d}	3.75±0.31^{e}
Control site**	4.07	6.10	Spinach	4.20	0.00	1.77	1.58
Control site	4.46	6.34	Potato	1.48	0.31	1.00	0.94
Control site	3.47	5.98	Union	0.40	0.29	0.22	1.01
Control site	3.75	6.46	Cabbage	0.37	0.30	0.24	0.75
Control site	3.90	6.19	Garlic	0.97	0.26	0.32	1.91

Within column, values with different uppercase letters are significantly different at P≤0.01. – represents no data. ** control site (Duki city) was 63 km away from Loralai

Figure 3. *Croplands of study site for sample set 2*

http://www.aloki.hu ● ISSN 1589 1623 (Print) ● ISSN1785 0037 (Online)
DOI: http://dx.doi.org/10.15666/aeer/2003_23652379

Macrofauna that were found on the surface of soil within each plot, as well as in the soil samples from upper soil layer (0-10 cm depth), were collected in 5% formalin-containing bottles. One bottle was used for one sampling site (cropland) as a pool sample of five replicates of a given sampling site. The sampling for data set 2 for vegetation, soil and soil fauna was carried out from 2 – 13 September 2019.

Chemical analysis of plant samples

Vegetables of data set 1 were rinsed with deionized water (Fluoride 0 ppm) to remove dust particles and oven-dried for 48 hours at 60°C. Samples were homogeneously grinded. Samples were thereafter analyzed for the concentration of fluoride with potentiometric ion selective electrode method (McQuaker and Gurney, 1977; D'Alessandro et al., 2008). Briefly, fluoride was extracted from the plant samples with HNO_3, followed by aqueous KOH. A fluoride-specific ion electrode was used to determine the concentration of fluoride in the solution. These were registered in an ion analyzer instrument which was calibrated with standards of known concentrations of NaF in distilled and deionized water. The supernatant was mixed at 1:1 ratio with a total ionic strength adjustment buffer (TISAB-IV) to dissociate F-Complexes and stabilize pH. The buffer was prepared by mixing 84 ml conc. HCl, 242 g TRIS (hydroxymethyl aminomethane, and 239 g sodium tartrate (FW=230.08), in about 500 ml water, cooled, and transferred to 1-liter volumetric flask and made to I L.

The vegetables of data set 2 were oven-dried at 60°C for 48 hours and the dry biomass was calculated. The analysis of nitrogen and phosphorus was carried out by digesting plant samples in sulfuric acid with repeated addition of hydrogen peroxide (30%) (Wolf, 1982). The concentration of nitrogen was assessed by Kjeldahl method of Jones (1991). The digested samples were analyzed for the concentration of phosphorus by vanadomolybdate phosphoric acid yellow color method of Cottenie (1980). The nitrogen efficiency and phosphorus efficiency ratios, as indicators of nutrient use efficiency for these nutrients (Baligar et al., 2001) were calculated as;

$$Nutrient\ efficiency\ ratio\ (NER\ or\ PER) = \frac{Plant\ biomass}{Concentration\ of\ N\ or\ P\ in\ plant\ tissue} \quad \text{(Eq.1)}$$

Chemical analysis of soil samples

The chemical analysis of soil samples of data set 1 was done at Geo Science Advance Research Laboratory, Geological Survey of Pakistan; whereas chemical analysis of soil samples of data set 2 for the concentration of fluoride was carried out at the Quaid-e-Azam University, Islamabad. The air-dried soil samples were crushed, passed through 2 mm mesh size sieve to remove pebbles and other debris. Thereafter, samples were burned in crucibles by fusion with 10 mL NaOH, and placing in furnace for 30 minutes at 600^0C. These fused samples were dissolved with 20 mL deionized water followed by their mixing in TISAB buffer solution to determine the concentration of fluoride with the ion selective electrode method (Zhang et al., 2010). The organic matter and soluble inorganic phosphorus of soil was analyzed according to the protocol described in Estefan et al. (2013) and D'Angelo et al. (2001), respectively. The pH and electrical conductivity were analyzed with ORION ion analyzer (5-Star series). Macrofauna were analyzed in the Department of Zoology, University of Balochistan, Pakistan.

http://www.aloki.hu ● ISSN 1589 1623 (Print) ● ISSN1785 0037 (Online)
DOI: http://dx.doi.org/10.15666/aeer/2003_23652379

Statistical analysis

The data sets of individual research parameters (except for soil fauna due to pooled samples) were screened for normal distribution with D'Agostino-Pearson K2 test before analysis of variance (ANOVA). The differences between mean values of a given data set were analyzed using least significance difference test. The relationship of concentration of water soluble fluoride in soil with the concentration of fluoride in various tissues of tested vegetables was measured with Pearson correlation coefficient (Pearson's *r*). Data analysis was performed on CoStat and Microsoft Excel software.

Results

The concentration of water soluble fluorite in 0-20 cm depth of soil (sample set 1) ranged from 7.42 – 23.3 mg kg^{-1} soil and 0-10 cm depth the range was 37 – 74 mg kg^{-1} soil (sample set 2). The concentration of fluoride in leaves, fruits, stems and roots of tested crops showed positive and significant relationship with the concentration of water soluble fluoride in soil (*Figure 4*). The 17 croplands sampled had diverse cropping systems; however, almost all croplands were under mouldboard tillage practice. The application of manure with synthetic fertilizer and the addition of ash of crop residues in soil were common practices (*Table 1*). The concentration of soil organic matter varied significantly between croplands and ranged between 3.59 – 12.6 mg kg^{-1} soil (*Table 2*). The number of soil fauna m^{-2} and total number of species per cropland varied between sampling sites (*Table 3*). Total of 25 different species of soil fauna were observed (*Table 3*). The number of soil fauna m^{-2} between sampling sites ranged from 0 – 6 while number of species of soil fauna between sampling sites ranged from 0 – 8 (*Table 3*). The growth performance parameters of crops i.e. biomass, NER and PER varied significantly between croplands (*Table 4*). The lowest NER and PER were found in garden pea of Dargai F2 field, whereas the highest NER and PER were found in maize of Gulab karez 2 and chili of Mahiwal F1 fields respectively (*Table 4*). No relationship was observed between SOM and the NER and PER of crops except for garden pea of Dargai F2, which had the lowest SOM and lowest NER and PER. Likewise, no relationship was observed between number of soil fauna and species with NEW and PER of crops (*Table 5*).

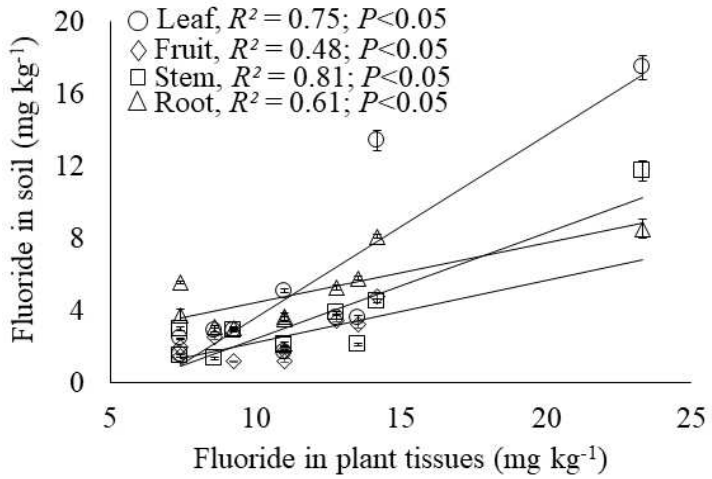

Figure 4. *Regression analysis to measure relationship between concentration of fluoride in soil and concentration of fluoride in leaves, fruits, stems and roots of tested crops*

http://www.aloki.hu ● ISSN 1589 1623 (Print) ● ISSN1785 0037 (Online)
DOI: http://dx.doi.org/10.15666/aeer/2003_23652379

Table 2. *Type of harvested crop, cropping history and fertilizer management of study sites*

Sampling villages with their names	Age (yrs)	Crop sampled and tested	Cropping history of agricultural land	Fertilizer management
Mahiwal F1	~ 50	Chili	Crop rotation, (Vegetable-cereals) fallow period for a season or year	Manure + synthetic fertilizer, deep tillage, ash of plant residues returned to field after burning for cooking
Mahiwal F2	~ 50	Cauliflower	Crop rotation, (vegetables-cereals) fallow period for a season or year	Manure + synthetic fertilizer, deep tillage, ash of plant residues returned to field after burning for cooking
Bukhara F1	> 100	Ladyfinger	Crop rotation (cereals-vegetables) fallow period for a season or year	Manure + synthetic fertilizer, deep tillage, ash of plant residues returned to field after burning for cooking
Bukhara F2	> 100	Tomato	Crop rotation, (vegetables-cereals) fallow period for a season or year	Manure + synthetic fertilizer, deep tillage, ash of plant residues returned to field after burning for cooking
Chapri F1	> 100	Chili	Crop rotation, (cereals- vegetables)	Manure + synthetic fertilizer, deep tillage, ash of plant residues returned to field after burning for cooking
Chamoos	~ 30	Chili, ladyfinger, bringel	Intercropping, crop rotation, (vegetables-cereals)	Manure + synthetic fertilizer, deep tillage, ash of plant residues returned to field after burning for cooking
Chapri F2	6 yrs	Chili	Crop rotation, (cereals-vegetables)	Synthetic fertilizer, deep tillage, ash of plant residues returned to field after burning for cooking
Mahiwal F3	~ 50	Carrot	Tree-based intercropping + crop rotation	Manure + synthetic fertilizer, deep tillage, ash of plant residues returned to field after burning for cooking
Gulab Karez F1	~ 60	Carrot	Crop rotation (cereals-vegetables)	Synthetic fertilizer, deep tillage, ash of plant residues returned to field after burning for cooking
Gulab Karez F2	~ 60	Maize	Crop rotation (vegetables-cereals)	Synthetic fertilizer, deep tillage, ash of plant residues returned to field after burning for cooking
Chinjwala	~ 60	Chili	Crop rotation (cereals-vegetables)	Manure + synthetic fertilizer, deep tillage, ash of plant residues returned to field after burning for cooking
Wahar	~ 30	Cauliflower	Crop rotation (cereals-vegetables)	Synthetic fertilizer but also amend manure every 2-3 yrs, deep tillage, ash of plant residues returned to field after burning for cooking
New Wiala	~ 20	Maize	Crop rotation	Fallow period of 2-3 yrs, synthetic fertilizer, deep tillage, ash of plant residues returned to field after burning for cooking
Baharwala	~ 30	Cauliflower	Crop rotation (vegetables-cereals)	Synthetic fertilizer, deep tillage, ash of plant residues returned to field after burning for cooking
Watagan	6	Carrot	Crop rotation (cereal-vegetables)	Synthetic fertilizer, deep tillage, ash of plant residues returned to field after burning for cooking
Dargai F1	2	Chili	Crop rotation	Synthetic fertilizer, deep tillage, ash of plant residues returned to field after burning for cooking
Dargai F2	1	Garden pea	No crop rotation	Synthetic fertilizer, deep tillage

http://www.aloki.hu ● ISSN 1589 1623 (Print) ● ISSN1785 0037 (Online)
DOI: http://dx.doi.org/10.15666/aeer/2003_23652379

Table 3. *Soil organic matter (g kg^{-1}), water soluble fluoride (mg kg^{-1} soil in 0-10 cm depth soil) and olson P (mg kg^{-1}) of soils collected from study field sites*

Field site	Vegetable	Soil type*	F	SOM	Olson P
Mahiwal F1	Chili	Loamy	43	9.34 ± 1.00^{b}	1.09 ± 0.51^{ab}
Mahiwal F2	Cauliflower	Loamy	37	7.75 ± 0.85^{b}	0.26 ± 0.58^{ab}
Bukhara F1	Ladyfinger	Sandy loam	51	3.59 ± 0.56^{e}	1.13 ± 0.32^{ab}
Bukhara F2	Tomato	Sandy loam	40	3.62 ± 0.98^{cde}	1.86 ± 1.34^{a}
Chapri F1	Chili	Sandy loam	62	12.5 ± 1.37^{a}	1.02 ± 0.65^{ab}
Chamoos	Chili, ladyfinger, eggplant	Loamy	41	7.40 ± 0.58^{b}	1.49 ± 0.66^{ab}
Chapri F2	Chili	Sandy loam	50	4.33 ± 1.28^{cde}	1.38 ± 1.33^{ab}
Mahiwal F3	Carrot	Loamy	48	6.84 ± 1.22^{bc}	1.33 ± 0.60^{ab}
Gulab Karez F1	Carrot	Sandy loam	54	6.23 ± 2.15^{bcde}	1.52 ± 0.54^{ab}
Gulab Karez F2	Maize	Sandy loam	63	7.28 ± 1.86^{b}	3.32 ± 1.29^{a}
Chinjwala	Chili	Sandy loam	68	12.6 ± 1.36^{a}	1.42 ± 0.62^{ab}
Wahar	Cauliflower	Loamy	71	10.8 ± 1.79^{ab}	2.59 ± 0.93^{a}
New Wiala	Maize	Riverbank deposits	59	5.64 ± 0.51^{cd}	0.62 ± 0.32^{b}
Baharwala	Cauliflower	Riverbank deposits	74	7.52 ± 1.54^{bc}	1.41 ± 0.39^{a}
Watagan	Carrot	Sandy loam	68	7.62 ± 0.60^{b}	1.00 ± 0.41^{ab}
Dargai F1	Chili	Loamy	63	8.77 ± 0.83^{b}	0.86 ± 0.54^{ab}
Dargai F2	Garden pea	Loamy	59	4.04 ± 068^{de}	1.00 ± 0.60^{ab}

Within column, values with different letters are significantly different at $P \leq 0.05$. *soils of all tested sites had gravels

http://www.aloki.hu ● ISSN 1589 1623 (Print) ● ISSN1785 0037 (Online)
DOI: http://dx.doi.org/10.15666/aeer/2003_23652379

Table 4. *Number of soil fauna (m^{-2}), number of fauna species and types of soil fauna found in different study field sites*

Field site (village names)	Vegetable	Number of soil fauna (m^{-2})	Total number of species	Names of animals
Mahiwal F1	Chili	6	6	*Trimeroptropis Sp., Orthoptera tetrigigae, Orthoptera tetrigigae, Acheta domesticus, Iridomyrmex purpureus,* Family-lycosidae
Mahiwal F2	Cauliflower	3.2	5	*Schistocera geregaria Trimeroptropis Sp., Iroxals afghana Iridomyrmex purpureus Euborellia annulipes*
Bukhara F1	Ladyfinger	2.0	3	*Orthoptera tetrigigae* Family-lycosidae *Iridomyrmex purpureus*
Bukhara F2	Tomato	2.0	5	*Schistocera geregaria Trimeroptropis Sp., Iroxals afghan, Orthoptera tetrigigae, Hepyllus ecclesiasticus,*
Chapri F1	Chili	4.0	6	*Euborellia annulipes, Pepsis thibse, Oniscus asellus,* Family- Carabidae, *Dysdera corocata*, Family-lycosidae
Chamoos	Chili, ladyfinger, eggplant	4.4	8	*Schistocera geregaria Orthoptera tetrigigae Iridomyrmex purpureus Euborellia annulipes Oniscus asellus, Coccinella septempuntata, Blattela germanica,* Family-lycosidae
Chapri F2	Chili	3.6	5	*Trimeroptropis sp., Iroxals afghan, Orthoptera tetrigigae Euborellia annulipes,* Order-Lepidoptera
Mahiwal F3	Carrot	2.4	4	*Trimeroptropis sp., Iroxals afghan, Orthoptera tetrigigae* Order- Lipidoptera
Gulab Karez F1	Carrot	5.2	7	*Schistocera geregaria Trimeroptropis sp., Iroxals afghana Orthoptera tetrigigae Iridomyrmex purpureus, Camponotus pennsylvanicus, Pyrgomorpha conica*
Gulab Karez F2	Maize	0	0	--
Chinjwala	Chili	0	0	--
Wahar	Cauliflower	2.8	4	*Schistocera geregaria Trimeroptropis sp., Iroxals afghana Orthoptera tetrigigae*
New Wiala	Maize	0	0	--
Baharwala	Cauliflower	4.0	7	*Schistocera geregaria Trimeroptropis sp., Iroxals afghana, Orthoptera tetrigigae, Gryllus sp.(gryllinae) Dysdera corocata, Vostox sp.*
Watagan	Carrot	5.2	6	*Trimeroptropis sp., Orthoptera tetrigigae, Coccinella septempuntata Camponotus pennsylvanicus, Agelenopsis sp., Pyrgomorpha conica*
Dargai F1	Chili	2.8	4	*Schistocera geregaria Trimeroptropis sp., Acheta domesticus, Gryllus sp.(gryllinae)*
Dargai F2	Garden pea	4.0	6	*Trimeroptropis sp., Iroxals afghan, Orthoptera tetrigigae Iridomyrmex purpureus, Camponotus consobrinus* Family-Apidae

http://www.aloki.hu ● ISSN 1589 1623 (Print) ● ISSN1785 0037 (Online)
DOI: http://dx.doi.org/10.15666/aeer/2003_23652379

Table 5. *Mean ± SD dry biomass of vegetables (t ha^{-1}), total N, total P, nutrient efficiency ratio of crops for N and P*

Sampling sites (villages with their names)	Vegetable	Dry biomass	Total N	Total P	NER	PER
Mahiwal F1	Chili	147 ± 33.4^{ab}	26.4 ± 3.9^{ab}	2.68 ± 1.2^{c}	5.6 ± 1.4^{bc}	0.71 ± 0.47^{a}
Mahiwal F2	Cauliflower	118 ± 58.9^{ab}	29.2 ± 7.5^{ab}	5.06 ± 2.9^{bc}	4.1 ± 2.2^{bcd}	0.30 ± 0.20^{abc}
Bukhara F1	Ladyfinger	88.8 ± 36.5^{b}	16.4 ± 2.1^{c}	4.36 ± 1.2^{bc}	5.3 ± 1.7^{bc}	0.23 ± 0.14^{abc}
Bukhara F2	Tomato	135.7 ± 37.6^{ab}	20.7 ± 6.6^{abc}	3.89 ± 2.2^{bc}	6.9 ± 2.1^{bc}	0.46 ± 0.34^{abc}
Chapri F1	Chili	165 ± 35.9^{ab}	23.9 ± 1.2^{b}	6.39 ± 2.5^{bc}	6.8 ± 1.1^{b}	0.31 ± 0.20^{abc}
Chamoos	Chili, ladyfinger, eggplant	123 ± 50^{abc}	20.5 ± 6.5 ^{abc}	6.46 ± 2.7^{bc}	5.9 ± 2.2^{bcd}	0.23 ± 0.14^{abc}
Chapri F2	Chili	188 ± 42.2^{ab}	28.6 ± 6.7^{ab}	5.18 ± 1.6^{bc}	6.9 ± 2.6^{bc}	0.40 ± 0.19^{abc}
Mahiwal F3	Carrot	177 ± 53^{ab}	36.1 ± 7.5^{a}	8.28 ± 5.1^{abc}	5.1 ± 1.8^{bcd}	0.39 ± 0.46^{abc}
Gulab Karez F1	Carrot	98.7 ± 32^{b}	30.8 ± 4.9^{ab}	7.04 ± 2.8^{b}	3.1 ± 0.7^{cd}	0.16 ± 0.08^{c}
Gulab Karez F2	Maize	234 ± 50^{a}	13.5 ± 1.9^{c}	5.77 ± 3.5^{bc}	17.4 ± 3.9^{a}	0.55 ± 0.28^{abc}
Chinjwala	Chili	160 ± 39.3^{ab}	25.8 ± 2.3^{ab}	3.9 ± 1.3^{bc}	6.2 ± 1.7^{b}	0.51 ± 0.42^{ab}
Wahar	Cauliflower	106 ± 50.6^{ab}	24.8 ± 10.4^{abc}	5.9 ± 3.9^{bc}	5.5 ± 4.1^{bcd}	0.32 ± 0.30^{abc}
New Wiala	Maize	100 ± 22.4^{b}	13.6 ± 1.9^{c}	4.9 ± 1.7^{bc}	7.3 ± 1.4^{b}	0.23 ± 0.12^{abc}
Baharwala	Cauliflower	123 ± 18^{b}	28.0 ± 6.6^{ab}	4.6 ± 1.5^{bc}	4.6 ± 1.4^{bcd}	0.29 ± 0.12^{abc}
Watagan	Carrot	101 ± 18.7^{b}	25.8 ± 2.9^{ab}	6.1 ± 3.1^{b}	3.9 ± 0.8^{bcd}	0.19 ± 0.09^{bc}
Dargai F1	Chili	140 ± 31.2^{ab}	25.0 ± 9.4^{ab}	6.6 ± 1.3^{b}	5.6 ± 1.3^{b}	0.21 ± 0.04^{c}
Dargai F2	Garden pea	35.8 ± 8.2^{c}	25.9 ± 10.5^{abc}	12.6 ± 2.4^{a}	1.7 ± 1.1^{d}	0.02 ± 0.01^{d}

Within column values with different letters are significantly different (P≤0.05)

http://www.aloki.hu ● ISSN 1589 1623 (Print) ● ISSN1785 0037 (Online)
DOI: http://dx.doi.org/10.15666/aeer/2003_23652379

Discussion

The concentration of fluoride in the soils ranged between 7.42 – 23.3 mg kg^{-1}; whereas, the concentration of fluoride in edible parts of vegetable crops ranged between 1.2 – 11.7 mg g^{-1} plant tissue. The data collected from the soil and vegetables of local gardens in the Kpogame and Hahotoe phosporite mining area, Togo West Africa, Tanouayi et al. (2016) reported that the concentration of fluoride in soil ranged between 5.1 – 11.2 mg g^{-1} soil. The concentration of fluoride in vegetables (eggplant, carrot, onion, cucumber, chili pepper) ranged between 1.6 – 20.6 mg g^{-1} plant tissue (Tanouayi et al., 2016). The concentration values for fluoride, in the soils of agricultural lands of our study site, are lower than the published reports. We attribute this to the fact that, soils of agricultural lands of Loralai mining sites are transported. However, because the concentration of fluoride in irrigated waters are very high (1.5 – 18.9 mg L^{-1}, data unpublished), and the possible deposition of this heavy metal from air, as has been frequently reported for other heavy metals from mining activities (Bislimi et al., 2021; He et al., 2021), these factors might be the reason of still high concentration of fluoride in soils and vegetables.

As hypothesized, concentration of fluoride in soil had a significantly positive influence on its concentration in all tissues of crops (i.e. leaf, fruit, stem and roots) (R^2 = 0.75, 0.48, 0.81 and 0.61 for leaf, fruit, stem and root tissues of crops respectively; P<0.05). Our results are consistent with published empirical evidences, which demonstrated positive relationship between the concentration of heavy metals in soil with their concentration in edible plant tissues (Avila et al., 2017; Kaninga et al., 2020, Kaninga et al., 2021; Filimon et al., 2021) including fluoride (Bhat et al., 2015). The set limit for fluoride concentration in edible parts of crops (leafy vegetables, corn and maize) by FAO/WHO is 1.5 mg kg^{-1} plant tissue (FAO/WHO, 2011). Our data show fluoride concentration in the range of 1.2 – 11.2, depending on the concentration of fluoride in soil samples. Filimon et al. (2021) found that the concentration of copper (Cu) and lead (Pb) in leafy vegetables such as celery roots, sorrel and dill, grown in the agricultural lands near Bor Copper Mining site, Eastern Serbia Europe, exceeded the safe limit of Cu 40 mg kg^{-1} plant dry weight and Pb 0.3 mg kg^{-1} plant dry weight, set by WHO/FAO. Empirical evidences support our finding that concentration of heavy metals in soil from mining activities directly increase their concentration in crops.

A negative relationship was found between concentration of fluoride and number of soil surface or soil fauna and number of ants. The sites Baharwala, Wahar and Dargai F1 had water soluble fluoride concentration as 74, 71 and 63 mg kg^{-1} soil respectively. Interestingly, in these sites, presence of ants was not observed; however, macrofauna such as *Schistocera geregaria Trimeroptropis sp., Iroxals afghan* and *Orthoptera tetrigigae* were the most common in these highly polluted soils. These species were however found in other soils also, which indicates their high tolerance to fluoride toxicity. The ants such as *Iridomyrmex purpureus*, *Camponotus pennsylvanicus* and *Camponotus consobrinus* were found in the soils of study sites Mahiwal F1, Mahiwal F2, Bukhara F1, Dargai F2, Gulab Karez F1 and Chamoos. The concentration of fluoride in these soils were 43, 37, 51, 59, 54 and 41 mg kg^{-1} soil respectively. This finding shows that these ant species can tolerate concentrations of fluoride less than 55 mg kg^{-1}. The sites such as Gulab Karez F2, Chinjwala and New Wiala had fluoride concentrations as 63, 68 and 59 mg kg^{-1} soil and no macrofauna was found, which may be due to fluoride toxicity. Our findings are in agreement to the results of Madden and Fox (1997) regarding high sensitivity of ants to fluoride concentration.

http://www.aloki.hu ● ISSN 1589 1623 (Print) ● ISSN1785 0037 (Online)
DOI: http://dx.doi.org/10.15666/aeer/2003_23652379

Soil organic matter plays an important role in the health of soil and crop growth performance (Kane et al., 2021; Wulanningtyas et al., 2021). No relationship of SOM was seen with crop growth performance. For example, two sites; Chapri F1 and Chinjwala had the highest concentration of SOM (12.5 and 12.6 mg kg^{-1} respectively) but it did not positively influence the NER or PER of crops. These sites also had high concentration of fluoride in soil (62 and 68 mg kg^{-1} soil, respectively), which may explain this result. Contrary to these sites, PER of crop of Mahiwal F1 site was significantly higher. This site had lower SOM but also had lower concentration of fluoride (43 mg kg^{-1} soil) and also had higher abundance of soil fauna. These factors may explain high crop growth performance of this site than most of other sites. The difference in NER and PER between crops and their no relationship with SOM and concentration of soil fluoride may be due to differential tolerances of crops to heavy metal toxicity (Kumar et al., 2016) besides diverse management history, irrigation water and difference in soil texture. The croplands that had loamy texture generally had the highest number of soil fauna and greater number of species of soil fauna such as Mahiwal and Chamoos croplands and the crops of these sites tend to have higher PER. Another interesting observation can be seen regarding age of a cropland. The newly grown croplands such as Chapri F2 and Dargai F2 had the lowest concentration of SOM, the lowest yield t ha^{-1} and lower NER and PER but this observation was not consistent for other new fields such as Chapri F2, Watagan and Dargai F1.

Conclusions

The concentration of fluoride in vegetables was positively related to its concentration on soil. Ants were sensitive to the high concentration of fluoride in soil. Grasshoppers, crickets, spiders and toothed earwigs were tolerant to the high concentration of fluoride. No clear relationship between concentration of fluoride in soil and crop growth performance parameters (biomass yield, NER and PER) was found. Likewise, relationship of SOM with soil fauna and crop growth performance parameters was also not observed. Future research is required to assess soil quality and crop growth performance parameters of croplands of this region, and the same needs to be done on croplands of other regions, within same climatic zone, but with no mining activity. Such study will help get an insight into influence of fluoride mining on agroecosystem processes.

Acknowledgement. We thank Agriculture Research Institute, Quetta, Balochistan, Pakistan for laboratory facilities for chemical analysis of plants.

REFERENCES

[1] Avila, P. F., Silva, E. F., Candeias, C. (2017): Health risk assessment through consumption of vegetables rich in heavy metals: the case study of the surrounding villages from Panasqueira mine, Central Portugal. – Environmental Geochemistry and Health 39: 565-589.

[2] Baligar, B. C., Fageria, N. K., He, Z. L. (2001): Nutrient use efficiency in plants. – Communications in Soil Science and Plant Analysis 32(7-8): 921-50. doi:10.1081/CSS-100104098.

http://www.aloki.hu ● ISSN 1589 1623 (Print) ● ISSN1785 0037 (Online)
DOI: http://dx.doi.org/10.15666/aeer/2003_23652379

[3] Bhat, N., Jain, S., Asawa, K., Tak, M., Shinde, K., Singh, A., Gandhi, N., Gupta, V. V. (2015): Assessment of fluoride concentration of soil and vegetables in vicinity of zinc smelter, Debari, Udaipur, Rajasthan. – Journal of Clinical and Diagnostic Research 9(10): 63-66.
[4] Bislimi, K., Halili, J., Sahiti, H., Bici, M., Mazreku, I. (2021): Effect of Mining Activity in Accumulation of Heavy Metals in Soil and Plant (*Urtica dioica* L). – Journal of Ecological Engineering 22(1): 1-7.
[5] Cottenie, R. (1980): Soil and Plant testing as a basis of fertilizer recommendations. – FAO Soil Bulletin 38(2).
[6] D'Alessandro, W., Bellomo, S., Parello, F. (2008): Fluoride speciation in topsoils of three active volcanoes of Sicily (Italy). – Environmental Geology 56: 413-423.
[7] D'Angelo, E., Crutchfield, J., Vendivere, M. (2001): Rapid, sensitive, microscale determination of phosphate in water and soil. – Journal of Environmental Quality 30: 2206-2209. doi:10.2134/jeq2001.2206.
[8] Davies, T. C. (1994): Water quality characteristics associated with fluorite mining in the Kerio Valley area of Western Kenya. – International Journal of Environmental Health Research 4: 165-175. DOI: 10.1080/09603129409356814.
[9] Djebbi, C., Chaabani, F., Font, O., Queralt, I., Querol, X. (2017): Atmospheric dust deposition on soils around an abandoned fluorite mine (Hammam Zriba, NE Tunisia). – Environmental Research 158: 153-166.
[10] Estefan, G., Sommer, R., Ryan, J. (2013): Methods of soil, plant, and water analysis: A manual for the West Asia and North Africa region. Beirut, Lebanon. – In: Sommer, R., Ryan, J. (eds.) International Center for Agricultural Research in the Dry Areas (ICARDA).
[11] FAO/WHO (2011): Summary report of the seventy-third meeting of JECFA. – Joint FAO/WHO Expert Committee on Food Additives. Geneva.
[12] Filimon, M. N., Caraba, I. V., Popescu, R., Dumitrescu, G., Verdes, D., Ciochina, L. P., Sinitean, A. (2021): Potential ecological and human health risks of heavy metals in soils in selected copper mining areas - A case study: the bor area. – International Journal of Environmental research and Public Health 18: 1516. https://doi.org/10.3390/ijerph18041516.
[13] Gao, Y., Liu, H., Liu, G. (2017): The spatial distribution and accumulation characteristics of heavy metals in steppe soils around three mining areas in Xilinhot in Inner Mongolia, China. – Environmental Science and Pollution Research 24: 25416-25430.
[14] Gil-Loaiza, J., White, S. A., Root, R. A., Solís-Dominguez, F. A., Hammond, C. M., Chorover, J., Maier, R. M. (2016): Phytostabilization of mine tailings using compost-assisted direct planting: Translating greenhouse results to the field. – Science of the Total Environment 565: 451-461. https://doi.org/10.1016/j.scitotenv.2016.04.168.
[15] He, B., Wang, W., Geng, R., Ding, Z., Luo, D., Qiu, J., Zhen, G., Fan, Q. (2021): Exploring the fate of heavy metals from mining and smelting activities in soil-crop system in Baiyin, NW China. – Ecotoxicology and Environmental Safety 207: 111234.
[16] Jones, J. B. (1991): Kjeldahl method for nitrogen determination. – Athens, GA: Micro-macro Publishing Inc.
[17] Kane, D. A., Bradford, M. A., Fuller, E., Oldfield, E. E., Wood, S. A. (2021): Soil organic matter protects US maize yields and lowers crop insurance payouts under drought. – Environmental Research Letters 16: 044018.
[18] Kaninga, B. K., Chishala, B. H., Maseka, K. K., Sakala, G. M., Lark, M. R., Tye, A., Watts, M. J. (2020): Review: mine tailings in an African tropical environment - mechanisms for the bioavailability of heavy metals in soils. – Environmental Geochemistry and Health 42: 1069-1094.
[19] Kaninga, B., Lark, R. M., Chishala, B. H., Maseka, K. K., Sakala, G. M., Young, S. D., Tye, A., Hamilton, E. M., Watts, M. J. (2021): Crop uptake of heavy metals in response to the environment and agronomic practices on land near mine tailings in the Zambian Copperbelt Province. – Environmental Geochemistry and Health 43: 3699-3713.

http://www.aloki.hu ● ISSN 1589 1623 (Print) ● ISSN1785 0037 (Online)
DOI: http://dx.doi.org/10.15666/aeer/2003_23652379

[20] Kumar, R., Mishra, R. K., Mishra, V., Qidwai, A., Pandey, A., Shukla, S. K., Pandey, M., Pathak, A., Dikshit, A. (2016): Detoxification and Tolerance of Heavy Metals in Plants. – In: Parvaiz, A. (ed.) Plant Metal Interaction. Chapter 13, Emerging Remediation Techniques, Elsevier, pp. 335-359. ISBN 9780128031582, https://doi.org/10.1016/B978-0-12-803158-2.00013-8.

[21] Limei, Z., Liao, X., Chen, T., Yan, X., Xie, H., Wu, B., Wang, L. (2008): Regional assessment of cadmium pollution in agricultural lands and the potential health risk related to intensive mining activities: A case study in Chenzhou City, China. – Journal of Environmental Sciences 20: 696-703.

[22] Madden, K. E., Fox, B. J. (1997): Arthropods as indicators of the effects of fluoride pollution on the succession following sand mining. – Journal of Applied Ecology 34: 1239-1256.

[23] Malkani, M. S. (2011): Stratigraphy, mineral potential, geological history and paleobiogeography of Balochistan Province, Pakistan. – Sindh University Research Journal (Science Series) 43: 269-290.

[24] Malkani, M. S., Mahmood, Z., Shaikh, S. I., Arif, S. J. (2017): Mineral Resources of Balochistan Province, Pakistan. – Government of Pakistan, Ministry of Petroleum & Natural Resource, Geological Survey of Pakistan. Information Release No. 1001.

[25] McQuaker, N. R., Gurney, M. (1977): Determination of total fluoride in soil and vegetation using an alkali fusion–selective ion electrode technique. – Analytical Chemistry 49: 53-56.

[26] Mendez, G. O., Zafra, D. L., Vassilev, N. B., Silva, I. R., Ribeiro, J., Costa Jr, M. D. (2014): Biochar enhances *Aspergillus niger* rock phosphate solubilization by increasing organic acid production and alleviating fluoride toxicity. – Applied and Environmental Microbiology 80: 3081-3085. doi:10.1128/AEM.00241-14.

[27] Takac, P., Szabova, T., Kozakova, L., Benkova, M. (2010): Heavy metals and their bioavailability from soils in the long-term polluted Central Spiš region of SR. – Plant, Soil and Environment 55: 167-172.

[28] Tanouayi, G., Gnandi, K., Ouro-Sama, K., Aduayi-Akue, A. A., Ahoudi, H., Nyametso, Y., Solitoke, H. D. (2016): Distribution of fluoride in the phosphorite mining area of Hahotoe–Kpogame (Togo). – Journal of Health and Pollution 6: 84-94.

[29] Wolf, B. (1982): The comprehensive system of leaf analysis and its use for diagnosing crop nutrient status. – Communications in Soil Science and Plant Analysis 3: 1035-1059. doi:10.1080/00103628209367332.

[30] Wulanningtyas, H. S., Gong, Y., Li, P., Sakagami, N., Nishiwaki, J., Komatsuzaki, M. (2021): A cover crop and no-tillage system for enhancing soil health by increasing soil organic matter in soybean cultivation. – Soil and Tillage Research 205: 104749.

[31] Zhang, C., Li, Z., Gu, M., Deng, C., Liu, M., Li, L. (2010): Spatial and vertical distribution and pollution assessment of soil fluorine in a lead-zinc mining area in the Karst region of Guangxi, China. – Plant, Soil and Environment 56(6): 282-7.

[32] Zhang, X., Zhu, Y., Zhang, Y., Liu, Y., Liu, S., Guo, J., Li, R., Wu, S., Chen, B. (2014): Growth and metal uptake of energy sugarcane (Saccharum spp.) in different metal mine tailings with soil amendments. – Journal of Environmental Sciences 26: 1080-1089. https://doi.org/10.1016/S1001-0742(13)60543-4.

http://www.aloki.hu ● ISSN 1589 1623 (Print) ● ISSN1785 0037 (Online)
DOI: http://dx.doi.org/10.15666/aeer/2003_23652379

APPENDIX

Table A1. *Coordinates of data set 1*

Sampling site	Latitude	Longitude
Tor Thana	30°26'33.6"	69°06'10.8"
Terrag	30°25'32.8"	69°03'22.9"
Kotakai	30°25'11.3"	69°02'41.4"
Chamaza	30°24'51.8"	69°02'21.4"
Saper Chamaza	30°24'40.3"	69°01'55.3"
Chijan Wa	30°24'20.2"	69°01'50.1"
Sagri	30°24'07.5"	69°01'24.6"
Shabozai	30°38'22.0"	69°12'29.9"
Mahiwal	30°37'30.0"	69°12'8.0"
Cheena Alizai	30°37'48.7"	69°11'34.2"
Nail walizai	30°38'48.8"	69°10'21.6"
Agberg	30°37'27.0"	69°09'58.1"
Cheena Alizai	30°35'42.0"	69°07'43.8"
Zarra	30°34'31.2"	69°4'16.1"
Kochan	30°32'29.8"	68°56'53.2"
Zara kalam	30°32'48.5"	68°55'57.1"
Darai	30°30'07.9"	68°56'35.2"
Marra tangi	30°28'30.7"	68°56'37.9"
Juma Killi	30°27'07.9"	69°00'50.1"
Manzaki	30°28'04.3"	69°00'37.8"
Control site 1**	31° 21' 00''	69° 34' 07''
Control site 2**	31° 21' 33''	69° 33' 59''
Control site 3**	31° 23' 10''	69° 34' 58''
Control site 4**	31° 25' 07''	69° 35' 06''
Control site 5**	31° 25' 40''	69° 35' 14''

**Duki city, Balochistan, Pakistan, 63 kilometers away from Loralai

Table A2. *Coordinates of data set 2*

Sampling site	Latitude	Longitude
Mahiwal F1	30°42'37.9"	68°98'34.1"
Mahiwal F2	30°42'36.3"	68°98'28.3"
Bukhara F1	30°41'35.1"	67°03'63.6"
Bukhara F2	30°41'32.6"	69°03'61.6"
Safar F1	30°41'90.0"	69°04'37.4"
Chamoos	30°43'02.5"	69°05'87.2"
Safar F2	30°42'29.2"	69°02'96.7"
Mahiwal F3	30°42'67.4"	69°99'49.8"
Gulab karez F1	30°39'71.1"	68°99'65.0"
Gulab karez F2	30°39'70.7"	68°99'57.1"
Chinjwala	30°40'15.1"	69°02'80.9"
Wahar	30°40'77.9"	68°96'09.5"
New wiala	30°38'47.0"	68°97'85.4"
Baharwala	30°50'91.4"	69°03'69.6"
Watagan	30°49'63.7"	69°02'97.4"
Dragai F1	30°41'83.5"	69°20'50.0"
Dragai F2	30°43'22.5"	69°19'94.9"
Mining site 1 Mahiwal	30°41'16.0"	69°00'30.1"
Mining site 2 Baharwala	30°50'47.6"	69°04'49.2"
Mining site 3 Dargai	30°41'39.7"	69°25'57.4"

http://www.aloki.hu ● ISSN 1589 1623 (Print) ● ISSN1785 0037 (Online)
DOI: http://dx.doi.org/10.15666/aeer/2003_23652379

PERFORMANCE OF HIGH YIELDING VARIETIES OF CASHEW (*ANACARDIUM OCCIDENTALE* L.) UNDER DIFFERENT PLANTING DENSITIES

JANANI, P.* – ADIGA, J. D. – MOG, B. – KALAIVANAN, D. – MEENA, R. K. – REJANI, R. – YADUKUMAR, N.

ICAR - Directorate of Cashew Research, Puttur 574202, Karnataka, India

**Corresponding author*
e-mail: jananiswetha@gmail.com; phone: +91-825-123-1530

(Received 18th Nov 2021; accepted 25th Mar 2022)

Abstract. The effect of four planting densities on plant growth and yield of nine cashew varieties in India were studied. The results revealed the significant influence of planting densities and varieties on plant growth and yield of cashew. The tree height (6.90 m) and canopy coverage (185.46%) were maximum under planting density S_4 (500 trees ha^{-1}) while density at S_1 (200 trees ha^{-1}) recorded the minimum tree height (5.86 m) and canopy coverage (77.04%). The maximum cumulative nut yield was recorded under plant densities S_4 (8.86 t ha^{-1}) and S_3 (8.19 t ha^{-1}) respectively. The variety Bhaskara under 200 trees ha^{-1} and adoption of HDP (500 trees ha^{-1}) with Ullal-3 and Bhaskara varieties could be recommended for high production until up to the 10th year of planting under the West coast conditions of Karnataka. The less vigorous varieties VRI-3 and NRCC Selection-2 are suitable for HDP. Furthermore, the present study demonstrated that the adoption of high-density planting for cashew and proper pruning practices increases the yield and net income from cashew plantation.
Keywords: *cashew, plant density, tree growth, canopy coverage, LAI and yield*

Introduction

The cashew (*Anacardium occidentale* L.), an important export-oriented high-value commodity crop was introduced into India by the Portuguese in the 16th century for afforestation and soil conservation purposes. Presently, the total production of cashew in India is 7,38,000 MT from 11.36 lakh ha of land with a productivity of 665 kg/ha (Hubballi, 2021). India exports 67,647 MT of cashew kernel and 4,605 MT of cashew nut shell liquid to over 65 countries worldwide. Cashew orchards in India are mostly characterized by widespread plantations with low-density orchards (156 to 175 trees ha^{-1}) and low productivity**.** Indian cashew industries face a shortage of raw cashew nuts due to low productivity (665 kg/ha). To meet the rising demand, India imports raw cashews worth Rs. 8,861.59 crores annually (Hubballi, 2021). Therefore, to improve the productivity of cashew, it is necessary to adopt important strategies such as the use of quality planting material, proper canopy management, integrated nutrient management and integrated pest and disease management. By adopting High Density Planting (HDP) system (500 plants ha^{-1}), the cashew yield can be increased by 2.2 compared to normal density planting (156 plants ha $^{-1}$) for the first ten years (Yadukumar et al., 2011). Varietal selection is the most critical decision in the high-density planting system (Salam, 1999). There are more than 50 varieties of cashew widely cultivated in various agroecological conditions of India (Nayak and Muralidhara, 2018). Variations in morphological and yield characteristics of cashew varieties indicate the need for a different density for different varieties for optimal yield. Beneficial effects of combining planting density with varieties have been demonstrated in mango (Gunjate et al., 2009) and almond (Kumar et

http://www.aloki.hu ● ISSN 1589 1623 (Print) ● ISSN 1785 0037 (Online)
DOI: http://dx.doi.org/10.15666/aeer/2003_23812392

al., 2012). In the light of the circumstances mentioned above, a field experiment was carried out to find out the effect of planting density on growth and yield of cashew varieties under west coast conditions to recommend the best combination of variety and planting density to realize highest returns from cashew in the first decade of plantation.

Methodology

Experimental site

This study (2006-07 to 2016-17) was conducted at the Experimental Station of ICAR-Directorate of Cashew Research (DCR), Puttur, Dakshina Kannada District, Karnataka, India (latitude 12°46′36″N, longitude 75°16′08″ and altitude 72 m above MSL) in the west coast region of India. The climate of this study site was tropical, with an annual rainfall of 3500 mm per year. The average temperature was 27.6 °C with a relative humidity of 60–70%. The soil was characterized by sandy loam with acidic pH (4.8–5.3) and available nutrients ranged from 203–247 kg ha^{-1} for nitrogen, 7.0 to 7.3 kg ha^{-1} for phosphorous and 112 to 198.0 kg ha^{-1} for potassium.

Experimental layout and treatment details

The experiment was laid out in a split-plot design consisting of four plant densities as main plot *viz*., 200 (S_1-10 m × 5 m), 236 (S_2-6.5 m × 6.5 m), 384 (S_3-6.5 m × 4 m) and 500 (S_4-5m × 4m) trees ha^{-1} and nine cashew varieties as sub-plot treatments such as T_1-VRI-3, T_2-Ullal-3, T_3-Vengurla-4, T_4-Bhaskara, T_5-Madakkathara-2, T_6- NRCC Sel-2, T_7-Vengurla-7, T_8-Ullal-1 and T_9-Dhana with three replications and nine plants per treatment. One-year-old grafts of cashew seedlings of nine varieties were planted in July 2007 at a spacing of 10 m × 5 m, 6.5 m × 6.5 m, 6.5 m × 4 m and 5 m × 4 m which gives a tree density of 200, 236, 384 and 500 trees/ha under rainfed conditions. The recommended dose of fertilizer is 500 g N, 125 g each of P and K per tree per year. During the first year of planting, 1/5 of a full dose of fertilizer was applied annually during October. Similarly, in the second, third and fourth year of planting, 2/5, 3/5 and 4/5 of the dose and from the 5th year onwards the full dose of fertilizer was applied. Lower branches of cashew trees are removed uniformly during the first 3-4 years to facilitate proper canopy shape to the plantation.

Measurements of morphological and growth parameters

The vegetative parameters (tree height, trunk girth and canopy spread) were measured on four randomly selected trees (in December 2016). The tree trunk cross-sectional area (TCSA) was calculated according to Westwood et al. (1963). The rate of canopy ground coverage was calculated according to Rejani et al. (2013) and expressed in percentage. Leaf Area Index (LAI) and light extinction coefficient (k) were measured inside the canopies of trees in four directions (east, west, north and south directions) using a canopy analyzer (CI-110, CID international, USA) between 10 AM to 12 PM during January/February of 2017.

Measurements of yield parameters

Cashew nut yield was recorded year wise from four trees in each treatment under each replication. The nuts were collected manually and separated from cashew, sun-

http://www.aloki.hu ● ISSN 1589 1623 (Print) ● ISSN 1785 0037 (Online)
DOI: http://dx.doi.org/10.15666/aeer/2003_23812392

dried for three days and weighed. The mean nut weight (g/tree) and nut yield (kg/tree) were calculated for the periods 2009-10 to 2016-17. The economics of plant densities with different varieties was calculated based on production cost and economic benefits per year.

Statistical analysis

The experimental data were analyzed using the SAS software (SAS Institute Inc., 2011). ANOVA was performed using the PROC GLM procedure of SAS. The mean differences were separated with Fisher's protected least significant difference (LSD) test at the probability ($p \leq 0.05$).

Results

The vegetative growth of different varieties under different planting densities

The results indicated that increasing plant population from 200 to 500 trees ha^{-1} had marked influences on the growth parameters of cashew (*Table 1*). Plants under HDP (S_4) recorded the highest plant height (6.90 m), which was on par with S_3 and S_2 (6.73 m and 6.59 m) whereas, the minimum plant height increment (4.68 m) was recorded in plants of S_1. The data revealed that by the 10^{th} year of planting, trees under S_1 (200 trees ha^{-1}) had a significantly lower percentage (77.04) of ground coverage by the canopy as compared to S_3 (137.08) and S_4 (185.46). The cashew varieties had a significant impact on tree height, trunk girth and TCSA, yet the interaction of plant densities x varieties had no significant influence on vegetative traits. The maximum plant height (7.95 m), trunk girth (73.08 cm) and TCSA (429.72 cm^2) were recorded with Madakkathara-2, mainly due to the inherent vigor of variety. VRI-3 recorded minimum plant height (4.68 m), trunk girth (53.79 cm), TCSA (235.00 cm^2), canopy spread (6.36 m) and ground coverage of canopy (108%) indicating its suitability for high-density planting.

Variability of LAI and k in different varieties under different densities of planting

The LAI values increased with increasing plant densities (*Table 2*). The varieties under study had a significant influence on LAI values and the highest (1.74) and lowest (1.45) LAI values were recorded in T_5 (Madakkathara-2) and T_6 (NRCC Selection-2) respectively. The data revealed the negative influence of plant densities on *k* values as it increased with decreasing plant densities (*Table 3*). Among the combinations, 200 trees ha^{-1} with Madakkathara-2 (S_1T_5) recorded the highest *k* value (0.95) and 384 trees ha^{-1} with Vengurla-7 (S_3T_7) recorded the least *k* value (0.79).

Effect of planting density and varieties on yield and benefits derived from cashew

The wide range of variation was observed for the yield of different varieties of cashew in different plant densities during the growing season (*Table 4*). Plant densities at S_3 and S_1 (384 and 200 trees ha^{-1}) recorded relatively higher nut yield which accounted for 1.51 and 1.44 t ha^{-1} respectively at 10^{th} year after planting (*Table 4*). Among the varieties, Bhaskara recorded the highest nut yield (1.65 t ha^{-1}) while it was least in NRCC Selection- 2 and VRI-3 (1.20 and 1.15 t ha^{-1}), which were on par with each other. However, the synergistic effect of plant density and varieties had no

http://www.aloki.hu ● ISSN 1589 1623 (Print) ● ISSN 1785 0037 (Online)
DOI: http://dx.doi.org/10.15666/aeer/2003_23812392

significant effect on nut yield in 10th year of planting. The effect of density on the nut yield showed significant variation during the experiment period, except in the two initial years and eighth years after planting (*Fig. 1*). The highest (8.86 t ha^{-1}) and the lowest (4.97 t ha^{-1}) cumulative nut yield up to 10th year of planting was recorded at plant densities 500 and 200 trees ha^{-1} respectively.

Table 1. *Effect of plant densities and varieties on vegetative growth of cashew at 8th harvest (10th year after planting)*

Treatments	Plant height (m)	Plant girth (cm)	TCSA (cm^2)	Canopy spread (m)	Ground coverage by canopy (%)
Spacing					
S_1	5.86 ± 1.07	64.57 ± 9.58	3364.42 ± 981.38	6.93 ± 0.86	77.04
S_2	6.59 ± 0.93	62.22 ± 6.45	3089.31 ± 621.17	7.35 ± 1.18	103.19
S_3	6.73 ± 1.00	64.76 ± 4.98	3363.25 ± 523.00	6.67 ± 0.86	137.08
S_4	6.90 ± 1.08	62.94 ± 7.09	3160.39 ± 714.77	6.81 ± 0.85	185.46
Mean	6.52	63.63	3244.34	6.94	125.69
SE (d)	0.44	3.03	307.80	2.32	16.29
LSD ($p \leq 0.05$)	0.40**	ns	ns	ns	19.06**
Varieties					
T_1	4.68 ± 0.87	53.79 ± 6.91	2317.04 ± 627.49	6.36 ± 0.59	108.00
T_2	6.94 ± 0.88	66.83 ± 5.39	3525.57 ± 571.82	7.31 ± 0.81	138.58
T_3	6.07 ± 0.51	57.29 ± 10.22	2651.22 ± 980.95	7.01 ± 1.28	129.53
T_4	6.97 ± 0.93	65.83 ± 7.44	3442.42 ± 807.38	7.16 ± 1.14	133.01
T_5	7.95 ± 1.66	73.08 ± 6.60	4236.91 ± 742.46	6.82 ± 0.76	122.52
T_6	5.73 ± 1.15	59.08 ± 9.37	2802.61 ± 914.60	6.44 ± 1.21	109.25
T_7	6.83 ± 1.14	63.21 ± 6.19	3160.07 ± 620.31	7.21 ± 0.93	134.95
T_8	6.91 ± 1.09	64.42 ± 6.58	3296.05 ± 645.08	6.93 ± 0.63	121.33
T_9	6.60 ± 0.98	69.08 ± 4.52	3767.18 ± 480.62	7.24 ± 1.09	134.05
Mean	6.52	63.63	3244.34	6.94	125.69
SE (d)	0.44	3.03	307.80	2.32	16.29
LSD ($p \leq 0.05$)	0.88**	6.05**	614.91**	ns	ns
Interaction effect for S X T (densities × varieties)					
LSD ($p \leq 0.05$)	ns	ns	ns	ns	ns

The data are represented as mean values ± standard deviation for triplicates. **Statistical significance was at 0.05 p value, ns: not significant, LSD = least significant difference at 5% level of significance

Cumulative nut yield was also significantly influenced by the varietal response. Among the varieties, T_4 (Bhaskara) recorded maximum cumulative nut yield (7.90 tha^{-1}) while a lower nut yield of 5.67 t ha^{-1} was recorded in T_1 (VRI-3) (*Fig. 2*). The highest cumulative nut yield (10.43 and 10.39 t ha^{-1}) was recorded in S_4T_2, closely followed by S_4T_4 (500 trees ha^{-1} with Ullal-3 and Bhaskara) while the lowest cumulative yield of 3.64 t ha^{-1} with S_1T_1 (200 trees ha^{-1} with VRI-3) (*Fig. 3*). T_6 and T_9 (NRCC Selection-2 and Dhana) performed better under hedgerow planting (9.13 and 8.80 t ha^{-1}) and other

http://www.aloki.hu ● ISSN 1589 1623 (Print) ● ISSN 1785 0037 (Online)
DOI: http://dx.doi.org/10.15666/aeer/2003_23812392

varieties performed better in HDP. The cumulative yield performance of the varieties also indicated that the varieties such as Ullal-3 (T_2) Bhaskara (T_4), Madakkathara-2 (T_5) and Vengurla-7(T_7) were constantly high yielding compared to other varieties

Table 2. *Effect of plant density and varieties on leaf area index (LAI)*

Treatments	T_1	T_2	T_3	T_4	T_5	T_6	T_7	T_8	T_9	Mean
S_1	1.46 ± 0.20	1.36 ± 0.07	1.34 ± 0.04	1.47 ± 0.20	1.75 ± 0.25	1.38 ± 0.09	1.62 ± 0.25	1.36 ± 0.09	1.80 ± 0.10	1.50
S_2	1.46 ± 0.08	1.55 ± 0.18	1.52 ± 0.34	1.59 ± 0.10	1.67 ± 0.08	1.54 ± 0.27	1.53 ± 0.10	1.47 ± 0.24	1.48 ± 0.11	1.53
S_3	1.46 ± 0.18	1.46 ± 0.04	1.57 ± 0.23	1.70 ± 0.05	1.89 ± 0.57	1.30 ± 0.23	1.73 ± 0.31	1.50 ± 0.17	1.55 ± 0.12	1.58
S_4	1.69 ± 0.19	1.53 ± 0.01	1.63 ± 0.04	1.57 ± 0.07	1.65 ± 0.15	1.59 ± 0.03	1.44 ± 0.02	1.58 ± 0.16	1.63 ± 0.11	1.59
Mean	1.52	1.48	1.52	1.58	1.74	1.45	1.58	1.48	1.61	1.55
		S	T	S X T						
SE (d)		0.05	0.08	0.15						
LSD ($p \leq 0.05$)		ns	0.15**	ns						

The data are represented as mean values ± standard deviation for triplicates. **Statistical significance was at 0.05 p value, ns: not significant, LSD = least significant difference at 5% level of significance

Table 3. *Effect of plant density and varieties on k (Light extinction coefficient) value*

Treatments	T_1	T_2	T_3	T_4	T_5	T_6	T_7	T_8	T_9	Mean
S_1	0.88 ± 0.08	0.90 ± 0.05	0.84 ± 0.12	0.94 ± 0.02	0.95 ± 0.03	0.82 ± 0.07	0.89 ± 0.08	0.83 ± 0.04	0.85 ± 0.04	0.88
S_2	0.84 ± 0.02	0.94 ± 0.04	0.84 ± 0.06	0.92 ± 0.02	0.91 ± 0.07	0.83 ± 0.11	0.85 ± 0.02	0.83 ± 0.06	0.90 ± 0.04	0.87
S_3	0.91 ± 0.02	0.79 ± 0.04	0.87 ± 0.06	0.83 ± 0.02	0.90 ± 0.07	0.82 ± 0.06	0.90 ± 0.10	0.91 ± 0.06	0.93 ± 0.01	0.87
S_4	0.84 ± 0.08	0.83 ± 0.02	0.90 ± 0.06	0.86 ± 0.05	0.84 ± 0.11	0.89 ± 0.05	0.81 ± 0.03	0.83 ± 0.09	0.86 ± 0.06	0.85
Mean	0.87	0.86	0.86	0.89	0.90	0.84	0.86	0.85	0.89	0.87
		S	T	S X T						
SE (d)		0.01	0.02	0.04						
LSD ($p \leq 0.05$)		ns	ns	0.09**						

The data are represented as mean values ± standard deviation for triplicates. **Statistical significance was at 0.05 p value, ns: not significant, LSD = least significant difference at 5% level of significance

The cost-benefit analysis of cashew has revealed that the highest cumulative total return of USD 5928/ha was obtained in S_4 (5 m × 4 m) with BCR of 2.54. However, the highest B:C ratio (2.77) with cumulative total return (USD 5854/ha) was recorded in S_3, followed by S_1 (2.48) (*Table 5*). Meanwhile, the maximum BCR (3.10) was obtained in normal density with Bhaskara variety (S_1T_4) followed by S_2T_4 (2.98) and the lowest 1.78 in S_1T_1 (*Table 6*).

http://www.aloki.hu ● ISSN 1589 1623 (Print) ● ISSN 1785 0037 (Online)
DOI: http://dx.doi.org/10.15666/aeer/2003_23812392

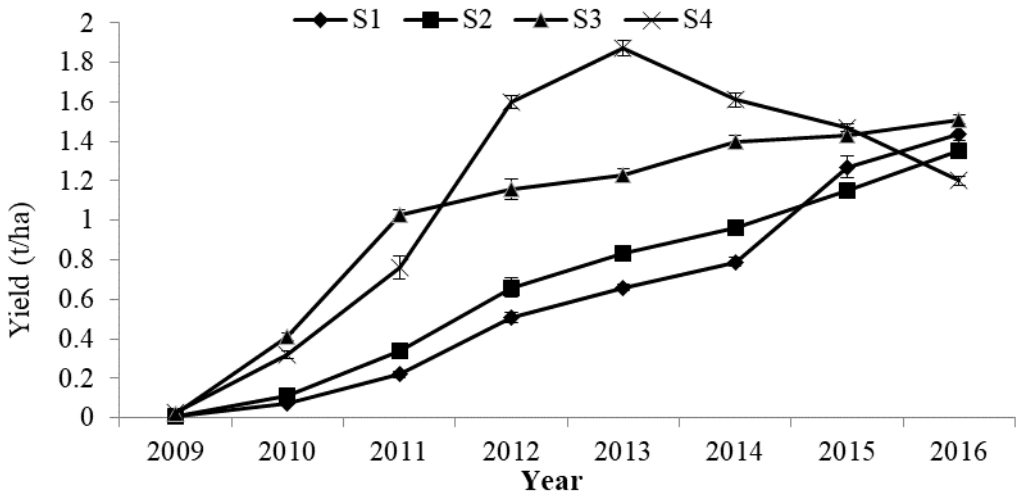

Figure 1. *Effect of plant densities on raw cashew nut yield (t ha $^{-1}$)*

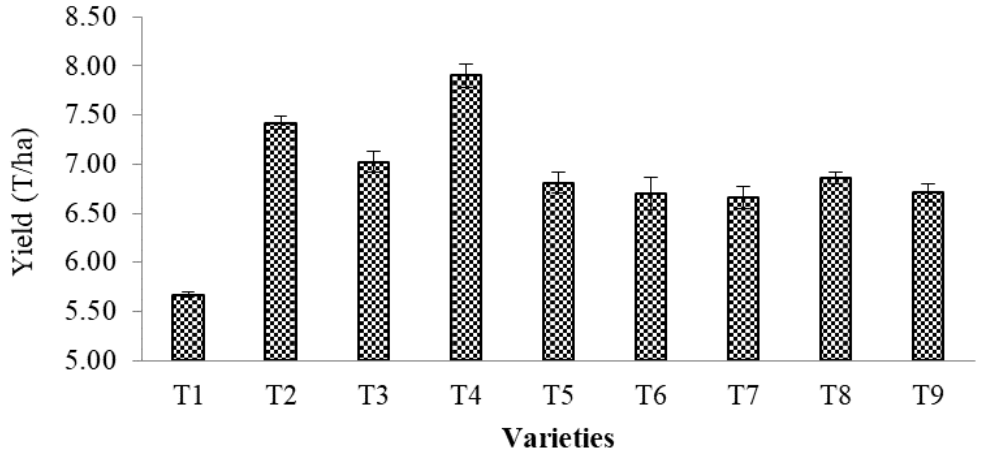

Figure 2. *Effect of varieties on cumulative nut yield (t ha^{-1}) of cashew*

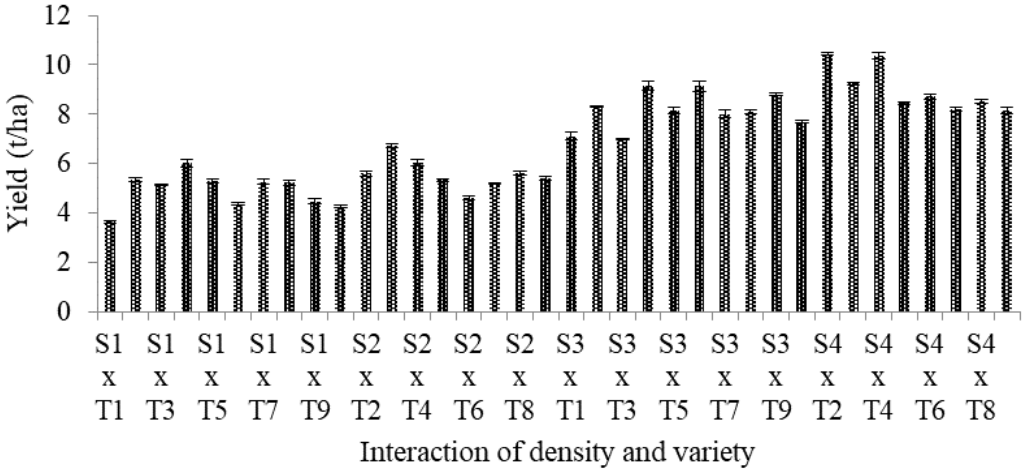

Figure 3. *Combined effect of planting densities and varieties on cumulative cashew nut yield (t ha $^{-1}$) (2009-10 to 2016-17)*

http://www.aloki.hu ● ISSN 1589 1623 (Print) ● ISSN 1785 0037 (Online)
DOI: http://dx.doi.org/10.15666/aeer/2003_23812392

Table 4. *Effect of planting density and varieties on raw cashew nut yield (t ha^{-1}) (10thyear)*

Treatments	T_1	T_2	T_3	T_4	T_5	T_6	T_7	T_8	T_9	Mean
S_1	1.09 ± 0.06	1.61 ± 0.03	1.49 ± 0.04	1.70 ± 0.04	1.59 ± 0.03	1.23 ± 0.03	1.57 ± 0.04	1.31 ± 0.06	1.33 ± 0.04	1.44
S_2	1.07 ± 0.07	1.45 ± 0.07	1.40 ± 0.02	1.71 ± 0.05	1.41 ± 0.03	1.13 ± 0.04	1.36 ± 0.05	1.37 ± 0.05	1.28 ± 0.05	1.35
S_3	1.33 ± 0.08	1.58 ± 0.33	1.44 ± 0.10	1.75 ± 0.16	1.63 ± 0.10	1.36 ± 0.14	1.51 ± 0.05	1.53 ± 0.20	1.48 ± 0.06	1.51
S_4	1.13 ± 0.22	1.28 ± 0.22	1.38 ± 0.01	1.45 ± 0.11	1.23 ± 0.20	1.10 ± 0.08	1.12 ± 0.13	1.03 ± 0.20	1.06 ± 0.02	1.20
Mean	1.15	1.48	1.43	1.65	1.47	1.20	1.39	1.31	1.29	1.37
		S		T		S X T				
SE (d)		0.03		0.05		0.09				
LSD ($p \leq 0.05$)		0.07**		0.10**		ns				

The data are represented as mean values ± standard deviation for triplicates. **Statistical significance was at 0.05 p value, ns: not significant, LSD = least significant difference at 5% level of significance

Table 5. *Economics of different plant density planting based on cumulative yield (2006-2016)*

Spacing (density)	Nut yield (t/ha)	Cost of cultivation (USD/ha)	Total return (USD/ha)	Net return (USD/ha)	BCR
S_1	4.97	2369	5873	3505	2.48
S_2	5.42	2529	6247	3718	2.47
S_3	8.19	3298	9152	5854	2.77
S_4	8.86	3853	9781	5928	2.54

Table 6. *Effect of planting density and varieties on economics of raw cashew nut cumulative yield (2006-2016)*

Treatments	BC ratio				Mean
	S_1	S_2	S_3	S_4	
T_1	1.78	1.92	2.42	2.22	2.09
T_2	2.67	2.46	2.92	2.95	2.75
T_3	2.68	2.80	2.52	2.64	2.66
T_4	3.10	2.98	2.93	2.85	2.97
T_5	2.58	2.45	2.76	2.53	2.58
T_6	2.14	2.25	2.87	2.44	2.43
T_7	2.55	2.39	2.74	2.42	2.53
T_8	2.59	2.57	2.77	2.47	2.60
T_9	2.23	2.43	2.95	2.35	2.49
Mean	2.48	2.47	2.77	2.54	

Discussion

Adopting appropriate planting density combined with high yielding varieties has been found to contribute towards a significant increase in yield per unit area. The yield

http://www.aloki.hu ● ISSN 1589 1623 (Print) ● ISSN 1785 0037 (Online)
DOI: http://dx.doi.org/10.15666/aeer/2003_23812392

of cashew in response to density depends on the choice of variety, integrated nutrient management and environmental factors (Yadukumar et al., 2001; Mini Poduval and Yadukumar, 2011; Tripathy et al., 2015a; Yuvaraj et al., 2015; Mangalassery et al., 2019). The results indicated that increasing plant population from 200 to 500 trees ha^{-1} had marked influences on the growth parameters of cashew. In the 10^{th} year, data on plant height and ground coverage by the canopy showed an increasing trend with increasing plant density. Under HDP, tree height increased to compete with one another in search of a light for photosynthesis that could be due to stem elongation and overlapping of plant canopies, reducing the penetration of light into the leaves (Policarpo et al., 2006). While a wider spacing exhibited a decrease in plant height, which is due to the maximum availability of space for the spread of plants and less competition for natural resources leading to reduced height as there was enough space for spreading of the canopy (Gaikwad et al., 2017). The relatively higher trunk girth and trunk cross-sectional area under wider spacing are due to lesser competition for natural resources, nutrients and photosynthates. A similar trend was reported by Tripathy et al. (2015a, b) and Yuvaraj et al. (2015) in cashew, Nath et al. (2007) in mango, Kundu (2007) in guava and Kumar et al. (2012) in almond**.**

During the early years, the canopy spread of the varieties under different densities recorded significant differences between the widest spacing and closer spacing (Rejani et al., 2013). The present results indicated that canopy spread did not show any significant variations which could be due to the stabilization of the canopy spread in all the treatments. A similar pattern of results was observed by Das and Jana (2012) in mango. The results revealed that under wider spacing, there is still 23% of available space for canopy growth, which indicates the possibility of obtaining a higher yield in subsequent harvests. While under HDPs, tree canopy coverage exceeded the allocated space by an additional 35% to 85%, which indicates the unsustainability of HDP system over a long period (i.e., by 10^{th} year). These findings are in accordance with the findings of Balasimha and Yadukumar (1993); Tripathy et al. (2015a, b) in cashew.

The maximum plant height, girth of collar and TCSA of the tree were recorded with the Madakkathara-2 variety (T_5), mainly due to the inherent vigor of the tree. The trees of NRC Selection-2 (T_6) and VRI-3 (T_1) varieties grew slowly and less vigorous than other varieties. The results revealed that Madakkathara-2, Bhaskara, Ulla-3 and Vengurla -7 were vigorous varieties and VRI-3 and NRCC Selection -2 were the least vigorous varieties, indicating their suitability for high-density planting. A similar variation of vegetative growth parameters was reported by Hanumanthappa et al. (2014) and Chandrasekhar et al. (2018). Yadukumar (2016) recommended that VRI-3, NRCC Selection-2, K-22-1 and Ullal-1 cashew varieties are highly suitable for HDP.

At different plant densities, LAI and *k* values were negatively related as LAI values increased with decreasing *k* values while LAI and *k* were positively related under the different varietal influence. The canopies overgrew in the allotted space under high density, which led to an overlapping of adjacent canopies, resulting in a LAI that is on par with normal density. In the present experiment, higher *k* value was associated with the low-density planting system, indicating that canopy light interception was lower than that in HDP. Similarly, previous studies reported that light extinction coefficient has decreased through plant density in guava (Kumawat et al., 2014). Yadukumar et al. (2001) observed that light interception by the canopy was approximately 70-80% which determined cashew yield. The differences in LAI among the varieties were significant due to their genetic variability. The results indicated that Madakkathara-2 and Dhana

http://www.aloki.hu ● ISSN 1589 1623 (Print) ● ISSN 1785 0037 (Online)
DOI: http://dx.doi.org/10.15666/aeer/2003_23812392

had a denser canopy with more foliage components, while NRCC Selection- 2 exhibited the least foliage component. In mango, Rajan et al. (2001) found that the variation in canopy characters of mango cultivars depended on vegetative growth, crop regularity, and growth cycle. These results provide an idea for the researcher to select varieties for optimal canopy architecture for improving photosynthetic efficiency suitable for HDP and achieving higher yields.

Cashew nut yield (t ha^{-1}) increased with an increase of plant density up to the sixth year and then decreased with a further increase in plant density. The present data indicated that during initial years in S_1, S_2 and S_3, the yield of an individual tree was low, this showed an increasing trend in subsequent years. However, in normal and medium density orchards, the yield stabilized after 7-8 years. The response of yield to plant density was not constant, as it varied according to the variety and geographical location. In the 10^{th} year, individual trees showed a high yield potential under medium and low density because there was less competition among trees for natural resources. Balasimha and Yadukumar (1993) found that photosynthesis and transpiration were higher in widely spaced trees, parallel with higher irradiances. In the present study, the highest nut yield and optimum ground coverage by the canopy and light interception were obtained in hedgerow planting. From the results, hedgerow planting (S_3) could be considered as a threshold level of cashew. The results are supported by Gaikwad et al. (2017), Kerutagi et al. (2017) Rajbhar et al. (2016) in mango, Zec et al. (2015) in peach and nectarines Kumar et al. (2012) in almond, Milosevic et al. (2008) in plum, Elkins et al. (2008) and Robinson (2010) in pear reported that the maximum yield was recorded under high plant density than traditional planting. For ten years of study, the maximum mean nut yield of 7.90 t ha^{-1} was recorded in Bhaskara, while it was least in VRI-3 (5.67 t ha^{-1}) over the years. Sundararaju et al. (2006) confirmed that Bhaskara variety performed better under normal density and HDP in the coastal region of Karnataka. The cumulative yield performance of the varieties also indicated that the varieties such as Bhaskara, Vengurla-7, Madakkathara-2 and Ullal-3 (T_4, T_7, T_5 and T_2) were constantly high yielding compared to other varieties. The present results are in agreement with the findings of Hanumanthappa et al. (2014) reported that the varieties Vengurla -7, Vengurla-4, Dhana, Ullal-1 and Ullal-3 performed better in coastal Karnataka. Similarly, Odisha conditions in BPP-8 by Dasmohapatra et al. (2012) Chandrasekhar et al. (2018) and Konkan region of Maharashtra, H-303 hybrids recorded highest nut yield (Gajbhiye et al., 2018). The synergetic effect of density and variety significantly influenced the cumulative nut yield, the highest cumulative net yield (10.43 and 10.39 t ha^{-1}) was recorded in an Ullal-3 and Bhaskara at a density of 500 trees ha^{-1}. Thus, it may be concluded that the highest cumulative yield was under HDP due to accommodating more plants and higher production per unit area. The results of present investigation corroborate the findings of Samal et al. (2006) and Tripathy et al. (2015a) under Odisha condition, Yadukumar et al. (2011), Mangalassery et al. (2019) in Karnataka; Mini Poduval and Yadukumar (2011) in West Bengal; Anon (2011) under Tamil Nadu. According to Caliskan et al. (2007), the increase in plant density decreased growth and yield per plant but an increase in productivity per unit area.

Conclusion

In the present study, planting density and varieties had a significant influence on the growth and yield of cashews. Based on observations on various aspects, it may be

http://www.aloki.hu ● ISSN 1589 1623 (Print) ● ISSN 1785 0037 (Online)
DOI: http://dx.doi.org/10.15666/aeer/2003_23812392

concluded that cashew growers can adopt the hedgerow planting system to achieve higher productivity per unit area (higher B: C ratio: 2.77) under the West coast of India. For variety- wise spacing recommendation, cultivating Dhana, NRCC Selection 2, Madakkathara-2, Ullal-1, Vengurla-7, and VRI-3 varieties under hedgerow planting (S_3) Bhaskara with low-density planting (S_1), Vengurla-4 with medium density planting (S_2) Ullal-3 under high density planting (S_4) performed better with a BCR of 2.95, 2.87, 2.76, 2.77, 2.74, 2.42, 3.10, 2.80 and 2.95 respectively. The highest cumulative nut yield ha^{-1} with the highest BCR (3.10) can be realized under low-density planting accommodating 200 plant ha^{-1} with Bhaskara variety, for 8 harvests (first decade of the plantation) in cashews under West coast conditions. In conclusion, the results showed that the selection of varieties and planting density should take into account the vigor and productivity per unit area. Strong research is needed on timing and intensity of pruning, use of dwarfing rootstocks, development of dwarf varieties that have an erect growth with lower canopy area and application of plant growth regulators need to be further investigated.

Acknowledgments. The authors are grateful to Indian Council of Agricultural Research and ICAR-Directorate of Cashew Research, Puttur, Karnataka, India for providing the financial support and necessary facilities for conducting the experiments.

Conflict of interests. The authors declare that they have no conflict of interests.

REFERENCES

[1] Anonyomus (2011): High Density Planting System in Cashew. – In: Directorate of Research, Tamil Nadu (ed.) New Crop Implements and Management Technologies. Agricultural University, Coimbatore.

[2] Balasimha, D., Yadukumar, N. (1993): Effect of plant density on photosynthesis in cashew. – Indian Journal of Plant Physiology XXXVI(1): 5-7.

[3] Caliskan, S. M., Aslan, M., Uremis, I., Caliskan, M. E. (2007): The effect of row spacing on yield and yield components of full season and double-cropped soybean. – Turkish Journal of Agriculture and Forestry 31: 147-154.

[4] Chandrasekhar, M., Sethil, Tripathy, K., Mukherjee, P. S. K., Panda, P. K., Roy, A. (2018): Performance of released cashew (Anacardium occidentale L.) varieties under hot and humid climatic zone of Odisha. – Indian Journal of Agricultural Research 52(2): 152-156.

[5] Das, B., Jana, B. (2012): Effect of canopy management on growth and yield of mango cv. Amrapali planted at close spacing. – Journal of Food, Agriculture and Environment 10(3): 328-33.

[6] Dasmohapatra, R., Rath, S., Pattnaik, A. K. (2012): Performance of cashew entries/varieties under eastern coastal plain of Odisha. – Environment and Ecology 30(3): 770-772.

[7] Elkins, R. B., Klonsky, K., DeMoura, R., DeJong, T. M. (2008): Economic evaluation of high density versus standard orchard configurations; case study using performance data for Golden Russet Bosc pear. – Acta Horticulturae 800(2): 739-746.

[8] Gaikwad, S. P., Chalak, S. U., Kamble, A. B. (2017): Effect of spacing on growth, yield and quality of mango. – Journal of Krishi Vigyan 5(2): 50-53.

[9] Gajbhiye, R. C., Pawar, S. N., Salvi, S. P., Zote, V. K., Haldavanekar, P. C. (2018): Performance of different cashew (*Anacardium occidentale* L.) genotypes under Konkan region of Maharashtra. – International Journal of Chemical Studies 6(5): 1939-1942.

http://www.aloki.hu ● ISSN 1589 1623 (Print) ● ISSN 1785 0037 (Online)
DOI: http://dx.doi.org/10.15666/aeer/2003_23812392

[10] Gunjate, R. T., Kumbhar, A. R., Thiamaiah, I. M., Amin, S. M. (2009): Growth and fruiting of some mango cultivars under high density plantation in arid conditions of Gujarat (India). – Acta Horticulturae 820: 463-467.
[11] Hanumanthappa, M., Patil, R. S., Sudhir Kamath, K. V., Vinod, V. R., Dhananjaya, B., Shankar, M. (2014): Performance of different cashew cultivars in coastal Karnataka. – Environment and Ecology 32(3): 891-895.
[12] Hubballi, N. V. (2021): Cashew Development in India - Challenges and Opportunities. – In: Souvenir of National Conference on Cashew Development in India "Challenges and Opportunities," Panaji, Goa, pp. 9-14.
[13] Kerutagi, M. G., Deshetti, M. B., Abhilash, K. (2017): Comparative economics of traditional *viz* high density mango cultivation in Karnataka. – Asian Journal of Agricultural Extension, Economics and Sociology 18(3): 1-12.
[14] Kumar, D., Ahmed, N., Verma, M. K. (2012): Studies on high density planting in almond in Kashmir valley. – Indian Journal of Horticulture 69(3): 328-32.
[15] Kumawat, K. L., Sarolla, D. K., Kaushik, R. A., Jodha, A. S. (2014): Effect of different spacing on newly planted guava cv. L-49 under high density planting system. – African Journal of Agricultural Research 9(51): 3729-3735.
[16] Kundu, S. (2007): Effect of High Density Planting on Growth, Flowering and Fruiting of Guava (*Psidium guajava* L.). – In. Singh, G., Kishun, R., Chandra, E. (eds.) Proceedings of the First International Guava Symposium. Acta Horticulture 735: 267-270.
[17] Mangalassery, S., Rejani, R., Singh, V., Adiga, J. D., Kalaivanan, D., Rupa, T. R., Prabha, S. P. (2019)**:** Impact of different irrigation regimes under varied planting density on growth, yield and economic return of cashew (*Anacardium occidentale* L.). – Irrigation Science 37: 483-494.
[18] Milosevic, T., Zornic, B., Glisic, I. (2008): A comparison of low-density and high-density plum plantings for differences in establishment and management costs, and in returns over the first three growing seasons - a mini-review. – Journal of Horticultural Science and Biotechnology 83(5): 539-542.
[19] Minipoduval, Yadukumar, N. (2011): Effect of different doses of fertilizers on different densities of cashew plantation. – Journal of Plantation Crops 39: 35-40.
[20] Nath, V., Das, B., Rai. M. (2007): Standardization of high-density planting in mango (*Mangifera indica* L.) under sub-humid Alfisols of Eastern India. – Indian Journal of Agricultural Sciences 77: 3-7.
[21] Nayak, M. G., Muralidhara, B. M. (2018): Cashew Varieties: Recent Developments in India. – In: Handbook of Cashew, pp. 11-13.
[22] Policarpo, M., Talluto, G., Bianco, R. L. (2006): Vegetative and productive responses of 'Conference' and 'Williams' pear trees planted at different in-row spacing's. – Scientia Horticulture 109: 322-331.
[23] Rajan, S., Ram Kumar, Negi, S. S. (2001): Variation in canopy characteristics of mango (*Mangifera indica* L.) cultivars from diverse eco-geographical regions. – Journal of Applied Horticulture 3(2): 95-97.
[24] Rajbhar, Y. P., Singh, S. D., Lal, M., Singh, G., Rawat, P. L. (2016): Performance of high density planting of mango (*Mangifera indica* L.) under a mid-western plain zone of Uttar Pradesh. – Indian Journal of Agricultural Sciences 12: 298-301.
[25] Rejani, R., Adiga, J. D., Yadukumar, N. (2013): Performance of different varieties of cashew under high density planting system. – Journal of Plantation Crops 41(1): 28-33.
[26] Robinson, T. L. (2010): High-density pear production: an opportunity for NY growers. – New York Fruit Quarterly 18: 5-9.
[27] Salam, A. M. (1999): Cashew and pepper live in harmony. – The Cashew 13(3): 54-55.
[28] Samal, S., Lenka, P. C., Rout, G. R. (2006): Evaluation of cashew varieties under Bhubaneswar condition for major plant characters and nut yield. – The Cashew 2: 8-13.
[29] SAS Institute Inc. (2011): SAS Statistical Software. – SAS Institute Inc., Cary.

http://www.aloki.hu ● ISSN 1589 1623 (Print) ● ISSN 1785 0037 (Online)
DOI: http://dx.doi.org/10.15666/aeer/2003_23812392

[30] Sundararaju, D., Yadukumar, N., Shivarama Bhat, P., Raviprasad, T. N., Venkattakumar, R., Sreenath Dixit. (2006): Yield performance of Bhaskara cashew variety in coastal Karnataka. – Journal of plantation crops 34(3): 216-219.
[31] Tripathy, P., Sethi, K., Patnaik, A., K., Mukherjee, S. K. (2015a): Nutrient Management in High-Density Cashew Plantation under Coastal Zones of Odisha. – International Journal of Bio-resource and Stress Management 6(1): 93-97.
[32] Tripathy, P., Sethi, K., Patnaik, A., K., Mukherjee, S. K., Saroj, P. L. (2015b): Efficacy of plant density and nutrient management in cashew (*Anacardium occidentale* L.). – Progressive Horticulture 47(2): 2015213-217.
[33] Westwood, M. N., Reimer, F. C., Quackenbush, V. L. (1963): Long term yield as related to ultimate tree size of three pears varieties grown on rootstocks of five *Pyrus* species. – Proceedings of the American Society for Horticultural Science 82: 103-8.
[34] Yadukumar, N. (2016): High Density and Ultra-High Density in Cashew - Merits and Demerits. – In: Souvenir of National Conference on Cashew and Cocoa: Production to Marketing, Panaji, Goa, pp. 4507-4508.
[35] Yadukumar, N., Bhaskara Rao, E. V. V., Mohan, E. (2001): High density planting of cashew (*Anacardium occidentale* L.). – Tropical Agriculture 78(1): 19-28.
[36] Yadukumar, N., Rejani, R., Rupa, T. R., Srividya, B. R. (2011): Optimal nutrient requirement and plant density for enhancing cashew productivity. – Journal of Plantation Crops 30(1): 26-29.
[37] Yuvaraj, K. M., Reddy, M. L. N., Umamaheswararao, K. (2015): Nutrient management in high density cashew plantation under coastal sandy soils of Andhra Pradesh. – Advances in Life Sciences 4(1): 26-28.
[38] Zec, G., Solic, S., Vulic, T., Milatovic, D., Djordjevic, B., Djurovic, D., Velickovic, M. (2015): Influence of planting density on yield of peach and nectarine. – In: Fifth International Scientific Agricultural Symposium, University of East Sarajevo, Faculty of Agriculture, Jahorina, pp. 204-208.

http://www.aloki.hu ● ISSN 1589 1623 (Print) ● ISSN 1785 0037 (Online)
DOI: http://dx.doi.org/10.15666/aeer/2003_23812392

DISTRIBUTION OF HEAVY METALS (Pb, Zn, Cu, Cd AND Cr) FORM THE SOURCE OF THE PEARL RIVER, CHINA

YAN, Y. H.[1] – TANG, L. Z.[1] – DING, X. M.[2] – PENG, L. J.[1] – LI, Q.[1,3*]

[1]*School of Biological Resources and Food Engineering, Qujing Normal University, Qujing, Yunnan 655000, China*

[2]*School of Ecology and Environmental Science, Yunnan University, Kunming, Yunnan 650500, China*

[3]*Key Laboratory of Yunnan Province Universities of Qujing Natural History and Early Vertebrate Evolution，Qujing Normal University, Qujing, Yunnan 655000, China*

[*]*Corresponding author*
e-mail: LQ@mail.qjnu.edu.cn; phone: +86-183-1398-1795

(Received 22nd Nov 2021; accepted 15th Feb 2022)

Abstract. The present paper has a research on the distribution and bioaccumulation of heavy metals (Pb, Zn, Cu, Cd and Cr) in the water, sediments, and three endemic fish species from the Huashan Reservoir, source of the Pearl River. The results showed that the water of Huashan Reservoir was under the grade II standard for most of the heavy metals according to the national environmental quality standard for surface water (GB3838-2002) launched by the State Environmental Protection Administration of China, and the metal concentrations of most surface sediments have exceeded the background values of the local soil in Yunnan Province. Furthermore, the Pb, Zn, Cu, Cd and Cr content in the sediment cores increased abruptly around early 1970s. Notably, most metals in all collected fish in this study didn't exceed the safety thresholds according to the national standards. Finally, the results found that the concentrations of heavy metals in the muscles of three fishes were all safe for human consumption, and the mean concentration in the fish organs followed the sequence of liver>gill>muscle.
Keywords: *Huashan Reservoir, heavy metals, water sediment, endemic fish*

Introduction

Heavy metals are normal constituents of the environment and widely present in aquatic ecosystems on a global scale. The heavy metal pollutions of rivers and reservoirs mainly come from the sewage discharge (Frascareli et al., 2018; Lan et al., 2019). Besides, geochemical structure, mining activity, metal smelting, industrial wastes, incineration of garbage and urban sewage discharge create potential sources of heavy metal pollution in the water bodies, too (Kumar et al., 2019; Kostka and Leśniak, 2020; Zhou et al., 2020). Heavy metals are deposited, assimilated or incorporated in water, sediments which can't be degraded by aquatic animals due to their chemical properties (Sobhanardakani et al., 2018; Debnath et al., 2021). Heavy metals will enter and accumulate in the food chain and they are non-biodegradable, persistent and potentially accumulated in organisms, causing extremely harmful to human bodies (Li et al., 2014; Isangedighi and David, 2019). Once above bioavailable threshold levels, they become toxic to human bodies (Ali et al., 2019; Singh et al., 2020).

Despite many municipal sewage treatments were established, water bodies and sediments are continuously being loaded with a large number of heavy metals. Especially the external physicochemical conditions might affect the enrichment of heavy metals in the sediments (Tian et al., 2020; Miranda et al., 2021). Sediments are significant sinks of heavy metals in the aquatic environment, but the heavy metals will release from sediments to the water bodies with the environment changed, leading the sediments as a monitor of the aquatic ecosystems

http://www.aloki.hu ● ISSN 1589 1623 (Print) ● ISSN1785 0037 (Online)
DOI: http://dx.doi.org/10.15666/aeer/2003_23932407

(Al-Edresy et al., 2019; Ayodele et al., 2021). Sediment cores can provide an archive of environmental changes and show temporal and spatial differences in the concentrations of different heavy metals (Liu, R. et al., 2019; Liu, H. et al., 2022). Determining heavy metal content in water or sediments only can not provide information on heavy metal bioaccumulation or biomagnification. So clarifying the concentrations of heavy metal in sediment cores can provide a valuable historical record of heavy metal contamination.

Fish often accumulate large amounts of heavy metals from the water. Fish is not only long-living and absorb a variety of pollutants over time, but also normally occupy high positions in aquatic trophic webs so that they can be used as a biomonitor of heavy metal contamination, too (Kumar et al., 2020; Łuczyńska et al., 2020; Abu Shnaf et al., 2021). Fish optimally reflect the consequences of heavy metal pollution in the water (Adams et al., 1992; Merciai et al., 2014; Rajeshkumar and Li, 2018). Heavy metals can be classified as toxic (e.g., lead, cadmium and chromium) or essential (e.g., copper, zinc) for living organisms, but essential metals are toxic with a higher concentration (Munoz-Olivas and Camara, 2001). For this reason, to evaluate the potential risk to human health of fish consumption, determining the content of heavy metals in fish is extremely necessary (Buffle and DeVitre, 1993; Xie et al., 2020).

The study of heavy metal accumulation in fish tissues (muscle, liver and gills) is therefore interesting in assessing pollutions in natural water bodies. These tissues in fish were chosen because of that (1) the muscle was selected for its importance in case of fish consumption by humans; (2) liver is a crucial organ in the metabolism and storage of metals (Miller et al., 1992); (3) the gills reflect the metal levels in the water since they are the primary sites of gas exchange, acid-base regulation and ion transfer (Salem et al., 2014).

Pearl River is the third largest river in China, derived from southern Maxiong Mountain in Qujing, with an elevation of 1998 m, and then flows through the Huashan Reservoir. The Huashan Reservoir was finished in 1958, and the capacity of the reservoir was 80 million cubic meters. Nanpan River, the first stream upriver from the Pearl River, will cutoff if the Huashan Reservoir dries up. The local people have developed the fish farm in this reservoir; the *Cyprinus carpio*, *Carassius auratus* and *Anabarilius alburnops* can be found here easily. But there are many large chemical plants around the Huashan Reservoir. The annual production value of the industrial parks is nearly 50 billion. So there may be some heavy metal pollution in the reservoir. This area is important not only for the local people but also for the whole Pearl River basin. However, no research has been conducted on the distribution and behavior of metals in this area. In addition, the potential health risk should be concerned for intaking the endemic fish for local people. In a word, the line of study is lacking, specifically in the source of Pearl River.

The present study indicated Lead (Pb), Zinc (Zn), Cuprum (Cu), Cadmium (Cd) and Chromium (Cr) concentrations in water, sediments and some endemic fish (*Cyprinus carpio*, *Carassius auratus* and *Anabarilius alburnops*) in water of Hushan Reservoir. It should be noted that these fish species are considered an essential part of the diet in this region.

Material and methods

Collection of water and sediment samples

Water samples and sediment core samples were collected from 8 sites across the reservoir in June 2019. The coordinates of sampling were recorded with a global position system (*Table 1, Figure 1*). Water samples were collected with 4 L amber glass bottles. Nitric acid (1% by volume) was immediately added into the samples to suppress the metals binding with the container wall. Sediment core samples were collected up to a depth of 110 cm by a sampling

http://www.aloki.hu ● ISSN 1589 1623 (Print) ● ISSN1785 0037 (Online)
DOI: http://dx.doi.org/10.15666/aeer/2003_23932407

vessel with a stainless steel gravity corer (*Figure 2*). The core was sectioned into twenty-two and finished at 5 cm intervals with a pre-cleaned stainless steel knife. All of the sectioned sediment core samples were placed into the labeled and sealed plastic pack, respectively. Both water and sediment core samples were placed into ice-packed coolers and transported to the laboratory as soon as possible. Water samples were refrigerated at 4°C until analysis, while sediment core samples were frozen at -35°C for further analysis.

Table 1. *GPS sites of water samplings and core samples in Huashan Reservoir*

Location	X (Longitude)	Y (Latitude)
C1	103.9158	25.7895
C2	103.9181	25.7826
C3	103.9210	25.7769
C4	103.9212	25.7710
C5	103.9024	25.7670
C6	103.9110	25.7674
C7	103.9314	25.7690
C8	103.9387	25.7755

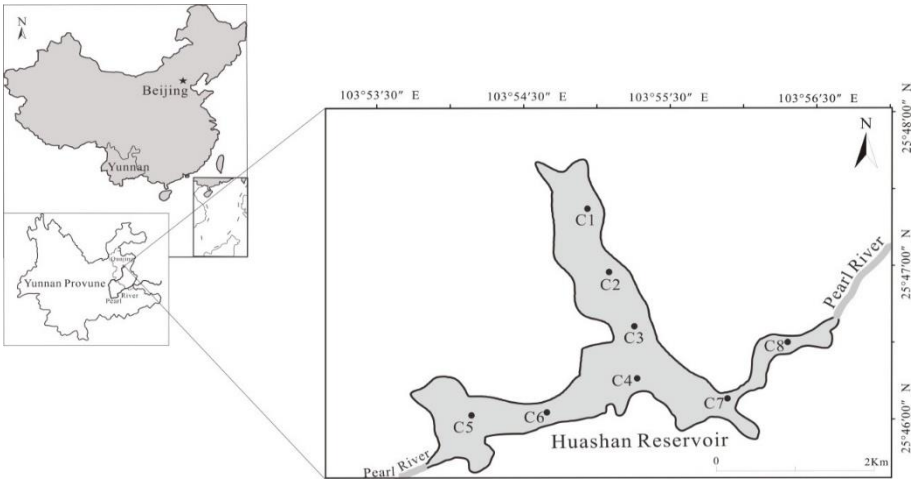

Figure 1. *Water and sediment core sampling sites in the Huashan Reservoir*

Collection of fish samples

Fish samples were collected from local fishermen across the reservoir, after they had been interviewed to ensure that the species had been caught in the area of interest for this study. Fish species were selected for analysis basing on several considerations (Keith et al., 2001) and considering the availability in the food chain from sampling sites, including their size (weight), migratory behavior and placement. As the fish species were meant to represent an area within a reservoir, fewer migratory species were preferred (Liu et al., 2011). Fish species analyzed in this paper include carp (*Cyprinus carpio,* body length 14.0-28.3 cm and body weight 98.0-507.5 g), crucian carp (*Carassius auratus,* body length 9.5-15.6 cm and body weight 56.2-211.0 g) and silvery minnow (*Anabarilius alburnops,* body length 5.3-6.8 cm and body weight 15.4-116.0 g), which were common in the reservoir and placed in the same position in the food chain. A total of 102 specimens, representing 3 species, were collected from six sites. Fish was immediately placed in coolers with ice and carried to the laboratory for sample preparation. All

http://www.aloki.hu ● ISSN 1589 1623 (Print) ● ISSN1785 0037 (Online)
DOI: http://dx.doi.org/10.15666/aeer/2003_23932407

the equipment used for sample collection, transportation and preparation were free from contamination. The data of analyzed fish from each site were presented in *Table 2*.

Table 2. *Data of analyzed fish from Hushan Reservoir*

Species	Sampling sites					
	Huashan Town (F1)	The estuary of Nanpan River (F2)	Around the area of China Xuantian Grade I Road (F3)	Industrial Park (F4)	The East of Huashan Reservoir (F5)	The East of Huanshan Town (F6)
carp	5	6	7	4	7	6
crucian carp	7	5	3	5	3	4
silvery minnow	8	9	5	7	6	5

Chemicals and apparatus

All solvents in this study were of pure analytical grade or pure chromatographic grade. The standard stock solutions (1,000 μg ml^{-1}) of Pb, Zn, Cu, Cd and Cr were used. Solutions for standard curve preparation were made by appropriate dilution prior to use. All the plastic containers and glassware were soaked in dilute nitric acid (1+9) and rinsed with distilled water before use.

Microwave-assisted extraction was performed by ETHOS 1 advanced microwave extraction system (Milestone, Italy) equipped with a 12-sample tray and temperature control system. A flame/graphite atomic absorption spectrometer (AAFS, Varian Instruments AA240; Varian, America) was used for sample analysis in this study.

Sample preparation and analysis

Water samples were taken on-site and immediately measured for pH using Microwave-assisted extraction equipment (Milestone, Italy). Water samples were filtered through Millipore 0.45 μm glass fiber filters (Billerica, MA, USA) to remove algae, zooplankton, and suspended particles and then stored at 0-4 ºC. After that 15 ml water samples were digested with 2 ml of concentrated HNO_3 (65%) and 1 ml H_2O_2 (30%) at 180ºC for 10 min. A blank digestion was carried out in the same way.

Sediment samples were freeze-dried and passed through a 1 mm clean plastic sieve to remove shell fragments. Sieved sediments were ground with an agate mortar until all particles passing a 100-mesh nylon sieve (pore diameter: 0.147 mm). For the total content determination of heavy metals in sediments, our previous report about microwave-assisted digestion (MAD) procedures with some modifications was adopted (Li et al., 2014). Firstly, 0.2 g sediment samples were digested with 4 ml HNO_3 (65%), 2 ml H_2O_2 (30%) and 1 ml HF (40%) at 200 ºC for 5 min. It took 26 minutes to accomplish the set program process. A blank digestion process was carried out in the same way. After cooling, the supernatant was separated from the solid phase by filtration and then diluted into a colorimetric cylinder until the requisite volume arrived with double deionized water (Milli-Q Millipore 18.2 M cm^{-1} resistivity) (Liu et al., 2012). Eight sediment samples were subjected to three technical replications. The dating of the sediment samples was extrapolated utilizing a 137Cs chronology, which refers to the magnitude of 137 Cs activity having two peaks at all core sampling points. This procedure provides the possibility of calculating sedimentation rates from 1963-1986 and 1986 to the present (Xue et al., 2007).

Total nitrogen (TN) and total phosphorus (TP) was measured using potassium persulfate digestion-UV spectrophotometric method (GB11894-89, GB11893-89). An oxidising agent is

http://www.aloki.hu ● ISSN 1589 1623 (Print) ● ISSN1785 0037 (Online)
DOI: http://dx.doi.org/10.15666/aeer/2003_23932407

added to the water, and after the oxidation is completed, the oxidised solution is subjected to an atomic absorption spectrometer for colorimetric measurement of total nitrogen and total phosphorus.

For the determination of heavy metals, after the samples were collected, the water samples were firstly digested with a combination of HNO_3-H_2O_2 acid system and elevated temperature; For the sediment, a certain amount of sediment was first taken, wrapped in aluminium foil and placed in an oven and dried at 105ºC. After drying, the sediment was grounded and passed through a 100 mesh sieve, and the soil samples were retained by the quadratic method. The sediment sample was weighed to 0.1 g and subjected to microwave digestion using a combined HNO_3-H_2O_2 acid system and elevated temperature. The water and sediment were determined using atomic absorption for Pb, Zn, Cu, Cd and Cr.

Fish was killed in a lethal dose of anesthetic (MS-222) and dissected with a clean scalpel blade to separate the tissues from the bones. Muscles of some individuals were dissected, pooled, homogenized and freeze-dried (Eyela FDU-1200, Japan) for four days. Each organ tissue was homogenized and kept separately. Due to their small size (< 12 cm), they only separate muscles of silvery minnow*s* and internal organs. After lyophilization, the samples were ground to powder, sieved to1 mm, and then stored in the sealed plastic pack at room temperature until digestion. 1 g dry fish samples were digested with 6 ml HNO_3 (65%) and 2 ml H_2O_2 (30%) in a microwave digestion system and diluted to 10 ml with double deionized water (Milli-Q Millipore 18.2 M cm^{-1} resistivity) (Liu et al., 2012). The digestion conditions for the microwave system were applied as 2 min for 250 W, 2 min for 0 W, 6 min for 250 W, 5 min for 400 W, 8 min for 550 W, vent: 8 min, respectively. A blank digest was carried out the same way (Tuzen, 2009).

Pb, Zn, Cu Cd and Cr levels in the water sediments, and fish tissues were measured by a flame/graphite atomic absorption spectrometer (AAFS, Varian Instruments AA240, Varian America). All the samples were analyzed as soon as possible.

Statistical analysis

All statistical analyses were conducted by IBM SPSS (Statistical Product and Service Solutions) Statistics, 5 Version 20.0. One-way analysis of variance (ANOVA) was implemented to test the differences between all sites for each water, sediment and fish. The relationships between metal concentrations and other water chemistry variables were explored with Spearman's rank correlation analysis (rho). A one-way ANOVA also compared differences in mean metal concentrations between different species, tissues and locations. Multiple comparisons were conducted using Tukey's Honestly Significant Difference test (HSD) by the program of ANOVA. Differences were considered significant if $P<0.05$, and all data were expressed as means ± standard error.

Results

Water and surface sediment

The concentrations heavy metals in water from the Huashan Reservoir were shown in *Table 3*. The concentrations of Pb, Zn, Cu, Cd and Cr in water were 14.33 ± 0.60-46.31 ± 2.07 μg L^{-1} (mean, 32.59 μg L^{-1}), 214.78 ± 1.51-491.72 ± 3.50 μg L^{-1} (mean, 370.23 μg L^{-1}), 84.15 ± 1.75-126.36 ± 2.54 μg L^{-1} (mean, 105.32 μg L^{-1}), 1.02 ± 0.22-3.22 ± 0.12 μg L^{-1} (mean, 1.94 μg L^{-1}) and 86.72 ± 5.28-127.83 ± 2.90 μg L^{-1} (mean, 112.29 μg L^{-1}), respectively. The heavy metal concentrations in water have a big difference in different locations (ANOVA, $p<0.001$).

http://www.aloki.hu ● ISSN 1589 1623 (Print) ● ISSN1785 0037 (Online)
DOI: http://dx.doi.org/10.15666/aeer/2003_23932407

Table 3. *Water quality and mean heavy metal concentrations (μg L^{-1} ± standard deviation) at each sampling site surveyed in Huashan Reservoir. Grade II standards of the environmental quality standards for surface water in China (GB3838-2002) was also included. The letters (a, b, c, d, e, f) group sites by heavy metal, considered homogenous at $p<0.05$*

Location	C1	C2	C3	C4	C5	C6	C7	C8	Environmental quality standard (Grade II)
Water depth(m)	4.56	5.20	4.80	5.80	5.10	4.00	5.10	3.60	-
Temperature(°C)	22.5	22.0	22.1	21.9	22.0	22.7	22.5	22.3	-
pH	7.79	7.67	7.74	7.87	7.83	8.04	8.01	7.85	6-9
Total phosphorus(mg L^{-1})	0.243	0.171	0.208	0.203	0.178	0.216	0.208	0.176	≤0.025
Total nitrogen(mg L^{-1})	2.26	2.56	2.66	2.64	2.64	3.17	2.67	2.47	≤0.5
Pb(μg L^{-1})	36.58 ± 2.03^{ab}	20.96 ± 1.84^{c}	46.31 ± 2.07^{d}	42.84 ± 1.82^{bd}	44.85 ± 3.50^{d}	33.62 ± 3.13^{a}	14.33 ± 0.60^{e}	21.22 ± 1.62^{c}	≤10
Zn(μg L^{-1})	466.77 ± 4.86^{a}	491.72 ± 3.50^{b}	355.92 ± 3.43^{c}	316.48 ± 3.41^{d}	384.02 ± 4.07^{e}	345.22 ± 4.08^{f}	214.78 ± 1.51^{g}	386.97 ± 1.56^{e}	≤1000
Cu(μg L^{-1})	93.20 ± 1.88^{a}	105.28 ± 5.20^{b}	84.15 ± 1.75^{c}	125.34 ± 3.06^{d}	107.20 ± 1.83^{b}	100.43 ± 4.94^{ab}	100.58 ± 0.88^{ab}	126.36 ± 2.54^{d}	≤1000
Cd(μg L^{-1})	2.78 ± 0.09^{ab}	3.22 ± 0.12^{b}	1.62 ± 0.09^{c}	2.54 ± 0.34^{a}	1.56 ± 0.23^{c}	1.45 ± 0.05^{cd}	1.02 ± 0.22^{d}	1.36 ± 0.13^{cd}	≤5
Cr(μg L^{-1})	105.73 ± 0.85^{a}	127.83 ± 2.90^{b}	115.89 ± 3.46^{c}	113.48 ± 2.75^{ac}	115.26 ± 3.98^{ac}	118.25 ± 2.18^{bc}	86.72 ± 5.28^{d}	115.19 ± 3.87^{ac}	≤50

Table 4. *Surface sediment mean heavy metal concentrations (mg kg^{-1} dw ± standard deviation) at 8 sites surveyed in Huashan Reservoir. Heavy metal background values in soils from Yunnan Province (State Environmental Protection Agency Administration of China, 1990) was also included. The letters (A, B, C, D, E, F) group sites by environmental variable, considered homogenous at $p < 0.05$*

Location	C1	C2	C3	C4	C5	C6	C7	C8	Background value
Pb(mg kg^{-1})	75.03 ± 4.42^{A}	96.18 ± 3.39^{B}	98.10 ± 4.19^{B}	111.76 ± 7.51^{BC}	112.13 ± 7.05^{BC}	100.90 ± 8.69^{BC}	119.13 ± 6.36^{CD}	135.37 ± 8.01^{D}	26.2
Zn(mg kg^{-1})	210.18 ± 6.02^{A}	225.04 ± 3.27^{A}	165.39 ± 5.59^{B}	172.42 ± 6.71^{B}	190.09 ± 9.87^{C}	189.66 ± 5.51^{C}	157.67 ± 8.55^{B}	171.80 ± 5.71^{B}	88.4
Cu(mg kg^{-1})	118.26 ± 2.16^{AD}	104.96 ± 5.00^{ABC}	120.73 ± 3.96^{D}	115.46 ± 5.06^{ABD}	193.30 ± 6.12^{E}	102.09 ± 7.10^{BC}	99.97 ± 8.05^{C}	86.59 ± 5.71^{F}	35.1
Cd(mg kg^{-1})	2.21 ± 0.09^{ABC}	2.54 ± 0.08^{BC}	2.09 ± 0.14^{ABD}	2.29 ± 0.14^{ABC}	2.33 ± 0.24^{ABC}	2.58 ± 0.08^{C}	1.68 ± 0.31^{D}	1.86 ± 0.09^{AD}	0.28
Cr(mg kg^{-1}))	134.39 ± 5.16^{A}	148.80 ± 3.68^{B}	132.68 ± 4.06^{AC}	122.62 ± 5.42^{ACD}	127.00 ± 6.08^{AC}	123.78 ± 4.34^{ACD}	110.51 ± 9.45^{D}	119.70 ± 10.65^{CD}	58.6

http://www.aloki.hu ● ISSN 1589 1623 (Print) ● ISSN1785 0037 (Online)
DOI: http://dx.doi.org/10.15666/aeer/2003_23932407

Compared to all sites, the highest values of Zn, Cd and Cr were observed at site C2 ($p<0.05$), and the highest values of Cu were observed at site C8 ($p<0.05$). Total phosphorus concentration was also positively related to total nitrogen concentration in water ($r=0.808$, $p=0.015$). In addition, pH was some negatively related to all metal concentrations in water ($r<-0.454$, $p<0.258$), with the exception of Cu ($r=0.147$, $p=0.05$) and Pb ($r=-0.039$, $p=0.928$).

The heavy metal concentrations of surface sediments from the Huashan Reservoir were shown in *Table 4*. The concentrations of Pb, Zn, Cu, Cd and Cr in surface sediments were 75.03 ± 4.42-135.37 ± 8.01 mg kg^{-1} (mean, 106.07 mg kg^{-1}), 157.67 ± 8.55-225.04 ± 3.27 mg kg^{-1} (mean, 185.28 mg kg^{-1}), 86.59 ± 5.71-193.30 ± 6.12 mg kg^{-1} (mean, 117.67 mg kg^{-1}), 1.68 ± 0.31-2.54 ± 0.08 mg kg^{-1} (mean, 2.13 mg kg^{-1}) and 110.51 ± 9.45-148.80 ± 3.68 mg kg^{-1} (mean, 127.43 mg kg^{-1}), respectively. The heavy metal concentrations in the surface sediments also varied significantly at different locations (ANOVA, $p<0.001$). The highest concentration of Zn, Cd and Cr was observed at site C2, which was one of the closest sites near the industrial park. The concentrations of Zn, Cd and Cr in surface sediment were higher than other sites.

The correlation coefficients between heavy metals in water and surface sediments were shown in *Table 5*. A significant positive correlation (0.873) of Zn was found between the water and sediments. And significant positive correlations (0.872) between Zn level in the water and Cr level in the sediments. Cd content of water showed significant positive relationships with Zn and Cr content in surface sediments with correlation coefficients 0.778 and 0.800, respectively. Furthermore, the Cr level in the water correlated positively with Cr (0.759) and Cd (0.742) in surface sediments of the same site.

Table 5. *Pearson's correlation coefficient (r) between heavy metals level in water (μg L^{-1}) and sediment (mg kg^{-1} dw) samples collected from all sites (n = 8)*

		Water				
		Pb	Zn	Cu	Cd	Cr
Sediment	Pb	-0.364	-0.526	0.683	-0.619	-0.155
	Zn	-0.023	0.873**	-0.129	0.778*	0.554
	Cu	0.627	-0.114	-0.141	-0.026	0.110
	Cd	0.403	0.562	-0.072	0.562	0.759*
	Cr	0.193	0.872**	-0.307	0.800*	0.716*

* Correlation is significant at the 0.05 level (2-tailed), ** Correlation is significant at the 0.01 level (2-tailed)

Sediment cores

The vertical distribution patterns for Pb, Zn, Cu, Cd and Cr in the sediment cores from the reservoir were shown in *Figure 2*. Overall, the mean metal concentrations approximately equaled the background levels in the local soils from 30 to 110 cm depth. The metal concentrations in sediment cores markedly increased from 10 to 30 cm depth and placidly increased from 10 cm depth to the surface.

http://www.aloki.hu ● ISSN 1589 1623 (Print) ● ISSN1785 0037 (Online)
DOI: http://dx.doi.org/10.15666/aeer/2003_23932407

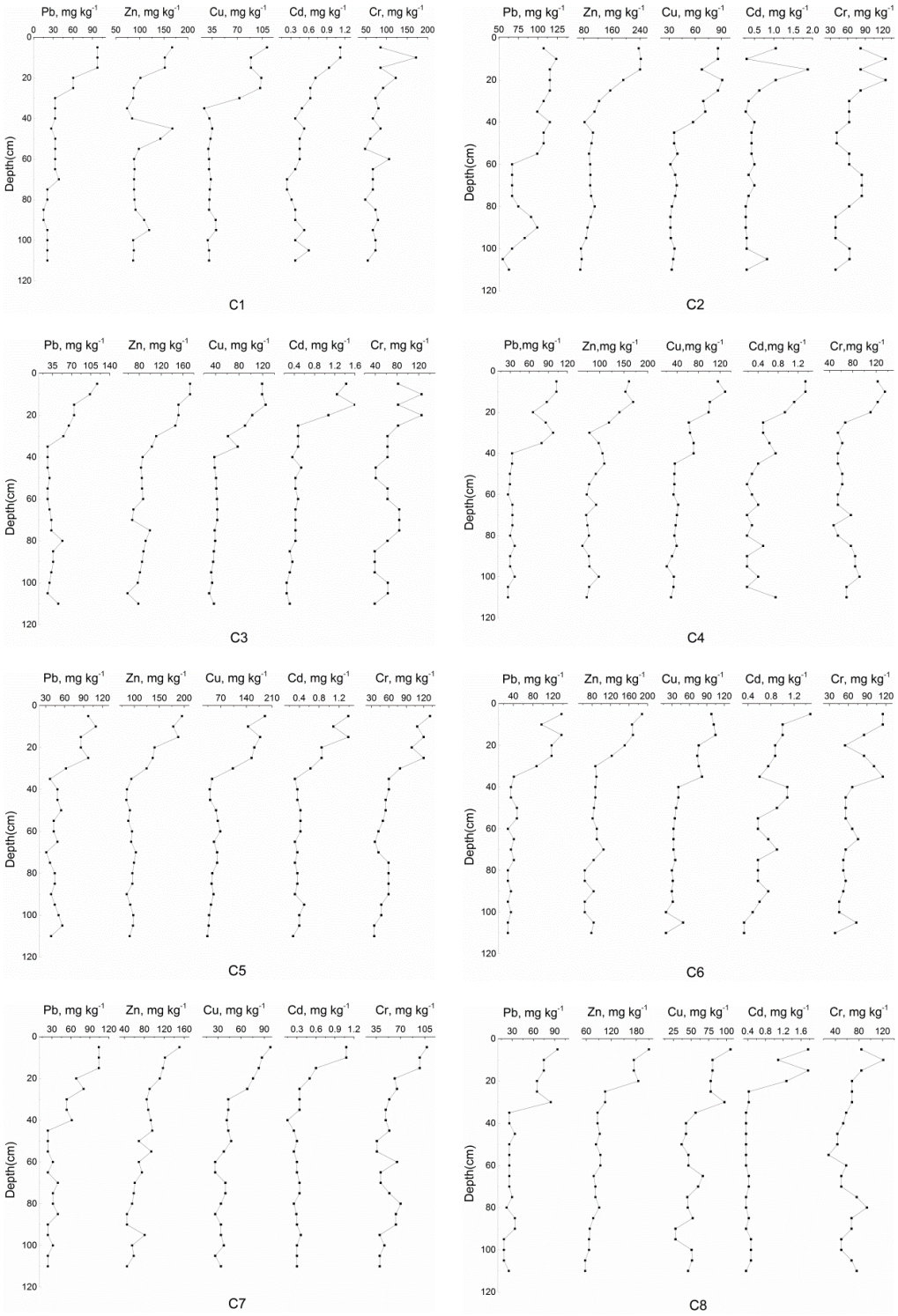

Figure 2. *The concentration of heavy metals changed with depth in sediment cores*

Fish

The concentrations of all the metals differed significantly between different locations (ANOVA, F5, 12<12.761, p<0.01), tissues (ANOVA, F2, 51>7.410, p<0.01) and significantly negative between species. The concentrations of heavy metals in fish muscle

http://www.aloki.hu ● ISSN 1589 1623 (Print) ● ISSN1785 0037 (Online)
DOI: http://dx.doi.org/10.15666/aeer/2003_23932407

samples from Hushan Reservior were shown in *Figure 3*. All metal concentrations were determined on a dry weight basis. For all sampling sites, the mean concentrations of Pb, Zn, Cu, Cd and Cr in muscle samples were 0.10-0.78 mg kg^{-1}, 21.79-67.87 mg kg^{-1}, 0.48-1.47 mg kg^{-1}, 0.03-0.16 mg kg^{-1} and 0.13-0.94 mg kg^{-1}, respectively. Compared to all the sites F1, F2, F3, F4, F5 and F6, shown in *Table 2*), the three fish species at site F4 had a higher concentration of Pb, Zn, Cu, Cd and Cr ($p<0.05$) except the concentrations of Pb in crucian carp, which was the closest site to the industrial park. Similarly, concentrations of Pb, Zn and Cu were much higher ($p<0.05$) at F1 and F4 sites, and concentrations of Cd were much higher ($p<0.05$) at F4 and F6 sites comparing to the other sites.

For all sampling sites, organs (liver and gill) from the same species (carp and crucian carp) were anatomized and pooled to determine Pb, Zn, Cu, Cd and Cr concentrations.

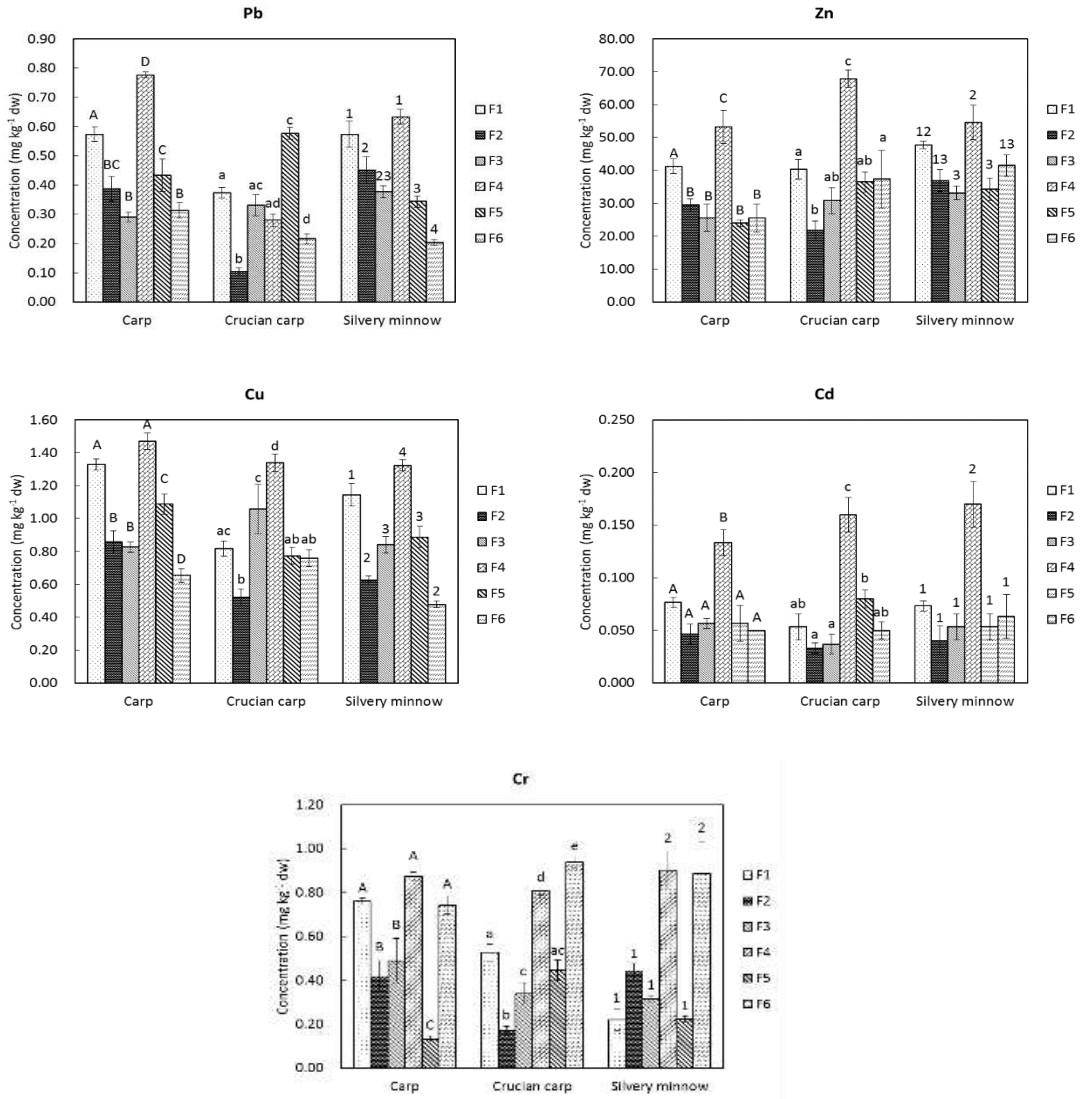

Figure 3. *Concentrations of Pb, Zn, Cu, Cd and Cr in fish muscle samples collected from Huashan Reservoir. The different letters (A, B, C, D) represent significant differences ($p<0.05$) between different sites for carp. The different letters (a, b, c, d) represent significant differences ($p<0.05$) between sites for crucian carp. The different numbers (1, 2, 3, 4) represent significant differences ($p<0.05$) between sites for silvery minnow*

http://www.aloki.hu ● ISSN 1589 1623 (Print) ● ISSN1785 0037 (Online)
DOI: http://dx.doi.org/10.15666/aeer/2003_23932407

Specifically, carp had the highest mean values of Pb (1.63 ± 0.32 mg kg^{-1}), Zn (85.67 ± 7.70 mg kg^{-1}), Cu (1.97 ± 0.42 mg kg^{-1}), Cd (0.20 ± 0.05 mg kg^{-1}) and Cr (1.09 ± 0.54 mg kg^{-1}) and crucian carp had the highest mean values of Pb (1.35 ± 0.45 mg kg^{-1}), Zn (68.68 ± 21.23 mg kg^{-1}), Cu (1.41 ± 0.35 mg kg^{-1}), Cd (0.16 ± 0.03 mg kg^{-1}) and Cr (0.98 ± 0.43 mg kg^{-1}) in liver. According to the national food safety standard (GB 2762-2012). The Pb, Cd Cr Zn and Cu values of threshold established were 0.5 mg kg^{-1} ww, 0.1 mg kg^{-1} ww 2.0 mg kg^{-1} ww, 100 mg kg^{-1} ww and 10 mg kg^{-1} ww, respectively. This illustrated that the metal concentrations of Pb, Zn, Cu, Cd and Cr in all fish species collected from the reservoir didn't exceed those standards by the Ministry of Health of the People's Republic of China. The present levels observed in fish species were safe for human consumption from this reservoir.

Discussion

Water and surface sediment analysis

Based on the national environmental quality standard for surface water (GB3838-2002) launched by the State Environmental Protection Administration of China, the results showed that the content of metals in water was under the grade II standards except for Pb and Cr. The highest concentrations for Zn, Cd and Cr occurred closest to the industrial park, and the highest concentration of Cu occurred closest to the Huashan town, which is also adjacent to a major industrial park. This high concentration of heavy metals maybe due to the urban runoff, sewage outfallsand and wastewater discharges. In addition, there were many industries near those sampling sites. The presence of some industrial resources such as phosphorus chemical industry, machinery, and steel smelting in this area may directly or indirectly contaminated the reservoir. The average value of pH was 7.85, indicating a weak alkaline environment. In this pH condition, minimal metal would be bound and not be released from the sediment (Atkinson et al., 2007). The average values of total nitrogen(TN) and total phosphorus(TP) were 2.63 mg/L and 0.200 mg/L, which were the grade V standards based on the national environmental quality standard for surface water (GB3838-2002). This pollution of TN and TP may also come from domestic sewage and chemical plants.

The metal concentrations of most surface sediments had exceeded the background values of local soils. The contamination of this area with heavy metals was caused by the higher population densities of urbanization and industrialization. It was apparent that the sediments with higher metal concentrations were influenced by anthropogenic discharge. The heavy metal concentrations in the sediments were higher in the reservoir because humic substances present in sediments creating metal complexes.

Therefore, heavy metals of Cd, Zn and Cr in waters and surface sediments may come from similar sources. The primary source of heavy metals was anthropogenic activities and weathering of bedrocks. Sediments act as the most important sink of metals in the aquatic environment. Some metals may interact with organic matter in the water and settle down, causing the precipitation of metals in the sediments (Gupta et al., 2009; Debnath et al., 2021). The detected positive correlation of each metal between the water and the sediment supported this argument.

http://www.aloki.hu ● ISSN 1589 1623 (Print) ● ISSN1785 0037 (Online)
DOI: http://dx.doi.org/10.15666/aeer/2003_23932407

Sediment cores analysis

Because the sediment deposition and burial rates were characterized, concentrations within each sediment slice can be characterized on a temporal basis. The chronology of the sediment samples was inferred according to the 137Cs method (Xue et al., 2007; Abbasi, 2019). The 5-10 cm and 25-30 cm of cores layers referred to the 2000s and 1970s, respectively. The historical changes of heavy metals were relatively small before the 1970s. Pb, Zn, Cu, Cd and Cr concentrations increased abruptly around early 1970s. It was apparent that the Huashan Reservoir was more polluted with anthropogenic source metals from the 1970s. During this period, the heavy metal pollution was also caused by urbanization and industrialization in Huashan Town. In addition, the results showed that the concentrations of these metals tended to remain unchanged from the 2000s to now. This phenomenon may be due to the environment administered engineering with the Qujing government from 2003.

Fish analysis

It can be seen from the figures that the concentrations of Pb, Zn, Cu, Cd and Cr in fish muscle samples were in agreement with some other research (Tuzen, 2009; Xie et al., 2020) and concentrations of Cd were in agreement with these reported by Canli and Atli (2003). Similarly, the mean concentrations of Pb and Zn observed in the current study might be considered comparable with those reported in the muscle of Cyprinidae by Yang et al. (2014). In addition, the Pb, Cu and Cr concentrations detected in fish muscle samples in our study were lower than the data reported by Chale (2002). The Zn concentrations found in muscle samples resemble to the data from the paper finished by Merciai et al. (2014), who reported that similar concentrations ranged from 32.91 to 114.2 mg kg^{-1} in fish collected from the Llobregat River, which flows into the Mediterranean Sea.

The lowest and highest Pb levels in fish muscles were found as 0.10 ± 0.01 mg kg^{-1} in crucian carp at site F2 and 0.78 ± 0.01 mg kg^{-1} in carp at site F4, respectively. Pb is known to induce increase of blood pressure and cardiovascular disease in adults and reduce children's intellectual performance and cognitive development. Zn (21.79-67.87 mg kg^{-1}) and Cu (0.48-1.47 mg kg^{-1}) concentrations were comparatively high in muscles of all species studied during the present investigation. However, Zn and Cu in analyzed fish samples were lower than limits. Zn and Cu are usually essential elements, but it can cause adverse health problems under very high intake, such as liver and kidney damage (Ikem and Egiebor, 2005; Attar, 2020). Cd (0.03-0.16 mg kg^{-1}) concentrations were comparatively low in muscles for all species studied during the present investigation. Compared to all sites, the three fish species at site F4 had 2-3 times higher concentrations of Cd. These results are in accordance with the higher concentrations of Cd in surface sediment in this site. To some degree, industrial effluents contribute to the Cd pollution in this area, which was the closest site to the industrial park. Cr is an essential mineral in humans and has been related to carbohydrate, lipid and protein metabolism (Biswas et al., 2012). The lowest and highest Cr levels in fish muscles of species were found as 0.13 ± 0.01 mg kg^{-1} in carp and 0.89 ± 0.15 mg kg^{-1} in a silvery minnow.

As the results obtained in our study, the mean concentrations of metal were comparatively higher in the livers, while the lowest concentration was obtained in the edible muscles. For the most part, the higher concentrations of the studied metals were found in the gills of carp, crucian carp and silvery minnow collected from the Huashan Reservoir. Overall, the mean concentration in fish organs followed the sequence of

http://www.aloki.hu ● ISSN 1589 1623 (Print) ● ISSN1785 0037 (Online)
DOI: http://dx.doi.org/10.15666/aeer/2003_23932407

liver>gill>muscle. For the tissues, the liver was confirmed as the best metal depository for all elements determined (Çoğun et al., 2006; Sattari et al., 2020). The adsorption of metals into the gill surface could also be an important influence on the total metal levels of the gill (Heath, 1995).

Conclusion

This study may increase our knowledge of the geochemistry of water, sediment and some fish of the Huashan Reservoir, a part of the Pearl River source. The results showed that the water and sediment samples of Huashan Reservoir were polluted by a certain extent, especially from the waste water of industrial parks. From the results, we concluded that concentrations of Pb, Zn, Cu, Cd and Cr increased abruptly from around early 1970s. This study fills a gap by providing information on heavy metal concentrations in different fish species from the Huashan Reservoir. Fortunately, metal concentrations found in edible parts of carp, crucian carp and silvery minnow were not heavily burdened based on the samples collected. Metal quantities were higher in liver and gills than that in muscle. The liver was confirmed as the best metal depository for all elements determined. However, fish livers were very seldom consumed in the area.

Further work is necessary to decide on the form of storage of metals in the liver of the studied fish species. Proper management is needed to sustain the quality of this lake for the coming generations. Therefore, we need to investigate the levels and spatial variations of heavy metals in water, sediment and fish and to provide baseline information on the pollution situation in this basin. The information could contribute to the knowledge and rational management of this region in the future.

Acknowledgements. This work was supported by a grant from the Surface Programs of Science and Technology Commission of Yunnan Province (Grant No. 202101BA070001-076) and the fund from Meemann Chang Academician Workstation of Yunnan Province.

REFERENCES

[1] Abbasi, A. (2019): 210 Pb and 137 Cs based techniques for the estimation of sediment chronologies and sediment rates in the Anzali Lagoon, Caspian Sea. – Journal of Radioanalytical and Nuclear Chemistry 322(2): 319-330.

[2] Abu Shnaf, A. S. M., Abd El-Aziz, S. H., Ata, A. M. (2021): Cyto-histopathological and Protein Polymorphism Alterations in Five Populations of Nile Tilapia (Oreochromis niloticus) as biomonitor for water heavy metal pollution. – Journal of Fish Biology 99(3): 999-1009.

[3] Adams, W. J., Kimerle, R. A., Barnett, J. W. (1992): Sediment quality and aquatic life assessment. – Environmental science and technology 26(10): 1864-1875.

[4] Al-Edresy, M. A., Wasel, S. O., Al-Hagibi, H. A. (2019): Ecological risk assessment of heavy metals in coastal sediments between Al-Haymah and Al-Mokha, south red sea, Yemen. – International Journal of Hydrology 3(2): 159-173.

[5] Ali, H., Khan, E., Ilahi, I. (2019): Environmental chemistry and ecotoxicology of hazardous heavy metals: environmental persistence, toxicity, and bioaccumulation. – Journal of chemistry 2019: 1-14.

[6] Atkinson, C. A., Jolley, D. F., Simpson, S. L. (2007): Effect of overlying water pH, dissolved oxygen, salinity and sediment disturbances on metal release and sequestration from metal contaminated marine sediments. – Chemosphere 69(9): 1428-1437.

http://www.aloki.hu ● ISSN 1589 1623 (Print) ● ISSN1785 0037 (Online)
DOI: http://dx.doi.org/10.15666/aeer/2003_23932407

[7] Attar, T. (2020): A mini-review on importance and role of trace elements in the human organism. – Chemical Review and Letter 3(3): 117-130.
[8] Ayodele, O. S., Madukwe, H. Y., Adelodun, A. A. (2021): Geoenvironmental evaluation of toxic metals in the sediments of Araromi coastal area, Southwestern Nigeria. – Environmental Quality Management 31(3): 101-119.
[9] Biswas, S., Prabhu, R. K., Hussain, K. J., Selvanayagam, M., Satpathy, K. K. (2012): Heavy metals concentration in edible fishes from coastal region of Kalpakkam, southeastern part of India. – Environmental Monitoring and Assessment 184(8): 5097-5104.
[10] Buffle, J., DeVitre, R. R. (1993): Chemical and biological regulation of aquatic systems. – CRC Press. The Los Angeles.
[11] Canli, M., Atli, G. (2003): The relationships between heavy metal (Cd, Cr, Cu, Fe, Pb, Zn) levels and the size of six Mediterranean fish species. – Environmental pollution 121(1): 129-136.
[12] Chale, F. (2002): Trace metal concentrations in water, sediments and fish tissue from Lake Tanganyika. – Science of the Total Environment 299(1): 115-121.
[13] Çoğun, H. Y., Yüzereroğlu, T. A., Firat, Ö., Goek, G., Kargin, F. (2006): Metal concentrations in fish species from the northeast Mediterranean Sea. – Environmental monitoring and assessment 121(1-3): 431-438.
[14] Debnath, A., Singh, P. K., Sharma, Y. C. (2021): Metallic contamination of global river sediments and latest developments for their remediation. – Journal of Environmental Management 298(15): 1-20.
[15] Frascareli, D., Cardoso-Silva, S., De Oliveira Soares Silva Mizael, J., Rosa, A. H., Pompeo, M. L. M., Lopez-Doval, J. C., Moschini-Carlos, V. M. (2018): Spatial distribution, bioavailability, and toxicity of metals in surface sediments of tropical reservoirs, Brazil. – Environmental monitoring and assessment 190(4): 1-15.
[16] Gupta, A., Rai, D. K., Pandey, R. S., Sharma, B. (2009): Analysis of some heavy metals in the riverine water, sediments and fish from river Ganges at Allahabad. – Environmental Monitoring and Assessment 157(1-4): 449-458.
[17] Heath, A. G. (1995): Water pollution and fish physiology. – CRC Press. The Los Angeles.
[18] Ikem, A., Egiebor, N. O. (2005): Assessment of trace elements in canned fishes (mackerel, tuna, salmon, sardines and herrings) marketed in Georgia and Alabama (United States of America). – Journal of food composition and analysis 18(8): 771-787.
[19] Isangedighi, I. A., David, G. S. (2019): Heavy metals contamination in fish: effects on human health. – Journal of Aquatic Science and Marine Biology 2(4): 7-12.
[20] Keith, T. L., Snyder, S. A., Naylor, C. G., Staples, C. A., Summer, C., Kannan, K., Giesy, A. P. (2001): Identification and quantitation of nonylphenol ethoxylates and nonylphenol in fish tissues from Michigan. – Environmental science and technology 35(1): 10-13.
[21] Kostka, A., Leśniak, A. (2020): Spatial and geochemical aspects of heavy metal distribution in lacustrine sediments, using the example of Lake Wigry (Poland). – Chemosphere 240: 1-12.
[22] Kumar, V., Parihar, R. D., Sharma, A., Bakshi, P., Sidhu, G. P. S., Bali, A. S., Karaouzas, L., Bhardwaj, R., Thukral, A. K., Gyasi-Agyei, Y., Rodrigo-Comino, J. (2019): Global evaluation of heavy metal content in surface water bodies: A meta-analysis using heavy metal pollution indices and multivariate statistical analyses. – Chemosphere 236: 1-30.
[23] Kumar, M., Gupta, N., Ratn, A., Awasthi, Y., Prasad, R., Trivedi, A., Trivedi, S. P. (2020): Biomonitoring of heavy metals in river ganga water, sediments, plant, and fishes of different trophic levels. – Biological trace element research 193(2): 536-547.
[24] Lan, X., Ning, Z., Liu, Y., Xiao, Q., Chen, H., Xiao, E., Xiao, T. (2019): Geochemical distribution, fractionation, and sources of heavy metals in dammed-river sediments: The Longjiang River, Southern China. – Acta Geochimica 38(2): 190-201.
[25] Li, Q., Zhou, J. L., Chen, B., Huang, B., Zeng, X. D., Zhan, J. H., Pan, X. J. (2014): Toxic metal contamination and distribution in soils and plants of a typical metallurgical industrial area in southwest of China. – Environmental Earth Sciences 72(6): 2101-2109.

http://www.aloki.hu ● ISSN 1589 1623 (Print) ● ISSN1785 0037 (Online)
DOI: http://dx.doi.org/10.15666/aeer/2003_23932407

[26] Liu, J. L., Wang, R., Huang, B., Lin, C., Wang, Y., Pan, X. J. (2011): Distribution and bioaccumulation of steroidal and phenolic endocrine disrupting chemicals in wild fish species from Dianchi Lake, China. – Environmental pollution 159(10): 2815-2822.
[27] Liu, J. L., Pan, X. J., Huang, B., Fang, K., Yu, W., Gao, J. (2012): An improved method for simultaneous analysis of steroid and phenolic endocrine disrupting chemicals in biological samples. – International Journal of Environmental Analytical Chemistry 92(10): 1135-1149.
[28] Liu, R., Guo, L., Men, C., Wang, Q., Miao, Y., Shen, Z. (2019): Spatial-temporal variation of heavy metals' sources in the surface sediments of the Yangtze River Estuary. – Marine pollution bulletin 138: 526-533.
[29] Liu, H., Liu, E., Yu, Z., Lin, Q., Zhang, E., Shen, J. (2022): Spatio-temporal accumulation patterns of trace metals in sediments of a large plateau lake (Erhai) in Southwest China and their relationship with human activities over the past century. – Journal of Geochemical Exploration 234: 106943.
[30] Łuczyńska, J., Tońska, E., Paszczyk, B., Łuczyński, M. J. (2020): The relationship between biotic factors and the content of chosen heavy metals (Zn, Fe, Cu and Mn) in six wild freshwater fish species collected from two lakes (Łańskie and Pluszne) located in northeastern Poland. – Iranian Journal of Fisheries Sciences 19(1): 421-442.
[31] Merciai, R., Guasch, H., Kumar, A., Sabater, S., Garcia-Berthou, E. (2014): Trace metal concentration and fish size: variation among fish species in a Mediterranean river. – Ecotoxicol Environment Safe 107: 154-161.
[32] Miller, P., Munkittrick, K., Dixon, D. (1992): Relationship between concentrations of copper and zinc in water, sediment, benthic invertebrates, and tissues of white sucker (Catostomus commersoni) at metal-contaminated sites. – Canadian Journal of Fisheries and Aquatic Sciences 49(5): 978-984.
[33] Miranda, L. S., Wijesiri, B., Ayoko, G. A., Egodawatta, P., Goonetilleke, A. (2021): Water-sediment interactions and mobility of heavy metals in aquatic environments. – Water Research 202: 1-9.
[34] Munoz-Olivas, R., Camara, C. (2001): Speciation related to human health. – In: Trace element speciation for environment food and health, pp. 331-353.
[35] Rajeshkumar, S., Li, X. (2018): Bioaccumulation of heavy metals in fish species from the Meiliang Bay, Taihu Lake, China. – Toxicology reports 5: 288-295.
[36] Salem, B. Z., Capelli, N., Laffray, X., Elise, G., Ayadi, H., Aleya, L. (2014): Seasonal variation of heavy metals in water, sediment and roach tissues in a landfill draining system pond (Etueffont, France). – Ecological Engineering 69: 25-37.
[37] Sattari, M., Bibak, M., Bakhshalizadeh, S., Forouhar Vajargah, M. (2020): Element accumulations in liver and kidney tissues of some bony fish species in the Southwest Caspian Sea. – Journal of Cell and Molecular Research 12(1): 33-40.
[38] Singh, B. R., Tindwa, H., Kashem, A. M., Panghaal, D., Semu, E. (2020): Heavy Metals Bioavailability in Soils and Impact on Human Health. – In: The Soil–Human Health Nexus, pp. 249-273.
[39] Sobhanardakani, S., Tayebi, L., Hosseini, S. V. (2018): Health risk assessment of arsenic and heavy metals (Cd, Cu, Co, Pb, and Sn) through consumption of caviar of Acipenser persicus from Southern Caspian Sea. – Environmental Science and Pollution Research 25(3): 2664-2671.
[40] Tian, K., Wu, Q., Liu, P., Hu, W., Huang, B., Shi, B., Zhou, Y., Kwon, B., Choi, K., Ryu, J., Khim, J., Wang, T. (2020): Ecological risk assessment of heavy metals in sediments and water from the coastal areas of the Bohai Sea and the Yellow Sea. – Environment international 136: 1-15.
[41] Tuzen, M. (2009): Toxic and essential trace elemental contents in fish species from the Black Sea, Turkey. Food and chemical toxicology. – Food and Chemical Toxicology 47(8): 1785-1790.

http://www.aloki.hu ● ISSN 1589 1623 (Print) ● ISSN1785 0037 (Online)
DOI: http://dx.doi.org/10.15666/aeer/2003_23932407

[42] Xie, Q., Gui, D., Liu, W., Wu, Y. (2020): Risk for Indo-Pacific humpback dolphins (Sousa chinensis) and human health related to the heavy metal levels in fish from the Pearl River Estuary, China. – Chemosphere 240: 1-10.
[43] Xue, C. D., Liu, X., Qi, C. Y., Wei, H. X., Song, X. L., Liu, Y. Q., Hao, B. W. (2007): Element geochemical characteristics of modern sediments in the Dianchi Lake, Kunming, and their environmental significance. – Acta Petrologica et Mineralogica 26(6): 582-590.
[44] Yang, R., Zhang, S., Wang, Z. (2014): Bioaccumulation and regional distribution of trace metals in fish of the Tibetan Plateau. – Environmental geochemistry and health 36(1): 183-191.
[45] Zhou, Q., Yang, N., Li, Y., Ren, B., Ding, X., Bian, H., Yao, X. (2020): Total concentrations and sources of heavy metal pollution in global river and lake water bodies from 1972 to 2017. – Global Ecology and Conservation 22: e00925.

http://www.aloki.hu ● ISSN 1589 1623 (Print) ● ISSN1785 0037 (Online)
DOI: http://dx.doi.org/10.15666/aeer/2003_23932407

CHARACTERIZATION OF EXTRACELLULAR PROTEASE FROM *STENOTROPHOMONAS RHIZOPHILA* MT1 ISOLATED FROM AQUACULTURE SLUDGE WASTE

LICH, N. Q.[1*] – THAO, T. T. P.[2] – HUY, N. D.[3]

[1]*School of Engineering and Technology, Hue University, 49000 Hue, Thua Thien Hue, Vietnam*

[2]*Jeonbuk National University, Jeonju-si, Jeollabuk-do 54896, Republic of Korea*
(e-mail: ttpthao@jbnu.ac.kr)

[3]*Institute of Biotechnology, Hue University, 49000 Hue, Thua Thien Hue, Vietnam*
(e-mail: ndhuy@hueuni.edu.vn)

**Corresponding author*
e-mail: nguyenquanglich@hueuni.edu.vn; phone: +84-93-575-7273

(Received 25th Nov 2021; accepted 2nd May 2022)

Abstract. A protease-producing *Stenotrophomonas rhizophila* MT1 isolated from sludge samples of shrimp ponds was selected to evaluate extracellular proteases. Enzyme activity reached the highest value of 139.02 U/mL after 60 h of culture. The isolate produced the highest protease activity in the culture medium containing 1% casein (w/v) with an inoculum size of 10% (v/v) and an agitation speed of 180 rpm. Zymography indicated two proteolytic bands with estimated molecular weights of 30 kDa and 110 kDa, respectively. The protease activity increased in Ca^{2+}, Mg^{2+}, Co^{2+} and K^{+} ions and was partially inhibited in the presence of Mn^{2+}, Zn^{2+}, Cu^{2+} and Fe^{2+} ions. Meanwhile, acetone and hexane solvents enhanced protease activity. This is the first report that evaluated the extracellular proteases produced by *S. rhizophila*. The isolate is a promising candidate for application in the removal of protein residues in aquaculture sludges, minimizing the negative effect of aquaculture sludges on the environment.
Keywords: *bioremediation, hydrolytic enzyme, organic pollutants, proteolytic activity, shrimp wastewater*

Introduction

Aquaculture is an important food production industry and has become a significant economic activity in many countries (Hamza et al., 2017; Santos and Ramos, 2018). However, a large amount of excess feed, animal carcasses and manure have been generated, exacerbating the accumulation of organic matters in the aquaculture ponds causing the blossom of harmful microorganisms as well as problem in waste sludge treatment (Li et al., 2020; Mariane De Morais et al., 2020). The major nitrogen sources of aquaculture ponds contain large amounts of protein and amino acids. Thus, sludge waste has higher organic matters, total nitrogen and phosphorus values than regular soils. Shrimp pond solid waste comprises 1.92% organic C, 0.54% total N and 1.70% P (Tangguda et al., 2015). Interestingly, the high levels of organic matters, nitrogen and phosphorus in the sediments make pond sediments a potential organic material for fertilizer use. Production of organic fertilizers from solid waste and its later use in agriculture and fisheries is recommended to reduce waste disposal volumes, environmental degradation and increase soil productivity (Suwoyo et al., 2020).

In particular, organic matters should be first decomposed into dissolved form. Then, ammonification, nitrification and denitrification possess organic matters into nitrogen gas. Bacteria play an important role in these processes by secreting enzymes such as

http://www.aloki.hu ● ISSN 1589 1623 (Print) ● ISSN 1785 0037 (Online)
DOI: http://dx.doi.org/10.15666/aeer/2003_24092423

protease, nitrate reductase, nitrite reductase, nitric-oxide reductase and nitrous oxide reductase … (Su et al., 2020). Extracellular proteases produced by bacteria are important enzymes that efficiently hydrolyze organic matters into peptides and amino acids (Su et al., 2020). Protease-producing bacteria not only improve protein digestibility and host growth but also reduce organic pollutants in aquaculture (Shi et al., 2016; Amin, 2018). Protease-producing bacteria belong to four major phyla of Proteobacteria, Firmicutes, Actinobacteria and Bacteroidetes (Su et al., 2020).

The genus *Stenotrophomonas* belongs to the class Gamma-proteobacteria and becomes interesting due to its wide prevalence in diverse habitats with biotechnological applications (Ryan et al., 2009). Their plant growth-promoting properties and antagonistic activity against soil pathogens have been reported (Ryan et al., 2009). The genus *Stenotrophomonas* includes several species, including *S. maltophilia, S. africana, S. rhizophila, S. pavanii, S. humi, S. koreensis, S. chelatiphaga, S. dokdonesis, S. panacihumi, S. terrae, S. nitritireducens, S. acidaminiphila, S. bentonitica, S. ginsengisoli and S. daejeonensis* ... (Patil et al., 2016). Among them, *S. maltophilia* is the most studied species that produces alkaline protease and a variety of beneficial extracellular metabolites (Wang et al., 2016b). However, development for commercial use of *S. maltophilia* has been hampered by its ability to cause infections in human (Brooke, 2012) *S. rhizophila* is closely related both phylogenetically and ecologically to *S. maltophilia* (Pinski et al., 2020). However, unlike *S. maltophilia*, *S. rhizophila* has no pathogenic features for human (Berg and Martinez, 2015). *S. rhizophila* offers biotechnological applications that do not pose any risk to human health.

Although Stenotrophomonas is ubiquitous, *S. rhizophila* is commonly associated with plant rhizomes, such as maize, wheat, rice, canola, potatoes, strawberries, alfalfa, and sunflower (Ryan et al., 2009). Because of beneficial plant interactions that promote plant growth, *S. rhizophila* has become essential for agricultural biotechnology applications. On the other hand, *S. rhizophila* produces many hydrolytic enzymes such as chitinase (Jankiewicz et al., 2020), endoglucanase (Singh et al., 2015), lipase (Said et al., 2019) and protease (Steinmann et al., 2018; Singh et al., 2015). However, there is no report on the production or characterization of extracellular protease of *S. rhizophila*. Furthermore, its wide conversion properties of organic compounds combined with high metal tolerance make *S. rhizophila* is more attractive for bioremediation (Sun et al., 2021). To facilitate application of wastes into fertilizers, the selection of microbial strains that have both the properties of converting wastes into fertilizers and plant growth promotion has greater advantages value. On the other hand, the quality of fertilizers obtained from wastes depends on the extracellular enzymes including protease. Thus, the present study focused on isolating and characterizing the protease producing bacteria isolated from aquaculture sludge waste which could be interesting for converting aquaculture wastes into agriculture fertilizers.

Materials and methods

Isolation and identification of protease produced strain

The waste sludges were collected from shrimp pond in Phong Dien district, Thua Thien Hue province, Vietnam. The composition of the solid waste included 190.8 ± 4.4 mg/kg of total organic carbon, 22.6 ± 0.1 g/kg of total phosphorus and 32.0 ± 0.9 g/kg of total nitrogen. One milliliter of shrimp pond sludge waste was mixed with 9 mL of sterile distilled water, then serially diluted to 10^{-4}. One hundred

http://www.aloki.hu ● ISSN 1589 1623 (Print) ● ISSN 1785 0037 (Online)
DOI: http://dx.doi.org/10.15666/aeer/2003_24092423

microliters of the sample from the last dilution were placed onto the surface of casein agar in a petri dish (1% casein and 2% agar) and incubated at 35 °C for 72 h. The clear zone around the colonies was assessed as indication for protease activity. The colony with the greatest clearance zone on casein agar was selected and purified on LB medium.

Bacterial strains with strong protease activity were identified by molecular techniques. The bacterial DNA was extracted according to Sambrook et al. (2001). Total DNA was used as a template for PCR amplification of 16S rRNA sequences using primer pairs of 27-F (5'-AGAGTTTGATCCTGGCTCAG-3') and 1492-R (5'-GGTTACCTTGTTACGACTT-3'). PCR components included 6 µL GoTaq Green master mix (Promega, USA), 10 pmol per primer, 50 ng genomic DNA and 12 µL distilled water. PCR reaction was performed on an MJ Mini^{TM} Gradient Thermal Cycler (BioRad, USA). The PCR cycles was carried out by denaturing at 95 °C for 5 min, flowing thermal cycle included steps of denaturation of 95 °C for 1 min, annealing at 55 °C for 1 min, extension of 72 °C for 1 min 30 s, repeat with 30 cycles, and final extension of 72 °C for 10 min. PCR products were qualified on 0.8% agarose gel electrophoresis. PCR products were performed nucleotide sequencing using a commercial sequencing service (Firstbase, Malaysia). Nucleotide sequences were compared with data on GenBank. Phylogenetic trees were constructed using MEGA 11 software with the Maximum Likehihood method (Tamura et al., 2021).

The growth and protease production of bacterial strain

The highest protease producing isolate was selected for further investigation. The strain was cultured in LB medium for 16 h. Then, cells suspension (1%, v/v) was transferred to protease production medium containing 1% casein, 0.2% $(NH_4)_2SO_4$; 0.1% K_2HPO_4; 0.1% $MgSO_4.7H_2O$; 0.05% NaCl, pH 7.5 and continuously cultured at 35 °C for 96 h, 180 rpm of shaking. Extracellular proteases were collected every 12 h by centrifugation at 10.000 rpm for 15 min at 4 °C. Cell growth was monitored by measuring absorbance at 600 nm (Wang et al., 2016a).

Protease activity assay

Protease activity of bacterial strains was determined by Sigma's method using casein as a substrate. One unit of protease activity was defined as the amount of casein hydrolyzing enzyme releasing an amino acid equivalent of 1 µmole of tyrosine in 1 min at pH 7.5, temperature of 37 °C (Cupp-Enyard, 2008; Marathe et al., 2018). Briefly, five milliliters of 0.65% casein substrate were incubated at 37 °C for 5 min. Then, one milliliter of crude enzyme was added and incubated for 10 min. The reaction was terminated by the adding of 5 mL of 5% trichloroacetic acid and kept for 30 min at room temperature. The mixture was then centrifuged at 6000 rpm for 10 min, 4 °C and harvested supernatant. Color was developed by adding 5 mL of 0.5 M Na_2CO_3 and 1 mL of 1 M Folin reagent into reaction supernatant, then incubated for 30 min in the dark. After incubation, the sample absorbances were measured at 660 nm using a UV-2650 Spectro UV-VIS RS Auto Spectrophotometer (Labomed, USA). Use the Tyrosine standard curve to calculate the enzyme activity according to *Equation 1:*

$$U = \frac{\mu mole\ Tyrosine * 11}{10 * 2 * 1} \quad \text{(Eq.1)}$$

http://www.aloki.hu ● ISSN 1589 1623 (Print) ● ISSN 1785 0037 (Online)
DOI: http://dx.doi.org/10.15666/aeer/2003_24092423

where: U is enzyme unit; 11 is the total volume (in milliliters) of assay; 10 is the time of assay (in minutes); 1 is volume of enzyme used (in milliliters); 2 is volume used (in milliliters).

Effect of culture conditions on protease production

Effect of casein concentration

The effect of substrate concentration on protease production was determined by culturing the isolate in the protease-producing medium as described above containing casein at concentrations of 0, 1, 2, or 5% (w/v). Culture was performed in 96 h at 180 rpm of shaking. Extracellular proteases were collected every 12 h by centrifugation at 10.000 rpm for 15 min at 4 °C and enzyme activity was measured according to the protease activity assay.

Effect of inoculum size

To determine the effect of inoculum size, culture was incubated in the medium with inoculum ranging from 1, 5, 10 or 15% (v/v). Reaction mixtures were incubated at 35 °C by shaking at 150 rpm for 96 h. Enzyme activity was measured every 12 h as mentioned above.

Effect of agitation rate

After determining the casein concentration and inoculum size, the effect of agitation rate on protease production was investigated. Agitation rates were investigated at 120, 150, 180 or 210 rpm for 96 h at 35 °C. Extracellular protease activity was determined for every 12 h.

Zymogram

Zymogram was performed according to Wang et al. (2016). Fifteen microliters of the cell-free supernatant were mixed with 2X loading dye buffer. The mixture is then subjected to SDS-PAGE with 5% stacking gel and 12% separating gel containing 0.8 mg/mL of casein. The gel was washed twice with Triton X-100 2.5% (v/v) for 30 min at room temperature and three times with distilled water, then incubated in the reaction buffer (50 mmol/L Tris - HCL pH 8.3, 50 mmol/L $CaCl_2$) at 35 °C for 2 h. Gel was stained with Coomassie Brilliant Blue R-250 and destained in acetate methanol solution. The appearance of a clear zone on the blue background of the gel was accessed for protease activity (Wang et al., 2016a).

Effects of pH and temperature on protease activity

The optimal pH for protease activity was determined using casein 0.65% (w/v) as substrate at different pH values. Enzyme was incubated with reaction buffers of pH ranged from 2 to 12 using difference buffers including glycine-HCl buffer (pH 2-3), sodium acetate (pH 4-5), sodium phosphate buffer (pH 6–8) and glycine-NaOH (pH 9–12)). The reactions were performed at 37 °C.

To determine the effect of temperature on protease activity, the incubation time of enzyme substrate mixture was maintained at 10 min and the temperatures for which activity of enzyme was conducted at 20 °C, 30 °C, 40 °C, 50 °C, 60 °C and 70 °C. The

http://www.aloki.hu ● ISSN 1589 1623 (Print) ● ISSN 1785 0037 (Online)
DOI: http://dx.doi.org/10.15666/aeer/2003_24092423

relative activities of the protease were measured. The maximum activity of crude enzyme was expressed as 100%.

Effects of inhibitors and metal ions on protease activity

The effect of metal ions on protease was examined by incubating the reaction mixture including enzyme solution, casein substrate with ion metals of Cu^{2+}, Ca^{2+}, Mg^{2+}, Co^{2+}, Zn^{2+}, Fe^{2+}, Mn^{2+} and K^{+} at a concentration of 1 mM with optimum pH (pH 9) and temperature (50 °C) for 1 h. The control sample was carried out as no metal ion presence in reaction solution.

The effects of different enzyme inhibitors on protease activity were examined using ethylenediaminetetraacetic acid (EDTA) and β-mercaptoethanol. The protease was pre-incubated at 25 °C for 1 h with each agent at a final concentration of 1 mM. Controls were pre-incubated without inhibitors.

Effect of organic solvents on protease activity

The protease activity was determined in the presence of 30% organic solvent (v/v) at an optimum temperature of 50 °C and pH 9. Methanol, ethanol, isopropanol, acetone and hexane were used as organic solvents in the reaction mixture. Protease activity in the solvent-free sample was used as a control.

Statistical analysis

All experiments were performed in triplicate. Absorbances were recorded three times and average values were accessed for statistical analysis of experimental replication. Data were analyzed using Statgraphics 19 software and presented as mean ± SD. The difference between means was assessed by ANOVA and Duncan's test then was used to compare data among treatments. Statistical significance between treatments was based on $p < 0.05$.

Results and discussion

Isolation and identification of protease producer

Waste sludge was collected from shrimp ponds in Phong Dien district, Thua Thien Hue province, Vietnam and delivered to the laboratory to be diluted to 10^{-4} and spread on a plate containing medium Casein agar. Three distinct bacterial colonies with the zone of clearance on casein agar were obtained after incubation, named MT1, MT2 and MT3, respectively. Among them, strain MT1 had the greatest zone of clearance on casein agar, showing that it is a good protease producer (*Fig. 1D*). The isolate was grown on protease production medium and enzyme activity was evaluated on an agar plate. *Figure 1D* showed that strain MT1 had a halo ring diameter of 25.67 ± 1.2 mm after 48 h of incubation at 35 °C (*Fig. 1D*).

The isolate MT1 was Gram negative, catalase positive, motility and rod shape. The 16S rRNA sequence of the MT1 strain was amplified, sequenced and compared with other bacterial strains available in NCBI database by BLAST analysis. The results indicated the sequence of isolate had high homology (100%) with other *S. rhizophila* species. The phylogenetic tree based on the 16S rRNA gene sequence was shown in *Figure 2*. The MT1 strain was identified as *S. rhizophila* (accession number: MZ396455).

http://www.aloki.hu ● ISSN 1589 1623 (Print) ● ISSN 1785 0037 (Online)
DOI: http://dx.doi.org/10.15666/aeer/2003_24092423

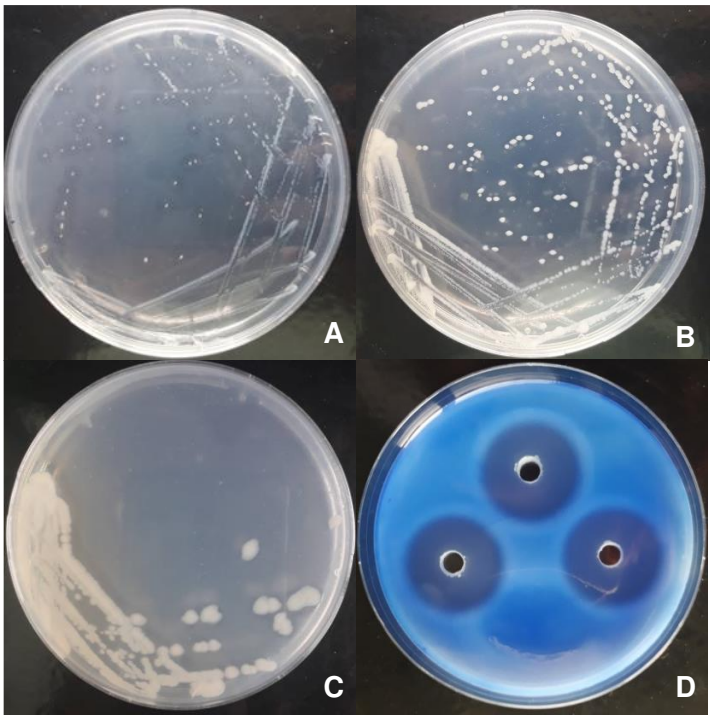

Figure 1. *Colony formation and extracellular protease activity of isolates. Colony formation of isolate MT1 (A), MT2 (B), and MT3 (C) grow on LB medium containing 1% casein. Casein hydrolytic activities are indicated as clear zones around colonies. (D) Extracellular protease activity of MT1*

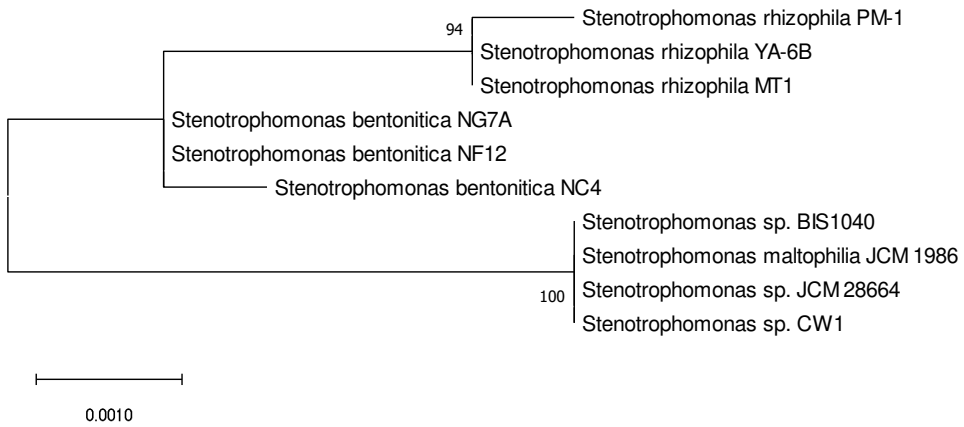

Figure 2. *Phylogenetic tree between S. rhizophila MT1 and other Stenotrophomonas species. The evolutionary history was inferred by using the Maximum Likelihood method and Tamura-Nei model. The percentage of trees in which the associated taxa clustered together is shown next to the branches*

The growth and protease production

The growth and enzyme production of *S. rhizophila* MT1 were examined on medium supplemented with 1% casein (w/v) for 96 h at 35 °C. The results shown in *Figure 3* indicated proteolytic activity was hardly detectable in the early stages of culture. Meanwhile, protease production started only up-regulated at the log phase to the end of

http://www.aloki.hu ● ISSN 1589 1623 (Print) ● ISSN 1785 0037 (Online)
DOI: http://dx.doi.org/10.15666/aeer/2003_24092423

the growth curve. The proteolytic activity reached the highest activity between 48 h to 60 h culture (no significant difference) with a peak at 60 h (139.02 U/mL) and then decreased. The production of protease was observed to be proportional to the growth of the organism. The results are consistent with the study by Wang et al. (2016) whereas protease production of *S. maltophilia* FF11 is proportional to the growth and reaches maximal activity at the peak of the growth (Wang et al., 2016a).

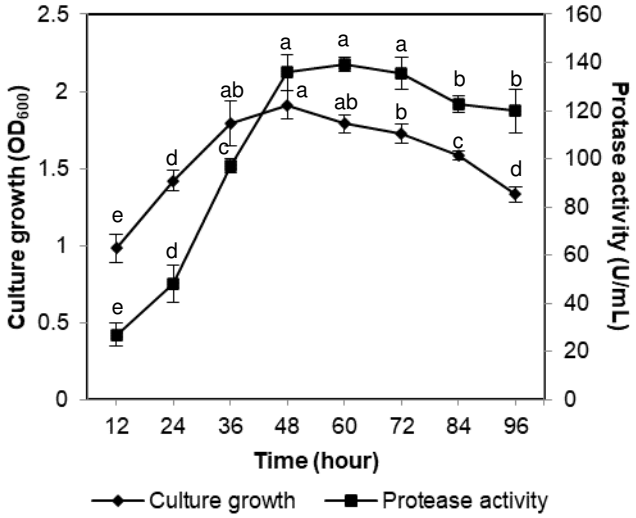

Figure 3. *The growth and extracellular protease activity by S. rhizophila MT1. Error bars represent the standard deviations of the mean (n = 3). Different letters indicate significant differences ($p < 0.05$)*

Effect of culture conditions on protease production

Effect of casein concentration

The concentration of casein was investigated by conducting experiments with increasing the concentration of casein in the medium. *Figure 4A* showed that protease achieved the highest activity of 139.02 ± 2.87 U/mL in the medium supplemented with 1% casein. When the casein concentration increased to 2 and 5%, the enzyme activity dramatically decreased to 135.16 ± 5.31 and 76.21 ± 3.79 U/mL, respectively. Casein has been reported as major nitrogen source for many microorganisms for maximal protease production. Jayasree et al. (2009) reported 1% casein as the major nitrogen source for the alkaline protease produced by *Streptomyces pulveraceus* (Jayasree et al., 2009). *Streptomyces halstedii* Salh-12 and *Streptomyces endus* Salh40, the two most proteolytic thermophilic strains used 1% casein as major nitrogen source for protease production, respectively (El Zawahry et al., 2007). Meanwhile, Asha et al. (2018) reported *Bacillus cereus* FT1 secreted the highest enzyme activity under cultivation in medium supplemented with 3.5% casein concentration (Asha and Palaniswamy, 2018).

Effect of inoculum size

The finite volume of the culture medium means that it contains only limited nutrients for microorganisms. The consumption of nutrients gradually depends on the bacterial population. Inoculum size is important in optimizing production because very low

http://www.aloki.hu ● ISSN 1589 1623 (Print) ● ISSN 1785 0037 (Online)
DOI: http://dx.doi.org/10.15666/aeer/2003_24092423

initial biomass concentrations may lead to long incubation times, while high inoculum levels lead to rapid biomass gain, resulting in nutritional stress affecting product formation (Khursade et al., 2019). Therefore, to ensure the production of enzymes in a limited media, it is necessary to control the initial stocking bacterial population. The maximal protease activity achieved at 188.56 ± 1.77 U/mL with inoculum size of 10% (v/v). The results showed that the *S. rhizophilia* MT1 required a higher initial inoculum size than *Bacillus licheniformis* NK reported by Ramkumar et al. (2018) and *B. cereus* AT reported by Vijayaraghavan et al. (2014) with the inoculum size of 5 and 6% (v/v), respectively (Ramkumar et al., 2018; Vijayaraghavan et al., 2014). A higher inoculum size of 15% (v/v) reduced protease production by *S. rhizophilia* MT1 than that inoculum size of 1% (v/v) (*Fig. 4B*). Therefore, high inoculum sizes do not enhance protease yield. The increase in the production of protease using small inoculum sizes is due to the higher surface area to volume ratio, which results in increasing protease production (Rahman et al., 2005). In addition, the improved distribution of dissolved oxygen and more efficient nutrient uptake also contributes to higher protease production. On the contrary, if the inoculum sizes are too small, insufficient bacterial population will reduce in the amount of protease secreted (Shafee et al., 2005).

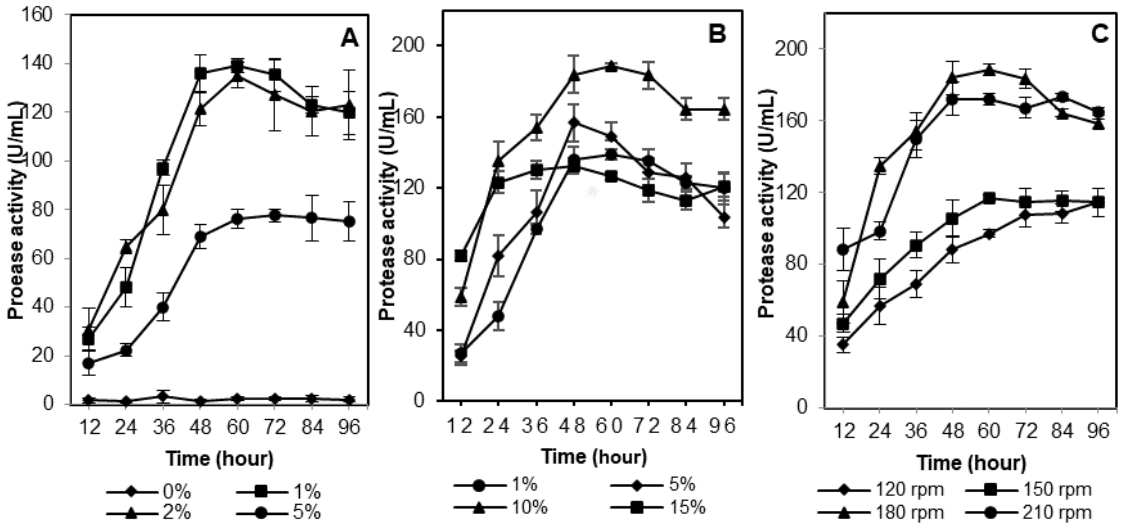

Figure 4. *Effect of casein concentration (A), inoculum size (B) agitation rate (C) on extracellular protease production by S. rhizophila MT1. Error bars represent the standard deviations of the mean (n = 3)*

Effect of agitation rate

Microorganisms differ in their oxygen requirements. In particular, oxygen acts as a terminal electron acceptor for oxidation reactions to provide energy for cellular activities. Variation in agitation speed was found to affect the degree of mixing in a shaker or bioreactor (Nascimento and Martins, 2004). The results showed that protease increases with increasing shaking speed and reached its highest at 180 rpm (188.56 ± 1.77 U/mL) (*Fig. 4C*). At this rate, aeration of the culture medium is increased, leading to an adequate supply of dissolved oxygen in the medium. Although protease production was found to decrease with shaking at 210 rpm, low shaking conditions most likely restricted protease production. Therefore, a higher shaking speed

http://www.aloki.hu ● ISSN 1589 1623 (Print) ● ISSN 1785 0037 (Online)
DOI: http://dx.doi.org/10.15666/aeer/2003_24092423

might increase the oxygen pressure of the system but not the yield, possibly because at high shaking speed, the enzyme's structure may not be stable (Abusham et al., 2009). Reducing the aeration rate significantly decreased protease production, showing reducing oxygen supply is an important limiting factor for growth and protease synthesis (Nascimento and Martins, 2004).

Effects of pH and temperature on protease activity

pH and temperature are factors that significantly change enzyme activity due to the abilities on modifying the catalytic groups in enzyme active sites as well as enzyme structure. Thus, each enzyme only catalyzes at a suitable temperature and pH range, where the reaction rate occurs fastest (Harris and Turner, 2002; Arcus and Mulholland, 2020). The effect of pH on protease activity was investigated with a pH range of 2.0–12.0. The protease was active with a board pH range of 7.0–10.0. The optimal pH was 9.0 (*Fig. 5A*). When pH increased from 5.0 to 8.0, the protease activity gradually increased with the relative activity increasing from 25.32 ± 3.44 to $96.82 \pm 6.02\%$, respectively. In the alkaline conditions (pH 10.0–12.0), the relative activity gradually decreased from 77.76 ± 9.43 to $27.36 \pm 2.1\%$ compared to the protease activity at pH 9.0. Protease lost $\geq 90\%$ activity at an acidic pH of 2.0-4.0. These results are in accordance with previous reports on alkaline proteases from *S. maltophilia* JSHY3 (Wang et al., 2016b), *S. maltophilia* FF11 (Wang et al., 2016a), *B. firmus* Tap5 (Joshi, 2010) and *Beauveria* sp. MTCC 5184 (Shankar et al., 2011).

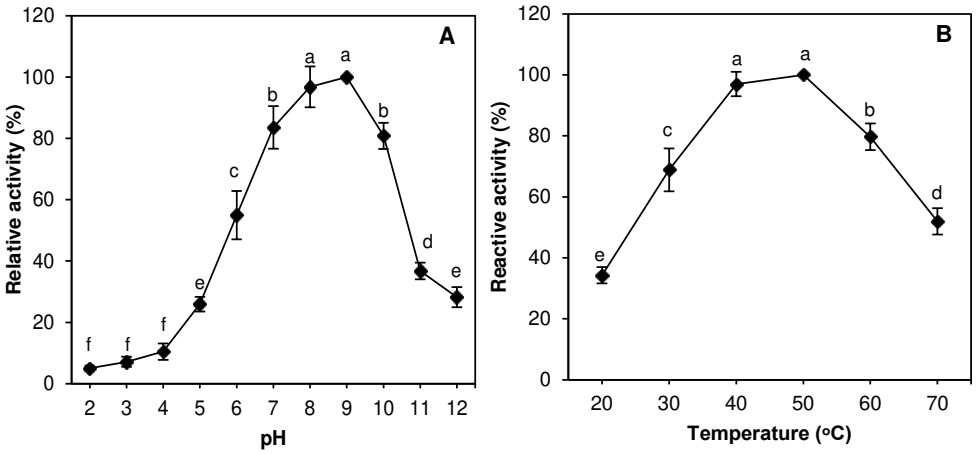

Figure 5. *Effect of pH (A) and temperature (B) on extracellular protease activity produced by S. rhizophila MT1. Error bars represent the standard deviations of the mean (n = 3). Different letters indicate significant differences ($p < 0.05$)*

The enzyme is active over a wide temperature range from 20 °C to 70 °C. A linear increase in protease activity was observed with increasing temperature. Maximum enzyme activity reached at 50 °C and maintained $\geq 50\%$ activity at temperature ranges of 30–70 °C. The lowest activity occurred when enzyme reaction was conducted at a temperature of 20 °C, reaching $34.31 \pm 2.67\%$. The relative protease activity of $51.94 \pm 4.3\%$ remained at 70 °C (*Fig. 5B*). The results are similar to previous study conducted on alkaline proteases from *Serratia marcescens subsp. sakuensis* TKU019 with maximum activity at 50 °C (Liang et al., 2010). Shankar et al. 2011 reported an

http://www.aloki.hu ● ISSN 1589 1623 (Print) ● ISSN 1785 0037 (Online)
DOI: http://dx.doi.org/10.15666/aeer/2003_24092423

optimum temperature of 50 °C for protease derived from *Beauveria* sp. MTCC 5184 (Shankar et al., 2011). Similar result was reported on protease from *S. maltophilia* S-1 with an optimum temperature of 50 °C (Miyaji et al., 2005).

Effects of inhibitors and metal ions on protease activity

Various metal ions have been reported to affect protease activity. Metal ions play an important role in enhancing thermal stability and maintaining the active conformation of enzymes, and influencing enzyme activity by binding at the catalytic site (Mechri et al., 2017). Calcium ion is an inducer and stabilizer of many enzymes and protecting them from structural changes (Sharma et al., 2017). The influence of various metal ions on the enzyme is presented in *Figure 6*A. The protease activity was not significantly ($p > 0.05$) affected by 1 mM of Zn^{2+}, Mg^{2+} and Cu^{2+} while the activity of enzyme was decreased in the presence of Mn^{2+}, Fe^{2+}. Meanwhile, Co^{2+}, K^{+} increased enzyme activity of 107.7%, and 108.37%, respectively. However, these increases were not significant in compared with control. On the contrary, Ca^{2+} significantly enhanced protease activity up to 116.51%. The results are equivalent to study Wang et al. (2016). However, protease of *S. rhizophilia* MT1 retained ≥ 90% activity in the presence of metal ions such as Zn^{2+}, Mn^{2+}, Cu^{2+} and Fe^{2+}, while Mn^{2+} and Fe^{2+} ions decreased protease activity of *S. maltophilia* FF11. Zn^{2+} and Cu^{2+} inhibited protease activity of *S. maltophilia* FF11 (Wang et al., 2016a). A serine protease from *B. safensis* is activated by Ca^{2+}, Co^{2+} and Mg^{2+} and inhibited by Ni^{2+} and Hg^{2+} ions (Rekik et al., 2019). Alkaline proteases from *Aeribacillus pallidus* are enhanced by Ca^{2+}, Cu^{2+} and Fe^{2+} ions (Mechri et al., 2017).

Proteins can be classified based on their susceptibility to inhibitors. The relative protease activity increased to 104.48 ± 3.91% in the presence of EDTA, a well-known inhibitor of metalloprotease and unaffected by β-mercaptoethanol (98.69 ± 4.2%), a cysteine protease inhibitor. The protease of *S. rhizophilia* MT1 expresses optimal activity at pH 9, suggesting it belongs to the alkaline protease class.

Effect of organic solvents on protease activity

The organic solvent stability of an enzyme depends on its nature (Matkawala et al., 2019). The effect of different organic solvents on protease activity was investigated at 30% (v/v) concentration. *Figure 6B* showed that the protease was not affected significantly ($p > 0.05$) by hydrophilic solvents such as methanol, ethanol and isopropanol. The enzyme activity was significantly increased to 114.81 ± 6.42 and 121.56 ± 11.6% in the presence of acetone and hexane, respectively. The effect of organic solvents on protease activity varies with protease types and solvents. It is known that proteases are more active and stable in hydrophobic solvents than in hydrophilic solvents (Wang et al., 2016a). For example, protease activities of *B. pumilus* 115b and 146 increase in hydrophobic solvents such as hexane, 1-decanol, isooctane, and n-dodecane (25%, v/v) (Rahman et al., 2005). The organic solvent stability of *S. rhizophila* MT1 protease is similar to that of protease from *S. maltophilia* FF11 (Wang et al., 2016a) and higher than other alkaline proteases produced by *Aeribacillus pallidus* C10 (Yildirim et al., 2017), *Neocosmospora* sp. N1 (Matkawala et al., 2019). In the presence of organic solvents, the ability of natural proteases to remain stable without making any modifications to enzyme stability is important for various applications (Doukyu and Ogino, 2010). The strong stability of *S. rhizophilia* MT1 protease in organic solvents leads to a great applicability advantage.

http://www.aloki.hu ● ISSN 1589 1623 (Print) ● ISSN 1785 0037 (Online)
DOI: http://dx.doi.org/10.15666/aeer/2003_24092423

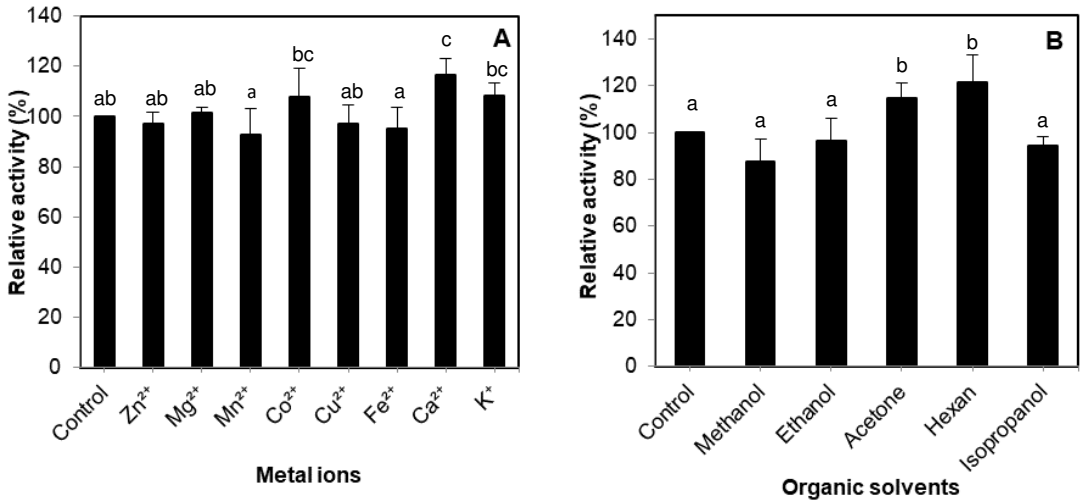

Figure 6. *Effect of metal ions (A) and organic solvents (B) on extracellular protease activity produced by S. rhizophila MT1. Error bars represent the standard deviations of the mean (n = 3). Different letters indicate significant differences (p < 0.05)*

Zymogram

Molecular mass and enzyme activity were assessed using zymogram electrophoresis. The cell-free supernatant of *S. rhizophila* MT1 was subjected to polyacrylamide gel electrophoresis to separate and determine the molecular weight of the extracellular proteases. The zymogram showed two distinct casein-resolution luminous areas on the gel with molecular masses of 30 and 110 kDa (*Fig. 7*). Previous studies reported that alkaline proteases from *S. maltophilia* G2 (Huang et al., 2009), *B. licheniformis* MP1 (Jellouli et al., 2011), *Beauveria* sp. MTCC 5184 (Shankar et al., 2011), *B. halodurans* JB 99 (Shrinivas and Naik, 2011) exhibit similar small protease band of *S. rhizophila* MT1. Meanwhile, alkaline proteases of *P. fluorescens* (Kandasamy et al., 2012); *S. maltophilia* FF11 (Wang et al., 2016a) are differed. Numerous higher molecular weight of alkaline proteases have been reported from *B. halotolerans* CT2 (Dorra et al., 2018) and *Aspergillus fumigatus* TKU003 (Wang et al., 2005).

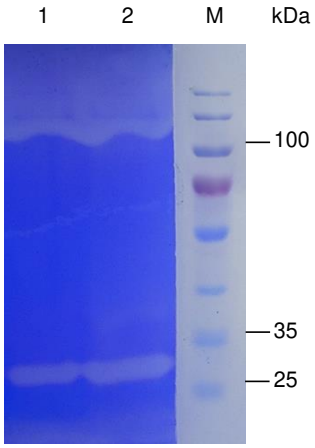

Figure 7. *Proteolytic zymogram of S. rhizophila MT1 cell-free supernatant. Lane M: PageRuler™ Prestained Protein (Thermo Scientific, USA); Lane 1, 2: S. rhizophila MT1 cell-free supernatant*

http://www.aloki.hu ● ISSN 1589 1623 (Print) ● ISSN 1785 0037 (Online)
DOI: http://dx.doi.org/10.15666/aeer/2003_24092423

Conclusion

The *S. rhizophila* MT1 isolate shows strong protease production. The maximum enzyme activity occurs in the culture medium containing 1% casein (w/v), inoculum size of 10% (v/) and agitation rate of 180 rpm. Two clear caseinolytic activity protein bands had molecular weights of 30 kDa and 110 kDa. The optimum activity of this enzyme expressed at temperature of 50 °C and pH of 9. Ca^{2+}, Co^{2+} and K^{+} ions greatly enhanced enzyme activity. The enzyme was stable in the presence of the metal ions Mn^{2+}, Zn^{2+}, Cu^{2+} and Fe^{2+} with protease activity maintained $\geq 90\%$ maximal activity. Organic solvents such as acetone and hexane solvents increased enzyme activity. The present study demonstrates that *S. rhizophila* MT1 protease is stable in the environment containing various metal ions and organic solvents, promising the potential to convert aquaculture sludge to agriculture fertilizers, which minimizes the negative effect of aquaculture sludge waste to environment.

Acknowledgements. The study received funding support from Vietnam Ministry of Education and Training under grant number B2020-DHH-18.

REFERENCES

[1] Abusham, R. A., Rahman, R. N., Salleh, A. B., Basri, M. (2009): Optimization of physical factors affecting the production of thermo-stable organic solvent-tolerant protease from a newly isolated halo tolerant *Bacillus subtilis* strain Rand. – Microbial Cell Factories 8: 20.

[2] Amin, M. (2018): Marine protease-producing bacterium and its potential use as an abalone probiont. – Aquaculture Reports 12: 30-35.

[3] Arcus, V. L., Mulholland, A. J. (2020): Temperature, dynamics, and enzyme-catalyzed reaction rates. – Annual Review of Biophysics 49: 163-180.

[4] Asha, B., Palaniswamy, M. (2018): Optimization of alkaline protease production by *Bacillus cereus* FT 1 isolated from soil. – Journal of Applied Pharmaceutical Science 8: 119-127.

[5] Berg, G., Martinez, J. L. (2015): Friends or foes: can we make a distinction between beneficial and harmful strains of the *Stenotrophomonas maltophilia* complex? – Frontiers in Microbiology 6: 241.

[6] Brooke, J. S. (2012): *Stenotrophomonas maltophilia*: an emerging global opportunistic pathogen. – Clinical Microbiology Reviews 25: 2-41.

[7] Cupp-Enyard, C. (2008): Sigma's non-specific protease activity assay - casein as a substrate. – Journal of Visualized Experiments. DOI: 10.3791/899.

[8] Dorra, G., Ines, K., Imen, B. S., Laurent, C., Sana, A., Olfa, T., Pascal, C., Thierry, J., Ferid, L. (2018): Purification and characterization of a novel high molecular weight alkaline protease produced by an endophytic *Bacillus halotolerans* strain CT2. – International Journal of Biological Macromolecules 111: 342-351.

[9] Doukyu, N., Ogino, H. (2010): Organic solvent tolerant enzymes. – Biochemical Engineering Journal 48: 270-282.

[10] El Zawahry, Y., Awny, M., Tohamy, E., Abou Zeid, A., Reda, F. (2007): Optimization, characterization and purification of protease production by some Actinomycetes isolated under stress conditions. – Proceeding of the Second Scientific Environmental Conffer, Zagazig Uni., pp. 153-175.

http://www.aloki.hu ● ISSN 1589 1623 (Print) ● ISSN 1785 0037 (Online)
DOI: http://dx.doi.org/10.15666/aeer/2003_24092423

[11] Hamza, F., Satpute, S., Banpurkar, A., Kumar, A. R., Zinjarde, S. (2017): Biosurfactant from a marine bacterium disrupts biofilms of pathogenic bacteria in a tropical aquaculture system. – FEMS Microbiology Ecology. DOI: 10.1093/femsec/fix140.
[12] Harris, T. K., Turner, G. J. (2002): Structural basis of perturbed pKa values of catalytic groups in enzyme active sites. – IUBMB Life 53: 85-98.
[13] Huang, X., Liu, J., Ding, J., He, Q., Xiong, R., Zhang, K. (2009): The investigation of nematocidal activity in *Stenotrophomonas maltophilia* G2 and characterization of a novel virulence serine protease. – Canadian Journal of Microbiology 55: 934-42.
[14] Jankiewicz, U., Baranowski, B., Swiontek Brzezinska, M., Frak, M. (2020): Purification, characterization and cloning of a chitinase from *Stenotrophomonas rhizophila* G22. – 3 Biotech 10: 16.
[15] Jayasree, D., Sandhya Kumari, T., Kavi Kishor, P., Vijayalakshmi, M., Lakshmi Narasu, M. (2009): Optimization of production protocol of alkaline protease by *Streptomyces pulvereceus*. – Inter JRI Sci Technol 1: 79-82.
[16] Jellouli, K., Bellaaj, O., Ayed, H., Manni, L., Agrebi, R., Nasri, M. (2011): Alkaline-protease from *Bacillus licheniformis* MP1: Purification, characterization and potential application as a detergent additive and for shrimp waste deproteinization. – Process Biochemistry 46: 1248-1256.
[17] Joshi, B. H. (2010): Purification and characterization of a novel protease from *Bacillus Firmus* Tap5 isolated from tannery waste. – Journal of Applied Sciences Research 6: 1068-1076.
[18] Kandasamy, N., Punitha, V., Amsamani, S., Raghava, R. J., Bangaru, C., Palanisamy, T. (2012): Eco-benign enzymatic dehairing of goatskins utilizing a protease froma *Pseudomonas fluorescens* species isolated from fish visceral waste. – Journal of Cleaner Production 25: 27-33.
[19] Khursade, P. S., Galande, S. H., Shiva Krishna, P., Prakasham, R. S. (2019): *Stenotrophomonas maltophilia* Gd2: a potential and novel isolate for fibrinolytic enzyme production. – Saudi Journal of Biological Sciences 26: 1567-1575.
[20] Li, Y., Wang, L., Yan, Z., Chao, C., Yu, H., Yu, D., Liu, C. (2020): Effectiveness of dredging on internal phosphorus loading in a typical aquacultural lake. – Science of the Total Environment 744: 140883.
[21] Liang, T. W., Kuo, Y. H., Wu, P. C., Wang, C. L., Dzung, N. A., Wang, S. L. (2010): Purification and Characterization of a chitosanase and a protease by conversion of shrimp shell wastes fermented by *Serratia Marcescens Subsp. Sakuensis* TKU019. – Journal of the Chinese Chemical Society 57: 857-863.
[22] Marathe, S. K., Vashistht, M. A., Prashanth, A., Parveen, N., Chakraborty, S., Nair, S. S. (2018): Isolation, partial purification, biochemical characterization and detergent compatibility of alkaline protease produced by *Bacillus subtilis*, *Alcaligenes faecalis* and *Pseudomonas aeruginosa* obtained from sea water samples. – Journal of Genetic Engineering and Biotechnology 16: 39-46.
[23] Mariane De Morais, A. P., Abreu, P. C., Wasielesky, W., Krummenauer, D. (2020): Effect of aeration intensity on the biofilm nitrification process during the production of the white shrimp *Litopenaeus vannamei* (Boone, 1931) in Biofloc and clear water systems. – Aquaculture 515: 734516.
[24] Matkawala, F., Nighojkar, S., Kumar, A., Nighojkar, A. (2019): A novel thiol-dependent serine protease from Neocosmospora sp. N1. – Heliyon 5: e02246.
[25] Mechri, S., Ben Elhoul Berrouina, M., Omrane Benmrad, M., Zarai Jaouadi, N., Rekik, H., Moujehed, E., Chebbi, A., Sayadi, S., Chamkha, M., Bejar, S., Jaouadi, B. (2017): Characterization of a novel protease from *Aeribacillus pallidus* strain VP3 with potential biotechnological interest. – International Journal of Biological Macromolecules 94: 221-232.
[26] Miyaji, T., Otta, Y., Shibata, T., Mitsui, K., Nakagawa, T., Watanabe, T., Niimura, Y., Tomizuka, N. (2005): Purification and characterization of extracellular alkaline serine

http://www.aloki.hu ● ISSN 1589 1623 (Print) ● ISSN 1785 0037 (Online)
DOI: http://dx.doi.org/10.15666/aeer/2003_24092423

protease from *Stenotrophomonas maltophilia* strain S-1. – Journal of Applied Microbiology 41: 253-257.
[27] Nascimento, W., Martins, M. (2004): Production and properties of an extracellular protease from thermophilic *Bacillus* sp. – Brazilian Journal of Microbiology 35: 91-96.
[28] Patil, P. P., Midha, S., Kumar, S., Patil, P. B. (2016): Genome sequence of type strains of genus Stenotrophomonas. – Frontiers in Microbiology 7: 309.
[29] Pinski, A., Zur, J., Hasterok, R., Hupert-Kocurek, K. (2020): Comparative genomics of *Stenotrophomonas maltophilia* and *Stenotrophomonas rhizophila* revealed characteristic features of both species. – International Journal of Molecular Sciences 21: 4922.
[30] Rahman, R. N., Geok, L. P., Basri, M., Salleh, A. B. (2005): Physical factors affecting the production of organic solvent-tolerant protease by *Pseudomonas aeruginosa* strain K. – Bioresource Technology 96: 429-436.
[31] Ramkumar, A., Sivakumar, N., Gujarathi, A. M., Victor, R. (2018): Production of thermotolerant, detergent stable alkaline protease using the gut waste of *Sardinella longiceps* as a substrate: optimization and characterization. – Scientific Reports 8: 12442.
[32] Rekik, H., Zarai Jaouadi, N., Gargouri, F., Bejar, W., Frikha, F., Jmal, N., Bejar, S., Jaouadi, B. (2019): Production, purification and biochemical characterization of a novel detergent-stable serine alkaline protease from *Bacillus safensis* strain RH12. – International Journal of Biological Macromolecules 121: 1227-1239.
[33] Ryan, R. P., Monchy, S., Cardinale, M., Taghavi, S., Crossman, L., Avison, M. B., Berg, G., Van Der Lelie, D., Dow, J. M. (2009): The versatility and adaptation of bacteria from the genus *Stenotrophomonas*. – Nature Reviews Microbiology 7: 514-525.
[34] Said, M., Faizal, M., Yudono, B., Hasanudin, Estuningsih, S. P. (2019): Isolates of lipolytic, proteolytic and cellulolytic bacteria from palm oil mill effluent and their potency as consortium. – International Journal on Advanced Science, Engineering and Information Technology 9: 390-396.
[35] Sambrook, J., Maccallum, P., Russell, D. (2001): Molecular Cloning: A Laboratory Manual. – Cold Spring Harbor Press, New York.
[36] Santos, L., Ramos, F. (2018): Antimicrobial resistance in aquaculture: current knowledge and alternatives to tackle the problem. – International Journal of Antimicrobial Agents 52: 135-143.
[37] Shafee, N., Aris, S., Rahman, R., Basri, M., Salleh, A. (2005): Optimization of environmental and nutritional conditions for the production of alkaline protease by a newly isolated bacterium Bacillus cereus strain 146. – Journal of Applied Sciences Research 1: 1-18.
[38] Shankar, S., Rao, M., Laxman, R. (2011): Purification and characterization of an alkaline protease by a new strain of *Beauveria* sp. – Process Biochemistry 46: 579-585.
[39] Sharma, K. M., Kumar, R., Panwar, S., Kumar, A. (2017): Microbial alkaline proteases: optimization of production parameters and their properties. – Journal of Genetic Engineering and Biotechnology 15: 115-126.
[40] Shi, Z., Li, X.-Q., Chowdhury, M. K., Chen, J.-N., Leng, X.-J. (2016): Effects of protease supplementation in low fish meal pelleted and extruded diets on growth, nutrient retention and digestibility of gibel carp, *Carassius auratus* gibelio. – Aquaculture 460: 37-44.
[41] Shrinivas, D., Naik, G. (2011): Characterization of alkaline thermostable keratinolytic protease from thermoalkalophilic *Bacillus halodurans* JB 99 exhibiting dehairing activity. – International Biodeterioration and Biodegradation 65: 29-35.
[42] Singh, S., Thavamani, P., Megharaj, M., Naidu, R. (2015): Multifarious activities of cellulose degrading bacteria from Koala (*Phascolarctos cinereus*) faeces. – Journal of Animal Science and Technology 57: 23.
[43] Steinmann, J., Mamat, U., Abda, E. M., Kirchhoff, L., Streit, W. R., Schaible, U. E., Niemann, S., Kohl, T. A. (2018): Analysis of phylogenetic variation of

http://www.aloki.hu ● ISSN 1589 1623 (Print) ● ISSN 1785 0037 (Online)
DOI: http://dx.doi.org/10.15666/aeer/2003_24092423

Stenotrophomonas maltophilia reveals human-specific branches. – Frontiers in Microbiology 9: 806.

[44] Su, H., Xiao, Z., Yu, K., Huang, Q., Wang, G., Wang, Y., Liang, J., Huang, W., Huang, X., Wei, F., Chen, B. (2020): Diversity of cultivable protease-producing bacteria and their extracellular proteases associated to *scleractinian corals*. – PeerJ 8: e9055.

[45] Sun, S.-C., Chen, J.-X., Wang, Y.-G., Leng, F.-F., Zhao, J., Chen, K., Zhang, Q.-C. (2021): Molecular mechanisms of heavy metals resistance of *Stenotrophomonas rhizophila* JC1 by whole genome sequencing. – Archives of Microbiology 203: 2699-2709.

[46] Suwoyo, H. S., Tuwo, A., Haryati, Anshar, H., Syah, R. (2020): The utilizations of solid waste originating from super intensive shrimp farm as organic fertilizers for natural feed productions. – IOP Conf. Series: Earth and Environmental Science 473: 012110.

[47] Tamura, K., Stecher, G., Kumar, S. (2021): MEGA11: Molecular evolutionary genetics analysis version 11. – Molecular Biology and Evolution 38: 3022-3027.

[48] Tangguda, S., Diana, A., Arning, W. E. (2015): Utilization of solid waste from White Shrimp (*Litopenaeus vannamei*) farm on the growth and Chlorophyll content in *Chlorella* sp. – Journal of Life Science and Biomedicine 5: 81-85.

[49] Vijayaraghavan, P., Lazarus, S., Vincent, S. G. (2014): De-hairing protease production by an isolated *Bacillus cereus* strain AT under solid-state fermentation using cow dung: biosynthesis and properties. – Saudi Journal of Biological Sciences 21: 27-34.

[50] Wang, S. L., Chen, Y. H., Wang, C. L., Yen, Y. H., Chern, M. K. (2005): Purification and characterization of a serine protease extracellularly produced by *Aspergillus fumigatus* in a shrimp and crab shell powder medium. – Enzyme and Microbial Technology 36: 660-665.

[51] Wang, Q., Ji, F., Wang, J., Jiang, B., Li, L., An, L., Li, Y., Bao, Y. (2016a): Characterization of a salt-activated protease with temperature-dependent secretion in *Stenotrophomonas maltophilia* FF11 isolated from frozen Antarctic krill. – Journal of Industrial Microbiology and Biotechnology 43: 829-840.

[52] Wang, Z., Sun, L., Cheng, J., Liu, C., Tang, X., Zhang, H., Liu, Y. (2016b): The optimization of fermentation conditions and enzyme properties of *Stenotrophomonas maltophilia* for protease production. – Biotechnology and Applied Biochemistry 63: 292-299.

[53] Yildirim, V., Baltaci, M. O., Ozgencli, I., Sisecioglu, M., Adiguzel, A., Adiguzel, G. (2017): Purification and biochemical characterization of a novel thermostable serine alkaline protease from *Aeribacillus pallidus* C10: a potential additive for detergents. – Journal of Enzyme Inhibition and Medicinal Chemistry 32: 468-477.

http://www.aloki.hu ● ISSN 1589 1623 (Print) ● ISSN 1785 0037 (Online)
DOI: http://dx.doi.org/10.15666/aeer/2003_24092423

DROUGHT STRESS AT FLOWERING STAGE REGULATES PHOTOSYNTHESIS, AROMA AND GRAIN YIELD IN FRAGRANT RICE

GUI, R. F.[1,2] – JIANG, H. L.[1,2] – ASHRAF, U.[3] – LI, S. Y.[1,2] – DUAN, M. Y.[1,2] – PAN, S. G.[1,2] – TIAN, H.[1,2] – TANG, X. R.[1,2] – MO, Z. W.[1,2*]

[1]*State Key Laboratory for Conservation and Utilization of Subtropical Agro-bioresources, College of Agriculture, South China Agricultural University, Guangzhou 510642, China*

[2]*Scientific Observing and Experimental Station of Crop Cultivation in South China, Ministry of Agriculture and Rural Affairs, Guangzhou 510642, China*

[3]*Department of Botany, Division of Science and Technology, University of Education, Lahore, 54770 Punjab, Pakistan*

[*]*Corresponding author*
e-mail: scaumozhw@126.com

(Received 25th Nov 2021; accepted 17th Mar 2022)

Abstract. Fragrant rice is widely consumed worldwide due to its pleasant aroma and better cooking qualities, however external plant factors such as drought could their yield and quality characteristics of fragrant rice. Drought-induced reductions in morphological and yield attributes of rice were previously reported, nevertheless effects of drought stress imposed at flowering stage on 2-acetyl-1-pyrroline (2AP) contents, grain yield, and related morphophysiological attributes of fragrant rice were rarely investigated. The present study, two fragrant rice cultivars, Yuxiangyouzhan and Guixiangzhan, were exposed to two water levels i.e., (i) well-watered treatment (CK), during the whole plant growth period with a 2-4 cm water layer was maintained until one week before harvest, and (ii) drought stress treatment (Drought) imposed only at 50% heading of the main stem for one week. Results indicated that drought stress substantially improved the grain the 2AP content. The grain yield was decreased by 15.02-20.49% in both rice cultivars owing to substantial reduction in morphological and biochemical attributes, total dry weight, relative water contents, leaf weight per unit area, photosynthesis, and antioxidant activities. Overall, development of drought resistant fragrant rice cultivars is necessary to get grains with strong aroma without compromising grain yield under water deficit conditions.
Keywords: *physiological measurement, drought stress, fragrant rice, yield*

Introduction

Fragrant rice (*Oryza sativa* L.) is globally famous for its unique fragrance and 2-acetyl-1-pyrroline (2AP) was recognized as the key compound responsible for perfumed smell in fragrant rice (Wakte et al., 2017). Physiologically, various enzymes and precursors such as proline, proline dehydrogenase, $^{\Delta}$1-pyrroline are actively involved in 2AP biosynthesis which have been reported in previous studies (Mo et al., 2015, 2019, 2019a; Liu et al., 2020; Xie et al., 2020). Moreover, the enzymes and precursors involved in 2AP formation such as proline, $^{\Delta}$1-pyrroline-5-carboxylate synthetase, $^{\Delta}$1-pyrroline-5-carboxylate, were also involved in the metabolic pathway of plants in response to adverse environments (Xie et al., 2020).

Drought and/or water-deficit conditions not only affect the rice growth and yield traits but also the grain aroma contents in fragrant rice. For example, occurrence of drought during rice growth period could result in poor seed development and yield loss in rice

http://www.aloki.hu ● ISSN 1589 1623 (Print) ● ISSN1785 0037 (Online)
DOI: http://dx.doi.org/10.15666/aeer/2003_24252438

(Yang et al., 2013). The inhibition of photosynthetic carbon metabolism under drought stress conditions could make the conditions more adverse in rice (Ambavaram et al., 2014). Previous studies suggested that mild drought (within safe limits) could promote the accumulation of 2AP in fragrant rice without yield loss, whilst shallow-water irrigations/ alternate wetting and drying at tillering, booting stage and grain filling stage could improve the grain 2AP contents (Wang et al., 2013a,b), however, the effects of mild drought stress at flowering stage, the most critical phase for rice yield formation in related to the changes in agronomical and physiological processes under drought stress (Yang et al., 2013; Hinge et al., 2016) on aroma, grain yield, gas exchange parameters and antioxidant activities in fragrant rice have not been well reported. Hence, present study was conducted to evaluate the effects of drought stress at flowering stage on 2AP accumulation in the leaves and grains as well as the gas exchange attributes, antioxidant capacities and grain yield of elite Chinese fragrant rice cultivars.

Materials and methods

Experimental details

A pot experiment was conducted in greenhouse at Experimental Research Farm, South China Agricultural University, Guangzhou, China during 2015. Two regionally popular and widely grown fragrant rice cultivars, i.e., Yuxiangyouzhan and Guixiangzhan having growth periods of 128 and 118 days for early season (March-July), were exposed to two water levels i.e., (i) well water treatment (CK), during the whole plant growth period with 2-4 cm water layer was maintained till one week before harvest, and (ii) drought stress treatment (Drought) imposed only at 50% heading of the main stem (Yang et al., 2013) for one week and then re-watering at the same time before and after treatment. The soil moisture content was measured by oven-drying method. The ratio of the water mass lost to the mass of the dried soil when the samples were dried to a constant weight at 110°Cand expressed as percentage. The pots were arranged in completely randomized design (CRD) with 24 pots per treatment. Rice seedlings (20-days-old) were transplanted into the pots (31 cm in diameter and 29 cm in height), with five hills per pot. All treatments kept shallow water layer 1cm when transplanting, in addition, drought treatment was strictly controlled as required, and all treatments were cut off water one week before harvest. The experimental soil was sandy loam containing 20.45 g kg^{-1} soil organic matter, 1.09 g kg^{-1} total nitrogen, 1.03 g kg^{-1} total phosphorus, 19.68 g kg^{-1} total potassium. The drought was imposed by with-holding irrigation to reduce the water contents at flowering stage and the respective changes of relative soil water content and plant growth of aromatic rice in 7 days after drought stress treatment was shown in (*Figure 1*).

Plant sampling and measurements

The leaves and grains 2AP content were extracted according to (Mo et al., 2019) whereas extract was added for sodium sulfate, filtered with 0.22 μm filter paper (Shimadzu, Japan) and then directly used to detected the 2AP content by using GC-MS QP 2010 Plus (Shimadzu Corporation, Japan) by following the methods of (Hinge et al., 2016). The 2AP content was expressed as μg kg^{-1}. We sampled 6 of 24 pots from each treatment to determine 2AP content.

Yield and yield related traits were estimated according to (Mo et al., 2017). At maturity, grain yield was measured from six pots in each treatment, threshed manually,

http://www.aloki.hu ● ISSN 1589 1623 (Print) ● ISSN1785 0037 (Online)
DOI: http://dx.doi.org/10.15666/aeer/2003_24252438

and then sun dried (adjusted to moisture content of ~14%). Panicle number per pot was measured by counting the panicle numbers of each hill in six different pots in each treatment and averaged. Five random samples from filled grains were counted, weighed and averaged. The plant height and total dry weight were measured at maturity stage and the harvest index was calculated as the dry yield weight divided by the total dry aboveground biomass. The leaf weight per unit area was also calculated according to the following formula: specific leaf weight =leaf weight/leaf area.

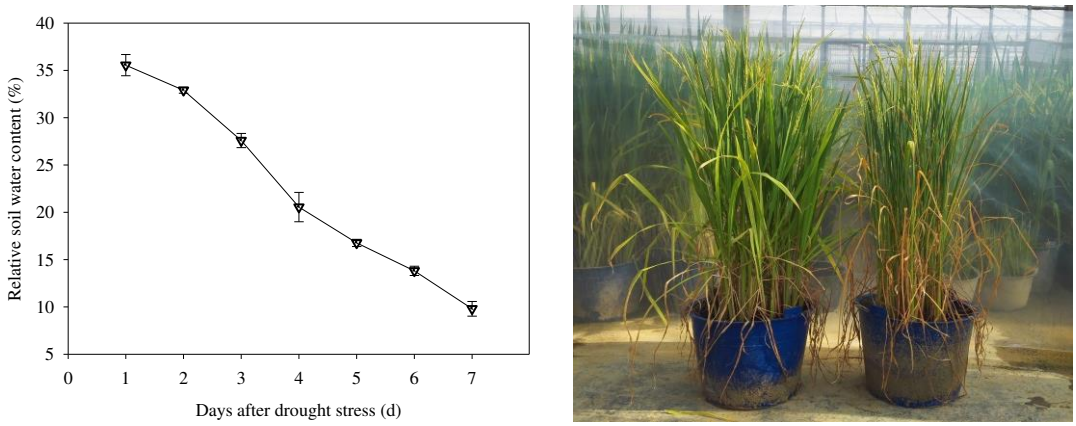

Figure 1. *Changes of the relative soil water content within 7 days after drought stress treatment and the plant growth of aromatic rice*

Net photosynthetic rate and gas exchange attributes i.e., stomatal conductance, intercellular CO_2 and transpirational rates was determined in three plants from each pot and nine from each treatment by using portable photosynthesis system (LI-6400, LI-COR, USA). Photosynthesis and gas exchange attributes were measured at 09:00-11:00 am after treatment application and after 5 days of drought recovery with the following adjustments: photosynthetically active radiation at leaf surface was up to 1200 µmol m^{-2} s^{-1}, molar flow of air per unit leaf area was about 500 µmol s^{-1}, ambient CO_2 concentration almost 400 µmol mol^{-1} (Pan et al., 2016).

In addition, it was cut from after treatment and after 5 days of recovery fresh leaf samples (0.3 g) were homogenized in 6 ml of 50 mM sodium phosphate buffer (pH 7.8) with a mortar and pestle in an ice bath and homogenate were centrifuged at 10000 rpm for 20 min at 4°C and an aliquot of the supernatant was used to record the enzymatic activities. Superoxide dismutase (SOD) was determined according to (Zhang and Kirkham, 1996) by following the inhibition of photochemical reduction due to nitro blue tetrazolium (NBT) and the absorbance was read at 560 nm. SOD activity per units was the amount of enzyme required to inhibit NBT photochemical reduction to 50% as an activity unit (U) and expressed as U g^{-1} protein min^{-1}. Peroxidase (POD) activity was estimated according to Zhang and Kirkham (1996) by using guaiacol method and the absorbance was read at 470 nm. One unit of POD activity was the amount of enzyme that caused absorption variation at 470 nm and expressed as U g^{-1} protein min^{-1}. Catalase activity (CAT) was measured according to the protocols of Zhang and Kirkham (1996). The absorbance was read at 240 nm. One unit of enzyme activity (U) was calculated as the absorption changed at A240 and express as U g^{-1} protein min^{-1}. All were determined by (Shimadzu, Japan UV2600 UV) spectrophotometer.

http://www.aloki.hu ● ISSN 1589 1623 (Print) ● ISSN1785 0037 (Online)
DOI: http://dx.doi.org/10.15666/aeer/2003_24252438

Protein contents were estimated according to Bradford (1976) using G-250. The absorbance of the reaction mixture was read at 595 nm in triplicate. The Malondialdehyde (MDA) contents were estimated according to methods advised by Zhang and Kirkham (1996). It was cut from after treatment and after 5 days of recovery fresh leaf samples (0.2 g) were homogenized in 2 ml of 0.5% thiobarbituric acid (TBA) solution in 10% trichloroacetic acid (TCA) and boiled in the water bath at 100°C for 30 min. The boiled samples were then cooled down in an ice bath and centrifuged at 4000 rpm for 15 min. The absorbance of the reaction mixtures was read by spectrophotometer and the final contents were expressed as μmol g^{-1}.

The relative water contents (RWC) of the leaves were determined according to Nauš et al. (2016). To determine the total nitrogen content in after treatment the leaves and grains, the dried samples (0.3 g) were digested using the 5 ml of H_2SO_4 and a few drops of $HClO_4$ to clear the solution. The total N contents were determined by the Kjeldahl method with a 2300 Kjeltec Analyzer Unit (Foss Tecator AB, Sweden).

Statistical analysis

The pots were arranged in completely randomized design (CRD) with 24 pots per treatment. Analyses of variances (ANOVA) were performed by Statistix version 8 (Statistix 8, Analystical, Tallahassee, Florida, USA). Comparisons of means among different treatments were separated according to the least significant difference (LSD) test at the 5% probability level. The figures were made by using the SigmaPlot for windows version 10. 0 and Microsoft Excel 2010.

Results

2AP content in grains and leaves

The 2AP contents for both rice cultivars i.e., Guixiangzhan and Yuxiangyouzhan were substantially enhanced after drought treatment. For instance, the 2AP content in grains were enhanced by 298.84% and 20.52% for Guixiangzhan and Yuxiangyouzhan, respectively, whereas the 2AP contents in leaves were enhanced by 33.46% of Guixiangzhan whereas a marginal increase was noted in the leaves of Yuxiangyouzhan at the end of treatment only. Moreover, no significant increase in 2AP content in leaves of both rice cultivars was detected after 5 days of drought recovery (*Figure 2*).

Agronomic traits

Compared to CK, drought decreased plant height, grain yield and total dry weight in Guixiangzhan by 4.88%, 15.02%, and 14.03%, respectively, as well as by 4.81%, 22.99%, and 20.49% in Yuxiangyouzhan, respectively. No significant effect of drought on harvest index was recorded for both fragrant rice cultivars (*Figure 3*).

Photosynthetic rate and gas exchange parameters

Drought substantially reduced photosynthetic rate, stomatal conductance, intercellular CO_2 concentration and transpiration rate in both fragrant rice cultivars (*Figure 4*). The photosynthetic rate, stomatal conductance and transpiration rate for Guixiangzhan was reduced even after 5 days of recovery. Drought significantly decreased the photosynthetic rate in Yuxiangyouzhan whereas the intercellular CO_2 concentration for both fragrant rice cultivars were enhanced under after 5 days of recovery stress. Moreover, photosynthetic

http://www.aloki.hu ● ISSN 1589 1623 (Print) ● ISSN1785 0037 (Online)
DOI: http://dx.doi.org/10.15666/aeer/2003_24252438

rate, stomatal conductance and transpiration rate were remained higher under CK (except intercellular CO_2 concentration) (*Figure 5*).

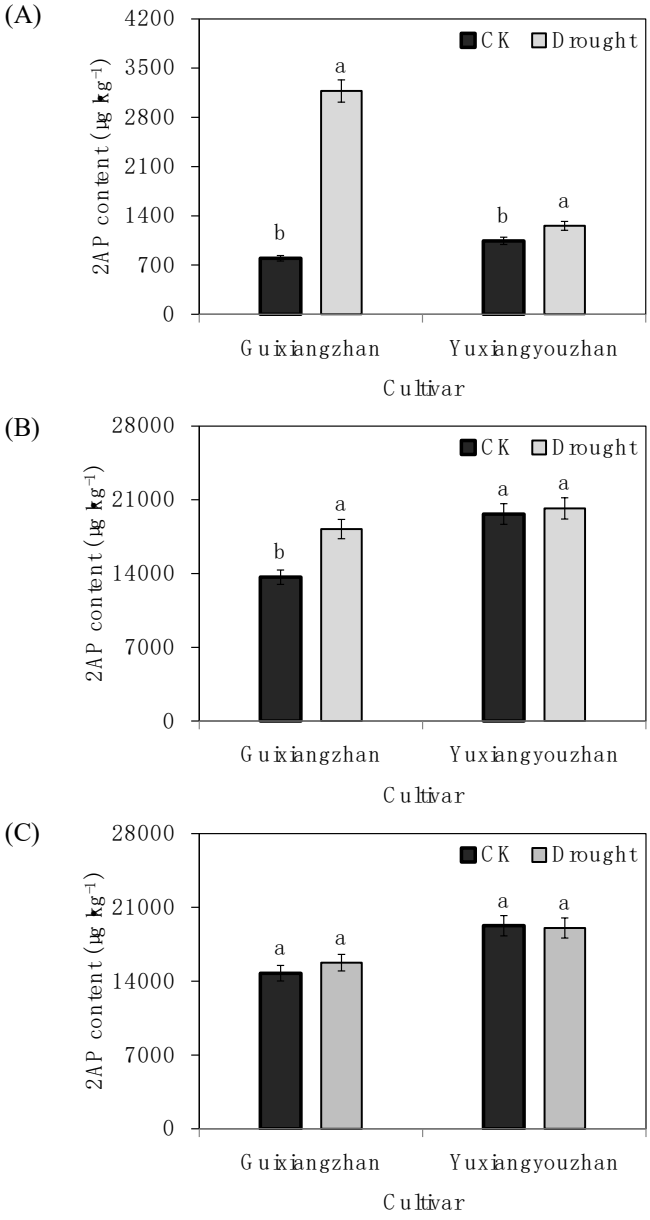

Figure 2. *Effects of drought stress on 2AP content in grains (A) and leaves at the end of treatment(B) and after 5 days recovery(C) of two fragrant rice cultivars. Vertical bars with different lower case letters above are significantly different at P<0.05 by LSD tests. Capped bars represent S.D (n=3).CK:Well water treatment*

Physio-biochemical attributes and leaf N contents

The protein contents in the leaves were substantially increased after drought but decreased significantly after 5 days of recovery. No significant difference in terms of MDA concentration after drought was found, however, the MDA concentration was remained noticeably higher after 5 days of recovery (*Figure 6*).

http://www.aloki.hu ● ISSN 1589 1623 (Print) ● ISSN1785 0037 (Online)
DOI: http://dx.doi.org/10.15666/aeer/2003_24252438

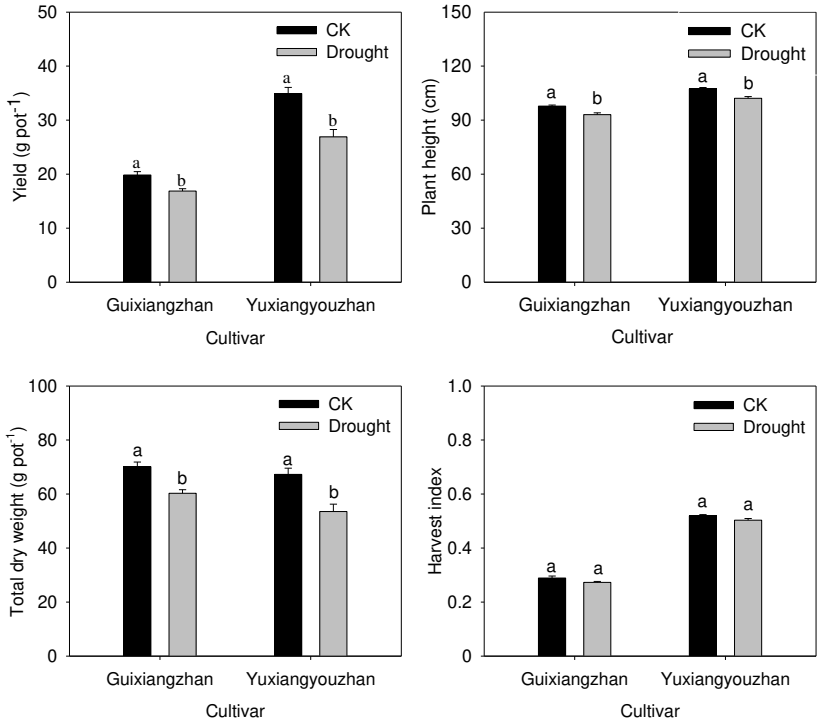

Figure 3. *Effects of drought stress on yield, plant height, total dry weight and harvest index of two fragrant rice cultivars. Vertical bars with different lower case letters above are significantly different at P<0.05 by LSD tests. Capped bars represent S.D (n=6). CK: Well water treatment*

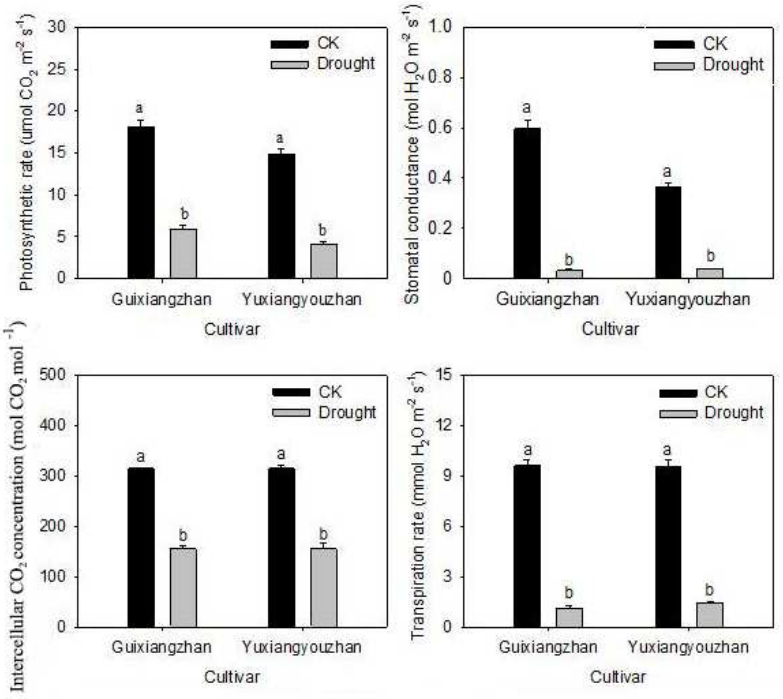

Figure 4. *Effects of drought stress treatment on photosynthetic rate, stomatal conductance, intercellular CO_2 concentration and transpiration rate of two fragrant rice cultivars at the end of treatment. Vertical bars with different lower case letters above are significantly different at P<0.05 by LSD tests. Capped bars represent S.D (n=6). CK: Well water treatment*

http://www.aloki.hu ● ISSN 1589 1623 (Print) ● ISSN1785 0037 (Online)
DOI: http://dx.doi.org/10.15666/aeer/2003_24252438

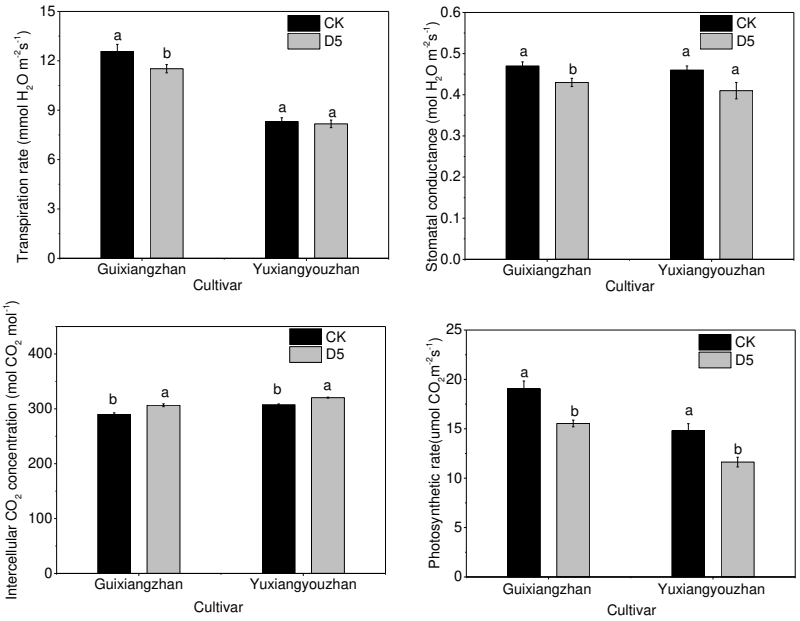

Figure 5. *Effects drought stress treatment on photosynthetic rate, stomatal conductance, intercellular CO_2 concentration and transpiration rate of two fragrant rice cultivars after 5 days recovery. Vertical bars with different lower case letters above are significantly different at $P<0.05$ by LSD tests. Capped bars represent S.D (n=6).CK: Well water treatment. D5: After 5 days of recovery*

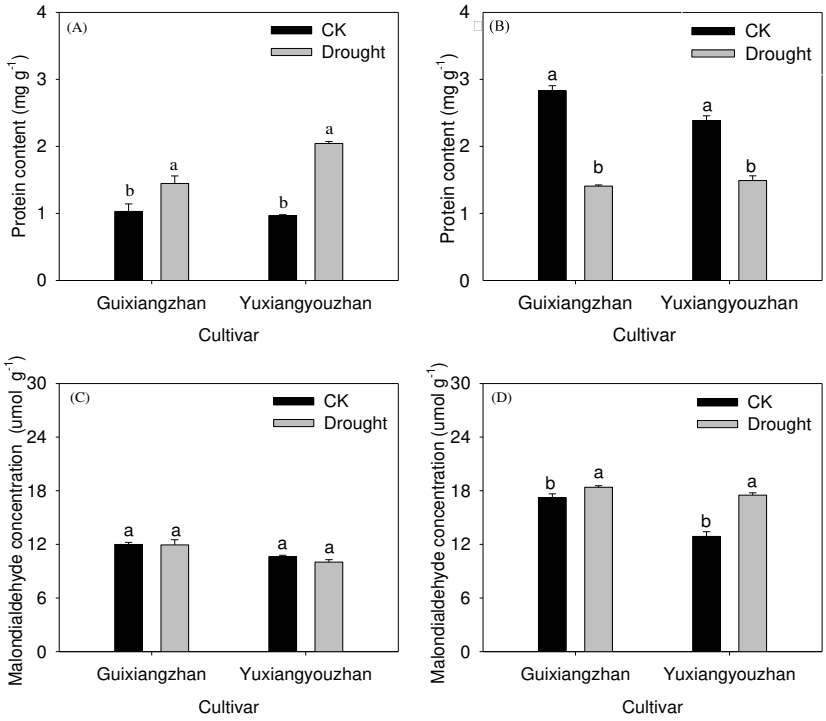

Figure 6. *Effects of drought stress treatment on protein content and malondialdehyde concentration of two fragrant rice cultivars. A, C, sampling at the end of drought stress treatment and B, D, sampling at 5 days after recovery. Vertical bars with different lower case letters above are significantly different at $P<0.05$ by LSD tests. Capped bars represent S.D (n=6) CK: Well water treatment*

http://www.aloki.hu ● ISSN 1589 1623 (Print) ● ISSN1785 0037 (Online)
DOI: http://dx.doi.org/10.15666/aeer/2003_24252438

Drought stress decreased the activities of SOD, POD, and CAT activities by 31.22%, 32.86%, and 35.70%, respectively in the leaves of Guixiangzhan whilst decreased by 48.71%, 34.03%, and 33.49% for Yuxiangyouzhan under drought stress treatment. After 5 days of recovery, SOD, POD and CAT activities were remained higher under drought stress than CK. Moreover, the activities of SOD, POD, and CAT activities were increased by 42.39%, 64.97%, and 67.65% for Guixiangzhan and 33.04%, 54.49%, and 47.13% for Yuxiangyouzhan (*Figure 7*).

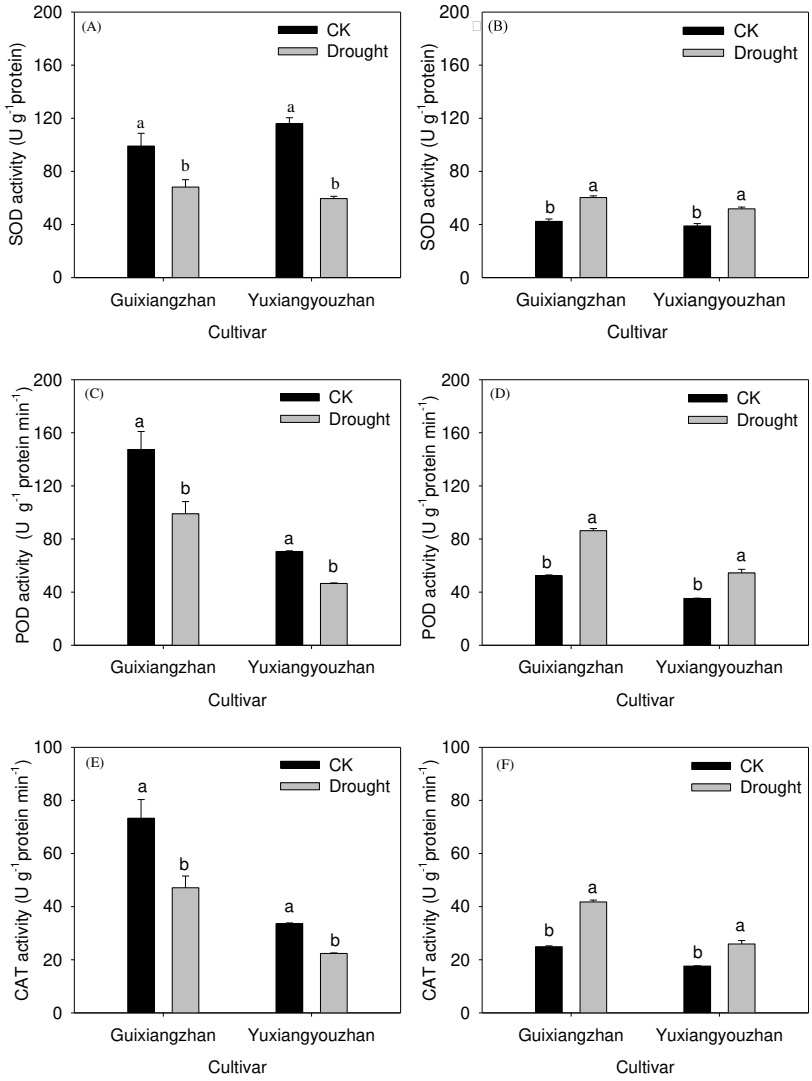

Figure 7. *Effects of drought stress treatment on SOD, POD and CAT activity of two fragrant rice cultivars. A, C, E sampling at the end of drought stress treatment and B, D, F sampling at 5 days after recovery. Vertical bars with different lower case letters above are significantly different at P<0.05 by LSD tests. Capped bars represent S.D (n=6). CK: Well water treatment*

The leaf RWC and the leaf weight per unit area of both fragrant rice cultivars were noticeably decreased under drought stress (*Figure 8*). Likewise, the total nitrogen contents in leaves were decreased by 10.19% for Yuxianyouzhan whilst no significant effect of drought was observed on total nitrogen content in leaves for Guixiangzhan (*Figure 9*).

http://www.aloki.hu ● ISSN 1589 1623 (Print) ● ISSN1785 0037 (Online)
DOI: http://dx.doi.org/10.15666/aeer/2003_24252438

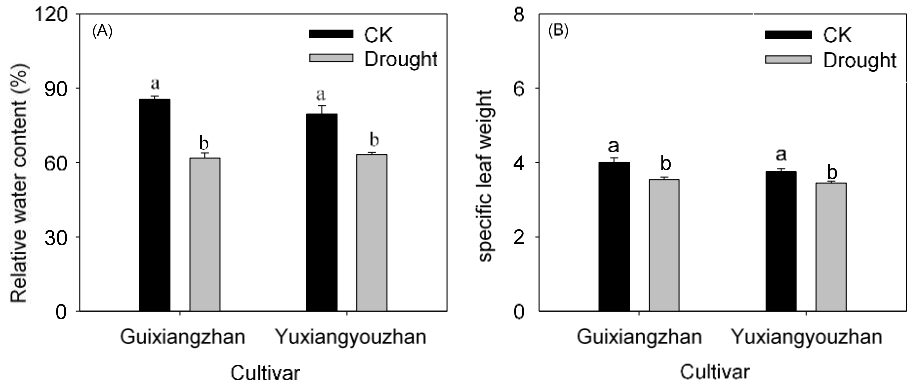

Figure 8. *Effects of drought stress treatment on relative water content and specific leaf weight of two fragrant rice cultivars. Vertical bars with different lower case letters above are significantly different at P<0.05 by LSD tests. Capped bars represent S.D (n=10). CK: Well water treatment*

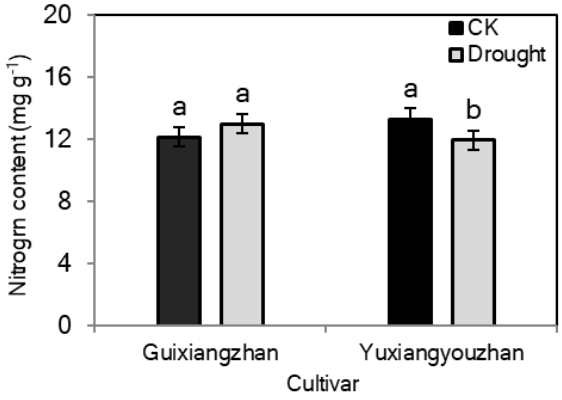

Figure 9. *Nitrogen content in leaves after drought stress treatment of two fragrant rice cultivars. Vertical bars with different lower case letters above are significantly different at P<0.05 by LSD tests. Capped bars represent S.D (n=6). CK: Well water treatment*

Analysis of variance for the investigated parameters

Cultivars (C) were remained statistically different regarding plant height, grain yield, harvest index, photosynthetic rate, stomatal conductance, intercellular CO_2 concentration, and protein and MDA contents as well as for POD and CAT activity in the leaves after drought treatment. Drought significantly affected plant height, grain yield, total dry weight, harvest index, photosynthetic rate, stomatal conductance, intercellular CO_2 concentration, transpiration rate, protein content, POD, SOD and CAT activities, relative water contents, leaf weight per unit area in leaves as well as photosynthetic rate, stomatal conductance, intercellular CO_2 concentration, transpiration rate, protein and MDA contents, and the activities of POD, SOD and CAT in the leaves after 5 days of recovery. For C×T interaction was significantly affected the grain yield, stomatal conductance, intercellular CO_2 concentration, protein and nitrogen contents and SOD activity in the leaves after drought treatment and the protein and MDA contents, POD and CAT activity in leaves after 5 days of recovery whereas no significant difference was observed for other parameters (*Table 1*).

http://www.aloki.hu ● ISSN 1589 1623 (Print) ● ISSN1785 0037 (Online)
DOI: http://dx.doi.org/10.15666/aeer/2003_24252438

Table 1. *Analysis of variance of the investigated parameters*

Investigated parameters	Cultivar (C)	Water treatment (T)	C×T
Yield	164.72**	64.03**	13.46**
Plant height	340.72**	27.80**	0.04^{ns}
Total dry weight	2.25^{ns}	38.56**	1.08^{ns}
Harvest index	2255.23**	8.99*	0.00^{ns}
Photosynthesis rate in leaves after treatment	15.78*	485.84**	1.66^{ns}
Stomatal conductance in leaves after treatment	51.75**	561.45**	40.11**
Intercellular CO_2 concentration in leaves after treatment	16.31**	292.92**	41.84**
Transpiration rate in leaves after treatment	0.46^{ns}	705.94**	0.45^{ns}
Protein content in leaves after treatment	9.17*	170.14**	33.05**
MDA concentration in leaves after treatment	9.21*	1.88^{ns}	1.37^{ns}
POD activity in leaves after treatment	51.20**	26.96**	3.06^{ns}
SOD activity in leaves after treatment	0.45^{ns}	80.80**	6.92*
CAT activity in leaves after treatment	48.43**	27.82**	4.41^{ns}
Photosynthetic rate in leaves after 5 days of recovery	27.16**	30.40**	0.08^{ns}
Stomatal conductance in leaves after 5 days of recovery	5.98^{ns}	9.43*	0.27^{ns}
Intercellular CO_2 concentration in leaves after 5 days of recovery	71.04**	89.26**	1.22^{ns}
Transpiration rate in leaves after 5 days of recovery	100.97**	6.64*	3.90^{ns}
Protein content in leaves after 5 days of recovery	30.07**	223.38**	11.57**
MDA concentration in leaves after 5 days of recovery	24.85**	72.64**	25.87**
POD activity in leaves after 5 days of recovery	136.00**	258.02**	19.93**
SOD activity in leaves after 5 days of recovery	29.12**	57.64**	1.57^{ns}
CAT activity in leaves after 5 days of recovery	152.10**	252.16**	29.10**
Relative water content in leaves after treatment	0.82^{ns}	86.87**	2.88^{ns}
Specific leaf weight after treatment	3.70^{ns}	27.37**	1.00^{ns}
Nitrogen content in leaves after treatment	0.04^{ns}	0.93^{ns}	17.97**
2AP content of grains after treatment	338.44**	1462.8**	1031.36.00**
2AP content of leaves after treatment	0.08^{ns}	0.01^{ns}	2.85^{ns}
2AP content of leaves after 5 days of recovery	507.74**	3.36^{ns}	6.48^{ns}

*, significant at P<0.05; **, significant at P<0.01; ns, no significant at P<0.05 level

Discussion

Cultivar, drought stress and their interactive effect on fragrant rice have been detected in this study (*Table 1*). Previously, Fitzgerald et al. (2010) reported that the fragrance in rice was related to yield reduction under salt treatment. In this study, drought stress significantly increased 2AP content in mature grain, and enhanced the 2AP content in leaves (*Figure 2*) whereas the 2AP of Guixiangzhan and Yuxiangyouzhan was remained higher than CK under drought stress. Moreover, the yield of both rice cultivars was significantly higher under CK than drought treatment, which indicates that the content of 2AP is negatively correlated with the yield under drought stress. In addition, it can also

http://www.aloki.hu ● ISSN 1589 1623 (Print) ● ISSN1785 0037 (Online)
DOI: http://dx.doi.org/10.15666/aeer/2003_24252438

be inferred that the yield of Yuxiangyouzhan under drought conditions is higher than that of Guixiangzhan, which is mainly related to its higher harvest index (*Figure 3*).

In addition, the 2AP possibly transports from leaves and other above ground plant parts to grains (Mo et al., 2016) whilst the grain 2AP content is related to the nitrogen content in plants (Mo et al., 2018, 2019a). Thus, higher 2AP content in leaves could result in high 2AP content in mature grains. Furthermore, the regulations in the N content, Na content, rice yield, shoot dry weight and tiller number are linked to the dynamics in grain 2AP contents (Funsueb et al., 2016). In this study, the agronomic parameter such as grain yield, N content, relative water content, gas exchange parameters, protein content and antioxidative capacities of the fragrant rice were regulated by drought stress (*Figures 2-11*). The gas exchange parameters contribute to rice photosynthesis that lead to dry matter accumulation in fragrant rice thus could affect the morpho-physiological and yield traits under drought stress. Moreover, the physiological traits such as protein, relative water contents, as well as antioxidant activities regulated the drought-resistant metabolism in fragrant rice, which affects rice yield as well as the aroma accumulation. Overall, these results suggested that changes in 2AP content in leaves, total dry weight, plant height, harvest index, gas exchange parameters, protein content, relative water content, N content and antioxidant activities were related to 2AP in grains under drought stress.

Rice yield formation substantially affected in response to drought stress at flowering stage as a consequence of the change of the agronomic and physiological attributes (Fu et al., 2010). Drought stress at flowering stage decreased photosynthetic rate in rice (Yang et al., 2013). In this study, drought stress substantially reduced photosynthetic rate, stomatal conductance, intercellular CO_2 concentration and transpiration rate in both fragrant rice cultivars after drought stress treatment (*Figure 4*). The photosynthetic rate, stomatal conductance and transpiration rate for Guixiangzhan was substantially lower even after 5 days of recovery. Drought stress treatment significantly decreased the photosynthetic rate in Yuxiangyouzhan whereas intercellular CO_2 concentration for both fragrant rice cultivars were enhanced under after 5 days of recovery (*Figure 5*). Therefore, yield reduction in fragrant rice is related to alteration in photosynthesis and gas exchange attributes under drought stress at flowering stage.

Drought stress at flowering stage led to excessive accumulation of reactive oxygen species (ROS) that may cause oxidative damage and thus lead to substantial reduction in photosynthetic rate (Zhou et al., 2015). The ROS are scavenged through the enzymatic antioxidant defense system i.e., SOD, POD, and CAT and non-enzymatic components i.e., ASA, GSH, vitamin (Ashraf et al., 2015, 2017a; Ashraf and Tang, 2017). In general, antioxidants such as SOD, POD and CAT play an important role in eliminating ROS in plant cells (Ashraf et al., 2017b, 2018). Our results indicated that the activities SOD, POD, CAT were decreased under drought stress treatment (*Figure 7A,C,E*), which indicated that the water-deficit conditions might damage antioxidant defense system, however, after 5 days of drought recovery, SOD, POD, CAT activity have been improved. Dynamics in the activities of antioxidants under water deficit conditions were previously reported (Yang et al., 2014; Anjum et al., 2016). Besides, the changes in protein synthesis and degradation are regarded as direct responses of plants to drought stress (Shanker et al., 2014). The protein contents were substantially increased under drought treatment and was reduced after 5 days of recovery (*Figure 6A,B*), which implicated that the trial cultivars may maintain water balance via altered protein contents to adapt the irreversible condition. Interestingly, no significant difference in terms of MDA concentration after

http://www.aloki.hu ● ISSN 1589 1623 (Print) ● ISSN1785 0037 (Online)
DOI: http://dx.doi.org/10.15666/aeer/2003_24252438

drought stress treatment was found whereas MDA concentration was remarkably increased after 5 days of recovery (*Figure 6C,D*). Thus, morpho-physiological changes and regulations in 2AP contents of fragrant rice in response to drought stress at flowering stage were quite prominent. Therefore, close relationships exist among the investigated parameters in fragrant rice such as the rice yield, gas exchange parameters and antioxidative capacities, and all those parameters were also associated with aroma in fragrant rice. In addition, limited water application and/or water deficit conditions could substantially reduce the rice yield as compared to normal irrigation application which might be due to drought stress induced the closure of leaf stomata and gaseous exchange between leaf mesophyll cells and the external environment (Du et al., 2020). Hence, reduced photosynthetic rate could result in reduced yield production under drought conditions. No doubt, drought stress often results in yield reduction in rice. Some studies have shown that appropriate application of nitrogen can promote the development of rice root system and improve the rice yield under drought conditions (Cao et al., 2017). In this experiment, under drought treatment, the content of total nitrogen in leaves of yuxiang oil decreased significantly (*Figure 9*). This suggests that fertilization of the Yuxiangyouzhanl during this period may help to increase the yield. However, as there is lack of evidence to support this; much work should be done in future studies.

Conclusion

In conclusion, the 2AP contents were substantially enhanced under drought stress in both rice cultivars whereas the 2AP contents were varied between grains and leaves. On the other hand, the drought stress decreased grain yield in fragrant rice cultivars as a consequence of the reduction related morphological traits i.e., plant height, the total dry weight, the relative water content, the leaf weight per unit area, the photosynthetic capacity, and the antioxidant enzyme activities. Therefore, in the future, we need research temporal transcription dynamics during plant drought needs to be further investigated to unravel the drought tolerant genes to develop drought - tolerant and high - yielding fragrant rice cultivars.

Acknowledgements. We acknowledge the funding provided by Special Fund for the National Natural Science Foundation of China (31601244, 31271646).

REFERENCES

[1] Ambavaram, M. M., Basu, S., Krishnan, A., Ramegowda, V., Batlang, U., Rahman, L., Baisakh, N., Pereira, A. (2014): Coordinated regulation of photosynthesis in rice increases yield and tolerance to environmental stress. – Nat. Commun 5: 5302.

[2] Anjum, S. A., Tanveer, M., Ashraf, U., Hussain, S., Shahzad, B., Khan, I., Wang, L. (2016): Effect of progressive drought stress on growth, leaf gas exchange, and antioxidant production in two maize cultivars. – Environ. Sci. Pollut. R 23: 17132-17141.

[3] Ashraf, U., Kanu, A. S., Mo, Z. W., Hussain, S., Anjum, S. A., Khan, I., Abbas, R. N., Tang, X. R. (2015): Lead toxicity in rice: effects, mechanisms, and mitigation strategies - a mini review. – Environ. Sci. Pollut. R 22: 18318-18332.

[4] Ashraf, U., Tang, X. R. (2017): Yield and quality responses, plant metabolism and metal distribution pattern in aromatic rice under lead (Pb) toxicity. – Chemosphere 176: 141-155.

http://www.aloki.hu ● ISSN 1589 1623 (Print) ● ISSN1785 0037 (Online)
DOI: http://dx.doi.org/10.15666/aeer/2003_24252438

[5] Ashraf, U., Hussain, S., Anjum, S. A., Abbas, F., Tanveer, M., Noor, M. A., Tang, X. R. (2017a): Alterations in growth, oxidative damage, and metal uptake of five aromatic rice cultivars under lead toxicity. – Plant Physiol Bioch 115: 461-471.
[6] Ashraf, U., Kanu, A. S., Deng, Q. Q., Mo, Z. W., Pan, S. G., Tian, H., Tang, X. R. (2017b): Lead (Pb) Toxicity; Physio-Biochemical Mechanisms, Grain Yield, Quality, and Pb Distribution Proportions in Scented Rice. – Front Plant Sci 8: 259.
[7] Ashraf, U., Hussain, S., Akbar, N., Anjum, S. A., Hassan, W., Tang, X. R. (2018): Water management regimes alter Pb uptake and translocation in fragrant rice. – Ecotox Environ Safe 149: 128-134.
[8] Bradford, M. M. (1976): A rapid and sensitive method for the quantitation of microgram quantities of protein utilizing the principle of protein-dye binding. – Anal Biochem 72: 248-254.
[9] Cao, X. C., Zhong, C., Sajid, H., Zhu, L. F., Zhang, J. H., Wu, L. H., Jin, Q. Y. (2017): Effects of watering regime and nitrogen application rate on the photosynthetic parameters, physiological characteristics, and agronomic traits of rice. – Acta Physiologiae Plantarum 39: 135.
[10] Du, J., Shen, T. H., Xiong, Q. Q., Zhu, C. L., Peng, X. S., He, X. P., Fu, J. R., Ouyang, L. J., Bian, J. M., Hu, L. F., Sun, X. T., Zhou, D. H., He, H. H., Zhong, L., Chen, X. R. (2020): Combined proteomics, metabolomics and physiological analyses of rice growth and grain yield with heavy nitrogen application before and after drought. – Bmc Plant Biol 20: 556.
[11] Fitzgerald, T. L., Waters, D. L. E., Brooks, L. O., Henry, R. J. (2010): Fragrance in rice (*Oryza sativa*) is associated with reduced yield under salt treatment. – Environmental and Experimental Botany 68: 292-300.
[12] Fu, G. F., Song, J., Li, Y. R., Yue, M. K., Xiong, J., Tao, L. X. (2010): Alterations of panicle antioxidant metabolism and carbohydrate content and pistil water potential involved in spikelet sterility in rice under water-deficit stress. – Rice Sci 17: 303-310.
[13] Funsueb, S., Krongchai, C., Mahatheeranont, S., Kittiwachana, S. (2016): Prediction of 2-acetyl-1-pyrroline content in grains of thai jasmine rice based on planting condition, plant growth and yield component data using chemometrics. – Chemometrics & Intelligent Laboratory Systems 156: 203-210.
[14] Hinge, V. R., Patil, H. B., Nadaf, A. B. (2016): Aroma volatile analyses and 2AP characterization at various developmental stages in basmati and non-basmati scented rice (*Oryza sativa* L.) cultivars. – Rice 9: 38.
[15] Liu, X. W., Huang, Z. L., Li, Y. Z., Xie, W. J., Li, W., Tang, X. R., Ashraf, U., Kong, L. L., Wu, L. L., Wang, S. L., Mo, Z. W. (2020): Selenium-silicon (Se-Si) induced modulations in physio-biochemical responses, grain yield, quality, aroma formation and lodging in fragrant rice. – Ecotoxicology and Environmental Safety 196: 110525.
[16] Mo, Z. W., Li, W., Pan, S. G., Fitzgerald, T. L., Xiao, F., Tang, Y. J., Wang, Y. L., Duan, M. Y., Tian, H., Tang, X. R. (2015): Shading during the grain filling period increases 2-acetyl-1-pyrroline content in fragrant rice. – Rice 8: 9.
[17] Mo, Z. W., Huang, J. X., Xiao, D., Ashraf, U., Duan, M., Pan, S. G., Tian, H., Xiao, L. Z., Zhong, K., Tang, X. R. (2016): Supplementation of 2-Ap, Zn and La improves 2-acetyl-1-pyrroline concentrations in detached aromatic rice panicles in Vitro. – Plos one 11(2): e0149523.
[18] Mo, Z. W., Lei, S., Ashraf, U., Khan, I., Li, Y., Pan, S. G., Duan, M. Y., Tian, H., Tang, X. R. (2017): Silicon fertilization modulates 2-acetyl-1-pyrroline content, yield formation and grain quality of aromatic rice. – J. Cereal Sci 75: 17-24.
[19] Mo, Z. W., Ashraf, U., Tang, Y. J., Li, W., Pan, S. G., Duan, M. Y., Tian, H., Tang, X. R. (2018): Nitrogen application at the booting stage affects 2-acetyl-1-pyrroline, proline, and total nitrogen contents in aromatic rice. – Chilean Journal of Agricultural Research 78: 165-172.
[20] Mo, Z. W., Li, Y. H., Nie, J., He, L. X., Pan, S. G., Duan, M. Y., Tian, H., Xiao, L. Z., Zhong, K. Y., Tang, X. R. (2019): Nitrogen application and different water regimes at

http://www.aloki.hu ● ISSN 1589 1623 (Print) ● ISSN1785 0037 (Online)
DOI: http://dx.doi.org/10.15666/aeer/2003_24252438

booting stage improved yield and 2-acetyl-1-pyrroline (2ap) formation in fragrant rice. – Rice 12: 74.

[21] Mo, Z. W., Tang, Y. J., Ashraf, U., Pan, S. G., Duan, M. Y., Tian, H., Wang, S. L., Tang, X. R. (2019a): Regulations in 2-acetyl-1-pyrroline contents in fragrant rice are associated with water-nitrogen dynamics and plant nutrient contents. – Journal of Cereal Science 88: 96-102.

[22] Nauš, J., Šmecko, S., Špundová, M. (2016): Chloroplast avoidance movement as a sensitive indicator of relative water content during leaf desiccation in the dark. – Photosynth. Res 129: 217-225.

[23] Pan, S. G., Liu, H. D., Mo, Z. W., Patterson, B., Duan, M. Y., Tian, H., Hu, S. J., Tang, X. R. (2016): Effects of nitrogen and shading on root morphologies, nutrient accumulation, and photosynthetic parameters in different rice genotypes. – Sci. Report 6: 32148.

[24] Shanker, A. K., Maheswari, M., Yadav, S. K., Desai, S., Bhanu, D., Attal, N. B., Venkateswarlu, B. (2014): Drought stress responses in crops. – Functional & integrative genomics 14: 11-22.

[25] Wakte, K., Zanan, R., Hinge, V., Khandagale, K., Nadaf, A., Henry, R. (2017): Thirty-three years of 2-acetyl-1-pyrroline, a principal basmati aroma compound in scented rice (*Oryza sativa* L.): a status review. – J. Sci. Food Agri. 97: 384-395.

[26] Wang, P., Tang, X. R., Tian, H., Pan, S. G., Duan, M. Y., Nie, J., Luo, Y. M., Xiao, L. Z. (2013a): Effects of different irrigation modes on aroma content of aromatic rice at booting stage. – Guangdong Agri. Sci. 8: 1-3.

[27] Wang, P., Xiao, L. Z., Tang, X. R., Tian, H., Pan, S. G., Duan, M. Y., Nie, J., Luo, Y. M. (2013b): Effects of different irrigation modes on aroma content of aromatic rice at tillering stage. – J. Irrigation Drainage 32: 103-105.

[28] Xie, W. J., Kong, L. L., Ma, L., Ashraf, U., Pan, S. G., Duan, M. Y., Tian, H., Wu, L. M., Tang, X. R., Mo, Z. W. (2020): Enhancement of 2-acetyl-1-pyrroline (2AP) concentration, total yield, and quality in fragrant rice through exogenous γ-aminobutyric acid (GABA) application. – J Cereal Sci 91: 102900.

[29] Yang, Y. J., Zhang, C. X., Song, J., Xiong, J., Wang, X., Zhang, X. F., Fu, G. F., Tao, L. X. (2013): Effects of drought stress on water and photosynthetic physiology activities of near-isogenic indica rice lines at flowering stage. – Sci. Agri. Sin 46: 1481-1491.

[30] Yang, P. M., Huang, Q. C., Qin, G. Y., Zhao, S. P., Zhou, J. G. (2014): Different drought-stress responses in photosynthesis and reactive oxygen metabolism between autotetraploid and diploid rice. – Photosynthetica 52: 193-202.

[31] Zhang, J., Kirkham, M. B. (1996): Antioxidant responses to drought in sunflower and sorghum seedlings. – New Phytol 132: 361-373.

[32] Zhou, S. S., Li, M. J., Guan, Q. M., Liu, F. L., Zhang, S., Chen, W., Yin, L. H., Qin, Y., Ma, F. W. (2015): Physiological and proteome analysis suggest critical roles for the photosynthetic system for high water-use efficiency under drought stress in Malus. – Plant Sci 236: 44-60.

http://www.aloki.hu ● ISSN 1589 1623 (Print) ● ISSN1785 0037 (Online)
DOI: http://dx.doi.org/10.15666/aeer/2003_24252438

RENEWABLE ENERGY CONSUMPTION AND OUTPUT GROWTH IN AFRICA: A NEW EVIDENCE

CHUKWU, A. B.[1] – ANOCHIWA, L. I.[1] – AGBANIKE, T. F.[1*] – ENYOGHASIM, M. O.[1] – OGBUAGU, A. R.[1] – UWAJUMOGU, N. R.[1] – OGBONNAYA, I. O.[1] – OGWURU, H. O. R.[2] – ONOJA, T. C.[1] – OTTA, N. N.[1] – MATTHEW, E.[1] – AGU, G. C.[1]

[1]*Department of Economics and Development Studies, Alex Ekwueme Federal University, Ndufu-Alike, Ebonyi State, Nigeria*
(e-mails: basilchukwu@gmail.com – A. B. Chukwu; lanochiwa@yahoo.com – L. I. Anochiwa; mic_martserve@yahoo.com – M. O. Enyoghasim; anulireg@gmail.com – A. R. Ogbuagu; ketchyus@yahoo.com – N. R. Uwajumogu; ioogbons@yahoo.com – I. O. Ogbonnaya; musheshe@yahoo.co.uk – T. C. Onoja; ottankama@gmail.com – N. N. Otta; matthew.enyinnaya@funai.edu.ng – E. Matthew; aguglorychibuzo@gmail.com – G. C. Agu)

[2]*Department of Economics, Novena University, Delta State, Nigeria*
(e-mail: profeca@yahoo.com)

**Corresponding author*
e-mail: basilchukwu@gmail.com, basil.chukwu@funai.edu.ng
phone: + 234-908-267-8797

(Received 27th Nov 2021; accepted 21st Mar 2022)

Abstract. Previous studies have shown that Africa's growing weight in energy production is felt mainly in the non-renewable energy sources such as coal, oil and natural gas. However, recently, studies have started to emerge showing that renewable energy sources in bioenergy, hydropower, wind and solar photovoltaic (PV) are fast developing and contribute to growth at some economic units within the region. This study adopted the system generalized method of moments (Sys-GMM), pooled ordinary least squares (POLS) and fixed effects (FE) models to examine the impact of renewable energy consumption on inclusive growth in a cross-sectional panel of 47 African countries, spanning 1990–2019. Our findings revealed that there is a weak convergence rate of inclusive growth between low-income countries and high-income countries of the African region. This implies that although renewable energy is fast developing, growth in the sector is not yet sufficient to promote inclusive growth in the entire region. A policy thrust towards strengthening the macroeconomic environment so as to reap from the investments into the renewable energy sector will lead to an improvement in Africa's growth architecture.
Keywords: *inclusive growth, renewable energy, carbon dioxide (CO_2) emissions, GMM, Africa*

Introduction

The demand for energy is borne out of the need to grow productivity in any economy. Energy demand therefore, is derived from the numerous activities (economic or non-economic) needed to accomplish growth. Most developed countries are working assiduously to completely migrate from carbon emission prone energy to alternative energy supplies like solar, wind, hydro, and biomass among others to meet their daily energy needs. Regrettably, in Africa, the energy need of the region centres mostly on fossil fuel whose cost of production is persistently high and environmentally inimical (Bhattacharya, et al., 2016; Adewuyi and Awodumi, 2017a; Agbanike et al., 2019). Africa houses a greater percentage of the poor in the world; therefore, the opportunity to overcome the development divide will depend on how fast the region takes advantage of the renewable energy mix for which the cost of production is rapidly declining, as is the

http://www.aloki.hu ● ISSN 1589 1623 (Print) ●ISSN1785 0037 (Online)
DOI: http://dx.doi.org/10.15666/aeer/2003_24392456

case with advanced economies which have leveraged the declining cost of production of renewable energy to drive their growth structures.

In the recent times, studies have started to emerge showing that renewable energy sources in bioenergy, hydropower, solar, and wind are contributing to the rapid growth of certain economies within the African region- a clear departure from the concentration of traditional use of biomass (Adewuyi and Awodumi, 2017a, b;Adu and Denkyirah, 2018). This is commendable but has to be stepped up. Thus, the link between energy consumption demand and national output growth abound in the literature (Apergis and Payne, 2014; Shahbaz et al., 2015; Bouznit, et al., 2016; Mitic et al., 2017; Paramati et al., 2018). Notwithstanding, there are still numerous studies and findings also on the relationship between energy consumption demand and economic growth which showed that either energy consumption does not lead to economic growth, or ambiguous or inconclusive (see Ozturk, Aslan and Kalyoncu, 2010; Yasar,2017; Ahmed and Shimada,2019).

This paper is driven by two main reasons; firstly, the absence of consensus in the literature on the relationship between renewable energy and economic growth in Africa. The second motivation resides on the necessity to reduce greenhouse gases emissions from the consumption of fossil fuel which characterizes energy consumption mix in Africa. There is the need to grow the share of renewable energy mix (wind, solar, hydropower, biomass and geo-thermal energy) in the total energy mix in Africa to achieve sustainable and inclusive development. According to Energy information administration report (EIA, 2016), renewable energy accounts for a paltry 22% of the world energy consumption and this is far less in the case of Africa, despite her huge potentials in renewable energy. Thus, increasing the share of renewable energy becomes a priority. Subsequently, for the desire to promote and achieve 'green growth' and less emission of carbon in Africa, cleaner energy sources through wind, solar, and biomass, become paramount (Waziri et al., 2018) and highly imperative. No doubt this paper contributes to the inconclusive debate in the literature regarding the exact link between renewable energy and economic growth.

To achieve this purpose, we employ more robust econometric techniques – system generalized method of moments (Sys-GMM), pooled ordinary least squares (POLS) and fixed effects (FE) models to evaluate our results and make policy prescriptions. Furthermore, this study disaggregates the entire African data into two components (Low-medium income and Low-income countries) following the World Bank (2020) classification. This is to take into account the diverse economic statuses of the countries in the different income classifications. The rest of this paper is structured as follows: The next section presents some stylized facts on Africa's energy demand mix and energy-related carbon dioxide (CO_2) emissions structure, which is followed by review of relevant literature on the energy-growth relations. The subsequent section is Data and Methodology which describes the data, model specification and estimation technique, followed by presentation and discussion of the results from empirical analyses, while the last section concludes the study with policy prescription.

Stylized facts on Africa's energy demand mix and energy-related carbon dioxide (CO_2) emissions structure

Africa is regarded as energy intensive growing economies. A focus on Africa's energy structure shows that energy demand within the region has grown twice as fast as the global average in the past two decades. With a growing population and rapid demand for energy

http://www.aloki.hu ● ISSN 1589 1623 (Print) ●ISSN1785 0037 (Online)
DOI: http://dx.doi.org/10.15666/aeer/2003_24392456

consumption especially for industrial production, transport, building and domestic uses, Africa is projected to emerge as a major force in global energy markets, higher than China and second to India by 2040 (IEA, 2019). Africa's growing weight in energy production is felt in non-renewable energy sources -coal, oil and natural gas. A cursory observation of Africa's primary energy demand mix shows that these sources of energy contribute to more than 80% of total energy demand (see *Table 1*).

Table 1. *Energy demand – Africa*

Africa case										
	Energy demand (Mtoe)							**Shares (%)**		**CAAGR* (%)**
	2010	**2017**	**2018**	**2025**	**2030**	**2035**	**2040**	**2018**	**2040**	**2018-40**
Total primary demand	681	817	838	872	888	1 024	1 204	100	100	1.7
Coal	108	110	112	110	105	104	100	13	8	-0.5
Oil	161	193	194	257	304	335	362	23	30	2.9
Natural gas	90	126	133	171	198	229	290	16	24	3.6
Nuclear	3	4	4	4	7	9	19	0	2	7.6
Hydro	9	11	12	19	27	36	44	1	4	6.3
Bioenergy	308	368	378	280	180	197	212	45	18	-2.6
Other renewables	2	6	7	31	68	115	179	1	15	16.1

*Compound average annual growth rate
Source: IEA: Africa Energy Outlook, 2019

Although Africa is richly endowed with abundant renewable sources of energy such as bioenergy, hydropower, wind and solar photovoltaic (PV), current contributions from these sources to total energy demand is still very negligible. Available statistics show that the region is endowed with over 10 (TW) of PV, 350 (GW) of hydroelectric, 110 (GW) of wind and geothermal energy sources of 15 (GW), United Nations Environment Programme (UNEP, 2017). However, despite these huge endowments, Africa has not been able to meet successfully its energy needs. Some of the reasons adduced by energy experts for this challenging situation are weak economic growth, weak energy policies and lack of adequate investments into the different energy sources (UNEP, 2017). Within the last two decades, Africa's total investment in the energy sector is about 5.5% of the global total share; one of the lowest when compared with other regions. An International Energy Agency (IEA, 2019) report on Africa stated that in 2018, about $100 billion was invested in the Africa's energy sector. Of this amount, $70 billion was invested in fossil fuels; $13 billion was invested each in electricity networks and renewable energy respectively. However, these amounts of investment in renewables are meagre when compared to other regions.

United Nations Environment Program report (UNEP, 2017) posits that for Africa to solve the issue of low energy production and supply, and fast-track energy sufficiency, Africa's renewable energy sector investment requires between $43-55 billion per year through 2040. In the bid to fast-track energy sufficiency, the new comprehensive African Union's (AU) energy strategic framework was adopted in 2015. The strategic framework is divided into two critical structures – the Program for Infrastructure Development in Africa (PIDA) and the Africa Renewable Energy Initiative (AREI). While the PIDA aimed at closing Africa's vast infrastructure gap across transport, energy and water

http://www.aloki.hu ● ISSN 1589 1623 (Print) ●ISSN1785 0037 (Online)
DOI: http://dx.doi.org/10.15666/aeer/2003_24392456

sectors, information and communication technologies, AREI is expected to accelerate the exploitation of the continent's huge renewable energy potential. *Inter alia*, the AREI policy framework is expected to achieve at least 10 gigawatts (GW) of new renewable energy generation capacity by 2020 and least 300 GW by 2030 (AfDB, 2015).

The increase in the renewable energy capacity is expected to impact positively on energy supply and improved access to electricity, especially in major cities and rural communities. A report by IRENA (2015) posits that "modern renewables can eliminate power shortages, bring electricity and development opportunities to rural villages, spur industrial growth, create entrepreneurs, and support the ongoing lifestyle changes across the continent" (p.7). However, with the current state of electricity infrastructure coupled with weak economic growth challenges, the region's electricity generation capacity (supply) has remained low and unable to help Africa meet its social and economic needs. Between 2017 and 2018, an average of 236 (GW) electricity was generated with the non-renewable sources contributing to a greater percentage of total electricity generation (see *Table 2*).

Received statistics show that over 600 million persons living in Africa have no access to electricity- with over 57% of this population coming from sub-Saharan (International Energy Agency IEA, 2018). A robust, uninterrupted electricity supply is a key prerequisite for improvement in economic activities, the functioning of the healthcare system and the maintenance of social welfare in an economy. In Africa, several thousand households, hospitals and healthcare facilities and private businesses have no access to electricity. Africa has the world's lowest per capita energy consumption which is far below the world average. With 17% of the world's population, the region consumes about 3.3% of global primary energy. Received statistics show that Africa consumes 42% of its oil production, 28% of gas, 22% of coal, 6% hydro, and 1% of renewable and nuclear energy respectively (UNEP, 2017).

Table 2. *Africa's electricity generation (GW)*

Africa case									
	Electrical capacity (GW)						**Shares (%)**		**CAAGR(%)**
	2017	**2018**	**2025**	**2030**	**2035**	**2040**	**2018**	**2040**	**2018-40**
Total capacity	228	244	398	550	709	924	100	100	6.2
Coal	48	48	53	50	45	37	20	4	-1.2
Oil	42	43	48	51	52	53	18	6	1
Natural gas	92	103	148	167	183	228	42	25	3.7
Nuclear	2	2	2	4	5	10	1	1	7.6
Renewables	44	48	144	273	414	579	20	63	12
Hydro	35	36	57	77	99	117	15	13	5.5
Bioenergy	1	1	4	7	9	11	0	1	13
Wind	5	5	25	51	72	94	2	10	13.8
Geothermal	1	1	2	5	9	14	0	2	14.9
Solar PV	3	4	52	124	209	316	2	34	21.5
CSP	1	1	4	9	17	26	0	3	16.2
Marine	-	-	0	0	0	0	-	0	n.a.

*Compound average annual growth rate
Source: IEA: Africa Energy Outlook, 2019

http://www.aloki.hu ● ISSN 1589 1623 (Print) ●ISSN1785 0037 (Online)
DOI: http://dx.doi.org/10.15666/aeer/2003_24392456

In terms of carbon emission, Africa contributes only sparingly to global energy-related carbon dioxide (CO_2) emissions as a result of the underdeveloped nature of the energy and industrial sectors. *Table 3* presents carbon emission structure for the African region. Between 2017 and 2018, an average of 1198 million tonnes (Mt) of carbon emission was generated by the region and this is projected to increase to 1797 (Mt) by 2040. Received statistics show that as at today, the Asian continent is the highest global emitter of CO_2 (53%), North America (18%), Europe (17%), Africa and South America account for 3-4% of global emissions each (Ritchie and Roser, 2017). International Energy Agency (IEA, 2019) report on Africa's Energy Outlook stated that Africa's global share of CO_2 emissions in 2018 stands at 3.7% or 1.2 gigatonnes (Gt) CO_2.

Table 3. *Africa's CO_2 emissions (million tonnes)*

Stated policies scenario										
	CO_2 emissions (Mt)							**Shares (%)**		**CAAGR (%)**
	2010	**2017**	**2018**	**2025**	**2030**	**2035**	**2040**	**2018**	**2040**	**2018-40**
Total CO_2	1 017	1 181	1 215	1 357	1 464	1 621	1 797	100	100	1.8
Coal	385	391	395	382	346	332	318	32	18	-1
Oil	450	541	551	668	750	846	948	45	53	2.5
Natural gas	182	248	269	307	368	443	532	22	30	3.1
Power sector	420	466	480	495	490	508	530	100	100	0.4
Coal	263	257	261	275	255	239	215	54	41	-0.9
Oil	54	59	62	63	59	62	60	13	11	-0.2
Natural gas	103	150	158	157	176	208	256	33	48	2.2
Final consumption	496	620	641	776	892	1 021	1 163	100	100	2.7
Coal	66	83	85	84	85	89	96	13	8	0.5
Oil	382	472	480	590	675	767	871	75	75	2.8
Transport	257	345	351	436	495	549	603	55	52	2.5
Natural gas	48	65	76	102	131	165	197	12	17	4.4

*Source: IEA: Africa Energy Outlook, 2019

North Africa and South Africa account for Africa's highest CO_2 emissions with 40% (about 490 million (Mt) CO_2) and 35% (about 420 Mt CO_2) respectively. The high CO_2 emissions from these two regions is as a result of the developed nature of their energy sectors relative to the other regions of the continent and the number of persons having access to electricity. In North and South Africa, about 98% and 85% respectively of the population have access to electricity (IRENA, 2017). However, despite the relatively small amount of carbon emission by Africa, the region is disproportionately exposed to the challenges of climate change.

Literature review

The link between energy (i.e. renewable energy) consumption and economic growth is often associated with four main hypotheses- the growth hypothesis, conservation hypothesis, the feedback hypothesis, and the neutrality hypothesis. These hypotheses give different directions of causality between energy consumption and economic growth (uni-directional, bi-directional and neutral). The growth hypothesis postulates that it is energy consumption that causes economic growth. This presupposes that a decline in energy

http://www.aloki.hu ● ISSN 1589 1623 (Print) ●ISSN1785 0037 (Online)
DOI: http://dx.doi.org/10.15666/aeer/2003_24392456

consumption will lead to a decrease in economic growth (Adewuyi and Awodumi, 2017a). The second hypothesis is more like a reverse of the first; the conservation hypothesis posits that it is economic growth that causes the demand for renewable energy (Shahbaz and Feridum, 2012). When an economy is growing, income per head also increases and also the energy required for the growth, thus, it is economic growth that drives renewable energy consumption. Feedback hypothesis asserts the existence of a bi-directional causal relationship between energy consumption and economic growth. That renewable energy drives economic growth just as economic growth can drive renewable energy consumption. Lastly, the Neutrality hypothesis postulates no causality between energy consumption and economic growth. In other words, that causality does not run from economic growth to renewable energy and vice versa (Stern and Cleveland, 2004).

In the recent times, a huge number of studies has attempted different methodologies to establish the empirical relationship between energy consumption and output growth. Some of the methodologies employed include the bootstrap panel analysis, the bivariate or multivariate error correction model, the Toda–Yamamoto analytical procedure that is within a production function framework, and the forecast error variance decomposition model. However, in spite of all these different methodologies, research findings showed that there are no clear-cut consensus on the impact or direction of causality between energy consumption and economic growth. Ighodaro (2010) adopted the Johansen cointegration and bivariate Granger causality methods to examine the relationship between energy consumption and economic growth in Nigeria. The study included monetary and fiscal policy variables and found a unidirectional causality running from energy consumption to economic growth. Akinlo (2008) examined the energy consumption and economic growth link for 11 Sub-Sahara African countries using the vector error correction model (VECM). The study found mixed results. While bi-directional relationship exists between energy consumption and economic growth for Gambia, Ghana and Senegal, a unidirectional causal relationship occurs for Sudan and Zimbabwe.

Ocal and Aslan (2013) investigated the relationship between renewable energy consumption and income growth in Turkey between 1990 and 2010 using the ARDL and Toda–Yamamoto causality tests approach. Findings showed that while the result of the ARDL presented a negative impact of renewable energy on economic growth, Toda–Yamamoto causality tests showed a unidirectional causality running from output growth to renewable energy consumption. Similarly, Pao and Fu (2013) examined renewable-non-renewable-growth nexus in Brazil from 1980-2010, using the multivariate error correction model. The results showed that while the cointegration test reveals that a long-run relationship exists from real GDP to renewable and non-renewable energy sources, the vector error correction model presents a bidirectional causality between economic growth and renewable energy, and a unidirectional causality from economic growth to non-renewable energy sources.

Ahmed and Shimada (2019) selected a panel of 30 emerging and developing countries using data from the World Development Indicators (WDI) of the World Bank, Renewable Energy Country Attractiveness Index (RECAI) by Ernst and Young, and employed the Cobb-Douglas production function. The findings show a significant long-run relationship between renewable energy consumption and economic growth for selected South Asian, Asian and most of the African countries (Ghana, Tunisia, South Africa, Zimbabwe and Cameroon). But for the Latin American and the Caribbean countries, economic growth

http://www.aloki.hu ● ISSN 1589 1623 (Print) ●ISSN1785 0037 (Online)
DOI: http://dx.doi.org/10.15666/aeer/2003_24392456

depends on non-renewable energy consumption. Renewable energy consumption in the selected countries of these two regions is still at the initial stage.

Other studies with differentiated methodology found a bidirectional relationship between renewable energy consumption and economic growth. Ozcana and Ozturk (2019) examined the renewable energy consumption-economic growth relations in 17 emerging countries, covering the period of 1990–2016. The study adopted the bootstrap panel causality test and found no causal relationship between renewable energy demand and economic growth.

Zafar et al. (2019) investigated the impact of non-renewable and renewable energy on economic growth among Asia-Pacific Economic Cooperation countries (APEC) during the period of 1990–2015. The study adopted the second-generation panel unit root test and Westerlund cointegration test and found that a bidirectional causal relationship runs between economic growth, renewable and non-renewable energy consumption. Rahman and Velayutham (2020) adopted the panel Fully Modified Ordinary Least Squares (FMOLS) and panel Dynamic Ordinary Least Squares (DOLS) estimation techniques to examine the renewable and non-renewable energy consumption- economic growth connection among five South Asian countries from 1990–2014. The study found a positive relationship between renewable and non-renewable energy consumption on economic growth.

Aydin (2019) examined the relationship between renewable and non-renewable electricity consumption and economic growth in 26 OECD countries from 1980–2015, adopting the Time and Frequency domain Granger causality tests. The study found that while Time and domain Granger causality test showed that a bidirectional relationship runs from non-renewable electricity energy consumption and economic growth, the Frequency domain Granger causality test presents a bidirectional temporary and permanent causality relationship between output growth and renewable-non-renewable electricity consumption. Sarkodie and Adams (2020) applied the Bayesian and nonlinear autoregressive distributed lag (NARDL) estimation approach to investigate the relationship between electricity access and income inequality in South Africa from 1990-2017. They included corruption index as a determinant of the level of development of government and political institutions and found that although the level of corruption is high, there is a long-run unequal effects between income level and access to electricity.

Kouton (2021) examined the impact ofrenewable energy consumption on growth in some African countries using Generalized Method of Moments (GMM) estimation technique for a period of 1991–2015. The study found a significant positive relationship between renewable energy consumption and aggregate growth in the region.

Following the ambiguousness of results of different studies on renewable energy-growth mix, it is necessary to further extend the investigation for 47 African countries, within the period of 1990–2019 using the system generalized method of moments (Sys-GMM), pooled ordinary least squares (POLS) and fixed effects (FE) model. The essence of adopting these estimation techniques is to obtain a more robust result that provides policymakers appropriate information in the crafting of policy interventions that would strengthen Africa's growth and development architectures.

http://www.aloki.hu ● ISSN 1589 1623 (Print) ●ISSN1785 0037 (Online)
DOI: http://dx.doi.org/10.15666/aeer/2003_24392456

Data and methodology

Model specification

This study adopts the endogenous growth model (Solow, 1956) which has capital and labour as main factors of production to analyse the impact of energy consumption demand on aggregate national income. The justification for adopting the endogenous growth model is consistent with the energy–growth literature where multivariate growth models have widely been used (see, Akinlo (2008) Bhattacharya et al., 2016; Koçak and Şarkgüneşi, 2017; Maji et al., 2019). According to the growth theory, national wellbeing is mostly achieved and sustained when technological progress interacts with the stock of human capital. As investment in capital stock interacts with human capital, a critical mass of inclusive growth is achieved. However, in the absence of appropriate investment in the capital stock and a weak human capital formation, inclusive aggregate growth is affected negatively.

According to Khan and Chaudhry (2019), human capital formation is essential for aggregate economic growth. Hur (2014) posits that sustainable investment in critical mass of human capital promotes inclusive growth through the creation of additional employment. However, a poor human capital formation creates limited employment opportunities in the environment with high unemployment. A reduced employment opportunity is therefore inimical to growth of national output. The energy sector is one of the sectors that have the highest capacity to create several forms of additional employment (both skilled and unskilled) and cause economic growth when adequate investments are made. Building on the endogenous growth framework, the neoclassic production function is therefore stated as follows:

$$Y = f(K, L) \quad \text{(Eq.1)}$$

where, the output produced (Y) is a function of the combined input of capital (K) (henceforth, KAP) and Labour (L) (henceforth, LABF). Since endogenous growth model comprises technology, this study incorporates the renewable energy (REN) variable as an input factor. This study further augments the function by including variables of health and monetary policy (broad money) as control variables. While the health variable (government expenditure) provides insight of the state of the health sector within the countries, broad money (BRM) provides information on the level of macroeconomic instability in the different economies (see Omotor, 2008; Kouton (2021). A highly volatile business environment occasioned by high price volatility impacts negatively on aggregate growth over time (see Kumah and Sandy, 2013). Thus:

$$Y = f(KAP, LABF, REN, HEX, BRM) \quad \text{(Eq.2)}$$

From *Equation 2* a new production function with time period is stated as:

$$Y_{it} = f(KAP_{it}, LABF_{it}, REN_{it}, HEX, BRM_{it}) \quad \text{(Eq.3)}$$

where*Y* stands for output growth, proxied by the GDP per person employed (at Constant 2011 Purchasing Power Parity $USD) (Raheem etal., 2018; Oyinlola andAdedeji, 2019; Kouton, 2021). Unlike GDP growth rate which previous studies adopted (for example; Maji et al., 2019), this study adopted the GDP per person employed, which is a broader concept

http://www.aloki.hu ● ISSN 1589 1623 (Print) ●ISSN1785 0037 (Online)
DOI: http://dx.doi.org/10.15666/aeer/2003_24392456

of inclusive growth than the regular GDP growth rate (Kouton, 2021). *KAP* stands for physical capital measured by gross capital formation (GRCF); *LABF* represents the labour force in country *i*, time *t. REN*, represents total renewable energy demand by country *i,* time *t*. *HEX* represents government expenditure on the health sector; while *BRM*, denotes broad money rates in country *i,* time *t* (Ighodaro, 2010).

From *Equation 3* above, we re-specified the function as follows (all the variables are specified in log-linear form):

$$\hat{y}_{it} = \alpha + \widehat{\delta_i y}_{it-1} + \beta_i kap_{it} + \beta_i labf_{it} + \beta_i ren_{it} + \beta_i hex_{it} + \beta_i brm_{it} + \gamma_i + \varepsilon_{it} \quad \text{(Eq.4)}$$

where$i$ = 1,…, N is the number of countries (N = 47); time period (t = 29); δ_i, is the intercept β_i, and represents the coefficient of the parameters; γ_i captures the country-specific effect. $\varepsilon_{it}$is the error term in period *i*at time *t*.

Data

Secondary data were sourced for 47 countries from 1990-2019[1]. This period captures the period where virtually all the countries witnessed a positive economic growth and development in their energy sectors. Specifically, Energy data classified into renewable and non-renewable and expressed in tera-joule (TJ), were sourced from Word Development Indicators (WDI) (World Bank, 2020). Data for capital (proxied by gross capital formation and expressed as a percentage of GDP), broad money, GDP (per person employed) and the labour force data were also sourced from the World Bank database (WDI, 2020).

Estimation technique

Equation 4 above is estimated using the System Generalized Method of Moments (Sys-GMM) estimation technique. However, the pooled ordinary least squares (POLS) and fixed effects (FE) estimation methods are adopted to ascertain the robustness of the GMM results. Unlike in other instrument variables such as ordinary least square (OLS) and Two-stage least square (TSLS), GMM provides a more superior and efficient estimates. According to Hansen (1982) and (Bond etal., 2001), GMM estimates are known to be superiorly efficient asymptotically, compared to the estimates of other estimators. The application of GMM in a panel data framework, enables us include the initial level of our dependent variable (GDP) at lag level in order to correct for misspecification bias and account for conditional convergence across countries (see Eggoh, 2009). Although, the lag of the initial level of the dependent variable (GDP) leads to the issue of endogeneity and causes measurement errors, GMM estimator removes the presence of the endogeneity between the lagged dependent variable and the other regressors.

Secondly, the adoption of GMM as an estimator takes care of the challenges of country-specific effects or time-invariant country-specific variables, by taking into account the first differences of the equation. However, studies have shown that at first difference, the level of variables show some level of limitation and weakness. Solving

[1]See *Appendix 1* for list of selected countries and *Appendices 2* and *3* for country classifications into Low-medium and Low-income respectively.

http://www.aloki.hu ● ISSN 1589 1623 (Print) ●ISSN1785 0037 (Online)
DOI: http://dx.doi.org/10.15666/aeer/2003_24392456

this limitation, requires that the estimate of level and first-difference regression to be treated as a "system" in the presence of persistency (see Blundell and Bond, 1998). To solve the limitations of the first-difference estimator, two-step System GMM is applied. According to Windmeijer (2005), Roodman (2009a) and Hauk and Wacziarg (2009), the two-step System GMM provides better results than the first-difference GMM because it presents unbiased lower standard errors.

In this study, we adopt the two-step System GMM approach to investigate the energy consumption–economic growth nexus. In order to avoid the problem related to misspecification or over-identification of parameters which is likely to *overfit* the endogenous variables[2] and weaken the informative power of the Hansen-J test (Roodman, 2009b), we follow the rule of thumb which stipulates that the number of instruments should be close to the number of countries (Roodman, 2009a) and the number of lags of endogenous variables limit to t-1 and t-2. To check for the joint validity of the GMM estimator and of the instruments variable, the J-Statistics test is employed. The study also tests for the absence of serial correlation in the model, using the Arellano-Bond Serial Correlation Test. Following the rule of thumb, we reject the null hypothesis in the absence of a negative first-order correlation of the residuals and accept the null hypothesis in the absence of a second-order correlation of residuals at a probability value greater than 5% level of significance.

Results and discussion

Table 4 provides the descriptive statistics and correlation analysis of the variables used in the regression analysis. From the table, it is shown that the average GDP per person employed (Y) during the period is US$3.920, with a median value of US$ 3.864. The consumption of renewable energy (REN) has an average value of 1.710 TJ and a median value of 1.885TJ. Broad money (BRM) presents the highest mean, average and maximum values.

Overall, all the variables in the study present positive mean values, suggesting an overall upward trend in all the countries in the sample. It is also observed that variability is highest for gross capital formation (KAP), while health expenditure (HEX) appears to be the least volatile variable among the series. The correlation matrix shows that there is no high correlation between the explanatory variables, suggesting that there is no multi-collinearity challenge. The highest and lowest values of the correlation coefficients is 0.604 and 0.015 respectively, and are observed between gross capital formation (KAP) and labour force (LABF); and labour force and health expenditure (HEX) respectively.

Table 5 presents the results of the analysis from *Equation4*. From the table, it is shown that the coefficient of the dependent variable (GDP per person employed) is positive and significant. A positive coefficient of the dependent variable implies weak convergence rate of inclusive growth between low-income countries and high-income countries of the region. Whereas this result is consistent with the findings of Maji et al. (2019), it is inconsistent with Kouton (2021) that found negative and significant relationship. A negative and significant coefficient of inclusive growth as posits by growth theorists, suggest that countries of low levels of economic inclusion experience high rates of

[2]Over-fitting of endogenous variables occurs when the model is too complex. This gives rise to wrong coefficients of the p-values (Roodman, 2009).

http://www.aloki.hu ● ISSN 1589 1623 (Print) ●ISSN1785 0037 (Online)
DOI: http://dx.doi.org/10.15666/aeer/2003_24392456

inclusive growth faster than countries with high levels of economic inclusion (see Kouton, 2021).

Table 4. *Descriptive statistics and correlation matrix*

	Y	KAP	LABF	REN	HEX	BRM
Mean	3.920	9.346	6.528	1.710	0.695	11.068
Median	3.864	9.336	6.613	1.885	0.690	11.294
Maximum	5.074	10.950	7.777	1.993	1.310	13.541
Minimum	2.988	6.575	5.050	-1.229	0.102	0.460
Std. dev.	0.440	0.698	0.592	0.445	0.170	1.348
Skewness	0.366	0.118	-0.332	-3.518	-0.001	-1.280
Kurtosis	2.242	3.013	2.426	18.466	3.097	7.844
Jarque-Bera	64.825	2.619	45.249	16960.745	0.555	1748.950
Probability	0.000	0.270	0.000	0.000	0.758	0.000
Sum	5488.271	10532.716	9203.937	2411.340	979.554	15473.145
Sum sq. dev.	270.813	547.924	493.306	278.399	40.805	2537.347
Observations	1400	1127	1410	1410	1410	1398
Correlation matrix						
Y	1.000					
KAP	0.525*	1.000				
LABF	-0.280*	0.604*	1.000			
REN	-0.619*	-0.488*	-0.041	1.000		
HEX	-0.267*	-0.235*	0.015	0.136*	1.000	
BRM	0.043	0.431*	0.389*	-0.135*	-0.055***	1.000
Observations	1127	1127	1127	1127	1127	1127

Y, stands for gross domestic product (GDP) per person employed; KAP, represents gross capital formation; LABF, represents total labour force; REN, is the total renewable energy consumption from all renewable energy resources; HEX, stands for government expenditure in the health sector; BRM, stands for broad money which explains the structure of government monetary policy framework. All variables are in log-form. *, ** significant at 1% and 10% respectively

Table 5. *Energy demand and output growth. Dependent variable: GDP per person employed*

Variable	GMM result (first differences)	GMM orthogonal deviation test
	Coefficient	Coefficient
Y(-1)	0.698* (0.051)	0.956* (0.014)
KAP	0.042** (0.023)	0.011 (0.008)
LABF	-0.040 (0.044)	-0.027 (0.019)
REN	-0.070** (0.036)	-0.019** (0.011)
HEX	-0.013 (0.018)	0.000 (0.014)
BRM	-0.007** (0.004)	0.005* (0.001)
Mean dependent var	0.004	-0.044
S.E. of regression	0.025	0.021
J-statistic	12.672	13.191
Prob (J-statistic)	0.000	0.000
S.D. dependent var	0.020	0.064
Sum squared resid	0.674	0.459
No of Observation	1049	1049
Cross section included	43	43

http://www.aloki.hu ● ISSN 1589 1623 (Print) ●ISSN1785 0037 (Online)
DOI: http://dx.doi.org/10.15666/aeer/2003_24392456

Standard errors in parentheses, * p < 0.01, ** p < 0.1. All explanatory variables were lagged by one period (t-1). E-views 10.All variables are in log-form

This outcome is a true reflection of the African situation. For many decades, economic activities and growth performance of low-income economies are still far away from those of the dominant economies like Nigeria, South Africa, Egypt and Morocco.

The renewable energy (REN) result showed a negative and significant coefficient at 5%. This result implies that Africa's renewable energy sector is still underdeveloped and unable to cause inclusive growth unlike in the case of the non-renewable energy sector (Omotor, 2008; Ighodaro, 2010). An undeveloped renewable energy sector indicates that: few persons are employed into the sector; and the cost of production of energy in the sector will remain high. High cost of production translates to high price of energy which, leads to low energy consumption. While this result is consistent with Maji et al. (2019) who also found that renewable energy sector demand in 15 African countries reduces output growth, it does not collaborate with the findings of Kouton, (2021) that found positive relationship. Although recent development reports have shown that Africa's renewable energy sector is fast developing, the level of growth is still very low compared to the contributions of the non-renewable energy sector (see EIA, 2016).

One of the fundamental reasons for the weak growth in the renewable energy sector is the issue of level of investment within the sector. An IEA report on Africa's energy outlook (IEA, 2019) stated that in 2018, about $100 billion worth of investment went into the Africa's entire energy sector. Of this amount, USD$70 billion was invested in fossil fuels with USD$13 billion invested each in electricity networks and renewable energy development. This level of investment in the renewable energy sector is low and inadequate to develop the sector to the level where it can cause inclusive growth that reduces the high rates of poverty and inequality facing the region. The coefficient of capital (KAP) conforms to apriori expectation with a positive and significant value at 10%. Although the coefficient is rightly signed and significant, the magnitude is low (0.042%). This low magnitude of capital reinforces our earlier view that the level of capital (investment) in the renewable sector is weak and requires an average investment of US$ 70 billion per year of investment between 2015 and 2030 (IRENA, 2015).

The result of the labour force meets our apriori expectation in terms of magnitude and direction. Although the result is not significant, the negative outcome of the coefficient is similar to those obtained by Raheem et al. (2018) and, Oyinlola and Adedeji (2019). The underlying reason for this result is possibly that Africa's labour force is not only weak to stimulate growth, but it is characterised with low productivity and profit (Gupta, 1993). Pertaining to the coefficient of health variable (HEX), although the parameter presents a negative relationship with the dependent variable, it is not significant at any level. This result conforms to that of Ighodaro (2010) and it underlines the fact that the health sector in Africa is underdeveloped to meet the health needs of the continent. Similarly, the result of broad money is negative and significant, implying that Africa's macroeconomic environment is weak and not favourable to inclusive growth (Ighodaro, 2010; Oyinlolaand Adedeji, 2019).

Table 6 presents the result of the disaggregated data into Low-medium and Low-income countries. From the result it shows that there is not much significant difference in the outcomes of the variables both in terms of magnitude and direction. However, the result of the orthogonal deviation showed that broad money (BRM) is positive and significant for Low-medium countries. This result therefore implies that macroeconomic

http://www.aloki.hu ● ISSN 1589 1623 (Print) ●ISSN1785 0037 (Online)
DOI: http://dx.doi.org/10.15666/aeer/2003_24392456

environment among the Low-medium countries is robust enough to drive economic growth within the region.

Table 6.*Energy demand and output growth (disaggregated data). Dependent variable: GDP per person employed*

	Low-medium income		**Low-income**	
Variable	**GMM Result (first differences)**	**GMM orthogonal deviation test**	**GMM result (first differences)**	**GMM orthogonal deviation test**
	Coefficient		**Coefficient**	
Y(-1)	0.771*(0.076)	0.969*(0.022)	0.513*(0.044)	0.834*(0.029)
KAP	0.028(0.033)	0.022(0.066)	0.099**(0.042)	0.055**(0.022)
LABF	-0.173(0.389)	-0,099(0.075)	-0.751***(0.438)	-0.446***(0.240)
REN	-0.024(0.017)	0.000(0.010)	-0.057(0.084)	-0.021(0.054)
HEX	0.028(0.024)	0.004(0.013)	-0.061***(0.032)	0.022(0.015)
BRM	-0.002(0.005)	0.005*(0.002)	0.013(0.017)	-0.010(0.013)
Mean depend var	0.013	-0.073	0.017	-0.072
S.E. of regression	0.046	0.035	0.052	0.047
J-statistic	11.699	12.718	7.165	7.594
Prob (J-statistic)	0.001	0.000	0.007	0.006
S.D. dependent var	0.038	0.093	0.044	0.109
Sum squared resid	0.780	0.444	0.629	0.514
No of Observation	371	371	242	242
Cross section	26	26	19	19

Standard errors in parentheses, * p < 0.01,** p < 0.05. *** p < 0.1. All explanatory variables were lagged by one period (t-1). All variables are in log-form. E-views 10

Robustness tests

To validate the consistency of our results, GMM orthogonal deviation and Arellano-Bond Serial Correlation tests were employed. From the results of GMM orthogonal deviation test, our findings show that apart from the capital variable (KAP), the results of other variables are not significantly different from those obtained from first difference. Arellano-Bond Serial Correlation test results in*Table 7* show that at first lag period (AR(1)), there exists a serial correlation since the probability value is less than the 5% threshold. However, the second-order result (AR (2)) produced no serial correlation, implying that our model is of good fit.

Table 7. *Arellano-Bond serial correlation test (observations: 1049)*

Test order	**m-Statistic**	**rho**	**SE(rho)**	**Prob.**
AR(1)	-3.783	-0.289	0.076	0.000
AR(2)	-1.388*	-0.039	0.028	0.165

E-views 10. Probability value > 5%. H_0 = There is no serial correlation

We also further subjected the GMM results by estimating two additional models using pooled ordinary least squares (POLS) and fixed effects (FE) following Bond (2002) and Kouton (2021). According to Bond, if in dynamic panel estimation, the results of the

http://www.aloki.hu ● ISSN 1589 1623 (Print) ●ISSN1785 0037 (Online)
DOI: http://dx.doi.org/10.15666/aeer/2003_24392456

lagged dependent variable lies between those of the POLS and FE, then the dynamic panel result is robust and appropriate. This is because while the estimation from FE model in the dynamic form leads to a downward bias of the lagged dependent variable coefficient, the POLS lead to an upward bias (Kouton, 2021). *Table 8* presents the two supplementary results from POLS and FE models. Our results show that the coefficient of the lagged dependent variable (0.698) lies between those of the POLS (0.976) and FE (0.885) as suggested in Bond (2002).

Table 8. *GMM, GMM orthogonal, fixed effects and pooled OLS results*

Variable	GMM result[a] (first differences) (1)	GMM orthogonal[b] deviation test (2)	Fixed effects result (3)	Pooled OLS result (4)
	Coefficient	**Coefficient**	**Coefficient**	**Coefficient**
Y(-1)	0.698* (0.051)	0.956* (0.014)	0.885* (0.025)	0.976* (0.010)
KAP	0.042*** (0.023)	0.011 (0.008)	0.034** (0.014)	0.021* (0.007)
LABF	-0.040 (0.044)	-0.027 (0.019)	-0.156* (0.055)	-0.017**(0.008)
REN	-0.070*** (0.036)	-0.019*** (0.011)	0.004 (0.010)	0.000 (0.002)
HEX	-0.013 (0.018)	0.000 (0.014)	-0.011 (0.013)	0.012**(0.005)
BRM	-0.007*** (0.004)	0.005* (0.001)	0.002 (0.002)	0.000 (0.001)
Constant			1.144* (0.355)	0.000 (0.027)
R^2			0.998	0.998
Adjusted R^2			0.998	0.998
Mean dependent var	0.004	-0.044		
S.E. of regression	0.025	0.021		
J-statistic	12.672	13.191		
Prob (J-statistic)	0.000	0.000		
No of observation	1049	1049	1093	1093
Cross section included	43	43	44	44

All variables are in log-form. E-views 10
[a,b]Results as earlier stated in *Table 5*
*, **, *** significant at 1%, 5%, 10% respectively.Standard errors in parentheses

Conclusion and policy prescription

In this study, the relationship between renewable energy demand and inclusive growth was examined. The study adopted the system generalized method of moments (Sys-GMM), pooled ordinary least squares (POLS) and fixed effects (FE) models to examine this relationship in a cross-sectional panel of 47 African countries, spanning 1990–2019. The variables included in the models are GDP per person employed which measured inclusive growth, capital, measured by gross capital formation, labour force ratio, health expenditure which captures government activities in the health sector and broad money which captures the macroeconomic effectiveness. Our findings revealed that there is a weak convergence rate of inclusive growth between low-income countries and high-income countries of the African region. This implies that although the renewable energy is fast developing, the growth in the sector is not yet sufficient enough to promote inclusive growth in the region.

The levels of labour productivity and capital investment (domestic and foreign) in the African economy, most especially in the renewable energy sector, are weak. From the

http://www.aloki.hu ● ISSN 1589 1623 (Print) ●ISSN1785 0037 (Online)
DOI: http://dx.doi.org/10.15666/aeer/2003_24392456

forgoing, to foster inclusive growth and promote social development, African governments need to create the enabling structure that increases capital investments into the renewable energy sources that has the capacity to create employments (especially in manufacturing renewable energy-based products) and provide income that would improve the living conditions of the most vulnerable households. Currently, the sector is challenged with difficulties in attracting adequate and affordable finance from both domestic and foreign agencies. Increase in renewable energy demand will allow Africa to unlock and fully realize its growth potential. To achieve this objective, this study suggests that various governments, through public-private partnership, should embark on aggressive renewable energy projects across the continent.

Since the availability of renewable energy sources varies from one country to another, these projects should be country specific. Projects related to power generation from geothermal sources should be implemented in parts of Africa with huge abundance of renewable energy sources. However, the success of implementation of these projects will mostly depend on policy frameworks that integrate local communities to own the projects. The policy frameworks should be such that target major stakeholders (that is, local workers, businesses and communities) who are willing to invest in the renewable sector and provide cheap energy to the communities. Secondly, the successful implementation of the project will also depend on the framework that integrates the renewable energy sector with other sectors with high absorptive capacity. Sectors with higher absorptive capacities have been documented in development studies literature as sector that creates more resources and foresters inclusive growth. Lastly, there is the urgent need for African governments to revitalize their different health sectors to meet modern day challenges. The COVID-19 pandemic has exposed the sorry state of the healthcare system in Africa and creates huge uncertainty around the sector. However, this study is limited to panel data analysis, and policies are prescribed for the entire panel and sub-panels; hence, future studies can utilize time-series analyses for country-specific findings and policies.

Acknowledgements. The authors would like to thank the Editor-in-Chief and anonymous reviewers for their time and suggestions which were most helpful in improving this article.

Conflicting interests. The authors declare that they have no potential conflicting interests with respect to the research, authorship, and/or publication of this article.

Funding information. The authors received no financial support for the research, authorship,and/or publication of this article.

Disclaimer. The views expressed in this article are those of the authors and not an official position of their institutions.

REFERENCES

[1] Adewuyi, A.O., Awodumi, O.B. (2017a): Biomass energy consumption, economic growth and carbon emissions: fresh evidence from West Africa using a simultaneous equation model. – Energy 119: 453-471.

[2] Adewuyi, A.O., Awodumi, O.B. (2017b): Renewable and non-renewable energy-growth-emissions linkages: review of emerging trends with policy implications. – Renew. Sustain. Energy Rev. 69(2017): 275-291.

[3] Adu, D.T., Denkyirah, E.K. (2018): Economic growth and environmental pollution in West Africa: testing the environmental Kuznets curve hypothesis. – Kasetsart. Journal of Social Science 2018: 8-15.

http://www.aloki.hu ● ISSN 1589 1623 (Print) ●ISSN1785 0037 (Online)
DOI: http://dx.doi.org/10.15666/aeer/2003_24392456

[4] African Development Bank (2015): Annual Report. – Abidjan, Côte d'Ivoire.
[5] Agbanike, T. F., Chinazaekpere, N., Uwazie, I., Anochiwa, L., Enyoghasim (2019): Banking sector development and energy consumption in Nigeria: exploring the causal relationship and its implications. – African Development Review 31(3): 292-306.
[6] Ahmed, M.M., Shimada, K. (2019): The effect of renewable energy consumption on sustainable economic development: evidence from emerging and developing economies. – Energies 12(15): 2954.
[7] Akinlo, A. E. (2008): Energy consumption and economic growth: evidence from 11 Sub-Sahara African countries. – Energy Economics 30(5): 2391-2400.
[8] Apergis, N., Payne, J.E. (2014): The causal dynamics between renewable energy, real GDP, emissions and oil prices: evidence from OECD countries. – Appl. Econ. 46: 4519-4525.
[9] Aydin, M. (2019): Renewable and non-renewable electricity consumption–economic growth nexus: evidence from OECD countries. – Renewable Energy 136: 599-606.
[10] Bhattacharya, M., Paramati, S. R., Ozturk, I., Bhattacharya, S. (2016): The effect of renewable energy consumption on economic growth: evidence from top 38 countries. – Applied Energy 162:733-741.
[11] Blundell, R., Bond, S. (1998): Initial conditions and moment restrictions in dynamic panel data models. – JEconom 87:115-143.
[12] Bond, S. (2002): Dynamic panel data models: a guide to micro data methods and practice. – Port Econ J1:141-162.
[13] Bond, S., Hoefer, A., Temple, J. (2001): GMM estimation of empirical growth models. – CEPR Discussion Paper no. 3048.
[14] Bouznit, M., Pablo-Romero, M.d.P.(2016): CO2 emission and economic growth in Algeria. – Energy Policy 96: 93-104.
[15] Eggoh, J.C. (2009):Croissanceéconomiqueetdéveloppementfnancier: elements d'analyse théorique et empirique. – Doctoral Dissertation, Orléans.
[16] EIA (2016): Energy information administration of United States. – https://www.eia.go.
[17] Gupta, D. (1993): On measurement and valuation of manufacturing flexibility. – The International Journal of Production Research 31(12): 2947-2958.
[18] Hansen, L. P. (1982): Large sample properties of generalized method of moments estimators. – Econometrica: Journal of the Econometric Society 50(4): 1029-1054.
[19] Hauk, W. R., Wacziarg, R. (2009): A Monte Carlo study of growth regressions. – Journal of Economic Growth 14(2): 103-147.
[20] Hur, S. (2014): Govt. spending and inclusive growth in developing Asia. – ADB working Paper Series 415: 4-39.
[21] Ighodaro, C. A. (2010): Co-integration and causality relationship between energy consumption and economic growth: further empirical evidence for Nigeria. – Journal of Business Economics and Management 1: 97-111.
[22] International Energy Agency (IEA) (2018): Report "World Energy Outlook".– IEA, Paris. https://www.iea.org/reports/world-energy-outlook-2018. Accessed online 8/11/2019.
[23] International Energy Agency (IEA) (2019):Report "Africa Energy Outlook, 2019". – IEA, Paris.
[24] International Renewable Energy Agency (IRENA) (2015): Renewable Energy Capacity Statistics. – https://www.irena.org/publications/2015/Jun/Renewable-Energy-Capacity-Statistics-2015. Accessed online 8/11/2019.
[25] International Renewable Energy Agency (IRENA) (2017): Renewable Energy Capacity Statistics. – https://www.irena.org/publications/2017/Jul/Renewable-Energy-Statistics-2017. Accessed online 8/11/2019.
[26] Khan, R., Chaudhry, I. S. (2019): Impact of human capital on employment and economic growth in developing countries. – Review of Economics and Development Studies 5(3): 487-496.
[27] Koçak, E., Şarkgüneşi, A. (2017): The renewable energy and economic growth nexus in black sea and Balkan countries. – Energy Policy 100:51-57.

http://www.aloki.hu ● ISSN 1589 1623 (Print) ●ISSN1785 0037 (Online)
DOI: http://dx.doi.org/10.15666/aeer/2003_24392456

[28] Kouton, J. (2021): The impact of renewable energy consumption on inclusive growth: panel data analysis in 44 African countries. – Econ Change Restruct. https://doi.org/10.1007/s10644-020-09270-z.
[29] Kumah, F., Sandy, M. (2013): In search of inclusive growth: the role of economic institutions andpolicy. – Modern Economy 4(11): 758-775.
[30] Maji, I. K., Sulaiman, C., Abdul-Rahim, A. (2019): Renewable energy consumption and economic growth nexus: a fresh evidence from West Africa. – Energy Reports 5:384-392.
[31] Mitic, P., Ivanovic, O.M., Zravkovic, A. (2017): A co-integration analysis of real GDP and CO2 emissions in transitional countries. – Sustainability 9: 568.
[32] Ocal, O., Aslan, A. (2013): Renewable energy consumption–economic growth nexus in Turkey. – Renewable and Sustainable Energy Reviews 28: 494-499.
[33] Omotor, D. G. (2008): Causality between energy consumption and economic growth in Nigeria. – Pakistan Journal of Social Sciences 5(8): 827-835.
[34] Oyinlola, M. A., Adedeji, A. (2019): Human capital, financial sector development and inclusive growth in sub-Saharan Africa. – Economic Change and Restructuring 52(1): 43-66.
[35] Ozcan, B., Ozturk, I. (2019): Renewable energy consumption-economic growth nexus in emerging countries: a bootstrap panel causality test. – Renew Sustain Energy Rev 104:30-37.
[36] Ozturk, I., Aslan, A., Kalyoncu, H. (2010): Energy consumption and economic growth relationship: evidence from panel data for low and middle income countries. – Energy Policy 38(8): 4422-4428.
[37] Pao, H. T., Fu, H. C. (2013): Renewable energy, non-renewable energy and economic growth in Brazil. – Renewable and Sustainable Energy Reviews 25: 381-392.
[38] Paramati, S.R., Apergis, N., Ummalla, M. (2018): Dynamics of renewable energy consumption and economic activities across the agriculture, industry and service sectors: evidence in the perspective of sustainable development. – Environ. Sci. Pollut. Res. 25: 1375-1387.
[39] Raheem, I. D., Isah, K. O., Adedeji, A. A. (2018): Inclusive growth, human capital development and natural resource rent in SSA. – Economic Change and Restructuring 51(1): 29-48.
[40] Rahman, M. M., Velayutham, E. (2020): Renewable and non-renewable energy consumption-economic growth nexus: new evidence from South Asia. – Renewable Energy 147: 399-408.
[41] Ritchie, H., Roser, M. (2017): Fossil fuels. – https://ourworldindata.org/fossil-fuels.
[42] Roodman, D. (2009a): How to do xtabond2: an introduction to difference and system GMM in Stata. – Stata Journal 9: 86-136.
[43] Roodman, D. (2009b): A note on the theme of too many instruments. – Oxford Bulletin of Economics and Statistics 71: 135-158.
[44] Sarkodie, S. A., Adams, S. (2020): Electricity access and income inequality in South Africa: evidence from Bayesian and NARDL analyses. – Energy Strategy Reviews 29: 100480.
[45] Shahbaz, M., Feridun, M. (2012): Electricity consumption and economic growth empirical evidence from Pakistan. – Quality & Quantity 46(5): 1583-1599.
[46] Shahbaz, M., Loganathan, N., Zeshan, M., Zaman, K. (2015): Does renewable energy consumption add in economic growth? An application of auto-regressive distributed lag model in Pakistan. – Renew Sustain Energy Rev 44:576-585.
[47] Solow, R. M. (1956): A contribution to the theory of economic growth. – The quarterly Journal of Economics 70(1): 65-94.
[48] Stern, D.I., Cleveland, C.J. (2004): Energy and economic growth. – https://econpapers.repec.org/paper/rpirpiwpe/0410.htm (accessed on 26 October, 2021).
[49] UNEP Emissions of Gas Report (2017): https://www.unep.org/resources/emissions-gap-report-2017. – Accessed online 8/11/2021.

http://www.aloki.hu ● ISSN 1589 1623 (Print) ●ISSN1785 0037 (Online)
DOI: http://dx.doi.org/10.15666/aeer/2003_24392456

[50] Waziri, S. I., Nor, N. M., Hook, L. S., and Hassan, A. (2018): Access to safe drinking water, good sanitation, occurrence of under-five mortality and standard of living in developing countries: system GMM approach. – Journal Ekonomi Malaysia 52(2): 279-289.
[51] WDI (World Bank) (2020): https://datatopics.worldbank.org/world-development-indicators/ https://databank.worldbank.org/source/world-development-indicators. – World Bank, Washington, DC.
[52] Windmeijer, F. (2005): A finite sample correction for the variance of linear efficient two-step GMM estimators. – J Econom 126(1):25-51.
[53] Yasar, N. (2017): The relationship between energy consumption and economic growth: evidence from different income country groups. – International Journal of Energy Economics and Policy 7(2).
[54] Zafar, M. W., Shahbaz, M., Hou, F., Sinha, A. (2019): From non-renewable to renewable energy and its impact on economic growth: the role of research & development expenditures in Asia-Pacific Economic Cooperation countries. – Journal of Cleaner Production 212: 1166-1178.

APPENDIX

Appendix 1.*List of countries*

Algeria, Angola, Benin, Botswana, Burundi, Cabo Verde, Cameroon, Central Africa Republic, Chad, Congo Republic, Congo DR, Cote d'Ivoire, Djibouti, Egypt, Equatorial Guinea, Eswatini, Ethiopia, Gabon, Gambia, Ghana, Guinea, Guinea Bissau, Kenya, Lesotho, Liberia, Madagascar, Malawi, Mali, Mauritania, Mauritius, Morocco, Mozambique, Niger, Nigeria, Papua New Guinea, Rwanda, Senegal, Sierra Leone, South Africa, Seychelles, Sudan, Tanzania, Togo, Tunisia, Uganda, Zambia, Zimbabwe

Appendix 2.*Low-medium countries according to World Bank (2020) classification*

Algeria, Angola, Benin, Botswana, Cabo Verde, Cameroon, Congo Republic, Congo DR, Cote d'Ivoire, Egypt, Eswatini, Ethiopia, Gabon, Ghana, Kenya, Lesotho, Mauritania, Mauritius, Morocco, Nigeria, Papua New Guinea, Senegal, Sierra Leone, South Africa, Seychelles, Tanzania, Tunisia, Zambia, Zimbabwe

Appendix 3.*Low-income countries according to World Bank (2020) classification*

Burundi, Central Africa Republic, Chad, Congo Republic, Djibouti, Equatorial Guinea, Ethiopia, Gambia, Guinea, Guinea Bissau, Liberia, Madagascar, Malawi, Mali, Mozambique, Niger, Rwanda, Sudan, Togo

http://www.aloki.hu ● ISSN 1589 1623 (Print) ●ISSN1785 0037 (Online)
DOI: http://dx.doi.org/10.15666/aeer/2003_24392456

DYNAMICS OF UNFOLDED LEAVES IN MAIZE (*ZEA MAYS* L.) AND THEIR MODEL ESTABLISHMENT BASED ON ACCUMULATED TEMPERATURE

LIU, Y. H. – HAO, J. P.* – DU, T. Q. – MA, L. L.

College of Agriculture, Shanxi Agricultural University; Crop Ecology and Dry Cultivation Physiology Key Laboratory of Shanxi Province, Taigu County, Shanxi Province 030801, China

**Corresponding author*
e-mail: hjpsxau@163.com

(Received 29th Nov 2021; accepted 17th Mar 2022)

Abstract. The dynamic relationship between unfolding leaves and active accumulated temperature (AAT) of different maize (*Zea mays* L.) varieties was studied under different sowing dates, which would provide a theoretical basis for the realization of the informatization and digitalization of maize production on the Loess Plateau of China. Results showed that as the number of unfolded leaves increased, the number of days and the required active accumulated temperature to unfold one leaf showed a single peak trend. The unfolding of the 1st and the last leaves need the least time and AAT, while the 8th-15th leaves need the most. With the delay of sowing date, the peak value of the variation trend of the days and active accumulated temperature to unfold one leaf basically decreased gradually. Among different fitting models, the 3rd degree polynomial fitting model $y = a + bx + cx^2 + dx^3$ may have better biological significance and was thus adopted. As a result, the established models showed great variations in c and d parameters for different varieties, a and c for different sowing dates. The model was tested and showed that the simulated values were in good agreement with the actual values. The above results can provide valuable reference for the quantitative leaf unfolding and AAT requirement for maize and its adaptation to climate change.
Keywords: *number of unfolded leaves, simulation model, sowing date, climate change, Loess Plateau*

Introduction

Since the Industrial Revolution, global climate change caused by anthropogenic greenhouse gas emissions, e.g., CO_2, CH_4, N_2O, has led to a rise in global temperatures of approximately 1.25 °C (Voosen, 2021). Crop production can be affected by global warming, threatening the world-wide food production (Renard and Tilman, 2019; Gomez-Zavaglia et al., 2020). Climate change would have major negative impacts on crop production due to a decrease in crop growth duration and an increase in extreme events (Chen et al., 2018).

Identifying effects of warming on the maize (*Zea mays* L.) growth is particularly important as food security is highly dependent on maize production (Tigchelaar et al., 2018; Rotundo et al., 2019; Liu et al., 2020). Leaf growth and wilting could change the leaf area of maize and affect its photosynthesis and dry matter accumulation, thus affecting maize growth and yield (Testa et al., 2016; Meena et al., 2021; Yan et al., 2021). Active accumulated temperature (AAT) plays a decisive role in the growth of leaves (Zhou et al., 2020), being an important condition to improve the yield of maize.

As a major variable, accumulated temperature has been widely used in many mechanistic crop models to describe or simulate crop growth (Li et al., 2010, 2011; Liu et al., 2019; Wang et al., 2022), especially in leaf area dynamics. Recently, many studies have been conducted to determine the relationship between accumulated temperature and maize leaf area. For example, Zhang et al. (2007) studied and

http://www.aloki.hu ● ISSN 1589 1623 (Print) ● ISSN 1785 0037 (Online)
DOI: http://dx.doi.org/10.15666/aeer/2003_24572470

established a dynamic simulation model of relative leaf area index for spring maize, rice, and winter wheat. Li et al. (2011) reported the dynamic characteristics of leaf area coefficient under different sowing dates and planting densities with maize cultivars differing in maturity; the study also established a corresponding accumulated temperature model. The change of leaf area is determined by the unfolding and wilting of leaves, while leaf growth could be affected by the change of accumulated temperature, thus affecting crop yield (Zhu et al., 2021). To establish a mathematical model between unfolding leaves and AAT would be of great significance to study efficiently the growth and development of the maize, which can promote the quantification and digitalization of maize production.

Currently, many studies have been conducted on the relationship between the change of the maize leaf area index and accumulated temperature demand (Li et al., 2011; Wang et al., 2017), but few study have investigated the relationship between maize leaf unfolding and demand of accumulated temperature. In addition, climate change alters the phenology of maize, and the demand for accumulated temperature varies greatly among maize cultivars at different stages of maturity. The main purpose of this study is to improve the accuracy of leaf unfolding and accumulated temperature simulation, by increasing the observation frequency of leaf unfolding. Additionally, a dynamic model of the relationship between leaf unfolding and accumulated temperature would be established to analyze the effect of different sowing dates on the model, to determine the maize leaf growth dynamics in response to climate change, and to provide a theoretical basis for the digitization of maize production information.

Materials and methods

Site description

This study was conducted in the experimental station of Shanxi Agricultural University (112°59′E, 37°42′N) in Taigu, Jinzhong, Shanxi Province, China in 2012 and 2013. The field experiment located in the Jinzhong Basin, which has a temperate monsoon climate. The annual average temperature of this area is approximately 10 °C, the annual average precipitation is approximately 450 mm with precipitation mainly concentrated in June to August. The precipitation and air temperature in the growth and development stage of the maize were showed in *Figure 1* in both 2012 and 2013. The AAT was 3959.5 °C and 3801.9 °C, the total precipitation was 428 mm and 479.4 mm, and the total sunshine was 1760.8 h and 1378.7 h during the maize growing season in 2012 and 2013, respectively. The substance content in the 0-20 cm soil layer included 23.84 $g \cdot kg^{-1}$ of soil organic matter, 8.01 of pH, 0.775 $g \cdot kg^{-1}$ of total salt content, 0.750 $g \cdot kg^{-1}$ of total nitrogen, 1.227 $g \cdot kg^{-1}$ of total phosphorus, 24.74 $g \cdot kg^{-1}$ of total potassium, 42.41 $mg \cdot kg^{-1}$ of available nitrogen, 31.35 $mg \cdot kg^{-1}$ of available phosphorus, and 229.8 $mg \cdot kg^{-1}$ of available potassium.

Experimental design

In 2012, six maize cultivars were tested including the early maturity cultivars Xieyu Early 1 (ChongNongZuoPinShen 11) and Xinnong Early 3 (YuShenYu 2005008), medium maturity cultivars Xianyu 335 (GuoShenYu 2006026) and Zhengdan 958 (GuoShenYu 20000009), and mid-late maturity cultivars Dafeng 26 (JinShenYu 2009003) and Luyu 36 (JinShenYu 2012009). Five sowing dates (April 26, May 6, May

http://www.aloki.hu ● ISSN 1589 1623 (Print) ● ISSN 1785 0037 (Online)
DOI: http://dx.doi.org/10.15666/aeer/2003_24572470

16, May 26, and June 5) were set for 30 treatments. The maize cultivars tested in 2013 were the same as those in 2012, but the sowing dates were adjusted. In general, the conventional sowing date ranged from late-April to early-May in the region of the study. Six sowing dates (April 1, April 11, April 21, May 1, May 11, and May 21) were used in 2013 for a total 36 treatments. Thereto, the normal and late sowing dates were set in 2012, excluding the early sowing date. In order to assess the effect of sowing date on unfolding leaves, the sowing dates were optimized and added the early sowing dates, i.e., April 1 and April 11 in 2013. Each plot covered an area of 36 m^2 (length 10 m × width 3.6 m) and included eight rows with the planting technique of alternating wide to narrow rows (50 cm: 40 cm). The row spacing was 29.6 cm and the planting density was 75, 000 plants·ha^{-1}.

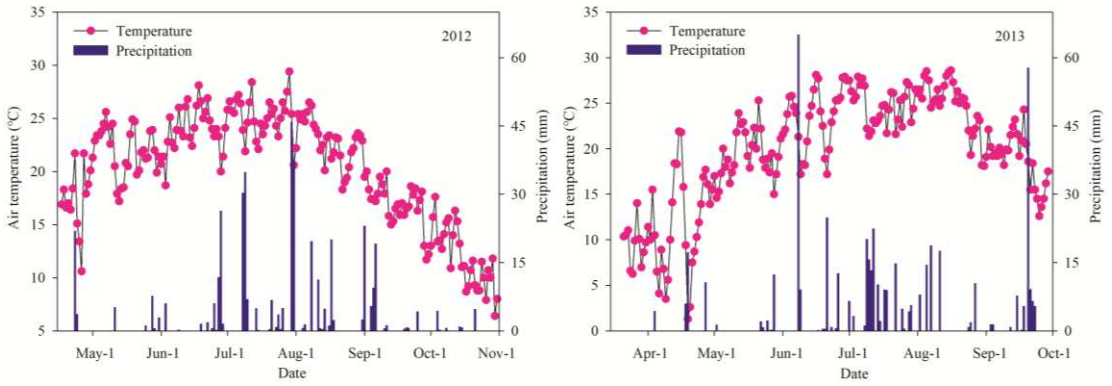

Figure 1. *The distribution of the precipitation and air temperature in the growth and development stage of the maize in both 2012 and 2013*

In 2012, the experimental field was well irrigated on April 20. Around 600 kg·ha^{-1} of phosphorus-potassium nitrate fertilizer (N-P_2O_5-K_2O = 22-9-9), provided by Shanxi Tianji Coal Chemical Group Co., Ltd., was used as basal fertilizers for all plots on the afternoon of April 22. The field was rotovated to a depth of ~8-10 cm on the morning of April 23. The insecticide Dursban was used to prevent underground insects on April 25. After the herbicide of butachlor (4%) -propisochlor (20%) -atrazine (18%) was applied to prevent the weeds on April 26, the film was mulched over the ground all plots. Then, the maize was sown at different sowing dates according to the experiment design. Above farming practices were inconsistent because of the precipitation during this period. Moreover, the film was removed after the maize emerged for each plot. Around 375 kg·ha^{-1} of urea (46% N) as topdressing was used for each plot, which was carried out for the first three sowing dates (i.e., April 26, May 6, May 16) on June 29, and the last two sowing dates (i.e., May 26, and June 5) on July 9. The maize in all the plots had been harvested by October 31.

In addition, in order to ensure soil moisture content for sowing in 2013, a series of farming operations were conducted on November 9, 2012. First of all, the soil was plowed to a depth of ~25-30 cm. Then, around 600 kg·ha^{-1} of compound fertilizer (N-P_2O_5-K_2O = 30-10-0), provided by Yunan Yuntianhua Co., Ltd., was used as basal fertilizers for all plots. Whereafter, the field was rotovated to a depth of ~8-10 cm and leveled. The insecticide Dursban was applied, then the film was mulched over the ground all the plots. In 2013, after the maize was sown at different sowing dates

http://www.aloki.hu ● ISSN 1589 1623 (Print) ● ISSN 1785 0037 (Online)
DOI: http://dx.doi.org/10.15666/aeer/2003_24572470

according to the experiment design, the herbicide was applied. Likewise, we removed the film for each plot after the maize emerged. And around 375 kg·ha^{-1} of urea was used as topdressing for each plot, which was carried out for the first five sowing dates (i.e., April 1, April 11, April 21, May 1, May 11) on June 12, and the last one sowing dates (i.e., May 21) on June 20. The maize in all the plots had been harvested by September 28, 2013.

Determination items and methods

After germination, 10 plants with identical growth were selected and marked for each treatment, and the number of visible leaves and unfolded leaves were recorded daily until all the leaves unfolded. Visible leaf refers to a leaf with the heart leaf exposed 1–2 cm before the jointing stage and exposed 5 cm after the jointing stage. A leaf was considered unfolded leaf when the leaf pulvinus extended out of the leaf sheath of the adjacent lower leaves and the blade completely unfolded. The days required for maize leaf unfolding referred to the time from the heart leaf being visible to the lower leaf completely growing out of the ligule and the leaf sheath being exposed. The accumulated temperature was measured as the accumulation of daily mean temperature (≥10 °C) of maize leaves from the visible to unfolded leaf periods.

The temperature record and accumulated temperature calculation were conducted by an automatic weather station in the test field, and the daily basic meteorological data were automatically measured hourly. A Watch Dog Data Logger (United States) was hung in a louver at the weather station approximately 1.5 m above ground to record the temperature at the test field hourly. The daily mean temperature (T_{mean}) was calculated by using the temperature recorded every two hours from 0 o'clock every day (*Eq. 1*). The AAT (T_{accum}) was the accumulation of daily mean temperature (≥10 °C) (*Eq.* 2) (McMaster and Wilhelm, 1997; Liu et al., 2019).

$$T_{mean} = \sum_{i=1}^{12} T_i/12 \quad \text{(Eq.1)}$$

where T_{mean} is the daily mean temperature (°C), and T_i is the temperature recorded every 2 h from 0 o'clock (°C).

$$T_{accum} = \sum_{j=1}^{n} T_{mean,\, j(\geq 10^{o}\mathrm{C})} \quad \text{(Eq.2)}$$

where T_{accum} is active accumulated temperature (°C), j is the daily mean temperature ≥ 10 °C.

Data analysis

Using the data measured in 2012 and the method of normalization, the AAT and total number of leaves from the emergence stage to leaf unfolding were set to 1 in all treatments, so that the relative AAT and relative unfolded leaf numbers could range from 0 to 1. In this study, Curve Expert 1.4 was used to dynamically simulate the relative number of unfolded leaves and relative AAT of all cultivars and sowing date, and different maize maturities and different sowing dates. The model was tested using

http://www.aloki.hu ● ISSN 1589 1623 (Print) ● ISSN 1785 0037 (Online)
DOI: http://dx.doi.org/10.15666/aeer/2003_24572470

the unfolded leaf number of maize measured in 2013. Normalized Root Mean Square Error (*NRMSE*) was used to evaluate the relative difference between measured and simulated values, and Index of Agreement (I) was used to test the consistency between measured and simulated values. *NRMSE* and *I* were calculated using *Equations 3–6,* respectively (Bai et al., 2011).

$$NRMSE = \sqrt{\frac{\sum_{i=1}^{n}(S_i - R_i)^2}{n}} \times \frac{100}{\overline{R}} \quad \text{(Eq. 3)}$$

$$I = 1 - \left[\frac{\sum_{i=1}^{n}\left(S_i - R_i\right)^2}{\sum_{i=1}^{n}\left(\left|S_i^{'}\right| + \left|R_i^{'}\right|\right)^2} \right] \quad \text{(Eq.4)}$$

$$S_i^{'} = S_i - \overline{R} \quad \text{(Eq.5)}$$

$$R_i^{'} = R_i - \overline{R} \quad \text{(Eq.6)}$$

where S_i is the simulated value, R_i is the measured value, $\overline{R}$ is the average measured value, and n is the sample number of the simulated value. When $NRMSE < 10\%$, the fit was considered excellent; when $10\% \leq NRMSE \leq 20\%$, the fit was good; when $20\% \leq NRMSE \leq 30\%$ the fit fell in the middle; and when $NRMSE > 30\%$, the fit was considered bad. When the value of '*I*' is closer to 1, the consistency between the simulated and measured number is better, otherwise the this is the contrary. All figures in the study were drawn by Sigmaplot 12.0.

Results

The number of days and AAT needed for leaf unfolding

As shown in *Figure 2*, under different sowing dates of six maize cultivars, the number of days needed for leaf unfolding fit a unimodal curve that first increased and then decreased with the increase of leaf position. The number of days needed for each leaf unfolding ranged from 1 day to 18 days, of which the first, second, and last leaves needed less than a day to unfold, while the eighth to 14th leaves required additional days. With the postponement of the sowing date, the peak value of the days needed for leaf unfolding of different maize cultivars showed a decreasing trend, namely, April 26 > May 6 > May 16 > May 26 > June 5.

Similar to the above results, the AAT of each leaf unfolding increased first and then decreased with the increase of leaf position (*Fig. 3*). The AAT required for one leaf to unfold ranged from 16.6 °C to 388.1 °C, of which the first, second, and last leaves needed less AAT, while the ninth to 15th leaves needed additional time and accumulated temperature. Similar to the results of days required for leaf unfolding, the peak value of accumulated temperature for leaf unfolding of different maize cultivars gradually decreased with the delay of sowing date, which was April 26 > May 6 > May 16 > May 26 > June 5.

http://www.aloki.hu ● ISSN 1589 1623 (Print) ● ISSN 1785 0037 (Online)
DOI: http://dx.doi.org/10.15666/aeer/2003_24572470

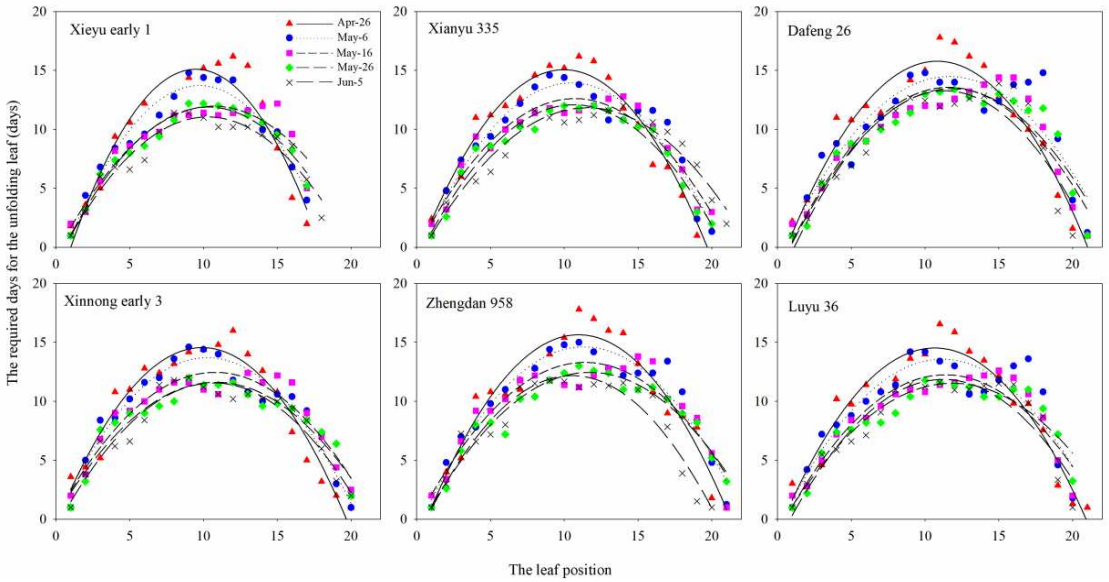

Figure 2. *The number of days to unfold each leaf for different sowing dates and cultivars in 2012*

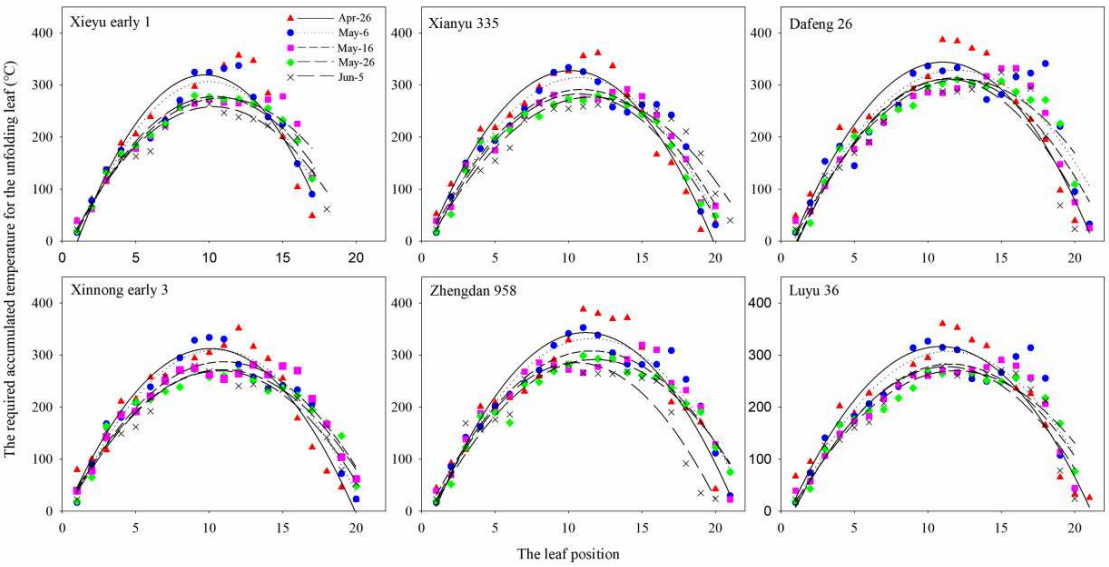

Figure 3. *The AAT needed to unfold each leaf for different sowing dates and cultivars in 2012*

Establishment of a model of relative number of unfolded leaves

The AAT and the number of unfolded leaves required for leaf unfolding of maize cultivars with different maturities in five sowing dates in 2012 were normalized. Each cultivar and sowing date was also normalized. Curve Expert 1.4 was used to simulate the relative number of unfolded leaves and relative AAT. The six models with the best simulations were selected including cubic equation, rational function, Hoerl model, quadratic equation, Shifted power fitting, and sinusoidal function. The determinant coefficients of these models were over 0.9900, and their standard deviations were less than 0.03 (*Table 1*).

http://www.aloki.hu ● ISSN 1589 1623 (Print) ● ISSN 1785 0037 (Online)
DOI: http://dx.doi.org/10.15666/aeer/2003_24572470

Table 1. *Models employed to fit the observed relative number of unfolded leaves against the relative accumulated temperature and the parameters obtained for each model*

Simulated model	Parameters of each model				Standard deviation	Determination coefficient
	a	***b***	***c***	***d***		
$y = a + bx + cx^2 + dx^3$	0.0368	0.9203	-0.6774	0.6873	0.0236	0.9934**
$y = (a + bx)/(1 + cx + d x^2)$	0.0392	0.9109	0.7472	0.7882	0.0235	0.9933**
$y = a*(b\text{^}x)*(x\text{^}c)$	0.3234	3.0264	0.4428	-	0.0242	0.9930**
$y = a + bx + cx^2$	0.0727	0.4739	0.4181	-	0.0275	0.9909**
$y = a(x\text{-}b)\text{^}c$	0.5389	-0.3658	1.8755	-	0.0279	0.9907**
$y = a + b*cos(cx + d)$	1.7490	1.7589	0.7923	3.4548	0.0286	0.9902**

In the model, x and y represent the relative accumulated temperature and relative number of unfolded leaves, respectively. **Significance is at a probability level of 0.01

The results of the six simulation models all performed well (*Table 1*), thus the clearer physical meaning of simple polynomials, quadratic, and cubic polynomial equations were chosen. Based on this, a fitting diagnosis (*Fig. 4*) was conducted using the relative number of unfolded leaves and the standardized residuals obtained from the relative number of unfolded leaves. Two equations showed that the standardized residual distribution of the cubic polynomial equation was more uniform than that of the quadratic polynomial equation. Therefore, the cubic polynomial equation was used in this study for the simulation analysis. In the cubic polynomial equation, when $x = 0$, $y = a$, which means the value of 'a' was the relative number of unfolded maize leaves at the emergence stage; when $x = 1$, $y = a + b + c + d$, of which the $(a + b + c + d)$ was the relative number of maize leaves completely unfolded. By using the cubic polynomial equation, any relative number of unfolded leaves corresponding to relative AAT can be simulated, and the dynamic change of unfolded leaf number can be observed over time.

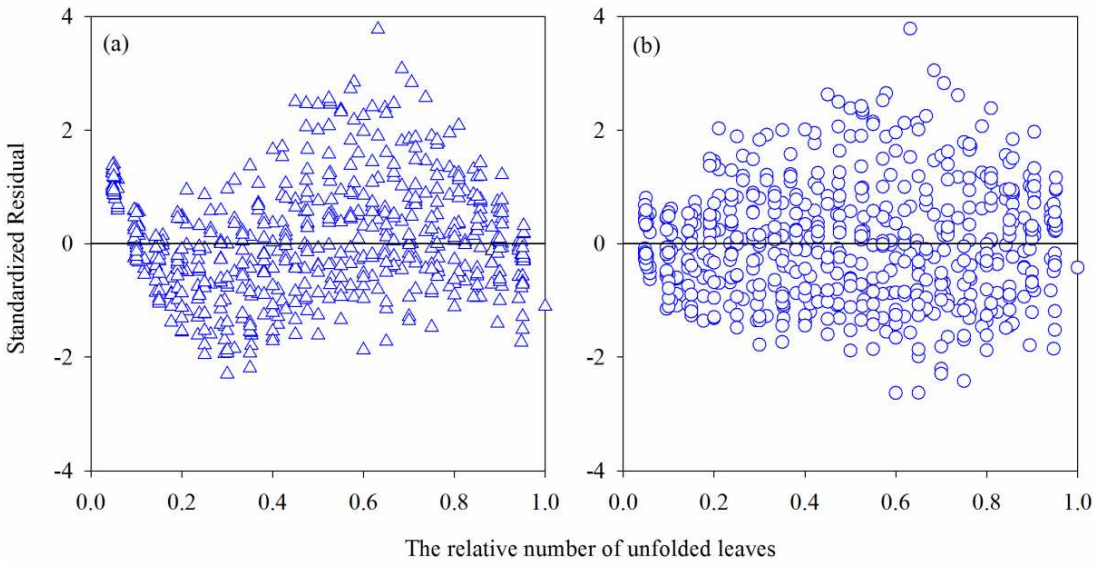

Figure 4. *The standardized residual distribution between the relative number of unfolded leaves with quadratic (a) and cubic (b) regression equations, respectively*

http://www.aloki.hu ● ISSN 1589 1623 (Print) ● ISSN 1785 0037 (Online)
DOI: http://dx.doi.org/10.15666/aeer/2003_24572470

Analysis of key parameters for the dynamic model of the relative number of unfolded maize leaves of different cultivars and sowing dates

Based on the above analysis, the parameters of the dynamic model of the relative number of unfolded leaves of maize cultivars with different maturities and sowing dates were further studied. The results showed that the simulation effects of relative AAT and the relative number of unfolded leaves in all treatments in 2012 reached a very significant level, and the coefficient of variation (CV) was higher than 0.9900. In *Table 2*, the CVs of model parameters '*c*' and '*d*' of maize with different maturities were large, -28.66% and 21.80%, respectively, while those of '*a*' and '*b*' were relatively small, which indicated that '*c*' and '*d*' were the main parameters to explain the variation of simulated equation of relative unfolded leaf number of maize with different maturities. The CVs of various parameters of maize cultivars with the same maturity were different. The variation of parameters '*a*', '*b*', and '*c*' in the early maturity maize cultivars was relatively high, while that of '*a*', '*c*', and '*d*' in the medium maturity cultivars was also higher. The variation of '*c*' and '*d*' in the mid-late maturity cultivars was also high. Comparing the model parameters of all maize cultivars, the variations of parameters '*c*' and '*d*' were larger, -24.72% and 18.52%, respectively, while those of parameters '*a*' and '*b*' were smaller. This indicates that '*c*' and '*d*' were the dominant parameters affecting the simulation equation of the relative unfolded leaf number of different maize cultivars, but the dominant parameters of the simulation of different maize cultivars at the same level of maturity were different.

Table 2. *Models employed to fit the observed relative number of unfolded leaves against the relative accumulated temperature and the parameters obtained for each model of different maize cultivars*

Cultivar	Parameters of each model				Standard deviation	Determination coefficient
	a	*b*	*c*	*d*		
Early maturity	0.0349	0.9590	-0.8698	0.8640	0.0237	0.9934**
Xieyu Early 1	0.0316	1.0727	-0.9835	0.8695	0.0169	0.9968**
Xinnong Early 3	0.0271	0.9167	-0.8610	0.9047	0.0180	0.9964**
CV for early maturity*	10.84	11.09	-9.39	2.81		
Medium maturity	0.0369	0.8491	-0.5061	0.6067	0.0214	0.9946**
Zhengdan 958	0.0361	0.8743	-0.5965	0.6650	0.0232	0.9937**
Xianyu 335	0.0321	0.8688	-0.5103	0.6061	0.0179	0.9964**
CV for medium maturity*	8.29	0.45	-11.01	6.55		
Mid-late maturity	0.0383	0.9485	-0.6002	0.6002	0.0184	0.9960**
Luyu 36	0.0328	0.9952	-0.6297	0.5944	0.0167	0.9968**
Dafeng 26	0.0340	0.9757	-0.7145	0.6882	0.0177	0.9964**
CV for mid-late maturity*	2.54	1.40	-8.92	10.34		
CV among maturities#	4.66	6.60	-28.66	21.80		
CV among cultivars※	9.31	8.31	-24.72	18.52		

* is the coefficient of variation (CV) among different cultivars under a certain maturity, # is the CV among different maturities, ※ is the CV among six maize cultivars. ** Significance is at a probability level of 0.01

http://www.aloki.hu ● ISSN 1589 1623 (Print) ● ISSN 1785 0037 (Online)
DOI: http://dx.doi.org/10.15666/aeer/2003_24572470

In addition, the analysis of the dynamic regression model parameters of the relative unfolded leaf number of maize under different sowing dates (*Table 3*) showed that the CVs of parameters '*a*', '*c*', and '*d*' were very large; the model parameters simulated at the sowing date of April 26 were quite different from the others. If the data from April 26 were not taken into account, the variation of parameters '*a*' and '*c*' was larger, while that of '*b*' and '*d*' was smaller. Therefore, '*a*' and '*c*' were the main parameters explaining the variation of the relative number of unfolded maize leaves in the models under different sowing dates. Theoretically, the value of parameter '*a*' in the model should be 0, and its fitted value in this study was close to 0. The '*b*' value should change at approximately 1, which is determined by the normalization. Thus, the range of the dependent variable (*y*) and independent variable (*x*) varied from 0 to 1. In summary, except for the sowing date of April 26, the parameters '*a*' and '*b*' of the models under different cultivars and other sowing dates were relatively stable, while the relative changes of '*c*' and '*d*' were largely variable.

Table 3. *Models employed to fit the observed relative number of unfolded leaves against the relative accumulated temperature and the parameters obtained for each model of different sowing dates*

Sowing date	Parameters of each model				Standard deviation	Determination coefficient
	a	***b***	***c***	***d***		
April 26th	0.0099	1.0680	-1.0949	1.0017	0.0195	0.9956**
May 6th	0.0377	0.9215	-0.6805	0.7047	0.0216	0.9946**
May 16th	0.0321	0.9367	-0.5862	0.6096	0.0185	0.9961**
May 26th	0.0433	0.8513	-0.5301	0.6248	0.0228	0.9940**
June 5th	0.0378	0.9907	-0.7270	0.6901	0.0202	0.9953**
Coefficient of variation	40.61#	8.49	-30.59	21.94		
	12.12※	6.21	-14.13	7.17		

# indicates the coefficient of variation (CV) among all sowing dates, ※ indicates the CV except for April 26th. ** Significance is at a probability level of 0.01

Inspection and application of dynamic models of the relative number of unfolded leaves

Generally, the AAT required by a certain maize cultivar is constant (Li et al., 2011), therefore, the relative AAT after normalization is also considered stable. Combined with the daily investigation of maize leaf unfolding, the observed accumulated temperature was substituted into the simulation equation to get the corresponding relative unfolded leaf number, and then the real-time unfolded leaf number could be calculated by multiplying the total leaf number of this cultivar by the relative unfolded leaf number at the growing period. The model established by different cultivars and sowing dates was tested with the data in 2013, and the 1:1 test chart of measured and simulated values of unfolded leaf number was obtained (*Figs. 5* and *6*). When validating the measured and simulated number of different cultivars, the equations established by different cultivars and those established by all cultivars together were also tested in this study. The results showed that NRMSE was less than 15%, and I and I1 were close to 1, indicating that the measured number of unfolded leaves of six maize cultivars was in good agreement with the simulated number of the two equations, but the simulated number was slightly

http://www.aloki.hu ● ISSN 1589 1623 (Print) ● ISSN 1785 0037 (Online)
DOI: http://dx.doi.org/10.15666/aeer/2003_24572470

higher than the measured number. Because of the difference of sowing dates between years, the number of unfolded leaves under different sowing dates was simulated based on the equation established by all sowing dates in this study, and this fit the measured numbers. The results indicated that NRMSE was less than 15%, and I and I1 were close to 1, which showed that the consistency between simulated and measured numbers was good. The fitted value was slightly higher than the measured value when the number of unfolded leaves was less than five, while the simulated value was lower than the measured value when the number of unfolded leaves was more than five. In summary, the model parameters established by the relative unfolded leaves of different cultivars were slightly different from those established by all cultivars together, but the simulation level of these two models was very high, which indicated that the model has wide application.

Discussion

The dynamic of unfolded maize leaves affects the leaf area index, photosynthesis, and yield of crop plants (Wang et al., 2018). Temperature is one of the most important environmental and ecological factors affecting the dynamics of unfolded maize leaves and yield formation (Yan et al., 2009), which determines the yield of maize and whether a maize variety can be planted in a certain area (Daiet al., 2008). The AAT is an important reflection of the effect of temperature change on crop growth (Pan et al., 2011).

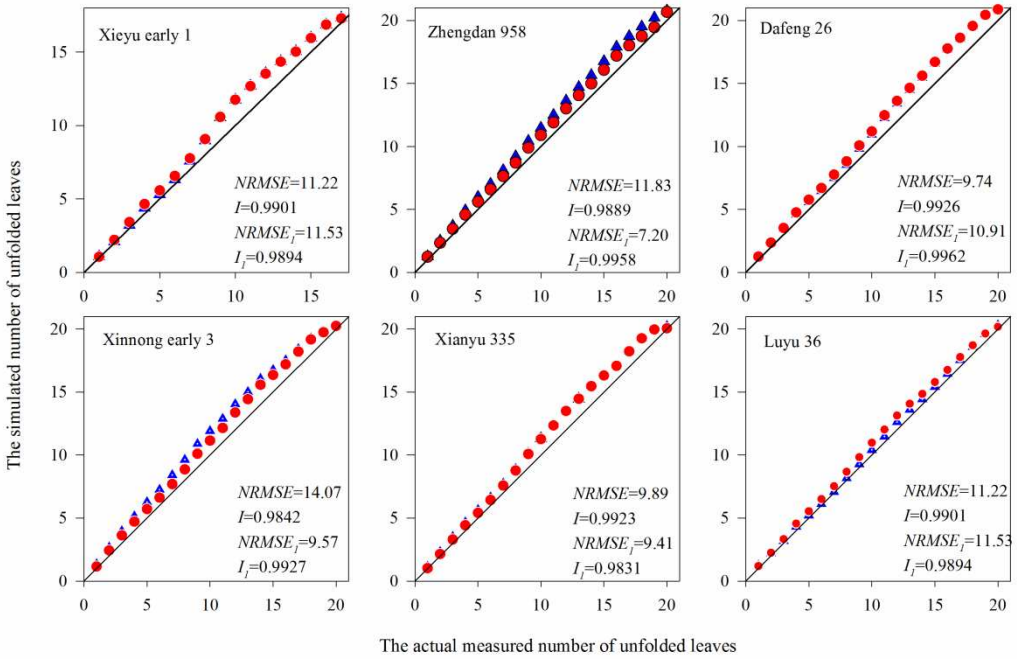

Figure 5. *The test chart of the simulated number of unfolded leaves and the actual measured number of unfolded leaves in maize for different cultivars. NRMSE and I indicate the normalized root mean square error and index of agreement, respectively. The "1" in lower right-hand corner of NRMSE and I is the value based on the model of each maize cultivar. The blue triangle indicates the simulated value through the mathematical model which was establish by all maize cultivars, while the red circle indicates the simulated value through the mathematical model which was establish by each maize cultivar*

http://www.aloki.hu ● ISSN 1589 1623 (Print) ● ISSN 1785 0037 (Online)
DOI: http://dx.doi.org/10.15666/aeer/2003_24572470

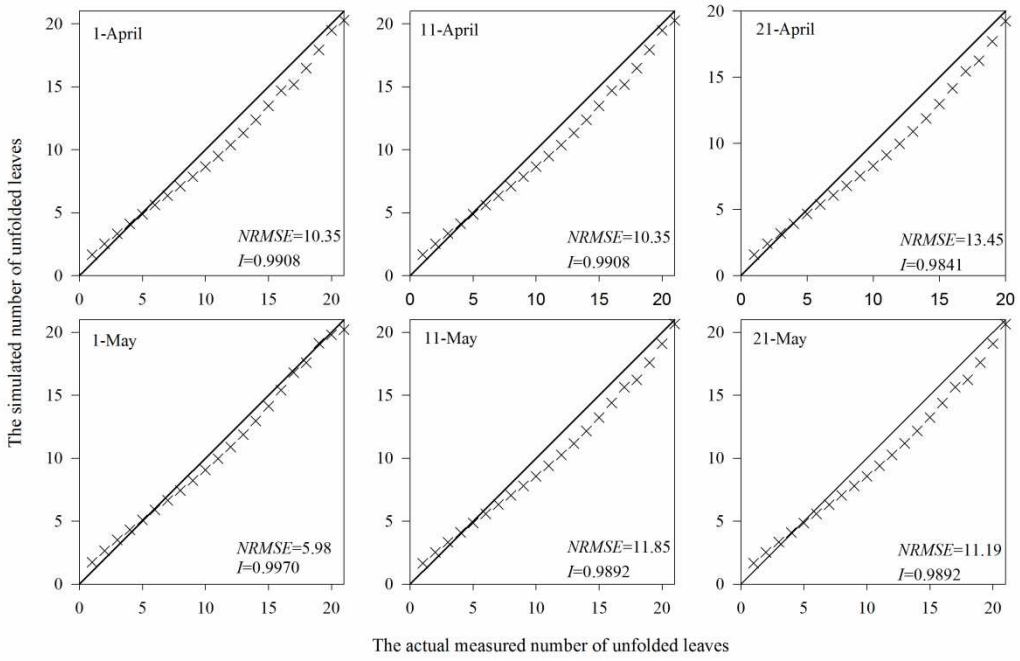

Figure 6. *The test chart of the simulated number of unfolded leaves and the actual measured number of unfolded leaves in maize under different sowing dates. NRMSE and I indicate the normalized root mean square error and index of agreement, respectively. The "1" in lower right-hand corner of NRMSE and I is the value based on the model of each maize cultivar*

The results of this study showed that the number of days and accumulated temperature, needed for leaf unfolding of six maize varieties, presented a unimodal trend with the increase of leaf position. The first, second, and last leaves needed fewer days and less AAT to unfold, while the eighth to fifteenth leaves needed additional days and AAT. This result might be mainly due to the following reasons. First of all, there were usually larger leaves from the eighth to fifteenth leaves, which would require the absorption of more nutrients to accumulate dry matter. Then, the larger the unfolded leaves were, the more days they needed to absorb nutrients for dry matter accumulation. Furthermore, the effects of the environmental factors could be stronger by those larger leaves. Lower air temperature could inhibit the development of the first leaves compared with larger leaves.

This study showed that with the postponement of the sowing date, the peak value of the days and AAT required for maize leaf unfolding decreased. With the delay of the sowing date, the growth process of maize was accelerated and the growth period was gradually shortened (Xie et al., 2005), reducing the number of days needed for most leaves to unfold. Although the accumulated daily temperature was greater during leaf unfolding, the accumulated active temperature decreased in general.

The study of crop growth models is of great significance to the development of modern agriculture (Boote et al., 2018). In this study, maize leaves were observed daily, with an average of 12 observations per day and 12 measurements for the standard value of daily average temperature per day. The AAT and total number of leaves required for maize varieties with different stages of maturity from emergence to leaf unfolding at different sowing dates were normalized. The relative number of unfolded leaves and relative AAT after normalization were simulated, by establishing the dynamic model of

http://www.aloki.hu ● ISSN 1589 1623 (Print) ● ISSN 1785 0037 (Online)
DOI: http://dx.doi.org/10.15666/aeer/2003_24572470

the relative number of unfolded leaves: $y = a + bx + cx^2 + dx^3$. The parameters of the model have great biological significance, where the value of 'a' is the relative unfolded leaf number of maize at the emergence stage, and the value of $(a + b + c + d)$ is the relative unfolded leaf number at the heading stage.

In this study, comparisons of models established by six maize varieties showed that the variation of model parameters between varieties was mainly '*c*' and '*d*' and that of model parameters at different stages of maturity presented similar results. However, the model parameters among varieties at three maturities (early maturity, middle maturity, and mid-late maturity) was different, in which the CV of '*a*' and '*c*' was the largest and '*b*' was the smallest.

By comparing the values, the simulated values of the model established by all varieties together and those made by each variety separately were slightly higher than the measured values, which may be resulted from the difference of maize growth and development between years. The results of *NRMSE* and *I* tests demonstrated that these two models were in good agreement, indicating that the models based on all varieties can be applied to the simulation of unfolded leaf number of different varieties. When the required AAT and the total number of leaves are known, the relative number of unfolded leaves corresponding to any relative AAT can be accurately obtained. This provides a timely method to control the dynamic changes of the number of unfolded leaves and provides the corresponding basis for the digitization of maize production information.

At present, global climate change has become the focus of scientists from all fields. Considering the overall temperature increase in the future, late sowing can be regarded as an environmental condition of the future, so it can be used to evaluate the adaptation of maize leaf growth to climate change to a certain extent. The results of this study showed that the rising temperature in the future could reduce the number of days and accumulated temperature required for most maize leaves to unfold. In addition, besides the leaf unfolding, leaf withering also has a great impact on the leaf area index. Therefore, it is necessary to further analyze the combined dynamics of the processes of leaf unfolding and withering to analyze and predict the change of the leaf area index.

In current study, the mathematical relationships between unfolding leaves and AAT were assessed, which would be more efficient and concise to study the growth and development of the maize. However, leaf area index, depended on the unfolding and wilting of leaves, is a very important indicator in the general research. Then, there would be much more meaningful to establish the mathematical relationships between leaf area index and AAT. In addition, in order to testify the applicability and validity of the current model widely, more field trials would be carried out in different ecological zones in future study. Furthermore, the dynamic relationship between unfolding leaves and AAT under other cultivation practices would be considered in the future research.

Conclusions

Based on different cultivars and sowing dates, the number of days required for each leaf unfolding and the needed accumulated temperature were analyzed. A dynamic model of the relative number of unfolded leaves was established. The main conclusions are as follows:

(1) With the increase in the number of unfolded leaves, the number of days needed for leaf unfolding and accumulated temperature of different maize cultivars showed a

http://www.aloki.hu ● ISSN 1589 1623 (Print) ● ISSN 1785 0037 (Online)
DOI: http://dx.doi.org/10.15666/aeer/2003_24572470

unimodal trend. The eighth to the fifteenth leaves needed more days and a higher accumulated temperature compared to that needed by the first, second, and last leaves. With the postponement of the sowing date, the peak value of the variation of days needed for leaf unfolding and AAT showed a decreasing trend.

(2) The cubic polynomial equation $y = a + bx + cx^2 + dx^3$ showed the best simulation effect between the relative number of unfolded leaves and relative AAT of maize. The parameters of this model have great biological significance, which can accurately predict the dynamic changes of the number of unfolded leaves.

(3) The result could provide a theoretical support that through the optimization of sowing date promoting effectively the adaptation of maize production to climate change in the future.

Acknowledgements. This research was funded by China Spark Program (2011GA630001), Research Program Sponsored by State Key Laboratory of Integrative Sustainable Dryland Agriculture (in preparation), Shanxi Agricultural University (202105D121008-3-1) and Scientific and Technological Innovation Fund of Shanxi Agricultural University (2017YJ25). We would like to extend our sincere appreciation to Jian-Fu Xue for revising and polishing English.

REFERENCES

[1] Bai, C. Y., Li, S. K., Bai, J. H., Zhang, H. B., Xie, R. Z. (2011): Characteristics of accumulated temperature demand and its utilization of maize under different ecological conditions in Northeast China. – Chinese Journal of Applied Ecology 22(9): 2337-2342 (in Chinese with English abstract).

[2] Boote, K. J., Jones, J. W., Hoogenboom, G. (2018): Simulation of Crop Growth: CROPGRO Model. – In: Peart, R. M., Curry, R. B. (eds.) Agricultural Systems Modeling and Simulation. CRC Press, Boca Raton, FL, pp. 651-692.

[3] Chen, Y., Zhang, Z., Tao, F. (2018): Impacts of climate change and climate extremes on major crops productivity in China at a global warming of 1.5 and 2.0 °C. – Earth System Dynamics 9(2): 543-562.

[4] Dai, M. H., Tao, H. B., Binder, J., Wang, L. N., Claupein, W., Wang, P. (2008): Comparing grain production and utilization of solar, heat resources between spring maize and summer maize. – Journal of Maize Sciences 16(4): 82-85 (in Chinese with English abstract).

[5] Gomez-Zavaglia, A., Mejuto, J. C., Simal-Gandara, J. (2020): Mitigation of emerging implications of climate change on food production systems. – Food Research International 134: 109256.

[6] Li, X., Zhao, M., Li, C., Ge, J., Hou, H., Li, Q., Hou, L. (2010): Effect of sowing-date and planting density on dry matter accumulation dynamic and establishment of its simulated model in maize. – Acta Agronomica Sinica 36(12): 2143-2153 (in Chinese with English abstract).

[7] Li, X., Zhao, M., Li, C., Ge, J., Hou, H. (2011): Dynamic characteristics of leaf area index in maize and its model establishment based on accumulated temperature. – Acta Agronomica Sinica 37(2): 321-330 (in Chinese with English abstract).

[8] Liu, Y., Zhang, J., Qin, Y. (2020): How global warming alters future maize yield and water use efficiency in China. – Technological Forecasting and Social Change 160: 120229.

[9] Liu, Y., Zhou, W., Ge, Q. (2019): Spatiotemporal changes of rice phenology in China under climate change from 1981 to 2010. – Climatic Change 157: 261-277.

http://www.aloki.hu ● ISSN 1589 1623 (Print) ● ISSN 1785 0037 (Online)
DOI: http://dx.doi.org/10.15666/aeer/2003_24572470

[10] McMaster, G. S., Wilhelm, W. W. (1997): Growing degree–days: one equation, two interpretations. – Agricultural and Forest Meteorology 87: 291-300.
[11] Meena, R. K., Reddy, K. S., Gautam, R., Maddela, S., Reddy, A. R., Gudipalli, P. (2021): Improved photosynthetic characteristics correlated with enhanced biomass in a heterotic F1 hybrid of maize (*Zea mays* L.). – Photosynthesis Research 147: 253-267.
[12] Pan, G. X., Gao, M., Hu, G. H., Wei, Q. P., Yang, X. G., Zhang, W. Z., Zhou, G. S., Zou, J. W. (2011): Impacts of climate change on agricultural production of China. – Journal of Agro-Environment Science 30(9): 1698-1706 (in Chinese with English abstract).
[13] Renard, D., Tilman, D. (2019): National food production stabilized by crop diversity. – Nature 571: 257-260.
[14] Rotundo, J. L., Tang, T., Messina, C. D. (2019): Response of maize photosynthesis to high temperature: Implications for modeling the impact of global warming. – Plant Physiology and Biochemistry 141: 202-205.
[15] Testa, G., Reyneri, A., Blandino, M. (2016): Maize grain yield enhancement through high plant density cultivation with different inter-row and intra-row spacings. – European Journal of Agronomy 72: 28-37.
[16] Tigchelaar, M., Battisti, D. S., Naylor, R. L., Ray., D. K. (2018): Future warming increases probability of globally synchronized maize production shocks. – Proceedings of the National Academy of Sciences of the United States of America 115(26): 6644-6649.
[17] Voosen, P. (2021): Global temperatures in 2020 tied record highs. – Science 371(6527): 334-335.
[18] Wang, D., Li, G., Mo, Y., Cai, M., Bian, X. (2017): Effect of planting date on accumulated temperature and maize growth under mulched drip irrigation in a middle-latitude area with frequent chilling injury. – Sustainability 9(9): 1500.
[19] Wang, N., Wang, E., Wang, J., Zhang, J., Zheng, B., Huang, Y., Tan, M. (2018): Modelling maize phenology, biomass growth and yield under contrasting temperature conditions. – Agricultural and Forest Meteorology 250: 319-329.
[20] Wang, R., Sun, Z., Yang, D., Ma, L. (2022): Simulating cucumber plant heights using optimized growth functions driven by water and accumulated temperature in a solar greenhouse. – Agricultural Water Management 259: 107170.
[21] Xie, T., Ceng, C., Xu, S. A. (2005): A primary test of suitable sowing date of spring corn in southern Hunan. – Crop Research 19(4): 216-218 (in Chinese with English abstract).
[22] Yan, P., Yang, M., Wang, P., Ji, Y. H. (2009): Precise division of accumulated temperature on GIS in Heilongjiang province. – Heilongjiang Meteorol 26(1): 26-27 (in Chinese).
[23] Yan, Y., Hou, P., Duan, F., Niu, L., Dai, T., Wang, K., Zhao, M., Li, S., Zhou, W. (2021): Improving photosynthesis to increase grain yield potential: an analysis of maize hybrids released in different years in China. – Photosynthesis Research 150: 295-311.
[24] Zhang, B., Zhao, M., Dong, Z. Q., Li, J. G., Chen, C. Y., Sun, R. (2007): Establishment and test of LAI dynamic simulation model for high yield population. – Acta Agronomica Sinica 33(4): 612-619 (in Chinese with English abstract).
[25] Zhou, H., Zhou, G. S., He, Q., Zhou, L., Ji, Y., Zhou, M. (2020): Environmental explanation of maize specific leaf area under varying water stress regimes. – Environmental and Experimental Botany 171: 103932.
[26] Zhu, T., Fonseca de Lima, C. F., De Smet, I. (2021): The heat is on: how crop growth, development and yield respond to high temperature. – Journal of Experimental Botany 72(21): 7359-7373.

http://www.aloki.hu ● ISSN 1589 1623 (Print) ● ISSN 1785 0037 (Online)
DOI: http://dx.doi.org/10.15666/aeer/2003_24572470

EFFECT OF SPLIT BAMBOO SUBSTRATE ON PERIPHYTON AND GROWTH PERFORMANCE OF PACIFIC WHITE SHRIMP, *PENAEUS VANNAMEI* (BOONE, 1931) IN LOW SALINE GROUNDWATER CULTURE

VIJAY AMIRTHARAJ, K. S.[1*] – AHILAN, B.[2] – RAJAGOPALSAMY, C. B. T.[3] – ROSALIND GEORGE, M.[4] – JAWAHAR, P.[5]

[1]*Mariculture Research Farm Facility, Department of Aquaculture, Fisheries College and Research Institute, TNJFU, Thoothukudi 628008, India*

[2]*Dr. M.G.R Fisheries College and Research Institute, TNJFU, Ponneri 601204, India*

[3]*Department of Aquaculture, Dr. M.G.R. Fisheries College and Research Institute, Ponneri 601204, India*

[4]*Department of fish Pathology and Health Management, Fisheries College and Research Institute, Thoothukudi 628008, India*

[5]*Tamil Nadu Dr. J. Jayalalithaa Fisheries University, Nagapattinam 611002, India*

[*]*Corresponding author*
e-mail: vijayamirtharaj@tnfu.ac.in, ksvijay444@gmail.com; phone: +91-999-445-0248

(Received 25th Nov 2021; accepted 25th Feb 2022)

Abstract. An experimental study was undertaken to assess the impact of substrate and periphyton on the growth, survival and feed utilization of *Penaeus vannamei*. This study was conducted in cement tanks with bamboo as substrate. The average submersion depth of the substrates was maintained at 85.16 ± 0.26 cm in the treatment tanks. There was significant difference (P value < 0.05) observed in the values of Chlorophyll a (3.12 ± 0.32 µg/cm^2 minimum and 16.29 ± 1.15 µg/cm^2 maximum values), dry weight (2.49 ± 1.46 mg/cm^2), ash (0.78 ± 0.46 mg/cm^2), ash free dry weight (1.71 ± 1.0 mg/cm^2) and autotrophic index (146 ± 18) in terms of submersion time but there was no significance observed in terms of substrate depth. The bio growth parameters (Average Body Weight - 15.4 ± 4.9 g, Average Daily Growth - 0.165 ± 0.01 g, Specific Growth Rate - 7.67 ± 0.03, Protein Efficiency Ratio - 3.12 ± 0.15 and Food Conversion Ratio - 0.92 ± 0.00018) were also observed to be high in treatments with the substrate. Feed usage in the treatment tank was found to be reduced by 19% compared to the control tank. The Periphyton community recorded on the treatment tanks with split bamboo poles as substrate comprised of 4 groups (Bacillariophyceae, Chlorophyceae, Cyanophyceae and Euglenophyceae). The results on the depth-wise analysis of microbial load on the split bamboo substrate have shown a significant difference between 10 cm and 40 cm depth and 10 cm and 70 cm depth of the substrate (P<0.05), whereas, there was no significance observed between 40 cm and 70 cm depth of the substrate in the microbial load. Under the low saline condition, substrate-based vannamei farming has shown better performance compared to the tanks without substrate.
Keywords: *periphyton, specific growth rate, protein efficiency ratio, food conversion ratio, substrate*

Introduction

Aquaculture continues to grow faster than any other major food sector. Inland aquaculture production contributes to around 64% of the total aquaculture production with different production systems (FAO, 2018). Aquaculture contributes 1.07% to the total GDP and 5.23 % to the agricultural GDP of India. Inland saline ground water-based aquaculture also offers the potential to increase the production of euryhaline and marine

http://www.aloki.hu ● ISSN 1589 1623 (Print) ● ISSN1785 0037 (Online)
DOI: http://dx.doi.org/10.15666/aeer/2003_24712484

species. In more than 100 countries saline soil occurs in arid regions and the surface water and groundwater in such areas have a salinity of more than 1 ppt (Keren, 2000). Most efforts on the culture of marine shrimp in inland ponds have focused on the use of inland saline groundwater in U.S.A, Israel and India (DattaMunshi, 2010). The commercial farming of shrimps in Inland saline water was done with 2 – 7 ppt in Alabama, Florida, Texas, Arizona and Arkansas. In Texas *Penaeus vannamei* farming in saline, quarry waters started in the 1970s and in Israel culture of finfishes in deep geothermal brackish water aquifers was in practice from the late 1980s and this is known as "desert aquaculture" (Allan et al., 2009). Low saline groundwater refers to the farming of marine shrimps in salinity less than 15 ppt and this inland saline farming of marine shrimp is in practice for more than 10 years in some farms in the states of Florida, Alabama, Arizona and Texas in USA (DattaMunshi, 2010).

Inland saline-based farming of Pacific white shrimp, *Penaeus vannamei* is in trend worldwide, which is native to the pacific coast from Northern Peru to Mexico (Liao and Chien, 2011). The inland-based vannamei farming is more successful compared to seawater or brackish water-based culture. In 2018, the world farmed production of *Penaeus vannamei* was recorded at 4.156 million tonnes, which is 53% of the total farmed crustacean production (FAO, 2018). The Pacific white shrimp is a euryhaline species, it can tolerate a wide range of salinity from 0.5 to 45 g L^{-1} [6,7]. *Penaeus vannamei* can even grow with salinity less than 0.5 g L^{-1} in water (Araneda, 2008; Cuvin-Aralar, 2009). *Penaeus vannamei* has now become the candidate species for low saline inland farming due to its ability to survive and grow in different saline conditions.

Periphyton refers to the total assemblage of sessile or attached organisms on any substrate (Reid and Wood, 1976; Weitzel, 1979). In many water bodies, the contribution of the Periphyton community to production is greater than that of the phytoplankton. In a study that compared the primary productivity of a turbid and clear lake, phytoplankton was found to account for 96% of the total annual production in the turbid lake while epipelon contributed 77% in the clear lake. The contribution of Periphyton to annual primary productivity is as high as 1 kg cm^2 (Azim et al., 2005). The development of periphyton depends on different factors like time, depth and type of substrate used. Based on different studies by different authors have proved bamboo substrate to have better growth of periphyton both quantitatively and quantitatively (Azim et al., 2003; Khatoon et al., 2007; Keshavanath et al., 2017). The present investigation was undertaken to assess the impact of split bamboo substrate on the growth and survival of Pacific white shrimp in low saline groundwater culture conditions.

Materials and methods

Experimental site and design

The experimental study was conducted at the Fisheries College and Research Institute, Thoothukudi, Tamil Nadu, India during the months of September 2019. This investigation was done in outdoor circular cement tanks each with 13 tons water holding capacity. The trial was conducted for 90 days. Groundwater with salinity 5 g L^{-1} was used for this investigation. Split Bamboo poles with 4 cm width were used as the substrate for this study, throughout the trial the mean submersion depth of the split bamboo poles was maintained at 85.16 ± 0.26 cm Split bamboos were provided with cement stones as sinkers in the bottom of the pole to maintain it in the vertical hanging position. These substrates were erected inside the circular tanks and one week before the tanks were stocked with

http://www.aloki.hu ● ISSN 1589 1623 (Print) ● ISSN1785 0037 (Online)
DOI: http://dx.doi.org/10.15666/aeer/2003_24712484

Penaeus vannamei seed (*Figure 1*). The control tanks were filled with water and maintained without substrate.

Figure 1. *Fabricated split bamboos and their erection in 13 ton circular tanks*

Periphyton sampling

Quantitative and qualitative analysis of periphyton was done every 10 days once from the split bamboo substrate erection in the treatment circular cement tanks, where the substrate samples were analyzed for dry matter (DM), pigment Chlorophyll *a* (Chl *a*), ash free dry matter (AFDM) and autotrophic index (AI) every 10 days once with following standard methods (APHA, 1992). The water sample from the control tank was also analyzed for plankton and Chlorophyll *a* for every 10 days once. From each treatment tank, one substrate was taken and 2 x 2 cm^2 samples of periphyton were taken at three different depths (10, 40 and 70 cm). The area was scrapped carefully using a scalpel blade to remove all the periphyton without affecting the substrate (visually). After sampling, the substrates were replaced in their original position, marked and excluded from subsequent sampling.

Bio growth sampling of Penaeus vannamei

Penaeus vannamei shrimps of Post Larval stage 12 (0.015 gm) were purchased from Coastal Aquaculture Authority (CAA) approved hatchery and stocked in all control and treatment tanks. Stocking density was done as per the norms of CAA, India (60/m^3), stocking density was maintained at the same levels for control and treatment tanks also. Initial feeding for the shrimps was done as per the recommendation of the feed company using commercial vannamei feed with 38% protein content. The sampling was done every 10 days once and weekly weight gain and the average of daily growth parameters were recorded.

http://www.aloki.hu ● ISSN 1589 1623 (Print) ● ISSN1785 0037 (Online)
DOI: http://dx.doi.org/10.15666/aeer/2003_24712484

Sample analysis

Water quality parameters

Water quality parameters like water temperature, pH and dissolved oxygen were measured daily using YSI professional handheld multi-parameter kit at the water depth of 30 cm. Salinity was checked initially before pumping and checked at an interval of 10 days. Other water quality parameters were checked at an interval of 7 days till the end of the study. The water chlorophyll contents were also determined using the standard method by collecting samples once every 10 days. All the water quality parameters were observed at optimal levels both in control and treatment tanks through out the study (*Figure 2*).

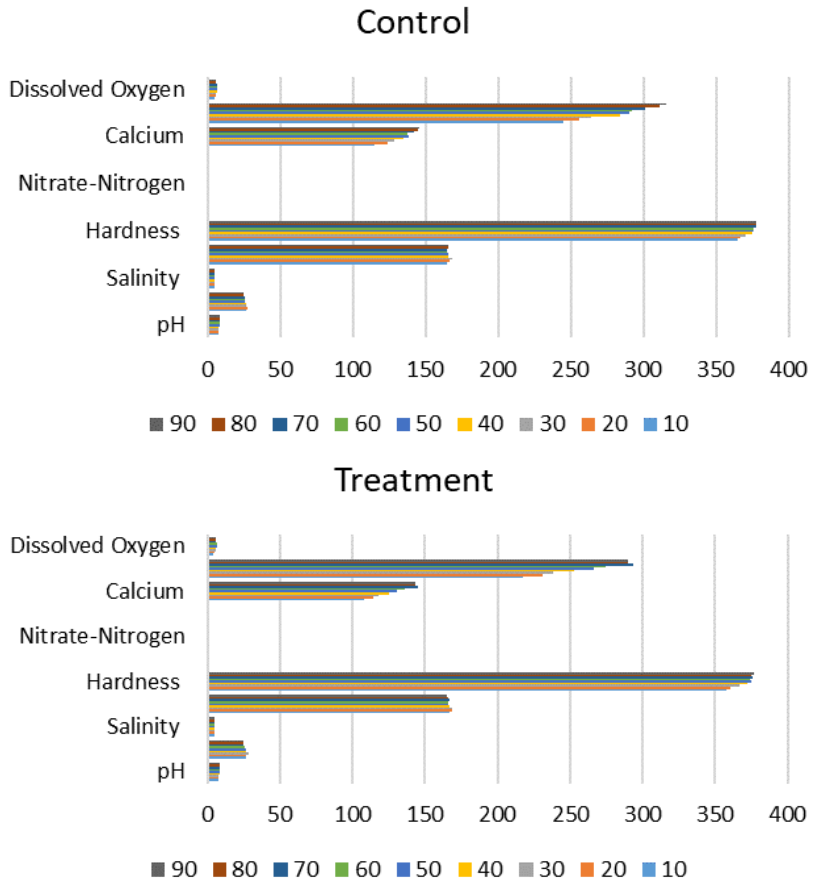

Figure 2. *Water quality parameters*

Chlorophyll a

Periphyton sample collected for estimation of Chl *a* and the sample was transferred into tubes containing 10 ml of 90% acetone, labeled and stored in refrigerator for overnight (APHA, 1992). The next day morning, samples were homogenized for 30 sec in a tissue grinder, again refrigerated for 4 hours and centrifuged for 10 minutes at 2000 rpm. The supernatant was carefully transferred to 1 cm glass cuvettes and absorbance is measured at 663, 645 and 630 nm using an UV spectrophotometer (Perkin Elmer).

http://www.aloki.hu ● ISSN 1589 1623 (Print) ● ISSN1785 0037 (Online)
DOI: http://dx.doi.org/10.15666/aeer/2003_24712484

Dry matter and ash free dry matter

From the collected periphyton samples, one sample was used for the determination of total dry matter and ash content of the periphyton. Further, pre-weighed and labeled with aluminum foil and dried at 105 °C in a hot air oven (Technico) for 1 hour until constant weight and kept in a desiccator until weighed. The dry matter is transferred to a muffle furnace (Technico) and ashed at 450 °C for 6 hours and weighed. Dry matter, ash free dry matter and ash content were determined by weight difference.

Taxonomic analysis of periphyton

The periphyton samples collected were suspended in 50 ml distilled water and preserved in 5% buffered formalin in a sealed plastic vials for taxonomic analysis of periphyton. From the preserved sample 1 ml was transferred to Sedgwick-Rafter cell (S-R cell) divided in 1,000 squares after vigorous shaking. Using Nikon Inverted Microscope (Eclipse TS 100) 10 squares were randomly selected for identification of the algae. Taxa were identified using keys from manual of freshwater biota (DattaMunshi, 2010). Plankton was also determined every ten days once by filtering 5 liters of water from the circular tanks, samples were taken at 2 different locations of the tank using 45µm plankton net and preserved in 5% formalin further analysis of the taxa were done as it was done for the periphyton.

Bio growth parameter analysis of Penaeus vannamei

The weight of the 100 numbers of *Penaeus vannamei* shrimps/sampling from the treatment and control tanks were measured every 10 days once and documented for statistical analysis. The bio growth parameters like Specific Weight Gain (SGR), Protein Efficiency Ratio (PER), Average Daily Weight Gain (ADG) and Food Conversion Ratio (FCR) were calculated after the completion of the trial study following the standard calculation methods.

$$\text{Specific weight gain} = (\text{InFw} - \text{InIw})/t \quad \text{(Eq.1)}$$

where,
InFw is the log value final weight gain;
InIw is the log value Initial weight;
t is the time duration of experiment in days.

$$\text{Protein Efficiency Ratio} = \text{Gain in body mass (g)}/\text{Protein intake (g)} \quad \text{(Eq.2)}$$

$$\text{Average Daily Weight Gain} = \text{Final weight gain (g)}/\text{Days of culture} \quad \text{(Eq.3)}$$

$$\text{Food Conversion Ratio} = \text{Total feed consumed}/\text{Total harvest} \quad \text{(Eq.4)}$$

Statistical Analysis

The normality and homogeneity of chlorophyll *a* data, DW, Ash, AFDW and AI were checked using Shapiro-Wilk and Levene Statistic respectively. ANOVA test was performed for all the variables and evaluated for its significance using SPSS 25.0 statistical analysis software. Chl *a*, dry matter, ash, ash free dry matter, autotrophic index

http://www.aloki.hu ● ISSN 1589 1623 (Print) ● ISSN1785 0037 (Online)
DOI: http://dx.doi.org/10.15666/aeer/2003_24712484

depending on time and depth and day wise plankton taxa were also analyzed for its significance using one-way ANOVA. Bio growth parameters were analyzed using descriptive statistics and two-way ANOVA using excel.

Results

Submersion time and periphyton

The overall maximum values of Chl a, DW, Ash, AFDW and AI values were observed as 16.29 ± 1.15 µg/cm^2, 4.28 ± 0.04 mg/cm^2, 1.37 ± 0.01 mg/cm^2, 2.91 ± 0.02 mg/cm^2 and 186 ± 12.8, respectively. The maximum mean values of Chl a, DW, Ash, and AFDW were observed in the experiment tank during the 90th day of sampling and the maximum value of AI was reported on the 80th day of sampling. There was a significant difference (*Figure 3*) observed in the Chl *a* development on the split bamboo substrates with an increase in the submersion time (*P* value <0.05). In the multiple comparisons made for Chl a it was observed that there was no significant difference observed in the levels of Chl *a* in the comparison made between 70th day vs 80th day (P value – 0.559) and 80th day vs 90th day (P value – 0.865). In the case of the multiple comparisons made for DW, Ash, AFDW and AI with submersion time there was a significant difference observed (*Table 1*).

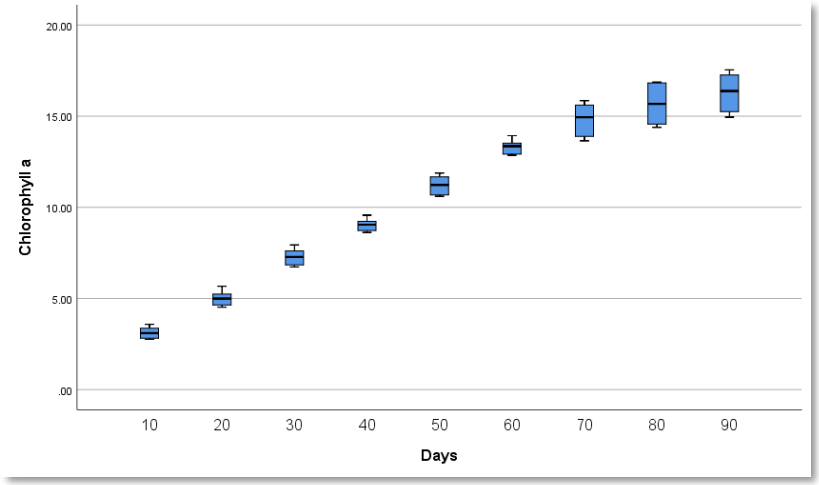

Figure 3. *Submersion time and chlorophyll a concentration in bamboo substrate*

Submersion depth and periphyton

In the present study, the one-way ANOVA analysis on the impact of depth on Chl *a* has not shown any significant differences (*Figure 4*). The mean values observed at different depths of substrate 10 cm, 40 cm and 70 cm were 10.55 µg cm^{-2}, 10.84 µg cm^{-2} and 10.51 µg cm^{-2}, respectively. The highest mean value was observed at 40 cm depth.

Taxonomic composition of periphyton on the split bamboo substrate

This study for periphyton in low saline groundwater using split bamboo substrate has recorded with only eight genera of periphyton taxa which belong to Bacillariophyceae, Chlorophyceae, Cyanophyceae and Euglenophyceae. The overall mean values were

http://www.aloki.hu ● ISSN 1589 1623 (Print) ● ISSN1785 0037 (Online)
DOI: http://dx.doi.org/10.15666/aeer/2003_24712484

observed to be higher for genera Euglena (7919 ± 2685) followed by Ankistrodesmus (6291 ± 2270) (*Figure 5*). There was a significant difference observed in the levels of plankton taxa concerning increase in days and between genera (*P* value <0.05).

Table 1. *Turkey HSB multiple comparisons of submersion time (days) showing the significance and non-significance*

Submersion Time (Days)		Dry Weight (P value)	Ash (P value)	AFDW (P value)	AI (P value)
10	20	0.967	0.999	0.936	0.172
10	30	*	*	*	0.517
30	40	*	*	*	0.244
30	50	*	*	*	0.072
40	50	*	*	*	0.986
40	60	*	*	*	0.774
40	70	*	*	*	0.108
40	80	*	*	*	0.054
40	90	*	*	*	0.149
50	60	*	*	*	0.997
50	70	*	*	*	0.350
50	80	*	*	*	0.183
50	90	*	*	*	0.457
60	70	*	*	*	0.703
60	80	*	*	*	0.435
60	90	*	*	*	0.822
70	80	*	0.159	*	1.000
70	90	*	*	*	1.000
80	90	0.967	*	1.000	0.996

AFDW – Ash Free Dry Weight, AI – Autotrophic Index, * P value <0.05 (Significance)

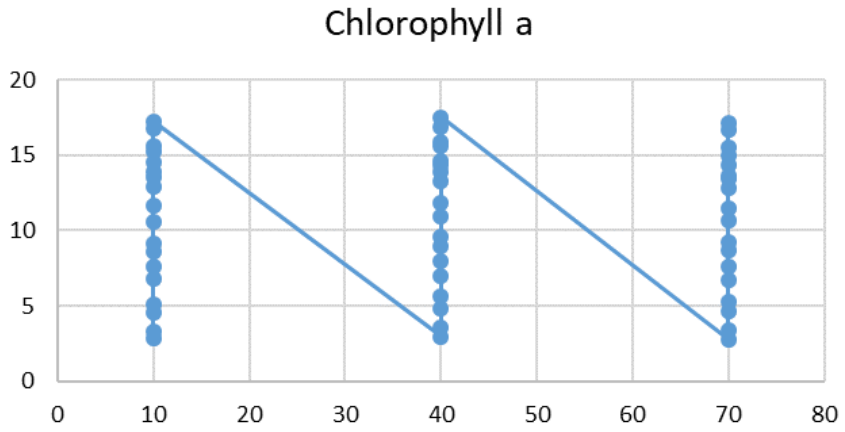

Figure 4. *Chlolophyll a concentration at different depths in the substrate*

http://www.aloki.hu ● ISSN 1589 1623 (Print) ● ISSN1785 0037 (Online)
DOI: http://dx.doi.org/10.15666/aeer/2003_24712484

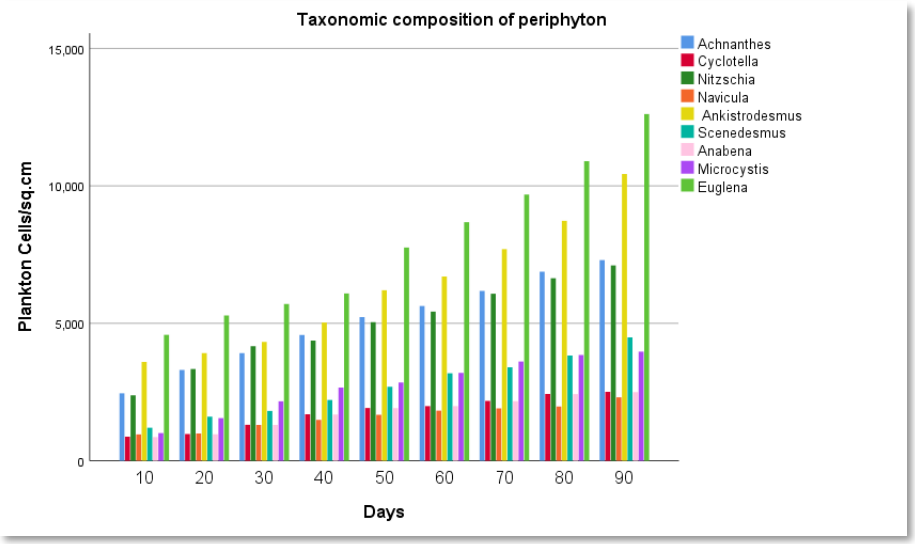

Figure 5. *Taxonomic composition of plankton on split bamboo substrate*

Bio-growth parameters of Penaeus vannamei

The growth performance of *P.vannamei* was observed to be high in treatments with substrate compared to the control tank without substrate (*Table 2*). There was a significant difference observed in growth between treatment and control based on ANOVA test (*P* value < 0.05) (*Table 3*). The growth of *P.vannamei* in the treatment tank was observed to be high by 71% in with substrate compared to the control (*Figure 6*) tank without substrate.

Table 2. *Bio-growth parameters of Penaeus vannamei*

Growth parameters	Control	Treatment
Stocking density (Per m ^{3})	60	60
Total stocking (Numbers)	780	780
Initial weight (g)	0.015	0.015
Days of Culture	90	90
Initial weight	0.015 ± 0.011	0.015 ± 0.011
Initial biomass (g)	11.7 ± 0.43	11.7 ± 0.43
Final weight (g)	8.8 ± 0.14	15.1 ± 0.17
Final biomass (g)	6107 ± 150	11189 ± 225
Feed	12850 ± 250	10244 ± 208
Average Daily Growth (ADG)	0.09 ± 0.0005	0.16 ± 0.007
Specific Growth Rate (SGR)	7.07 ± 0.02	7.67 ± 0.03
Protein Efficiency Ratio (PER)	1.36 ± 0.0003	3.12 ± 0.0006
Food Conversion Ratio (FCR)	2.10 ± 0.0004	0.92 ± 0.00018
Survival rate	89 ± 0.56	95 ± 0.70

http://www.aloki.hu ● ISSN 1589 1623 (Print) ● ISSN1785 0037 (Online)
DOI: http://dx.doi.org/10.15666/aeer/2003_24712484

Table 3. *Significant difference observed between control and treatment in growth*

ANOVA						
Source of Variation	*SS*	*df*	*MS*	*F*	*P-value*	*F crit*
Control x Treatment	41.0368519	2	20.51843	11.13941	0.000932	3.633723
Error	29.4714815	16	1.841968			

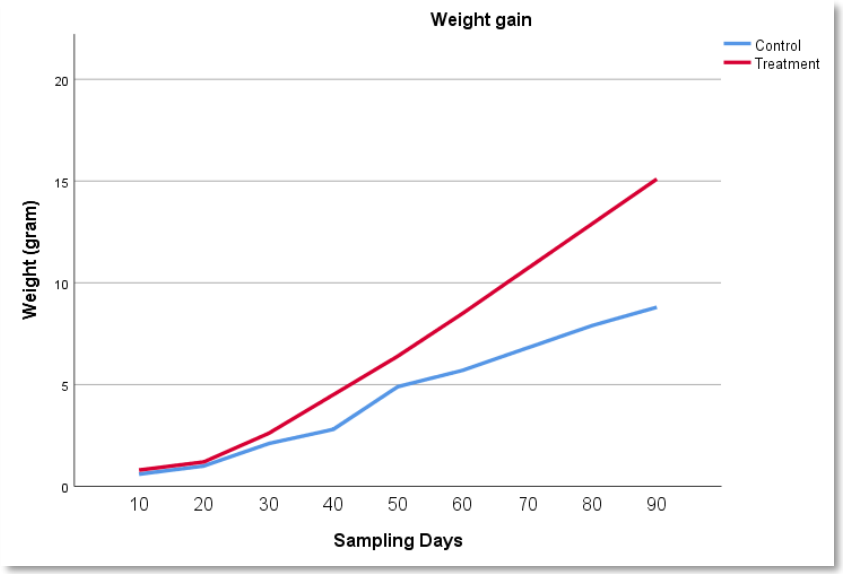

Figure 6. *Penaeus vannamei weight gain in control and treatment tanks*

In the present study, at the end of the 90 days trial, *P.vannamei* in treatment with substrate attained an ABW of 15.4 ± 4.9 and in control, the ABW was 8.8 ± 3.5. Average daily growth gain was observed to be high in treatment tanks with the substrate (0.165 ± 0.01) and relatively less in control (0.09 ± 0.008). In the present trial, the total consumption of feed has been observed to be reduced by 25% (*Figure 7*) in the substrate-based tank (10.24 kg feed) compared to the control tank (12.8 kg feed). The Protein Efficiency Ratio was observed to be high in treatment with the substrate (3.12 ± 0.15) and less in the control tank (1.36 ± 0.12). No specific difference was observed in treatment and control in terms of survival of vannamei shrimp.

Microbiology of split bamboo substrate

The swab samples collected from the split bamboo pole at different depths of 10 cm, 40 cm and 70 cm were analyzed for microbial load by enumerating the total plate count (TPC). The result has shown that there was a significant difference observed between 10 cm and 40 cm depth and 10 cm and 70 cm depth of the substrate ($P<0.05$), whereas, there was no significance observed between 40 cm and 70 cm depth of the substrate in the microbial load. The Shapiro-Wilk analysis on the data has shown the normal distribution of the data, the highest mean value was recorded at 70 cm depth of the split bamboo pole (4.97 ± 0.98 x 10^6 cfu/ml) with minimum and maximum values of 3.6 x 10^6 cfu/ml and 6.6 x 10^6 cfu/ml followed by 40 cm depth with mean value of

http://www.aloki.hu ● ISSN 1589 1623 (Print) ● ISSN1785 0037 (Online)
DOI: http://dx.doi.org/10.15666/aeer/2003_24712484

4.76 ± 0.97 x 10^6 cfu/ml and minimum and maximum values of 3.4 x 10^6 cfu/ml and 6.4 x 10^6 cfu/ml. Mean values, minimum and maximum values recorded at 10 cm depth of the substrate was 3.88 ± 1.0 x 10^6 cfu/ml, 2.3 x 10^6 cfu/ml and 5.8 x 10^6 cfu/ml (*Figure 8*).

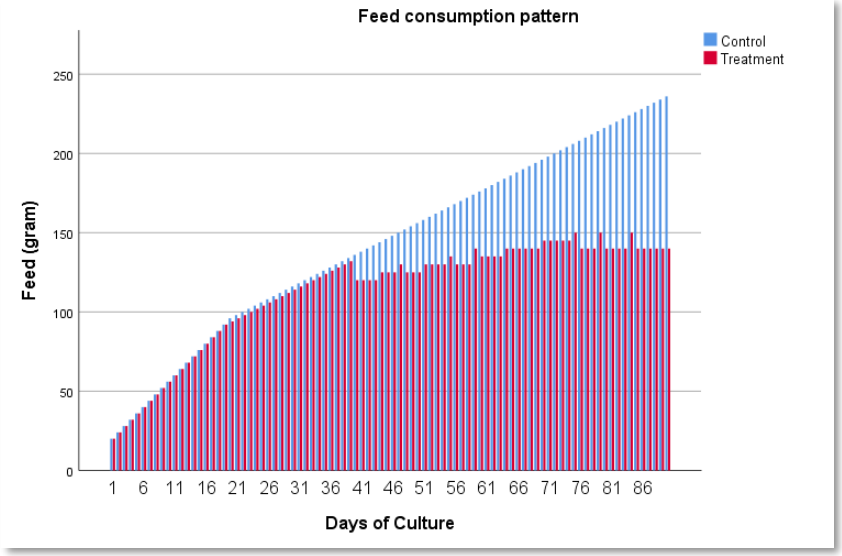

Figure 7. *Comparative feed consumption pattern in control and treatment tank*

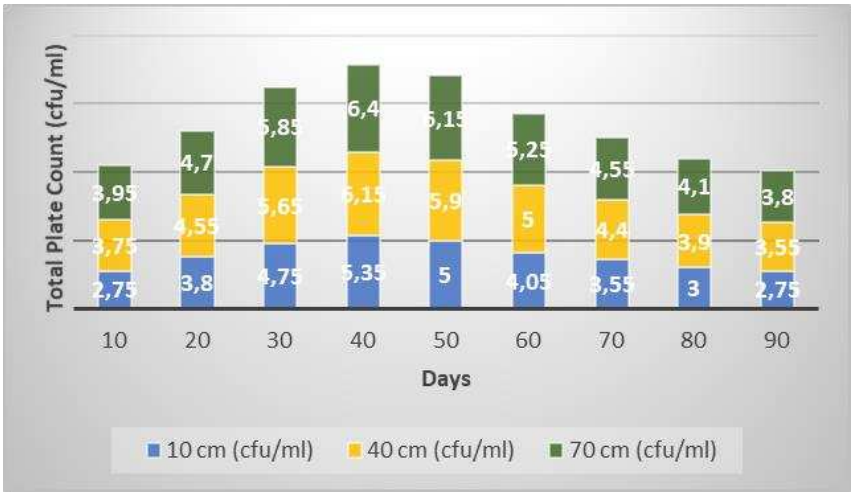

Figure 8. *Total Plate Count (cfu/ml) at different depths of the substrate*

Discussion

Submersion time and periphyton

The mean value of Chl a (10.64 ± 1.59 µg/cm^2) reported from the present study is in line with the Chl a value (11.5 µg/cm^2) reported by Azim et al. (2002a) in hizol substrate and lower than the Chl a value (39.59 µg/cm^2) documented by Keshavanath et al. (2017) in the bamboo substrate from freshwater. Multiple comparisons of AI with submersion time have not shown any significant difference in the increase in AI value with time. The

http://www.aloki.hu ● ISSN 1589 1623 (Print) ● ISSN1785 0037 (Online)
DOI: http://dx.doi.org/10.15666/aeer/2003_24712484

significant increase in the levels of periphytic algae in terms of Chl a, DW, Ash and AFDW with submersion time observed in the present investigation in low saline groundwater was is in line with the results reported from other authors in freshwater (Hoagland et al., 1982; Biggs, 1996; Steinman, 1996; Azim et al., 2001, 2002b, 2003), brackish (Khatoon et al., 2007) and marine waters (Richard et al., 2007).

Submersion depth and periphyton

At greater depth, the periphyton standing stock gets reduced due to a reduction in light intensity (Konan-Brou and Guiral, 1994; Azim et al., 2002). According to Kirk (1994), the intensity of light and the spectral composition has a considerable impact on the quality and composition of flora and periphyton with change in depth. Irradiance induced more difference in the epilithic biomass, a higher level of irradiance leading to a higher level of biomass and change in the taxonomic composition of epilithic assemblage (DeNicola and Hoagland, 1996). Similarly, Konan-Brou and Guiral (1994) have reported minimal horizontal heterogeneity of algae in brackish water using Acadja as substrate; Azim et al. (2002b) have reported on the vertical distribution of Chl a in bamboo substrates have no significance with depth in freshwater polyculture system is following the present report of non-significance with the growth of periphyton in terms of depth and the present observation Chl *a* with depth is not accordance with Kirk (1994). The present study is in acceptance with DeNicola and Hoagland (1996). Overall, the irradiance concentration influenced the occurrence of the higher level of periphytic algae throughout the substrate length and also due to the influence of vigorous aeration and water movement in the experiment tank.

Taxonomic composition of periphyton on the split bamboo substrate

In pond habitat, the periphyton taxa are dominated by Bacillariophyceae, Chlorophyceae, Cyanophyceae, Euglenophyceae, Zooplankton and Invertebrates. However, in the Estuary and seawater environment, the periphyton taxa are dominated by Bacillariophyceae, Chlorophyceae, Cyanophyceae, Rhodophyceae and Phaeophyceae (Azim et al., 2005). The plankton taxa generic composition observed in this investigation in low saline groundwater was comparatively very less to those reported by other authors in freshwater (Azim et al., 2001; Algarte et al., 2017; Sunil Rai et al., 2018) and marine waters (Richard et al., 2007). The genera of planktons found in low saline groundwater are similar to those reported from freshwater.

Bio-growth parameters of Penaeus vannamei

The difference in growth observed in treatment tanks in the present study with the substrate is in line with Schveitzer et al. (2013), who has reported that the presence of substrate corresponds to shrimp biomass production. Khatoon et al. (2007b) observed that the specific growth rate of shrimp post-larvae increased 28% in the presence of substratum. Ballester et al. (2007) determined that growth and survival of *Farfantepenaeus paulensis* post-larvae did not enhance in the presence of artificial substrata that had their biofilm periodically removed, indicating the importance of biofilm as food. The FCR was observed to be better in tanks with substrates and this matches with the earlier findings in the culture of *P.vannamei* (Audelo-Naranjo et al., 2011) and *F.paulensis* (Ballester et al., 2007). Bratvold and Browdy (2001) have also reported high shrimp production and low feed conversion ratio (FCR) during the culture of *P.vannamei*

http://www.aloki.hu ● ISSN 1589 1623 (Print) ● ISSN1785 0037 (Online)
DOI: http://dx.doi.org/10.15666/aeer/2003_24712484

in a high-density culture system with artificial substrata (Aquamats™). The SGR values obtained in the present trial were on par with the results reported by Correia et al. (2014) and Legarda et al. (2018) in a biofloc based nursery rearing of shrimp system.

Microbiology of split bamboo substrate

The Total Plate Count (TPC) values in the present study are in accordance with the other authors (Sanli et al., 2015; Yingshun et al., 2017) report on heterotrophic bacterial composition in submerged substrates. The trial conducted on the growth of *P.vannamei* using bamboo substrate in cement tank has shown an increase in the values of TPC with submersion time which is in line with Haglund and Hillebrand (2005) statement on the impact of grazing on the exponential growth of bacteria.

Conclusion

The substrate-based farming of *P.vannamei* in low saline groundwater has proved with higher production, low FCR, high SGR, higher ABW and higher ADG in substrate-based culture compared to substrate-free culture system. Apart from this, the present trial has also proved the reduction in feed consumption in substrate-based culture compared to substrate-free system. The growth of periphyton in low saline water and its quantitative and qualitative analysis has been reported to be in line with the production reported by other authors in fresh, brackish and marine water culture systems. The taxonomic composition of periphyton was observed to be very limited compared to other reports. Further studies on substrate-based pond culture of *Penaeus vannamei* in low saline groundwater system is essential for field-level validation of this present investigation.

REFERENCES

[1] Algarte, V. M., Siqueira, T., Landeiro, V. L., Rodrigues, L., Bonecker, C. C., Rodrigues, L. C., Santana, N. F., Thomaz, S. M., Bini, L. M. (2017): Main predictors of periphyton species richness depend on adherence strategy and cell size. – PLoS ONE 12(7): e0181720.

[2] Allan, G. L., Fielder, G. S., Fitzsimmons, K. M., Applebaum, S. L., Raizada, S. (2009): Inland Saline Aquaculture. – In: New Technologies in Aquaculture. Woodhead Publishing, pp. 1119-1147.

[3] APHA. (1992): Standard Methods for the Examination of Water and Wastewater. – American Public Health Association, Washington DC.

[4] Araneda, M., Perez, E. P., Gasca-Leyva, E. (2008): White shrimp Penaeus vannamei culture in freshwater at three densities: condition state based on length and weight. – Aquaculture 283: 13-18.

[5] Audelo-Naranjo, J. M., Martinez-Cordova, L. R., Voltolina, D., Gomez-Jimenez, S. (2011): Water quality, production parameters and nutritional condition of Litopenaeus vannamei (Boone, 1931) grown intensively in zero water exchange mesocosms with artificial substrates. – Aquaculture Research 42: 1371-1377.

[6] Azim, M. E., Wahab, M. A., Van Dam, A. A., Beveridge, M. C. M., Verdegem, M. C. J. (2001): The potential of periphyton-based culture of two Indian major carps, rohu, Labeo rohita (Hamilton) and gonia, Labeo gonius (Linnaeus). – Aquaculture Research 32: 209-216.

[7] Azim, M. E., Wahab, M. A., Verdegam, M. C. J., Van Dam, A. A., Van Rooij, J. M., Beveridge, M. C. M. (2002a): The effect of artificial substrates on freshwater pond

http://www.aloki.hu ● ISSN 1589 1623 (Print) ● ISSN1785 0037 (Online)
DOI: http://dx.doi.org/10.15666/aeer/2003_24712484

productivity and water quality and the implications for periphyton-based aquaculture. – Aquatic Living Resources 15: 231-241.

[8] Azim, M. E., Verdegem, M. C. J., Rahman, M. M., Wahab, M. A., Van Dam, A. A., Beveridge, M. C. M. (2002b): Evaluation of polyculture with Indian major carps in periphyton-based pond. – Aquaculture 213: 131-149.

[9] Azim, M. E., Wahab, M. A., Verdegem, M. C. J. (2003): Periphyton-water quality relationships in fertilized fishponds with artificial substrates. – Aquaculture 228: 169-187.

[10] Azim, M. E., Verdegem, M. C. J., Singh, M., Van Dam, A. A., Beveridge, M. C. M. (2003): The effects of periphyton substrate and fish stocking density on water quality, phytoplankton, periphyton and fish growth. – Aquaculture Research 34(9): 685-695.

[11] Azim, M. E., Verdegem, M. C. J., Van Dam, A. A., Beveridge, M. C. M. (2005): Periphyton Ecology, Exploitation and Management. – Cambridge, CABI Publishing 319: 15-33.

[12] Ballester, E. L. C., Wasielesky Jr., W., Cavalli, R. O., Abreu, P. C. (2007): Nursery of the pink shrimp Farfantepenaeus paulensis in cages with artificial substrates: biofilm composition and shrimp performance. – Aquaculture 269: 355-362.

[13] Biggs, B. J. F. (1996): Patterns in benthic algae of streams. – In: Stevenson, R. J., Bothwell, M. L., Lowe, R. L. (eds.) Algal Ecology: Freshwater Benthic Ecosystems. Academic Press, San Diego, California, pp. 31-56.

[14] Bratvold, D., Browdy, C. L. (2001): Effect of sand sediment and vertical surfaces (AquaMats™) on production, water quality and microbial ecology in an intensive Litopenaeus vannamei culture system. – Aquaculture 195: 81-94.

[15] Correia, E. S., Wilkenfeld, J. S., Morris, T. C., Wei, L. Z., Prangnell, D. I., Samocha, T. M. (2014): Intensive nursery production of the Pacific white shrimp Litopenaeus vannamei using two commercial feeds with high and low protein content in a biofloc-dominated system. – Aquacultural Engineering 59: 48-54.

[16] Cui, Y., Jin, L., Ko, S-R., Chun, S-J., Oh, H-S., Lee, C. S., Srivastava, A., Oh, H-M., Ahn, C-Y. (2017): Periphyton effects on bacterial assemblages and harmful cyanobacterial blooms in a eutrophic freshwater lake: a mesocosm study. – Scientific Reports 7: 7827. doi:10.1038/s41598-017-08083-x.

[17] Cuvin-Aralar, M. L. A., Lazartigue, A. G., Aralar, E. V. (2009): Cage culture of the Pacific white shrimp Litopenaeus vannamei (Boone, 1931) at different stocking densities in a shallow eutrophic lake. – Aquaculture Research 40: 181-187.

[18] DattaMunshi, J. S. (2010): Manual of Freshwater Biota. – Narendra Publishing House, 455p.

[19] DeNicola, M., Hoagland, K. D. (1996): Effects of Solar Spectral Irradiance (Visible to UV) on a Prairie Stream Epilithic Community. – Freshwater Science 15(2). doi: 10.3389/fmicb.2015.01192.

[20] FAO. (2018): The State of World Fisheries and Aquaculture - Meeting the sustainable development goals. – Rome.

[21] Haglund, A.-L., Hillebrand, H. (2005): The effect of grazing and nutrient supply on periphyton associated bacteria. – FEMS Microbiology Ecology 52(1): 31-41.

[22] Hoagland, K. D., Roemer, S. C., Rosowski, J. R. (1982): Colonization and community structure of two periphyton assemblages with emphasis on the diatoms (Bacillariophyceae). – American Journal of Botany 69: 188-213.

[23] Keren, R. (2000): Salinity. – In: Summer, M. E. (ed.) Handbook of Soil Science. CRC Press, Boca Raton, pp. 1-26.

[24] Keshavanath, P., Leao da Fonseca, F. A., Affonso, E. G., Nobre, A. D., Jeffson, N. P. (2017): Periphyton growth on three bio-substrates and its influence on the performance of Jaraqui (Semaprochilodus insignis). – International Journal of Aquaculture 7(13): 86-93.

[25] Khatoon, H., Yusoff, F., Banerjee, S., Shariff, M., Sidik Bujang, J. (2007a): Formation of periphyton biofilm and subsequent biofouling on different substrates in nutrient enriched brackishwater shrimp ponds. – Aquaculture 273: 470-477.

http://www.aloki.hu ● ISSN 1589 1623 (Print) ● ISSN1785 0037 (Online)
DOI: http://dx.doi.org/10.15666/aeer/2003_24712484

[26] Khatoon, H., Yusoff, F. M., Banerjee, S., Shariff, M., Mohamed, S. (2007b): Use of periphytic cyanobacterium and mixed diatoms coated substrate for improving water quality, survival and growth of Penaeus monodon Fabricius postlarvae. – Aquaculture 271: 196-205.
[27] Kirk, J. T. O. (1994): Light and Photosynthesis in Aquatic Ecosystems. – Cambridge University Press, Cambridge, Massachussetts.
[28] Konan-Brou, A. A., Guiral, D. (1994): Available algal biomass in tropical brackish water artificial habitats. – Aquaculture 119: 175-190.
[29] Legarda, E. C., Barcelos, S. S., Redig, J. C., Ramírez, N. C. B., Guimarães, A. M., do Espirito Santo, C. M., Seiffert, W. Q., do Nascimento Vieira, F. (2018): Effects of stocking density and artificial substrates on yield and water quality in a biofloc shrimp nursery culture. – Brazilian Journal of Animal Science, R. Bras. Zootec 47.
[30] Liao, I. C., Chien, Y-H. (2011): The Pacific White Shrimp, Litopenaeus vannamei, in Asia: The World's Most Widely Cultured Alien Crustacean. – In: Galil, B., Clark, P., Carlton, J. (eds.) In the Wrong Place - Alien Marine Crustaceans: Distribution, Biology and Impacts. Springer, pp. 489-519.
[31] Rai, S., Gharti, K., Shrestha, M., Ranjan, R., Diana, J., Egna, H. (2018): Potential substrates for periphyton enhancement in Carp-SIS polyculture. – Our Nature 16(1): 8-16.
[32] Reid, G. K., Wood, R. D. (1976): Ecology of Inland waters and Estaries. – 2nd ed. D. van Nostrand company, New York.
[33] Richard, M., Trottier, C., Verdegem, M. C. J., Hussenot, J. M. E. (2009): Submersion time, depth, substrate type and sampling method as variation sources of marine periphyton. – Aquaculture 295: 209-217.
[34] Roy, L. A., Davis, D. A., Saoud, I. P., Boyd, C. A., Pine, H. J., Boyd, C. E. (2010): Shrimp culture in inland low salinity waters. – Reviews in Aquaculture 2: 191-208.
[35] Sanli, K., Bengtsson-Palme, J., Nilsson, R. H., Kristiansson, E., Rosenblad, M. A., Blanck, H., Eriksson, K. M. (2015): Metagenomic sequencing of marine periphyton: taxonomic and functional insights into biofilm communities. – Frontiers in Microbiology 6(1192): 1-14.
[36] Schveitzer, R., Arantes, R., Baloi, M. F., Costódio, P. F. S., Aranaa, L. V., Seiffert, W. Q., Andreatta, E. R. (2013): Use of artificial substrates in the culture of Litopenaeus vannamei (Biofloc System) at different stocking densities: Effects on microbial activity, water quality and production rates. – Aquacultural Engineering 54: 93-103.
[37] Steinman, A. D. (1996): Effect of Grazers on Freshwater Benthic Algae. – In: Stevenson, R. J., Bothwell, M. L., Lowe, R. L. (eds.) Algal Ecology: Freshwater Benthic Ecosystems. Academic Press, San Diego, California, pp. 341-373.
[38] Weitzel, R. L. (1979): Periphyton measurements and applications. – In: Weitzal, R. L. (ed.) Methods and Measurements of Periphyton communities: a Review. American Society for Testing and Materials, special Technical Publication (ASTM, STP) 690: 3-33.

http://www.aloki.hu ● ISSN 1589 1623 (Print) ● ISSN1785 0037 (Online)
DOI: http://dx.doi.org/10.15666/aeer/2003_24712484

ANALYSIS OF MUNICIPAL SOLID WASTE MANAGEMENT IN AFGHANISTAN, CURRENT AND FUTURE PROSPECTS: A CASE STUDY OF KABUL CITY

ULLAH, S.[1,2,9] – BIBI, S. D.[2] – ALI, S.[3] – NOMAN, M.[4] – RUKH, G.[5] – NAFEES, M. A.[6] – BIBI, H.[7] – ALI, S.[8] – QIAO, X. C.[9*] – KHAN, S.[2] – HAMIDOVA, E.[10]

[1]*Department of Water Resources and Environmental Engineering, Nangarhar University, Jalalabad 2600, Nangarhar, Afghanistan*

[2]*Department of Environmental Sciences, Abdul Wali Khan University, Mardan 23200, Pakistan*

[3]*Department of Environmental Sciences, Karakoram Internationasl University, Gilgit 15100, Pakistan*

[4]*Colleges of Environmental Science and Engineering, Donghua University, Shanghai 201620, China*

[5]*Department of Chemistry, Women University Swabi, Swabi 23430, Pakistan*

[6]*Department of Animal Sciences, Karakoram International University, Gilgit 15100, Pakistan*

[7]*Department of Soil and Environmental Sciences, The University of Agriculture, Peshawar 25130, Pakistan*

[8]*Department of Environmental Sciences, University of Baltistan, Gilgit-Baltistan, Pakistan*

[9]*School of Resources and Environmental Engineering, East China University of Science and Technology, Shanghai 200237, China*

[10]*Landscape-Azerbaijan State Pedagogical University, Baku AZ1000, Azerbaijan*

[*]*Corresponding author*
e-mail: xiuchenqiao@ecust.edu.cn; phone: +86-21-6425-2171; fax: +86-21-6425-2826

(Received 3rd Dec 2021; accepted 17th Mar 2022)

Abstract. In Asian countries like Afghanistan, the quantity of municipal solid waste (MSW) is rapidly increasing because of increasing population and economic developments. This increased MSW amount and its inappropriate management has severe impacts on Kabul city. The purpose of the current study was to find out the MSW sources, generation rate, physiochemical properties, current and future management practices in Kabul city, Afghanistan. A questionnaire survey of a total number with 1,150 questionnaires was conducted on the basis of stratified random sampling in January, 2021. Quantification/composition of waste was determined by using a standard method of ASTM-D5231-92. The average MSW generation ratio of four (04) categories of residential areas such as (high, middle, low income and rural areas) were considered and ranged from 0.28±0.10 kilograms per capita per day (kg/c/d) for low income or rural areas to 0.48±0.10 kg/c/d for high income areas with the maximum quantity of food waste (FW) at 52.4% of the total waste, followed by paper 20.3% and plastic 17.4% in residential areas. Hence, the total generation of MSW was 3,200 tons/day. The mean per capita FW production in Kabul city was 0.35 kilograms/day or 120.10 kilograms/year. MSW includes of fifteen (15) different types, with organic waste >70% as a major constituent of the MSW in the Kabul city. Outcomes of the current study might help the government to design and operate a complete municipal solid waste management (MSWM) structure for Kabul city and other growing cities all over the country.

Keywords: *solid waste, physiochemical analysis, solid waste management, 3R's approach, awareness*

http://www.aloki.hu ● ISSN 1589 1623 (Print) ● ISSN 1785 0037 (Online)
DOI: http://dx.doi.org/10.15666/aeer/2003_24852507

Introduction

Proper solid waste management (SWM) is the most important method for environmental protection and resources management (Sandulescu, 2004; Ilyas et al., 2017). In SWM, the municipal solid waste management (MSWM) is a significant factor affecting the environment which is ignored in most of the Asian countries like Bangladesh, China, Nepal, Pakistan and Afghanistan (Murtaza and Rahman, 2000; Ghaforzai et al., 2021). In developed countries the generation amount of MSW is equal to collection amount, but in Asian countries like Afghanistan, Bangladesh, Pakistan and India etc., the situation is completely different and MSWM consist of only collection and open dumping (Ali et al., 2016).

There is little census data for Afghanistan but Afghanistan's Central Statistics Office (ACSO) assessed that Kabul city had a population of 720,000 in 1978, which has recently increased to 4 million in 2012 (Mack et al., 2013). The Kabul city population has increased to 4.8 and 5 million in 2015 and 2018 respectively, which shows a total 15% of Afghanistan population. According to United Nations report it is estimated that the population in the Kabul city will rise to about 9 million by the year 2057 (Mack, 2018). This is the maximum ratio of population in any one city in Central or South Asia. Due to this fast growth in population, that extending the boundaries of Kabul city and specifies greater waste generation quantity. This growing quantity of MSW is one of the key challenges to controlling organizations to keep the Kabul city clean (Mack, 2018).

Urbanization, developmental activities, population growth and current living standards are the basic causes behind the increasing growth in MSW generation in Kabul city (Khoshbeen et al., 2020). This increased solid waste total causes trouble in effective MSWM method (collection, storage, transportation and disposal) (Ozcan et al., 2016). Globally the amount and composition of MSW differs with area, climatic as well as socio-economic conditions (Ciuta et al., 2015). In many of the Afghanistan big cities and towns only 50% of the MSW is collected and stored and >80% of the collected MSW goes to open dumping sites around the cities (Khoshbeen et al., 2020). But, for the cities to be comparatively hygienic at least > 80% of the MSW should be collected.

The MSW generation in Kabul city in 2017 was about 0.4 kg/c/d with total amount of 2,000 tons per day (Haidaree and Lukumwena, 2017). In 2020, the MSW generation rate further increased to 0.5 kg/c/d with total amount of 2,563 tons/d. Moreover, it is expected that the sum of MSW generated within the Kabul city will be increase to 0.6 kg/c/d with total generation of 3,300 tons/d by the year 2025 (Khoshbeen et al., 2020). Consequently, the quantity of MSW is expected to rise extremely in the near future while there is no proper management system in Kabul Municipality (KM) to overcome with it. Absence of reliable facts, improper institutional measures, non-compliance of rules, inadequate resources (equipment and money), and absence of specialists are the main limitations for suitable MSWM in Kabul city. In Afghanistan throughout the last two decades due to migration of societies from rural to urban regions the household ratio in Kabul city has enlarged from 3.8-9.2%.

Currently, there is no well-designed and effective MSWM system, necessary data on the sources, generation rate, characterization and composition about MSW in Kabul city. Moreover, there is no well-planned landfill facility in the study area and all the MSW is dumped near to households and causes problems to human health, water quality both surface and underground and also sustainable development. The overall purpose of the current study was to develop a sound and sustainable MSWM for Kabul city. To achieve this purpose, the current MSWM systems have been examined and MSWM practices

http://www.aloki.hu ● ISSN 1589 1623 (Print) ● ISSN 1785 0037 (Online)
DOI: http://dx.doi.org/10.15666/aeer/2003_24852507

were found. All the important data about sources, generation rate, physiochemical properties, current and future prospects of MSWM in Kabul city of Afghanistan have been investigated.

Materials and Methods

Study area

Kabul city lies in the middle of Kabul province, with an expected population of 5 million with in 22 districts, with a total number of households are 694,756; commercial units 70,720 and administrative units are 761 (CSO, 2018). A comprehensive map of study area is available in *Figure 1*. KM is the organization in charge for all the hygienic actions in the Kabul city comprising regular collection, transport and dumping of MSW, as well as drainage cleaning and street sweeping under the control of Directorate of Sanitation (DoS). As of 2019, the DoS met challenges with insufficient technical manpower with a total number of officials are 119 for administration, with a total number of workers/staff 3,625 divided into three (03) sub units transportation, central unit and district offices in DoS. DoS collects the MSW from all the districts excluding district 14 from municipal collection bins. The DoS presently lacks technical staff to plan a well-designed a landfill and operate on international standards (Khoshbeen et al., 2020).

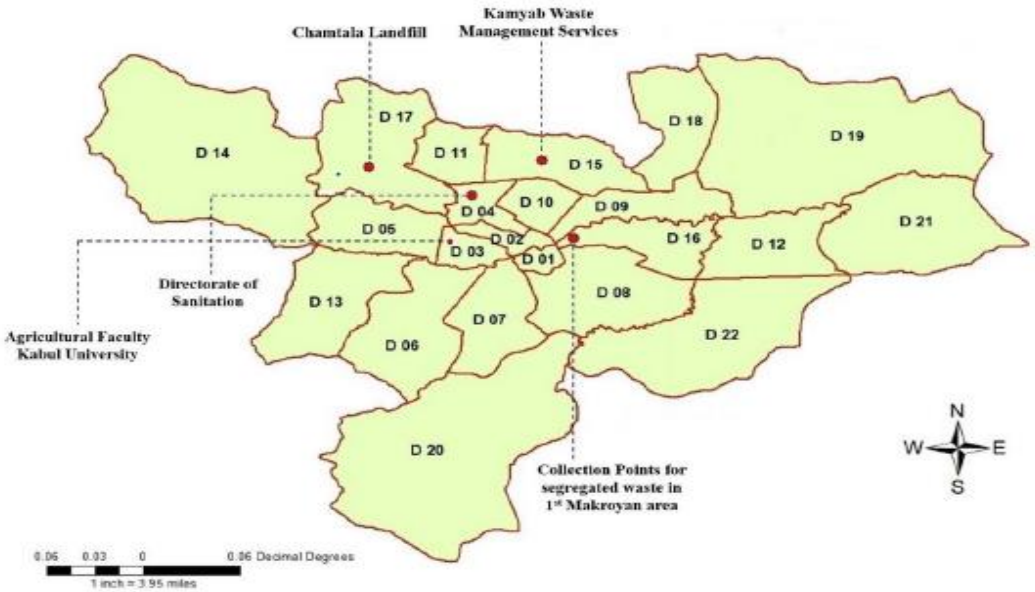

Figure 1. *Location of the study area with district boundaries & important locations of SWM. Map adopted from Khoshbeen et al. (2020)*

Sampling design

In current study MSW samples of the Kabul city were collected from both the main city and rural zones. The benefit of this sampling analysis was to measure the quantity of MSW produced and to identify its sources, generation rate, physiochemical properties and current management practices that will help to recommend a MSWM strategy/system. A total ten (10) sources of waste for the current study were considered, as shown in *Table 1*. Household sources were classified into four (04) main categories

http://www.aloki.hu ● ISSN 1589 1623 (Print) ● ISSN 1785 0037 (Online)
DOI: http://dx.doi.org/10.15666/aeer/2003_24852507

(high, medium, low income and rural families) for stratified sampling. For each source type a total 115 sampling points were selected see in *Table 1*, and waste quantity ratio to discharge was measured. The total sampling was done in ten (10) days (from 20th to 29th of January, 2021) and a total of 1,150 questionnaires and 750 waste samples were considered from all type sources for the current study. Out of the total 1,150 questionnaires about 600, 150, 120, 120, 100 and 60 from residential, markets, commercial, parks, institutions and street sweepings respectively. Moreover, the data about houses, individuals per family, number of staffs and total house area were collected from the questionnaire study.

Table 1. *Sampling design for solid waste generation sources in Kabul city*

Types		Questionnaire Survey for Solid Waste in Kabul City				
		Locations	**Samples/location**	**No of samples**	**Sampling days**	**Total samples**
Residential	High income	05	03	15	10	150
	Middle income	05	03	15	10	150
	Low income	05	03	15	10	150
	Rural areas	05	03	15	10	150
Commercial	Hotels	02	04	08	10	80
	Others	01	04	04	10	40
Markets		05	03	15	10	150
Institutions		05	02	10	10	100
Street sweepings		03	02	06	10	60
Parks		04	03	12	10	120
Total				115		1,150

Solid waste amount

For the determination of MSW generation rate in Kabul city, we used output technique or load count analysis (Ilyas et al., 2017), and it is reported from the literature that this technique requires less works and cost-effective as compared to Input method. Waste samples were collected in plastic bags from each source assigned with a different source code, and these waste samples were collected in specific allotted vehicles. MSW generation rate was measured by weighing the waste amount from each source (Di Maria et al., 2013; Suthar and Singh, 2015). To determine MSW generation rate the mean household size was used seven (07) persons. The relative proportion of each waste component was estimated as percent by weight on wet basis (Di Maria et al., 2015).

Analysis of solid waste composition

Physical properties of waste

Physiochemical properties of MSW show an important role in selection of suitable MSWM approach (Ilyas et al., 2017). For physical composition analysis of the MSW of the Kabul city a standard method ASTM-D5231-92 was used (ASTM, 2008). American Society for Testing Materials (ASTM) has termed this technique as ASTM-D5231-92 standard technique for the analysis of the MSW composition (Worrell and Vesilind, 2011). This method comprises unloading and analyzing the amount of MSW at a disposal

http://www.aloki.hu ● ISSN 1589 1623 (Print) ● ISSN 1785 0037 (Online)
DOI: http://dx.doi.org/10.15666/aeer/2003_24852507

location, in the absence of winds. A representative sample of size 100-200 kg resulting from the collection of waste in residential area is necessary for analysis.

Moreover, reduction process was done for huge MSW producing sources to get a sample of about 200 kg and the samples <200 kg segregation method was used directly. The physical composition percentage of each MSW sample in wet base, Xi (%), was measured as given below.

$$\text{Xi} = \frac{\text{Weight of each weight composition (kg)}}{\text{Total amount of each waste composition (kg)}} \times 100 \quad \text{(Eq.1)}$$

Once the representative sample was prepared, the MSW is full into a plastic container. The plastic container containing the MSW is fallen 03 times to ground from a 30 cm of height, and then the volume is calculated using measuring tape and mass by a balance. The Apparent Specific Gravity (ASG) is calculated as follow.

$$\text{ASG} = \frac{\text{Weight of the MSW in container (kg)}}{\text{Volume of the MSW (m3)}} \quad \text{(Eq.2)}$$

The waste samples were separated into fifteen (15) different physical components after measuring AGS, see in *Table 4*.

Chemical properties of waste

In the present study 100 samples of waste were collected from 20 different sources at Kabul city as shown in *Table 2*. Chemical composition analysis includes the analysis of carbon: nitrogen (C: N), moisture content (MC) of MSW, and three component analysis such as ash, combustible and moisture content were investigated. All analyses were carried out at Centralized Resource Laboratory (CRL), University of Peshawar, Pakistan. For the analysis of MC, minimum 1-1.5 kg of MSW was used of each composition. First of all, the samples were packed in a plastic bags to overcome the loss of MC and kept at a temperature range of 95-100°C for almost five to six (5-6) days in incubator (ASTM, 2008; Nadeem et al., 2016; Ilyas et al., 2017). Later MC was measured as given below.

$$\text{MC}(\%) = \frac{\text{Weight of sample before drying(kg)} - \text{Weight of sample after drying (kg)}}{\text{Weight of sample before drying (kg)}} \times 100 \quad \text{(Eq.3)}$$

Table 2. *Number of samples for chemical composition survey for MSW in Kabul City*

Types		Chemical composition Survey for Solid Waste in Kabul City			
		Source of generation	**Moisture Content (MC)**	**Carbon: Nitrogen (C: N)**	**Three component analysis**
		Locations	**Samples/Location**	**Samples/Location**	**Samples/Location**
Residential	High income	05	5 × 5 = 25	5 × 5 = 25	5 × 5 = 25
	Middle income	05	5 × 5 = 25	5 × 5 = 25	5 × 5 = 25
	Low income	05	5 × 5 = 25	5 × 5 = 25	5 × 5 = 25
Markets (Fruits and Vegetables)		05	5 × 5 = 25	5 × 5 = 25	5 × 5 = 25
Total		20	100	100	100

http://www.aloki.hu ● ISSN 1589 1623 (Print) ● ISSN 1785 0037 (Online)
DOI: http://dx.doi.org/10.15666/aeer/2003_24852507

To analyze the Nitrogen ratio of MSW samples Total Kjeldahl Nitrogen method was used using Mercury (Hg) as a catalyst (Olsen et al. 1982). MC of combustible waste was calculated for MSW category (01, 02, 03, 04, 05 and 08); C: N ratio for (01, 02, 03 and 05) and three component analyses were carried out for (01 to 15). For three component analyses ash, combustible and moisture were analyzed for MSW types ranging from 01-15. For this purpose, 5-7 g of MSW was measured in crucible furnace of 150 ml. The samples were heated at a temperature of 820-850°C for almost two (02) hours and then kept in desiccator for 30-40 min to cool down and weighted. Then ash component (A) and combustible (V) were measured.

$$A(\%) = \frac{\text{Weight of sample after heating (g)}}{\text{Weight of sample (g)}} \times 100 \quad \text{(Eq.4)}$$

$$V(\%) = \frac{\text{Weight of sample (g)} - \text{Weight of sample after heating (g)}}{\text{Weight of sample (g)}} \times 100 \quad \text{(Eq.5)}$$

Data analysis

For MSW generation rate and its composition, 95% confidence interval of the means was calculated. Analysis of data was done using GraphPad Prism (GraphPad Software, Inc., San Diego, CA, USA) (Prism) and Microsoft Excel.

Results and Discussion

The outcomes of the current study show the sources, generation rate, physiochemical properties and current management practices of MSW from study area which is a combination of various constituents. The major ratio of the MSW in Kabul city is organic waste (compostable) more than 70%. Greater amount of this waste indicates a suitable idea for composting method, regular collection and removal of MSW from generation points.

Characterization of MSW in Kabul city

MSW generation, composition and characterization

The mean household size of low, middle, high and rural areas was seven (07) persons (Osama and Kajita, 2020). Average MSW generation rate of these 04 categories of residential parts ranged from 0.28±0.10 kg/c/d for low income or rural regions to 0.48±0.10 kg/c/d for high income regions as given in *Figure 2(a)*. High income areas generate more MSW as related to low income or rural regions; it reveals that living standard greatly affect the quantity of MSW generated.

In *Figure 2(b)* has shown the average MSW generation from commercial sources. Due to insufficient information about the exact number of individuals generating MSW in these regions we have to suggest the mean weight of MSW produced in 10 sampling days. In other sources of MSW, restaurants/hotels are the leading generator of MSW with a total amount of 12.2 kg/d following open parks with 8.4 kg/d of MSW amount. Street sweepings show less role and about 1.8 kg/d of MSW generated. Markets generate 2.5 kg/d of the MSW and institutes 5.3 kg/d individually. Also, MSW quantity study has been done in vegetable and fruit market places of Kabul city. There are some vegetables and fruit market places where KM has sited a communal container of 3 m^3. While other

http://www.aloki.hu ● ISSN 1589 1623 (Print) ● ISSN 1785 0037 (Online)
DOI: http://dx.doi.org/10.15666/aeer/2003_24852507

shops, which are illegal selling points of vegetables and fruits, are distributed in the Kabul city. Ten (10) major points were selected for the collection of samples in these selling places.

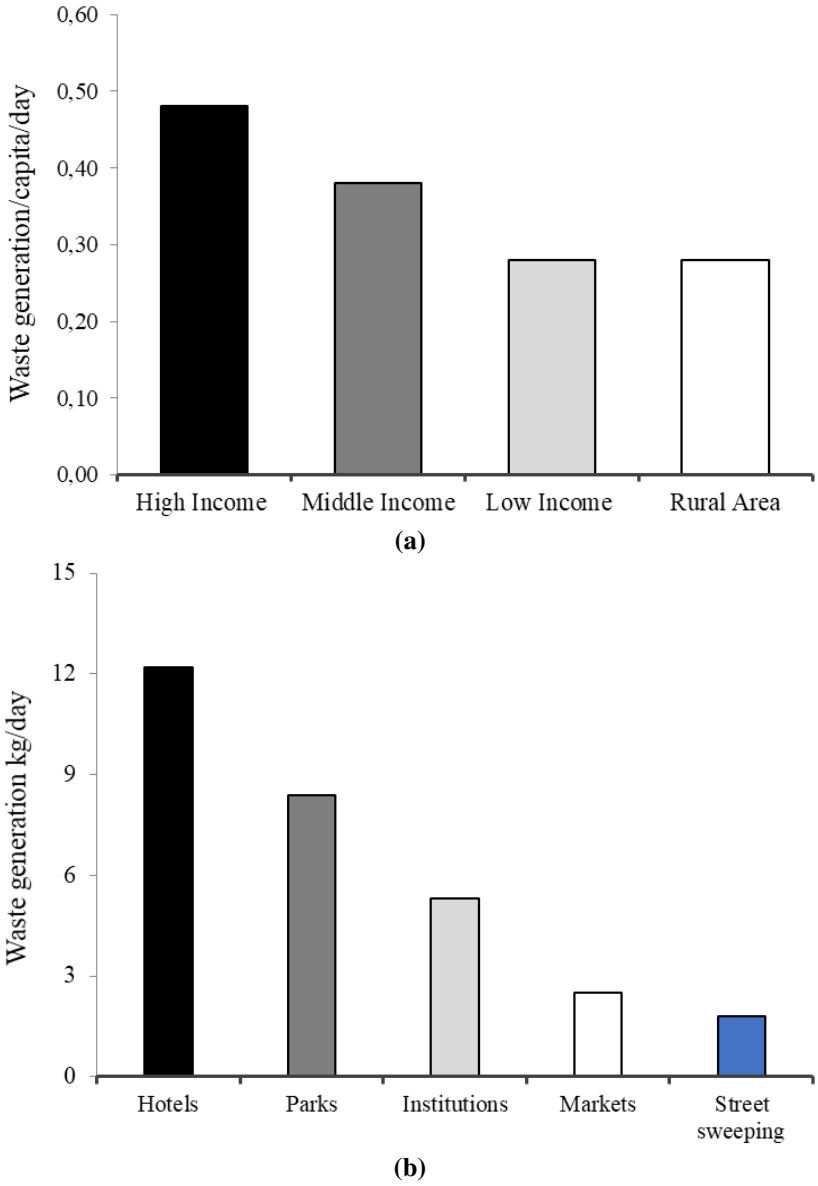

Figure 2. *Solid waste generation per capita per day (kg/d) in* ***(a)*** *residential areas and* ***(b)*** *in commercial areas*

The ASG for each MSW type was analyzed and listed in *Figure 3*. The ASG of MSW from these four (04) residential areas reported 272 kg/m^3 for high income, 280 kg/m^3 for middle income and 278 kg/m^3 for low income areas while 260 kg/m^3 has been reported for rural areas, but commercial MSW from hotels have peak rate of ASG of around 550 kg/m^3. The mean per capita generation of MSW in Afghanistan was expected to be 0.44 and 0.61 kg/c/d in 2016 and 2018, respectively (Kaza et al., 2018). The major cause of this rapid growth is a consequence of current economic development in the Kabul city. With mean per capita MSW production of 0.61 kg/c/d, with expected 5 million population

http://www.aloki.hu ● ISSN 1589 1623 (Print) ● ISSN 1785 0037 (Online)
DOI: http://dx.doi.org/10.15666/aeer/2003_24852507

the total MSW production was approximately 3,050 tons/d. The per capita MSW generation in Bangkok and Delhi was reported 0.82 and 0.41 kg/c/d, respectively (Kumar et al., 2017; Khoshbeen et al., 2020). Significant, Bangkok city has mostly high to middle income families and thus the per capita generation of MSW was greater than Kabul city which generally has low and middle-income families. Remarkably, the high and middle-income families of Kabul city produced MSW at the equal ratio of the Bangkok city. Worldwide, MSW is consisting of 44% organic and food waste followed by cardboard and paper 17% both and plastics 12% (Kaza et al., 2018). A study by Marashlian and El-Fadel (2005) found that food waste grinders can reduce the total solid waste generation by 12 to 43%.

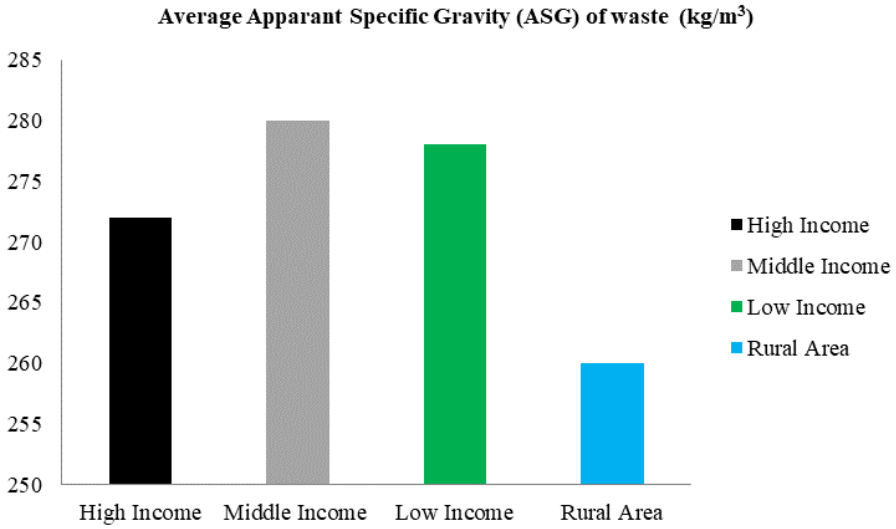

Figure 3. *The average (ASG) (kg/m^3) for residential areas*

Quantification and characterization of MSW generation are obligatory for effective management plan. Geographic area, living standards, food preferences, energy sources, industrial practices, and weather conditions all have an effect on MSW composition (Sahariah et al., 2015). Developing countries MSW contains more organic wastes, while developed countries MSW contains a greater proportion of plastics and paper. The proportion of organic constituents in MSW varies relatively between developed and developing countries like the United States (24%), the European Union (34%), China (67%), Malaysia (55%) and Japan (40%). Organic waste accounted for 60-70% of the total MSW in Indonesia (Sudibyo et al., 2017). Depending on the waste composition, different methods and MSW systems may be considered. Characterizing and classifying MSW for its suitable management requires knowledge of its physical composition. *Table 3* shows a complete list of MSW materials generated by various major cities in developed and developing countries, as classified by the USEPA and EUROSTAT. The important components in MSW produced by major cities in various developing countries do not always conform to the classifications developed by environmental agencies based in the United States and Europe. The composition of MSW generated in most of these cities was found to be dominated by FW and other decomposable materials. Moreover, some slowly decomposable materials like paper, wood, textiles, leather and rubber were reported in all cities, see in *Table 3*.

http://www.aloki.hu ● ISSN 1589 1623 (Print) ● ISSN 1785 0037 (Online)
DOI: http://dx.doi.org/10.15666/aeer/2003_24852507

Table 3. *Average composition of MSW in major cities in developed and developing nations*

S.No.	City/ (Country)	Food waste	Paper	Wood	Textile	Glass	Plastic	Rubber/ Leather	Metal	Others	References
01	Nottingham (UK)	21	32	-	2	9	11	-	8	10	Wang et al. (2018)
02	Mazowieckie (Poland)	38	8	0.04	1	10	8	-	2	6	Baran (2018)
03	Mexico City (Mexico)	28	12	-	-	5	17	-	3	33	Tsydenova et al. (2018)
04	Chengdu (China)	67	9	3	3	-	-	-	-	19	Huang et al. (2015)
05	Kolkata (India)	51	6	1.2	2	0.34	5	0.7	0.2	3	Paul et al. (2019)
06	Terengganu (Malaysia)	12	8	-	-	10	9	-	2	3	Jaafar et al. (2018)
07	Lampang (Thailand)	34	15	-	2	8	24	1	3	2	Outapa and na roiet (2018)
08	Kuala Lumpur (Malayasia)	55	13	1	4	2	19	-	3	3	Bashir et al. (2018)
09	Tehran (Iran)	-	7	-	6	-	6	-	-	-	Dehghanifard and Dehghani (2018)
10	Chittagong (Bangladesh)	21	2	-	4	-	-	1	1	-	Sarkar and Bhuyan (2018)
11	Muscat (Oman)	34	25	2	6	8	16	0.4	3	1	Baawain et al. (2017)
12	Jakarta (Indonesia)	35	11	18	3	14	14	4	4	7	Indrawati and Purwaningrum (2018)
13	Lagos (Nigeria)	10	12	-	3	-	6	-	9	4	Olukanni et al. (2018)
14	Kerbala (Iraq)	57	12	-	-	4	15	-	4	9	Abdulredha et al. (2018)
15	Kumasi (Ghana)	17	21	-	-	-	6	-	2	30	Edjabou et al. (2017)

It was also clear that the composition of MSW differed significantly between big cities and small towns. Organic components, for instance, about 55% of total MSW in Kuala Lumpur, Malaysia, related to 12.2% of total MSW in Terengganu, Malaysia, with a total population of 1.84 and 0.5 million people respectively (Jaafar et al., 2018). MSW in Qatar consisted primarily of organic components (60%) and recyclables (40%) (Rehrah et al., 2016).

FW generation rate, composition and characterization

FW is presently one of the biggest issue in the Kabul city. As explained previously, FW contributes 52.4% of total MSW produced in Kabul city. Hence, the total generation of MSW was 3,200 tons/d; the contribution of FW was 1,677 tons/d. The mean per capita FW production in Kabul city was 0.35 kg/d or 120.10 kg/y. According to Dung et al. (2014) the average FW generation in developing and devolped countries was about 56 and 107 kg/y respectivley obviously showing that the people in Kabul city are producing

http://www.aloki.hu ● ISSN 1589 1623 (Print) ● ISSN 1785 0037 (Online)
DOI: http://dx.doi.org/10.15666/aeer/2003_24852507

FW more than developing and devolped countries. FW was cosist of vegetables at maximum fraction of 35% followed by fruits 30%. Rice waste 20% was mostly produced at resturatnts and high income families. The whole constiuants of FW shows that the FW was mostly organic and thus appropriate for composting purposes.

The mean density of FW was reported 300 kg/m^3, greater than unsegregated waste, which was reported 221 kg/m^3. The mean MC of FW was reported 80% which may possibly generate leachate after dumping in adjecent landfills. Since MC of Kabul city FW was great, thus anaerobic digestion and composting are appropriate to get rid of FW.

Physiochemical properties of MSW

The physiochemical properties of MSW were analyzed for four residential areas. *Figure 4a*,*b*,*c* and *d* show the physical composition of waste for residentail areas includes the maximum quantity of food waste which was 52.4% of the total MSW, followed by paper 20.3% and plastic 17.4% see in *Table 4*. Metals are reported in fewer amounts due to segregation at household level (Batool et al., 2008). The physical composition of MSW in rural areas was changed from urban regions and includes of 36% of FW, followed by soil and stones 23% and wood and grass 12%. Recyclable plastic is less in low and rural areas waste which was associated with socio-economic situation of the region. Non-recyclable plastic and textile waste also reported in great quantity in household waste. The physical composition of wastes from commercial sources such as restaurants generated FW, paper and plastic 60%, 12% and 08% respectively.

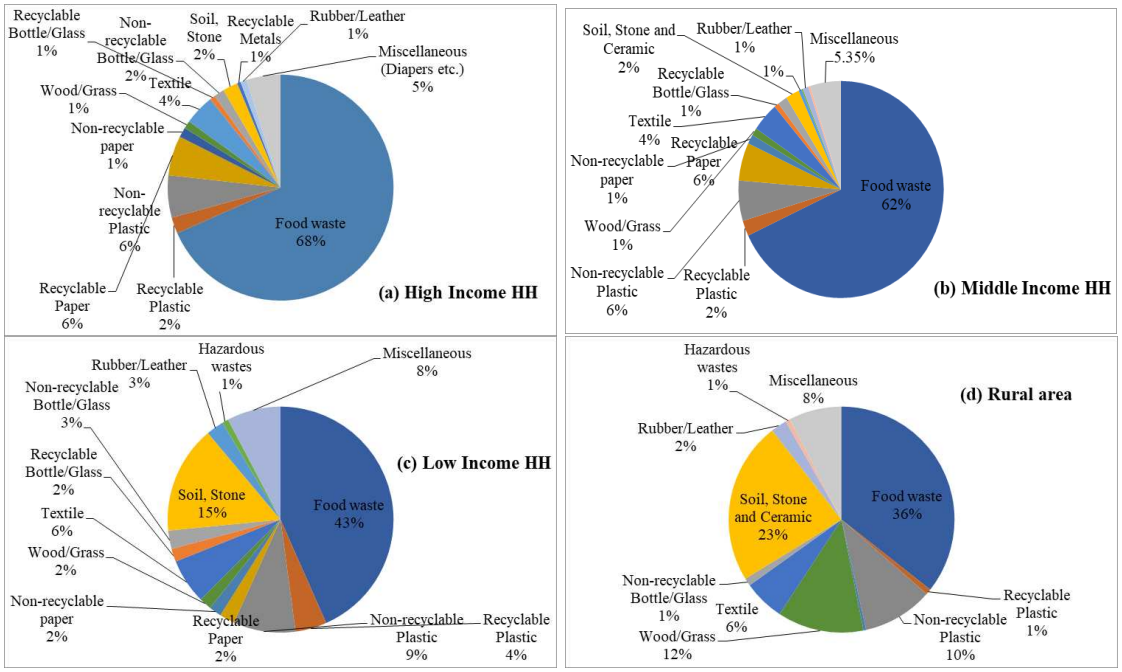

Figure 4. *Physical composition of waste generated from (a) high income household, (b) middle income household, (c) low income household, and (d) rural area*

Waste from commercial markets and shopping centers were mostly contained of FW 48%, followed by paper waste 42%, non-recyclable plastic 30% and wood and grass 25% each.

http://www.aloki.hu ● ISSN 1589 1623 (Print) ● ISSN 1785 0037 (Online)
DOI: http://dx.doi.org/10.15666/aeer/2003_24852507

Table 4. *Average physical composition of waste for residential areas in Kabul city*

S.No.	Physical components	High income areas	Middle income areas	Low income areas	Rural areas
		Average %	Average %	Average %	Average %
01	Food waste	68.02	62.10	43.98	35.5
02	Recyclable Plastic	2.30	2.60	4.56	0.80
03	Non-recyclable Plastic	6.02	6.75	9.02	10.05
04	Recyclable Paper	5.65	6. 03	2.2	0.00
05	Non-recyclable paper	1.40	1.10	1.8	0.38
06	Wood/Grass	1.10	1.50	1.8	12.32
07	Textile	4.32	5.12	6.55	5.85
08	Recyclable Bottle/Glass	0.75	1.80	1.87	0.00
09	Non-recyclable Bottle/Glass	1.50	0.55	2.68	1.10
10	Soil, Stone and Ceramic	2.15	4.75	15.65	23.15
11	Recyclable Metals	0.50	0.20	0.00	0.00
12	Non-recyclable Metals	0.20	0.10	0.42	0.35
13	Rubber/Leather	0.89	1.50	2.55	2.30
14	Hazardous wastes	0.35	0.55	0.92	0.65
15	Miscellaneous (Diapers etc.)	4.85	5.35	7.80	7.55
16	Total	100.00	100.00	100.00	100.00

Offices and institutions waste comprise 40% wood and grass, 28% soil, stones and ceramic and 10% paper waste. While in street sweeping 67% soil, stone and ceramic and 15% wood and grass, however park waste only contain wood and grass about 70% followed by recyclable plastic about 10% and FW 5% due to food stalls in the park area.

The chemical composition analysis of the MSW was carried out for MC, C: N ratio as well as three component analysis. Mean value for MC of the residential regions was reported 64%. The MC for MSW of high, middle, low-income and market areas were reported about 70.2%, 68.4%, 55.8% and 61.3%, respectively as shown in *Figure 5(a)*. The mean value for C: N ratio for MSW was reported to be 120.50. While C: N ratio for MSW of high, middle, low income region and market waste were 140.66, 130.44, 121.58 and 89.32 were observed respectively as given in *Figure 5(b)*.

For the three-component analysis; ash, combustible and moisture content were investigated. MC for MSW of high, middle, low income areas and market areas have detected about 73.2%, 65.5%, 67.6% and 70.2%, respectively as shown in *Figure 5(c)*, while the average value was found to be 69.2% in three component analysis for 100 samples. The mean value of combustible content (V) was detected about 81.8%, with maximum rate of 88.8% for high income region. In middle and low-income areas, (V) was observed to be comparable 80.6% and 81.2%, respectively, however lowest (V) was detected 76.4% in MSW of market areas. Likewise, the mean ash content (A) for the same samples were checked and found to be 14.2%. Maximum (A) is detected for market areas

http://www.aloki.hu ● ISSN 1589 1623 (Print) ● ISSN 1785 0037 (Online)
DOI: http://dx.doi.org/10.15666/aeer/2003_24852507

waste 20.4% and lower most for high income areas 8.3%. The values for (A) waste from middle and low-income areas were reported 13.5-14.6% respectively. *Table 5* shows the physiochemical properties of MSW produced in some big cities in several developing countries.

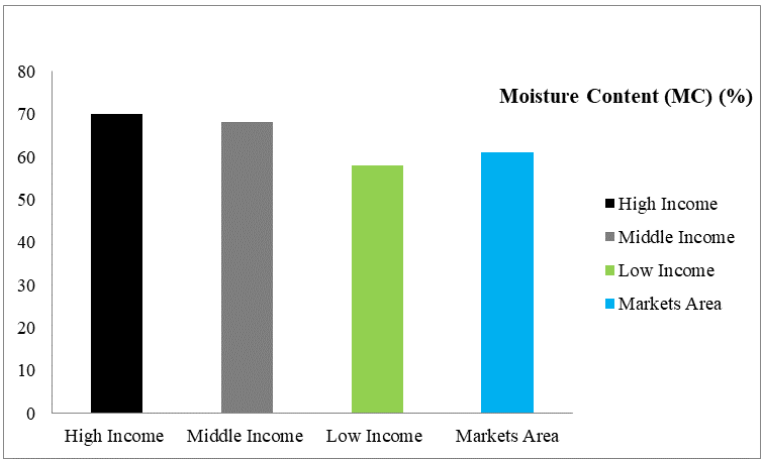

(a)

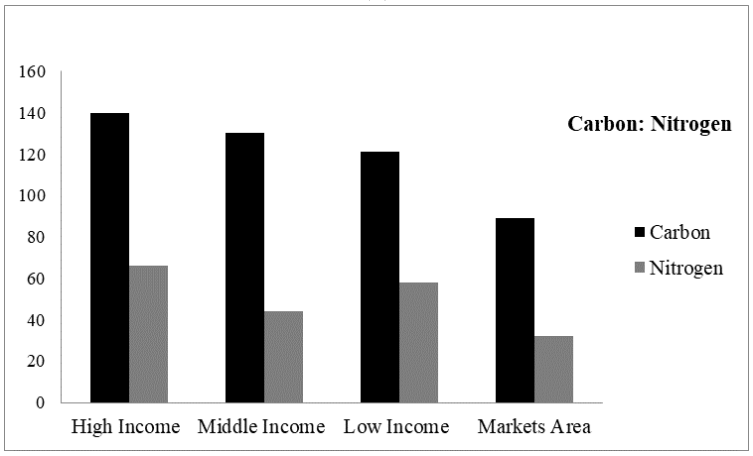

(b)

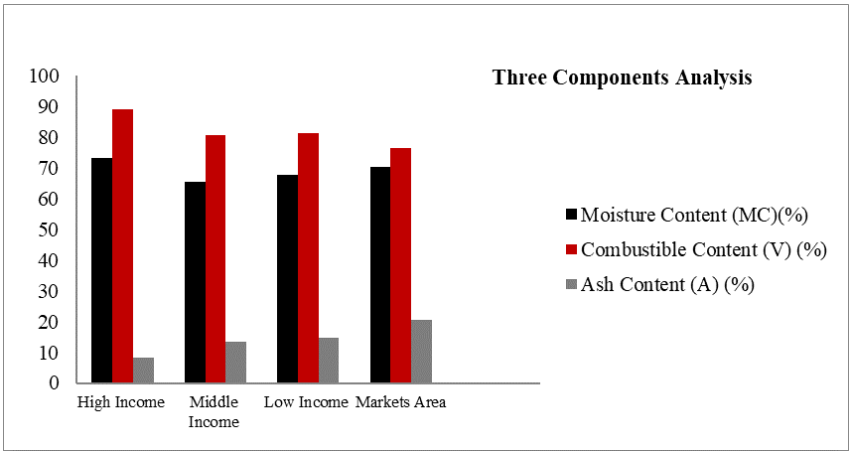

(c)

Figure 5. *(a) Average moisture content (MC) of the waste samples, (b) Average Carbon and Nitrogen (C: N) ratio of solid waste in Kabul city, and (c) Three components analysis of solid waste in Kabul city*

http://www.aloki.hu ● ISSN 1589 1623 (Print) ● ISSN 1785 0037 (Online)
DOI: http://dx.doi.org/10.15666/aeer/2003_24852507

Table 5. *Physiochemical properties of MSW produced by major cities in developing nations (source: Das et al. (2019))*

S.No.	Parameters	Lahore	Dhaka	Numan	Kumasi	Delhi	Kuala Lumpur	Cap-Haïtien	Zanjan	Kolkata
01	pH	-	8.0	-	7.0	8.2	9.1	8.2	5.2	9.01
02	Carbon: Nitrogen (C: N)	44:3	10:1	-	37:1	-	-	31:1	14:1	32:2
03	Ash content (%)	11.7	-	1.50	11.2	5.5	9.3	21.0	6.8	24.0
04	Moisture content (%)	75	-	8.5	51	40	55	56	68	46
05	Organic matter (%)	67	-	-	14	24	-	-	58	-
06	Volatile matter (%)	80	-	-	60	28	32	79	-	-
07	Organic C (%)	-	-	4	-	8.4	-	53	45	22
08	Hydrogen (H) (%)	8.2	-	-	-	1.2	-	-	3.1	2.0
09	Potassium (K) (%)	-	0.6	-	-	0.9	-	1.1	-	0.5
10	Phosphorus (P) (%)	-	0.3	-	-	0.6	-	-	-	0.8
11	Oxygen (O) (%)	27	15	-	9	-	31	-	-	-
12	Total Nitrogen (N) (%)	0.6	0.9	0.04	1.0	0.9	1.3	0.9	-	0.8
13	Fixed carbon (%)	7.2	6.1	-	-	-	-	4.2	-	5.4
14	Sulphur (S) (%)	0.4	-	0.006	-	0.01	0.2	-	0.14	-
15	Lead (Pb) (ppm)	0.8	0.13	-	-	0.04	26	1.1	-	-
16	Zinc (Zn) (ppm)	33.08	0.3	-	-	0.4	-	9.1	-	4.2
17	Cadmium (Cd) (ppm)	1.1	-	-	0.8	0.2	8.8	-	3.9	-
18	Manganese (Mn) (ppm)	0.2	-	-	2.0	1.9	10.3	-	4.9	3.3
19	Mercury (Hg) (%)	0.3	-	-	-	-	1.0	-	-	-
20	Chromium (Cr) (%)	59.1	6.0	-	8.2	1.9	14.4	-	3.0	8.0

MSW collection and transportation in Kabul city

According to Khoshbeen et al. (2020) in the year 2019, there were approximately 4,273 MSW collection bins in the Kabul city. Out of the total MSW bins, 857 are 7 m^3, 1,116 are 1 m^3 and 2,300 are 0.1 m^3 bins. The 0.1 m^3 bins were set up at private points such as walkways, schools, markets, public parks, universities and hospitals etc., to avoid the problems of waste scattering. The information and facts collected from the weighing machine that were installed at Gazak 2 landfill in 2017 revealed that in working days

http://www.aloki.hu ● ISSN 1589 1623 (Print) ● ISSN 1785 0037 (Online)
DOI: http://dx.doi.org/10.15666/aeer/2003_24852507

(Saturday – Thursday) the mean MSW transported to Gazak 2 landfill was about 1,738 tons/d however in weekends (Thursday and Friday) the MSW transported was about 448 tons/d.

The collection efficiency was greatly minor on holidays as associated to working days, as the DoS does not assign period for employees on holidays as well as overtime payment for truck drivers. The DoS had only 477 vehicals in 2018 end and only 384 were active out of the total. Among the active vehicals, 374 were allocated for hygiene purposes though 10 were employed for organizational purposes. In May 2019, 76 new vehicals were added and it is estimated that the MSW transference to Gazak 2 landfill could rise to 2,500 tons/d. Vehicals with volume of 3,218 tons or lesser transported MSW to the handover station however vehicals of greater volume transported MSW to Gazak 2 landfill directly.

Disposal of MSW in Kabul city

For the final disposal of the MSW collected from the whole Kabul city by DoS is transported to Gazak 2 landfill. This Gazak 2 landfill was opened in 2012 for MSW disposal when the other 02 landfills such as (Gazak 1 and Chamtala landfills) were filled. The total area of Gazak 2 landfill is approximately 1, 60, 225 hectares and presently more than half is already filled. All the MSW are dumped collectively in the Gazak 2 landfill and the soil protection is barely obvious at landfill.

This Gazak 2 landfill is worked like a dumpsite, where the total MSW thrown openly neither dumped with soil cover or any proper compaction on daily basis. This MSW contain more MC hence leachate generated and enters to the ground water while the greenhouse gases are released into the air due to lack of treatment method. However, no communities close to landfill site up to 1 km range, the people living outside have been complaining about the bad odor, and other soical problems. With that the dumped leftover frequently catches fire, particularly in winter period, producing great quantity of smoke.

Current management practices of MSW in Kabul city

Recycling of MSW

The native scavengers in Kabul city including children, old men and drug addicts collected the MSW around the city. All these scavengers have personal two, three, or four-wheel carts to gather MSW. DoS predict that there could be about 2,250 to 2,750 scavengers in the Kabul city gathering approximately 215 to 320 tons of MSW/day that is about 9 to 12% of total MSW produced in the city. When the FW (Dry bread) is collected and vended to livestock farm. Even although this might aid to decrease the possibilities of FW stored in the landfill but it frequently causes health problems in the livestock (Leib et al., 2016). Recyclable MSW such as glass bottles, paper, plastic and aluminum can etc., are vended by these scavengers to the private recycling services natively called Kabar Khana (shops that purchase waste and recompense them with money). Previous studies reveals that that if FW, paper waste, HDPE and PET bottles, glass bottles and aluminum cans are vended on regular basis to the recycling services instead of transferring to landfill sites, it might generate an expected profit of around USD 182,590/day (Khoshbeen et al., 2020).

A well planned implementation of 3R's technique of MSW turn into a responsibility via education, awareness, training and practice for better MSWM and cleaner environment (Azimi Jibril et al., 2012). This 3R's approach are introduced to achieve

http://www.aloki.hu ● ISSN 1589 1623 (Print) ● ISSN 1785 0037 (Online)
DOI: http://dx.doi.org/10.15666/aeer/2003_24852507

synergistic effects with national polices and laws which aim control of GHG emissions, resources procurement and landfill prevention (Sakai et al., 2011). Hence, it is vital that a proper MSWM strategy for Kabul city should be focused on 3R's methods. Therefore, the current study suggested that the 3R's methods must be selected over the traditional method of collection, management and disposal.

Hospital waste management

According to previous studies about SWM in study area there was no perfect checking of hospital waste dumping both by DoS and by the Ministry of Public Health (MoPH). Maximum of the government hospitals used burners to burn all the hospital waste that is produced. While, the waste generated from private hospitals have managed by a private service named Kamyab Waste Management Services. More than five private hospitals were monitored and all of them confirmed that they refer their hospital waste to the private company for management. Though, it was also found via the survey that great quantity of hospital waste was mixed with MSW in the containers. It shows that private hospitals are transferring their hospital waste combine with MSW into the communal bins in Kabul city.

Construction and destruction waste

The fast-developmental growth in study area causing a rapid rise in the construction and demolition (C&D) waste. Till date no appropriate controlling of such type of wastes. The parts of steel bars are vended to industries where these parts are recycled. The timber waste that is usually not recyclable is vended to local people for heating and cooking purposes in winter period. The brick, stone and soil waste are recycled for houses filling. If not applied for filling purposes, then the construction companies pay to truck drivers for the removal afar from the Kabul city. Truck drivers move this C&D waste to the rural regions and used in the flood ways to safeguard farming land from flood disasters. But this method was not applied by wholly construction companies. Usually, this waste is discarded into the communal bins for final disposal or goes to drainage system. The soil and stone that go into the near streams and canals blocks the flow of water in heavy rainfalls and thus causes urban floods in Kabul city.

Role of private companies & public in MSWM

There are various private facilities in the Kabul city that offer Households (HH) waste collection facilities. In the current study, some of these companies were visited to evaluate their MSWM system. These facilities regularly collect waste from HH and get money in back. The selected companies that were visited charge about 100-200 AFN/month each HH. These facilities adopted Door-to-door collection approach for waste collection. Presently, around 51,347 HH are offered with this approach. Out of the total 52,570 HH, approximately 27,585 HH, 52.47%, 9,700 HH 18.45% and 5, 987 HH 11.38% willingly pays 100, 150 and 200 AFN/month respectively for Door-to-door collection facility.

Residents' willingness to pay

The MSW operations and management expenses are currently covered by the central government national treasury. For the MSWM, the DoS also receives international grants and loans. One of the most critical requirements for a well-developed SWM system is cost recovery. A cost recovery method has several phases, but the first and most important

http://www.aloki.hu ● ISSN 1589 1623 (Print) ● ISSN 1785 0037 (Online)
DOI: http://dx.doi.org/10.15666/aeer/2003_24852507

is determining the overall system's actual cost. *Table 6* shows the overall cost analysis of the present SWM scheme in the Kabul city.

Table 6. *Cost of different components in SWM of Kabul city*

Amount of MSW	Component	Cost in AFN	Cost in USD
For 1,850 tons of MSW that is presently collected	Collection and transfer cost/ton	700	8.93
	Disposal cost/ton	15	0.19
	Additional cost/ton	550	7.02
	Total cost/ton	1265	16.14
	Total cost/ton/month	70.20 million	0.90 million
	Total cost/ton/year	842.40 million	10.75 million
For 100 % collection efficacy (3,200 tons of MSW)	Total cost/ton/month	121.44 million	1.55 million
	Total cost/ton/year	1457.28 million	18.59 million

For the calculation of per ton collection and transferring expense, the cost of fuel consumed by vehicles that collect and transfer waste from collection points, as well as the wages of sanitation workers who were directly involved in waste collection and transportation, were taken into account.

The cost of fuel consumed by disposal site vehicles such as excavators and compactors, as well as the wages of sanitation staff (disposal officers, workers, guards, and so on) is factored into the per ton disposal cost estimate. The cost of fuel consumed by administrative vehicles, the wages of sanitation staffs engaged in administrative work, and the extra costs incurred from GPS, power bills, spare parts, repairs, hydraulics, and other factors were taken into account.

The cost of transporting one ton of waste is 1,265 AFN, as shown in *Table 6*. The overall transfer cost is 70.20 million AFN because only 1,850 tons of waste are collected and transferred each month. The overall monthly cost of transferring the waste produced, which is 3,200 tons per day, rises to 121.44 million AFN, with a per year cost of 1457.28 million AFN. People's willingness to pay for services was examined. Municipalities should impose a tax on solid waste collection in Kabul city.

On the application of the levy, 80% and 20% (920 and 230 respondents) were agreed and disagreed respectively, while high-income HH said they were willing to pay more than 200 AFN.

The lower ranges, 50-100 AFN and 100-150 AFN, were mostly chosen by low-income households, while the higher ranges, 150-200 AFN and more than 200 AFN, were mostly chosen by high-income, middle-income, and commercial units, as shown in *Figure 6*.

MSWM plan for Kabul city

All the major issues and challenges regarding to MSWM in study area were noted in this current study. Various risks to local public, climate, aesthetics values and environment, and thus demand for a proper MSWM strategy to effectively control the MSW of the Kabul city. The main aim of this MSWM strategy is the preparation and operation of a safe, sound and sustainable MSWM system to change the Kabul city in to a smart and clean city.

http://www.aloki.hu ● ISSN 1589 1623 (Print) ● ISSN 1785 0037 (Online)
DOI: http://dx.doi.org/10.15666/aeer/2003_24852507

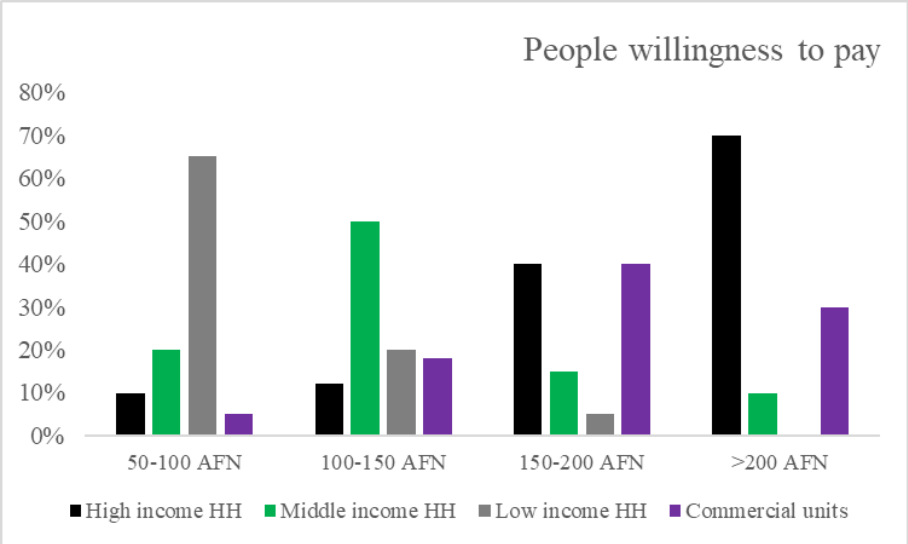

Figure 6. *People willingness to pay for SW collection in Kabul city*

Proper awareness programs

Unawareness and absence of environmental interests leads to the failure of MSWM strategies in South Asia countries (Visvanathan et al., 2003). A proper awareness program should be planned and focus on social changes of residents to suitable MSWM practices like reduction of waste, separation of waste at household level, not burning or scattering waste onto roads and sewage, willingness to pay for collection services and finally implementation of 3R's approach. Hospitals should separate their wastes in to three (03) types such as hazardous, wet and dry wastes. Door-to-door collection facility will improve collection and recycling efficacy, as well as generate revenue. DoS must monitor MSWM services at district level. Scavengers must be listed and observable. For better capacity building proper trainings and seminar sessions must be organized at regular intervals of time in Kabul city.

Implementation of 3R's approach

The principle of waste minimization reduces the quantity and negative consequences of waste generation by decreasing waste volume, reusing waste products with easy treatments, and recycling wastes by using them as tools to generate the same or changed products (Obi et al., 2016).This approach commonly called the '3R's'process. Some waste materials may be used as tools for the manufacture of other goods or the same product, implying that the same resource can be recycled. This decreases the waste production and reduces the exploitation of fresh resources.

Overall, the 3R's method save new resource utilization and exploitation, bring value to resources that have already been used, and, most significantly, reduce waste quantity and its negative effects individually and collectively. The 3R's theory seeks to achieve effective waste minimization by reducing waste, reusing and recycling waste products and resources by: (a) to minimize the amount of waste produced, choose to use products with care. (b) usage of substances or parts of substances that are still available on a regular basis. (c) using waste as a resource itself.

http://www.aloki.hu ● ISSN 1589 1623 (Print) ● ISSN 1785 0037 (Online)
DOI: http://dx.doi.org/10.15666/aeer/2003_24852507

3R's obstacles and constraints

However, there are several limitations and barriers that produce problems in the implementation of 3R's approach. From survey it was reported that the household's willingness to contribute in 3R's approach was comparatively low and need much improvement. High cost for the transportation limited the recycling and reusing rate of recycled and reused materials in the Kabul city. Local people are unaware of which materials might be reuse, or recycled and which might be vended to scavengers. Demand for these materials is also low in market places and thus leads to the limitation of 3R's approach. Absence of specialists to run and sustain the recycling technologies is also a major concern and no one ready to invest in large recycling technologies. A total 500 households were interviewed for this purpose, and out of the total 70% claimed that they are known of this 3R's programs while 30% claimed that they are unaware of the 3R's approach. This shows a good sign for the adaptation of 3R's approach because most of households are known of the profits of 3R's programs and only few numbers of households need to adopt this approach.

Therefore, DoS need to take some proper steps for 3R's approach. The usage of cloth or paper bags should be prioritized over plastic bags in the markets and local shops. Number of waste collection bins should be increased to a larger number around the city to overcome the MSW issues. DoS must conduct awareness campaigns in the Kabul city to aware the households about wet and dry MSW separation. DoS need to install the GPS system in all running vehicles to monitor the landfill routes and to resolve the fuel stealing problems. As well as, suitable MSWM practices should be initiated to overcome the scattering of MSW by residents along roadsides and canals to control urban floods. Hospital waste and C&D waste should be dumped separately from other waste and MSW must be disposed suitably in to communal containers at each collection points. Burning of MSW should be banned in Kabul city to avoid the issues of air pollution.

Policy enhancement and implementation for SWM in Kabul city

The amount of MSW produced in urban regions of developing countries is low as compared to developed countries though, the system of MSWM is not good and sustainable. Problems includes lack of appropriate policies, encouraging regulations, insufficient collection facilities, open dumping without any treatment and open burning of MSW are at the major roots of waste management issues (Khajuria et al., 2008; Manaf et al., 2009). The above-mentioned problems have been reported in various under and developing counties such as: Asia (Agamuthu et al., 2009), Afghanistan (Haidaree and Lukumwena, 2017), Bangladesh (Shams et al., 2017), Cameroon (Manga et al., 2008), Kenya (Henry et al., 2006), Malaysia (Manaf et al., 2009), Pakistan (Batool et al., 2008), Palestinian (Al-Khatib et al., 2007) and South Africa (Simatele et al., 2017).

Mostly Asian and developing countries have applied laws and policies cover MSWM but their function showed to be unreliable and insufficient, such as Afghanistan (Khoshbeen et al., 2020), Bangladesh (Shams et al., 2017), Cameroon (Manga et al., 2008), Kenya (Henry et al., 2006), Pakistan (Ilyas et al., 2017) and South Africa (Simatele et al., 2017). These laws and policies covering a series of works and efforts to take improvements for human health and environmental sustainability. However, even with the approved quality and significance, the regulations implementation still doesn't ensure the enhancements in MSWM. To guarantee all these objectives of MSWM laws and policies are have been attained, now it is compulsory to observe and monitor its outcomes

http://www.aloki.hu ● ISSN 1589 1623 (Print) ● ISSN 1785 0037 (Online)
DOI: http://dx.doi.org/10.15666/aeer/2003_24852507

to find out the requirements for other significant management involvements. Like other laws and policies, same these policies should be evaluated and enhanced through the object of achievement and appropriate standards and measures (Crabbe and Leroy, 2008).

National Environmental Protection Agency (NEPA) of Afghanistan made the law and policy of waste management of Afghanistan in 2010. Since 2010 no improvements have been made in that law which required important modifications. There should be a separate law and policy for plastic bags. The ban of plastic bags must be extended from bread shops to stores and pharmacies and finally to market places. With that, efforts are required to be applied to avoid the MSW imported from another nation. The disposing of hospital waste and C&D waste together with MSW must be banned strictly and persons who not obeying must be charged. Scattering of such type of wastes onto roadsides or sewage must be banned immediately. All those construction companies who's produce C&D waste of >20-25 tons/day or 300-350 tons/project/month must to submit a MSWM plan and to get proper approvals from local government authorities before starting of work. Moreover, MSWM laws and policies should be regularly improved through outputs (policies, plans, programs and capitals) and outcomes efficiency evaluations. Through this method, targets might be recognized and updated rules and instruments such as reduce, reuse and recycle (3R's) waste to energy (WTE), waste disposition charge (WDC) and extended producer responsibility (EPR) principle might be adopted.

Composting method for MSW in Kabul city

Composting is basically a method that is done by a series of microbes related with several decomposition methods (López-González et al., 2015). Switching organic waste of MSW from landfills to composting has several environmental values. Amongst them, reduction of greenhouse gases from landfills and enhancement of soil quality via composting method have been reported (Bernstad et al., 2016). The efficiency of the composting method is mainly affected by some factors like oxygen (O_2) amount, temperature, MC, pH, C: N, compaction and particle size (Li et al., 2013). Suitable O_2 amount is the significant factor to be count in composting method; hence, aeration is significant. The effectiveness of this method is greatly influenced by O_2 amount as this method is completely linked with bacterial population (Nakasaki and Hirai, 2017).

Luckily, the MSW of Kabul city is mainly consisting of approximately more than 70% of organic waste mainly consist of food waste, paper and wood and grass which is compostable, hence, composting turns out to be a significant part of the MSWM strategy. Meanwhile aerobic composting is efficient, easy to use and cost-effective method as compared to anaerobic composting, however, the suitable option of MSW composting in Kabul city might be aerobic composting. The Gazak 2 landfill which is currently operative must be improved in to a sanitary landfill. If the government of Afghanistan implements MSWM strategy, about 5-11% (125–300 tons/day) of the total waste, mostly non-recyclable waste, will be ends up into Gazak 2 landfill related to the present condition in which approximately more than 85% of the MSW is openly dumped in the Gazak 2 landfill.

Conclusion

Solid waste sources, generation rate, physiochemical properties and its management practices in Kabul city had revealed some interesting results. The average household size in Kabul city was seven (07). MSW generation rate ranged from 0.28±0.10 kg/c/d for

http://www.aloki.hu ● ISSN 1589 1623 (Print) ● ISSN 1785 0037 (Online)
DOI: http://dx.doi.org/10.15666/aeer/2003_24852507

low-income or rural areas to 0.48±0.10 kg/c/d for high-income in residential areas. Also, waste generation rate from commercial sources reported as 12.2 kg/d, 8.4 kg/d, 5.3 kg/d, 2.5 kg/d and 1.8 kg/d for restaurants/hotels, parks, institutions, shops and street sweeping respectively. Results revealed that ASG of MSW from four (04) residential areas reported as 272 kg/m^3, 280 kg/m^3, 278 kg/m^3 and 260 kg/m^3 for high, middle, low-income areas and rural areas respectively, however, commercial MSW from hotels/restaurants have a peak value of ASG of about 550 kg/m^3. The average value for MC, C:N ratio, combustible and ash content were reported to be 64%, 120.50%, 81.8% and 14.2%, respectively. This study shows that MSW generated from the Kabul city has maximum possibility for composting because >70% of the MSW was consist of organic wastes. Moreover, there is no proper management of MSW in Kabul city, hence, it is important that a proper MSWM strategy for Kabul city should be focused on 3R's approach. Therefore, the current study suggested that the Kabul city must take initiatives such as awareness programs, policy enhancement and implementation, composting method and 3R's approach must be selected over the traditional method of solid waste management in Kabul city and other growing cities around the country.

Conflict of interests. The authors declare no conflict of interests.

Funding. The authors received no financial support for the research, authorship or publication of this article.

REFERENCES

[1] Abdulredha, M., Kot, P., Alkhaddar, R., Jordan, D., Abdulridha, A. (2018): Investigating Municipal Solid Waste Management System Performance during the Arba'een Event in the City of Kerbala, Iraq. – Environment, Development and Sustainability 22: 1431-1454. https://doi.org/10.1007/s10668-018-0256-2.

[2] Agamuthu, P., Khidzir, K. M., Hamid, F. S. (2009): Drivers of sustainable waste management in Asia. – Waste Manag. Res. 27: 625-633. https://doi.org/10.1177/0734242X09103191.

[3] Al-Khatib, I. A., Arafat, H. A., Basheer, T., Shawahneh, H., Salahat, A., Eid, J., Ali, W. (2007): Trends and problems of solid waste management in developing countries: a case study in seven Palestinian districts. – Waste Manag. 27: 1910-1919. https://doi.org/10.1016/j.asman.2006.11.006.

[4] Ali, M., Wang, W., Chaudhry, N. (2016): Management of wastes from hospitals: A case study in Pakistan. – Waste Management & Research 34(1): 87-90.

[5] ASTM Committee D-34 on Waste Management (2008): Standard test method for determination of the composition of unprocessed municipal solid waste. – ASTM International.

[6] Azimi Jibril, J. D., Sipan, I. B., Sapri, M., Shika, S. A., Isa, M., Abdullah, S. (2012): 3R's critical success factor in solid waste management system for higher educational institutions. – Procedia-Social and Behavioral Sciences 65: 626-631.

[7] Baawain, M., Al-Mamun, A., Omidvarborna, H., Al-Amri, W. (2017): Ultimate composition analysis of municipal solid waste in Muscat. – J. Clean. Prod. 148: 355-362. https://doi.org/10.1016/j.jclepro.2017.02.013.

[8] Baran, J. (2018): Municipal Waste Management in Rural Areas in Poland. – https://doi.org/10.22616/ESRD.2018.113.

http://www.aloki.hu ● ISSN 1589 1623 (Print) ● ISSN 1785 0037 (Online)
DOI: http://dx.doi.org/10.15666/aeer/2003_24852507

[9] Bashir, M., Tao, G., Abu, S., Amr, T. (2018): Public concerns and behaviors towards solid waste minimization using composting in Kampar district, Malaysia. – Global NEST J. 20: 316-323.
[10] Batool, S. A., Chaudhry, N., Majeed, K. (2008): Economic potential of recycling business in Lahore, Pakistan. – Waste Management 28(2): 294-298.
[11] Bernstad, A., Wenzel, H., la Cour Jansen, J. (2016): Identification of decisive factors for greenhouse gas emissions in comparative life cycle assessments of food waste management – An analytical review. – Journal of Cleaner Production 119: 13-24.
[12] Central Statistic Organization (CSO) (2018): Analysis of population projections 2017-18. – Available at: http://cso.gov.af/en/page/demography-and-socile-statistics/demograph-statistics/3897111. Accessed on May 2019.
[13] Ciuta, S., Apostol, T., Rusu, V. (2015): Urban and rural MSW stream characterization for separate collection improvement. – Sustainability 7(1): 916-931.
[14] Crabbe, A., Leroy, P. (2008): The Handbook of Environmental Policy Evaluation. – Earthscan, London, 202p.
[15] Das, S., Lee, S. H., Kumar, P., Kim, K. H., Lee, S. S., Bhattacharya, S. S. (2019): Solid waste management: Scope and the challenge of sustainability. – Journal of cleaner production 228: 658-678.
[16] Dehghanifard, E., Dehghani, M. H. (2018): Evaluation and Analysis of Municipal Solid Wastes in Tehran, Iran. – MethodsX 5: 312-321. https://doi.org/10.1016/j.mex.2018.04.003.
[17] Di Maria, F., Sordi, A., Micale, C. (2013): Experimental and life cycle assessment analysis of gas emission from mechanically–biologically pretreated waste in a landfill with energy recovery. – Waste Management 33(11): 2557-2567.
[18] Di Maria, F., Micale, C., Morettini, E., Sisani, L., Damiano, R. (2015): Improvement of the management of residual waste in areas without thermal treatment facilities: A life cycle analysis of an Italian management district. – Waste management 44: 206-215.
[19] Dung, T. N. B., Sen, B., Chen, C. C., Kumar, G., Lin, C. Y. (2014): Food waste to bioenergy via anaerobic processes. – Energy Procedia 61: 307-312.
[20] Edjabou, M. E., Martín-Fernandez, J. A., Scheutz, C., Astrup, T. F. (2017): Statistical analysis of solid waste composition data: arithmetic mean, standard deviation and correlation coefficients. – Waste Manag. 69: 13-23. https://doi.org/10.1016/j. wasman.2017.08.036.
[21] Ghaforzai, A., Ullah, S., Asir, M. (2021): Household waste management in formal housing developments in Afghanistan: a case study of Kabul city. – Aust. J. Eng. Innov. Technol. 3(4): 64-72. https://doi.org/10.34104/ajeit.021.064072.
[22] Haidaree, G. H., Lukumwena, N. (2017): Solid waste management challenges and possible solution in Kabul city. – Int J Environ Chem Ecol Geol Geophys Eng 11: 262-266.
[23] Henry, R. K., Yongsheng, Z., Jun, D. (2006): Municipal solid waste management challenges in developing countries: kenyan case study. – Waste Manag. 26: 92-100. https://doi.org/10.1016/j.wasman.2005.03.007.
[24] Hidayat, O., Kajita, Y. (2020): Influences of Culture in the Built Environment; Assessing Living Convenience in Kabul City. – Urban Science 4(3): 44.
[25] Huang, H., Singh, V., Qureshi, N. (2015): Butanol production from food waste: a novel process for producing sustainable energy and reducing environmental pollution. – Biotechnol. Biofuels 8: 147. https://doi.org/10.1186/s13068-015-0332-x.
[26] Ilyas, H., Ilyas, S., Ahmad, S. R., Nawaz, M. (2017): Waste generation rate and composition analysis of solid waste in Gujranwala city, Pakistan. – Int. J. Waste Resour 7(3): 97.
[27] Indrawati, D., Purwaningrum, P. (2018): Identification and analysis the illegal dumping spot of solid waste at Ciliwung segment 5 riverbanks. – IOP Conf. Ser. Earth Environ. Sci. 106: 012043.

http://www.aloki.hu ● ISSN 1589 1623 (Print) ● ISSN 1785 0037 (Online)
DOI: http://dx.doi.org/10.15666/aeer/2003_24852507

[28] Jaafar, I., Ibrahim, T., Awanis Ahmad, N., Abdul Kadir, K., Tomari, R. (2018): Waste Generation and Characteristization: Case Study of Seberang Takir. Kuala Nerus, Terengganu, Malaysia. – Journal of Physics 1049: 012029. https://doi.org/10.1088/1742-6596/1049/1/012029.
[29] Kaza, S., Yao, L., Bhada-Tata, P., Van Woerden, F. (2018): What a waste 2.0: a global snapshot of solid waste management to 2050. – World Bank Publications.
[30] Khajuria, A., Yamamoto, Y., Morioka, T. (2008): Solid waste management in Asian countries: Problems and 531 issues. – WIT Trans Ecol Environ 109: 643-653.
[31] Khoshbeen, A. R., Logan, M., Visvanathan, C. (2020): Integrated solid-waste management for Kabul city, Afghanistan. – Journal of Material Cycles and Waste Management 22(1): 240-253.
[32] Kumar, S., Smith, S. R., Fowler, G., Velis, C., Kumar, S. J., Arya, S., Rena, Kumar, R., Cheeseman, C. (2017): Challenges and opportunities associated with waste management in India. – Royal Society open science 4(3): 160764.
[33] Leib, E., Balkus, O., Rice, C., Maley, M., Taneja, R., Cheng, R., Civita, N., Alvoid, T. (2016): Leftovers for livestock: a legal guide for using food scraps as animal feed. – FLPC, in partnership with the Food Recovery Project.
[34] Li, Z., Lu, H., Ren, L., He, L. (2013): Experimental and modeling approaches for food waste composting: A review. – Chemosphere 93(7): 1247-1257.
[35] López-González, J., Vargas-García, M., López, M., Suárez-Estrella, F., Jurado, M., Moreno, J. (2015): Biodiversity and succession of mycobiota associated to agricultural lignocellulosic waste-based composting. – Bioresource Technology 187: 305-313.
[36] Mack, T. J. (2018): Groundwater Availability in the Kabul Basin, Afghanistan. – In: Groundwater of South Asia, Springer, Singapore, pp. 23-35.
[37] Mack, T. J., Chornack, M. P., Taher, M. R. (2013): Groundwater-level trends and implications for sustainable water use in the Kabul Basin, Afghanistan. – Environment Systems and Decisions 33(3): 457-467.
[38] Manaf, L. A., Samah, M. A. A., Zukki, N. I. M. (2009): Municipal solid waste management in Malaysia: practices and challenges. – Waste Manag. 29: 2902-2906. https:// doi.org/10.1016/j.wasman.2008.07.015.
[39] Manga, V. E., Forton, O. T., Read, A. D. (2008): Waste management in Cameroon: a new policy perspective? – Resour. Conserv. Recycl. 52: 592-600. https://doi.org/10. 1016/j.resconrec.2007.07.003.
[40] Marashlian, N., El-Fadel, M. (2005): The effect of food waste disposers on municipal waste and wastewater management. – Waste management & research 23(1): 20-31.
[41] Murtaza, G., Rahman, A. (2000): Solid waste management in Khulana City and a case study of a CBO: Amader Paribartan. – Maqsood Sinha, A. H. Md., Enayetullah, I. (eds.) Community Based Solid Waste Management: The Asian Experience. Waste Concern, Dhaka, Bangladesh.
[42] Nadeem, K., Farhan, K., Ilyas, H. (2016): Waste amount survey and physio-chemical analysis of municipal solid waste generated in Gujranwala-Pakistan. – International Journal of Waste Resources 6: 196.
[43] Nakasaki, K., Hirai, H. (2017): Temperature control strategy to enhance the activity of yeast inoculated into compost raw material for accelerated composting. – Waste Management 65: 29-36. Available on-line: doi: 10.1016/j.wasman.2017.04.019.
[44] Obi, F. O., Ugwuishiwu, B. O., Nwakaire, J. N. (2016): Agricultural waste concept, generation, utilization and management. – Nigerian Journal of Technology 35(4): 957-964.
[45] Olsen, S., Sommers, L., Page, A. (1982): Methods of soil analysis, Part 2. – Soil Science Society of America, Inc., pp. 403-430.
[46] Olukanni, D., Aipoh, A., Kalabo, I. (2018): Recycling and Reuse Technology: Waste to Wealth Initiative in a Private Tertiary Institution, Nigeria. – Recycling 3(3): 44. https://doi.org/10.3390/recycling3030044.

http://www.aloki.hu ● ISSN 1589 1623 (Print) ● ISSN 1785 0037 (Online)
DOI: http://dx.doi.org/10.15666/aeer/2003_24852507

[47] Outapa, P., Na Roiet, V. (2018): Evaluation of greenhouse gas emissions from municipal solid waste (MSW) management: case study of Lampang municipality, Thailand. – Appl. Environ. Res. 40: 46-56.
[48] Ozcan, H. K., Guvenc, S. Y., Guvenc, L., Demir, G. (2016): Municipal solid waste characterization according to different income levels: A case study. – Sustainability 8(10): 1044.
[49] Paul, K., Chattopadhyay, S., Dutta, A., Krishna, A. P., Ray, S. (2019): A comprehensive optimization model for integrated solid waste management system: a case study. – Environ. Eng. Res. 24: 220-237. https://doi.org/10.4491/eer.2018.132.
[50] Prism, G., 5.0. GraphPad Software Inc., San Diego, CA, USA.
[51] Rehrah, D., Bansode, R. R., Hassan, O., Ahmedna, M. (2016): Physico-chemical characterization of biochars from solid municipal waste for use in soil amendment. – J. Anal. Appl. Pyrolysis 118: 42-53. https://doi.org/10.1016/j.jaap.2015.12.022.
[52] Sahariah, B., Goswami, L., Farooqui, I. U., Raul, P., Bhattacharyya, P., Bhattacharya, S. (2015): Solubility, hydrogeochemical impact, and health assessment of toxic metals in municipal wastes of two differently populated cities. – J. Geochem. Explor. 157: 100-109. https://doi.org/10.1016/j.gexplo.2015.06.003.
[53] Sakai, S. I., Yoshida, H., Hirai, Y., Asari, M., Takigami, H., Takahashi, S., Tomoda, K., Peeler, M. V., Wejchert, J., Schmid-Unterseh, T., Douvan, A. R. (2011): International comparative study of 3R's and waste management policy developments. – Journal of Material Cycles and Waste Management 13(2): 86-102.
[54] Sandulescu, E. (2004): The contribution of waste management to the reduction of greenhouse gas emissions with applications in the city of Bucharest. – Waste Management & Research 22(6): 413-426.
[55] Sarkar, M., Bhuyan, M. (2018): Analysis of physical and chemical composition of the solid waste in Chittagong city. – Jr. Ind. Poll. Control 34: 1984-1990.
[56] Shams, S., Sahu, J. N., Rahman, S. M. S., Ahsan, A. (2017): Sustainable waste management policy in Bangladesh for reduction of greenhouse gases. – Sustain. Citie. Soc. 33: 18-26. https://doi.org/10.1016/j.scs.2017.05.008.
[57] Simatele, D. M., Dlamini, S., Kubanza, N. S. (2017): From informality to formality: perspectives on the challenges of integrating solid waste management into the urban development and planning policy in Johannesburg, South Africa. – Habitat Int. 63: 122-130. https://doi.org/10.1016/j.habitatint.2017.03.018.
[58] Sudibyo, H., Majid, A. I., Pradana, Y. S., Budhijanto, W., Deendarlianto, Budiman, A. (2017): Technological evaluation of municipal solid waste management system in Indonesia. – Energy Procedia 105: 263-269. https://doi.org/10.1016/j.egypro.2017.03.312.
[59] Suthar, S., Singh, P. (2015): Household solid waste generation and composition in different family size and socio-economic groups: A case study. – Sustainable Cities and Society 14: 56-63.
[60] Tsydenova, N., Vazquez Morillas, A., Cruz Salas, A. A. (2018): Sustainability assessment of waste management system for Mexico City (Mexico) based on analytic hierarchy process. – Recycling 3: 45. https://doi.org/10.3390/recycling3030045.
[61] Visvanathan, C., Trankler, J. (2003): Municipal Solid Waste Management in Asia: A Comparative Analysis. – Presented at the National Workshop on Sustainable Solid Waste Landfill Management in Asia, Bangkok, Thailand.
[62] Wang, D., He, J., Tang, Y.-T., Higgitt, D. (2018): The EU Landfill Directive Drove the Transition of Sustainable Municipal Solid Waste Management in Nottingham City, UK. – 7th International Symposium on Energy from Biomass and Waste, Venice.
[63] Worrell, W., Vesilind, P. (2011): Solid Waste Engineering. – SI Version. Nelson Education.

http://www.aloki.hu ● ISSN 1589 1623 (Print) ● ISSN 1785 0037 (Online)
DOI: http://dx.doi.org/10.15666/aeer/2003_24852507

AEROBIC COMPOSTING OF OIL PALM FRONDS – A REVIEW

SABIANI, N. H. M. – AWANG, N.*

School of Civil Engineering, Universiti Sains Malaysia, 14300 Nibong Tebal, Pulau Pinang, Malaysia

**Corresponding author*
e-mail: cenikazimatol@usm.my; phone: +60-45-996-290; fax: +60-45-996-906

(Received 5th Dec 2021; accepted 21st Mar 2022)

Abstract. The palm oil industry is a major agricultural industry in Malaysia and is also one of the major suppliers of palm oil in the world. The growth of this industry has also increased the quantity of waste generated. Lignocellulosic biomass produced from the palm oil industry, such as oil palm fronds (OPF), oil palm trunks (OPT), mesocarp fibers (MF), palm kernel shells (PKS), and palm oil mill effluent (POME), can affect air, water, soil, and environmental ecosystems. Of the total biomass waste generated, OPF is generated at a higher rate than others. Therefore, composting is the most viable treatment for reusing and recycling OPF, an environmentally friendly treatment that provides economic potential. This review focuses on OPF composting studies and provides important insights into the possible use of this waste as an alternative approach to treat biomass produced by the palm oil industry and resolve pollution issues in the environment. Furthermore, this review covers the use of inoculum in the composting process, including white-rot fungi (WRF), sewage sludge, palm oil mill effluent (POME), and thickened POME anaerobic sludge for rapid decomposition of lignocellulose OPF while exploring the effects of composting on the environment.
Keywords: *lignocellulosic biomass, OPF compost, white-rot fungi, palm oil mill effluent sludge, lignocellulolytic microorganisms, lignin degradation*

Abbreviations: OPF: oil palm fronds, OPT: oil palm trunks, MF: mesocarp fibers, PKS: palm kernel shells, POME: palm oil mill effluent, WRF: white-rot fungi, WWF: World Wildlife Fund, GHG: greenhouse gas, EFB: empty fruit bunches, MPOB: Malaysia Palm Oil Board, AIM: Agensi Inovasi Malaysia, EM: effective microbe, VOCs: volatile organic compounds, PF: phenol formaldehyde, OLPG: organosolv lignin phenol glyoxal, COD: chemical oxygen demand, BOD: biochemical oxygen demand, TSS: total suspended solids, RH: relative humidity, AKD: alkyl ketene dimer, OCC: old corrugated container, CM: chicken manure, RB: rice bran, N: nitrogen, P: phosphorus, K: Potassium, PL: poultry litter, POB: palm oil biowaste, CD: cow dung, EC: electrical conductivity, PCR-DGGE: polymerase chain reaction-denaturant gel gradient electrophoresis, CEC: cation exchange capacity, CCD: coconut coir dust, CCDP: CCD and peat mixes, $CCDC_A$: CCD and OPF compost A, $CCDC_B$: CCD and OPF compost B, $CCDC_C$: CCD and OPF compost C, OM: organic matter, HS: humic substance, LiP: lignin peroxidase, Lac: laccase, MnP: manganese peroxidase, VP: versatile peroxidase, GLOX: glyoxal oxidase, AAO: aryl alcohol oxidase, MSW: municipal solid waste, C/N: carbon to nitrogen ratio, SSB: solid-state bioconversion, SEM: scanning electron microscope, WWTPs: wastewater treatment plants, SS: sewage sludge, GW: green waste, OMW: olive mill waste, GI: germination index, Ni: nickel, Pb: lead, Cd: cadmium, Cr: chromium, 16S rRNA: 16S ribosomal RNA, 18S rRNA: 18S ribosomal RNA, USEPA: United States Environmental Protection Agency

Introduction

The worldwide palm oil sector is predicted to expand significantly to meet the escalating global demand for edible oil, which is utilised in various industries. The palm oil processing sector is expected to increase its overall production to 25 million tonnes by 2035 (Arisht et al., 2020). Over the past four decades, palm oil has experienced a tremendous and consistent expansion in the world market, with a projected average annual output of 15.4 million tonnes in Malaysia between 2016 to 2020 (Abdullah and

http://www.aloki.hu ● ISSN 1589 1623 (Print) ● ISSN 1785 0037 (Online)
DOI: http://dx.doi.org/10.15666/aeer/2003_25092533

Sulaiman, 2013). Palm oil has been reported to contribute to the socioeconomic sustainability of Malaysia; however, several international pressure groups, such as the Rainforest Action Network, Greenpeace, and World Wildlife Fund (WWF), have deemed the industry unsustainable due to industry practices that contribute to increased greenhouse gas (GHG) emissions, deforestation, and biodiversity loss (Dalton et al., 2017; Bateman et al., 2010). High solid waste production, such as oil palm fronds (OPF), oil palm trunks (OPT), empty fruit bunches (EFB), mesocarp fibers (MF), palm kernel shells (PKS), and palm oil mill effluent (POME), are all the environmental implications of unsustainable palm oil production practices (Foo and Hameed, 2010; Abdullah and Sulaiman, 2013).

As previously noted, most of the biomass is abandoned in the plantations, indicating that this primary lignocellulose feedstock is underutilised. OPF and OPT, which are abundantly accessible in plantations, account for about 75% of the solid waste, while the remaining 25% is contributed by EFB, MF, and PKS that are typically available at the mills (AIM, 2013). According to Awalludin et al. (2015), during oil palm fruit harvesting, over 44 million tonnes of OPF (dry weight) are produced annually, and during the replanting season, around 15 tonnes of dry OPF are typically chopped off and allowed to deteriorate naturally. Dalton et al. (2017) reported that OPF produced through pruning represents the majority of solid waste generated in the palm oil sector at 58.8%. The sector has attempted sustainable approaches such as mulching and enriching soil nutrients by laying frond piles in plantations (MPOB, 2014). According to the results of the field experiments, these methods could recover 7.5 kg of nitrogen into the soil, with 106 kg of phosphorus, 9.81 kg of potassium, and 2.79 kg of magnesium which also benefit soil enrichment. It reduces dependence on inorganic fertiliser, alleviates fertiliser costs, and improves environmental conservation (MPOB, 2014). Moreover, OPF has been reported as a viable raw material for producing paper through the chemical pulping process. In addition, OPF is also used as livestock feed, biofuel regeneration, heavy metal ion absorber in wastewater, renewable sugars, and composite boards (Hussin et al., 2013). Abandoning OPF in the plantation without further treatment can cause environmental issues due to the large accumulated organic content on the ground. According to Ahmad et al. (2011), the traditional method of OPF disposal for oil palm replanting through the burning method at the plantation can result in air pollution. Furthermore, allowing OPF to decompose naturally inhibits the replantation process and increases the spreading of diseases such as *Ganoderma* as well as insects such as rhinoceros beetles (*Dynastinae)*, which could damage the oil palm trees (Abdullah and Sulaiman, 2013). Due to the increased availability of OPF during harvesting and replanting, an alternative strategy for disposing of OPF is required. As a result, composting is recommended as an alternative method to convert bulky biomass such as OPF into profitable and manageable products for use in plantations or as market products (Shafawati and Siddique, 2013).

Organic waste composting is now recognised as a feasible strategy for enhancing soil health, establishing soil ecosystems, and assuring the sustainability of agricultural output. Composting is an alternate method of dealing with agricultural and industrial wastes created worldwide. Composting of agricultural waste is a recycling technology that has been proven to be used to make biofertilisers and soil conditioners. Stable compost products help replenish plant nutrients, maintain soil organic matter and improve soil physical and microbiological characteristics (Fadzilah et al., 2017). Composting is a series of interconnected biological processes involving various types of microorganisms required for the degradation of organic materials. The composting process involves

http://www.aloki.hu ● ISSN 1589 1623 (Print) ● ISSN 1785 0037 (Online)
DOI: http://dx.doi.org/10.15666/aeer/2003_25092533

numerous biological, chemical, and physical changes. Erwan et al. (2012) revealed that in the existence of microorganisms, great numbers of organic compounds, such as carbohydrates, sugars, and cellulose, will undergo biochemical changes and in turn produce heat, water, and CO_2. Aerobic, anaerobic, and vermicomposting are the three most common composting methods. Aerobic composting refers to the biological degradation of organic waste under controlled aerobic conditions. Aerobic composting requires the presence of oxygen during the decomposition process and is characterised by high temperatures, the absence of bad odors, and brief stabilisation. Weed seeds and other pathogenic organisms will be eliminated by high temperatures. In general, factors influencing aerobic composting consist of moisture content, carbon to nitrogen (C/N) ratio, particle size, pH, temperature, lignin degradation, and oxygen content (aeration) covering important aspects of physical, chemical, and biological properties. Three main composting methods that are often practiced in the organic waste composting process which includes windrow, aerated static pile (ASP), and mechanical or in-vessel composting. *Table 1* shows the comparison between the characteristics of these three methods. Composting of oil palm biomass, particularly OPF, into microbial-based biofertilisers is critical to reducing the impact of pollution and waste generation in the oil palm industry (Ahmad et al., 2012). Composting is becoming increasingly popular as a disposal method of solid waste or oil palm biomass. The main purpose of composting is to produce a stable product rich in nutrients that are easily absorbed by plants. Several academics have looked at the possibility of using OPF as an organic source of compost (Nahrul Hayawin et al., 2010; Ahmad et al., 2012; Erwan et al., 2012; Vakili et al., 2014; Fadzilah et al., 2015; Fadzilah et al., 2017).

Table 1. *The comparison between the characteristics of the windrow, aerated static pile, and in-vessel composting methods*

Characteristics	Windrow composting	Aerated static pile (ASP) composting	In-vessel or mechanical composting
Definition	• the organic wastes are mixed and piled in a long, thin heap, frequent turning is manually performed for aeration purposes. • requires a large area of land	• a method similar to the windrow method but the air is supplied through a network of porous pipes and an air blower built under the pile. • requires a medium space of land	• entails restricting the composting process to various containers or vessels • more efficiently than windrow and ASP methods and requires minimal land space.
Operation control	• Moisture content: 50-60% (optimum) • C/N: 25-30 (optimum) • pH: 6.5 – 7.5 (optimum), 7.0-8.0 (final) • Aeration control: Limited. Unless forced ventilation is performed	• Aeration control: Not limited.	• Aeration control: Not limited.
Duration	Long	Long	Short
Compost quality	Medium to good	Medium to good	Good
Capital cost	Low	Medium	High
Environmental impact	High	Medium	Medium

Source: Lim et al. (2017), Sabiani (2008), Huang et al. (2004), Liang et al. (2003), Agamuthu (2001), Wong et al. (2001)

http://www.aloki.hu ● ISSN 1589 1623 (Print) ● ISSN 1785 0037 (Online)
DOI: http://dx.doi.org/10.15666/aeer/2003_25092533

Inoculum is an additive material in composting through the addition of specific organisms to improve population growth known as the compost inoculation process. According to Rastogi et al. (2020), inoculum can be extracted from microbial communities based on certain degradative activities or produced from a mixture of cow dung, straw, soil, and so on. Inoculum can also be obtained from mature compost, an effective microbe (EM), or a mixture of commercial strains. Because of the existence of mesophilic and thermophilic bacterial populations in considerable proportions, the addition of inoculum into the composting mixture will result in changes in temperature distribution and ammonia emission, increased enzymatic activity, shortened the biological process's initial lag period, and hastened the composting process (Rastogi et al., 2020). It can also minimise odorous emissions, particularly volatile organic compounds (VOCs), and generate compost with greater nutrient content.

This review highlights the studies on the composting of OPF and alternative treatment methods that will provide useful information on the potential use of this waste for the production of value-added products. This review also discusses the utilisation of inoculum in the composting processes such as lignocellulolytic microorganisms, namely white-rot fungi (WRF), sewage sludge, palm oil mill effluent (POME), and thickened POME anaerobic sludge for rapid breakdown of lignocellulosic OPF. Furthermore, the environmental consequences of composting are also investigated in this review since the composting process might indirectly minimise problems associated with environmental pollution affecting air, water, and soil.

Oil palm

Oil palm (*Elaeis guineensis*) is a native plant from West Africa that is beneficial for a variety of applications and is now extensively cultivated, notably in the South American and Asian continents (Onoja et al., 2018). Nigeria was the world's largest producer of palm oil until the mid-1960s when Malaysian palm oil production exceeded Nigeria's due to the fast expansion of the oil palm sector (Oviasogie et al., 2010). Malaysia was the world's biggest palm oil producer and exporter and related goods until 2007 when Indonesia surpassed that position (Paterson et al., 2009; Mazaheri et al., 2010; Rupani et al., 2010). Tropical weather conditions and high rainfall reception cause oil palm trees to grow fertile (Yaap et al., 2010); promising the success of its cultivation in Malaysia and Indonesia. Mohammad et al. (2010) revealed that these two countries produce almost 85% of the world's palm oil, with Indonesia and Malaysia accounting for 44% and 41% of output, respectively.

The British initially introduced oil palm trees to Malaysia in 1871 as ornamental plants (Onoja et al., 2018). The commercial-scale farming of oil palm trees in Malaysia began almost 100 years ago, with the initiation of the first palm oil plantation at Tenamaran Estate in Selangor in 1917 (Awalludin et al., 2015). After achieving independence in 1957, Malaysia experienced a continuous expansion in the cultivation of oil palm trees. This achievement was made possible by the Malaysian government's introduction of several initiatives, which resulted in the rapid growth of the oil palm sector (Awalludin et al., 2015), with oil palm plantations occupying more than 16% of the country’s accessible land by 2014 (Hosseini and Wahid, 2014).

In 2012, solid and liquid wastes from oil palm biomass totaled 83 million tonnes of solid waste, and 60 million tonnes of liquid waste were produced (AIM, 2013). This amount is predicted to reach 85–110 million tonnes for dry solid waste and 70–

http://www.aloki.hu ● ISSN 1589 1623 (Print) ● ISSN 1785 0037 (Online)
DOI: http://dx.doi.org/10.15666/aeer/2003_25092533

110 million tonnes for liquid waste by 2020 (AIM, 2013). This forecast is in line with the continued expansion of oil palm plantation areas in Malaysia. The planting and cutting of oil palm trees to produce palm oil in Malaysia have indirectly increased the generation of solid waste such as OPF and OPT. Meanwhile, EFB, MF and PKS resulting from palm oil processing activities also have adverse implications for the environment.

Oil palm fronds (OPF)

Oil palm fronds (OPF) are the most abundant biomass available in the world surpassing rice straw and corn stover, particularly in South-East Asia (Tan et al., 2016). OPF has sponge-like fibres. As illustrated in *Figure 1*, OPF consists of four primary parts: petiole, stem, rachis, and leaflet (Roslan et al., 2014). The petiole portion is responsible for half of the weight of the OPF. SEM micrographs of stem and petiole indicated the presence of porous lignocellulosic fibres with silica bodies comparable to those of EFB (Simarani et al., 2009). Rachis, stem, and petiole are mostly composed of cellulose, whereas leaflet is mostly composed of hemicellulose and lignin.

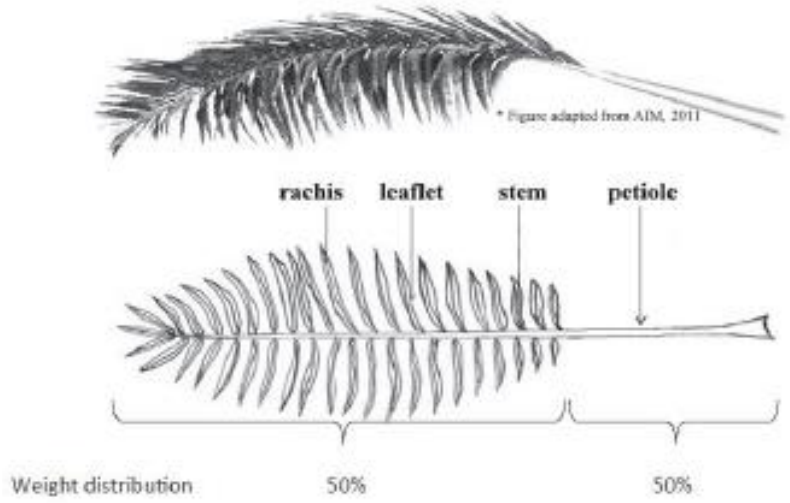

Figure 1. *Oil palm fronds (OPF) parts (Roslan et al., 2014)*

The major components of OPF are extractives, cellulose, hemicellulose, and lignin, which are found in vascular bundles and parenchyma (Kumneadklang et al., 2019). OPF contains 2.4-2.8% nitrogen, 0.15-0.18% phosphorus, 0.90-1.20% potassium, 0.25-0.4% magnesium and other trace elements (Sunarti et al., 2016). According to Onoja et al. (2018), the cellulose, hemicellulose, and lignin contents of OPF are 40.01%, 30.78%, and 29.50%, respectively. Carbon (C), hydrogen (H), nitrogen (N), sulfur (S), and oxygen (O) have been identified in the ultimate analysis of OPF. Several researchers such as Guangul et al. (2012), Abnisa et al. (2013), and Loh (2016) reported that the percentage ranges of C, H, N, S, and O contents observed in OPF were 42.76-48.43%, 4.53-10.48%, 0.39-12.40%, ND-0.07%, and 46.75-50.88%, respectively. According to Ho et al. (2015), one of the benefits of OPF is that it contains a high proportion of oxygen which requires less external air for complete combustion, thus making it a cost-effective fuel source together with other parts of the oil palm, such as leaves, trunks and empty fruit bunches. Because of its low nitrogen and sulfur content, OPF can be an environmentally friendly source of energy with a reduced risk of greenhouse gas emissions (Onoja et al., 2018). From

http://www.aloki.hu ● ISSN 1589 1623 (Print) ● ISSN 1785 0037 (Online)
DOI: http://dx.doi.org/10.15666/aeer/2003_25092533

proximate analysis, OPF has been reported to contain 13.84% moisture content, 82.70% volatile matter, 0.24% ash, and 3.22% fixed carbon (Abnisa et al., 2013). The presence of volatile matter and fixed carbon in OPF indicates that it has a high calorific value and can be ignited, gasified, or oxidized to some extent (McKendry, 2002). OPF has been recognised as an excellent source of fuel that can be converted into biogas (Mekbib et al., 2013; Herbert and Unni Krishnan, 2016) and biofuels through appropriate technology by referring to data related to volatile matter and fixed carbon. Furthermore, research on the volatile matter has revealed that OPF is composed of organic compounds such as cellulose, hemicellulose, and lignin. Because OPF is lignocellulose, it is easily transformed into simple sugars, which are subsequently processed into important biochemicals and biofuels (Loh, 2016).

Utilisation of oil palm fronds

Earlier, OPF was mostly utilised as soil mulching and allowed to degrade naturally in the plantation (Sulaiman et al., 2010; Mulakhudair et al., 2016), cattle feed (Daud and Law, 2010), and hydrogen gas supplies (Kelly-Yong et al., 2007). The application of OPF has expanded in numerous fields as a result of recent technological breakthroughs and research. Efforts in utilising OPF lignocellulose biomass in Malaysia are supported by the Malaysian National Biomass Strategy. Conversion of OPF into more valuable products has recently been reported, such as the production of bio-oil and biochar (Jadhav et al., 2019; Lawal et al., 2020), adsorbent for dye removal (Chew and Husni, 2019), wood adhesive production (Hussin et al., 2018), wastewater filtration media (Lee et al., 2021), renewable sugars (Manaf et al., 2018), composite boards (Iling et al., 2019), activated carbon production (Maulina and Anwari, 2018), bioethanol production (Syed Abdullah et al., 2021) and papermaking (Jarupan et al., 2021).

Jadhav et al. (2019) used the hydrothermal liquefaction method to create biochar solid and bio-oil liquid from OPF in a batch autoclave reactor. The results demonstrated that the percentage of bio-oil yield increased from 27.3% at 160°C to 41.9% at 260°C, whereas the percentage of biochar yield declined from 65.2% at 160°C to 43.2% at 260°C. Moreover, the percentage of carbon in biochar and bio-oil increased from 42.73% in OPF to 59.42% and 60.47%, respectively. In contrast, the percentage of oxygen in biochar and bio-oil declined from 52.51% to 36.30% and 35.61%, respectively. Phenolic compounds and their derivatives, alcohols, ketones, and esters are the most common chemical compounds found in bio-oil. The application of biochar in wastewater treatment has expanded due to advances in biochar synthesis and modification. Lawal et al. (2020) synthesized biochar from OPF using the pyrolysis method at a steam temperature of 500°C, which was then mashed into granulated and micro-fine particles. These biochar particles were characterised and employed as adsorbents in the final discharge treatment of POME. By raising the dosage of micro-fine biochar from 5 to 30 g/L, they discovered that the adsorption capacity reduced chemical oxygen demand (COD) and color. The micro-fine biochar effectively reduced the COD and color of wastewater by 81.4% and 95.6%, respectively, making it appropriate for recycling in processing plants and harmless for discharge into the natural water bodies at a concentration of 30 g/L.

The disposal of industrial wastewater containing dye leftovers that are detrimental to persons and the environment is one of the environmental challenges. The search for low-cost and environmentally friendly adsorbents that can help eliminate dye appears challenging. Therefore, Chew and Husni (2019) conducted a study to investigate the ability of OPF as an absorbent to eliminate Janus Green B dye. In the study, the adsorption

http://www.aloki.hu ● ISSN 1589 1623 (Print) ● ISSN 1785 0037 (Online)
DOI: http://dx.doi.org/10.15666/aeer/2003_25092533

capacity of OPF-based adsorbent was investigated based on the concentration of initial dye solution (50-250 mg/L), OPF loading (1–7 g/L), and pH (2–8) employed. Chew and Husni (2019) observed that the OPF-based adsorbent has an initial dye solution concentration of 150 mg/L, an adsorption capacity of 67 mg/g at pH 8, and an organic loading of 1 g/L for eliminating Janus Green B dye. Hussin et al. (2018) explored the use of lignocellulosic materials such as OPF in the production of environmentally friendly wood adhesives. In their research, they employed organosolv lignin generated from black liquor by organosolv pulping of OPF and regarded it as an alternative to phenol to manufacture glyoxal-phenolic resins for plywood. When compared with commercial phenol-formaldehyde (PF) adhesives, they discovered that the adhesive composition of 50% organosolv lignin phenol glyoxal (OLPG) with 50% (w/w) phenol replaced by organosolv lignin had maximum adhesive strength.

The amount of wastewater and biomass waste generated by palm oil processing activities has increased in tandem with the increasing demand for palm oil. Lee et al. (2021) employed OPF fiber as a media filter material to treat POME as an alternative strategy. OPF fiber was chosen for its unique properties, including high cellulose content, availability, biodegradability, and non-toxic. Chemical oxygen demand (COD), biochemical oxygen demand (BOD), total suspended solids (TSS), and pH were the criteria used to determine the pollutant reduction performance in their study. To identify optimal treatment results, OPF filters were arranged in various ratios, particle sizes and also coupled with other filter media materials such as activated carbon and sand. The findings of the study showed that pH 5.77 recorded the best results for BOD, COD, and TSS removal at 26.44%, 55.21%, and 98%, respectively. OPF has become increasingly popular as a source of sustainable fermentation feedstock. Manaf et al. (2018) studied the potential utilisation of soluble OPF bagasse products during dilute acid hydrolysis. Evaluation of experimental parameters such as nitric acid concentration, temperature, and contact duration resulted in optimal xylose release from OPF. Using 4% (v/v) HNO_3 at 130°C for 20 minutes, the maximum sugar levels obtained were 18.4 g xylose and 8.9 g glucose per 100 g OPF. There were 22.1 g/L xylose, 8.9 g/L glucose, and 4.6 g/L total inhibitors in the liquid fraction. In the fermentability test of xylitol production utilising OPF hydrolysate, the highest production of 0.35 g xylitol per gram of sugar was achieved. The study deduced that the use of dilute nitric acid to hydrolyse xylitol is a cost-effective and environmentally friendly method in biorefinery.

The selection of raw materials and fabrication variables has a significant impact on the performance of composite boards. Iling et al. (2019) evaluated the impact of various amounts of applied pressure on the performance of the OPF composite board as the end product. Using a crusher machine, OPF was crushed into small particles. Composite boards having a density of 0.7 g/cm^3 were made from sieved OPF particles retained on a 0.60 mm sieve screen. Composite boards with dimensions of 20 cm x 20 cm x 0.50 cm were produced at 160°C for three distinct applied pressures, namely 5 MPa, 6 MPa, and 7 MPa. The results showed that when the applied pressure increased, the performance of OPF composite boards improved. Composite boards produced from OPF are widely applied as base materials, decorative boards, and teaching aids. The presence of cellulose, hemicellulose, and lignin in OPF highlights its potential to be processed into a more valuable product. Therefore, using pyrolysis and impregnation methods, Maulina and Anwari (2018) utilized this waste to produce activated carbon. The OPF was pyrolyzed in reactors for 60 minutes at temperatures of 1500°C, 2000°C, and 2500°C. Subsequently, the pyrolyzed charcoal was smoothed using a ball mill, sieved to 140 meshes, and

http://www.aloki.hu ● ISSN 1589 1623 (Print) ● ISSN 1785 0037 (Online)
DOI: http://dx.doi.org/10.15666/aeer/2003_25092533

impregnated for 24 hours with sodium carbonate (Na_2CO_3) at concentrations of 0, 2.5, 5, and 7.5% (w/v). The activated carbon produced was porous, coarse and uniformly distributed in addition to having 72.75% fixed carbon, 35.13% charcoal yield, 24.75% volatile matter, 14.25% ash content, 8.6% water content, and 492.29 iodine number.

On the other hand, OPF juice is an effective fermentation feedstock for bioethanol production due to its high fermentable sugar content. The rapid deterioration of fermentable sugars in the juice during storage is a key drawback of using it as a feedstock. Thus, Syed Abdullah et al. (2021) investigated the impact of OPF juice concentration and moderate temperature storage on the juice's glucose content. Squeezing fresh OPF petiole was used to extract the juice, which was then concentrated by evaporating 30–70% (v/v) of the water. The juice was kept at varying temperatures (30 – 60ºC) for 20 days before being utilised for bioethanol production. The results showed that although there were various concentrations of OPF juice, the glucose content remained unchanged at storage temperatures of 50°C and 60°C. Furthermore, when OPF juice was stored at 50°C, bacterial deterioration was significantly reduced, and when kept at 60°C, it was destroyed. When compared to freshly made OPF juice, bioethanol production utilising OPF juice stored at 50ºC yielded about 15% higher bioethanol. Previously, the mold pulp trays used were made from newspaper waste. The transition to the digital age has resulted in a decline in this key feedstock. Therefore, alternative fiber sources such as OPF are beginning to be explored. Jarupan et al. (2021) found that fibers from OPF have great potential for waterproof containers in humid environments. Fibers were recovered from petioles with a yield of 30.72% using sulfate pulping in their investigation. The high α-cellulose content (38%) proved to be beneficial for papermaking. Properties such as Runkle's ratio (0.63), rigidity coefficient (38.46), and slenderness value (100) of the resulted paper all showed that it would have good mechanical quality. In cold chain logistics, packaging must withstand high humidity and low temperatures (90% RH, 12°C). Significant increases in water absorption resistance (from 59 to 23250 s), burst (6.68%), and tensile index (26.47%) were recorded when the addition of 1.4% cationic starch and 0.5% alkyl ketene dimer (AKD) was performed. The compressive strength of the mold pulp trays made of 70% sized frond fibers and 30% old corrugated container (OCC) fiber was 7.71% higher than that of a neat OCC tray.

Composting of oil palm fronds

The unique physical, chemical and biological characteristics of each organic matter provide a significant influence on the aerobic composting process. *Table 2* briefly shows the comparison of characteristics between OPF and typical softwood waste. Factors such as moisture content, pH, carbon, hydrogen, nitrogen, sulfur, oxygen, and organic content of lignin, cellulose, and hemicellulose were found to be interrelated with each other. The presence of high carbon and oxygen content will produce compost rich in organic matter and these elements play an important role in microbial activity during the composting process. Garcia et al. (2012) reported that the nitrogen present in OPF will be converted to ammonia gas which adversely affects the environment. Thus, the composting method is seen as the best alternative to manage OPF while solving the disposal problem and providing economic potential.

The biological characteristics of OPF consist of a high percentage of cellulose and hemicellulose, which are primary carbon sources and are followed by lignin. A study by Garcia et al. (2012) showed that enzyme degradation is an essential element in the degradation of lignocellulose via the aerobic composting method. A sufficient additional

http://www.aloki.hu ● ISSN 1589 1623 (Print) ● ISSN 1785 0037 (Online)
DOI: http://dx.doi.org/10.15666/aeer/2003_25092533

amount of nitrogen in the mixture corresponding to the amount of carbon is needed, where an appropriate C/N ratio can be achieved. Therefore, a precise understanding of OPF properties will ensure the practical configuration of composting towards a rapid degradation rate as well as producing a valuable final compost product.

Table 2. *A brief comparison of characterisation between OPF and typical softwood biomass*

Type of analysis	Oil palm fronds (OPF)		Typical softwood biomass	
	Value	References	Value	References
Physical characteristics (mf wt %)				
Moisture content	37.5	Omar et al. (2018)	n/d	Telmo et al. (2010)
pH	3	Atnaw et al. (2012)	2.5	
Chemical characteristics (mf wt%)				
C	42.4		47.0-54.0	
H	5.8		5.6-7.0	
N	3.6	Atnaw et al. (2012)	0.1-0.5	Telmo et al. (2010)
S	0.03		0.01-0.05	
O	48.2		40.0-44.0	
Biological characteristics (mf wt%)				
Lignin	20.5		25-35	
Cellulose	49.8	Atnaw et al., (2012)	45-50	Telmo et al. (2010)
Hemicellulose	23.5		25-35	

Notes: mf wt % is weight fraction percentage of dry material; n/d refers to not defined

Efficient biomass waste management can reduce the problems associated with environmental pollution caused by the disposal of large amounts of waste resulting from the oil palm industry, particularly OPF. Since OPF has a high content of organic matter, the compost resulting from the composting process has great potential to increase soil fertility (Vakili et al., 2014). It can also substitute the role of chemical fertilisers in agricultural activities. Composting is a valuable biomass recycling technology for producing compost that is easy to handle, stable, and high in plant-nutrient content. The conversion of OPF into compost is very interesting and has gained the attention of previous researchers. The studies have encompassed various aspects, including (1) characteristics, physicochemical and biological changes that occur during OPF composting and co-composting of other substrates (Erwan et al., 2012; Vakili et al., 2012, 2014; Ahmad et al., 2014); (2) microbial succession during co-composting of OPF with other substrates (Ahmad et al., 2016); (3) activity and diversity of fungal populations on OPF during the composting process (Fadzilah et al., 2015); (4) chemical and physical properties of OPF inoculated with fungi during composting (Fadzilah et al., 2017); and (5) utilisation of OPF compost (Kala et al., 2009; Erwan et al., 2013; Stevanus et al., 2016; Sunarti et al., 2016).

Erwan et al. (2012) investigated the physicochemical and biological changes that have occurred during OPF composting. Compost A, B, and C were prepared by mixing OPF, chicken manure (CM), and rice bran (RB) in the following proportions: 40:40:20, 40:30:30, and 40:20:40. Compost A had the lowest C/N ratio and the greatest amounts of nitrogen (N), phosphorus (P), and potassium (K) after 21 days, with values of 15.79, 2.33, 2.02, and 1.80, respectively. Compost A also had more bacteria than the other two composts, indicating that by day 21, OPF in compost A had matured enough to be used as soil supplements in agricultural areas. Vakili et al. (2012) examined the optimum ratios

http://www.aloki.hu ● ISSN 1589 1623 (Print) ● ISSN 1785 0037 (Online)
DOI: http://dx.doi.org/10.15666/aeer/2003_25092533

of poultry litter (PL) to palm oil biowaste (POB) composting process while observing the properties and physicochemical changes in bin composting of POB and PL. The POB utilised throughout their study was a combination of OPF and EFB. To achieve nutrient balance in the compost mixture, PL was combined with POB in three different ratios, namely 3:1, 1:1, and 1:3, and the moisture content was set to 40%. The composting materials were watered and turned periodically. Then, the materials were left under the shade for 11 weeks to decompose. The pH of all samples at the end of the process was close to natural. All samples exhibited a C: N ratio in the optimal range (25:1); however, the POB and PL ratio of 1:3 had the lowest C: N ratio. Moreover, Vakili et al. (2015) used a co-substrate different from previous to obtain the best ratio when conducting composting of POB (mixture of OPF and EFB) and cow dung (CD) to produce compost suitable for use in agriculture. In the study, Vakili and his co-workers provided four different POB and CD ratios, namely 4:0, 3:1, 1:1, and 1:3. The composting process, which took 11 weeks, was performed in plastic bins under the shade. Throughout this process, the composting materials were moistened to maintain optimum moisture content and the turning process was performed periodically. From the study, it was found that the 1:3 ratio (POB: CD) produced better quality compost than other ratios with C: N ratio, electrical conductivity (EC), and pH for mature compost recorded were 22.2, 2.83 mS/m, and 7.81, respectively. The use of POME as a co-substrate in the composting of chipped-ground OPF was investigated by Ahmad et al. (2014). The co-composting of chipped-ground OPF and POME took 60 days and had an average C/N ratio of 23. The temperature of the compost rose to a thermophilic phase (53.5°C) after 4 days of composting. On the 21st day, the maximum temperature recorded during the thermophilic phase was 56°C. The oxygen level, moisture content, and pH of the compost were sustained at 1.7 - 12.2%, 60.6 - 70.7%, and 7.9 - 8.5, respectively, during the 60-day composting period. The initial bacteria count was $55x10^{10}$ cfu/mL, which decreased to $14.7x10^{10}$ cfu/mL on on the 25th day and $3.7x10^{10}$ cfu/mL on the 60th day. The C/N ratio began at 63.9 and decreased to 24 on the 60th day.

Composting is a self-heating aerobic process involving microbial organic breakdown and stabilisation. This process can also be interpreted as a microbial succession that is constantly adapting to nutritional changes and ambient conditions. Mesophilic bacteria, which rapidly use decomposing materials, generally dominate the composting process initially. However, high metabolic activity contributes to heat production, resulting in a rapid temperature rise. As a result, thermophilic bacteria have taken over the mesophilic population. According to Baffi et al. (2006), a composting process involves lignocellulose biomass occurring in the thermophilic phase. In the maturation phase, new mesophilic populations will reappear to replace thermophilic populations. Microbial succession during co-composting of chipped ground OPF with POME was studied by Ahmad et al. (2016). Succession and phylogenetic profiles of microbial communities during the composting process were studied using polymerase chain reaction-denaturant gel gradient electrophoresis (PCR-DGGE) analysis. The findings revealed that the dominating microbial population was ɤ-*Probacteria* (e.g., *Pseudomonas sp.*) throughout the composting process. Meanwhile, *Bacillales* (e.g., *Bacillus psychrodurans*) were also detected in compost heaps when the composting process was heading towards the final stage. *Pedobacter solani* from the *Bacteroidetes* group was detected in the compost heap during the final stage of composting.

Improper and inefficient disposal of OPF will contribute to environmental problems. With proper compost management, OPF has the potential to be converted into organic

http://www.aloki.hu ● ISSN 1589 1623 (Print) ● ISSN 1785 0037 (Online)
DOI: http://dx.doi.org/10.15666/aeer/2003_25092533

compost that can be used as a soil amendment to promote crop growth. OPF is reported to have the potential to be utilised as an organic fertiliser that helps the growth of crops such as organic rice, rubber, cauliflower, and ornamental plants. Stevanus et al. (2016) examined the optimum dosage of OPF-based compost to promote the growth of rubber plants. The study analysed the OPF composting process as well as applied the resulting compost as a medium to improve the soil in the rubber plantation area. They stated that, except for K_2O concentration, the resulting compost met the Indonesian National Standard for compost quality. When compared with other treatments, the application test indicated that 20% compost + 80% subsoil treatment was the best dosage to enhance rubber plant growth. The final cation exchange capacity (CEC) value of the control declined compared to the initial value, but the CEC value of compost-added media increased with higher compost dosages. Compost-added media also had higher levels of P, K, Ca, and Mg than control media. Sunarti et al. (2016) made a comparison of three types of fertilisers consisting of OPF compost, cow manure, and synthetic fertiliser in organic rice cultivation. All these three treatments were evaluated at three distinct dosage levels, namely 60, 90, and 120 kg N/ha. In terms of quantity of tillers and productive tillers, the study found that OPF compost outperformed cow dung and synthetic fertiliser. However, there were no significant differences in plant height or rice production in the three fertilising treatments. On the other hand, an increase in nitrogen concentration will improve rice growth and production. Erwan et al. (2013) investigated the feasibility of using coconut coir dust (CCD) mixed with OPF compost soilless growth medium for cauliflower cultivation. In a tropical humid plant house, five distinct soilless growth media were evaluated: CCD alone, CCD and peat (CDP) mixes, CCD and OPF compost A ($CCDC_A$), CCD and OPF compost B ($CCDC_B$), and CCD and OPF compost C ($CCDC_C$). Due to superiority in physiological characteristics (stomatal conductance, photosynthesis rate, and chlorophyll content in leaves) and higher nutrient uptake rate. Throughout the growing phase, $CCDC_A$ treatment offered optimal plant development conditions for cauliflower, resulting in maximum total dry mass production and economic yield, i.e. the largest curd production (302 g/plant). Plants grown on a $CCDC_A$ medium also matured six days quicker than control plants. As a result, plants grown in soilless media, such as $CCDC_A$, may be appropriate for commercial cauliflower production in tropical conditions.

Factors such as acid reaction, high organic acid content as well as low micronutrient and macronutrient content contribute to low crop production rate. To overcome this problem, the use of OPF with ameliorants such as Cu^{2+}, Fe^{3+}, and Zn^{2+} can enhance peat soil while having a low environmental effect. Zahrah (2020) investigated the effects of ameliorants, namely Cu^{2+}, Fe^{3+}, and Zn^{2+} as well as OPF compost treatments on the growth of mung beans. The first factor was the application of four-level ameliorants (Cu^{2+}, Fe^{3+}, and Zn^{2+} without ameliorant). The second factor was the four levels of OPF compost dosages (0, 12, 24, and 36 g per plant). The combination of Cu^{2+}, Fe^{3+}, and Zn^{2+} with OPF compost considerably affected the percentage of filled pods, seed dry weight, and root volume of mung beans. According to the findings, the mixture of Cu^{2+} with 24 g/plant OPF compost yielded 26.67 g/plant seed dry weight, 94.7% filled pods, and 27.4 cm^3 root volume, representing a 175.5%, 32.8%, and 109.2% increase, respectively, over untreated soils.

http://www.aloki.hu ● ISSN 1589 1623 (Print) ● ISSN 1785 0037 (Online)
DOI: http://dx.doi.org/10.15666/aeer/2003_25092533

Utilisation of white-rot fungi (WRF), sewage sludge (SS), palm oil mill effluent (POME), and POME anaerobic sludge in lignocellulose biomass composting

According to Awasthi et al. (2017), organic matter (OM) is digested and transformed into a stable humic substance (HS) during composting under suitable circumstances. Organic macromolecules including lignocellulose, protein, and lipid are commonly found in the composting of raw materials. Because of its complicated physicochemical composition and structure, lignocellulose is the most stable organic component in composts. The presence of lignocellulose materials not only decelerates composting but also inhibits HS production. As a result, improving lignocellulose biodegradation is critical for enhancing organic waste composting efficiency and compost quality (Zhu et al., 2021).

Inoculation with lignocellulolytic microorganisms, such as bacteria and fungi, is a potential method to improve lignocellulose decomposition. Fungi that are active in the biodegradation of lignocellulose biomass can be divided into three major categories, namely white-rot, brown-rot, and soft-rot fungi. White-rot and brown-rot fungi belong to *Basidiomycetes*, whereas soft-rot fungi belong to *Ascomycetes* (Isroi et al., 2011). White-rot fungi (WRF) break down lignin using two mechanisms: selective and non-selective decays. The selectivity of WRF lignin degradation is affected by lignocellulose species, culture period, and other variables (Hatakka and Hammel, 2010). *Ceriporiopsis subvermispora, Dichomitus squalens, Phanerochaete chrysosporium*, and *Phlebia radiata* are examples of WRFs that exhibit selective decay under specific conditions, while *Trametes versicolor* and *Fomes fomentarius* are two WRFs with non-selective decay. Lignin peroxidase (LiP), laccase (Lac), manganese peroxidase (MnP), versatile peroxidase (VP), and H_2O_2-forming enzymes such as glyoxal oxidase (GLOX), and aryl alcohol oxidase (AAO) are enzymes involved in lignin breakdown (Hatakka, 2001; Wong, 2009). WRF generates a variety of enzymes involved in the breakdown of lignin, cellulases, xylanases, and other hemicellulases. Most WRFs produce manganese peroxidase (MnP) and laccase (Lac), but only a few produce lignin peroxidase (LiP) (Isroi et al., 2011). WRF has a great potential for delignification, although its effectiveness varies depending on the species selected for pretreatment (Rouches et al., 2016).

For example, Heidarzadeh et al. (2019) found a drop in the C/N ratio and a decrease in process time when *Aspergillus Niger* was inoculated to municipal solid waste (MSW) compost. Due to the enhanced diversity of fungal populations, Hu et al. (2019) discovered that incorporating lignocellulolytic microbial consortia into swine manure and mushroom waste co-composting improved lignocellulose breakdown by 8.77–34.45%. According to Awasthi et al. (2014), inoculating thermophilic fungal consortia (Trichoderma and Aspergillus) in the MSW composting mixture dramatically increased organic carbon mineralisation and expedited compost maturity. After WRF (*Phanerochaete chrysosporium, Trametes versicolor,* and *Fomes fomentarius*) was inoculated in the organic fraction of MSW, Voberkova et al. (2017) discovered that solid waste degradation was expedited, as demonstrated by modifications in the C/N ratio, electrical conductivity, pH, greater degradation ratio, better maturity degree, and enhanced enzymatic activity. During the second fermentation stage of rice straw composting, Zeng et al. (2010) discovered that inoculation of *Phanerochaete chrysosporium* enhanced cellulase and ligninase activities.

Inoculation with WRF during oil palm biomass composting is an approach that could positively affect lignocellulose degradation. Alam et al. (2006) conducted solid-state bioconversion (SSB) of mixed substrates consisting of EFB and POME in a laboratory-

http://www.aloki.hu ● ISSN 1589 1623 (Print) ● ISSN 1785 0037 (Online)
DOI: http://dx.doi.org/10.15666/aeer/2003_25092533

scale rotary drum bioreactor. In the study, different lignocellulolytic microorganisms such as *Trichoderma, Aspergillus, Penicillium,* and *Phanerocheate chrysosporium* (a type of WRF) were inoculated in composting materials (EFB and POME) in the drum. Four distinct fungal species were involved in the composting process through SSB depending on their activity in the rotary drum bioreactor for 2 months. They found that after 20 days of composting, the C/N ratio decreased from 70 to 25. A germination index of 50-70 showed that the compost generated was phytotoxic-free and only attained mature compost after 45 days of composting time. Fadzilah et al. (2015) employed a scanning electron microscope (SEM) and traditional identification methods to assess the activity and diversity of fungal populations on OPF during the composting process. Two WRF species, *Trametes versicolor* and *Schizophyllum commune*, were used as inoculants to shorten the composting time and produce high-quality compost. OPF was composted for 14 weeks in four distinct treatments: control (untreated OPF), OPF treated with *T. versicolor*, OPF treated with *S. commune* and OPF treated with both *T. versicolor* and *S. commune*. Each treatment was repeated four times. From the composted OPF, they isolated and identified eight fungi genera, including *Aspergillus, Trichoderma, Absidia, Geotrichum, Trametes, Schizophyllum, Syncephalastrum,* and *Beauveria.* Although *T. versicolor* and *S. commune* were added as accelerating agents, other fungal species were also present which could be due to the indigenous microflora in OPF, resulting in the succession of various fungal species depending on the complexity of biological processes in composting feedstock. Through the same study, the chemical and physical characteristics of OPF for 14 weeks of composting were also examined. They discovered that the finished compost was brown in colour, consistent in appearance, and odourless. When compared with other treatments, *S. commune* inoculation produced the lowest C/N ratio of 63.2 at the end of the composting period (Fadzilah et al., 2017). A single inoculation of *S. commune* produced a greater volume reduction percentage of 62.8% than other treatments. They conclude that a single *S. commune* inoculation offers an appropriate medium for OPF composting.

In addition, sewage sludge is also seen to have the potential to play a role as an inoculum in organic waste composting to produce compost or organic soil amendments. Municipal wastewater treatment plants produce a large volume of sewage sludge as a secondary waste product. It is a semi-solid or liquid residue generated during residential wastewater treatment and must be disposed of or removed from the system regularly to ensure the biological treatment process functions optimally (Ivanov et al., 2004). The use of sewage sludge for other applications often results in cost savings over disposal. According to Samaras (2007), sludge management via aerobic/anaerobic digestion, mechanical dewatering, and incineration often account for half of the total investment in wastewater treatment facilities. Sewage sludge contains a high amount of microbial diversity, which may impact the efficiency of wastewater treatment plants (WWTPs) and soil quality if used as fertiliser. Using molecular biology, Nascimento et al. (2018) investigated the diversity and structure of microbial communities in 19 sewage sludges from Sao Paulo, Brazil, as well as their connections to sources, biological treatments, and chemical properties. Although all sludges had a great amount of bacterial diversity, the sources, redox operating conditions, and liming did not have a consistent effect on the bacterial community structures. The main phylum was *Proteobacteria*, followed by *Bacteroidetes* and Firmicutes, while the leading genus was *Clostridium*, followed by *Treponema*, *Propionibacterium, Syntrophus*, and *Desulfobulbus.* As the biological sludge produced during the activated sludge process contained a wide variety of potentially

http://www.aloki.hu ● ISSN 1589 1623 (Print) ● ISSN 1785 0037 (Online)
DOI: http://dx.doi.org/10.15666/aeer/2003_25092533

heterotrophic bacteria, it is an appropriate microbial consortium for the decomposition of MSW organic waste fractions. For example, Deepesh et al. (2014) claimed that by using sewage sludge as an inoculum, the segregated MSW may be efficiently valorized, and the quality of the compost produced is equivalent to compost intended for unrestricted applications. During chicken manure-cornstalk composting, Li et al. (2017) found that inoculum derived from sewage sludge exhibited the best performance in terms of composting stability and maturity (the C/N ratio was lowered from 15.5 to 10, while the germination index was increased to 109%).

In addition, co-composting of lignocellulosic biomass and sewage sludge can also produce quality compost and is suitable for use as a natural fertiliser for crops. For example, Dzulkurnain et al. (2017) used a pilot-scale bioreactor system of 10 m^3 to co-compost municipal sewage sludge and landscaping waste as a soil amendment. Throughout the composting process, temperature, oxygen level, moisture content, and pH were all recorded. They found that the finished compost has 3.01% nitrogen, 0.27% phosphorus, and 0.68% potassium, making it ideal for ornamental plant growth. The Solvita® compost maturity kit produced an index result of 7, indicating that the product has reached maturity. The compost pathogenicity test revealed that coliforms and *Escherichia coli* were eradicated after 15 days of composting at the thermophilic stage, proving that the compost was safe for use in the natural environment. Kebibeche et al. (2019) studied the influence of co-composted sawdust with sewage sludge and wheat straw on seed germination. For 90 days, the two mixes were heaped and composted. The first mixture (C1) contained sewage sludge and wheat straw, whereas the second mixture (C2) contained sewage sludge, wheat straw, and wood sawdust. Temperature (> 55°C in the thermophilic phase), moisture content (30%), pH (6.73 for C1 and 7.19 for C2) and EC (1.81 mS/cm for C1 and 1.32 mS/cm for C2) of both composts met the necessary maturity level. The compost produced also showed a high level of maturity with C: N value below 12. In addition, no pathogenic bacteria were found in the finished compost. As shown by a germination index of over 80%, the concentration of total heavy metals dropped, allowing the elimination of sewage sludge toxicity. The addition of wood sawdust then increased the nitrogen content of the compost, resulting in slightly alkaline conditions. Meanwhile, Asses et al. (2018) evaluated the possibility of co-composting sewage sludge with organic waste in terms of management and agricultural value of the end product as a treatment technique. Two composting cycles (P1 and P2) were performed using sewage sludge (SS) to generate two mixtures, one with olive mill waste (OMW) and the other with green waste (GW). The co-composting of SS with both organic wastes resulted in hygienic compost of sufficient agronomic grade. The buildup of phenols from OMW-containing mixture resulted in a significant reduction of pathogens in the compost. These products were distinguished by the concentrations of P and K comparable to commercial composts as well as an advanced maturity suitable for direct application in agriculture. The germination index (GI) values for maize and tomato seeds treated with P1 were 79.68% and 97.36%, respectively. However, the GI values declined to 74.45% (maize) and 81.45% (tomato seeds) when using P2.

Several previous researchers in Malaysia have performed studies on the utilisation of oil palm wastes, namely EFB, OPF, and OPT as compost. Sewage sludge is another organic waste that must be disposed of properly in Malaysia. Co-composting of these waste materials has the potential to be converted into value-added products. Kala et al. (2009) examined the optimum ratio of oil palm waste aggregation (EFB, OPF, OPT) with sewage sludge (SS). Experiments were conducted in a glass greenhouse using a

http://www.aloki.hu ● ISSN 1589 1623 (Print) ● ISSN 1785 0037 (Online)
DOI: http://dx.doi.org/10.15666/aeer/2003_25092533

polystyrene box to produce mature compost, which was then used as potting media in horticulture. The oil palm wastes were chopped and blended with SS in three different ratios of 1:0, 3:1, and 4:1. The moisture content was set at 60%. From the experiments, they concluded that the OPT and SS ratio of 4:1 is the best to be used as an ornamental plant medium as its texture is most suitable as potting media. This ratio gave the following results: pH of 6.2, low C/N ratio of 19, and high nutrient levels such as nitrogen (2.05%), phosphorus (0.640%), potassium (1.39%), calcium (0.705%) and magnesium (0.229%).

Due to its significant level of OM and nutrients such as nitrogen, phosphorous, and potassium, SS can be used as fertiliser to increase crop production (Wu et al., 2010). Utilization of SS directly as a fertilizer is restricted due to the hygienic instability and immaturity of SS as well as the existence of pathogenic organisms and heavy metals. Composting is considered an appropriate SS management method as it converts OM into stable humic compounds via mineralisation and humification while decreasing harmful bacteria during the thermophilic phase (Yanez et al., 2009). To achieve compost maturity, many environmental parameters such as temperature, pH level, aeration, moisture content, the particle size of composting materials, and free air space should be carefully managed (Ge et al., 2015; Kim et al., 2016). A phytotoxicity test is usually conducted to determine the toxicity and maturity of the compost before the compost is used for agricultural purposes as well as to avoid any risk to the environment. According to Brewer and Sullivan (2003), unstable and immature compost use will contribute to problems such as inhibiting seed germination, inhibiting crop growth, and the occurrence of competition for oxygen due to insufficient OM decomposition. SS cannot be composted alone owing to its high moisture content and small particle size (Zhao et al., 2016). Furthermore, its low C/N ratio is detrimental to the composting process and results in a high volume of ammonia volatilization (Wang et al., 2014; Kulikowska, 2016). To increase gas permeability and minimise ammonia volatilisation, SS should be composted with dry material rich in carbon sources to modify the moisture content and C/N ratio (Awasthi et al., 2016). Co-composting may offer ideal composting conditions, such as a good C/N ratio, high porosity, and substantial active biomass, and it could also dispose of two or more types of solid waste simultaneously (Meng et al., 2017).

In Malaysia, the majority of research on co-composting of palm oil waste using EFB, OPF, and MF with POME produced from the palm oil milling process or POME anaerobic sludge from the anaerobic reactor or anaerobic pond at the mill. Raw POME is classified as high-strength agro-based wastewater with 95–96% water, 4–5% total solids (Vakili et al., 2014), COD and BOD concentrations of 69,500 mg/L and 25,000 mg/L, respectively (Abdullah et al., 2013), and high oil and grease (8370 mg/L) (Nik Kob, 2017). Raw POME is a hot and acidic brownish colloidal suspension. As Malaysia is one of the world's largest palm oil producers, POME anaerobic sludge is in large volumes and is easily available. The palm oil production process generates a large amount of waste in the form of POME which is subsequently treated through anaerobic digestion and finally produces POME anaerobic sludge. Sabiani (2019) reported that the COD concentrations, total solids, volatile solids, and water content of POME anaerobic sludge were 57,768 mg/L, 8.43%, 68.3%, and 91.5%, respectively. According to Zainuddin et al. (2013), thickened POME anaerobic sludge has high nutrient content comprising nitrogen (4.7%), phosphorus (1.3%), and potassium (6.5%) as well as indigenous microorganisms, making it an excellent microbial seed for the composting process. The application of thickened POME sludge during the composting process may shorten the composting duration while increasing compost yield.

http://www.aloki.hu ● ISSN 1589 1623 (Print) ● ISSN 1785 0037 (Online)
DOI: http://dx.doi.org/10.15666/aeer/2003_25092533

Alkarimiah and Suja' (2019) used a mechanical rotary drum reactor with a partial sequence feeding approach for co-composting of EFB and POME. According to their findings, the pH value increased during the composting process from 7.6 to 9.74, but as the process progressed, the pH profile began to decline to 7.59, which is the optimal and recommended pH value for final compost. The initial C/N ratio of 22.73 has dropped substantially to 9.11 after 14 days of treatment. After 111 days of composting, the C/N ratio was 10.29, indicating that the compost had matured and could be utilised as a natural fertiliser for agriculture. Furthermore, extremely low amounts of heavy metals (Ni, Pb, Cd, and Cr) were identified in the final compost, and all elements were undetectable. Understanding the role of different microorganisms (fungi, bacteria) in composting is critical to evaluating the efficacy of composting and producing high-quality compost. Krishnan et al. (2017) studied the microbial diversity of the EFB-POME co-composting process. Temperature, pH, and moisture content of the EFB-POME co-compost were determined. Microbial diversity was discovered by metagenomic sequencing analysis of 16S rRNA and 18S rRNA genes. The temperature, pH, and moisture content were 30°C, 7.43, and 58.76% for surface compost, and 45°C, 7.94, and 60.56% for inside compost. According to 16S rRNA gene sequencing for bacterial identification, the main genera in POME are *Parabacteroides, Bellilinea, Levilinea, Smithella,* and *Prolixibacter.* Meanwhile, *Nitriliruptor, Delftia, Filomicrobium, Steroidobacter,* and *Ohtaekwangia* are the predominant genera in surface compost. Major genera in inside compost include *Steroidobacter, Nitriliruptor, Anaeromyxobacter, Filomicrobium,* and *Filomicrobium.* According to 18S rRNA gene sequencing to identify fungi, *Remersonia, Inonotus, Kluyveromyces, Chaetomium, Thermomyces,* and *Candida* are the major genera in the surface compost. On the other hand, *Remersonia, Inonotus, Saccharomycopsis, Chaetomium,* and *Saccobolus* are the main genera present in the inside compost. The most common genera in POME are *Kluyveromyces, Inonotus, Kazachstania, Candida,* and *Cystofilobasidium.* Owing to their capacity to produce ligninolytic and cellulolytic enzymes, the microbial diversity observed in EFB-POME compost and POME may enhance the effectiveness of co-composting. Zainuddin et al. (2017) used 454-pyrosequencing to analyse the bacterial community succession at different phases of pilot-scale co-composting for EFB-POME anaerobic sludge, which was then associated with changes in physicochemical parameters such as temperature, oxygen level, and moisture content. According to the findings, species belonging to *Devosia yakushimensis* and *Desemzia incerta* appeared as dominating bacteria during the thermophilic stage, while *Planococcus rifietoensis* was related to the later stage of co-composting. This proves that the changes in physicochemical properties are parallel to the change of bacterial community at each stage of co-composting and this condition is very useful in monitoring the co-composting progress and as well as the level of compost maturity. In addition to EFB, co-composting of oil palm waste, such as OPF and MF, with POME anaerobic sludge was also conducted by several researchers. Lim et al. (2009) conducted a pilot-scale investigation on the characteristics and physicochemical changes in the windrow co-composting process for MF and POME anaerobic sludge. They found that the utilisation of POME anaerobic sludge as a nutrient source and microbial seeding into MF compost resulted in a thermophilic state (50-68°C) being maintained until day 39 of treatment. The pH value remained constant (6.8-7.8) during the entire process, while the moisture level decreased towards the completion of treatment, with a final moisture content of about 50%. The finished compost was produced in 50 days and has a C/N ratio of 12.6. Furthermore, significant amounts of nutrients and low levels of heavy metals

http://www.aloki.hu ● ISSN 1589 1623 (Print) ● ISSN 1785 0037 (Online)
DOI: http://dx.doi.org/10.15666/aeer/2003_25092533

were discovered in the final compost. They concluded that windrow co-composting for MF and POME anaerobic sludge could generate acceptable grade compost for fertiliser or soil amendment applications. Meanwhile, the co-composting process of OPF with POME anaerobic sludge has been discussed in the previous section (Ahmad et al., 2011, 2012, 2014, 2016).

Environmental impacts of composting

Composting converts organic matter into more stable compounds that have numerous benefits and can be applied to the soil. The finished product is environmentally safe, clean, and low in hazardous content. Composting has many advantages, including (i) producing a cleaner environment in which the composting process can reduce methane gas production at landfills, (ii) producing soil improvement materials that are useful and suitable for agricultural activities, (iii) reducing the need for solid waste transportation, (iv) increasing the effectiveness of fertiliser application, (v) a process that is flexible and can be implemented at various levels ranging from in-house efforts to large-scale levels, and (vi) may be started with low operational and capital expenditures.

In general, using mature compost made from agricultural waste as a natural fertiliser is less expensive than using chemical fertilisers. Long-term use of chemical fertilisers will adversely affect water, soil, and air as well as ecosystems. Inappropriate and persistent use of chemical fertilisers will cause soil structure degradation, reduction of organic components, and ultimately affects soil aggregation strength, which limits field crop output (Vakili et al., 2014). Easy and fast crop growth increased interest among farmers in using chemical fertilisers and pesticides instead of compost. Compost has long been utilised as a beneficial soil improver. Its more efficient application will improve the agricultural product quality, minimise the need for artificial fertilisers, be cost-effective, and indirectly protect natural resources. Due to its ability to alter the physical, chemical, and biological aspects of the soil, compost has a high potential to improve soil quality and crop productivity. Nevertheless, compost is not only used for crop fertilisation, it is also used to control soil erosion (USEPA, 1997a), landfill cover, landscape improvement (USEPA, 1997a), turf remediation (USEPA, 1997a), road construction projects (USEPA, 1997a), bioremediation and pollution prevention (USEPA, 1997b), disease control for plants and pest control (USEPA, 1997c), reforestation and wetlands restoration (USEPA, 1997d), and energy fuel source via compost palletization (Chia et al., 2020).

The oil palm waste (OPF, EFB, OPT MF, and others) which is largely generated from plantation activities and palm oil processing is seen to have great potential to produce compost. It can substitute chemical fertilisers in oil palm plantations and can be used as organic fertiliser for other agricultural activities such as vegetable farms and nurseries. Furthermore, compost made from oil palm waste has a high potential to be used for purposes other than as crop fertilizer in Malaysia. The conversion of oil palm waste into compost through the composting process can indirectly avoid problems related to environmental pollution involving air, water, and soil.

Conclusion

Research on OPF composting in resolving issues associated with the management of biomass from the oil palm industry has been discussed in detail in this article. Composting is a treatment process that decomposes organic materials in the presence of a group of

http://www.aloki.hu ● ISSN 1589 1623 (Print) ● ISSN 1785 0037 (Online)
DOI: http://dx.doi.org/10.15666/aeer/2003_25092533

microorganisms under specified conditions to convert organic materials into a stable soil-like product, namely compost. This method can be considered old technology and has been extensively reported in the literature. However, in the case of oil palm waste management focusing on OPF, this approach needs to be further investigated. The OPF pruning process in oil palm plantations is the highest contributor to oil palm waste generation. Various environmental issues will arise if OPF is left untreated as dumping of OPF will increase the organic content in the soil. Typically, the burning method is used to dispose of OPF which in turn results in air pollution. In addition, the problems of Ganoderma infestation and infectious insects will damage oil palm trees if OPF is allowed to decompose naturally on the ground. Therefore, composting is an alternative to disposing of OPF which has the potential to convert lignocellulose OPF into a product that benefits the soil and can generate profit. OPF has high amounts of cellulose and hemicellulose, which are the major carbon sources, followed by lignin. Degrading enzymes are critical components in the aerobic composting process for lignocellulose breakdown. The presence of lignocellulose materials not only delays composting but also limits the generation of humic substances. As a result, increasing lignocellulose decomposition is essential to enhance organic waste composting efficacy and compost quality. To enhance the decomposition of lignocellulose, the inoculation process of lignocellulolytic microorganisms such as white-rot fungi (WRF) can be performed. WRF is a type of fungi that can produce various types of enzymes such as lignin peroxidase, manganese peroxidase, and laccase for the breakdown of lignin, cellulose, and hemicellulose. Apart from WRF, sewage sludge is considered to have the potential to be utilized as an inoculum in organic waste composting. Co-composting of lignocellulose biomass and sewage sludge can also result in high-quality compost that can be used as a natural fertiliser for crops. On the other hand, the use of thickened POME anaerobic sludge as microbial seed may reduce composting time while increasing compost production. Even though a large number of studies have been conducted in this field, given the massive quantity of oil palm biomass produced annually, there are still many gaps in this area that other researchers may address. Among the future studies in OPF composting that can be conducted is by producing biofuels from OPF compost. Biofuel production through compost palletization is one of the ways to address the issues of low-quality compost and compost overproduction. In addition, studies related to the maturity of OPF compost include physical (eg: pile temperature, color, odor), biological (eg: respiration, phytotoxicity, enzyme activity), and chemical tests (eg: C/N ratio, organic matter, cation exchange capacity, electrical conductivity) needs to be done before the resulting OPF compost is applied to the crop. Future studies should also take into account the use of OPF compost so that it is not just limited to organic fertilizer for crops or agricultural activities only. The use of OPF compost can be further expanded to other uses such as soil erosion control, landfill cover, turf remediation, wetland restoration, and also in road construction projects.

Acknowledgments. The authors would like to acknowledge the research funding support received from the Fundamental Research Grant Scheme (FRGS), Ministry of Education Malaysia on Correlations between OPF Pre-treatment Using White Rot Fungi and Methane Generation in Temperature-Phased AD (1001/PAWAM/8014038).

http://www.aloki.hu ● ISSN 1589 1623 (Print) ● ISSN 1785 0037 (Online)
DOI: http://dx.doi.org/10.15666/aeer/2003_25092533

REFERENCES

[1] Abdullah, N., Sulaiman, F. (2013): The oil palm wastes in Malaysia. In Biomass Now Sustainable Growth and Use. – InTech Open, United Kingdom.

[2] Abdullah, N., Yuzir, A., Curtis, T. P., Yahya, A., Ujang, Z. (2013): Characterization of aerobic granular sludge treating high strength agro-based wastewater at different volumetric loadings. – Bioresource Technology 127: 181-187.

[3] Abnisa, F., Arami-Niya, A., Wan-Daud, W. M. A., Sahu, J. N., Noor, I. M. (2013): Utilization of oil palm tree residues to produce bio-oil and bio-char via pyrolysis. – Energy Conversion and Management 76: 1073-1082.

[4] Agamuthu, P. (2001): Solid Waste: Principals and Management with Malaysian case studies. – University of Malaya Press, Kuala Lumpur.

[5] Ahmad, M. N., Mokhtar, M. N., Baharuddin, A. S., Lim, S. H., Ahmad Ali, S. R., Abd-Aziz, S. (2011): Changes in physicochemical and microbial community during co-composting oil palm frond with palm oil mill effluent anaerobic sludge. – BioResources 6(4): 4762-4780.

[6] Ahmad, M. N., Baharuddin, A. S., Lim, S. H. (2012): Co-composting of chipped oil palm frond enriched with palm oil mill effluent anaerobic sludge. – Malaysian International Conference on Trends in Bioprocess Engineering (MICOTriBE) 2012, 3-5 July 2012, Meritus Pelangi Beach Resort & Spa Langkawi, Kedah, Malaysia.

[7] Ahmad, M. N., Ahmad Ali, S. R., Hassan, M. A. (2014): Physicochemical changes during co-composting of chipped-ground oil palm frond and palm oil mill effluent. – Oil Palm Bulletin 69: 1-4.

[8] Ahmad, M. N., Ahmad Ali, S. R., Hassan, M. A. (2016): Microbial succession in co-composting of chipped-ground oil palm frond and palm oil mill effluent. – Journal of Oil Palm Research 28(2): 191-197.

[9] AIM. (2013): National Biomass Strategy 2020: New wealth creation for Malaysia's biomass industry: Version 2.0, Agensi Inovasi Malaysia, Kuala Lumpur. – Available at: http://etp.pemandu.gov.my/upload/Biomass_Strategy_2013.pdf.

[10] Alam, M. Z., Kabbashi, N. A., Othman, A. A. (2006): Development of composting process by different lignocellulolytic fungi using oil palm industrial waste in rotary drum bioreactor. – International Conference on Agricultural Wastes, March 21-23, 2006, Putrajaya Marriott Hotel, Malaysia.

[11] Alkarimiah, R., Suja', F. (2019): Co-composting of EFB and POME using rotary drum reactor by partially sequence feeding strategy. – In: Mohamed Nazri, F. (ed.) Proceedings of AICCE'19. AICCE 2019. Lecture Notes in Civil Engineering, Vol 53. Springer, Cham.

[12] Arisht, S. N., Abdul, P. M., Jasni, J., Yasin, N. H. M., Lin, S. K., Wu, S. Y., Takriff, M. S., Md. Jahim, J. (2020): Dose-response analysis of toxic effect from palm oil mill effluent (POME) by-products on biohydrogen producing bacteria - A preliminary study on microbial density and determination of EC50. – Ecotoxicology and Environmental Safety 203: 110991.

[13] Asses, N., Farhat, A., Cherif, S., Hamdi, M., Bouallagui, H. (2018): Comparative study of sewage sludge co-composting with olive mill wastes or green residues: Process monitoring and agriculture value of the resulting composts. – Process Safety and Environmental Protection 114: 25-35.

[14] Atnaw, S., Sulaiman, S., Moni, M. (2012): Experimental study on temperature profile of fixed-bed gasification of oil palm fronds. – International Journal of Technology 1: 93-94.

[15] Awalludin, M. F., Othman, S., Rokiah, H., Wan, N. A., Wan, N. (2015): An overview of the oil palm industry in Malaysia and its waste utilization through thermochemical conversion, specifically via liquefaction. – Renew. Sustain. Energy Rev. 50: 1469-1484.

[16] Awasthi, M. K., Pandey, A. K., Khan, J., Bundela, P. S., Wong, J. W. C., Selvam, A. (2014): Evaluation of thermophilic fungal consortium for organic municipal solid waste composting. – Bioresource Technology 168: 214-221.

http://www.aloki.hu ● ISSN 1589 1623 (Print) ● ISSN 1785 0037 (Online)
DOI: http://dx.doi.org/10.15666/aeer/2003_25092533

[17] Awasthi, M. K., Wang, Q., Huang, H., Li, R., Shen, F., Lahori, A. H., Wang, P., Guo, D., Guo, Z., Jiang, S., Zhang, Z. (2016): Effect of biochar amendment on greenhouse gas emission and bio-availability of heavy metals during sewage sludge co-composting. – Journal of Cleaner Production 135: 829-835.
[18] Awasthi, M. K., Li, J., Kumar, S., Awasthi, S. K., Wang, Q., Chen, H., Wang, M., Ren, X., Zhang, Z. (2017): Effects of biochar amendment on bacterial and fungal diversity for co-composting of gelatin industry sludge mixed with organic fraction of municipal solid waste. – Bioresource Technology 246: 214-223.
[19] Baffi, C., Abate, M. T. D., Nassisi, A., Silva, S., Benedetti, A., Genevini, P. L., Adani, L. (2006): Determination of biological stability in compost: A comparison of methodologie. – Soil Biology & Biochemistry 39: 1284-1293.
[20] Bateman, I. J., Fisher, B., Fitzherbert, E., Glew, D., Naidoo, R. (2010): Tigers, markets and palm oil: market potential for conservation. – Oryx 44(2): 230-234.
[21] Brewer, L. J., Sullivan, D. M. (2003): Maturity and stability evaluation of composted yard trimmings. – Compost Science & Utilization11(2): 96-112.
[22] Chew, T. L., Husni, H. (2019): Oil palm frond for the adsorption of Janus Green dye. – Materials Today: Proceedings 16: 1766-1771.
[23] Chia, W. Y., Chew, K. W., Le, C. F., Lam, S. S., Chee, S. C. C., Ooi, M. S. L., Show, P. L. (2020): Sustainable utilization of biowaste compost for renewable energy and soil amendments. – Environmental Pollution 267: 115662.
[24] Dalton, O. S., Mohamed, A. F., Chikere, A. O. (2017): Status Evaluation of Palm Oil Waste Management Sustainability in Malaysia. – OIDA International Journal of Sustainable Development, Ontario International Development Agency, Canada, 41-47. Available at http://www.ssrn.com/link/OIDA-Intl-Journal-Sustainable-Dev.html.
[25] Daud, W. R. W., Law, K. N. (2010): Oil palm fibers as papermaking material: potentials and challenges. – BioResources 6: 901-917.
[26] Deepesh, V., Verma, V. K., Suma, K., Ajay, S., Gnanavelu, A., Madhusudanan, M. (2014): Evaluation of an organic soil amendment generated from municipal solid waste seeded with activated sewage sludge. – Journal of Material Cycles and Waste Management 18(2).
[27] Dzulkurnain, Z., Hassan, M. A., Zakaria, M. R. (2017): Co-composting of municipal sewage sludge and landscaping waste: a pilot scale study. – Waste Biomass Valorization 8: 695-705.
[28] Erwan, I. M. R., Mohd Saud, H., Habib, S. H., Siddiquee, S., Kausar, H. (2012): Physical, chemical and biological changes during the composting of oil palm frond. – African Journal of Microbiology Research 6(19): 4084-4089.
[29] Erwan, I. M. R., Saud, H. M., Othman, R., Habib, S. H., Kausar, H., Naher, L. (2013): Effect of oil palm frond compost amended coconut coir dust soilless growing media on growth and yield of cauliflower. – International Journal of Agriculture and Biology 15(4): 732-736.
[30] Fadzilah, K., Saini, H. S., Atong, M. (2015): Identification of microbial population during oil palm frond (OPF) composting using light and scanning electron microscopy. – Journal of Agrobiotechnology 6.
[31] Fadzilah, K., Saini, H. S., Atong, M. (2017): Physicochemical characteristics of oil palm frond (OPF) composting with fungal inoculants. – Pertanika Journal of Tropical Agricultural Science 40(1): 143-160.
[32] Foo, K. Y., Hameed, B. H. (2010): Insight into the applications of palm oil mill effluent: A renewable utilization of the industrial agricultural waste. – Renewable and Sustainable Energy Reviews 14(5): 1445-1452.
[33] Garcia, R., Pizarro, C., Lavin, A. G., Bueno, J. L. (2012): Characterization of Spanish biomass wastes for energy use. – Bioresource Technology 103(1): 249-258.
[34] Ge, J., Huang, G., Huang, J., Zeng, J., Han, L. (2015): Mechanism and kinetics of organic matter degradation based on particle structure variation during pig manure aerobic composting. – Journal of Hazardous Materials 292: 19-26.

http://www.aloki.hu ● ISSN 1589 1623 (Print) ● ISSN 1785 0037 (Online)
DOI: http://dx.doi.org/10.15666/aeer/2003_25092533

[35] Guangul, F. M., Sulaiman, S. A., Ramli, A. (2012): Gasifier selection, design and gasification of oil palm fronds with preheated and unheated gasifying air. – Bioresource Technology 126: 224-232.
[36] Hatakka, A. (2001): Biodegradation of lignin. – In: Biopolymer: Biology, Chemistry, Biotechnology, Applications. Vol 1. Lignin, Humic Substances and Coal, Hofrichter, M. and Steinbuchel (eds.), Wiley-WCH.
[37] Hatakka, A., Hammel, K. E. (2010): Fungal biodegradation of lignocellulose. – In: The Mycota, A Comprehensive Treatise on Fungi as Experimental Systems for Basic and Applied Research. Esser, K. (series ed.), Industrial Applications, 2nd Edition, Hofrichter, M. (volume ed.), Springer Berlin Heidelberg.
[38] Heidarzadeh, M. H., Amani, H., Javadian, B. (2019): Improving municipal solid waste compost process by cycle time reduction through inoculation of *Aspergillus Niger*. – Journal of Environmental Health Science & Engineering 17(1): 295-303.
[39] Herbert, G. M. J., Unni Krishnan, A. (2016): Quantifying the environmental performance of biomass energy. – Renewable & Sustainable Energy Reviews 59: 292-308.
[40] Ho, W. S., Khor, C. S., Hashim, H., Lim, J. S., Ashina, S., Herran, D. S. (2015): Optimal operation of a distributed energy generation system for a sustainable palm oil-based eco-community. – Clean Technologies and Environmental Policy 17: 1597-1617.
[41] Hosseini, S. E., Wahid, M. A. (2014): Utilization of palm solid residue as a source of renewable and sustainable energy in Malaysia. – Renewable & Sustainable Energy Reviews 40: 621-632.
[42] Hu, T., Wang, X., Zhen, L., Gu, J., Zhang, K., Wang, Q., Ma, J., Peng, H., Lei, L., Zhao, W. (2019): Effects of inoculating with lignocellulose-degrading consortium on cellulose-degrading genes and fungal community during co-composting of spent mushroom substrate with swine manure. – Bioresource Technology 291: 121876.
[43] Huang, G. F., Wong, J. W. C., Wu, Q. T., Nagar, B. B. (2004): Effect of C/N on composting of pig manure with sawdust. – Waste Management 2: 805-813.
[44] Hussin, M. H., Abdul Rahim, A., Ibrahim, M. N. M., Brosse, N. (2013): Physicochemical characterization of alkaline and ethanol organosolv lignins from oil palm (*Elaeis guineensis*) fronds as phenol substitutes for green material applications. – Industrial Crops and Products 49: 23-32.
[45] Hussin, M. H., Abdul Samad, N., Abd. Latif, N. H., Rozuli, N. A., Yusoff, S. B., Gambier, F., Brosse, N. (2018): Production of oil palm (Elaeis guineensis) fronds lignin-derived non-toxic aldehyde for eco-friendly wood adhesive. – International Journal of Biological Macromolecules 113: 1266-1272.
[46] Iling, E., Siti, D., Ali, H., Osman, M. S. (2019): Effect of pressing pressure on physical and mechanical properties of Elaeis Guineensis fronds composite board. – J Soc Sci Humanity 16(3): 1-12.
[47] Isroi, Millati, R., Syamsiah, S., Niklasson, C., Cahyanto, M. N., Lundquist, K., Taherzadeh, M. J. (2011): Biological pretreatment of lignocelluloses with white-rot fungi and its applications: A review. – BioResources 6(4): 5224-5259.
[48] Ivanov, V. N., Wang, J. Y., Stabnikova, O. V., Tay, S. T. L., Tay, J. H. (2004): Microbiological monitoring in the biodegradation of sewage sludge and food waste. – Journal of Applied Microbiology 96: 641-647.
[49] Jadhav, A., Ahmed, I., Baloch, A. G., Jadhav, H., Nizamuddin, S., Siddiqui, M. T. H., Baloch, H. A., Qureshi, S. S., Mubarak, N. M. (2019): Utilization of oil palm fronds for bio-oil and bio-char production using hydrothermal liquefaction technology. – Biomass Conversion and Biorefinery 11: 1465-1473.
[50] Jarupan, L., Hunsa-Udom, R., Bumbudsanpharoke, N. (2021): Potential use of oil palm fronds for papermaking and application as molded pulp trays for fresh product under simulated cold chain logistics. – Journal of Natural Fibers. DOI:10.1080/15440478.2021.1889433.

http://www.aloki.hu ● ISSN 1589 1623 (Print) ● ISSN 1785 0037 (Online)
DOI: http://dx.doi.org/10.15666/aeer/2003_25092533

[51] Kala, D. R., Rosenani, A. B., Fauziah, C. I., Thohirah, L. A. (2009): Composting oil palm wastes and sewage sludge for use in potting media of ornamental plants. – Malaysian Journal of Soil Science 13(1): 77-91.
[52] Kebibeche, H., Khelil, O., Kacem, M., Harche, M. K. (2019): Addition of wood sawdust during the co-composting of sewage sludge and wheat straw influences seeds germination. – Ecotoxicology and Environmental Safety 168: 423-430.
[53] Kelly-Yong, T. L., Lee, K. T., Mohamed, A. R., Bhatia, S. (2007): Potential of hydrogen from oil palm biomass as a source of renewable energy worldwide. – Energy Policy 35: 5692-5701.
[54] Kim, E., Lee, D. H., Won, S., Ahn, H. (2016): Evaluation of optimum moisture content for composting of beef manure and bedding material mixtures using oxygen uptake measurement. – Asian-Australasia Journal Animal Science 29(5): 753-758.
[55] Krishnan, Y., Bong, C. P. C., Azman, N. F., Zakaria, Z., Othman, N., Abdullah, N., Ho, C. S., Lee, C. T., Hansen, S. B., Hara, H. (2017): Co-composting of palm empty fruit bunch and palm oil mill effluent: Microbial diversity and potential mitigation of greenhouse gas emission. – Journal of Cleaner Production 146: 94-100.
[56] Kulikowska, D. (2016): Kinetics of organic matter removal and humification progress during sewage sludge composting. – Waste Management 49: 196-203.
[57] Kumneadklang, S., O-Thong, S., Larpkiattaworn, S. (2019): Characterization of cellulose fiber isolated from oil palm frond biomass. – Materials Today: Proceedings 17: 1995-2001.
[58] Lawal, A. A., Hassan, M. A., Farid, M. A. A., Yasim-Anuar, T. A. T., Yusoff, M. Z. M., Zakaria, M. R., Roslan, A. M., Mokhtar, M. N., Shirai, Y. (2020): Production of biochar from oil palm frond by steam pyrolysis for removal of residual contaminants in palm oil mill effluent final discharge. – Journal of Cleaner Production 265: 121643.
[59] Lee, M. D., Mohamad, N. F. A., Abu Hassan, N., Lee, P. S. (2021): Performance of oil palm frond fiber as filtration material in palm oil mill effluent treatment. – IOP Conf. Series: Earth and Environmental Science 690: 012039.
[60] Li, S., Li, J., Yuan, J., Li, G., Zang, B., Li, Y. (2017): The influences of inoculants from municipal sludge and solid waste on compost stability, maturity and enzyme activities during chicken manure composting. – Environmental Technology 38: 13-14, 1770-1778.
[61] Liang, C., Das, K. C., McClendon, R. W. (2003): The influence of temperature and moisture contents regimes on the aerobic microbial activity of biosolids composting blend. – Bioresource Technology 86: 131-137.
[62] Lim, S. H., Baharuddin, A. S., Ahmad, M. N., Md Shah, U. K., Abdul Rahman, N. A., Abd-Aziz, S., Hassan, M. A., Shirai, Y. (2009): Physicochemical changes in windrow co-composting process of oil palm mesocarp fiber and palm oil mill effluent anaerobic sludge. – Australian Journal of Basic and Applied Sciences 3(3): 2809-2816.
[63] Lim, L. Y., Bong, C. P. C., Lee, C. T., Klemes, J. J., Sarmidi, M. R., Lim, J. S. (2017): Review on the current composting practices and the potential of improvement using two-stage composting. – Chemical Engineering Transactions 61: 1051-1056.
[64] Loh, S. K. (2016): The potential of the Malaysian oil palm biomass as a renewable energy source. – Energy Conversion and Management 141: 285-298.
[65] Manaf, S. F. A., Md Jahim, J., Harun, S., Luthfi, A. A. I. (2018): Fractionation of oil palm fronds (OPF) hemicellulose using dilute nitric acid for fermentative production of xylitol. – Industrial Crops & Products 115: 6-15.
[66] Maulina, S., Anwari, F. N. (2018): Utilization of oil palm fronds in producing activated carbon using Na_2CO_3 as an activator. – IOP Conf. Series: Materials Science and Engineering 309: 012087.
[67] Mazaheri, H., Lee, K. T., Bhatia, S., Mohamed, A. R. (2010): Sub/supercritical liquefaction of oil palm fruit press fiber for the production of bio-oil: effect of solvents. – Bioresource Technology 101: 7641-7647.
[68] McKendry, P. (2002): Energy production from biomass (part1): Overview of biomass. – Bioresource Technology 83: 37-46.

http://www.aloki.hu ● ISSN 1589 1623 (Print) ● ISSN 1785 0037 (Online)
DOI: http://dx.doi.org/10.15666/aeer/2003_25092533

[69] Mekbib, S., Anwar, S., Yusup, S. (2013): Syngas production from downdraft gasification of oil palm fronds. – Energy 61: 491-501.
[70] Meng, L., Li, W., Zhang, S., Wu, C., Lv, L. (2017): Feasibility of co-composting of sewage sludge, spent mushroom substrate and wheat straw. – Bioresource Technology 226: 39-45.
[71] Mohammad, N., Alam, M. Z., Kabbashi, N. A., Ahsan, A. (2012): Effective composting of oil palm industrial waste by filamentous fungi: a review. – Resource Conservation and Recycling 58: 69-78.
[72] MPOB (2014): Oil Palm & The Environment. – Malaysian Palm Oil Board, available at: http://www.mpob.gov.my/en/palm info/environment/520-achievements.
[73] Mulakhudair, A. R., Hanotu, J., Zimmerman, W. (2016): Exploiting microbubble-microbe synergy for biomass processing: Application in lignocellulosic biomass pretreatment. – Biomass Bioenergy 93: 187-193.
[74] Nahrul Hayawin, Z., Abdul Khalil, H. P. S., Jawaid, M., Hakimi Ibrahim, M., Astimar, A. A. (2010): Exploring chemical analysis of vermicompost of various oil palm fibre wastes. – The Environmentalist 30(3): 273-278.
[75] Nascimento, A. L., Souza, A. J. P., Andrade, A. M., Andreote, F. D., Coscione, A. R., Oliveira, F. C., Regitano, J. B. (2018): Sewage sludge microbial structures and relations to their sources, treatments, and chemical attributes. – Frontiers in Microbiology 9: 1-11.
[76] Nik Kob, N. N. (2017): Conversion of palm oil mill effluent (POME) into bio-hydrogen. – Master Thesis. University Putra Malaysia, Malaysia.
[77] Omar, N. N., Abdullah, N., Mustafa, I. S., Sulaiman, F. (2018): Characterisation of oil palm frond for bio-oil production. – ASM Science Journal 11(1): 9-22.
[78] Onoja, E., Chandren, S., Abdul Razak, F. I., Mahat, N. A., Abdul Wahab, R. (2018): Oil Palm (Elaeis guineensis) Biomass in Malaysia: The Present and Future Prospects. – Waste and Biomass Valorization.
[79] Oviasogie, P., Aisueni, N., Brown, G. (2010): Oil palm composted biomass a review of the preparation, utilization, handling and storage. – African Journal of Agricultural Resources 5: 1553-1571.
[80] Paterson, R. R., Moen, S., Lima, N. (2009): The feasibility of producing oil palm with altered lignin content to control Ganoderma disease. – Journal of Phytopathology 157: 649-656.
[81] Rastogi, M., Nandal, M., Khosla, B. (2020): Microbes as vital additives for solid waste composting. – Heliyon 6: e03343.
[82] Roslan, A. M., Zahari, M. A. K. M., Hassan, M. A., Shirai, Y. (2014): Investigation of oil palm frond properties for use as biomaterials and biofuels. – Tropical Agricultural Development 58(1): 26-29.
[83] Rouches, E., Zhou, S., Steyer, J. P., Carrere, H. (2016): White-rot fungi pretreatment of lignocellulosic biomass for anaerobic digestion: Impact of glucose supplementation. – Process Biochemistry 51: 1784-1792.
[84] Rupani, P. F., Singh, R. P., Ibrahim, M. H., Esa, N. (2010): Review of current palm oil mill effluent (POME) treatment methods: vermicomposting as a sustainable practice. – World Applied Science Journal 11: 70-81.
[85] Sabiani, N. H. M. (2019): Pretreatment study of food waste using sonication for enhancement of methane production. – Ph.D. Thesis. University Putra Malaysia. Malaysia.
[86] Sabiani, N. H. M. (2008): Pengkomposan sisa taman menggunakan kaedah timbunan statik berudara dan deram berputar. – MSc thesis. University Sains Malaysia. Malaysia. (Malay version).
[87] Samaras, P. (2007): Management of wasted sludge from municipal wastewater treatment plants. – ''Modern technologies for water and wastewater treatment'', Workshop. INTERREG III A/CARDS, Greece-FYROM.
[88] Shafawati, S. N., Siddiquee, S. (2013): Composting of oil palm fibres and Trichoderma spp. as the biological control agent: A review. – International Biodeterioration & Biodegradation 85: 243-253.

http://www.aloki.hu ● ISSN 1589 1623 (Print) ● ISSN 1785 0037 (Online)
DOI: http://dx.doi.org/10.15666/aeer/2003_25092533

[89] Simarani, K., Hassan, M. A., Abd-Aziz, S., Wakisaka, M., Shirai, Y. (2009): Effect of palm oil mill sterilization process on the physicochemical characteristics and enzymatic hydrolysis of empty fruit bunch. – Asian Journal Biotechnology 1(2): 57-66.
[90] Stevanus, C. T., Bintarti, A. F., Setiawan, N. (2016): The effect of oil palm frond-based compost as growing media amendment for rubber (*Hevea brasiliensis,* Müll. Arg.) planting material. – Malaysian Journal of Soil Science 20: 195-209.
[91] Sulaiman, F., Abdullah, N., Gerhauser, H., Shariff, A. (2010): A perspective of oil palm and its wastes. – Journal of Physical Science 21: 67-77.
[92] Sunarti, Hasibuan, I., Suzanna, E. (2016): Application of organic fertiliser made of oil palm fronds on organic rice. – The 2nd International Conference On Food Agriculture And Natural Resources 2016, 2-4 August 2016, Universitas Brawijaya, Malang, East Java, Indonesia.
[93] Syed Abdullah, S. S., Bahrin, E. K., Shirai, Y., Hassan, M. A. (2021): Influence of storage conditions on oil palm frond juice as a renewable feedstock for bioethanol production. – Biomass and Bioenergy 150: 106101.
[94] Tan, J. P., Jahim, J. M., Harun, S., Wu, T. Y., Mumtaz, T. (2016): Utilization of oil palm fronds as a sustainable carbon source in biorefineries. – International Journal of Hydrogen Energy 41(8): 4896-4906.
[95] Telmo, C., Lousada, J., Moreira, N. (2010): Proximate analysis, backwards stepwise regression between gross calorific value, ultimate and chemical analysis of wood. – Bioresource Technology 101(11): 3808-3815.
[96] USEPA (1997a): Innovative Uses of Compost Erosion Control, Turf Remediation, and Landscaping. – EPA530-F-97-043. Solid Waste and Emergency Response (5306W). United State Environmental Protection Agency.
[97] USEPA (1997b). Innovative Uses of Compost Bioremediation and Pollution Prevention. – EPA530-F-97-042. Solid Waste and Emergency Response (5306W). United State Environmental Protection Agency.
[98] USEPA (1997c). Innovative Uses of Compost Disease Control for Plants and Animals. – EPA530-F-97-044. Solid Waste and Emergency Response (5306W). United State Environmental Protection Agency.
[99] USEPA (1997d). Innovative Uses of Compost Reforestation, Wetlands Restoration, and Habitat Revitalization. – EPA530-F-97-046. Solid Waste and Emergency Response (5306W). United State Environmental Protection Agency.
[100] Vakili, M., Haque, A. A. M. (2012): Potentiality of palm oil biowaste with poultry litter for composting. – Awam International Conference on Civil Engineering (AICCE'12) Geohazard Information Zonation (GIZ'12). August 28-30, 2012. Park Royal Penang Resort. Penang, Malaysia.
[101] Vakili, M., Rafatullah, M., Ibrahim, H. M., Salamatinia, B., Gholami, Z., Zwain, M. H. (2014): A review on composting of oil palm biomass. – Environment, Development and Sustainability.
[102] Vakili, M., Zwain, H. M., Rafatullah, M., Gholami, Z., Mohammadpour, R. (2015): Potentiality of palm oil biomass with cow dung for compost production. – KSCE Journal of Civil Engineering 19: 1994-1999.
[103] Voberkova, S., Vaverkova, M. D., Buresova, A., Adamcova, D., Vrsanska, M., Kynicky, J. (2017): Effect of inoculation with white-rot fungi and fungal consortium on the composting efficiency of municipal solid waste. – Waste Management 61: 157-164.
[104] Wang, J., Hu, Z., Xu, X., Jiang, X., Zheng, B., Liu, X., Pan, X., Kardol, P. (2014): Emissions of ammonia and greenhouse gases during combined pre-composting and vermicomposting of duck manure. – Waste Management 34(8): 1546-1552.
[105] Wong, D. (2009): Structure and action mechanism of ligninolytic enzymes. – Applied Biochemistry and Biotechnology 157: 174-209.

http://www.aloki.hu ● ISSN 1589 1623 (Print) ● ISSN 1785 0037 (Online)
DOI: http://dx.doi.org/10.15666/aeer/2003_25092533

[106] Wong, J. W. C., Mak, K. F., Chan, N. W., Lam, A., Fang, M., Zhou, L. X., Wu, Q. T., Liao, X. D. (2001): Co-composting of soybean residues and leaves in Hong Kong. – Bioresource Technology 76: 99-106.
[107] Wu, D. L., Liu, P., Luo, Y. Z., Tian, G. M., Mahmood, Q. (2010): Nitrogen transformations during co-composting of herbal residues, spent mushrooms, and sludge. – Journal of Zheijang University SCIENCE B 11(7): 497-505.
[108] Yaap, B., Struebig, M. J., Paoli, G., Koh, L. P. (2010): Mitigating the biodiversity impacts of oil palm development. – CAB Reviews 5: 1-11.
[109] Yanez, R., Alonso, J. L., Diaz, M. J. (2009): Influence of bulking agent on sewage sludge composting process. – Bioresource Technology 100(23): 5827-5833.
[110] Zahrah, S. (2020): Effects of ameliorant Cu^{2+}, Fe^{3+}, and Zn^{2+} and palm oil frond compost applications on the growth and production of mung bean (*Vigna radiata* (L.) R. Wilczek) grown on peat soil in Riau. – Applied Ecology and Environmental Research 18(4): 5199-5209.
[111] Zainudin, M. H. M., Hassan, M. A., Tokura, M., Shirai, Y. (2013): Indigenous cellulolytic and hemicellulolytic bacteria enhanced rapid co-composting of lignocellulose oil palm empty fruit bunch with palm oil mill effluent anaerobic sludge. – Bioresource Technology 147: 632-635.
[112] Zainudin, M. H. M., Ramli, N., Hassan, M. A., Shirai, Y., Tashiro, K., Sakai, K., Tashiro, Y. (2017): Bacterial community shift for monitoring the co-composting of oil palm empty fruit bunch and palm oil mill effluent anaerobic sludge. – Journal of Industrial Microbiology and Biotechnology 44: 869-877.
[113] Zeng, G., Yu, M., Chen, Y., Huang, D., Zhang, J., Huang, H., Jiang, R., Yu, Z. (2010): Effects of inoculation with *Phanerochaete chrysosporium* at various time points on enzyme activities during agricultural waste composting. – Bioresource Technology 101: 222-227.
[114] Zhao, X. L., Li, B. Q., Ni, J. P., Xie, D. T. (2016): Effect of four crop straws on transformation of organic matter during sewage sludge composting. – Journal of Integrative Agriculture 15(1): 232-240.
[115] Zhu, N., Zhu, Y., Li, B., Jin, H., Dong, Y. (2021): Increased enzyme activities and fungal degraders by *Gloeophyllum trabeum* inoculation improve lignocellulose degradation efficiency during manure-straw composting. – Bioresource Technology 337: 125427.

http://www.aloki.hu ● ISSN 1589 1623 (Print) ● ISSN 1785 0037 (Online)
DOI: http://dx.doi.org/10.15666/aeer/2003_25092533

EFFECT OF EDTA ON ACCUMULATION OF HEAVY METALS FROM MINING TAILINGS AND ITS RELATIONSHIP WITH ON GROWTH, PHYSIOLOGICAL RESPONSE AND ANTIOXIDANT ACTIVITY OF *GRINDELIA TARAPACANA* PHIL.

HUILLCA, Y. – MEDINA, F. J. – POCOHUANCA, S. – VIVEROS, P. – MARIN, A. L. – ESCOBAR, P. – MARTÍNEZ, L. A. – LAZO, H. O.*

Universidad Nacional de San Agustín de Arequipa, Av. Alcides Carrión N°501-A, Peru

*Corresponding author
e-mail: hlazor@unsa.edu.pe; phone: +51-054-215-946

(Received 6th Dec 2021; accepted 21st Mar 2022)

Abstract. Wild plants that grow in areas contaminated with heavy metals can be used in phytoremediation due to the adaptation processes they use. In this work, the phytoremediation capabilities of *Grindelia tarapacana* in the presence of the chelating agent Ethylenediamine tetraacetic acid (EDTA) was evaluated. The effect of EDTA (50, 100, and 150 mg/kg) on the accumulation of heavy metals from mining tailings and its relationship with the physiological response and metabolism of greenhouse plants were tested. It was found that the biomass was increased in the treatment with 50 mg / Kg of EDTA. But the growth was decreased by up to 10% in treatments with higher concentrations. The photosynthetic pigments did not vary significantly in content. In the treatments with higher EDTA content, soluble carbohydrates were decreased significantly ($p < 0.05$), and soluble protein content changed significantly ($p < 0.05$). However, an opposite effect is observed for the antioxidant activity which increases with higher concentrations of EDTA in the substrate; consequently, lipid peroxidation also was decreased. The application of EDTA favored the accumulation of heavy metals in this species, in the order of roots> leaves> stems. Finally, it is concluded that *Grindelia* is a stabilizer and phytoextractor plant.
Keywords: *contaminated soil, antioxidative enzymes, phytoremediation, phytoextraction, toxicity*

Introduction

Phytoremediation is a technique that uses plant species to extract, volatilize, or stabilize heavy metals present in soils and water. Compared to other remediation techniques, this method requires lower resources while maintaining the integrity of soils due to their ecological safety (Chakravarty et al., 2017).

In this context, wild plant species growing around mines and mining tailings can be used as potential candidates for phytoremediation (Varun et al., 2015). These particular species may be well adapted to those polluted environments (Bech et al., 2002; Varun et al., 2015), therefore being capable of absorbing and accumulating appreciable amounts of heavy metals, specifically in the tissues of the tips of roots, stems, and spongy mesophyll cells (Islam et al., 2008). Additionally, due to their source area, these species may also require lower special care than crop plant species, such as frequent watering, fertilization, or pesticide treatments (Conesa et al., 2007).

However, the increased concentration of heavy metals in plants potentially results in decreased growth, physiological alterations, and oxidative stress. Consequently, cell and tissue damage (Gupta et al., 2013; Fryzova et al., 2017), is expressed as the increase in malondialdehyde, degradation of photosynthetic pigments contents; and the increase in compatible solutes such as soluble carbohydrates and proline. Other countable signals also include the increase in the synthesis of soluble protein and oxidative stress enzymes

http://www.aloki.hu ● ISSN 1589 1623 (Print) ● ISSN 1785 0037 (Online)
DOI: http://dx.doi.org/10.15666/aeer/2003_25352552

such as superoxide dismutase (SOD), peroxidases such as ascorbate peroxidase (APX), guaiacol oxidase (GPX), catalase (CAT), and glutathione reductase (GR) (Hameed et al., 2016; Khan and Khan, 2017).

The use of various chelating agents such as EDTA, diethylenetriaminepentaacetic acid (DTPA), Hydroxyethylethylenediaminetriacetic acid (HEDTA), Nitrilotriacetic acid (NTA) and different organic acids have been studied in field and laboratory conditions in order to improve the accumulation of metals by plants (Solhi et al., 2005). EDTA is considered one of the most effective chelators for mobilizing heavy metals, especially for Pb (Khalid et al., 2017), because of its ability to form ion-complex (Zhou et al., 2011; Dipu et al., 2012). Then, this chelating effect increasing the solubility of heavy metals present in soil solution, is a favorable process for remediation by plants (Chandra et al., 2018).

The genus *Grindelia*, from the Asteraceae family, is found in arid and semi-arid zones of Chile, Peru, Uruguay, southern Brazil and Argentina. Being most of its species found in regions whit annual rainfall lower than 250 mm (Castro et al., 1995). *Grindelia tarapacana* Phil. known as "chiri-chiri" is a perennial shrub with deep roots. It has been reported in other experiences because of its foliar bioaccumulation capacity for heavy metals, such as, Cu, Pb and Fe (Vásquez, 1998). Contrarily, studies on growth, physiological and metabolic factors associated with the ability of this plant for accumulation of heavy metals, are scarce. Therefore, the objective of this research was to evaluate the phytoremediation potential of *G. tarapacana* in the presence of increasing concentrations of the chelating agent EDTA.

Material and methods

Description of area for biological sample collection

Seeds of *G. tarapacana* and the mine tailings samples were collected from Kiowa mine, (south latitude 16 ° 32 '4.4 ", west longitude 71 ° 28' 23.7"), altitude 2450 m a.s.l. located in the province of Arequipa, Peru. All the tests were carried out in the Plant Physiology and Biotechnology laboratory, and greenhouse of the Faculty of Biological Sciences of Universidad Nacional de San Agustín de Arequipa.

Vegetal material

The seeds with healthy appearance, uniformity, and greater size were selected for the tests. First, the biological material was disinfected by soaking in commercial NaClO 5% (v/v) for 10 min and rinsed three times with distilled water, followed by a soaking process with distilled water at 40°C for three days (Hartman et al., 2002). Finally, the seeds were sown in beds with a substrate (sand: moss; 3:1 volume ratio), and were located in a growth chamber until the seedlings were 4-5 cm long.

Treatments of EDTA-Na

Substrates of treatments were prepared by mixing sand and soils (2:1) with 10 g of cattle manure and 20 g of moss per kg of substrate (Barrutia et al., 2009). The mine tailings were added to obtain its final concentration at 10%. After 10 days, fertilization was carried out by watering with 200 ml of Hoagland's solution ½, up to field capacity (FC). Then, the prepared substrate was watered for 15 days with distilled water in intervals of 3 days up to FC, and at the end of this period, the soil analysis was performed

http://www.aloki.hu ● ISSN 1589 1623 (Print) ● ISSN 1785 0037 (Online)
DOI: http://dx.doi.org/10.15666/aeer/2003_25352552

(*Table 1*). The substrate was placed in 1.5 kg pots and watered with distilled water, and the pots were kept in greenhouse conditions for two weeks prior to transplanting.

For each experimental unit, one seedling was transplanted for each pot; after 7 days, the EDTA treatments were applied at increasing concentrations of 50, 100, and 150 mg / Kg. The treatment with the substrate mentioned above and without application of EDTA was labelled as "Control"; and the treatment with field soil, "Blank". Then, the plants were grown in a greenhouse for 60 days. To avoid leaching and loss of nutrient and metals, a tray was placed under each pot, and the excess water was collected daily and returned to the pot (Ali et al., 2003). Finally, the plants were acclimatized to the substrate media in 7 days in a growth chamber (*Fig. 1*). with fluorescent lighting (40 Watts), the irradiance of 35 µmol m^{-2} s^{-1}, photoperiod 12 h / 12 h (D / N), the temperature of 22ºC and 18ºC (D / N) and relative humidity 40/70%.

Figure 1. *G. tarapacana plants with different EDTA treatments in acclimatization chamber*

Dry mass determination

The plants were carefully extracted from the pots. The roots, stems, and leaves of individual plants were separated, packaged, and labeled according to each treatment and repetition; for the specific case of roots, this material was carefully washed with distilled water, then all samples were put to desiccation at 70°C for 48 h in an oven to obtain the dry weight.

Physiological response

Malondialdehyde content (MDA)

The content of MDA or lipid peroxidation, was determined according to Chen et al. (2021). Briefly, 30 mg of fresh leaves were homogenized with 2 mL Trichloroacetic acid (TCA) 0.1% (p / v) and centrifuged at 5000 rpm for 10 minutes at 4°C. The supernatant (1 mL) was removed, and 2 mL of 20% TCA: 0.5% Thiobarbituric Acid was added. The sample was then heated in a water bath at 95°C for 30 minutes. The absorbance was measured at 440, 532, and 600 nm (UV-VIS Spectroquant Pharo 300 spectrophotometer).

http://www.aloki.hu ● ISSN 1589 1623 (Print) ● ISSN 1785 0037 (Online)
DOI: http://dx.doi.org/10.15666/aeer/2003_25352552

As the final step, the non-specific turbidity was corrected by subtracting the absorbance score obtained at 600 nm.

Photosynthetic pigments content

The content of chlorophylls and carotenoids was determined according to Steubing et al. (2001); for this purpose, 30 mg of fresh leaves were homogenized with 3 mL 85% acetone maintaining cold mortar. The homogenized sample was filtered with filter paper Whatman No. 2 and rinsed with 3 mL of cold acetone at 80%. The content of chlorophylls and carotenoids was calculated by using the absorbance of the extract measured with a UV-VIS spectrophotometer (Spectroquant Pharo 300) at 662 nm for chlorophyll A (chl a), 644 nm for chlorophyll B (chl b) and 440 nm for carotenoids (Nikolic et al., 2016).

Soluble Carbohydrate content

The total soluble carbohydrate content was determined according to Steubing et al. (2001). Briefly, 30 mg of fresh leaves were homogenized with 10 mL 5% TCA. The mixture was placed in a water bath for 3 h at 90°C, and it was centrifuged at 7500 rpm for 10 min. Then, 0.2 mL of the supernatant, 0.5 mL of 5% phenol, and 2.5 mL of concentrated sulfuric acid were mixed in a test tube. For the determination of soluble carbohydrates, the absorbance score data was obtained by spectrophotometry at 485 nm.

Soluble protein content

The total soluble protein content was determined as follows. Fresh leaves (30 mg) were homogenized with 2 mL of 100 mM potassium phosphate buffer pH 7.5. It was centrifuged at 6000 rpm for 30 min, at 4°C. A sample of 70 µl of supernatant and 2.5 mL of Bradford's reagent were mixed. The data from the analysis was obtained at an absorbance of 595 nm (Moreno et al., 2002).

Antioxidant enzymes activity

The extract for further activity determinations was obtained from 30 mg of fresh leaves. Briefly, the biological material was homogenized with 2 mL of 100 mM potassium phosphate buffer pH 7.5 and centrifuged at 6000 rpm for 30 minutes at 4°C (Moreno et al., 2002); then, the supernatant was isolated and stored for determination antioxidant enzymes.

Determination of SOD activity

SOD activity was determined according to Donahue et al. (1997), where 1188 uL of potassium phosphate buffer, 20 uL of 20 mM EDTA, 50 uL of methionine, 154 uL of Nitro blue tetrazolium (NBT), 200 uL of the supernatant, and 338 uL of riboflavin were mixed in a tube. The result of the reaction was measured at an absorbance of 560 nm.

Determination (estimation) APX activity

The APX activity was determined according to Zhao and Blumwald (1998). In a tube, 2 mL of potassium phosphate buffer, 80 uL of the supernatant, 80 uL of ascorbic acid, and 10 uL of H_2O_2 30% were mixed. The absorbance was measured at 290 nm for 1 minute.

http://www.aloki.hu ● ISSN 1589 1623 (Print) ● ISSN 1785 0037 (Online)
DOI: http://dx.doi.org/10.15666/aeer/2003_25352552

Determination (estimation) of GPX activity

GPX activity was determined according to Pinhero et al. (1997). In a tube, 2 mL of potassium phosphate buffer, 30 uL of the supernatant, 10 uL of Guaiacol, and 10 uL of H_2O_2 30% were mixed. Then, it was measured at 470 nm for 1 min.

Determination of CAT activity

The CAT activity was determined according to Pinhero et al. (1997). In a tube, 1 mL of 100 mM potassium phosphate buffer pH 7, 10 uL of the extract, and 10 uL of 30% H_2O_2 were mixed. It was measured at 240 nm for 1 min.

Determination (estimation) of GR activity

In a tube, 5 mL of potassium phosphate buffer 100 mM, pH 7.5, was mixed with 5 ml of DTT 1 mM and 5 ml of disodium salt of EDTA 1 mM. This solution was mixed with the extract containing PVPP, and the mix was incubated at 4ºC /1 hour and then centrifuged. The supernatant was mixed with 100 mM Phosphate Buffer,1 mM EDTA, 540 ul distilled water, and 100 ul of 2 mM NADPH. The absorbance was measured at 300-340 nm for 240 sec.

Metal absorption

Determination of the bioabsorption coefficient factor (BAC), bioconcentration factor (BCF) and translocation factor (TF).

BAC, BCF, and TF were determined (*Eqs. 1-3*) to quantify the efficiency of heavy metal phytoextraction (Ebrahimi, 2013; Varun et al., 2015).

$$BAC = C\ stem \div C\ soil \quad \text{(Eq.1)}$$

$$BCF = C\ root \div C\ soil \quad \text{(Eq.2)}$$

$$TF = C\ stem \div C\ root \quad \text{(Eq.3)}$$

where: C is the heavy metal content for each case (Varun et al., 2015).

A number of 5 plants was used for each analysis.

Statistical analysis

The design applied was completely randomized. The statistical analysis was carried out by applying ANOVA, and the mean differences were established using the Tuckey test ($p < 0.05$). The statistical software STATISTICA version 10 was used, considering that all reported results correspond to the mean of five repetitions per treatment and controls.

Results

Soil characteristics

Table 1 presents the characteristics of the soil (Blank) and the substrate with tailings (Control). Concerning previous reports from the area where the soil material was obtained

http://www.aloki.hu ● ISSN 1589 1623 (Print) ● ISSN 1785 0037 (Online)
DOI: http://dx.doi.org/10.15666/aeer/2003_25352552

(INIA, 2017), both (blank and control) presented sandy texture, alkaline pH, and moderate salinity. The Electrical Conductivity (EC) for both controls was in the average of soils from the study area, with low organic matter content, low $CaCO_3$ content, low Cation exchange capacity (CEC) (meq / 100 g) score, similar nitrogen content, exchangeable cations (low Na, medium K, low Ca, low Mg), and high phosphorus content.

Table 1. *Physicochemical characterization of agricultural soil and substrates prepared at the beginning of the experiment*

Physicochemical parameters	Treatment	
	Blank	**Control**
pH	8.01	8.01
Calcium carbonate (%)	0.35	0.44
Cation exchange capacity (meq/100g)	5.8	6.2
Conductivity (dS/m)	2.52	2.76
Organic material (%)	1.39	1.44
Sand (%)	78.4	79.8
Silt (%)	16.5	14.2
Clay (%)	5.0	6.0
Nitrogen (%)	0.193	0.179
Available Phosphorus (ppm)	66.97	72.98
Potassium (meq/100g)	0.61	0.95
Calcium (meq/100g)	4.19	4.26
Magnesium (meq/100g)	0.83	0.84
Sodium (meq/100g)	0.17	0.15
Percentage of interchangeable sodium (%)	2.93	2.42
Heavy metal		
Total As (mg kg^{-1})		63.19893
Total Hg (mg kg^{-1})		0.02820
Total Cd (mg kg^{-1})		0.23285
Total Cr (mg kg^{-1})		11.83308
Total Cu (mg kg^{-1})		196.95120
Total Fe (mg kg^{-1})		4317.84000
Total Mn (mg kg^{-1})		62.33994
Total Ni (mg kg^{-1})		2.46189
Total Pb (mg kg^{-1})		261.44817
Total Zn (mg kg^{-1})		36.96600

Biomass

Treatments with mine tailings containing metals and metalloids (As and Hg) increased the biomass (dry matter) by 30% compared to the blank. However, increasing concentrations of EDTA and mine tailings in the substrate, resulted in a significant decrease of biomass ($p < 0.05$), being the lowest value obtained in the treatment with EDTA 150 mg / Kg (*Fig. 2*). Specifically, the biomass of *G. tarapacana* decreased 1, 12, and 30% compared to the control, being affected at the level of stems and roots with significant differences between each tissue.

Photosynthetic pigments

The levels of photosynthetic pigments in *G. tarapacana* leaves, treated with mine tailings in increasing concentrations of EDTA, are shown in *Fig. 3*. The content of Chl a and Chl b increased significantly ($p < 0.05$) as the concentration of EDTA increased up to

http://www.aloki.hu ● ISSN 1589 1623 (Print) ● ISSN 1785 0037 (Online)
DOI: http://dx.doi.org/10.15666/aeer/2003_25352552

100 mg / Kg. Carotenoids decreased significantly ($p < 0.05$) in control compared to the blank, and the Chl a / Chl b ratio increased in the mine tailing treatments with EDTA (50 mg / kg). Furthermore, higher content of EDTA among treatments showed an increase in the Chl b content compared to the blank.

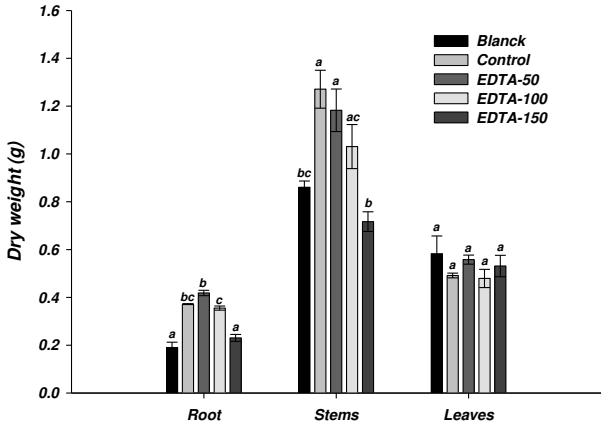

Figure 2. *Biomass of G. tarapacana plants under EDTA treatments (50-100-150 mg Kg-1) after 60 days of cultivation; and biomass in Blank: no tailing; and Control: with tailing. The values correspond to the average of 5 repetitions per treatment; Different letters indicate significant differences evaluated by the Tukey test ($p < 0.05$) after performing the ANOVA analysis*

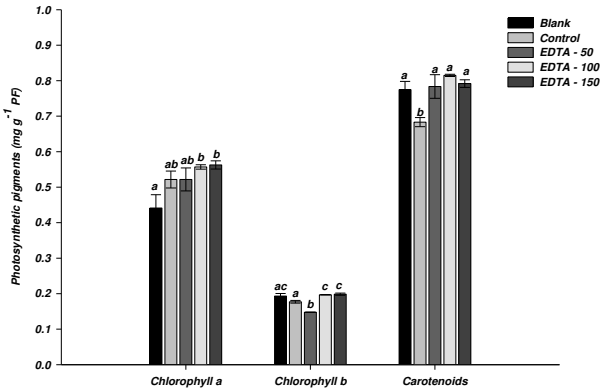

Figure 3. *Effect of different concentrations of EDTA on the content of chl a, chl b and carotenoids in G. tarapacana leaves, after 60 days of cultivation. Blank: agricultural land, Control: substrate with tailings. The values correspond to the average of 5 repetitions. Different letters indicate significant differences according to Tukey's test ($p < 0.05$)*

Carbohydrates and soluble protein

The mine tailing in the substrate and the application of EDTA significantly influenced ($p < 0.05$) the content of carbohydrates and total soluble proteins in leaves (*Fig. 4*). The control and the treatment with 50 mg / kg of EDTA increased the concentration of soluble sugars by 42 and 20%, respectively, about blank. Higher concentrations of EDTA, 100 and 150 mg / kg decreased soluble sugar content by 2 and 25%, respectively, if compared to blank. Additionally, the protein content decreased in control and the treatments between 6.5-8% compared to blank.

http://www.aloki.hu ● ISSN 1589 1623 (Print) ● ISSN 1785 0037 (Online)
DOI: http://dx.doi.org/10.15666/aeer/2003_25352552

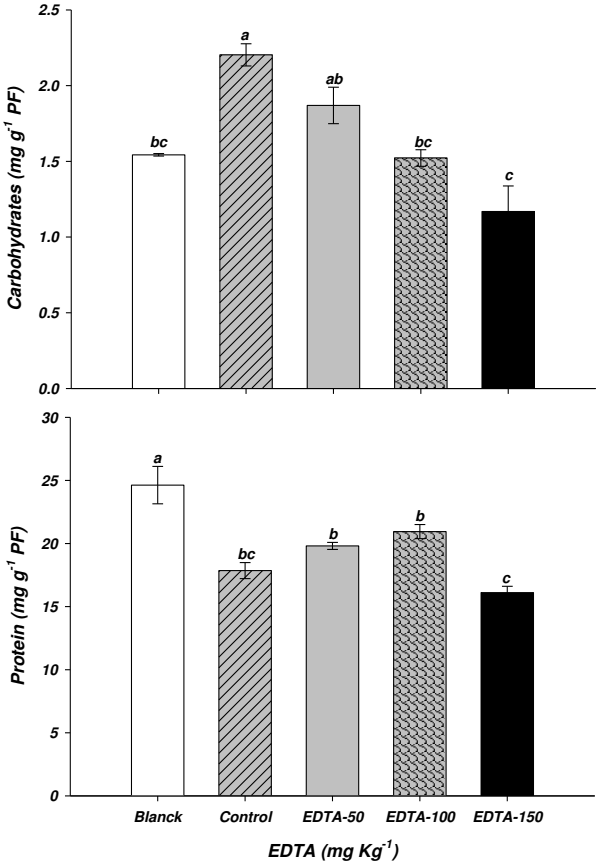

Figure 4. *Effect of different concentrations of EDTA (mg Kg-1) on the content of carbohydrates (upper) and total soluble proteins (lower) in G. tarapacana leaves, after 60 days of cultivation. Blank: agricultural soil, Control: substrate with tailings. The values correspond to the average of 5 repetitions. Different letters indicate significant differences according to Tukey's test ($p<0.05$)*

Lipid peroxidation and antioxidant enzymes

The breakdown of the cell membrane by lipid peroxidation is measured by the detection of the MDA, which is present when the vegetal organism is exposed to conditions of high oxidative stress (Fryzova et al., 2017). From our results, no significant differences were found between the control and treatment with 50 mg / Kg of EDTA concerning the blank (*Fig. 5*). However, the treatments with 100 and 150 mg / Kg of EDTA showed significant differences ($p < 0.05$), having lectures of MDA for the treatment with 100 mg / kg in 236% and decrease in 36% with 150 mg / kg of EDTA to the blank.

The mine tailing in substrate and EDTA treatments affected significantly ($p < 0.05$) the SOD, APX, CAT, GPX and GR enzymatic activity (*Fig. 5*). In specific, the Superoxide dismutase activity in the treatment with EDTA at 150 mg / kg presented the highest SOD enzymatic activity (476%); meanwhile, the control presented the lowest activity (51.54%). The highest GPX enzymatic activity was obtained with the EDTA treatment (150 mg / kg, with 0.000300 µmol g protein^{-1} min^{-1}) up to 1034% compared to the control (with 0.000029 µmol g protein^{-1} min^{-1}). The least activity was presented in the blank.

http://www.aloki.hu ● ISSN 1589 1623 (Print) ● ISSN 1785 0037 (Online)
DOI: http://dx.doi.org/10.15666/aeer/2003_25352552

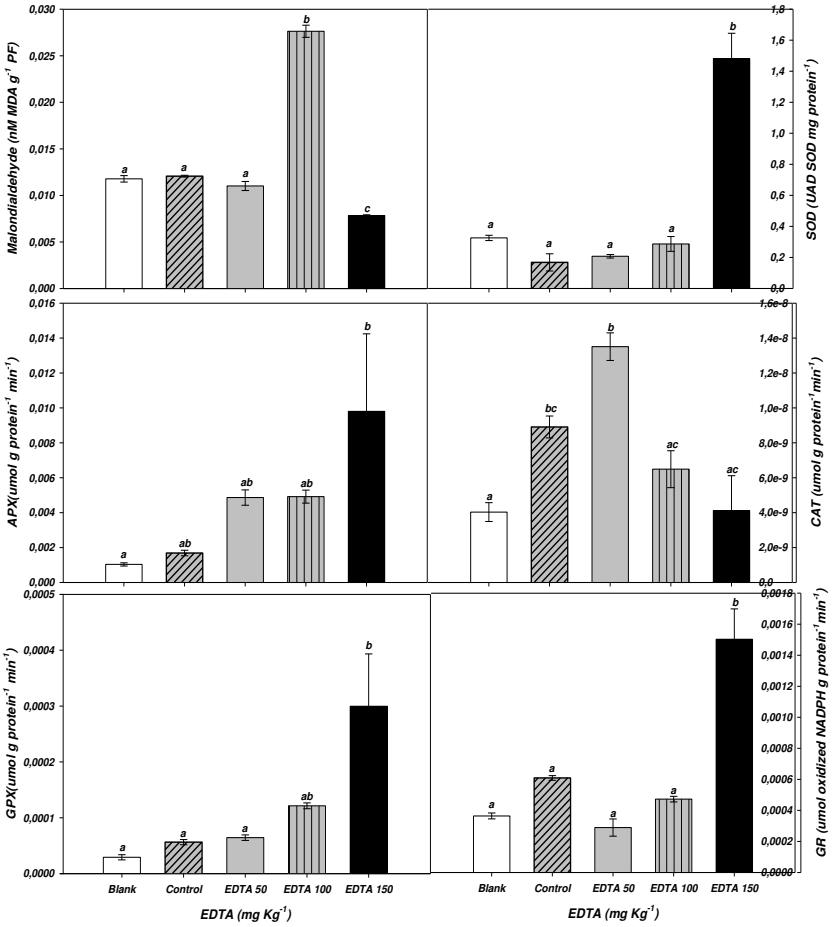

Figure 5. *Effects of EDTA in MDA content, activity of antioxidant enzymes SOD, APX, CAT, GPX and GR in G. tarapacana under substrates treatments with mine tailings (10%), treatments with EDTA (50 mg / kg, 100 mg / kg and 150 mg / kg), control without EDTA, and blank without mine tailing. Duration: 60 days. Values are means of 5 repetitions. Different letters indicate significant differences evaluated by the Tukey test (p <0.05) after performing the ANOVA analysis*

Bioaccumulation of heavy metals

Table 2 presents the total concentration of metals absorption from the soil with mine tailing (10%) in root, stem, and leaves. Being from highest to lowest, Fe> Pb> Cu> Mn> As> Zinc> Cr> Ni> Cd> Hg. After applying the EDTA treatments, the highest absorption was found in root> leaves> stem. Accumulation varies by metal and EDTA treatments. The highest percentage of accumulation in the stem samples was, Pb> Cu> As> Zn> Ni with 209%, 135%, 134%, 60% and 32%, respectively for EDTA 150 mg / kg. The other metals presented accumulation scores lower than 20%. Furthermore, the metals Fe, Cu, and Pb were found at toxic levels in the leaves.

Table 3 shows the heavy metal bioaccumulation factors BAC, BCF and TF. The BAC values varied for Hg> Zn> Mn> Ni, with 5.86, 3.38, 1.81 and 1.80, respectively; and TF Hg> Zn> Ni> Mn, with 2.26, 1.85, 1.21 and 1.20, respectively. These values, according to the BAC> 1 and TF> 1 criteria, show this plant as a phytoextractor for these metals. Additionally, the BCF values show Cd> Cr> As> Cu> Pb> Fe with 8.82, 1.96, 1.7, 1.56, 0.91, 0.79, respectively, classifying this plant as a Phyto stabilizer.

http://www.aloki.hu ● ISSN 1589 1623 (Print) ● ISSN 1785 0037 (Online)
DOI: http://dx.doi.org/10.15666/aeer/2003_25352552

Table 2. *Improvement of the phytoremediation potential: concentration of metals in the soil and accumulation in roots, stems, and leaves of G. tarapacana (mg kg-1), treated with EDTA (50,100 and 150 mg kg-1), after 60 growing days*

	Treatments	Heavy metal									
		As	Hg	Cd	Cr	Cu	Fe	Mn	Ni	Pb	Zn
SOIL	Blank	2.99 ± 0.34	0.04 ± 0.02	0.04 ± 0.02	7.20 ± 0.20	21.8 ± 0.94	2600.9 ± 9.05	69.46 ± 0.95	2.91 ± 0.04	3.4 ± 0.93	19.43 ± 2.11
	Control	60.98 ± 1.15	0.04 ± 0.02	0.24 ± 0.14	6.38 ± 0.09	178.9 ± 1.60	4417.3 ± 3.16	65.55 ± 0.77	2.96 ± 0.03	266.0 ± 2.52	47.79 ± 0.79
	EDTA 50	62.55 ± 1.01	0.01 ± 0.01	0.21 ± 0.12	7.04 ± 0.01	186.4 ± 2.05	4509.3 ± 4.35	65.72 ± 0.89	2.41 ± 0.01	280.6 ± 3.13	41.39 ± 2.06
	EDTA 100	61.35 ± 0.67	0.07 ± 0.04	0.22 ± 0.12	4.41 ± 0.13	179.0 ± 2.17	4531.8 ± 6.73	69.61 ± 0.82	2.60 ± 0.03	260.5 ± 0.97	41.20 ± 0.80
	EDTA 150	56.81 ± 1.52	0.04 ± 0.02	0.23 ± 0.13	2.74 ± 0.33	161.1 ± 2.50	4568.4 ± 5.57	61.29 ± 0.79	2.41 ± 0.02	248.7 ± 3.14	50.54 ± 0.76
	F value	*	*	*	*	*	*	*	*	*	*
ROOT	Blank	12.88 ± 1.53	0.08 ± 0.05	0.45 ± 0.25	3.02 ± 0.02	31.8 ± 2.01	1209.5 ± 4.25	92.68 ± 1.94	2.59 ± 0.04	4.62 ± 1.42	29.95 ± 2.17
	Control	101.42 ± 1.29	0.14 ± 0.07	1.82 ± 0.37	5.82 ± 0.31	234.6 ± 2.66	3087.0 ± 6.67	78.12 ± 1.35	3.53 ± 0.03	255.13 ± 1.93	60.00 ± 1.46
	EDTA 50	64.46 ± 1.90	0.10 ± 0.05	1.14 ± 0.55	4.76 ± 0.32	145.9 ± 2.73	2057.5 ± 5.41	49.35 ± 2.61	2.84 ± 0.03	165.25 ± 4.29	50.00 ± 1.89
	EDTA 100	93.10 ± 0.74	0.11 ± 0.06	1.91 ± 0.99	5.61 ± 0.25	280.0 ± 3.24	3622.8 ± 4.95	81.78 ± 2.63	3.49 ± 0.04	238.04 ± 1.88	75.09 ± 1.37
	EDTA 150	96.61 ± 0.83	0.10 ± 0.05	1.45 ± 0.73	5.39 ± 0.10	246.1 ± 4.23	2774.1 ± 7.08	92.40 ± 0.91	3.59 ± 0.04	216.40 ± 0.91	75.93 ± 1.01
	F value	*	*	*	*	*	*	*	*	*	*
STEM	Blank	0.69 ± 0.10	0.04 ± 0.03	0.31 ± 0.17	1.45 ± 0.16	11.74 ± 0.90	79.42 ± 2.04	37.53 ± 0.95	1.12 ± 0.01	0.97 ± 0.03	29.01 ± 1.35
	Control	4.54 ± 0.78	0.05 ± 0.03	0.61 ± 0.35	1.77 ± 0.46	20.00 ± 0.51	140.60 ± 3.71	26.20 ± 1.37	1.28 ± 0.03	5.11 ± 0.77	42.86 ± 0.97
	EDTA 50	4.33 ± 0.09	0.04 ± 0.02	0.55 ± 0.32	1.70 ± 0.49	26.17 ± 1.19	164.49 ± 1.25	33.01 ± 0.77	1.31 ± 0.01	8.65 ± 1.05	44.39 ± 0.90
	EDTA 100	5.12 ± 0.19	0.06 ± 0.04	0.37 ± 0.20	2.12 ± 0.17	36.20 ± 1.20	198.84 ± 2.66	34.19 ± 0.67	1.72 ± 0.02	9.04 ± 0.67	55.02 ± 0.66
	EDTA 150	6.64 ± 0.85	0.04 ± 0.02	0.37 ± 0.20	1.89 ± 0.33	41.24 ± 0.61	167.78 ± 1.85	42.57 ± 1.01	1.97 ± 0.03	8.81 ± 0.87	53.42 ± 0.71
	F value	*	*	*	ns	*	*	*	*	*	*
LEAVES	Blank	5.55 ± 0.79	0.18 ± 0.09	0.33 ± 0.18	2.61 ± 0.25	35.18 ± 1.36	435.26 ± 2.05	41.85 ± 2.09	1.73 ± 0.01	11.33 ± 1.22	60.48 ± 0.96
	Control	1.46 ± 0.16	0.17 ± 0.09	0.23 ± 0.12	2.95 ± 0.42	26.78 ± 1.13	461.03 ± 1.30	65.75 ± 1.12	2.01 ± 0.01	3.87 ± 2.13	51.41 ± 0.72
	EDTA 50	6.21 ± 0.24	0.19 ± 0.10	0.40 ± 0.23	3.13 ± 0.07	47.35 ± 0.88	575.56 ± 3.11	59.98 ± 1.60	2.19 ± 0.04	16.47 ± 1.24	71.54 ± 1.00
	EDTA 100	6.22 ± 0.13	0.19 ± 0.11	0.47 ± 0.25	3.14 ± 0.09	49.61 ± 0.82	505.81 ± 0.94	50.53 ± 1.59	2.32 ± 0.01	14.95 ± 1.02	84.30 ± 0.89
	EDTA 150	7.36 ± 0.11	0.17 ± 0.09	0.41 ± 0.23	2.97 ± 0.40	68.74 ± 2.05	551.63 ± 3.14	68.73 ± 0.89	2.38 ± 0.04	19.00 ± 1.02	97.51 ± 0.77
	F value	*	ns	*	ns	*	*	*	*	*	*

http://www.aloki.hu ● ISSN 1589 1623 (Print) ● ISSN 1785 0037 (Online)
DOI: http://dx.doi.org/10.15666/aeer/2003_25352552

Table 3. *Evaluation of the phytoremediation potential of Grindelia tarapacana exposed to mining tailings (10%) and increasing concentrations of EDTA (50, 100 and 150 mg kg-1): Characteristics of metal accumulation, BAC (Cstem/ Csoil), BCF (Croot / Csoil) and TF (Cstem/ Csoil), after 60 days of growth*

Treatment	Factors	Heavy metals									
		As	Hg	Cd	Cr	Cu	Fe	Mn	Ni	Pb	Zn
Blank	BAC	2.07 ± 0.06	5.35 ± 0.02	15.67 ± 0.03	0.56 ± 0.04	2.15 ± 0.01	0.20 ± 0.00	1.14 ± 0.03	0.98 ± 0.01	3.69 ± 0.05	4.69 ± 0.04
	BCF	4.31 ± 0.03	1.96 ± 0.00	11.11 ± 0.01	0.42 ± 0.01	1.46 ± 0.03	0.47 ± 0.00	1.33 ± 0.01	0.89 ± 0.00	1.32 ± 0.06	1.55 ± 0.06
	TF	0.48 ± 0.01	2.72 ± 0.01	1.41 ± 0.00	1.35 ± 0.13	1.48 ± 0.02	0.43 ± 0.00	0.86 ± 0.02	1.10 ± 0.01	3.11 ± 0.78	3.01 ± 0.14
Control	BAC	0.10 ± 0.01	5.49 ± 0.02	3.50 ± 0.00	0.74 ± 0.13	0.26 ± 0.01	0.14 ± 0.00	1.40 ± 0.02	1.11 ± 0.00	0.03 ± 0.01	1.97 ± 0.00
	BCF	1.66 ± 0.01	3.45 ± 0.01	7.61 ± 0.28	0.91 ± 0.04	1.31 ± 0.00	0.70 ± 0.00	1.19 ± 0.01	1.19 ± 0.00	0.96 ± 0.01	1.26 ± 0.01
	TF	0.06 ± 0.01	1.59 ± 0.05	0.46 ± 0.02	0.81 ± 0.11	0.20 ± 0.00	0.19 ± 0.00	1.18 ± 0.01	0.93 ± 0.00	0.04 ± 0.01	1.57 ± 0.01
EDTA 50	BAC	0.17 ± 0.00	17.14 ± 0.04	4.48 ± 0.00	0.69 ± 0.08	0.39 ± 0.01	0.16 ± 0.00	1.41 ± 0.02	1.45 ± 0.01	0.09 ± 0.01	2.80 ± 0.05
	BCF	1.03 ± 0.01	6.97 ± 0.01	5.35 ± 0.03	0.68 ± 0.04	0.78 ± 0.00	0.46 ± 0.00	0.75 ± 0.03	1.18 ± 0.01	0.59 ± 0.01	1.21 ± 0.05
	TF	0.16 ± 0.00	2.46 ± 0.00	0.84 ± 0.00	1.01 ± 0.05	0.50 ± 0.00	0.36 ± 0.00	1.88 ± 0.05	1.23 ± 0.00	0.15 ± 0.01	2.32 ± 0.05
EDTA 100	BAC	0.18 ± 0.00	3.76 ± 0.00	3.87 ± 0.00	1.19 ± 0.02	0.48 ± 0.01	0.16 ± 0.00	1.22 ± 0.02	1.55 ± 0.01	0.09 ± 0.01	3.38 ± 0.03
	BCF	1.52 ± 0.00	1.62 ± 0.00	8.82 ± 0.02	1.27 ± 0.02	1.56 ± 0.00	0.80 ± 0.00	1.17 ± 0.02	1.34 ± 0.00	0.92 ± 0.01	1.82 ± 0.00
	TF	0.12 ± 0.00	2.32 ± 0.01	0.44 ± 0.00	0.94 ± 0.00	0.31 ± 0.00	0.19 ± 0.00	1.04 ± 0.01	1.16 ± 0.00	0.10 ± 0.01	1.86 ± 0.01
EDTA 150	BAC	0.25 ± 0.01	5.86 ± 0.01	3.36 ± 0.01	1.78 ± 0.06	0.68 ± 0.01	0.16 ± 0.00	1.82 ± 0.01	1.80 ± 0.01	0.11 ± 0.01	2.99 ± 0.02
	BCF	1.70 ± 0.03	2.58 ± 0.01	6.20 ± 0.03	1.97 ± 0.21	1.53 ± 0.00	0.61 ± 0.00	1.51 ± 0.00	1.49 ± 0.01	0.87 ± 0.01	1.50 ± 0.00
	TF	0.14 ± 0.01	2.27 ± 0.01	0.54 ± 0.00	0.90 ± 0.12	0.45 ± 0.0	0.26 ± 0.00	1.20 ± 0.01	1.21 ± 0.00	0.13 ± 0.01	1.99 ± 0.01
Treatment	***F value***	*	*	*	*	*	*	*	*	*	*
Factors	***F value***	*	*	*	ns	*	*	*	*	ns	*
Interaction	***F value***	*	*	*	*	*	*	*	*	*	*

http://www.aloki.hu ● ISSN 1589 1623 (Print) ● ISSN 1785 0037 (Online)
DOI: http://dx.doi.org/10.15666/aeer/2003_25352552

Discussion

Heavy metals cause toxicity and adverse effects on mineral nutrition, photosynthesis and cell metabolism, decreasing growth (Antoniadis et al., 2017). However, *G. tarapacana* had a favorable response to the mine tailings by increasing its growth and tolerance to high concentrations of metals (As, Fe, Cu and Pb). Response which has also been reported in *Poa annua, Helianthus annuus* and other species (Nouri et al., 2009; Vamerali et al., 2010; Varun et al., 2015).

The results show that theTreatments with mine tailings increased the biomass compared to the blank (*Fig. 2*), this may be because some metals can stimulate cell proliferation (Kadukova and Kavulicova, 2010). The biomass was decreased at higher concentrations of EDTA, altering the root/shoot ratio (0.18) to the blank (0.13) (*Fig. 2*). This response would be consistent with descriptions from Hadi et al. (2010) in *Zea mays* treated with Pb + EDTA + AG3 and Greman et al. (2001) in *Brassica rapa* and *Trifolium pratense* treated with low concentrations of EDTA. This response may be attributed to the effect of how higher concentrations of EDTA increase solubility, breaking the physiological barriers in the roots, and a further indiscriminately translocation of heavy metals as described in *Chrysanthemum coronarium* and *Vigna radiata* (Luo et al., 2006); in consequence, reducing the activity of "Plant Growth Promoting Rhizobacteria," dubbed PGPRs, involved in stem growth (Ali et al., 2003; Bahadur et al., 2017).

In this study, the toxic concentrations of heavy metals in the mine tailings did not affect the content of chlorophylls in leaves but decreased carotenes (*Fig. 3*). The EDTA treatments increased the contents of Chl a and Chl b and carotenes. This response is because a fraction of the heavy metals binds to EDTA. Another fraction forms complexes with the xylem pathway and cell walls of the leaf mesophyll, reducing their mobility and preventing toxicity and cell damage (Zhao et al., 2010; Tian et al., 2011).

The results show how mine tailings increase the content of total soluble sugars in *G. tarapacana*. This trend coincides with reports from studies on *Oryza sativa* (Mishra and Dubey, 2013), *Pisum sativum* (Devi et al., 2007), and *Cucumis sativus* (Burzynsky and Klobus, 2004), where the increase in sucrose synthase and invertase acidic activity was also found. Toxic concentrations of heavy metals affect the light phase of photosynthesis and alter the carbon fixation process, controlled by several enzymes, regenerating the Calvin-Benson Cycle, in consequence affecting plant growth (Verma and Duvey, 2001; Burzynski and Klobus, 2004). At higher EDTA concentrations, total sugar levels decreased. This can be explained because of the degradation of starch and the synthesis of sucrose as crucial processes in the release of energy, originating hexoses to be metabolized in the glycolytic pathway, together with the pentose phosphate, which is strongly involved in tolerance processes to ROS caused by heavy metals (Devi et al., 2007; Rosa et al., 2009; Van den Ende and Valluru, 2009).

The soluble protein content of *G. tarapacana* decreases in the presence of mine tailings. The most significant effect was observed in the treatments with the highest concentration of EDTA (150 mg / L). This response would be related to the toxic content of Fe, Cu, and Pb in leaves, which could be associated with the greater protease activity (Palma et al., 2002; Hasan et al., 2017) or various structural alterations caused by protein denaturation (John et al., 2009; Hassan et al., 2017). This result coincides with investigations in *Digitaria sanguinalis*, where the soluble protein content decreased significantly by exposure to Pb and less effective with Cd and Ni (Ewais, 1997). However, in *Lemna minor*, an increase in soluble protein content was also observed by the effect of

http://www.aloki.hu ● ISSN 1589 1623 (Print) ● ISSN 1785 0037 (Online)
DOI: http://dx.doi.org/10.15666/aeer/2003_25352552

Cu and Cd (Hou et al., 2007); furthermore, a similar response was observed in pea plants exposed to Ni (Gajewska and Sklodowska, 2006; Romero-Puertas et al., 2007).

The results evidence the negative relationship between lipid peroxidation and antioxidant enzyme activity. In circumstances of low activity of antioxidant enzymes, high lipid peroxidation was found, and vice versa. This could be explained as the response to heavy metals. High concentrations of metals increase the content of MDA (Kumar and Prasad, 2018). Toxic concentrations of heavy metals produce alterations in cell permeability due to membrane decomposition related to lipid peroxidation that increases MDA formation, indicating high oxidative stress (Fryzova et al., 2017). Similar effects have been observed in plants treated with Cu and Pb, such as *Ceratophyllum demersum* (Devi et al., 2007), *Salsola passerina, Chenopodium album* (Hu et al., 2012) and *Lemna minor* (Hou et al., 2007). Similar responses were found with Pb and Cd in *Zea mays* (Gupta et al., 2013) and *Triticum aestivum* (Dey et al., 2007).

The oxidative stress caused by heavy metals has a first line of defense in the antioxidant enzymes SOD, APX, GPX, CAT, and GR (Gratao et al., 2005; Hameed et al., 2016). The results in this study show how SOD decreased in the control, but increased with EDTA. This increase in SOD activity in *G. tarapacana* leaves could be related to defensive mechanisms against oxidative stress, probably related to the specific concentration of metals such as Fe, As, Cu, and Pb (Gratao et al., 2005; Antoniadis et al., 2017).

The APX activity increased in *G. tarapacana* due to the mine tailings in the substrate. Similarly, high APX enzymatic activity was found in the presence of Cd, Cu, Zn, Al or Ni in *Avena sativa, Pisum sativum, Phaseolus vulgaris, Cucumis sativus* (Yruela, 2009). From the results, the APX activity increased in conditions of mixed metals compared to a separate application. This coincides with other experiences, such as in the case of *Ceratophyllum demersum*, where Cd and Zn was applied in mixed and separate solution (Chibuike and Obiora, 2014). And with other experiences where APX activity was higher with the treatment of 150 mg / Kg of EDTA, due to the higher availability of heavy metals (Raza et al., 2021).

The GPX activity in *G. tarapacana* was low, differing of what has been found in other studies, where under exposition to Pb and Cu, *Lupinus luteous, Triticum aestivum, Helianthus annuus*, and *Macrotyloma uniflorum*, showed higher activity of GPX (Jouili and Ferjani, 2003; Reddy et al., 2005; Dey et al., 2007; Mourato et al., 2009).

The results show how CAT activity in *G. tarapacana*, increased its activity in treatments with mine tailing; on the contrary, higher concentrations of EDTA decreased its activity for the blank. This would be explained by the fact that CAT activity has been reported as efficient at low concentrations of heavy metals (Gratao et al., 2005). In addition, the CAT activity has evident variation under the effect of the different heavy metals under study, also depending on the species and type of tissue. The activity of this enzyme in the presence of Cd was reported to decrease in *Phaseolus vulgaris, Lemna minor* and *Capsicum spp*., but increased in the presence of Cu and Ni in *Agropyrum repen, Raphanus sativus, Saccharum officinarum*, and *Helianthus annuus* (Jouili and El Ferjani, 2003). Finally, in experiences with *Glicine maxima*, the treatments with Cd have not presented changes in the activity (Gratao et al., 2005).

The GR activity in *G. tarapacana* increased by the effect of the mine tailings in the substrate. Our results are consistent with what has been described by Gratao et al. (2005), where the exposition to heavy metals increased GR activity, specifically in the presence of Pb (*Oryza sativa*), Hg (*Arabidopsis thaliana*), Cd (*Phaseolus vulgaris, Solanum*

http://www.aloki.hu ● ISSN 1589 1623 (Print) ● ISSN 1785 0037 (Online)
DOI: http://dx.doi.org/10.15666/aeer/2003_25352552

tuberosum), Ni (*Coffea arabica*), and As (*Brassica napus*) (Zuccarelli and Freschi, 2018). However, the GR activity reached its maximum activity with the highest EDTA, increasing the availability of heavy metals (Raza et al., 2021).

The bioaccumulation of heavy metals varies among the different organs of the plant, being influenced by the type of metal and the concentration in the soil (Varun et al., 2015). The greatest accumulation of heavy metals in *Grindelia* occurred in the roots. This response was consistent with the structure and function of roots in various species (Islam et al., 2008). In this case, the roots act as selective barriers, decreasing toxicity in the apoplastic and symplastic pathways (Jhon et al., 2009). Additionally, the combinations of mine tailings with EDTA reduced root growth due that EDTA facilitates the penetration of some metals into the root tissue, reducing growth (Evangelou et al., 2007; Antoniadis et al., 2017).

The results indicate differences in the accumulation of heavy metals in the stem. Which is explained by the different translocation indices (ITF). In *Grindelia*, ITFs were improved by EDTA, showing differences among the different metals. These variations may be related to concentration, mobility, speciation, and competition for cell transporters, with essential mineral elements such as K, Ca, Mg, P, Fe, and Zn (Ke et al., 2007; Antoniadis et al., 2017). This coincides with other experiences in different species of grasses (Chami et al., 2015; Varum et al., 2015).

The phytoremediation capacity as phytoextractor or Phyto stabilizer species depends on the values obtained for the Bio adsorption coefficient (BAC), Bioconcentration Factor (BCF), and Translocation Factor (TF) (Vamerali et al., 2010; Varum et al., 2015). In this study, *G. tarapacana* showed an accumulative capacity for not exceeding 1000 mg / Kg of dry weight, but it has shown phytoextraction capacity for Hg, Zn, and Mn; and Phyto stabilization capacity for Cd, Cr, As, Cu, Pb, and Fe. The growth response, tolerance, and bioaccumulation of this species, suggest its potential as a phytoremediation species of Fe, Cu, and Pb using EDTA, as it has been described in the Asteraceae family (Nouri et al., 2009; Doncheva et al., 2012) and other plant species (Luo et al., 2006; Meers et al., 2007; Vamerali et al., 2010; Chami et al., 2015).

Conclusion

The growth response showed decrement due to treatment with heavy metals and the application of EDTA in higher concentration. The availability of heavy metals increased by effect of EDTA, improving its absorption by the roots, translocation and accumulation in stems and leaves. The activity of antioxidant enzymes increased in the presence of heavy metals and was affected by the concentration of EDTA. The bioaccumulation of heavy metals establishes the potential use of *G. tarapacana* as an accumulator species. Furthermore, this species responded as Phyto-extractor for Hg, Zn and Mn; and as a Phyto stabilizer for Cd, Cr, As, Cu, Pb and Fe. Finally, the growth responses, physiology and antioxidant activity under high concentrations of heavy metals, suggest the potential use of this specie in phytoremediation for Cu and Pb metals. We recommend evaluating the use of EDTA in combination with phytohormones and microorganisms to improve plant growth and increase phytoremediation capacity.

Acknowledgement. We acknowledge the financing provided by the Universidad Nacional de San Agustín de Arequipa, through UNSA-INVESTIGA with contract IBA-0025-2016.

http://www.aloki.hu ● ISSN 1589 1623 (Print) ● ISSN 1785 0037 (Online)
DOI: http://dx.doi.org/10.15666/aeer/2003_25352552

REFERENCES

[1] Ali, M. B., Vajpayee, P., Tripathi, R. D., Rai, U. N., Singh, S. N., Singh, S. P. (2003): Phytoremediation of lead, Nickel, and Copper by Salix acmophylla Boiss.: Role of antioxidant enzymes and antioxidant subtances. – Bull Environmen. Contam. Toxicol. 70: 462-469. doi: 10.1007/s00128-003-0009-1.

[2] Antoniadis, V., Levizou, E., Shaheen, S. M., Ok, Y. S., Sebastian, A., Baum, C., Prasad, N. V., Wenzel, W. W., Rinklebe, J. (2017): Trace elemnts in the soil-plant interface: Phytoavailabilitu, translocation, and phytorremediatión - A review. – Earth-Science Reviews 171: 621-645.

[3] Bahadur, A., Ahmad, R., Afzal, A., Feng, H., Suthar, V., Batool, A., Khan, A., Mahmood-ul-Hassan, M. (2017): The influences of Cr-tolerant rhizobacteria in phytoremediation and attenuation of Cr (VI) stress in agronomic sunflower (*Helianthus annuus* L.). – Chemosphere 179: 112-119.

[4] Barrutia, O., Artetxe, U., Hernández, A., Olano, J., García-Plazaola, J., Garbisu, C., Becerril, J. (2009): Native plant communites in an abandoned Pb-Zn miningarea of Northern Spain: Implications for Phytoremediation and germplasm preservation. – International Journal of Phytoremediation 13: 256-270.

[5] Bech, J., Poschenreider, C., Barcelo, J., Lansac, A. (2002): Plants from mine spoils in the South American área as potential sources of germplasm for phytorremediation technologies. – Acta Biotechnology 22(1-2): 5-11.

[6] Burzynski, M., Klobus, G. (2004): Changes of photosynthetic parameters in cucumber leaves under Cu, Cd, and Pb stress. – Photosynthetica 42(4): 505-510.

[7] Castro, S., Fuentes, E., Timmermann, B. (1995): Germination responses and resin production of Grindelia glutinosa and G. tarapacana from the Atacama Desert. – Journal of arid Environments 29: 25-32.

[8] Chakravarty, P., Bauddh, K., Kumar, M. (2017): Phytoremediation: a multidimensional and ecologically viable practice for the cleanup of environmental contaminants. – In: Bauddh, K., Singh, B., Korstad, J. (eds.) Phytorremediation Potential of bioenergy plants. Springer, doi: 10.1007/978-981-10-3084-0_1.

[9] Chami, Z., Amer, N., Bitar, A., Cavoski, I. (2015): Potential use of Sorghum bicolor and Cartahamus tinctorius in phytoremediation of nickel, lead and zinc. – Int. J. Environ. Sci. Technol. 12: 3957-3970.

[10] Chandra, R., Kumar, V., Singh, K. (2018): Hyperaccumulator versus nonhyperaccumulator plants for environmental waste management. – In: Chandra, R., Dubey, N. K., Kumar, V. (eds.) Phytoremediation of environmental pollutants. CRC Press.

[11] Chen, G., Ran, Y., Ma, Y., Chen, Z., Li, Z., Chen, Y. (2021): Influence of *Rahnella aquatilis* on arsenic accumulation by *Vallisneria natans* (Lour.) Hara for the phytoremediation of arsenic-contaminated water. – Environmental Science and Pollution Research 28(32): 44354-44360.

[12] Chibuike, G. U., Obiora, S. C. (2014): Heavy metal polluted soils: effect on plants and bioremediation methods. – Hindawi Publishing Corporation Applied and Environmental Soil Science, doi: http://dx.doi.org/10.1155/2014/752708.

[13] Conesa, H. M., Schulin, R., Nowack, B. (2007): A laboratory study on revegetation and metal uptake in native plant species from neutral mine tailings. – Water air soil Polut 183: 201-212.

[14] Devi, R., Munjral, N., Gupta, A. K., Kaur, N. (2007): Cadmium indiced changes in carbohydrate status and enzymes of carbohydrate metabolism, glycolisis and pentose phospahte pathway in pea. – Environmental and Experimental Botany 61: 167-174.

[15] Dey, S. K., Dey, J., Patra, S., Pothal, D. (2007): Changes in the antioxidative enzyme activities and lipid peroxidation in wheat seedlings exposed to cadmium and lead stress. – Braz. J. Plant Physiol. 19(1): 53-60.

http://www.aloki.hu ● ISSN 1589 1623 (Print) ● ISSN 1785 0037 (Online)
DOI: http://dx.doi.org/10.15666/aeer/2003_25352552

[16] Dipu, S., Kumar, A., Gnana, S. (2012): Effect of chelating agents in phytoremediation of heavy metals. – Remediation Journal 22(2): 133-146. http://onlinelibrary.wiley.com/doi/10.1002/rem.21304/abstract.
[17] Donahue, J., Moses, C., Cramer, C., Brabau, E., Grene, R. (1997): Responses of antioxidants to paraquat in Pea Leaves. – Plant Physiol. 113: 249-257. Recuperado de: http://www.plantphysiol.org/content/113/1/249.long.
[18] Doncheva, S., Moustakas, M., Ananieva, K., Chavdarova, M., Gesheva, E., Vassilevska, R., Mateev, P. (2012): Plant response to lead in the presence or absence EDTA in two sunflower genotypes (cultivated H. annuus cv. 1114 and interspecific line H. annuus x H. argophyllus). – Environ Sci Pollut Res Int. 20(2): 823-833. doi: 10.1007/s11356-012-1274-5.
[19] Ebrahimi, M. (2013): Effect of EDTA application on heavy metals uptake and germination of Echinochloa cruz galii (L.) Beave in contaminated soil. – International Journal of Agriculture and Crop Sciences 6(4): 197-202.
[20] Evangelou, M., Ebel, M., Schaeffer, A. (2007): Chelate assisted phytoextraction of heavy metals from soil. Effect, mechanism, toxicity, and fate of chelating agents. – Chemosphere 68: 989-1003.
[21] Ewais, E. A. (1997): Effects of cadmium, nickel and lead on growth, chlorophyll content and proteins of weeds. – Biologia Plantarum 39(3): 403-410.
[22] Fryzova, R., Pohanka, M., Martinkova, P., Cihlarova, H., Brtnicky, M., Hladky, J., Kynicky, J. (2017): Oxidative stress and heavy metals in plants. – Rev. Environ Contam Toxicol. 245: 129-156. doi: 10.1007/398_2017_7.
[23] Gajewska, E., Sklodowska, M., Slaba, M., Mazur, J. (2006): Effect of nickel on antioxidative enzyme activities, proline and chorophyll contents in wheat shoots. – Biologia Plantarum 50(4): 653-659.
[24] Gratao, P., Polle, A., Lea, P., Azebedo, R. (2005): Making the life of heavy metal-stressed plants a Little easier. – Functional Plant Biology 32: 481-494.
[25] Greman, H., Veliconja-Bolta, S., Vodnik, D., Kos, B., Lestan, D. (2001): EDTA enhanced heavy metal phytoextraction: metal accumulation, leaching and toxicity. – Plant and Soil 235: 105-114.
[26] Gupta, D., Corpas, F., Palma, J. (2013): Heavy metal stress in plants. – España doi: 10.1007/978-3-642-38469-1.
[27] Hadi, F., Bano, A., Fuller, M. P. (2010): The improved phytoextraction of lead (Pb) and the growth of maize (*Zea mays* L.): the role of plant growth regulators (GA3 and AIA) and EDTA alone and in combinations. – Chemosphere 80: 457-462.
[28] Hameed, A., Rasool, S., Azooz, M., Anwar, M., Abass, M., Ahmad, P. (2016): Heavy metal stress: plant responses and signaling. – In: Ahmad, P. (ed.) Plant Metal Interaction, emerging remediation techniques. Elsevier, Amsterdam.
[29] Hartman, H., Kester, D., Davies, F. T., Geneve, R. (2002): Plant Propagation: Principles and Practices. – 6th ed. Prentice Hall.
[30] Hasan, K., Cheng, Y., Kanwar, M. K., Chu, X. Y., Ahammed, G. J., Qi, Z. Y. (2017): Responses of Plant Proteins to Heavy Metal Stress - A Review. – Frontiers in Plant Science 8(1-16).
[31] Hou, W., Chen, X., Song, G., Wang, Q., Chang, Ch. (2007): Effects of copper and cadmium on heavy metal polluted waterbody restoration by duckweed (lemna minor). – Plant Physiol and Biochemistry 45: 62-69.
[32] Hu, R., Sun, K., Pan, Y., Zhang, Y. X., Wang, X. P. (2012): Physiological responses and tolerance mechanism to Pb in two xerophils: Salsola passerina Bunge and *Chenopodium álbum* L. – Journal of Hazardous materials 205: 131-138.
[33] INIA (2017): Manual de procedimientos de los análisis de suelos y agua con fines de riego. – Ministerio de Agricultura y Riego, Lima-Perú, 80p.

http://www.aloki.hu ● ISSN 1589 1623 (Print) ● ISSN 1785 0037 (Online)
DOI: http://dx.doi.org/10.15666/aeer/2003_25352552

[34] Islam, E., Liu, D., Li, T., Yang, X., Jin, X., Mahmood, Q., Tian, S., Li, J. (2008): Effect of Pb toxicity on leaf growth, physiology and ultrastructure in the two ecotypes of Elsholtzia argyi. – Journal of Hazardous Materials 154: 914-926.
[35] John, R., Ahmad, P., Gadgil, K., Sharma, S. (2009): Heavy metal toxicity: Effect on plant growth, biochemical parameters and metal accumulation by *Brassica juncea* L. – International Journal of Plant Production 3(3).
[36] Jouili, H., El Ferjani, E. (2003): Changes in antioxidant and lignifying enzyme activities in sunflower roots (*Helianthus annuus* L.) stressed with copper excess. – C. R. Biologies 326: 639-644.
[37] Kadukova, J., Kavulicova, J. (2010): Phytoremediation and stress. Evaluation of heavy metal-induced stress in plants. – Nova Science Publishers, Inc. ISBN 978-1-61761-319-7. New York.
[38] Ke, W., Xiong, Z. T., Chen, S., Chen, J. (2007): Effects of copper and mineral nutrition on growth, copper accumulation and mineral element uptake in two Rumex japonicus populations from a copper mine and an uncontaminated field sites. – Environmental and Experimental Botany 59: 5967.
[39] Khalid, S., Shahid, M., Khan, N., Murtaza, B., Bibi, I., Dumat, C. (2017): A comparison of technologies for remediation of heavy metal contaminated soils. – Journal of Geochemical Exploration 182: 247-268. Doi: 10.1016/j.gexplo.2016.11.021.
[40] Khan, M. I., Khan, N. A. (2017): Reactive Oxygen species and antioxidant systems in plants: role and regulation under abiotic stress. – Springer Nature Singapore. Doi: 10.1007/978-981-10-5254-5.
[41] Kumar, A., Prasad, M. N. (2018): Plant-lead: interactions: transport, toxicity, tolerance, and detoxification mechanism. – Ecotoxicology and Environmental Safety 166: 401-418. Doi: 10.1016/j.ecoenv.2018.09.113.
[42] Luo, Ch., Shen, Z., Lou, L., Li, X. (2006): EDDS and EDTA-enhanced phytoextraction of metals from artificially contaminated soil and residual effects of chelant compounds. – Environmental Pollution 144: 862-871. Doi: 10.1016/j.envpol.2006.02.012.
[43] Meers, E., Vandecasteele, B., Ruttens, A., Vangronsveld, J., Tack, F. M. (2007): Potential of five willow species (Salix spp.) for phytoextraction of heavy metals. – Environmental and Experimental Botany 60: 57-68.
[44] Mishra, P., Dubey, R. S. (2013): Excess nickel modulates activities of carbohydrate metabolizing enzymes and induces accumulation of sugars by upregulating acid invertase and sucrose synthase in rice seedlings. – Biometals 26: 97-111.
[45] Moreno, L., Crespo, S., Pérez, W., Melgarejo, L. (2002): Pruebas Bioquímicas como herramientas para estudios de fisiología. En: Experimentos en Fisiología Vegetal. – Universidad Nacional de Colombia, Bogotá, Departamento de Biología, pp. 187-248.
[46] Mourato, M. P., Martins, L. L., Campos-Andrada, M. P. (2009): Physiological responses of Lupinus luteous to different copper concentrations. – Biologia Plantarum 53(1): 105-111.
[47] Nikolic, N., Zoric, L., Cvetkovic, I., Pajevic, S., Borisev, M., Orlovic, S., Pilipovic, A. (2016): Assessment of cadmium tolerance and phytoextraction ability in Young Populus deltoides L. and Populus x euramericana plants through morpho-anatomical and physiological responses to growth in cadmium enriched soil. – iForest Biogeosciences and Forestry 10(3): 635-644. doi: 10.3832/ifor2165-010.
[48] Nouri, J., Khorasani, N., Lorestani, B., Karami, M., Hassani, A. H., Yousefi, N. (2009): Accumulation of heavy metals in soil and uptake by plant species with phytoremediation potential. – Environ. Earth Sci 59: 315-323.
[49] Palma, J., Sandalio, L., Corpas, F., Romero-Puertas, M., McCarthy, I., Del Río, L. (2002): Plant proteases, protein degradation, and oxidative stress: role of peroxisomes. – Plant Physiol. Biochem. 40(6-8): 521-530. Doi: 10.1016/S0981-9428(02)01404-3.

http://www.aloki.hu ● ISSN 1589 1623 (Print) ● ISSN 1785 0037 (Online)
DOI: http://dx.doi.org/10.15666/aeer/2003_25352552

[50] Pinhero, R., Rao, M., Paliyath, G, Murr, D., Fletcher, A. (1997): Changes in activities of antioxidant enzymes and their relationship to genetic and Paclobutrazol-induced chilling tolerance of Maize seddlings. – Plant Physiol. 114: 695-704.
[51] Raza, A., Hussain, S., Javed, R., Hafeez, M. B., Hasanuzzaman, M. (2021): Antioxidant defense systems and remediation of metal toicity in Plants. – Approaches to the Remediation of Inorganic Pollutants 1: 91-124. Doi: 10.1007/978-981-15-6221-1_6.
[52] Reddy, A. M., Kumar, S. G., Jyothsnakumari, G., Thimmanaik, S., Sudhaker, C. (2005): Lead induced changes in antioxidant metabolism of horsegram (Macrotyloma uniflorum (Lam.) Verdc.) and bengalgram (Cicer arietinum L.). – Chemophere 60: 97-104.
[53] Romero-Puertas, M. C., Corpas, F. J., Rodriguez-Serrano, M., Gomez, M., del Rio, L. A., Sandalio, L. M. (2007): Differential expresión and regulation of antioxidative enzymes by cadmium in pea plants. – Journal of Plant Physiology 164: 1346-1357.
[54] Rosa, M., Prado, C., Podazza, G., Internodato, R., Gonzalez, J. A., Hilal, M., Prado, F. (2009): Soluble sugars Metabolism, sensing and abiotic stress. – Plant Signaling and Behavior 4(5): 388-393.
[55] Solhi, M., Hajabbasi, M., Shareatmadari, H. (2005): Heavy metals extraction potential of Sunflower (Helianthus annuus) and canola (Brassica napus). – Caspian Journal of environmental sciences 3(1): 35-42.
[56] Steubing, L., Godoy, R., Alberdi, M. (2001): Métodos de ecología vegetal. – Editorial Universitaria S.A. ISBN 956-11-1589-1. Chile.
[57] Tian, S., Lu, L., Yang, X., Huang, H., Brown, P., Labavitch, J., Liao, H., He, Z. (2011): The impact of EDTA on lead distribution and speciation in the accumulator Sedum alfredii by synchrotron X-ray investigation. – Environmental Pollution 159: 782-788.
[58] Vamerali, T., Bandiera, M., Mosca, G. (2010): Field crops for phytoremediation of metal-contaminated land. A review. – Environ. Chem. Lett. 8(1-17). Doi: 10.1007/s10311-009-0268-0.
[59] Van den Ende, W., Valluru, R. (2009): Sucrose, sucrosyl oligosaccharides, and oxidative stress: scavenging and salvaging? – Journal of Experimental Botany 60(1): 9-18.
[60] Varun, M., D'Souza, R., Favas, P., Pratas, J., Paul, M. (2015): Utilization and supplementation of phytoextraction potential of some terrestrial plants in metal-contaminated soils. – Phytoremediation: Management of Environmental Contaminats 1: 177-200. Doi: 10.1007/978-3-319-10395-2_13.
[61] Vásquez, K. (1998): Identificación de plantas hiperacumuladoras de cobre, plomo y hierro en los yacimientos de Yarabamba. – Facultad de Ciencias Biológicas, Universidad Nacional de San Agustín.
[62] Verma, S., Dubey, R. S. (2001): Effect of cadmium on soluble sugars and enzymes of their metabolism in rice. – Biologia Plantarum 44(1): 117-123.
[63] Yruela, I. (2009): Copper in plants: acquisition, transport and interactions. – Functional Plant Biology 36: 409-430.
[64] Zhao, S., Blumwald, E. (1998): Changes in oxidation-reduction state and antioxidant enzymes in the roots of Jack pine seedlings during cold acclimation. – Physiologia Plantarum 104: 134-142.
Recuperado de: https://doi.org/10.1034/j.1399-3054.1998.1040117.x.
[65] Zhao, Z., Xi, M., Jiang, G., Liu, X., Bai, Z., Huang, Y. (2010): Effects of IDSA, EDDS and EDTA on heavy metals accumulation in hydroponically grown maize (*Zea mays* L.). – Journal of Hazardous Materials 181: 455-459.
[66] Zhou, J., Deng, C., Si, S., Shi, Y., Zhao, X. (2011): Study on the effect of EDTA on the photocatalytic reduction of mercury onto nanocrystalline titania using quartz crystal microbalance y differential pulse voltammetry. – Electrochimica 56(5): 2062-2067.
[67] Zuccarelli, R., Frechi, L. (2018): Glutathione Reductase: safeguarding plant cells against oxidative damage. – In: Gupta, D., Palma, J. M., Corpas, F. J. (eds.) Antioxidants and antioxidants enzymes in higher plants. Springer International Publishing.

http://www.aloki.hu ● ISSN 1589 1623 (Print) ● ISSN 1785 0037 (Online)
DOI: http://dx.doi.org/10.15666/aeer/2003_25352552

DETERMINATION OF SEED-BORNE FUNGI IN SOME MEDICINAL AND AROMATIC PLANTS

KAYGUSUZ, T.[1] – COŞKUNTUNA, A.[2*]

[1]*Agricultural Credit Cooperatives of Turkey, Sarkoy, Tekirdag, Turkey*

[2]*Department of Plant Protection, Faculty of Agriculture, Tekirdag Namik Kemal University, Tekirdag 59030, Turkey*

[*]*Corresponding author*
e-mail: acoskuntuna@nku.edu.tr

(Received 10th Dec 2021; accepted 21st Mar 2022)

Abstract. The aim of this study was to identify as well as to determine and pathogenicity of fungi, using the agar plate and blotter method, associated with the seeds of anise (*Pimpinella anisum*), coriander (*Coriandrum sativum*), flax (*Linum usitatissimum*), fenugreek (*Trigonella foenumgraecum*), fennel (*Foeniculum vulgare*), and lemon balm (*Melissa officinalis*). A total of six fungi namely *Alternaria alternata*, *Aspergillus niger*, *Arthrinium arundinis*, *Botrytis cinerea*, *Cladosporium sphaerospermum*, and *Penicillium* spp. isolated from seeds of the medicinal and aromatic plants. Pathogenicity tests demonstrated that *A. alternata* was pathogenic in lemon balm and fenugreek seeds at the rates of 70 and 75%, respectively. *B. cinerea* was determined as a pathogen in lemon balm seed at the rate of 35%. *A. arundinis* was detected at rates of 96 and 67% pathogen in coriander and lemon balm seeds, respectively. *A. niger* was determined as pathogen in coriander seed at the rate of 100%. *C. sphaerospermum* was found as pathogen in fennel and flax seeds at the rates of 86 to 90%, respectively. To our knowledge this is the first report on *A. alternata, B. cinerea* and *A. arundinis* isolated from melissa seeds in Turkey. This study also represents the first reported cases of *C. sphaerospermum* in flax and fennel seeds and *A. alternata* in fenugreek seeds and *A. niger* and *A. arundinis* on coriander seeds for Turkey.
Keywords: *anise, coriander, flax, fennel, fenugreek, lemon balm, fungal disease, pathogenicity*

Introduction

Anise, coriander, flax, fennel, fenugreek and lemon balm are among the most important medicinal aromatic plants that can be propagated by seeds. In recent years, interest in the use of herbal medicine has increased in the world (Singh et al., 2016). Those products are more environment friendly or understanding the method of action could lead to develop more efficient and less harmful drugs. On the other hand, some of the synthetic drug raw materials used in various treatments may have very dangerous side effects for human health. Thus, scientific studies on the field of alternative medicine that focus on medicinal and aromatic plants make products derived from these species (Faydaoğlu and Sürücüoğlu, 2011). According to the data of the World Health Organization (WHO), 80% of the population in underdeveloped countries are using traditional medicines for treatment, while this rate is about 40% in developed countries. The utilization rate of medicinal plants is expected to increase all over the world in the future (Acıbuca and Budak, 2018). In addition to the use of medicinal and aromatic plants in the pharmaceutical industry; the refreshing effect of spices, cleaning products, toothpaste, chewing gum and herbal teas and their natural presence in cosmetics is of great importance. Besides that, the use of medicinal and aromatic plants as organic fertilizers in organic agriculture also increases the beneficial microbial population, helping to improve yield and quality in plant production (Badalingappanavar et al., 2018).

http://www.aloki.hu ● ISSN 1589 1623 (Print) ● ISSN 1785 0037 (Online)
DOI: http://dx.doi.org/10.15666/aeer/2003_25532564

According to the information belonging to 12000 plant taxa in Turkey, which naturally occur and approximately one third of those taxa are endemic. In Turkey, 347 medicinal and aromatic plant species are traded in domestic and foreign trade and 139 the plant are exported. Medicinal and aromatic plants collected in Turkey often provided by nature. This situation makes it difficult to keep healthy statistical data on this issue (Bingol et al., 2019).

The exports of medicinal and aromatic plants increased from 112 million dollars in 2002 to 280 million dollars at the end of 2015 with a change of 150%. The most important crops for export are thyme, poppy, laurel, tea, anise, cumin, sage, mahaleb, red pepper and herbal teas (lime, rosehip, sage, mixed fruits, etc.) in Turkey (Temel et al., 2018). In accordance with 2020 data of Turkey Statistical Institute, annual lemon balm, coriander, fenugreek, fennel and anise production in Turkey were 150, 188, 713, 4365 and 10716 tons, respectively (TUIK, 2020).

In nature, various pathogenic fungi, bacteria, viruses and phytoplasmas can infect foliage, fresh stems and rhizosphera plant parts of the medicinal and aromatic plants. Air-borne fungal diseases such as powdery mildew, rust, and some leaf blight affect the development of these plants negatively. Medicinal and aromatic plants are also affected by disease caused by soil-borne fungi and bacteria pathogens such as damping off, root rot, wilt, anthracnose, and dieback (Sing et al., 2016). Seed-borne fungal pathogens cause a decrease in seed quality, germination capability and a decrease in the amount of product to be taken from the plant. Researches on the detection of seed-borne fungal diseases focus mostly on anise, coriander, fennel, cumin and mustard seeds among medicinal aromatic plants. In seed-borne fungi isolations realised on coriander, fennel, cumin and anise seeds, *A. dauci*, *A. radicina*, *A. petroselini* and *A. alternata* species belong to the genus *Alternaria* were identified in previous studies (Demirci and Hancıoğlu, 1994; Bulajić et al., 2009; Özer and Bayraktar, 2015). *Aspergillus*, *Botrytis, Colletotrichum*, *Fusarium*, *Penicillium*, *Trichoderma*, *Cladosporium*, *Mucor*, *Epicoccum*, *Phoma*, *Rhizoctonia*, *Acremonium*, *Curvularia* and *Rhizopus* are among the genus of pathogen fungi most isolated from medicinal aromatic plant seeds (Sing et al., 2013; Özer and Bayraktar, 2015; Pavlović et al., 2016; Akhtar et al., 2017; Gahukar, 2018; Mangwende et al., 2018). The objective of this study was to identify seed-borne fungi and their pathogenicity on anise, coriander, flax, fennel, fenugreek, and lemon balm seeds.

Materials and methods

Detection of seed-borne mycoflora of medicinal and aromatic plant seeds

Seeds of anise (*P. anisum*), coriander (*C. sativum*), flax (*L. usitatissimum*), fennel (*F. vulgare*), fenugreek (*T. foenumgraecum*), and lemon balm (*M. officinalis*) were obtained from Tekirdag Namik Kemal University, Department of Field Crops in Turkey. The seeds were stored in 50 g paper bags for isolation at 4 °C in a refrigerator. Four hundred seeds of each the medicinal and aromatic plant seeds were randomly selected. The seeds were surface sterilized in 2% sodium hypochlorite for 3 minutes, and then rinsed in sterile distilled water (SDS) twice and dried on sterile filter paper in a sterile bench. The surface sterilized seeds were transferred on potato dextrose agar (PDA) medium (Merck, Darmstad, Germany) (containing streptomycin 0.1 g/1000 ml SDS and chloramphenicol 0.05 g/1000 ml SDS: Sigma-Aldric, Germany) in 9 cm diameter sterilized Petri plates. The Petri plates were incubated for 7-10 days at 23 °C under for a 12 h dark/light cycle. There were 10 seeds in each Petri plates. Each treatment was replicated 40 times. After 7-10 days of

http://www.aloki.hu ● ISSN 1589 1623 (Print) ● ISSN 1785 0037 (Online)
DOI: http://dx.doi.org/10.15666/aeer/2003_25532564

incubation period, fungal colonies growing on the seeds were individually examined with the aid of a stereomicroscope. The single spore isolations of seed-borne fungi were done by Agar Plate Methods in which pre-sterilized (hot air) petri plates were taken and plated either with sterilized PDA, Potato Carrot Agar (PCA), Water Agar and Oat Flour Agar. Each of the purified fungus isolates was examined at 40× to 100× with a Zeiss light microscope according to their growth rate, culture colors, conidiophore and conidia structures and their taxonomic characteristics were identified, and grouped based on morphological appearance and recorded (Domsch et al., 1980; Ellis and Ellis, 1997; Lawrence et al., 2016).

The percentage frequency of occurrence of various fungal species was calculated as follows (*Eq.1*):

$$\text{Frequency of occurrence (\%)} = \frac{\text{Number of seeds on which a fungal species occurs}}{\text{Total Number of seeds}} \text{ x } 100 \qquad \text{(Eq.1)}$$

For the pathogenicity tests of the isolates grouped at the species or genus level, isolates representing each group were selected and single spore isolations were made. The isolation of fungi studies was carried out in Mycology Laboratory Department of Plant Protection, Faculty of Agriculture, Tekirdag Namik Kemal University.

In vitro pathogenicity test

Fungi species isolated from each seed variety were grouped primarily at the genus and species level. Single spore isolates of the isolate representing each group were prepared, and their morphological diagnosis was made by examining them under a microscope. Pathogenicity testing was performed with a representative isolate of each morphologically diagnosed fungus species. As described in the determination of fungal flora, first of all, surface sterilization was applied to all the seeds. For the pathogenicity test of *Alternaria alternata* and *Cladosporium sphaerospermum* spore concentration were adjusted to 1 x 10^5 spores/ml by diluting in SDS. Inoculum concentration of *Aspergillus niger*, *Arthrinium arundinis* and *Botrytis cinerea* were adjusted to a final concentration of 1 x 10^4 spores / ml (Noelting et al., 2012; Singh et al., 2013; Akhdar et al., 2017). The seeds were dipped into the prepared conidia suspensions, 10 µl Tween 20 was added and shaken with a rotary shaker for 1 hour. The seeds inoculated with fungal isolates were placed on sterile blotting papers and allowed to dry for 30 minutes. Four layers of blotter (in size equivalent to each petri plate) were soaked in SDS. Ten seeds were placed in each petri dishes. After planting the seeds in the petri plates were incubated for 7-10 days at 24±1°C with a cycle of 12 hours light and 12 hours darkness. The experiment was conducted in a completely randomized design with four replicates and repeated twice. Observed et the end of the incubation period, each seed was evaluated as disease-healthy. The pathogenic fungi were re-isolated from diseased seed. Conversely, the control petri plate which contain only sterilized seeds did not show any symptoms. Pathogenicity test was performed on the all seeds included in the experiment for all isolates that were diagnosed morphologically.

Molecular identification

Molecular diagnosis was performed for 3 isolates among the morphologically identified isolates. A representative fungal isolate was selected for the diagnosis of the molecular properties of *A. alternata* and *Arthrinium arundinis* from lemon balm seeds

http://www.aloki.hu ● ISSN 1589 1623 (Print) ● ISSN 1785 0037 (Online)
DOI: http://dx.doi.org/10.15666/aeer/2003_25532564

and *C. sphaerospermum* isolated from fennel seeds. Identity confirmation of *A. alternata* isolate TR-MeAa3 and *C. sphaerospermum* isolate TR-ReCs13 and *A. arundinis* TR-MeArtA5 isolate were realised by the polymerase chain reaction (PCR). Ribosomal fungal DNA extraction was conducted using the method from Özer and Bayraktar (2015). Fungal isolates were grown on PDA medium at 25±1°C for 7-10 days. Fungal mycelia of each isolate were gently scraped with a sterile spatula from the surface of PDA medium and suspended in 500 µl extraction buffer (50 mM Tris-HCl pH: 7.5, 50 mM EDTA, 3% SDS). Two times extractions with phenol/chloroform/isoamylalcohol (24:1:1; v/v/v) were done, DNA was precipitated by addition of 0.5 volume of 7.5 M ammonium acetate and 1.5 volume of isopropanol. The resultant pellet was rinsed with ethanol suspended in ddH_2O, and stored at -20°C. The identification of the isolates representing different fungal species was confirmed by DNA sequence analysis with the primer pairs ITS1/4 and Alt for /rev described by White et al. (1990) and Hong et al. (2005), respectively. PCR reaction was carried out in 50 ml mixture containing 5 µl reaction buffer (10×), 1.5 mM of $MgCl_2$, 0.4 µl of each primer, 0.2 mM of dNTPs, 1.5 unit of Taq DNA polymerase (MBI; Fermentas, Leon-Rot, Germany) and remaining deionised water. PCR amplification was performed in a thermal cycler programmed as follows: one cycle of 94°C for 1 min, 35 cycles of 94°C for 30 s, 57°C for 30 s, 72°C for 1 min, and during 10 min at 72°C. The amplified DNA products were sequenced in both directions using the same primers in NABILTEM Laboratory. For the identification of the fungal isolates, the sequences were subjected to BLAST searches within NCBI database. Sequence analysis and comparison of the fungus isolates were conducted using MEGA 6.0 software (Tamura et al., 2013).

Statistical analysis

In the study, the data obtained as a result of the pathogenicity tests were statistically analyzed using the one-way ANOVA procedures in SPSS (Statistical Package for Social Sciences, Inc., 2001, Model 11.0. Chicago). The differences between the the treatment means were compared according to the Duncan Multiple Comparison test ($P \leq 0.01$).

Results

Detection test

Six fungal species namely *Alternaria alternata*, *Aspergillus niger, Arthrinium arundinis, Botrytis cinerea, Cladosporium sphaerospermum* and *Penicillium spp.* were detected from the seeds of medicinal and aromatic plants. *A. alternata* was the first species has the highest incidence isolated from in leman balm (19%) and fenugreek (25%) seeds, respectively has many in host plants and producing toxins (*Table 1*).

The second species of higher frequency in fennel, anise and flax seeds was *Penicillium* spp. But, *Penicillium* species isolated from all seeds, especially anise seeds, were thought to be saprophytes. Preliminary pathogenicity tests (results no given) showed that *Penicillium* spp. did not caused disease and so was not used other pathogenicity test in this study. Highest percentage of *A. arundinis* was also found in lemon balm seeds (2.25%) followed by coriander seeds (0.25%). *A. niger* had low incidence (0.50%) only in coriander seeds examined. Percentage of occurence of *B. cinerea* (1.00%) was also recorded only in lemon balm seeds. Percentage of occurence of *C. sphaerospermum* was higher frequency in fennel (2.25%) than flax seeds (1.75%) (*Table 1*).

http://www.aloki.hu ● ISSN 1589 1623 (Print) ● ISSN 1785 0037 (Online)
DOI: http://dx.doi.org/10.15666/aeer/2003_25532564

Table 1. *Percentage of occurrence of seed-borne fungi (%) associated with seeds of the medicinal and aromatic plants*

Seeds	*A. alternata*	*A. arundinis*	*A. niger*	*B. cinerea*	*C. sphaerospermum*	*Penicillium* spp.
Anise	0.00*	0.00	0.00	0.00	0.00	5.00
Coriander	0.00	0.25	0.50	0.00	0.00	0.00
L. balm	19.00	2.25	0.00	1.00	0.00	1.25
Fennel	0.00	0.00	0.00	0.00	2.25	7.50
Fenugreek	25.00	0.00	0.00	0.00	0.00	0.00
Flax	0.00	0.00	0.00	0.00	1.75	5.00

*Each value is the average of four repetitions

Among the medicinal and aromatic plant seeds examined in terms of fungal flora, lemon balm had the highest contamination rate in terms of hosting fungi belong to different species and genera (*Table 1*).

Pathogenicity test

According to the results of the pathogenicity test, the only fungus species growing in fenugreek seeds is *A. alternata* was found to be pathogenic at a rate of 75.00± 3.53%. *A. alternata* was also isolated from lemon balm seeds and its pathogenicity was calculated as 70.00± 2.54% (*Table 2*, *Fig. 1*).

Table 2. *Pathogenicity of the fungi associated with medicinal and aromatic seeds (%)*

Seeds	*A. alternata*	*A. arundinis*	*A. niger*	*B. cinerea*	*C. sphaerospermum*
Coriander	0.00±0.00 ^{b}*	96.00 ± 2.16 ^{a}	100 ± 0.00 ^{a}	0.00 ± 0.00 ^{b}	0.00 ± 0.00 ^{b}
L. balm	70.00±2.54 ^{a}	67.00 ± 6.04 ^{b}	0.00 ± 0.00 ^{b}	35.00 ± 2.04 ^{a}	0.00 ± 0.00 ^{b}
Fennel	0.00±0.00 ^{b}	0.00 ±0.00 ^{c}	0.00 ± 0.00 ^{b}	0.00 ± 0.00 ^{b}	86.00 ± 2.16 ^{a}
Fenugreek	75.00±3.53 ^{a}	0.00 ±0.00 ^{c}	0.00 ± 0.00 ^{b}	0.00 ± 0.00 ^{b}	0.00 ± 0.00 ^{b}
Flax	0.00±0.00 ^{b}	0.00 ±0.00 ^{c}	0.00 ± 0.00 ^{b}	0.00 ± 0.00 ^{b}	90.00 ± 2.16 ^{a}

*: Each value in the same column is the average of four repetitions and the values shown with different letters are significantly different according to Duncan Multiple Comparison Test (P≤0.01)

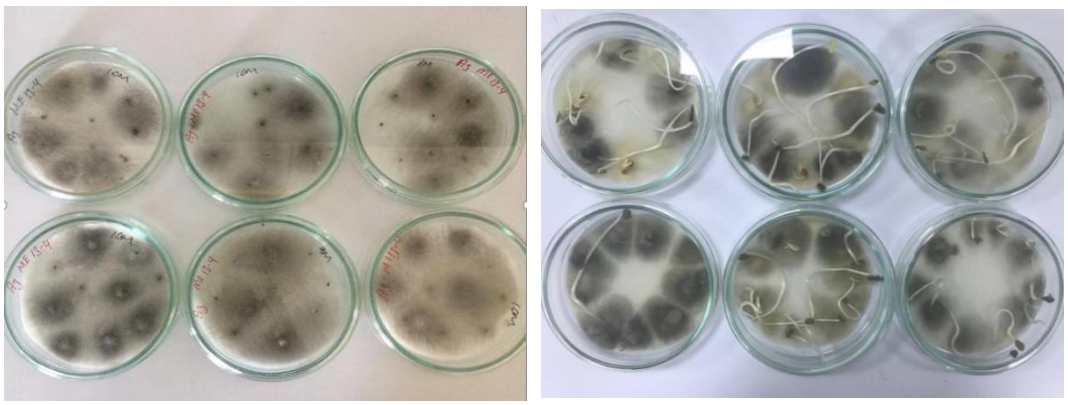

Figure 1. *Pathogenicity of A. alternata TR-MeAa3 in lemon balm (left) and fenugreek seeds (right)*

http://www.aloki.hu ● ISSN 1589 1623 (Print) ● ISSN 1785 0037 (Online)
DOI: http://dx.doi.org/10.15666/aeer/2003_25532564

There is no statistically significant difference between the disease severity of *A. alternata* developed in fenugreek and lemon balm ($p \geq 0.01$) (*Table 2*). It was recorded that *B. cinerea* only developed in lemon balm seeds and showed disease severity of 35± 2.04%. *A. arundinis* was also found to be 67± 6.04% pathogen in lemon balm seeds (*Fig. 2*). This fungus was also recorded pathogen in coriander seeds, and the disease severity was found to be statistically significant at a rate of 96± 2.16% compared to lemon balm seeds ($p \leq 0.01$). It was detected that *A. niger* has a high rate of pathogen (100± 0.00%) only from coriander seeds. *C. sphaerospermum* was noted as pathogen fungi at the rate of 86± 2.16% in fennel seeds and at the rate of 90± 2.16% in flax seeds (*Fig. 3*). Statistically, the difference in disease severity between them is not significant ($p \geq 0.01$) (*Table 2*). There was discolaration and brown symptoms on the diseased seeds caused by *A. alternata*, *A. arundinis*, and *C. sphaeraspermum*. These seeds, including those that germinated, rotted at the end of the pathogenicity test.

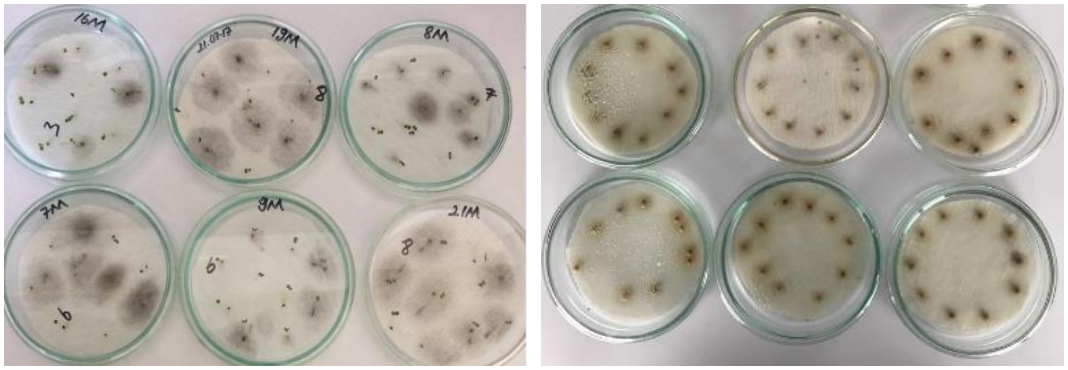

Figure 2. *Pathogenicity of A. arundinis TR-MeArtA5 in lemon balm (left) and coriander seeds (right)*

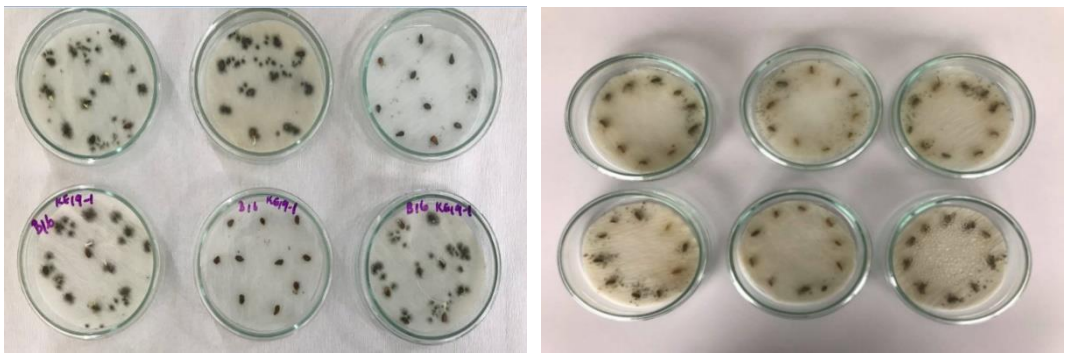

Figure 3. *Pathogenicity of C. sphaerospermum TR-ReCs13 in flax (left) and fennel seeds (right)*

Phylogenetic analyses

The isolates of *Alternaria alternata* TR-MeAa3 (GenBank Acc. No. MK806694) and *Cladosporium sphaerospermum* TR-ReCs13 (GenBank Acc. No. MK806696) and *Arthrinium arundinis* TR-MeArtA5 (GenBank Acc. No. MK806695) were identified based on morphological characters (*Figs. 4,5,6*) were also confirmed to sequenced and checked against the NCBI database. PCR amplification with primers ITS1 and ITS4 yielded a single RNA fragment approximately ranging in length from 525-bp to 591-bp

http://www.aloki.hu ● ISSN 1589 1623 (Print) ● ISSN 1785 0037 (Online)
DOI: http://dx.doi.org/10.15666/aeer/2003_25532564

from *C. sphaerospermum* TR-ReCs13 (525 bp) and *A. alternata* TR-MeAa3 (591 bp) and *A. arundinis* TR-MeArtA5 (580 bp). According to phylogenetic trees of partial sequencing of 18S rRNA gene of the fungal isolates verified the sequences producing significant alignments of partial sequencing of 18S rRNA gene of the fungal isolates compared to those similar strain and isolate in GenBank. *A. alternata* TR-MeAa3 isolate was isolated from lemon balm seeds showed 99 to 100% similarities with 26 *A. alternata* isolates registered in GenBank (*Fig. 4*) (Kleczewski et al., 2012; Woudenberg et al., 2013, 2015; Kovaceć et al., 2016; Mohamed et al., 2016; Vu et al., 2019). *C. sphaerospermum* TR-ReCs13 was isolated from fennel seeds exhibited 99 to 100% similarities with 18 *C. sphaerospermum* isolates and strain registered in GenBank (*Fig. 5*; Zalar et al., 2007). *A. arundinis* TR-MeArtA5 was isolated from lemon balm seeds demonstrated 85 to 100% similarities with 17 *A. arundinis* isolates registered in GenBank (*Fig. 6*; Crous and Groenewald, 2013; Jiang et al., 2018).

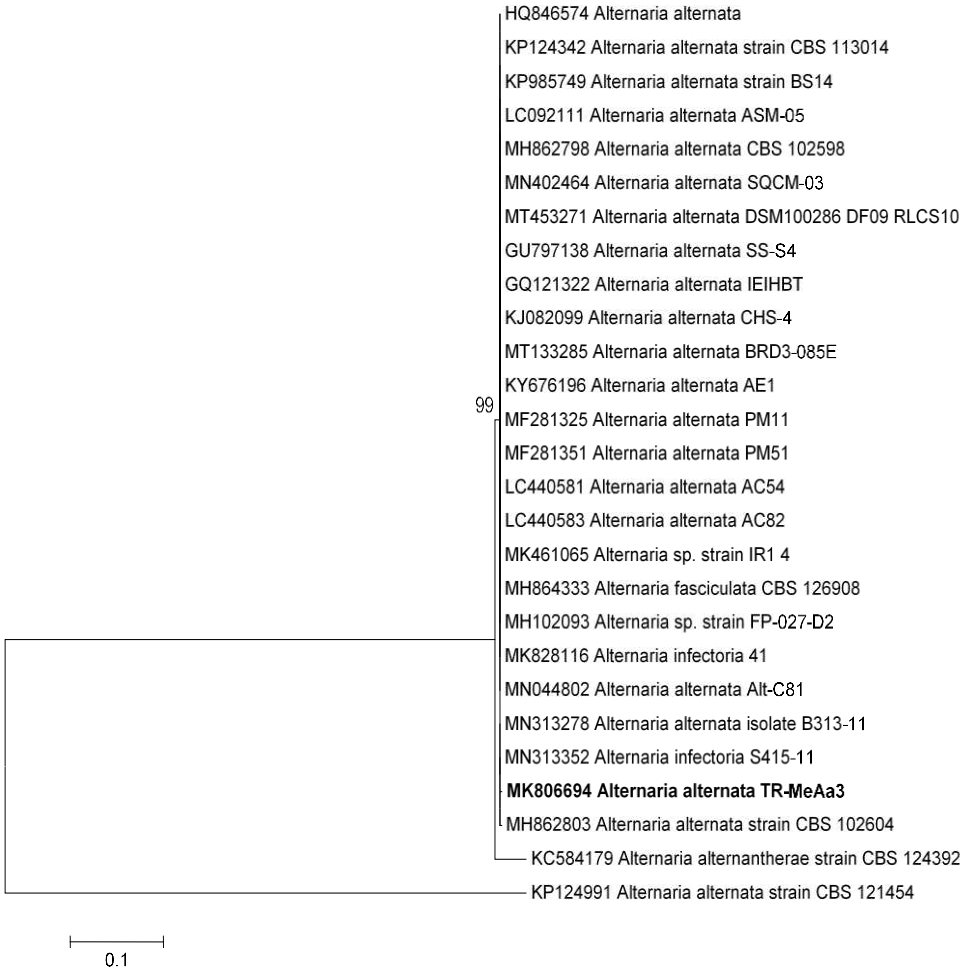

Figure 4. *Phyllogenetic and molecular evolutionary analyses were carried out using MEGA version 6 (Tamura et al. 2013). Maximum likelihood analysis method based on the Kimura-2 model of 27 Alternaria spp. isolates. The sequence of the Turkish isolate from this study is shown in bold. Numbers represent the bootstrap values out of 1000 replicates. Only bootstrap values bigger than 50 are shown*

http://www.aloki.hu ● ISSN 1589 1623 (Print) ● ISSN 1785 0037 (Online)
DOI: http://dx.doi.org/10.15666/aeer/2003_25532564

Figure 5. *Phyllogenetic and molecular evolutionary analyses were carried out using MEGA version 6 (Tamura et al. 2013). Maximum likelihood analysis method based on the Kimura-2 model of 19 Cladosporium spp. isolates. The sequence of the Turkish isolate from this study is shown in bold. Numbers represent the bootstrap values out of 1000 replicates. Only bootstrap values bigger than 50 are shown*

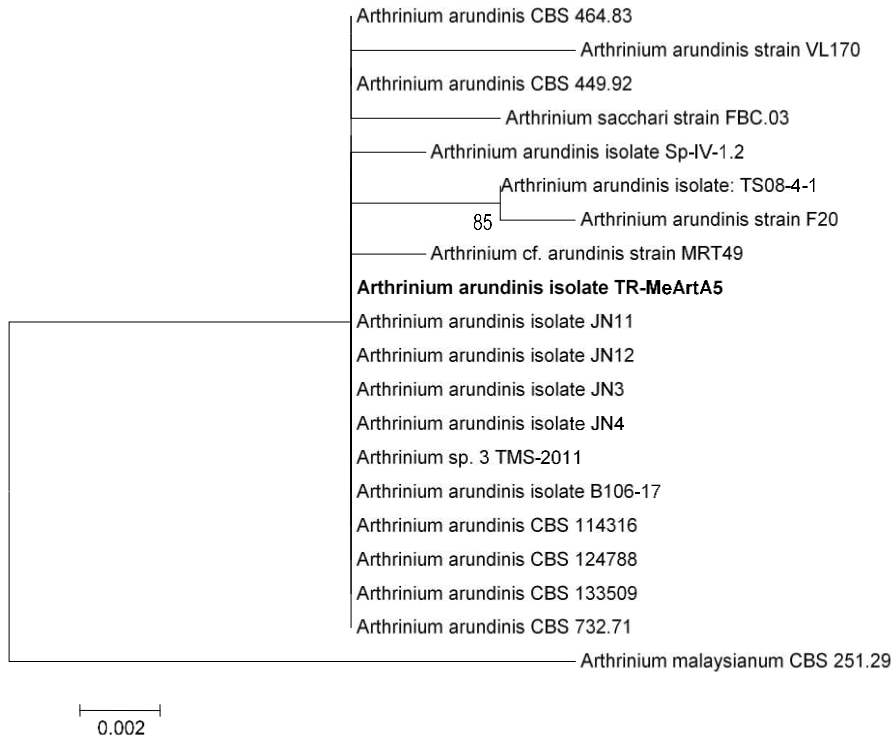

Figure 6. *Phyllogenetic and molecular evolutionary analyses were carried out using MEGA version 6 (Tamura et al. 2013). Maximum likelihood analysis method based on the Kimura-2 model of 20 Arthirinium spp. isolates. The sequence of the Turkish isolate from this study is shown in bold. Numbers represent the bootstrap values out of 1000 replicates. Only bootstrap values bigger than 50 are shown*

http://www.aloki.hu ● ISSN 1589 1623 (Print) ● ISSN 1785 0037 (Online)
DOI: http://dx.doi.org/10.15666/aeer/2003_25532564

Discussion

In this study for the determination of fungal flora in some medicinal and aromatic plant seeds, it was found that the seeds were contaminated with saprophytes and some pathogenic fungi. Among the seeds examined in our study, it was observed that the highest contamination rates in terms of the number of infected seeds were in lemon balm and fenugreek seeds. It has also been found that there are different species of fungi in lemon balm seeds. *A. niger* and *B. cinerea*, *C. sphaerospermum*, *A. alternata*, *A. arundinis*, which grow from flax, lemon balm, coriander, fenugreek, anise, fennel seeds, were observed to be pathogens at different rates. In addition, molecular identification of *A. alternata*, which has a high rate of pathogen in both fenugreek and lemon balm seeds, was also carried out in this study. *A. alternata* showed similar pathogenicity in lemon balm and fenugreek seeds. Similarly, this pathogen was the most isolated fungus from medicinal and aromatic plant seeds in previous studies (Bulajić et al., 2009; Singh et al., 2013; Seyyedi and Moghaddam, 2016; Mangwende et al., 2018). Although literature on seed-borne fungal diseases in medicinal and aromatic plants are restricted, there is more research on fungal diseases caused problem in the leaf, stems and roots of medicinal and aromatic plants (Singh et al., 2016).

The presence of *A. arundinis* in both lemon balm (11.5%) and coriander (5%) seeds was detected, but this rate was higher in lemon balm seeds. It was noted that coriander seeds of the same fungi are more pathogenic than lemon balm seeds. *A. arundinis* showing 96% pathogenicity in coriander seeds, 67% pathogen was found in lemon balm seeds. Although *C. sphaerospermum* was found at lower rates (1.75%) in flax seeds, its pathogenicity was higher (90%), but there was no significant difference with its pathogenicity (86%) in fennel.

It is observed that *A. arundinis* and *A. niger* were isolated from coriander seed and they had high disease severity in the pathogenicity experiment.

A. alternata was detected in previous studies from coriander, fennel, anise, cumin, lemon balm and fenugreek seeds as the same as in our study (El-Nagerabi, 2002; Szczeponek and Mazur, 2006; Sumanth et al., 2010; Singh et al., 2013; Özer and Bayraktar, 2015; Mangwende et al., 2018). At the end of the pathogenicity test of *A. alternata*, the seeds that could germinate from the infected fenugreek seeds were completely rotted after a while due to the infection by the pathogenic fungus. Similarly, *A. alternata* has been reported seed-borne pathogen, and led to brownish necrotic symptoms and death of cumin seed (Özer and Bayraktar, 2015). In other studies, *A. alternata*, *Aspergillus*, *Fusarium*, *Penicillium* and *Rhizopus* species were reported to be isolated from coriander seeds (Singh et al., 2013; Mangwende et al., 2018). Singh et al. (2013), 54 different fungus species were identified in coriander, foeniculum, cumin and brassica seeds, and similar to our study, other than *Aspergillus niger*, *A. flavus* and *A. parasiticus* species were also identified in coriander seeds.

A. arundinis was not isolated from lemon balm and coriander seeds in previous studies. *C. sphaerospermum* was not isolated from fennel and flax seeds in previous studies and its pathogenicity was not investigated the studies on the seeds before. So, these isolates were included in molecular diagnosis. *A. alternata* was detected in previous studies from coriander, fennel, anise, cumin, lemon balm and fenugreek seeds (El-Nagerabi, 2002; Szczeponek and Mazur, 2006; Sumanth et al., 2010; Singh et al., 2013; Mangwende et al., 2018). In addition, *A. alternata* caused leaf spot on coriander plants, and was confirmed to be seed transmitted by Mangwende et al. (2018). As a result, in this research demonstrated that it also represented the *Alternaria alternata* TR-MeAa3 (GenBank Acc.

http://www.aloki.hu ● ISSN 1589 1623 (Print) ● ISSN 1785 0037 (Online)
DOI: http://dx.doi.org/10.15666/aeer/2003_25532564

No. MK806694) isolate was isolated from lemon balm seeds showed 99% similarity to *Alternaria alternata* strain CBS 113014 (GenBank Acc. No. KP124342). However, *A. alternata* isolate (GenBank Acc. No. KT895947.) was isolated on coriander seeds by Mangwende et al. (2018) was recorded to similar to *A. alternata strain* CBS 113014 (GenBank Acc. No. KP124342) 73%.

However, in previous studies in Turkey, only *Alternaria* sp. was isolated from coriander seeds and research was carried out on its chemical control (Demirci and Hancıoğlu, 1994).

A. alternata, *B. cinerea* and *A. arundinis* isolated from melissa seeds were first reports in Turkey. *C. sphaerospermum* was the pathogen on both of flax and fennel seeds. *A. niger* and *A. arundinis* were isolated on coriander seeds that was confirmed as pathogens were first recorded in Turkey. *A. alternata* was detected on fenugreek seeds was also first reported in Turkey.

Conclusions

Medicinal and aromatic plants are used in the medicine, food and cosmetics industries, and the market demand for natural products based on these plants is increasing every year. The use of medicinal and aromatic plants as raw materials for important drugs is increasing. It is known that approximately 25% to 30% of all drugs today are obtained directly or indirectly from the plants.

In this study, the fungi detected as pathogens in medicinal aromatic plants significantly inhibited the seeds germination. It is not possible to grow healthy seedlings from the diseased seeds. Pathogenic fungi reduce yield and quality in medicinal and aromatic plants. In order to be able to control these pathogenic fungi, it is very important to know which fungi species are capable of causing disease.

Therefore, the genetic resistance of the seed varieties of medicinal and aromatic plants to be used in production against these pathogens should be examined and the production of non-resistant seeds should not be allowed. Considering the studies conducted in the world in general, molecular studies on the detection of seed-borne fungi in medicinal and aromatic plant seeds are very few. This research is the first detailed study in seed-borne fungi on medicinal and aromatic plant seeds. *Alternaria alternata*, *Botrytis cinerea* and *A. arundinis*, isolated from lemon balm seeds; *C. sphaerospermum* in flax seeds; *A. alternata* in fenugreek; It is the first registration for Turkey. The study is an enlightening nature for the next researches to be carried out for the detection of seed-borne disease factors and their pathogenicity. Considering the pathogen host relationships in disease development, the data we obtained in this study will form the basis for future research on the control of these diseases.

Acknowledgements. We wish to thank Professor Canan Sağlam for providing medicinal and aromatic plant seeds. We wish to thank Professor Gassan Köklü and Professor Harun Bayraktar for help with phylogenetic analysis.

REFERENCES

[1] Acıbuca, V., Budak, D. B. (2018): The place and importance of medicinal and aromatic plants in Turkey and in the world. (Dünya'da veTürkiye'de tıbbi ve aromatik bitkilerin yeri ve önemi.). – Çukurova Tarım Gıda Bil. Dergisi 33(1): 37-44.

http://www.aloki.hu ● ISSN 1589 1623 (Print) ● ISSN 1785 0037 (Online)
DOI: http://dx.doi.org/10.15666/aeer/2003_25532564

[2] Akhtar, J., Sing, B., Kandan, A., Kumar, P., Maurya, A. K., Chand, D., Gupta, V., Dubey S. C. (2017): Status of seed-borne fungi in some indigenous medicinal and aromatic plants conserved in National Gene Bank, India. – Indian Pyhtopathology 70: 206-215.
[3] Badalingappanavar, R., Hanumanthappa, M., Veeranna, H. K., Kolakar, S., Khidrapure, G. (2018): Organic fertilizer management in cultivation of medicinal and aromatic crops: a review. – Journal of Pharmacognosy and Phytochemistry SP3: 126-129.
[4] Bingol, M. U., Balpınar, N., Guney, K., Guven, F., Ketenoglu, O., Arslan, M., Karakas, M. (2019): Evaluation of threat categories of the endemic plants of deveci mountains (Yozgat-Tokat/Turkey). – Commun. Fac. Sci. Univ. Ank. Series C 28 Number 1: 22-34.
[5] Bulajić, A., Djekić, I., Lakić, N., Krstić, B. (2009): The presence of *Alternaria* spp. on the seed of *Apiaceae* plants and their influence on seed emergence. – Archives of Biological Sciences, Belgrade 61(4): 871-881.
[6] Crous, P., Groenewald, J. (2013): A Phylogenetic re-evaluation of *Arthrinium*. – International Mycological Association 4(1): 133-154.
[7] Demirci, F., Hancıoğlu, Ö. (1994): Control of *Alternaria Blight* of cumin (*Cuminum cyminum* L.) by seed treatement. – 9th Congress of the Mediterranean Phytopathological Union- Kuşadası-Aydın Turkey, pp. 381-382.
[8] Domsch, K. H., Gams, W., Anderson, T. H. (1980): Compedium of soil fungi. – Academic Press, London, 860p.
[9] El-Nagerabi, S. A. F. (2002): Determination of Seedborne Fungi and Detection of Aflatoxins in Sudanese Fenugreek Seeds. – Phytoparasitica 30(1): 61-66.
[10] Ellis, B. M., Ellis, J. P. (1997): Microfungi on landplants: An identification handbook, new (enlarged ed.). – Slough: Richmond Publishing 868p.
[11] Faydaoğlu, E., Sürücüoğlu, M. (2011): The use and economic importance of medicinal and aromatic plants from past to present. (Geçmişten günümüze tıbbi ve aromatik bitkilerin kullanılması ve ekonomik önemi.). – Kastamonu Üniversitesi Orman Fakültesi Dergisi 11(1): 52-67.
[12] Gahukar, R. T. (2018): Management of pests and diseases of important tropical/subtropical medicinal and aromatic plants: A review, India. – Journal of Applied Research on Medicinal and Aromatic Plants 9: 1-18.
[13] Hong, S. G., Cramer, R. A., Lawrence, C. B., Pryor, B. M. (2005): Alt a1 allergen homologs from *Alternaria* and related taxa: analysis of phylogenetic content and secondary structure. – Fungal Genetics and Biology 42: 119-129.
[14] Jiang, N., Li, J., Tian, C. M. (2018): *Arthrinium* species associated with bamboo and reed plants in China. – Fungal Systematics and Evaluation 2: 1-9.
[15] Kleczewski, N. M., Bauer, J. T., Bever, J. D., Clay, K., Reynolds, H. L. (2012): A survey of endophytic fungi of switchgrass (*Panicum virgatum*) in the Midwest, and their putative roles in plant growth. – Fungal Ecology 5(5): 521-529.
[16] Kovaceć, E., Likar, M., Regvar, M. (2016): Temporal changes in fungal communities from buckwheat seeds and their effect in germination and seedling secondary metabolism. – Fungal Biology 120: 666-678.
[17] Lawrence, D. P., Rotondo, F., Ganniba, P. B. (2016): Biodiversity and taxonomy of the pleomorphic genus *Alternaria*. – Mycological Progress 15: 1-22.
[18] Mangwende, E., Kritzinger, Q., Aveling, T. A. S. (2018): *Alternaria alternata*: A new seed-transmitted disease of coriander in South Africa. – European Journal of Plant Pathology 152: 409-416.
[19] Mohamed, S., Al-Yami, M., Sadik, A. (2016): Detection of mycophages associated with fungal strains isolated from soil of KSA and identified via 18S rRNA Gene. – Research Journal of Pharmaceutical Biological Chemical Science 7: 1375-1380.
[20] Noelting, M. C., Molina, M. C., Monaco, C. I., Sandoval, M. C., Perello, A. (2012): First report of *Alternaria infectoria* on amaranth (*Amaranthus caudatus* spp. *mantegazzianus*) in Argentina. – New Disease Reports 25: 11.

http://www.aloki.hu ● ISSN 1589 1623 (Print) ● ISSN 1785 0037 (Online)
DOI: http://dx.doi.org/10.15666/aeer/2003_25532564

[21] Özer, G., Bayraktar, H. (2015): Determination of fungal pathogens associated with *Cuminum cyminum* in Turkey. – Plant Protection Science 51(2): 74-79.
[22] Pavlović, S., Ristić, D., Vucurović, I., Stevanović, M., Stojanović, S., Kuzmanović, S., Starović, M. (2016): Morphology, pathogenicity and molecular identification of *Fusarium* spp. associated with anise seeds in Serbia, Belgrade. – Notulae Botanicae Horti Agrobotanici Cluj-Napoca 44: 411-417.
[23] Seyyedi, S. M., Moghaddam, P. R. (2016): Evaluating the ability of some medicinal plants for controlling *Rhizopus* (*Rhizopus nigricans*) and black spot rot (*Alternaria alternate*) as postharvest diseases in tomato produced under conventional and organic cropping systems. – Iran Journal of Agroecology 8: 318-328.
[24] Singh, B., Gitansh, Bhadauria, S. (2013): Prevalence of seed mycoflora from different seed of spices under field and storage conditions of Agra region. – Asian Journal of Plant Science and Research 3(2): 93-98.
[25] Singh, A., Gupta, R., Saikia, S. K., Pant, A., Pandey, R. (2016): Diseases of medicinal and aromatic plants, their biological impact and management. – Plant Genetic Resources: Characterization and Utilization 14(4): 370-383.
[26] Sumanth, G. T., Bhagawan, M. W., Surendra, R. S., (2010): Incidence of mycoflora from the seeds of Indian main spices. – African Journal of Agricultural Research 5(22): 3122-3125.
[27] Szczeponek, A., Mazur, S. (2006): Occurence of fungal diseases on lemon balm (Mellisa officinalis L.) and peppermint (Mentha x piperita L.) in the region of Malopolska. – Commun Agric Appl Biol Sci. 71(3 Pt B): 1109-1118.
[28] Tamura, K., Stecher, G., Peterson, D., Filipski, A., Kumar, S. (2013): MEGA6: Molecular evolutionary genetics analysis version 6.0. – Molecular Biology and Evolution 30: 2725-2729.
[29] Temel, M., Tınmaz, A. B., Öztürk, M., Gündüz, O. (2018): Production and trade of medicinal-aromatic plants in the Turkey and in the world. (Dünyada ve Türkiye'de tıbbi-aromatik bitkilerin üretimi ve ticareti.). – KSU Journal of Agriculture and Nature 21 (Special Issue): 198-214.
[30] TUIK (2020): Plant Production Statistics. Turkey Prime Ministry, Turkish Statistical Institute. – https://data.tuik.gov.tr/Bulten/Index?p=Crop-Production-2nd-Estimation-2020-33736 (Date of access: 16.02.2021).
[31] Vu, D., Groenewald, M., de Vries, M., Gehrmann, T., Stielow, B., Eberhardt, U., Al-Hatmi, A., Groenewald, J. Z., Cardinali, G., Houbraken, J., Boekhout, T., Crous, P. W., Robert, V., Verkley, G. J. M. (2019): Large-scale generation and analysis of filamentous fungal DNA barcodes boosts coverage for kingdom fungi and reveals thresholds for fungal species and higher taxon delimitation. – Studies in Mycology 92: 135-154.
[32] White, T. J., Bruns, T. D., Lee, S., Taylor, J. (1990): Amplification and direct sequencing of fungal ribosomal genes form phylogenetics. – In: Innis, M. A., Gelfrand, D. H., Sninsky, J. J., White, T. J. (eds.) PCR Protocols. San Diego, Academic Press, pp. 315-322.
[33] Woudenberg, J. H., Groenewald, J. Z., Binder, M., Crous, P. W. (2013): *Alternaria* redefined. – Studies in Mycology 75(1): 171-212.
[34] Woudenberg, J. H., Seidl, M. F., Groenewald, J. Z., de Vries, M., Stielow, J. B., Thomma, B. P., Crous, P. W. (2015): *Alternaria* section *Alternaria*: Species, formae speciales or pathotypes? – Studies in Mycology 82: 1-21.
[35] Zalar, P., Hoog, G. S., Schroers, H.-J., Crous, P. W., Groenewald, J. Z., Gunde-Cimerman, N. (2007): Phylogeny and ecology of the ubiquitous saprobe *Cladosporium sphaerospermum,* with descriptions of seven new species from hypersaline environments. – Studies in Mycology 58: 157-183.

http://www.aloki.hu ● ISSN 1589 1623 (Print) ● ISSN 1785 0037 (Online)
DOI: http://dx.doi.org/10.15666/aeer/2003_25532564

MILLET (*BRASSICA NAPUS* L.) ROTATION MODEL PROMOTED THE YIELD OF MILLET BY IMPROVING THE FUNGAL COMMUNITY STRUCTURE IN DRYLANDS IN CHINA

YU, G. H.[1,2#] – LIU, P. C.[1,2#] – LU, G. L.[1,2] – GUO, A. Q.[1,2] – HAO, H. B.[1,2] – ZHOU, J.[3] – LI, M. Z.[1,2*]

[1]*Institute of Dry Farming, Hebei Academy of Agriculture and Forestry Sciences/Key Lab of Crop Drought Tolerance Research of Hebei Province, Hengshui 053000, P. R. China*
(e-mail: guangwen19840104@163.com – Yu, G. H.)

[2]*Key Lab of Crop Drought Tolerance Research of Hebei Province, Hengshui 053000, P. R. China*
(e-mail: guziketi@163.com – Li, M. Z.)

[3]*School of Life Sciences, Qufu Normal University, Jining 273165, P. R. China*
(e-mail: jingzhou-2004@163.com – Zhou, J.)

[#]*These authors contributed equally to this study.*

[*]*Corresponding author*
e-mail: guziketi@163.com

(Received 13th Dec 2021; accepted 25th Mar 2022)

Abstract. Plant-crop rotation model plays an important regulatory role in effectively avoiding the occurrence of continuous cropping obstacles in drylands. However, it is not clear how fungal communities change in soils with some different rotation models. To solve this question, we determined the soil nutrient contents, and compared the composition of fungi from soils (0-20 cm) using fungal ITS pyrosequencing techniques. We also tested different crop rotation regimes, including *Triticum aestivum* L. and millet rotation (TaSi), small rye (*Triticale Secalotriticum*) and millet rotation (TsSi), one season of leisure (no any crop) and one season of millet (Si), rape (*Brassica napus* L.) and millet rotation (BnSi). The results showed that BnSi significantly improved soil available potassium contents, the activity of soil catalase, and yields of *Setaria italica,* while reduced soil Alkali-hydrolyzed nitrogen contents compared with other three groups. Fungal alpha-diversity index in BnSi was the highest. The relative abundances of Ascomycota in BnSi (61.53%) and TsSi (62.6%) were higher than that in Si (58.65) and TaSi (55.67%), while Basidiomycota exhibited the opposite trend. Available potassium and organic matter were significant factors affecting fungal communities, explaining 61.4% of total variation. Our findings shed new light on the response of the soil fungal communities to long-term green manure regimes.
Keywords: *Setaria italica, green manure, crop rotation model, soil nutrient, ITS pyrosequencing*

Introduction

The negative effects of continuous cropping on crop production are mainly a reflection of the adverse effects on soil. Continuous cropping changes the physical and chemical properties of soil, and further causes nutrient imbalance (Bending et al., 2000; Yao et al., 2006; Zhang et al., 2019), accelerates the decomposition rate of organic carbon, causes rapid nutrient loss (West et al., 2002; Liu et al., 2003), and destroys the structure of soil aggregates (Six et al., 1999; Nayya et al., 2009). Continuous cropping can cause changes in soil microbial biomass and microbial community structure, resulting in imbalance of microbial community structure, the accumulation of pathogenic bacteria as well as serious diseases (Bever et al., 2012; Zhou et al., 2017), and thus seriously affect the yield and quality of millet.

http://www.aloki.hu ● ISSN 1589 1623 (Print) ● ISSN1785 0037 (Online)
DOI: http://dx.doi.org/10.15666/aeer/2003_25652576

Compared with continuous cropping, crop rotation system could effectively avoid the occurrence of continuous cropping obstacles and increased crop yields (Zhao et al., 2020). Rotation system could improve soil structure and soils organic matter (Govaerts et al., 2008; Detheridge et al., 2016), and Rotation system could also improve soil microbial diversity, change community structure and biological activity (Chaparro et al., 2012; Trivedi et al., 2015), decreased disease levels (Ai et al., 2018). In addition, the researchers found that fungi are more sensitive than bacteria to crop rotation (Guo et al., 2020). In terms of prevention and control of plant diseases, it was found that in the rotation system, the pathogenic micro-generation was significantly less than that in the continuous cropping system, and can reduce the occurrence of some important crop diseases (Jawson et al., 1993; Li et al., 2014; Palojärvi et al., 2020).

Millet (*Setaria italica*) is one of the main grains for people in northern China. It is widely cultivated in the middle and upper reaches of the Yellow River, and with a small amount cultivated in other areas. Grain of *Setaria italica* has high nutritional value, rich in protein, fat and vitamins.

Due to its important position in agricultural production, people use unreasonable cultivation system in order to pursue yield benefits in limited land, such as continuous cropping or unreasonable crop rotation, and so on. However, long-term continuous cropping has negative impaction on agricultural production, which decreased significantly the yield or quality of major grain crops, such as wheat, corn and rice, under continuous cropping conditions (Johnson et al., 1992; Ladha et al., 2000; Lithourgidis et al., 2006). In addition, continuous cropping could also result in yield decline on other main crops, such as soybean, Peanut, and so on (Chen et al., 2014).

The objectives of this investigation were to clarify the effect of different continuous cropping and crop rotation system on soil physical and chemical properties, microbial community structure and enzyme activities, and further to assess the effect on *Setaria italica* production.

Material and methods

Experimental materials and soil sampling

The experimental plants millet (*Setaria italica* Henggu 13) was used as the test material, and the experiment was carried out at the Shenzhou Experimental Station of Dry Farming Agricultural Research Institute (37°44´N, 115°42´E, 20 m a.s.l.) of Hebei Academy of Agricultural and Forestry Sciences from 2016 to 2019. The soil type is loam, the average precipitation is 373.1 mm and the average temper is 24.85℃. There were four treatments in a random block design with three replicates: wheat (*Triticum aestivum* L.) and millet rotation (TaSi), small rye (*Triticale secalotriticum*) and millet rotation (TsSi), one season of leisure (no any crop) and one season of millet (Si), rape (*Brassica napus* L.) and millet rotation (BnSi). The management, fertilization and watering of all treatments during millet planting are consistent, and the management measures during wheat, triticale, leisure and rape are consistent. The area of each replicate plot was 12 m×7 m. Soil samples were collected before *Setaria italica* was harvest at the third year (in October of 2019). Five bulk soil (5~10 cm) samples from each treatment were randomly collected and sieved through a 2.0-mm sieve and stored at -80°C for further molecular analysis. The yield of millet in four rotation planning patterns were calculated by per acre.

http://www.aloki.hu ● ISSN 1589 1623 (Print) ● ISSN1785 0037 (Online)
DOI: http://dx.doi.org/10.15666/aeer/2003_25652576

Analyses of soil physicochemical properties

For physicochemical characterization, soil samples were air dried at room temperature and sieved through a 2-mm screen. Soil pH value was determined by pHS3C pH meter with soil : water=1 : 2.5, and electric conductivity was determined by electrode method. The content of organic matter (OM), alkali-hydrolyzed nitrogen (AN), the effective phosphorus (AP) and available potassium (AK) were determined by external heating method of potassium dichromate, alkaline hydrolysis diffusion method, colorimetric method and flame photometry, respectively.

The activity of soil urease, cellulase and catalase were determined by sodium phenol-sodium hypochlorite colorimetric method, 3, 5-dinitrosalicylic acid colorimetric method and potassium permanganate titration method, respectively.

The concentrations of soil physicochemical properties in soil samples were tested for differences among samples using one-way analysis of variance (ANOVA) by SPSS BASE ver. 21.1 statistical software (SPSS, Chicago, IL, USA).

Soil DNA extraction and Illumina MiSeq sequencing

Soil genomic DNA was extracted using the MoBio PowerSoil® DNA isolation kit (MoBio Laboratories, Solana Beach, CA, USA), DNA concentration was quantified on a NanoDrop spectrophotometer (Thermo Scientific). Polymerase chain reaction (PCR) was performed using the primers ITS1F (5- CTTGGTCATTTAGAGGAAGTAA -3) and ITS2 (5- TGCGTTCTTCATCGATGC-3) (Zhang et al., 2015) for Fungal ITS region. High-throughput sequencing was performed on the Illumina MiSeq platform (Illumina Inc., San Diego, CA, USA) at Beijing Allwegene Technology Co., Ltd. (Beijing, China).

The raw data were deposited into the NCBI short reads archive database (accession number : PRJNA733686) The raw sequence reads were initially trimmed using Mothur, and sequences met all the three criteria were kept: (1) the sequence with precise primers and bar-codes; (2) quality score >20; (3) the sequences >230 bp in length. The software package Vsearch was then used to further filter out sequences which were erroneous, chimeric. The remaining high-quality sequences were queried against the GenBank non-redundant nucleotide database (nt) in NCBI using local Blastn. The MEGAN program (Huson et al., 2007) was used to assign BLAST hits to taxa of the NCBI taxonomy. After removing non-fungal sequence reads, the fungal sequences were clustered into operational taxonomic units (OTUs) at a 97% similarity level using Uclust. Low-abundance OTUs (fewer than 2 reads, including singletons), which might influence richness and diversity estimates (Dickie, 2010), were excluded from the subsequent analyses. Rarefaction, diversity indices (Shannon and Simpson) of each sample were calculated using the software Mothur. The weighted and unweighted unifrac tests were performed using Mothur to determine the statistical significance of structural similarity among communities across sampling locations. Visualization of beta-diversity information was achieved via ordination plotting with PCA. To compare community characteristics in greater detail, heat maps at the species and genus level were constructed and Venn diagrams were created with R package. The correlations between fungal communities (at the genus level) and physical and chemical properties were determined with redundancy analysis (RDA), by using CANOCO 5.0.

http://www.aloki.hu ● ISSN 1589 1623 (Print) ● ISSN1785 0037 (Online)
DOI: http://dx.doi.org/10.15666/aeer/2003_25652576

Results

Effects of different planting patterns on soil physico-chemical properties, enzyme activities and yields of Setaria italica

For analysis whether there was difference of available nutrients among in soils with different green mature plant and *Setaria italica* rotation modes. BnSi significantly improved the contents of soil available potassium, and reduced the contents of soil Alkali-hydrolyzed nitrogen compared to other three groups. And compared with Si, the soil conductivity was decreased (down 42.26%) significantly in BnSi. However, there was no significant difference for pH value, contents of organic matter and available phosphorus among the four planting patterns (*Table 1*).

Table 1. *Soil physical and chemical properties*

Planting patterns	pH value	Electric Conductivity	Organic Matter (%)	Available Potassium(mg/kg)	Effective Phosphorus (mg/kg)	Alkali-hydrolyzed nitrogen (mg/kg)
BnSi	7.10a	0.08b	2.00abc	130.07a	29.08a	87.15bc
Si	7.44a	0.13a	2.08ab	104.63b	29.95a	91.18ab
TaSi	7.44a	0.11ab	1.98abc	102.04b	31.06a	92.31a
TsSi	7.14a	0.11ab	2.11a	98.78b	30.84a	91.95ab

BnSi is *Brassica napus* L. and *Setaria italica* rotation group; Si is *Setaria italica* continuous group; TsSi is *Triticum secale* and *Setaria italica* rotation group; TaSi is *Triticum aestivum* L. and *Setaria italica* rotation group. Values within the same column followed by the different letters indicate significant differences ($P < 0.05$)

BnSi and Si group significantly improved the activity of soil catalase, but there was no significant difference in activity of urease and phosphatases among the four planting patterns (*Table 2*). Yields of *Setaria italica* in BnSi and TaSi were the highest in the four treatments, and were higher than those in Si and TsSi (*Fig. 1*).

Table 2. *Soil enzyme activities*

Planting patterns	Urease (mg/(g.24h))	Catalase (0.1mol/L KMnO4)/(h.g)	Phosphatases (mg/g.h)
BnSi	0.34a	0.97a	2.98a
Si	0.32a	0.96a	3.19a
TaSi	0.26a	0.65c	3.20a
TsSi	0.27a	0.72bc	3.14a

BnSi is *Brassica napus* L. and *Setaria italica* rotation group; Si is *Setaria italica* continuous group; TsSi is *Triticum secale* and *Setaria italica* rotation group; TaSi is *Triticum aestivum* L. and *Setaria italica* rotation group. Values within the same column followed by the different letters indicate significant differences ($P < 0.05$)

Planting patterns changed fungal diversity

A total of 2,024,148 high quality fungal ITS sequences were obtained from all 20 soil samples. and these were classified into 1,416 OTUs. Good's coverage values were > 0.99 for all samples, indicated that the current numbers of sequences in this study was

http://www.aloki.hu ● ISSN 1589 1623 (Print) ● ISSN1785 0037 (Online)
DOI: http://dx.doi.org/10.15666/aeer/2003_25652576

sufficient to reveal the diversity of fungal community. Shannon and Simpson indexes were all significantly affected by different planting patterns, Shannon and Simpson indexes in BnSi were highest, followed by Si group, Tasi group and TsSi group (*Fig. 2*).

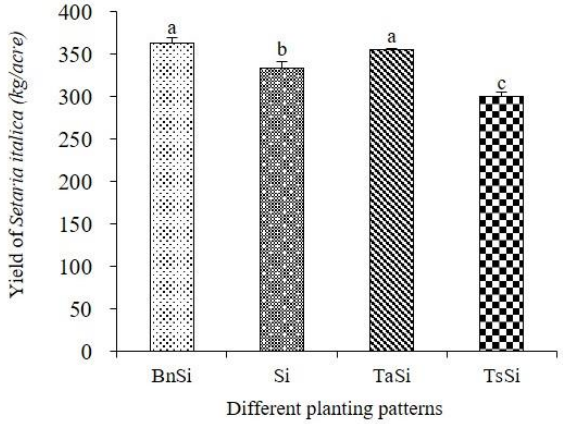

Figure 1. *Yields of Setaria italica in different planting patterns. BnSi is Brassica napus L. and Setaria italica rotation group; Si is Setaria italica continuous group; TsSi is Triticum secale and Setaria italica rotation group; TaSi is Triticum aestivum L. and Setaria italica rotation group. Values within the same column followed by the different letters indicate significant differences ($P < 0.05$)*

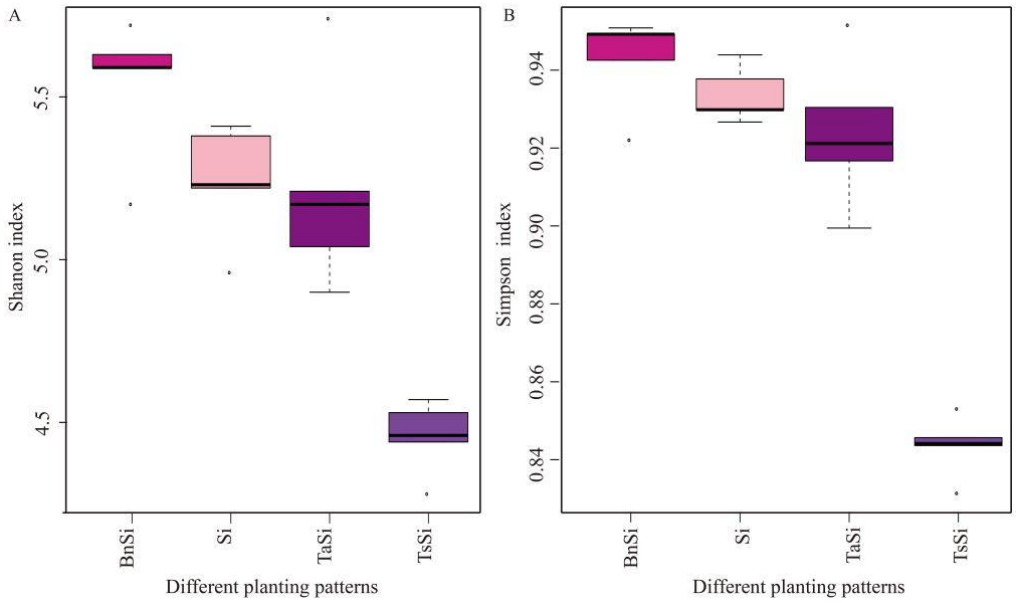

Figure 2. *Alpha diversity indexes in four groups. BnSi is Brassica napus L. and Setaria italica rotation group; Si is Setaria italica continuous group; TsSi is Triticum secale and Setaria italica rotation group; TaSi is Triticum aestivum L. and Setaria italica rotation group*

The PCA result revealed that fungal communities clustered according to different treatments. Based on the fungal beta-diversity, the four groups of samples were divided into two groups by the first PCA axis, and the left were BnSi and Si, and the right side were TaSi and TsSi (*Fig. 3*).

http://www.aloki.hu ● ISSN 1589 1623 (Print) ● ISSN1785 0037 (Online)
DOI: http://dx.doi.org/10.15666/aeer/2003_25652576

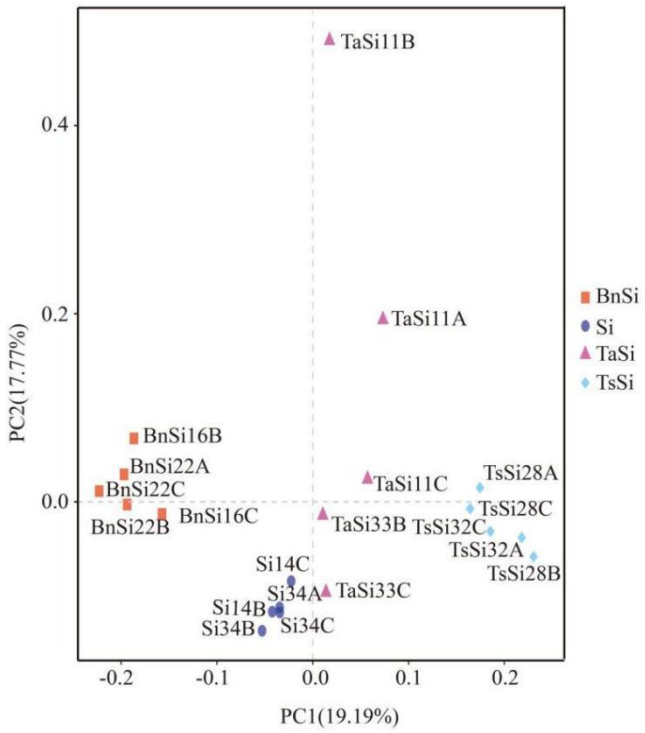

Figure 3. *Principal Component Analysis (PCA). PCA of the pyrosequencing reads obtained from soils subjected to different fertilization regimes based on the weighted Fast UniFrac metric. Different colors or shapes represent different samples or groups. The scales of horizontal and vertical axes are relative distance and have no practical significance. PC1 and PC2 respectively represent the suspected influencing factors of the genetic composition deviation of the two groups of samples, which need to be summarized by combining the characteristic information of the samples. The closer the distance between the two points, the smaller the difference of gene abundance composition between the two samples, and the higher the similarity. BnSi is Brassica napus L. and Setaria italica rotation group; Si is Setaria italica continuous group; TsSi is Triticum secale and Setaria italica rotation group; TaSi is Triticum aestivum L. and Setaria italica rotation group*

Fungal community composition

The relative abundance of different phyla in the four groups are shown in *Fig. 4*. The dominant fungi phyla in soils were Ascomycota (55.67%-62.6%), Mortierellomycota (4.73%-9.36%), Basidiomycota (3.15%-4.40%) and Glomeromycota (1.20%-1.90%).

Different planting patterns significantly changed the relative abundance of the main phyla. For phyla Mortierellomycota, their relative abundance was significantly =lower from BnSi, Si, Tasi than TsSi. The relative abundance of Ascomycota in BnSi (61.53%) and TsSi (62.6%) were higher than in Si (58.65) and TaSi (55.67%), while Basidiomycota showed the opposite trend.

Distribution of the fungal community at the genus level

At the genus level, we compared the differences in the top ten abundant genera in different groups. Mortierella was typically declined in relative abundance, while Chrysosporium increased. the relative abundance of genera Tomentella in BnSi was highest than other groups (*Fig. 5*).

http://www.aloki.hu ● ISSN 1589 1623 (Print) ● ISSN1785 0037 (Online)
DOI: http://dx.doi.org/10.15666/aeer/2003_25652576

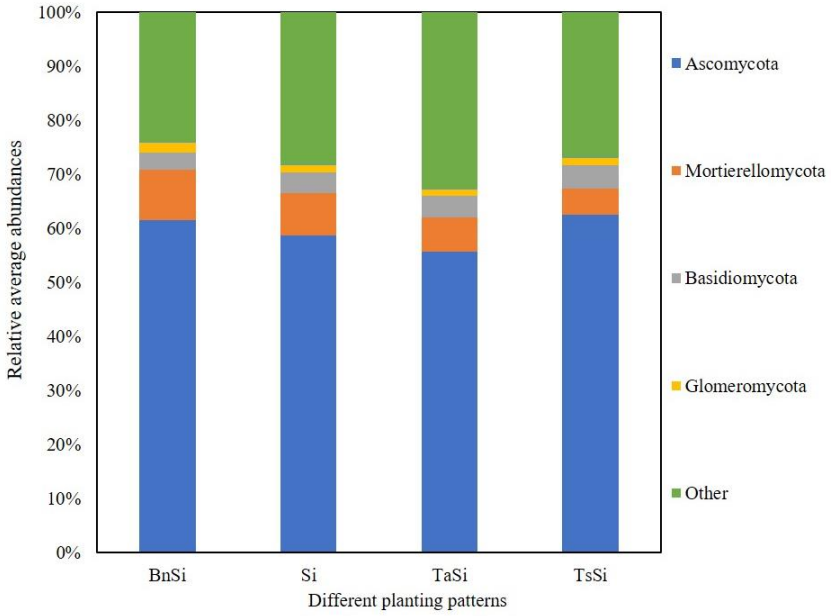

Figure 4. *Relative average abundances of the four most abundant phyla across different planting patterns. BnSi is Brassica napus L. and Setaria italica rotation group; Si is Setaria italica continuous group; TsSi is Triticum secale and Setaria italica rotation group; TaSi is Triticum aestivum L. and Setaria italica rotation group*

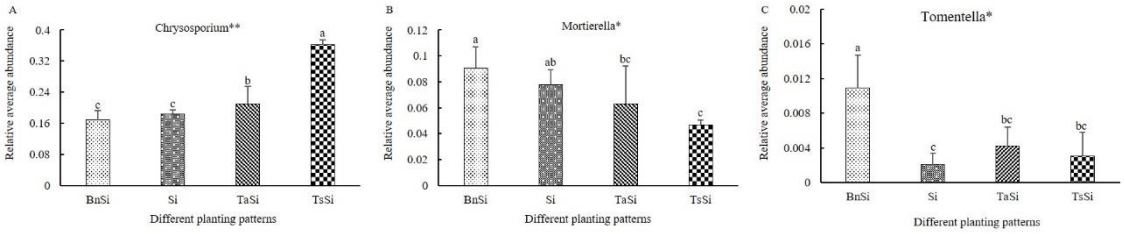

Figure 5. *Relative average abundances of the top three abundant genera under different planting patterns. A: The relative average abundance of the Chrysosporium genus; B: The relative average abundance of the Mortierella genus; C: The relative average abundance of the Tomentella genus. Error bars indicate the standard deviation of relative abundance between five replicate samples (**P<0.01， *P<0.05). BnSi is Brassica napus L. and Setaria italica rotation group; Si is Setaria italica continuous group; TsSi is Triticum secale and Setaria italica rotation group; TaSi is Triticum aestivum L. and Setaria italica rotation group*

Redundancy analysis

RDA showed that physicochemical parameters explained 28.49% of changes in fungal communities. The axis1 explained 15.43%, while the axis 2 explained 13.06% of the changes (*Fig. 6*). AK (F = 2.2, *P* = 0.016), OM (F = 1.8, *P* = 0.022) (*Table 3*) were significant factors affecting fungal communities, explaining 61.4% of total variation.

http://www.aloki.hu ● ISSN 1589 1623 (Print) ● ISSN1785 0037 (Online)
DOI: http://dx.doi.org/10.15666/aeer/2003_25652576

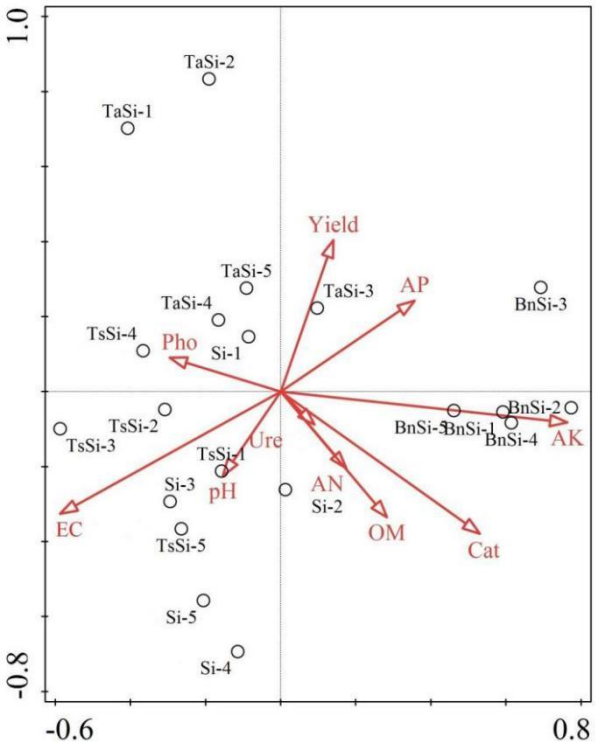

Figure 6. *Results from redundancy analysis (RDA) of different nitrogen added treatments bacterial and soil chemical characteristic. pH is pH Value; EC is electric conductivity; OM is organic matter; AP is available potassium; available phosphorus; AN is alkali-hydrolyzed nitrogen; Pho is phosphatases; Cat is catalase; Ure is Urease*

Table 3. *Analysis of constrained forward selection results*

Name	Explains (%)	Contribution (%)	pseudo-F	P-value
AK	10.7	17.4	2.2	0.016
OM	8.6	14	1.8	0.022
AP	6.4	10.4	1.4	0.168
Alkali hydrolyzed nitrogen	6.1	9.9	1.3	0.142
Conductivity	6.4	10.4	1.4	0.126
Yield	5.3	8.6	1.2	0.26
Catalase	5.4	8.9	1.3	0.218
pH	3.8	6.2	0.9	0.578
Urease	4.1	6.6	0.9	0.504
Phosphatase	4.6	7.4	1.1	0.388

pH is pH Value; OM is organic matter; AK is available potassium; AP is available phosphorus

Discussion

Our study explored the effects of soil physicochemical property analyses and soil fungal communities under different crop rotation combinations, and further to clear which crop rotation combinations was better.

http://www.aloki.hu ● ISSN 1589 1623 (Print) ● ISSN1785 0037 (Online)
DOI: http://dx.doi.org/10.15666/aeer/2003_25652576

Effect of crop rotation on soil physicochemical properties

Soil enzyme activities and soil physical and chemical properties, are greatly related with soil microorganisms (Sun et al., 2013). In our study, we measured the activity of urease, catalase and phosphatases under four crop rotation combinations, the result showed the activity of catalase was higher in BnSi and Si than in Tasi and TsSi. Catalase was important oxidoreductases, which could break down hydrogen peroxide to water and oxygen, and reduced the toxic effects of hydrogen peroxide produced by plant or micro-organisms metabolism on organisms and soil. In addition, Catalase was also reported involving in soil antimicrobial defense, and was positive related to plant disease resistance (Zhou et al., 2012; Xu et al., 2013), this was consisted with the previous research that the activities of catalase were significantly increased in the healthy soil (Wang et al., 2017).

In modern intensive agriculture, potassium depletion is a biggest cause of crop yield stagnation and low nutrient efficiency in the soil (Hahane et al., 2020), Soil available potassium is a kind of potassium that can be absorbed easily by plant, increased content of available potassium in BnSi showed *Setaria italica*-oilseed rotation combination was more sustainable agricultural system. Electric conductivity was lowest in BnSi may suggest that *Brassica napus* L. could have positive effects in reducing salinity levels (Gura and Mnkeni, 2019).

Effects of crop rotation combinations on soil fungal diversity

Compared with continues cropping, crop rotation system could also improve soil microbial diversity, change community structure and biological activity (Chaparro et al., 2012; Detheridge et al., 2016), But the intensity of improvement was different under different crop rotation combinations (Ai et al., 2018). Microbial diversity had positive impacts of soil environment. Rich microbial diversity in soil can lead to a more stable and heathy soil ecological system (Chaer et al., 2009; Pietras et al., 2013; Wang et al., 2017). In our study Soil samples in BnSi (*Setaria italica*- oilseed rotation combination) had highest fungal diversity, followed by Si and Tasi. TsSi significant decreased the soil fungal diversity. These results were consistent with PCA, compare to TaSi and TsSi, BnSi and TsSi significantly changed the fungal diversity and the sample clustering were separated far from the other two groups.

Effect of crop rotation on fungal community composition

In our study Ascomycota was dominant fungal phylum in all bulk soils, but there was significant difference in Mortierellomycota. Besides, Mortierella is an important genus of Mortierellomycota shown significant changes in different crop rotation, Mortierella has been shown to be a beneficial fungi for crops, and can assist crops and mycorrhizal fungi in phosphorus acquisition (Wang et al., 2020; Etesami et al., 2021), and some members of Mortierella was plant fungal endophyte can enhances biosynthesis and stress tolerance in the host plant (Wani et al., 2017), Tomentella belongs to Ectomycorrhizal fungi, increasing abundance of Tomentella can facilitate nutrient and water supply to the plants.

http://www.aloki.hu ● ISSN 1589 1623 (Print) ● ISSN1785 0037 (Online)
DOI: http://dx.doi.org/10.15666/aeer/2003_25652576

Conclusion

In conclusion, the soil phy-chemical characteristics, soil enzyme activities, yields of millet, and the composition of fungal communities in soils were clearly affected by long term plant-millet rotations. The microbial community data presented support the idea that rape (*Brassica napus* L.) and millet rotation have positive effects (i.e. higher alpha-diversity index) on fungal communities, yields of millet, and the activity of soil catalase. Therefore, we preliminarily concluded that millet and rape rotation is a good choice for the stability of soil ecosystem and sustainable development of production under drought conditions.

Acknowledgments. This work was Funded by Basic Research Funds of Hebei Academy of Agriculture and Forestry Sciences, [No.2021040202], Key Research and Development Program of Hebei Province, [No. 20326321D], and Construction of Modern Agricultural Industrial Technology System [NO. CARS-06-13.5-B3].

REFERENCES

[1] Ai, C., Zhang, S., Zhang, X., Guo, D., Zhou, W., Huang, S. (2018): Distinct responses of soil bacterial and fungal communities to changes in fertilization regime and crop rotation. – Geoderma 319: 156-166.
[2] Bending, G., Putland, C., Rayns, F. (2000): Changes in microbial community metabolism and labile organic matter fractions as early indicators of the impact of management on soil biological quality. – Biology and Fertility of Soil 31: 7884.
[3] Bever, J., Platt, T., Morton, E. (2012): Microbial population and community dynamics on plant roots and their feedbacks on plant communities. – Annual Review of Microbiology 66: 265-283.
[4] Chaer, G., Fernandes, M., Myrold, D., Bottomley, P. (2009): Comparative resistance and resilience of soil microbial communities and enzyme activities in adjacent native forest and agricultural soils. – Microbial Ecology 58: 414-424.
[5] Chaparro, J., Sheflin, A., Manter, D., Vivanco, J. (2012): Manipulating the soil microbiome to increase soil health and plant fertility. – Biology Fertility and Soils 48: 489-499.
[6] Chen, M., Li, X., Yang, Q., Pan, L., Chen, N., Yang, Z., Wang, T., Wang, M., Yu, S. (2014): Dynamic succession of soil bacterial community during continuous cropping of peanut (*Arachis hypogaea* L.). – PLoS One 9: e101355.
[7] Detheridge, A., Brand, G., Fychan, R., Crotty, F., Sanderson, R., Griffith, G., Marley, C. (2016): The legacy effect of cover crops on soil fungal populations in acereal rotation. – Agriculture Ecosystems & Environment 228: 49-61.
[8] Dickie, I. (2010): Insidious effects of sequencing errors on perceived diversity in molecular surveys. – New Phytologist 188: 916-918.
[9] Etesami, H., Jeong, B., Glick, B. (2021): Contribution of arbuscular mycorrhizal fungi, phosphate-solubilizing bacteria, and silicon to P uptake by plant. – Frontiers in Plant Science 12: 699618.
[10] Govaerts, B., Mezzalama, M., Sayre, K., Crossa, J., Lichter, K., Troch, V., Vanherck, K., De Corte, P., Deckers, J. (2008): Long-term consequences of tillage, residue manage-ment, and crop rotation on selected soil microflora groups in the subtropical highlands. – Appl. Soil Ecology 38: 197-210.
[11] Guo, Z., Wan, S., Hua, K. (2020): Fertilization regime has a greater effect on soil microbial community structure than crop rotation and growth stage in an agroecosystem. – Applied Soil Ecology 149: 103510.

http://www.aloki.hu ● ISSN 1589 1623 (Print) ● ISSN1785 0037 (Online)
DOI: http://dx.doi.org/10.15666/aeer/2003_25652576

[12] Gura, I., Mnkeni, P. (2019): Crop rotation and residue management effects under no-till on the soil quality of a haplic cambisol in Alice, Eastern Cape, South Africa. – Geoderma 337: 927-934.
[13] Hahane, A., Shivay, Y., Prasanna, R., Kumar, D. (2020): Nutrient removal by rice-wheat cropping system as influenced by crop establishment techniques and fertilization options in conjunction with microbial inoculation. – Scientific Reports 10(1): 21944.
[14] Huson, D., Richter, D., Rausch, C., Dezulian, T., Franz, M., Rupp, R. (2007): Dendroscope: An interactive viewer for large phylogenetic trees. – BMC Bioinformatics 8(1): 1-6.
[15] Jawson, M., Franzluebbers, A., Galusha, D., Aiken, R. M. (1993): Soil fumigation within monoculture and rotations: response of corn and mycorrhiza. – Agronomy Journal 85: 1174-1180.
[16] Johnson, N., Copeland, P., Crookston, R., Pfleger, F. (1992): Mycorrhizae: possible explanation for yield decline with continuous corn and soybean. – Agronomy Journal 84: 387-390.
[17] Ladha, J., Radanielson, A., Rutkoski, J., Buresh, R., Dobermann, A., Angeles, O., Pabuayon, I. L. B., Santos-Medellín, C., Fritsche-Neto, R., Chivenge, P., Kohli, A. (2000): Steady agronomic and genetic interventions are essential for sustaining productivity in intensive rice cropping. – Proceeding of the National Academe of the United States of America 118(45): e2110807118.
[18] Li, X., Ding, C., Zhang, T., Wang, X. (2014): Fungal pathogen accumulation at the expense of plant-beneficial fungi as a consequence of consecutive peanut monoculturing. – Soil Biology & Biochemistry 72: 11-18.
[19] Lithourgidis, A., Damalas, C., Gagianas, A. (2006): Long-term yield patterns for continuous winter wheat cropping in northern Greece. – European Journal of Agronomy 25: 208-214.
[20] Liu, X., Han, X., Song, C., Herbert, S., Xing, B. (2003): Soil organic carbon dynamics in black soils of China under different agricultural management systems. – Communications in Soil Science Plant Analysis 34: 973-984.
[21] Nayyar, A., Hamel, C., Lafond, G., Gossen, B., Hanson, K. (2009): Soil microbial quality associated with yield reduction in continuous-pea. – Applied Soil Ecology 43: 115-121.
[22] Palojärvi, A., Kellock, M., Parikka, P., Jauhiainen, L., Alakukku, L. (2020): Tillage System and Crop Sequence Affect Soil Disease Suppressiveness and Carbon Status in Boreal Climate. – Frontiers in microbiology 11: 534786.
[23] Pietras, M., Rudawska, M., Leski, T., Karliński, L. (2013): Diversity of ectomycorrhizal fungus assemblages on nursery grown European beech seedlings. – Annals of Forest Science 70: 115-121.
[24] Six, J., Elliott, E., Paustian, K. (1999): Aggregate and soil organic matter dynamics under conventional and no-tillage systems. – Soil Science Society America Journal 63: 1350-1358.
[25] Sun, J., Peng, M., Wang, Y., Li, W., Xia, Q. (2013): The effects of different disease-resistant cultivars of banana on rhizosphere microbial communities and enzyme activities. – FEMS Microbiology Lett 345: 121-126.
[26] Trivedi, P., Rochester, I., Trivedi, C., Van Nostrand, J., Zhou, J., Karunaratne, S., Anderson, I., Singh, B. (2015): Soil aggregate size mediates the impacts of crop-ping regimes on soil carbon and microbial communities. – Soil Biology & Biochemistry 91: 169-181.
[27] Wang, R., Zhang, H., Sun, L. G., Qi, G., Chen, S., Zhao, X. (2017): Microbial community composition is related to soil biological and chemical properties and bacterial wilt outbreak. – Scientific Reports 7(1): 1-10.
[28] Wang, S., Cheng, J., Li, T., Liao, Y. (2020): Response of soil fungal communities to continuous cropping of flue-cured tobacco. – Scientific Reports 10(1): 19911.
[29] Wani, Z. A., Kumar, A., Sultan, P., Bindu, K., Riyaz-Ul-Hassan, S., Ashraf, N. (2017): Mortierella alpina CS10E4, an oleaginous fungal endophyte of *Crocus sativus* L. enhances

http://www.aloki.hu ● ISSN 1589 1623 (Print) ● ISSN1785 0037 (Online)
DOI: http://dx.doi.org/10.15666/aeer/2003_25652576

apocarotenoid biosynthesis and stress tolerance in the host plant. – Scientific Reports 7(1): 8598.

[30] West, T., Post, W. (2002): Soil organic carbon sequestration rates by tillage and crop rotation: a global data analysis. – Soil Science Society of America Journal 66: 1930-1946.

[31] Xu, W., Wu, F., Chang, C., Liu, S., Zhou, Y. (2013): Effects of wheat as companion cropping on growth, soil enzymes and disease resistance of watermelon. – Allelopathy Journal 32: 267-278.

[32] Yao, H., Jiao, X., Wu, F. (2006): Effects of continuous cucumber cropping and alternative rotations under protected cultivation on soil microbial community diversity. – Plant and Soil 284(1): 195-203.

[33] Zhang, W., Yuan, Y., Yang, S., Huang, J., Huang, L. (2015): ITS2 secondary structure improves discrimination between medicinal "Mu Tong" species when using DNA barcoding. – PLOS One 10: e0131185.

[34] Zhang, P., Sun, J., Li, L. (2019): Effect of soybean and maize rotation on soil microbial community structure. – Agronomy 9: 42.

[35] Zhao, J., Yang, Y., Zhang, K. (2020): Does crop rotation yield more in China? A meta-analysis. – Field Crops Research 245: 107659.

[36] Zhou, B., Chen, Z., Du, L., Ye, X., Liu, Y. (2012): Resistance of eggplant (*Solanum melongena* L.) to verticillium wilt correlates to microbial abundance and soil enzyme activities. – Am J Exp Agric 2: 557-572.

[37] Zhou, X., Liu, J., Wu, F. (2017): Soil microbial communities in cucumber monoculture and rotation systems and their feedback effects on cucumber seedling growth. – Plant and Soil 415: 507-520.

http://www.aloki.hu ● ISSN 1589 1623 (Print) ● ISSN1785 0037 (Online)
DOI: http://dx.doi.org/10.15666/aeer/2003_25652576

THE FINANCIAL INCLUSION, RENEWABLE ENERGY AND CO_2 EMISSIONS NEXUS IN THE BRICS NATIONS: NEW EVIDENCE BASED ON THE METHOD OF MOMENTS QUANTILE REGRESSION

BASKAYA, M. M.* – SAMOUR, A.* – TURSOY, T.

Near East University, Department of Banking and Finance, 99138 Nicosia, Mersin 10, Turkey (phone: +90-(392)-223-6464)

**Corresponding authors*
e-mail: minebaskaya@yahoo.com; ahmad.samour@neu.edu.tr

(Received 16th Dec 2021; accepted 25th Mar 2022)

Abstract. This paper aims to examine the nexus between financial inclusion, renewable and non-renewable energy consumption, and carbon emissions according to the Environmental Kuznets Curve (EKC) hypothesis in the BRICS nations, employing the Method of Moments Quantile Regression (M.M.Q.R.) approach for 2002-2019. The causal linkages among the tested variables in heterogeneous panel data are investigated by utilising the Dumitrescu and Hurlin test. The empirical outcomes validate the EKC hypothesis for the BRICS nations. Furthermore, the findings from the panel quantile estimations (M.M.Q.R.) showed that the coefficients for the consumption of renewable energy and financial inclusion are negative through all quantiles (1st to 9th quantiles) for the emissions of CO_2. Thus, this suggests CO_2 emission levels are reduced by financial inclusion and renewable energy. In addition, the current analysis indicates that the volume of renewable energy investment in overall energy improves due to economic enlargement in the BRICS economies. Hence, financial inclusion is a catalyst for growth while mitigating carbon emissions. Therefore, financial inclusion should be included in the climate change paradigm strategies of the BRICS countries. To reach sustainable economic growth, we conclude that policy-makers should improve incentives for inclusive green finance.
Keywords: *inclusive green finance, banking, sustainable development, pollution, environment*

Introduction

Financial inclusion, utilisation of renewable energy and reducing carbon intensity are crucial elements of the sustainable development goals (S.D.G.s). A financial inclusion policy that aims to augment a low-carbon economy is defined as inclusive green finance (IGF), as stated by Alliance for Financial Inclusion (A.F.I.) (2020). IGF is the primary mechanism contributing to financial development through financial inclusion by considering environmental health and societal well-being. The Universal Financial Access (U.F.A.) proposes that financial inclusion is the first pillar in the fight against poverty and considering opportunities for economic development (The World Bank, 2020). Its purpose is to provide everybody with affordable access to the financial system. Hence, it leads to the improvement of the monetary framework of the country. Also, it is a holistic aspect of economic development. All countries depend on different types of energies according to their natural resources during their development period. Energy is the primary catalyst of industrial, technological, economic and social development. Some countries have natural resources and use primary energy sources, including those obtained from fossil fuels (natural gas, oil and coal), to obtain a competitive advantage. Both the economic growth of countries and common energy utilisation have a significant effect on

http://www.aloki.hu ● ISSN 1589 1623 (Print) ● ISSN1785 0037 (Online)
DOI: http://dx.doi.org/10.15666/aeer/2003_25772595

environmental pollution. Traditional energy utilization leads to the emission of carbon dioxide (CO_2).

CO_2 outflows are the primary ozone harming substances that add to the global increase in temperature. This leads to negative externalities for the environment and directly affects ecology, including natural water sources, natural resources, lands, animals, oxygen in the air, and the overall biodiversity and economy of the country. Thus, it is the main driving force behind implementing new environmentally-friendly power generation for low-carbon economies with sustainable economic growth. Sadorsky (2010) stated that the essential factors of energy demand construct the path for formulating decarbonisation mechanisms in the current economy through financial development. The transition to a renewable energy sector improves every country's economic growth and competitiveness, as stated by Simionescu et al. (2020), Blazejczak et al. (2014), and Wu et al. (2016).

Nevertheless, energy transformation is the most important innovation to mitigate environmental pollution in developed and developing countries (Saleem Jabari et al.,2022). Hence, green finance represents one of the critical factors driving green expansion to mitigate the adverse effects caused by environmental degradation. Since 1972, the United Nations has resolved to find solutions to solve environmental issues. In 2005, the Kyoto protocol came into effect to mitigate greenhouse gas (GHG) emissions, with the target of decreasing emissions by 5% between 2008 and 2012 (Samour et al., 2022a). In 2015, the Paris Agreement accepted and offered climate change mitigation, energy transformation rules and climate finance. It was adopted by 186 parties nationally, and 90 countries are still working on national adaptation plans to address the changing climate. Thus, policy-makers should adopt more incentives to implement renewable energy investments projects to maintain the global warming target level at 2^{o}C. The U.S. Energy Information Administration, International Energy Outlook 2019 (IEO 2019) proposes that by 2050, energy utilisation will increase by 50%. According to the European Green Deal agreement, the aim is to achieve a 60% reduction in greenhouse gases (GHG) by 2030, maintain global warming below 1.5^{o}C, and reach a long-term objective of establishing a zero-carbon strategy by 2050.

The BRICS countries are categorised as rapidly growing emerging economies with some of the world's highest greenhouse gas (GHG) emission levels. BRICS is an abbreviation for five countries whose economies are defined as emerging, namely Brazil, Russia, India, China and South Africa. A 2019 report published by the International Renewable Energy Association (I.R.E.N.A.) stated that Brazil meets 42% of its energy needs by using clean energy sources, and 41% of its primary energy supply is generated by oil. According to Nationally Determined Contributions (N.D.C.), Brazil proclaims to decrease its emissions of greenhouse gases (GHG) by 43% by 2030, below the 2005 level. By 2030, Russia intends to lower its emissions of greenhouse gases (GHG) by 25%-30% below the level recorded in 1990. India plans to reduce the emission level by 2030 to 33%-35% below the 2005 level. One of the highest carbon emitters globally with a 28% share, China dominates over 14.84% of the world economy. China's primary energy source is oil, and its share of the energy supply is 64%, whereas the renewable energy supply accounts for only 8%. China intends to reduce its emission levels by 2030 to around 60%-65% below the 2005 level. South Africa proposes to decrease its greenhouse gas (GHG) emissions to 26% by 2030. *Figure 1* shows the carbon emissions from 1990 until 2019 in the BRICS countries.

http://www.aloki.hu ● ISSN 1589 1623 (Print) ● ISSN1785 0037 (Online)
DOI: http://dx.doi.org/10.15666/aeer/2003_25772595

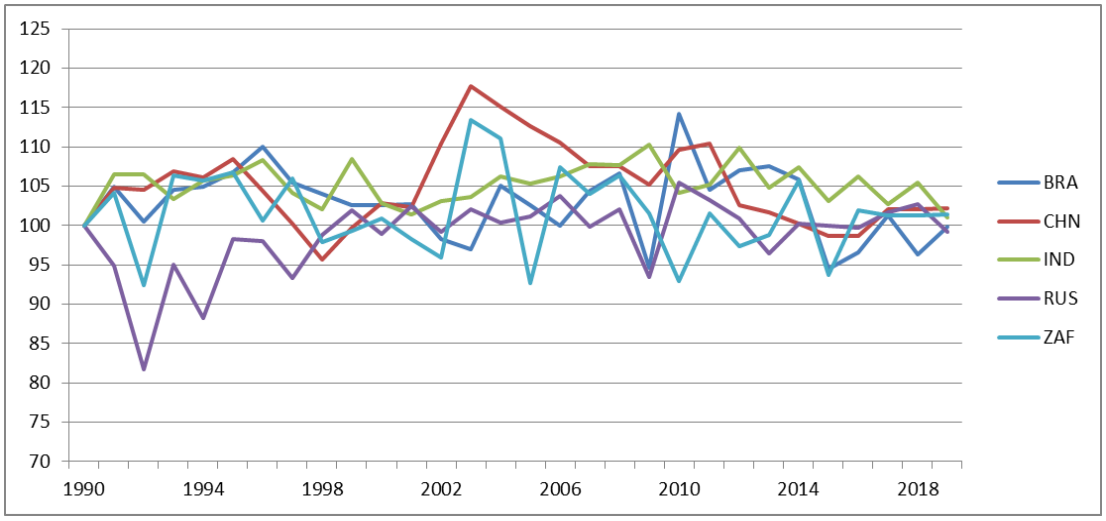

Figure 1. *Carbon emissions for BRICS countries (Million Tons, since 1990=100). (Source: World Bank, 2021)*

Scientific and academic studies have increasingly focused on these negative impacts, and policy-makers have also encouraged studies on technological innovations for low-carbon energy sources like nuclear and renewables. Therefore, to achieve economic sustainability and social development in the long term, energy sources with low carbon emissions should be utilised worldwide. However, this study aims to contribute extant research: The number of studies in the literature about the linkage between economic expansion, financial inclusion, consumption of renewable energy, and emissions of CO_2 for the BRICS nations to achieve sustainable development is limited. First, it provides new insights for the literature regarding financial inclusion and carbon emissions nexus in the light of the Environmental Kuznets Curve hypothesis (EKC) in the context of the BRICS nations. Second, this study considers inclusive green finance for sustainable development. Third, this research employs the newly-developed Method of Moments quantile regression test to analyse the associations. Hence, this research aims to resolve the deficiency in the extant literature by answering the following question: Do financial inclusion, and renewable energy mitigate the emissions of CO_2 in the BRICS nations? Multiple estimation methods are used to investigate the short and long run cause-and-effect relationships to answer the previous question.

The study structure is organised as follows: the second section depicts a review of previous studies on the topic, while the third part presents the model's data and specifications. The fourth presents a discussion of the findings, and finally, the fifth part offers a conclusion.

Literature Review

The relevant scientific studies can be grouped into the following three sub-categories: the affiliation among economic expansion and carbon emissions, the connection among the consumption of renewable energy and non-renewable energy and carbon emissions, and finally, the interrelation between financial inclusion and emissions of carbon.

http://www.aloki.hu ● ISSN 1589 1623 (Print) ● ISSN1785 0037 (Online)
DOI: http://dx.doi.org/10.15666/aeer/2003_25772595

Economic growth and CO_2 emissions

Analysing the interconnection between economic growth and carbon emissions has been one of the critical areas of focus in the energy economics domain in recent years. As suggested by the EKC hypothesis, as a country develops, its level of pollution rises, and when the income level increases to a turning point, the carbon emissions reach the highest level and then diminish as a result of economic growth over a specific period. The EKC suggests that an inverse relationship exists between pollution and income. The EKC hypothesis confirmed that industrialised countries become aware of environmental degradation and invest in renewable energy resources through green finance. Many studies have supported the EKC hypothesis. In this field, Apergis and Ozturk (2015) showed that carbon acid gas and income per capita have a reverse U-shape connection and validated the EKC hypothesis. Narayan et al. (2016) investigated the economic enlargement and carbon outflow nexus for 181 nations to validate the EKC hypothesis for 1960 to 2008 using the cross-correlation estimation approach. Haseeb et al. (2018) employed Dynamic Seemingly Unrelated Regression (D.S.U.R.), the Dumitrescu-Hurlin Granger causality test and the FMOLS test, and investigated the interconnection among energy utilisation, monetary expansion, globalisation, economic enhancement, and urbanisation and carbon dioxide outflow, and affirmed the validity of the EKC hypothesis for the BRICS nations. Ike et al. (2020) utilised the new "Method of Moments Quantile Regression" (M.M.Q.R.) approach with fixed effects. The findings showed a significant link between economic development and carbon gas outflow in 15 nations that produced oil from 1980 to 2010. Bibi and Jamil (2021) employed the random effect and fixed effect panel estimations test and validated the EKC among G.D.P. per capita and additional main variables and carbon dioxide emissions in MENA regions from 2000 to 2018. In addition, Sun et al. (2021) examined the linkage among economic expansion, renewable energy technologies, and carbon emissions in the Chinese context for 1990 to 2017 using the V.A.R., V.E.C.M., and Granger causality testing techniques. The outcomes revealed an inverted U-shaped association between economic enlargement and carbon emissions. The results suggested that green technology is the best practice to reduce carbon emissions. Abumunshar et al. (2020) used the A.R.D.L. model to show that G.D.P. has a positive impact on Turkey's level of carbon emissions over the tested period from 1981 to 2015.

However, there are contrary findings related to the EKC hypothesis in the literature. Chakravarty and Mandal (2016) studied the effect of income and carbon emissions for the BRICS nations using the EKC hypothesis between 1997 and 2011, employing the fixed products and G.M.M. testing technique. The findings indicated that the EKC was not valid in the BRICS nations over the tested period. Dogan and Lotz (2020) investigated the linkage between economic systems and carbon emissions according to the EKC hypothesis in several countries in Europe from 1980 to 2014. The author's employed FMOLS and O.L.S. and the S.T.R.I.P.A.T. testing techniques. The empirical analysis revealed that the EKC hypothesis had no validity. Finally, Aydın and Turan (2020) analyzed the importance of economic growth, free trade, and energy intensity on carbon gas outflow for the BRICS countries from 1996 to 2016 using the A.M.G. and C.C.E.M.G. testing models. The empirical findings provided no evidence supporting the presence of the EKC hypothesis in all of the BRICS nations. Recently, several studies confirmed that GDP has powerful impact on the level of carbon emissions in different countries (e.g., Rehman et al., 2021; Pata, 2021;Kirikkaleli et al., 2022; Alola et al., 2022; Adebayo, 2022; Adebayo et al., 2022a,b; Awosusi et al., 2022; Fareed et al., 2022; Miao

http://www.aloki.hu ● ISSN 1589 1623 (Print) ● ISSN1785 0037 (Online)
DOI: http://dx.doi.org/10.15666/aeer/2003_25772595

et al., 2022; Akadiri et al., 2022; Pata and Samour, 2022; Yan et al., 2022; Shahzad et a., 2022; Akram et al., 2022; Samour et al., 2022b).

Energy consumption and CO_2 emissions

Various researchers have tested how energy consumption (renewable and non-renewable energy) impacts carbon emission levels. On this subject, Boluk and Mert (2015) investigated the validity of the Environmental Kuznets Curve (EKC) hypothesis by exploring how the consumption of renewable energy impacted decreasing greenhouse gas (GHG) outflow from 1961 to 2010 for Turkey. The findings suggested that the utilisation of renewable energy decreased greenhouse gas (GHG) emissions in Turkey. Using the A.R.D.L. model, Altarhouni et al. (2021) and Qashou et al. (2022) also confirmed that renewable energy decreased greenhouse gas (GHG) emissions in Turkey over the period from 1988-2018 and 1981-2015, respectively. Ummalla and Goyari (2020) validated the EKC hypothesis for the BRICS nations by applying FMOLS and the Dumitrescu–Hurlin panel causality test from 1992 to 2014. The results indicated that the consumption of clean energy significantly decreases carbon emissions. Altinoz and Dogan (2021) employed the quantile regressions estimation method on a panel of 82 countries from 1990 to 2014. The findings revealed that renewable energy consumption negatively influences carbon emission levels. In addition, Aziz et al. (2021) analysed the effects of natural resources, renewable energy and globalisation on carbon emission according to the EKC in the MINT countries by employing the new Method of Moments quantile regression model and Dumitrescu-Hurlin causality test. The outcomes verified the EKC hypothesis among income and carbon outflow except for higher quantiles. At the same time, renewable energy consumption caused a rise in carbon outflow at over half quantiles and reversed in below half quantiles. Thus, the analysis showed that energy supply from renewable sources did not meet the demand for energy consumption from 1995 to 2018.

Dogan and Seker (2016) tested the impact of renewable and non-renewable energy, real income and trade openness on carbon emissions in the European Union according to the EKC hypothesis throughout 1980 to 2012. The findings showed that non-renewable energy positively affects carbon emissions. Zhang et al. (2017) utilised the FMOLS, DOLS and C.C.R. approaches for Pakistan from 1970 to 2012 and validated the EKC hypothesis, reporting that renewable energy significantly and negatively affects carbon emissions. In contrast, the effect of the consumption of non-renewable energy on carbon emissions is significant and positive. Souza et al. (2018) explored the relationship among economic growth, renewable and non-renewable energy and carbon emissions according to the EKC hypothesis for the Southern Common Market (MERCOSUR) from 1990 to 2014. The outcomes indicated that the consumption of clean energy diminished carbon emissions and supported the EKC hypothesis, whereas non-renewable energy usage caused carbon emissions to increase. Chen et al. (2019) analysed the relationship among economic expansion, renewable energy and non-renewable energy consumption and carbon emissions within the EKC hypothesis concerning the regions of China from 1995 to 2012. Using both FMOLS and DOLS approaches, this study indicated that renewable energy negatively impacts carbon emissions in the regions to the east and west of the country, whereas in the central area, the effect is insignificant. However, in all areas, non-renewable energy positively impacts carbon emissions. Zafar et al. (2019) employed the V.E.C.M., CUP-FM, and CUP-BC models to examine the interaction among energy usage, trade openness, and carbon emissions for different emerging economies from 1990

http://www.aloki.hu ● ISSN 1589 1623 (Print) ● ISSN1785 0037 (Online)
DOI: http://dx.doi.org/10.15666/aeer/2003_25772595

to 2015. The study showed that the consumption of non-renewable energy positively influences carbon emissions. Anwar et al. (2021) used the FMOLS, DOLS, FE-OLS approaches to test how energy consumption impacts carbon emission levels in the ASEAN countries between 1990 and 2018. The presented evidence verified the presence of the EKC hypothesis based on all approaches. In addition, the results demonstrated that non-renewable energy usage positively affects carbon emission levels.

Financial inclusion and CO_2 emissions

The existing literature highlighted that financial inclusion significantly affects economic variables. Sharma (2015) employed vector auto-regression (V.A.R.) models in this field, and the results indicated that economic growth and financial inclusion variables were positively correlated. Maune et al. (2020) used a regression model and examined how financial inclusion impacts the economic growth of Zimbabwe from 2011 to 2017. The study revealed that financial inclusion causes financial development to improve in Zimbabwe. Ratnawati (2020) examined the nexus between financial inclusion and income inequality, poverty, economic enlargement and financial stability in 10 developing countries in Asia for the period 2009 to 2018 by using G.M.M. methods. The findings showed that financial inclusion creates economic development and improves financial stability, thus diminishing poverty and income inequality. Van et al. (2021) studied financial inclusion and economic improvement in emerging markets using econometric panel techniques and found that economic development and inclusive finance were positively related. Barık and Pradhan (2021) explored how financial inclusion affects financial stability concerning the BRICS nations from 2005 to 2015 by using G.M.M. methods and the Dumitrescu and Hurlin panel Granger causality test. The authors stated that financial inclusion significantly impacts the financial stability of the BRICS nations. Huang et al. (2021) analysed how inclusive finance and trade openness impacted the economic development of 27 members of the European Union (E.U.) from 1995 to 2015 through the use of fully modified least squares (FMOLS). The study revealed that financial inclusion driven policies could be used as a catalyst to improve the financial system, which directly causes economic growth. Conversely, only a few studies have tested the effect of financial inclusion on pollution of the environment. Based on the literature review, financial inclusion policies can mitigate carbon emissions. Samour et al. (2019) used A.R.D.L. and FMOLS to examine how the banking industry impacted Turkish emissions of carbon between 1980 and 2014. The outcomes revealed that banking sector development has a significant positive effect on carbon emissions. Le et al. (2020) analysed how financial inclusion influences carbon emissions from 2004 to 2014 for 31 Asian countries by utilising S.T.I.R.P.A.T. The findings indicated that financial inclusion gradually increased carbon emissions in 31 Asian countries. Renzhi and Baek (2020) explored the presence of the Environment Kuznets curve (EKC) based on financial inclusion in 103 countries between 2004 and 2014. Pooled O.L.S. and fixed effects, G.M.M. and Arellano-Bond and Hansen tests were applied in the analysis. The findings validated the EKC and demonstrated that financial inclusion negatively influences carbon emissions. Also, financial inclusion development, which considers different customer segments, is a significant factor in mitigating environmental degradation. *Table 1* presents a summary of the primary outcomes of the empirical research that have tested the EKC hypothesis.

http://www.aloki.hu ● ISSN 1589 1623 (Print) ● ISSN1785 0037 (Online)
DOI: http://dx.doi.org/10.15666/aeer/2003_25772595

Table 1. *Summary of the review of the literature on economic growth, energy consumption and financial inclusion*

	Authors	Period	Methodology	Country	The Results
1	Apergis and Ozturk (2015)	1990-2011	GMM	Asian Countries	EKC is valid
2	Boluk and Mert (2015)	1961-2010	ARDL	Turkey	EKC is valid
3	Al-Mulali et al. (2016)	1980-2010	DOLS-VECM Granger causality test	7 regions	EKC is valid
4	Chakravarty and Mandal (2016)	1997-2011	GMM	BRICS countries	EKC is not valid
5	Dogan and Seker (2016)	1980-2012	DOLS and Dumitrescu–Hurlin panel causality test	EU	EKC is valid
6	Narayan et al. (2016)	1960-2008	Cross correlation estimation approach	181 countries	EKC is valid
7	Zhang et al. (2017)	1970-2012	FMOLS, DOLS and C.C.R. approach	Pakistan	REC-CO_2 emissions
8	Haseeb et al. (2018)	1995-2014	D.S.U.R., and Dumitrescu-Hurlin Granger causality test	BRICS countries	EKC is valid
9	Souza et al. (2018)	1990-2014	Panel	MERSOCUR	REC-CO_2 emissions
10	Chen et al. (2019)	1995-2012	FMOLS, DOLS	China	REC-CO_2 emissions
11	Samour et al. (2019)	1980-2014	ARDL and FMOLS, CCR	Turkey	Banking sector+CO_2 emissions
12	Zafar et al.(2019)	1990-2015	VECM, CUP-FM, CUP-BC	Emerging economies	NREC+CO_2 emissions
13	Aydin and Turan (2020)	1996-2016	AMG, CCEMG	BRICS countries	EKC is not valid
14	Dogan and Lotz (2020)	1980-2014	FMOLS, OLS, STRIPAT technique	European countries	EKC is not valid
15	Ike et al. (2020)	1980-2010	M.M.Q.R. with fixed effects	15 oil producing countries	EKC is valid
16	Le et al. (2020)	2004-2014	STIRPAT	31 Asian countries	FC+CO_2 emissions
17	Ummalla and Goyari (2020)	1992-2014	FMOLS and Dumitrescu–Hurlin panel causality test	BRICS countries	EKC is valid
18	Renzhi and Baek (2020)	2004-2014	Pooled O.L.S. and fixed effects, G.M.M. and Arellano-Bond and Hansen tests	103 countries	FC-CO_2 emissions
19	Altınoz and Dogan (2021)	1990-2014	M.M.Q.R.	82 countries	REC-CO_2 emissions
20	Anwar et al. (2021)	1990-2018	MMQR	ASEAN countries	NREC+CO_2 emissions
21	Aziz et al.(2021)	1995-2018	M.M.Q.R., FMOLS, DOLS, FE-OLS	MINT countries	REC-CO_2 emissions
22	Bibi and Jamil(2021)	2000-2018	Random effect and fixed effect panel estimations	Different Selected Countries	EKC is valid
23	Sun et al. (2021)	1990-2017	V.A.R., V.E.C.M., Granger causality test	China	EKC is valid
24	Altarhouni et al.,(2021)	1988-2018	ARDL	Turkey	REC-CO_2 emissions
25	Qashou et al.,(2022)	1981-2015	ARDL	Turkey	NREC+CO_2 emissions

http://www.aloki.hu ● ISSN 1589 1623 (Print) ● ISSN1785 0037 (Online)
DOI: http://dx.doi.org/10.15666/aeer/2003_25772595

Data Sources and Methodology of the Study

Data

Our data were sourced from the World Bank (W.B.) database and International Monetary Fund (I.M.F.) and consisted of annual observations for the BRICS countries covering 2002 to 2019. Moreover, the obtained data series included gross domestic product (G.D.P.) per capita as a proxy of economic growth, and financial inclusion (F.C.) is an index that is calculated using four sub-indices, including the number of A.T.M.s per 100,000 adults, the number of bank branches per 100,000 adults, the number of credit cards per 1,000 adults, and the number of debit cards per 1,000 adults. In addition, carbon dioxide (CO_2) emissions per capita were used as an indicator of environmental pollution, oil, coal and natural gas power utilisation (N.R.E.C.), and renewable energy consumption (R.E.C.). The details of the data are presented in *Table 2* variables of the study.

Table 2. *Study variables*

Variable	Symbol	Scale Unit	Definition	Source
Renewable energy consumption	R.E.C.	Quad B.T.U.	Consumption of renewable energy per capita	World Bank
Non-renewable energy consumption	N.R.E.C.	Billion B.T.U.s	Oil, coal, natural gas usage	World Bank
GDP	GDP	(constant 2010 US$)	Real GDP per capita (constant 2010US$)	World Bank
Financial Inclusion	F.C.	Calculation index on 4 sub-indices in the banking sector	The calculation of this index is based on 4 sub-indices: the amount of A.T.M.s for every 100,000 adults, the number of banking centres for every 100,000 adults, the number of credit cards for every 100,000 adults, and the number of debit cards for every 100,000 adults.	IMF
Carbon Emissions	CO_2	kiloton (kt)	Carbon emissions in metric tons	World Bank

Empirical methodology

Inspired by the existing literature, the effects of income, renewable energy and non-renewable energy, and financial inclusion on the emissions of CO_2 is formulated as follows (*Eq.1*):

$$CO_{2\,it} = f(\text{G.D.}P_{it}, \text{G.D.}P_{it}^2, \text{N.R.E.}C_{it}, \text{RE}C_{it}, \text{F}C_{it}) \quad \text{(Eq.1)}$$

The investigated variables $CO_{2\,it}$, G.D.P_{it}, G.D.P_{it}^2, N.R.E.C_{it}, REC_{it}, FC_{it} represent CO_2 emissions, G.D.P., and the square of G.D.P., non-renewable energy, consumption of renewable energy and financial inclusion, respectively. The proxy used for REC_{it} is the usage of solar, hydroelectricity, and wind energy (Cui et al., 2022). The proxy used for N.R.E.C_{it} is the consumption of coal, oil, and natural gas—the proxy used for G.D.P_{it} is measured in constant US$. The proxy used for G.D.P_{it}^2 is the square of G.D.P. (Samour and Pata, 2022). The proxy used for FC_{it} is an index, the calculation of which is based on 4 sub-

http://www.aloki.hu ● ISSN 1589 1623 (Print) ● ISSN1785 0037 (Online)
DOI: http://dx.doi.org/10.15666/aeer/2003_25772595

indices: the amount of A.T.M.s for every 100,000 adults, the number of banking centres for every 100,000 adults, the number of credit cards for every 100,000 adults, and the number of debit cards for every 100,000 adults. The variables mentioned above were acquired from the World Development Indicators (World Bank, 2021) and I.M.F.

Before assessing the unspecified parameters, various conventional introductory tests are employed to detect the time-series attributes of the factors. From this perspective, this study uses the cross-sectional dependence (CD) test as well as the augmented cross-sectional I.P.S. (C.I.P.S.) test proposed by Pesaran (2007) to measure cross-sectional dependence in the panel data as well as to generate superior outcomes that are probably unmeasured when conducting the first-generation test of Levin, Lin and Chu, Im, Pesaran, and Shin (Aziz et al., 2021).

We simultaneously used three progressive panel estimation approaches for heterogeneous panels called Dynamic O.L.S. (DOLS), Fully Modified O.L.S. (FMOLS), and the Fixed Effects O.L.S. (FE-OLS) testing models to examine the estimation coefficients amongst the investigated variables. The DOLS testing model was developed by Kao and Chiang (2001). Monte Carlo simulations settings form the framework of this test. On the other hand, the FMOLS testing model was developed by Pedroni (2004). The intercepts are unique for each series in the panel. The FE-OLS testing model was created with the standard errors of Driscoll and Kraay, and this test exhibits robustness to standard kinds of cross-sectional dependence.

In this case, models such as O.L.S. built on the assumption of normal distribution may reveal biased estimates. This study utilised a novel estimation approach to overcome this issue, namely the M.M.Q.R. test that was first proposed in the study of Machado and Santos Silva (2019). Unlike earlier regression methods, M.M.Q.R. is used to estimate results through moment conditions that do not assume the presence of the moment function or make distribution assumptions. The M.M.Q.R. approach has superiority as it considers conditional heterogeneous covariance effects of the components of the endogenous explanatory variables. M.M.Q.R. shows the nexus among the variables through different quantiles. Hence, the distributional and heterogeneous effects are ascertained by the panel quantile regression model across quantiles (Aziz et al., 2020). In addition, it reflects factual observations about the linkage between tested variables that consider the fixed effects of distribution heterogeneity. Hence, the testing model shows multiple conditions between tested variables in different conditional distributions that cannot be obtained using conventional regressions based on average factors estimates. However, it is essential to evaluate the tested variables at the conditional distribution within conditional quantiles to delineate the distributive impact of the independent variable on the dependent variable in various quantile ranges (Alhodiry et al., 2021).

To estimate the conditional quantiles $Q_y(\tau|X)$ for the model of the a location-scale variant, the equation (*Eq.2*) below is formulated:

$$Y_{it} = \alpha_{it} + X_{it}^{'} \beta + (\delta_i + Z_{it}\, \gamma)\mu_{it} \quad \text{(Eq.2)}$$

where the probability, $P\{\delta_i + Z_{it}\, \gamma > 0\} = 1$. $(\alpha, \beta', \delta_i, \gamma')$ are estimated parameters. The object *i* fixed is reflected by $(\alpha_i\, , \delta_i{}')$. $i = 1, \ldots,$ n, and Z is K-vector selected components of X that can be seen in a different format with particular l represented in *Eq.3*:

$$Z_I = Z_I(\mathrm{X}),\ I = 1, \ldots., \mathrm{k} \quad \text{(Eq.3)}$$

http://www.aloki.hu ● ISSN 1589 1623 (Print) ● ISSN1785 0037 (Online)
DOI: http://dx.doi.org/10.15666/aeer/2003_25772595

$X_{it}^{'}$ is identically and independently disposed of for any stabilised i and independent through time (t). μ_{it} is identically and independently disposed within time (t), and are orthogonal to $X_{it}^{'}$ and normalised to verify the present status in Machado and Santos Silva (2019) that amongst other variables do not indicate rigid exogeneity. Thus, *equation (2)* designates by *Eq.4* stated below:

$$Q_y(\tau|X_{it}) = \left(\alpha_{it} + \delta_{iq}\,(\tau)\right) + X_{it}^{'}\,\beta + Z_{it}\,\gamma' q\,(\tau) \qquad \text{(Eq.4)}$$

In *Eq.4*, independent variables' vectors are indicated by $X_{it}^{'}$, which in the current study are defined as the natural logarithms of G.D.P_{it}, G.D.P_{it}^2, N.R.E.C_{it}, REC_{it}, FC_{it}. $Q_y(\tau|X)$ reflects the quantile distribution of the response variable Y_{it} (the natural log of $CO_{2\,it}$) which is subject to the position of the independent variable $X_{it}^{'}$. $\alpha_{it}(\tau) = \alpha_{it} + \delta_i q\,(\tau)$ is the scalar coefficient, which is significant of the quantile –τ fixed effect for individual *i.*

The particular impact indicates no intercept change, unlike the typical fixed least-squares results. These parameters are fixed within time, whose heterogonous degrees are fitted to deviant the conditional distributional quantiles of the selected variables within the model. The τ-the sample quantile is symbolised by q(τ), which is regarded by referencing the issue of optimisation (*Eq.5*):

$$min_q \sum_i \sum_t \rho_\tau\,(R_{it} - (\delta_i + Z_{it}'\,\gamma)\,q) \qquad \text{(Eq.5)}$$

In *Eq.4*, $\rho_\tau\,(A) = (\tau - 1)\,AI\,\{A \leq 0\} + \tau AI\,\{A > 0\}$ denotes the check function. To confirm the cause-and-effect relationship among the inspected factors, another method of the Dumitrescu and Hurlin (2012) test is utilised to examine the interconnection among the investigated variables in heterogeneous panel information models. In this model, there are two dimensions: the causal link's heterogeneity and the employed regression model's heterogeneity. The hypothesis of non-homogeneous causality H_0 is compared by two subclass options: The first one categorises the cause-and-effect interconnection among two variables, while the second subclass is constructed by two variables that have no relationship.

Empirical Results and Discussion

Unit root test of the second generation and panel co-integration test

The cross-sectional dependence and the C.I.P.S., Im, Pesaran, and Shin tests are presented in *Tables 3. and 4*. The C.I.P.S. test outcomes confirmed that ($CO_{2\,it}$, G.D.P_{it}, G.D.P_{it}^2, N.R.E.C_{it}, REC_{it}, FC_{it}) have an order of integration of I(1) at a 1% level of significance. The outcomes of the CD test indicated that the investigated variable series all have significant differences across panels at a significance level of 1%.

Table 5. presents the findings of the Pedroni (2004) and bootstrap Westerlund's (2007) co-integration tests. The test results indicate it is not possible to reject the null hypothesis of "no co-integration". Contrastingly, it is possible to accept the alternative hypothesis. These findings specify and affirm that the tested model variables have a long-run co-integration.

Table 3. *Results of the CD and C.I.P.S. unit root tests*

http://www.aloki.hu ● ISSN 1589 1623 (Print) ● ISSN1785 0037 (Online)
DOI: http://dx.doi.org/10.15666/aeer/2003_25772595

Variables	CD test	p-value	C.I.P.S. test	
			Level	1st difference
$CO_{2\ it}$	12.15	0.00	- 1.953	- 5.211***
G.D.P_{it}	13.16	0.00	-1.201	- 6.008***
G.D.P_{it}^2	12.99	0.00	-0.951	- 5.698***
N.R.E.C_{it}	16.18	0.00	- 0.985	- 6.889***
REC_{it}	13.85	0.00	- 0.790	- 6.761***
FC_{it}	19.14	0.00	-1.1985	- 5.448***

Note: ***denotes that the null hypothesis is rejected at the 1% significance level

Table 4. *Stationary analysis outcomes*

	Im, Pesaran, and Shin			
	I(0) Cons	I(0) constant and tend	I(1) constant	I(1) constant and tend
$CO_{2\ it}$	-0.151	-0.250	-5.151***	-6.309***
G.D.P_{it}	-0.131	-0.231	-6.559***	-7.021***
G.D.P_{it}^2	-0.239	-0.320	-5.299***	-6.829***
N.R.E.C_{it}	0.315	0.322	6.315***	5.891***
REC_{it}	-0.589	-0.695	-6.589***	-6.021***
FC_{it}	1.210	1.158	5.210***	7.791***

Note: *** indicates that the null hypothesis is rejected at the 1% significance level

Table 5. *Pedroni co-integration test outcomes*

Test	Statistic	Prob
$CO_{2\ it}$= f(GDP_{it}, G.D.P_{it}^2, N.R.E.C_{it}, REC_{it}, FC_{it})		
Panel v	-0.623	0.650
Panel rho	-0.695	0.350
Panel PP	-3.985***	0.000
Panel ADF	-4.998***	0.000
Panel ADF	0.311	0.573
Group PP	-5.995***	0.000
Group ADF	-4.010***	0.000

Note: *, **, ***means significance of the tested variables at 10%, 5%, 1% levels, respectively

Panel estimation results

After proving that the tested variables are cointegrated, the research employed the DOLS, FMOLS, FE-OLS testing models. The findings of DOLS, FMOLS and FE-OLS presented in *Table 6*. show the influence of G.D.P_{it}, G.D.P_{it}^2, N.R.E.C_{it}, REC_{it}, and FC_{it} on the emissions of CO_2. The results show that at the 5% statistical significance level, G.D.P. positively and significantly influences CO_2 emissions. In contrast, G.D.P^2 negatively and significantly affects CO_2 according to the FMOLS, DOLS and FE-OLS testing models. The model specifications imply that a 1% rise in G.D.P. positively affects emissions by 2.9% according to the DOLS model, 2.3% according to the FMOLS model and 2.5% according to the FE-OLS model.

Table 6. *Results of panel estimation for BRICS nations*

http://www.aloki.hu ● ISSN 1589 1623 (Print) ● ISSN1785 0037 (Online)
DOI: http://dx.doi.org/10.15666/aeer/2003_25772595

	DOLS		FMOLS		FE-OLS	
	Coef	**t-stats**	**Coef**	**t-stats**	**Coef**	**t-stats**
GDP_{it}	2.915**	9.795	2.315***	10.980	2.513***	9.889
G.D.P_{it}^2	-0.951**	-5.350	-0.7985***	-5.430	-0.651***	-6.002
REC_{it}	-0.250**	-6.235	-0.557***	-6.005	-0.995***	-5.563
N.R.E.C_{it}	0.884**	7.980	0.7985***	7.980	0.651***	6.851
FC_{it}	-0.410*	-5.621	-0.751	-5.985**	-0.215	3.995*

Note: *, **, ***means significance of the tested variables at 10%, 5%, 1% levels, respectively

Besides, the model specifications imply a 1% increase in G.D.P_{it}^2 negatively affects emissions by 0.95% according to the DOLS model, 0.79% according to the FMOLS model and 0.65% according to the FE-OLS model. The outcomes of this study validate the EKC hypothesis in the context of the BRICS nations. The results of the current research concur with those of empirical research conducted by Boluk and Mert (2015), Al-Mulali et al. (2016), and Narayan et al. (2016).

Across the model specifications, the findings for renewable energy consumption show that at the 5% statistical significance level, a 1% increase in REC_{it} causes CO_2 emissions to be negatively and significantly affected by 0.25% in the DOLS model, 0.55% in FMOLS and 0.99% in the FE-OLS testing models. This is aligned with the findings of existing empirical studies conducted by Zafar et al. (2019), Anwar et al. (2021), and Aziz et al. (2021). The energy transformation paradigm represents an important challenge for the sustainability of human well-being and economic growth. Clean energy utilisation is the primary driver in efforts to mitigate carbon emissions. Our outcomes are consistent with existing empirical studies, which confirm that environmental sustainability can be reached by producing clean energy.

In contrast, the findings for non-renewable energy consumption imply a 1% expansion in N.R.E.C_{it} consumption escalates the carbon emissions by 0.88% according to the DOLS model, 0.79% according to the FMOLS model and 0.65% according to the FE-OLS model. Hence, non-renewable energy consumption positively and significantly affects carbon emissions. The BRICS countries are therefore heavily dependent upon coal-based conventional energy supply. Thus, this indicates that the BRICS countries emit carbon dioxide. In this line, the BRICS nations should promote green finance to mitigate carbon emissions. The findings of the current research are consistent with the empirical studies conducted by Zhang et al. (2017), Souza et al. (2018), and Chen et al. (2019).

Conversely, the financial inclusion outcomes suggest that at the 5% level of statistical significance, the impact of FC_{it} on CO_2 emissions is negative and significant according to the FMOLS, DOLS and FE-OLS testing models. The results imply that as financial inclusion increases, this causes CO_2 to decrease by 0.41%, 0.75%, 0.21% in FMOLS, DOLS and FE-OLS, respectively. The outcomes of the current research are consistent with the empirical studies conducted by Renzhi and Baek (2020), who explored the existence of the Environment Kuznets curve (EKC) based on financial inclusion in 103 countries for the period between 2004 and 2014, using Pooled O.L.S. and fixed effects, G.M.M. and Arellano-Bond and Hansen tests.

http://www.aloki.hu ● ISSN 1589 1623 (Print) ● ISSN1785 0037 (Online)
DOI: http://dx.doi.org/10.15666/aeer/2003_25772595

Method of moments of quantile regression results

This paper investigates the effects of G.D.P., consumption of non-renewable energy, renewable energy usage, and financial inclusion on the emissions of carbon for the BRICS Panel by employing the M.M.Q.R. model. In *Table 7*, the findings of panel quantile estimations (M.M.Q.R.). The outcomes show that the effect of G.D.P_{it} on CO_2 emissions is positive across all quantiles (1st to 9th quantiles). G.D.P_{it} causes CO_2 emissions to increase from the lower to middle quantiles, decreasing from 219% to 165%. Thus, the findings show that the emissions of CO_2 rise from the lower to middle quantiles, and the emission intensity decreases throughout the middle and upper quantiles. While G.D.P_{it}^2 negatively affects the level of carbon emissions across each of the quantiles (1st to 9th quantiles). Hence, the testing model outcome provides empirical findings that validate the EKC hypothesis in the BRICS countries. The outcomes of the quantile regression confirm the conclusions of the FMOLS, DOLS, FE-OLS tested models. The empirical findings demonstrate that as economic growth occurs, this initially accelerates carbon emissions but decreases carbon emissions.

Table 7. *Panel quantile estimations (M.M.Q.R.) results*

Variables	Location	Scale	Quantiles								
			0.10	**0.20**	**0.30**	**0.40**	**0.50**	**0.60**	**0.70**	**0.80**	**0.90**
G.D.P_{it}	0.711**	0.322***	1.889***	2.210***	2.235***	2.791***	2.191***	2.099***	1.981***	1.881***	1.651***
G.D.P_{it}^2	-0.631*	-0.299**	-0.890**	-0.931**	-0.860**	-0.880**	-0.832**	-0.795***	-0.733**	-0.652**	-0.611**
REC_{it}	-0.251**	-0.195**	-0.250**	-0.281**	-0.290***	-0.325**	-0.350***	-0.315***	-0.299**	-0.290**	-0.271**
N.R.E.C_{it}	0.650**	0.351***	0.291***	0.298***	0.396***	0.321***	0.299***	0.250***	0.248***	0.232***	0.202***
FC_{it}	-0.391**	-0.298*	-0.315*	-0.395*	-0.441**	-0.488**	-0.480**	-0.431**	-0.401	-0.388	-0.381

Note: *, **, ***means significance of the tested variables at 10%, 5%, 1% levels, respectively

The findings from the panel quantile estimations (M.M.Q.R.) show that the coefficient of REC_{it} for CO_2 emissions is significant and negative through all quantiles (1st to 9th quantiles), implying that renewable energy causes CO_2 emissions to decrease. The quantile regression finding confirms the conclusions of the FMOLS, DOLS, FE-OLS tested models. However, the BRICS economies are growing, which has caused a dramatic transformation in demand for energy due to pressure on the environmentally-friendly power generations. From medium to upper quantiles, there are sustainable levels on the effect of carbon emissions; thus, the incentives for a low carbon economy should be increased.

However, the findings show that N.R.E.C_{it} is significant and positive for the emissions of CO_2 throughout all quantiles (1st to 9th quantiles), and it is evident that more non-renewable energy consumption causes pollution to rise. The findings of the quantile regression confirm the findings of the F.M.L.O.S., DOLS, FE-OLS tested models. Moreover, the (M.M.Q.R.) findings show a significant and negative coefficient of FC_{it} impact emissions of CO_2 across quantiles (1st to 9th quantiles), which demonstrates that financial inclusion causes CO_2 emissions to decrease. However, our study provides new empirical evidence that financial inclusion negatively affects carbon emissions in the BRICS nations using the new M.M.Q.R. technique.

Furthermore, the heterogeneous causality technique for panel data (Dumitrescu and Hurlin, 2012) is employed for verifying the causality among the tested variables. The

http://www.aloki.hu ● ISSN 1589 1623 (Print) ● ISSN1785 0037 (Online)
DOI: http://dx.doi.org/10.15666/aeer/2003_25772595

causality test results are shown in *Table 8*. A uni-directional cause-and-effect relationship is ascertained among G.D.P., G.D.P_{it}^2 , N.R.E.C_{it}, REC_{it} , FC_{it} and the levels of carbon emissions. Hence, G.D.P., G.D.P_{it}^2 , N.R.E.C_{it}, REC_{it}, FC_{it} cause $CO_{2\,it}$ in the BRICS economies.

Table 8. *Granger heterogeneous causality*

Null hypotheses	Z-bar	P-Value
G.D.P_{it} does not homogenously cause $CO_{2\,it}$	8.511***	0.000
$CO_{2\,it}$ does not homogenously cause G.D.P_{it}	1.511	0.211
G.D.P_{it}^2 does not homogenously cause $CO_{2\,it}$	7.511***	0.000
$CO_{2\,it}$ does not homogenously cause G.D.P_{it}^2	0.211	0.293
N.R.E.C_{it} does not homogenously cause $CO_{2\,it}$	8.511***	0.000
$CO_{2\,it}$ does not homogenously cause N.R.E.C_{it}	1.850	0.251
REC_{it} does not homogenously cause $CO_{2\,it}$	4.1251*	0.051
$CO_{2\,it}$ does not homogenously cause REC_{it}	0.151	0.399
FC_{it} does not homogenously cause $CO_{2\,it}$	7.150***	0.000
$CO_{2\,it}$ does not homogenously cause FC_{it}	1.991	0.319

Note: **, ***means the significance of the tested variables at 10%, 5% levels, respectively

However, the findings show that the EKC is valid in the BRICS countries. Furthermore, the results show that non-renewable energy consumption positively affects the levels of carbon emissions. In contrast, the findings from these tests show that renewable energy consumption negatively affects the levels of carbon emissions. Financial inclusion mitigates CO_2 emissions. The BRICS countries have extensive resources for renewable energy. In this context, China has extensive resources of wind and biomass, which have been assuming a significant share of the total capacity over the last years; the total generation capacity in the country experienced six-fold growth, reaching 91,400 MW. However, the renewable energy supply accounts for only 8%. China intends to reduce its emission levels by 2030 to around 60%-65%.

Brazil has extensive resources in wind energy sources; with the help of increased funding and technology, wind energy will provide around 10% of total electricity in 2023. A 2019 report published by the International Renewable Energy Association (I.R.E.N.A.) stated that Brazil meets 42% of its energy needs by using clean energy sources, and 41% of its primary energy supply is generated by oil. According to Nationally Determined Contributions (N.D.C.), Brazil proclaims to decrease its emissions of greenhouse gases (GHG) by 43% by 2030.

South Africa and India also have extensive resources for solar energy. South Africa became the first country with installed P.V. capacity approaching 1000 MW. The wind energy program in this country contributed much to this success. In this context, large-scale wind generators were constructed in the Darling Wind Farm in the country over the last few years. On the other hand, India is a tropical country with an average annual temperature of between 25 °C and 27 °C; the country receives around 5000 trillion kW h equivalents in the source of solar energy; this condition is suitable for the development of solar energy in India.

Despite the BRICS countries having extensive resources in renewable energy, they should promote the consumption and production of renewable energy. Therefore, one primary requirement is investment and financing in these sources to develop and promote

http://www.aloki.hu ● ISSN 1589 1623 (Print) ● ISSN1785 0037 (Online)
DOI: http://dx.doi.org/10.15666/aeer/2003_25772595

renewable energy. Hence, the study suggests that policy-makers should develop energy strategies to reduce non-clean energy use through efficient energy use channels, and they should design systems to support projects and investments that use renewable energy resources. In this line, the policy-makers need to formulate conducive and investment-friendly environment policies to boost more green investment. Furthermore, the Policies should enhance new consumer influxes to accelerate financial inclusion and investment in renewable energies to implement zero-carbon production processes to mitigate pollution in the BRICS countries. Thus, this will lead to sustainable development in these countries.

Conclusion and Policy Implications

In this empirical study, the effects of financial inclusion, as well as the consumption of renewable and non-renewable energy on the emissions of carbon are examined according to the EKC hypothesis in the BRICS for 2002 and 2019, using multivariate structure techniques including DOLS and FMOLS FE-OLS and D-H panel causality estimation and M.M.Q.R. approaches. It is the first study to use the Method of Moments quantile regression technique to explore the connection among the selected variables according to the EKC hypothesis in the BRICS nations. The outcomes of the M.M.Q.R. model exhibit more sensitivity than the DOLS, FMOLS, FE-OLS approaches.

The findings of the DOLS, FMOLS, FE-OLS, M.M.Q.R. tests show that G.D.P. positively affects the levels of carbon emissions, while the impacts of GDP^2 on carbon emissions are adverse. However, the G.D.P. and GDP^2 results confirm that the EKC is valid for the BRICS nations. Furthermore, the DOLS, FMOLS, FE-OLS, and M.M.Q.R. test findings reveal that non-renewable energy consumption positively influences the levels of carbon emissions. In contrast, the conclusions of these tests reveal that renewable energy usage negatively affects the levels of carbon emissions. Therefore, based on the research findings, it is recommended that policy-makers develop energy strategies to reduce non-clean energy use through efficient energy use channels, and they should design systems to support projects and investments that use green energy resources. In this line, the policy-makers need to formulate conducive and investment-friendly environment policies to boost more green investment.

On the other hand, the findings of the DOLS, FMOLS, FE-OLS, and M.M.Q.R. tests show that financial inclusion mitigates carbon emissions. Renewable energy coefficients are significant and negative, which indicates that FC_{it} decreases the CO_2 emissions. THE RESULTS OF the D-H panel approach show that a uni-directional association exists among all variables and CO_2 emissions. According to the research findings, the BRICS must incentivise green investment for the sustainability of economic growth. This indicates that the BRICS countries should offer environmental and financial initiatives associated with CO_2 reduction, particularly by considering financial inclusion and renewable energies. Policies should promote the willingness of people to accelerate financial inclusion and investment in renewable energies to implement zero-carbon production processes to mitigate pollution in the BRICS countries. Thus, this will lead to sustainable development in these countries. Furthermore, further studies could also incorporate the digital financial inclusion variables for particular countries, and a similar study may also apply identical indicators for developing nations.

http://www.aloki.hu ● ISSN 1589 1623 (Print) ● ISSN1785 0037 (Online)
DOI: http://dx.doi.org/10.15666/aeer/2003_25772595

REFERENCES

[1] Abumunshar, M., Aga, M., Samour, A. (2020): Oil price, energy consumption, and CO_2 emissions in Turkey. New evidence from a Bootstrap A.R.D.L. Test. – Energies 13(21): 5588.

[2] Adebayo, T. S. (2022): Renewable Energy Consumption and Environmental Sustainability in Canada: Does Political Stability Make a Difference? – Environmental Science and Pollution Research 1-16.

[3] Adebayo, T. S., Oladipupo, S. D., Adeshola, I., Rjoub, H. (2022a): Wavelet analysis of impact of renewable energy consumption and technological innovation on CO2 emissions: evidence from Portugal. – Environmental Science and Pollution Research 29(16): 23887-23904.

[4] Adebayo, T. S, Saint Akadiri, S., Haouas, I., Rjoub, H. (2022b): A time-varying analysis between financial development and carbon emissions: evidence from the MINT countries. –Energy & Environment 0958305X221082092.

[5] A.F.I. (2020). Alliance for Financial Inclusion. Inclusive Green Finance: A Survey of the Policy Landscape. – Second edition.

[6] Akadiri, S. S., Adebayo, T. S., Asuzu, O. C., Onuogu, I. C., Oji-Okoro, I. (2022): Testing the role of economic complexity on the ecological footprint in China: a nonparametric causality-in-quantiles approach. – Energy & Environment 0958305X221094573.

[7] Akram, R., Fareed, Z., Xiaoli, G., Zulfiqar, B., Shahzad, F. (2022): Investigating the existence of asymmetric environmental Kuznets curve and pollution haven hypothesis in China: Fresh evidence from QARDL and quantile Granger causality. – Environmental Science and Pollution Research 1-17.

[8] Alhodiry, A., Rjoub, H., Samour, A. (2021): Impact of oil prices, the U.S. interest rates on Turkey's real estate market. New evidence from combined co-integration and bootstrap A.R.D.L. tests. – Plos one 16(1): e0242672.

[9] Al-Mulali, U., Ozturk, I., Solarin, S. A. (2016): Investigating the environmental Kuznets curve hypothesis in seven regions: The role of renewable energy. – Ecological indicators 67: 267-282.

[10] Alola, A. A., Adebayo, T. S., Onifade, S. T. (2022): Examining the dynamics of ecological footprint in China with spectral Granger causality and quantile-on-quantile approaches. – International Journal of Sustainable Development & World Ecology 29(3): 263-276.

[11] Altarhouni, A., Danju, D., Samour, A. (2021): Insurance Market Development, Energy Consumption, and Turkey's CO2 Emissions. New Perspectives from a Bootstrap A.R.D.L. Test. – Energies 14(23): 7830.

[12] Altinoz, B., Dogan, E. (2021): How renewable energy consumption and natural resource abundance impact environmental degradation? New findings and policy implications from quantile approach. – Energy Sources, Part B: Economics, Planning, and Policy 16(4): 345-356.

[13] Anwar, A., Siddique, M., Dogan, E., Sharif, A. (2021): The moderating role of renewable and non-renewable energy in environment-income nexus for ASEAN countries: Evidence from Method of Moments Quantile Regression. – Renewable Energy 164: 956-967.

[14] Apergis, N., Ozturk, I. (2015): Testing Environmental Kuznets Curve in Asian countries. – Ecological Indicators 52: 16-22.

[15] Awosusi, A. A., Adebayo, T. S., Altuntaş, M., Agyekum, E. B., Zawbaa, H. M., & Kamel, S. (2022): The dynamic impact of biomass and natural resources on ecological footprint in BRICS economies: A quantile regression evidence. – Energy Reports (8): 1979-1994.

[16] Aydın, M., Turan, Y. E. (2020): The influence of financial openness, trade openness, and energy intensity on ecological footprint: revisiting the environmental Kuznets curve

http://www.aloki.hu ● ISSN 1589 1623 (Print) ● ISSN1785 0037 (Online)
DOI: http://dx.doi.org/10.15666/aeer/2003_25772595

hypothesis for BRICS countries. – Environmental Science and Pollution Research 27: 43233-43245.

[17] Aziz, N., Mihardjo, L. W. W., Sharif, A., Jermsittiparsert, K. (2020): The role of tourism and renewable energy in testing the environmental Kuznets curve in the BRICS countries: fresh evidence from methods of moments quantile regression. – Environmental Science and Pollution Research 27: 39427-39441.

[18] Aziz, N., Sharif, A., Raza, A., Jermsittiparsert, K. (2021): The role of natural resources, globalisation, and renewable energy in testing the EKC hypothesis in MINT countries: new evidence from Method of Moments Quantile Regression approach. – Environmental Science and Pollution Research 28: 13454-13468.

[19] Barik, R., Pradhan, A. K. (2021): Does Financial Inclusion Affect Financial Stability: Evidence from BRICS nations? – The Journal of Developing Areas 55(1): 341-356.

[20] Bashir, M. F., Ma, B., Bashir, M. A., Radulescu, M., Shahzad, U. (2021): Investigating the role of environmental taxes and regulations for renewable energy consumption: evidence from developed economies. – Economic Research-Ekonomska Istraživanja, DOI: 10.1080/1331677X.2021.1962383.

[21] Bibi, F., Jamil, M. (2021): Testing Environment Kuznets Curve (EKC) Hypothesis in Different Regions. – Environmental Science and Pollution Research 28: 13581-13594.

[22] Blazejczak, J., Braun, F. G., Edler, D., Schill, W.-P. (2014): Economic effects of renewable energy expansion: A model-based analysis for Germany. – Renewable and Sustainable Energy Reviews 40: 1070-1080.

[23] Boluk, G., Mert, M. (2015): The renewable energy, growth and environmental Kuznet curve in Turkey: An A.R.D.L. approach. – Renewable and Sustainable Energy Reviews 52: 587-595.

[24] Chakravarty, D., Mandal, S. K. (2016): Estimating the relationship between economic growth and environmental quality for the BRICS economies - A Dynamic Panel Data Approach. – The Journal of Developing Areas 50(5): 119-130.

[25] Chen, Y., Zhao, J., Lai, Z., Wang, Z., Xia, H. (2019): Exploring the effects of economic growth, and renewable and non-renewable energy consumption on China's CO_2 emissions: Evidence from a regional panel analysis. – Renewable Energy 140: 341-353.

[26] Cui, L., Weng, S., Nadeem, A. M., Rafique, M. Z., Shahzad, U. (2022): Exploring the role of renewable energy, urbanisation and structural change for environmental sustainability: Comparative analysis for practical implications. – Renewable Energy 184: 215-224.

[27] Dogan, E., Lotz, R. I. (2020): The impact of economic structure to the environmental Kuznets curve (EKC) hypothesis: evidence from European countries. – Environmental Science and Pollution Research 27: 12717-12724.

[28] Dogan, E., Seker, F. (2016): Determinants of CO_2 emissions in the European Union: The role of renewable and non-renewable energy. – Renewable Energy 94: 429-439.

[29] Dumitrescu, E. I., Hurlin, C. (2012): Testing for Granger non-causality in heterogeneous panels. – Economic Modelling 29(4): 1450-1460.

[30] Fareed, Z., Rehman, M. A., Adebayo, T. S., Wang, Y., Ahmad, M., Shahzad, F. (2022): Financial inclusion and the environmental deterioration in Eurozone: the moderating role of innovation activity. – Technology in Society 69: 101961.

[31] Haseeb, A., Xia, E., Danish, Baloch, M. A., Abbas, K. (2018): Financial development, globalisation, and CO_2 emission in the presence of EKC: evidence from BRICS countries. – Environmental Science and Pollution Research 25(31): 31283-31296.

[32] Huang, R., Kale, S., Paramati, S. R., Taghizadeh-Hesary, F. (2021): The nexus between financial inclusion and economic development: Comparison of old and new E.U. member countries. – Economic Analysis and Policy 69: 1-15.

[33] IEO (2019). U.S. Energy Information Administration, International Energy Outlook 2019.

http://www.aloki.hu ● ISSN 1589 1623 (Print) ● ISSN1785 0037 (Online)
DOI: http://dx.doi.org/10.15666/aeer/2003_25772595

[34] Ike, G. N., Usman, O., Sarkodie, S. A. (2020): Testing the role of oil production in the environmental Kuznets curve of oil producing countries: New insights from Method of Moments Quantile Regression. – Science of the Total Environment 711: 135208.
[35] Kao, C., Chiang, M.-H. (2001): On the estimation and inference of a cointegrated regression in panel data. – In: Baltagi, B. H., Fomby, T. B., Carter Hill, R. (eds.) Nonstationary panels, panel co-integration, and dynamic panels. Emerald Group Publishing Limited. Bingley, pp. 179-222.
[36] Kirikkaleli, D., Güngör, H., Adebayo, T. S. (2022): Consumption-based carbon emissions, renewable energy consumption, financial development and economic growth in Chile. – Business Strategy and the Environment 31(3): 1123-1137.
[37] Le, T. H., Le, H. C., Taghizadeh-Hesary, F. (2020): Does financial inclusion impact CO_2 emissions? Evidence from Asia. – Finance Research Letters 34: 101451.
[38] Machado, J. A. F., Santos Silva, J. M. C. (2019): Quantiles via moments. – Econometrics 213: 145-173.
[39] Maune, A., Matanda, E., Mundonde, J. (2020): Does financial inclusion cause Economic growth in Zimbabwe? An Empirical Investigation. – Economica 16(1): 195-215.
[40] Miao, Y., Razzaq, A., Adebayo, T. S., Awosusi, A. A. (2022): Do renewable energy consumption and financial globalisation contribute to ecological sustainability in newly industrialized countries? – Renewable Energy 187(29).
[41] Narayan, P. K., Saboor, B., Soleymani, A. (2016): Economic growth and carbon emissions. – Economic Modelling 53: 388-397.
[42] Pata, U. K. (2021): Renewable and non-renewable energy consumption, economic complexity, CO2 emissions, and ecological footprint in the USA: testing the EKC hypothesis with a structural break. – Environmental Science and Pollution Research 28(1): 846-861.
[43] Pata, U. K., Samour, A. (2022): Do renewable and nuclear energy enhance environmental quality in France? A new EKC approach with the load capacity factor. – Progress in Nuclear Energy 149: 104249.
[44] Pedroni, P. (2004): Panel co-integration: asymptotic and finite sample properties of pooled time series test with an application to the P.P.P. hypothesis. – Economic Theory 20: 597-625.
[45] Pesaran, M. H. (2007): A simple panel unit root test in the presence of crosssection dependence. – Applied Economics 22: 265-312.
[46] Qashou, Y., Samour, A., Abumunshar, M. (2022): Does the Real Estate Market and Renewable Energy Induce Carbon Dioxide Emissions? Novel Evidence from Turkey. – Energies 15(3): 763.
[47] Ratnawati, K. (2020): The Impact of Financial Inclusion on Economic Growth, Poverty, Income Inequality, and Financial Stability in Asia. – Journal of Asian Finance, Economics and Business 7(10): 73-85.
[48] Rehman, M. A., Fareed, Z., Salem, S., Kanwal, A., Pata, U. K. (2021): Do diversified export, agriculture, and cleaner energy consumption induce atmospheric pollution in Asia? Application of method of moments quantile regression. – Frontiers in Environmental Science 497.
[49] Renzhi, N., Baek, Y. J. (2020): Can financial inclusion be an effective mitigation measure? evidence from panel data analysis of the environmental Kuznets curve. – Finance Research Letters 37: 101725.
[50] Sadorsky, P. (2010): The impact of financial development on energy consumption in emerging economies. – Energy Policy 38: 2528-2535. doi:10.1016/j.enpol.2009.12.048.
[51] Saleem Jabari, M., Aga, M., Samour, A. (2022): Financial sector development, external debt, and Turkey's renewable energy consumption. – Plos one 17(5): e0265684.

http://www.aloki.hu ● ISSN 1589 1623 (Print) ● ISSN1785 0037 (Online)
DOI: http://dx.doi.org/10.15666/aeer/2003_25772595

[52] Samour, A., Isiksal, A. Z., Resatoglu, N. G. (2019): Testing the impact of banking sector development on Turkey's CO_2 emissions. – Applied Ecology and Environmental Research 17(3): 6497-6513.
[53] Samour, A., Baskaya, M., Tursoy, T. (2022a): The Impact of Financial Development and FDI on Renewable Energy in the U.A.E.: A Path towards Sustainable Development. – Sustainability 14(3): 1208.
[54] Samour, A., Moyo, D., Tursoy, T. (2022b): Renewable energy, banking sector development, and carbon dioxide emissions nexus: A path toward sustainable development in South Africa. – Renewable Energy 193:1032-1040.
[55] Samour, A., Pata, U. K. (2022): The impact of the US interest rate and oil prices on renewable energy in Turkey: a bootstrap ARDL approach. – Environmental Science and Pollution Research 1-10.
[56] Shahzad, U., Fareed, Z., Shahzad, F., Shahzad, K. (2021): Investigating the nexus between economic complexity, energy consumption and ecological footprint for the United States: New insights from quantile methods. – Journal of Cleaner Production 279: 123806.
[57] Sharma, D. (2015): Nexus between financial inclusion and economic growth Evidence from the emerging Indian economy. – Financial Economic Policy 8(1): 13-36.
[58] Simionescu, M., Pauna, C. B., Diaconescu, T. (2020): Renewable energy and economic performance in the context of the European Green Deal. – Energies 13(23):6440.
[59] Souza, E. S., Freire, F. S., Pires, J. (2018): Determinants of CO_2 emissions in the MERCOSUR: The role of economic growth, and renewable and non-renewable energy. – Environmental Science and Pollution Research 25: 20769-20781.
[60] Sun, Y., Li, M., Zhang, M., Khan, H. S. U. D., Li, J., Li, Z., Sun, H. (2021): A study on China's economic growth, green energy technology, and carbon emissions based on the Kuznets curve (EKC). – Environmental Science and Pollution Research 28: 7200-7211.
[61] Ummalla, M., Goyari, P. (2020): The impact of clean energy consumption on economic growth and CO_2 emissions in BRICS countries: Does the environmental Kuznets curve exist? – Journal of Public Affairs 21(1): e2126.
[62] Van, T.-H. L., Vo, A. T., Nguyen, N. T., Vo, D. H. (2021): Financial Inclusion and Economic Growth: An International Evidence. – Emerging Markets Finance and Trade 57(1): 239-263.
[63] Westerlund, J. (2007): Testing for error correction in panel data. – Oxford Bulletin of Economics and Statistics 69(6): 709-748.
[64] World Bank (2020). UFA2020 Overview: Universal Financial Access by 2020. – https://www.worldbank.org/en/topic/financialinclusion/brief/achieving-universal-financial-access-by-2020.
[65] World Bank (2021). DataBank, World Development Indicators (W.D.I.). https://databank.worldbank.org/reports.aspx?source=world-development-indicators.
[66] Wu, Q., Zhou, J., Liu, S., Yang, X., Ren, H. (2016): Multi-objective optimisation of integrated renewable energy system considering economics and CO_2 emissions. – Energy Procedia 104: 15-20.
[67] Yan, Y., Shah, M. I., Sharma, G. D., Chopra, R., Fareed, Z., Shahzad, U. (2022): Can tourism sustain itself through the pandemic: nexus between tourism, COVID-19 cases and air quality spread in the 'Pineapple State'Hawaii. – Current Issues in Tourism 25(3): 421-440.
[68] Zafar, M. W., Mirza, F. M., Zaidi, S. A. H., Hou, F. (2019): The nexus of renewable and non-renewable energy consumption, trade openness, and CO_2 emissions in the framework of EKC: evidence from emerging economies. – Environmental Science and Pollution Research 26: 15162-15173.
[69] Zhang, D. B., Wang, B., Wang, Z. (2017): Role of renewable energy and non-renewable energy consumption on EKC: Evidence from Pakistan. – Journal of Cleaner Production 156: 855-864.

http://www.aloki.hu ● ISSN 1589 1623 (Print) ● ISSN1785 0037 (Online)
DOI: http://dx.doi.org/10.15666/aeer/2003_25772595

NATURAL DISTRIBUTION OF WEED SEEDBANK IN DIFFERENT LAND ACTIVITIES DUE TO ABANDONED LAND RECLAMATION FOR AGRICULTURE

MD-AKHIR, A. H. B. – ISA, N. – MISPAN, M. S.*

Institute of Biological Sciences, Faculty of Science, Universiti Malaya, 50603 Kuala Lumpur, Malaysia
(phone: +603-7967-6757; fax: +603-7967-4376)

**Corresponding author*
e-mail: shakirin@um.edu.my

(Received 17th Dec 2021; accepted 21st Mar 2022)

Abstract. Most studies on weed infestation mainly focused on the aboveground infestation despite the fact that the importance of the seedbank dynamics in influencing weed abundance is well acknowledged. Effective weed management for development or rejuvenation of an abandoned land should consider the potential of weed seed emergence from the seedbank. Soil samples from three different locations were collected from abandoned agriculture lands in Glami Lemi Biotechnology Research Center, Negeri Sembilan (GLBRC), Malaysia to determine the density and distribution pattern of the weed seedbank using seed separation and seedling emergence methods. A total of 53 weed species, mainly broadleaves, were identified in the area. Broadleaf weeds showed a higher number of emerged seedlings compared to grasses which reflected the aboveground weed vegetation composition. Seedling emergence method provided better representation of weed seedbank composition in this study compared to separation method. Lloyd's patchiness index (*lp*) determined that the majority of survey sites displayed cluster distribution pattern for the seedbank of both broadleaf and grass weeds indicating the robust weed seedbank composition of the area. The weed seedbank management could be effectively employed for the development of abandoned lands based on the clustering areas and precise prediction of seedbank density.
Keywords: *distribution pattern, land management, soil seedbank, tillage, weed management*

Introduction

Periodical weed field emergence strongly depends on the amount, botanical composition and vertical arrangement of the seedbank (Benvenuti and Perdossi, 2017). The vertical arrangement is key for weed survival via seedbank where light-dependent small seeds are capable of germination and seedling emergence at the shallowest seed bank possible (Batlla and Benech-Arnold, 2014). In addition, high seed longevity is typical for many weeds (Gu et al., 2006) which facilitates their long-term persistence in the soil (Mispan et al., 2019).

The number of viable seeds in the soil can be affected by ecological conditions and agronomic practices ranges from about 2300 seeds per m^2 in the conventional cropping systems (Sosnoskie et al., 2006), to almost 10,000–50,000 seeds per m^2 in the organic management systems (Albrecht, 2005; Graziani et al., 2012). In Malaysian rice agro-ecosystem for instance, weedy rice seedbank plays a crucial role in weedy rice infestation for future successive seasons (Mispan et al., 2019).

This seedbank accumulation occurs since most annually produced weed seeds undergo dormancy in the soil due to genetic, species, and/or environmental soil-depth mediated mechanisms (Gu et al., 2006; Benvenuti and Mazzoncini, 2019). Consequently, knowing the quantity, botanical composition and vertical distribution of buried seeds can play a crucial role in predicting the likeliness of the dynamics of weed emergence. As seedbank

http://www.aloki.hu ● ISSN 1589 1623 (Print) ● ISSN 1785 0037 (Online)
DOI: http://dx.doi.org/10.15666/aeer/2003_25972607

plays an important role for plant species survivability and viability, this phenomenon also brings several impacts towards many human activities such in the agriculture practices (Hossain et al., 2014), and forestry (Meers et al., 2012). This information facilitates planning on weed control strategies before weed emergence. In other words, a seedbank evaluation acts as a non-chemical weed management method, thus making it a useful agronomic tool.

Malaysia is a tropical country with warm climate and adequate rainfall. These conditions permit the luxuriant growth of various weed species almost all year round. Today, the Malaysian agro-ecosystems are homes of more than 500 weed species including nine of the world's worst weed species (Heap, 2014; Ruzmi et al., 2017). Some of these species are classified as scheduled pests under the Malaysia Plant Quarantine Act 1976 and Plant Quarantine Regulation 1981. Farmers in Malaysia normally employ a battery of control methods to achieve satisfactory results in managing weeds. These include, principally, the agro-technical and preventive methods comprising land preparation and tillage, water management, crop manipulation through competitive cultivars, chemical control, and in certain cases, biological control using bio-control agents and bio-herbicides is instituted (Mispan et al., 2015). The aim of these weed management strategies was not only eliminating the weeds that emerge but also include limiting the seed production and dispersal (Nichols et al., 2015) to minimize the input of weed seeds in the soil – the seedbank (Mispan et al., 2019).

Abandoned land was known to be infested with weed flora and volunteer crop species when not more in use for any anthropogenic activities. The abilities of these weeds and vegetation to continue to infest the land are supported by the dynamics of their respective seedbank to provide adequate seedling to continue its survival even after abandonment (Valko et al., 2016). Therefore, reclamation of the land for agriculture activities will need to consider the potential of weed infestation from the existing seedbank. Thus, the seedbank dynamics play an important role as a developmental potential for future weeds infestation and vegetation species in the region (Bajwa et al., 2016).

The objective of this study was to observe and determine the ecology of seedbank via seed distribution patterns at different types of soils in an abandoned agricultural land. Such information will be useful for decision making for future weed management based on potential risks and incurred costs for further development of the area. The results can be used for future land-use weed control program for a given types of abandoned land.

Materials and Methods

Study sites

This study was conducted in June 2018 at the Glemi Lemi Biotechnology Research Center (GLBRC), Universiti Malaya (3.053361N, 102.063997E) which is in the district of Jelebu, Negeri Sembilan, Malaysia. This 120-acre facility was built on an abandoned farming land and an ex-tin mining site with the purpose to be a field-research hub for agricultural biotechnology. A total of 10 sampling sites were randomly selected across the land (*Fig. 1*) and was grouped into three categories based on the current land activities (*Table 1*).

Sites I to IV were located within approximately 30 m from the facility's buildings parameter. These areas were regularly maintained from weed infestation mainly by mowing and scheduled herbicide (mainly glyphosate) application. Soil for these areas were sandy with mostly from foreign soil brought in for development and construction

http://www.aloki.hu ● ISSN 1589 1623 (Print) ● ISSN 1785 0037 (Online)
DOI: http://dx.doi.org/10.15666/aeer/2003_25972607

purpose. Sites V to VII were located near field research experiment sites. During this study, these areas were growing Napier grass and pineapple. Weed management of these sites followed standard weed management practices. Sites VIII to X were located on undeveloped areas where there were no active agricultural practices on the land since the opening of the facility in 2012.

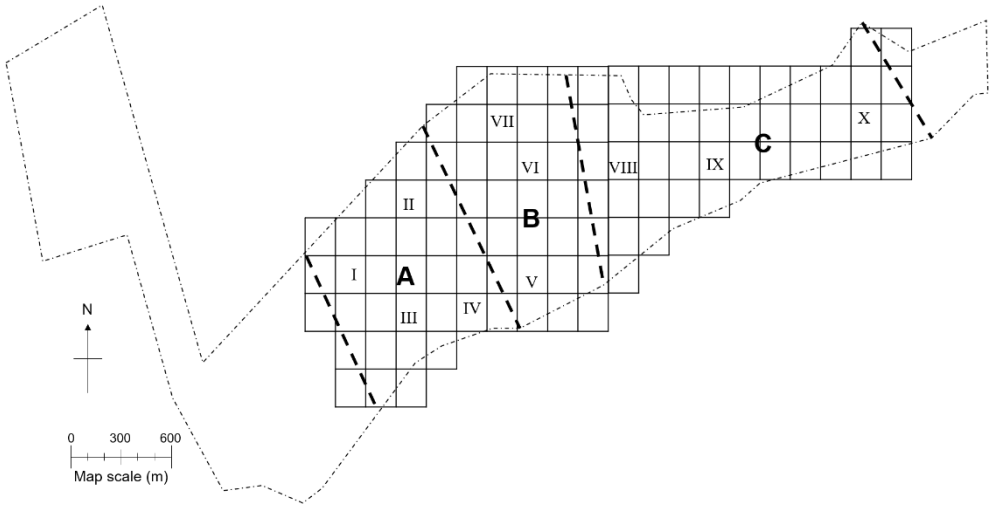

Figure 1. *Locations (A-C) of the seedbank collection at ten sampling sites (I-X). The sampling sites were randomly determined from the aerial grid*

Table 1. *Description of seedbank survey locations in Glami Lemi Biotechnology Research Center, Universiti Malaya, Jelebu, Negeri Sembilan*

Locations	Sites	Description
A	Site I - IV	• Near building areas. No vegetation. Mainly primary succession. • Mostly foreign soil brought in for development purpose.
B	Site V – VII	• Active research sites. • Various type of vegetation being planted: corn, napier, pumpkin. • Vegetation grown for research project.
C	Site VII – X	• Near active location (*B*). • No active agricultural practices or crop grown. • Primarily covered with shrubs and weeds.

Vegetative recording

The weed species of GLBRC were identified and recorded. The species were characterized as grasses, broadleaves, sedges and ferns. Some species were identified directly by observing their taxonomical characteristics, but some were sampled and brought back to lab for further identification.

Seedbank sampling

Distribution of seedbank in GLBRC was accessed by two methods, namely germination test and direct seed counting. A total of five (5) spots were randomly plotted at every sampling site for soil collection. Distance for each spot was more than 20 m apart. Soil was extracted in a 10 cm x 10 cm square and 1 cm deep at each spot. The

http://www.aloki.hu ● ISSN 1589 1623 (Print) ● ISSN 1785 0037 (Online)
DOI: http://dx.doi.org/10.15666/aeer/2003_25972607

samples were immediately put in a plastic bag and placed in a greenhouse to be air-dried for three days.

To estimate composition of the seedbank by germination test, each soil sample was concentrated by washing the soil with water through a course (4.0 mm mesh width) and a fine sieve (0.212 mm mesh width), to remove both coarse and fine soil material, roots and vegetative parts. The concentrated samples were mixed with water until they became fluid then thinly and evenly (~ 5 mm thick) poured in a plastic container (15 cm x 15 cm x 10 cm) filled with 1 cm thick steam-sterilized potting soil and 5 mm thick layer of sterile sand preventing contact between sample and the potting soil. The sand and potting soil were separated with a fine nylon mesh net. The samples were placed in the greenhouse at natural temperatures and humidity. Germinated seedlings were counted at every 3-day interval for six weeks. The containers were kept moist for the entire experiment. Germinated seeds were identified as grass or broadleaf weed based on seedling leaf morphological characteristic.

Additional soil samples from the similar plots for germination test were used for direct seed counting. A 1 cm thick layer of soil samples were collected and placed in a 9 mm petri dish. The samples were air-dried for 3 days in the greenhouse. The presence of seed in the soil was directly counted under light microscope.

Lloyd's patchiness index (*lp*) was used to assess the distribution pattern of soil seedbank on all sites from the relationship between mean crowding (m*) and mean density (m) (Baki and Shakirin, 2010). The distribution pattern can be determined using the Iwao line from the m*/m plotting. Values located close to the line indicate a random distribution. Values plotted above and below the line correspond to clustered and uniform distribution, respectively.

Results

Aboveground weed composition and seedbank composition

Survey of the aboveground vegetation identified and recorded a total of 53 weed species within the facility. There were 17 families of weed characterized as broadleaf, grass, sedge and fern with 36, 14, 2 and 1 number of species, respectively (*Fig. 2*). This information will be the base to corroborate with the seedbank composition.

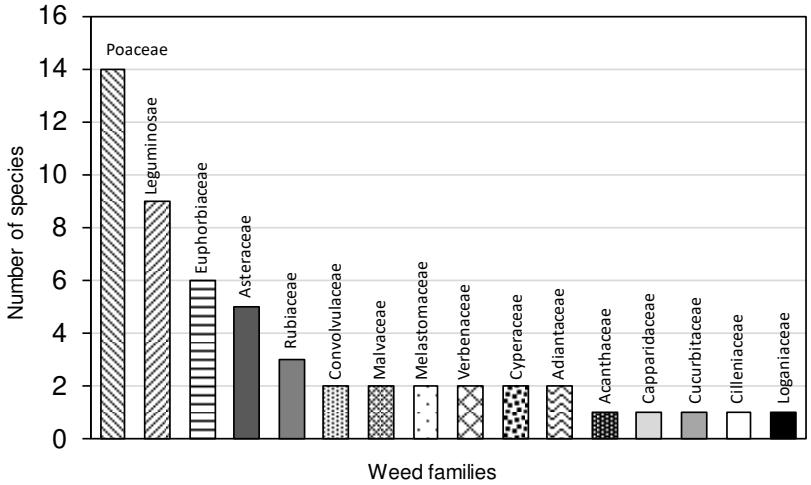

Figure 2. *Number of weed species according to respective family identified in survey sites*

http://www.aloki.hu ● ISSN 1589 1623 (Print) ● ISSN 1785 0037 (Online)
DOI: http://dx.doi.org/10.15666/aeer/2003_25972607

Germination test on the soil samples showed that the seedlings started to emerge from the soil at 3 d after soaking and reached full germination at 9 d (*Fig. 3*). No new seedlings emerged after 9 d of imbibition. Sites VI and VII displayed the highest number of germinated seedlings with an average of 212.0 (±352.26) and 144.0 (±352.26) seedlings, respectively especially in Plots 6.1 and 7.1.

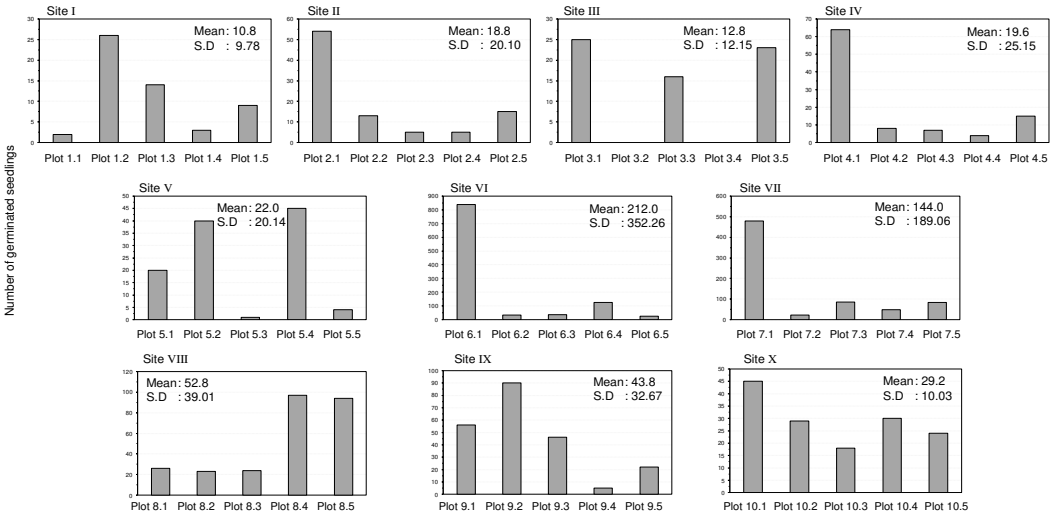

Figure 3. *Number of emerged seedlings recorded at every site (I-X). Mean and standard deviation (S.D.) were calculated based on five plots in each site*

Due to high standard deviation of number of seedlings in the majority of the sites, numbers for all plots at each site were combined to represent the site. Emerged seedlings were differentiated as grasses and broadleaves, based on their seedlings leaf characteristics (*Fig. 4*). Site VI recorded the highest density of both grass and broadleaf seedlings, while Sites I and II displayed the lowest density for broadleaf and grass seedlings, respectively. Majority of the sites showed higher density for broadleaves than grasses except at Sites II. The biggest difference was shown within location B where agriculture activities were located.

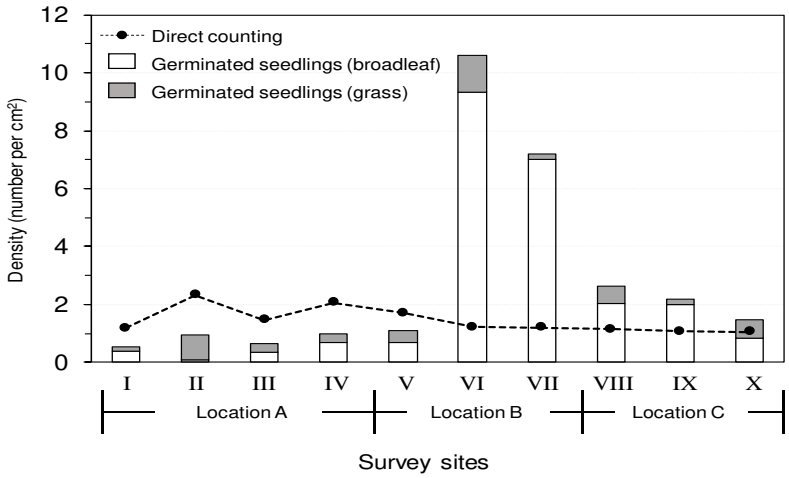

Figure 4. *Density (number per cm^2) of germinated seedlings for grass and broadleaf weeds (bar) and number of seeds from direct counting (dotted line) from the sampling sites (I-X)*

http://www.aloki.hu ● ISSN 1589 1623 (Print) ● ISSN 1785 0037 (Online)
DOI: http://dx.doi.org/10.15666/aeer/2003_25972607

Seeds from the seedbank were hand sorted and directly counted (*Fig. 4*). Across all sites, locations B (except Site V) and C displayed higher density of seedling emergence compared to direct counting, while location A displayed the opposite. Soil composition in location A was primarily foreign sand that were brought in for development purpose as compared to other locations which has diverse compositions of higher silt and clay. Location A also was highly maintained from weeds. The difference ratio between emerged seedlings and counted seeds can be used as indicator to the potential of seedbank to germinate once the environment favors, depending on dormancy status and/or the viability of the seedbanks

Seedling spatial distribution

None of the weed seedbanks for both broadleaf and grass types form uniform distribution at all sites based on Lloyd's patchiness index (*Fig. 5*). Majority of the sites displayed cluster or clump distribution pattern for both grass and broadleaf weeds. Broadleaves showed random distribution at sites I, IV and VII, while grasses only displayed random distribution at site II.

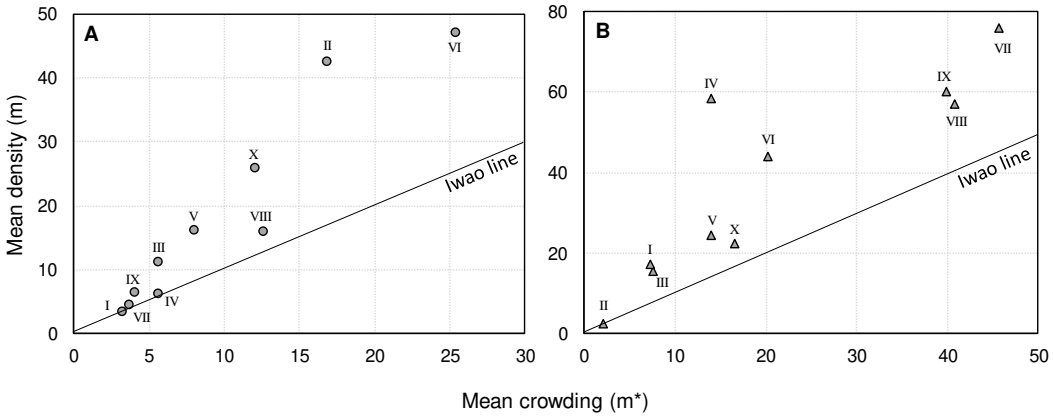

Figure 5. *Distribution pattern of broadleaf (A) and grass (B) weeds based on mean density (m) and mean crowding (m*) for every survey site (I-X). Sites located on, above, and below Iwao line indicate random, clustered and uniform distribution pattern, respectively*

Discussion

An effective management plan for invasive weed infestation must consider the potential for the emergence of weeds from the soil seedbank (Head et al., 2015). Weeds can persist in an agricultural land through their seed's survivability in the seedbank. Maintaining viability over longer periods in the seedbank might provide several adaptive advantages for weed seeds to survive heat and high humidity and escape seed deterioration especially in tropical areas. Therefore, knowing the composition of weed in the seedbank is crucial to allow effective management strategies to be designed to reduce or ultimately eliminate the possible seed escape (Mispan et al., 2019).

This study showed that the aboveground weed vegetation can be reflected to the seedbank composition of grass and broadleaf weeds. Broadleaf weeds displayed higher density of germinated seedling compared to grasses (*Fig. 4*) which tallied with our aboveground weed composition findings in *Fig. 2*. Takim et al. (2013) reported that

http://www.aloki.hu ● ISSN 1589 1623 (Print) ● ISSN 1785 0037 (Online)
DOI: http://dx.doi.org/10.15666/aeer/2003_25972607

broadleaf weed seeds were easy to germinate in the agricultural fields. Continuous cultivated maize farm has significantly higher density of broadleaf weed seedlings when compared with cultivated cowpea farm and closely followed by natural fallow fields that show to be the least significant in term of density of broadleaf weed (Takim et al., 2013).

In contrast, Tozer et al. (2010) reported that aboveground weed composition did not reflect the seedbank germinated seedling in a pasture. Weed assessment in a pasture recorded domination of grass weeds in all regions, but only one grass weed species germinated from the seedbank. Weedy herb (broadleaf) species were the most frequent seedlings emerging from the seedbank but not the most frequent species found aboveground in all surveyed regions.

Sites at locations B and C showed higher density of germinated seedlings as compared to direct counting from separation method (*Fig. 4*). At the same time, average frequency of direct counting for all locations was not significantly different despite variation in germination data. This indicates that determination of composition of seeds in the soil cannot be highly dependent on physically count the seeds. Determination of seedbank composition in the soil by separation method is a tedious process with some inadequacies (Ter Heerdt et al., 1996). Problems of this method are the residue still contains soil material, and hand-sorting under a binocular microscope to collect the seeds is needed which was very time consuming and only suitable for finding large-seeded species but ineffective for small-seeded species, especially in large-scale studies (Price et al., 2010). At the same time, seeds in the soil has diverse morphological characteristics with huge magnitude of sizes (Price et al., 2010; Leslie et al., 2017).

While germination data provides better representation of seeds information in the seedbank, many other factors can contribute towards seeds germination ability which the extent of variation is still unknown (Price et al., 2010; Leslie et al., 2017). Seedlings emergence from the seedbank can be affected by field management practices (Chauhan et al., 2012), weed seedbank diversity (Mesquita et al., 2013), seed dormancy and viability (Kleemann and Gill, 2013), and seed placement (Mohler et al., 2006). Chauhan et al. (2006) reported that seed decay in no-tillage systems (48 to 60%) was much higher than under minimum tillage (12 to 39%). As these factors and their impacts are considered, the efficiency and efficacy of weed seedbank management can be increased.

It was also clear that sites at Location A displayed significantly the lowest density for emerged seedlings compared to other locations. Active weed control of the areas might have resulted in the low seedbank number. Application of herbicide for instance can suppress germination or might push toward death of the weed seed itself. Kumar et al. (2013) reported that herbicide usage produced a shift in the weed seedbank in favor of germination of weed species that are less susceptible compared with other species. However, Smith et al. (2016) showed that pesticide seed treatment can reduce the abundance of the seed natural enemies such as pathogens (bacteria, fungi) and soil dwelling predator that able to damage or destroy seeds in the soil seedbank thus treated plot had much higher but less diverse weed seedbank compared to untreated plot. Herbicides significantly able to suppress seedling emergence from the seedbank and can harm both non-native and native plants at some growth stages such as seed stage (Wagner and Nelson, 2014).

High standard deviation at each site (*Fig. 2*) indicates the variation of seedbank distribution in the field. Analysis of spatial distribution of the seedbank might provide new insight on how the seeds of the weeds dispersed into the seedbank. The cluster distribution pattern at the majority of the sites suggests a robust seedbank in the area

http://www.aloki.hu ● ISSN 1589 1623 (Print) ● ISSN 1785 0037 (Online)
DOI: http://dx.doi.org/10.15666/aeer/2003_25972607

which can provide suitable environments for further germination (Mohammadvand et al., 2007). Moreover, it may indicate that the grass and broadleaf weeds only cluster at certain specific areas since weed seeds are generally dispersed in less than two meters away from the parent plant (Roham et al., 2014). However, for seeds to travel further from mother plant, they will require dispersal agent to help facilitate their dispersion (McConkey et al., 2012). It can be assumed that the seedbank is most likely to form a cluster in a low-density weed population. This is possible since the seedbank samples of this study, despite being random sampling, were taken only at the accessible areas where the vegetations were not dense due to safety issue.

In general, weed vegetations always clusters at various densities with various patchiness sizes (Roham et al., 2014). Seeds of the weed can be easily dispersed by multiple agents according to the size and shape of reproductive organs, environmental conditions (e.g. wind, water, animals), and anthropological activities including planting patterns, tillage system or management and harvesting practices (McConkey et al., 2012). As the distribution of weed seeds are dynamically changing due to various dispersion factors mentioned, some seedbank of the abandoned fields may contain seeds below the economic thresholds while the other parts may have higher abundance of seedbank (López-Toledo and Martínez-Ramos, 2011) which are often overlooked in agricultural practices (Mispan et al., 2015, 2019).

Weed management especially by herbicide application is typically applied uniformly throughout the field. It was always assumed that weeds are distributed homogeneously (Roham et al., 2014). Conversely in this study, it has been shown that the seedbanks were heterogeneously distributed. The weed seedbank management could be effectively improved if the control methods (e.g. herbicide application) has been based on the clumping locations (Loghavi and Mackvandi, 2008) and precise prediction on seedbank density.

Although this study could give a fair estimation of future weed emergence in the field, the result is only a representation of a small and variable fraction of weed seed in the soil seedbank. Therefore, it is proposed, the assessment on seed content in the soil especially in a large-scale study needs a reliable, quick and space-savvy method. A new approach can be developed to determine seedbank composition in the soil using molecular methods. Molecular techniques have been developed to detect and quantify a range of organisms in soil (Ophel-Keller et al., 2008) but very limited studies are available on seeds in the soil. Riley et al. (2010) developed quantitative DNA assays for *Lolium perenne* (ryegrass) and *Trifolium subterraneum* (subterranean clover) to include seeds determination in the soil in mixed plant populations. DNA extraction from seeds in general is feasible (Barrett et al., 2005) indicating the potential of using molecular techniques on seeds. Osterbauer and Rehms (2002) used Polymerase Chain Reaction (PCR) techniques to detect single seed of broomrape (*Orobanche minor* Smith.), which are extremely small, averaging 200 to 300 μm in size. This method was expanded by Rolland et al. (2016) by using High Resolution Melting assay where they successfully and accurately determined the targeted broomrape species from the soil. Accurate seedbank information will assist in decision support system in the future for weed management via seedbank.

Conclusion

Effective weed management for development or rejuvenation of an abandoned land should consider the potential of weed seed emergence from the soil seedbank. This study

http://www.aloki.hu ● ISSN 1589 1623 (Print) ● ISSN 1785 0037 (Online)
DOI: http://dx.doi.org/10.15666/aeer/2003_25972607

shows that broadleaf weeds were highly likely to emerge first under favorable condition. Any potential weed management including application of pre-emergence herbicide should consider this possibility. Different activities also influenced soil seedbank distribution. Active weed management will reduce weed seedbank capability to emerge as the density was significantly reduced. On the other hand, abandonment of the land produced patchiness or clustering of weed seeds in the seedbank which contributes to uncertainties of future weed infestation. Molecular techniques are proposed as a way forward to determine weed seedbank composition in agricultural soils to overcome the limitations in the seedling emergence and seed separation methods. Understanding the nature on how seed of weeds dispersed and settled in the soil as seedbank is significant to provide better strategy(s) to manage/control weeds.

Acknowledgements. This study was supported by the Bantuan Kecil Penyelidikan [grant number: BK004-2015], Universiti Malaya and Fundamental Research Grant Scheme [grant number: FP001-2015A], Ministry of Higher Education Malaysia.

REFERENCES

[1] Albrecht, H. (2005): Development of arable weed seedbanks during the 6 years after the change from conventional to organic farming. – Weed Research 45(5): 339-350. DOI: https://doi.org/10.1111/j.1365-3180.2005.00472.x.

[2] Bajwa, A. A., Chauhan, B. S., Farooq, M., Shabbir, A., Adkins, S. W. (2016): What do we really know about alien plant invasion? A review of the invasion mechanism of one of the world's worst weeds. – Planta 244(1): 39-57. DOI: 10.1007/s00425-016-2510-x.

[3] Baki, B. B., Shakirin, M. M. (2010): Spatio-temporal distribution pattern of new biotypes of weedy rice (*Oryza sativa* L.) in Selangor North-West Project, Malaysia. – Korean Journal of Weed Science 30(2): 68-83.

[4] Barrett, L. G., He, T., Lamont, B. B., Krauss, S. L. (2005): Temporal patterns of genetic variation across a 9-year-old aerial seed bank of the shrub Banksia hookeriana (Proteaceae). – Molecular Ecology 14(13): 4169-4179.

[5] Batlla, D., Benech-Arnold, R. L. (2014): Weed seed germination and the light environment: Implications for weed management. – Weed Biology and Management 14(2): 77-87. https://doi.org/10.1111/wbm.12039.

[6] Benvenuti, S., Pardossi, A. (2017): Weed seedbank dynamics in Mediterranean organic horticulture. – Scientia Horticulturae 221: 53-61. DOI: 10.1016 /j. scienta.2017.04.011.

[7] Benvenuti, S., Mazzoncini, M. (2019): Soil Physics Involvement in the Germination Ecology of Buried Weed Seeds. – Plants 8(1): 7. DOI: 10.3390/plants8010007.

[8] Chauhan, B. S., Gill, G. S., Preston, C. (2006): Tillage system effects on weed ecology, herbicide activity and persistence: a review. – Australian Journal of Experimental Agriculture 46(12): 1557-1570. https://doi.org/10.1071/EA0529187100.

[9] Chauhan, B. S., Singh, R. G., Mahajan, G. (2012): Ecology and management of weeds under conservation agriculture: a review. – Crop Protection 38: 57-65. DOI: 10.1016/j.cropro.2012.03.010.

[10] Graziani, F., Onofri, A., Pannacci, E., Tei, F., Guiducci, M. (2012): Size and composition of weed seedbank in long-term organic and conventional low-input cropping systems. – European Journal of Agronomy 39: 52-61. DOI: 10.1016/j.eja.2012.01.008.

[11] Gu, X. Y., Kianian, S. F., Foley, M. E. (2006): Dormancy genes from weedy rice respond divergently to seed development environments. – Genetics 172(2): 1199-1211. DOI: 10.1534/genetics.105.049155.

http://www.aloki.hu ● ISSN 1589 1623 (Print) ● ISSN 1785 0037 (Online)
DOI: http://dx.doi.org/10.15666/aeer/2003_25972607

[12] Head, L., Larson, B. M., Hobbs, R., Atchison, J., Gill, N., Kull, C., Rangan, H. (2015): Living with invasive plants in the Anthropocene: the importance of understanding practice and experience. – Conservation and Society 13(3): 311-318. DOI: 10.4103/0972-4923.170411.
[13] Heap, I. (2014): Global perspective of herbicide-resistant weeds. – Pest Management Science 70(9): 1306-1315. DOI: 10.1002/ps.3696.
[14] Hossain, M. M., Begum, M., Hashem, A., Rahman, M. M., Bell, R. W., Haque, M. E. (2014): Yield response of mustard as influenced by weed management practice under conservation agriculture system. – Bangl J Weed Sci. 4: 87-92. DOI: 10.5281/zenodo.5002940.
[15] Kleemann, S. G. L., Gill, G. S. (2013): Seed dormancy and seedling emergence in ripgut brome (Bromus diandrus) populations in southern Australia. – Weed Science 61(2): 222-229. DOI: https://doi.org/10.1614/WS-D-12-00083.1.
[16] Kumar, V., Singh, S., Chhokar, R. S., Malik, R. K., Brainard, D. C., Ladha, J. K. (2013): Weed management strategies to reduce herbicide use in zero-till rice–wheat cropping systems of the Indo-Gangetic Plains. – Weed Technology 27(1): 241-254. DOI: https://doi.org/10.1614/WT-D-12-00069.1.
[17] Leslie, A. B., Beaulieu, J. M., Mathews, S. (2017): Variation in seed size is structured by dispersal syndrome and cone morphology in conifers and other nonflowering seed plants. – New Phytologist 216(2): 429-437. DOI: 10.1111/nph.14456.
[18] Loghavi, M., Mackvandi, B. B. (2008): Development of a target-oriented weed control system. – Computer Electronic in Agriculture 63(2): 112-118.
[19] López-Toledo, L., Martínez-Ramos, M. (2011): The soil seed bank in abandoned tropical pastures: source of regeneration or invasion? – Revista Mexicana de Biodiversidad 82(2): 663-678.
[20] McConkey, K. R., Prasad, S., Corlett, R. T., Campos-Arceiz, A., Brodie, J. F., Rogers, H., Santamaria, L. (2012): Seed dispersal in changing landscapes. – Biological Conservation 146(1): 1-13. DOI: 10.1016/j.biocon.2011.09.018.
[21] Meers, T. L., Enright, N. J., Bell, T. L., Kasel, S. (2012): Deforestation strongly affects soil seed banks in eucalypt forests: generalisations in functional traits and implications for restoration. – Forest Ecology and Management 266: 94-107. DOI: 10.1016/j.foreco.2011.11.004.
[22] Mesquita, M. L. R., Andrade, L. A. D., Pereira, W. E. (2013): Floristic diversity of the soil weed seed bank in a rice-growing area of Brazil: in situ and ex situ evaluation. – Acta Botanica Brasilica 27(3): 465-471. DOI: http://dx.doi.org/10.1590/S0102-33062013000300001.
[23] Mispan, M. S., Jalaluddin, A., Majrashi, A. A., Baki, B. B. (2015): Weed Science in Malaysia: An Analysis. – In: Rao et al. (eds.) Weed Science in the Asian Pacific Region. Asian-Pacific Weed Science Society.
[24] Mispan, M. S., Bzoor, M., Mahmod, I., Md-Akhir, A. H., Zulrushdi, A. (2019): Managing weedy rice (*Oryza sativa* L.) in Malaysia: challenges and ways forward. – Journal of Research in Weed Science 2: 149-167.
[25] Mohammadvand, E., Rashe, M. M., Nasiri, M. M., Pourtousi, N. (2007): Characterizing Distribution and Stability of Purple Nutsedge Population Using Geostatistics over two Growing Seasons. – Iranian Journal of Weed Research 3: 1-21.
[26] Mohler, C. L., Frisch, J. C., McCulloch, C. E. (2006): Vertical movement of weed seed surrogates by tillage implements and natural processes. – Soil and Tillage Research 86(1): 110-122. DOI: https://doi.org/10.1016/j.still.2005.02.030.
[27] Nichols, V., Verhulst, N., Cox, R., Govaerts, B. (2015): Weed dynamics and conservation agriculture principles: A review. – Field Crops Research 183: 56-68. DOI: https://doi.org/10.1016/j.fcr.2015.07.012.

http://www.aloki.hu ● ISSN 1589 1623 (Print) ● ISSN 1785 0037 (Online)
DOI: http://dx.doi.org/10.15666/aeer/2003_25972607

[28] Ophel-Keller, K., McKay, A., Hartley, D., Curran, J. (2008): Development of a routine DNA-based testing service for soilborne diseases in Australia. – Australasian Plant Pathology 37(3): 243-253. DOI: 10.1071/AP08029.
[29] Osterbauer, N. K., Rehms, L. (2002): Detecting single seeds of small broomrape (*Orobanche minor*) with a polymerase chain reaction. – Plant Health Progress 3(1): 1. doi:10.1094/PHP-2002-1111-01-RS.
[30] Price, J. N., Wright, B. R., Gross, C. L., Whalley, W. R. (2010): Comparison of seedling emergence and seed extraction techniques for estimating the composition of soil seed banks. – Methods in Ecology Evolution 1(2): 151-157. DOI:https://doi.org/10.1111/j.2041-210X.2010.00011.x.
[31] Riley, I. T., Wiebkin, S., Hartley, D., McKay, A. C. (2010): Quantification of roots and seeds in soil with real-time PCR. – Plant and Soil 331(1-2): 151-163. DOI: 10.1007/s11104-009-0241-5.
[32] Roham, R., Pirdashti, H., Yaghubi, M., Nematzadeh, G. (2014): Spatial distribution of nutsedge (*Cyperus* spp. L.) seed bank in rice growth cycle using geostatistics. – Crop Protection 55: 133-141.
[33] Rolland, M., Dupuy, A., Pelleray, A., Delavault, P. (2016): Molecular identification of broomrape species from a single seed by high resolution melting analysis. – Frontiers in Plant Science 7: 1838. DOI: 10.3389/fpls.2016.01838.
[34] Ruzmi, R., Ahmad-Hamdani, M. S., Bakar, B. B. (2017): Prevalence of herbicide-resistant weed species in Malaysian rice fields: A review. – Weed biology and management 17(1): 3-16.
[35] Smith, R. G., Atwood, L. W., Morris, M. B., Mortensen, D. A., Koide, R. T. (2016): Evidence for indirect effects of pesticide seed treatments on weed seed banks in maize and soybean. – Agriculture Ecosystem and Environment 216: 269-273. DOI: 10.1016/j.agee.2015.10.008.
[36] Sosnoskie, L. M., Herms, C. P., Cardina, J. (2006): Weed seedbank community composition in a 35-yr-old tillage and rotation experiment. – Weed science 54(2): 263-273. DOI: https://doi.org/10.1043/0043-1745(2006)54[263:WSCCIA]2.0.CO;2.
[37] Takim, F. O., Fadayomi, O., Amosun, J. O., Ekeleme, F. (2013): Influence of Land use Intensity and Weed Management Practice on Field Emergence, Characterization and Growth of Weeds in Southern Guinea Savanna of Nigeria. – Journal of Agriculture Research and Development 12(2): 13-32. DOI: 10.4314/jard.vl2i2.2.
[38] Ter Heerdt, G. N. J., Verweij, G. L., Bekker, R. M., Bakker, J. P. (1996): An improved method for seed-bank analysis: seedling emergence after removing the soil by seiving. – Functional Ecology 10: 144-151.
[39] Tozer, K. N., Barker, G. M., Cameron, C. A., James, T. K. (2010): Relationship between seedbank and above-ground botanical composition during spring. – New Zealand Plant Protection 63: 90-95.
[40] Valkó, O., Deák, B., Török, P., Kelemen, A., Miglécz, T., Tóth, K., Tóthmérész, B. (2016): Abandonment of croplands: problem or chance for grassland restoration? Case studies from Hungary. – Ecosystem Health and Sustainability 2(2): 2-8. DOI: https://doi.org/10.1002/ehs2.1208.
[41] Wagner, V., Nelson, C. R. (2014): Herbicides can negatively affect seed performance in native plants. – Restoration Ecology 22(3): 288-291. DOI: https://doi.org/10.1111/rec.12089.

http://www.aloki.hu ● ISSN 1589 1623 (Print) ● ISSN 1785 0037 (Online)
DOI: http://dx.doi.org/10.15666/aeer/2003_25972607

ANALYSIS THE RELATIONSHIP OF DIFFERENT YIELD LEVELS AND WATER USE OF DRYLAND WHEAT (*TRITICUM AESTIVUM* L.) UNDER DIFFERENT FALLOW TILLAGE TYPES

DONG, S. – NOOR, H. – YANG, L. –REN, A. – LIN, W. – YU, S. – REN, J. – SUN, M.* – GAO, Z.

College of Agriculture, Shanxi Agricultural University, Taigu 030801, China

**Corresponding author*
e-mail: sm_sunmin@126.com

(Received 19th Dec 2021; accepted 25th Feb 2022)

Abstract. Tillage method does exert a certain regulatory effect on yield of rainfed crops. A field experiment was established on the Loess Plateau and was for 8 years during 2009–2017. Three types of fallow tillage (no-tillage, deep plough and subsoiling) were used, and divided the yield with cluster analysis, studied the relationship of the main yield components and precipitation, soil water storage and water use. The results showed that the yield of wheat was influenced by the adjustment of the distribution of yield components in different precipitation years, and the number of plural was the main factor to obtain higher yield, which was influenced by the precipitation during the fallow-period and the sowing-anthesis period, the reasonable distribution of grain number per spike and 1000-grain weight is the factor of high yield, which is mainly affected by precipitation and soil water consumption at the later growth stage. In addition, cultivation during fallow-period can achieve higher yield, but under the influence of precipitation type, DP during growth-dry year type was more favorable to the increase of field evapotranspiration, the growth-wet type of SS was more beneficial to the improvement of water use efficiency.
Keywords: *Loess Plateau, tillage regulation, yield components, water use efficiency, precipitation use efficiency*

Introduction

The Loess Plateau is one of the main wheat-producing areas in China, and food security is dependent on its yield. In this region, the dry-farming wheat area accounted for 80% of wheat farming and was the key that affected the yield (Su et al., 2007). Water is the main factor limiting the yield of the region by low precipitation, high variability in precipitation, high evaporation, and uneven concentration; 60% of the precipitation in the fallow period is inconsistent with the growth and development of wheat (Qiu et al., 2017; Kang et al., 2002; Ren et al., 2019). In the region, intensive agriculture has long been used to ensure food security, which has led to the destruction of soil structures, reduced fertility and severe soil erosion, and increased environmental damage; these are detrimental to the sustainable development of agriculture (Su et al., 2007; Hungria et al., 2009; Zhang et al., 2016).

Conservation tillage is an agricultural measure that reduces mechanical or non-tillage of the soil and provides a permanent organic mulch, which has an outstanding performance in increasing wheat yields in drylands (Friedrich et al., 2017). These techniques include no-tillage (NT), subsoiling (SS), and deep plowing (DP). NT (usually including Straw mulching) improves soil degradation and farmland erosion caused by intensive agriculture (Zhang et al., 2016; Camarotto et al., 2018), but long-term use may increase soil bulk density and permeability resistance and decrease total porosity, which are detrimental to water conservation. DP (depth of 25-30 cm) and SS (depth of 30–40 cm) are often used to reduce and break soil compaction and reduce soil bulk density

http://www.aloki.hu ● ISSN 1589 1623 (Print) ● ISSN 1785 0037 (Online)
DOI: http://dx.doi.org/10.15666/aeer/2003_26092623

(Unger et al., 1994; López-Garrido et al., 2014; Costa et al., 2015). These reduced tillage practices positively affected rain penetration into the soil and soil water storage, thus improving soil water content and increasing tiller number, wheat grain yield, and plant water-use efficiency (WUE); however, the yield varied enormously from year to year.

Wheat yield components include tiller number, grain number per ear, and 1000-grain weight. Increased coordination among yield components is required to improve crop yield potential (Qin et al., 2015; Slafer et al., 2003; Sadras et al., 2012). However, some studies have shown that the contribution of the various yield components to the total yield differs for different yield-range levels, and correlation analysis between any single variable and yield does not fully explain the importance of each component to yield (Dewey et al., 1959; Singh et al., 1979; Cao et al., 2019). Furthermore, some studies have shown a significant correlation influenced by field water consumption between wheat yield and soil moisture status over multiple growth stages from sowing to maturity (Ozturk, 2004; Seddaiu et al., 2016; Wang et al., 2018).

In this study, the main objective was to determine the correlation between yield and soil water content and water consumption at different yield levels. Grain yield differences in dryland can be large, and the effects from different years and tillage methods on wheat yield are known to vary significantly. Therefore, studying the relationship between water content and yield components at different yield levels will help guide yield promotion at different yield levels and provide more detailed ideas for increasing yield. Based on this rationale, a long-term experiment was established in a typical semi-arid Loess Plateau region using fallow tillage (DP, SS, and NT). Based on production data, the objectives of this study were: 1) to clarify the correlation between yield and water during the growth period under different yield levels, 2) to compare the effects of year and tillage on yield components and water use, and 3) to evaluate the correlation differences between yield components and yield and water sources at different stages under different yield levels.

Materials and methods

Description of the study site

Field experiments were conducted during the winter wheat growing season from 2009 through 2017 in the Experimental Station at Shanxi Agricultural University, located in Wenxi County (34° 35′ N; 110° 15′ E), Shanxi Province, China. The site is characterized by the semi-arid climate of the northeast region of the Loess Plateau, with an average annual ambient temperature of 11–13 °C and annual p^{r}ecipitation of 335.0–671.30 mm (2009–2017). The elevation ranges between 450 and 700 m above sea level, and the annual precipitation tends to concentrate in the months from July through September. According to Guo et al. (2012), based on the precipitation distribution from 1987-2017, the follow period and growth period were divided according to the drought index (normal, dry, and wet), the results shown in *Table 1*. Monthly temperature and precipitation distribution during 2009–2017 are shown in *Figure 1*.

Experimental design and field management

During the winter-wheat fallow season, three different tillage methods were tested: 1) DP (stirring at a depth of 25–30 cm), 2) SS (loosening at a depth of 30–40 cm), and 3) NT (*Fig. 2*). When winter wheat was harvested at the end of June, 20–30 cm of

http://www.aloki.hu ● ISSN 1589 1623 (Print) ● ISSN 1785 0037 (Online)
DOI: http://dx.doi.org/10.15666/aeer/2003_26092623

stubble was retained in the field to reduce water evaporation and to provide soil organic matter for the next crop. In mid-late July, two different tillage machines were used for fallow cultivation, compared with no-tillage. Rotary tillage was conducted in late August to level the land to prepare it for sowing. All treatments were designed with complete block randomization and repeated 3 times with an area of 300 m^2 (6 m × 50 m). Before sowing, 150 kg N ha^{-1} (urea, 46%), P_2O_5 (38 kg ha^{-1}), and K_2O (75 kg ha^{-1}) were applied. The test material was 'Hanyun20410,' which was mechanically sown with a row spacing of 20 cm and a planting density of 315 × 10^4 plant ha^{-1}. Field management measures were adopted in Dryland, weeds were controlled artificially, and no irrigation was carried out during the growing period. The date of sowing is shown in *Table 2*.

Table 1. *Annual precipitation amount and type in the fallow, growth, and whole cropping seasons at the Wenxi Dryland Agriculture Research Station from 2007 to 2017*

Planting season	Fallow season (Late June - Mid September)			Growth season (Late September - Mid June)		
	Precipitation	Drought index	Type	Precipitation	Drought index	Type
2009-2010	173.1	-0.75	dry	161.9	-1.25	dry
2010-2011	401.5	1.65	wet	133.2	-1.84	dry
2011-2012	459.9	2.27	wet	213.2	-0.21	normal
2012-2013	171.1	-0.77	dry	171.8	-1.05	dry
2013-2014	283.7	0.41	wet	190.5	-0.67	dry
2014-2015	365.6	1.28	wet	151.1	-1.47	dry
2015-2016	94.7	-1.58	dry	292.1	1.40	wet
2016-2017	165.4	-0.83	dry	240.9	0.36	wet

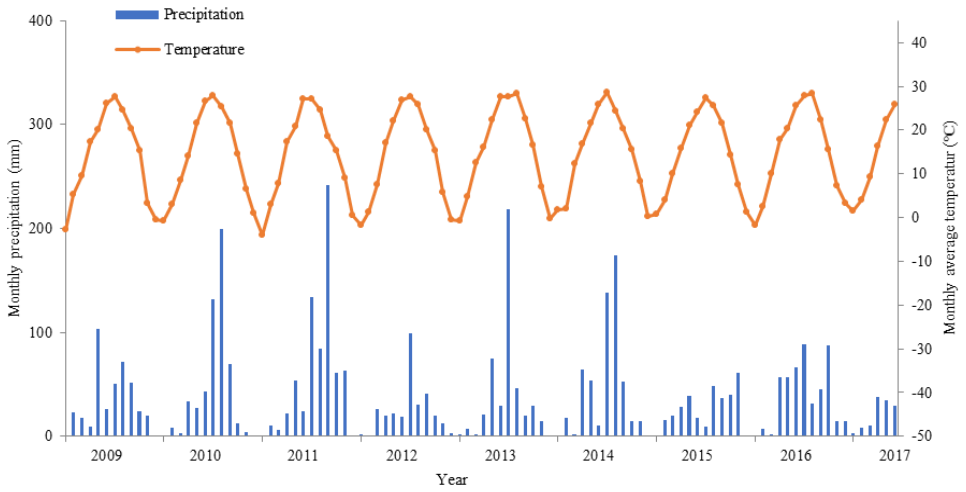

Figure 1. *Temporal distribution of monthly precipitation and temperature from 2009 to 2017*

Table 2. *Information on experimental land preparation*

Items	Growing season							
	2009-2010	2010-2011	2011-2012	2012-2013	2013-2014	2014-2015	2015-2016	2016-2017
Date of subsoiling and deep plowing	15 July	15 July	10 July	15 July	15 July	15 July	15 July	15 July
Date of rotary tillage and land leveling	20 Aug	28 Aug	25 Aug	25 Aug	23 Aug	22 Aug	26 Aug	27 Aug

http://www.aloki.hu ● ISSN 1589 1623 (Print) ● ISSN 1785 0037 (Online)
DOI: http://dx.doi.org/10.15666/aeer/2003_26092623

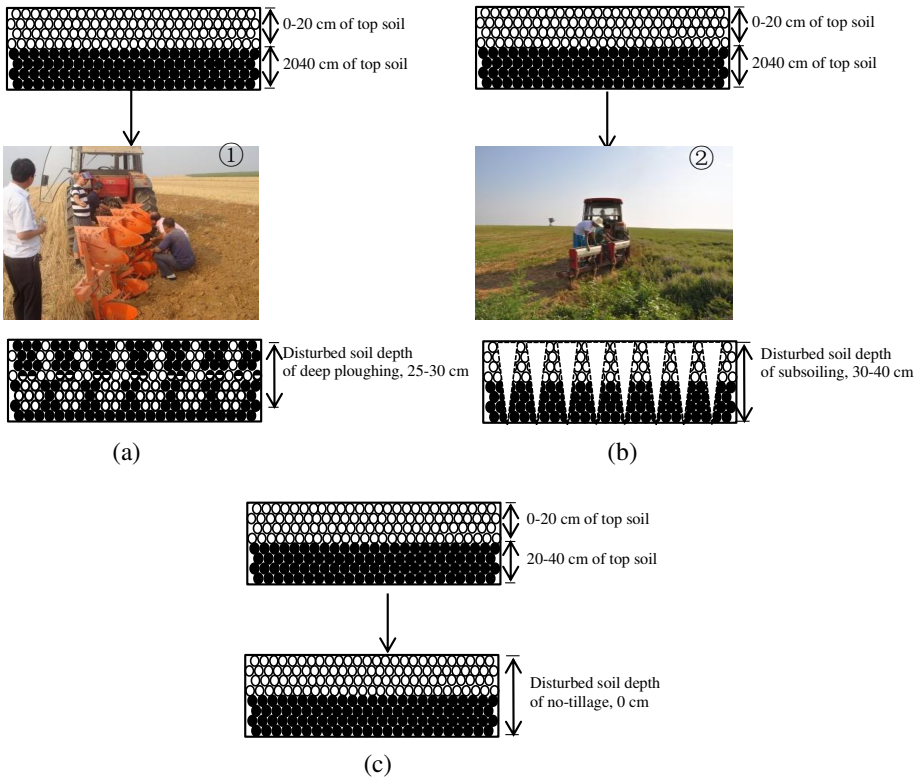

Figure 2. *Sketch map of topsoil structure of 0–40 cm after deep plowing, subsoiling, and no-tillage. ◯ Sketch map structure of 0–20 cm soil particle before tillage. ● Sketch map structure of 20–40 cm soil particle before tillage. ▽ Sketch map of the voids in the soil after subsoiling*

Cluster analysis in 2009–2017 of wheat yield

The distribution of yield and cluster analysis for wheat yields from 2009–2017 were analyzed. Wheat yields ranged from 1.50 t ha^{-1} to 6.50 t ha^{-1} (*Fig. 3*). According to the method of cluster analysis, the yield was divided into three levels: low yield (2.14–2.92 t ha^{-1}), medium yield (3.64–4.27 t ha^{-1}), and high yield (4.58-6.01 t ha^{-1}) (*Fig. 4*).

Measurements

Soil moisture

Soil gravimetric moisture content (GSW, %) and soil water storage (SWS, mm) were measured gravimetrically at each plant growth stage. Soil samples were collected to a depth of 300 cm at 20-cm intervals, as described by (Sun et al., 2019). One sample was considered as one replicate. GSW and SWS were obtained using *Equations 1* and *2,* respectively:

$$GSW(\%) = \frac{Mw - Md}{Md} \times 100 \quad \text{(Eq.1)}$$

$$SWS\ (mm) = GSW\ (\%) \times \rho b\ (g\ cm^{-3}) \times SD\ (cm) \quad \text{(Eq.2)}$$

where M_w and M_d are the weights (g) of wet and dry soil, respectively; ρb is soil bulk density of the given soil layer, and SD refers to soil depth.

http://www.aloki.hu ● ISSN 1589 1623 (Print) ● ISSN 1785 0037 (Online)
DOI: http://dx.doi.org/10.15666/aeer/2003_26092623

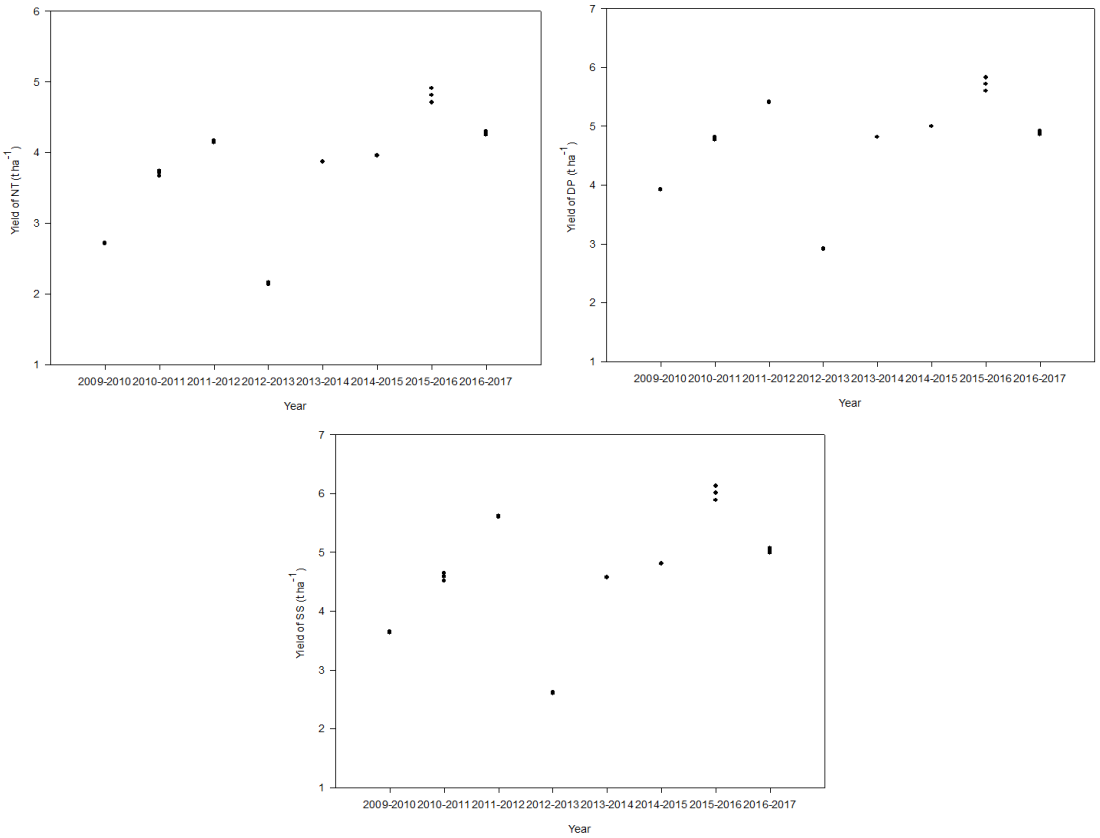

Figure 3. *Distribution of wheat yield from 2009 to 2017*

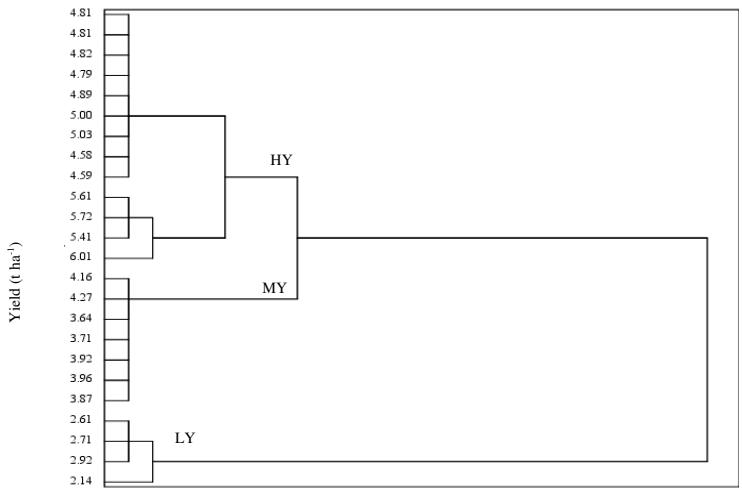

Figure 4. *Yield cluster analysis under different tillage methods (deep plowing, subsoiling, no-tillage). LY = Low yield level; MY = Medium yield level; HY = High yield level*

Evapotranspiration, precipitation, and WUE

Evapotranspiration (ET) over the whole growing season, WUE, and precipitation use efficiency (PUE) were calculated using *Equations 3, 4* and *5:*

http://www.aloki.hu ● ISSN 1589 1623 (Print) ● ISSN 1785 0037 (Online)
DOI: http://dx.doi.org/10.15666/aeer/2003_26092623

$$ET = SW_0 - SW_1 + P - R - D \quad \text{(Eq.3)}$$

$$WUE\ (kg\ ha^{-1}\ mm^{-1}) = \text{grain yield}/ET \quad \text{(Eq.4)}$$

$$PUE\ (kg\ ha^{-1}\ mm^{-1}) = \text{grain yield}/P \quad \text{(Eq.5)}$$

where SW_0 is soil water storage before sowing and SW_1 is soil water storage after harvest. P is precipitation during the wheat growth period, R is soil surface runoff, D is deep percolation, and Pt is the total precipitation from tillage to harvest. Because the field was flat and the experimental plots were surrounded by ridges to prevent runoff, R was estimated to be 0 in this research. The ground water table was deeper than 50 m in the research region and there was no water percolated to the deep soil layers; therefore, D was also considered to be 0.

Yield and yield components

Fifty plants from each plot were randomly sampled at maturity from the inner rows to determine yield components, including spike numbers, grains per spike, and 1000-grain weight. Plot grain yield was determined by harvesting all plants in a 20 m^2 area, shelling them mechanically, and determining grain yield after air-drying.

Statistical analysis

Analysis of variance and the least significant difference were performed using SPSS 25.0 (SPSS Inc., Chicago, IL, USA) to determine treatment effects and to identify significant differences among treatments. Differences were considered significant at $P < 0.05$. Figures and tables were designed using Microsoft Excel 2015.

Results

Differences in SWS and yield formation at different growth stages

The correlation between yield formation and SWS differed for different yield levels (*Fig. 5*). At the low yield level, the yield was not significantly related to SWS at sowing, jointing, or anthesis, but with increasing SWS, the yield decreased first and then increased. This indicated that SWS higher than 388.2 mm, 331.2 mm, and 258.0 mm at sowing, jointing, and anthesis, respectively, was beneficial for yield formation (*Fig. 5A–C*). At the medium yield level, the yield showed an increasing trend with increasing SWS, and the correlation between yield and SWS at the jointing stage was higher (*Fig. 5B*). Lastly, at the high yield level, the yield was mainly related to SWS at jointing, anthesis, and maturity, and the trend was similar to that observed for the medium yield level (*Fig. 5A–C*). These results indicate that higher SWS during the late growth period is crucial for the formation of a higher yield.

Correlation between field water consumption and yield formation

The correlation between yield formation and water consumption during growth was different for each yield level (*Fig. 6*). Thus, at the low yield level, yield increased with increasing soil water consumption at each growth stage, although differences were not significant (*Fig. 6A–C*). In turn, yield increased with increasing field water consumption

http://www.aloki.hu ● ISSN 1589 1623 (Print) ● ISSN 1785 0037 (Online)
DOI: http://dx.doi.org/10.15666/aeer/2003_26092623

and correlated with water consumption from jointing to anthesis at the medium yield level (*Fig. 6B*). On the other hand, at the high yield level, yield correlated with water consumption at anthesis and maturity and increased with increasing water consumption (*Fig. 6A–C*). These results indicate that higher field water consumption during late growth is essential to high yield.

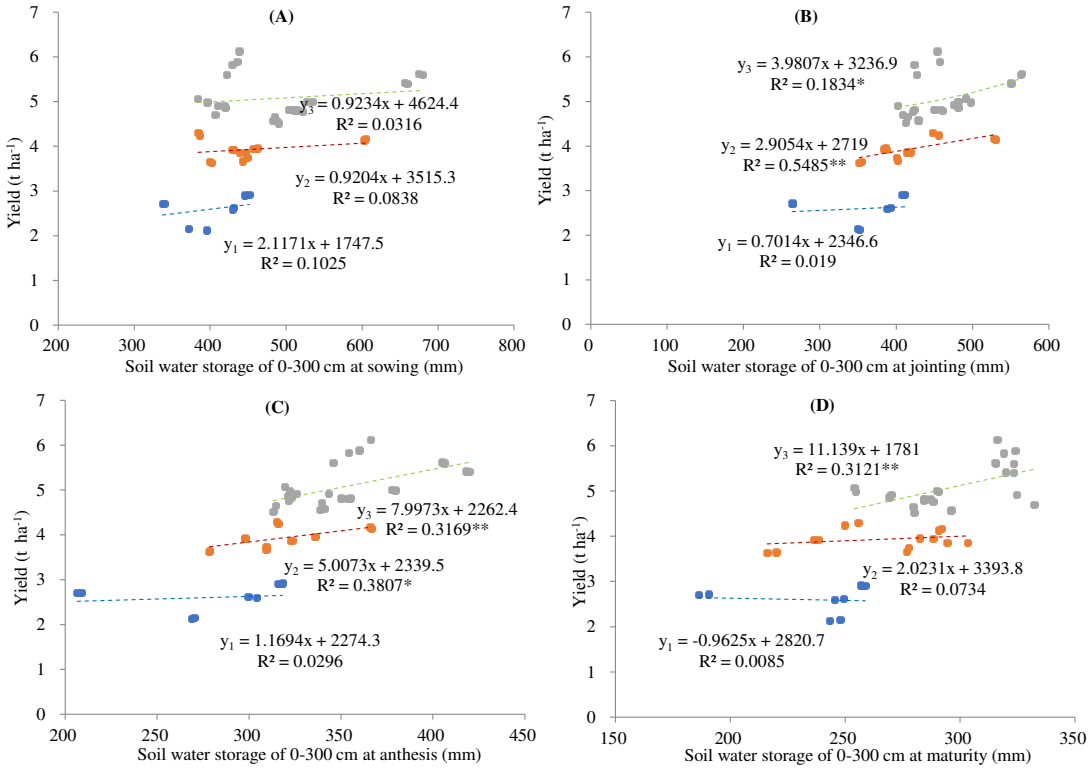

Figure 5. *Correlation between soil water content at sowing and anthesis and low, medium, and high yield levels of winter wheat. y_1 = Low yield; y_2 = Medium yield; y_3 = High yield; * and ** indicates difference at the 0.05 and 0.01 probability levels, respectively*

Yield components and WUE

In 2009-2017, the fluctuation range of wheat yield was large, and the yield varied with different treatments in the same year (*Table 3*). No-tillage treatment, 2009-2010, 2012-2013 in low-yield level, 2010-2012, 2013-2015, 2016-2017 in the middle-yield level, 2015-2016 in high-yield level. The precipitation patterns were similar at the same yield level, the low-yield level included dry of all the season, the middle-yield level included wet-fallow and dry-growth season, dry-fallow and wet-growth season, the high-yield level included dry-fallow and wet-growth season. Compared with NT, SS and DP were conducive to crop production, especially between 2009-2010 and 2010-2012, 2013-2015, 2016-2017, the level of output changes, low yield to middle, middle to high yield. Compared with SS, DP had higher yield in 2009-2011 and 2012-2015, and had similar annual pattern, all of which were dry-growth season types. But in other years, the yield of SS was higher, and the annual pattern was normal-growth or wet-growth season types. In dry-growth, DP was more advantageous to improve the PUE and increase the ET. In normal-growth, SS was more advantageous to improve the PUE and increase the ET. In wet-growth, SS was more advantageous to improve the PUE and WUE.

http://www.aloki.hu ● ISSN 1589 1623 (Print) ● ISSN 1785 0037 (Online)
DOI: http://dx.doi.org/10.15666/aeer/2003_26092623

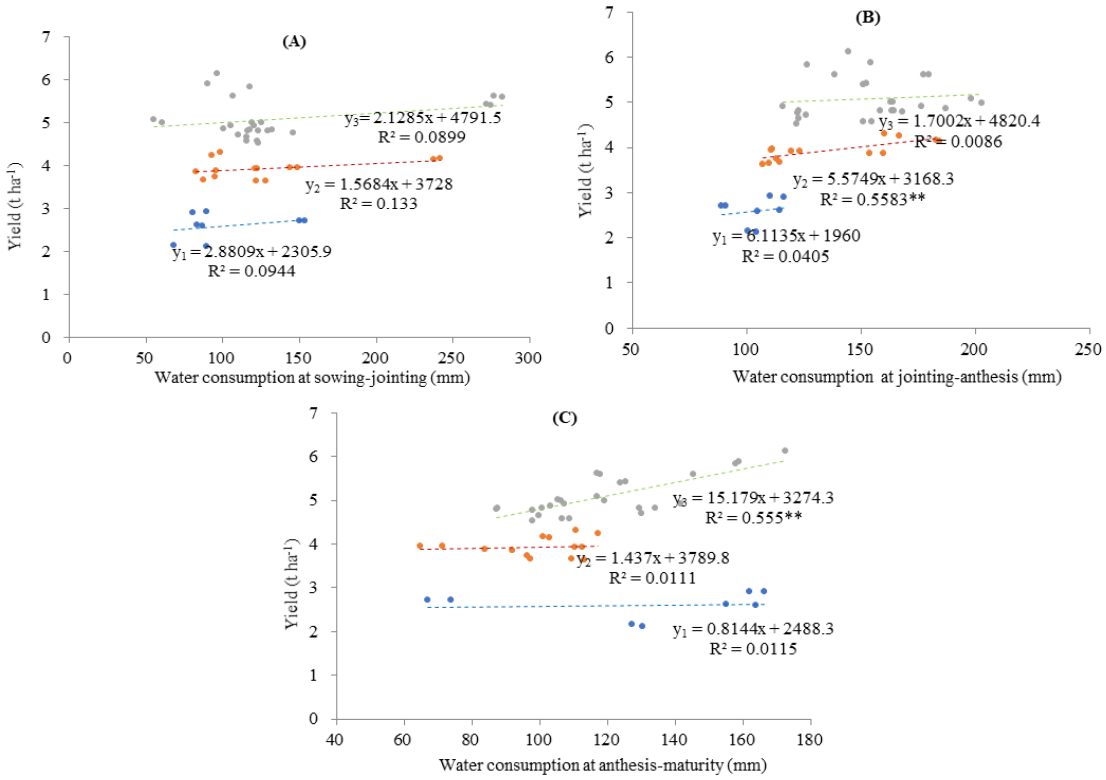

Figure 6. *Correlation between field water consumption at different growth stages and yield at y_1 = Low yield; y_2 = Medium yield; y_3 = High yield; * and ** indicates difference at the 0.05 and 0.01 probability levels, respectively*

Tillage method, the year, and their interaction significantly affected water consumption, WUE, and PUE, all of which showed an increasing trend with increasing production level. At the low yield level, average field water consumption, WUE, and PUE were 334.7 mm, 7.8 kg ha^{-1} mm^{-1}, and 7.6 kg ha^{-1} mm^{-1}, respectively, and water consumption was highest in the year with the highest yield, while WUE was also relatively high. WUE and PUE were also significantly higher at all yield levels when the yield was higher, compared to years when the yield was low. In addition, compared with NT, DP and SS effectively improved WUE by 11.7%-11.9%, and PUE by 24.2%-26.7%, respectively, in the same year.

Correlation analysis of yield, yield components, and contribution of water sources

The contribution of the various yield components to yield formation varied with yield level (*Table 4*). Thus, at the low yield level, tillers, grain number per ear, and 1000-grain weight were positively correlated with yield. Meanwhile, at the medium yield level, 1000-grain weight was negatively correlated with yield, while tiller number and grain number per ear were the key components for increasing grain yield. Lastly, at the high yield level, the correlation between the 1000-grain weight and yield was non-significant, but the latter was significantly increased by tiller number and grain number per ear.

At the low yield level, the fallow precipitation and precipitation from sowing to jointing and jointing to anthesis were positively correlated with tillers. However, from anthesis to maturity, the correlation was negative (*Table 5*)—the grain number per ear and 1000-grain weight correlated negatively with precipitation. Soil water consumption

http://www.aloki.hu ● ISSN 1589 1623 (Print) ● ISSN 1785 0037 (Online)
DOI: http://dx.doi.org/10.15666/aeer/2003_26092623

from sowing to jointing was positively correlated with tillers, but it was negative from jointing to anthesis. Grain number per ear and 1000-grain weight were positively correlated with soil water consumption from jointing to anthesis and from anthesis to maturity. In turn, at the medium yield level, the precipitation from sowing to jointing was positively correlated with tiller number, but from jointing to anthesis and from anthesis to maturity, the correlation was negative. Precipitation from sowing to jointing was negatively correlated with grain number per ear. Finally, the correlation between precipitation and tillers at the high yield level was similar to that detected at the low yield level, and fallow precipitation and precipitation from sowing to jointing were negatively correlated with grain number per ear. In contrast, the correlations were positive with precipitation from jointing to anthesis and from anthesis to maturity. On the other hand, soil water consumption from sowing to jointing and jointing to anthesis was positively correlated with the tiller number, whereas the same variables correlated negatively with water consumption from anthesis to maturity.

Table 3. *Differences in yield components and water use efficiency among LY, MY, HY*

Yield level	Treatment	Tillers (10^4 ha^{-1})	Grain number per ear	1000-grains weight (g)	Yield (t ha^{-1})	ET (mm)	WUE (kg ha^{-1} mm^{-1})	PUE (kg ha^{-1} mm^{-1})
LY	2009-2010 NT	407.71 a	20.38 c	36.14 c	2.71 b	311.98 c	8.70 a	8.10 b
	2012-2013 NT	300.25 d	20.37 c	36.46 c	2.14 d	310.17 c	6.90 d	6.24 d
	2012-2013 SS	341.50 c	22.29 b	38.81 b	2.61 c	354.10 b	7.37 c	7.61 c
	2012-2013 DP	350.25 b	23.17 a	40.67 a	2.92 a	362.43 a	8.04 b	8.50 a
Mean		349.93	21.55	38.02	2.59	334.67	7.75	7.61
MY	2009-2010 SS	427.18 c	21.70 f	39.04 c	3.64 f	344.88 d	10.55 f	10.87 b
	2009-2010 DP	453.72 b	23.78 e	42.08 a	3.92 c	354.37 c	11.07 e	11.71 a
	2010-2011 NT	401.04 e	26.22 c	40.51 b	3.71 e	301.65 g	12.28 a	6.93 f
	2011-2012 NT	485.50 a	24.33 d	35.44 d	4.12 b	525.20 a	7.91 g	6.17 g
	2013-2014 NT	386.65 f	27.55 b	39.12 c	3.87 d	334.05 e	11.58 c	8.15 d
	2014-2015 NT	417.00 d	27.48 b	39.14 c	3.96 c	325.22 f	12.16 b	7.66 e
	2016-2017 NT	452.12 b	33.36 a	35.66 d	4.27 a	373.02 b	11.46 d	10.52 c
Mean		431.89	26.35	38.71	3.93	365.48	11.00	8.86
HY	2010-2011 SS	446.58 k	28.24 g	40.59 cd	4.59 h	340.81 j	13.46 c	8.58 i
	2010-2011 DP	481.08 h	28.38 fg	42.58 a	4.80 g	361.01 i	13.28 c	8.97 h
	2011-2012 DP	603.00 b	26.56 h	37.15 f	5.41 d	549.04 b	9.86 h	8.04 k
	2011-2012 SS	616.50 a	26.74 h	38.63 e	5.61 c	575.02 a	9.76 h	8.34 j
	2013-2014 SS	454.41 j	28.31 fg	41.04 bc	4.58 h	379.48 f	12.06 f	9.65 f
	2013-2014 DP	466.00 i	29.63 e	41.55 b	4.82 fg	409.82 c	11.76 g	10.16 e
	2014-2015 SS	488.33 fg	28.79 f	40.30 d	4.81 fg	380.16 f	12.64 e	9.30 g
	2014-2015 DP	522.98 c	29.72 e	41.01 bc	5.00 e	391.54 e	12.77 de	9.68 f
	2015-2016 NT	425.75 l	34.78 d	39.06 e	4.81 fg	371.90 h	12.94 d	12.44 c
	2015-2016 DP	484.50 gh	36.23 b	39.11 e	5.72 b	396.09 d	14.44 b	14.79 b
	2015-2016 SS	493.25 ef	37.80 a	41.26 b	6.01 a	408.60 c	14.71 a	15.54 a
	2016-2017 DP	496.25 e	35.57 c	33.12 h	4.90 f	390.33 e	12.53 e	12.04 d
	2016-2017 SS	503.36 d	35.54 c	34.21 g	5.03 e	376.52 g	13.36 c	12.38 c
Mean		498.61	31.25	39.20	5.08	410.02	12.58	10.76
ANOVA results								
Tillage (T)		< 0.001						
Year (Y)								
T×Y								

WUE = water use efficiency, PUE = precipitation use efficiency, LY = Low yield level, MY = Medium yield level, HY = High yield level, NT = no-tillage, SS = subsoiling, DP = deep plowing, Significant difference between different yield level groups are indicated with different letters in the same treatment ($P < 0.05$)

http://www.aloki.hu ● ISSN 1589 1623 (Print) ● ISSN 1785 0037 (Online)
DOI: http://dx.doi.org/10.15666/aeer/2003_26092623

Table 4. *Correlation between yield and yield components*

Yield level	Y1	Y2	Y3	Simulation equation
LY	0.676**	0.661*	0.634*	$Y = 5.694*Y1 + 111.949*Y3-3653.974$, $R^2 = 0.999$
MY	0.626**	0.641**	-0.700**	$Y = 4.558*Y1 + 42.942*Y2 + 831.857$, $R^2 = 0.999$
HY	0.540**	0.375*	-0.088	$Y = 8.836*Y1 + 111.52*Y2 + 93.9*Y3-6489.48$, $R^2 = 0.999$

Y = Yield, Y1 = Tillers, Y2 = Number per ear, Y3 = 1000-grains weight, * and ** indicates the correlation level $P < 0.05$ and $P < 0.01$

Table 5. *Correlation between yield components and water source contribution*

Yield level	Yield composition	X1	X2	X3	X4	X5	X6	X7
LY	Y1	0.869**	0.951**	0.869**	-0.698**	0.869**	-0.199	-0.869**
	Y2	-0.551*	-0.338	-0.551*	0.765**	-0.551*	0.949**	0.551*
	Y3	-0.585*	-0.370	-0.585*	0.779**	-0.585*	0.944**	0.585*
MY	Y1	0.012	-0.033	0.812**	0.665**	-0.611**	0.939**	-0.483*
	Y2	-0.112	-0.785**	0.368	0.242	0.120	-0.167	0.069
	Y3	-0.212	0.360	-0.869**	-0.730**	0.259	-0.470*	0.356
HY	Y1	0.345*	0.630**	0.819**	0.524**	0.629**	-0.482**	-0.559**
	Y2	-0.872**	-0.099	-0.478**	-0.949**	0.311*	0.253	0.695**
	Y3	0.605**	-0.708**	-0.211	0.269*	-0.822**	0.451**	0.160

LY = Low yield level, MY = Medium yield level, HY = High yield level, Y1 = Tillers, Y2 = grain number per ear, Y3 = 1000-grain weight, X1 = Precipitation of fallow period, X2 = Soil water consumption of sowing–jointing, X3 = Precipitation of sowing–jointing, X4 = Soil water consumption of jointing–anthesis, X5 = Precipitation of jointing–anthesis, X6 = Soil water consumption of anthesis–maturity, X7 = Precipitation of anthesis–maturity; * and ** indicates the correlation level $P < 0.05$ and $P < 0.01$

The simulation equation (*Table 4*) indicated that soil water consumption from anthesis to maturity mainly influenced the formation of grain number per ear and 1000-grain weight at the low yield level. Furthermore, at the medium yield level, tiller number was positively affected by soil water consumption from jointing to maturity; grain number per ear was affected by soil water consumption from anthesis to maturity, and 1000-grain weight was affected by precipitation from seeding to jointing, and soil water consumption from anthesis to maturity. Finally, tiller number was positively affected by fallow precipitation from seeding to anthesis at the high yield level; grain number per ear was affected by water consumption from seeding to anthesis and precipitation from jointing to maturity, while 1000-grain weight was affected by fallow precipitation and precipitation at each growth stage.

Discussion

Effect of water on wheat yield

Precipitation is the important source of water supply in arid and semi-arid regions; therefore, it is the main limiting factor for winter wheat production (He et al., 2016).

http://www.aloki.hu ● ISSN 1589 1623 (Print) ● ISSN 1785 0037 (Online)
DOI: http://dx.doi.org/10.15666/aeer/2003_26092623

Field water consumption, WUE, and PUE were all affected by year and tillage treatment, thereby affecting wheat yield (Sun et al., 2019, 2018). In addition, wheat yield was significantly correlated with soil water status at various developmental stages from sowing to maturity. Wang et al. (2017) reported that soil water storage from jointing to maturity was the key factor for increasing wheat yield in the Loess Plateau. Further, Lin and Wang et al. (2017) suggested that the key periods for water demand of winter wheat were sowing, jointing, and anthesis. Meanwhile, according to Deng et al. (2006) and Su et al. (2007), soil moisture from jointing to heading stage is particularly important in determining yield formation. The correlation between yield and soil water storage at each growth stage was different, which is not only related to regional differences but to wheat growth stage and yield level. In this study, when yield was lower than 3.00 t ha^{-1}, it was more strongly related to soil water storage at sowing, jointing, and anthesis. In contrast, when yield reached between 3.00 and 4.50 t ha^{-1} it was more related to soil water storage at jointing and anthesis; whereas, when it reached over 4.50 t ha^{-1} it was more related to soil water storage at jointing, anthesis, and maturity. Sufficient soil moisture is beneficial for providing water for wheat growth, especially under the conditions of low precipitation. Tillage in the fallow period improved soil water storage, field evapotranspiration, and WUE in the same year, which was conducive to the improvement of yield (Xue et al., 2019). In addition, this study also showed that DP was more advantageous to the formation of wheat yield in growth-dry year, possibly because DP water moved down shallowly, water supply was more convenient in early growth period, and promoted the formation of crop yield components, higher ET was also evidence. In growth-normal or growth-wet years, SS was more effective, probably because SS water moved down more deeply, and precipitation was adequate for yield construction in the early growth stage, and soil water construction consumed less water, which could mainly serve for grain formation, higher WUE could be demonstrated.

Effects of yield components on wheat grain yield

Optimizing spike number per hectare is a important method to maximize yield in most cereal crops beside of genotype-specific because it can increase plant vigor and hence plant grain yield (Weiner et al., 2001). Both, the number of tillers and yield were positively correlated at different yield levels, indicating that a larger number of tillers may guarantee a higher yield from winter wheat. These results are consistent with previous studies (Del Blanco et al., 2001; Cao et al., 2019). However, grain number per ear and 1000-grain weight showed different correlations with yield at different yield level. Thus, for example, Duan et al. (2018) suggested that at a low yield level (less than 7.50 t ha^{-1}), yield was positively correlated with the number of grains per ear but negatively correlated with 1000-grain weight, whereas at high yield level (i.e., yields greater than 7.50 t ha^{-1}), yield was correlated with grain number per ear, but not with 1000-grain weight. In the present study, a significant relationship was found between yield and tiller number. However, when yield was lower than 3.00 t ha^{-1}, it was correlated with 1000-grain weight, and when yield was between 3.00 and 4.50 t ha^{-1}, it was significantly and negatively correlated with 1000-grain weight. In addition to number of tillers, at low and intermediate yield levels, 1000-grain weight and number of grains per ear were the key yield components responsible for increasing crop yield. Similarly, at the high yield level, the key to high crop yield was higher grain number per ear and 1000-grain weight, in addition to number of tillers. Compared with NT, fallow

http://www.aloki.hu ● ISSN 1589 1623 (Print) ● ISSN 1785 0037 (Online)
DOI: http://dx.doi.org/10.15666/aeer/2003_26092623

tillage can improve PUE, regulate water and promote the formation of yield components. In growth-dry or growth-normal years, water mainly regulated the growth factors of wheat, and the ET was higher, but in growth-wet years, it promoted wheat filling and WUE was higher.

Effects of water and wheat yield formation

The key yield components responsible for the formation of yield are well known to be affected by soil moisture at each growth stage and to influence each other (Li et al., 2017; Yao et al., 2015; Dong et al., 2019; Slafer, 2003). The early growth stage is conducive to the formation of spike number, while the latter growth stage is important for the formation of spike number and 1000-grain weight (Hochman, 1982). At different yield levels, the correlation between components and water sources in the different stages varied. In the low-yielding years, ear-forming stage precipitation was less in 2009–2010 and 2012–2013. Especially in 2012–2013, when fallow cultivation was adopted, it was difficult to make up for the deficit in the grain number per ear caused by the lack of precipitation in the sowing–jointing stage. In 2009–2010, the precipitation in the sowing–jointing period was 31 mm higher than that in 2012–2013, and the precipitation in the fallow period was accumulated to make up the inadequate water consumption under NT to ensure that the yield reached the medium-level of the same year. The medium-yield years were distributed in 2010–2012, 2013–2015, and 2016–2017, among which 2010–2012 and 2014–2015 rainfall distribution was similar, its follow period rainfall was sufficient, reaching 360 mm and above; although the growth stage rainfall was less. However, DP and SS accumulated water in the soil during the fallow period, ensured water consumption in the later period and increased the yield. The precipitation in 2013–2014 and 2016–2017 was similar, although the precipitation in the fallow period was less and that in the key growth stage was more. DP and SS could improve the physical and chemical properties of soil, absorb more precipitation in the fallow and key growth periods, reduce water stress in wheat, and promote high yield in the same year. The high-yield years were mainly from 2015 to 2016, with precipitation being less in the fallow period. However, in the two key periods sowing–jointing and flowering–maturing periods, the precipitation was sufficient to meet the needs of population construction and grain filling of wheat. During the fallow period, tillage increased the spike number and 1000-grain weight slightly, which mainly regulated the formation of grain number per spike and increased the yield. Although precipitation varied with year, water supply in the key stages was still the primary factor affecting yield components. In the fallow period, DP and SS had the advantage of increasing yield at different levels, which may be attributed to the improvement of soil structure that promoted the PUE and then made up for the difference caused by the lack of precipitation, especially in the low–medium yield years.

Conclusions

At different yield levels, precipitation distribution is different in fallow and growth periods. Using DP and SS in the fallow period, PUE can be improved and yield components negatively affected by precipitation can be improved. In low and medium yield years, DP and SS were mainly responsible for 1000-grain weight and grain number per spike. In the high-yield years, fallow cultivation can help adjust the relationship among the components, promote reasonable distribution, and improve

http://www.aloki.hu ● ISSN 1589 1623 (Print) ● ISSN 1785 0037 (Online)
DOI: http://dx.doi.org/10.15666/aeer/2003_26092623

yield. In addition, this study also found that under growth-dry, DP was more beneficial to the contribution of water to the growth of wheat and to the improvement of yield, while SS was more effective under the growth-normal or growth-wet, it may be that water accumulation is more favorable for the use of grain filling. However, whether the yield components of different wheat genotypes have the same effect on the response to water stress needs further study.

Acknowledgements. This research was partially supported by the "Modern Agriculture Industry Technology System Construction" (No. CARS-03-01-24), the National Key Research and Development Program of China (No. 2018YFD020040105), National Natural Science Foundation of China (No. 31771727), the "Crop Ecology and Dry Cultivation Physiology Key Laboratory of Shanxi Province" (No. 201705D111007), and the "1331" Engineering Key Innovation Cultivation Team-Organic Dry Cultivation and Cultivation Physiology Innovation Team (No. SXYBKY201733), 2019 Graduate Education Innovation Plan Project (No. 2019SY222), the scientific and technological innovation project of Shanxi University (2019l0385), the science and technology innovation fund project of Shanxi Agricultural University (2019001), and the scientific research project of Shanxi excellent doctor working in Shanxi Province (sxybky2018044).

REFERENCES

[1] Camarotto, C., Ferro, N. D., Piccoli, I., Polese, R., Morari, F. (2018): Conservation agriculture and cover crop practices to regulate water, carbon and nitrogen cycles in the low-lying Venetian plain. – Catena 167: 236-249.

[2] Cao, H., Li, Y., Chen, G., Chen, D., Qu, H., Ma, W. (2019): Identifying the limiting factors driving the winter wheat yield gap on smallholder farms by agronomic diagnosis in North China Plain. – Journal of Integrative Agriculture 18(8): 1701-1703.

[3] Costa, J. L., Aparicio, V., Cerda, A. (2015): Soil physical quality changes under different management systems after 10 years in the Argentine humid pampa. – Solid Earth 6(1): 361-371.

[4] Del Blanco, I. A., Rajaram, S., Kronstad, W. E. (2001): Agronomic potential of synthetic hexaploid wheat-derived populations. – Crop Science 41: 670-676.

[5] Deng, X., Shan, L., Zhang, H., Turner, N. C. (2006): Improving agricultural water use efficiency in arid and semiarid areas of China. – Agricultural Water Management 80: 23-40.

[6] Dewey, D. R., Lu, K. (1959): A correlation and path-coefficient analysis of components of crested wheatgrass seed production. – Agronomy Journal 51: 70-74.

[7] Dong, Z., Zhang, X., Li, J., Zhang, C., Wei, T., Yang, Z., Cai, T., Zhang, P., Ding, R., Jia, Z. (2019): Photosynthetic characteristics and grain yield of winter wheat (Triticum aestivum L.) in response to fertilizer, precipitation, and soil water storage before sowing under the ridge and furrow system: a path analysis. – Agricultural and Forest Meteorology 272: 12-19.

[8] Duan, J., Wu, Y., Zhou, Y., Ren, X., Shao, Y., Feng, W., Zhu, Y., Wang, Y., Guo, T. (2018): Grain number responses to pre-anthesis dry matter and nitrogen in improving wheat yield in the Huang-Huai Plain. – Scientific Reports 8: 1-10.

[9] Friedrich, T., Derpsch, R., Kassam, A. (2017): Overview of the global spread of conservation agriculture, sustainable development of organic agriculture. – Apple Academic Press, Palm Bay, FL, pp. 75-90.

[10] Guo, S., Zhu, H., Dang., T., Wu, J., Liu, W., Hao, M., Li, Y., Syers, J. K. (2012): Winter wheat grain yield associated with precipitation distribution under long-term nitrogen fertilization in the semiarid Loess Plateau in China. – Geoderma 189: 442-450.

http://www.aloki.hu ● ISSN 1589 1623 (Print) ● ISSN 1785 0037 (Online)
DOI: http://dx.doi.org/10.15666/aeer/2003_26092623

[11] He, G., Wang, Z., Li, F., Dai, J., Li, Q. (2016): Soil water storage and winter wheat productivity affected by soil surface management and precipitation in dryland of the Loess Plateau. – China. Agricultural Water Management 171: 1-9.
[12] Hochman, Z. (1982): Effect of water stress with phasic development on yield of wheat grown in a semi-arid environment. – Field Crops Research 5: 55-67.
[13] Hungria, M., Franchini, J. C., Brandão-Junior, O., Kaschuk, G., Souza, R. A. (2009): Soil microbial activity and crop sustainability in a long-term experiment with three soil-tillage and two crop-rotation systems. – Applied Soil Ecology 42: 288-296.
[14] Kang, S. Z., Zhang, L., Liang, Y., Hu, X., Cai, H., Gu, B. (2002): Effects of limited irrigation on yield and water use efficiency of winter wheat in the Loess Plateau of China. – Agricultural Water Management 55: 203-216.
[15] Lin, X., Wang, D. (2017): Effects of supplemental irrigation on water consumption characteristics, grain yield and water use efficiency in winter wheat under different soil moisture conditions at seeding stage. – Acta Agronomica Sinica 43(09): 1357-1369.
[16] López-Garrido, R., Madejón, E., León-Camacho, M., Girón, I., Moreno, F., Murillo, J. M. (2014): Reduced tillage as an alternative to no-tillage under Mediterranean conditions: a case study. – Soil and Tillage Research 140: 40-47.
[17] Ozturk, A., Aydin, F. (2004): Effect of water stress at various growth stages on some quality characteristics of winter wheat. – Journal of Agronomy and Crop ence 190: 93-99.
[18] Qin, X., Zhang, F., Liu, C., Yu, H., Cao, B., Tian, S., Liao, Y., Siddique, K. H. M. (2015): Wheat yield improvements in China: past trends and future directions. – Field Crops Research 177: 117-124.
[19] Qiu, L., Hao, M., Wu, Y. (2017): Potential impacts of climate change on carbon dynamics in a rain-fed agroecosystem on the Loess Plateau of China. – Science of the Total Environment 577: 267-278.
[20] Ren, A., Sun, M., Xue, L., Deng, Y., Wang, P., Lei, M., Lin, W., Yang, Z., Gao, Z. (2019): Spatio-temporal dynamics in soil water storage reveals effects of nitrogen inputs on soil water consumption at different growth stages of winter wheat. – Agricultural Water Management 216: 379-389.
[21] Sadras, V. O., Slafer, G. A. (2012): Environmental modulation of yield components in cereals: heritabilities reveal a hierarchy of phenotypic plasticities. – Field Crops Research 127: 215-224.
[22] Seddaiu, G., Iocola, I., Farina, R., Orsini, R., Iezzi, G., Roggero, P. P. (2016): Long term effects of tillage practices and N fertilization in rainfed Mediterranean cropping systems: durum wheat, sunflower and maize grain yield. – European Journal of Agronomy 77: 166-178.
[23] Singh, D., Singh, M., Sharma, K. C. (1979): Correlation and path coefficient analysis among flag leaf area, yield and yield attributes in wheat (Triticum aestivum L.). – Cereal Research Communications 7(2): 145-152.
[24] Slafer, G. A. (2003): Genetic basis of yield as viewed from a crop physiologist's perspective. – Annals of Applied Biology 142: 117-128.
[25] Su, Z., Zhang, J., Wu, W., Cai, D., Lv, J., Jiang, G., Huang, J., Gao, J., Hartmanne, Roger., Gabrielset, Donald. (2007): Effects of conservation tillage practices on winter wheat water-use efficiency and crop yield on the Loess Plateau, China. – Agricultural Water Management 87: 307-314.
[26] Sun, M., Ren, A., Gao, Z., Wang, P., Mo, F., Xue, L., Lei, M. (2018): Long-term evaluation of tillage methods in fallow season for soil water storage, wheat yield and water use efficiency in semiarid southeast of the loess plateau. – Field Crops Research 218(9): 24-32.
[27] Sun, L., Wang, R., Li, J., Wang, Q., Lyu, Wei., Wang, X., Cheng, K., Mao, H., Zhang, X. (2019): Reasonable fertilization improves the conservation tillage benefit for soil water use and yield of rain-fed winter wheat: a case study from the Loess Plateau, China. – Field Crops Research 242-253.

http://www.aloki.hu ● ISSN 1589 1623 (Print) ● ISSN 1785 0037 (Online)
DOI: http://dx.doi.org/10.15666/aeer/2003_26092623

[28] Unger, P. W., Kaspar, T. C. (1994): Soil compaction and root growth: a review. – Agronomy Journal 86: 759-766.
[29] Wang, D. (2017): Water use efficiency and optimal supplemental irrigation in a high yield wheat field. – Field Crops Research 217: 213-220.
[30] Wang, Y., Zhang, Y., Zhou, S., Wang, Z. (2018): Meta-analysis of no-tillage effect on wheat and maize water use efficiency in China. – Science of the Total Environment 635: 1372-1382.
[31] Weiner, J., Griepentrog, H. W., Kristensen, L. (2001): Suppression of weeds by spring wheat Triticum aestivum increases with crop density and spatial uniformity. – Journal of Applied Ecology 38: 784-790.
[32] Xue, L., Khan, S., Sun, M., Anwar, S., Ren, A., Gao, Z., Lin, W., Xue, J., Yang, Z., Deng, Y. (2019): Effects of tillage practices on water consumption and grain yield of dryland winter wheat under different precipitation distribution in the loess plateau of China. – Soil and Tillage Research 191: 66-74.
[33] Zhang, Q., Liu, D., Cheng, S., Huang, X. (2016): Combined effects of runoff and soil erodibility on available nitrogen losses from sloping farmland affected by agricultural practices. – Agricultural Water Management 176: 1-8.

http://www.aloki.hu ● ISSN 1589 1623 (Print) ● ISSN 1785 0037 (Online)
DOI: http://dx.doi.org/10.15666/aeer/2003_26092623

STUDY OF THE FLAVONOIDS OF ROUND-LEAVED ANEMONE (*ANEMONE OBTUSILOBA*) ON ALPINE MEADOW AND THE MECHANISM OF ITS ADAPTATION TO THE ENVIRONMENT BASED ON METABOLIC PATHWAYS

LV, W.[1,2*] – LIU, Z.[2]

[1]*Tianshui Normal University, Tianshui 741000, China*

[2]*School of Life Science and Engineering, Lanzhou University of Technology, Lanzhou 730050, China*

**Corresponding author*
e-mail: 413958876@qq.com

(Received 21st Dec 2021; accepted 21st Mar 2022)

Abstract. The article aimed to investigate the main pigment composition of the A. obtusiloba, focusing on the changes in absorbance spectra in relation to environmental factors of the alpine meadows of Maqu County, China, using UV-vis spectrophotometry, High Performance Liquid Chromatography (HPLC), and liquid chromatography-mass spectrometry (LC-MS). The results showed that there were two kinds of pigments in A. obtusiloba, carotenoids, and flavonoids. The absorbance spectra regularly changed with the depth of flower colour. Based on HPLC and LC-MS analyses, seven kinds of flavonoids were inferred, including luteolin-3-7-O-glucoside, quercetin-3-O-rutoside, quercetin-3-O-galactoside, quercetin-3-O-glucoside, quercetin-3-O-rhamnoside, kaempferol-3-O-sophoroside, and myricetin-3-O-rhamnose, and the derivative of quercetin was identified as the main component in A. obtusiloba. Additionally, according to the analysis of the flavonoid metabolism pathway, it could be determined that flavonoid 3'-hydroxylase (F3′H) was the key enzyme in increasing quercetin content. This paper speculates that A. obtusiloba increases the content of quercetin by regulating flavonoid F3′H, so that it can deepen the flower colour to adapt to the environment.
Keywords: *Qinghai Tibet Plateau, flower colour, adaptability, HPLC, LC-MS*

Introduction

Anemone obtusiloba, commonly known as Padar, Rattanjog, or Kawashud, is a flowering plant of the family Ranunculaceae and a densely tufted perennial herb (Thu et al., 2018). It is native to the Himalayan and mountainous regions of Myanmar occurring in the Alpine Himalaya from Kashmir to Sikkim at 2100-4200 m altitude and in the Nilgiri hills at an altitude above 1800 m (Tan, G. L. et al., 2002). It bears buttercup hermaphrodite plural and the stem is short and tufted with a single terminal flower, generally producing one to three individual stems with yellow, light-yellow, or white colour. At present, research mainly focuses on the medicinal value of *A. obtusiloba*, whose ethanolic extract contains saponins (Masood et al., 1979). It also contains protoanemonin, which is an irritating acrid oil and is an enzymatic breakdown product of the glycoside ranunculin (Savita, R. et al., 2011). *A. obtusiloba* is used as a purgative and in the treatment of rheumatic joints, jaundice, spleen disorders, and anxiety neurosis. Besides, it is also used as an antidote to snakebite, while its seed oil is used to cure arthritis (Gupta et al., 2005). Studies have shown that the petal colour of *A. obtusiloba* is related to reproductive characteristics and reproductive distribution. During the flowering period, with the deepening of flower colour, the reproductive characteristics and reproductive distribution of *A. obtusiloba* have been adjusted to

http://www.aloki.hu ● ISSN 1589 1623 (Print) ● ISSN 1785 0037 (Online)
DOI: http://dx.doi.org/10.15666/aeer/2003_26252638

improve its own nutritional growth and male function. However, in the fruit stage, with the deepening of flower colour, the related phenotypic characteristics and resource allocation of *A. obtusiloba* made adjustments to improve reproductive function and female function. From flowering to fruiting, dark flowers are more competitive and more adaptable to the environment (Li, 2012). However, there are few studies on the mechanism of petal colour adaptation to the environment.

In the Tibetan Plateau, *A. obtusiloba* has its own adaptive mechanism to the local environment. During the past years, affected by global warming, there have been significant environmental changes in the plateau area—The temperature rises and the precipitation increases (Zheng, 2015). After years of observation by our research team, we find an obvious decrease of white flowers and an increase of yellow and light-yellow flowers of *A. obtusiloba*. It is speculated that this phenomenon may be related to its adaptability to the environment and biological evolution. Flower colour is one of the most important traits of plants and is attributed to various pigments that are composed of three major classes of compounds including flavonoids, carotenoids, and anthocyanin (Grotewold, 2006). Among these compounds, flavonoids are responsible for the yellow colour. At the same time, the number and position of phenolic groups in the chemical structure have a certain influence on the flower colour. The colour of the flower will change from yellow to orange and to red by the hydroxylation at C_3 (Yu et al., 2002). However, increasing the hydroxylation of the B ring will change the colour to blue, and the methylation of the B ring will make it red (Harborne 1993). Carotenoids are responsible for colours ranging from yellow to red (Tanaka et al., 2008). Cyanidin, which controls red, blue, purple, and other colours, can be divided into three types: pelargonidin, delphinidin, and anthocyanins (Hall, 1897).

Flavonoids represent a large subgroup of plant secondary metabolites including flavones, isoflavones, anthocyanins, flavanols, flavonols, and derivatives (Gao et al., 2019) with various biological activities such as anti-inflammation, anti-cancer, etc. (Arora et al., 2015). Over the past decade, studies have revealed the core biosynthesis pathways of flavonoids in various plants such as *Arabidopsis* (Tohge et al., 2017), *Lactuca sativa* (Zhang et al., 2017), *Camellia sinensis* (Liu et al., 2018), *Salvia miltiorrhiza* (Deng et al., 2018), *Oroxylum indicum* (Deshmukh et al., 2018), *Chrysanthemum morifolium* (Yue et al., 2018), *Chrysanthemum indicum* (Jiang et al., 2019), and *Scutellaria baicalensis* (Zhao et al., 2016). Flavones are synthesized via the flavonoid pathway, which is part of phenylpropanoid metabolism (Ferreyra et al., 2012). Naringenin is a central intermediate in the biosynthesis of normal 4'-hydroxyflavones (Martens and Mithöfer, 2005). The enzymatic properties related to flavonoid accumulation in vitro have been confirmed (Zhu, et al., 2020). Flavonoid biosynthetic genes can be classified into two categories: (i) early biosynthetic genes, such as genes encoding phenylalanine ammonia lyase (PAL), chalcone synthase (CHS), and chalcone isomerase (CHI); (ii) late biosynthetic genes, such as those encoding flavanone 3-hydroxylase (F3′H), dihydroflavonol reductase (DFR), and anthocyanidin synthase (ANS) (Patra et al., 2013). CHS, the first key enzyme in the anthocyanin synthesis pathway, is affected by multiple factors, such as environmental stress, light, inducer, etc. (Takeuchi et al., 1995). There are six genes involved in anthocyanin synthesis in different tissues of grape, CHS, CHI, F3′H, DFR, leucoanthocyanidin reductase (LAR), and flavonoids glycosyltransferase (UFGT), while the accumulation of anthocyanidin is absent in white grape. Therefore, the accumulation of anthocyanidin is not only related to tissue, but also related to the alternative gene expression. The study aimed to

http://www.aloki.hu ● ISSN 1589 1623 (Print) ● ISSN 1785 0037 (Online)
DOI: http://dx.doi.org/10.15666/aeer/2003_26252638

qualitatively and quantitatively identify the chemical composition using different analytical methods including ultraviolet-visible (UV-vis) spectroscopy, HPLC, and LC-MS, and to further analyse the key enzyme synthesizing this pigment.

Materials and methods

Materials

The experimental materials light-yellow and yellow *A. obtusiloba* fresh petals about 10 gwere collected in early July at the peak of flowering from Maqu County, Gansu Province of China in 2018 (101.52E, 33.40N, altitude 3500 m). The flowers were rinsed, and the stamens were removed. After fixating at 80 °C for 30 min, they were dried at 60 °C and crushed into powder with a pulveriser (Tianjin Taisite Instrument Co. Ltd., Tianjin, China). Then the powder sample was stored in a sealed bag and kept in a dark place before using.

Spectral analysis by UV-vis spectroscopy

Spectral analysis of flavonoids

The flavonoid extraction was identified according to the method of Deepika et al. (2018) with some modifications. To extract flavonoids, 0.1 g of flower powder was treated with methanol/formic acid (98:2, v/v) for 24 h in a Soxhlet apparatus under dark conditions. The filter residue was repeatedly extracted by the solvent. After the filtrate was combined and diluted to 10 mL, the spectral scanning was carried out by a UV spectrophotometer (UV-3000, Shanghai JiaPeng technology Co., Ltd., Shanghai, China) with a range of 200–700 nm. The measurements was repeated three times for each sample.

Content calculation (Cai et al., 2010):

$$\text{Total flavonoids content (mg/g)} = A_{max} \times 320 \times V_1/(V_2 \times 1000 \times m) \quad \text{(Eq.1)}$$

A_{max}: Maximum absorbance; V_1: Total sample volume; V_2: Sample volume; m: Weight of flower powder.

Spectral analysis of carotenoids

The carotenoids of *A. obtusiloba* were extracted based on the method reported by Cai et al. (2010) with necessary modifications. Briefly, each sample of flower powder (0.1 g) was mixed with acetone/ethanol (1:1, v/v), and the mixture was repeatedly extracted 24 h in a Soxhlet apparatus under dark conditions. After the filtrate was combined and diluted to 10 mL, the spectral scanning was carried out with a range of 200–700 nm. The measurements was repeated three times for each sample.

Content calculation (Cai et al., 2010):

$$\text{Total carotenoid content (mg/g)} = 4 \times A_{max} + 3.28 \times A_{665} - 11.64 \times A_{649} \quad \text{(Eq.2)}$$

Qualitative and quantitative analysis of petal pigments

Flavonoids in petals of *A. obtusiloba* were extracted with methanol/formic acid (98:2, v/v) in darkness at 4 °C for 24 h. Then the mixture was centrifuged at 12,000 rpm

http://www.aloki.hu ● ISSN 1589 1623 (Print) ● ISSN 1785 0037 (Online)
DOI: http://dx.doi.org/10.15666/aeer/2003_26252638

for 5 min at 4 °C to remove the precipitants. The supernatant was collected and filtered through a 0.45 μm micropore membrane, and the as-prepared sample was stored for qualitative and quantitative analysis (Wang et al., 2018).

The quantitative analysis of flavonoids was performed on HPLC-PAD (Waters 2685, USA) and HPLC-MS (Agilent 6460, USA). A C18 column of Inertsil Zorbax SB (4.6 mm × 250 mm, 5 μm, Shimadzu GL, Shanghai, China) was used to separate the individual flavonoids with mobile phase A (double distilled water containing 0.1% phosphoric acid) and mobile phase B (acetonitrile). The elution gradient was set as follows: 0 min, 1% B; 15 min, 8% B; 35 min, 22% B; 45 min, 42% B; 55 min, 75% B; 65 min, 100% B. Then, 2 μL of the sample was injected for HPLC analysis. The chromatogram showed horizontal coordinate and vertical coordinate, corresponding to the retention time (min) and response value (m AU), respectively. The flow rate was 0.2 mL/min, and the column temperature was 30 °C. Since flavonoids are expected to be observed at a 300 nm wavelength by UV detector, the spectra were scanned in the range of 190–700 nm.

The MS conditions were set as follows: High purity nitrogen (99.999%) was used as a nebulizing (60 psi) and drying gas at a flow rate of 9.0 L/min. The vaporizer temperature was set at 350 °C. Other parameters were rationally set including an Ion spray voltage of 70–205 V and a scanning range of 100–1000 m/z.

Statistical analysis

The data were processed and presented as mean ± standard deviation (SD). Measurements were performed in triplicates and the statistical analysis was executed by one-way analysis of variance (ANOVA). Significant differences between groups were discerned at $p \leq 0.05$. Statistic software Graph Pad Prism 6.0 (Graph Pad Software Inc., San Diego, USA) was used for all the graphical and statistical evaluations.

Results

Spectral analysisusing UV-vis spectrometer

Spectral analysis of flavonoids

As shown in the UV-vis spectrum of the flavonoid fraction of *A. obtusiloba* (*Fig. 1A*), the maximum absorption peaks were observed at 268 nm (band II) and 330 nm (band I), respectively. There are two typical absorbance bands of flavonoids, band B (310–350 nm) for flavones and band A (250–290 nm) for flavonols (Arora and Itankar, 2018). Generally speaking, band II absorption could be caused by ring A-cyclobenzoic acid system, while band I was caused by ring B-cyclocinnamic acid system (Hu et al., 2008). As shown in *Figure 1A,* the absorption peak at 268 nm indicated the presence of the A-cyclobenzoyl system, while the absorption peak at 300 nm suggested that there was a B-cyclocinnamoyl system in the flavonoid fraction of the flower extract. Based on the observation that band II was the main peak while band I was weak, we speculated that the cinnamoyl system might be destroyed (Liu et al., 2007). This result showed that the extract from *A. obtusiloba* had the basic structure of flavonoids C6-C3-C6.

Spectral analysis of carotenoids

According to the UV-vis spectrum of the carotenoids sample from *A. obtusiloba* (*Fig. 1B*), the maximum absorption peak was at 268 nm, which was consistent with the

http://www.aloki.hu ● ISSN 1589 1623 (Print) ● ISSN 1785 0037 (Online)
DOI: http://dx.doi.org/10.15666/aeer/2003_26252638

characteristic absorption peak of the carotenoid. With the deeper colour, the absorption peak of the carotenoid sample gradually increased. The total content changed regularly with the shading of the colour (*Fig. 1B*). The maximum light absorption value of the pale-yellow sample was 18.36%less than that of the yellow sample (4.112 and 3.357 of the optical density (OD), respectively).

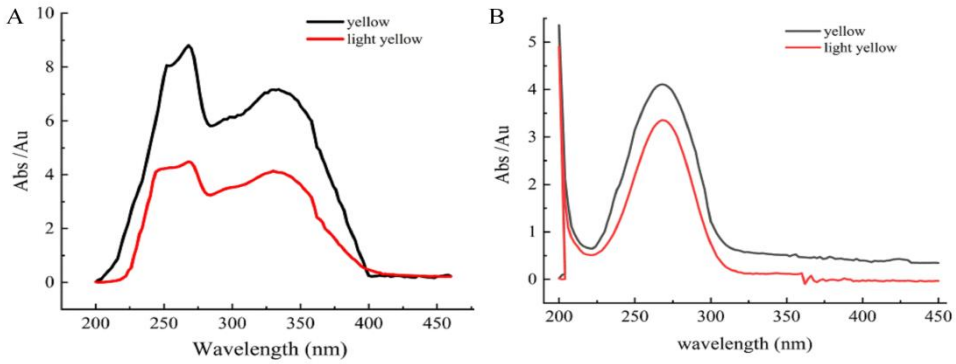

Figure 1. *The UV-visible spectra of petal pigments in Anemone obtusiloba, Flavonoid (A), Carotenoid (B)*

According to the Total flavonoid content and total carotenoid content ANOVA tables (*Table 1*), significant differences between groups were discerned at $p \leq 0.05$. However, differences of total flavonoid content between groups was more significant, and the content of total flavonoids is higher than that of total carotenoids. Flavonoids were identified as the main components of flower colour, and the specific components were analysed and determined.

Table 1. *Total flavonoid content and total carotenoid content ANOVA tables*

Total flavonoid content ANOVA table					
Source	**SS**	**df**	**MS**	**F**	**P-value**
Group	127.1716882	1	127.1716882	11137.17493	4.83E-08
Error	0.045674667	4	0.011418667		
Total	127.2173628	5			
Total carotenoid content ANOVA table					
Source	**SS**	**df**	**MS**	**F**	**P-value**
Group	0.02535	1	0.02535	13.82727273	0.020501259
Error	0.007333333	4	0.001833333		
Total	0.032683333	5			

Qualitative and quantitative analysis of petal pigments

Qualitative analysis of petal pigments from Maqu

Based on the HPLC-PDA analysis of the flavonoid extract of yellow flowers of *A. obtusiloba* (*Fig. 2*), 7 kinds of compounds were detected at 300 nm with a retention time ranging from 30 to 50 min. Meanwhile, there were 8 kinds of compounds detected in light-yellow of flavonoid fraction of *A. obtusiloba*. Zhao et al. (2005) reported that

http://www.aloki.hu ● ISSN 1589 1623 (Print) ● ISSN 1785 0037 (Online)
DOI: http://dx.doi.org/10.15666/aeer/2003_26252638

the different colour of flowers were not determined by the structure of the compound, but by the change in the content of some pigment molecules. Studies have also found that the red colour of cotton is mainly caused by flavonoid accumulation. Except for the flavonoid-related enzyme genes in red cotton such as CHS and F3'H, other genes that regulate flavonoid biosynthesis have higher transcription levels than those in white cotton (Long et al., 2019). In the HPLC chromatogram (*Fig. 2A*), peaks 3 and 8 were close to each other, suggesting that they might be isomers. Therefore, the flavonoid components of the two coloured flowers are supposed to be the same. Mostly, the peak intensity (response value) of yellow flowers (B) was higher than that of the light yellow (B) ones. Therefore, it could be suggested that the colour intensity of *A. obtusiloba* was caused by the content of pigment molecules. The components (*Fig. 2A*) at peaks 3 (1.775 mg/g), 6 (1.56 mg/g), and 7 (2.687 mg/g) were more dominant in light-yellow flowers, whereas peaks 3 (4.124 mg/g), 4 (2.754 mg/g), and 7 (2.651 mg/g) were more dominant in yellow flowers (*Fig. 2B*).

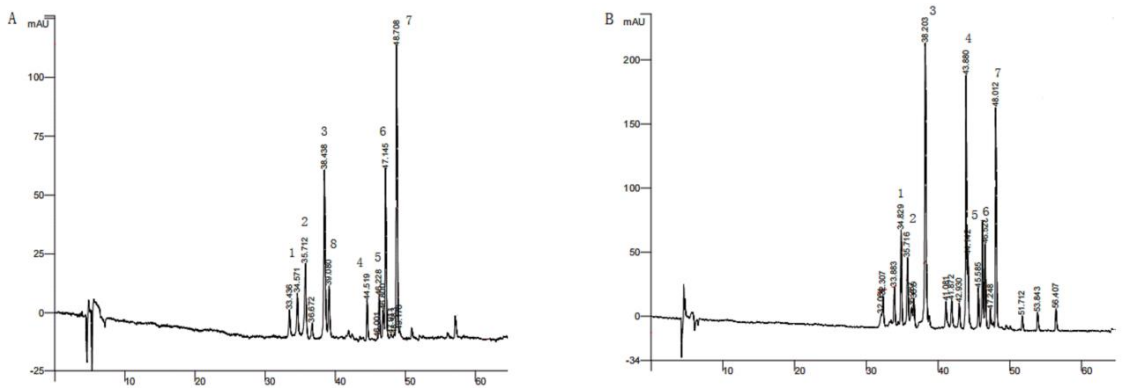

Figure 2. *HPLC chromatogram of flavonids from Anemone obtusiloba, Light yellow (A), Yellow (B)*

Quantitative analysis of petal pigments from Maqu

To further determine the specific type of pigment molecules, HPLC-MS analysis was carried out on yellow flowers with high total contents. The MS peaks of four standards (Quercetin, Kaempherol, Luteolin, and Rutin) were shown in *Figure 3*. According to the total ion chromatogram and positive ion mode of flavonoid from the yellow flower (*Figs. 4* and *5*), the analysis results in *Table 2* were obtained.

Table 2. *HPLC-MS analysis results of flavonid from Anemone obtusiloba yellow flower*

Peak No.	Retention time (min)	Molecular ion (m/z)	Fragment ions (m/z)	Identification
7	31.88	645.18([M + H]$^+$)	465, 287, 248	luteolin-3-7-O-glucoside
6	33.24	625.15([M]$^+$)	465, 303, 274	quercetin-3-O-rutoside
5	36.19	611.2([M + H]$^+$)	445, 287, 263	kaempferol-3-O-sophoroside
4	42.58	483.1([M + 3H]$^+$)	318, 146	myricetin-3-O-rhamnose
3	45.31	465.1([M + H]$^+$)	303, 287, 274	quercetin-3-O-galactoside
2	45.74	465.1([M + H]$^+$)	303, 287, 274	quercetin-3-O-glucoside
1	47.40	449.2([M + H]$^+$)	303, 274, 179	quercetin-3-O-rhamnoside

http://www.aloki.hu ● ISSN 1589 1623 (Print) ● ISSN 1785 0037 (Online)
DOI: http://dx.doi.org/10.15666/aeer/2003_26252638

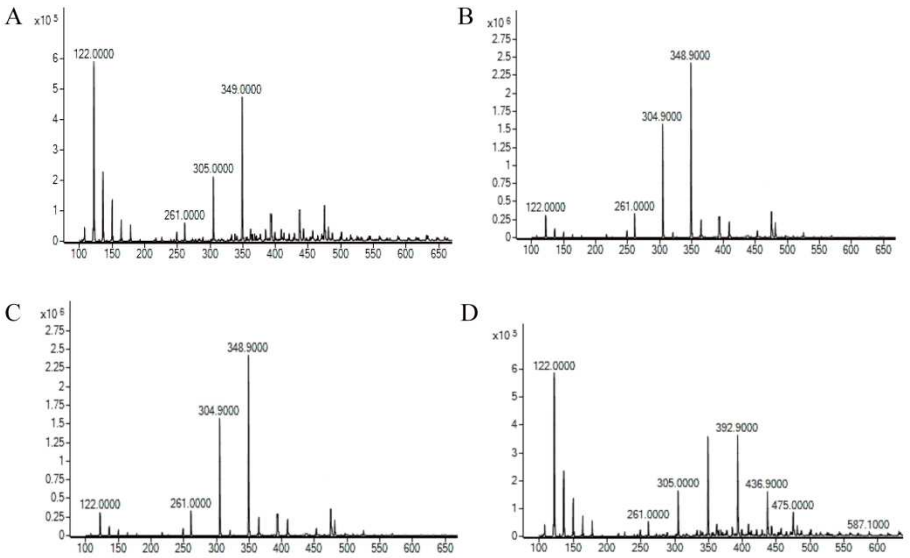

Figure 3. *Total ion chromatogram of standards Lquercetin (A), Kaempherol (B), Luteolin (C), and quercetin-3-O-rutinoside (D)*

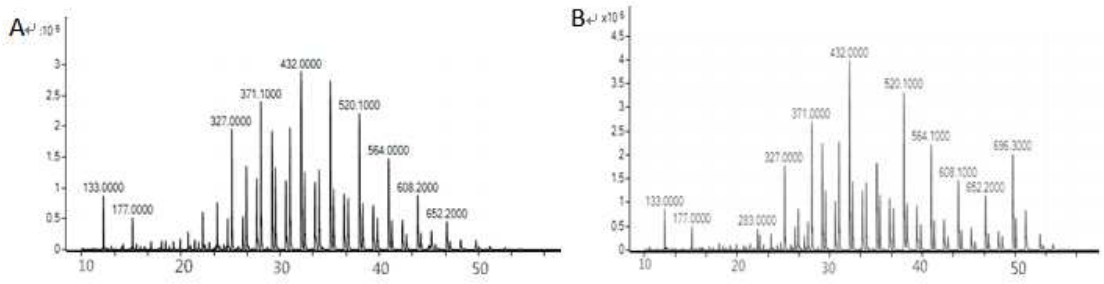

Figure 4. *Total ion chromatogram of flavonoid from Anemone obtusiloba Light yellow (A), yellow (B)*

The molecular ion peak was observed at m/z 645.18 [M + H]+ of peak 7. The fragment at m/z 465 represented the loss of one glucose molecule. Then one glucose molecule was removed to obtain a fragment m/z 287, which was luteolin aglycone. It was speculated to be luteolin-3-7-O-glucoside since it was consistent with the result reported by Susan (1985).

The fragment at m/z 303 corresponded to quercetin aglytin and its cleaved m/z 274 fragments were found the MS of peaks 6, 3, 2, and 1, which were presumed to be derivatives of quercetin. The [M + H]+ of peak 6 was m/z 625.15, which contained fragment ions m/z 465 and 303, indicating that two molecules of six-carbon sugar have been removed. As a result, it could be quercetin-3-O-rutoside (Susan et al., 1985). Besides, a molecular ion peak was observed at m/z 465.1 [M + H]+ of peaks 3 and 2, and the removal of one six-carbon sugar molecule obtained m/z 303. This result could indicate that peak 3 was quercetin-3-O-galactoside (Harborne 1986) and peak 2 was quercetin-3-O-glucoside (Yu et al., 2007). Fragments at m/z 303 showed that the removal of rhamnose and fragments at m/z 179 could be the loss of one water molecule representing the [M + H]+ peak 1. The result indicated that it might be quercetin-3-O-

http://www.aloki.hu ● ISSN 1589 1623 (Print) ● ISSN 1785 0037 (Online)
DOI: http://dx.doi.org/10.15666/aeer/2003_26252638

rhamnoside (Li et al., 2008). The fragment ion m/z 287 matched the molecular weight of kaempferol. Therefore, it could be speculated that kaempferol was contained in its structure. The fragment m/z 445 indicated the loss of two molecules of glucose, which was consistent with the peak of kaempferol-3-O-sophoroside reported previously (Li et al., 2008). The molecular ion peak 4 was observed at m/z 483.1 [M + H]+. Based on the characteristic ion of myricetin at m/z 318, and the glycosyl ion at m/z 146, the data were found to be consistent with the result of myricetin-3-O-rhamnose (Chosson et al., 1998). The content of the flavonoids was measured (*Table 3*). The content of quercetin-3-O-galactoside (4.124 mg/g) was found to be relatively higher than the other components. As a result, quercetin derivatives were dominant in flavonoids of *A. obtusiloba* flowers.

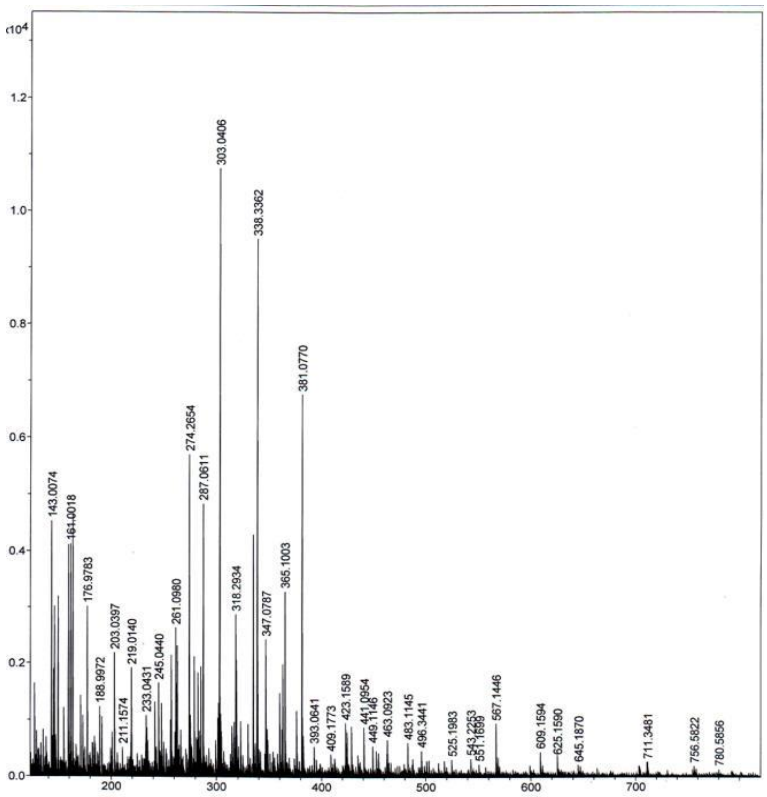

Figure 5. *Cationic mass spectrograms of flavonoid from yellow Anemone obtusiloba*

Table 3. *The content of main components of anthocyanin in Maqu Anemone obtusiloba (mg/g)*

Peak No.	Component	Yellow flowers	Light yellow flower
7	luteolin-3-7-O-glucoside	2.754	2.687
6	quercetin-3-O-rutoside	0.982	1.56
5	kaempferol-3-O-sophoroside	1.2	0.394
4	myricetin-3-O-rhamnose	2.651	0. 34
3	quercetin-3-O-galactoside	4.124	1.775
2	quercetin-3-O-glucoside	0.867	0.815
1	quercetin-3-O-rhamnoside	1.05	0.461

http://www.aloki.hu ● ISSN 1589 1623 (Print) ● ISSN 1785 0037 (Online)
DOI: http://dx.doi.org/10.15666/aeer/2003_26252638

The keyenzyme analysis in the regulation of anthocyanin in A. obtusiloba

Although the anthocyanins of *A. obtusiloba* are mainly composed of four sugar derivatives of luteolin, kaempferol, myricetin and quercetin. In these major flavonoids, quercetin with the highest relative abundance may be one of the main active ingredients. According to the metabolic pathway of flavonoids (*Fig. 6*) (He et al., 2020), quercetin could only be synthesized from dihydroquercetin and catalysed by flavonol synthetase (FLS). There were two pathways of dihydroquercetin synthesis: one was eriodictyol catalysed by flavanone-3-hydroxylase (F3H), and the other was dihydrokaempferol catalysed by flavonoid-3'-hydroxylase (F3'H). However, eriodictyol could be also catalysed by flavone synthase II (FNSII) to form luteolin. In the study, the derivatives of luteolin (2.754 mg/g) were observed. Therefore, luteolin pathway was not prohibited, and the activity of FNSII might be reduced or the gene expression of FNSII was down regulated to reduce the decomposition of luteolin. F3'H catalysed the synthesis of dihydrokaempferol and dihydroquercetin from senkyolin and naringenin, respectively. According to the reactions in *Figure 6,* F3'H showed a higher affinity with naringenin. So it was speculated that the affinity of FLS with dihydroquercetin was enhanced in the pathway of the synthesis of luteolin, which competed with dihydrokaempferol and dihydromyricetin to increase the content of quercetin. According to the content of flavonoids in *A. obtusiloba*, it was speculated that the dihydrokaempferol pathway improved the translation of F3'H to increase the content of dihydroquercetin. And the affinity between FLS and dihydroquercetin was enhanced, so quercetin content could be eventually increased.

Therefore, enhancing the translation of F3'H gene could not only increase the content of dihydroquercetin, but also increase the content of eriodictyol, which could indirectly increase the content of dihydroquercetin and finally achieve the purpose of increasing the content of quercetin.

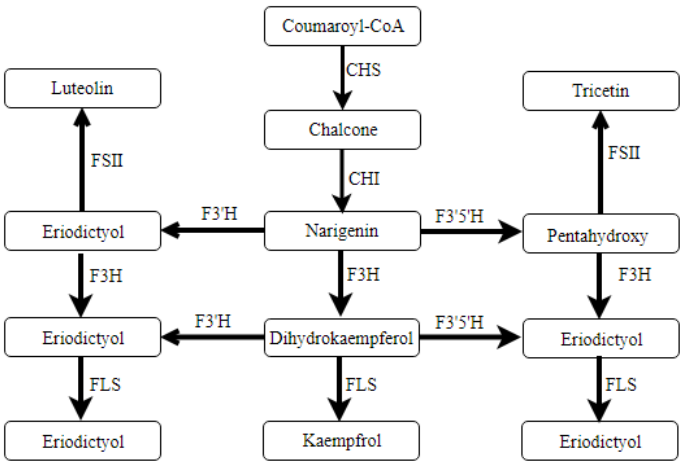

Figure 6. *The metabolic pathway of flavonoid*

Discussion

In recent years, with changes in the environment in the alpine region—The temperature rises and the precipitation increases (Zheng, 2015), the pigment of the unique plant *A. obtusiloba* has also been changed. The pigment of *A. obtusiloba* has

http://www.aloki.hu ● ISSN 1589 1623 (Print) ● ISSN 1785 0037 (Online)
DOI: http://dx.doi.org/10.15666/aeer/2003_26252638

undergone significant changes to adapt to the environment. In the Hezuo plot with lower altitudes (altitude 3000 m), the pigment of the *A. obtusiloba* is obviously darkened, white flowers are not easily observed. Compared with low altitude Hezuo plot, the higher the altitude, the deeper the colour, in the Maqu plot with higher altitudes, and even no white flowers are observed (*Fig. 7*) (Lan, 2016). The same experiment was carried out in the HeZuo sample plot, and the results were consistent with this study. Seven kinds of components in flavonoids were speculated by HPLC-MS, increases the content of quercetin by regulating the expression or activity of F3'H to deepen the flower colour so that it could adapt to the environment (Lv et al., 2019). The side shows that, the evolutionary direction and adaptive mechanism of *A. obtusiloba* at different altitudes are the same.

Studies have shown that the petal colour of *A. obtusiloba* is related to reproductive characteristics and reproductive distribution, moreover, with the increase of reproductive pressure (altitude), yellow flowers are more competitive than other colours (Li, 2012). Therefore, the number of yellow flowers increased with the increase of altitude, this is consistent with our observations. There is also a certain relationship between petal colour and genetic diversity. The research shows that there are more genetic diversity polymorphic loci in anemone with deeper flower colour in different regions (Liu, 2017). Moreover, the number of seeds per fruit and seed setting rate of yellow plants in the same population were significantly higher than those of white plants (Hu, 2013). It can be inferred that the yellow flower of *A. obtusiloba* is the direction of its adaptive evolution.

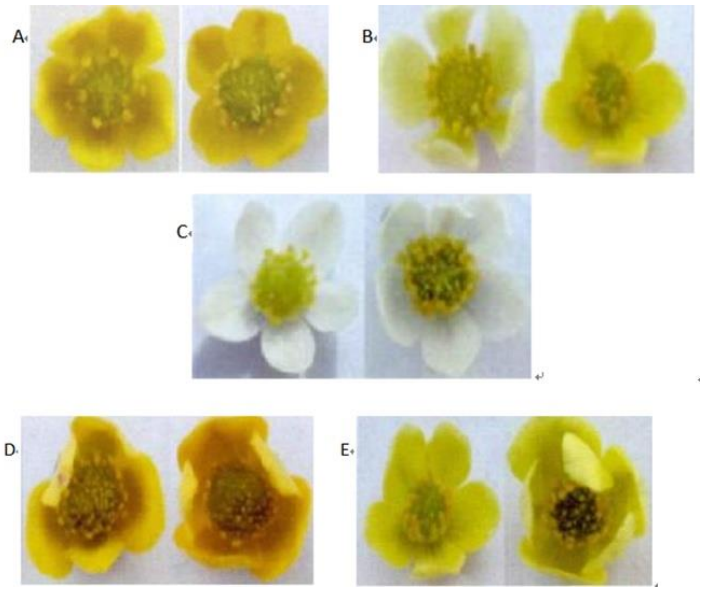

Figure 7. *Three Pigment of Anemone obtusiloba. (A) Hezuo Yellow, (B) Hezuo Pale Yellow, (C) Hezuo White, (D) Maqu Yellow and (E) Maqu Pale Yellow*

Conclusion

In this study, the main components and their key enzymes in different colourful flowers of *A. obtusiloba* were analysed by UV-vis spectroscopy, HPLC-PAD, and HPLC-MS. Seven kinds of components in flavonoids were speculated by HPLC-MS, including luteolin-3-7-O-glucoside, quercetin-3-O-rutoside, quercetin-3-O-galactoside,

http://www.aloki.hu ● ISSN 1589 1623 (Print) ● ISSN 1785 0037 (Online)
DOI: http://dx.doi.org/10.15666/aeer/2003_26252638

quercetin-3-O-glucoside, quercetin-3-O-rhamnoside, kaempferol-3-O-sophoroside, and myricetin-3-O-rhamnose. According to the results of qualitative and quantitative analysis, quercetin showed the largest proportion of sugar derivatives and the most obvious change of flower colour, it is the main chromogenic pigment that causes the difference in flower colour of *A. obtusiloba*. According to the flavonoid metabolic pathways, there are three main ways to increase the content of quercetin: (1) reducing the activity of FNSII or attenuating the translation of FNSII gene to reduce the path of eriodictyol; (2) enhancing the affinity of FLS binding with dihydroquercetin to make dihydroquercetin superior in substrate competition; (3) enhancing the translation of F3'H genes, such as increasing the transcription factor in the promoter region to increase the content or activity of F3'H to increase the contents of dihydroquercetin and saugenin. This paper speculates that *A. obtusiloba* increases the content of quercetin by regulating the expression or activity of F3'H to deepen the flower colour so that it could adapt to the environment.

Through this study, the evolution of *A. obtusiloba* response to the environment was analysed. This conjecture is also applicable to the adaptation to altitude changes. It provides a theoretical basis for the study of the evolution mechanism of plateau plants responding to the environment and provides a reference for the relationship between plateau environmental change and vegetation, it also provides a research direction for studying the adaptive evolution of plateau plants. In the future, the adaptability of *A. obtusiloba* to the environment can be studied from the perspective of molecular biology, especially F3'H related genes, and further study its evolutionary direction, genetic diversity and the impact of environment on its evolution.

Acknowledgements. Thanks for the financial support provided by Lanzhou University of Technology.

Conflict of interests. No conflict of interests exits in the submission of this manuscript, and all the authors listed have approved the manuscript that is enclosed.

REFERENCES

[1] Arora, S., Itankar, P. (2018): Extraction, isolation and identification of flavonoid from *Chenopodium album* aerial parts. – Journal of Traditional and Complementary Medicine 8(4): 476-482.

[2] Cai, X., Su, F., Jin, H. X., Yao, C. H., Wang, C. Y. (2010): Components and extraction methods for petal pigments of *Osmanthus fragrans* 'Siji Gui'. – Journal of Zhejiang Forestry College 27(4): 559-564.

[3] Chosson, E., Chaboud, A., Chulia, A. J., Raynaud, J. (1998): A phloracetophenone glucoside from *Rhododendron ferrugineum*. – Phytochemistry 47(1): 87-88.

[4] Deepika, S. M., Thangam, R., Sakthidhasan, P., Arun, S., Sivasubramanian, S., Thirumurugan, R. (2018): Combined effect of a natural flavonoid rutin from Citrus sinensis and conventional antibiotic gentamicin on Pseudomonas aeruginosa biofilm formation. – Food Control 90(1): 282-294.

[5] Deng, Y., Li, C., Li, H., Lu, S. (2018): Identification and characterization of flavonoid biosynthetic enzyme genes in *Salvia miltiorrhiza* (*Lamiaceae*). – Molecules 23(6): 1467-86.

[6] Deshmukh, A. B., Datir, S., Bhonde, Y., Kelkar, N., Samdani, P. (2018): De novo root transcriptome of a medicinally important rare tree *Oroxylum indicum* for characterization of the flavonoid biosynthesis pathway. – Phytochemistry 156: 201-213.

http://www.aloki.hu ● ISSN 1589 1623 (Print) ● ISSN 1785 0037 (Online)
DOI: http://dx.doi.org/10.15666/aeer/2003_26252638

[7] Ferreyra, M. L. F., Rius, S. P., Casati, P. (2012): Flavonoids: biosynthesis, biological functions, and biotechnological applications. – Frontiers in Plant Science 3(1): 222-237.
[8] Gao, G., Chen, P., Chen, J. K., Chen, K. M., Wang, X. F., Shehu, A. A., Liu, N., Yu, C. M., Zhu, A. G. (2019): Genomic survey, transcriptome, and metabolome analysis of apocynum venetum and apocynum hendersonii to reveal major flavonoid biosynthesis pathways. – Metabolites 9(12): 1-15.
[9] Grotewold, E. (2006): The genetics and biochemistry of floral pigments. – Annual Review of Plant Biology 57(1): 761-780.
[10] Gupta, A. K., Sharma, M., Chandha, A. (2005): Reviews on Indian Medicinal Plants. – Journal of Ethnopharmacology 96(3): 0972-7957.
[11] Hall, M. A. (1897): Plant Structure, Function and Adaptation. – Science Press, Beijing, pp. 221-258.
[12] Harborne, J. B. (1986): Flavonoid patterns and phytogeography: the genus Rhododendron section Vireya. – Phytochemistry 25(7): 1641-1643.
[13] Harborne, J. B. (1993): Introduction to Ecological Biochemistry. – Academic Press, London, pp. 36-70.
[14] He, J., Yang, W. J., Cheng, B., Ma, L., Tursunjiang, D., Ding, Z. M., Li, Y., Wang, Z. F., Ma, Y. M., Li, G. (2020): Integrated metabolomic and transcriptomic profiling reveals the tissue-specific flavonoid compositions and their biosynthesis pathways in Ziziphora bungeana. – Chinese Medicine 15(73): 73-73.
[15] Hu, C. (2013): Reproductive Ecology of Anemone Obtusiloba in Alpine Meadow of Qinghai Tibet Plateau. – College of Life Science and Engineering, Lanzhou University of Technology, China.
[16] Hu, H. P., Han, Y. L., Zhang, F., Zhang, D. M., Li, S. J. (2008): Extraction of *Pawpaw* flavoids and its ultraviolet spectrum characteristic. – Modern Food Science and Technology 24(3): 250-252.
[17] Jiang, Y., Ji, X., Duan, L., Ye, P., Yang, J., Zhan, R., Chen, W. W., Ma, D. M. (2019): Gene mining and identification of a flavone synthase II involved in flavones biosynthesis by transcriptomic analysis and targeted flavonoid profiling in *Chrysanthemum indicum* L. – Industrial Crops and Products 134(1): 244-256.
[18] Lan, W. L. (2016): Studies on the Allelopathy of Anemone Obtusiloba. – College of Life Science and Engineering, Lanzhou University of Technology, China.
[19] Li, B. (2012): Reproductive Strategies of Anemone Obtusiloba Under Different Environmental Conditions. – College of Life Science and Engineering, Lanzhou University of Technology, China.
[20] Li, C. H., Wang, L. S., Shu, Q. Y., Xu, Y. J., Zhang, J. (2008): Pigments composition of petals and floral color change during the blooming period in Rhododendron mucronulatum. – Acta Horticulturae Sinica 35(1): 1023-1030.
[21] Liu, Z. P. (2017): Genetic Diversity of Anemone Obtusiloba Population in Alpine Meadow of Qinghai Tibet Plateau and Its Correlation with Ecological Factor. – College of Life Science and Engineering, Lanzhou University of Technology, China.
[22] Liu, J. B., Lin, S. Y., Wang, Z. Z., Wang, E. L. (2007): Study on structure identification of flavonoids in *Vaccinium uliginosum.* L. – Food Science 28(9): 89-91.
[23] Liu, L., Li, Y., She, G., Zhang, X., Jordan, B., Chen, Q. (2018): Metabolite profiling and transcriptomic analyses reveal an essential role of UVR8-mediated signal transduction pathway in regulating flavonoid biosynthesis in tea plants (*Camellia sinensis*) in response to shading.–BMC Plant Biol 18: 233-250.
[24] Long, L., Liu, J., Gao, Y., Xu, F. C., Zhao, J. R., Li, B., Gao, W. (2019): Flavonoid accumulation in spontaneous cotton mutant results in red coloration and enhanced disease resistance. – Plant Physiology and Biochemistry 143(1): 40-49.
[25] Lv, W. L., Liu, Z. J., Zhang, X. R., Wang, Y. X. (2019): Research of Anemone obtusiloba main pigment composition and mechanism of adaptation. – Natural Product Research and Development 31: 395-400.

http://www.aloki.hu ● ISSN 1589 1623 (Print) ● ISSN 1785 0037 (Online)
DOI: http://dx.doi.org/10.15666/aeer/2003_26252638

[26] Martens, S., Mithöfer, A. (2005): Flavones and flavone synthases. – Phytochemistry 66(20): 2399-2407.
[27] Masood, M., Ashok, P., Tiwari, K. P. (1979): Obtusilobinin and obtusilobin, two new triterpene saponins from *Anemone obtusiloba.* – Phytochemistry 18(9): 1539-1542.
[28] Patra, B., Schluttenhofer, C., Wu, Y., Pattanaik, S., Yuan, L. (2013): Transcriptional regulation of secondary metabolite biosynthesis in plants. – Biochim Biophys Acta 1829(11): 1236-1247.
[29] Savita, R., Sanjeev, K., Mudassir, J. S., Santosh, K., Chand, G. R. (2011): Cytological studies in some members of family Ranunculaceae from Western Himalayas (India). – Caryologia 64(4): 408-415.
[30] Susan, K. W., Paul, A. H. (1985): Quercetin 3-O-galactosyl-(1→6)-glucoside, a compound from narrowleaf vetch with antibacterial activity. – Phytochemistry 24(2): 243-245.
[31] Takeuchi, A., Matsumoto, S., Hayatsu, M. (1995): Effects of shading treatment on the expression of the genes for Chalcone synthase and phenylalanine ammonialyase in tea plant (*Camellia sinensis*). – Bulletin of the National Research Institute of Vegetable Ornamental Plants and Tea 8(1): 1-9.
[32] Tan, G. L., Du, G. Z., Li, Z. Z., Yang, G. Y., Ma, J. Y., Niang, M. J. (2002): Relationship between productivity and species diversity in alpine meadow plant community. – J Plant Ecol 26: 57-62.
[33] Tanaka, Y., Sasaki, N., Ohmiya, A. (2008): Biosynthesis of plant pigments: anthocyanins, betalains and carotenoids. – The Plant Journal 54(4): 733-749.
[34] Thu, Z. M., Aye, M. M., Aung, H. T., Sein, M. M., Vidari, G. (2018): a review of common medicinal plants in Chin State, Myanmar. – Natural Product Communications 13(11): 1557-1567.
[35] Tohge, T. D., Souza, L. P., Fernie, A. R. (2017): Current understanding of the pathways of flavonoid biosynthesis in model and crop plants. – Journal of Experimental Botany 68(15): 4013-28.
[36] Wang, Y., Zhang, C., Dong, B., Fu, J., Hu, S., Zhao, H. (2018): Carotenoid accumulation and its contribution to flower coloration of *Osmanthus fragrans*. – Frontiers in Plant Science 9: 1-17.
[37] Yu, X. N., Zhang, Q. X. (2002): Anthocyanins and flower colors of ornamental plants. – Forestry Science (03): 147-153.
[38] Yu, Y. Q., Gong, Z. J., Li, R. (2007): Simultaneous determination of hyperosid, isoquercitrin and quercetin in kendir extracturm by high performance liquid chromatographic method. – Journal of Fudan University (Natural Science) 46: 417-420.
[39] Yue, J., Zhu, C., Zhou, Y., Niu, X., Miao, M., Tang, X., Chen, F. D., Zhao, W. P., Liu, Y. S. (2018): Transcriptome analysis of differentially expressed unigenes involved in flavonoid biosynthesis during flower development of Chrysanthemum morifolium 'Chuju'. – Scientific Reports 28(1): 13414-13441.
[40] Zhang, L., Su, W., Tao, R., Zhang, W., Chen, J., Wu, P. (2017): RNA sequencing provides insights into the evolution of lettuce and the regulation of flavonoid biosynthesis. – Nature Communications 8(1): 1-12.
[41] Zhao, C. L., Guo, W. M., Chen, J. Y. (2005): Formation and regulation of flower color in higher plants. – Chin Bull Bot 22(1): 70-81.
[42] Zhao, Q., Zhang, Y., Wang, G., Hill, L., Weng, J., Chen, X., Xue, H. W., Martin, C. (2016): A specialized flavone biosynthetic pathway has evolved in the medicinal plant, *Scutellaria baicalensis*. – Science Advances 2(4): e1501780-e1501780.
[43] Zheng, R. (2015): Climate Change Characteristics of Qinghai Tibet Plateau and its Impact on Desertification Under the Background of Global Warming. – College of Atmospheric Sciences, Nanjing University of Information Engineering, China.

http://www.aloki.hu ● ISSN 1589 1623 (Print) ● ISSN 1785 0037 (Online)
DOI: http://dx.doi.org/10.15666/aeer/2003_26252638

[44] Zhu, J. Y., Xu, Q. S., Zhao, S. Q., Xia, X. B., Yan, X. M., An, Y. L., Mi, X. Z., Guo, L. X., Samarina, L., Wei, C. L. (2020): Comprehensive co-expression analysis provides novel insights into temporal variation of flavonoids in fresh leaves of the tea plant (*Camellia sinensis*). – Plant Science 290(1): 110306-110317.

http://www.aloki.hu ● ISSN 1589 1623 (Print) ● ISSN 1785 0037 (Online)
DOI: http://dx.doi.org/10.15666/aeer/2003_26252638

RESPONSE OF SALT-TOLERANT SOYBEAN (*GLYCINE MAX* (L.) MERR.) GENOTYPES TO PHOSPHORUS FERTILIZER ON SALINE SOILS OF INDONESIA

PURWANINGRAHAYU, R. D. – TAUFIQ, A. – HARSONO, A. – SUNDARI, T. – KUNTYASTUTI, H. – SUSANTO, G. W. A. – HARNOWO, D. – MEJAYA, M. J.*

Indonesian Legumes and Tuber Crop Research Institute, Jl. Raya Kendalpayak km 8. PO. Box 66 Malang 65101, East Java, Indonesia

**Corresponding author*
e-mail: mmejaya@yahoo.com, madejmejaya@gmail.com

(Received 24th Dec 2021; accepted 21st Mar 2022)

Abstract. Due to global climate change the salt-affected agricultural land has enlarged in Indonesia, especially in coastal areas. Chemical soil properties, such as pH, Na and Cl contents, as well as soil nutrients including availability of soil phosphorus, are changed by higher soil salinity. Phosphorus fertilizer management on saline soils must be done properly since improper dosage of P can worsen the severity of the effects of salinity. The study aimed to determine appropriate dose of P fertilization for salt-tolerant soybean genotypes in saline soil. The experiment was conducted on an agricultural field during dry season 2018 in Tuban District, East Java Province, Indonesia. The treatment consisted of two P fertilizer dosage (72 and 108 kg P_2O_5/ha) on two salt-tolerant of soybean genotypes (Anjasmoro variety and K-13 line). The treatment was arranged in randomized complete block design, with fourteen replicates. Soil EC at the study site during the growing season was 9-17 dS/m, while EC of irrigation water was 6-16 dS/m. Results showed that among the two tested salt-tolerant genotype, Anjasmoro variety revealed better performance than K-13 line according to growth parameters, as well as yield and yield attributes. Appropriate P fertilizer dosage for both genotypes was 108 kg P_2O_5/ha.
Keywords: *application, dosage, nutrient, salinity, yield*

Introduction

Vulnerability to sea level rise, drought and flooding are new criteria in land suitability evaluation in the global climate change era (Sukarman et al., 2018). Climate change caused sea level rise and increased soil or groundwater salinity, especially in coastal areas. Indonesia has a large coastal area with about a 100,000 km coastline, which is the second longest in the world following Canada. Based on vulnerability to sea level rise, there is 12.02 million ha lands that is prone to salinization (Karolinoerita and Yusuf, 2020). The problem of salinity stress for plants is not only related to the adverse direct effects of salinity and toxicity of Na or Cl elements, but also to the indirect effect related to high pH and nutrient immobilization, especially phosphorus.

Phosphorous deficiency often occurs in saline soils because of absorption inhibition (Kaya et al., 2001; Hirpara et al., 2005), low availability due to Ca fixation and high soil pH (Chhabra and Thakur, 2000; Mahmood et al., 2013; Penn and Camberato, 2019; Tang et al., 2019). Increasing the availability of P in saline soils through fertilization improves growth and increases yield (Zribi et al., 2018; Belouchrani et al., 2020). The P fertilizer effectiveness and crop yield increase are higher when combined with organic fertilizers (Mahmood et al., 2013; Meena et al., 2018; Ding et al., 2020).

The use of salinity-tolerant genotypes is the key to increase crop productivity. Soybean (*Glycine max* (L.) Merr.) line IAC100/Bur/Malabar-10-KP-21-50 and K-13 were identified tolerant to salinity up to 12.2 dS/m (Purwaningrahayu et al., 2015,

http://www.aloki.hu ● ISSN 1589 1623 (Print) ● ISSN 1785 0037 (Online)
DOI: http://dx.doi.org/10.15666/aeer/2003_26392650

2016). Soybean line K-13 and Anjasmoro variety were also reported tolerant to salinity in different mechanism. Salt-tolerance of Anjasmoro was due to more K uptake, while in K-13 it was due to inhibition of Na uptake (Taufiq et al., 2016).

Combining salinity-tolerant genotypes with best soil management resulted in better effect as well as yield. Soybean yield of Anjasmoro variety and K-13 line increased by 36% in saline soil with salinity of 10 dS/m amended with 2.5 t/ha manure and 1.5 t/ha gypsum (Taufiq et al., 2016; Purwaningrahayu and Taufiq, 2018). In previous studies on saline soil with soil conductivity 6- > 10 dS/m, soybean K-13 line productivity reached 1.5 t/ha in saline soil with fertilization at 46 kg N/ha and 108 kg P_2O_5/ha (Purwaningrahayu and Taufiq, 2018a). Phosphorous fertilization of saline soil must be done properly. Tang et al. (2019) showed that maize in saline environment absorbed more Na from well P supplied soil compared with low P or P deficient soil. This research aimed to determine the optimum dosage of P fertilization in saline soil for two saline-tolerant of soybean genotypes.

Methodology

Place and time of study

Field trial was conducted in saline land at Gesikharjo Village, Palang Sub District, Tuban District, East Java Province (6°54'19.5196"S; 112°8'17.7947"E; 4 m asl) from July to October 2018 (dry season). The trial site was located at about 500 m from coastline with soil properties presented in *Table 1*. There was no rainfall during the field trial, and average air temperature was 27.9 °C (*Fig. 1*). Soybean planted in paddy field after rice following planting pattern of rice-soybean. In fact, farmer in this land only grow rice once during rainy season and then fallow because of high salinity of soil as well as irrigation water.

Research design

The treatment consisted of two factors. The first factor was two dosages of P fertilizer (72 kg P_2O_5/ha and 108 kg P_2O_5/ha) using SP36 (36% P_2O_5), and the second factor was two soybean genotypes (Anjasmoro variety and K-13 line). Treatment of P fertilizer dosage use was based on the optimum dosage of a previous research. Each treatment combination was applied in a plot of 24 m^2 (4 m wide and 6 m length) that were laid out according to randomized complete block design, with 14 replications.

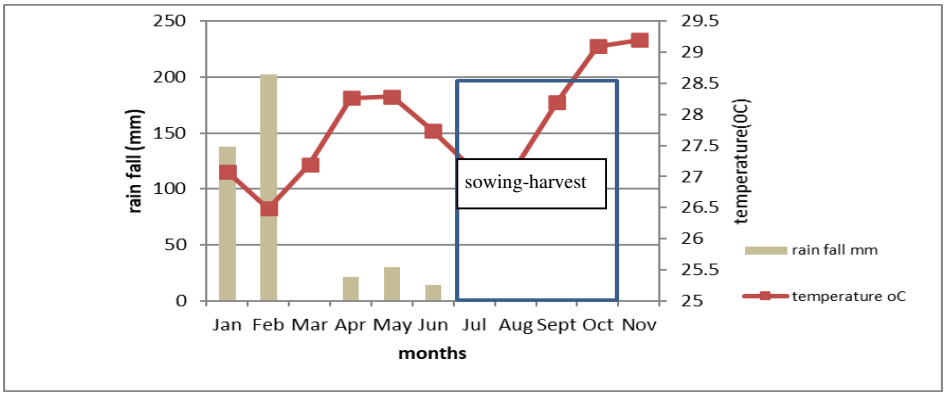

Figure 1. *Rain fall and air temperature in Palang Sub District, Tuban District in 2018*

http://www.aloki.hu ● ISSN 1589 1623 (Print) ● ISSN 1785 0037 (Online)
DOI: http://dx.doi.org/10.15666/aeer/2003_26392650

Table 1. *Chemical and physical properties of top 0-20 cm composite soil sample at preplanting. Tuban, dry season 2018*

Properties	Methods	Value	Classification[1)]
Soil fraction (%)	Pipet		
• Clay		74	
• Silt		23	
• Sand		3	
• Texture class		Clay	
Bulk density (g/cm^3)		1.1	
Moisture content (%w/w)			
• pF 2.5	Pressure plate	44.5	
• pF 4.2		24.5	
Salinity (dS/m)	Field measurement (Portable EC meter)	14.4	VH
pH-H_2O	1:5[2)]	8.2	Slight alkaline
Total-N (%)	Kjedahl[3)]	0.12	L
C-organic (%)	Walky & Black[4)]	1.70	L
P_2O_5 (mg/kg)	Olsen[5)]	17.73	L
SO_4 (mg/kg)	1 N NH_4OAc pH 4,8[6)]	997	VH
Cu (mg/kg)	DTPA extraction	4.9	M
Fe (mg/kg)	DTPA extraction	1.12	L
Exchangeable cations (cmol$^+$/kg)	1 N NH_4OAc pH 7.07[7)]		
• K		3.05	VH
• Na		3.55	VH
• Mg		4.87	VH
• Ca		24.97	VH
CEC (cmol$^+$/kg)	1 N NH_4OAc pH 7	48.04	H
Na saturation (ESP, %)	(Na/CEC)*100%	7.38	H

[1)]L: low; H: high; VH: very high; M: moderate according to Sulaeman et al. (2005); [2)]Mclean (1982); [3)]Bremner (1960); [4)]Walkley and Black (1934); [5)]Olsen and Sommers (1982); [6)]Tabatabai (1982); [7)]Peech (1945)

Rice straw clearing, as well as soil tillage, were conducted before planting. Prior to planting, soybean seeds treated with insecticide of thiametoxam active ingredient for protection against pest. Seed planting was done manually by dibbling 2-3 seeds into the hole at planting distance of 40 cm interrow and 15 cm interplant, and then covered with manure at a dosage of 5 t/ha. All plots were fertilized with 46 kg N/ha as urea (46% N) and 60 kg K_2O/ha as MOP (60% K_2O). Phosphorous fertilizer at dosage according to the treatment and all dosage of MOP fertilizer broadcast applied once at planting time, and then 3.5 t/ha of rice straw applied as mulch. Urea fertilizer applied at 15 DAP and 30 DAP (days after planting) with 50% of the dosage, respectively. Weeding was done twice (20 and 45 DAP) using herbicide, and chemical pesticide sprayed five times for pest control. Soybean crops were irrigated five times during the growth using water from well around at the trial site.

http://www.aloki.hu ● ISSN 1589 1623 (Print) ● ISSN 1785 0037 (Online)
DOI: http://dx.doi.org/10.15666/aeer/2003_26392650

Data collection and analysis

Moisture content (gravimetric method) and electrical conductivity (portable EC meter Hanna instruments) were measured at 0-20 cm soil depth starting from 15 DAP to 75 DAP with 15 days interval. Plant height and Chlorophyll content index (CCI) were observed from 15 DAP to 75 DAP with 15 days interval. The CCI was measured in the second and the third top leaves of ten samples using SPAD-502 (Minolta instruments). Proline, K and Na content of leaf were measured at 60 DAP (pod filling stage). Considering yield and yield attributes (number of filled and empty pods, weight of a 100 seeds) yield was measured based on dry seed (12% moisture content) from the plot, while yield attributes from 10 samples of each plot. The population of growing plants was calculated on an experimental plot of 24 m^2 (6 m × 2.4 m) or about 780 plants at plant spacing of 40 cm × 15 cm, 2 plants per hole. Plant population growth was calculated at 15 DAP, then the percentage was determined by the number of plants growing theoretically (780 plants). Similarly, at harvest time, the number of harvested plants was calculated on a 24 m^2 tiled plot, then the percentage was calculated by the number of growing plants.

The collected data were analyzed according to analysis of variance (ANOVA), and the mean comparison analysis using LSD 5%. All statistical analyses were proceeded with a statistical program package.

Results and discussion

Soil properties

In the soil of the study site clay fraction dominated, and so that the percentage of available water was low (20%) even water content at field capacity was quite high. Soil salinity, pH, exchangeable cations, CEC, S, and Na saturation were high, N, P and C-organic content were low. Micronutrient Cu was sufficient, but Fe was low, which might have been due to high soil pH (*Table 1*). Based on pH, salinity, and Na saturation values, soil in the study site was classified as high salinity soil according to Jones (2003). High soil salinity, Na, and pH as well as low P might be a limiting factor for soybean growth. Deficiency of P become more severe because of high soil salinity, pH, Na and Ca content. These soil properties not only inhibit P uptake, but also immobilized P due to Na and Ca fixation (Chhabra, 2002; Qadir et al., 2003; Ghafoor et al., 2004).

Soil salinity vs soil moisture

Soil EC (ECs), soil moisture content (SMC), as well as EC of irrigation water (ECw) changed during crop growth (*Fig. 2*). SMC tend to decrease linearly as soybean crop become older, and the lowest SMC was about physiological maturity stage. In contrast, ECs increased as SMC became lower. ECs was relatively stable and lower at 15 days after planting (DAP) and 30 DAP, then increased drastically at 45 DAP, but it was a little bit lower and relatively constant after 45 DAP (*Fig. 2A*). ECs at study site was about 9 dS/m during vegetative stage and increased to 15-17 dS/m during generative stage. ECw increased from 6 dS/m at planting to 14-16 dS/m at 15-60 DAP (*Fig. 2B*). Irrigation sources were wells located in the research location, because during the period of growth to harvest there was no additional rainwater (*Fig. 1*). Irrigation was carried out eight (8) times during the plant growth period at 0, 18, 23, 27, 29, 32, 44 and 51 DAP (*Fig. 2B*). Means that soybean experiencing higher salinity stress during generative stage than

http://www.aloki.hu ● ISSN 1589 1623 (Print) ● ISSN 1785 0037 (Online)
DOI: http://dx.doi.org/10.15666/aeer/2003_26392650

vegetative stage. Soybean was also subjected to double salinity stress, namely soil and irrigation water, and also sudden peak salinity stress that resulted in more adverse effect than constant salinity according to Bustingorri and Lavado (2011).

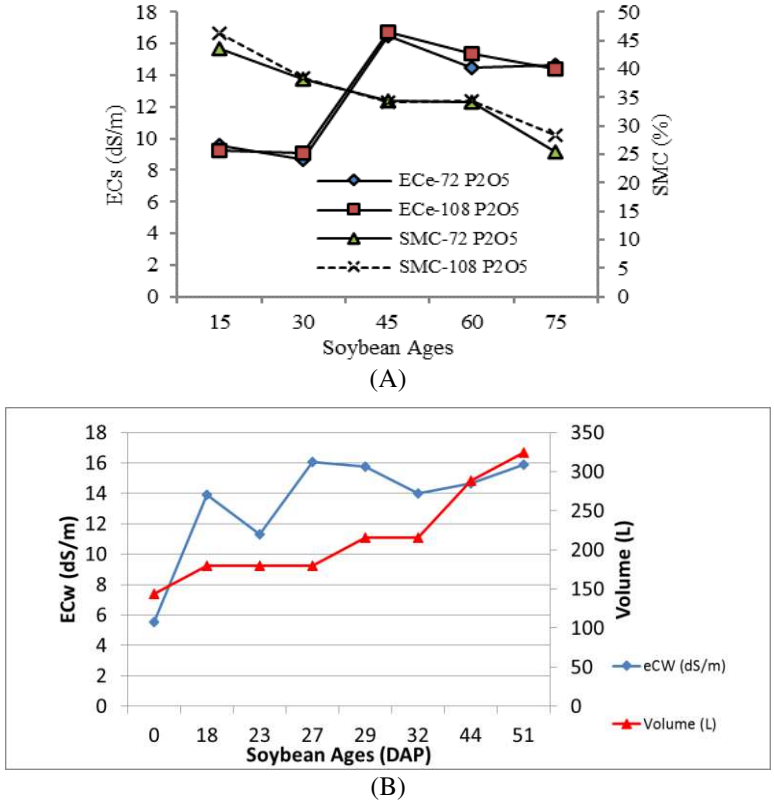

Figure 2. *Soil EC and moisture content (A) in saline soil and EC and volume of irrigation water (B) during soybean growth. Tuban, dry season 2018*

Application of P fertilizer had no effect on ECs or SMC (*Fig. 2A*). Therefore, increasing ECs during crop growth could be related to reducing SMC and increasing ECs. Soybeans were irrigated five times during their growth, using water from bored wells located in the experimental site. During the dry season bore wells were the only source of irrigation water in this area. Unfortunately, ECw in the dry season was almost twice higher than in the rainy season. EC from water irrigation could have an adverse effect to crop growth according to Aydinşakir et al. (2015), and even plant death (Singh et al., 2004).

Plant growth

Soybean growth as indicated by plant height and shoot biomass at 45 DAP and at harvest was affected significantly by P fertilization. Application of 108 kg P_2O_5/ha increased plant height by 29.6% at 45 DAP and by 16.4% at harvest compared to a dose of 72 kg P_2O_5/ha (*Fig. 3A*), and hence shoot biomass at 45 DAP and at harvest was 30.9% and 38.8% higher than at a dose of 72 kg P_2O_5/ha (*Fig. 3B*). It means that increasing P fertilizer rates improve soybean growth. This result is in accordance with Faozi et al. (2019) from their trial in sandy saline soil in coastal land in Yogyakarta. Phosphorous nutrient has an important role in photosynthetic activity of soybean (Marschner et al., 1996).

http://www.aloki.hu ● ISSN 1589 1623 (Print) ● ISSN 1785 0037 (Online)
DOI: http://dx.doi.org/10.15666/aeer/2003_26392650

The genotype factor as well as its interaction with P fertilization had no significant effect on plant height and shoot biomass at all observation dates. Anjasmoro variety grows taller than K-13 line and higher shoot biomass than K-13 line at all observation dates, but the difference in shoot biomass was not significant (*Fig. 3C*, *D*). Anjasmoro and K-13 were tolerant to high salinity stress (Taufiq et al., 2016). Salinity stress reduced root, stem, and shoot biomass, and the reduction of salt-tolerant soybean genotype was lower than susceptible genotype (Hamayun et al., 2019). The result indicates that Ajasmoro variety seems to be more tolerant to salinity stress than K-13 line.

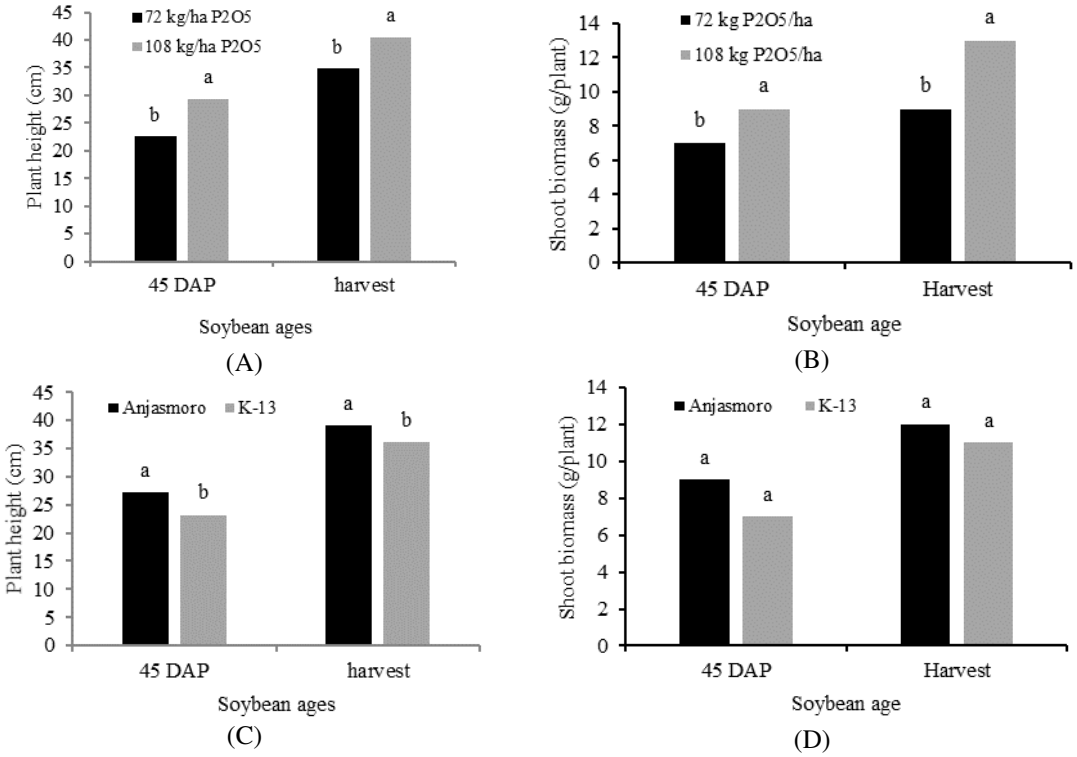

Figure 3. *Effect of P fertilization on plant height (A), shoot biomass (B), and effect of soybean genotype on plant height (C) and shoot biomass (D) in saline soil. (Same letter above bar in every chart and observation date means no significant difference based on LSD 5% test)*

Chlorophyll content index (CCI)

Soil salinity increases with the age of the crop, and this condition was also followed by a decrease in CCI (*Fig. 5*). Increasing salinity levels indicate increasing salt content, and this condition reduces chlorophyll content (Ghassemi-Golezani et al., 2011), because of the ultra-structure of leaf chloroplast damage the effect becomes severe as crop becomes older (Mitsuya et al., 2003). The CCI at different P fertilization dosage showed different trend, even though it was not significant statistically. The CCI at P fertilizer dosage of 72 kg P_2O_5/ha decreased continuously. However, CCI at P dosage of 108 kg P_2O_5/ha tended to increase and stabiles after 30 DAP, even the CCI was lower than in the early growth (*Fig. 4A*). Leaves analysis at 60 DAP showed that P and K content were significantly higher and Na content was significantly lower at P fertilizer dosage of 108 kg P_2O_5/ha compared to 72 kg P_2O_5/ha (*Table 2*). Phosphorous nutrient beside being important for photosynthetic activity, it also has an important role in increasing activity of

http://www.aloki.hu ● ISSN 1589 1623 (Print) ● ISSN 1785 0037 (Online)
DOI: http://dx.doi.org/10.15666/aeer/2003_26392650

nitrogenase enzyme (Marschner et al., 1996). However, leaf N content did not significantly differ between the two dosages of P fertilizer as indicted in *Table 2*. In contrast, proline content of leaf was lower at 108 kg P_2O_5/ha compared to 72 kg P_2O_5/ha (*Table 2*), and this fact is in accordance with Al-Karaki et al. (1996) that *Phaseolus vulgaris* L. and *P. acutifolius* accumulate lower proline at lower dosage of P application. Application of P fertilizer on black paper (*Paper nigrum*) reduce salt stress through increasing assimilation of N, P, K, Mg, Ca, Fe, Zn, Mn, and Cu (Cimrin et al., 2010*).* This result indicates that application of high P fertilizer dosage preventing chlorophyll damage, and it might be due to lower Na and higher K content, so that the adverse effect of Na can be prevented and hence the relatively higher CCI can be maintained.

CCI of the two genotypes tested were quite the same during germination stage (0-15 DAP), but the CCI of K-13 was higher than Anjasmoro after 15 DAP (*Fig. 4B*). Leaf of K-13 contained lower N, higher K and Na, but had no difference in K/Na ratio, and K-13 also had higher proline than Anjasmoro (*Table 2*). Adverse effect of higher Na in K-13 could be minimized by high K content. Increasing K uptake is a mechanism of crop tolerance to salt stress because K has a competitive property against Na in maintaining water status in the crop (Capula-Rodríguez et al., 2016). Proline is an organic substance in plants with a function to maintain turgor pressure of cells. This result indicates that higher K and proline content in K-13 line than in Anjasmoro might be responsible to higher CCI.

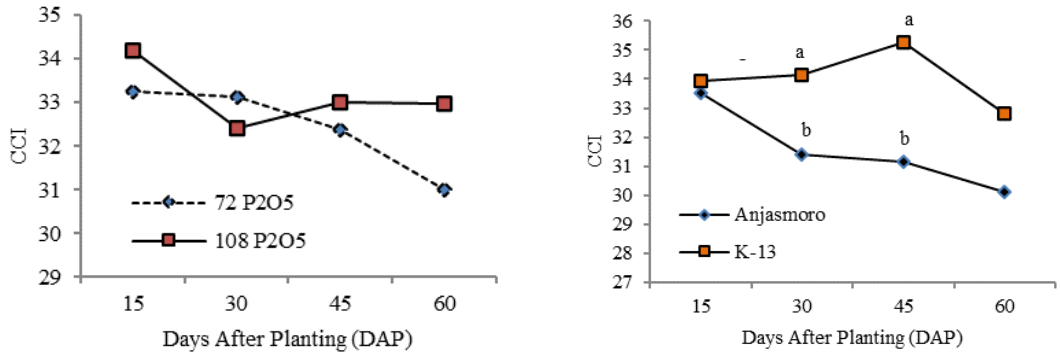

Figure 4. *Effect of different of P fertilization dosage (A) and different soybean genotype (B) on chlorophyll content index in saline soil. Tuban, second dry season 2018 (point in the graph with the same letter or without letter means no significant difference according to LSD 5%)*

Table 2. *N, P, K, Na content, K/Na ratio, and proline content of soybean leaf at 60 DAP at different P fertilizer rate and genotype in saline soil. Tuban, 2018*

Treatment	Proline (µg/g)	N (%)	P (%)	K (%)	Na (%)	K/Na ratio
P dosage						
• 72 kg/ha	119.5 a	1.51 a	0.14 b	1.33 b	0.054 a	24.8 b
• 108 kg/ha	70.0 b	1.49 a	0.17 a	1.52 a	0.047 b	32.7 a
Genotype						
• Anjasmoro	87.5 B	1.70 A	0.16 A	1.33 B	0.048 B	27.7 A
• K13	102.5 A	1.30 B	0.15 A	1.52 A	0.052 A	29.8 A

Numbers in the same column with the same letter means no significant difference according to LSD 5% test

http://www.aloki.hu ● ISSN 1589 1623 (Print) ● ISSN 1785 0037 (Online)
DOI: http://dx.doi.org/10.15666/aeer/2003_26392650

Yield and yield attributes

Phosphorus and genotype factors significantly affected yield and yield attributes, but there was no significant interaction effect between the factors (*Table 3*). Application of 108 kg P_2O_5/ha increased soybean grain yield by 77% compared to 72 kg P_2O_5/ha. The higher grain yield was in accordance with increasing number of filled pods, grain weight per plant, and a 100 seeds weight by 27%, 54%, and 25%, respectively. Phosphorus fertilization at dosage of 108 kg P_2O_5/ha increased P and K content, and hence improved soybean growth as indicated by high shoot biomass and CCI resulting in better pod setting and seed development.

Both genotypes tested survive and complete their life cycle even under high salinity of soil and irrigation water stress. This indicates that the two genotypes tested (Anjasmoro and K-13) can tolerate soil salinity of 9-17 dS/m. Some other research studies also showed that these genotypes are tolerant to soil EC of 14.4 dS/m (Purwaningrahayu et al., 2015; Susanto et al., 2016; Taufiq et al., 2016; Putri et al., 2017, 2019).

Table 3. *Effect of P fertilization and genotype on yield and yield attributes of soybean in saline soil. Tuban, second dry season 2018*

Treatment	Number of filled pods/plant	Grain weight (g/plant)	Weight of a 100 seeds (g)	Grain yield (kg/ha)
P dosage				
• 72 kg/ha	23.1 b	4.38 b	8.74 b	430.52 b
• 108 kg/ha	29.5 a	6.77 a	11.00 a	763.46 a
Genotype				
• Anjasmoro	28.8 A	6.15 A	9.58 A	733.59 A
• K-13	23.7 B	5.00 A	9.15 A	460.39 b
CV (%)	27.34	30.78	13.54	20.72

Numbers in the same column with the same letter means no significant difference according to LSD 5% test

Soybean yield positively correlates with plant population (r = 0.75 and 0.81**, n = 28, respectively for Anjasmoro variety and K-13 line, at harvest, *Fig. 5A, B*). Plant stands during germination stage were relatively similar (73%) among the two P fertilization dosage (*Fig. 6A*). However, the final plant stand was 10% higher with P fertilization of 108 kg/ha P_2O_5 than 72 kg P_2O_5/ha (*Fig. 6B*). This indicates that higher dosage of P fertilization improves soybean survival under saline circumstance, and hence reduces the number of dead-plant.

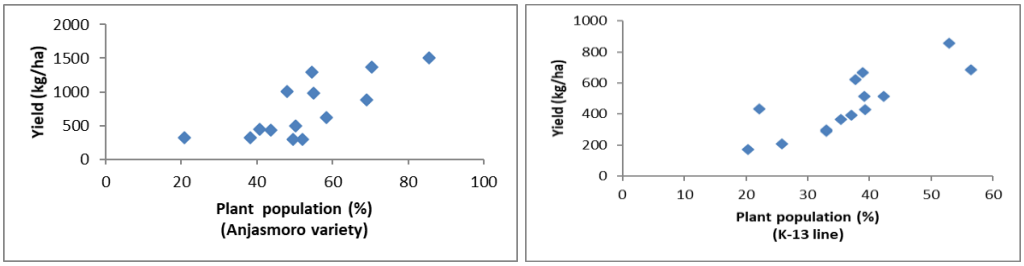

(A) (B)

Figure 5. *Correlation between number of harvested-plant and soybean grain yield Anjasmoro variety (A) r = 0.75 and K-13 line (B) r = 0.81 in saline soil. Tuban, second dry season 2018*

http://www.aloki.hu ● ISSN 1589 1623 (Print) ● ISSN 1785 0037 (Online)
DOI: http://dx.doi.org/10.15666/aeer/2003_26392650

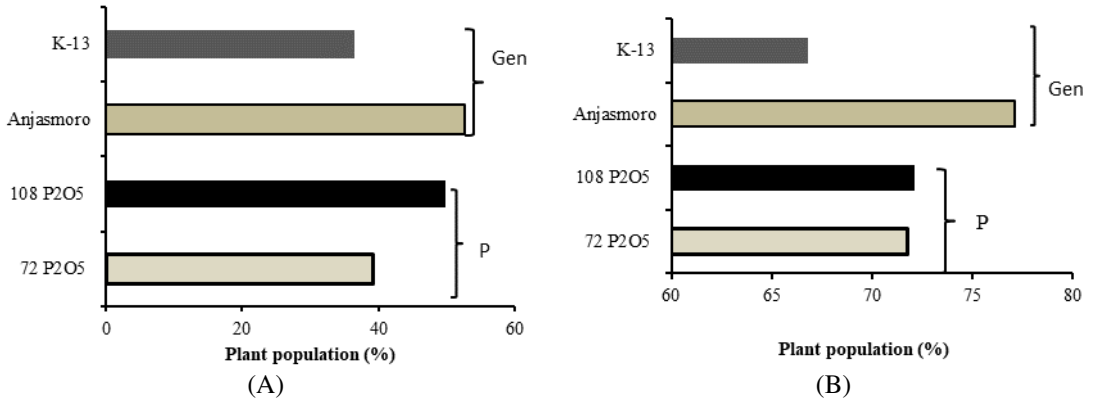

Figure 6. *Effect of P fertilization and soybean genotype on plant population percentage in germination stage (A) and at harvest (B) in saline soil. Tuban, second dry season 2018*

The two tested genotypes had different germination capability under high saline condition. Soil ECs during seedling stage was 9.0 dS/m, and germination percentage observed at 15 DAP of Anjasmoro variety was higher than that of K-13 line (*Fig. 6A*). Plant stands at harvest of Anjasmoro variety were also higher than that of K-13 (*Fig. 6B*). Grain weight per plant and 100 seeds of Anjasmoro variety did not differ from K-13, but Anjasmoro had filled pods 21.5% higher than K-13. So that Anjasmoro yielded 59.4% higher than K-13 (*Table 3*). Salt-tolerant genotypes has better germination capability and growth under saline condition than salt-sensitive genotypes (Putri et al., 2017a), and this phenomenon is related to the decreasing GA/ABA ratio (Shu et al., 2017). Based on plant population in early growth stage and at harvest, growth parameters, as well as grain yield, it seems that Anjasmoro variety is more tolerant to high soil salinity than K-13. However, soybean yield in this experiment is very low when compared with soybean productivity in optimal land. The yield potential of the Anjasmoro variety in optimal land is 2.03-2.25t/ha (Balitkabi, 2021). The average yield of soybean in saline soil/suboptimal land in this study can be categorized as moderate (430-760 kg/ha), from previous studies at ECs 8.19 dS/m Anjasmoro yield: 121.6 kg/ha, K-13 yield: 119.7 kg/ha; in saline soil at ECs 13.20 dS/m Anjasmoro yield: 77.4 kg/ha and K-13 yield 289.7 kg/ha; K-13 line yield: 800-1,090 kg/ha in saline soils at ECs 11-13 dS/m (Putri et al., 2017; Taufiq et al., 2017; Purwaningrahayu and Taufiq, 2018).

Conclusion

Plant growth during the vegetative and generative phases was severely hampered, with soil EC reaching 9.0-17.0 dS/m and EC of irrigation water reaching 6.0-16.4 dS/m. P fertilizer at a dose of 108 kg P_2O_5/ha in saline soil on tolerant soybean genotypes could improve tolerance by increasing P and K absorption and reducing Na uptake thereby reducing the number of dead plants. P fertilization at this dose also improved plant growth and seed development, thereby increasing the number of filled pods and yields. Based on seed germination, survival plant population and yield, the Anjasmoro variety was more saline tolerant than the K-13 line. The use of Anjasmoro variety and P fertilization as much as 108 kg/ha P_2O_5 could increase the growth and yield of soybeans in saline soil ECs up to 17 dS/m. It is recommended for future studies to repeat these treatments in other locations with different salinity levels in saline soil of Indonesia.

http://www.aloki.hu ● ISSN 1589 1623 (Print) ● ISSN 1785 0037 (Online)
DOI: http://dx.doi.org/10.15666/aeer/2003_26392650

Acknowledgements. The authors are thankful to the Director of the Indonesian Legumes and Tuber Crops Research Institute (ILETRI), the Indonesian Agency for Agricultural Research and Development (IAARD), and the Ministry of Agriculture of the Republic of Indonesia for providing the funding of this research.

REFERENCES

[1] Al-Karaki, G. N., Al-Karaki, C. Y. (1996): Phosphorus nutrition and water stress effects on proline accumulation in sorghum and bean. – Plant Physiology 148(6): 745-751.
[2] Aydinşakir, K., Büyüktaş, D., Dinç, N., Karaca, C. (2015): Impact of salinity stress on growing, seedling development and water consumption of peanut (Arachis hypogaea cv. NC-7). – Akdeniz Üniversitesi Ziraat Fakültesi Dergisi 28(2): 77-84.
[3] Balitkabi. (2021): Deskripsi Varietas Aneka Kacang dan Umbi. – https://balitkabi. litbang. pertanian.go.id/produk/deskripsi-varietas/.
[4] Belouchrani, A. S., Latati, M., Ounane, S. M., Drouiche, N., Lounici, H. (2020): Study of the interaction salinity: phosphorus fertilization on sorghum. – Journal of Plant Growth Regulation 39: 1205-1210.
[5] Bremner, J. M. (1960): Determination of nitrogen in soil by the Kjeldahl method. – The Journal of Agricultural Science 55(1): 11-33. DOI: 10.1017/S0021859600021572.
[6] Bustingorri, C., Lavado, R. S. (2011): Soybean growth under stable versus peak salinity. – Scientia Agricola (Piracicaba, Braz.) 68(1): 102-108.
[7] Capula-Rodríguez, R., Valdez-Aguilar, L. A., Cartmill, D. L., Cartmill, A. D., Alia-Tejacal, I. (2016): Supplementary calcium and potassium improve the response of tomato (Solanum lycopersicum, L.) to simultaneous alkalinity, salinity, and boron stress. Commun. – Soil Science and Plant Analysis 47(4): 505-511.
[8] Chhabra, R. (2002): Salt-affected soils and their management for sustainable rice production - key management issues: a review. – Agricultural Reviews 23: 110-126.
[9] Chhabra, B. S., Thakur, D. S. (2000): Base saturation of rice growing soils of eastern part of central India. – Journal of Soils and Crops: 10(2): 189-194.
[10] Cimrin, K. M., Türkmen, O., Turan, M., Tuncer, B. (2010): Phosphorus and humic acid application alleviate salinity stress of pepper seedling. – African Journal of Biotechnology 9: 5845-5851.
[11] Ding, Z., Kheir, A. M. S., Ali, M. G. M., Ali, O. A. M., Abdelaal, A. I. N., Xin'e, L., Zhou, N., Wang, B., Liu, B., He. Z. (2020): The integrated effect of salinity, organic amendments, phosphorus fertilizers, and deficit irrigation on soil properties, phosphorus fractionation and wheat productivity. – Scientific Reports 10: 2736.
[12] Faozi, K., Yudono, P., Indradewa, D., Ma'as, A. 2019. Effectiveness of phosphorus fertilizer on soybean plants in the coastal sands soil. – *IOP* Conference Series: Earth Environment Science 250: 1-7.
[13] Ghafoor, A., Qadir, M., Sadiq, M., Murtaza, M., Brar, M. S. (2004): Lead, copper, zinc and iron concentrations in soils and vegetables irrigated with city effluent on urban agricultural lands. – Journal of the Indian Society of Soil Science *52*(1): 114-117.
[14] Ghassemi-Golezani, K., Taifeh-Noori, M., Oustan, S., Moghaddam, M., Rahmani, S. S. (2011): Physiological performance of soybean cultivars under salinity stress. – Journal of Plant Physiology and Breeding 1(1): 1-7.
[15] Hamayun, M., Khan, S. A., Iqbal, A., Hussain, A., Lee, I. J. (2019): Screening of soybean cultivars for salinity tolerance under hydroponic conditions. – Fresenius Environmental Bulletin 28(11): 7955-7963.
[16] Hirpara, K. D., Ramoliya, P. J., Patel, A. D., Pandey, A. N. (2005): Effect of salinisation of soil on growth and macro- and micro-nutrient accumulation in seedlings of Butea monosperma (Fabaceae). – Anales de Biología 27: 3-14.

http://www.aloki.hu ● ISSN 1589 1623 (Print) ● ISSN 1785 0037 (Online)
DOI: http://dx.doi.org/10.15666/aeer/2003_26392650

[17] Jones, B. J. (2002): Agronomic Handbook: Management of Crops, Soils, and Their Fertility. – CRC press, Boca Raton, FL.
[18] Karolinoerita, V., Yusuf, W. A. (2020): Land salinization and the problems in Indonesia. – *Jurnal Sumberdaya Lahan* 14(2): 91-99 (in Indonesian).
[19] Kaya, C., Kirnak, H., Higgs, D. (2001): Enhancement of growth and normal growth parameters by foliar parameters by foliar application of potassium and phosphorus in tomato cultivars grown at high (NaCl) salinity. – Journal of Plant Nutrition 24: 357-367.
[20] Mahmood, I. A., Ali, A., Aslam, M., Shahzad, A., Sultan, T., Hussain, F. (2013): Phosphorus availability in different salt-affected soils as influenced by crop residue incorporation. – International Journal Agriculture Biology 15: 472–478.
[21] Marschner, H., Kirkby, E. A., Cakmak, I. (1996): Effect of mineral nutritional status on shoot-root partitioning of photoassimilates and cycling of mineral nutrients. – Journal of Experimental Botany 47: 1255-1263.
[22] Mclean, E. O. (1982): Soil pH and Lime Requirement. – In: Page, A. L., Miller, R. H., Keeney, D. R. (eds.) Methods of Soil Analysis Part 2: Chemical and Microbiological Properties. 2nd Ed. Soil Science Society of America, Inc. Madison, WI, pp. 199-223.
[23] Meena, M. D., Narjary, B., Sheoran, P., Jat, H. S., Joshi, A. T., Chinchmalatpurea, A. R., Yadav, G., Yadav, R. K., Meena, M. K. (2018): Changes of phosphorus fractions in saline soil amended with municipal solid waste compost and mineral fertilizers in a mustard-pearl millet cropping system. – CATENA 160 (January): 32-40.
[24] Mitsuya, S., Kawasaki, M., Taniguchi, M., Miyake, H. (2003): Relationship between salinity-induced damages and aging in rice leaf tissues. – Plant Production Science 6(3): 213-218.
[25] Olsen, S. R., Sommers, L. E. (1982): Phosphorus. – In: Page, A. L., Miller, R. H., Keeney, D. R. (eds.) Methods of Soil Analysis Part 2: Chemical and Microbiological Properties. 2nd Ed. Soil Science Society of America, Inc. Madison, WI, pp. 403-427.
[26] Peech, M. (1945): Determination of exchangeable cations and exchange capacity of soils - rapid micro methods utilizing centrifuge and spectrophotometer. – Soil Science 59(1): 25-38.
[27] Penn, C. J., Camberato, J. J. (2019): A critical review on soil chemical processes that control how soil ph affects phosphorus availability to plants. – Agriculture 9(120): 1-18.
[28] Purwaningrahayu, R. D., Taufiq, A. (2018a). Mulching and amelioration saline soil for growth and yield of soybean. – Jurnal Agronomi Indonesia 46(2): 182-188 (in Indonesian).
[29] Purwaningrahayu, R. D., Taufiq, A. (2018b): Efektivitas pemupukan N dan P pada Kedelai di Tanah Salin. – In: Rukmowati B., dan Widodo, P. (eds.) Prosiding Seminar Nasional "Pembangunan Pertanian Indonesia dalam Memperkuat Lumbung Pangan Fundamental Ekonomi dan Daya saing Global" UPN Veteran Yogyakarta 17 Nov 2018 (in Indonesian).
[30] Purwaningrahayu, R. D., Sebayang, H. T., Syekhfani, Aini, N. (2015): Resistance level of some soybean (*Glycine max* L. Merr) genotypes toward salinity stress. – Journal of Biological Researches 20: 7-14**.**
[31] Purwaningrahayu, R. D., Sebayang, H. T., Syekhfani, Aini, N. (2016): Physiological renspons and seed yield of various soybean genotype to salinity stress. – Buletin Palawija 14(1): 18-27 (in Indonesian).
[32] Putri, P. H., Susanto, G. W. A. (2019): Performance of soybean lines (*Glycine max*) of F2 generation crossing in saline land. – Prosiding Seminar Nasional Masyarakat Biodiversitas Indonesia 5(1): 101-106 (in Indonesian).
[33] Putri, P. H., Susanto, G. W. A., Taufiq (2017a): Soybean genotype tolerance to salinity stress. – Jurnal Penelitian Pertanian Tanaman Pangan 1(3): 233-242 (in Indonesian).
[34] Putri, P. H., Susanto, G. W. A., Artari, R. (2017b). Response of soybean genotypes to salinity in germination stage. – Nusantara Bioscience 9(2): 133-137.

http://www.aloki.hu ● ISSN 1589 1623 (Print) ● ISSN 1785 0037 (Online)
DOI: http://dx.doi.org/10.15666/aeer/2003_26392650

[35] Qadir, M., Steffens, D., Yan, F., Schubert, S. (2003): Sodium removal from a calcareous saline–sodic soil through leaching and plant uptake during phytoremediation. – Land Degradation & Development 14(3): 301-307.
[36] Shu, K., Qi, Y., Chen, F., Meng, Y., Luo, F., Shuai, Y., Zhou, Y., Ding, J., Du, J., Liu, D., Yang, F., Wang, Q., Liu, W., Yong, X., Wang, X., Feng, Y., Yang, W. (2017): Salt stress represses soybean seed germination by negatively regulating GA biosynthesis while positively mediating ABA biosynthesis. – Frontiers in Plant Science 8(1372): 1-12.
[37] Singh, A. L., Basu, M. S., Singh, B. H. (2004): Mineral Disorders of Groundnut. – National Research Centre for Groundnut (ICAR), Junagadh, India.
[38] Sukarman, Mulyani, A., Purwanto, S. (2018): Modification of climate change-oriented land suitability evaluation methods. – Jurnal Sumberdaya Lahan 12(1): 1-11 (in Indonesian).
[39] Sulaeman, Suparto, Eviati. (2005): Technical Guidelines for Soil, Plant, Water and Fertilizer Chemical Analysis. – Soil Research Institute. Agricultural Research and Development Agency, Ministry of Agriculture, Jakarta (in Indonesian).
[40] Susanto, G. W. A., Taufiq, A., Putri, P. H. (2016): Evaluation of Soybean Genotypes (*Glycine max* (L.) Merr.) of Germ Plasm Collection in Saline Environment. – In: Taryono, Supriyanta, dan Kristamtini (eds.) Pemanfaatan Sumber Daya Genetik Lokal dalam Mendukung Keberhasilan Program Pemuliaan. – Prosiding Seminar Nasional PERIPI Komda Jateng-DIY, Yogyakarta, 2 Juni 2016. Fakultas Pertanian Universitas Gadjah Mada, Yogyakarta (in Indonesian).
[41] Tabatabai, M. A. (1982): Sulfur. – In: Page, A. L., Miller, R. H., Keeney, D. R. (eds.) Methods of Soil Analysis Part 2: Chemical and Microbiological Properties. 2nd Ed. Soil Science Society of America, Inc. Publisher. Madison, WI, pp. 501-534.
[42] Tang, H., Niu, L., Wei, V., Chen, X., Chen, Y. (2019): Phosphorus limitation improved salt tolerance in maize through tissue mass density increase, osmolytes accumulation, and Na^+ uptake inhibition. – Frontier Plant Science 10: 856.
[43] Taufiq, A., Wijanarko, A., Kristiono, A. (2016): Effect of genotype and amelioration to soybean growth and yield in saline soil. – Buletin Palawija 14(1): 1-8 (in Indonesian).
[44] Walkley, A., Black, I. A. (1934): An examination of the Degtjareff method for determining soil organic matter, and a proposed modification of the chromic acid titration method. – Soil Science 37(1): 29-38.
[45] Zribi, O. T., Slama, I., Trabelsi, N., Hamdi, H., Smaoui, A., Abdelly, C. (2018): Combined effects of salinity and phosphorus availability on growth, gas exchange, and nutrient status of Catapodium rigidum. – Arid Land Research and Management 32(3): 277-290.

http://www.aloki.hu ● ISSN 1589 1623 (Print) ● ISSN 1785 0037 (Online)
DOI: http://dx.doi.org/10.15666/aeer/2003_26392650

PHYTOEXTRACTION OF HEAVY METALS FROM A DECOMMISSIONED TANNERY WASTE DISPOSAL AREA BY PIONEER HERBACEOUS PLANTS

LI, X.[1] – SHAO, X.-L.[2*] – XIE, F.[3]

[1]*Hubei Xiaohuan Environmental Technology Co., Ltd, Xiaogan 432100, China*
(phone: +86-712-211-0967)

[2]*Hubei Provincial Academy of Eco-Environmental Sciences, Wuhan 430072, China*
(phone: +86-27-8721-1953; fax: +86-27-8765-2858)

[3]*Hubei Hengkun Environmental Protection Engineering Technology Co., Ltd, Xiaogan 432100, China*
(phone: +86-712-211-1533)

**Corresponding author*
e-mail: 53849750@qq.com

(Received 27th Dec 2021; accepted 2nd May 2022)

Abstract. A field survey of pioneer herbaceous plants growing on a decommissioned tannery waste disposal area in Hubei Province, China, was conducted to identify the species extracting heavy metals especially accumulating Cr in their tissues. The results show that the soil in the area was extremely contaminated with soil Cr range of 1300–3100 mg/kg, which was 13–30 times higher than that of unpolluted soil. Besides, 18 herbaceous species belonging to 11 families were found in the polluted area, among which 8 species, were identified as the dominant adaptive species with Cr > 200 mg/kg in their shoots and occupying dominant biomass. *Cynodon dactylon* L. was found to have the highest Cr concentration 774 mg/kg and 2335 mg/kg respectively in its shoot and root. The Cr bioaccumulation coefficients and translocation factors of dominant herbaceous plants both were lower than 1, indicating that the plants were possibly tolerant-stratified to the high Cr environment. *Cynodon dactylon* L. was considered as the suitable candidate for bioremediation of Cr-contaminated soils in the area.
Keywords: *chromium, soil contamination, phytoremediation, Cynodon dactylon L., field survey*

Introduction

Pollution of the biosphere with heavy metal has accelerated dramatically and has been attracting considerable public attention during the last century (Boularbah et al., 2006; Minkina et al., 2017). Removal of heavy metals from soil has been a subject of major concern to scientists for many years (Garbisu and Alkorta, 2001; Tong et al., 2020). The rapid development in economics together with the unplanned disposal of effluent from metallurgy, tanneries, electroplating, textile and other industries have increased the threat of soil pollution in China (Sun et al., 2016; Jia et al., 2019; Xiao et al., 2019; Zhang et al., 2020). For many years, China has remained one of the top countries with great tannery industry in the world, from which numerous hazardous tannery effluent and solid waste containing chromium and its compounds are introduced into natural ecosystems, resulting in an acute problem of chromium pollution in China (Xiao et al., 2019). Increasingly widespread heavy metal pollution has caused vast areas of land to become non-arable and hazardous for both wildlife and human populations. There is, therefore, an urgent need for research on the remediation of chromium polluted soil in tannery areas (Zhou et al., 2019).

Unlike many organic pollutants, heavy metals are persistent environmental contaminants, which cannot be chemically or biologically destroyed, and tend to

http://www.aloki.hu ● ISSN 1589 1623 (Print) ● ISSN 1785 0037 (Online)
DOI: http://dx.doi.org/10.15666/aeer/2003_26512662

accumulate in organisms, thereby eventually entering the food chains (Siegel, 2002). The restoration methods for heavy metal contaminated soil can be categorized into physical remediation (i.e, washing, extraction, solidification and stabilization of heavy metals), chemical remediation (i.e., chemical leaching, chemical fixation, electrokinetic remediation, vitrifying technology), biological remediation (i.e., phytoremediation, bioremediation and animal remediation) and cocktails of the above remediation methods (Rajendran et al., 2022). However, considering the cost effectiveness of remediation, the physical or/and chemical strategies face some challenges such as cost, machine and logistics (Dhaliwal et al., 2020). Furthermore, such physicochemical methods render the land useless as a medium for plant growth, as they remove all biological activity including useful symbiotic microbes such as nitrogen-fixing bacteria and mycorrhizal fungi as well as fauna in the process of decontamination, thus decreasing their biodiversity (Lombi et al., 2001). Phytoremediation is a potential solution to the problem of heavy metal pollution using plants, and is considered as a cost-effective and environmentally-friendly green technique for heavy metal polluted soil, attracting interest and attention world widely (Mahar et al., 2016). This technology employs plants with ecophysiological adaptations to metalliferous soils to filter (rhizofiltration) or absorb (phytoextraction/phytoaccumulation) heavy metal(s) followed by their harvest. The major limitations to this powerful technology include small biomass of plants adapted to grow on nutrient-poor contaminated soils and disposal of the heavy metal-enriched biomass. The type of plants can also make a significant difference in pollutant removal (Khan, 2001).

The early phytoremediation studies focused on the hyperaccumulator species, which are plants able to accumulate unusually high levels of metals in their tissues (Shrivastava et al., 2020). The hyper accumulators plants such as trees and grasses are now being actively evaluated (Pasricha et al., 2021). In extremely contaminated areas such as disposal fields of tannery wastes, there generally exists only pioneer plant species which could be adaptive to the heavy metal contaminated soil and could be potential candidates for elementary phytoremediation of the contaminated soil, though the metal accumulation capability of pioneer plants might not be able to meet the standard of that of hyper accumulator plants (Navarro-Noya et al., 2010; Sun et al., 2016). It is therefore necessary for the phytoremediation of heavy metal contaminated soil to evaluate the metal accumulation capability of the adaptive pioneer plants.

In this study, soils and herbaceous plants in a decommissioned tannery waste disposal area polluted by tannery waste in Jingzhou, Hubei Province, China, were collected and analyzed. The contamination level of Cr, Cu, Zn and Pb of soil and pioneer plants were evaluated. Besides, the Cr accumulators and species with relatively high Cr tolerant capacity and large biomass were confirmed and identified. Furthermore, contamination levels of Cr, Cu, Zn and Pb of soil and pioneer plants were evaluated.

Materials and methods

Field survey and sampling

The survey was conducted in a decommissioned tannery waste disposal area located in Jingzhou, Hubei Province, China, which belongs to a subtropical continental zone with a warm, wet climate and annual average temperatures of 15.9–16.6 °C and average precipitations of 1100–1300 mm.

The tannery waste disposal area (*Fig. 1*) covers an area of 1.4×10^6 m^2, holding a center point GPS information about 30.008° North latitude and 111.607° East longitude.

http://www.aloki.hu ● ISSN 1589 1623 (Print) ● ISSN 1785 0037 (Online)
DOI: http://dx.doi.org/10.15666/aeer/2003_26512662

The tannery waste disposal area was constructed in 1970 s and decommissioned 1990 s. During the operation of the tannery waste disposal area, numerous hazardous tannery wastewater effluent and solid waste was introduced into natural ecosystems. Furthermore, because of the seasonal floodwater overflow in the area, chromium-contained hazardous waste was dispersed along the river coast wise, resulting widespread pollution. In the most seriously polluted areas, there exist hardly wood plants but some pioneer herbaceous plant species adapted to the chromium-contaminated soil. Therefore, a very reduced plant cover on the tannery waste-contaminated site was noted, suggesting a strong selection pressure.

In September 2019, a detailed investigation on the soils and pioneer herbaceous plant species was conducted. Four sampling sites were selected: wastewater treatment plant and nearby, wastewater outfall and riverside, deserted tannery and nearby, and the uncontaminated area as comparison. At each site, almost all species of herbaceous plants were sampled, and all the plant samples included roots and shoots (defined as the above-ground parts in this paper). The roots sampling were carried out according to the procedure of excavation method (Bertin et al., 2003). At least 15 single individual plants of each species were randomly collected within the sampling area and mixed in 3 independent samples. Plant samples were placed loosely in a labeled polythene bag, and were transported to the lab as quickly as possible. Soil samples (0–15 cm) were collected from each site, with benchmark soil samples taken from uncontaminated forest sites around the tanning area (*Fig. 2*).

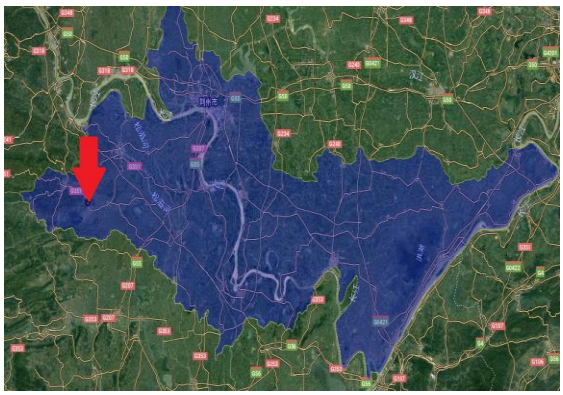

Figure 1. *Map showing the study area*

Figure 2. *Two grasses sampling. (a) Cynodon dactylon L., (b) Eleusine indica L. Gaertn*

http://www.aloki.hu ● ISSN 1589 1623 (Print) ● ISSN 1785 0037 (Online)
DOI: http://dx.doi.org/10.15666/aeer/2003_26512662

Heavy metal analysis

Soil samples were air-dried at room temperature and milled to pass through a 100-mesh nylon sieve. Whole plants were washed thoroughly with running tap water to remove adhering substrate materials, rinsed twice for 30 s with distilled water (Liu et al., 2006), air-dried for 5 h, then separated into shoot and root parts. The samples were first oven-dried at 105 °C for 30 min, then at 70 °C for 48 h to constant weight, milled in a metal-free mill, and passed through a 100-mesh nylon sieve.

The samples (soil: ~0.40 g, shoot: ~0.40 g, root: ~0.30 g) were digested in a microwave digestion reactor (HP1510, Shanghai HengPing Instrument & Meter Co., Ltd. China) equipped with a temperature control microwave power system of differential procedures, holding a mixture of 8 ml HNO_3 (G.R. 65%) + 2 ml H_2O_2 (G.R. 30%), 7 ml HNO_3 + 2 ml H_2O_2 and 7 ml HNO_3 + 1 ml H_2O_2, respectively. The digests were brought to 50 ml with deionized distilled water after cooling to room temperature. Then the aqueous solutions were filtered through filter paper, serially diluted and analyzed on a Hitachi Z-2000 flame atomic absorption spectrometer (Hitachi, Japan) for metals (Cr, Cu, Zn and Pb). Standard materials were included for assurance control.

The dry weight of the digested soil or plant sample was presented in the milligram per kilogram dry weight (mg/kg DW). The mean value of three samples of each plant species were taken as the heavy metal concentration of the corresponding species.

Soil pH and organic matter analysis

The slurry soil samples (5 g dry matter/25 ml water) were prepared for pH measurement using a pH meter (model pHS-2C, Beijing shanghai Instrument Co., Ltd., Beijing, China). Organic matter measurements were performed according to the literature (Liu et al., 2006).

Data analysis

Bioaccumulation coefficient (BC) and translocation factor (TF) were employed to describe the heavy metal accumulation capacity of plants, which were defined as the ratio of heavy metal concentration of plant shoot/root to that in soil, and the ratio of the metal concentration of the shoots to the metal concentration of the roots of dry biomass bases, respectively (Baker et al., 1994). Pearson's correlation analysis was undertaken to assess the relationship of concentrations of heavy metals between shoots and roots (Zhou et al., 2015). The data in this paper were analyzed by MATLAB 9.0 (MathWorks. Inc, USA).

Results

Metal concentration in soil

The heavy metal content, pH and organic matter of the soil samples in the investigated areas are listed in *Table 1*. It is described that pH of three sites of polluted zone were higher than that of the uncontaminated area, and the contaminated soil contained significantly more organic matter than that of the uncontaminated soil, due to the emission of tannery waste with high organic matter content.

The heavy metal content, pH and organic matter of the soil samples in the investigated areas are listed in *Table 1*. It was described that the pH of three sites of polluted zone was higher than that of the uncontaminated area. The contaminated soil

http://www.aloki.hu ● ISSN 1589 1623 (Print) ● ISSN 1785 0037 (Online)
DOI: http://dx.doi.org/10.15666/aeer/2003_26512662

contained significantly more organic matter than that of the uncontaminated soil, due to the emission of tannery waste with high organic matter content.

Table 1. *Heavy metal content, pH and organic matter of samples (mg/kg)*

Site	pH	Organic matter (%)	Cu	Pb	Zn	Cr
Sewage treatment plant and nearby	7.24	8.73	71.45	50.72	97.78	3109.98
Sewage outfall and riverside	6.64	5.68	60.76	43.81	118.97	1477.89
Deserted tannery and nearby	7.02	7.04	68.20	41.91	43.74	1361.39
Uncontamined area	5.74	2.83	48.16	34.70	23.05	104.69
Standard for soils*	—	—	150–200[a] 50–100[b]	100–140[a] 90–120[b]	200–250	250–300[a] 150–200[b]

*Soil environmental quality—risk control standard for soil contamination of agricultural (GB 15618-2018) of the People's Republic of China
[a]Standards for paddy field
[b]Standards for other agricultural field except paddy field

Cu, Pb and Cr contents in the investigated area were greater than soil environmental background values in China. Compared with the unpolluted soils, the tanning zone cannot be considered contaminated with Cu, Pb and Zn. However, extremely high concentrations of Cr (the maximum value was 3109.98 mg/kg DW in the wastewater treatment plant and nearby) were found in the soil of the tanning area, with 13–30 times higher than that of unpolluted soil, indicating that the tanning zone has been severely contaminated by Cr.

Cu, Pb and Cr contents in the investigated area were greater than soil environmental background values in China. Compared with the unpolluted soils, the tanning zone has not been contaminated with Cu, Pb and Zn. However, extremely high concentrations of Cr (the maximum value was 3109.98 mg/kg DW in the wastewater treatment plant and nearby) were found in the soil of the tanning area, with 13–30 times higher than that of unpolluted soil, indicating that the tanning zone has been severely contaminated by Cr.

Heavy metals in the plants

During the investigation, 18 herbaceous plant species belonging to 11 families were found in deserted tannery and nearby. All species and their total Cu, Pb, Zn, Cr concentrations for shoots and roots are showed in *Table 2*. It can be seen that different plants had different metal-enrichment capabilities, and metal concentrations in different parts of the plants were different. Generally, most of the above heavy metals in the aerial part and root of plants were of significant difference. Cu and Zn concentrations in all shoots and roots from four sites were within the scope of normal contents in plants. Pb concentrations of some plants were slightly higher than that of the normal content. However, Cr concentrations in shoots and roots of most plants were extremely greater than the normal contents. The Cr concentration maximum values (774.05 mg/kg DW and 2334.56 mg/kg DW in shoot and root, respectively) were found in *Cynodon dactylon* L., which holds an extremely wide distribution of all warm countries. Besides, no species investigated in this paper could be qualified as chromium hyper-accumulator, according to the criterion of Cr hyper-accumulator suggested by Baker and Brooks holding the Cr concentration > 1000 mg/kg dry leaf tissue (Baker and Brooks, 1989).

http://www.aloki.hu ● ISSN 1589 1623 (Print) ● ISSN 1785 0037 (Online)
DOI: http://dx.doi.org/10.15666/aeer/2003_26512662

As shown in *Table 2*, there were 11 herbaceous species whose Cr concentrations of shoots were higher than 200 mg/kg. However, the field investigation showed that there existed only very small number of individuals and low biomass for three herbaceous species, i.e., *Humulus scandens* (Lour.) Merr*, Rumex acetosa* L., and *Fimbristylis aestivalis* (Retz.) Vahl. Thus 8 herbaceous species (*Cynodon dactylon* L., *Chenopodium glaucum* L., *Rorippa montana* (Wall.) Small, *Malachium aquaticum* (L.) Fries., *Oenanthe javanica* (Blume) DC., *Agerarum houstonianum* Mill., *Eleusine indica* (L). *Gaertn*, *Saccharum officenarum* L.) were identified as the dominant adaptive species or hyper-tolerant plants in the area. The averages concentrations of heavy metals of all the pioneer species were 10 times higher than the plants from non-polluted environments.

Table 2. *Heavy metal concentrations in different plants of deserted tannery and nearby (mg/kg)*

Plant species	Cu		Pb		Zn		Cr	
	Aerial part	Root	Aerial part	Root	Aerial part	Root	Aerial part	Root
Cynodon dactylon L.	31.59	13.26	54.75	56.24	143.51	135.24	774.05	2334.56
Humulus scandens (*Lour.*) *Merr.*	28.05	33.99	23.60	15.24	65.37	51.04	216.90	1235.46
Solidago decurens Lour.	12.85	38.56	62.01	50.13	73.50	115.26	75.90	1265.35
Chenopodium glaucum Linn.	29.43	35.26	21.27	30.22	104.48	75.21	552.95	1925.34
Rorippa montana (*Wall.*) *Small*	24.47	15.24	9.70	7.56	65.20	75.20	294.07	1156.35
Arrhenatherum elatius (*Linn.*) *Pressl*	13.82	42.44	58.89	47.62	110.55	136.52	196.85	1392.62
Malachium aquaticum (*L.*) *Fries.*	21.39	20.75	67.96	26.70	113.43	79.51	219.50	983.40
Oenanthe javanica (*Blume*) *DC.*	19.78	16.25	61.77	41.86	67.98	60.26	242.40	1005.22
Boehmeria nivea (*Linn.*) *Gaudich*	21.82	15.42	59.57	36.59	57.52	63.21	78.04	1123.21
Eragrostis pilosa (*L.*) *Beauv.*	21.83	9.62	2.91	15.83	31.30	86.00	55.66	784.84
Rumex acetosa Linn.	30.44	39.58	3.97	18.59	93.11	55.94	218.27	799.08
Amaranthus retroflexus L.	16.52	2.01	53.30	29.44	74.67	36.44	181.70	932.67
Agerarum houstonianum Mill.	18.21	3.57	30.70	18.76	50.25	64.44	242.44	1035.08
Fimbristylis aestivalis Retz.	10.53	8.97	29.60	20.87	64.32	43.56	234.60	1008.23
Eleusine indica L. Gaertn	19.08	13.25	30.90	24.48	79.97	56.78	241.48	1178.34
Zizania aquatica L.	9.99	3.01	4.88	19.35	23.78	21.38	10.62	936.49
Saccharum officenarum L.	21.20	1.56	6.11	25.01	68.38	73.22	364.18	1251.06
Aster ageratoides Turcz.	7.95	3.15	24.96	23.20	192.49	30.71	110.26	1017.41
Plants grow in uncontaminated area	3.67-24.4	3.21-18.32	0.88-40.66	18.37-43.4	14.69-156.87	13.46-123.87	1.98-75.11	70.51-118.76

Bioaccumulation coefficient and translocation factor

Bioaccumulation coefficient (BC) is generally employed to depict the enrichment capacity of plants to heavy metal (Hu et al., 2020). The greater the coefficient, the higher the capacity. The chromium BCs of 8 dominant pioneer plants are shown in *Figure 3*. All the BCs values of plants for Cu were no more than 1. The BCs for Pb and Zn of some plants were higher than 1. There existed only one species, *Chenopodium glaucum* L., whose BCs for Cr in roots were higher than 1. All the BCs for Cr in shoots were much lower than 1. The Cr bioaccumulation capacities of roots were much higher than those of homologous shoots. *Chenopodium glaucum* L. held the greatest BC for Cu and Cr. *Oenanthe javanica* (Blume) DC. showed the greatest BC for Pb. As shown in *Figure 4*, the TFs of most plants were higher than 1, indicating that these plants favored translocation of Cu, Pb and Zn to the shoots of their own. However, the TFs for Cr of all the 8 species were lower than 0.4, implying that the plants did not prefer their translocation of Cr an extreme Cr pollution pressure.

http://www.aloki.hu ● ISSN 1589 1623 (Print) ● ISSN 1785 0037 (Online)
DOI: http://dx.doi.org/10.15666/aeer/2003_26512662

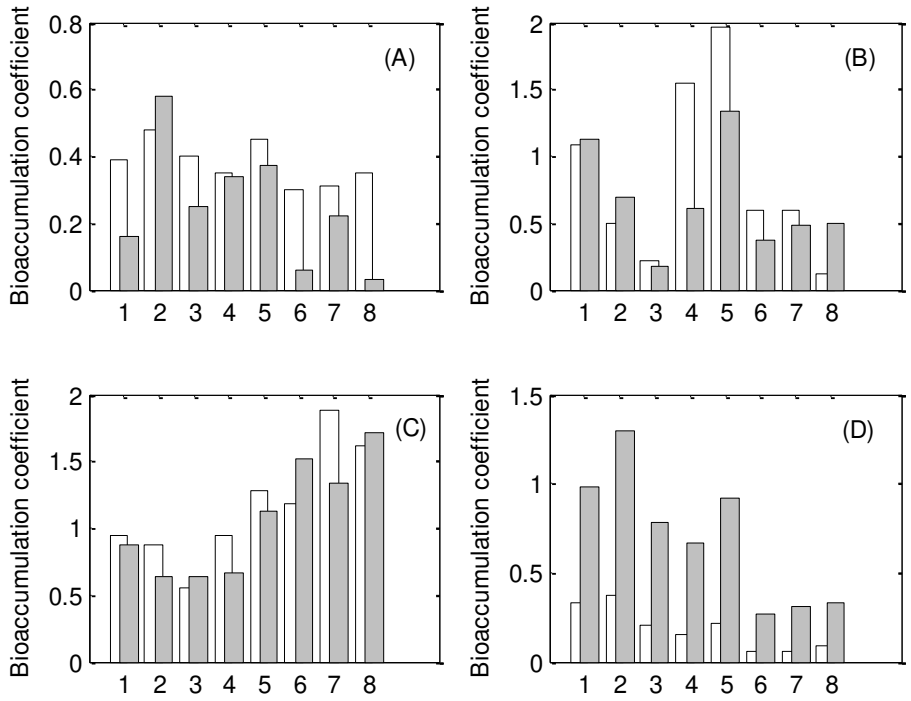

Figure 3. *BCs of heavy metals. Opened bar: shoots; filled bar: roots. (A) Cu, (B) Pb, (C) Zn, (D) Cr. 1. Cynodon dactylon L.; 2. Chenopodium glaucum Linn.; 3. Rorippa montana (Wall.) Small; 4. Malachium aquaticum (L.) Fries.; 5. Oenanthe javanica (Blume) DC.; 6. Agerarum houstonianum Mill.; 7. Eleusine indica L. Gaertn; 8. Saccharum officenarum L.*

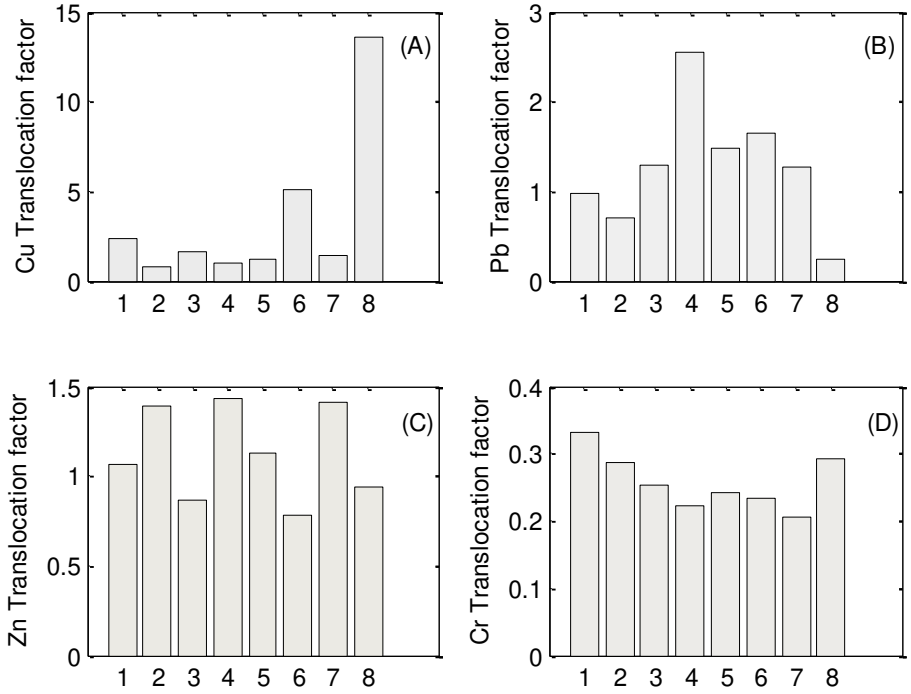

Figure 4*. TFs of heavy metals. (A) Cu; (B) Pb; (C) Zn; (D) Cr. 1. Cynodon dactylon L.; 2. Chenopodium glaucum Linn.; 3. Rorippa montana (Wall.) Small; 4. Malachium aquaticum (L.) Fries.; 5. Oenanthe javanica (Blume) DC.; 6. Agerarum houstonianum Mill.; 7. Eleusine indica L. Gaertn; 8. Saccharum officenarum L.*

http://www.aloki.hu ● ISSN 1589 1623 (Print) ● ISSN 1785 0037 (Online)
DOI: http://dx.doi.org/10.15666/aeer/2003_26512662

Correlation of heavy metal bioaccumulation

The correlation coefficient matrix of heavy metal concentrations of plant shoots and roots is shown in *Table 3*. The Cr concentrations of shoots were significantly correlated with that in roots ($r = 0.99$) in these highly polluted sites, and the scatter plot together with ordinary least square regression further depicted the significant correlation relationship (*Fig. 5A*). The Cr BC held almost the same way (*Fig. 5B*) as Cr concentration, indicating that the Cr bioaccumulation in shoots was greatly depended on that in roots. It is worth noting from *Table 3* that the Cr accumulation was positively correlated with Cu and Zn both in shoots and in roots, implying probably the synergistic absorption of these heavy metals.

Table 3. *Correlation coefficient matrix of heavy metal concentrations between shoots and roots of 8 dominant pioneer species (Cynodon dactylon L., Chenopodium glaucum Linn., Rorippa montana (Wall.) Small, Malachium aquaticum (L.) Fries., Oenanthe javanica (Blume) DC., Agerarum houstonianum Mill., Eleusine indica L. Gaertn, Saccharum officenarum L.)*

	Cu		**Pb**		**Zn**		**Cr**	
	Shoot	**Root**	**Shoot**	**Root**	**Shoot**	**Root**	**Shoot**	**Root**
Cu-shoot	1.00							
Root	0.52	1.00						
Pb-shoot	-0.00	0.20	1.00					
Root	0.48	0.14	0.62	1.00				
Zn-shoot	0.76*	0.46	0.49	0.69	1.00			
Root	0.80*	0.04	0.27	0.64	0.81*	1.00		
Cr-shoot	0.92**	0.26	0.01	0.66	0.74*	0.86**	1.00*	
Root	0.92**	0.35	0.00	0.63	0.75*	0.81*	0.99*	1.00*

*$p < 0.05$; **$p < 0.01$

Discussion

The plant response to heavy metals in soil depends on the plant species, total soil metal concentration, bioavailability of the metal itself of soils, etc. Accumulation and exclusion were suggested as the two basic strategies by which plants respond to elevated concentration of heavy metals (Vogel-Mikuš et al., 2005), and the corresponding categories of plants were considered as accumulators and excluders (Sun et al., 2016) respectively. In metal accumulator species, TF greater than 1 was common, indicating a very efficient capability to transport metal from roots to shoots, most likely due to efficient metal transporter systems (Zhang et al., 2007). The TFs of heavy metal excluder species were typically lower than 1 (Baker and Brooks, 1989), showing an exclusive strategy of heavy metal accumulation.

Chromium is an essential trace element in metabolism of human beings and animals. However, excess Cr is highly toxic to animals and plants and may induce cancer and separatism. Hyperaccumulator plants can accumulate extremely high levels of metals in their tissues compared to accumulators (Baker and Brooks, 1989). Three chromium hyperaccumulators, i.e., *Dicoma niccolifera* Wild (Wang et al., 2012), *Brassica campestris* L. ssp. *Pekinensis* (Zhao et al., 2019) and *Leersia hexandra* Swartz (Zhang et al., 2007) in China, were reported. With the maximum Cr concentration 2978 mg/kg

http://www.aloki.hu ● ISSN 1589 1623 (Print) ● ISSN 1785 0037 (Online)
DOI: http://dx.doi.org/10.15666/aeer/2003_26512662

in the dry leaf matter, *Leersia hexandra* Swartz, a hydrophilous plant, mostly grows in the swamp, paddy field and riverside and is widely distributed over China. However, none individual of *Leersia hexandra* Swartz was found in the investigated area, and neither reported on other tanning areas in China, perhaps due to inadaptable to the soil polluted by tannery waste or the earth environment.

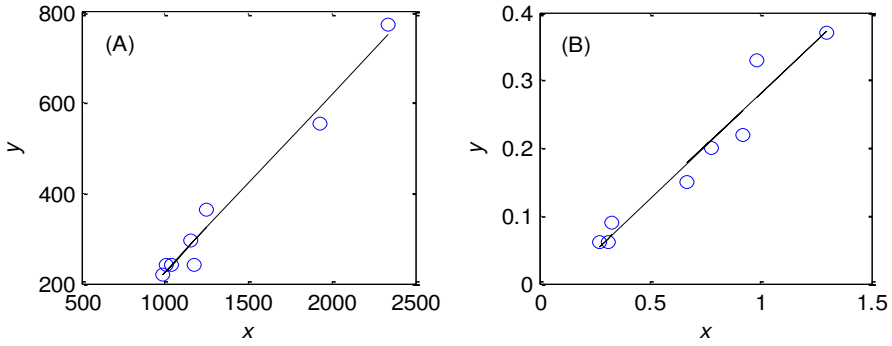

Figure 5. *Scatter plot of Cr concentration/bioaccumulation coefficient in shoots and roots of 8 dominant pioneer species (Cynodon dactylon L., Chenopodium glaucum Linn., Rorippa montana (Wall.) Small, Malachium aquaticum (L.) Fries., Oenanthe javanica (Blume) DC., Agerarum houstonianum Mill., Eleusine indica L. Gaertn, Saccharum officenarum L.), together with ordinary least square regression. (A) Cr concentration, the solid line stands y = 0.39x-167.98, r = 0.99. (B) Bioaccumulation coefficient, the solid line stands y = 0.30x-0.03, r = 0.97*

A comparison of our results with the criterion used to classify the hyperaccumulator plants indicates that plants collected from tanning area under study were not Cr hyperaccumulators but hyper-tolerant (Boularbah et al., 2006). This was confirmed by bioaccumulation coefficients and translocation factors generally lower than 1 (*Figs. 2* and *3*).

However, it is found in the present study that the Cr concentration of *Cynodon dactylon* L. reached 774 mg/kg DW in shoots, indicating that it had a stronger Cr-extraction ability than other plant species in the area. *Cynodon dactylon* L. was a representative plant blooming on the tanning zone. In fact, this grass has an extremely wide distribution, being found in all warm countries and even persisting in colder climates. It is the most widely used lawn grass and an important pasture grass in warm parts of the world. It can grow in very diverse conditions of soil and moisture, withstanding drought well and also tending to eliminate other plants and forming dense cover. Moreover, it is reported that *Cynodon dactylon* L. may be a potentially source of bio-based energy due to its vast acreage (Cantrell et al., 2009). It can be cut for hay when in full bloom. Normally 4 cuttings per year are possible. These characteristics thus make it possible for *Cynodon dactylon* L. to be considered as the potential suitable candidate for bioremediation of Cr-contaminated soils in the area. However, the exploration on the biochemical mechanisms of chromium hyper-tolerance and detoxification of such species should be taken into further research.

Conclusions

The phytoextraction of heavy metals by pioneer herbaceous plants from a decommissioned tannery waste disposal area in south central China was researched. The Cr concentrations were ranged 1300–3100 mg/kg in the surveyed soils, 13–30 times

http://www.aloki.hu ● ISSN 1589 1623 (Print) ● ISSN 1785 0037 (Online)
DOI: http://dx.doi.org/10.15666/aeer/2003_26512662

higher than the unpolluted control soil, indicating the area was severely contaminated by Cr from tannery waste. In this area, 18 species of plants were identified as the dominant plants with the ability to tolerate high concentrations of Cr, implying that they can be considered as the adaptive pioneer species for ecological restoration of Cr contaminated soils, although none of them were found to be the hyperaccumulators of Cr. With the advantages of high Cr tolerance, universality, value, etc., *Cynodon dactylon* L. is more suitable for Cr contaminated soil remediation than other herbaceous plants. Additionally, the microbial dynamics of heavy metal contaminated soils along with herbaceous plants should be considered for further studies.

REFERENCES

[1] Baker, A. J. M., Brooks, R. R. (1989): Terrestrial higher plants which hyperaccumulate metallic elements. A review of their distribution, ecology and phytochemistry. – Biorecovery 1: 81-126.

[2] Baker, A. J. M., Reeves, R. D., Hajar, A. S. M. (1994): Heavy metal accumulation and tolerance in British populations of the metallophyte *Thlaspi caerulescens* J. & C. Presl (Brassicaceae). – New Phytologist 127: 61-68.

[3] Bertin, C., Yang, X., Weston, L. A. (2003): The role of root exudates and allelochemicals in the rhizosphere. – Plant and Soil 256: 67-83.

[4] Boularbah, A., Schwartz, C., Bitton, G., Aboudrar, W., Ouhammoud, A., Morel, J. L. (2006): Heavy metal contamination from mining sites in South Morocco: 2. Assessment of metal accumulation and toxicity in plants. – Chemosphere 63: 811-817.

[5] Cantrell, K. B., Stone, K. C., Hunt, P. G., Ro, K. S., Vanotti, M. B., Burns, J. C. (2009): Bioenergy from Coastal bermudagrass receiving subsurface drip irrigation with advance-treated swine wastewater. – Bioresource Technology 100: 3285-3292.

[6] Dhaliwal, S. S., Singh, J., Taneja, P. K., Mandal, A. (2020): Remediation techniques for removal of heavy metals from the soil contaminated through different sources: a review. – Environmental Science and Pollution Research 27: 1319-1333.

[7] Garbisu, C., Alkorta, I. (2001): Phytoextraction: a cost-effective plant-based technology for the removal of metals from the environment. – Bioresource Technology 77: 229-336.

[8] Hu, B., Xue, J., Zhou, Y., Shao, S., Fu, Z., Li, Y., Chen, S., Qi, L., Shi, Z. (2020): Modelling bioaccumulation of heavy metals in soil-crop ecosystems and identifying its controlling factors using machine learning. – Environmental Pollution 262: 114308.

[9] Jia, X., Hu, B., Marchant, B. P., Zhou, L., Shi, Z., Zhu, Y. (2019): A methodological framework for identifying potential sources of soil heavy metal pollution based on machine learning: a case study in the Yangtze Delta, China. – Environmental Pollution 250: 601-609.

[10] Khan, A. G. (2001): Relationships between chromium biomagnification ratio, accumulation factor, and mycorrhizae in plants growing on tannery effluent-polluted soil. – Environment International 26: 417-423.

[11] Liu, Y., Zhang, H., Zeng, G., Huang, B., Li, X. (2006): Heavy metal accumulation in plants on Mn mine tailings. – Pedosphere 16: 131-136.

[12] Lombi, E., Zhao, F. J., Dunham, S. J., McGrath, S. P. (2001): Phytoremediation of heavy metal-contaminated soils: natural hyperaccumulation versus chemically enhanced phytoextraction. – Journal of Environmental Quality 30: 1919-26.

[13] Mahar, A., Wang, P., Ali, A., Awasthi, M. K., Lahori, A. H., Wang, Q., Li, R., Zhang, Z. (2016): Challenges and opportunities in the phytoremediation of heavy metals contaminated soils: a review. – Ecotoxicology and Environmental Safety 126: 111-121.

http://www.aloki.hu ● ISSN 1589 1623 (Print) ● ISSN 1785 0037 (Online)
DOI: http://dx.doi.org/10.15666/aeer/2003_26512662

[14] Minkina, T. M., Fedorov, Yu A., Nevidomskaya, D. G., Pol'shina, T. N., Mandzhieva, S. S., Chaplygin, V. A. (2017): Heavy metals in soils and plants of the don river estuary and the Taganrog Bay coast. – Eurasian Soil Science 50: 1033-1047.
[15] Navarro-Noya, Y. E., Jan-Roblero, J., González-Chávez, M. C., Hernández-Gama, R., Hernández-Rodríguez, C. (2010): Bacterial communities associated with the rhizosphere of pioneer plants (Bahia xylopoda and Viguiera linearis) growing on heavy metals-contaminated soils. – Antonie van Leeuwenhoek 97: 335-349.
[16] Pasricha, S., Mathur, V., Garg, A., Lenka, S., Verma, K., Agarwal, S. (2021): Molecular mechanisms underlying heavy metal uptake, translocation and tolerance in hyperaccumulators-an analysis: heavy metal tolerance in hyperaccumulators. – Environmental Challenges 4: 100197.
[17] Rajendran, S., Priy, T. A. K., Khoo, K. S., Hoang, T. K. A., Ng, H. S., Munawaroh, H. S. H., Karaman, C., Orooji, Y., Show, P. L. (2022): A critical review on various remediation approaches for heavy metal contaminants removal from contaminated soils. – Chemosphere 287: 132369.
[18] Shrivastava, M., Khandelwal, A., Srivastava, S. (2020): Heavy Metal Hyperaccumulator Plants: The Resource to Understand the Extreme Adaptations of Plants Towards Heavy Metals. – In: Srivastava, S., Srivastava, A. K., Suprasanna, P. (eds.) Plant-Metal Interactions. Springer, Cham.
[19] Siegel, F. R. (2002): Heavy Metals Mobility/Immobility in Environmental Media. – In: Siegel, F. R. (ed.) Environmental Geochemistry of Potentially Toxic Metals. Springer, Berlin.
[20] Sun, Z., Chen, J., Wang, X., Lv, C. (2016): Heavy metal accumulation in native plants at a metallurgy waste site in rural areas of Northern China. – Ecological engineering 86: 60-68.
[21] Tong, S., Li, H., Wang, L., Tudi, M., Yang, L. (2020): Concentration, spatial distribution, contamination degree and human health risk assessment of heavy metals in urban soils across China between 2003 and 2019—a systematic review. – International Journal of Environmental Research and Public Health 17: 3099.
[22] Vogel-Mikuš, K., Drobne, D., Regvar, M. (2005): Zn, Cd and Pb accumulation and arbuscular mycorrhizal colonisation of pennycress *Thlaspi praecox* Wulf. (Brassicaceae) from the vicinity of a lead mine and smelter in Slovenia. – Environmental Pollution 133: 233-242.
[23] Wang, A., Huang, S., Zhong, G., Xu, G., Liu, Z., Shen, X. (2012): Effect of Cr(VI) stress on growth of three herbaceous plants and their Cr uptake. – Environmental Science 33: 2028-2037 (in Chinese).
[24] Xiao, L., Guan, D., Chen, Y., Dai, J., Ding, W., Peart, M. R., Zhang, C. (2019): Distribution and availability of heavy metals in soils near electroplating factories. – Environmental Science and Pollution Research 26: 22596-22610.
[25] Zhang, X. H., Liu, J., Huang, H. T., Chen, J., Zhu, Y. N., Wang, D. Q. (2007): Chromium accumulation by the hyperaccumulator plant *Leersia hexandra* Swartz. – Chemosphere 67: 1138-1143.
[26] Zhang, C., Cai, X., Xia, Z., Jin, X., Wu, H. (2020): Contamination characteristics of heavy metals in a small-scale tanning area of southern China and their source analysis. – Environmental Geochemistry and Health 04. https://doi.org/10.1007/s10653-020-00732-x.
[27] Zhao, Y., Hu, C., Wang, X., Qing, X., Wang, P., Zhang, Y., Zhang, X., Zhao, X. (2019): Selenium alleviated chromium stress in Chinese cabbage (*Brassica campestris* L. ssp. *Pekinensis*) by regulating root morphology and metal element uptake. – Ecotoxicology and Environmental Safety 173: 314-321.
[28] Zhou, H., Zeng, M., Zhou, X., Liao, B., Peng, P., Hu, M., Zhu, W., Wu, Y., Zou, Z. (2015): Heavy metal translocation and accumulation in iron plaques and plant tissues for 32 hybrid rice (*Oryza sativa* L.) cultivars. – Plant and Soil 386: 317-329.

http://www.aloki.hu ● ISSN 1589 1623 (Print) ● ISSN 1785 0037 (Online)
DOI: http://dx.doi.org/10.15666/aeer/2003_26512662

[29] Zhou, W., Zhang, L., Peng, J., Ge, Y., Tian, Z., Sun, J., Cheng, H., Zhou, H. (2019): Cleaner utilization of electroplating sludge by bioleaching with a moderately thermophilic consortium: a pilot study. – Chemosphere 232: 345-355.

http://www.aloki.hu ● ISSN 1589 1623 (Print) ● ISSN 1785 0037 (Online)
DOI: http://dx.doi.org/10.15666/aeer/2003_26512662

THE WESTERN CHIMPANZEE (*PAN TROGLODYTES VERUS*) IN THE ANTENNA ZONE (NIOKOLO KOBA NATIONAL PARK, SENEGAL): NESTING ECOLOGY AND SYMPATRICS WITH OTHER MAMMALS

SYLLA, S. F.[1] – NDIAYE, P. I.[1*] – LINDSHIELD, S. M.[2] – BOGART, S. L.[3] – PRUETZ, J. D.[4]

[1]*Département de Biologie Animale, Faculté des Sciences et Techniques, Université Cheikh Anta Diop, BP 25178, Dakar, Senegal*
(ORCID: 0000-0001-8461-2319 – S. F. Sylla; 0000-0002-9978-564X – P. I. Ndiaye)

[2]*Department of Anthropology, Purdue University, West Lafayette, IN, USA*
(ORCID: 0000-0002-4507-1502 – S. M. Lindshield)

[3]*Department of Anthropology, University of Florida, Gainesville, FL, USA*
(ORCID: 0000-0001-9971-8968 – S. L. Bogart)

[4]*Department of Anthropology, Texas State University, San Marcos, TX, USA*
(ORCID: 0000-0002-9151-8571 – J. D. Pruetz)

**Corresponding author*
e-mail: ibnou.ndiaye@ucad.edu.sn; phone: +221-77-814-2834

(Received 27th Dec 2021; accepted 21st Mar 2022)

Abstract. The western chimpanzee (*Pan troglodytes verus*) is "Critically Endangered" due to a gradual decrease of its population and a continuous degradation of their habitats. Niokolo Koba National Park is considered an important biodiversity area in West Africa and has high conservation value for western chimpanzees. However, Niokolo Koba National Park has been inscribed on the World Heritage list as being in Danger since 2007 due to anthropogenic factors. Over the last 40 years, only sporadic and short-term studies on the ecology and behavior of chimpanzees in the park have occurred. For this reason, we studied the nesting ecology of a putative chimpanzee community in the Antenna zone. We also identified sympatric medium and large mammals using a camera trap. Chimpanzees mostly used *Hexalobus monopetalus* for nesting, followed by *Pterocarpus erinaceus*. Nest heights in the Antenna zone were lower than they are in Assirik, and outside the park at Fongoli and Diaguiri sites despite the presence of potential predators in the park. Predator presence influences nesting height behavior. These data deepen our knowledge about chimpanzees in Senegal, and are useful for the management plan of the park and will contribute to an action plan for their conservation there.
Keywords: *great apes, protected area, nest behavior, large wild mammals, Senegal*

Introduction

Nest building behaviors of wild chimpanzees have been reported by primatologists at various sites (e.g., Fruth and Hohmann, 1996; Hernandez-Aguilar et al., 2013; McGrew, 2021). The nests consist of vegetative structures that can remain visible for weeks or months according to the nest decay rate which depends on the site type, season, tree species bearing nest and sun exposure (i.e., degree of openness) in general (Kühl et al., 2008; Kouakou et al., 2009; Ndiaye et al., 2018a). Thus, due to the difficulty of making direct contacts with unhabituated great apes, many research projects and protected area monitoring programs have been carried out using nest counts to collect data for

http://www.aloki.hu ● ISSN 1589 1623 (Print) ● ISSN 1785 0037 (Online)
DOI: http://dx.doi.org/10.15666/aeer/2003_26632681

ecological and behavioral purposes (Furuichi and Hashimoto, 2004; Ogawa et al., 2007; Kühl et al., 2008; van Casteran et al., 2012; Dutton et al., 2017).

Chimpanzees learn to build day nests during their first three years of life (Fruth and Hohmann, 1996). Weaned individuals build nests in which they sleep at night or sometimes rest during the day (Goodall, 1968). Many studies are focused on nests for a better understanding of the ecology and behavior of chimpanzees (Basabose and Yamagiwa, 2002; Pruetz et al., 2002; Ogawa et al., 2007; Koops et al., 2012; Dutton et al., 2017). These authors agree that nest site selection is related to environmental factors, such as predator avoidance, human hunting pressure, climatic conditions, habitat types, tree species and the availability of ripe fruits among others. For example, chimpanzees rarely build night nests in trees offering ripe fruits, but instead stay close enough to reoccupy the tree early in the morning (Fruth and Hohmann, 1994; Basabose and Yamagiwa, 2002; Hernandez-Aguilar, 2009; Hernandez-Aguilar et al., 2013). Selection of nesting sites and tree species bearing nests by chimpanzees has been described by several authors. For example, Stanford and O'Malley (2008) found that chimpanzees used only 38 of at least 163 available tree species for nesting in Bwindi (Uganda) and, of these, they only used four tree species heavily. In Toro-Semliki in Uganda, chimpanzees prefered *Cynometra alexandri* for the majority of their sleeping nests (Samson and Hunt, 2014). Some studies have focused on the nest building ecology and behavior of chimpanzees in Senegal but most stem from outside of protected areas (Pruetz et al., 2002, 2008; Ndiaye et al., 2013a, 2018a, b; Stewart and Pruetz, 2013; Badji et al., 2018). There exists only relatively old data of nesting behavior of chimpanzees in Niokolo Koba National Park (NKNP), focusing on Mt Assirik in the late 1970s and 2000 (Baldwin et al., 1981; Pruetz et al., 2008). Baldwin et al. (1981), described that environmental factors, namely season, habitat type, tree height, tree species and predation also risk influence nesting behavior, comparing Equatorial Guinea and Senegal. Baldwin et al. (1981) examined many other variables, such as nest height, nest-group size, nests per tree, minimum distance between nests, whether or not the nest was open and girth of the tree bearing the nests. Primatologists have recognized recently the importance of documenting the potential effects of climate change on primates (Sesink et al., 2015; Korstjens and Hillyer, 2016; Sales et al., 2020). Range of mean annual rainfall in Assirik in 1976-79 was between 824 and 1224 mm and the mean annual rainfall was 954 mm (McGrew et al., 1981). Now, in the face of global habitat loss of mammals due to land-use and climate change (Baisero et al., 2020), we think that data on the ecology of chimpanzee in the hot and dry environment of Assirik (NKNP) is needed.

Danger from terrestrial predators is often hypothesized to influence chimpanzee nesting behavior (Baldwin, 1979; Tutin et al., 1981; Pruetz et al., 2008; Stewart and Pruetz, 2013). Stewart and Pruetz (2013) investigated nesting behavior at Issa (Tanzania) where chimpanzees lived in a predator-rich habitat and compared it to a habitat relatively devoid of predators at Fongoli (Senegal) outside of NKNP. These authors found that in Issa, chimpanzees nested more frequently within the same tree as other community members and they built their nests proportionately higher and more peripherally within trees than in Fongoli (Stewart and Pruetz, 2013). A somewhat similar pattern was found by Pruetz et al. (2008) in their comparison of nesting behavior at Fongoli and Assirik. These authors found that Assirik chimpanzees constructed nests higher in the tree canopy and individuals nested in closer proximity to each other, as expected in the environment with higher predator species richness.

http://www.aloki.hu ● ISSN 1589 1623 (Print) ● ISSN 1785 0037 (Online)
DOI: http://dx.doi.org/10.15666/aeer/2003_26632681

In a larger survey of chimpanzees in Senegal, Ndiaye et al. (2013a, b) found that chimpanzees made their nests mostly in gallery forests during the dry season and showed a preference for particular trees, with *Pterocarpus erinaceus* being the most preferred tree species.

However, in Bagnomba, a site close to the NKNP, the most preferred tree species is *Diospyros mespiliformis* (Badji et al., 2018), which shows that nesting tree preference varies among sites in Senegal. Multiple studies outside of the NKNP in Senegal have described the influence of habitat, season, and tree species on the western chimpanzee nesting behavior (Stewart and Pruetz, 2013; Badji et al., 2018; Ndiaye et al., 2018a, b).

Since the early 1980s, there has been relatively little research in the NKNP, the only national park in Senegal with this "Critically Endangered" species. According to Hunt and McGrew (2002), the study of chimpanzees at the edges of the species' range may also have conservation implications. Documenting behaviors associated with dry-habitats should extend our knowledge of the capacities of chimpanzees to adapt to their environment. Therefore, we stress the importance of investigating chimpanzees in the NKNP, and their ecology and behavior in accordance with the consideration that the NKNP is an area of high conservation value for the western chimpanzee (Heinicke et al., 2019).

The western chimpanzee is one of the more threatened species in the world (Schwitzer et al., 2019), and Niokolo Koba National Park is at the northwestern limit of its geographic distribution. The NKNP is one of the largest natural parks in West Africa, with an area of 913 000 ha. It was added to the list of UNESCO World Heritage Sites in 1981 and classified as "In Danger" in 2007 (UNESCO, 2019). The park contains a significant diversity of mammals, including the western chimpanzee, West African red colobus (*Procolobus badius temminckii*), Lion (*Panthera leo*), African wild dog (*Lycaon pictus*), Leopard (*Panthera pardus*), Spotted hyena (*Crocuta crocuta*), African elephant (*Loxodonta africana*), Hippopotamus (*Hippopotamus amphibious*), Western giant eland (*Taurotragus derbianus*), Roan antelope (*Hippotragus equinus*), and African buffalo (*Syncerus caffer*) (Papaco – International Union for Conservation of Nature, 2009; UNESCO, 2011). However, the park is under heavy pressure related to an international highway running through it and the rapid growth of extractive mining in Kedougou, which is southeast of NKNP (Ndiaye et al., 2018b; Lindshield et al., 2019). Chimpanzees are one of the flagship species of the park. Due to the decline of the western chimpanzee populations (Kühl et al., 2017), the species is listed in Annex I and II of the Convention on the Conservation of the Migratory Species of Wild Animals (CMS) in 2017 (UNEP/CMS/COP 12, 2017), Appendix 1 of the Convention on International Trade in Endangered Species of Wild Fauna and Flora (CITES, 2018) and was reclassified as "Critically Endangered" in the red list of the International Union for Conservation of Nature in 2016 (IUCN, 2018).

Studies that have been done to date of the western chimpanzee in NKNP have focused on the Mont Assirik site (Baldwin, 1979; Baldwin et al., 1981; McGrew et al., 1981, 2014; Tutin et al., 1981, 1983; Pruetz et al., 2008, 2012; Ndiaye et al., 2018b; Lindshield et al., 2019). Chimpanzee nests have also been reported in the southeastern part of NKNP, in the Antenna zone, near the international highway (Pruetz et al., 2012). However, there is a lack of information about chimpanzees at this site.

Additionally, little is known about the relationships between chimpanzees and sympatric mammals, particularly other primate species, in this area of the NKNP. Chimpanzees share habitats with many other large mammals such as leopard, buffalo,

http://www.aloki.hu ● ISSN 1589 1623 (Print) ● ISSN 1785 0037 (Online)
DOI: http://dx.doi.org/10.15666/aeer/2003_26632681

elephant, lion, other primates species that may potentially influence nesting behavior here. In general, the influence of large sympatric mammals on nesting behavior of chimpanzees is poorly known (Basabose and Yamagiwa, 2002; McGrew et al., 2014; Piel et al., 2019). Information about nesting behavior in a protected area of Senegal is needed for a better understanding of relationships between the chimpanzees and their environment in this extremely hot and dry savannah region, and in comparison with chimpanzees living in other countries and habitat types (Anderson et al., 1983; Brownlow et al., 2001; Hernandez-Aguilar, 2009; Koops et al., 2012; Hernandez-Aguilar et al., 2013; Carvalho et al., 2015; Hakizimana et al., 2015; Dutton et al., 2017). We aim to provide information on a putative new chimpanzee community in the Antenna zone of southeastern NKNP and compare their nesting ecology with that of chimpanzees at other sites. Given the known big ranges of savanna chimpanzees, this is possible and deserves testing that Antenna chimpanzees community could be the same community that is at Assirik, which is only 17.5 km (as a crow flies) from Antenna zone, and which is accessible to it via tributaries of the Niokolo Koba River. Thus, we provide new data on chimpanzees nesting behavior in NKNP in Senegal and how these data can help the conservation of western chimpanzees and their habitats in Senegal. We also present a preliminary assessment of the presence of other medium and large mammals in the Antenna zone, using three months of data from one camera trap as well as data from previous occasional surveys.

Materials and methods

Study site

We conducted our study in the "Antenna zone" (UTM Zone 28N; 752139E, 1442478N) of NKNP, near the Dakar-Kedougou-Bamako transportation corridor (N7 highway) (*Fig. 1*). We collected field data during July 2017, January-March 2018, and September-November 2018.

NKNP is in southeastern Senegal (West Africa) and the region is characterized by a hot and dry climate with mixed tree and grass vegetation (McGrew et al., 1981; Pruetz et al., 2002; Ndiaye et al., 2018a). The vegetation classification falls within a transitional Sudano-Guinean savanna system that is dominated by woodlands and grasslands (Ba et al., 1997). The majority of this savanna landscape consists of open-canopy vegetation (e.g., gallery forest, ecotone forest). The most common tree species include *Adansonia digitata, Afzelia africana, Anogeissus leiocarpus, Bombax costatum, Combretum glutinosum, Combretum nigricans, Daniellia oliveri, Hexalobus monopetalus, Parkia biglobosa, Piliostigma thoningii, Khaya senegalensis, Sterculia setigera, Pterocarpus erinaceus, Tamarindus indica, Terminalia macroptera* and *Vitellaria parkii* (Ba et al., 1997; Pruetz et al., 2002; Ndiaye et al., 2018b). The Kedougou region is one of the rainiest parts of Senegal and the gallery forests here are seasonally flooded. Annual rainfall ranged 900-1800 mm in 1995-2015, with a long-term mean of approximately 1200 mm. During the same period, the mean annual temperature was 28.6 °C (Agence Nationale de l'Aviation Civile et de la Météorologie 2015; Faye et al., 2019). The dry season occurs from November to April and the rainy season occurs from June to October (Ndiaye et al., 2018a), with May as a transitional month. According to Korstjens and Hillyer (2016), rainfall has decreased generally in sub-Saharan Africa since 1901. In recent years, temperature variations have increased in general in Senegal in relation to regional climate change (Funk et al., 2012; Sarr et al., 2013, 2015).

http://www.aloki.hu ● ISSN 1589 1623 (Print) ● ISSN 1785 0037 (Online)
DOI: http://dx.doi.org/10.15666/aeer/2003_26632681

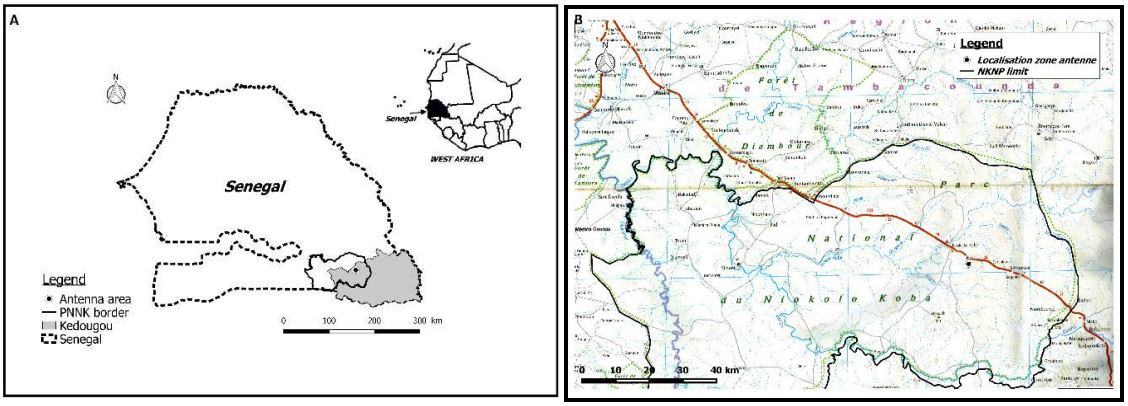

Figure 1. *Locations of Niokolo Koba National Park in Senegal, West Africa (A), and the Antenna zone in the park in relation to the N7 highway and to the Assirik chimpanzee site (labeled "Hassirik") (B). (Projection: UTM Zone 28 datum WGS 84; Data source: Database of Global Administrative Areas, created by PI Ndiaye)*

Data collection and analysis

Recce-transect survey

Primatologists concur that counting chimpanzee nests along line transects is one of the best methods for identifying the presence or absence of wild, unhabituated chimpanzees (Kühl et al., 2008; Junker et al., 2009; Arandjelovic et al., 2014) but applying this method to the savanna environments in Senegal involves intensive sampling of vegetation types that can be poorly suited for nesting, such as plateau grasslands with scattered trees and shrubs (Pruetz et al., 2002). For this reason, we used a recce-transects approach (Maisels et al., 2008) to search opportunistically for nests on the edges of gallery forest in the Antenna zone following Ndiaye et al. (2013a, b; 2018b) in order to maximize the number of nests encountered during the study. The recce-walk method is a survey on foot in a predetermined direction along a path of least resistance, which can deviate by any degree, through the survey area (Kühl et al., 2008; Maisels et al., 2008; Ndiaye et al., 2018b). Recce-transects were conducted in July 2017 and January-March 2018 to record fresh and recent nests, and follow-up surveys were conducted from September 5-November 12, 2018 to additionally sample old and rotting nests (*Fig. 2*). During the last survey period in 2018, we sampled in both the dry and wet seasons. Data collected during the all survey periods were used to visualize the distribution of nests within the study area, while only data collected from September to November 2018 were used for statistical analyses with Excel software (see below) to avoid duplicating data on fresh or recent nests surveyed in January-March 2018.

For each nest we encountered during surveys, including single or multiple nests in close proximity, we recorded the date and time, and the geographic coordinates using a GPS Garmin etrex 10. The accuracy Garmin etrex 10 is about 3 meters 95% of the time. We used the tracking option of the GPS to ensure we measured each nest only once, in case recce-transects overlapped. In addition, we recorded the vegetation type (gallery forest, plateau, woodland, grassland and bamboo) following McGrew et al. (1981), and tree species bearing each nest, using our personal experience and identification keys (Arbonnier, 2009). We measured the height of the nest above the ground using a Tracker 670 laser rangefinder and determined the nest age class according to Tutin and

http://www.aloki.hu ● ISSN 1589 1623 (Print) ● ISSN 1785 0037 (Online)
DOI: http://dx.doi.org/10.15666/aeer/2003_26632681

Fernandez (1984). We identified fresh nests as being used the night before, with the presence of copious green and moist leaves. In addition, we often found fresh feces or urine on the ground beneath new nests. Recent nests had green leaves that were wilted and drying. Old nests had a mixture of green and brown dried leaves or consisted entirely of brown leaves. Rotted nests ranged from disintegrating brown leaves to leafless structures consisting only of the branchy frame.

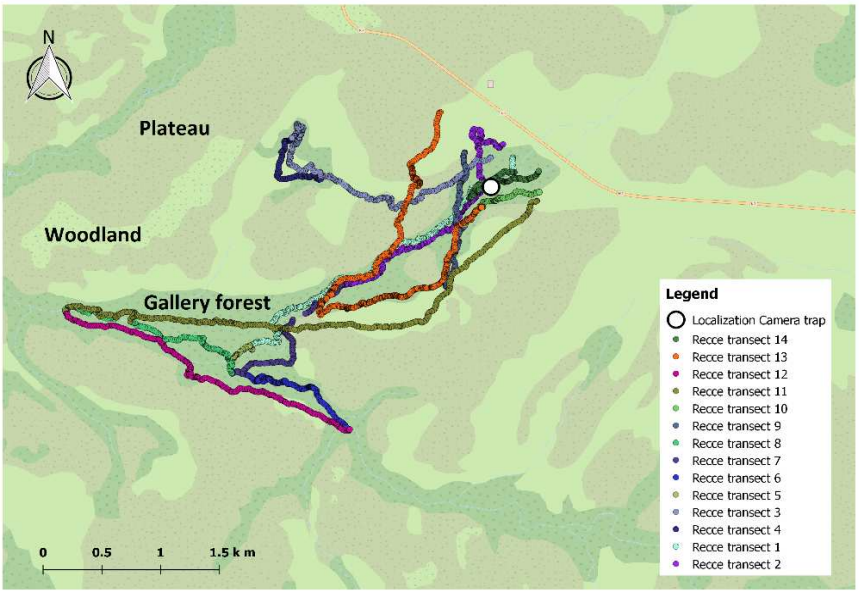

Figure 2. *Locations of recce-transects in the Antenna zone of Niokolo Koba National Park, Senegal, from September 5 to November 12, 2018. (Projection: UTM Zone 28 datum WGS 84; Data source: OpenStreetMap standard, created by PI Ndiaye)*

We used the nests we recorded to determine the chimpanzees' nest encounter rate (Kiszka et al., 2007; Gurarie and Ovaskainen, 2013) as *Equation 1:*

$$N/L \qquad \text{(Eq.1)}$$

where "*N*" is the number of censused nests and "*L*" is the total distance surveyed (km).

Vegetation survey

To assess nesting tree species preference, we conducted vegetation surveys at nesting sites and along the recce-walks in a total of 26 quadrats, each measuring 20 × 20 m (400 m^2) with a total quadrat zone of 10,400 m^2. We measured all trees with a diameter at breast height ≥ 10 cm in each quadrat. The relative abundance of each species was calculated to identify common and rare tree species at nesting sites, identifying species based on personal experience and identification keys (McGrew et al., 1981; Arbonnier, 2009). We determined whether a tree species was preferred for nesting by plotting a histogram comparing the proportion of nests in each tree species with the relative abundance of each tree species. We used a simple linear regression test to evaluate relationships between nesting tree species and the tree species abundances and to determine if chimpanzees prefer certain tree species for nest building in the Antenna zone**.** All the maps are done with Qgis 2.18.28 software.

http://www.aloki.hu ● ISSN 1589 1623 (Print) ● ISSN 1785 0037 (Online)
DOI: http://dx.doi.org/10.15666/aeer/2003_26632681

Camera trap

Medium and large mammal presence was determined using one camera trap (Bushnell Trophy Cam HD Essential) in order to survey for sympatric mammals. The camera was positioned at a nesting site in a large gallery forest from September, 05 to November, 12, 2018 (N = 68 camera trap days) (*Fig. 2*). We calculated the relative abundance of each species using the equation: (l/L) x 100 according to Hedwig et al. (2018) where "l" is the number of all the individuals of one species captured with the camera trap and "L" is the number of all individuals of all species captured during the survey.

Results

During the preliminary surveys, we recorded 14 fresh and 76 recent nests in July 2017 and 41 fresh and 112 recent nests from January to March 2018 (*Fig. 3A*). During the last data collection period (from September 5 to November 12, 2018), we conducted 14 recce-transects (*Fig. 2*), totaling 34 km in length in a 12 km^2 area and recorded 262 chimpanzee nests including 16 fresh (6%), 23 recent (8.8%), 18 old (6.9%) and 205 (78.3%) rotten nests (*Fig. 3B*). The encounter rate is 7.70 nests/km. Most nests (n = 254; 97%) were in the gallery forests that connect to the Gambia River via "Bo ko", a tributary of the Niokolo Koba River. Only 8 nests (3%) are encountered in woodland. We have not encountered chimpanzee's nest in plateau, grassland and bamboo.

Nest location and nesting tree species preference

The locations of nests in *Figure 3A* and *B* indicate that chimpanzees built their sleeping nests in the same area in the Antenna zone between July 2017 and November 2018.

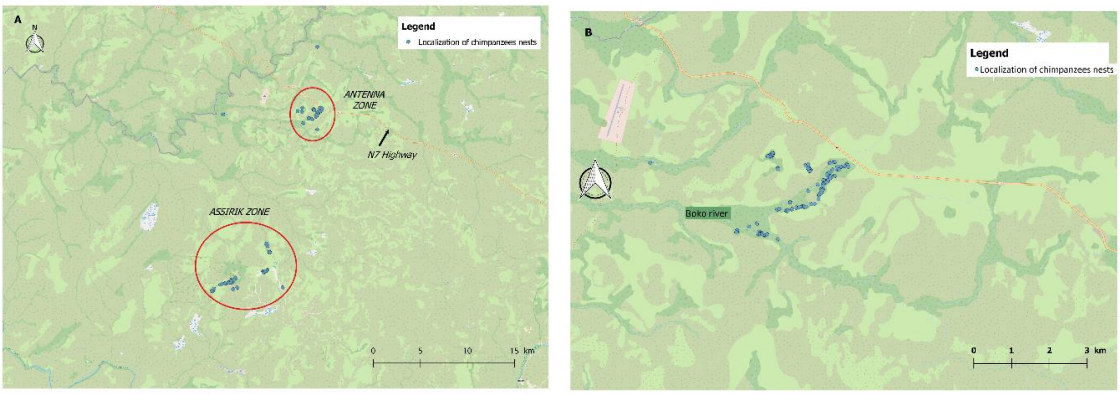

Figure 3. *Location of chimpanzee nests in the Antenna zone, Niokolo Koba National Park, Senegal (A) in 2017 and 2018, in relation to the Assirik zone (unpublished data); (B) from September to November 2018, showing Antenna zone only. (Projection: UTM Zone 28 datum WGS 84; Data source: OpenStreetMap standard, created by PI Ndiaye)*

Chimpanzees in the Antenna zone have at least 34 tree species to construct sleeping nests. Most of the nests (84%) were associated with four tree species, including

http://www.aloki.hu ● ISSN 1589 1623 (Print) ● ISSN 1785 0037 (Online)
DOI: http://dx.doi.org/10.15666/aeer/2003_26632681

Hexalobus monopetalus (46%), *Pterocarpus erinaceus* (22%), *Anogeissus leiocarpus* (9%), and *Combretum* sp. (7%). The remaining 16% of nests were associated with 30 other species, such as *Malacanta alnifolia* (4.6%), *Khaya senegalensis* (2.7%), *Diospyros mespiliformis* (1.9%) and *Cola cordifolia* (1.5%) among others (*Fig. 4*). We counted 711 trees in the sample quadrats and identified a total of 34 species (*Fig. 4*). Eight of these 34 tree species comprised 73% of the sample, namely *H. monopetalus* (17.7%), *Combretum* sp. (17.9%), *P. erinaceus* (17%), *Piliostigma thonningii* (7.6%), *Lannea microscarpa* (4.9%), *Vitex guineensis* (4.3%), *M. alnifolia* (4.5%) and *A. leiocarpus* (3.5%). These results suggest that *H. monopetalus, P. erinaceus* and *A. leiocarpus* are respectively the most used tree species by chimpanzee to bear their nests in this site. But the most abundant tree species in the study site are respectively *H. monopetalus, Combretum* sp., *P. erinaceus* and *P. thonningii.*

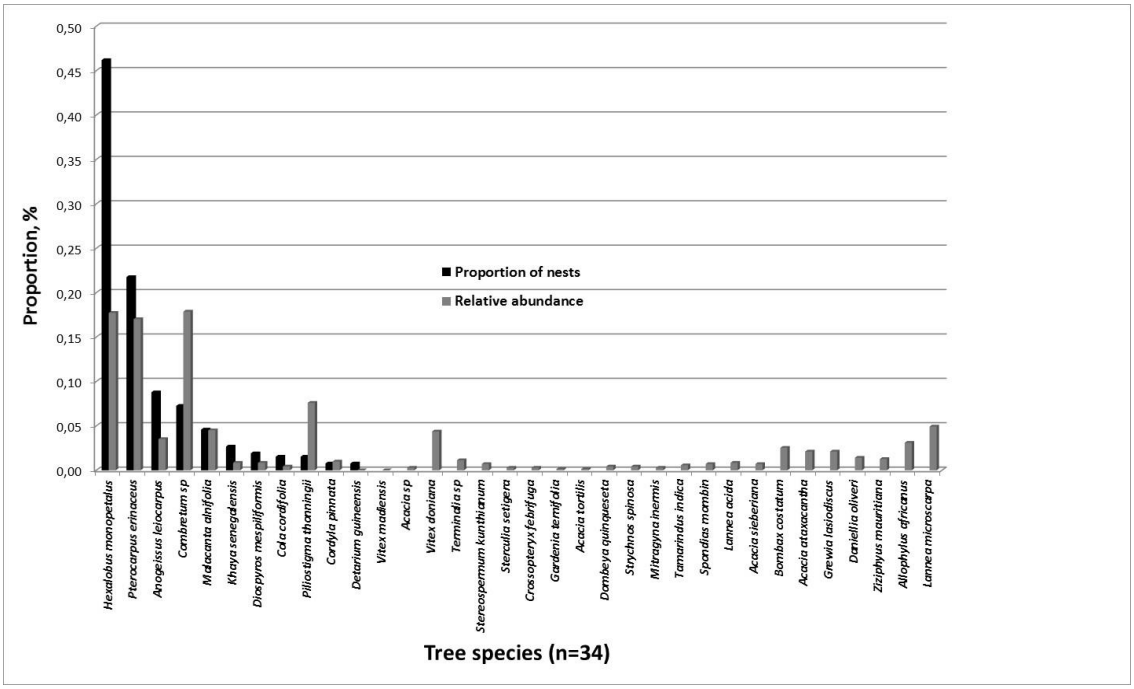

Figure 4. *Tree abundance (%) of 34 tree species (n = 711 trees) and abundance (%) of nests (n = 505) in the Antenna zone (NKNP, Senegal)*

Simple linear regression permitted us to have the values indicated in *Table 1* and *Figure 5*.

Table 1. *Statistical data of linear regression between relative abundance of nests (n = 505 nests) to abundance of trees (n = 711 trees) in Antenna zone, NKNP (Senegal)*

R square	Adjusted R	Standard error	P-value	Ecart-type	Confidence intervals
0.6061	0.5937	22.2803	5.9364	0.1707	95%

Nest height

We did not encounter ground nests during this study. The majority of nests (246 nests; 94%) were between 3 to 14 m above the ground and 36% (94 nests) of these nests

http://www.aloki.hu ● ISSN 1589 1623 (Print) ● ISSN 1785 0037 (Online)
DOI: http://dx.doi.org/10.15666/aeer/2003_26632681

were between 6 to 9 m (*Fig. 6*). Mean nest height was 8.7 ± SD 3.34 m with a range of 1-30 m and median range of 8 m. More than half of the nests (n = 163 nests; 62%) were at 5-10 m.

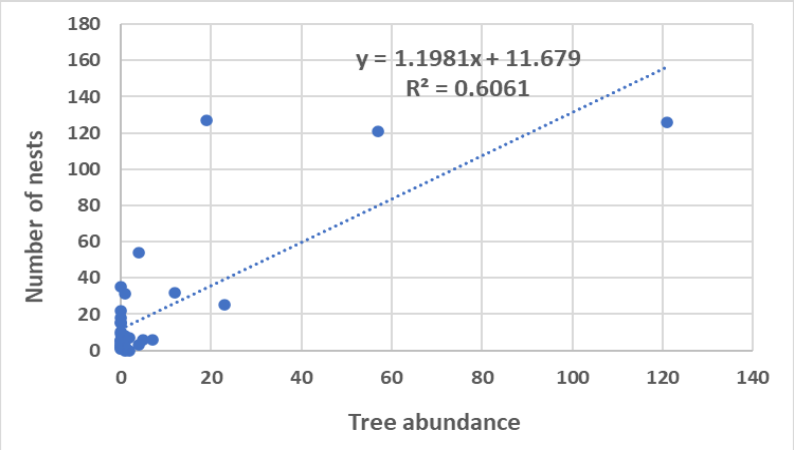

Figure 5. *Overall relationship between relative abundance of nests (n = 505 nests) to abundance of trees (n = 711 trees) in Antenna zone, NKNP (Senegal)*

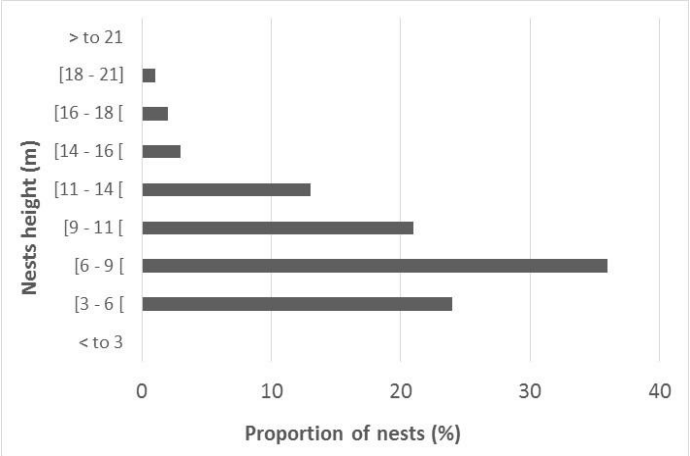

Figure 6. *Proportion (%) and number (n = 262) of chimpanzees nests over four height classes in Antenna zone, NKNP*

Sympatric mammals

We identified nine mammal species in the Antenna zone in addition to the West African chimpanzee (*Pan troglodytes verus*), including, three large carnivore species: the spotted hyena (*Crocuta crocuta*), the lion (*Panthera leo*), the leopard (*Panthera pardus*); four large herbivores: the roan antelope (*Hippotragus equinus*), the warthog (*Phacochoerus africanus*), the African buffalo (*Syncerus caffer*), the bushbuck (*Tragelaphus scriptus*); one small ungulate: the red-flanked duiker (*Cephalophus rufilatus*) and one monkey species: the Guinea baboon (*Papio papio*) (*Table 2*). Guinea baboons (*Papio papio*) and western chimpanzees account for 27.6% and 10.3% of camera trap images, respectively, at our study site (*Fig. 7*). The presence of leopard (*Panthera pardus*) was verified with a camera trap during the preliminary survey.

http://www.aloki.hu ● ISSN 1589 1623 (Print) ● ISSN 1785 0037 (Online)
DOI: http://dx.doi.org/10.15666/aeer/2003_26632681

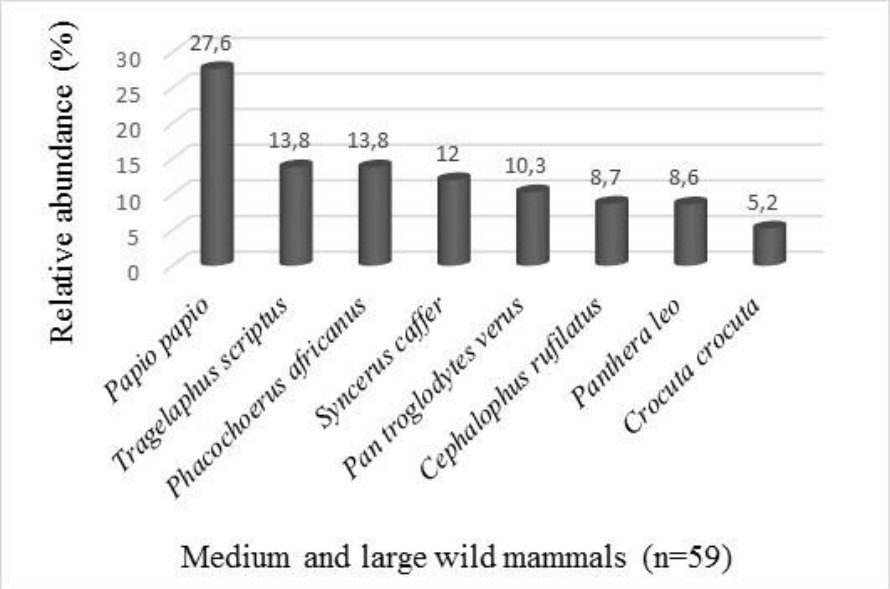

Figure 7. *Relative abundance (%) of medium to large mammalian species recorded on a camera trap in Antenna zone, NKNP*

Table 2. *List of sympatric mammals detected using a camera trap in the Antenna zone, Nokolo Koba National Park between September 5 to November 12, 1998*

Order	Family	Species	English name	French name	IUCN Status	Absolute abundances of species in CT images (n = 59)
Cetartiodactyla	Suidae	*Phacochoerus africanus*	Warthog	Phacochère	LC decreasing	8
	Bovidae	*Tragelaphus scriptus*	Bushbuck	Guib harnaché	LC	8
		Syncerus caffer	African buffalo	Buffle de savane	LC decreasing	7
		Cephalophus rufilatus	Red-flanked duiker	Cephalophe à flanc roux	LC decreasing	5
		Hippotragus equinus	Roan antelope	Hippotrague	LC decreasing	**
Carnivora	Felidae	*Panthera leo*	Lion	Lion	VU decreasing	5
		Panthera pardus	Leopard	Léopard	VU decreasing	*
	Hyenidae	*Crocuta crocuta*	Spotted hyena	Hyène tachetée	LC decreasing	3
Primates	Cercopithecidae	*Papio papio*	Guinea baboon	Babouin de Guinée	NT	16
	Hominidae	*Pan troglodytes verus*	Chimpanzee	Chimpanzé de l'Ouest	CR	6

CR = Critically Endangered; NT = Near threatened; LC = Least Concern; VU = Vulnerable
*Leopard was not included in the calculation of "frequencies of species in CT images" because the picture was recently taken from another camera trap dataset from Antenne and at the time of writing the species identifications from this dataset were incomplete
**We have only one direct observation of roan antelope during the prospections

http://www.aloki.hu ● ISSN 1589 1623 (Print) ● ISSN 1785 0037 (Online)
DOI: http://dx.doi.org/10.15666/aeer/2003_26632681

Discussion

The simultaneous presence of fresh and recent nests indicates the presence of chimpanzees in the Antenna zone in NKNP over the period of our study. The high percentage of rotten nests may be because we carried out the study towards the end of the rainy season. Chimpanzee nests generally decay relatively fast during the rainy season and in gallery forests in the nearby non-protected area of Kedougou (Diaguiri: Ndiaye et al., 2018a; PI Ndiaye, unpublished data).

In this study, within the Antenna zone chimpanzees nest in the most abundant tree species found in this area of NKNP, namely *Hexalobus monopetalus, Pterocarpus erinaceus* and *Combretum* sp., together comprising 84% of the total nests. These patterns are similar to those at other sites in Senegal (Ndiaye et al., 2013b, 2018a; Badji et al., 2018), but differ mostly in the percentage of nests in other species, such as *K. senegalensis, A. digitata, Diospyros mespiliformis* and *H. monopetalus,* at Bagnomba and Diaguiri (Ndiaye et al., 2018a, b). Sousa et al. (2014) also highlighted that chimpanzees in Guinea-Bissau made the majority of their nests in sub-humid forests with sparse canopy and in forest with dense canopy. Dutton et al. (2017) are also described that environmental factors affected nest site and species bearing choices by chimpanzees in Nigeria. According to these authors, *P. t. ellioti* made 52.9% of their nests in only five tree species of the 123 tree species recorded. Many authors, including Ndiaye et al. (2013a, 2018a), Hakizimana et al. (2015) and Badji et al. (2018), have described that chimpanzees prefer certain tree species for sleeping nests in Senegal, Burundi and Cameroon. Physical characteristics of the wood, particularly the hardness and flexibility are one of the most determining properties in this choice. We also recorded several tree species that had nests in them more than we expected based on their abundance at Antenna, including *K. senegalensis*, *D. mespiliformis* and *C. cordifolia*. These data indicate that chimpanzees prefer to nest in these tree species at the Antenna site. These species usually grow up to 7-8 m in height (Arbonnier, 2009), which is lower than the average of the nesting tree height at two sites in unprotected areas of Senegal, including Diaguiri (Ndiaye et al., 2018a) and Bagnomba (Badji et al., 2018). Simple lineaire regression showed a positive value of the correlation coeficience ($R^2 = 0.6061$; $0 < r < 1$). Thus, we can deduce a low relationship between trees species bearing nests and their abundance in the case of Antenna zone. In this case, the number of nests on *H. monopetalus, P. erinaceus* and *Combretum* sp. seem to increase with this tree species abundance. But we trust strongly that chimpanzees have preference for tree and sites bearing nests similar to the others sites in Senegal (Baldwin, 1979; Ndiaye et al., 2013a, 2018a; Badji et al., 2018). Baldwin (1979) found huge differences in nest frequency across vegetation types, at the nearest site to Antenna zone. In the case of our study, we have not focused on the division of nests between vegetation types, although we have not recorded this information. *A. leiocarpus* and *P. thonningii* are generally one of the most tree bearing chimpanzees' nest in Senegal. But we note that *A. leiocarpus* is the third most common tree species bearing chimpanzees' nest in this site and is not among the four most abundant species. *P. thonningii* is the fourth abundant tree species in this site but bear only few nests. It is not listed among the four most common species bearing the nest. Thus, we can hypothesize that the choice of tree species bearing nests by chimpanzee does not depend only on the tree abundance in the sleeping site. Others factors such as the habitat type, presence or absence of predator, social organization and food availability can influence the selection of tree species bearing chimpanzee's nests (Baldwin et al., 1981; Carvalho et al., 2015; Badji et al., 2018). Concentration of nests

http://www.aloki.hu ● ISSN 1589 1623 (Print) ● ISSN 1785 0037 (Online)
DOI: http://dx.doi.org/10.15666/aeer/2003_26632681

near a major highway also could indicate avoidance of predators, if the letter are discouraged by human activity, such as traffic. Fatal costs to chimpanzees of living near highways has been shown by Cibot et al. (2015) and Krief et al. (2020) at Kibale, Uganda.

While *Hexalobus monopetalus* is among the top species used at other sites, such as Bagnomba and Diaguiri (Ndiaye et al., 2018a, b), it is not the preferred species elsewhere outside the NKNP. *Pterocarpus erinaceus* is the most used species in the Kedougou region (Baldwin, 1979; Ndiaye et al., 2013a, 2018a, b), probably due to the quality of its wood, and particularly its hardness (which explains why this species is often used by woodworkers) (Ndiaye et al., 2013a). In Assirik (NKNP), Baldwin (1979) have described *Pseudospondias microcarpa* and *Erythrophloem suaveoleus* were the most used species to bear nests in forest habitats. But in grassland and woodland, *Pterocarpus erinaceus* was used the most used species. However, *H. monopetalus* is the most abundant species at the Antenna zone, fruits at the beginning of the rainy season, and also has a high-quality wood (Arbonnier, 2009), which may explain why the chimpanzees preferred it in our study. Fruit abundance and vegetation type had much stronger influences on site selection than did other factors for chimpanzees at Kalinzu (Uganda) (Furuichi and Hashimoto, 2004) and we hypothesize that similar factors could promote the high use of *H. monopetalus* by Antenna chimpanzees. Additional long-term research on chimpanzee nesting behavior in Antenna zone might confirm or reveal differences about nesting trees species preferences.

Although chimpanzees select particular trees species for nesting, the principles that guide species preferences are poorly understood. For example, in Semliki (Uganda), another savanna chimpanzee site, *Cynometra alexandri* (Fabaceae, which is the same family as *P. erinaceus*) constitutes only 9.6% of trees in the gallery forest in which their study population range but represented 73.6% of the chimpanzee nests (Samson and Hunt, 2014). However, most authors agree that structural properties of the tree species, their height and feeding are also key choice features in chimpanzees nesting behavior (Hunt and McGrew, 2002; Ogawa et al., 2007; Ndiaye et al., 2013a; Stewart and Pruetz, 2013; Badji et al., 2018). Chimpanzees at the Antenna site may make similar choices in choosing nesting species (Samson, 2012; Ndiaye et al., 2013a; Samson and Hunt, 2014).

The chimpanzees of the Antenna zone continued to build their nests on the edges of gallery forest during and immediately following the rainy season. This contrasts with previous studies showing that chimpanzees nest in higher elevations during the rainy season in most unprotected areas across Kedougou (Ndiaye et al., 2013b) and elsewhere in Africa (e.g., Koops et al., 2012). We hypothesize that the topographic relief in the Antenna zone explains this difference, as the area includes numerous elevated areas at the edges of the gallery forests (Gessain, 1963). However, using only nests may fail to consider the seasonality of chimpanzees ranging and should not imply that only areas where nests are observed are valuable for conservation. Data on human pressures and the availability of fruiting trees are required for a better understanding of chimpanzee distribution.

Chimpanzees in the Antenna zone built the majority of their nests (62%) at 5-10 m in height. This is similar to findings for chimpanzees in the non-protected area of Bagnomba, to the south-east of NKNP (Badji et al., 2018). Despite the presence of potential predators (lion, spotted hyena and leopard), nest heights in the Antenna zone in this study seem to be lower than those described for Assirik, situated only about

http://www.aloki.hu ● ISSN 1589 1623 (Print) ● ISSN 1785 0037 (Online)
DOI: http://dx.doi.org/10.15666/aeer/2003_26632681

16 km to the west (Baldwin, 1979). But, we want to repeat this study in the same periods and at the same time in these different sites before making a strong hypothesis. The range of heights of nests at Assirik is greater than those recorded in Guinea and Equatorial Guinea (Baldwin, 1979; Baldwin et al., 1981). However, further research is needed to verify if this is still true. In Senegal, the chimpanzees mean nest height is lower than the mean tree height at Fongoli, Assirik and Diaguiri (Baldwin, 1979; Pruetz et al., 2008; Ndiaye et al., 2013a; Badji et al., 2018; Ndiaye et al., 2018).

At Assirik, chimpanzees face four species of large carnivore (Pruetz et al., 2008; McGrew et al., 2014), while at Fongoli, humans have exterminated almost all natural predators, although leopard and hyena persist at low densities (Pruetz, unpublished data). Chimpanzees at Fongoli nested at lower heights and farther apart than did chimpanzees at Assirik and sometimes made nests on the ground (Pruetz et al., 2008). Many researchers have also investigated the relation between chimpanzee nest height and the presence of terrestrial predators elsewhere in Africa (Koops et al., 2012). For example, Gombe (Tanzania) chimpanzee nests may be constructed at any height above 4 m from the ground up to 25 m (Baldwin et al., 1981; Hernandez-Aguilar, 2006). The chimpanzees of Issa (Tanzania) prefer tall trees with high first branches for nesting, thus supporting the hypothesis that elevated height of a sleeping place is a predator defense strategy (Hernandez-Aguilar et al., 2013; Hernandez-Aguilar and Reitan, 2020). Chimpanzees in Issa, where several potential predators exist, did not nest more frequently in forest vegetation than chimpanzees in Fongoli, although forest vegetation is expected to provide greater opportunity for escape from terrestrial predators (Stewart and Pruetz, 2013). According to Baldwin (1979) and Stewart and Pruetz (2013), nest height correlated weakly with tree height, suggesting that height from the ground to the first branch may be a more important factor than tree height alone in selecting a tree in which to nest. Many factors influence nest site selection in chimpanzees, of which danger from terrestrial predators is likely to be one (Tutin et al., 1981). Further study of nesting tree characteristics and preferences is necessary to improve our understanding of the ecology and behavior of chimpanzees in the hot and dry habitat of Antenna zone. The distance between Assirik and Antenna zone is about 16 km. Mt Assirik's environment fulfills all three criteria for savanna with mean annual rainfall range about 824 to 1224 during the long-term study project SAPP 1976-1979 (McGrew et al., 1981; Russak and McGrew, 2008; McGrew et al., 2014). Nest heights in the Antenna zone seem to be lower than Assirik and the presence of predators (lion and leopard) has also been described in this site since many years (Baldwin, 1979; McGrew et al., 2014; Lindshield et al., 2019). Thus, we can hypothesize that nest height does not only depend on rainfall and the presence or absence of predators.

The influence of competitors on chimpanzee behavior in Senegal is relatively unstudied. Therefore, competition may be high between the two non-human primates most frequently captured by cameras in the Antenna zone, chimpanzees and Guinea baboons, for resources related to sleeping mostly. Repeated visits by lions and spotted hyenas to this area may be related to the abundance of their potential prey, especially baboons. The high frequency of baboons at the site may also imply competition for food with the chimpanzees (Matsumoto-Oda and Kasagula, 2000). Thus, there are many reasons (e.g., predation, competition) to examine the diversity of sympatric mammalian fauna that live sympatrically with wild chimpanzees (Russak and McGrew, 2008; Piel et al., 2019).

http://www.aloki.hu ● ISSN 1589 1623 (Print) ● ISSN 1785 0037 (Online)
DOI: http://dx.doi.org/10.15666/aeer/2003_26632681

Conclusion, recommendations and future studies

Our study provides new data about the nesting behavior of chimpanzees in NKNP. The location of nests near the N7 highway highlights the possible acclimation of chimpanzees to anthropogenic pressures because we encountered the nesting sites not far from the N7 highway (within 500 m to 3 km from the road). We found that *Hexalobus monopetalus* was used most frequently for chimpanzee nests, unlike in other studies in Senegal.

These results will contribute to the ongoing management of NKNP and to the construction of a national action plan for chimpanzees in Senegal.

Further we think that long-term studies are needed for a better understanding of chimpanzee nesting behavior in Antenna zone and of broader, community-ecological relationships to better understand how chimpanzees and other species share landscapes and mutually exploit resources.

Acknowledgements. We would like to thank the authorities of the Niokolo Koba National Park, namely the Director of "Parcs Nationaux du Sénégal" and the conservator of "Parc National du Niokolo Koba" for the authorization and facilities to carry out the present study and all the NKNP agents for their contribution during the study process. We also thank Cheikh Loucoubar and Cheikh Talla of the "Groupe de Biostatistique, bio-informatique et modélisation de l'Institut Pasteur à Dakar" for their assistance during the statistical analysis, Texas State University, Purdue University, University of Florida and Université Cheikh Anta Diop for their institutional support. Many thanks to the anonymous reviewers, particularly for their important and helpful comments and suggestions contributing to improve the quality of the earlier version of this manuscript.

Funding. This study was supported by the Faculté des Sciences et Techniques de l'Université Cheikh Anta Diop de Dakar, Purdue University, the National Science Foundation, Primate Conservation, Inc., and the Leakey Foundation.

Compliance with ethical standards. This study was carried out following the code of best practices for field primatology of the International Primatological Society (Riley et al., 2014) and recommendations for minimizing risk of disease transmission between humans and great apes by the International Union for Conservation of Nature (Gilardi et al., 2015).

REFERENCES

[1] Agence Nationale de l'Aviation Civile et de la Météorologie (2015): Données climatique de la station de Kédougou. – www.anacim.sn/meteorologie.

[2] Anderson, J. R., Williamson, E. A., Carter, J. (1983): Chimpanzees of Sapo Forest, Liberia: density, nests, tools and meat-eating. – Primates 24: 594-601. doi.org/10.1007/BF02381692.

[3] Arandjelovic, M., Boesch, C., Campbell, G., Hohmann, G., Junker, J., Kouakou, Y. C., Kühl, H., Leendertz, F., Leinert, V., Möbius, Y., Murai, M., Oelze, V., Rabanal, L., Robbins, M., Vergnes, V., Wagner, O., Head, J. (2014): Guidelines for Research and Data Collection. Pan African Programme, The Cultured Chimpanzee. – Pan African Programme Data Collection, Leipzig.

[4] Arbonnier, M. (2009): Arbres, arbustes et lianes des zones sèches d'Afrique de l'Ouest. – MNHN Service de Publications Scientifiques, Paris.

[5] Ba, A. T., Sambou, B., Finn, E., Goudiaby, A., Camara, C., Diallo, D. (1997): Végétation et Flore. – Parc transfrontalier Niokolo Badiar. Ed, Projet FED Niokolo-Badiar et Institut des Sciences de l'Environnement (UCAD), Dakar.

http://www.aloki.hu ● ISSN 1589 1623 (Print) ● ISSN 1785 0037 (Online)
DOI: http://dx.doi.org/10.15666/aeer/2003_26632681

[6] Badji, L., Ndiaye, P. I., Lindshield, S. M., Ba, C. T., Pruetz, J. D. (2018): Savanna chimpanzee (*Pan troglodytes verus*) nesting ecology at Bagnomba (Kedougou, Senegal). – Primates 59: 235-241. doi.org/10.1007/s10329-017-0647-2.

[7] Baisero, D., Visconti, P., Pacifici, M., Cimatti, M., Rondinini, C. (2020): Projected global loss of mammal habitat due to land-use and climate change. – One Earth 2: 578-585. doi.org/10.1016/J.oneear.2020.05.015.

[8] Baldwin, P. J. (1979): The Natural History of the Chimpanzee (*Pan troglodytes verus*) at Mt. Assirik, Senegal. – PhD Dissertation, University of Stirling, Stirling, Scotland.

[9] Baldwin, P. J., Sabater Pi, J., McGrew, W. C., Tutin, C. E. G. (1981): Comparison of nest made by different populations of chimpanzees (*Pan troglodytes*). – Primates 22: 474-486. Doi.org/10.1007/BF02381239.

[10] Basabose, A. K., Yamagiwa, J. (2002): Factor affecting nesting site choice in chimpanzees at Tshibati, Kahuzi-Biega National Park: influence of sympatric gorillas. – International Journal of Primatology 23: 263-282. dx.doi.org/10.1023/A:1013879427335.

[11] Brownlow, A. R., Plumptre, A. J., Reynolds, V., Ward, R. (2001): Sources of variation in the nesting behavior of Chimpanzees *(Pan troglodytes schweinfurthii)* in the Budongo forest, Uganda. – American Journal of Primatology 55: 49-55. dx.doi.org/10.1002/ajp.1038.

[12] Carvalho, J. S., Meyer, C. F., Vicente, L., Marques, T. A. (2015): Where to nest? Ecological determinants of chimpanzee nest abundance and distribution at the habitat and tree species scale. – American Journal of Primatology 77: 186-199. Doi.org/10.1002/ajp.22321.

[13] Cibot, M., Bortolamiol, S., Seguya, A., Krief, S. (2015): Chimpanzees Facing a Dangerous Situation: A High-Traffic Asphalted Road in the Sebitoli Area of Kibale National Park, Uganda. – International Journal of Primatology 77: 1-11. DOI: 10.1002/ajp.22417.

[14] Convention on International Trades in Endangered Species of wild fauna and flora (2018): Great Apes (Hominidae spp.). – Report of the Secretariat. Seventieth Meeting of the Standing Committee Rosa Khutor, Sochi (Russian Federation).

[15] Dutton, P., Moltchanova, E., Chapman, H. (2017): Nesting Ecology of a Small Montane Population of the Nigerian / Cameroon Chimpanzee (*Pan troglodytes ellioti*) in Nigeria. – Folia Primatologica 87: 361-374. doi.org/10.1159/000454921.

[16] Faye, M., Fall, A., Tine, D., Faye, C. S., Faye, B., Ndiaye, A. (2019): Evolution pluvio-thermique de 1950 à 2013 au Sénégal Oriental: cas de la region de Tambacounda. – International Journal of Advanced Research 7(12): 270-287.

[17] Fruth, B., Hohmann, G. (1994): Comparative Analyses of Nest Building Behaviour in Bonobos and Chimpanzees. – In: Wrangham, R. W., McGrew, W. C., deWaal, F. B. M., Heltne, P. G. (eds.) Chimpanzee Cultures. Harvard University Press, Cambridge, MA, pp. 109-128.

[18] Fruth, B., Hohmann, G. (1996): Nest Building Behaviour in the Great Apes: The Great Leap Forward? – In: McGrew, W. C., Marchant, L. F., Nishida, T. (eds.) Great Ape Societies. Cambridge University Press, Cambridge, pp. 225-240.

[19] Funk, C., Michaelsen, J., Marshall, M. (2012): Mapping Recent Decadal Climate Variations in Precipitation and Temperature Across Eastern Africa and the Sahel. Chap. 14. – In: Wardlow, B., Anderson, M., Verdin, J. (eds.) Remote Sensing of Drought—Innovative Monitoring Approaches. CRC Press, Boca Raton. https://doi.org/10.1201/b11863.

[20] Furuichi, T., Hashimoto, C. (2004): Botanical and topographical factors influencing nesting-site selection by chimpanzees in Kalinzu Forest, Uganda. – International Journal of Primatology 25: 755-765. 0164-0291/04/0800-0755/0.

[21] Gessain, R. (1963): Introduction à l'étude du Sénégal Oriental (Cercle de Kédougou). – In: Cahiers du Centre de recherches anthropologiques, XI^{e} série. Tome 5 fascicule 1-2, pp. 5-85.

http://www.aloki.hu ● ISSN 1589 1623 (Print) ● ISSN 1785 0037 (Online)
DOI: http://dx.doi.org/10.15666/aeer/2003_26632681

[22] Gilardi, K. V., Gillespie, T. R., Leendertz, F. H., Macfie, E. J., Travis, D. A., Whittier, C. A., Williamson, E. A., Cameron, K., Cranfield, M., Gaffikin, L., Kalema-zikusoka, G., Köndgen, S., Leendertz, S., Lonsdorf, E., Muehlenbein, M., Mugisha, L., Bosco nizeyi, J., Nutter, F., Petrzelkova, K., Reed, P., Rwego, I., Ssebide, B., Unwin, S. (2015): Best practice guidelines for health monitoring and disease control in great ape populations. – IUCN SSC Primate Specialist Group, Gland, Switzerland.

[23] Goodall, J. (1968): The behaviour of free-living chimpanzees in the Gombe Stream Reserve. – Annales of Behaviour Monography 1: 161-311. doi.org/10.1016/S0066-1856(68)80003-2.

[24] Gurarie, E., Ovaskainen, O. (2013): Towards a general formalization of encounter rates in ecology. – Theoretical Ecology 6: 189-202. DOI 10.1007/s12080-012-0170-4.

[25] Hakizimana, D., Hambuckers, A., Brotcorne, F., Huynen, M. (2015): Characterization of Nest Sites of Chimpanzees in Kibira National Park, Burundi. – African Primates 10: 1-12.

[26] Hedwig, D., Kienast, I., Bonnet, M., Curran, B. K., Courage, A., Boesch, C., Kühl, H. S., King, T. (2018): A camera trap assessment of the forest mammal community within the transitional savannah-forest mosaic of the Batéké Plateau National Park, Gabon. – African Journal of Ecology 56: 777-790. DOI: 10.1111/aje.12497.

[27] Heinicke, S., Mundry, R., Boesch, C., Hockings, K. J., Kormos, R., Ndiaye, P. I., Tweh, C., Williamson, E. A., Kühl, H. S. (2019): Towards systematic and evidence-based conservation planning for western chimpanzees. – American Journal of Primatology 81: 1-13. DOI: 10.1002/ajp.23042.

[28] Hernandez-Aguilar, R. A. (2006): Ecology and nesting pattern of Chimpanzees (*Pan troglodytes*) in Issa, Ugalla, Tanzania. – PhD Thesis, University of Southern California, Los Angeles.

[29] Hernandez-Aguilar, R. A. (2009): Chimpanzee nest distribution and site reuse in a dry habitat: implications for early hominin ranging. – Journal of Human Evolution 57: 350-364. DOI: 10.1016/j.jhevol.2009.03.007.

[30] Hernandez-Aguilar, R. A., Reitan, T. (2020): Deciding where to sleep: spatial levels of nesting selection in chimpanzees (*Pan troglodytes*) living in Savanna at Issa, Tanzania. – International Journal of Primatology 41: 870-900. doi.org/10.1007/s10764-020-00186-z.

[31] Hernandez-Aguilar, R. A., Moore, J., Stanford, C. B. (2013): Chimpanzee nesting patterns in savanna habitat: environmental influences and preferences. – American Journal of Primatology 75: 979-994. DOI: 10.1002/ajp.22163.

[32] Hunt, K. D., McGrew, W. C. (2002): Chimpanzees in the Dry Habitats of Assirik, Senegal and Semliki Wildlife Reserve, Uganda. – In: Boesch, C., Hohmann, G., Marchant, L. F. (eds.) Behavioural Diversity in Chimpanzees and Bonobos. Cambridge University Press, Cambridge, pp. 35-51.

[33] International Union for Conservation of Nature (2018): The IUCN RedList of Threatened Species. – IUCN, Gland, Switzerland.

[34] Junker, J., N'Goran, K. P., Kouakou, Y. C., Kühl, H. (2009): Biomonitoring Guide—Survey Training Workshop. – Taï National Park, Côte d'Ivoire.

[35] Kiszka, J., Macleod, K., Van Canneyt, O., Walker, D., Ridoux, V. (2007): Distribution, encounter rates, and habitat characteristics of toothed cetaceans in the Bay of Biscay and adjacent waters from platform of opportunity data. – ICES Journal of Marine Sciences 64: 1033-1043. DOI: 10.1093/icesjms/fsm067.

[36] Koops, K., McGrew, W. C., De Vries, H., Matsuzawa, T. (2012): Nest-building by chimpanzees (*Pan troglodytes verus*) at Seringbara, Nimba Mountains: antipredation, thermoregulation, and antivector hypotheses. – International Journal of Primatology 33: 356-380. dx.doi.org/10.1007/s10764-012-9585-4.

[37] Korstjens, A. H., Hillyer. A (2016): Primates and Climate Change: A Review of Current Knowledge. – In: Wich, S. A., Marshall, A. J. (eds.) An Introduction to Primate Conservation. Oxford University Press, Oxford, pp. 175-192. DOI 10.1093/acprof:oso/9780198703389.003.0011.

http://www.aloki.hu ● ISSN 1589 1623 (Print) ● ISSN 1785 0037 (Online)
DOI: http://dx.doi.org/10.15666/aeer/2003_26632681

[38] Kouakou, C. Y., Boesch, C., Kuehl, H. (2009): Estimating chimpanzee population size with nest counts: validating methods in Taï National Park. – American Journal of Primatology 71: 447-457. DOI 10.1002/ajp.20673.
[39] Krief, S., Iglesias-González, A., Appenzeller, B. M. R., Okimat, J. P., Fini, J. B., Demeneix, B., Vaslin-Reimann, S., Lardy-Fontan, S., Guma, N., Spirhanzlova, P. (2020): Road impact in a protected area with rich biodiversity: the case of the Sebitoli road in Kibale National Park, Uganda. – Environment Science Pollution Resources 27: 27914-27925. Doi.org/10.1007/s11356-020-09089-0.
[40] Kühl, H., Maisels, F., Ancrenaz, M., Williamson, E. A. (2008): Best Practice Guidelines for Surveys and Monitoring of Great Ape Populations. – IUCN SSC Primate Specialist Group (PSG), Gland, Switzerland.
[41] Kühl, H. S., Sop, T., Williamson, E. A., Mundry, R., Brugière, D., Campbell, G., Cohen, H., Danquah, E., Ginn, L., Herbinger, I., Jones, S., Junker, J., Kormos, R., Kouakou, C. Y., Goran, P. K. N., Normand, E., Tickle, A., Vendras, E., Welsh, A., Wessling, E. G., Boesch, C. (2017): The Critically Endangered western chimpanzee declines by 80%. – American Journal of Primatology 79: 1-15. doi.org/10.1002/ajp.22681.
[42] Lindshield, S., Bogart, S. L., Gueye, M., Ndiaye, P. I., Pruetz, J. D. (2019): Informing protection efforts for critically endangered chimpanzees (*Pan troglodytes verus*) and sympatric mammals amidst rapid growth of extractive industries in Senegal. – Folia Primatologica 90: 124-136. doi.org/10.1159/000496145.
[43] Maisels, F., Colom, A., Inogwabini, B. I. (2008): Section 6: Training. – In: Best Practice Guidelines for Surveys and Monitoring of Great Ape Populations. IUCN SSC Primate Specialist Group (PSG), Gland, Switzerland.
[44] Matsumoto-Oda, A., Kasagula, M. B. (2000): Preliminary study of feeding competition between baboons and chimpanzees in the Mahale Mountains National Park, Tanzania. – African Study Monographs 21: 147-157. doi.org/10.14989/68200.
[45] McGrew, W. C. (2021): Sheltering chimpanzees. – Primates 62: 445-455. doi.org/10.1007/s10329-021-00903-z.
[46] McGrew, W., Baldwin, P. J., Tutin, C. E. G. (1981): Chimpanzee in a hot, dry and open habitat: Mt Assirik, Senegal, West Africa. – Journal of Human Evolution 10: 227-244.
[47] McGrew, W., Baldwin, P. J., Marchant, L. F., Pruetz, J. D., Tutin, C. E. G. (2014): Chimpanzees (*Pan troglodytes verus*) and their mammalian sympatriates: Mt Assirik, Niokolo-Koba National Park, Senegal. – Primates 55: 525-532. DOI: 10.1007/s10329-014-0434-2.
[48] Ndiaye, P. I., Galat-luong, A., Galat, G., Nizinski, G. (2013a): Endangered West African chimpanzees (*Pan troglodytes verus*) (Schwarz, 1934) (Primates : Hominidae) in Senegal prefer Pterocarpus erinaceus , a threatened tree species, to build their nests : implications for their conservation. – Journal of Threatened Taxa 5: 5266-5272.
[49] Ndiaye, P. I., Galat, G., Galat-luong, A. (2013b): Note on the seasonal use of lowland and highland habitats by the West African Chimpanzee *Pan troglodytes verus* (Schwarz, 1934) (Primates: Hominidae): Implications for its conservation. – Journal of Threatened Taxa 5: 3697-3700. doi.org/10.11609/JoTT.o3229.3697-700.
[50] Ndiaye, P. I., Badji, L., Lindshield, S. M., Pruetz, J. D. (2018a): Nest-building behaviour by chimpanzees (*Pan troglodytes verus*) in the non-protected area of Diaguiri (Kedougou, Senegal): implications for conservation. – Folia Primatologica 89: 316-326. doi.org/10.1159/000490945.
[51] Ndiaye, P. I., Lindshield, S. M., Badji, L., Pacheco, L., Wessling, E. G., Boyer, K. M., Pruetz, J. D. (2018b): Survey of chimpanzees (*Pan troglodytes verus*) outside protected areas in southeastern Senegal. – African Journal of Wildlife Research 3: 1-14. doi.org/10.3957/056.048.
[52] Ogawa, H., Idani, G., Moore, J., Pintea, L., Hernandez-Aguilar, A. (2007): Sleeping parties and nest distribution of chimpanzees in the savanna woodland, Ugalla, Tanzania. –

http://www.aloki.hu ● ISSN 1589 1623 (Print) ● ISSN 1785 0037 (Online)
DOI: http://dx.doi.org/10.15666/aeer/2003_26632681

International Journal of Primatology 28: 1397-1412. dx.doi.org/10.1007/s10764-007-9210-0.

[53] Piel, A. K., Bonnin, N., Amaya, S. R., Wondra, E., Stewart, F. A. (2019): Chimpanzees and their mammalian sympatriates in the Issa Valley, Tanzania. – African Journal of Ecology 57: 31-40. DOI 10.1111/aje.12570.

[54] Programme on African protected Areas and Conservation (Papaco)—International Union for Conservation of Nature (2009): Sénégal: Parc National du Niokolo Koba. Evaluation de l'efficacité de gestion du Parc National du Niokolo Koba, Enhancing our Heritage (EoH) du Programme des Aires Protégées de l'Afrique du Centre et de l'Ouest. – IUCN-Regional Protected Areas, West Africa.

[55] Pruetz, J. D., Marchant, L. F., Arno, J., McGrew, W. C. (2002): Survey of Savanna Chimpanzees (*Pan troglodytes verus*) in Southeastern Senegal. – American Journal of Primatology 58: 35-43. doi.org/10.1002/ajp.10035.

[56] Pruetz, J. D., Fulton, S. J., Marchant, L. F., McGrew, W. C., Schiel, M., Waller, M. (2008): Arboreal nesting as anti-predator adaptation by savanna chimpanzees (*Pan troglodytes verus*) in southeastern Senegal. – American Journal of Primatology 70: 393-401. doi.org/10.1002/ajp.20505.

[57] Pruetz, J. D., Ballahira, R., Camara, W., Lindshield, S., Marshack, J. L., Sahdiako, M., Villalobos-flores, U. (2012): Update on the Assirik chimpanzee (*Pan troglodytes verus*) population in Niokolo Koba National Park, Senegal. – Pan African News 19: 8-11.

[58] Riley, E. P., Mackinnon, K., Fernandez-Duque, E., Setchell, J. M., Garber, P. A. (2014): Code of best practices for field primatology. – Resour doc, International Primatology Society, American Society of Primatologist. https://www.asp.org/resources/docs/Code%20of_Best_Pratices%20Oct%202014pdf.

[59] Russak, S. M., McGrew, W. C. (2008): Chimpanzees as fauna: comparisons of sympatric large mammals across long-term study sites. – American Journal of Primatology 70: 402-409. DOI: 10.1002/ajp.20506.

[60] Sales, L., Ribeiro, B. R., Chapman, C. A., Loyola, R. (2020): Multiple dimensions of climate change on the distribution of Amazon primates. – Perspective Ecology Conservation 18: 83-90. doi.org/10.1016/j.pecon.2020.03.001.

[61] Samson, D. R. (2012): The chimpanzee nest quantifield: morphology and ecology of arboreal sleeping platforms within the dry habitat site of Toro-Semliki Wildlife Reserve, Uganda. – Primates 53: 357-364. doi.org/10.1007/s10329-012-0310-x.

[62] Samson, D. R., Hunt, K. D. (2014): Chimpanzees preferentially select sleeping platform construction tree species with biomechanical properties that yield stable, firm, but compliant nests. – PLoS One 9. doi.org/10.1371/journal.pone.0095361.

[63] Sarr, M. A., Zorome, M., Seidou, O., Bryant, C. R., Gachon, P. (2013): Recent trends in selected extreme precipitation indices in Senegal—a change-point approach. – Journal of Hydrology 505: 326-334. DOI: http://dx.doi.org/10.1016/j.jhydrol.2013.09.032.

[64] Sarr, M. A., Seidou, O., Tramblay, Y., El Adlouni, S. (2015): Comparison of downscaling methods for mean and extreme precipitation in Senegal. – Journal of Hydrology 4: 369-385. dx.doi.org/10.1016/j.ejrh.2015.06.005.

[65] Schwitzer, C., Mittermeier, R. A., Rylands, A. B., Chiozza, F., Williamson, E. A., Byler, D., Wich, S., Humle, T., Johnson, C., Mynott, H., McCabe G (eds.) (2019): Primates in Peril: The World's 25 Most Endangered Primates 2018-2020. – IUCN SSC Primate Specialist Group, International Primatological Society, Global Wildlife Conservation, and Bristol Zoological Society, Washington, DC.

[66] Sesink Clee, P. R., Abwe, E. E., Ambahe, R. D., Anthony, N. M., Fotso, R., Locatelli, S., Maisels, F., Mitchell, M. W., Morgan, B. J., Pokempner, A. A., Gonder, M. K. (2015): Chimpanzee population structure in Cameroon and Nigeria is associated with habitat variation that may be lost under climate change. – BMC Evolution Biology 15: 1-13. doi.org/10.1186/s12862-014-0275-z.

http://www.aloki.hu ● ISSN 1589 1623 (Print) ● ISSN 1785 0037 (Online)
DOI: http://dx.doi.org/10.15666/aeer/2003_26632681

[67] Sousa, J., Casanova, C., Barata, A. V., Sousa, C. (2014): The effect of canopy closure on chimpanzee nest abundance in Lagoas de Cufada National Park, Guinea-Bissau. – Primates 55: 283-292. doi.org/10.1007/s10329-013-0402-2.
[68] Stanford, C. B., O'Malley, R. C. (2008): Sleeping tree choice by Bwindi chimpanzees. – American Journal of Primatology 70: 642-649. DOI 10.1002/ajp.20539.
[69] Stewart, F. A., Pruetz, J. D. (2013): Do chimpanzee nests serve an anti-predatory function? – Am J Primatol 75: 593-604. DOI 10.1002/ajp.22138.
[70] Tutin, C. E. G., Fernandez, M. (1984): Nationwide census of Gorilla (*Gorilla g. gorilla*) and Chimpanzee (*Pan t. troglodytes*) Populations in Gabon. – American Journal of Primatology 6: 313-336. doi.org/10.1002/ajp.1350060403.
[71] Tutin, C. E. G., McGrew, W. C., Baldwin, P. J. (1981): Responses of Wild Chimpanzees to Potential Predators. – In: Chiarelli, A. B., Corruccini, R. S. (eds.) Primate Behavior and Sociobiology. Proceedings in Life Sciences. Springer, Berlin, pp. 136-141. doi.org/10.1007/978-3-642-68254-4_19.
[72] Tutin, C. E. G., McGrew, W. C., Baldwin, P. J. (1983): Social ORGAxNIZATION of Savanna-dwelling Chimpanzees *Pan troglodytes verus,* at Mont Assirik, Senegal. – Primates 24: 154-173.
[73] United Nations Educational, Scientific and Cultural Organization/International Union for Conservation of Nature World Heritage Sites (2011): Niokolo Koba National Park (Senegal). – UNESCO, Paris.
[74] United Nations Educational, Scientific and Cultural Organization (2019): State of conservation of the properties inscribed on the List of the World Heritage in Danger. – 43rd Session of the World Heritage Committee (WHC/19/43. COM/7A.Add), Baku, Republic of Azerbaijan.
[75] United Nations Environment Programme/Convention on the Conservation of Migratory Species of Wild Animals/The twelfth Session of the Conference of the Parties (2017): Proposal for a concerted action for the nut-cracking chimpanzees of West Africa (*Pan troglodytes verus*) already listed on appendices I and II of the convention. – 12th Meeting of the Conference of the Parties, Manilla, Philippines, p. Doc. 25.1.1.
[76] van Casteran, A., Sellers, W. I., Thorpe, S. K. S., Coward, S., Crompton, R. H., Myatt, J. P., Ennos, R. (2012): Nest-building orangutans demonstrate engineering know-how to produce safe, comfortable beds. – PNAS (USA) 109: 6873-6877. DOI: 10.1073/pnas.1200902109.

http://www.aloki.hu ● ISSN 1589 1623 (Print) ● ISSN 1785 0037 (Online)
DOI: http://dx.doi.org/10.15666/aeer/2003_26632681

CONSEQUENCES OF CLIMATE CHANGE ON THE FLORISTIC COMPOSITION OF KHULAIS REGION, SAUDI ARABIA

ALSHERIF, E. A.[1,2*] – ALMAGHRABI, O. A.[3]

[1]*Biology Department, College of Science and Arts at Khulis, University of Jeddah, Jeddah, Saudi Arabia*

[2]*Department of Botany and Microbiology, Faculty of Science, Beni-Suef University, Beni Suef, Egypt*

[3]*Department of Biology, College of Science, University of Jeddah, Jeddah, Saudi Arabia*

[*]*Corresponding author*
e-mail: eaalsherif@uj.edu.sa; phone: +96-656-097-3189

(Received 4th Jan 2022; accepted 25th Feb 2022)

Abstract. Climate change has resulted in profound changes in biodiversity throughout the globe. It has also become a serious source of worry for environmentalists and governments alike. The goal of this study is to provide first-hand information about the effects of climate change on floristic composition in the Khulais region, Saudi Arabia, during the last decade. Data obtained from the metrological station showed that the amount of annual precipitation decreased, while the mean annual temperature exhibited an increase. The results showed that Lange, De Martonne and Emberger's drought indices, ranged between ($3x10^{-5}$ to 2.8), ($3x\ 10^{-5}$ to 2.0), and ($2x\ 10^{-4}$ to 14.8), respectively, which decreased in 2020 by between 50% and 230% from 2011. Most plant species in the studied region showed a decrease in their frequency. 50 out of 251 species showed a frequency change of more than ten percent, which was recorded in the first survey. Species that showed the largest declines were mostly a variety of agricultural weeds and valley plants, while species of rocky and mountain habitats were less affected. Only seven species showed a relative increase in their frequency, *Prosopis Juliflora* and *Trianthema portulacastrum* L. recording the highest change in their frequency. This work serves as a warning to those interested in wild plants and to governments to take appropriate measures to protect the arid environment threatened by the impact of climate change.
Keywords: *Prosopis, biodiversity, drought indices, Trianthema, invasive*

Introduction

A major and direct biological consequence of climate change is the has led to of rising ambient temperatures on organisms' thermal performance. Climate change has influenced huge changes in biodiversity across the globe, and it is becoming a serious concern for environmentalists and governments alike. Higher plants are the principal producers in the majority of terrestrial ecosystems, and their distribution and diversity have a significant impact on the distribution and variety of most other creatures (Carvell et al., 2006; Jonason et al., 2010; Berg, 2012). Plant species, on the other hand, are susceptible to a wide variety of environmental changes, frequently to the point where plant communities as a whole or localized species pools are impacted (Arts, 2002; Maad et al., 2009; Cousins et al., 2015; Hedwall and Brunet, 2016; Sun et al., 2022). So, keeping a close eye on changes in the diversity and frequency of vascular plants should be a top goal (Nielsen et al., 2019). Climate change has caused significant alterations in species distributions and abundances during the last 30 years (Parmesan et al., 2003; Root et al., 2003) and has been linked to one species-level extinction (Root et al., 2003). Pounds et al. (1999) stated that flora composition is often used to forecast site circumstances, such as temperature

http://www.aloki.hu ● ISSN 1589 1623 (Print) ● ISSN 1785 0037 (Online)
DOI: http://dx.doi.org/10.15666/aeer/2003_26832695

and site characteristics (Berges et al., 2006). Due to its continental climate, cold winters, scorching summers, and sporadic rainfall, the Kingdom of Saudi Arabia (KSA) is one of the nations most sensitive to climate change (Al-Wabel et al., 2020).

Despite the fact that the Mediterranean and its surrounding territories have been extensively studied in recent decades (Hoskins and Pedder, 1980; Trigo et al., 2002; Lee et al., 2011). Saudi Arabia's scientific knowledge and literature on climate and climate change is dispersed, fragmentary, and inadequate. Future regional climate change and its impacts on Saudi Arabia have received little attention in study. Alkolibi (2002) looked at how general circulation models predicted climate change, as well as the consequences of increasing temperatures and decreased precipitation on Saudi Arabia's water resources and agriculture. With the exception of a narrow tong running from the north to the center of KSA, Meehl et al. (2007) forecast a 0.1 mm/day increase in mean annual surface evaporation throughout most of KSA by the end of the twenty-first century. Williams et al. (2012) reviewed the effect of climate change on animal in Saudi Arabia, Zekâi (2013) studied the probable links between desertification and climate change in dry areas. Elnesr and Alazba (2010) carried out a study to understand the behavior of its temperature climatology in Saudi Arabia. Climate change and water resources were researched by Tarawneh and Chowdhury (2018), who reported an increase in temperature in all regions and a decrease in rainfall in many regions. According to Al-Wabel et al. (2020), the Kingdom of Saudi Arabia (KSA) is one of the most susceptible nations to climate change owing to its continental climate, harsh winters, scorching summers, and unpredictable rainfall. Many studies (Muller, 1982; Moore, 1986) provided brief and sound climatological information on the Arabian Peninsula, demonstrating that the Arabian Peninsula has a wide climatic spectrum, ranging from the snows of the Asir Province in Saudi Arabia to the overpowering humidity of the Arabian Gulf, from the searing heat of the Rub Al Khali to the monsoon precipitation in the Qara mountains in Dhofar. Plant diversity and distribution data, which must be gathered on a continuous basis due to continuing climate change, are critical for conservation biology and resource management at all scales. The diversity of plant species may be used to determine the sustainability of an ecosystem (Gamoun et al., 2012). The goal of this research is to get firsthand knowledge of the impacts of climate change on floristic composition in the Khulais region, Saudi Arabian.

Materials and methods

Study area

The region under investigation, the Khulais region, is situated between longitudes 15 and 39 degrees east and latitudes 22 and 30 degrees north in the Arabian Shield, which encompasses the western chains of Hijaz and Asir highlands, as well as the western portion of the Nagd plateau (*Figure 1*). Its soils are made up of basaltic volcanic rocks with textures varying from silty clay to coarse sandy, pH levels ranging from 7.2 to 7.6, and salinity levels ranging from 0.4 to 7.4 mM/cm. With an annual average rainfall of 35.1 mm, the climate is hot in the summer and warm in the winter. Rainfall is irregular and unpredictable, in addition to its paucity.

http://www.aloki.hu ● ISSN 1589 1623 (Print) ● ISSN 1785 0037 (Online)
DOI: http://dx.doi.org/10.15666/aeer/2003_26832695

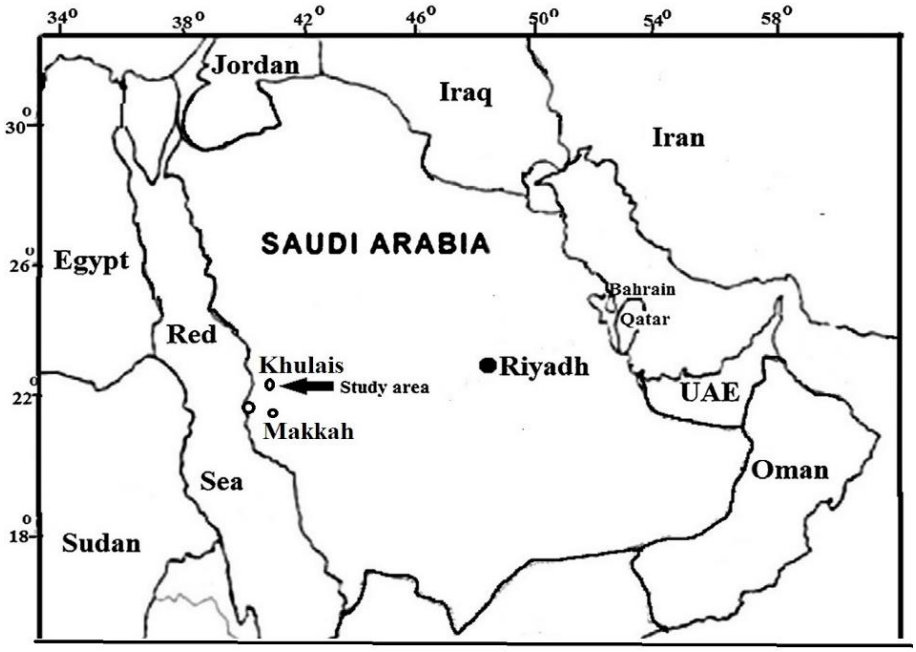

Figure 1. *Location map showing the study area*

Field survey and the data sets

Two surveys of the flora of Khulais, conducted in 2010–2011 and 2020–2021, were compared in this report. The first survey was carried out during the period of September 2010 to the September 2011, while the second one was carried out between September 2020 to September 2021. The species recorded in the first survey were published by Alsherif et al. (2013). Four study sites were selected to do the second survey, the GPS positions of the sampling sites are as follows: 22° 7'38.41"N 39°17'46.00"E, 22° 7'30.21"N 39°28'49.43"E, 22° 7'47.68"N47.68 '31°39 "E and 21°55'47.29"N 0.02'19°39"E. It was taken into account that the second survey should be in the same areas as the first survey, with the exclusion of areas in which human activity appeared, such as road construction, land use for agriculture and housing construction. Frequency detection was carried out using the quadrat point approach (Daget et al., 1995). The research sites' plant species compositions were obtained by randomly planting one square meter quadrat at ten different locations at each site. Frequency (F), the distribution of a certain species was estimated as % of occurrence:

Frequency (F%) = (Total number of quadrates studied/number of quadrates where the species occurred) X100. With the use of standard flora reference books, plant species within each quadrat were collected and identified (Collenette, 1989, 1999; Chaudhary, 2001; Miller, 2007). Life form categories were constructed according to Raunkiaer's guidelines (Raunkiaer, 1934).

Drought indices determination

The study area's climate data for the previous ten years was obtained from the Jeddah meteorological station. In many locations of Saudi Arabia, aridity knowledge is required to explain landscape features and the efficient use of water resources. Aridity indices provide a straightforward approach to represent the precipitation-to-evaporation ratio.

http://www.aloki.hu ● ISSN 1589 1623 (Print) ● ISSN 1785 0037 (Online)
DOI: http://dx.doi.org/10.15666/aeer/2003_26832695

The regional variation of three climatic indices, the Lang index, Martonne index, and Emberger aridity index, was explored in this work to establish the climate structure of the Khulais area.

De Martonne index

The Martonne index calculated as described in the following equation:

$$\mathrm{IDM} = \frac{\mathrm{Pav}}{\mathrm{Tav}} + 10 \qquad \text{(Eq.1)}$$

where IDM= De Martonne's index, Pav= average rainfall, Tav= average temperature.

Lang index

Lang index was calculated as described in the following equation:

$$\mathrm{L} = \mathrm{R}/\mathrm{T} \qquad \text{(Eq.2)}$$

where L= Lang's rainfall factor, R = Average rainfall, T= Average temperature.

Emberger aridity

Emberger aridity was calculated as described in the following equation:

$$\mathrm{IP} = \frac{100\mathrm{x}\ \mathrm{P}}{\mathrm{T} - \mathrm{t}} \qquad \text{(Eq.3)}$$

where Ip is the Emberger index, P is the average annual precipitation, T is the average maximum temperature for the hottest month, while t is the average lowest temperature for the coldest month.

Results

General climate and arid indices of the region

Data obtained from the metrology station showed that the amount of annual precipitation that has been recorded in the last decade in general is very small. It is not fixed, it changes from year to year, but it is very clear that it is decreasing. The past ten years have varied in recording the amount of rain and have ranged between 0.001 and 86.4 milliliters throughout the year (*Table 1*). The results also showed that the amount of rain decreased by 85% in the years following the year 2011, except for the year 2018. It's worth noting that the mean annual temperature is constantly increasing from year to year. The average annual temperatures increased by between 0.7 and 1.3 degrees Celsius. A decrease in the relative humidity was observed during the last three years compared to the first three years of this decade by an amount of 7%. The relative humidity showed slightly changing, it ranged between 51% and 57%.

In addition, the three drought indices measured in the current study for the last decade confirmed that the study area is an arid area. The results also showed that Lange, De Martonne and Emberger's indices, ranged between (3x10-5 to 2.8), (3x 10-5 to 2.0) and (2x 10-4 to 14.8), respectively (*Table 2*). All drought indices decreased in 2020 by between 50 and 230% from 2011.

http://www.aloki.hu ● ISSN 1589 1623 (Print) ● ISSN 1785 0037 (Online)
DOI: http://dx.doi.org/10.15666/aeer/2003_26832695

Table 1. *The annual total precipitation (ml), mean temperature (°C) and mean relative humidity (%) of the studied area. ± S.D*

Year	2011	2012	2013	2014	2015	2016	2017	2018	2019	2020	2021
Total Precipitation	80.6 ±21.8	12.5 ±2.5	0.001 ±0.0	52.0 ±9.5	33.0 ±6.4	10.5 ±1.7	24.0 ±4.8	86.4 ±20.1	35.3 ±8.5	40 ±5.8	10.1 ±1.8
Mean Temperature	28.4 ±3.4	29.1 ±3.4	29.2 ±2.8	29.5 ±2.9	29.4 ±3.4	29.7 ±3.0	29.3 ±3.3	29.7 ±3.2	29.6 ±3.7	29.3 ±3.7	26.0 ±2.9
Mean relative humidity	57 ±1.2	55 ±2.0	56 ±1.6	53 ±1.4	53 ±1.7	54 ±1.1	55 ±1.1	54 ±1.5	51 ±1.6	52 ±1.3	52 ±1.4

Table 2. *Aridity indices for the study area during last decade*

	2011	2012	2013	2014	2015	2016	2017	2018	2019	2020	2021
Lange index	2.8	0.4	$3X10^{-5}$	1.72	1.1	0.3	0.8	2.9	1.1	1.3	1.3
De Martonne Aridity Index	2.0	0.3	$3X10^{-5}$	1.3	0.8	0.2	0.6	2.1	0.8	1.0	1.0
Emberger Index	13.5	2.0	$2x10^{-4}$	9.8	5.0	1.7	4.0	14.8	6.5	6.1	6.1

Change in frequency of plant species

The majority of plant species in the studied region showed a decrease in their frequency. 50 out of 251 species showed a frequency change of more than ten percent, which was recorded in the first survey. The species that showed the largest declines over the last decade are mostly a collection of arable weeds and valley plants, while species of rocky and mountain habitats were less affected (*Table 3*).

The greatest changes were noted for the following items when compared to their frequency in the second survey. Digera muricata, Capsella pursa pastoris, Cleome paradoxa, and Indigofera hoschstettei all of which decreased by more than 15%. Only seven species showed relative increases, and the invasive species Prosopis Juliflora and Trianthema portulacastrum L. showed the highest increase, both of which increased by more than 15%. Many common species in open/agricultural lands have also seen severe reductions, but to a lesser extent, such as Convolvulus Fatemensis, Euphorbia granulate, Glinus lotoides, and Lolium perenne (*Table 3*). It is not only the invasive plants that have increased their frequency, but also some native species such as Tamarix aphylla, Portulaca oleracea and Suaeda monica which increased its frequency by 10 to 12%.

Life forms of the changed species

The current results showed that the proportions of the life forms of species that recorded a change in their frequencies slightly differed from the proportions that were recorded in the initial survey of the area (*Table 4*). Therophytes recorded the highest percentage (50.9%) of plants that changed their frequency, followed by chaemophytes, while geophytes recorded the lowest percentage (3.7%). It is also noted that most of the species that showed a change in their frequency were annuals, while perennials recorded the lowest percentage.

http://www.aloki.hu ● ISSN 1589 1623 (Print) ● ISSN 1785 0037 (Online)
DOI: http://dx.doi.org/10.15666/aeer/2003_26832695

Table 3. *The species that showed a highest change during the study period*

Family	Species	Change %	Habitat	Life form	Chorology
Aizoaceae	*Aizoon canariense* L.	-11	Sandy soil- Wadi	Th	SU
	Sesuvium sesuviodes(Fenzl) Verdc.	13	sabkha- salt affected soil	Ch	TR
	Trianthema portulacastrum L.	15	Cultivated lands-Garden	Th	AM
Amaranthaceae	*Digera muricata* (L.) Mast.	-17	Wadi	Th	TR
Apocynaceae	*Rhazya stricta* Decne.	-12	Wadi	Ch	SA+SU
Asclepiedaceae	*Caralluma acutangula* (Decne.) N.E.Br.	-10	Rocky habitats	Th	SA+SU
	Odontanthera radians (Forssk.) D.V.Field	-14	Wadi	Ch	TR
Asteraceae	*Asphodelus tenuifolius* (Cav.) Baker	-16	Wadi	Th	SA
	Asteriscus hierochunticus (Michon) Wiklund	-11	Wadi	Th	SA+SU
Boraginaceae	*Arnebia decumbens* (Vent.) Coss.&Kralik	-13	Wadi	Ch	SA
	Moltkiopsis ciliate (Forssk.) I.M.Johnst.	-13	Wadi	Th	Cosm
Brassicaceae	*Capsella pursa pastoris* (L.) Medik.	-18	Cultivated lands-Garden	Th	ME+SA
	Schouwia purpurea (F0rssk.) Schweinf.	-16	Wadi	Ch	SU
Capparaceae	*Cadaba farinosa* Frossk.	-11	Wadi	Th	SU
	Diptergium glaucum Decne.	-12	Wadi	Ch	IT
	Mareua oblongifolia (Frossk.) A.Rich.	-12	Wadi	Ch	SU
Chenopodiacea	*Haloxylon scoparium* Pomel	-16	Wadi	Ch	SU
	Suaeda monica Frossk.ex J.F. Gmel.	10	salt affected soil	Ch	SU
Cleomaceae	*Cleome droserfolia* (Forssk.)Delile	-12	Wadi- Cultivated lands	Ch	SU
	Cleome paradoxa R.Br.exDC.	-17	Wadi	Ch	SA
Convolvulaceae	*Convolvulus fatemensis* Kunze	-14	Wadi- Cultivated lands	Ch	Cosm
Euphorbiaceae	*Euphorbia granulata* Frossk.	-11	Wadi- Cultivated lands	Ge	SA
Liliaceae	*Dipcadi erythraeum* Webb & Berth.	-10	Wadi	Th	TR
Lythraceae	*Ammannia baccifera* L.	-16	Wadi	Ph	SA
Mimosaceae	*Prosopis juliflora* (Sw.) DC.	18	Wadi-swampy	Th	ME+IT
Molluginaceae	*Glinus lotoides* L.	-16	Wadi- Cultivated lands	Th	TR
	Mollugo cerviana (L.) Ser.	-14	Wadi	Th	SA
Papilionaceae	*Astragalus vogelii* (Webb) Bornm.	-12	Wadi	Th	SA+SU
	Crotalaria microphylla Vahl	-17	Wadi	Ch	SU
	Indigofera hoschstettei Baker	-19	Wadi	Th	SU
	Trigonella stellata Forssk.	-10	Wadi	Th	SA
	Tephorosia nubica (Boiss.) Baker	-10	Wadi	He	SA+SU
	Trigonella hamosa L.	-12	Wadi	Th	ME+IT

http://www.aloki.hu ● ISSN 1589 1623 (Print) ● ISSN 1785 0037 (Online)
DOI: http://dx.doi.org/10.15666/aeer/2003_26832695

Family	Species	Change %	Habitat	Life form	Chorology
Poaceae	*Cenchrus ciliaris* L.	-10	Wadi	He	ME+IT
	Lamarckia aurea (L.) Moench	-13	Wadi	He	SA+SU
	Lolium perenne L.	-13	Wadi- Cultivated lands	Th	Cosm
	Panicum turgidum Forssk.	-15	Wadi	He	SA
	Lolium rigidum Gaudin	-13	Cultivated lands	Ch	SA
	Polypogon monospliensis (L.)	-16	Cultivated lands	Ph	SA+SU
Portulacaeae	*Portulaca oleracea* L.	12	Cultivated lands	Ph	SU
Resedaceae	*Ochradenus baccatus* Del.	-10	Wadi	Ch	ME+SA
	Oligomeris linifolia (Fahl ex Hornen) J.F. Macbr.	-16	Wadi	Ch	SA
Rutaceae	*Haplophyllum tuberculatum* (Forssk.) A.Juss.	-11	Wadi	Th	ME+SU
Solanaceae	*Datura innoxia* Mill.	10	Wadi- Cultivated lands	Th	SA+SU
	Lycium shawii Roem. & Schult.	-10	Wadi	Th	SA
	Solanum incanum L.	-14	Wadi- Cultivated lands	Th	ME+IT
Tamaricaceae	*Tamarix aphylla (L.) Karst.*	10	Wadi- Salty habitat	Ph	SU
Tiliaceae	*Corchorus depressus* (L.) Stocks	-12	Cultivated lands	Th	SA+ME
Zygophyllaceae	*Fagonia indica* Burm. f.	-10	Wadi	Th	ME+IT
	Tripulus terrestris L.	-11	Wadi	Th	SU

Table 4. *Life forms and chorotype % of the species that showed the highest change*

Life form		Chorotype	
Hemi-cryptophytes	7.6	Cosmopolitan	5.88
Chamaephytes	30.2	Tropical	9.88
Geophytes	3.7	Mediterranean+ Sudano-Zambezian	15.71
Phanerophytes	7.6	Mediterranean + Sudano-Zambezian	17.64
Therophytes	50.9	Saharo-Arabian	21.56
		Sudano-Zambezian	23.52
		Pluriregional	5.81

Chorological types of the changed species

Table 4 shows the chorological types of species that have a higher (more than 10%) change in their frequency. Sudanian elements had the greatest percentage (23.5%), followed by Saharo-Arabian elements (21.5%), which was the polar opposite of the original survey, which had Saharo-Arabian components scoring higher than Sudanian elements. The largest change occurred in the biregional type which included the Mediterranean type; their change was 17%, while their percentage in the initial survey was 8%.

http://www.aloki.hu ● ISSN 1589 1623 (Print) ● ISSN 1785 0037 (Online)
DOI: http://dx.doi.org/10.15666/aeer/2003_26832695

Discussion

Since the previous decade, the present research found a rise in mean temperatures and a reduction in total precipitation in the analyzed region. It was fascinating to see whether the flora's makeup mirrored these unusual circumstances. The race between climate change and vegetation has already begun, according to various studies (Hughes, 2000; Walther et al., 2005; Lenoir, 2008). The study of plant diversity in dry regions is crucial for determining their ecological and economic worth, as well as the necessity for conservation and restoration in the face of current climate change. The collected data confirms that the study area is a dry area in general due to the low values of drought indices. It also showed that the area was drier during the second survey compared to the timing of the initial survey. Areas are classified as arid areas if the De Martonne index is less than 10, the Emberger index is less than 30 and the Lange index is less than 40 (De Martonne, 1923; Emberger, 1932).

It was intriguing to see whether these circumstances were mirrored in the flora composition. Adaptations to these environmental changes were certainly reflected in the shift in species frequency, according to the current research. Our findings demonstrate that the overall frequency of the majority of common ground flora species has altered. The key trends show that wadi, garden, and arable weeds are declining, while invasive species are increasing. Climate change has had a substantial impact on changes in the flora during the past century, according to a prior research based on data from Swedish regions (Auffret and Thomas, 2019). Large reductions in arable weeds recorded in the present study could be explained owing to lower water availability and increased evaporation as a consequence of higher average temperatures and lower rainfall. The results of the current study are in agreement with IPCC (2019) who reported that the loss of species variety, decreased plant production, reduction of soil structure and fertility, and an increase in water loss, soil erosion, and sand movements are the major consequences of arid and semiarid ecosystem degradation. Species with a poor tolerance for warmth, limited acclimation capacity, and restricted dispersion ability are at the highest danger of extinction as a result of fast climate change (Williams et al., 2007). The life form therophytes exhibited the most changed life form, because they blossom and produce lush growth after adequate rain (AlSherif et al., 2013, 2022). In the present study, valley habitats showed the highest change in plant species frequency because valleys in arid and semi-arid environments are the most affected sites when it comes to water stress due to drought and high temperatures (Eheart and Tornil, 1999). Smooth rocks in rocky environments help to condense water vapor and thus increase the soil water content (Le Houe´rou, 1998), which explains the small change in the frequency of species inhabiting the rocky habitats in the current study. In the absence of precipitation, Le Houe´rou (1998) observed that species living in dry settings use several techniques to gather water from humid air. When mountains or steep slopes obscure the clouds, a fog zone forms. This wetness encourages the growth of plant communities (Moore, 1986; Rundel et al., 1991). The current results indicate the decrease in the amount of rain, which led to the previous result. Although several studies have shown that desert ecosystems are among the least infested in the world, at least in terms of invasive and naturalized species (Lonsdale, 1999; Brooks and Pyke, 2001), the current study contradicts this due to the large spread of *P. juliflora*. Four of the recorded species with an increased frequency were considered invasive species in the area (Jacob et al., 2016). The sudden rise in frequency might be a sign of a changing environment. It was documented that climate change has been linked to extinction in the past via beneficial impacts on species that have unfavorable

http://www.aloki.hu ● ISSN 1589 1623 (Print) ● ISSN 1785 0037 (Online)
DOI: http://dx.doi.org/10.15666/aeer/2003_26832695

interactions with a target species, such as competitors (Wethey, 2002; Suttle et al., 2007). Warming temperatures, according to Stachowicz et al. (2002), may benefit imported species while aggravating their detrimental impacts on local flora and fauna. *Prosopis juliflora* was reported as one of the currently recorded Saudi invasive species by Jacob et al. (2016). It has a significant impact on ecosystems and agriculture, eradicating or displacing many native species from areas rich in vegetation, especially in valley habitats. *P. juliflora* is characterized by large amount of seeds, fast growth, desirable and diseased pods, seeds that maintain viability for farm animals and wild animal droppings, resistance to surfing (Shiferaw et al., 2004, 2022), extraordinary ability to re-germinate and build canopy quickly, and higher water use efficiency (Shaltout et al., 2013), all of this helps him to conquer new territories. The second most invasive species, *Trianthema portulacastum*, recorded in the current study, was reported as having a high invasion potential (Felker et al., 1983). Fahmy et al. (2019) stated that the characteristics of the seeds and seedlings of *T. portulacastrum* serve as indicators of the species' extensive ecological range. Among these characteristics is the ability to produce a high number of non-dormant seeds that germinate at a wide range of temperatures (20 - 45°C). Lee et al. (2001) documented that the global distribution of *T. portulacastrum*, which is characterized by warm or hot weather and high solar radiation, suggests that the seeds, seedlings, and adult plants are resistant and/or acclimated to stress conditions. The halophytic species *Tamarix aphylla* and *Sesuvium sesuviodes* are among the recorded invasive plants. It may be that changing climatic conditions led to an increase in soil salinity. Gaur and Squires (2018) stated that as a consequence of climate change, dry and semiarid zones where evaporation exceeds rainfall are being considerably worsened, causing soil erosion and salinization, leading to the increase of halophytes. It's important to remember, however, that changes in climate have direct effects on species, but they also have indirect effects on species through climate-induced changes in other environmental conditions like soil water shortage, soil chemistry, drainage, and erosion. The final effect of climate change on the structure and functioning of natural and semi-natural habitats and environments is determined by these abiotic impacts, as well as the direct response of plant species.

Conclusion

In the research area, average temperatures and yearly rainfall have changed, resulting in a decline in the frequency of most plant species and an increase in the frequency of invasive plants, indicating that climate change is having a significant influence on the region's flora. If this change continues, the negative impact on the plants of the region will increase. This phenomenon has a negative impact on not just agriculture, but the availability of water as well. Invasion from non-native plants is seen as a major danger to ecosystem structure and function.

Recommendations

The findings, suggestions, and guidance are supposed to be beneficial to administrators, both local and central in ensuring the environmental situation's long-term viability and maximum benefits. The sharp decline in biodiversity suggests that habitat conservation should be prioritized on a national level. Our results strongly support the need for broad-scale floristic diversity monitoring across both short and long-time scales.

http://www.aloki.hu ● ISSN 1589 1623 (Print) ● ISSN 1785 0037 (Online)
DOI: http://dx.doi.org/10.15666/aeer/2003_26832695

In addition, decision makers should implement a policy to reduce *P. juliflora*, and protect the native flora from the danger of this plant.

Acknowledgements. The authors extend their appreciation to the Deputyship for Research & Innovation, Ministry of Education in Saudi Arabia for funding this research work through the project number (MoE-IF-20-02/06).

REFERENCES

[1] Alkolibi, F. M. (2002): Possible effects of global warming on agriculture and water resources in Saudi Arabia: impacts and responses. – Climate Change 54: 225-245.

[2] Alsherif, E. A., Ayesh, A. M., Rawi, S. M. (2013): Floristic composition, life form and chorology of plant life at Khulais region western Saudi Arabia. – Pakistan Journal of Botany 45: 29-38.

[3] Alsherif, E. A., Al-Shaikh, T. M., AbdElgawad, H. (2022): Heavy Metal Effects on Biodiversity and Stress Responses of Plants Inhabiting Contaminated Soil in Khulais, Saudi Arabia. – Biology 11: 164. https://doi.org/10.3390/biology11020164.

[4] Al-Wabel, M. I., Sallam, A., Ahmad, M., Elanazi, K., Usman, A. R. A. (2020): Extent of Climate Change in Saudi Arabia and Its Impacts on Agriculture: A Case Study from Qassim Region. – In: Fahad, S. et al. (eds.) Environment, Climate, Plant and Vegetation Growth. Springer, Cham. https://doi.org/10.1007/978-3-030-49732-3_25.

[5] Arts, G. H. P. (2002): Deterioration of Atlantic soft water macrophyte communities by acidification, eutrophication and alkalinisation. – Aquatic Botany 73: 373-393. https://doi.org/10.1016/S0304 -3770(02)00031-1.

[6] Auffret, A. G., Thomas, C. D. (2019): Synergistic and antagonistic efects of land use and non-native species on community response to climate change. – Global Change Biology 25(12): 4303-4314. https://doi.org/10.1111/gcb.14765.

[7] Berg, Å. (2002): Composition and diversity of bird communities in Swedish farmland-forest mosaic landscapes. – Bird Study 49: 153-165.

[8] Berges, L., Gegout, J. C., Franc, A. (2006): Can understory vegetation accurately predict site index? A comparative study using floristic and abiotic indices in sessile oak (Quercus petraea Liebl.) stands in northern France. – Annals of Forest Science 63: 31-42.

[9] Brooks, M. L., Pyke, D. A. (2001): Invasive plants and fire in the deserts of North America. – In: Galley, K. E. M., Wilson, T. P. (eds.) Proceedings of the invasive species workshop: the role of fire in the control and spread of invasive species. Fire Conference 2000: The First National Congress on Fire Ecology, Prevention, and Management, Miscellaneous Publication No. 11, Tall Timbers Research Station, Tallahassee, Fl, pp. 1-14.

[10] Carvell, C., Roy, D. B., Smart, S. M., Pywell, R. F., Preston, C. D., Goulson, D. (2006): Declines in forage availability for bumblebees at a national scale. – Biological Conservation 132: 481-489.

[11] Chaudhary, S. (2001): Flora of the Kingdom o/Saudi Arabia. – Ministry of Agriculture and Water: Riyadh, Saudi Arabia, Volume 2, 432p.

[12] Collenette, S. (1985): An Illustrated Guide to the Flowers of Saudi Arabia. – Corpion Publishing Ltd.: London, UK.

[13] Collentette, S. (1999): Wild Flowers of Saudi Arabia. – National Commission for Wildlife Conservation and Development: Riyadh, Saudi Arabia.

[14] Cousins, S. A. O., Auffret, A. G., Lindgren, J., Trank, L. (2015): Regional-scale land-cover change during the 20th century and its consequences for biodiversity. – Ambio 44 (Suppl 1): 17-27. https ://doi.org/10.1007/s1328 0-014-0585-9.

[15] Daget, P., Godron, M. (1995): Pastoralisme: Troupeaux, Espaces et Sociétés. – Hatier-Aupelf: Uref, France, 510p.

http://www.aloki.hu ● ISSN 1589 1623 (Print) ● ISSN 1785 0037 (Online)
DOI: http://dx.doi.org/10.15666/aeer/2003_26832695

[16] De Martonne, E. (1923): Aréisme et indice d'aridité. – Compt. Rend. Séances Acad. Sci. 181: 1395-1398.
[17] Eheart, J. W., Tornil, D. W. (1999): Low-flow frequency exacerbation by irrigation withdrawals in the agricultural midwest under various climate change scenarios. – Water Resources Research 35: 2237-2246.
[18] Ellmouni, F. Y., Albach, D. C., Fouad, M. S., Fakhr, M. F. (2021): Genetic diversity analysis reveals weak population structure in invasive *Trianthema portulacastrum* L. at Fayoum depression, Egypt. – Turkish Journal of Botany 45: 541-552.
[19] Elnesr, M., Alazba, A. (2010): Spatio-Temporal Variability of Evapotranspiration over the Kingdom of Saudi Arabia. – Applied Engineering in Agriculture, ASABE, 26(5): 833-842.
[20] Emberger, E. (1932): Sur une formule climatique et ses applications en botanique. – La Météorologie, pp.423-432.
[21] Fahmy, G. M., Moussa, S. A., Farrag, H. F., Abd El Rehem, R. A. (2019): Seed and germination traits of the summer weed *Trianthema portulacastrum* L. – Egyptian Journal Experimental Biology (Bot) 15(2): 235-242. doi:10.5455/egyjebb.20190618082647.
[22] Felker, P., Cannell, G. H., Osborn, J. F., Clark, P. R., Nash, P. (1983): Effects of irrigation on biomass production of 32 *Prosopis* (mesquite) accessions. – Experimental Agriculture 19: 187-198. http://dx.doi.org/10.1017/S0014479700022638.
[23] Gamoun, M., Ouled-Belgacem, A., Hanchi, B., Neffati, M., Gill, F. (2012): Effet du pâturage sur la diversité floristique des parcours arides du Sud Tunisien. – Revue d'Ecologie (Terre Vie) 67: 271-282.
[24] Gaur, M. K., Squires, V. R. (eds.) (2018): Climate Variability Impacts on Land Use and Livelihoods in Drylands. – doi:10.1007/978-3-319-56681-8.
[25] Hedwall, P. O., Brunet, J. (2016): Trait variations of ground flora species disentangle the effects of global change and altered land-use in Swedish forests during 20 years. – Global Change Biology 22: 4038-4047. https ://doi.org/10.1111/gcb.13329.
[26] Hoskins, B. J., Pedder, M. A. (1980): The diagnosis of middle latitude synoptic development. – Quarterly Journal of the Royal Meteorological Society 106: 707-719.
[27] Hughes, L. (2000): Biological consequences of global warming: is the signal already apparent? – Trends in Ecology and Evolution 15(2): 56-61.
[28] IPCC (2019): Climate Change and Land. – In: Shukla, P. R., Skea, J., Calvo Buendia, E., Masson-Delmotte, V., Pörtner, H.-O., Roberts, D. C., Zhai, P., Slade, R., Connors, S., van Diemen, R., Ferrat, M., Haughey, E., Luz, S., Neogi, S., Pathak, M., Petzold, J., Portugal Pereira, J., Vyas, P., Huntley, E., Kissick, K., Belkacemi, M., Malley, J. (eds.) An IPCC special report on climate change, desertification, land degradation, sustainable land management, food security, and greenhouse gas fluxes in terrestrial ecosystems.
[29] Jacob, T., El-Sheikh, M. A., Alfarhan, A. H., Alatar, A. A., Mivadasan, M., Basahi, M., Al-Obaid, S., Rajakrishnan, R. (2016): Impact of alien invasive species on habitats and species richness in Saudi Arabia. – Journal of Arid Environments 127: 53-65.
[30] Jonason, D., Milberg, P., Bergman, K. O. (2010): Monitoring of butterflies within a landscape context in southeastern Sweden. – Journal for Nature Conservation 18: 22-33. https://doi.org/10.1016/j.jnc.2009.02.001.
[31] Lee, J., Chauhan, B. S., Johnson, D. E. (2011): Germination of fresh horse purslane (*Trianthema portulacastrum*) seeds in response to different environmental factors. – Weed Scence 59(4): 495-499.
[32] Le Houe´rou, H. N. (1998): Fog-dependent vegetation and ecosystems in the dry lands of Africa, paper presented at First Conference on Fog and Fog Collection. – International Development Research Centre, Vancouver, Canada, July 19-24, 1998.
[33] Lenoir, J., Gegout, J. C., Marquet, P. A., De Ruffray, P., Brisse, H. (2008): A significant upward shift in plant species optimum elevation during the 20th century. – Science 320(5884): 1768-1771.
[34] Lonsdale, W. M. (1999): Global patterns of plant invasions and the concept of invisibility. – Ecology 80: 1522-1536.

http://www.aloki.hu ● ISSN 1589 1623 (Print) ● ISSN 1785 0037 (Online)
DOI: http://dx.doi.org/10.15666/aeer/2003_26832695

[35] Maad, J., Sundberg, S., Stolpe, P., Jonsell, L. (2009): Floristic changes during the 20th century in Uppland, east central Sweden. – Svensk botanisk tidskrift 103: 67-104.
[36] Meehl, G. A., Stocker, T. F., Collins, W. D., Friedlingstein, P., Gaye, A. T., Gregory, J. M., Kitoh, A., Nutti, R. K., Murphy, J. M., Noda, A., Raper, S. C. B., Watterson, I. G., Weaver, A. J., Zhao, Z. C. (2007): Global climate projections. – In: Solomon, S., Qin, D., Manning, M., Chen, Z., Marquis, M., Averyt, K. B., Tignor, M., Miller, H. L. (eds.) Climate change 2007: the physical science basis. Contribution of working group I to the fourth assessment report of the Intergovernmental Panel on climate change. Cambridge University Press, Cambridge/New York.
[37] Miller, A. G., Cope, T. A. (2007): Flora of the Arabian Peninsula and Socotra. – Edinburgh University Press, 586p.
[38] Moore, E. (1986): Gardening in the Middle East. – Stacey International: London, UK, 144p.
[39] Mosallam, H. A. M. (2007): Comparative Study on the Vegetation of Protected and Nonprotected Areas, Sudera, Taif, Saudi Arabia. – International Journal of Agriculture and Biology 9(2): 202-214.
[40] Muller, M. J. (1982): Selected climatic data for a global set of standard stations for vegetation science. – In: Lieth, H. (ed.) Tasks for Vegetation Sciences. Kluwer Academic Publishers Group: Dordrecht, The Netherlands, pp. 143-285.
[41] Nielsen, T. F., Sand-Jensen, K., Dornelas, M., Bruun, H. H. (2019): More is less: net gain in species richness, but biotic homogenization over 140 years. – Ecology Letters 22(10): 1650-1657. https://doi.org/10.1111/ele.13361.
[42] Parmesan, C., Yohe, G. (2003): A globally coherent fingerprint of climate change impacts across natural systems. – Nature 421: 37-42.
[43] Pounds, J. A., Fogden, M. L. P., Campbell, J. H. (1999): Biological response to climate change on a tropical mountain. – Nature 398: 611-615.
[44] Raunkiaer, C. (1934): Life Forms of Plants and Statistical Geography. – Arno Press: Oxford, UK, 632p.
[45] Root, T. L., Price, J. T., Hall, K. R., Schneider, S. H., Rosenzweigk, C., Pounds, J. A. (2003): Fingerprints of global warming on wild animals and plants. – Nature 421: 57-60.
[46] Rundel, P. W., Dillon, M. O., Palma, B., Money, H. A., Gulmon, S. L., Ehleringer, J. R. (1999): The phytogeography and ecology of the coastal Atacama and Peruvian Deserts. – Aliso 13(1): 1-49.
[47] Shaltout, K., Baraka, D. M., Shehata, M. N., Ahmed, D., Arief, O. M. (2013): Distributional behavior and growth performance of *Trianthema portulacastrum* L. (Aizoaceae) in Nile Delta. – Egyptian Journal of Botany, pp. 183-199.
[48] Shiferaw, H., Teketay, D., Nemomissa, S., Assefa, F. (2004): Some biological characteristics that foster the invasion of *Prosopis juliflora* (Sw.). DC. at Middle Awash Rift Valley Area, northeastern Ethiopia. – Journal of Arid Environments 58: 134-153. http://dx.doi.org/10.1016/j.jaridenv.2003.08.011.
[49] Shiferaw, W., Demissew, S., Bekele, T., Aynekulu, E. (2022): Community perceptions towards invasion of Prosopis juliflora, utilization, and its control options in Afar region, Northeast Ethiopia. – PLoS ONE 17(1): e0261838. https://doi.org/101371/journal.pone.0261838.
[50] Stachowicz, J. J., Terwin, J. R., Whitlach, R. B., Osman, R. W. (2002): Linking climate change and biological invasions: ocean warming facilitates nonindigenous species invasions. – Proceedings of the National Academy of Sciences of the United States of America 99(24): 15497-15500. doi:10.1073/pnas.242437499.
[51] Sun, H., Wang, X., Fan, D., Sun, J. O. (2022): Contrasting vegetation response to climate change between two monsoon regions in Southwest China: The roles of climate condition and vegetation height. – Science of The Total Environment 802: 149643. https://doi.org/10.1016/j.scitotenv.2021.149643.

http://www.aloki.hu ● ISSN 1589 1623 (Print) ● ISSN 1785 0037 (Online)
DOI: http://dx.doi.org/10.15666/aeer/2003_26832695

[52] Suttle, K. B., Thomsen, M. A., Power, M. E. (2007): Species interactions reverse grassland responses to changing climate. – Science 315: 640-642. doi:10.1126/science.1136401.
[53] Tarawneh, Q. Y., Chowdhury, S. (2018): Trends of Climate Change in Saudi Arabia: Implications on Water Resources. – Climate 6(1): 8. doi:10.3390/cli6010008.
[54] Trigo, I. F., Bigg, G. R., Davis, T. D. (2002): Climatology of cyclogenesis mechanisms in the Mediterranean. – Monthly Weather Review 130: 549-569.
[55] Walther, G. R., Beissner, S., Burga, C. A. (2005): Trends in the upward shift of alpine plants. – Journal of Vegetation Science 16: 541-548.
[56] Wethey, D. S. (2002): Biogeography, competition, and microclimate: the barnacle Chthamalus fragilis in New England. – Integrative and Comparative Biology 42: 872-880. doi:10.1093/icb/42.4.872.
[57] Williams, J. W., Jackson, S. T., Kutzbacht, J. E. (2007): Projected distributions of novel and disappearing climates by 2100 AD. – Proceedings of the National Academy of Sciences of the United States of America 104: 5738-5742.
[58] Williams, J. B., Shobrak, M., Wilms, T. M., Arif, I. A., Khan, H. A. (2012): Climate change and animals in Saudi Arabia. – Saudi Journal of Biological Sciences 19: 121-130.
[59] Zekâi, Ş. (2013): Desertification and climate change: Saudi Arabian Case. – International Journal of Global Warming 5(3): 270-281.

http://www.aloki.hu ● ISSN 1589 1623 (Print) ● ISSN 1785 0037 (Online)
DOI: http://dx.doi.org/10.15666/aeer/2003_26832695

PHYSIOLOGICAL RESPONSES OF THE INVASIVE GREAT YELLOWCRESS (*RORIPPA AMPHIBIA* (L.) BESSERD) UNDER DIFFERENT WATER CONDITIONS

ZHOU, K. H. – KE, J. H. – WU, S. L. – WANG, J. X. – WANG, L. L. – WANG, Y.*

College of Life Science, Shenyang Normal University, No. 253 Huanghe North Street, Shenyang, LiaoNing 110034, China

**Corresponding author*
e-mail: wyancn2002@aliyun.com

(Received 6th Jan 2022; accepted 21st Mar 2022)

Abstract. The invasion plant *Rorippa amphibia* (L.) Besser native to Europe was first reported in China in 2009 and then it spread extensively in Liaoning Province. It natively grows in flooded or shallow habitats, but it actually appears in more broadly water-related habitats in Shenyang, Liaoning Province. Individuals of *Rorippa amphibia* were treated for 1 month under 4 water gradients with waterlogging, wet, moderate (CK) and drought in Shenyang Normal University, and their physiological indexes were measured. The results showed water stresses had some adverse effects on its physiological processes including the significantly decreasing of the transpiration rate, net photosynthetic rate and stomatal conductance, the increasing of malondialdehyde and electrolyte leakage. But the change of other physiological indexes as follows may alleviate the disadvantageous effects of water stresses. Compared with the CK, the chlorophyll content increased significantly, especially under the drought treatment. The activities of SOD, POD and CAT increased. SOD and POD activities were highest under the drought treatment and CAT activity was highest under the waterlogging treatment. The osmotic adjustment substance contents including proline, soluble protein and soluble sugar were significantly increased under water stresses, especially under the drought treatment and the waterlogging treatment. The root activities increased as soil water content declined and the activity under the drought treatment was significantly higher than the other 3 treatments. The result that all the individuals of *Rorippa amphibia* could survive under extreme soil water conditions meant that *Rorippa amphibia* had a strong invasive line because it could adapt to very different soil water conditions from waterlogging to extremely drought condition.
Keywords: *invasive mechanism, water stress, photosynthetic indexes, antioxidase, proline, soluble protein, soluble sugar, malondialdehyde (MDA), electrolyte leakage*

Introduction

With the development of globalization, many plants are brought to other parts of the world with the activities of people, so that plant invasion has become a common phenomenon. Water is an important ecological factor to influence the survival state of plants. To research the capability adapting to different water condition of invasive plants is very important to evaluate their expanding ability because water stress is a major limiting factor of plant growth and physiological process.

In general, water stress can inhibit the growth of plant. Water stress can be divided into waterlogging stress and drought stress. Chlorophyll is the predominant pigment of plants, and the quantity of chlorophyll determines plant growth capacity and is an indicator of stress level. Drought stress can change the quantity of chlorophyll a and chlorophyll b in plants leading to changes in photosynthesis capacity (Shukla et al., 2015; Yang et al., 2015). The study of Jennifer and Hulme (2021) on the invasive plant *Rumex obtusifolius* L. found that its chlorophyll content increased under drought stress. But the study of Pintó-Marijuan et al. (2016) on the invasive plant *Aptenia cordifolia*

http://www.aloki.hu ● ISSN 1589 1623 (Print) ● ISSN1785 0037 (Online)
DOI: http://dx.doi.org/10.15666/aeer/2003_26972716

(L.f.) Schwantes found that its chlorophyll content decreased under drought stress. Net photosynthetic rate has long been recognized as one of the most sensitive processes. Water stress can affect the indicators of photosynthesis. For example, stomatal closure limits air exchange and reduces photosynthetic CO_2 assimilation, whereas water deficiency decreases RuBP contents, thereby suppressing photosynthetic CO_2 assimilation, which becomes the dominant limitation at severe drought (Lewis et al., 1994). A study on invasive *Eriobotrya japonica* (Thunb.) Lindl. found a decrease in stomatal conductance (Cond) (Williams-Linera et al., 2021). Malondialdehyde (MDA) and Relative water content (RWC) ca n indicate the degree of stress. MDA, a product of lipid peroxidation, is an indicator of oxidative damage (Blokhina, 2003). RWC is also a key indicator to describe the water related physiological function in plants (Wang et al., 2019; Feizabadi et al., 2020). Under drought stress, plasma membrane permeability changes and electrolyte leakage had been found (Bajji et al., 2002).

Waterlogging stress is an important natural disturbance (Mack et al., 2000). Waterlogging can cause stunted growth or even death of plants. Because the decreasing of air exchange between soil and the atmosphere O_2 in the soil declines rapidly, and the soil may become hypoxic or anoxic within a few hours during waterlogging (Malik et al., 2002). One of the initial responses of plant to waterlogging stress appears to involve the closing of stomata, with a subsequent down-regulation of the photosynthetic machinery (García-Sánchez et al., 2007). The study of Jennifer and Hulme (2021) on the invasive plant *Rumex obtusifolius* L. found that its chlorophyll content increased under waterlogging stress. The study on invasive *Ligustrum sinense* Lour. found a decrease in stomatal conductance (Cond) and the net photosynthetic rate (Brown and Pezeshki, 2000). Similarly, Smaoui et al. (2011) found in their study on the invasive plant *Cotula coronopifolia* L. that chlorophyll content increased under waterlogging stress, while net photosynthetic rate and transpiration rate decreased. Many researchers found that waterlogging can facilitate invasion with exotic plants (Kercher and Zedler, 2004; Diez et al., 2012), mainly because of their tolerance to flooding, which is an another highly relevant factor for the success of invasive plant species (Dalmagro et al., 2013).

Some plants may have developed complex mechanisms to cope with water stress, such as adaptive morphology and structural changes (Moore et al., 2008; Lawlor, 2012; Komatsu and Yanagawa, 2013), enhanced biochemical and physiological responses such as solute accumulation, redox homeostasis, and changes in cellular turgor, membrane fluidity and composition (Reddy et al., 2004; Valliyodan and Nguyen, 2006). Plant tissues can reduce their cellular osmotic potential by synthesizing osmotic adjustment substances such as soluble protein (SP), proline (PRO) and soluble sugars to cope with water stress (Gao et al., 2008; Blum, 2016). Similarly, the antioxidant enzyme system is switched on. Superoxide dismutase (SOD), peroxidase (POD), catalase (CAT) are key enzymatic antioxidants. Some studies have indicated that enzymatic antioxidants increased in response to mild and/or moderate water deficit, but progressive severe drought stress impaired the function of these enzymes (Fan et al., 2009; Liu et al., 2011; Ge et al., 2014).

Rorippa amphibia (L.) Besser (yellowcress) is a perennial herb of the genus *Rorippa* Scop in the Brassicaceae family. Native to Europe, its invasion to the Caucasus, Central Asia, North Africa, North America and even New Zealand had been reported. Some studies have shown that it is most likely to invade with the introduced turf grass species (Elton, 1977). *Rorippa amphibia* have a strong ability of asexual reproduction and sexual reproduction, which is very helpful for them to become the dominant species in

http://www.aloki.hu ● ISSN 1589 1623 (Print) ● ISSN1785 0037 (Online)
DOI: http://dx.doi.org/10.15666/aeer/2003_26972716

lawns and other habitats. In addition, they have strong adaptability and expansibility, and the destructive power to some ecosystems is great (Ruprecht et al., 2013). *Rorippa amphibia* was first reported in China in 2009 and then it appeared in most areas of Liaoning Province, China, mainly distributed on the roadside and lawns (Zhang et al., 2009). In China, there are a few reports on the study of *Rorippa amphibia*. *Rorippa amphibia* grows in habitats are frequently flooded or where the groundwater level is relatively stable and shallow (Akman et al., 2012, 2014). But we found it appeared from moist and shade habitat to sunny and dry habitat in Shenyang, China. In this study, *Rorippa amphibia* was subjected to different gradient of soil water contents, and its physiological indexes under different water conditions were determined. We expect to reveal the adaptability of *Rorippa amphibia* to cope with water stress and to provide some theoretical basis for evaluating its potential invasive ability by this study.

Materials and methods

Plant material

This study was conducted from September to November in 2020 at Shenyang Normal University (Shenyang, Liaoning Province, China; 41°54′22″N 123°24′36″E). We put 15.0 kg mixed soil (loam soil: peat soil: perlite: vermiculite=15:4:3.5:1 v/v) in each pot (54*30*18 cm) and there were 8 pots to be used in this experiment. Well-grown and uniform in size individuals of *Rorippa amphibia* which were dominant species in a lawn in Shenyang Normal University were dug out and 40 individuals were transplanted in each pot. The pots were put in a greenhouse near windows for 30 days and plenty watered to guarantee the plants growing normally. Then 30 individuals which were similar in height and size were kept in each pot and they were nearly equidistant. The environmental indicators during the experiment were measured and the average temperature, humidity and illuminance were 20.17℃, 22.01%, 28853.67 lux respectively.

Experimental design and water treatments

Four different soil water contents were 5-10%, 15-20%, 25-30%, >100% (kept water surface higher than 2 cm over soil surface), which were equivalent to drought treatment, moderate treatment (CK), wet treatment and waterlogging treatment, respectively. There were two pots in each treatment (i.e., n=2 pots per treatment). The total 8 pots with 4 soil water gradients were random sorting (*Figs. 1,2*) in order to reduce the influence of other environmental factors on the experiment. When the water content was close to the high line of a specific designed treatment, the experiment began. The water content of soil samples in each pot was measured every day by drying method (Wang and Gao, 2006) and the overall weight of the whole pot was weighed to monitor the soil water condition. When the soil water content of each pot was close to the low line of each design water gradient, supplement water was given to meet the high line of the designed treatment. The *Rorippa amphibia* was treated under the designed water gradient for 1 month.

The superoxide dismutase, peroxidase, and catalase activities, soluble protein, soluble sugars, proline, malondialdehyde (MDA) content, electrolyte leakage, relative water content (RWC), chlorophyll content, photosynthetic indicators of the fresh fourth leaf and root activity were measured at the 35th days after the beginning of treatment.

http://www.aloki.hu ● ISSN 1589 1623 (Print) ● ISSN1785 0037 (Online)
DOI: http://dx.doi.org/10.15666/aeer/2003_26972716

There were 3 repetitions for each indicator in every water treatment and samples were taken from different pots (*Fig. 1*).

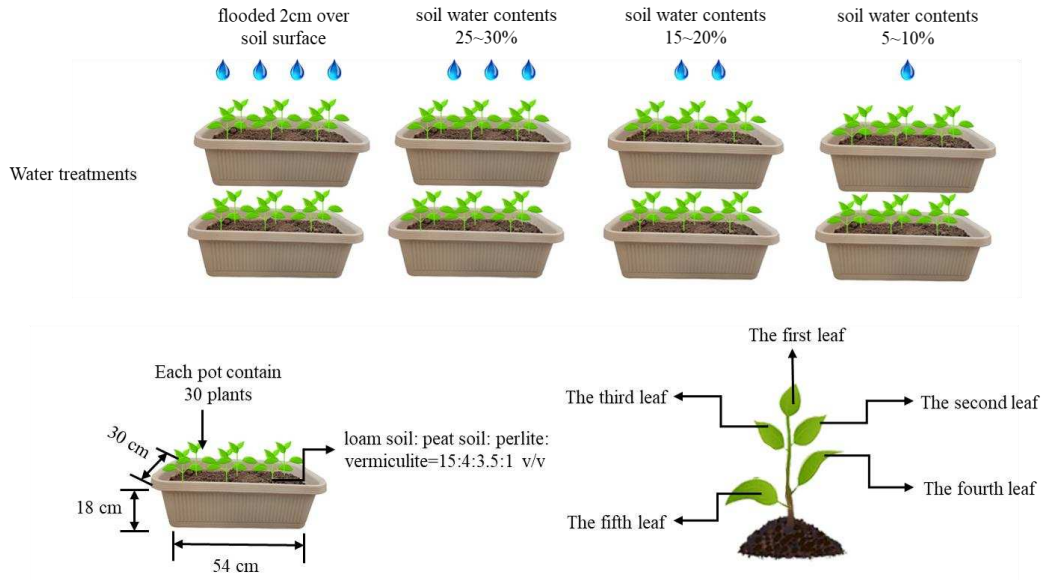

Figure 1. *Different water treatments*

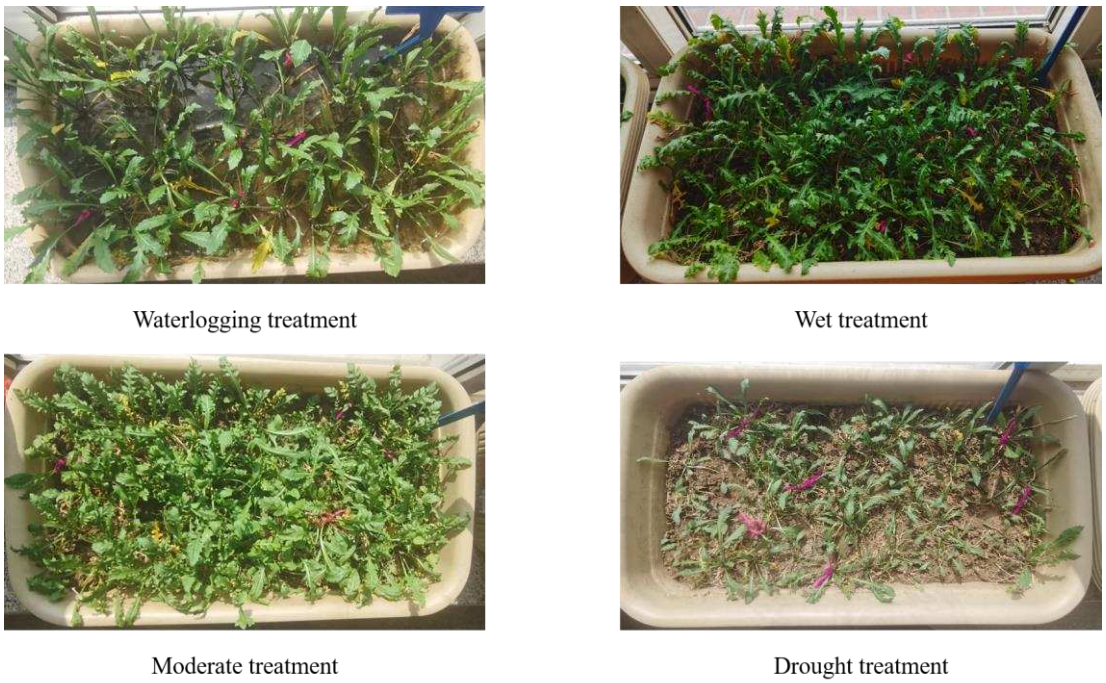

Figure 2. *Plants under different water treatments of the experiment*

Determination of activities of superoxide dismutase, peroxidase, and catalase

The leaves (0.2 g) were ground into homogenate in ice-bath using a mortar and pestle. 0.1 mol/L phosphate-buffered saline (pH 7.8) was added during grinding. After grinding,

http://www.aloki.hu ● ISSN 1589 1623 (Print) ● ISSN1785 0037 (Online)
DOI: http://dx.doi.org/10.15666/aeer/2003_26972716

the homogenate was centrifuged at 10,000 r/min for 20 min at 4°C by centrifuge (D-16C, Sartorius Lab Instruments GmbH & Co. KG 37070 Goettingen, Germany). The supernatant was collected to determine. Superoxide dismutase (SOD; EC 1.15.1.1) activity, assayed using the photochemical nitroblue tetrazolium (NBT) method (Beyer and Fridovich, 1987) measured estimate at 560 nm by spectrophotometer (UV-5900, Shanghai Metash Instruments Co., Ltd).

Fresh leaves (0.2 g) were ground into homogenate in ice-bath using a mortar and pestle. 20 mmol/L KH_2PO_4 was added during grinding. After grinding, the homogenate was centrifuged at 10,000 r/min for 20 min at 4°C. The supernatant was collected to determine. The peroxidase (POD; EC 1.11.1.7) activity use the Guaiacol method measured estimate at 470 nm (Chancea and Maehly, 1955).

The leaves (0.2 g) were ground into homogenate in ice-bath using a mortar and pestle. 0.1 mol/L phosphate-buffered saline (pH 7.0) was added during grinding. After grinding, the homogenate was centrifuged at 4,000 r/min for 15 min at 4°C. The catalase (CAT; EC 1.11.1.6) activity was determined by measuring the decomposition of H_2O_2 directly at 240 nm for 3 min as described by Aebi (1984).

Estimation of soluble protein content

For the contents of soluble proteins, 0.2 g fresh leaves were extracted in 2 mL buffer phosphate (0.1 M and pH = 7.8). The extract was then centrifuged at 3,000g for 10 min at 4°C and supernatant was collected. Soluble protein contents were determined according to the method of Bradford (1976), using the reagent Coomassie Brilliant Blue G-250, followed by absorbance readings at 595 nm using bovine serum albumin as standard.

Estimation of soluble sugars content

Fresh leaves (0.2 g) were homogenized in deionized water, heated to 100°C for 30 min and then cooled to room temperature, and this process was repeated twice. The extract was moved into 25 mL volumetric flasks and volume completed to scale. The anthrone-sulfuric acid method was used to quantify the total soluble sugars. The absorbance at 630 nm was measured using a spectrophotometer using sucrose as standard (Chen et al., 2007).

Estimation of proline content

Leaves (50 mg) were blended in 3% sulfosalicylic acid (10 mL) followed by filtration to determine the leaf proline contents. Taking 2 mL supernatant and acid ninhydrin reagent (2 mL) along with CH_3COOH (2 mL) were reacted in glass vials, subsequently cooled in ice and the resulting amalgam was extracted with toluene (4 mL) using a vortex shaker for 15-20 s. The change in color was measured at 520 nm using a spectrophotometer at room temperature with toluene as blank (Bates et al., 1973). A calibration curve based on proline standard was developed to assess the proline concentrations.

Estimation of malondialdehyde (MDA) content

Leaves (0.2 g) were ground with 5 mL 10% trichloroacetic acid and centrifuged at 10,000 g under 4 °C for 15 min. The reaction mixture containing 2 mL supernatant and 2 mL 0.6% thiobarbituric acid was incubated at 100 °C in water bath for 20 min and

http://www.aloki.hu ● ISSN 1589 1623 (Print) ● ISSN1785 0037 (Online)
DOI: http://dx.doi.org/10.15666/aeer/2003_26972716

then cooled quickly in an ice bath. The reaction mixture was centrifuged at 4,000 g and 4 °C for 10 min. The absorbance of supernatant was measured at 532, 600, and 450 nm. The content of MDA was calculated as the *Eq.1* showed (Li et al., 2012).

$$MDA\ content = 6.45 \times (A532 - A600) - 0.56 \times A450 \quad \text{(Eq.1)}$$

Estimation of root activity

A 0.25 mL of 0.4% TTC solution was prepared and put in a 10 mL container with a small amount of hyposulphuric acid sodium ($Na_2S_2O_4$) powder and shaken gently to homogenize the chemicals completely. Red color triphenylformazan (TPF) was produced immediately. Ethyle acetate was added to the container to the 10 mL level. The solution was stored in the dark. Six TPF solutions, respectively of 0, 0.25, 0.50, 1.00, 1.50, 2.00 mL concentration were put in 10 mL capacity containers. Ethyle acete was added to each container to the 10 mL level. A series of TPF concentrations were prepared. The TPF measurements were recorded with a spectrophotometer at 485 nm. Plot of standard curves was established.

Using a spatula, carefully dug 3 individuals out randomly from each treatment and then soaked them repeatedly in water and rinsed gently until no soil was left on the root surface. Using absorbent paper removed superfluous water from the surface of roots. Fresh root materials (0.5 g) were immersed in a mixture of 5 mL TTC and 5 mL 0.1 mol/L Phosphate-buffered saline (pH 7.8), incubated in the dark at 37 ℃ for 2 hours prior to addition of 2 mL 1 mol/L sulfuric acid to stop the reaction. Then roots were ground into homogenate using a mortar and pestle. Ethyl acetate and quartz sand (small amount) were added during grinding. After grinding, the homogenate was then measured at 485 nm with spectrophotometer (Wang et al., 2006). We determined the root activity using TTC as the standard.

Estimation of relative water content (RWC)

For relative water content (RWC) measurement, leaves were blotted dry on filter papers weighed (Fresh weight, FW); immersed in ice-cold water for 10 h to rehydrate, blotted on filter papers and reweighted (hydrated weight, HW). The plants were subsequently dried at 80℃ for 48 h prior to determination of dry weight (DW) by drying oven (DHG-9240A, Shanghai Yiheng Technical Co., Ltd.; Shanghai Bluepard). RWC was calculated as the *Eq.2* showed (Taheri-Garavand et al., 2021):

$$RWC = \left\{ {(FW - DW)} \Big/ {(HW - DW)} \right\} \times 100\% \quad \text{(Eq.2)}$$

Estimate electrolyte leakage

Leaves were washed with deionized water, each leaf was put into a marked vial filled with 20 mL deionized water respectively, and incubated at room temperature in the dark for 6 h. The electrolytic conductivity (EC_1) of the solution was measured using a conductivity meter (SA29-DDB11A, Midwest Group, Beijing, China). The solution was then heated to 100°C, cooled to room temperature, and the electrolytic conductivity (EC_2) was measured once again. The percentage electrolyte leakage (EL) of the leaf discs was calculated as the *Eq.2* showed (Dionisio-Sese and Tobita, 1998).

http://www.aloki.hu ● ISSN 1589 1623 (Print) ● ISSN1785 0037 (Online)
DOI: http://dx.doi.org/10.15666/aeer/2003_26972716

$$EL = \left({}^{EC_1}/_{EC_2}\right) \times 100\% \quad \text{(Eq.3)}$$

Determination of chlorophyll content (SPAD units)

Chlorophyll content was determined using a SPAD-calibrated portable chlorophyll meter (SPAD-502Plus, Konica Minolta (China) Investment LTD.) which can read chlorophyll content of leaf directly. 3 the fourth leaves of different *Rorippa amphibia* individuals per treatment were measured and the average value was used to represent the chlorophyll content of the whole leaf (Costa et al., 2015).

Determination of photosynthetic indicators

Photosynthetic indicators of the fourth leaf (3 repetitions per treatment) were measured using a portable photosynthetic system (LI-6400, Li-Cor Inc., Lincoln NE, USA) at ambient climatic conditions. During the measurement (10:00-12:00) the irradiance was 1,200 μmol•m^{-2}•s^{-1} and temperature was around 20°C (He et al., 2014). The net photosynthetic rate, transpiration rate (Tr), stomatal conductance (Cond) and intercellular carbon dioxide concentration (Ci) were measured.

Statistical methods

We performed our statistical analysis using version 26.0 of the SPSS statistics software. One-way ANOVA followed by LSD's multiple-range test for multiple comparisons was used to detect differences among treatments. We defined significance at $P<0.05$. We used version 9.0 of the Origin Pro software (https://www.originlab.com/) to prepare the graphs.

Result

Variations in the activities of superoxide dismutase (SOD), peroxidase (POD) and catalase (CAT)

SOD and POD activities of *Rorippa amphibia* reached maximum value under drought treatment (*Fig. 3A,B*), while CAT activity was maximum under waterlogging treatment (*Fig. 3C*). SOD activities under the drought and waterlogging treatments were significantly higher than those of the moderate and wet treatments ($P<0.01$). SOD under the drought treatment increased by 8.85%, 41.82%, 52.44% over the corresponding activity under the waterlogging, wet and moderate treatments, respectively. The corresponding increments of POD activity were 8.93%, 15.15%, 103.69%. CAT activity under the waterlogging treatment, on the other hand, displayed 38.10%, 141.67% and 7.41% increments over the wet, moderate and drought treatment, respectively. Under the moderate treatment, activity of POD was significantly lower than those displayed by the other 3 water stress treatments ($P<0.01$) and activity of CAT was very significantly lower than the drought and waterlogging treatments ($P<0.01$), and significantly lower than the wet treatment ($P<0.05$).

http://www.aloki.hu ● ISSN 1589 1623 (Print) ● ISSN1785 0037 (Online)
DOI: http://dx.doi.org/10.15666/aeer/2003_26972716

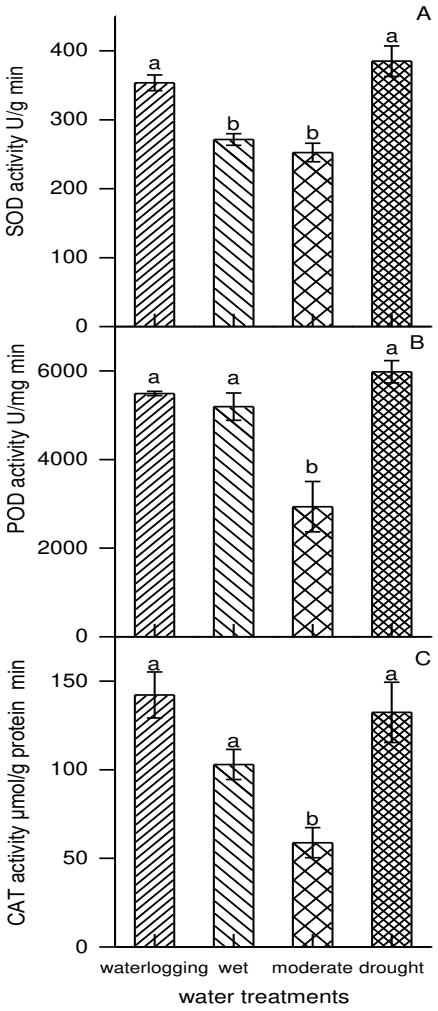

Figure 3. *Variations of the SOD, POD, and CAT activities of different water treatments. Bars indicate standard deviations (n = 3). Different lowercase letters in columns within the different treatments indicate significant difference. Note: the meaning of the bars and lowercase letters were the same as figure 3 for Figures 4~12*

Variations of proline content

Water stresses increased proline content in *Rorippa amphibia* (*Fig. 4*). The proline content was the highest under the drought treatment ($2.875 \cdot 10^{-4}$ μg/g), followed in descending order by the waterlogging treatment ($1.245 \cdot 10^{-4}$ μg/g), wet treatment ($6.267 \cdot 10^{-5}$ μg/g), and moderate treatment ($4.85 \cdot 10^{-5}$ μg/g). The drought treatment was significantly higher than the other 3 treatments ($P<0.01$). The waterlogging treatment were significantly higher than the wet and moderate treatments ($P< 0.01$).

Variations of soluble sugars content

The leaf soluble sugar contents were the lowest (0.0067 μg/g) and highest (0.0111 μg/g) for the moderate treatment and drought treatment, respectively (*Fig. 5*). The differences were significant among the treatments except between the waterlogging treatment and drought treatment. The drought treatment and waterlogging treatment

http://www.aloki.hu ● ISSN 1589 1623 (Print) ● ISSN1785 0037 (Online)
DOI: http://dx.doi.org/10.15666/aeer/2003_26972716

were significantly higher than moderate treatment (P<0.01), and the wet treatment was significantly higher than moderate treatment (P<0.05).

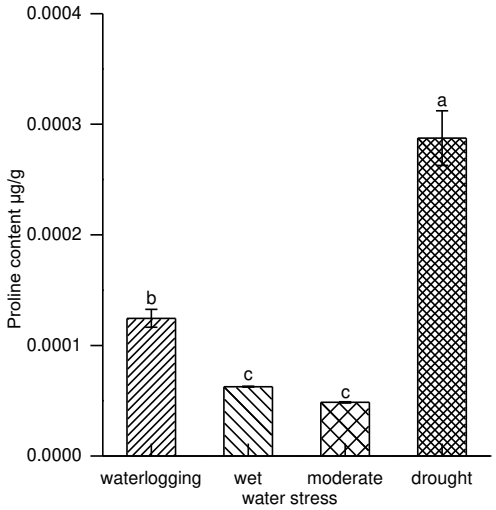

Figure 4. *Variations of proline content of different water treatments*

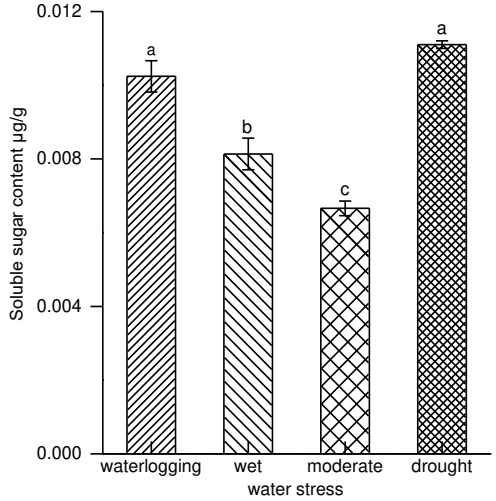

Figure 5. *Variations of soluble sugars content of different water treatments*

Variations of soluble protein content

The lowest (8.1675 mg/g) and highest (9.1895 mg/g) protein contents were displayed by the moderate treatment and waterlogging treatment, respectively (*Fig. 6*). The values for the waterlogging treatment and drought treatment were significantly higher than the moderate treatment (P < 0.01, P < 0.05, respectively) (*Fig. 6*).

Variations of malondialdehyde (MDA) content

Water stresses increased the MDA content of *Rorippa amphibia.* The MDA content was the highest under waterlogging treatment (12.2216 μmol/g) followed in descending order by the wet treatment (9.2333 μmol/g), drought treatment (7.4469 μmol/g),

http://www.aloki.hu ● ISSN 1589 1623 (Print) ● ISSN1785 0037 (Online)
DOI: http://dx.doi.org/10.15666/aeer/2003_26972716

moderate treatment (5.1248 μmol/g). The differences among the 4 treatments were significant, which was embodied in that the waterlogging treatment was much significantly higher than the other 3 treatments (P<0.01), and the moderate treatment was much significantly lower than the wet and drought treatments (P<0.01), while the difference between the wet and drought treatments was significant (P<0.05) (*Fig. 7*). Compared with the moderate treatment, MDA contents of the other 3 treatments were higher (P<0.01) which may generate higher lipid peroxidation and the damage of membrane.

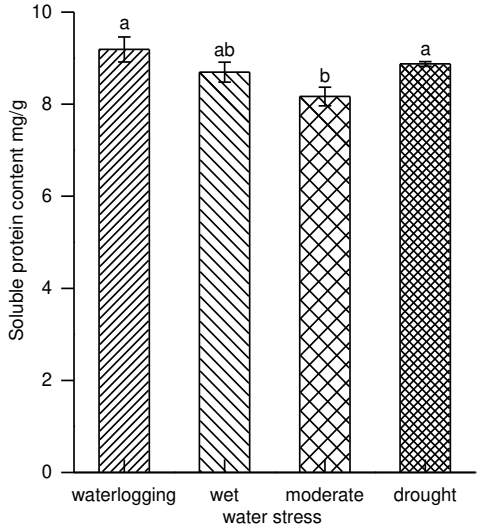

Figure 6. *Variations of soluble protein content of different water treatments*

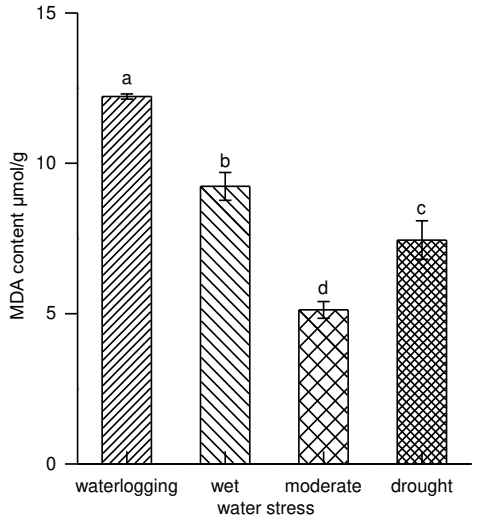

Figure 7. *Variations of MDA content of different water treatments*

Variations of root activity

The root activities of *Rorippa amphibia* increased as soil water content declined (*Fig. 8*). Root activity under the drought treatment was about 2.1 times as large as the waterlogging treatment. The differences of root activities were significant among

http://www.aloki.hu ● ISSN 1589 1623 (Print) ● ISSN1785 0037 (Online)
DOI: http://dx.doi.org/10.15666/aeer/2003_26972716

different treatments except between the wet treatment and moderate treatment, the wet treatment and waterlogging treatment. The drought treatment was significantly higher than the other 3 treatments (P<0.01).

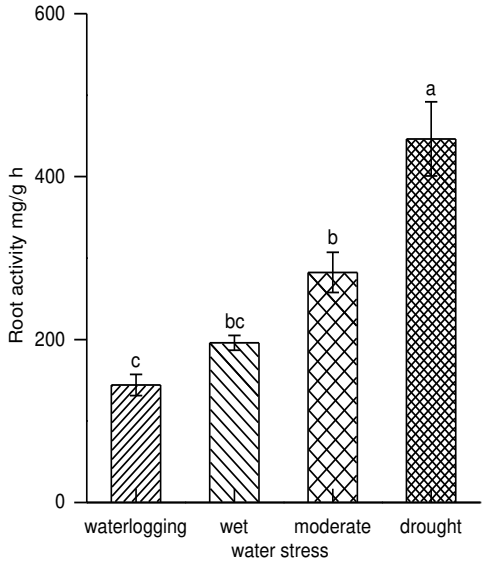

Figure 8. *Variations of root activity of different water treatments*

Variations of relative water content (RWC)

The RWC of leaves decreased with the decline of soil water contents. The RWC under the drought treatment was significantly lower than the other 3 treatments (P<0.01). The value of RWC was the highest under the waterlogging treatment and increased by 36.81% compared with the drought treatment (*Fig. 9*).

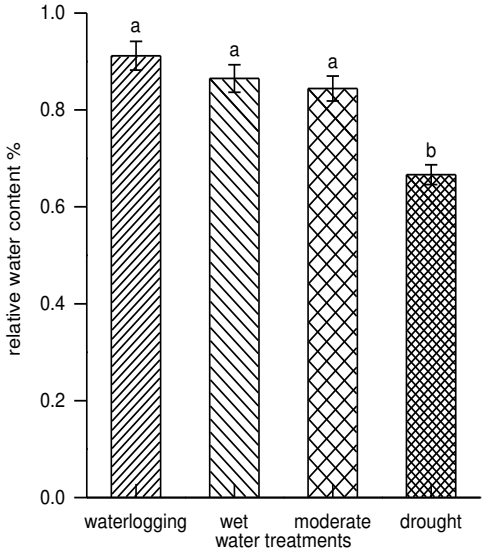

Figure 9. *Variations of relative water content of different water treatments*

http://www.aloki.hu ● ISSN 1589 1623 (Print) ● ISSN1785 0037 (Online)
DOI: http://dx.doi.org/10.15666/aeer/2003_26972716

Variations of electrolyte leakage

The waterlogging treatment evoked the highest electrolyte leakage and the value which was about 1.5 times as large as the lowest level of moderate treatment was significantly higher than other 3 treatments (P<0.01) (*Fig. 10*). The differences of electrical conductivity among the drought, wet and moderate treatments were not significant. The trend of electrolyte leakage was similar to MDA, which reflected the damage degree of membrane of *Rorippa amphibia* under different water treatments.

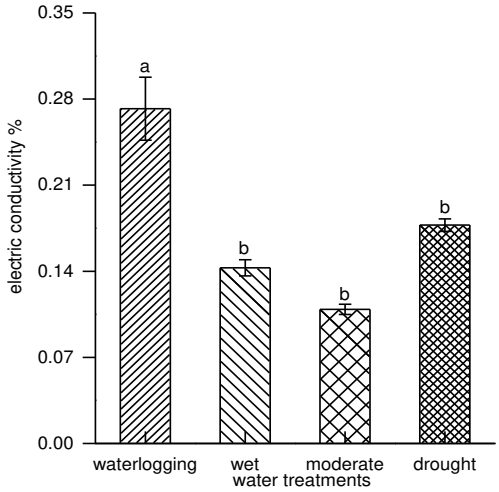

Figure 10. *Variations of electrolyte leakage of different water treatments*

Variations of chlorophyll content (SPAD units)

As shown in *Figure 11*, chlorophyll content was the highest for the drought treatment (44.00) followed in descending order by the wet treatment (39.20), waterlogging treatment (38.61), moderate treatment (36.28). Chlorophyll content of the drought treatment was significantly higher than those of the other 3 treatments (P<0.01), while chlorophyll content of the moderate treatment was significantly lower than those of the other 3 treatments (P<0.01).

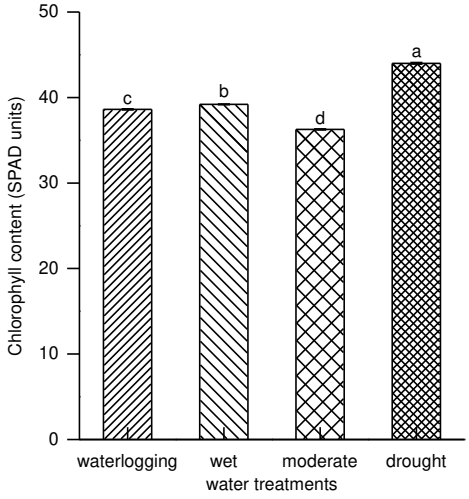

Figure 11. *Variations of chlorophyll content (SPAD units) of different water treatments*

http://www.aloki.hu ● ISSN 1589 1623 (Print) ● ISSN1785 0037 (Online)
DOI: http://dx.doi.org/10.15666/aeer/2003_26972716

Variations of photosynthetic indicators

Water stress had an obvious impact on the photosynthetic indicators of *Rorippa amphibia* (*Fig. 12*). Net photosynthetic rate (photo) was the highest under the moderate treatment (5.5960 μmol/m^2•s) followed in descending order by the wet treatment (5.2129 μmol/m^2•s), drought treatment (3.0701 μmol/m^2•s), waterlogging treatment (1.9714 μmol/m^2•s). The transpiration rate (Tr) and stomatal conductance (Cond) had the same changing trend as photo rate, while the intercellular carbon dioxide concentration (Ci) had just an opposite trend. All the photosynthetic indicators were significantly different among the 4 treatments (P<0.01).

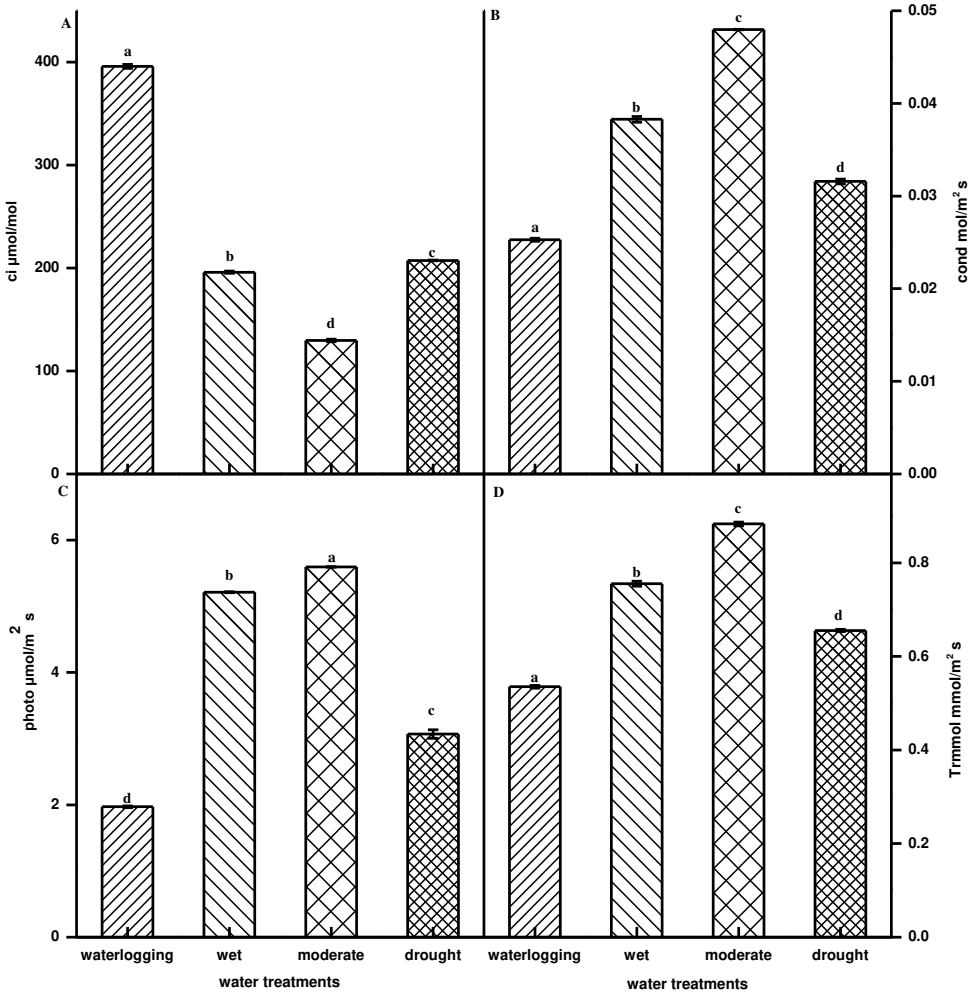

Figure 12. *Variations of photosynthetic indicators of different water treatments*

Discussion

Water stress is an important environmental factor that could influence the physiological and biochemical characteristics of plants. Water stress retards growth and metabolic activity (Pasala, 2016).

http://www.aloki.hu ● ISSN 1589 1623 (Print) ● ISSN1785 0037 (Online)
DOI: http://dx.doi.org/10.15666/aeer/2003_26972716

An increase in antioxidant enzyme activity is a common adaptive response of plants to water stress (Gill and Tuteja, 2010). The main function of SOD is to transform $O^{2\bullet-}$ into O_2 and H_2O_2, the latter is toxic, but can be eliminated by POD and CAT (Vince et al., 2004). The POD and CAT activities increased as a result of drought treatment in this study, which may protect plants from oxidation. POD also plays an important role in eliminating MDA, thus protecting permeability of cell membranes (Hojati et al., 2010). In this study, POD and CAT activity increased significantly under the waterlogging, wet and drought treatments, which may limit the increases of MDA. The increases of POD activity under the waterlogging, wet and drought treatments were in line with those reported by Hojati et al. (2010). Further, the increase of SOD activity was congruent with the report of Dehury et al. (2012).

Plants can reduce their cellular osmotic potential by synthesizing osmotic adjustment substances such as soluble protein (SP), proline (PRO) and soluble sugars to reduce effects of water stresses. The notable increase in proline content observed in this study in consistency with several reports (Pei et al., 2009; Liu et al., 2016; Li et al., 2020). The result that proline content increased significantly under waterlogging and drought treatments suggest that *Rorippa amphibia* may have a strong adaptability to extreme water conditions. Water stress induces soluble sugar accumulation, particularly sucrose, glucose, and fructose, which helps to improve osmoregulation (Praxedes et al., 2006). In this paper, the soluble sugar increased significantly under the drought treatment and waterlogging treatment compared with moderate treatment, which was similar to previous reported of Wu et al. (2016), Balsamo et al. (2015), and Pintó-Marijuan and Munné-Bosch (2013), but contradicted those reports for Li et al. (2020). Soluble protein contains some antioxidant enzymes. The significant increase in soluble proteins under the waterlogging and drought treatments showed by this study was consistent with the notable increase in some antioxidant enzymes. However, it was at variance with a previous report by Jalil et al. (2018). The observed discrepancy may be due to excessive stresses and/or to subtle difference between plants taxa and/or environments.

Malondialdehyde (MDA), which is a byproduct of enzymatic and oxygen radical-induced lipid peroxidation, is widely used as a biomarker of oxidative stress in plants (Davey, 2005). The increase of malondialdehyde content leads to the increase of plasma membrane peroxidation, which leads to electrolyte leakage. In this paper, MDA content increased significantly under the drought, wet and waterlogging treatments compared with the moderate treatment. This result was similar to Quinet's et al. (2015). Electrolyte leakage level had the same trend with MDA level. The results of this paper were similar to those of Zhang et al. (2020) and Faria et al. (2012). In addition, previous studies showed RWC as an eminent trait to measure stress tolerance (Dapanage and Bhat, 2017; Hemmati, 2018). RWC of *Rorippa amphibia* decreased significantly with the decrease of soil water content. In this paper, we found root activity reached the highest under the drought treatment, and this indicated that *Rorippa amphibia* continuously strengthened the water absorption capacity of root system in order to adapt to drought condition, which further indicated that *Rorippa amphibia* had strong adaptability.

Chlorophyll is another indicator of water stress level. A result showed that drought stress enhanced chlorophyll content in wheat leaves (Xu et al., 2017). In contrast, Li's study of *Lilium brownii* var. *viridulum* Baker found that reduced water content led to reduced chlorophyll content (Li et al., 2020). In this paper, the chlorophyll content of

http://www.aloki.hu ● ISSN 1589 1623 (Print) ● ISSN1785 0037 (Online)
DOI: http://dx.doi.org/10.15666/aeer/2003_26972716

Rorippa amphibia increased significantly under water stress conditions especially under drought treatment.

Photosynthesis is the most sensitive physiological process of plants to water stress (Centritto et al., 2011; He et al., 2017). Soil moisture and photosynthetically active radiation intensity affect plants by affecting plant photosynthesis, transpiration and respiration (Mitton et al., 1998; Deans et al., 2018). In this paper, the photosynthesis physiological parameters of *Rorippa amphibia* changed under different water conditions. Photosynthetic rate, stomatal conductance and transpiration rate decreased and intercellular carbon dioxide concentration increased under the drought and waterlogging treatments compared with the moderate treatment. The reason for the changes in these indicators under the drought treatment may be when water was scarce, root water intake reduced, and then stomatal conductance, photosynthetic rate, transpiration rate decreased, and intercellular carbon dioxide concentration increased. Some studies suggest *Rorippa amphibia* could even withstand submergence to some degree (Sasidharan et al., 2013; Akman, 2014). However, Prolonged flooding could have deleterious effects on nutrient uptake, carbohydrates translocation, hormonal balance, respiration of *Rorippa amphibia*. Then the root activity decreased and the water absorption was reduced, which led to the stomatal closure and the decreasing of stomatal conductance, photosynthetic rate as well as transpiration rate. So intercellular carbon dioxide concentration increased. The study of *Bupleurum chinense* DC also showed the same results (Yang et al., 2019).

Conclusion

The wet treatment had slight impact on the physiological indexes of *Rorippa amphibia*. The differences of most measured phyisiological indexes were not significant between the moderate treatment (CK) and wet treatment except the MDA content, soluble sugar content, activities of POD and CAT.

The drought and waterlogging treatments had some severe adverse effects on physiological process of *Rorippa amphibia.* The photosynthetic capacity and root activity were the lowest and the MDA content and electrical conductivity were the highest under the waterlogging treatment. The RWC of leaf was the lowest and the MDA content and electrical conductivity significantly increased under the drought treatment compared with CK.

But some changes of physiological indexes may alleviate the adverse effects of water stresses. *Rorippa amphibia* significantly increased the enzyme activities of antioxidant defense system, the contents of osmotic adjustment substance including proline, soluble sugar and soluble protein under the waterlogging and drought treatments. The activities of SOD and POD, chlorophyll content and root activity under drought treatment were the highest among all the treatments.

All the results indicated that *Rorippa amphibia* could tolerate extremely adverse soil water conditions. Its invasive capability to some ecosystems under different water conditions could not be ignored and further research should be carried out on *Rorippa amphibia*.

Acknowledgements. This work was funded by the National Natural Science Foundation of China (31600314).

http://www.aloki.hu ● ISSN 1589 1623 (Print) ● ISSN1785 0037 (Online)
DOI: http://dx.doi.org/10.15666/aeer/2003_26972716

REFERENCES

[1] Aebi, H. (1984): Catalase in vitro. – Oxygen Radicals in Biological Systems 105: 121-126.
[2] Akman, M., Bhikharie, A. V., McLean, E. H., Boonman, A., Visser, E. J. W., Schranz, M. E., Tienderen, P. H. (2012): Wait or escape? Contrasting submergence tolerance strategies of *Rorippa amphibia*, Rorippa sylvestris and their hybrid. – Annals of Botany 109: 1263-1276.
[3] Akman, M., Bhikharie, A. V., Mustroph, A., Sasidharan, R. (2014): Extreme flooding tolerance in *Rorippa*. – Plant Signaling & Behavior 9: e27847.
[4] Bajji, M., Kinet, J. M., Lutts, S. (2002): The use of the electrolyte leakage method for assessing cell membrane stability as a water stress tolerance test in durum wheat. – Plant Growth Regulation 36: 61-70.
[5] Balsamo, R., Boak, M., Nagle, K., Peethambaran, B., Layton, B. (2015): Leaf biomechanical properties in Arabidopsis thaliana polysaccharide mutants affect drought survival. – Journal of Biomechanics 48: 4124-4129.
[6] Bates, L. S., Waldren, R. P., Teare, I. D. (1973): Rapid determination of free proline for water-stress studies. – Plant and Soil 39: 205-207.
[7] Beyer, W. F., Fridovich, I. (1987): Assaying for superoxide dismutase activity: Some large consequences of minor changes in conditions. – Analytical Biochemistry 161: 559-566.
[8] Blokhina, O. (2003): Antioxidants, Oxidative Damage and Oxygen Deprivation Stress: A Review. – Annals of Botany 91: 179-194.
[9] Blum, A. (2016): Osmotic adjustment is a prime drought stress adaptive engine in support of plant production. – Plant, Cell & Environment 40: 4-10.
[10] Bradford, M. M. (1976): A rapid and sensitive method for the quantitation of microgram quantities of protein utilizing the principle of protein-dye binding. – Analytical Biochemistry 72: 248-254.
[11] Brown, C. E., Pezeshki, S. R. (2000): A study on waterlogging as a potential tool to control ligustrum sinense populations in western Tennessee. – Wetlands 20: 429-437.
[12] Bufford, J. L., Hulme, P. E. (2021): Increased adaptive phenotypic plasticity in the introduced range in alien weeds under drought and flooding. – Biological Invasions 23: 1-14.
[13] Centritto, M., Brilli, F., Fodale, R., Loreto, F. (2011): Different sensitivity of isoprene emission, respiration and photosynthesis to high growth temperature coupled with drought stress in black poplar (Populus nigra) saplings. – Tree Physiology 31: 275-286.
[14] Chance, B., Maehly, A. C. (1955): Assay of catalases and peroxidases. – Methods in Enzymology 2: 764-775.
[15] Chen, P., Chen, X., Wang, H., Qian, L. N., Zhang, C. C. (2007): Determination of polysaccharide from Panax japonicus of Hubei by anthrone-sulfuric acid Method. – Chinese Journal of Hospital Pharmacy 27: 1654-1656.
[16] Costa, J. P. R., Caputti, G. P., Galzerano, L., Silva, W. L., Ruggieri, A. C., Malheiros, E. B. (2015): Relative chlorophyll contents in the evaluation of the nutritional status of nitrogen from xaraes palisade grass and determination of critical nitrogen sufficiency index. – Acta Scientiarum Animal Sciences 37: 109-114.
[17] Dalmagro, H. J., Lobo, F. A., Vourlitis, G. L., Dalmolin, Â. C., Antunes, M. Z., Ortíz, C. E. R., Nogueira, J. S. (2013): Photosynthetic parameters of two invasive tree species of the Brazilian Pantanal in response to seasonal flooding. – Photosynthetica 51: 281-294.
[18] Dapanage, M., Bhat, S. (2017): Physiological responses of commercial sugarcane (Saccharum spp. hybrids) varieties to moisture deficit stress tolerance. – Indian Journal of Plant Physiology 23: 40-47.

http://www.aloki.hu ● ISSN 1589 1623 (Print) ● ISSN1785 0037 (Online)
DOI: http://dx.doi.org/10.15666/aeer/2003_26972716

[19] Davey, M. W., Stals, E., Panis, B., Keulemans, J., Swennen, R. L. (2005): High-throughput determination of malondialdehyde in plant tissues. – Analytical Biochemistry 347: 201-207.
[20] De Faria, A. P., Lemos-Filho, J. P., Modolo, L. V., França, M. G. C. (2012): Electrolyte leakage and chlorophyll a fluorescence among castor bean cultivars under induced water deficit. – Acta Physiologiae Plantarum 35: 119-128.
[21] Deans, R. M., Brodribb, T. J., Busch, F. A., Farquhar, G. D. (2018): Plant water-use strategy mediates stomatal effects on the light induction of photosynthesis. – New Phytologist 222: 382-395.
[22] Dehury, B., Sarma, K., Sarmah, R., Jagajjit, S., Smita, S., Mousumi, S., Priyabrata, S., Mahendra, K. M., Gauri, D. S., Manabendra, D. C., Madhumita, B. (2012): In silico analyses of superoxide dismutases (SODs) of rice (*Oryza sativa* L.). – Journal of Plant Biochemistry and Biotechnology 22: 150-156.
[23] Diez, J. M., D'Antonio, C. M., Dukes, J. S., Grosholz, E. D., Olden, J. D., Sorte, C. J., Cascade, J. B. S., Dana, M. B., Bethany, A. B., Regan, E., Inés, I., Sierra, J. J., Joshua, J. L., Miller, L. P. (2012): Will extreme climatic events facilitate biological invasions? – Frontiers in Ecology and the Environment 10: 249-257.
[24] Dionisio-Sese, M. L., Tobita, S. (1998): Antioxidant responses of rice seedlings to salinity stress. – Plant Science 135: 1-9.
[25] Elton, C. C. (1977): The Ecology of Invasions by Animals and Plants. – Journal of Range Management 47: 1601.
[26] Fan, X. W., Li, F. M., Song, L., Xiong, Y. C., An, L., Jia, Y., Fang, X. W. (2009): Defense strategy of old and modern spring wheat varieties during soil drying. – Physiologia Plantarum 136: 310-323.
[27] Feizabadi, A., Noormohammadi, G., Fatehi, F. (2020): Changes in Growth, Physiology, and Fatty Acid Profile of Rapeseed Cultivars Treated with Vermicompost Under Drought Stress. – Journal of Soil Science and Plant Nutrition 21: 200-208.
[28] Gao, J. M., Xiao, Q., Ding, L. P., Chen, M. J., Yin, L., Li, J. Z., Zhou, S. Y., He, G. Y. (2008): Differential responses of lipid peroxidation and antioxidants in Alternanthera philoxeroides and *Oryza sativa* subjected to drought stress. – Plant Growth Regulation 56: 89-95.
[29] García-Sánchez, F., Syvertsen, J. P., Gimeno, V., Botía, P., Perez-Perez, J. G. (2007): Responses to flooding and drought stress by two citrus rootstock seedlings with different water-use efficiency. – Physiologia Plantarum 130: 532-542.
[30] Ge, Y., He, X., Wang, J., Jiang, B., Ye, R., Lin, X. (2014): Physiological and biochemical responses of Phoebe bournei seedlings to water stress and recovery. – Acta Physiologiae Plantarum 36: 1241-1250.
[31] Gill, S. S., Tuteja, N. (2010): Reactive oxygen species and antioxidant machinery in abiotic stress tolerance in crop plants. – Plant Physiology and Biochemistry 48: 909-930.
[32] He, Q., Zhao, S., Ma, Q., Zhang, Y., Huang, L., Li, G., Hao, L. (2014): Endogenous Salicylic Acid Levels and Signaling Positively Regulate Arabidopsis Response to Polyethylene Glycol-Simulated Drought Stress. – Journal of Plant Growth Regulation 33: 871-880.
[33] He, F., Sheng, M., Tang, M. (2017): Effects of Rhizophagus irregularis on Photosynthesis and Antioxidative Enzymatic System in *Robinia pseudoacacia* L. under Drought Stress. – Frontiers in Plant Science 8: 183.
[34] Hemmati, K., Ebadi, A., Khomari, S., Sedghi, M. (2018): Influence of ascorbic acid and 24-epibrassinolide on physiological characteristics of pot marigold under water-stress condition. – Journal of Plant Interactions 13: 364-372.
[35] Hojati, M., Modarres-Sanavy, S. A. M., Karimi, M., Ghanati, F. (2010): Responses of growth and antioxidant systems in *Carthamus tinctorius* L. under water deficit stress. – Acta Physiologiae Plantarum 33: 105-112.

http://www.aloki.hu ● ISSN 1589 1623 (Print) ● ISSN1785 0037 (Online)
DOI: http://dx.doi.org/10.15666/aeer/2003_26972716

[36] Jalil, S. M., Movahhedi, D. M., Salehi, A., Bahreininejad, B. (2018): Physiological and yield responses of purple coneflower (*Echinacea purpurea* (L.) Moench) to nitrogen sources at different levels of irrigation. – Physiology and Molecular Biology of Plants 25: 177-187.
[37] Kercher, S. M., Zedler, J. B. (2004): Flood tolerance in wetland angiosperms: a comparison of invasive and noninvasive species. – Aquatic Botany 80: 89-102.
[38] Komatsu, S., Yanagawa, Y. (2013): Cell wall proteomics of crops. – Frontiers in Plant Science 4: 17.
[39] Lawlor, D. W. (2012): Genetic engineering to improve plant performance under drought: physiological evaluation of achievements, limitations, and possibilities. – Journal of Experimental Botany 64: 83-108.
[40] Lewis, J. D., Griffin, K. L., Thomas, R. B., Strain, B. R. (1994): Phosphorus supply affects the photosynthetic capacity of loblolly pine grown in elevated carbon dioxide. – Tree Physiology 14: 1229-1244.
[41] Li, Y., Zhang, S., Jiang, W., Liu, D. (2012): Cadmium accumulation, activities of antioxidant enzymes, and malondialdehyde (MDA) content in *Pistia stratiotes* L. – Environmental Science and Pollution Research 20: 1117-1123.
[42] Li, W., Wang, Y., Zhang, Y., Wang, R., Guo, Z., Xie, Z. (2020): Impacts of drought stress on the morphology, physiology, and sugar content of Lanzhou lily (*Lilium davidii* var. unicolor). – Acta Physiologiae Plantarum 42: 127.
[43] Liu, C., Liu, Y., Guo, K., Fan, D., Li, G., Zheng, Y., Yang, R. (2011): Effect of drought on pigments, osmotic adjustment and antioxidant enzymes in six woody plant species in karst habitats of southwestern China. – Environmental and Experimental Botany 71: 174-183.
[44] Liu, D., Hu, L. Y., Ali, B., Yang, A. G., Wan, G. L., Xu, L., Zhou, W. J. (2016): Influence of 5-aminolevulinic acid on photosynthetically related parameters and gene expression in *Brassica napus* L. under drought stress. – Soil Science and Plant Nutrition 62: 254-262.
[45] Mack, R. N., Simberloff, D., Mark, L. W., Evans, H., Clout, M., Bazzaz, F. A. (2000): Biotic invasions: causes, epidemiology, global consequences, and control. – Ecological Applications 10: 689-710.
[46] Malik, A. I., Colmer, T. D., Lambers, H., Setter, T. L., Schortemeyer, M. (2002): Short-term waterlogging has long-term effects on the growth and physiology of wheat. – New Phytologist 153: 225-236.
[47] Miao, Y., Zhu, Z., Guo, Q., Ma, H., Zhu, L. (2015): Alternate wetting and drying irrigation-mediated changes in the growth, photosynthesis and yield of the medicinal plant Tulipa edulis. – Industrial Crops and Products 66: 81-88.
[48] Mitton, J. B., Grant, M. C., Yoshino, A. M. (1998): Variation in allozymes and stomatal size in pinyon (Pinus edulis, Pinaceae), associated with soil moisture. – American Journal of Botany 85: 1262-1265.
[49] Moore, J. P., Vicré-Gibouin, M., Farrant, J. M., Driouich, A. (2008): Adaptations of higher plant cell walls to water loss: drought vs desiccation. – Physiologia Plantarum 134: 237-245.
[50] Pasala, R. K., Md, I. R. K., Paramjit, S. M., Farooq, M. A., Sultana, R. (2016): Can plant bio-regulators minimize crop productivity losses caused by drought, salinity and heat stress? An integrated review. – J Appl Bot Food Qual 89: 113-125.
[51] Pei, Z. F., Ming, D. F., Liu, D., Wan, G. L., Geng, X. X., Gong, H. J., Zhou, W. J. (2009): Silicon Improves the Tolerance to Water-Deficit Stress Induced by Polyethylene Glycol in Wheat (*Triticum aestivum* L.) Seedlings. – Journal of Plant Growth Regulation 29: 106-115.
[52] Pintó-Marijuan, M., Munné-Bosch, S. (2013): Ecophysiology of invasive plants: osmotic adjustment and antioxidants. – Trends in Plant Science 18: 660-666.

http://www.aloki.hu ● ISSN 1589 1623 (Print) ● ISSN1785 0037 (Online)
DOI: http://dx.doi.org/10.15666/aeer/2003_26972716

[53] Pintó-Marijuan, M., Cotado, A., Fleta-Soriano, E., Munné-Bosch, S. (2016): Drought stress memory in the photosynthetic mechanisms of an invasive CAM species, Aptenia cordifolia. – Photosynthesis Research 131: 241-253.
[54] Praxedes, S. C., DaMatta, F. M., Loureiro, M. E., Ferrão, M. A. G., Cordeiro, A. T. (2006): Effects of long-term soil drought on photosynthesis and carbohydrate metabolism in mature robusta coffee (*Coffea canephora* Pierre var. kouillou) leaves. – Environmental and Experimental Botany 56: 263-273.
[55] Quinet, M., Descamps, C., Coster, Q., Lutts, S., Jacquemart, A-L. (2015): Tolerance to Water Stress and Shade in the Invasive *Impatiens parviflora*. – International Journal of Plant Sciences 176: 848-858.
[56] Reddy, A. R., Chaitanya, K. V., Vivekanandan, M. (2004): Drought-induced responses of photosynthesis and antioxidant metabolism in higher plants. – Journal of Plant Physiology 161: 1189-1202.
[57] Ruprecht, E., Fenesi, A., Nijs, I. (2013): Are plasticity in functional traits and constancy in performance traits linked with invasiveness? An experimental test comparing invasive and naturalized plant species. – Biological Invasions 16: 1359-1372.
[58] Sasidharan, R., Mustroph, A., Boonman, A., Akman, M., Ammerlaan, A. M. H., Breit, T., Schranz, M. E., Voesenek, L. A. C. J., Tienderen, P. H. (2013): Root transcript profiling of two Rorippa species reveals gene clusters associated with extreme submergence tolerance. – Plant Physiology 163: 1277-1292.
[59] Shukla, P. S., Gupta, K., Agarwal, P., Jha, B., Agarwal, P. K. (2015): Overexpression of a novel SbMYB15 from Salicornia brachiata confers salinity and dehydration tolerance by reduced oxidative damage and improved photosynthesis in transgenic tobacco. – Planta 242: 1291-1308.
[60] Smaoui, A., Jouini, J., Rabhi, M., Bouzaien, G., Albouchi, A., Abdelly, C. (2011): Physiological and anatomical adaptations induced by flooding in Cotula coronopifolia. – Acta Biologica Hungarica 62: 182-193.
[61] Taheri-Garavand, A., Rezaei, N. A., Fanourakis, D., Fatahi, S., Ahmadi, M. M. (2021): Employment of artificial neural networks for non-invasive estimation of leaf water status using color features: a case study in Spathiphyllum wallisii. – Acta Physiologiae Plantarum 43: 1-11.
[62] Valliyodan, B., Nguyen, H. T. (2006): Understanding regulatory networks and engineering for enhanced drought tolerance in plants. – Current Opinion in Plant Biology 9: 189-195.
[63] Vince, G. H., Bendszus, M., Schweitzer, T., Goldbrunner, R. H., Roosen, K. (2004): Spontaneous regression of experimental gliomas - An immunohistochemical and MRI study of the C6 glioma spheroid implantation model. – Experimental Neurology 190: 478-485.
[64] Wang, Z. L., Gao, J. F. (2006): Practical soil moisture monitoring and forecasting technology. – China Water Power Press, Beijing. (A Chinese book).
[65] Wang, H. F., Zhu, Y. H., Sun, H. J. (2006): Determination of drought tolerance using root activities in Robinia pseudoacacia 'Idaho' transformed with mtl-D gene. – Forest Ecosystems 8: 75-81.
[66] Wang, N., Yuan, M. L., Chen, H., Li, Z. Z., Zhang, M. X. (2019): Effects on drought stress and rewatering on growth and physiological characteristic of invasive aegilops tauschii seedings. – Acta Prataculturae Sinica 28: 70-78. (In Chinese).
[67] Williams-Linera, G., Berry, Z. C., Díaz-Toribio, M. H., Espejel-Ontiveros, X. (2021): Drought responses of an exotic tree (*Eriobotrya japonica*) in a tropical cloud forest suggest the potential to become an invasive species. – New Forests 52: 1-15.
[68] Wu, X., Yuan, J., Luo, A., Chen, Y., Fan, Y. (2016): Drought stress and re-watering increase secondary metabolites and enzyme activity in dendrobium moniliforme. – Industrial Crops and Product 94: 385-393.

http://www.aloki.hu ● ISSN 1589 1623 (Print) ● ISSN1785 0037 (Online)
DOI: http://dx.doi.org/10.15666/aeer/2003_26972716

[69] Xu, L., Islam, F., Ali, B., Pei, Z., Li, J., Ghani, M. A., Zhou, W. (2017): Silicon and water-deficit stress differentially modulate physiology and ultrastructure in wheat (*Triticum aestivum* L.). – Biotech 7: 273.
[70] Yang, L., Zhao, Y., Zhang, Q., Cheng, L., Han, M., Ren, Y., Yang, L. (2019): Effects of drought-re-watering-drought on the photosynthesis physiology and secondary metabolite production of *Bupleurum chinense* DC. – Plant Cell Reports 38: 1181-1197.
[71] Zhang, S. M., Li, Z. X., Wang, Q., Chen, C., Jiang, X. P., Sun, H. K. (2009): A newly recorded species *Rorippa amphibia* (L.) Besser from China. – Journal of Tropical and Subtropical Botany 17: 176-178. (In Chinese).
[72] Zhang, X., Yang, Z., Li, Z., Zhang, F., Hao, L. (2020): Effects of drought stress on physiology and antioxidative activity in two varieties of Cynanchum thesioides. – Brazilian Journal of Botany 43: 1-10.

http://www.aloki.hu ● ISSN 1589 1623 (Print) ● ISSN1785 0037 (Online)
DOI: http://dx.doi.org/10.15666/aeer/2003_26972716

PERFORMANCE OF PRETREATMENTS AND MULTIVARIATE METHOD ON THE HYPERSPECTRAL ESTIMATION OF SOIL MOISTURE CONTENT

YAN, X. B.[1] – WANG, Y. X.[1] – ZHANG, X.[1] – WANG, Z. G.[1] – YANG, S.[1] – LI, Y.[1] – YANG, C. B.[1] – FENG, M. C.[1] – SONG, X. Y.[1] – ZHANG, M. J.[1] – XIAO, L. J.[1] – FAHAD, S.[2] – YANG, W. D.[1*] – WANG, C.[1*]

[1]*College of Agriculture, Shanxi Agricultural University, Taigu, China*

[2]*Institute of Molecular Biology and Biotechnology, The University of Lahore, Pakistan*

**Corresponding authors*
e-mail/phone: sxauywd@126.com/+86-138-3483-5129 – W. D. Yang;
wcqxx2005@126.com/+86-153-0354-3914 – C. Wang

(Received 6th Jan 2022; accepted 21st Mar 2022)

Abstract. Soil moisture controls the exchange of energy between the land surface and the atmosphere and is a significant factor affecting plant growth and productivity. Hyperspectral monitoring of soil water fraction could provide a theoretical basis for real-time estimation of spatial and temporal variations in soil moisture. To quantitatively evaluate the hyperspectral monitoring of soil moisture content (SMC): the SMC and its corresponding spectral reflectance were measured in the laboratory. In addition, the original spectral data was pre-processed by single and multiple transformations to study the effect of spectral preprocessing methods on the quantitative evaluation of soil moisture. The successive projections algorithm (SPA) was used to extract the corresponding wavelengths of soil moisture and the spectral monitoring model was established by using the partial least squares (PLS). The results show that (1) SMC and spectral reflectance show an obvious negative correlation, and the spectral reflectance gradually decreases with the increase of SMC. (2) Appropriate pretreatment methods can improve the correlation between SMC and spectral reflectance and improve the accuracy of the SMC monitoring model, of which T19 (R^2 + SNV + FD) is the best spectral pretreatment method. (3) The optimal SMC monitoring model is T19-SPA-PLS (R^2v = 0.986, RMSEv = 1.824, RPD = 8.239). This study provided a reference for spectral data processing and an effective method for the accurate estimation of SMC using hyperspectral remote sensing.
Keywords: *soil moisture content, multivariate statistical analysis, spectral features, partial least squares, remote sensing*

Introduction

Soil surface moisture plays an important role in the exchange of water and heat energy between the land surface and the atmosphere (Shepherd et al., 2002). Soil moisture content (SMC) is an important factor affecting crop growth and development as well as an indicator of drought stress (Yuan et al., 2019). Real-time accurate determination of soil moisture is extremely difficult as traditional approaches cannot be used on such a large scale under field conditions (Zhang et al., 2020). Soil hyperspectral technology is characterized by a huge amount of information, fast operation without damaging and pollution concerns; and is preferred in soil water content estimation (Zeng et al., 2017; Yu et al., 2017; Cai et al., 2018). Monitoring SMC on different spatial scales is of great significance for formulating scientific and reasonable irrigation plans, realizing efficient utilization of water resources, and to improve crop yields with efficient irrigation systems (Hasan., 2014).

http://www.aloki.hu ● ISSN 1589 1623 (Print) ● ISSN 1785 0037 (Online)
DOI: http://dx.doi.org/10.15666/aeer/2003_27172732

Hyperspectral techniques could be used to monitor SMC as there is a strong correlation between soil moisture content and hyperspectral reflectance (Qi et al., 2017). To be more precise, spectral reflectance will decrease with the increase of soil moisture content within a certain range (1400~1900 nm range). Based on the excellent correlation between soil moisture and spectral reflectance, many studies have established soil moisture monitoring models (Sanchez et al., 2014; Brosinsky et al., 2014). However, the accuracy of these soil moisture monitoring models is still needed to be improved (Yuan et al., 2019). It is pertinent to mention here that spectral data collection is often affected by instrumental errors, environmental changes, and extraneous factors (Liu et al., 2004). Therefore, it is imperative to preprocess the spectral data before modeling to improve the accuracy of the model (Xu et al., 2016; Wu et al., 2020). The common soil spectral pre-treatment methods mainly include smooth denoising, normalization, first-order derivative and multivariate scattering correction, and so on (Rinnan et al., 2009). The use of spectral pretreatment methods can in turn improve the accuracy of monitoring models (Guo et al., 2014; Wu et al., 2018). It has been proved that the spectral pretreatments and the combination of appropriate calibrated models can generally make a positive contribution to the predictive model (Li et al., 2014). By contrast, there is no single or combined of pre-processing method suitable for all different soil situations (Dotto et al., 2018). Therefore, exploration of different preprocessing methods before model calibration can provide a new perspective for the improvement of model accuracy (Zhang et al., 2014; Wang et al., 2017).

Soil texture and type can have a significant impact on the accuracy of soil moisture content monitoring models. He (2006) showed that soil type can seriously affect the reflectance of soil spectra because different types of soils have different physicochemical characteristics. For example, sandy soils have greater spectral reflectance than loamy soils. Lu (2018) showed that the accuracy and stability of the SMC prediction model improved as the soil particle size became smaller. Many studies have shown that it is difficult to analyze the effect of SMC on spectral reflectance when mixing different types of soils for a study (Liu et al., 2014). Therefore, in order to avoid the influence of factors other than SMC on the spectral properties of soils, the spectral reflectance of different soil moisture contents was measured under laboratory conditions in this study with a single soil type as the study object. In this study, we adopted a variety of pretreatment methods to transform the original spectral data and then used SPA to extract the characteristic wavelength of the preprocessed spectral data. Finally, we constructed PLS models of SMC on the full spectrum and on the characteristic wavelengths, respectively. The main objective of this study was to explore the best spectral pre-treatment method to achieve accurate monitoring of SMC.

Materials and methods

Soil sample collection and moisture treatments

The soil samples were collected from Jinzhong City, Shanxi Province, China (37.6874° N, 112.7527° E). The soil is calcareous yellow-brown soil developed from loess parent material with a medium soil fertility (Wang et al., 2016). The soil was collected from 0 – 20 cm depth, homogenized, passed through a 2 mm sieve, and finally dried in an incubator at 105 °C for 24 h. Briefly, 10 soil samples of 100 g each were placed inside a box (diameter of 9 cm and a height of 2 cm). After its surface is scraped

http://www.aloki.hu ● ISSN 1589 1623 (Print) ● ISSN 1785 0037 (Online)
DOI: http://dx.doi.org/10.15666/aeer/2003_27172732

flat, distilled water is slowly injected into the soil until soil saturation is achieved. Afterward, the soil samples were placed at room temperature to allow water evaporation naturally. Spectral information of soil samples was recorded regularly during the air-drying process and soil moisture content was determined on a gravimetric basis. A total of 120 soil spectral data were collected and we divided them into the calibration set (n = 80) and the validation set (n = 40).

Determination of soil moisture content

To avoid the error caused by water evaporation, the water content of the soil samples was estimated immediately after the soil spectral reflectivity data was collected. The SMC is expressed by θ and is calculated as follows:

$$\theta = (W_2 - W_0)/(W_0 - W_1) \times 100\% \quad \text{(Eq.1)}$$

where W_0 is the total weight of the dried soil sample and the black plastic box; W_1 is the weight of the black plastic box, and W_2 is the weight of the plastic box and the soil sample during air drying.

Spectral measurements

Spectral reflectance of soil was measured by using a Field Portable Spectrometer (ASD FieldSpec.3) inside a dark room. *Figure 1* shows the soil samples and experimental equipment. The device has a band range of 350~2500 nm, with a sampling interval of 1.4 nm (350~1000 nm) and 2 nm (1000~2500 nm): and a resampling interval of 1 nm, with a total of 2,151 bands. The light source of the spectrometer is a 50 W halogen lamp. When measuring the soil spectral reflectance, the light source was 30 cm away from the surface of the soil sample, and the zenith angle of the light source remained 15°. The sensor of the spectrometer was located 10 cm above the surface of the soil sample, the whiteboard calibration was carried out before each soil spectrometric determination. During the collection of spectral reflectance of soil, the frequency of our collection of spectral reflectance decreases as the moisture content of the soil decreases. When the SMC is high, the soil spectral reflectance is measured every 4 h because the water evaporates more quickly. When the SMC is low, the soil spectral reflectance is measured every 8 h because the soil evaporates more slowly. We set the scan time for a spectral curve to 5 s. While determining the spectral reflectance, four angles were measured for each soil sample. After an angle is determined, the soil sample was rotated 90 degrees to measure the next Angle, and therefore 10 spectral curves were collected from each angle. After the removal of abnormal soil spectra, the collected spectral data was averaged and processed as the final spectrum of the soil sample.

Spectral data preprocessing and analyses

We used ViewSpecPro software to remove outliers, rectify spectral breakpoints, and normalize the spectral data. Moreover, the Unscrambler X 10.4 software was used to preprocess spectral data, Matlab 2018 software was used to extract characteristic bands and establish models, and finally, the data was mapped using Origin 2021 software. Before the use of the spectral data, the spectral edge with low signal-noise ratio (350~399 nm and 2451~2500 nm) affected by the internal noise of the spectrometer was eliminated, and then the original spectral data were preprocessed with 20 methods in

http://www.aloki.hu ● ISSN 1589 1623 (Print) ● ISSN 1785 0037 (Online)
DOI: http://dx.doi.org/10.15666/aeer/2003_27172732

total, including conventional mathematical transformation, standard normal transformation (SNV) and First derivative (FD) as shown in *Table 1*.

Figure 1. *Spectroscopic equipment and soil samples*

Table 1. *The list and details of different methods used during preprocessing of soil spectral data*

Shortened form	Pre-processing method	Shortened form	Pre-processing method
T0	R	T10	R + FD
T1	1/R	T11	1/R + FD
T2	Log R	T12	Log R + FD
T3	$\sqrt{R}$	T13	$\sqrt{R}$ + FD
T4	R^2	T14	R^2 + FD
T5	R + SNV	T15	R + SNV + FD
T6	1/R + SNV	T16	1/R + SNV + FD
T7	Log R + SNV	T17	Log R + SNV + FD
T8	$\sqrt{R}$ + SNV	T18	$\sqrt{R}$ + SNV + FD
T9	R^2 + SNV	T19	R^2 + SNV + FD

R is the original spectral reflectance

The introduction of the partial least squares method

Partial least squares (PLS) is a powerful multivariate statistical tool that has been widely used in many fields. PLS is an effective statistical method, which can compress a large number of related spectral data into several uncorrelated principal components, and mainly solve the regression problem from multiple dependent variables to multiple independent variables. It is especially suitable for the situation where the variables in the prediction matrix are more than the observed values, and the values of independent variables exist multicollinearity. Studies have shown that the PLS0 method can establish a linear equation between soil properties and spectra, and successfully use laboratory or field spectra for soil spectral analysis and soil characterization (Xu et al., 2020).

http://www.aloki.hu ● ISSN 1589 1623 (Print) ● ISSN 1785 0037 (Online)
DOI: http://dx.doi.org/10.15666/aeer/2003_27172732

Statistical analyses and model evaluation parameters

The determination coefficient (R^2): root mean square error (RMSE): and relative percent deviation (RPD) were selected to evaluate the prediction accuracy of the model. The values of R^2 reflect the stability of model establishment and subsequent verification. The closer R^2 to 1, the better the model is stable and has a higher fitting degree. By contrast, the smaller RMSE values represent the better predictive ability of the model. Finally, the RPD also reflects the predictive ability of the model. If RPD < 1.4, the stability of the model is poor; if $1.4 \leq RPD < 2$, the model can make a rough assessment of the samples; if $RPD \geq 2$, the model can make a good prediction of the samples (Guo et al., 2014).

Results

Descriptive statistical analysis for the SMC

In this study, a total of 120 samples were collected, and the samples were sorted from high to low based on the value of SMC, and then, we divided the calibration set and validation set by 2:1. As shown in *Table 2,* the number of samples in the calibration set was 80, including the maximum and the minimum values of SMC with 65.1% and 0.1%, respectively. The number of validations set samples was 40, the maximum value of 65% while, the minimum value of 0.3%. In addition, the correction coefficient (CV) of the calibration set and validation set were 73.7% and 74.6%, respectively. Since the data distribution of SMC is relatively uniform and the share of data in the calibration set is 2/3, the range, minimum, maximum, mean, SD, and CV values of the calibration set and the total sample are basically the same. The validation set, on the other hand, has a smaller number of samples, 1/3 of the total sample, and therefore exhibits slight differences in SD and CV data between the calibration set and the total sample. The CV of SMC is exceeded 36%, which indicates a high dispersion of SMC values.

Table 2. *Statistical characteristics of the SMC*

	Samples	**range**	**Min**	**Max**	**Mean**	**SD (%)**	**Skewness**	**Kurtosis**	**CV**
Calibration set	80	65.0%	0.1%	65.1%	20.1%	14.839	0.765	0.207	73.7%
Validation set	40	64.7%	0.3%	65.0%	20.1%	15.028	0.836	0.566	74.6%
Total sample	120	65.0%	0.1%	65.1%	20.1%	14.839	0.779	0.259	73.7%

SD is the standard deviation. Range represents the difference between the maximum and minimum values. Min. and Max. express the minimum value and maximum value of soil moisture content, respectively

Spectral response on SMC

Figure 2 shows the spectral curves of soils in different moisture ranges. It can be seen that there are three distinct absorption valleys near the 1400 nm, 1900 nm, and 2200 nm bands of the spectral curve, respectively. The absorption valley near the 1900 nm band is the largest, while the absorption valley near the 2200 nm band is the smallest. Moreover, with the increase of SMC, the absorption valley near the 2200 nm band became gradually less obvious. In addition, it can be seen that the spectral reflectance shows a gradual decrease as the soil moisture increases, and it decreases

http://www.aloki.hu ● ISSN 1589 1623 (Print) ● ISSN 1785 0037 (Online)
DOI: http://dx.doi.org/10.15666/aeer/2003_27172732

sharply when the soil moisture range increases from 0~15% to 15~30%. It can be seen that the change in reflectance in the visible band (400-780 nm) is significantly smaller than that in the NIR band (780~2450 nm). And in the visible band, the spectral reflectance tends to increase significantly with the increase of wavelength, and the slope of the spectral reflectances decreases continuously with the increase of the soil moisture range.

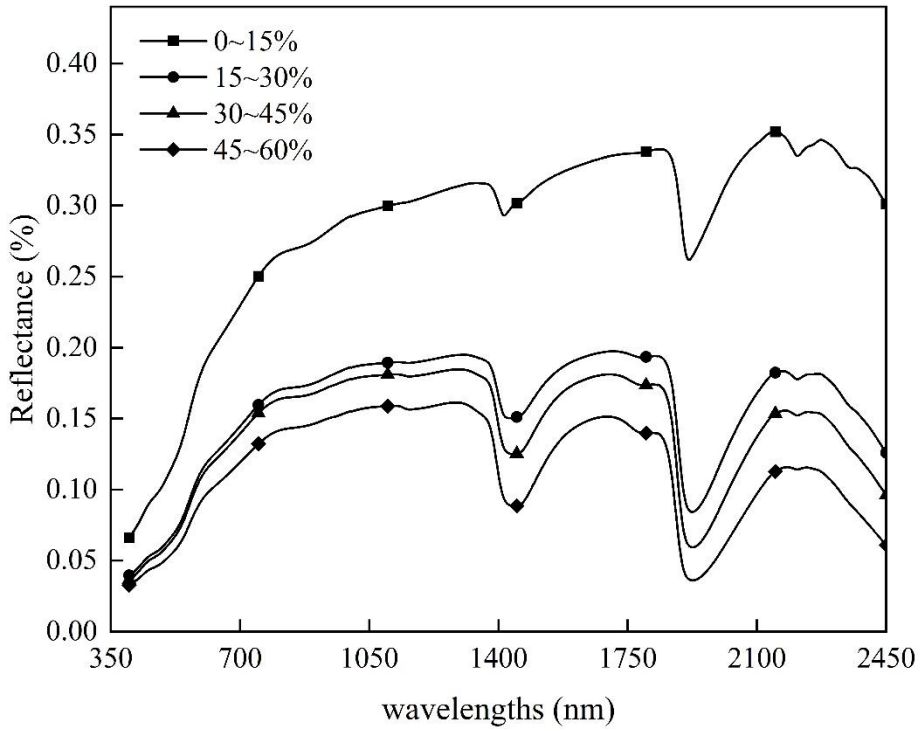

Figure 2. *Soil hyperspectral reflectance curves under different soil moisture ranges*

Correlation between soil spectral reflectance after pretreatment and soil moisture content

Figure 3a shows the correlation between the spectral reflectance and SMC after different pretreatments in the band of 400 nm to 2450 nm. *Figure 3b* shows the position of the highest correlation between the spectral reflectance and SMC with different pretreatments. It can be seen from *Figure 3* that the original spectral reflectance (T0) shows a significant negative correlation with the SMC, and its maximum absolute correlation coefficient (MACC) with SMC is 0.901. The MACC after T4 pretreatment was -0.838, which was significantly lower compared to the MACC of the original spectral reflectance with SMC. However, the MACC between the spectrum reflectance under other Pretreatment methods and the SMC improved to varying degrees. Among them, the MACC of spectral reflectance and SMC after T19 pretreatment showed the largest increase, with the MACC value of 0.991. It can be seen from *Figure 3b* that the MACC values of spectral reflectance and SMC after different pretreatments were distributed in three ranges, 1313~1495 nm, 1763~1943 nm, and 2188~2416 nm, respectively. As shown in the soil spectral reflectance curve in *Figure 2,* there are three obvious moisture absorption valleys in these three band ranges, therefore, these three bands must have a strong correlation with SMC.

http://www.aloki.hu ● ISSN 1589 1623 (Print) ● ISSN 1785 0037 (Online)
DOI: http://dx.doi.org/10.15666/aeer/2003_27172732

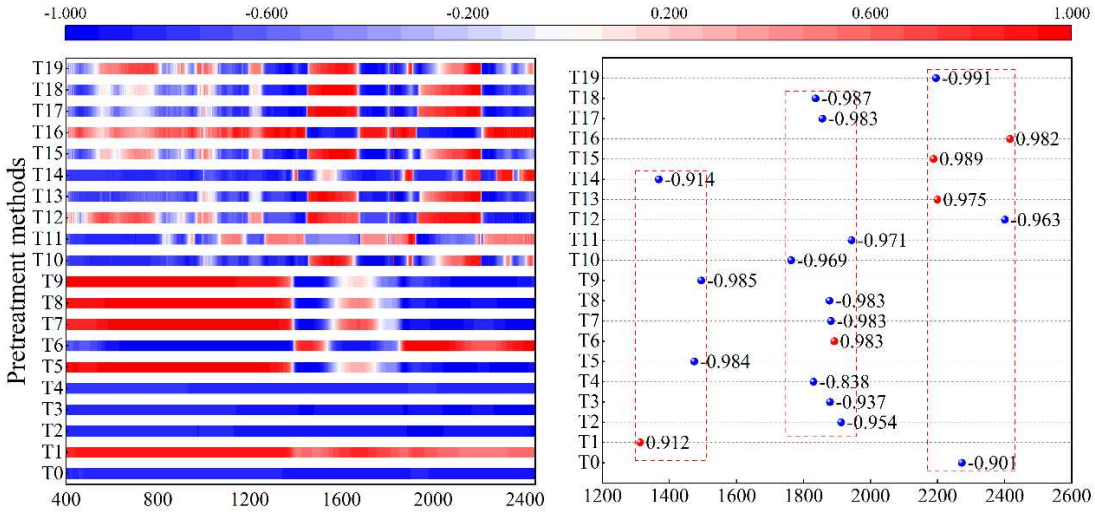

Figure 3. *Correlation of spectral reflectance with SMC after different pretreatments*

Establishment of SMC models based on the full spectrum.

With different pretreatment methods, we constructed full-spectrum PLS monitoring models for SMC, respectively. The models' performance were presented in *Table 3*. It can be seen that the accuracy of the SMC monitoring model decreases after applying the four classical mathematical variants from T1 to T4, as well as after applying FD preprocessing based on T1 to T4 (T11~T14). However, the accuracy of the SMC monitoring model improved after applying SNV preprocessing (T5): FD preprocessing (T10): SNV + FD preprocessing (T15): and applying SNV preprocessing based on T1~T4 (T6~T9). In addition, the accuracy of the SMC monitoring model improved after applying FD preprocessing based on T6~T9 (T16~T19). Comparing the SMC monitoring models constructed after applying different pretreatments, we can conclude that the SMC monitoring model constructed by applying the T19 pretreatment method is the best ($R^2v = 0.987$, RMSEv = 1.704, RPD = 8.819). To clearly show the PLSR model performance for SMC, the scatter plots and fitting lines of measured and predicted values for SMC were represented in *Figure 4*. As seen from the validation results, the data points in the scatter plot are near the 1:1 fit line, and the fit lines of the calibration and validation sets largely overlap with the 1:1 fit line. It indicates that the T19-PLS model has excellent monitoring ability for SMC.

Analysis of spectral variable selection results based on SPA

To screen out the characteristic wavelengths of SMC and further build the SMC monitoring model with lower complexity, as shown in *Figure 5,* SPA was used to screen the characteristic wavelengths under different pretreatments. It can be seen that the characteristic wavelengths under T0~T9 pretreatments are mainly distributed in four regions, which are 400~715 nm, 1256~1596 nm, 1799~1985 nm, and 2139~2278 nm, respectively. however, the characteristic wavelengths under T10~T19 pretreatment are mainly distributed in 402~585 nm, 805~1089 nm, 1805~1950 nm, and 2161~2278 nm. The reason for this phenomenon may be that T10~T19 applied the FD method, which led to the enhancement of the spectral features in the NIR short-wave region.

http://www.aloki.hu ● ISSN 1589 1623 (Print) ● ISSN 1785 0037 (Online)
DOI: http://dx.doi.org/10.15666/aeer/2003_27172732

Table 3. *Performance of SMC models constructed by using the full spectrum*

Model types	Calibration set		Validation set		
	R^2c	RMSEc	R^2v	RMSEv	RPD
T0-PLS	0.943	3.520	0.954	3.318	4.529
T1-PLS	0.845	5.815	0.735	11.080	1.356
T2-PLS	0.907	4.504	0.886	5.410	2.778
T3-PLS	0.930	3.907	0.953	3.258	4.613
T4-PLS	0.920	4.170	0.937	3.831	3.923
T5-PLS	0.981	1.998	0.983	1.944	7.730
T6-PLS	0.981	2.007	0.973	2.482	6.055
T7-PLS	0.974	2.376	0.977	2.265	6.635
T8-PLS	0.978	2.177	0.981	2.094	5.175
T9-PLS	0.983	1.936	0.983	1.943	7.734
T10-PLS	0.941	3.568	0.960	2.979	5.045
T11-PLS	0.936	3.741	0.908	5.262	2.856
T12-PLS	0.954	3.149	0.917	4.396	3.416
T13-PLS	0.927	3.991	0.932	4.066	3.696
T14-PLS	0.942	3.544	0.943	3.615	4.160
T15-PLS	0.988	1.617	0.979	2.149	4.157
T16-PLS	0.972	2.462	0.953	3.814	3.940
T17-PLS	0.989	1.538	0.982	2.009	7.480
T18-PLS	0.983	1.943	0.981	2.058	7.302
T19-PLS	0.999	0.517	0.987	1.704	8.819

R^2, RMSE, and RPD represent the determination coefficient, root means square error, and residual prediction deviation, respectively

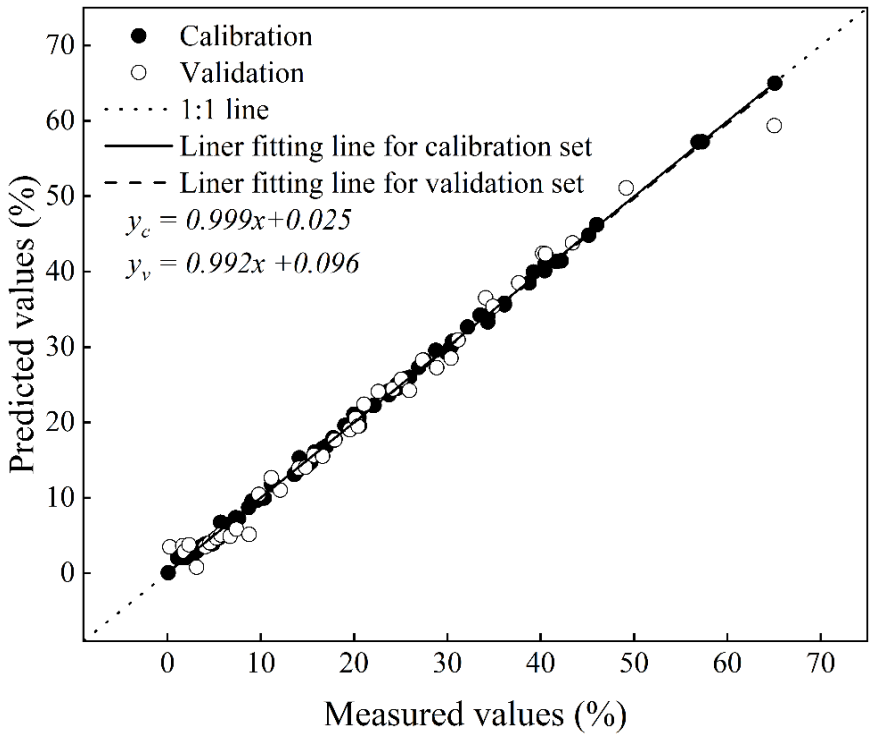

Figure 4. *Relationships between measured values and predicted values of SMC by using the T19-PLS model*

http://www.aloki.hu ● ISSN 1589 1623 (Print) ● ISSN 1785 0037 (Online)
DOI: http://dx.doi.org/10.15666/aeer/2003_27172732

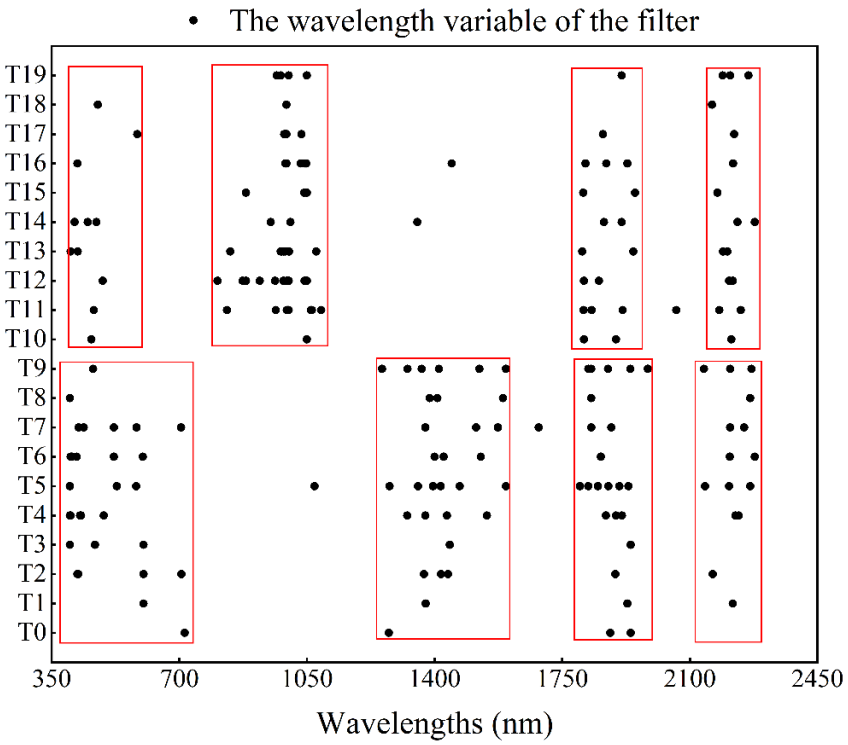

Figure 5. *Results of characteristic wavelengths filtered by SPA*

Establishment of SMC monitoring models based on characteristic wavelengths

Based on the above feature wavelengths screened using SPA under different pretreatments, we constructed SMC monitoring models based on the characteristic wavelengths, and the performance of these models is shown in *Table 4*. It can be seen that the accuracy of the T1-SPA-PLS, T2-SPA-PLS, T11-SPA-PLS, T13-SPA-PLS and T14-SPA-PLS models decreased compared with the T0-SPA-PLS model. However, the accuracy of all other models improved to different degrees, with the T19-SPA-PLS model having the highest accuracy ($R^2v = 0.986$, $RMSEv = 1.824$, $RPD = 8.239$). *Figure 6* is a scatter plot of the fit of the predicted and measured values of the T19-SPA-PLS model, from which it is clear that the performance of the T19-SPA-PLS model is outstanding. The fitted lines of the calibration and prediction set largely overlap with the 1:1 fit line. Comparing the models built from the full spectrum and the models built based on the characteristic wavelengths, it can be seen that T19 is the best spectral preprocessing method. Comparing the accuracy of the T19-PLS model and the T19-SPA-PLS model, it can be found that the accuracy of the two models is almost the same. However, compared to the model complexity, the T19-SPA-PLS model has few variables, so the model complexity is lower. Therefore, it can be concluded that the T19-SPA-PLS model is more valuable.

Discussion

Spectral response and character on SMC

The results of this study showed that the soil hyperspectral reflectance decreased with the increase of SMC, and there were two obvious absorption valleys near 1400 nm

http://www.aloki.hu ● ISSN 1589 1623 (Print) ● ISSN 1785 0037 (Online)
DOI: http://dx.doi.org/10.15666/aeer/2003_27172732

and 1900 nm, which is the same as previous studies (Tan et al., 2021). SMC showed a significant negative correlation with spectral reflectance (Babaeian et al., 2015). Generally, when the mass moisture content of the soil is below field capacity, the increase of soil moisture causes the soil surface particles to absorb moisture first and then become covered in a thin layer of water in the form of film around particles, and then, the light over the surface of the soil particles and water film exhibit multiple reflections resulting in decreased soil reflectance patterns (Yang et al., 2019). This may explain why the spectral reflectance is higher when the SMC is in the range of 0~15% and lower when the SMC is in the range of 15~60%. On the other hand, in terms of the effect of SMC on soil color, when the SMC is low, the soil color is lighter and the spectral reflectance is higher, and as the SMC increases, the soil color becomes darker and the spectral reflectance decreases. When the SMC is in the range of 0~15%, the change of soil color changes significantly with the increase of moisture content, and when the SMC exceeds 15%, the effect of moisture content on soil color becomes smaller. Therefore, it may lead to the difference of spectral curve changes in different soil moisture ranges. In addition, in the short-wave infrared region, water has a significant effect on reflectance due to the absorption of water at wavelengths above 1000 nm, and the increase in water has a significant effect on the spectral reflectance of the soil (Lobell et al., 2002). Therefore, in the near-infrared spectral region, the spectral profile exhibits a huge variation phenomenon.

Table 4. *Performance of SMC models constructed by using the characteristic wavelengths*

Model types	Calibration set		Validation set		
	R^2c	RMSEc	R^2v	RMSEv	RPD
T0-SPA-PLS	0.881	5.102	0.891	5.127	2.931
T1-SPA-PLS	0.846	5.845	0.762	9.625	1.561
T2-SPA-PLS	0.901	4.653	0.868	5.877	2.557
T3-SPA-PLS	0.938	3.721	0.961	3.015	4.984
T4-SPA-PLS	0.912	4.375	0.938	3.758	3.999
T5-SPA-PLS	0.981	1.987	0.982	1.961	7.663
T6-SPA-PLS	0.966	2.721	0.955	3.125	4.809
T7-SPA-PLS	0.975	2.305	0.974	2.387	6.296
T8-SPA-PLS	0.976	2.371	0.974	2.412	6.231
T9-SPA-PLS	0.979	2.206	0.978	2.189	6.865
T10-SPA-PLS	0.900	4.751	0.946	3.658	4.108
T11-SPA-PLS	0.892	4.831	0.803	9.068	1.657
T12-SPA-PLS	0.987	1.759	0.977	2.351	6.392
T13-SPA-PLS	0.921	4.132	0.866	5.924	2.537
T14-SPA-PLS	0.856	5.568	0.879	5.204	2.888
T15-SPA-PLS	0.980	2.139	0.984	1.935	7.766
T16-SPA-PLS	0.988	1.654	0.981	2.106	7.136
T17-SPA-PLS	0.967	2.758	0.983	1.938	7.754
T18-SPA-PLS	0.971	2.514	0.982	2.038	7.374
T19-SPA-PLS	0.988	1.682	0.986	1.824	8.239

R^2, RMSE, and RPD represent the determination coefficient, root means square error, and residual prediction deviation, respectively

http://www.aloki.hu ● ISSN 1589 1623 (Print) ● ISSN 1785 0037 (Online)
DOI: http://dx.doi.org/10.15666/aeer/2003_27172732

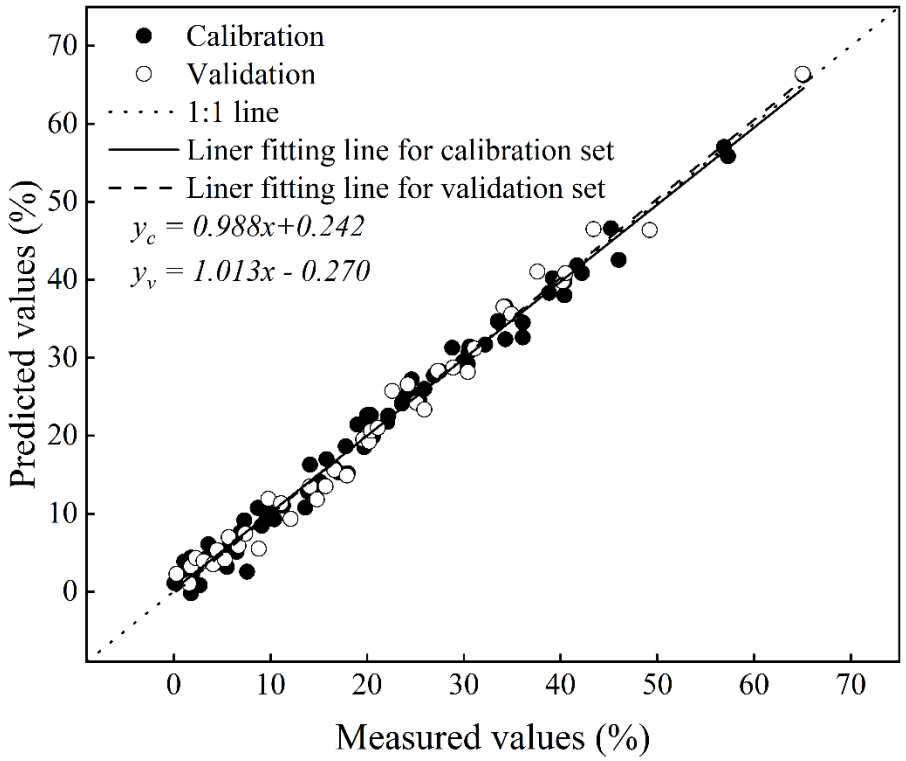

Figure 6. *Relationships between measured values and predicted values of SMC by using the T19-SPA-PLS model*

Correlation analysis of soil spectra data after different pretreatments with SMC

In the soil spectral pretreatment methods adopted in this study, when the SNV pretreatment method is used, the soil spectral characteristics before 1400 nm weakened whereas, soil spectral characteristics after 1400 nm were strengthened. After preprocessing the spectral data using the FD preprocessing method, the spectral characteristics of the soil greatly changed. The original weak spectral information was enhanced, and the spectral characteristics of some bands were highlighted (Wu et al., 2009; Sawut et al., 2014). From the positions of MACC about spectral reflectance and SMC under different pretreatments in *Figure 2,* the spectral characteristic regions of SMC are in three regions in the near-infrared band, where most of the MACC values appeared in the range of 1763~1943 nm, and in a previous study, it was also showed that the correlation between SMC and spectral reflectance was highest at 1969 nm, with the MACC value reached 0.94 (Zhai et al., 2020). Combined with the characteristic wavelengths of SMC screened using SPA in *Figure 5,* we found that the most obvious spectral characteristic region of SMC was near the 1900 nm band. In this study, compared with the original spectral reflectance (T0): except for T4, the correlation between soil spectral reflectance and soil moisture was improved after pretreatment. So, it can be concluded that suitable pre-processing methods can effectively enhance the soil spectral information and thus improve the correlation between soil spectral reflectance and SMC. For example, Yao (2011) used the spectral reflectance logarithm of the FD to estimate the SMC of black soil with a high prediction accuracy reaching 0.931. In this study, T19 was the best pretreatment method that maximized the correlation between SMC and spectral reflectance, and it is the superposition of three

http://www.aloki.hu ● ISSN 1589 1623 (Print) ● ISSN 1785 0037 (Online)
DOI: http://dx.doi.org/10.15666/aeer/2003_27172732

preprocessing methods: square, SNV, and FD. The squared original spectral reflectance was processed to highlight more clearly the positions of the peaks and troughs of the spectral curve, enhancing the effective information of the spectrum. Then, the squared spectral reflectance is further processed using SNV, which reduces the multiplicative effect of the scattering variation in the NIR spectrum and achieves the denoising effect (Diwu et al., 2019). Finally, the FD method is then applied to eliminate the spectral background noise, and it makes the spectral features more obvious (Zhang et al., 2020). T19 Applying a combination of methods to preprocess the original spectral reflectance provides a new horizon for enhancing the spectral information.

Spectral monitoring on SMC

Constructing the quantitative monitoring model of SMC by using spectral technology is essential for exploring their potential relationship and realizing their practical application in the future. In this study, PLS was used to build the SMC monitoring models. The PLS combined the characteristics of principal component analysis and multiple linear regression and can be used to resolve the collinearity problem of hyperspectral reflectance (Kuang et al., 2015; Xu et al., 2020). *Tables 3* and *4* show the SMC monitoring models built using the full spectrum and the characteristic wavelengths, respectively. It can be seen that the accuracy of both types of models constructed based on T1 and T11 is low, which indicates that the T1 and T11 methods are not suitable for dealing with spectral reflectance. The SMC monitoring models with full-spectrum constructed by applying other preprocessing methods have a good performance due to the great advantage of PLS in handling multidimensional data, and the application of PLS compresses a large amount of spectral data into a few uncorrelated principal components, which well solves the covariance problem of spectral data (Wold et al., 2001; Kahaer et al., 2020). However, SMC monitoring models constructed based on the characteristic wavelengths also perform well. SPA can eliminate the redundant information in the spectral matrix and extract some characteristic wavelengths across the band (Wei et al., 2020). In this study, the SMC model constructed based on the T19 preprocessing method has the highest accuracy due to the squared reflectance of the original spectrum, which amplifies the features of the soil spectrum, and further application of SNV to eliminate the baseline shift and improve the signal-to-noise ratio (Fearn et al., 2009; Bi et al., 2016). The application of FD amplified the effective information of the spectrum, and these three preprocessing methods were superimposed to maximize the effective information of the original spectrum. Considering the accuracy and complexity of the model, we can conclude that the SMC monitoring model based on the characteristic wavelength is better and has a higher application value because this type of model not only has very high accuracy but also low complexity. The best SMC monitoring model in this study is the T19-SPA-PLS ($R^2v = 0.986$, RMSEv = 1.824, RPD = 8.239). Most of the previous studies only used a single pretreatment method to process the original spectral reflectance and then established a prediction model. For example, Jia (2018) preprocessed the original spectral reflectance by first-order differentiation, and the R^2v of the SMC prediction model constructed was 0.903. In comparison, the T19-SPA-PLS model preprocessed the original spectral reflectance three times, and after greatly enhancing the spectral information, the SPA was used to extract the characteristic wavelength of the enhanced spectrum, which greatly reduced the wavelength variables and decreased the complexity of the model. Therefore, the T19-SPA-PLS model can achieve more accurate spectral

http://www.aloki.hu ● ISSN 1589 1623 (Print) ● ISSN 1785 0037 (Online)
DOI: http://dx.doi.org/10.15666/aeer/2003_27172732

monitoring of SMC compared with the models constructed in the previous studies. However, real field conditions are complex, and the collection of spectral reflectance can be affected by a variety of factors, such as soil texture, soil organic matter content, soil salinity, soil particle size, etc. Therefore, if complex field soils are collected for SMC monitoring studies, it is difficult to clarify the effect of SMC on spectral properties due to the differences in soil components. Therefore, this study was conducted under laboratory conditions simulating SMC, avoiding the interference of other factors besides soil moisture. Although the relationship between SMC and spectra was adequately elucidated, the applicability of the T19-SPA-PLS model in complex field environments needs further validation.

Conclusion

In this study, we investigated the effects of different pretreatment methods on the spectral characteristics of SMC, and then compared the full-spectrum SMC monitoring model with the SMC monitoring model built based on characteristic wavelengths, and finally constructed the best SMC monitoring model. It was found that SMC showed a significant negative correlation with spectral reflectance, and the response of SMC to the spectrum was most sensitive near the 1900 nm band. Proper preprocessing methods can improve the correlation between SMC and spectral reflectance, and improve the accuracy of the monitoring model as well. The SMC monitoring model based on the characteristic wavelengths screened by SPA is not only simple in model structure but also has high accuracy, among which, T19-SPA-PLS is the best SMC monitoring model ($R^2v = 0.986$, RMSEv = 1.824, RPD = 8.239). This study provided methodological and theoretical support for accurate monitoring of SMC by using hyperspectral. Future research should focus on the effects of soil properties interacting with soil moisture on the spectra, such as the interaction of soil grain size with moisture, soil organic matter content with moisture, and soil salinity with moisture. In addition, the quantitative effects of different soil components on the hyperspectral properties during the monitoring of SMC using hyperspectral should be explored.

Acknowledgements. This work was funded by the National Natural Science Foundation of China (31871571; 31371572): Outstanding Doctor Funding Award of Shanxi Province (SXYBKY2018040): Higher education Project of Scientific and Technological Innovation in Shanxi (2020L0132) and Scientific and Technological Innovation Fund of Shanxi Agricultural University (2018YJ17, 2020BQ32). The project was also supported by the Key Technologies R & D Program of Shanxi Province (201903D211002).

REFERENCES

[1] Babaeian, E., Homaee, M., Montzka, C., Vereecken, H., Norouzi, A. A. (2015): Towards retrieving soil hydraulic properties by hyperspectral remote sensing. – Vadose Zone Journal 14(3): 1-17.

[2] Bi, Y. M., Yuan, K. L., Xiao, W. Q. (2016): A local pre-processing method for near-infrared spectra, combined with spectral segmentation and standard normal variate transformation. – Analytica Chimica Acta 909: 30-40.

[3] Brosinsky, A., Lausch, A., Doktor, D. (2014): Analysis of spectral vegetation signal characteristics as a function of soil moisture conditions using hyperspectral remote sensing. – Journal of the Indian Society of Remote Sensing 42(2): 311-324.

http://www.aloki.hu ● ISSN 1589 1623 (Print) ● ISSN 1785 0037 (Online)
DOI: http://dx.doi.org/10.15666/aeer/2003_27172732

[4] Cai, L. H., Ding, J. L. (2018): Prediction for soil water content based on variable preferred and extreme learning machine algorithm. – Spectroscopy and Spectral Analysis 38(7): 2209-2214.
[5] Diwu, P. Y., Bian, X. H., Wang, Z. F. (2019): Study on the selection of spectral preprocessing methods. – Spectroscopy and Spectral Analysis 39(9): 2800-2806.
[6] Dotto, A. C., Dalmolin, R. S. D., Caten, A. T. (2018): A systematic study on the application of scatter-corrective and spectral-derivative preprocessing for multivariate prediction of soil organic carbon by Vis-NIR spectra. – Geoderma 314: 262-274.
[7] Fearn, T., Riccioli, C., Garrido-Varo, A. (2009): On the geometry of SNV and MSC. – Chemometrics and Intelligent Laboratory Systems 96(1): 22-26.
[8] Guo, D. D., Huang, S. M., Zhang, S. Q. (2014): Comparative analysis of various hyperspectral prediction models of fluvo-aquic soil organic matter. – Transactions of the Chinese Society of Agricultural Engineering (Transactions of the CSAE) 30(21): 192-200.
[9] Hasan, S., Montzka, C., Ruediger, C. (2014): Soil moisture retrieval from airborne L-band passive microwave using high resolution multispectral data. – ISPRS Journal of Photogrammetry & Remote Sensing 91(5): 59-71.
[10] He, T., Wang, J., Cheng, H. (2006): Spectral Features of Soil Moisture. – Acta Pedologica Sinica (6): 1027-1032.
[11] Jia, X. Q., Feng, M. C., Yang, W. D. (2018): Study on the spectral prediction model of soil moisture content based on SPA-MLR method. – Agricultural Research in the Arid Areas 36(3): 266-269 + 291.
[12] Kahaer, Y., Tashpolat, N., Shi, Q. D. (2020): Possibility of Zhuhai-1 hyperspectral imagery for monitoring salinized soil moisture content using fractional order differentially optimized spectral indices. – Water 12(12): 1-29.
[13] Kuang, B. Y., Tekin, Y., Mouazen, A. M. (2015): Comparison between artificial neural network and partial least squares for on-line visible and near infrared spectroscopy measurement of soil organic carbon, pH and clay content. – Soil & Tillage Research 146: 243-252.
[14] Li, J. M., Ye, X. J., Wang, Q. N. (2014): Development of prediction models for determining N content in citrus leaves based on hyperspectral imaging technology. – Spectroscopy and Spectral Analysis 34(1): 212-216.
[15] Liu, W. D., Baret, F., Zhang, B. (2004): Using hyperspectral data to estimate soil surface moisture under experimental conditions. – Remote Sensing 8: 434-442.
[16] Liu, Y., Ding, X., Liu, H. J. (2014): Quantitative analysis of reflectance spectrum of black soil as affected by soil moisture for prediction of soil moisture in black soil. – Acta Pedologica Sinica 51(5): 1021-1026.
[17] Lobell, D. B., Asner, G. P. (2002): Moisture effects on soil reflectance. – Soil Science Society of America Journal 66(3): 722-727.
[18] Lu, Y. L., Bai, Y. L., Wang, L. (2018): Spectral characteristics and quantitative prediction of soil water content under different soil particle sizes. – Scientia Agricultura Sinica 51(9): 1717-1724.
[19] Qi, H., Xiu, J., Liu, Z. (2017): Predicting sandy soil moisture content with hyperspectral imaging. – International Journal of Agricultural and Biological Engineering 10(2): 175-183.
[20] Rinnan, A., Van, D. B. F., Engelsen, S. B. (2009): Review of the most common pre-processing techniques for near-infrared spectra. – Trends in Analytical Chemistry 28(10): 1201-1222.
[21] Sanchez, N., Piles, M., Martinez-Fernandez, J. (2014): Hyperspectral optical, thermal, and microwave L-Band observations for soil moisture retrieval at very high spatial resolution. – Photogrammetric Engineering & Remote Sensing 80(8): 745-755.

http://www.aloki.hu ● ISSN 1589 1623 (Print) ● ISSN 1785 0037 (Online)
DOI: http://dx.doi.org/10.15666/aeer/2003_27172732

[22] Sawut, M., Ghulam, A., Tiyip, T. (2014): Estimating soil sand content using thermal infrared spectra in arid lands. – International Journal of Applied Earth Observation & Geoinformation 33: 203-210.
[23] Shepherd, A., Mcginn, S. M., Wyseure, G. (2002): Simulation of the effect of water shortage on the yields of winter wheat in North-East England. – Ecological Modelling 147(1): 41-52.
[24] Tan, Y., Jiang, Q. G., Yu, L. F. (2021): Reducing the moisture effect and improving the prediction of soil organic matter with VIS-NIR spectroscopy in black soil area. – IEEE Access 9: 5895-5905.
[25] Wang, C., Feng, M. C., Yang, W. D. (2016): A new method to decline the SWC effect on the accuracy for monitoring SOM with hyperspectral technology. – Spectroscopy and Spectral Analysis 35(12): 3495-3499.
[26] Wang, X. P., Zhang, F., Kung, H. T. (2017): Spectral response characteristics and identification of typical plant species in Ebinur lake wetland national nature reserve (ELWNNR) under a water and salinity gradient. – Ecological Indicators 81: 222-234.
[27] Wei, L. F., Pu, H. C., Wang, Z. X. (2020): Estimation of soil arsenic content with hyperspectral remote sensing. – Sensors-Basel 20(14): 1-16.
[28] Wold, S., Sjostrom, M., Eriksson, L. (2001): PLS-regression: a basic tool of chemometrics. – Chemometrics & Intelligent Laboratory Systems 58(2): 109-130.
[29] Wu, C. Y., Jacobson, A. R., Laba, M. (2009): Alleviating moisture content effects on the visible near-infrared diffuse-reflectance sensing of soils. – Soil Science 174(8): 456-465.
[30] Wu, L. G., Wang, S. L., He, J. G. (2018): Study on soil moisture mechanism and establishment of model based on hyperspectral imaging technique. – Spectroscopy and Spectral Analysis 38(8): 2563-2570.
[31] Wu, T. H., Yu, J., Lu, J. X. (2020): Research on inversion model of cultivated soil moisture content based on hyperspectral imaging analysis. – Agriculture-Basel 10(7): 292.
[32] Xu, C., Zeng, W. Z., Huang, J. S. (2016): Prediction of soil moisture content and soil salt concentration from hyperspectral laboratory and field data. – Remote Sensing 42(8): 1-20.
[33] Xu, L., Wang, Z., Hu, J. (2020): Estimation of soil salinity under various soil moisture conditions using laboratory based thermal infrared spectra. – Journal of the Indian Society of Remote Sensing (4): 1-11.
[34] Yang, X. G., Yu, Y., Li, M. Z. (2019): Estimating soil moisture content using laboratory spectral data. – Journal of Forestry Research 30(3): 1073-1080.
[35] Yao, Y., Wei, N., Tang, P. (2011): Hyper-spectral characteristics and modeling of black soil moisture content. – Transactions of the Chinese Society of Agricultural Engineering 27(8): 95-100.
[36] Yu, L., Hong, Y. S., Zhu, Y. X. (2017): Removing the effect of soil moisture content on hyperspectral reflectance for the estimation of soil organic matter content. – Spectroscopy and Spectral Analysis 37(7): 2146-2151.
[37] Yuan, J., Wang, X., Yan, C. X. (2019): A semi-empirical model for reflectance spectral of black soil with different moisture contents. – Spectroscopy and Spectral Analysis 39(11): 3514-3518.
[38] Zeng, W. Z., Lei, G. Q., Zhang, H. Y. (2017): Estimating root zone moisture from surface soil using limited data. – Ecological Chemistry & Engineering S 24(4): 501-516.
[39] Zhai, H. R., Li, X. C., Zhong, H. (2020): Hyperspectral indirect estimation model of soil water content in cultivated layer. – Chinese Agricultural Science Bulletin 36(11): 86-91.
[40] Zhang, D., Tashpolat·Tiyip, Zhang, F. (2014): Application of fractional differential in preprocessing hyperspectral data of saline soil. – Transactions of the Chinese Society of Agricultural Engineering 30(24): 151-160.

http://www.aloki.hu ● ISSN 1589 1623 (Print) ● ISSN 1785 0037 (Online)
DOI: http://dx.doi.org/10.15666/aeer/2003_27172732

[41] Zhang, X. G., Kong, F. C. (2020): Using hyperspectral imagery to estimate soil moisture and calculate evapotranspiration from coastal saline soil. – Journal of Irrigation and Drainage 39(9): 14-19.
[42] Zhang, Y., Tan, K., Wang, X. (2020): Retrieval of soil moisture content based on a modified Hapke photometric model: a novel method applied to laboratory hyperspectral and Sentinel-2 MSI data. – Remote Sensing 12(14): 2239.

http://www.aloki.hu ● ISSN 1589 1623 (Print) ● ISSN 1785 0037 (Online)
DOI: http://dx.doi.org/10.15666/aeer/2003_27172732

EFFECTS OF OXYTETRACYCLINE SUPPLEMENTATION ON CRYOPRESERVED SPERM QUALITY OF SHABOUT (*BARBUS GRYPUS* HECKEL 1843): APOPTOTIC ANALYSIS, DNA DAMAGE AND OXIDATIVE STRESS

DOĞU, Z.[1*] – ŞAHINÖZ, E.[1] – ARAL, F.[2] – KOYUNCU, I.[3] – EĞI, K.[4]

[1]*Department of Fisheries and Aquaculture, Bozova Vocational High School, Harran University, 63850 Bozova, Şanlıurfa, Turkey*

[2]*Independent Researcher, Çarşı PTT PK 138 Konya, Turkey*

[3]*Department of Medical Biochemistry, Faculty of Medicine, Harran University, Şanliurfa, Turkey*

[4]*Program of Medical Promotion and Marketing, Health Services Vocational School, Harran University, Şanliurfa, Turkey*

[*]*Corresponding author*
e-mail: zaferdogu@harran.edu.tr

(Received 6th Jan 2022; accepted 25th Mar 2022)

Abstract. The study aimed to examine the effects of oxytetracycline supplementation to glucose extender on the Oxidative Status, Glutathione (GSH), Malondialdehyde (MDA), 8-Hydroxydeoxyguanosine (8-OHdG) and Apoptotic Spermatozoa of *Barbus grypus* post-thaw sperm. The semen was frozen in diluents containing three different oxytetracycline concentrations (0.78, 1.56 and 3.12 mg). All the comparable levels of oxytetracycline linearly improved the post-thaw sperm motility rate and duration significantly ($p < 0.0001$). MDA and Total Oxidative Status (TOS) were linearly and quadratically decreased, however, Total Antioxidative Status (TAS) quadratically and GSH linearly and quadratically increased with oxytetracycline ($p < 0.001$). The increasing oxytetracycline levels typically resulted in a linear decline in DNA damage in the 8-OHdG assay. The determined percentage of apoptotic spermatozoa were linearly and quadratically reduced with Oxytetracycline (OTC) ($p < 0.0001$). These results showed that oxytetracycline can be used as an antibiotic additive in semen extender, providing better sperm freezing-thawing, without decreasing semen quality and antioxidant and increasing the oxidant, DNA damage and apoptotic sperm level of the *Barbus grypus*.
Keywords: *freezing, oxidative status, apoptosis, freshwater, Barbus grypus*

Introduction

Under poor environmental conditions, the uncontrolled production of ROS and capable microorganisms typically outstrips the antioxidant capacity of the diluted provided seminal plasma, resulting in oxidative stress (Brown and Mims, 1995; Boonthai et al., 2016; Vickham et al., 2017). However, antibiotics supplementation in different amounts to extenders, could increase the fertilization rate of semen freezing media and the motility duration of the sperm.

The biggest problem with antibiotics is bacterial resistance. Bacterial resistance to antibiotics is the biggest challenge in the treatment of fish diseases and semen extender, antibiotic choice. Antibiotics have become standard additions to the extender in the sperm reconstitution process. Antibiotics are also toxic chemicals for spermatozoa. Oxytetracycline (OTC) is a broad-spectrum and low-cost antibiotic used in the

http://www.aloki.hu ● ISSN 1589 1623 (Print) ● ISSN1785 0037 (Online)
DOI: http://dx.doi.org/10.15666/aeer/2003_27332746

treatment of many bacterial fish diseases (Long et al., 1989). It is routinely administered orally through direct addition to feeds moreover it is influential in strengthening the immune system (Rickers et al., 1980; Lunden et al., 2002; Serezli et al., 2005).

Sperm and eggs obtained from aquaculture with the desired characteristics are important in terms of breeding, as they affect fertilization. Sperm freezing allows the use of semen from these fish in the present and future. One of the factors affecting sperm quality is oxidative stress during sperm freezing and thawing (Bailey et al., 2008). However, excessive amounts of oxidative stress seem to typically represent the primary reason for the damage on polyunsaturated fatty acids (PUFA) in semen membrane structure of viable sperm. Researchers have revealed that oxidative stress reduces many sperm quality parameters such as sperm motility and DNA structure (Aramli et al., 2005). Hence, detection of DNA damage in cryopreservation studies conducted in fish semen today is among the most important criteria as it gives precise and sensitive results in determining sperm quality (Dhawan et al., 2009; Çavaş, 2011; Factori et al., 2014).

Current studies for the optimization of breeding and conservation of gene resources have focused on minimizing the molecular damage that occurs during freezing and thawing of semen (Li et al., 2010; Perez-Cerezales et al., 2010). Because both osmotic stress and oxidative stress caused by reactive oxygen species negatively affect sperm quality (Klaiwattana et al., 2016; Figueroa et al., 2019). From this point of view, it is thought that antibiotics supplementations to semen extenders may reduce cryoinjury damage (Cabrita et al., 2010; Figueroa et al., 2019). In addition, antioxidants can also control the production of intracellular reactive oxygen species (ROS), which occur in living organisms as a direct result of the possible effects of some essential metal and chemical oxidants (Wink et al., 1996; Ercal et al., 2001). Previous studies have typically suggested that these fertile cells produce a low profile, in terms of motility, morphology and DNA status, to viable sperm extended with some preventive antibiotics (Jasco et al., 1993; Hargreaves et al., 1998; Ercal et al., 2001; Li et al., 2007; Castillo et al., 2015).

As the proper ratio of steady-state concentration of oxidants to antioxidant increases oxidative stress, cellular response to it prominently causes DNA damage, cell cycle arrest and apoptosis (Aprioku, 2013; Agarwal et al., 2018). Spermatozoa are equipped with antioxidant defense mechanisms and are likely to eliminate ROS. Thus, it protects gonadal cells and mature sperm from oxidative damage (Henkel, 2011).

The researches about the effect of oxytetracycline on the genetic material in sperm are sparse. Li et al. (2007) reported that amoxicillin induced DNA lesions at the going like that of intracellular reactive oxygen species induction. ROS was accumulated after quinolone removal from alive cultures co-treated with chloramphenicol to sufficiently emphasize DNA-break-mediated killing (Hong et al., 2020). It has been demonstrated that idarubicin at elevated concentrations in the expanded range of 0.001 to 10 μM causes DNA damage in normal human lymphocytes. It has been showed that idarubicin typically causes the genotoxicity (Blasiak et al., 2002).

In previous studies, semen morphology and functions were tested while evaluating the effect of some antibiotics (Rahimi et al., 2015; Boonthai et al., 2016). But, OTC supplementation to semen extender has not been tried yet in *Barbus grypus*. In this study, the effects of oxytetracycline supplementation to the semen extender on DNA damage, oxidative stress parameters and semen quality of *B. grypus* were investigated.

http://www.aloki.hu ● ISSN 1589 1623 (Print) ● ISSN1785 0037 (Online)
DOI: http://dx.doi.org/10.15666/aeer/2003_27332746

Materials and Methods

Study area and semen collection

This study was carried out in the research laboratory of the Biochemistry Department of the Harran University Faculty of Medicine. Preliminary examinations of semen samples taken from the recently deceased Shabout (B. grypus) were carried out in the Fisheries Department laboratories of Harran University Bozova Vocational School, Şanlıurfa, Turkey.

In the study, the samples aged 4-5 years obtained from the fishermen in Atatürk Dam Lake, were used (n=~~9~~). Age estimates were obtained from the scales. The size of captive *B. grypus* changed between 2000.00 and 2850.00 g (mean 2400.00 ± 26.00 g) in body weight and 61.00 and 70.00 cm (mean 65.55 ± 3.59 cm) in total length. After, the urogenital papilla of the caught fish was carefully dried to prevent the contact of urea or feces to sperm. Then, semen was collected in 5 ml glass tubes by applying abdominal massage. As soon as the collection, they were placed in styrofoam containing ice (+4.00°C) and transferred to the laboratory without delay.

Chemicals

OTC, DMSO and all chemicals were obtained from Sigma-Aldrich (St. Louis, MO, USA).

Sperm evaluation

Sperm motility, duration and concentration

For the examination of spermatological characteristics, 5 µL samples of fresh and frozen-thawed milt was activated with 25 µL of sperm activating solution (0.29% NaCl) and analysed under a light microscope (400X magnification) to confirm the duration of motility of the spermatozoa and was expressed as percentage of motile spermatozoa before and after freezing (Tekin et al., 2003). For further use, the frozen-thawed milt was stored in fridge (1-4°C). The sperm concentrations were determined using Thoma haemocytometer (TH100; Hecht-Assistent, Sondheim, Germany) and expressed as $x10^9$ spz/ mL (Tvedt et al., 2001). Following the assay, examples were excluded from the research if they gave an unexpected appearing or macroscopical pathalogical conditions, owned spermatozoan motility below 80% or lack to a sperm concentration of 9.00×10^9 spz/mL (Ansari et al., 2012; Wang and Dong, 2017). Approximately 1.5 mL of semen was taken from each sample and centrifuged at 2000 *g* for 30 minutes to measure seminal plasma osmotic pressure and pH. Subsequently, all suitable semen samples were mixed to avoid individual variation, and a semen pool was created.

Cryopreservation protocols

Study design, extender composition, semen freezing and thawing

The pooled semen sample was divided into 5 portions of 5 groups. OTC was not added in the control and fresh semen group. Oxytetracycline supplemented extender groups were classified into 3 groups of 0.78, 1.56 and 3.12 mg of OTC (modified by Elia et al., 2014). Experimental and control group sperm were immediately diluted from each sperm samples with 1:3 v/v (sperm 1:diluents 3) with the Glucose extender (0.3 M Glucose) containing 10% dimethyl sulphoxide (DMSO).The extended semen was packaged in 0.25 ml straws, and equilibrated at 4ºC for 10 minutes. The straw was

http://www.aloki.hu ● ISSN 1589 1623 (Print) ● ISSN1785 0037 (Online)
DOI: http://dx.doi.org/10.15666/aeer/2003_27332746

frozen in a styrofoam box at 5 cm above the liquid nitrogen surface for 12 minutes. The frozen semen was stored for 2 weeks in liquid nitrogen for further evaluations. The frozen semen straws were placed in a 40°C water bath for 8 second (Kopeika et al., 2007).

The pooled semen sample was divided into 4 portions of 3 freezing groups and 1 fresh semen group. Thus, for the male *B. grypus*, there were 5 sperm pool samples in each time and the application was repeated 3 times, 4 parallel samples in each time (repetitions (n)=60).

Preparation of sperm samples for biochemical analysis

In this study, equal amount of sperm samples was taken from all trial groups. Sperm samples were diluted 1/10 with PBS, homogenized with a homogenizer (Tissue Lyser LT, Qiagen) and centrifuged to obtain supernatants.

Oxidative stress analysis

The effects of extenders containing oxytetracycline on the oxidative stress indices of semen were evaluated by examining the Total Antioxidant Status (TAS), Total Oxidant Status (TOS), Glutathione (GSH) and Malondialdehyde (MDA) parameters. GSH levels were assessed through reaction with OPA (1 mg/mL o-phthaldialdehyde in methanol) following to the modified technique of Kand'ar and Hajkova (2014) with GSH used as a standard. GSH samples were assessed via microplate reader (SpectraMax, M5, San Jose, California, USA), with excitation at 345 nm and emission at 425 nm. Results were expressed as nmol/g in sperm cell.

MDA levels in the sperm were assessed following the technique defined by Ohkawa et al. (1979). ELISA plates were read by a microplate reader (SpectraMax, M5, San Jose, California, USA), at 532 nm. The results were obtained as nmol/g in sperm.

Measurement of oxidative stress status

TOS and TAS were detected in sperm homogenates by using commercially available kits (Rel Assay®, Diagnostics kits, Mega Tıp, Gaziantep, Turkey) with an autoanalyzer (Cobas Integra 800, Roche Diagnostics, Indianapolis, IA, USA). TOS and TAS results were presented in mmol H_2O_2 equivalent/L (Erel, 2005) and mmol Trolox equivalent/L, respectively (Erel, 2004). The ratio of the TOS to the TAS revealed the Oxidative Stress Index (OSI), which is used as an indicator for total oxidative stress (Harma et al., 2003).

Apoptotic analysis by ELISA and DNA damage measurement

The protective effects of extenders containing oxytetracycline on spermatozoon DNA damage were investigated by intracellular 8-Hydroxydeoxyguanosine (8-OHdG) ELISA and comet assay. The results were obtained as ng/ml in sperm.

Apoptotic analysis by ELISA of fish sperm cells

Analysis of apoptosis in sperm samples was performed according to the protocol of the commercially available kit (Cell Death Detection ELISA^{PLUS}, Roche). The assay is based on the quantitative double-antibody sandwich enzyme immunoassay principle and uses monoclonal antibodies directed against DNA and histones, respectively. Anti-DNA POD antibody binds to single- and double-stranded DNA. Therefore, the ELISA allows

http://www.aloki.hu ● ISSN 1589 1623 (Print) ● ISSN1785 0037 (Online)
DOI: http://dx.doi.org/10.15666/aeer/2003_27332746

detection of mono- and oligonucleosomes from various species and can be applied to measure apoptotic cell death in many different cell systems.

Measurement of 8-hydroxydeoxyguanosine (8-OHdG) in fish sperm

8-OHdG is one of the very significant signs of oxidant-induced DNA damage. Quantification of 8-OHdG was done by using Fish 8-OHdG ELISA kit (BT-LAB). Protocol was followed as described in the manufacturer instructions.

Statistical analysis

Minitab 17.0 was used for analysis. Normality and homogeneity of variance of the data were checked by Kolmogorov-Simirnow's tests before analyses. The data that did not yield normal distribution underwent logarithmic transformation. Percent motility and apoptotic cell data were arcsine transformed. The data generated were analyzed with the one-way ANOVA test and the differences in the data of the trial groups were revealed by using the Tukey multiple comparison test. Linear or quadratic trends on OTC comparable levels and sperm variables were determined using orthogonal polynomials (Rosales et al., 2017). All mean values represent mean ± SE from triplicate.

Results

Evaluation of sperm parameters, oxidant and antioxidant status, DNA damage

In fresh sperm, spermatozoa motility rate (%), motility duration (s), concentration ($x10^9$ spz/mL) and ph were 87.86±1.28, 118.33±2.77, 11.92±0.12 and 8.14±0.12, respectively (*Table 1*). As shown in *Table 1, Table 2, Table 3 and Table 4,* motility rate and duration, oxidant and antioxidant status, DNA damage rates and the percentage of apoptotic spermatozoa were significantly changed through the use of a glucose extender with OTC ($p<0.0001$).

Table 1. *Post-thaw spermatological parameters of B. grypus semen frozen in diluents containing three different oxytetracycline concentrations*

Dose of Oxytetracycline (Groups)		Parameters	
		Motility Rate (%)	**Motility Duration (s)**
Fresh		87.86±1.28[a]	118.33±2.77[a]
Control		31.12±3.42[d]	36.50±4.86[d]
0.78 mg		50.83±3.58[b]	63.33±2.61[c]
1.56 mg		52.50±3.05[b]	71.08±2.99[b]
3.12 mg		59.17±2.60[b]	76.50±2.00[b]
Pr >F[1]	ANOVA	0.0001	0.0001
	Linear trend	0.001	0.0001
	Quatratic trend	0.0001	0.0001

Data are presented Mean ± SE of values. Different letters as a,b,c show differences between groups ($p< 0.001$), *post hoc* comparisons with Tukey multiple comparison test

http://www.aloki.hu ● ISSN 1589 1623 (Print) ● ISSN1785 0037 (Online)
DOI: http://dx.doi.org/10.15666/aeer/2003_27332746

Effect of oxytetracycline on post-thaw sperm motility and motility duration

Spermatozoa motility rate and motility duration are shown in *Table 1*. The freezing process typically had a significant negative effect on the motility and typical duration of it ($p<0.0001$). Increasing the levels of OTC significantly affected the spermatozoa motility rate and motility duration ($p< 0.05$). There were significant linear and quadratic trend levels of OTC for the spermatozoa motility rate and duration of motility ($p< 0.05$).

There were significant linear and quadratic trend levels of OTC for the spermatozoa motility rate and motility duration ($p< 0.001$). The spermatozoa motility rate and motility duration increased with the inclusion of OTC to extender compared with control ($p< 0.05$).

Effect of oxytetracycline on post-thaw antioxidant and oxidant status

The freezing process had a significant negative effect on both post-thaw antioxidant and oxidant status of sperm ($p<0.0001$). The post-thaw antioxidant level decreased markedly between 41.4 to 47.3% ($p<0.0001$). TAS and GSH were increased after thawing in high OTC doses compared to in no treatment group (*Table 2*). The post-thaw oxidant level in OTC proportionally raised with 9.0 to 14.0% after cryopreservation compared with in no treatment group ($p<0.05$).

Table 2. *Post-thaw oxidative stress parameters of B. grypus semen frozen in diluents containing three different oxytetracycline concentrations*

Dose of Oxytetracycline (Groups)		Parameters				
		TAS (mmol Trolox equiv/L)	**TOS (µmol H_2O_2 equiv/L)**	**OSI (AU)**	**GSH (nmol/g)**	**MDA (nmol/g)**
Fresh		1.88±0.07^{a}	12.11±1.09^{b}	1.02±0.01^{b}	44.90±0.60^{a}	16.28± 0.09^{a}
Control		0.99±0.08^{d}	13.85±0.08^{a}	1.23±0.01^{a}	26.29±0.34^{c}	15.42±0.42^{b}
0.78 mg		1.11±0.04^{cd}	10.97±0.62^{c}	0.81±0.03^{d}	27.63±0.08^{c}	13.10±0.35^{b}
1.56 mg		1.26±0.03c	11.34±0.06^{c}	0.90±0.01^{c}	36.29±0.19^{b}	8.66±0.33^{c}
3.12 mg		1.33±0.03^{b}	11.22±0.46^{c}	0.83±0.01^{cd}	37.56±0.23^{b}	8.27± 0.28^{d}
Pr >F[1]	ANOVA	0.0001	0.0001	0.0001	0.0001	0.0001
	Lineartrend	0.84	0.26	0.41	0.0001	0.0001
	Quatratic trend	0.01	0.05	0.05	0.0001	0.0001

Data are presented Mean ± SE of values. Different letters as a,b,c show differences between groups ($p< 0.001$), *post hoc* comparisons with Tukey multiple comparison test

Levels of TAS, GSH, MDA, TOS and Oxidative Stress Index (OSI) were significantly affected by the OTC supplementation ($p< 0.0001$). Significant linear and quadratic trends were found between the increasing levels of OTC and the levels of GSH and MDA ($p< 0.0001$). Moreover, a quadratic trend was found between the increasing levels of the OTC and levels of TAS, TOS and OSI ($p< 0.05$). (*Table 2*).

http://www.aloki.hu ● ISSN 1589 1623 (Print) ● ISSN1785 0037 (Online)
DOI: http://dx.doi.org/10.15666/aeer/2003_27332746

Changes in DNA damage paremeters and apoptosis

A significant increase in the level of 8-OHdG was observed in the control group and the fresh semen ($p<0.05$) (*Table 3*). And also, significant increase in the apoptotic spermatozoa rate was detected in the control groups ($p<0.0001$). As shown in *Table 4*, DNA damage in 8-OHdG was significantly decreased by the elevated OTC levels ($p<0.05$). All OTC doses had lower apoptosis levels ($p<0.0001$) (*Table 3*). A significant linear trend was found between the increasing OTC and the DNA damage levels ($p<0.0001$). Significant linear and quadratic trends were found between the increasing OTC levels and the percentage of apoptotic spermatozoa ($p< 0.0001$).

Table 3. *Post-thaw apoptosis analysis results of B. grypus semen frozen in diluents containing three different oxytetracycline concentrations*

Dose of Oxytetracycline (Groups)		**Parameters**
		Apoptozis (AR %)
Fresh		1.89±0.10[b]
Control		2.50±0.07[a]
0.78 mg		1.57±0.06[c]
1.56 mg		1.28±0.01[d]
3.12 mg		1.27±0.03[d]
Pr>F[1]	ANOVA	0.0001
	Linear trend	0.0001
	Quatratic trend	0.0001

Data are presented Mean ± SE of values. Different letters as a,b,c show differences between groups ($p< 0.001$), *post hoc* comparisons with Tukey multiple comparison test

Table 4. *Post-thaw DNA damage results of B. grypus semen frozen in diluents containing three different oxytetracycline concentrations (using by 8-Hydroxydeoxyguanosine (8-OHdG))*

Dose of Oxytetracycline (Groups)		**Parameters**
		8-OHdG (ng/mL)
Fresh		98.74±0.64[a]
Control		96.23±0.41[a]
0.78 mg		86.72±0.72[b]
1.56 mg		62.72±0.18[c]
3.12 mg		53.98±0.23[d]
Pr>F[1]	ANOVA	0.0001
	Linear trend	0.0001
	Quatratic trend	0.89

Data are presented Mean ± SE of values. Different letters as a,b,c show differences between groups ($p< 0.001$), *post hoc* comparisons with Tukey multiple comparison test

http://www.aloki.hu ● ISSN 1589 1623 (Print) ● ISSN1785 0037 (Online)
DOI: http://dx.doi.org/10.15666/aeer/2003_27332746

Discussion

Studies have properly shown different protocols for each properly recognized species in semen cryopreservation (Huang et al., 2009; Liu et al., 2018). Handling the protocol steps separately is important for the standardization process. Because, each stage is related to each other and affects the quality of sperm (Yang and Tiersch, 2009; Yang et al., 2018). From this point of view, we evaluated the effects of antibiotics, on semen quality after long-term storage by considering several different parameters. In our study, we investigated the effect of oxytetracycline supplementation to semen extenders at different rates on semen quality, oxidative stress status, DNA damage and apoptotic cell rates after sperm freezing-thawing process.

It was observed that freezing-thawing process decreased sperm motility rate and motility duration of treatment groups compared to fresh *B. grypus* semen. Motility rate in cryopreserved sperm of Atlantic salmon (*Salmo salar*) displayed significant reductions compared to fresh spermatozoa (Figueroa et al., 2019). All the treatment groups had better results in specific terms of motility duration and motility rate ($P<0.05$). The sperm motility rate and duration of *B. grypus* significantly improved with the apparent increase in the elevated OTC levels because the consistent trends were linear and quadratic in this comparative study. On the other hand, in previous studies, there were different results of other antibiotics supplementation studies to the semen extender. Jasko et al. (1993) highlighted the deleterious results of gentamicin on the motility of stallion spermatozoa at concentrations greater than 1 mg/mL. Besides, Ericsson and Baker (1967) reported that tetracyclines are toxic to ejaculated semen and bind strongly to the sperm head. Nevertheless, there efficiently was no difference in motility after incubation of human semen at 37°C for 48 hours following freeze-thawing by adding a synthetic oxytetracycline, the doxycycline hyclate (2.6 and 260 µg/mL) to the extender (King et al., 1997). Tetracycline at small concentrations as low as 2.5 µg/mL on human semen in vitro caused inhibition of the determined percentage of motile spermatozoa. It was determined that all spermatozoa were immobilized by using 50 µg/mL tetracycline (Hargreaves et al., 1998). Researchers suggest that the harmful result of tetracycline is due to its ability to chelate Ca^{2+} and the effect of this antibiotic is mostly irreversible.

Cryopreservation protocols are very important for post-thaw sperm quality due to the oxidative stress it naturally results in semen. For the possible time of the sperm storage, free radicals are properly produced, the created formation of oxidative stress results in a gradual decrease in antioxidant capacity (Aprioku, 2013; Agarwal et al., 2018; Riesco et al., 2020). Oxidative stress is believed concerning the critical influences that damage spermatozoa (Cho and Agarwal, 2018; Selwam and Agarwal, 2018; Alahmar, 2018). However, the mechanisms of this phenomenon have not been adequately explained (Krzysciak et al., 2020). In this comparative study, properly compared to the fresh semen, a significant decrease in the TAS and GSH levels, marked increase MDA, TOS and OSI were accurately detected in control groups. The decrease in MDA, TOS and OSI levels after thawing may result to the obvious quadratic increase in the TAS and linear and quadratic rise within GSH measures to here caused via the elevation in the OTC doses. The levels of TOS and OSI in in patients with moxifloxacin combination therapy were significantly decreased, while the levels of TAS were significantly increased after treatment ($p < 0.05$) (Yang et al., 2017).

Chemotherapeutic drugs, some metallic component and chemical agent can as well be resulted in the reactive oxygen species (Wink et al., 1996; Ercal et al., 2001). In the

http://www.aloki.hu ● ISSN 1589 1623 (Print) ● ISSN1785 0037 (Online)
DOI: http://dx.doi.org/10.15666/aeer/2003_27332746

preliminary examinations, controlled administration of penicillin, kanamycin, and gentamicin caused a marked reduction in ROS in rabbit semen (Duracka et al., 2019). On the contrary, tetracycline-induced testicular damage is associated with the induction of oxidative stress in testicular tissues as a result of a decrease in superoxide dismutase, catalase, glucose-6-phosphate dehydrogenase, glutathione-S-transferase activities, as well as significant decrease in GSH levels (Farombi et al., 2008). While this indicates an important relationship between GSH and OTC, other researchers have also stated high GSH levels in normozoospermia ejaculates (Krzysciak et al., 2020). The study findings show that high OTC dose contributes to the maintenance of GSH levels. Semen with high MDA values are associated with decreased sperm motility and higher percentages of necrotic and apoptotic sperm (Sahnoun et al., 2017; Hassanin et al., 2018). In addition, the present study is similar to the consistent findings of motility, oxidant and antioxidant levels of *B. grypus* viable sperm in observed treatment groups. The source of free radicals containing lipid peroxidation products such as MDA is non-mitochondrial sources found in mammalian spermatozoa (Aitken et al., 1989). Tetracycline-induced testicular damage has been reported to result from the development of MDA with the increased effect of γ-glutamyltranspeptidase (Farombi et al., 2008). Thus, the decrease in MDA levels as a result of its inclusion in a high OTC may be due to its effect on seminal plasma, spermatozoa or mitochondrial enzymes (Aitken et al., 1989). Oxidative stress shows the disproportion between the production of reactive oxygen species and antioxidant protections that buffer oxidative damage (Halliwell, 1994). Decreased antioxidative structures maintain the balance and buffer with increased oxidative structures (Baysal et al., 2009; Gülüm et al., 2011).

DNA damage detection has been frequently used in recent years for the detection of post-thaw sperm damage of different living species (Irvine et al., 2000). New markers for sperm quality assessment can strengthen the optimization of existing sperm analysis methods. Nuclear and mitochondrial DNA damage are serious consequences of oxidative stress. Thus, reduction of reactive oxygen species can decrease DNA damage (Venkatesh et al., 2009). In addition, free radicals, specifically reactive oxygen species, cause DNA damage after that lead to cellular apoptosis (Aitken et al., 1998; Zobeiri et al., 2012). In this study, the effective OTC doses kept the DNA damage at under of the comparable level of fresh semen. A linear trend could explain of the typically decreased its destruction variation of elevated OTC levels for sperm DNA damage. This means that we have a linear trend in the DNA damage in the OTC levels that can be interpreted as a response to recovering DNA intact. Previous studies had opposite results to our research findings. Of these, Zobeiri et al. (2012) showed that after administration of Ciprofloxacin to mice, the percentage of sperm with single-stranded DNA raised considerably. A considerable increase in DNA fragmentation in rabbit semen in culture medium supplemented with penicillin, kanamycin and gentamicin was shown (Duracka et al., 2019). It has also been shown that mitochondrial dysfunction severely increases nuclear DNA fragmentation in sperm (Donnelly et al., 2000). The DNA lesions were induced by only Amoxicillin reported by Li et al. (2007). ROS had been accumulated after quinolone removal with cultures co-treated with chloramphenicol for sufficiently emphasize DNA-break-mediated killing (Castillo et al., 2015). Quinolones are attacked to DNA, thereby blocking DNA gyrase causing further causing permanent destruction to DNA (Yang et al., 2017). It has been shown in normal human lymphocytes that different concentrations of idarubicin (0.001 to 10 μM) can cause an increase in the

http://www.aloki.hu ● ISSN 1589 1623 (Print) ● ISSN1785 0037 (Online)
DOI: http://dx.doi.org/10.15666/aeer/2003_27332746

percentage of damaged DNA. And also, this result of idarubicin shows that besides its various side effects, it is also important in terms of genotoxicity (Blasiak et al., 2002).

It is known that stress in cells leads to apoptosis. In our study, apoptotic cells were examined to determine the effects of sperm freezing stress. There was a significant difference in the comparable percentage of apoptotic cells ($p>0.05$) between fresh and cryopreserved sperm in control group. All the OTC levels resulted in significant ($p<0.0001$) decreases in apoptotic cells' percentage compared to determined values of control sperm. Therefore, OTC typically decreased the apoptosis of frozen sperm. This properly means that linear and quadratic trends typically has in the comparable percentage of apoptotic cells in the OTC levels that can be reasonably interpreted as a direct response to instantly recovering apoptosis. Antibiotics cause accumulation of DNA lesions and increased apoptotic response (Castillo et al., 2015). It has been reported that the negative consequences of doxorubicin occur due to increased DNA damage (L'Ecuyer et al., 2006).The decrease in the apoptosis after thawing may be due to the significant quadratic increase in the TAS, linear and quadratic rise GSH levels caused by the OTC levels. The essential fact that OTC increases TAS level, decreases DNA damage and meaningfully improves sperm criteria is evidence that it efficiently is a useful antibiotic. Because the possible formation of oxidative stress produce in a reduce in antioxidant capacity during the freezing-thawing process (Aprioku, 2013). Oxidative stress is also thought one of the primary variables that injury sperm (Selvam and Agarwal, 2018). In this manner, OTC may have slowed down apoptosis in viable sperm by sufficiently reducing oxidative stress during the freeze-thaw process.

Conclusions

As a result, spermatozoa motility rate and duration in post-thaw semen increased in all the OTC groups compared with control. The OTC supplementation to extender caused to increase TAS and GSH. In addition, it typically decreased TOS, OSI and MDA levels of post-thaw sperm. Considering the key findings of this comparative study, it was determined that the OTC not only decreased DNA damage but also reduced apoptosis. It was determined that the OTC supplementation to extender sufficiently protects the semen against pathophysiological events in post-thaw semen. On the other hand, we think that it would be useful to carry out more detailed studies in order to standardize the use of OTC in semen extenders.

Funding. This work was supported by the Harran University Scientific Research Coordination Unit [Project Number 20083]; Harran University, Turkey.

Institutional review board statement. All issues concerning the experimental methods and evaluation techniques were approved by the Scientific Ethical Committee, Harran University, Sanliurfa, Turkey (No: 11/02/2020-01/07).

Data availability statement. The datasets used and/or analyzed during in this study are available from the corresponding author upon reasonable request.

Conflicts of Interests. The authors declare no conflict of interests.

http://www.aloki.hu ● ISSN 1589 1623 (Print) ● ISSN1785 0037 (Online)
DOI: http://dx.doi.org/10.15666/aeer/2003_27332746

REFERENCES

[1] Agarwal, A., Qiu, E., Sharma, R. (2018): Laboratory assessment of oxidative stress in semen. – Arab J. Urol. 16: 77-86.
[2] Aitken, J., Clarkson, J. S., Fishel, J. (1989): Generation of reactive oxygen species, lipid peroxidation and human sperm function. – Biol Reprod. 40: 183-197.
[3] Aitken, R. J., Gordon, E., Harkiss, D., Twigg, J. P., Milne, P., Jennings, Z., Irvine, D. S. (1998): Relative impact of oxidative stress on the functional competence and genomic integrity of human spermatozoa. – Biol Reprod. 59(5): 1037-1046.
[4] Alahmar, A. T. (2018): The effects of oral antioxidants on the semen of men with idiopathic oligoasthenoteratozoospermia. – Clin Exp Reprod Med. 45(2): 57-66.
[5] Ansari, M. S., Rakha, B. A., Andrabi, S. M., Ullah, N., Iqbal, R., Holt, W. V., Akhter, S. (2012): Glutathione-supplemented tris-citric acid extender improves the post-thaw quality and in vivo fertility of buffalo (*Bubalus bubalis*) bull spermatozoa. – Reprod Biol. 12(3): 271-6.
[6] Aprioku, J. S. (2013): Pharmacology of free radicals and the impact of reactive oxygen species on the testis. – J. Reprod. Infertil. 14: 158-172.
[7] Aramli, M. S., Golshahi, K., Nazari, R. M., Aramli, S. (2005): Effect of freezing rate onmotility, adenosine triphosphate content and fertilizability in beluga sturgeon (*Huso huso*) spermatozoa. – Cryobiology 70: 170-174.
[8] Bailey, J. L., Lessard, C., Jacques, J., Breque, C., Dobrinski, I., Zeng, W., Galantino-Homer, H. L. (2008): Cryopreservation of boar semen and its future importance to the industry. – Theriogenology 70: 1251-1259.
[9] Baysal, Z., Cengiz, M., Ozgonul, A., Cakir, M., Celik, H., Kocyigit, A. (2009): Oxidative status and DNA damage in operating room personnel. – Clin Biochem. 42: 189-93.
[10] Błasiak, J., Gloc, E., Woźniak, K., Młynarski, W., Stolarska, M., Skórski, T., Majsterek, I. (2002): Genotoxicity of idarubicin and its modulation by vitamins C and E and amifostine. – Chem Biol Interact. 140(1): 1-18.
[11] Boonthai, T., Khaopong, W., Sangsong, J., Nimrat, S., Vuthiphandchai, V. (2016): Effect of antibiotic supplementation on the quality of cryopreserved fish sperm of silver barb (*Barbodes gonionotus*): sperm motility and viability, bacterial quality and fertilization. – Animal Reproduction Science 166: 36-46.
[12] Brown, G. G., Mims, S. D. (1995): Storage, transportation, and fertility of undiluted and diluted paddlefish milt. – Prog Fish-Cult. 57: 64-9.
[13] Cabrita, E., Sarasquete, C., Martínez-Paramo, S., Robles, V., Beirao, J., Pérez-Cerezales, S., Herraez, M. P. (2010): Cryopreservation of fish sperm: applications and perspectives. – J. Appl. Ichthyol. 26: 623-635.
[14] Castillo, D. S., Campalans, A., Belluscio, L. M., Carcagno, A. L., Radicella, J. P., Cánepa, E. T., Pregi, N. (2015): E2F1 and E2F2 induction in response to DNA damage preserves genomic stability in neuronal cells. – Cell Cycle 14(8): 1300-14.
[15] Çavaş, T. (2011): In vivogenotoxicity evaluation of atrazine and atrazine–based herbicide on fish *Carassius auratus* using the micronucleus test and the comet assay. – Food Chem Toxicol. 49(6): 1431-1435.
[16] Cho, C. L., Agarwal, A. (2018): Role of sperm DNA fragmentation in male factor infertility: A systematic review. – Arab J Urol. 16(1): 21-34.
[17] Dhawan, A., Bajpayee, M., Parmar, D. (2009): Comet assay: a reliable tool for the assessment of DNA damage in different models. – Cell Biol Toxicol. 25(1): 5-32.
[18] Donnelly, E. T., O'Connell, M., McClure, N., Lewis, S. E. (2000): Differences in nuclear DNA fragmentation and mitochondrial integrity of semen and prepared human spermatozoa. – Hum Reprod. 15(7): 1552-1561.
[19] Duracka, M., Lukac, N., Kacaniova, M. (2019): Antibiotics Versus Natural Biomolecules: The Case of In Vitro Induced Bacteriospermia by *Enterococcus faecalis* in Rabbit Semen. – Molecules (Basel, Switzerland) 24(23): 4329.

http://www.aloki.hu ● ISSN 1589 1623 (Print) ● ISSN1785 0037 (Online)
DOI: http://dx.doi.org/10.15666/aeer/2003_27332746

[20] Elia, A. C., Ciccotelli, V., Pacini, N., Dörr, A. J. M., Gili, M., Natali, M., Gasco, L., Prearo, M., Abete, M. C. (2014): Transferability of oxytetracycline (OTC) from feed to carp muscle and evaluation of the antibiotic effects on antioxidant systems in liver and kidney. – Fish Physiol. Biochem. 40: 1055-1068.
[21] Ercal, N., Gurer-Orhan, H., Aykin-Burns, N. (2001): Toxic metals and oxidative stress part I: mechanisms involved in metal-induced oxidative damage. – Curr Top Med Chem. 1(6): 529-39.
[22] Erel, O. (2004): A novel automated direct measurement method for total antioxidant capacity using a new generation, morestable ABTS radicalcation. – Clin Biochem. 37: 277-285.
[23] Erel, O. (2005): A new automated colorimetric method for measuring total oxidant status. – Clinical Biochemistry 38(12): 1103-1111.
[24] Ericsson, R., Baker, V. (1967): Binding of Tetracycline to Mammalian Spermatozoa. – Nature 214: 403-404.
[25] Factori, R., Leles, S. M., Novakowski, G. C., Rocha, C. L. S. C., Thomaz, S. M. (2014): Toxicity and genotoxicity of water and sediment from streams on dotted duckweed (*Landoltia punctata*). – Braz J Biol. 74(4): 769-778.
[26] Farombi, O., Morke, M., Ezenwadu, T., Oyeyemi, M., Ekor, M. (2008): Tetracycline-induced reproductive toxicity in male rats: Effects of vitamin C and N-acetylcysteine. – Experimental and toxicologic pathology: official journal of the Gesellschaft für Toxikologische Pathologie 60: 77-85.
[27] Figueroa, E., Lee-Estevez, M., Valdebenito, I., Watanabe, I., Oliveira, R. P. S., Romero, J. (2019): Effects of cryopreservation on mitochondrial function and sperm quality in fish. – Aquaculture 511: 634190.
[28] Gülüm, M., Yeni, E., Kocyigit, A., Taskin, A., Savas, M., Ciftci, H., Altunkol, A. (2011): Sperm DNA damage and seminal oxidative status after shock-wave lithotripsy for distal ureteral Stones. – Fertility and Sterility 96(5): 1087-1090.
[29] Halliwell, B. (1994): Free radicals, antioxidants, and human disease: curiosity, cause, or consequence? – Lancet 344: 721-724.
[30] Hargreaves, C. A., Rogers, S., Hills, F., Rahman, F., Howell, R. J. S., Homa, S. T. (1998): Effects of co-trimoxazole, erythromycin, amoxycillin, tetracycline and chloroquine on sperm function in vitro. – Human reproduction (Oxford, England) 13(7): 1878-86.
[31] Harma, M., Harma, M., Erel, O. (2003): Increased oxidative stress in patients with hydatidiformmole. – Swiss Med Wkly. 133: 563-566.
[32] Hassanin, A. M., Ahmed, H. H., Kaddah, A. N. (2018): A global view of the pathophysiology of varicocele. – Andrology 6(5): 654-661.
[33] Henkel, R. R. (2011): Leukocytes and oxidative stress: dilemma for sperm function and male fertility. – Asian J Androl. 13: 43-52.
[34] Hong, Y., Li, Q., Gao, Q., Xie, J., Huang, H., Drlica, K., Zhao, X. (2020): Reactive oxygen species play a dominant role in all pathways of rapid quinolone-mediated killing. – J. Antimicrob Chemother. 75(3): 576-585.
[35] Huang, C., Sun, C., Su, X., Zhao, X., Miao, M., Liu, Y., Dong, Q. (2009): Sperm cryopreservation in guppies and black mollies - a generalized freezing protocol for livebearers in Poeciliidae. – Cryobiology 59: 351-356.
[36] Irvine, D. S., Twigg, J. P., Gordon, E. L., Fulton, N., Milne, P. A., Aitken, R. J. (2000): DNA integrity in human spermatozoa: relationships with semen quality. – J Androl. 21: 33-44.
[37] Jasko, D. J., Bedfort, S. J., Cook, N. L., Mumfort, E. L., Squires, E. L., Pickett, B. W. (1993): Effect of antibiotics on motion characteristics ofcooled stallion spermatozoa. – Theriogenology 40: 885-93.

http://www.aloki.hu ● ISSN 1589 1623 (Print) ● ISSN1785 0037 (Online)
DOI: http://dx.doi.org/10.15666/aeer/2003_27332746

[38] Kandár, R., Hajkova, N. (2014): Assay of total glutathione and glutathione disulphide in seminal plasma of male partners of couples presenting for a fertility evaluation. – Andrologia 46(10): 1079-1088.
[39] King, K., Chan, P. J., Patton, W. C., King, A. (1997): Antibiotics: effect on cryopreserved-thawed human sperm motility in vitro. – Fertil Steril. 67(6): 1146-1151.
[40] Klaiwattana, P., Srisook, K., Srisook, E., Vuthiphandchai, V., Neumvonk, J. (2016): Effect of cryopreservation on lipid composition and antioxidant enzyme activity of seabass (*Lates calcarifer*) sperm. – Iranian Journal of Fisheries Sciences 15: 157-169.
[41] Kopeika, E., Kopeika, J., Zhang, T. (2007): Cryopreservation of Fish Sperm. – In: Day, J. G. (ed.) Methods in Molecular Biology. 2nd edition, Humana Press, New Jersey, United States, pp. 203-219.
[42] Krzyściak, W., Papież, M., Bąk, E. (2020): Sperm Antioxidant Biomarkers and Their Correlation with Clinical Condition and Lifestyle with Regard to Male Reproductive Potential. – J Clin Med. 9(6): 1785.
[43] L'Ecuyer, T., Sanjeev, S., Thomas, R., Novak, R., Das, L., Campbell, W., Heide, R. V. (2006): DNA damage is an early event in doxorubicin-induced cardiac myocyte death. – Am J Physiol Heart Circ Physiol. 291(3): 1273-1280.
[44] Li, P. Y., Chang, Y. C., Tzang, B. S., Chen, C. C., Liu, Y. C. (2007): Antibiotic amoxicillin induces DNA lesions in mammalian cells possibly via the reactive oxygen species. – Mutat Res. 629(2): 133-9.
[45] Li, P., Hulak, M., Koubek, P., Sulc, M., Dzyuba, B., Boryshpolets, S., Rodina, M., Gela, D., Manaskova-Postlerova, P., Peknicova, J., Linhart, O. (2010): Ice-age endurance:the effects of cryopreservation on proteins of sperm of common carp, *Cyprinus carpio* L. – Theriogenology 74: 413-423.
[46] Liu, Y., Torres, L., Tiersch, T. R. (2018): Cryopreservation of sperm bundles (spermatozeugmata) from endangered live bearing goodeids. – Cryobiology 82: 49-56.
[47] Long, A. R., Hsieh, L. C., Malbrough, M. S., Short, C. R., Barker, S. A. (1989): Matrix solidphase dispersion (MSPD) isolation and liquid chromatographic determination of oxytetracycline, tetracycline, and chlortetracycline in milk. – J Assoc Official Analytic Chem. 73(3): 379-84.
[48] Lundén, T., Lilius, E. M., Bylund, G. (2002): Respiratory burst activity of rainbow trout (*Oncorhynchus mykiss*) phagocytes is modulated by antimicrobial drugs. – Aquaculture 207(3-4): 203-212.
[49] Ohkawa, H., Ohishi, N., Yagi, K. (1979): Assay for lipid peroxides in animal tissues by thiobarbituricacid reaction. – Anal Biochem. 95: 351-358.
[50] Perez-Cerezales, S., Martínez-Paramo, S., Beirao, J., Herraez, M. P. (2010): Evaluation of DNA damage as a quality marker for rainbow trout sperm cryopreservation and use of LDL as cryoprotectant. – Theriogenology 74: 282-289.
[51] Rahimi, R., Hajirezaee, S., Shaluei, F., Katadj, J. K. (2015): Antibiotics, Penicillin and Sreptomycin improve semen quality indices of endangered Caspian brown trout, *Salmo trutta caspius* (Kessler, 1870) during in vitro short-term storage. – Aquaculture Research 47(11): 3662-3666.
[52] Riesco, F. M., Anel-Lopez, L., Neila-Montero, M., Palacin-Martinez, C., Montes-Garrido, R., Alvarez, M., de Paz, P., Anel, L. (2020): ProAKAP4 as Novel Molecular Marker of Sperm Quality in Ram: An Integrative Study in Fresh, Cooled and Cryopreserved Sperm. – Biomolecules 10(7): 1046.
[53] Rosales, M., Castillo, S., Pohlenz, C., Gatlin, D. M. (2017): Evaluation of dried yeast and threonine fermentation biomass as partial fish meal replacements in the diet of red drum *Sciaenops oceuatus*. – Anim. Feed Sci. Technol. 232: 190-197.
[54] Sahnoun, S., Sellami, A., Chakroun, N., Mseddi, M., Attia, H., Rebai, T., Lassoued, S. (2017): Human sperm Toll-like receptor 4 (TLR4) mediates acrosome reaction, oxidative stress markers, and sperm parameters in response to bacterial lipopolysaccharide in infertile men. – J Assist Reprod Genet. 34(8): 1067-1077.

http://www.aloki.hu ● ISSN 1589 1623 (Print) ● ISSN1785 0037 (Online)
DOI: http://dx.doi.org/10.15666/aeer/2003_27332746

[55] Selvam, M. K. P., Agarwal, A. (2018): A systematic review on sperm DNA fragmentation in male factor infertility, Laboratory assessment. – Arab J Urol. 16(1): 65-76.
[56] Serezli, R., Cagirgan, H., Okumus, I., Akhan, S., Balta, F. (2005): The effect of oxytetracyclineon non-specific immune response in sea bream (*Sparus aurata* L. 1758). – Turkish Journal of Veterinary and Animal Sciences 29: 31-35.
[57] Tekin, N., Secer, S., Akçay, E., Bozkurt, Y., Kayam, S. (2003): The effect of age on spermatological properties in rainbow trout (*Oncorhynchus mykiss* W. 1792). – Turkish Journal of Veterinary and Animal Scinces 27: 37-44.
[58] Tvedt, H. B., Benfey, T. J., Martin-Robichaud, D. J., Power, J. (2001): The relationship between sperm density, spermatocrit, sperm motility and fertilization success in Atlantic halibut, *Hipoglossus hippoglossus*. – Aquaculture 194: 191-200.
[59] Venkatesh, S., Riyaz, A. M., Shamsi, M. B., Kumar, R., Gupta, N. P., Mittal, S. (2009): Clinical significance of reactive oxygen species in semen of infertile Indian men. – Andrologia 41: 251-256.
[60] Wang, Y., Dong, S. (2017): Glutathione in combination with trehalose has supplementary beneficial effects on cryopreserved red deer (*Cervus elaphus*) sperm. – Am J Reprod Immunol. 77(1): 12610.
[61] Wink, D. A., Hanbauer, I., Grisham, M. B., Laval, F., Nims, R. W., Laval, J., Cook, J., Pacelli, R., Liebmann, J., Krishna, M., Ford, P. C., Mitchell, J. B. (1996): Chemical biology of nitric oxide: regulation and protective and toxic mechanisms. – Curr Top Cell Regul. 34: 159-87.
[62] Yang, H., Tiersch, T. R. (2009): Current status of sperm cryopreservation in biomedical research fish models: zebrafish, medaka, and Xiphophorus. – Comp. Biochem. Physiol. C Toxicol. Pharmacol. 149(2): 224-232.
[63] Yang, H., Zhao, Y., Ma, Y., Wen, Q., Zhang, M. (2017): Effect of moxifloxacin on oxidative stress, paraoxonase-1 (PON1) activity and efficacy of treatment in patients with multiple drug-resistant tuberculosis. – Tropical Journal of Pharmaceutical Research 16(10): 2515-2520.
[64] Yang, H., Hu, E., Buchanan, J. T., Tiersch, T. R. (2018): A strategy for sperm cryopreservation of Atlantic Salmon, *Salmo salar*, for remote commercial-scale high throughput processing. – J. World Aquacult. Soc. 49: 96-112.
[65] Zobeiri, F., Sadrkhanlou, R. A., Salami, S., Mardani, K., Ahmadi, A. (2012): The effect of ciprofloxacin on sperm DNA damage, fertility potential and early embryonic development in NMRI mice. – Vet Res Forum. 3(2): 131-135.

http://www.aloki.hu ● ISSN 1589 1623 (Print) ● ISSN1785 0037 (Online)
DOI: http://dx.doi.org/10.15666/aeer/2003_27332746

ASSESSMENT OF *LEGIONELLA PNEUMOPHILA* DEVELOPMENT THROUGH IRRIGATION SYSTEM MATERIALS

GEA-IZQUIERDO, E.

Pontificia Universidad Católica del Ecuador, Facultad de Medicina, 170143 Quito, Ecuador
e-mail: enriquegea@yahoo.es

(Received 6th Jan 2022; accepted 21st Mar 2022)

Abstract. *Legionella pneumophila* can cause a type of pneumonia called Legionnaires' disease. The bacterium is responsible for most cases of the disease and can multiply in man-made water systems, such as irrigation systems. The study analyzed the potential development of *Legionella pneumophila* in irrigation system materials of Spanish hotels. Sprinkler irrigation systems were analysed in hotel golf courses and compared with the Spanish regulation standards in order to establish sanitation criteria for the prevention and control of legionellosis. An analytical study and principal component methods were employed in the context of materials, type of water and legislative compliance. Lead, polybutylene and wastewater treatment plant had great relevance. There was a strong association between wastewater treatment plant-copper and well water-polyvinyl chloride. Polybutylene, iron, polyethylene, stainless steel and lead showed a great magnitude in the contribution biplot, while lead facilities had a very low level of compliance in the correspondence analysis. Materials and legislative compliance were not statistically significantly associated ($p<0.05$). Considering the material and type of water, deficiencies were identified in the hygienic-preventive maintenance of the facilities. Attending the sanitary control criteria, ease of colonization and results obtained, it´s suggested that there is a relationship between the different materials and the risk of bacterial development.
Keywords: *legionellosis, prevention and control, Spain, golf, construction materials*

Introduction

Legionellosis is an acute respiratory infection linked to the environment. It´s a disease caused by a bacterium belonging to the Legionellaceae family. It comprises a genus, *Legionella*, with a total of 52 species and 70 serogroups. For the *Legionella pneumophila* species 14 serogroups have been described. More than a half of the species have been implicated in human infection, however the most common legionellosis is cause by *Legionella pneumophila* serogroup 1 which is the most frequent in the environment. *Legionella pneumophila* is responsible for 90% of cases, being serogroups 1, 4 and 6 the most relevant, followed by *Legionella micdadei* (responsible for 10%), *Legionella bozemanii*, *Legionella longbeachae* and *Legionella dumoffii*. The most common form of transmission of the microorganism is through aerosolization of water (Nguyen et al., 2006) although more studies are required in this regard (O'Connor et al., 2007; Den Boer et al., 2015; Correia et al., 2016). The agent was initially identified in 1976 following an outbreak in Philadelphia (USA) (Cunha et al., 2016). Although the sources of development of the bacterium comprise a variety of devices related to human activity (Moritz et al., 2010), it has a natural presence in non-anthropic media (Van Heijnsbergen et al., 2015). Within the term "legionellosis" different forms are included: Legionnaires' disease, Pontiac and Lochgoilhead fever. Regarding clinical forms of presentation (Cunha, 2010), the most important are the first two.

Legionellosis shows a worldwide distribution with representation in North and South America, Asia, Africa, Australia and Europe. The purpose of the epidemiological surveillance is, among others, to control the occurrence of cases and outbreaks linked to risk facilities, which could be related to the environment (Kozak et al., 2013) or work

http://www.aloki.hu ● ISSN 1589 1623 (Print) ● ISSN1785 0037 (Online)
DOI: http://dx.doi.org/10.15666/aeer/2003_27472761

environment (Kozak-Muiznieks et al., 2014). The infection can be acquired fundamentally in two main areas: the community and nosocomial (Irons et al., 2013). In both the disease may be associated with various types of facilities and buildings, and can occur in the form of outbreaks, group of cases, and isolated or sporadic cases. It is worth noting cases link with travellers.

In Spain, legionellosis is a topic of special health interest, being a disease that is subject to specific monitoring by the government, essential (NNDSS Annual Report Working Group, 2016) for its prevention and control (Maini et al., 2012; Lee, 2018). The epidemiological surveillance of legionellosis is preferably based on the National Epidemiological Surveillance Network. Further, the purpose of legionellosis legislation is none other than control the appearance of cases and outbreaks linked to risky facilities. In recent years, the evolution and improvement of Royal Decree 909/2001 (Real Decreto 909, 2001) conduced to Royal Decree 865/2003 (Real Decreto 865, 2003), which established the hygienic-sanitary criteria for the prevention and control of legionellosis. Thus, legislative implementation together with the epidemiological surveillance system are synergistic elements that result in a better health protection (Campese et al., 2011).

In Spain around 50% of the hotels are somewhere colonized by *Legionella* spp. in the water network. This quantity is like those detected in Europe and other parts of the world and denote that it is a globally distributed and extraordinarily ubiquitous bacterium in natural and anthropic environments. The presence in these media of other microorganisms (bacteria, protozoa, algae) brings on their development by colonization, as well as iron, which acts as a development enhancer in some systems and facilities. The formation of biofilms, corrosion materials and incrustations in pipes is essential for the bacterium to find niches (Atlas, 1999; Ji et al., 2015) that protect it against certain conditions adverse in the aqueous medium.

This study was aimed to determine if the potential development of *Legionella pneumophila* may be related to irrigation system materials from hotels and the compliance of Spanish health legislation for prevention of legionellosis.

Materials and Methods

Sprinkler irrigation systems were analyzed in hotel golf courses (n=31) located in both inland and coastal communities of Malaga (Andalusia, Spain), comparing the results obtained with the Spanish regulation standards through which sanitary criteria is established for the prevention and control of legionellosis (Real Decreto 865, 2003).

The design of the study suggested gathering information through a self-administered survey (*Table A1* in the *Appendix*) aimed at directors and persons in charge of buildings with facilities at risk, as well as drawing water samples for a later analysis on laboratories authorized by the Spanish Sanitation Authority, in accordance to standardized regulations (ISO 11731, 2017). Forty variables were selected (*Table A1* in the *Appendix except * and non-selected in I*) for the sanitary control of the *Legionella pneumophila* development.

Exploratory data analysis and contingency tables were used to assess whether there was a dependence between categories. These tables drew a graphical matrix where each cell contained a dot whose size reflects the relative magnitude of the corresponding component. Particularly, materials with type of water and legislative compliance. To interpret the significant dependence a chi-square statistic was used between materials and the last. To obtain the nature of the dependence between the row and the column variables Pearson residuals (standardized residuals) were calculated and the contribution (%) of

http://www.aloki.hu ● ISSN 1589 1623 (Print) ● ISSN1785 0037 (Online)
DOI: http://dx.doi.org/10.15666/aeer/2003_27472761

each cell to the total chi-square score. Also, eigenvalues to determine the number of axes were considered in subsequent analysis.

An analytical study and principal components methods was carried out to explain the *n* observations (materials) and the *p* original variables (type of water), recycled water (Rw), wastewater treatment plant (Wwtp) and well water (Ww), according to a *biplot* graphic display (symmetric, asymmetric and contribution). To achieve this, their scores were represented in the coordinate axes of the principal components that characterize the *p* variables. To obtain factorial solutions, the principal component analysis considered the total variance, estimating the factors that contain low proportions of unique variance and, in specific cases, error variance. The study's interest focused on the prediction or on the minimum number of necessary factors to justify the maximum variance portion, represented on the original series of variables. As an objective means of interpretation, a vector model was used to capture the position degrees of irrigation pipe materials in the perceptual map. The bacterium potential development was considered in function of the material and physicochemical and microbiological water controls, in addition to the frequency of said controls and, in particular, of *Legionella* spp. and total aerobes. In the symmetric plot only the distance between row or column points can be interpreted, not the inter-distance between them. That´s why to interpret the mentioned distance an asymmetric plot was done, with column profiles presented in row space or vice versa. In the standard symmetric biplot it´s difficult to know the most contributing points to the solution of the correspondence analysis (Kassambara, 2017). In the asymmetric biplot, rows (or columns) points are plotted from the standard coordinates and the profiles of the columns (or the rows) are plotted from the principal coordinates (Bendixen, 2003). The argument used is a logical vector specifying if the plot should contain points (false, default) or arrows (true). The first value sets the rows and the second value sets the columns. The contribution biplot incorporates the contribution of points. In this display, points that contribute very little to the solution, are close to the center of the biplot and are relatively unimportant to the interpretation. We interpreted the contribution of rows to the definition of the axes. In this case, emphasize that columns are in principal coordinates and rows in standard coordinates multiplied by the square root of the mass. For a given row, the square of the new coordinate on an axis i is exactly the contribution of this row to the inertia of the axis i (Greenacre, 2013).

Likewise, the relation (correspondence analysis) between "materials" and "legislation fulfillment" was analyzed according to the observations corresponding to the number of hotels that include facilities at risk for bacterium. To this end, as we indicated above, a chi-square test of independence was carried out, where the null hypothesis was the independence between both variables. For the correspondence analysis, chi-square test of independence was used to analyze the frequency table formed by these variables, evaluating whether there was a significant association between the categories ($p<0.05$). Afterwards, the interdependence was presented through the dimensional reduction and perceptual map, the latter of which was based on the association between hotel fulfillment and the materials, expressing the correspondence of variable category with a unique capacity to represent rows and columns in a unique multidimensional space, and offering a multivariant interdependence expression for non-metric data. The observations were ordered according to the type of legislative compliance with the Spanish regulation standards to establish sanitation criteria for the prevention and control of legionellosis: very low (Vl, 0-10%), low (Lo, 11-40%), medium (Me, 41-70%), high (Hi, 71-90%) and very high (Vh, 91-100%). The analysis of the observations was carried out for the

http://www.aloki.hu ● ISSN 1589 1623 (Print) ● ISSN1785 0037 (Online)
DOI: http://dx.doi.org/10.15666/aeer/2003_27472761

materials of the different systems: copper (Co), lead (Le), iron (Ir), stainless steel (Ss), polybutylene (Pb), polyethylene (Pe) and polyvinyl chloride (Pv).

Analysis was conducted in R (R Core Team, 2019) using FactoMineR and FactoExtraR (ggplot2-based elegant visualization) packages.

Results

To assess whether there is a dependence between "type of water" and "legislative compliance" referred to "materials" two contingency tables were designed (*Figure 1*). Additionally, chi-square test of independence shows a Pearson λ value=27.04 (p-value=0.30), so materials and legislative compliance are not statistically significant associated. Pearson residuals can be visualized in *Figure 2*, in which cells with the highest absolute standardized residuals contribute the most to the chi-square score (size of the circle is proportional to the amount of the cell contribution). The positive values in cells specify a positive association between the corresponding row (materials) and column (legislative compliance) variables. The negatives values imply a repulsion among the corresponding. In *Figure 2A* it´s evident that there are an association between Vl-Ir, Hi-Ir and Hi-Ss. There is a strong positive association between Vl-Le. Negative residuals expressed that Vl and Lo are negatively associated with Co. There is a repulsion between Me-Ir and lighter between Vh-Ir and Vh-Ss. The contribution in percentage is in *Figure 2B*. The relative contribution of each cell to the total chi-square score gives some indication of the nature of the dependency between materials and legislative compliance of the contingency table. The most contributing cells to the chi-square are: Vl-Le (31.17%, strongly associated), Lo-Pe (7.88%), Hi-Ir and Hi-Ss (7.17%). These cells contribute about 53.39% to the total chi-square score. In this case, the contribution of one cell to the total chi-square score becomes a useful way of establishing the nature of dependency.

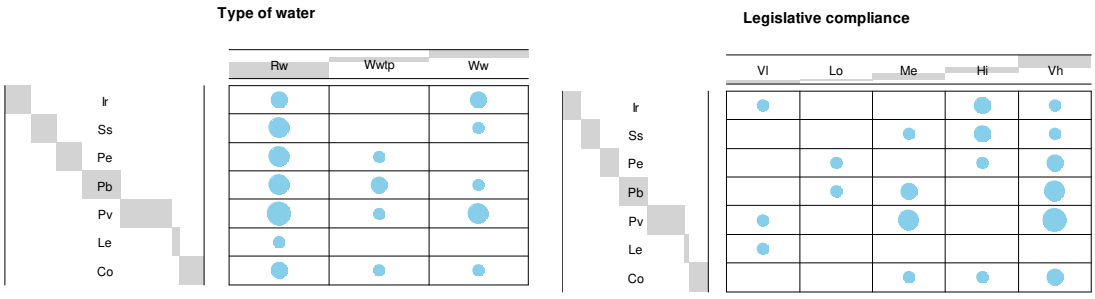

(A) (B)

Figure 1. *Dependence.* ***(A)*** *Materials and type of water.* ***(B)*** *Materials and legislative compliance*

The results of applying classification data to the perceptual compositional map are shown in a biplot (*Figure 3A*), in which three distinct types of attribute dimensions can be identified (each type of water), all in different directions. To highlight the most contributing row points for each dimension *Figure 3B* was done. The most contributing row points is spotlight on the scatter plot giving an idea of what pole of the dimensions the row categories are actually contributing to. It´s evident that row categories Pe and Pb have an important contribution to the positive pole of the first dimension, while the

http://www.aloki.hu ● ISSN 1589 1623 (Print) ● ISSN1785 0037 (Online)
DOI: http://dx.doi.org/10.15666/aeer/2003_27472761

categories Ir and Ss have a major contribution to the negative pole of the first dimension (Kassambara, 2017). Well water is almost perpendicular when compared to wastewater treatment plant, suggesting a separate and distinct dimension of its own. This representation is expressed on the biplot graphic display according to the initials corresponding to different materials and original variables. Regarding each type of water, the variance for the variables is very similar, since they have associated near length vectors. A correlation likewise exists, since the angle that separates the corresponding vectors is small. The direction of the axis corresponding to the first principal component arranges the data and it can be observed, through the scores obtained by the first two principal components in the observations, that the best materials regarding preventive compliance are Pv and Pb, always in respect to what the first principal component represents, which will be the most important one and will hold the largest data matrix variability. The approximation order is well and recycled water (Pv > Co/Ss > Pe > Ir > Pb > Le) and wastewater treatment plant (Pb > Pe > Co > Ss > Ir > Pb > Le).

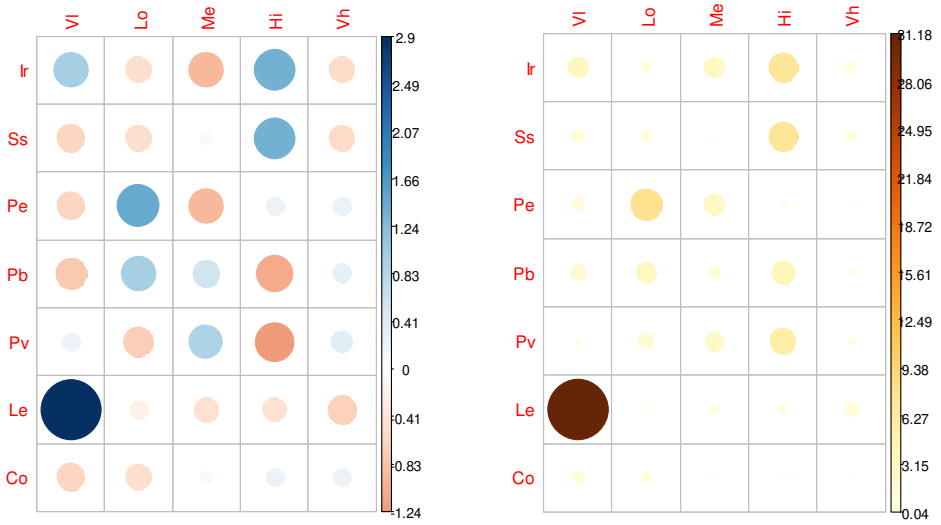

(A) (B)

Figure 2. ***(A)*** *Pearson residuals.* ***(B)*** *Contributions (%). Positive residuals are in blue and negative in red*

As mentioned before, first we represented the standard plot of correspondence analysis called symmetric biplot (*Figure 3C*). Materials (blue points) and type of water (red triangles) were represented in the same space using the principal coordinates (profiles). After, we calculated an asymmetric biplot (*Figure 3D*) to interpret the distance between column points and row points. As seen in contribution biplot (*Figure 3E*) the position of the column profile points is unchanged relative to that in the conventional biplot and the distances of the row points from the plot origin are related to their contributions to the two-dimensional factor map.

Through the analysis in two coordinates, the correspondence graph (*Figure 4*) was obtained. The representation of the two dimensions holds 77.8%, which is enough to conclude the two-dimensional representation is adequate. This means that the total inertia value is held at a 98.7% rate by the two-dimensional representation, which leads to the conclusion that said representation is valid. It is worth noting that the perceptual map obtained during the correspondences analysis is weighted by the existing inherent

http://www.aloki.hu ● ISSN 1589 1623 (Print) ● ISSN1785 0037 (Online)
DOI: http://dx.doi.org/10.15666/aeer/2003_27472761

interdependences and potential biases of a possible omitted attribute in a given "material", or of a single inappropriate attribute (or system). In the last *Figure*, irrigation system materials are located near the legislative compliance with which they are highly related, and apart from other categories with lower correspondences.

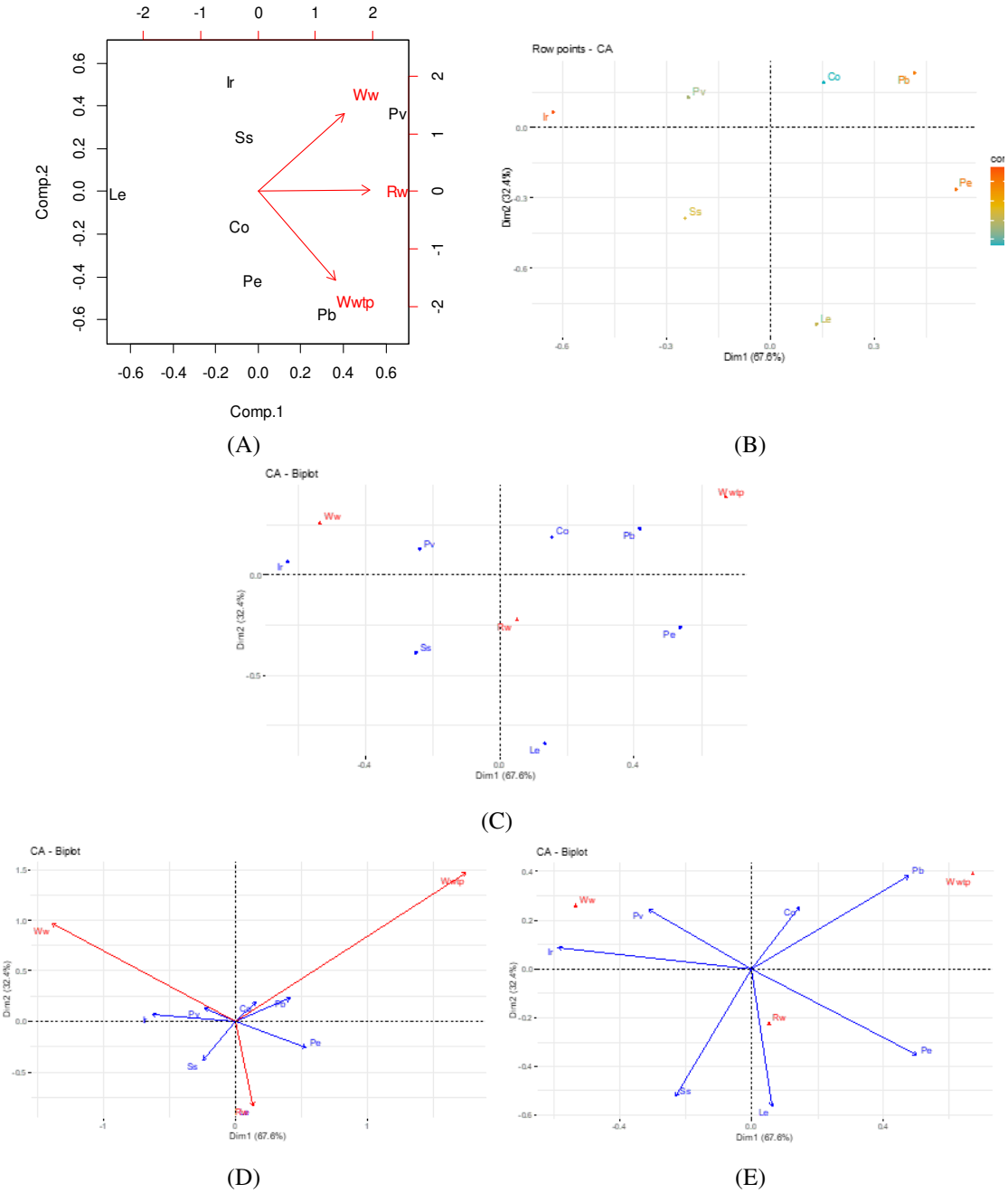

Figure 3. *Graphs of materials-type of water.* ***(A)*** *Biplot.* ***(B)*** *Contributions of rows (materials) to the dimensions.* ***(C)*** *Symmetric biplot.* ***(D)*** *Asymmetric biplot.* ***(E)*** *Contribution biplot*

http://www.aloki.hu ● ISSN 1589 1623 (Print) ● ISSN1785 0037 (Online)
DOI: http://dx.doi.org/10.15666/aeer/2003_27472761

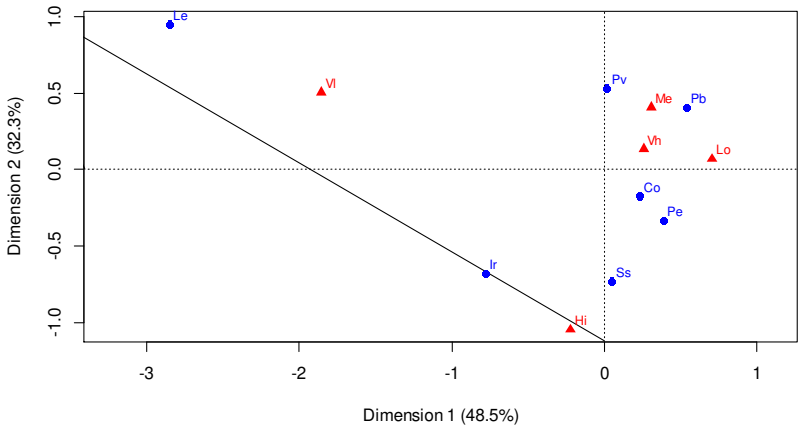

Figure 4. *Correspondence analysis: materials-legislative compliance*

Discussion

Considering the materials studied, it is mandatory to indicate that iron is a very critical material about *Legionella pneumophila*, easily colonizable, but in our study the facilities are protect by a high sanitary legislative compliance. The same occurs for stainless steel (van der Kooij et al., 2020), with less risk than the previous material. Likewise, polyethylene is a substrate that can be easily colonized by the bacterium, although to a lesser extent than iron, with intermediate preventive levels for the irrigation facilities studied. Regarding polybutylene, for the tests carried out for the survival and growth of *Legionella pneumophila* in the planktonic phases and in biofilm at 20ºC, the bacterium appears with a low proportion in the flora of the biofilm and in chlorinated polyvinyl chloride, but it is absent on copper surfaces. The pathogen is more abundant in biofilms in plastics at 40ºC, where it represents 50% of the total flora. Copper surfaces appear to be inhibitory to biological contamination and include only a low number of microorganisms, and polyvinyl chloride has low ease of being colonized (Lu et al., 2014). In fact, the pathogen can survive in biofilms on the surface of plastic materials at 50ºC but is absent from copper surfaces at the same temperature. In the presence of copper surfaces, biofilms formed on (adjacent) glass control surfaces are capable of "incorporating" copper ions, which subsequently inhibit colonization on their surfaces (Rogers et al., 1994), added to the low adhesion of the glass (Assaidi et al., 2018). It´s suggested that the use of copper pipes in water systems can help limit their colonization by *Legionella pneumophila*, an aspect that is acceptably controlled at a preventive level in the facilities analysed. It is worth noting the lead facilities, most of which are very old and deteriorated, which are not being performed hygienic-preventive maintenance, and could be subject to the formation of biofilms with growth of the specific bacterium studied. In fact, there is a relationship between this critical material and poor hygiene standards in Spanish neglected older irrigation systems, low-class hotels, and rural areas.

The chi-square test indicated whether there is a significant association between "materials" and the “preventive compliance intervals”. According to the Pearson´s chi-square test and because the p-value of the test is high, the null hypothesis of independence between the two variables was accepted. Likewise, it can be deduced that a certain material has no dependency to compliance or how these approaches can affect the growth and development of the bacterium.

http://www.aloki.hu ● ISSN 1589 1623 (Print) ● ISSN1785 0037 (Online)
DOI: http://dx.doi.org/10.15666/aeer/2003_27472761

The symmetric biplot showed a global pattern within the data. The distance between any material points or type of water points gave a measure of their similarity or not (general statements). In this way it can be stated that row and column points with similar profile were closed on the factor map. *Figure 3C* showed that Ir and Pv are more related to Ww, and Pb and Co with Wwtp. Additionally, the row variables with the larger value, contributed the most to the definition of the dimensions. Ir, Pe, Pb are the rows that contributed the most to dimension 1 and 2 and are the most important explaining the variability in the data set. Dimension 1 was mainly defined by the opposition of Pb-Co and Ir-Pv (positive and negative pole respectively). In the asymmetric biplot if the angle between two arrows was acute, then there was a strong association between the corresponding row and column, but to interpret the distance between rows and columns we perpendicularly project row points on the column arrow. In this biplot it´s evident that there was a strong association between Wwtp-Co and Ww-Pv. Wwtp had great relevance. Notice that in the contribution biplot the closer an arrow was (in terms of angular distance) to an axis the greater was the contribution of the row category on that axis relative to the other axis. If the arrow was near halfway between the two, its row category contributed to the two axes to the same extent (Kassambara, 2017). The variables that less stand out in magnitude were Co and Pv (explanatory power resides in the remaining), Ir was the most. Pe was the one that contributed the most to dimension 1.

From the correspondence analysis, the main conclusions were obtained due to the proximity or not of the representation of the variables. It should be noted that lead facilities had a very low level of compliance, being this material a nutrient that favors the development of the bacterium. Polybutylene and polyvinyl chloride materials presented a high risk (medium level of compliance) as well as copper (Rhoads et al., 2017) and polyethylene (medium-high level), not being associated with the bacterial growth studied.

Conclusions

Therefore, it can be concluded about the presence of materials easily colonizable by *Legionella pneumophila*, which do not have adequate hygienic-preventive maintenance, and which can be sources of development and proliferation of bacterium. It is worth highlighting Le and Pb with Rw (Fahrenfeld et al., 2013; Pepper and Gerba, 2018) and Wwtp (Kulkarni et al., 2018; Lequette et al., 2019), respectively. It´s estimated that the need for treatments according to the material (compatibility between the type of material, treatment used, condition and design) should be considered for a better control of the bacterium. Likewise, it is noteworthy the consideration of the origin of the irrigation water of the golf courses in the hotels studied (Papadakis et al., 2018; Gea-Izquierdo, 2020) and its need for treatment according to the physicochemical and microbiological characteristics of water (Gea-Izquierdo, 2018).

Recommendations

Possibility of expanding the Spanish sanitary legislative requirements for the prevention and control of legionellosis in irrigation systems is proposed (Mori et al., 2021), improving technical surveillance, increasing water quality controls, substituting materials for others with less risk of development and proliferation of the bacterium (Wang et al., 2012; Cullom et al., 2020), and vigilance regarding cross contamination with other facilities or water distribution systems (Blanky et al., 2015; De Giglio et al., 2019).

http://www.aloki.hu ● ISSN 1589 1623 (Print) ● ISSN1785 0037 (Online)
DOI: http://dx.doi.org/10.15666/aeer/2003_27472761

REFERENCES

[1] Assaidi, A., Ellouali, M., Latrache, H., Mabrouki, M., Timinouni, M., Zahir, H., Tankiouine, S., Barguigua, A., Mliji, E. M. (2018): Adhesion of Legionella pneumophila on glass and plumbing materials commonly used in domestic water systems. – International Journal of Environmental Health Research 28: 125-133. DOI: 10.1080/09603123.2018.1429580.

[2] Atlas, R. M. (1999): Legionella: from environmental habitats to disease pathology, detection and control. – Environmental Microbiology 1: 283-293. DOI: 10.1046/j.1462-2920.1999.00046.x.

[3] Bendixen, M. (2003): A practical guide to the use of correspondence analysis in marketing research. – Marketing Bulletin 14.

[4] Blanky, M., Rodríguez-Martínez, S., Halpern, M., Friedler, E. (2015): Legionella pneumophila: from potable water to treated greywater, quantification and removal during treatment. – The Science of the Total Environment 533: 557-565. DOI: 10.1016/j.scitotenv.2015.06.121. Epub 2015 Jul 17.

[5] Campese, C., Bitar, D., Jarraud, S., Maine, C., Forey, F., Etienne, J., Desenclos, J. C., Saura, C., Che, D. (2011): Progress in the surveillance and control of Legionella infection in France, 1998-2008. – International Journal of Infectious Diseases 15: 30-37. DOI: 10.1016/j.ijid.2010.09.007. Epub 2010 Nov 24.

[6] Correia, A. M., Ferreira, J. S., Borges, V., Nunes, A., Gomes, B., Capucho, R., Gonçalves, J., Antunes, D. M., Almeida, S., Mendes, A, Guerreiro, M., Sampaio, D. A., Vieira, L., Machado, J., Simões, M. J., Gonçalves, P., Gomes, J. P. (2016): Probable person-to-person transmission of Legionnaire's disease. – The New England Journal of Medicine 374: 497-498. DOI: 10.1056/NEJMc1505356.

[7] Cullom, A. C., Martin, R. L., Song, Y., Williams, K., Williams, A., Pruden, A., Edwards, M. A. (2020): Critical review: propensity of premise plumbing pipe materials to enhance or diminish growth of Legionella and other opportunistic pathogens. – Pathogens 9: 957. DOI: 10.3390/pathogens9110957.

[8] Cunha, B. A. (2010): Legionnaires' disease: clinical differentiation from typical and other atypical pneumonias. – Infectious Disease Clinics of North America 24: 73-105. DOI: 10.1016/j.idc.2009.10.014.

[9] Cunha, B. A., Burillo, A., Bouza, E. (2016): Legionnaires' disease. – Lancet 387: 376-385. DOI: 10.1016/S0140-6736(15)60078-2.

[10] De Giglio, O., Napoli, C., Apollonio, F., Brigida, S., Marzella, A., Diella, G., Calia, C., Scrascia, M., Pacifico, C., Pazzani, C., Felice Uricchio, V. F., Montagna, M. T. (2019): Occurrence of Legionella in groundwater used for sprinkler irrigation in Southern Italy. – Environmental Research 170: 215-221. DOI: 10.1016/j.envres.2018.12.041. Epub 2018 Dec 19.

[11] Den Boer, J. W., Euser, S. M., Brandsema, P., Reijnen, L., Bruin, J. P. (2015): Results from the National Legionella Outbreak Detection Program, the Netherlands, 2002-2012. – Emerging Infectious Diseases 21: 1167-1173. DOI: 10.3201/eid2107.141130.

[12] Fahrenfeld, N., Ma, Y., O'Brien, M., Pruden, A. (2013): Reclaimed water as a reservoir of antibiotic resistance genes: distribution system and irrigation implications. – Frontiers in Microbiology 28: 130. DOI: 10.3389/fmicb.2013.00130. eCollection 2013.

[13] Gea-Izquierdo, E. (2018): Water disinfection methods and their affect on legionellosis. – Tecnología y Ciencias del Agua 9: 29-46. DOI: 10.24850/j-tyca-2018-03-02.

[14] Gea-Izquierdo, E. (2020): Biological risk of Legionella pneumophila in irrigation systems. – Revista de Salud Pública 22: e208. DOI: 10.15446/rsap.v22n4.96429.

[15] Greenacre, M. (2013): Contribution biplots. – Journal of Computational and Graphical Statistics 22: 107-122. DOI: 10.1080/10618600.2012.702494.

[16] Irons, J. F., Dunn, M. J. G., Kefala, K., Thorn, S., Lakha, F., Caesar, D., Cameron, D. D., McCormick, D., McCallum, A., Helgason, K. O., Laurenson, I. F., Paterson, R. L.,

http://www.aloki.hu ● ISSN 1589 1623 (Print) ● ISSN1785 0037 (Online)
DOI: http://dx.doi.org/10.15666/aeer/2003_27472761

Greening, A., Fried, M., Hill, A. T., Hanson, M., Gillies, M. A. (2013): The effect of a large Legionnaires' disease outbreak in Southwest Edinburgh on acute and critical care services. – QJM 106: 1087-1094. DOI: 10.1093/qjmed/hct167. Epub 2013 Aug 22.

[17] ISO (2017): Water quality-Enumeration of Legionella. – ISO 11731:2017.

[18] Ji, P., Parks, J., Edwards, M. A., Pruden, A. (2015): Impact of water chemistry, pipe material and stagnation on the building plumbing microbiome. – PLoS One 10: e0141087. DOI: 10.1371/journal.pone.0141087. eCollection 2015.

[19] Kassambara, A. (2017): Principal guide to principal component methods in R: Practical Guide, 1st ed. – STHDA, Multivariate Analysis II.

[20] Kozak, N. A., Lucas, C. E., Winchell, J. M. (2013): Identification of Legionella in the environment. – Methods in Molecular Biology 954: 3-25. DOI: 10.1007/978-1-62703-161-5_1.

[21] Kozak-Muiznieks, N. A., Lucas, C. E., Brown, E., Pondo, T., Taylor Jr., T. H., Frace, M., Miskowski, D., Winchell, J. M. (2014): Prevalence of sequence types among clinical and environmental isolates of Legionella pneumophila serogroup 1 in the United States from 1982 to 2012. – Journal of Clinical Microbiology 52: 201-211. DOI: 10.1128/JCM.01973-13. Epub 2013 Nov 6.

[22] Kulkarni, P., Olson, N. D., Paulson, J. N., Pop, M., Maddox, C., Claye, E., Rosenberg Goldstein, R. E., Sharma, M., Gibbs, S. G., Mongodin, E. F., Sapkota, A. R. (2018): Conventional wastewater treatment and reuse site practices modify bacterial community structure but do not eliminate some opportunistic pathogens in reclaimed water. – The Science of the Total Environment 639: 1126-1137. DOI: 10.1016/j.scitotenv.2018.05.178.

[23] Lee, S. (2018): An Overview of the European Technical Guidelines for the prevention, control and investigation of infections caused by Legionella species. – Perspectives in Public Health 138: 241-247. DOI: 10.1177/1757913918790922.

[24] Lequette, K., Ait-Mouheb, N., Wéry, N. (2019): Drip irrigation biofouling with treated wastewater: bacterial selection revealed by high-throughput sequencing. – Biofouling 35: 217-229. DOI: 10.1080/08927014.2019.1591377. Epub 2019 Apr 2.

[25] Lu, J., Buse, H. Y., Gomez-Alvarez, V., Struewing, I., Santo Domingo, J., Ashbolt, N. J. (2014): Impact of drinking water conditions and copper materials on downstream biofilm microbial communities and Legionella pneumophila colonization. – Journal of Applied Microbiology 117: 905-918. DOI: 10.1111/jam.12578. Epub 2014 Jul 7.

[26] Maini, R., Naik, F., Harrison, Tg., Mentasti, M., Spala, G., Velonakis, E., Hadjichristodoulou, C., de Jong, B., Vatopoulos, A., Phin, N. (2012): Travel-associated Legionnaires' disease in residents from England and Wales travelling to Corfu, Greece, August to October 2011. – Euro Surveillance. 17, 20240. DOI: 10.2807/ese.17.32.20240-en.

[27] Mori, J., Uprety, S., Mao, Y., Koloutsou-Vakakis, S., Nguyen, T. H., Smith, R. L. (2021): Quantification and comparison of risks associated with wastewater use in spray irrigation. – Risk Analysis 41: 745-760. DOI: 10.1111/risa.13607.

[28] Moritz, M. M., Flemming, H. C., Wingender, J. (2010): Integration of Pseudomonas aeruginosa and Legionella pneumophila in drinking water biofilms grown on domestic plumbing materials. – International Journal of Hygiene and Environmental Health 213: 190-197. DOI: 10.1016/j.ijheh.2010.05.003.

[29] Nguyen, T. M., Ilef, D., Jarraud, S., Rouil, L., Campese, C., Che, D., Haeghebaert, S., Ganiayre, F., Marcel, F., Etienne, J., Desenclos, J. C. (2006): A community-wide outbreak of Legionnaire's disease linked to industrial cooling towers-how far can contaminated aerosols spread? – The Journal of Infectious Diseases 193: 102-111. DOI: 10.1086/498575. Epub 2005 Nov 28.

[30] NNDSS Annual Report Working Group (2016): Australia's notifiable disease status, 2014: annual report of the National Notifiable Diseases Surveillance System. – Communicable Diseases Intelligence Quarterly Report 40: 48-145.

http://www.aloki.hu ● ISSN 1589 1623 (Print) ● ISSN1785 0037 (Online)
DOI: http://dx.doi.org/10.15666/aeer/2003_27472761

[31] O'Connor, B. A., Carman, J., Eckert, K., Tucker, G., Givney, R., Cameron, S. (2007): Does using potting mix make you sick? Results from a Legionella longbeachae case-control study in South Australia. – Epidemiology and Infection 135: 34-39. DOI: 10.1017/S095026880600656X. Epub 2006 Jun 19.

[32] Papadakis, A., Chochlakis, D., Sandalakis, V., Keramarou, M., Tselentis, Y., Psaroulaki A. (2018): Legionella spp. risk assessment in recreational and garden areas of hotels. – International Journal of Environmental Research and Public Health 15: 598. DOI: 10.3390/ijerph15040598.

[33] Pepper, I. L., Gerba, C. P. (2018): Risk of infection from Legionella associated with spray irrigation of reclaimed water. – Water Research 139: 101-107. DOI: 10.1016/j.watres.2018.04.001. Epub 2018 Apr 2.

[34] R Core Team (2019): R: A language and environment for statistical computing. – R Foundation for Statistical Computing, Vienna, Austria. URL http://www.R-project.org/.

[35] Real Decreto 909/2001, de 27 de julio, por el que se establecen los criterios higiénico-sanitarios para la prevención y control de la legionelosis. B.O.E. núm. 180 de 28 de julio de 2001.

[36] Real Decreto 865/2003, de 4 de julio, por el que se establecen los criterios higiénico-sanitarios para la prevención y control de la legionelosis. B.O.E. núm. 171 de 18 de julio de 2003.

[37] Rhoads, W. J., Pruden, A., Edwards, M. A. (2017): Interactive effects of corrosion, copper, and chloramines on Legionella and mycobacteria in hot water plumbing. – Environmental Science & Technology 51: 7065-7075. DOI: 10.1021/acs.est.6b05616. Epub 2017 Jun 1.

[38] Rogers, J., Dowsett, A. B., Dennis, P. J., Lee, J. V., Keevil, C. W. (1994): Influence of temperature and plumbing material selection on biofilm formation and growth of Legionella pneumophila in a model potable water system containing complex microbial flora. – Applied and Environmental Microbiology 60: 1585-1592. DOI: 10.1128/aem.60.5.1585-1592.1994.

[39] Van der Kooij, D., Veenendaal, H. R., Italiaander, R. (2020): Corroding copper and steel exposed to intermittently flowing tap water promote biofilm formation and growth of Legionella pneumophila. – Water Research 183: 115951. DOI: 10.1016/j.watres.2020.115951. Epub 2020 Jun 23.

[40] Van Heijnsbergen, E., Schalk, J. A., Euser, S. M., Brandsema, P. S., den Boer, J. W., de Roda Husman, A. M. (2015): Confirmed and potential sources of Legionella reviewed. – Environmental Science & Technology 49: 4797-4815. DOI: 10.1021/acs.est.5b00142.

[41] Wang, H., Masters, S., Hong, Y., Stallings, J., Falkinham 3rd, J. O., Edwards, M. A., Pruden, A. (2012): Effect of disinfectant, water age, and pipe material on occurrence and persistence of Legionella, mycobacteria, Pseudomonas aeruginosa, and two amoebas. – Environmental Science & Technology 46: 11566-11574. DOI: 10.1021/es303212a. Epub 2012 Oct 25.

http://www.aloki.hu ● ISSN 1589 1623 (Print) ● ISSN1785 0037 (Online)
DOI: http://dx.doi.org/10.15666/aeer/2003_27472761

APPENDIX

Appendix 1. *The questionnaire used for monitoring prevention and control of legionellosis*

I)- Do you have any of the following facilities? Mark with a cross what applies.

	AVAILABILITY			**OPERATION**		**WORKING**	
FACILITY	YES	NO	**Number**	SEASONAL	NOT SEASONAL	DIURNAL	NIGHT
1.-Sanitary hot water							
2.-Accumulators ("boilers")							
3.-Sanitary cold water							
4.-Water tanks							
5.-Cooling towers							
6.-Evaporative condensers							
7.-Adiabatic condensers							
8.-Bathtubs without recirculation (single use)							
9.-Recirculating pools (collective use, spas o similar)							
10.-Humidifiers/evaporative cooling/ others							
11.-Water lines in dental units							
12.-Ornamental fountains							
13.-Tank trucks							
14.-Humidification in air ducts							
15.-Sprinkler irrigation (including aerosol)							
16.-Other industrial processes (with aerosol)							
17.-Thermal facilities							
18.-Aquariums (uncovered)							
19.-Fire fighting water systems							

http://www.aloki.hu ● ISSN 1589 1623 (Print) ● ISSN1785 0037 (Online)
DOI: http://dx.doi.org/10.15666/aeer/2003_27472761

20.- Origin of the water: Public ☐ Private ☐

Recycled water ☐ Wastewater treatment plant ☐ Well water ☐

	YES	NO
II) 21.- In the case of cooling towers, evaporative condensers or adiabatic, have they been notified to the competent health authority?		
22.- Have any modifications or improvements been made since its installation?		
23.- Do you usually carry out any control of the quality of the water?		
24.- If so, are the analysis carried out in an approved laboratory?		

III)-25.- What is the distance between the cooling towers or similar systems (unprotected) and the people who may be exposed to the aerosols?___meters.

26.- And regarding air conditioning or ventilation intakes?___meters.

	YES	NO
IV) 27.- The cooling system, can it be emptied completely?		

28.- What flow of circulating water exists?_____l/h.

29.- And of dragged water?_____l/h.

	YES	NO
30.- Do you have a continuous biocide dosing system?		

31.- Do you have any other disinfection system? Which one?

	YES	NO
- Chlorination		
- Ultraviolet radiation		
- Ozonation		
- Bromation		
- Copper-silver ionization		

V)- In cooling towers, evaporative and adiabatic condensers, others do you carry out water controls? (Please indicate facility type)

	YES	NO
32.-Physical-chemical		
33.-Microbiological		

With what periodicity?

	Annual	Biannual	Quarterly	Three-month	Bimonthly	Monthly	Weekly	Daily	Undefined
34.-Physical-chemical									
35.-*Legionella*									
36.-Total aerobes									

http://www.aloki.hu ● ISSN 1589 1623 (Print) ● ISSN1785 0037 (Online)
DOI: http://dx.doi.org/10.15666/aeer/2003_27472761

	YES	NO
VI) 37.- Do you have a facilities Maintenance Program?		
38.- And a Maintenance Registry?		

	YES	NO
VII) 39.-Staff performing hygienic-sanitary maintenance operations; have they completed the training courses, to that effect, approved by the Ministry of Health?		
40.- Do you have an external company to carry out the different treatments?		
41.- If so, is said company registered in the Official Register of Biocidal Establishments and Services?		

VIII) 42.- In the facilities marked by you in the box of the first question, is there any control of the water temperature?

43.- Is there water disinfection? What kind of disinfection?

	YES	NO
IX) 44.- Do you have a filtration system for drinking water?		

	YES	NO
X) 45.- Is access to drinking water equipment safe?		
46.- And for cooling towers and similar systems?		

XI) 47.- What material are the drinking water pipes made of?

Polybutylene ☐ Polyethylene ☐ Iron ☐ Lead ☐ Stainless steel ☐ Polyvinyl chloride ☐

Copper ☐ Other _____.

XII) 48.- What is the temperature of the sanitary cold water?_____ºC.

49.- Where are water tanks located?

	YES	NO
- Inside		
- Outside		
50.- Are they covered?		
51.- Do they have any access inside?		
52.-Are they isolated?		

http://www.aloki.hu ● ISSN 1589 1623 (Print) ● ISSN1785 0037 (Online)
DOI: http://dx.doi.org/10.15666/aeer/2003_27472761

XIII) 53.- What is the temperature of the sanitary hot water system?__ ºC.

54.- What is the temperature of the water in the accumulators?___ºC.

55.- Do accumulators have a drain valve?

YES	NO

XIV) 56.- Do you have respiratory therapy equipment?*

YES	NO

57.- How often do you disinfect reusable equipment?*

Monthly	Weekly	Daily	After use	Undefined	Never

XV) 58.- Do ornamental fountains have an automatic chlorination system?

YES	NO

XVI) 59.- Are the chemical products used in different water treatments approved?

60.- Do they have safety data sheet?

YES	NO

***STUDY CENTER*:**_____

OBSERVATIONS:

http://www.aloki.hu ● ISSN 1589 1623 (Print) ● ISSN1785 0037 (Online)
DOI: http://dx.doi.org/10.15666/aeer/2003_27472761

EFFECT OF SPRAYING WITH FOLIC ACID AND YEAST EXTRACT ON THE GROWTH, YIELD AND CALCIUM OXALATE CONCENTRATION OF SPINACH (*SPINACIA OLERACEA* L.)

AL-MHARIB, M. Z. K. – AL-UBAIDY, R. M. – MOHAMMED, M. M.*

Department of Horticulture and Landscape Gardening Design, College of Agricultural Engineering Sciences, University of Baghdad, Baghdad, Iraq
(phone: +964-781-871-4104)

**Corresponding author*
e-mail: mohammed.m@coagri.uobaghdad.edu.iq

(Received 7th Jan 2022; accepted 25 Mar 2022)

Abstract. An experiment was conducted according to randomized complete block design (RCBD) with three replications during the winter growing season of 2019-2020 at the Department of Horticulture and Landscape Gardening Design, College of Agricultural Engineering Sciences, University of Baghdad, Iraq, to investigate the response of spinach plants to different levels of exogenous application of Folic acid and yeast and their interactions in terms of growth, yield, and quality traits. The experiment included two factors the first was Folic acid (0,100 and150 mg.l^{-1}) symbolized as F0, F1 and F2, respectively. The second factor was foliar spraying with three levels of yeast extract (0,5 and10 g/l) symbolized as Y0, Y1 and Y2, respectively. According to the results the outcome of the F2 treatment (150 mg. l^{-1}) was a highly significant effect on all growth and yield traits. Also, Y1 (5 mg.l^{-1}) showed better results for all of the same characteristics except dry matter %, where Y2 treatment (10 g.l^{-1}) showed the highest value. Based on the results the F2Y1 treatment showed the best performance with a plant height of 46.47 cm, leaf width of 13.45 cm, number of leaves at 11.54 leaf.plant^{-1}, leaf area of 147.35 cm^2.plant^{-1}, oxalate at 61.36 mg.100^{-1} fresh weight, yield per plot at 8.29 kg and total yield of 27.63 ton.ha^{-1}, while F2Y2 treatment gave the highest percentage of dry matter 8.43% and the lowest percentage of nitrate 0.17%.
Keywords: *biostimulators, foliar application, vitamins, Saccharomyces cerevisiae, Chenopodiaceae*

Introduction

Leafy crops are of high nutritional value and stimulate human physiological processes (AL-Mharib et al., 2019). One of the most important crops of the Chenopodiaceae family is spinach (Spinacia oleracea L.). The cultivated area in Iraq is about 538 hectares with a total production of 3234 tons, with an average of 6.0112 ton.ha^{-1} annually (FAO, 2020). Spinach with a high content of beta-Carotene and lutein, has significant role in preventing heart diseases and cancer as it is considered to be an active antioxidant and also has a role in the health of the eyes, skin and hair, it increases immunity, and has significant roles in cell metabolism (Antunes et al., 2005). There are risks when eating spinach in large quantities due to the high accumulation of nitrates and oxalates, which may cause health problems when the permissible limit is exceeded. Al-Tayeb (2012) stated that spinach has high contents of oxalic acid, which causes its taste, its quantity was estimated at 100-400 mg.100 g^{-1} wet weight, while in some European varieties, it may reach more than 930 mg.100 gm^{-1}. There are many nutrients such as amino acids and acids of mineral elements that play an important role in the vegetative and yield traits of plants (Mariush and AL-Mharib, 2020). One of the most important sources of organic nutrients is the yeast extract (Saccharomyces cerevisiae) which had significant effects when it was applied on snap bean, summer squash and pea (Al-Amery and Mohammed, 2017; Salman and Alewi, 2017; Mohammed and Al-

http://www.aloki.hu ● ISSN 1589 1623 (Print) ● ISSN 1785 0037 (Online)
DOI: http://dx.doi.org/10.15666/aeer/2003_27632768

Ubaidy, 2020). Also, it showed an important role in plant alleviation under abiotic stress due to its contents of proteins, vitamins, and its ability to produce hormones such as (IAA, GA3) which significantly affect plants and symbiotic organisms (Shalaby and El-Nady, 2008; Mady, 2009). Both of Al-Khafaji (1990) and Tawfiq (2010) pointed to the importance of some chemical characters of yeast extract analysis (*Table 1*). Folic acid plays a function in delivering amino acids to their proper positions in protein chains, where it is involved in the methylation of amino and nucleic acids (Kelly, 1998; Lucock, 2004). There is a focus on using natural substances to improve the growth of plants where Folic acid has a synergistic effect on vegetative development and components of yield in many plants where it was so effective in reducing the free radicals (AL-maliky et al., 2019; Heo et al., 2019; Paucean et al., 2018; Sakr, 2009). The objective of this study was to investigate the effects of folic acid, yeast, and their interactions on growth, yield, and quality characteristics in spinach plants.

Table 1. *Chemical analysis of bread yeast extract*

Compounds*	**mg. g^{-1}**
Carb	82
Total nitrogen	90
Amino acids' nitrogen	40
Chlorides	1-13
Phosphate	38
Sodium	56
Potassium	30
Calcium	0.1
Iron	0.05
Magnesium	2
Copper	0.05
Zinc	0.05
Manganese	0.005
Cobalt	0.005
Produced hormones**	**mcg.ml^{-1}**
IAA	29.86 in 222 nm wavelength
IAA	198 in 280 nm wavelength
GA3	799 in 254 nm wavelength

*Source: Al-Khafaji (1990)
**Source: Tawfiq (2010)

Materials and methods

An experiment was conducted according to randomized complete blocks design (RCBD) with three replications at the Department of Horticulture and Landscape Gardening Design, College of Agricultural Engineering Sciences, University of Baghdad, Iraq, to investigate the response of spinach plants to different levels of exogenous application of Folic acid and yeast and their interactions on growth, yield, and quality traits. The experiment included two factors the first was Folic acid (0,100 and 150 mg.l^{-1}) symbolized as F0, F1 and F2, respectively. The second factor was foliar spraying with three levels of yeast extract (0,5 and10 g.l^{-1}) symbolized as Y0, Y1 and

http://www.aloki.hu ● ISSN 1589 1623 (Print) ● ISSN 1785 0037 (Online)
DOI: http://dx.doi.org/10.15666/aeer/2003_27632768

Y2, respectively. The field was divided into 2 m long and 1.5 m wide plots, and half a meter was left between each plot and another for the service and one meter at each 9 plots (block), the number of experimental units (plots) reached 27 plots for three replications. The spinach seeds were sown in the field directly in lines on the 21st October for the winter growing season of 2019 where the distance was of 25 cm between one line and another and each experimental unit contained 6 lines. A planted three seeds with an of average 30 kg.ha^{-1}, plant density reached 550000 plant.ha^{-1}, where the area of each experimental unit was 3 m^2, and all other cultural practices, such as irrigation and thinning out and fertilizer were uniform for all the experimental units according to (AL-Ansari, 2014). The estimation of nitrate as percentage was according to (Silveira et al., 2001) and calcium oxalate was measured according to (Mahadevan and Sridhar, 1982) and the other characters of vegetative growth and yield were estimated according to (Al-Mohammed, 2010). The collected data were analyzed statistically by Genstat statistical package software with two-way ANOVA (in Randomized Blocks) and L.S.D was used at 0.05 of probability for comparing the differences between various treatment means.

Results and discussion

The results in *Table 2* referred that spraying folic acid at F2 treatment (150 mg.l^{-1}) showed a highly significant increasing effect on plant height, leaf width, number of leaves, leaf area, dry matter, yield per plot and the total yield reached (42.98 cm.plant^{-1}, 12.6 cm.leaf^{-1}, 10.62 leaves.plant^{-1}, 129.61 cm^2.leaf^{-1}, 8.007%.leaf^{-1}, 7.75 kg.plot^{-1} and 25.843 ton.ha^{-1}) respectively. While it gave the lowest value of leaf content of oxalate, nitrate percentage in the leaf where reached (68.28 mg.100 gm^{-1} fresh weight, 0.2%.leaf^{-1}) respectively. The highest values were showed clearly in F2 treatment due to the positive effects of folic acid on the photosynthesis efficiency, activity of meristematic tissues, cell division and cell enlargement which led to increasing vegetative growth and then total yield and those results were agreed with Paucean et al. (2018) and AL-maliky et al. (2019).

Table 2. *Effect of folic acid on growth, yield, and oxalate in spinach*

Treatments	Plant height (cm)	Leaf width (cm)	Leaves number (leaf.plant^{-1})	Leaf area (cm^2.leaf^{-1})	Dry matter %	Oxalate (mg.100 gm^{-1} fresh weight)	Nitrate %	Yield per plot (kg)	Total yield (ton.ha^{-1})
F0	39.1	11.93	9.63	117.21	7.553	73.66	0.25	6.94	23.132
F1	42.06	12.4	10.36	124.9	7.707	69.72	0.22	7.48	24.937
F2	42.98	12.6	10.62	129.61	8.007	68.28	0.2	7.75	25.843
LSD 5%	0.633	0.147	0.095	1.091	0.1142	1.215	0.021	0.153	0.5077
SD	3.825	1.083	1.148	18.67	0.54	7.623	0.0404	0.781	2.604

The results in *Table 3* showed the superiority and significant effects of yeast foliar spraying at Y1 treatment (5 gm.l^{-1}) for plant height, leaf width, number of leaves, leaf area, yield per plot and total yield which reached (45.02 cm.plant^{-1}, 13.15 cm.leaf^{-1}, 11.13 leaf.plant^{-1}, 141.51 cm^2.leaf^{-1}, 7.96 kg.plot^{-1} and 26.533 ton.ha^{-1}) respectively. While Y2 treatment showed the highest value in leaf content of dry matter and the lowest value in nitrate percentage of leaves which reached (8.24%. leaf^{-1}, 0.19%. leaf^{-1}) respectively. The mentioned characters were increased as compared with control

http://www.aloki.hu ● ISSN 1589 1623 (Print) ● ISSN 1785 0037 (Online)
DOI: http://dx.doi.org/10.15666/aeer/2003_27632768

treatment due to increasing the dry matter content of leaves and decreasing the nitrate content of leaves by protein synthesis where nitrate was reduced to ammonia which reacted with the keto acids which were the products of carbohydrate metabolism during photosynthesis and that was agreed with Al-Dhalimi (2017).

Table 3. *Effect of yeast on growth, yield, and oxalate in spinach*

Treatments	Plant height (cm)	Leaf width (cm)	Leaves number (leaf.plant^{-1})	Leaf area (cm^2.leaf^{-1})	Dry matter %	Oxalate (mg.100 gm^{-1} fresh weight)	Nitrate %	Yield per plot (kg)	Total yield (ton.ha^{-1})
Y0	37.16	10.9	8.77	100.06	7.093	80.36	0.27	6.49	21.622
Y1	45.02	13.15	11.13	141.51	7.933	65.13	0.22	7.96	26.533
Y2	41.96	12.88	10.72	130.14	8.24	66.17	0.19	7.73	25.757
LSD 5%	0.633	0.147	0.095	1.091	0.1142	1.215	0.021	0.153	0.5077
SD	3.825	1.083	1.148	18.67	0.54	7.623	0.0404	0.781	2.604

The results in *Table 4* showed the superior effects of F2Y1 treatment (spraying 150 mg. l^{-1} of folic acid and 5g.l^{-1} of yeast) on the plant height, leaf width, the number of leaves, leaf area, yield per plot and the total yield reached (46.47 cm.plant^{-1}, 13.45 cm.leaf^{-1}, 11.54 leaf.plant^{-1}, 147.35 cm^2.leaf^{-1}, 8.29 kg.plot^{-1} and 27.63 ton.ha^{-1}) respectively. While it showed the lowest value of leaf content of oxalate reached 61.36 mg.100 gm^{-1} fresh weight. Also, F2Y2 treatment (spraying 150 mg. l^{-1} of folic acid and 10 g.l^{-1} of yeast) showed the highest percentage of dry matter 8.43% and the lowest percentage of nitrate 0.17% in leaves. While control treatment of interaction gave the least values for all the growth and yield indicators. The increasing values of studied characters by interaction treatments refer to the positive and significant effect of both folic acid and yeast in promoting and increasing enzyme activities and having an essential role in amino and nucleic acid synthesis, and similar results were obtained by Shalaby and El-Nady (2008), AL-Ansari (2014), Salman and Alewi (2017), Paucean et al. (2018) and Mohammed and Al-Ubaidy (2020).

Table 4. *Effect of folic acid and yeast interaction on growth, yield, and oxalate in spinach*

Treatments	Plant height (cm)	Leaf width (cm)	Leaves number (leaf.plant^{-1})	Leaf area (cm^2.leaf^{-1})	Dry matter %	Oxalate (mg.100 gm^{-1} fresh weight)	Nitrate %	Yield per plot (kg)	Total yield (ton.ha^{-1})
F0Y0	34.45	10.6	8.11	93.54	6.91	83.67	0.29	5.82	19.387
F0Y1	42.76	12.7	10.61	134.36	7.72	69.8	0.24	7.55	25.16
F0Y2	40.09	12.5	10.18	123.72	8.03	67.52	0.22	7.46	24.85
F1Y0	38.1	10.95	8.96	101.7	6.99	79.12	0.26	6.66	22.18
F1Y1	45.83	13.3	11.23	142.81	7.87	64.22	0.22	8.04	26.81
F1Y2	42.25	12.95	10.9	130.18	8.26	65.81	0.19	7.75	25.82
F2Y0	38.92	11.15	9.25	104.95	7.38	78.28	0.25	6.99	23.3
F2Y1	46.47	13.45	11.54	147.35	8.21	61.36	0.19	8.29	27.63
F2Y2	43.54	13.2	11.07	136.53	8.43	65.19	0.17	7.98	26.6
LSD 5%	1.096	0.255	0.164	1.889	0.1978	2.104	0.036	0.264	0.8793
SD	3.825	1.083	1.148	18.67	0.54	7.623	0.0404	0.781	2.604

Table 5 referred to the positive correlation of plant height, leaf width, number of leaves, leaf area, dry matter content of leaves with yield per plot where the highest value was showed between the number of leaves and yield per plot which reached (0.9697).

http://www.aloki.hu ● ISSN 1589 1623 (Print) ● ISSN 1785 0037 (Online)
DOI: http://dx.doi.org/10.15666/aeer/2003_27632768

Also, all the characters were correlated negatively with both oxalate concentration and nitrate percentage in leaves. While the correlation among oxalate and nitrate was positive. The results showed the ability to decrease the leaf content of oxalate and nitrate by improving the vegetative growth characters.

Table 5. *Correlation analysis of growth and yield among studied indicators of spinach*

Plant height (cm)								
Leaf width (cm)	0.9231							
Leaves number (leaf.plant^{-1})	0.957	0.9802						
Leaf area (cm^2.leaf^{-1})	0.9569	0.9786	0.9812					
Dry matter %	0.7561	0.888	0.8673	0.8365				
Nitrate %	-0.7202	-0.8008	-0.805	-0.7607	-0.839			
Oxalate (mg.100 gm^{-1} fresh weight)	-0.92	-0.976	-0.9674	-0.9609	-0.9089	0.8002		
Yield per plot (kg)	0.9543	0.9314	0.9697	0.9429	0.8368	-0.7905	-0.9414	
	Plant height (cm)	**Leaf width (cm)**	**Leaves number (leaf.plant^{-1})**	**Leaf area (cm^2.leaf^{-1})**	**Dry matter %**	**Nitrate %**	**Oxalate (mg.100 gm^{-1} fresh weight)**	**Yield per plot (kg)**

Conclusion

According to the obtained results in the current study, we could conclude that exogenous spraying with yeast at (5 g.l^{-1}), Folic acid at (150 mg. l^{-1}) and their interaction affected positively and significantly growth, yield, and quantitative characters. Treatments effectively decreased the nitrate and oxalate content of leaves, and in addition increased the growth and yield indicators. Therefore, we recommend future studies to investigate the different levels of yeast and folic interactions to improve the qualitative and quantitative characters of spinach.

REFERENCES

[1] Al-Amery, N. J., Mohammed, M. M. (2017): Influence of adding ascorbic acid and yeast on growth and yield and Rhizobium of snap bean (Phaseolus vulgaris L.) under irrigation with saline water. – J Agric Vet Sci 10: 23-28.

[2] Al-Ansari, H. R. M. (2014): Effect of spraying with some mineral nutrients and organic acids on growth, yield, and concentrations of some active compounds medicinally in spinach (*Spinacea oleracea L.*). – Ph.D. Dissertation, University of Baghdad, Iraq.

[3] Al-Dhalimi, A. M., Hussein, S. H., Gibbren, Q. K., Abdul-Hussein, A. K., Abas, Z. S. (2017): The effect of dry bread yeast Saccharomyces cerevisiae, in some qualities of vegetative growth and nutritional status of the faba bean Vicia fabd. – Al-Qadisiyah Journal of Pure Science 22(3): 121-128.

[4] Al-Khafaji, Z. M. (1990): Biotechnology. – University of Baghdad, Ministry of Higher Education and Scientific Research, Republic of Iraq.

[5] Al-maliky, A. W., Jerry, A. N., Obead, F. T. (2019): The Effect of Foliar Spraying with Folic Acid and Cysteine on Growth and Yield of Green Bean Plants (Vicia faba L.). – Journal of Al-Muthanna for Agricultural Sciences 7(4).

http://www.aloki.hu ● ISSN 1589 1623 (Print) ● ISSN 1785 0037 (Online)
DOI: http://dx.doi.org/10.15666/aeer/2003_27632768

[6] Al-Mharib, M. Z., Attalah, A. M., Ali, A. B. (2019): Effect of adding humic acid and phosphate fertilizer levels on growth and yield of lettuce. – J. Agric. and Veterinary Sci 12(4): 12-15.
[7] Al-Mohammed, M. H. S. (2010): Response of three cultivars of rocket (Eruca sativa Mill.) for nitrogen Fertilizer and kinetin spray on growth, content of some active compounds and their biochemical effects. – Ph.D. Thesis, College of Agriculture, University of Basra, Republic of Iraq.
[8] Al-Tayeb, F. A. S. (2012): Effect of using some factors on growth, yield and formation of calcium oxalate crystals in local variety of spinach (*Spinacea oleracea L.*). – Ph.D. dissertation, University of Kufa, College of Agriculture.
[9] Antunes, L. M., Pascoal, L. M., Bianchi, M. D. L., Dias, F. L. (2005) Evaluation of the clastogenicity and anticlastogenicity of the carotenoid bixin in human lymphocyte cultures. – Mutat Res 585(1-2): 113-119.
[10] Faostat, F. A. O. (2020): Crops. Food and Agriculture Organization of the United Nations. – https://www.fao.org/faostat/en/#compare.
[11] Heo, K., Gibson, G., Evans, R. (2019): Effects of bisphenol-A and folic acid on growth, reproductive development, and DNA methylation in snapdragons (Antirrhinum majus). – Botany 97(2): 149-160.
[12] Kelly, G. S. (1998): Folates: supplemental forms and therapeutic applications. – Alternative Medicine Review: A Journal of Clinical Therapeutic 3(3): 208-220.
[13] Lucock, M. (2004): Is folic acid the ultimate functional food component for disease prevention? – BMJ 328(7433): 211-214.
[14] Mady, M. A. (2009): Effect of foliar application with yeast extract and zinc on fruit setting and yield of faba bean (Vicia faba L.). – J. Biol. Chem. Environ. Sci. 4(2): 109-127.
[15] Mahadevan, A., Sridhar, R. (1982): Methods in Physiological Plant Pathology. 3rd Ed. – Center of Advanced Study in Botany, University of Madras.
[16] Mariush, A. H. K., AL-Mharib, Mohammed, Z. K. (2020): Effect of Nano-fertilizers and amino acids on the growth and yield of broccoli. – Int. J. Agricult. Stat. Sci. 16(Supplement 1): 1661-1665.
[17] Mohammed, M. M., Al-Ubaidy, R. M. (2020): Influence of yeast and intercropping system on growth and yield traits of pea. – Int. J. Agricult. Stat. Sci. 16(1): 1577-1580.
[18] Paucean, A., Moldovan, O. P., Mureșan, V., Socaci, S. A., Dulf, F. V., Alexa, E., Muste, S. (2018): Folic acid, minerals, amino-acids, fatty acids, and volatile compounds of green and red lentils. Folic acid content optimization in wheat-lentils composite flours. – Chemistry Central Journal 12(1): 1-9.
[19] Sakr, M. T., Arafa, A. A. (2009): Effect of some antioxidants on canola plants grown under soil salt stress condition. – Pakistan Journal of Biological Sciences PJBS 12(7): 582-588.
[20] Salman, F. A., Alewi, Z. H. (2017): Effect of spraying bread yeast extract and urea fertilizer on some vegetative and productivity indicators of summer squash plants (Cucurbita pepo L.). – Journal of University of Babylon 25(4): 1452-1462.
[21] Shalaby, M. E., El-Nady, M. F. (2008): Application of Saccharomyces cerevisiae as a biocontrol agent against Fusarium infection of sugar beet plants. – Acta Biologica Szegediensis 52: 275-271.
[22] Silveira, J. A. G., Matos, J. C. S., Cecatto, V. M., Viegas, R. A., Oliveira, J. T. A. (2001): Nitrate reductase activity, distribution, and response to nitrate in two contrasting Phaseolus species inoculated with Rhizobium spp. – Environmental and Experimental Botany 46(1): 37-46.
[23] Tawfiq, A. A. (2010): Estimation levels of Indol acetic acid (IAA) and Gibberellic acid (GA3) from dry bakery yeast Saccharomyces cereviciae. – Journal of Biotechnology Research Center 4(2): 94-100.

http://www.aloki.hu ● ISSN 1589 1623 (Print) ● ISSN 1785 0037 (Online)
DOI: http://dx.doi.org/10.15666/aeer/2003_27632768

SPATIAL AND TEMPORAL MODELING OF THE URBAN GROWTH AND LAND COVER CHANGES USING REMOTE SENSING, SPATIAL INDEXES AND GIS TECHNIQUES IN IRBID CITY, JORDAN

MASHAGBAH, A. F.[1*] – IBRAHIM, M.[1*] – AL-FUGARA, A.[2] – ALZABEN, H.[3]

[1]*Department of Geographic Information Systems and Remote Sensing, Institute of Earth and Environmental Sciences, Al Al-Bayt University, Mafraq, Jordan*
(e-mail: majed.ibrahim@aabu.edu.jo)

[2]*Department of Engineering Survey, Faculty of Engineering, Al Al-Bayt University, Mafraq, Jordan*
(e-mail: akifmohd @aabu.edu.jo)

[3]*Department of Mechanical Engineering, Faculty of Engineering, Al Hussein Technical University, Amman, Jordan*
(e-mail: heba.alzaben@htu.edu.jo)

*****Corresponding authors*
e-mail: atef.mashagbah@yahoo.com, atef.almashagbah@aabu.edu.jo, majed.ibrahim@aabu.edu.jo; phone: +962-77-678-7720

(Received 14th Jan 2022; accepted 2nd May 2022)

Abstract. This study examined the temporal and spatial changes in the urban land cover of the northern region of Jordan from 2000 to 2020. Automated processing of satellite images was carried out and different statistical indicators were applied to analyze the data. The data facilitated the monitoring of urban sprawl and determination of trends based on the Geographic Information System (GIS) and remote-sensing analysis of Landsat satellite images. The results revealed an increase in urban segments, population, and reverse migration compared to neighboring areas. The classified land use and land cover maps depicted an expansion of 19.22% from 2000 to 2010 and 8.04% from 2010 to 2020. In comparison to the areas at the urban saturation stage, more rapid urban growth was observed in the seven southwest and northwest districts. Thus, the study presents reliable information and a cartographic database to demonstrate the changes in urban cover of Irbid city, over the past 20 years.
Keywords: *land use, spatial and temporal patterns, sprawl, Landsat, urban expansion, Shannon entropy*

Introduction

Land use maps provide accurate and updated spatial information about the nature of land usage in the target areas. Their applications have become of key importance to plan and develop land resources and achieve maximum benefits for humans (Tewolde and Cabral, 2011). GIS and remote sensing are credible techniques to identify and study land usage. These techniques involve the linking of spatial data to the databases, which is analyzed to identify types and patterns of land usage. The patterns of land use form polygons where each type of land use contains a unit or group of cadastral units indicating industrial, commercial, and residential, areas. These methods provide reliable projections by identifying the empty spaces on the maps for future constructions and the expansion of cities (Eyoh et al., 2012; Kumar et al., 2015).

Urban sprawl is a contemporary global issue, especially in developing countries with higher population-increase rates. This phenomenon of urban sprawling leads to the significant encroachment of agricultural lands, which previously served as the source of

http://www.aloki.hu ● ISSN 1589 1623 (Print) ● ISSN 1785 0037 (Online)
DOI: http://dx.doi.org/10.15666/aeer/2003_27692781

economic activity by producing valuable human foods (Cohen, 2006; Al Mashagbah, 2016; Ibrahim and Al-Mashagbah, 2016; Ibrahim, 2016). Thus, urban sprawl refers to the expansion of cities and suburbs in agricultural and bare land, which transforms rural areas into city margins having high population densities. Urban sprawl is characterized by disorganized, uneven, and unplanned growth that results in unequal distribution of natural resources and services. The area covered by buildings also significantly increases during the urban expansion that decreases agricultural land area leading to reduced food stocks (Habibi, 2011). Multiple environmental problems are also associated with the increased urban constructions such as the lack of arable land, which reduces per-capita agricultural production of fruits and vegetables. The population growth and urban expansion raise the levels of water pollution and consumption, as well as air pollution due to increased traffic burdens. These factors ultimately accumulate to pose serious health concerns for the human population (Ren et al., 2013; Litman, 2020). Several factors such as erosion, human interference, and environmental factors contribute to land cover change. The tools of remote sensing and GIS techniques can effectively detect these changes by generating accurate reports and maps (Barkhordari, 2003; Ibrahim and Al-Mashagbah, 2016). The application of these systems becomes more crucial in areas under continuous urban development. These scientific and analytical tools facilitate the optimal utilization of available resources. Based on the generated information, the available resource could be managed accordingly to achieve the maximum output, which contributes towards a balanced and functional urban system through an easy and efficient decision-making process. Higher population growth rates leading to increased housing demands are the main factor affecting agricultural lands through urban sprawl. The constructions of roads for transportation, urban infrastructure, and factories near roads also result in the urbanization of agricultural lands (Zhao et al., 2006; Rawat and Puri, 2017). The recent increase in the Jordanian population is associated with the urbanization of either cultivated agricultural lands or lands under natural vegetation. The removal of vegetation cover over large areas has disturbed the ecological balance and reduced agricultural production. This study employed remote sensing, GIS, and statistical indicators to analyze the urban sprawl of the Irbid city and highlights the factors, which transformed its agricultural lands into residential areas.

Materials and methods

Study area

The selected area is Irbid city which is located in the northern region of Jordan, 71 km north of the capital city of Amman, and 15 km south of the Syrian-Jordanian border. It is in the central part of the Irbid Governorate within the Horan plain area. Population wise, Irbid is the third-largest city in the Kingdom of Jordan after the capital city of Amman and Zarqa. According to the recent census of 2017, the population of Irbid and its suburbs was over 530,200 (Norway, 2008). Irbid is an important industrial city of Jordan which, along with its population density and geographical location have made it a large commercial area. The study area extends between latitudes 32° 31’ 15″ and 32° 35’ 33″ north and longitudes 35° 48’ 00″ and 35° 53’ 00 East, covering a total of 36.86 km^2 across seven residential districts of varying size (Barha, Hashimiyah, Manara, Naser, Nozha, Rabea, and Rabea) as presented in *Figure 1*.

The altitude of the study area ranges between 324 m above sea level in the northwest and 677 m above sea level in the southwest districts**.** The climate of Irbid city significantly

http://www.aloki.hu ● ISSN 1589 1623 (Print) ● ISSN 1785 0037 (Online)
DOI: http://dx.doi.org/10.15666/aeer/2003_27692781

fluctuates between summer and winter, especially in areas well above the sea level. The city receives significant rainfall during winter and snowfalls in the high-altitude areas. The city and its surrounding areas are famous for soil fertility, being part of the Horan plains, where multiple field crops, grains, and fruit trees (especially olive trees) are grown.

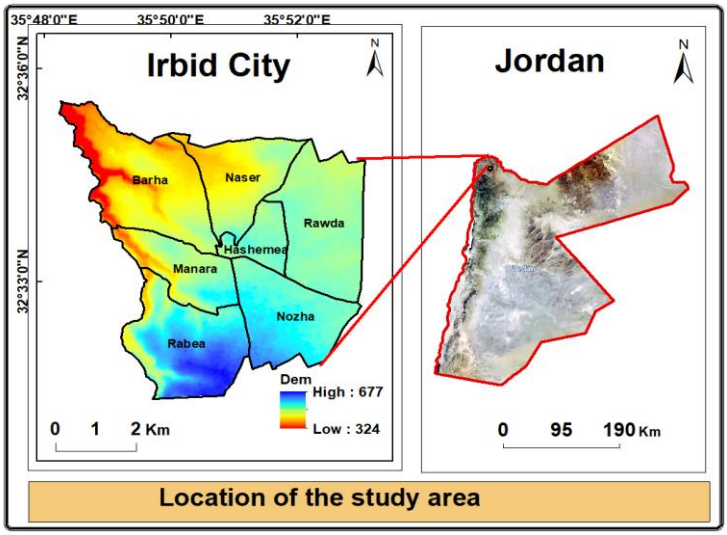

Figure 1. *The location of Irbid city districts*

Data collection

Three Landsat images with a cloud cover of less than 10% were selected to avoid classification errors, which were defined for path 174 and row 37 covering Irbid city. The first and second images from the Landsat-7 Enhanced Thematic Mapper Plus were captured on July 8, 2000, and September 6, 2010, respectively. The third image was obtained on August 24, 2020, using Landsat-8 Operational Land Imager. All images were downloaded from the USGS website (https://earthexplorer.usgs.gov/).

Image processing

Initially, before subjecting the images to classification, image pre-processing was carried out through image enhancement, geometric correction, and visual interpretation to make the images are more interpretable to human eye. The geometric correction process adjusted the distortion to produce a corrected image in the correct geographic location. The Landsat images were thus geo-referenced to UTM WGS 1984 Zone 36N using distinguishable points such as intersections, roads, and corners as seen on Google Earth maps, rectified digital topographical map, and a reference shapefile of the study area. All systematic errors and radiometric corrections were removed from the Landsat data, even though the land cover maps can be classified without performing any radiometric or atmospheric corrections (Kamal et al., 2020). The satellite images were reduced to a subset, covering Irbid city and a surrounding area of about 36.86 km^2. All bands of each satellite image were stacked into a single file to form an RGB multiband and a multi-color composite Tiff layer.

The digital classification technique divides the cells of the multi-spectral image into classes based on their spectral signature, which represents the reflectivity of the land

http://www.aloki.hu ● ISSN 1589 1623 (Print) ● ISSN 1785 0037 (Online)
DOI: http://dx.doi.org/10.15666/aeer/2003_27692781

cover in the spectral reflectance. Supervised and unsupervised classification techniques are used for satellite image classification through remote sensing. The unsupervised classification technique is purely statistical and does not require training data for the classification. Contrarily, the supervised classification requires user-defined training data from the field or high-resolution maps (Google Earth) before carrying out the classification process. A maximum likelihood supervised classification method is more accurate than the unsupervised classification method (Currit, 2005; Hasmadi et al., 2005; Ahmad and Quegan, 2013). This study aimed to extract satellite images based-classification of land use in Irbid city, therefore, a maximum likelihood supervised classification tool in ArcMap software was used. The three classified images were divided into two classes, (urban and non-urban land) to investigate temporal and spatial changes in the land use of the study area. The differences between the images were identified as natural or man-made changes between 2000 and 2020. The classified images were converted from raster to vector format using ArcGIS software to simplify the calculation of the area of each land-use class. The accuracy of classified maps was verified by generating 100 random samples for each image using ArcMap software. These points were compared with the equivalent Google Earth reference map through field surveys and a GPS device to evaluate the accuracy of classified images. An error matrix was produced for each classified image to calculate the overall accuracy and the Kappa coefficient.

Urban expansion intensity index

The urban expansion intensity index quantitatively analyses the ongoing differences in the spatial extension of an area. This method determines the tendency of urban growth over a particular period and projects potential future trends of urban expansion. It also compares the speed and intensity of changes in urban land use between different periods. (Zhao-ling et al., 2007), This index was divided as slow growth from 0 to 0.28 (Zhao et al., 2006), low-speed expansion from 0.28 to 0.59, medium-speed expansion from 0.59 to 1.05, high-speed expansion from 1.05 to 1.92, and very high-speed expansion at values greater than 1.92. The urban expansion intensity index of each period and direction was calculated as follows (*Eq. 1*).

$$UI = \frac{\Delta U}{\Delta T * TA} * 100 \quad \text{(Eq.1)}$$

where: UI is the urban expansion intensity index of the ith zone; ΔU is the difference between the urban area of the ith zone at time1 and time2; TA is the total land area of the ith zone; and Δt is time2-time1.

Pearson's chi-square and urban growth

A comparative analysis was conducted between observed, theoretical, or expected values of urban expansion in the study area. The expected growth of the urban area was calculated using *Equation 2*.

$$Mji = \frac{Mj \times Mi}{Mg} \quad \text{(Eq.2)}$$

where Mji is the expected growth, Mj is the column total, Mi is the row total, and Mg is the grand total.

http://www.aloki.hu ● ISSN 1589 1623 (Print) ● ISSN 1785 0037 (Online)
DOI: http://dx.doi.org/10.15666/aeer/2003_27692781

The chi-square calculation determined the degree of freedom for urban growth in the study area in different directions at different periods. The degree of freedom indicates the sustainability or unsustainability of the urban growth, whereas a high degree of freedom represents an unbalanced regional process of urban growth (Ren et al., 2013). The degrees of freedom for the entire study area and each direction were calculated using *Equation 3* (Ren et al., 2013):

$$X^2 = \sum_{i=1}^{n} \frac{(Oi-Ei)2}{Ei} \quad \text{(Eq.3)}$$

where X2 is the overall degree of freedom, Oi is the observed growth, and Ei is the expected growth.

Shannon's entropy index

The measures of contrast cannot be used for categorical data, as median or mean are not available for such data. However, Shannon's entropy index can be used for a random sample of data (*Eq. 4*). Shannon's index of diversity could calculate and compare biodiversity across communities to represent that how a geographic feature is distributed across a specific area (Kumar et al., 2020; Al Mashagbah, 2016; Wondrade et al., 2014).

$$Hn = \sum_{i=1}^{n} Pi * Ln(Pi) \quad \text{(Eq.4)}$$

Given $Pi = Xi / \sum_{i}^{n} Xi$; where n is the number of observations and Pi is the proportion of observations in the ith of n categories. The maximum value of entropy occurs when all proportions of observations are equal; as the sum of the pi is equal to $\sum_{i=1}^{n} Pi = kPi = 1$. In addition, Hmax = Ln (n), and the Relative entropy = Hn/Ln (n).

Annual urban expansion rate and average annual expansion

The annual urban expansion rate (AER) shows the relative dynamic change rate of urban expansion among different districts over the same period (*Eq. 5*), whereas the average annual expansion (AE) quantifies the overtime changes of urban areas and compares the urban growth of the same district over various periods. Following equations (*Eqs. 5* and *6*) were used for the calculation of these two indexes:

$$AER = ((LUj - LUi) / LUi) \times (1 / (\Delta t)) \times 100 \quad \text{(Eq.5)}$$

$$AE = (LUj - LUi) / \Delta t \quad \text{(Eq.6)}$$

where LUi and LUj represent the urban area at the initial and end period, respectively, whereas Δt represents the change in time.

Results

Urban growth and Pearson's chi-square statistics

The urban growth rate of each district was calculated from 2000-2010 and 2020-2020 (*Table 1*). The results demonstrated an overall declining trend in percentage

http://www.aloki.hu ● ISSN 1589 1623 (Print) ● ISSN 1785 0037 (Online)
DOI: http://dx.doi.org/10.15666/aeer/2003_27692781

growth rate except for the Manara district. Higher urban and residential saturation levels could justify this phenomenon. The lowest (0.11%) and the highest (46.36%) growth rates were observed in Hashimiyah and Rabea districts, respectively. *Equation 3* was followed to calculate Pearson's chi-square statistics for each temporal interval, and the degree of freedom for each district. The expected growth and the observed growth are considered closely related at a value near zero whereas they are considered significantly diverged at a higher chi-square value. The results reveal a balanced and sustainable urban growth of the study area between 2000 and 2020. A higher degree of freedom represents unbalanced urban growth at different intervals and places within the same area (Ren et al., 2013). The overall degree of freedom of the complete study area remained as 1.14 whereas lower degrees of freedom (0.38 and 0.76) at both temporal intervals (2000-2010 and 2010-2020) revealed a low variation between the expected and observed urban growth. A significantly low degree of freedom (less than 1) in all the districts indicates a higher similarity between expected and observed urban growth and expresses a coherent and balanced urban expansion. The degree of freedom values for Barha, Hashimiyah, Manara, Naser, Nozha, Rabea, and Rawda districts were noted as 0.17, 0.00, 0.08, 0.15, 0.04, 0.18, and 0.52, respectively. The highest degree of freedom (0.52) was recorded in the Rawda district, whereas the lowest (almost zero) value was observed for the Hashimiyah district.

Table 1. *Urban growth rates*

Period	Barha	Hashimiyah	Manara	Naser	Nozha	Rabea	Rawda	Total area
2010-2000	29.0%	0.2%	3.8%	15.8%	13.8%	46.4%	23.9%	19.2%
2020-2010	20.6%	0.1%	5.3%	1.6%	3.7%	28.9%	0.8%	8.0%

Shannon's entropy

Shannon's entropy analysis of different districts of Irbid city demonstrated a disparity among the urban areas of each district. The entropy values reflected the variations based on the area and density of urbanization in each district. *Table 2* presents the collective entropy values of all the districts at two intervals (2000-2010 and 2010-2020) whereas *Table 3* separately depicts the values of each district. The entropy values from 2000 to 2010 (1.61) and 2010 to 2020 (1.26) indicate the differences in the urban growth patterns for the specified years. These entropy values (1.95) were calculated to be greater than half of ln (n) representing that the Irbid city sprawled during the complete study period. However, the decreased entropy value during the second period (2010-2020) suggests that the city became more compact, especially in certain districts. In terms of individual districts, Shannon's entropy value for the Rawda district showed a lower degree of dispersion for build-up that indicates a higher urban density or more compact urban growth. The Barha and the Manara districts showed higher dispersion (close to Ln(n) (0.69)), thus indicating more dispersed distribution in these districts.

Table 2. *Shannon's entropy for both periods (n = 7)*

Time period	Entropy	Log (n)	1/2 Log(4)
2000-2010	1.61	1.95	0.97
2010-2020	1.26	1.95	0.97

http://www.aloki.hu ● ISSN 1589 1623 (Print) ● ISSN 1785 0037 (Online)
DOI: http://dx.doi.org/10.15666/aeer/2003_27692781

Table 3. *Shannon's entropy for the different districts (n = sum of both interval = 2)*

District	Barha	Hashimiyah	Manara	Naser	Nozha	Rabea	Rawda
Entropy	0.68	0.64	0.68	0.31	0.52	0.67	0.14
Log (n)	0.69	0.69	0.69	0.69	0.69	0.69	0.69

Intensity of urban expansion and rate of expansion

The intensity index was used to standardize the average of the annual expansion speeds of different districts at different times (Jianhua et al.,2003). Urban expansion intensity declined from 1.23 (2000-2010) to 0.61 (2010-2020). According to Zhao-ling et al. (2007), the first period displays high-speed urban expansion followed by medium-speed expansion during the second period that implies a decrease in urban sprawl (*Table 4*).

Table 4. *Area of expansion, urban expansion rate, and expansion intensity in Irbid City from 2000 to 2020*

Period	Area of expansion km^2/y	Expansion rate %	Expansion intensity %
2000-2010	0.45	1.92	1.23
2010-2020	0.23	0.80	0.61
2000-2020	0.34	1.44	0.92

The intensity of urban expansion in the seven urban districts is presented in *Figure 2*. The highest urban expansion intensity (0.34) was noted for Rawda district from 2000 to 2010 whereas the lowest value was observed for the Hashimiyah district because it had already reached its urban saturation point. However, a decline in urban expansion intensity during both periods was noticed in most of the districts.

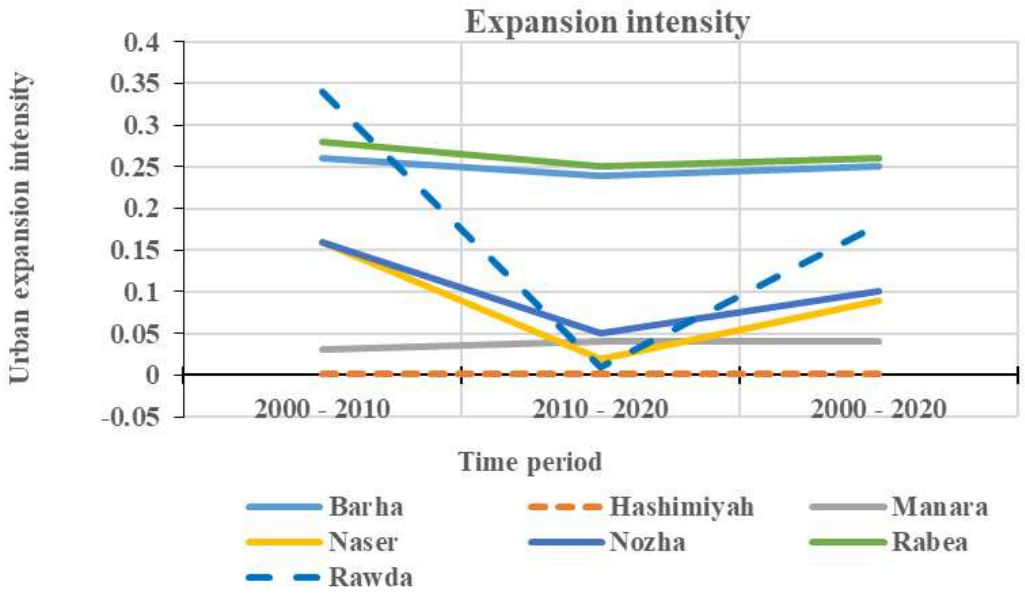

Figure 2. *Urban expansion intensities of the seven districts*

http://www.aloki.hu ● ISSN 1589 1623 (Print) ● ISSN 1785 0037 (Online)
DOI: http://dx.doi.org/10.15666/aeer/2003_27692781

The urban area collectively expanded from 23.6 km^2 in 2000 to 30.39 km^2 in 2020 at a rate of 0.34 km^2/year over the last two decades. The expansion in the urban land area was continuous even though the intensity of expansion comparatively decreased in the second period (2010-2020). The urban areas expanded by 4.53 km^2/year from 2000 to 2010 and decreased to 2.6 km^2/year from 2010 to 2020. The complete study area expanded at a rate of 0.45 km^2/year (1.92%) from 2000 to 2010 and at a relatively lower expansion rate of 0.23 km^2/year (0.8%) from 2010-2020. The highest expansion rates occurred in the southwest Rabea district (4.43%) and northeast Barha district (2.77%) from 2000 to 2020. Contrarily, the lowest expansion rates of 0.02% and 0.47% were noted for central Hashimiyah and Manara districts, with lower expansion intensities of 0.001% and 0.4%, respectively, due to urban saturation. Northwest and Southwest directions exhibited the highest urbanization trend as these areas are near to the already saturated.

Discussion

Land use/land cover change

Human activities lead to significant changes in land use. These land-use changes are detected by figuring out the changing class in comparison to others at a given time (Zubair, 2006; Pandy and Nathawat, 2006). The open-source U.S. Landsat data (ETM + and OLI) was utilized in this study to classify the land use and land cover. Satellite images with a 30 m spatial resolution captured in 2000, 2010, and 2020 were classified by following the supervised classification method in ArcMap 10.4 to detect and determine different classes of land in the study area. Two classes of land use (urban and non-urban) were selected based on the visual interpretations of the satellite images, Google Earth maps, field observations, and previous reports of land cover and land use of the study area. Urban areas consist of built-up areas including roads, commercial or industrial areas, and residential areas. The drylands, agricultural lands, uncultivated lands, and green spaces (irrigated vegetable crops, forests, or fruit trees) represent non-urban areas. The accuracy of classified maps was validated by creating a set of 100 random points in ArcMap software that were distributed across each image. These points were converted to KML format to open in Google Earth for verification with high-resolution Google images. Confusion matrices were generated for all classified images to calculate the Kappa coefficient and the overall accuracy between each classified map and reference data. The overall accuracy of classification images captured in 2000, 2010, and 2020 was calculated as 93%, 93%, and 94%, respectively. Simultaneously, the Kappa coefficient of 2000, 2010, and 2020 satellite images was estimated as 83.2%, 82.4%, and 84%, respectively. These values are in the acceptable range. According to Congalton and Green (2019), a Kappa value of 60% to 80% represents substantial agreement whereas greater than 80% indicates strong agreement between classified map and reference data. Similarly, a value of more than 0.75 indicates “a very good to an excellent” agreement according to (Monserud and Leemans, 1992). A continuous increasing trend of urban land cover was observed during the study period that accounted for 63.99%, 76.29%, and 82.42% of the land areas in 2000, 2010, and 2020, respectively. The proportion of bare and agricultural land reduced over time in contrast to urban areas. The land cover and land use maps indicated a significant increase in the urban areas at the expense of agricultural and bare lands. The main reasons for unregulated urban sprawl include the

http://www.aloki.hu ● ISSN 1589 1623 (Print) ● ISSN 1785 0037 (Online)
DOI: http://dx.doi.org/10.15666/aeer/2003_27692781

rising population during the past 20 years, the reverse migration from villages close to the city, and Syrian refugees. There was an increase of about 4.53 km^2 (19.22%) of the urban area during the first decade (2000-2010) whereas it increased by 2.26 km^2 (8.04%) from 2000-2010. The total increase in the urban area in bare and agricultural lands from 2000 to 2020 was estimated as 22.36%. The annual increase rate of urban areas in Irbid was calculated as 0.45 km^2/year from 2000 to 2010 and 0.23 km^2/year from 2010 to 2020. A higher urban saturation in Nozha (92.7%), Rawda (94.5%), Naser (97.8%), and Hashimiyah (99%) districts led to the decrease in urban expansion during the second decade (2010-2020). The economic development and increasing demographic pressure in the city center have urged the residents to move to the agricultural and bare lands of city surroundings. This phenomenon has resulted in increased residential areas in the city outskirts and the transformation is ultimately declining the agricultural and barren land areas. The Syrian civil war also led to a major migration of Syrian refugees to Jordan after 2010, especially to the northern governorates of Irbid and Mafraq that also contributed to an increase in the urban areas. The immigration from neighboring villages to Irbid for economic activities has also had an impact. The data analysis revealed that the urban area increased in all districts during the study period (2000-2020). Overall, the urban area increased from 23.60 km^2 in 2000 to 30.39 km^2 in 2020. The Population and commercial growth of the city has resulted in the rapid increase in industrial, residential, and commercial areas, and necessary infrastructure networks. The Rabea district, being the commercial and service center of the city, exhibited the highest level of urban growth. This area is near Yarmouk University and other buildable spaces. Urban sprawl is also quite significant in the Rabea, Barha, and Rawda districts as they have sufficient space for industrial, residential, and commercial growth. The land prices are also comparatively lower in these areas as compared to the areas near the city center. The significant expansion in the urban areas of various residential districts is presented in *Figure 3* from the years of 2000 to 2010 and years of 2010 to 2020. The results depict that the built-up areas expanded significantly in the Rabea, Barha, and Rawda districts, and at a comparatively lower rate in the Naser district. Contrarily, a horizontal expansion in the Manara and the Hashimiyah districts has now almost ceased due to the limited space and lack of construction land. Generally, only a minimal variation was observed among the growth patterns of urban sprawl and its trends in different districts. Horizontal urban sprawl has consumed some of the most fertile agricultural lands in several provinces and developing urban areas at the expense of olive and grape plantations, and wheat and barley fields are dangerous. The Rawda, Barha, and Nozha districts exhibited the highest expansion of urban area whereas the rate of urban expansion was noted to be lowest in Hashimiyah and Manara districts. The proportion of urban area in Rabea and Barha districts was less than 50% in 2000 in comparison to other districts. However, only the Rabea district had less than 50% area in 2010 whereas all other districts had more than 50% urban area by 2020. The urban areas of Hashimiyah, Naser, Nozha, and Rawda districts have reached up to more than 90% of their total areas. The urban growth was noted in all districts from 2000 to 2020, which can be attributed to population growth, and migration from the countryside to the city for jobs and accessing various services. Rabea and Barha districts proportionally showed the highest increase in the urban area during the study period as their urban land use grew from less than 50% in 2000 and 2010, to well over that in 2020. Hashimiyah and Manara districts demonstrated the lowest expansion of urban areas

http://www.aloki.hu ● ISSN 1589 1623 (Print) ● ISSN 1785 0037 (Online)
DOI: http://dx.doi.org/10.15666/aeer/2003_27692781

during the same period. During the second decade (2010 to 2020), urban areas rapidly increased in Rabea and Barha districts, whereas vertical construction mostly occurred in the Hashimiyah district leading to the least horizontal expansion of the urban area.

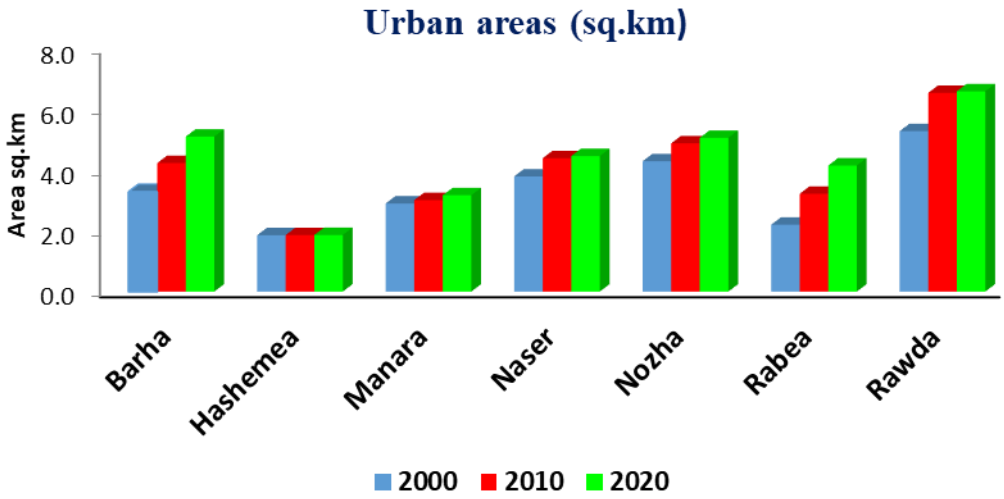

Figure 3. *Urban areas (km^2) included in the study*

According to the data of 2020, almost 88%, 93%, 95%, 98%, and 99% of the land in Manara, Nozha, Rawda, Naser, and Hashimiyah districts, respectively, could be considered urban. The lowest percentages of urban areas were noted in Rabea (63%) and Barha (65%) districts. Generally, 64%, 76.3%, and 82.4% of the overall land in 2000, 2010, and 2020, respectively, was residential and urban land, which increased by 19.22% from 2000 to 2010, and 8.04% from 2010 to 2020. The slowdown of urban growth during the second decade could be mainly attributed to the urban saturation in most of the districts within the city. Two main classes were extracted based on the data as shown in *Figure 4*.

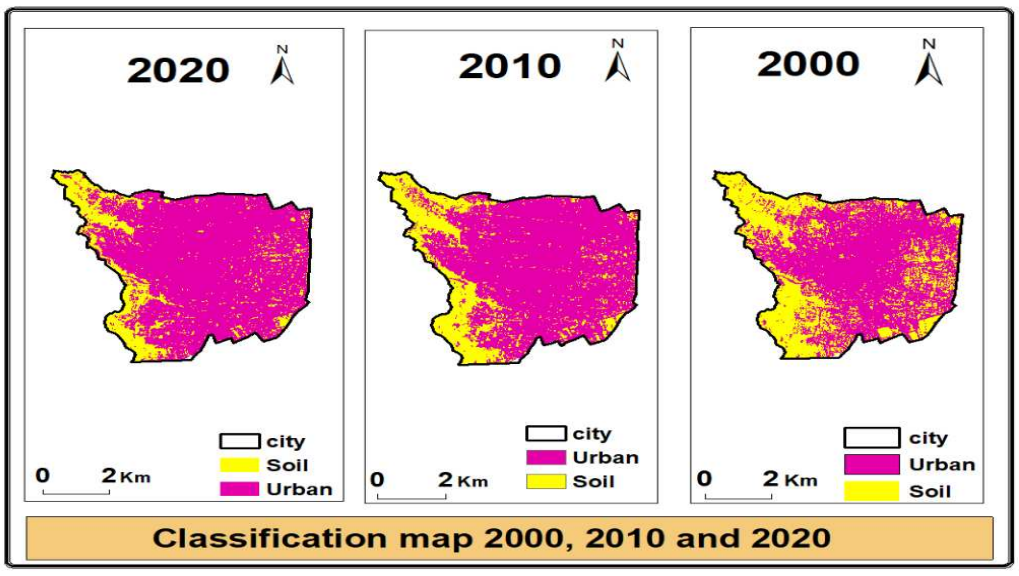

Figure 4. *Classified images of three periods depicting urban and non-urban lands*

http://www.aloki.hu ● ISSN 1589 1623 (Print) ● ISSN 1785 0037 (Online)
DOI: http://dx.doi.org/10.15666/aeer/2003_27692781

Conclusions

The study efficiently determined the land cover changes in Irbid city from the period of 2000 to 2020 by employing GIS and remote sensing techniques combined with different statistical indicators. The results revealed the effectiveness of GIS and remote-sensing techniques to produce accurate maps describing different types of land use. The Landsat satellite images were classified into two main classes of urban land and nonurban land. A map was extracted for the specific years of interest, and areas were calculated to compare the changes over time. A significant increase in urban areas corresponding to a decrease in the percentage of non-urban lands was observed in 2010 and 2020 as compared to the year 2000. The urban sprawl occurred by utilizing precious barren and agricultural lands, which could affect the agricultural produce in the future. The increase in urban lands and the decline of green lands may lead to some environmental problems such as increasing pollution; also the rapid urban growth may poses a serious burden on electricity, sewage, water, and transportation systems. However, the government has taken effective measures by establishing infrastructures in residential, industrial, agricultural, and commercial lands for the smooth conversion of lands into urban areas. This study will further facilitate the development of effective policies for managing urban sprawl in the future.

The use of geographic information systems requires effort, accuracy, and cost and gives accurate and fast results, and it can conduct spatial and attribute data analysis. The application of GIS, which provides the possibility of handling, processing, and analyzing a large volume of data, helps to increase the efficiency of land use studies; therefore, we recommend a similar and continuous future studies on the study area and on other similar areas to monitor urban development and its impact on the deterioration of agricultural land.

Funding. This research received no external funding.

Conflict of interests. The authors declare no conflict of interests.

REFERENCES

[1] Ahmad, A., Quegan, S. (2013): Comparative analysis of supervised and unsupervised classification on multispectral data. – Applied Mathematical Sciences 7(74): 3681-3694.

[2] Al Mashagbah, A. F. (2016): The use of GIS, remote sensing and Shannon's entropy statistical techniques to analyze and monitor the spatial and temporal patterns of urbanization and sprawl in Zarqa City, Jordan. – Journal of Geographic Information System 8(2): 293-300.

[3] Barkhordari, J. (2003): Assessing the effects of land use change on the hydrologic regime by RS and GIS. Assessing the effects of land use change on the hydrologic regime by RS and GIS. – Thesis, International Institute for Geo-Information Science and Earth Observation, Enschede.

[4] Cohen, B. (2006): Urbanization in developing countries: current trends, future projections, and key challenges for sustainability. – Technology in Society 28(1-2): 63-80.

[5] Currit, N. (2005): Development of a remotely sensed, historical land-cover change database for rural Chihuahua, Mexico. – International Journal of Applied Earth Observation and Geoinformation 7(3): 232-247.

http://www.aloki.hu ● ISSN 1589 1623 (Print) ● ISSN 1785 0037 (Online)
DOI: http://dx.doi.org/10.15666/aeer/2003_27692781

[6] Eyoh, A., Olayinka, D. N., Nwilo, P., Okwuashi, O., Isong, M., Udoudo, D. (2012): Modelling and predicting future urban expansion of Lagos, Nigeria from remote sensing data using logistic regression and GIS. – International Journal of Applied Science 2(5): 1-9.
[7] Habibi, S., Asadi, N. (2011): Causes, results and methods of controlling urban sprawl. – Procedia Engineering 21: 133-141.
[8] Hasmadi, M., Pakhriazad, H. Z., Shahrin, M. F. (2005): Evaluating supervised and unsupervised techniques for land cover mapping using remote sensing data. – Geografia-Malaysian Journal of Society and Space 5(1): 1-10.
[9] Ibrahim, M. M. (2014): The use of geoinformatics in investigating the impact of agricultural activities between 1990 and 2010 on land degradation in NE of Jordan. – PhD Dissertation, Faculty of Environmental and Natural Sciences, Freiburg University, Freiburg im Breisgau.
[10] Ibrahim, M. (2016): Temporal interpretation for land use/land cover changes using multispectral images: Irbid as a case study. – Journal of Natural Sciences Research 6(5): 100-104.
[11] Ibrahim, M., Al-Mashagbah, A. (2016): Change detection of vegetation cover using remote sensing data as a case study: Ajloun area. – Civil and Environmental Research 8(5).
[12] Jianhua, X., Changlin, F., Wenze, Y. (2003): An analysis of the mosaic structure of regional landscape using GIS and remote sensing. – Acta Ecologica Sinica 23(2): 365-75.
[13] Kamal, M., Muhammad, F. H., Mahardhika, S. A. (2020): Effect of image radiometric correction levels of Landsat images to the land cover maps resulted from maximum likelihood classification. – International Conference on Sustainability Science and Management: Advanced Technology in Environmental Research (CORECT-IJJSS 2019). https://doi.org/10.1051/e3sconf/202015302004.
[14] Kumar, K. S., Valasala, N. V., Subrahmanyam, J. V., Mallampati, M., Shaik, K., Ekkirala, P. (2015): Prediction of future land use land cover changes of Vijayawada city using remote sensing and GIS. – International Journal of Innovative Research in Advanced Engineering 2(3): 91-97.
[15] Litman, T. (2016): Determining optimal urban expansion, population and vehicle density, and housing types for rapidly growing cities. – World Conference on Transport Research - WCTR 2016 Shanghai, 10-15 July 2016.
[16] Monserud, R. A., Leemans, R. (1992): Comparing global vegetation maps with the Kappa statistic. – Ecological Modelling 62(4): 275-93.
[17] Norway, S. (2008): Population and housing census. Population and housing census. https://www.ssb.no/en/befolkning
[18] Pandy, A. C., Nathawat, M. (2006): Land use land cover mapping through digital image processing of satellite data. A case study from Panchkula Ambala and Yamunanagar districts, Haryana State, India. – Geospatial World.
[19] Rawat, V., Puri, M. (2017): Land use/land cover change study of district Dehradun, Uttarakhand using Remote sensing and GIS technologies. – International Journal of Advanced Remote Sensing and GIS 6(1): 2223-2233.
[20] Ren, P., Gan, S., Yuan, X., Zong, H., Xie, X. (2013): Spatial Expansion and Sprawl Quantitative Analysis of Mountain City Built-up Area. – In: Bian, F. et al. (eds.) Geo-informatics in Resource Management and Sustainable Ecosystem. International Symposium, GRMSE 2013, Wuhan, China, November 8-10, 2013, Proceedings, Part II. Springer, Berlin, Heidelberg, pp. 166-176.
[21] Tewolde, M. G., Cabral, P. (2011): Urban sprawl analysis and modeling in Asmara. – Remote Sensing 3(10): 2148-2165.
[22] Wondrade, N., Dick, O. B., Tveite, H. (2014): Landscape mapping to quantify degree-of-freedom, degree-of-sprawl, and degree-of-goodness of urban growth in Hawassa, Ethiopia. – Environment and Natural Resources 4(4): 223-237.

http://www.aloki.hu ● ISSN 1589 1623 (Print) ● ISSN 1785 0037 (Online)
DOI: http://dx.doi.org/10.15666/aeer/2003_27692781

[23] Zhao, S., Da, L., Tang, Z., Fang, H., Song, K., Fang, J. (2006): Ecological consequences of rapid urban expansion: Shanghai, China. – Frontiers in Ecology and the Environment 4(7): 341-346.
[24] Zubair, A. O. (2006): Change Detection in Land Use and Land Cover Using Remote Sensing Data and GIS (A Case Study of Ilorin and Its Environs in Kwara State). – Department of Geography, University of Ibadan, Nigeria.

http://www.aloki.hu ● ISSN 1589 1623 (Print) ● ISSN 1785 0037 (Online)
DOI: http://dx.doi.org/10.15666/aeer/2003_27692781

QUALITY OF STORED MELON (*CUCUMIS MELO* L.) SEEDS GROWN UNDER DIFFERENT IRRIGATION REGIMES

ÖZTOKAT KUZUCU, C.* – ÇIFTCI, H. N.

Canakkale Onsekiz Mart University, Faculty of Agriculture, Department of Horticulture, 17020 Canakkale/Turkey
(phone: +90-286-218-00-18)

**Corresponding author*
e-mail: cananoztokat@yahoo.com; phone: +90-286-218-00-18 (ext. 23088)

(Received 11th Jan 2022; accepted 25th Mar 2022)

Abstract. Ecological diversity is the richest heritage of the countries that they wish to hand down the next generations. Landraces constitute an important group of biodiversity resources. Especially the effects of stress on seed quality of landraces known to be resistant to abiotic and biotic stress factors is an important issue. Majority of producers preserve their seeds and serious quality losses are encountered in long-term storage of these seeds. In this sense, seeds obtained from Hırsız Kaçıran melon population grown under three different irrigation levels (50%, 100%, 150%) in Çanakkale province by Çiftci (2013) were stored for 5 years. In addition, new seeds (fresh seeds) were supplied from the experiments conducted under similar conditions with that previous study. Then, quality parameters of stored and fresh seeds were evaluated and compared. Seed color, germination rate, mean germination time, controlled deterioration test and electrical conductivity (EC), seed moisture, emergence rate and mean emergence time parameters were determined. According to the data obtained, germination and emergence rates were not affected on the other hand germination and emergence times were affected negatively by irrigation treatments. It was concluded that, Hırsız Kaçıran melon genotype is able to maintain germination rate for both irrigation regimes, whether the seeds could be stored at certain seed moisture condition without significant loss of vigor.
Keywords: *landraces, seed vigor, germination, seed storage, pan coefficient*

Introduction

Turkey is a prominent country in genetic diversity of melon (*Cucumis melo* L.) and thus is one of the centers within the area extending from the Mediterranean basin to Central Asia, then to Far East (Robinson and Decker-Walters, 1997). Several local melon varieties are still being grown by producers in Turkey. Landrace producers mostly continue their cultivation activities by producing their own seeds. Seed quality directly influences vegetable production and production costs. Use of qualified seeds is a pre-condition of successful production and plays a greater role in production of landraces over limited areas. Although landraces are preferred because of their resistance to harsh climate conditions of the region to where they were adapted, recent droughts pose a serious risk on entire agricultural activities. Adverse conditions caused by drought inevitably affect seed production and cause losses in seed yield (Szilagyi, 2003; El Balla et al., 2013) that makes the seed an expensive starting material. Therefore, majority of producers prefer to store seeds. However, during the storage process of seeds, cell membrane breakdown, lipid peroxidation, protein degradation and decrease in enzyme activities are encountered and seed vigor decreased due to the recess in respiration capacity (Walters, 1998; McDonald, 1999; Murthy et al., 2003; Finch-Savage and Bassel, 2016). Cucurbit seeds, like many orthodox seeds, can be stored for a long time by drying up to low moisture levels and slowing down relevant biochemical activities (Vertucci, 1989). Oluoch and Welbaum (1996) indicated that melon seeds maintained viability for 6 years under suitable conditions. Bass (1973)

http://www.aloki.hu ● ISSN 1589 1623 (Print) ● ISSN1785 0037 (Online)
DOI: http://dx.doi.org/10.15666/aeer/2003_27832799

conducted 12-year storage study with cantaloupe melons and reported that majority of the cultivars maintained germination rate at end of 12-year storage (10°C/60% humidity) and decrease in values of the cultivars with a loss of vigor was seen at the end of 7th year. On the other hand, Doijode (2006), stated that melon seeds stored at -20ºC maintained viability by 86% at the end of 15-year storage. Similarly, Nerson (2002) reported that watermelon seeds could be stored for 10 years without significant loss in quality traits. Ali et al. (1991) stored the seeds of Marketer, Marketmore, Wisconsin SMR-18, Tablegreen, Spotfree and China cucumber varieties at 3°C and 38% humidity for 26 years and indicated that varieties, except one, had 80% germination ratio in the 10th year, but germination was not encountered in the 13th and later years. Pandey (2016) preserved the seeds in hermetic containers with a solution containing glycerol and $CaCl_2$ to store them at room temperature for a long time and indicated that majority of cucurbit seeds maintained viability for 14 -16 years and some varieties remained viable even in the 24th year.

Various tests can be used to determine the long-term storage limit of cucurbit seeds. Abdalla and Roberts (1969) indicated that seed viability and vigor tests could be used to determine the storage life of seeds. It is also indicated for cucurbit family that controlled deterioration tests performed at 45ºC, 24% humidity and 48 hours could reliably be used to determine seed viability in melons and 45ºC, 24% humidity and 24 hours in cucumbers (Bhering et al., 2004; Torres, 2005). The tests designating seed quality, including controlled deterioration tests, enable the determination of changes in seed quality before and after storage. It was reported that viability of semi-ripe melon seeds increased after 6 months of storage at 10°C and 45% relative humidity and similar findings were also reported for cucumber seeds (Edwards et al., 1986; Nerson and Paris, 1988).

Quality loss is low and the storage life is at an acceptable level in seed production of landraces adapted to harsh conditions grown under non irrigated conditions. So the negative effects of drought on seed production will be alleviated and seed production in arid areas will be sustainable to a certain extent. Hırsız Kaçıran is a landrace which grown under non or limitedly irrigated in Aegean region of Turkey. And producers often adopt the method of obtaining their own seeds for production.

This study was conducted to determine the extent of quality loss with the aid of quality tests in seeds produced under different irrigated conditions and stored for a long time.

Material and Method

Seeds of the study was supplied from melon landrace “Hırsız Kaçıran” grown in Biga district of Çanakkale (Aegean part of Turkey) in 2013. Seeds were planted at 100 x 100 cm spaced plots irrigated in 7-day intervals by applying three different irrigation levels (multiplying Class-A pan evaporation by Kp1= 50%, Kp2= 100%, Kp3= 150% coefficients and cover percentage, which was taken as 30% at the beginning and increased accordingly later on) (Çiftci, 2013).

$$I = Epan \times Kp \times P \quad \text{(Eq.1)}$$

(Doorenbos and Pruitt, 1992; Kanber et al., 1994; Aslan and Tekıner, 2017)
where;
I: amount of irrigation water to be applied(mm), Epan: Pan evaporation (mm), Kp: Pan coefficient, P: plant cover percentage (%).

http://www.aloki.hu ● ISSN 1589 1623 (Print) ● ISSN1785 0037 (Online)
DOI: http://dx.doi.org/10.15666/aeer/2003_27832799

The amount of irrigation water applied and evaporation values in the two seasons is presented in *Table 1* and *Table 2*.

Table 1. *The amount of water given in irrigation treatments and evaporation values (I. seasons) (2013)*

Treatments	Evaporation (mm)	50% irrigation level	100% irrigation level	150% irrigation level
1	65	32.5	65	97.5
2	70	35	70	105
3	75	37.5	75	112.5
4	70	35	70	105
5	40	20	40	60
6	60	30	60	90
7	60	30	60	90
8	50	25	50	75
Total	490	245	490	735

Table 2. *The amount of water given in irrigation treatments and evaporation values (II. seasons) (2019)*

Treatments	Evaporation (mm)	50% irrigation level	100% irrigation level	150% irrigation level
1	30	15	30	45
2	32	16	32	48
3	53	26,5	53	79.5
4	28	14	28	42
5	43	21,5	43	64.5
6	35	17,5	35	52.5
7	41	20,5	41	61.5
Total	262	131	262	393

Melons were marked at full-bloom stage, harvested after 40-45 days, seeds were removed and stored for 5 years (10% (±1) relative humidity and +4 ºC). These seeds constituted the seed material of the present study. Newly produced Hırsız Kaçıran seeds were supplied from the stored seeds and grown in the same experimental design with similar agronomic practices. Harvested fruits were cut into half, seed cavity was removed and washed. Seeds were dried on drying papers (*Figure 1*). The seeds, passed through the same processes and stored were also taken out of the storage and analyzed similarly. Following equation was used for the performance of irrigation practices.

Seed Color (L value, chroma, hue^o)

Seed color of parameters (L, a and b) of each treatment were determined by chromameter Minolta CR400. Resultant a and b values were used to calculate chroma and hue^o values (McGuire, 1992).

http://www.aloki.hu ● ISSN 1589 1623 (Print) ● ISSN1785 0037 (Online)
DOI: http://dx.doi.org/10.15666/aeer/2003_27832799

Figure 1. *Experiment area and melon fruits*

Standard Germination Tests (%)

Germination tests were conducted in accordance with ISTA (International Seed Testing Association, 2003) criteria. Seeds were kept in between 20 x 20 cm moistened filter papers (Isolab – General Purpose 40 x 40 cm) in dark at 25ºC for 8 days and counted daily (ISTA, 2003). In present germination tests conducted in between papers (ISTA, 2008) two layers of paper were placed at the bottom, seeds were placed on these layers, another layer of paper was placed on top of seeds, papers were ~2 cm folded from the bottom corners and rolled. They were then closed to prevent loss of moisture and placed into growth chamber (Binder KBWF 240). About 6 ml distilled water was used to moisten each paper. Emergence of 2 mm rootlet was taken into consideration as the germination criterion.

Germination Rate (GR)

$$GR\ (\%) = (A/C) \times 100 \qquad \text{(Eq.2)}$$

A: Number of germinated seeds at the end of the test
C: Total number of seeds tested.

Mean Germination Time (MGT)

Mean germination time was calculated with the use of the following equation developed by Ellis and Roberts (1981).

$$MGT\ (day) = \Sigma dn / \Sigma n \qquad \text{(Eq.3)}$$

MGT: Mean germination time
d: Number of days counted
n: Number of seeds germinated in day d.

Seed Moisture Balance (%)

To eliminate the initial moisture-induced differences between the seed lots, moisture content of all lots (stored lots were 10% (±1)) was brought to 13%. In this sense, seeds were first kept on moist filter papers in petri dishes for certain periods and when the desired species-specific seed moisture content was reached (Mavi et al., 2010), they were kept at 5ºC for 3 days to provide the moisture balance. The following equation was used to increase moisture.

http://www.aloki.hu ● ISSN 1589 1623 (Print) ● ISSN1785 0037 (Online)
DOI: http://dx.doi.org/10.15666/aeer/2003_27832799

$$\text{Amount of water to be added (g)} = \text{Initial seed weight X } ((100 - \text{initial moisture}) / (100 - \text{moisture to be increased})) \quad \text{(Eq.4)}$$

To ensure the seed moisture balance and bring the seed moisture to desired level, seed initial moisture was determined according to gravimetric method of International Seed Testing Association (ISTA). Accordingly, 2 g seed samples were weighed in 2 replicates to get initial weights and the seed lots of all treatments were dried at 130ºC for 1 hour (High temperature oven method) (Memmert UNE 600) (ISTA, 2008). Seed samples were removed from the oven, cooled in a desiccator for about 30 minutes, then final weights were determined. The following equation was used to determine the moisture content.

$$\text{Moisture content (\%)} = ((\text{ISW-FSW}) / \text{ISW}) \times 100 \quad \text{(Eq.5)}$$

ISW: Initial seed weight
FSW: Final seed weight.

Electrical Conductivity (µs . cm^{-1} . g^{-1})

The seeds, the humidity of which was increased to 13%, were weighed in 4 replicates as to have 50 seeds in each replicate, they were placed in 500 mL glass beakers containing 250 ml distilled water and each beaker was closed with aluminum foil and placed into a growth chamber (Binder KBWF 240). Test materials were kept in dark conditions at 20°C for 24 hours. Then, the electrical conductivity values of the solutions were measured with the use of an EC-meter (CD-2005 Selecta). Resultant electrical conductivity values (µS . cm^{-1}) were subtracted from the electrical conductivity of test solution (should be less than 5 µS . cm^{-1}). The resultant value was divided by seed weight to get the electrical conductivity of the substances leaking from 1 gram seed (µS . cm^{-1} . g^{-1} seed) (Sivritepe at al., 2015).

Controlled Deterioration Test (%)

Controlled deterioration tests were conducted in 4 replications, each of having 25 seeds with equal moisture content. Seeds were placed in moisture-proof packages with aluminum mixture and hermetically sealed. Packages were kept under stress conditions (%20 seed moisture content and 45 °C (Memmert BE500) for 48, 72, 96 and 120 hours) (Mavi and Demir, 2007). Then, the seeds were taken to germination tests under the most suitable germination conditions according to ISTA rules (*Figure 2*). At the end of the germination test, normal and abnormal seedling ratios were determined (ISTA, 1995, 2012; Powell, 2006).

Emergence Rate (%) and Mean Emergence Time (day)

Emergence tests were conducted in a growth chamber (Binder KBWF 240) at 21±0.5ºC temperature, 75% relative humidity and 12:12 light:dark photoperiods. Tests were conducted in 4 replications with 50 seeds in each replicate. The seeds were sown to a depth of ~3-4 cm in peat-filled (Terraplant Compo) seedling multipots and placed into the growth chamber. Cotyledon leaves parallel to peat surface were accepted as emergence criteria. Emergences were countered daily and experiments were terminated when there was no emergence in 3 consecutive days. At the end of the experiment, seedlings were evaluated as normal and abnormal (Demir and Mavi, 2008).

http://www.aloki.hu ● ISSN 1589 1623 (Print) ● ISSN1785 0037 (Online)
DOI: http://dx.doi.org/10.15666/aeer/2003_27832799

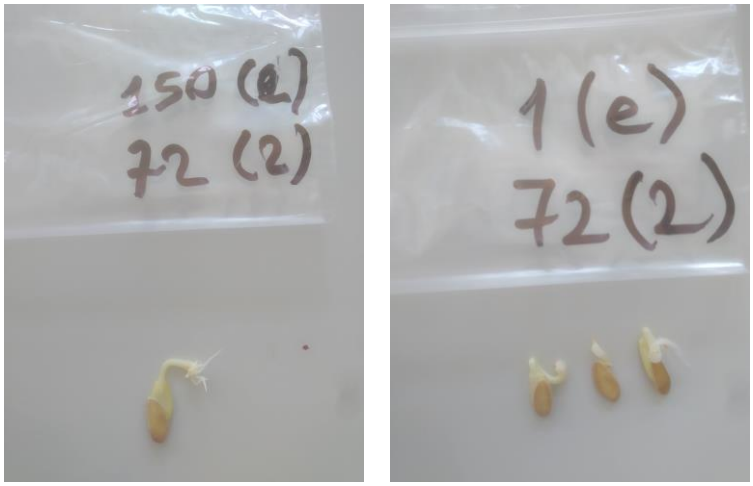

Figure 2. *Seedling samples from controlled deterioration tests 72 hours (%150 and %100 irrigation treatments)*

Peat- filled; Total nitrogen 80-280 mg/l, Water-soluble phosphorus 100-350mg/l, Water-soluble potassium 200-400mg/l, Organic matter 80%, pH 5.0-6.5, Humidity 65%, Salinity 0.7-1.8 g/l.

Mean emergence time

Mean emergence time was calculated in accordance with Ellis and Roberts (1981).

$$MET = \Sigma Dn / \Sigma n \qquad \text{(Eq.6)}$$

n: Number of emerged seeds in day D
D: Number of days counted from the beginning of emergences.

Statistical Analysis

Statistical analyses were conducted with the use of SPSS statistical software. While the controlled deterioration test was subjected to analysis of variance, only seed lots were compared. In this test, each time was considered as a separate test. Germination rate, controlled deterioration test and emergence test data were subjected to Arcsin transformation before the statistical analyses. Significant data were compared with the use of Duncan's test (0.05).

Results and Discussion

Seed Color (L value, chroma, hue°)

Color parameters (L, chroma and hue°) are shown in *Table 3*. In terms of color parameters, irrigation treatments were not found to be significant. However, storage was found significant for chroma ($p \leq 0.01$) and hue° ($p \leq 0.05$).

http://www.aloki.hu ● ISSN 1589 1623 (Print) ● ISSN1785 0037 (Online)
DOI: http://dx.doi.org/10.15666/aeer/2003_27832799

Table 3. *Effects of experimental treatments on color parameters*

TREATMENTS		L	Chroma	Hue°
Irrigation levels	50%	67.11	22.26	82.49
	100%	66.07	22.96	81.38
	150%	65.61	21.43	80.84
Storage	fresh seeds	66.33	21.45 b	82.75 a
	stored seeds	66.20	22.98 a	80.39 b
Irrigation levels		n.s.	n.s.	n.s.
Storage		n.s.	**	*
I X S		*	n.s.	*
Std. Dev		2,76	1,51	2,35

n.s.: not significant, *: p≤0.05, **: p≤0.01, Std. Dev.: Standard Deviation

In terms of interactions of the treatments, both L and hue° were found significant at p≤0.05 level.

The highest L value was obtained from the stored seeds subjected to 50% irrigation level and the lowest L value was obtained from the stored seeds subjected to 100% irrigation level (*Fig. 3*).

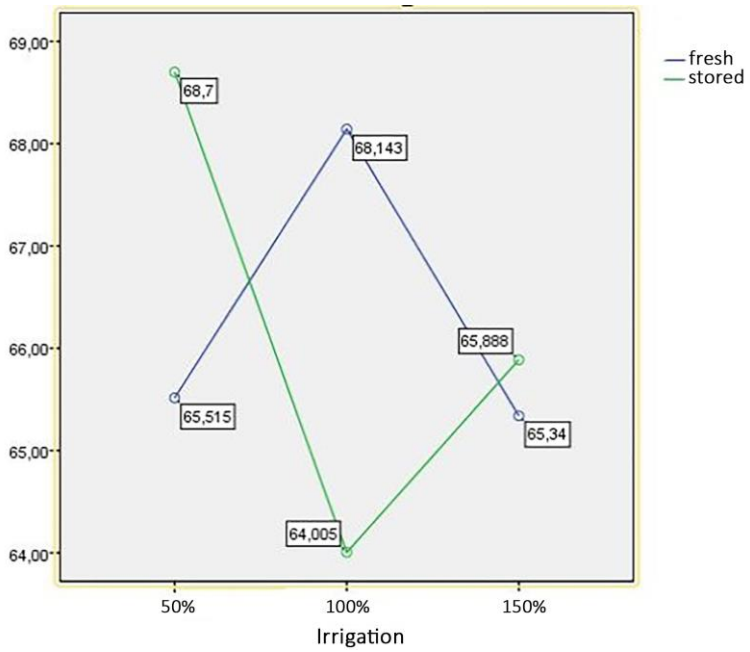

Figure 3. *Interaction graph for L value*

Chroma value was calculated as 22.98 for fresh seeds and 21.45 for stored seeds, forming two different groups. Contrary to chroma value, effects of storage treatment on hue° were higher in fresh seeds (82.75) than the hue° of stored seeds (80.39).

Interaction effects of experimental treatments on hue°, the highest value (83.61) was obtained from fresh seeds at 100% irrigation level. The lowest value (79.15) was obtained from stored seeds subjected to 100% and 150% irrigation levels (*Fig. 4*).

http://www.aloki.hu ● ISSN 1589 1623 (Print) ● ISSN1785 0037 (Online)
DOI: http://dx.doi.org/10.15666/aeer/2003_27832799

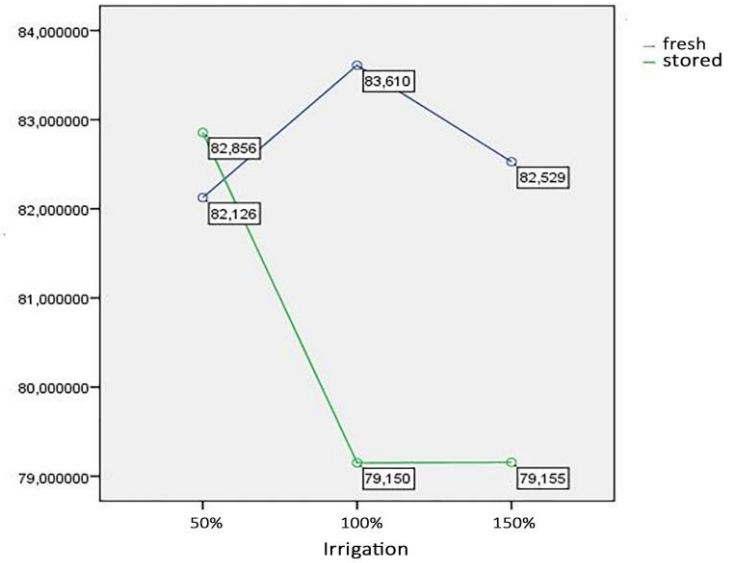

Figure 4. *Interaction graph for hue°*

Although the interaction was found significant for L value, indicating brightness - darkness of the color, the values were quite close to each other. Chroma values revealed more saturated color tones in stored seeds. Present hue° values revealed that seed colors were between yellow and orange, but closer to yellow. As compared to fresh seeds, stored seeds were closer to orange. In a previous study, aging-induced darkening - browning was encountered in red clover seeds (Velijević et al., 2017).

Mallek et al. (2017), stated that the color characteristics of melon seeds vary depending on both the variety and growing conditions, and the "a" value, which affects the chroma and hue values, is also affected by the storage period. Seed color has an importance as it affects the many factors but most importantly germination rate and mean germination time (Gairola et al., 2017).

Standard Germination Test (%)

Germination Rate (GR) (%); According to variance analysis for gemination rate of Hırsız Kaçıran melon seeds subjected to different irrigation water levels and storage conditions, storage treatments were found significant ($p \leq 0.05$), but irrigation water levels and irrigation x storage interactions were found insignificant (*Table 4*). Germination rate of stored seeds (96.08%) was greater than that of fresh seeds (85.62%).

Nerson (2002) conducted a study on watermelon seeds and reported that immature seeds harvested 28 days after flowering lost their germination ability after only 4-5 years of storage, but mature seeds (harvested 42-49 days after flowering) fully retained their germination potential even after 10 years of storage. In our study, seeds were harvested between 40-45 days and mature seeds were obtained. Therefore, stored seeds yielded high germination rates. The lower germination rates of fresh seeds could be attributed to negative effects of on-going climatic factors on agricultural practices of that year. Short-term dormancy, especially encountered in Cucurbit seeds, may have caused the seeds not to perform fully in germination of fresh seeds. Previous researchers, mentioning short-term dormancy in cucurbit seeds, indicated better test results for stored seeds (Nerson, 2007).

http://www.aloki.hu ● ISSN 1589 1623 (Print) ● ISSN1785 0037 (Online)
DOI: http://dx.doi.org/10.15666/aeer/2003_27832799

Table 4. *Effects of experimental treatments on germination parameters*

TREATMENT		Germination Rate (%)	Mean Germination Time (day)
Irrigation Levels	50%	90.06	1.88 a
	100%	92.50	1.91 a
	150%	90	1.72 b
Storage	fresh seeds	85.62 b	1.87
	stored seeds	96.08 a	1.80
Irrigation Level		n.s.	*
Storage		*	n.s.
I X S		n.s.	n.s.
Std. Dev		9,77	0,15

n.s.: not significant, *: p≤0.05, **: p≤0.01, Std. Dev.: Standard Deviation

Mean Germination Time (MGT) (day); Mean germination times obtained from different treatments are given in *Table 4*. In terms of mean germination times, storge treatments and irrigation x storage interactions were not found significant, but irrigation levels were found significant at $p \leq 0.05$ level. The lowest mean germination time (1.72 days) was obtained from 150% irrigation level, followed by 50% irrigation level (1.88 days) and the greatest value (1.91) was obtained from 100% irrigation level.

Hatzig et al. (2018) investigated the effect of drought stress on the mean germination time of different canola accessions. Mean germination time was higher in Okkai 3-Go, Pollen and Zephir seeds as a result of drought treatment, while mean germination time was higher in Musette and NK Nemax seeds in control treatments.

Seed Moisture Balance (%)

Initial moisture values were determined to ensure moisture balance of the seeds to be tested and results are shown in *Table 5*. While irrigation levels and irrigation x storage interactions were not found significant, storage treatments were found significant at $p \leq 0.01$ level. The lowest moisture level (8.17%) was observed in fresh seeds stored seeds had a moisture level of 11.18%, forming a separate group.

Table 5. *Effects of experimental treatments on initial moistures and electrical conductivity*

TREATMENTS		Moisture (%)	EC ($\mu s \cdot cm^{-1} \cdot g^{-1}$)
Irrigation Levels	50%	8.81	12.60
	100%	9.53	14.32
	150%	10.69	11.47
Storage	fresh seeds	8.17 b	12.86
	stored seeds	11.18 a	12.73
Irrigation Level		n.s.	n.s.
Storage		**	n.s.
I X S		n.s.	n.s.
Std. Dev		2,28	2,75

n.s.: not significant, *: p≤0.05, **: p≤0.01, Std. Dev.: Standard Deviation, Std. Dev.: Standard Deviation

As stated in the Materials and Methods section, moisture level of the seeds to be stored was brought to 10% (±1) level and stored in moisture-proof packages to preserve

http://www.aloki.hu ● ISSN 1589 1623 (Print) ● ISSN1785 0037 (Online)
DOI: http://dx.doi.org/10.15666/aeer/2003_27832799

their moisture levels. On the other hand, following the post-harvest cleaning processes, fresh seeds were dried at room temperature and no adjustments were made on their moisture levels. Mavi and Demır (2007) reported seed moisture contents of Kırkağaç melons as between 4.1 - 9.1%. Mallek-Ayadi et al. (2018) determined the moisture content as 7.16% in their study on Maazoun variety melon. Moisture values of fresh seeds were complying with previous literatures. Before to perform the seeds with known initial moisture content into the tests, moisture levels were brought to 13% and a moisture balance was then ensured.

Electrical Conductivity (µs . cm^{-1} . g^{-1})

Tissue electrical conductivity analysis results are shown in *Table 5*. Effects of experimental treatments and interactions on electrical conductivity were not found significant. The lowest electrical conductivity value (11.47 µs . cm^{-1} . g^{-1}) was obtained from 150% irrigation treatments and the greatest value (14.32 µs . cm^{-1} . g^{-1}) was obtained from 100% irrigation treatments.

Controlled Deterioration Test (%)

Controlled deterioration tests were applied for 4 different periods and resultant data are given in *Table 6* and *Table 7*. According to results of standard germination test conducted on seeds kept under stress conditions for 48 hours, normal seedling ratios varied between 71.25 - 92.50%. However, both treatments and interaction of experimental treatments were not found significant. Abnormal seedling ratios were found significant at $p \leq 0.05$ level only in terms of storage treatments.

Table 6. *Response of experimental treatments to controlled deterioration test (48-72 hours*

TREATMENTS		48-hour normal seedling ratio (%)	48-hour abnormal seedling ratio (%)	72-hour normal seedling ratio (%)	72-hour abnormal seedling ratio (%)
Irrigation Levels	50%	86.25	6.25	73.75	12.50 b
	100%	85.75	11.25	78.25	13.37 b
	150%	71.25	20.00	65.00	27.50 a
Storage	fresh seeds	76.67	17.50 a	74.17	19.17
	stored seeds	85.50	7.50 b	70.50	16.42
Irrigation Level		n.s.	n.s.	n.s.	*
Storage		n.s.	*	n.s.	n.s.
I X S		n.s.	n.s.	n.s.	n.s.
Std. Dev		16,95	12,60	19,65	13,17

n.s.: not significant, *: p≤0.05, **: p≤0.01, Std. Dev.: Standard Deviation

The abnormal seedling ratio was 7.50% in stored seeds and 17.50% in fresh seeds. As it was in seeds exposed to stress conditions for 48 hours, normal seedling ratios were not found significant as in seeds exposed to stress conditions for 72 hours. Effect of irrigation levels on abnormal seedling ratios were found significant at $p \leq 0.05$ level. Increasing abnormal seedling ratios were observed with increasing irrigation levels and the values formed two different groups. The lowest abnormal seedling ratios were observed in 50 and 100% irrigation levels respectively with 12.50% and 13.37%. The abnormal seedling ratio at 150% irrigation level was identified as 27.50%.

http://www.aloki.hu ● ISSN 1589 1623 (Print) ● ISSN1785 0037 (Online)
DOI: http://dx.doi.org/10.15666/aeer/2003_27832799

Table 7. *Response of experimental treatments to controlled deterioration tests (96-120 hours*

TREATMENTS		96-hour normal seedling ratio (%)	96-hour abnormal seedling ratio (%)	120-hour normal seedling ratio (%)	120-hour abnormal seedling ratio (%)
Irrigation Levels	50%	63.75	26.63	58.75	17.50
	100%	57.50	28.75	36.75	13.75
	150%	58.75	20.00	51.88	11.25
Storage	fresh seeds	45.00 b	31.08	33.75 b	14.17
	stored seeds	75.00 a	19.17	64.50 a	14.17
Irrigation Level		n.s.	n.s.	n.s.	n.s.
Storage		**	n.s.	*	n.s.
I X S		*	*	n.s.	**
Std. Dev		27,19	16,01	29,34	11,58

n.s.: not significant, *: p≤0.05, **: p≤0.01, Std. Dev.: Standard Deviation

The data for the rest hours are given in *Table 7*. In terms of normal seedling ratio at 96-hour stress conditions, storage treatments were found significant at *p≤0.01* level. While the normal seedling ratio was 75% in stored seeds, the value was 45% in fresh seeds. Interactions of experimental treatments were found significant at *p≤0.05* level.

Interaction graph (*Fig. 5 and Fig. 6*) revealed that stored seeds had greater germination rates at 150% irrigation, fresh seeds at 100% irrigation and stored seeds at 50% irrigation. The lowest normal seedling ratio (35%) was observed in stored seeds subjected to 150% irrigation level. Similarly, in seeds subjected to stress conditions for 96 hours, only the interaction of experimental treatments was found significant for abnormal seedling ratio (*p≤0.05*). The lowest abnormal seedling ratio (10%) was obtained from the stored seeds subjected to 50% irrigation level. The greatest values at 50% irrigation level were obtained from fresh seeds, the highest values at 100% irrigation level were obtained from stored seeds and the highest values at 150% irrigation level were obtained from fresh seeds.

In terms of normal seedling ratios of seed lots subjected to stress conditions for 120 hours, storage treatments were found significant (*p≤0.05*). The normal seedling ratio was measured as 43.70% in fresh seeds and 64.50% in stored seeds. In terms of abnormal seedling ratios, irrigation level x storage interactions (*Fig. 7*) were found significant (*p≤0.01*). The lowest abnormal seedling ratio (5%) was observed in stored seeds subjected to 50% irrigation level and fresh seeds subjected to 150% irrigation level. The highest abnormal seedling ratio was obtained from fresh seeds at 50% irrigation level, stored seeds at 100% irrigation level and fresh seeds at 150% irrigation level.

As compared to germination rates before the controlled deterioration, following the irrigation and storage treatments, germination loss was encountered in controlled deterioration tests. Number of normal seedlings decreased with increasing duration of exposure to controlled deterioration. Similar fluctuations between treatment durations were also reported by Mavi and Demir (2007).

http://www.aloki.hu ● ISSN 1589 1623 (Print) ● ISSN1785 0037 (Online)
DOI: http://dx.doi.org/10.15666/aeer/2003_27832799

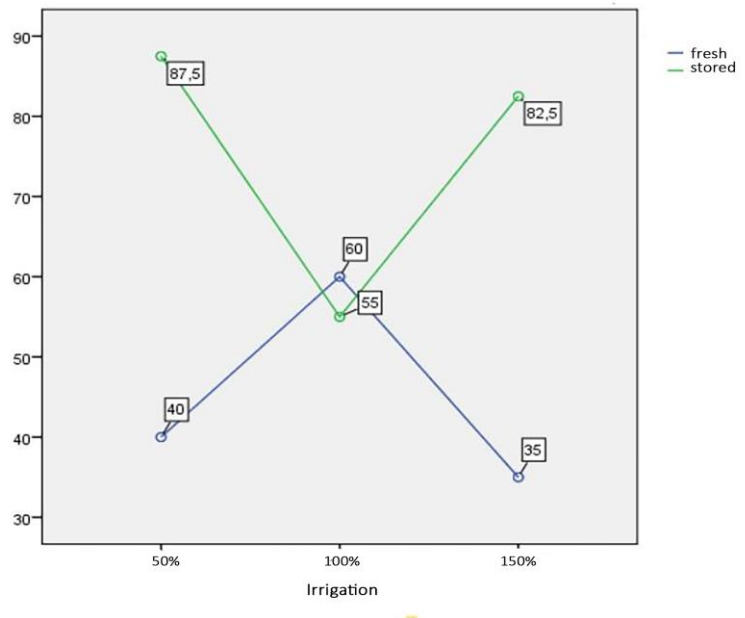

Figure 5. *Interaction graph for normal seedling ratio of controlled deterioration test (96 hours)*

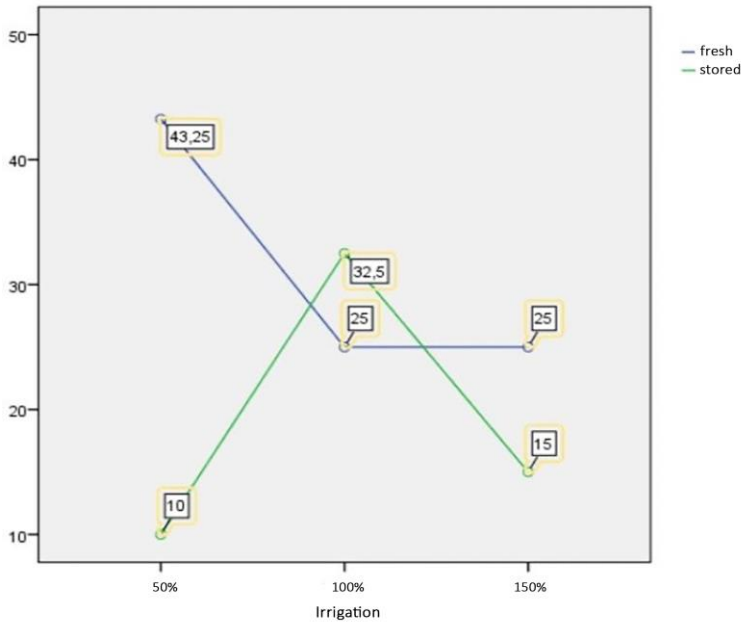

Figure 6. *Interaction graph for abnormal seedling ratio of controlled deterioration test (96 hours)*

http://www.aloki.hu ● ISSN 1589 1623 (Print) ● ISSN1785 0037 (Online)
DOI: http://dx.doi.org/10.15666/aeer/2003_27832799

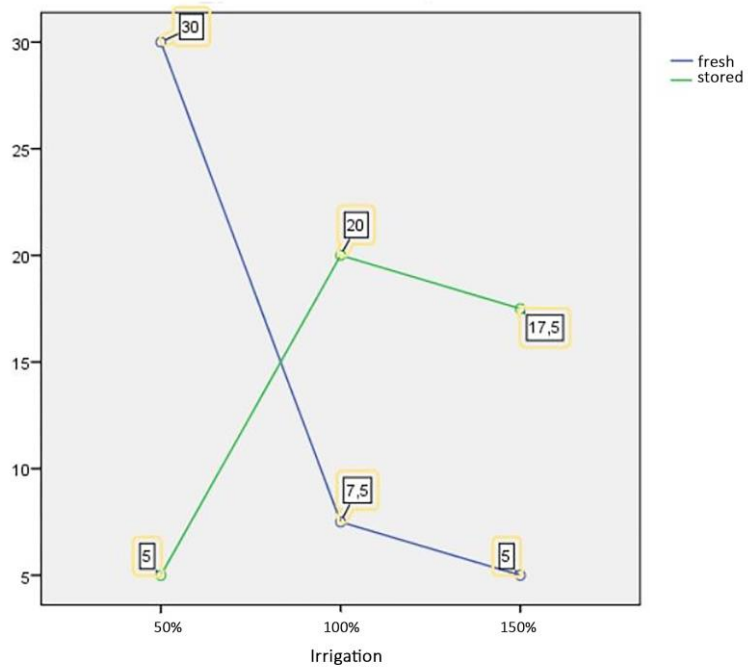

Figure 7. *Interaction graph for abnormal seedling ratio of controlled deterioration (120 hours) test*

Germination rate of vegetable seeds should be at least 75% (certified) – 80% (original) (Tarım and Bakanlığı, 2008). After 48 hours of controlled deterioration test, the germination rate of melon seeds irrigated at 150% irrigation level decreased by 20% to below 75%. After 72 hours of stress treatments, germination ratio of the seeds subjected to 50% irrigation level decreased below 75%. Mavi and Demir (2007) studied under similar conditions like this study and indicated that 48-hour stress treatments could be used in seed-aging. However, in our study, 85-86% germination rate was achieved in 48-hour controlled deterioration tests at 50% and 100% irrigation levels and sufficient aging was detected in longer stress durations.

Time-dependent changes were encountered in response of stored seeds to controlled deterioration tests. Stored seeds still had a high germination rate after 48 hours of controlled deterioration test. However, germination rate fluctuated throughout the test periods. As compared to initial values, about 2% germination loss was encountered at 120-hour controlled deterioration test. Fresh seeds, on the other hand, exhibited greater deterioration and had a germination rate of over 75% only after 48 hours of testing. The highest deterioration in fresh seeds was observed after 120 hours of testing as 60% loss in germination. The researchers noted that low germination of seed lots after the controlled deterioration test indicated low viability (Matthews, 1980; Matthews and Powell, 1981). Demir and Özçoban (2007) indicated that melon seeds still perform 90% germination after 5 years of storage at 20°C and 5% moisture content. Cucurbit seeds can be expected to show less loss of germination under suitable storage conditions.

Emergence Rate and Emergence Time (%)

In present study, emergence tests were conducted in peat media and emergence rate and time were determined (*Table 8*). Emergence rate tests were conducted by

http://www.aloki.hu ● ISSN 1589 1623 (Print) ● ISSN1785 0037 (Online)
DOI: http://dx.doi.org/10.15666/aeer/2003_27832799

considering number of normal / abnormal seedlings, but no abnormal seedlings were detected. In terms of emergence rate, both treatments were found insignificant, but interactions of experimental treatments were found significant at $p \leq 0.01$ level.

Table 8. *Effects of experimental treatments on emergence parameters*

TREATMENTS		Emergence rate (%)	Mean emergence time (day)
Irrigation Levels	50%	92.50	4.02
	100%	82.50	3.91
	150%	81.25	4.06
Storage	fresh seeds	83,33	4.02
	stored seeds	87.50	3.98
Irrigation level		n.s.	n.s.
Storage		n.s.	n.s.
I X S		**	n.s.
Std. Dev		12,85	0,14

n.s.: not significant, *: p≤0.05, **: p≤0.01, Std. Dev.: Standard Deviation

Interaction graph (*Fig. 8*) revealed that the greatest germination was achieved in stored seeds subjected to 50% irrigation level, thus it could be stated that seed storage at this irrigation regime did not result in negative outcomes. Considering 100% irrigation levels, it was observed that storage treatments did not negatively affect emergence. However, positive outcomes were achieved from the storage of the seeds subjected to 150% irrigation level. Delay in the seedling emergence time and decrease in the seedling emergence rate lead to non-uniform cultivation, which adversely affects the yield (Lawles et al., 2012). However, in our study, it was determined that the seeds obtained from over or deficit irrigation levels could be stored without significant loss in emergence rate.

Mean emergence time; variance analysis to determine the effects of experimental treatments on mean emergence times revealed that both treatments and interactions were insignificant. Mean emergence times varied between 3.85 - 4.09 days (*Table 8*).

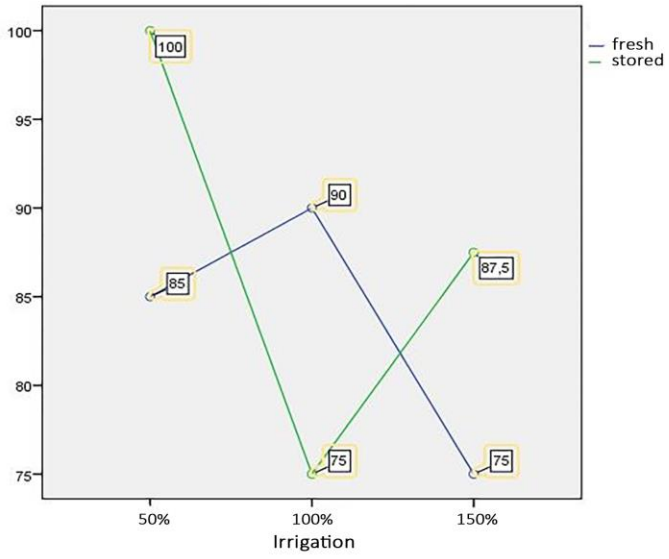

Figure 8. *Interaction graph for emergence rate*

http://www.aloki.hu ● ISSN 1589 1623 (Print) ● ISSN1785 0037 (Online)
DOI: http://dx.doi.org/10.15666/aeer/2003_27832799

Conclusion

Performance of cultivars resistant to stress conditions has always attracted the attention of researchers. However, it is not solely enough to obtain high quality and productive fruits under stress conditions. It is of great importance that the seed, which is a costly starting material, should be of high quality and maintain its quality for a long time in order to sustain vegetable production. Germination rate and emergence rate were not adversely affected by irrigation conditions and such a case indicated that seed production could be achieved under these conditions. On the other hand, low irrigation levels negatively influenced mean germination time of the seeds. Such a case then caused delays in germination and emergence. Seed lots produced with low irrigation level were found to be more resistant to vigour loss in controlled deterioration tests as compared to the seeds subjected to the other irrigation levels.

Storage treatments influenced hue and chroma values, thus darkened the seed color. Irrigation levels did not result in significant losses in color parameters. However, it should be considered that such a case was also influenced by factors such as effect of climatic factors and biotic factors on seed quality, ability of cucurbit seeds to maintain their viability for many years under suitable conditions and quality of the seeds.

It was concluded based on findings that, seeds of the Hırsız Kaçıran melon landrace able to maintain most of the seed quality traits and could be stored at 10± RH seed moisture (4°C temperature) conditions for approximately 5 years without significant loss of vigor. On the other hand, it can be suggested that, at least seeds of Hırsız Kaçıran genotype did not affected negatively while grown in different irrigation regimes and seed quality does not deteriorate.

It can be suggested to evaluate the potential of transferring genetic characteristics to other plants of the population, which was determined to be able to obtain quality products in arid conditions and can be stored without loss of vigor under producer conditions.

Acknowledgements. This study was supported by Scientific Research Project Department of Çanakkale Onsekiz Mart University (FBA-2018-2779).

REFERENCES

[1] Abdalla, F. H., Roberts, E. H. (1969): The effects of temperature and moisture on the induction of genetic changes in seeds of barley, broad beans, and peas during storage. – Annals of Botany 33(1): 153-167.

[2] Ali, N., Skirvin, R., Splittstoesser, W. E., George, W. L. (1991): Germination and regeneration of plants from old cucumber seed. – Hortscience 26(7): 917-918.

[3] Aslan, K. N., Tekiner, M. (2017): Assessment of irrigation practices of farmers receiving water from open-canal and piped irrigation networks. – Turkish Journal of Agriculture - Food Science and Technology 5(9): 1066-1070.

[4] Bass, L. N. (1973): Response of seeds of 27 *Cucumis melo* cultıvars to three storage condıtıons. – Proceedings of the Association of Official Seed Analysts 63: 83-87.

[5] Bhering, M. C., Dias, D. C. F. S., Tokuhisa, D., Dias, L. A. dos S. (2004): Vigor evaluation of melon seeds by controlled deterioration test. – Revista Brasileira De Sementes 26(1): 125-129.

[6] Çiftci, N. H. (2013): Farklı sulama seviyelerinin Çanakkale'de yetiştirilen yerel kavun populasyonun (Hırsız Kaçıran) gelişimi ve verimi üzerine etkileri, Yüksek Lisans Tezi. – Çanakkale Onsekiz Mart Üniversitesi Fen Bilimleri Enstitüsü Bahçe Bitkileri Anabilim Dalı, Çanakkale, Türkiye.

http://www.aloki.hu ● ISSN 1589 1623 (Print) ● ISSN1785 0037 (Online)
DOI: http://dx.doi.org/10.15666/aeer/2003_27832799

[7] Demir, I., Ozcoban, M. (2007): Dry and ultra-dry storage of pepper, aubergine, winter squash, summer squash, bean, cowpea, okra, onion, leek, cabbage, radish, lettuce and melon seeds at –20 °C and 20 °C over five years. – Seed Science and Technology 35: 165-175.
[8] Demir, I., Mavi, K. (2008): Seed vigour evaluation of cucumber (*Cucumis sativus* L.) seeds in relation to seedling emergence. – Research Journal of Seed Science 1(1): 19-25.
[9] Doijode, S. D. (2006): Long term seed storage studies in muskmelon (*Cucumis melo* L.). – J. Hort. Sci. 1(1): 58-60.
[10] Doorenbos, J., Pruitt, W. O. (1992): Crop water requirements. – FAO İrrigation and Drainage Paper 24.
[11] Edwards, M. D., Lower, R. L., Staub, J. E. (1986): Influence of seed harvesting and handling procedures on germination of cucumber seeds. – J. Amer. Soc. Hort. Sci. 111(4): 507-512.
[12] El Balla, M. M. A., Abdelbagi, H. A., Abdelmageed, A. H. A. (2013): Effects of time of water stress on flowering, seed yield and seed quality of common onion (*Allium cepa* L.) under the arid tropical conditions of Sudan. – Agricultural Water Management 121: 149-157.
[13] Ellis, R. H., Roberts, E. H. (1981): The quantification of ageing and survival in orthodox seeds. – Seed Sci. & Technol. 9: 373-409.
[14] Finch-Savage, W. E., Bassel, G. W. (2016): Seed vigour and crop establishment: extending performance beyond adaptation. – J. Exp. Bot 67: 567-591.
[15] Gairola, S., Shabana, H. A., Mahmoud, T., Santo, A. (2018): Effects of seed colour heterogeneity on germination behaviour of a desert plant, *Lotononis platycarpa* (Fabaceae). – Nordic Journal of Botany 36(3): njb–01617. doi:10.1111/njb.01617.
[16] Hatzig, S. V., Nuppenau, J., Snowdon, R. J., Schiessl, S. V. (2018): Drought stress has transgenerational effects on seeds and seedlings in winter oilseed rape (*Brassica napus* L.). – BMC Plant Biology 18: 297.
[17] ISTA (1995): Handbook of vigour test methods. – International Seed Testing Association, Zurich, Switzerland.
[18] ISTA (2003): International rules for seed testing. – International Seed Testing Association, Zurich, Switzerland.
[19] ISTA (2008): International Rules for Seed Testing. – International Seed Testing Association, Bassersdorf, Switzerland.
[20] ISTA (2012): International rules for seed testing. – International Seed Testing Association. Bassersdorf, Switzerland.
[21] Kanber, R., Köksal, H., Önder, S., Eylen, M. (1994): Farklı sulama yöntemlerinin genç portakal ağaçlarında verim, su tüketimi ve kök gelişimine etkileri. – J.of. Agriculture and Forestry 20: 163-172.
[22] Lawles, K., Raun, W., Desta, K., Freeman, K. (2012): Effect of delayed emergence on corn grain yields. – Journal of Plant Nutrition 35(3): 480-496.
[23] Mallek-Ayadi, S., Bahloul, N., Kechaou, N. (2018): Chemical composition and bioactive compounds of *Cucumis melo* L. seeds: Potential source for new trends of plant oils. – Process Safety and Environmental Protection II 3: 68-77.
[24] Mallek-Ayadi, S., Bahloul, N., Kechaou, N. (2019): Phytochemical profile, nutraceutical potential and functional properties of *Cucumis melo* L. seeds. – Sci Food Agric 99: 1294-1301.
[25] Matthews, S. (1980): Controlled deterioration-a new vigor test for crop seeds. – In: Hebblethwaite, P. D. (ed.) Seed production. Butterworth and Co. Ltd., London, UK.
[26] Matthews, S., Powell, A. A. (1981): Controlled deterioration test. – In: Perry, D. A. (ed.) Vigor Test Handbook. ISTA, Zurich, Switzerland.
[27] Mavi, K., Demir, İ. (2007): Controlled deterioration and accelerated aging tests predict relative seedling emergence potential of melon seed lots. – Hortscience 42(6): 1431-1435.
[28] Mavi, K., Demir, I., Matthews, S. (2010): Mean germination time estimates the relative emergence of seed lots of three cucurbit crops under stress conditions. – Seed Sci. & Technol. 38: 14-25.

http://www.aloki.hu ● ISSN 1589 1623 (Print) ● ISSN1785 0037 (Online)
DOI: http://dx.doi.org/10.15666/aeer/2003_27832799

[29] McDonald, M. B. (1999): Seed deterioration: physiology, repair and assessment. – Seed Sci. Technol. 27: 177-237.
[30] McGuire, G. R. (1992): Reporting of objective color measurements. – HortScience 27(12): 1254-1255.
[31] Murthy, U. M. N., Kumar, P. P., Sun, W. Q. (2003): Mechanisms of seed ageing under different storage conditions for *Vigna radiata L.* R. wilczek: lipid peroxidation, sugar hydrolysis, maillard reactions and their relationship to glass state transition. – J. Exp. Bot. 54: 1057-1067.
[32] Nerson, H., Paris, H. S. (1988): Effects of fruit age, fermentation and storage on germination of cucurbit seeds. – Scientia Horticulturae 35: 15-26.
[33] Nerson, H. (2002): Effects of seed maturity, extraction practices and storage duration on germinability in watermelon. – Scientia Horticulturae 93: 245-256.
[34] Nerson, H. (2007): Seed production and germinability of cucurbit crops. – Seed Science and Biotechnology 1(1): 1-10.
[35] Oluoch, M. O., Welbaum. G. E. (1996): Effect of postharvest washing and post- storage priming on viability and vigour of 6-year old muskmelon seeds from eight stages of development. – Seed Sci. Technol. 24: 195-209.
[36] Pandey, D. K. (2016): Liquid preservation of cucurbit seeds at ambient temperature. – Expl Agric. 53(4): 553-565.
[37] Powell, A. A. (2006): Seed vigor and its assessment. – In: Basra, A. S. (ed.) Handbook of Seed Science and Technology. The Haworth Press, New York, USA.
[38] Robinson, R. W., Decker-Walters, D. S. (1997): Cucurbits. – CAB International, Oxon, UK.
[39] Sivritepe, Ö. H., Senturk, B., Teoman, S. (2015): Electrical conductivity tests in maize seeds. – Advances in Plants & Agriculture Research 2(7): 00075.
[40] Szilagyi, L. (2003): Influence of drought on seed yıeld components in common bean. – Bulg. J. Plant Physiol. Special Issue 2003: 320-330.
[41] Tarim, T. C., Bakanliği, O. (2008): Sebze tohum sertifikasyonu ve pazarlaması yönetmeliği. – Retrieved from: https://www.tarimorman.gov.tr/Belgeler/Mevzuat/Yonetmelikler/Sebze.pdf.
[42] Torres, S. B. (2005): Controlled deterioration test on gherkin seeds. – Horticultura Brasilia 23(2): 307-310.
[43] Velijević, N., Štrbanović, R., Poštić, D., Stanisavljević, R., Đukanović, L. (2017): Effects of seed coat colour on the seed quality and initial seedling growth of red clover cultivars (*Trifolium pratense*). – Journal on Processing and Energy in Agriculture 21(3): 174-177.
[44] Vertucci, C. W. (1989): The effects of low water contents on physiological activities of seeds. – Physiologia Plantarum 77: 172-176.
[45] Walters, C. (1998): Understanding the mechanisms and kinetics of seed ageing. – Seed Sci. Res. 8: 223-244.

http://www.aloki.hu ● ISSN 1589 1623 (Print) ● ISSN1785 0037 (Online)
DOI: http://dx.doi.org/10.15666/aeer/2003_27832799

EFFECTS OF BIOCHAR ON MICROBIAL COMMUNITY DIVERSITY IN RHIZOSPHERE SOIL OF FARMLANDS IN NORTHEAST CHINA

DING, J.[1*] – LI, X.[2]

[1]*Heilongjiang Province Key Laboratory of Cold Region Wetland Ecology and Environment Research, Harbin University, Harbin 150086, Heilongjiang Province, PR China*

[2]*College of Resources and Environment, Northeast Agricultural University, Harbin 150030, Heilongjiang Province, PR China*

**Corresponding author*
e-mail: ding.junnan@163.com

(Received 12th Jan 2022; accepted 25th Mar 2022)

Abstract. The present study sought to study the effects of biochar application on the functional diversity of rhizosphere soil in the black and saline-alkaline rhizosphere soil. The results showed that biochar application to the black and saline-alkali soil could increase physical properties and enzymatic activity in the soil of northeast China. Biochar affected the bacterial community composition in the black and saline-alkali soil, of which Proteus, Bacteroides, Acidobacteria, and Actinobacteria were the dominant bacteria. Additionally, biochar inhibited the relative abundance of some bacteria. The relative abundance of Archaea and plant pathogenic functional bacteria and microorganisms affected the abundance of functional genes related to nitrification and the growth of various beneficial microorganisms, effectively inhibiting plant diseases. The canonical correspondence analysis results showed that saline alkaline soil and carbon application conditions were related to available phosphorus indicating a significant correlation between available phosphorus and the soil pH environmental factors. These results confirmed that the change in soil characteristics might indirectly affect the influence of biochar application. Overall, biochar is beneficial to relative abundance of the rhizosphere soil nutrient retention in the root system of black and saline-alkali soil of farmlands in northern China and could increase the growth-promoting bacterial community.
Keywords: *black soil, saline-alkali soil, biochar, bacterial community, functional diversity*

Introduction

Biochar is a carbon-rich material which can be prepared from various organic waste feedstock, such as agricultural wastes and municipal sewage sludge (Wang and Wang, 2019). Biochar has received increasing attention due to its unique feature such as high carbon content and cation exchange capacity, large specific surface area and stable structure (Chen et al., 2018; Yi et al., 2020). Application of biochar to soils changes soil physicochemical properties and stimulates the activities of soil microorganisms that influence soil quality and plant performance. Studying the response of soil microbial communities to biochar amendments is important for better understanding interactions of biochar with soil (Palansooriya et al., 2019). Soil microbes are key drivers of soil biological and chemical processes and critical for maintaining terrestrial ecosystem stability and ecological function, soil microbial community is the most important functional component in soil biota, soil microbial community is in the "plant-soil-soil microorganism" system (Nkongolo and Narendrula-Kotha., 2020). The interaction among plant, nutrients and carbon source supply (He et al., 2018). The formation of an effective feedback system has attracted the attention of scholars at home and abroad.

http://www.aloki.hu ● ISSN 1589 1623 (Print) ● ISSN 1785 0037 (Online)
DOI: http://dx.doi.org/10.15666/aeer/2003_28012816

Black soil is one of the most precious soil types, with the characteristics of high fertility that is suitable for plant growth (Ou et al., 2017). Hence, as an essential land resource, its protection has become highly necessitated. Northeast China is one of the major grain producing areas in China due to its typical back soil (Jiao et al., 2018). Unfortunately, the yearning for effective agricultural products, which requires excessive use of fertilizers for prolonged periods, has led to a gradual decrease in the quality of the black soil chernozem (Delang, 2018). Recently, the farmland soils of Northeast China are facing major problems, such as soil fertility decline, severe soil and water loss, soil acidification, drought and flood, salinization, desertification, physical and chemical properties deterioration, etc. (Gu et al., 2018). Generally, all types of saline soil, alkaline soil, and different degrees of saline and alkaline soils are well known as saline-alkali land (Wu et al., 2021). It has the characteristics of more saline and alkaline components and poor physical and chemical properties, resulting in the growth of most plants being inhibited to varying degrees, or even unable to survive (Kaltas and Javidoglu, 2019). Nowadays, with the increasing shortage of cultivated land resources, the sustainable utilization of saline-alkali land as a potential reserve resource of cultivated land has been highly concerned by researchers (Liu et al., 2019). As for the black soil of Northeast China, the location of the black soil area and the importance of black soil for agricultural production has limited the research on its distribution and its relationship with the physical and chemical properties of the farmland black and saline-alkali soil in terms of the changes in soil physical and chemical properties, enzyme activity, and biochar application-mediated microbial communities' diversity. Therefore, this study discussed the effect of biochar application on soil physiochemical properties, soil enzymes activities and soil bacterial community in two different types of soils in the northeast of China (Black and Saline-alkali soil), and provide a reference for the application of biochar in agriculture.

Materials and methods

Site description

This study was conducted in the pot experiment area of the Modern Agricultural Demonstration Park at Heilongjiang Academy of Agricultural Sciences in Harbin (126°50' E, 45°50' N), Heilongjiang Province in 2020. The geographical distribution of this region is as follows: the average temperature in the coldest month is -22 °C, while the hottest month has an average. Temperature of 20 °C; the annual ≥ 10 °C accumulated temperature is 2,000-2,800 °C and the frost-free period is 115-130 d; the annual average rainfall is 450-550 mm, of which more than 59% of the rainfall occurs between July-September; the soil type is typical black soil. During the study period, the soil condition was as follows: the organic nitrogen content (SOC) was 0.58 $g \cdot kg^{-1}$, the available nitrogen (A-N) content was 89.2 $mg \cdot kg^{-1}$, the available phosphorus (A-P) content was 128.2 $mg \cdot kg^{-1}$, the available kalium (A-K) content was 106.2 $mg \cdot kg^{-1}$, and its pH was 6.8.

Test materials

Test biochar: The test biochar is a kind of highly aromatic carbon rich material, which is transformed from rice husk by pyrolysis and carbonization at high temperature. Biochar was commercially supplied by Liao Ning Golden Future Agriculture

http://www.aloki.hu ● ISSN 1589 1623 (Print) ● ISSN 1785 0037 (Online)
DOI: http://dx.doi.org/10.15666/aeer/2003_28012816

Technology Co., Ltd. with the properties of pH 8.69, ≧34% of total nutrient content and N: P_2O_5: K_2O = 8:11:15.

Test soybean: the chosen soybean variety was Suinong 35 (*Glycine max* (L.) Merr.). The physiological characteristics of soybean are unlimited pod setting habit. The plant is about 90 cm high, with branches, white flowers, long leaves, gray hairs, slightly curved pods, sickle shape, and brown at maturity. The seeds are round, the seed coat is yellow, the navel is light yellow, matte, and the weight of 100 seeds is about 22 g. The protein content was 39.42%, and the fat content was 21.77% (Ma, 2018; Yu et al., 2017). Resistance to gray spot in inoculation identification. In the adaptive area, the number of days from emergence to maturity is about 120 days, which needs to be ≥ 10 °C and the active accumulated temperature is about 2450 °C, which was commercially provided by the Soybean Laboratory in the Institute of Tillage and Cultivation, Heilongjiang Academy of Agricultural Sciences. Routine water and fertilizer management and timely prevention and elimination of diseases, insects and grass.

Test soil: the black control soil (BC) samples were collected from the Modern Agricultural Demonstration Park at Heilongjiang Academy of Agricultural Sciences, and the soil type was typical black soil. The saline-alkali control (SAC) soils were collected from the Fanrong village in Zhaodong City, Heilongjiang Province (125°34’34″ E~46°23’58″ N), and the crops planted in the farmland were soybeans, collected saline-alkali test soil and brought it back to the demonstration park, the soil type was typical saline-alkali soil.

Experimental design

This study was based on the pot experiment. Pot experiments were performed using polypropylene plastic pots with a height and diameter of 30 cm. The biochar and air-dried black soil were well mixed and placed into the pots for soybean pot experiments. Four treatments were set as follows: (1) treatment 1 (BC): no biochar was added into the black soil; (2) treatment 2 (BB): 40 g of biochar was added into 1 kg of black soil, i.e., 160 g biochar/pot; (3) treatment 3 (SAC): no biochar was added into the saline-alkali soil; (4) treatment 4 (SAB): 40 g of biochar was added into 1 kg saline-alkali soil, i.e., 160 g biochar/pot.

In mid-May 2020, mature soybean seeding with relatively uniform size was selected and planted evenly into the pots containing different amounts of biochar. Each pot contained 6 seeds and each treatment was performed in triplicate.

The rhizosphere soil was collected at the maturity stage of soybean after different biochar treatments. The rhizosphere soil was obtained as follows: first the whole soybean plant was carefully excavated. Then the surface soil (0–5 cm) was gently shaken off of the roots, and the root surface was gently brushed to collect the soil attached to the root surface, which is the rhizosphere soil of soybean. After being sealed in sterile bags and returned to the laboratory in an ice box, fresh rhizosphere soil was prepared by grinding and sieving (2 mm) for subsequent tests.

Determination of soybean rhizospheric soil physical and chemical properties

The Walkley-Black titration method was carried out to determine the soil organic carbon content (Cha et al., 2019). The available nitrogen in the soil was measured by using the Alkali-diffusion method (Hurisso et al., 2018). Determination of the available phosphorus in soil was measured by using $NaHCO_3$ Extraction- Mo-Sb Anti-

http://www.aloki.hu ● ISSN 1589 1623 (Print) ● ISSN 1785 0037 (Online)
DOI: http://dx.doi.org/10.15666/aeer/2003_28012816

colorimetry (Ghorbanzadeh, 2020). Determination of available kalium in soil was measured by using NaOH melting--flame photometric method. Determination of soil pH, the soil samples were taken at mature soybean stages and all the samples were air dried for further determination. The water-soil leaching method with water: soil = 2.5:1 was used to determine soil samples using a table pH meter (Minkina et al., 2018).

Determination of soybean rhizospheric soil enzyme activity

The test soil was collected from the potted soybeans during the mature period. Urease was treated with sodium phenate colorimetry. Catalase was titrated by potassium permanganate. Saccharase was determined by 3, 5-dinitrosalicylic acid colorimetry. Phosphatase was measured by disodium phenyl phosphate colorimetry (Nannipieri, 2018).

Preparation of soybean rhizospheric microbial samples

The control and biochar treated soil samples were placed in a dry ice-box, then brought back to the laboratory for preservation, and stored in a refrigerator at - 80 °C to detect the soil microbial diversity. Herein, the soil microbial genomic DNA was extracted using the Omega e.z.n.a DNA kit (Omega Bio-Tek, Norcross, GA, U.S.).

Statistical analysis

Data were statistically analyzed using Excel 2003. One-way ANOVA analysis and PCA (α- = 0.05) were performed using SPSS 16.0 software. The differences in the soil microbial community composition among the soil samples were mapped using R language software.

Results

Effects of biochar on soybean rhizospheric soil physical and chemical properties

The effect of biochar on the physical and chemical properties of soybean rhizosphere soil is summarized in *Table 1*. The physical and chemical properties of the soybean rhizosphere soil were significantly influenced by biochar, which were all higher than BC and SAC.

Table 1. *Effects of biochar on soil physical and chemical properties*

Treatment	pH	A-N ($mg \cdot kg^{-1}$)	A-P ($mg \cdot kg^{-1}$)	A-K ($mg \cdot kg^{-1}$)	SOC ($g \cdot kg^{-1}$)
BC	6.52 ± 0.08 c	118.54 ± 3.04 b	25.46 ± 0.52 a	228 ± 7.22 b	11.26 ± 1.86 b
BB	6.85 ± 0.19 c	122.67 ± 5.98 a	25.98 ± 1.14 a	242 ± 8.56 a	13.68 ± 1.92 a
SAC	8.89 ± 0.15 b	99.41 ± 4.34 d	21.49 ± 1.08 b	204 ± 5.19 c	9.83 ± 1.53 d
SAB	9.05 ± 0.26 a	105.78 ± 5.44 c	22.65 ± 1.73 b	207 ± 4.23 c	10.92 ± 1.26 c

Note: Different lower-cases in the same column for differences at 0.05 level ($P < 0.05$), the same below

Effect of biochar on enzyme activity of soybean rhizospheric soil

As summarized in *Table 2,* the activities of urease and phosphatase in the soybean rhizosphere soil treated with biochar were significantly higher than the BC and SAC

http://www.aloki.hu ● ISSN 1589 1623 (Print) ● ISSN 1785 0037 (Online)
DOI: http://dx.doi.org/10.15666/aeer/2003_28012816

treatments. The change of catalase activity in the biochar treated soil was consistent with urease, of which the catalase activity in the BB and SAB treated rhizosphere soil was 7.85% and 3.46%, which were all higher than the control treatments. Additionally, the difference between the biochar and control treatments was significant ($P < 0.05$). With the increase of biochar application, the saccharase and phosphatase activity increased, showing significant differences between different treatments ($P > 0.05$).

Table 2. *Enzyme activity in rhizosphere soil treated with different amounts of biochar*

Treatment	Urease (NH_3-Nmg·100 g^{-1}·d^{-1})	Catalase (0.002 mol·L^{-1} $KMnO_4$·g^{-1})	Saccharase (mg·g^{-1})	Phosphatase (mg·g^{-1} ± ·24 h)
BC	24.08 ± 2.43 b	11.97 ± 1.45 a	26.47 ± 4.10 a	0.23 ± 0.02 b
BB	30.73 ± 1.18 a	12.99 ± 1.72 a	31.53 ± 8.22 a	0.27 ± 0.01 a
SAC	17.63 ± 3.65 d	7.79 ± 1.23 b	18.07 ± 2.01 d	0.14 ± 0.02 d
SAB	20.15 ± 2.13 c	8.07 ± 1.31 b	20.11 ± 2.02 c	0.16 ± 0.01 c

Effects of biochar on bacterial diversity in soybean rhizosphere soil

As depicted in *Figure 1,* the levels of bacterial OTUs in different soil samples were significantly different. A total of 5698 OTUs were obtained from all the samples. Of them, BB and BC contained 1414 and 1276 soil bacterial OTUs, respectively. SAB and SAC contained 1484 and 1524 bacterial OTUs, respectively. OTU401 accounted for 64.55% of all OTU species in the BC treatment, 48 species of bacterial unique to BC, others, and OTU487 accounted for 63.79% of all OTU species in BB, and 131 species unique to BB. OTU2214 and OTU2085 accounted for 53.46% of all OTU species in SAC, and there were 16 species unique to SAC. OTU1257, OTU1587, and OTU1717 accounted for 47.12% of all OTUs species in SAB, and there were 16 species unique to SAB.

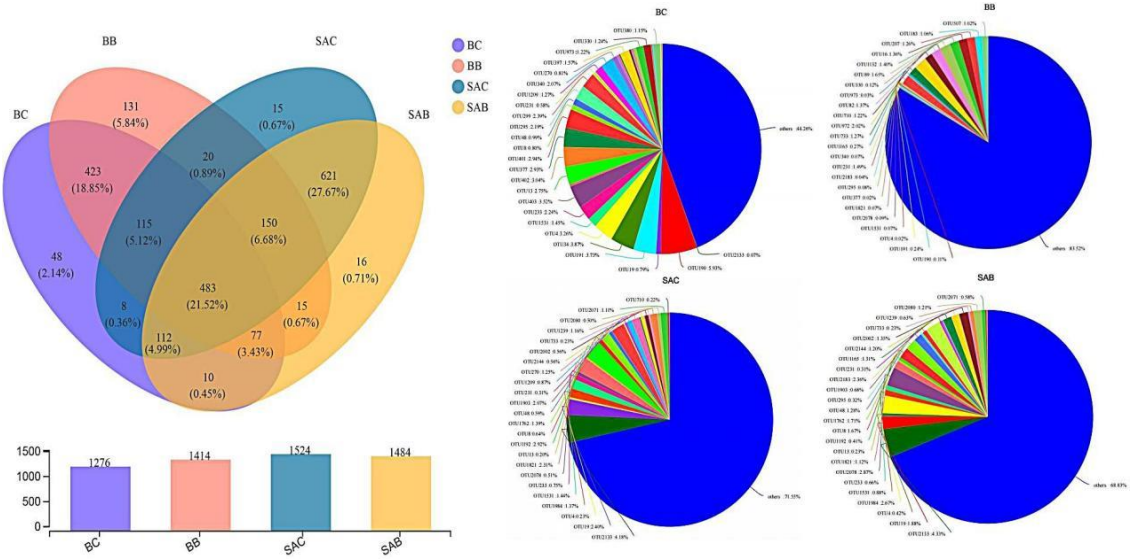

Figure 1. *OTUs numbers of bacterial communities in all samples*

As depicted in *Figure 2,* all the 23047 sequences belonged to 27 bacterial phyla, of which the primary bacterial microbial populations included *Proteobacteria*,

http://www.aloki.hu ● ISSN 1589 1623 (Print) ● ISSN 1785 0037 (Online)
DOI: http://dx.doi.org/10.15666/aeer/2003_28012816

Bacteroidetes, *Acidobacteria*, *Actinobacteria*, *Chloroflex*, *Gemmatimonades*, *Firmicutes*, *Saccharibacteria*, *Nitrospirae*, *Verrucomicrobia,* and others. The average proportion of flora structures in the BC and BB treatments was 42.91%, 22.41%, 9.99%, 6.11%, 7.24%, 2.97%, 2.25%, 1.98%, 0.59%, 0.82%, and 2.81%, respectively. Of which, the total number of sequences belonging to *Proteobacteria*, *Bacteroidetes*, *Acidobacteria*, *Actinobacteria,* and *Chloroflexi* accounted for 88.66% of all sequences, and the average proportion of structures in the saline-alkali soil was 39.32%, 15.97%, 16.42%, 10.76%, 3.59%, 3.34%, 2.25%, 2.45%, 1.97%, 2.95%, and 1.78%, respectively. The total number of sequences belonging to *Proteobacteria*, *Bacteroidetes*, *Acidobacteria*, *Actinobacteria,* and *Chloroflex* accounted for 86.06% of all sequences. *Armimondetes*, *Chlamydiae*, *Deferribacters,* and *Thermotogae* were the inferior flora, accounting for less than 0.5% of all sequences.

Effects of biochar on bacterial community composition in soybean rhizosphere soil

Moreover, the differences in bacterial community structure between the black and saline-alkali soil were analyzed, showing similar taxonomic profiles among various species. *Proteobacteria* accounted for a high bacterial proportion in all the samples (the proportion was between 35.81% and 48.08%), indicating *Proteobacteria* to be the dominant bacterial species in all the samples. Comparing the bacterial community structures of different soil types with biochar, *Proteobacteria* and *Bacteroidetes* were the dominant bacterial species in the BC treatment, while *Proteobacteria* and *Acidobacteria* were the dominant bacterial species in the BB treatment. After biochar application, the bacterial species of *Proteobacteria* and *Bacteroidetes* were decreased by 10.35% and 26.22%, respectively. Similarly, the bacteria species of *Acidobacteria* and *Chloroflexi* were increased by 16.05% and 10.41%. The bacterial species of *Proteobacteria*, *Bacteroidetes*, *Acidobacteria,* and *Actinobacteria* were the dominant bacteria species in the saline-alkali soil. After biochar application, the bacterial species of *Proteobacteria* and *Actinobacteria* were decreased by 6.98% and 1.2%, respectively, while the bacteria species of *Bacteroidetes* and *Acidobacteria* were increased by 0.92% and 9.98%, respectively.

Effects of biochar on community structure of soybean rhizosphere soil microorganisms

As depicted in *Figure 3,* the impact of biochar application on soil microorganisms in the black and saline-alkali soil was mainly manifested by two aspects. Firstly, biochar application promoted the abundance of soil bacteria, such as *Gemmatimonadetes*, *Nitrospirae*, *Chloroflexi*, *Acidobacteria*, *Aminicenantes*, *Parcubacteria*, *Ignavibacteriae*, *Planctomycetes*, *Latescibacteria*, *Deinococcus-Thermus*, *Caldiserica*, *Gracilibacteria*, *FCPU426*, *Armatimonadetes*, *Cyanobacteria*, *Spirochaetae* than the control. Secondly, biochar application inhibited the growth of *Bacteroidetes* and *FBP* in the black soil and *Saccharibacteria* and *Deinococcus-Thermus* in the saline-alkali soil. The bacterial richness in the biochar treated soil was lower than control.

Correlation analysis between soil bacterial community structure and environmental factors

The PCA results of soil bacterial community structure based on OTUs abundance are depicted in *Figure 4*. The contribution values of the PC1 axis and PC2 axis to the

http://www.aloki.hu ● ISSN 1589 1623 (Print) ● ISSN 1785 0037 (Online)
DOI: http://dx.doi.org/10.15666/aeer/2003_28012816

difference in sample composition were 41.69% and 17.81%, respectively. The sample points of biochar treatment and control treatment were significantly separated on the PC1 axis, indicating that biochar had a certain impact on the soil bacterial community structure. BB and SAB treatments had a significant correlation with the SOC and A-P environmental factors in the rhizosphere soil.

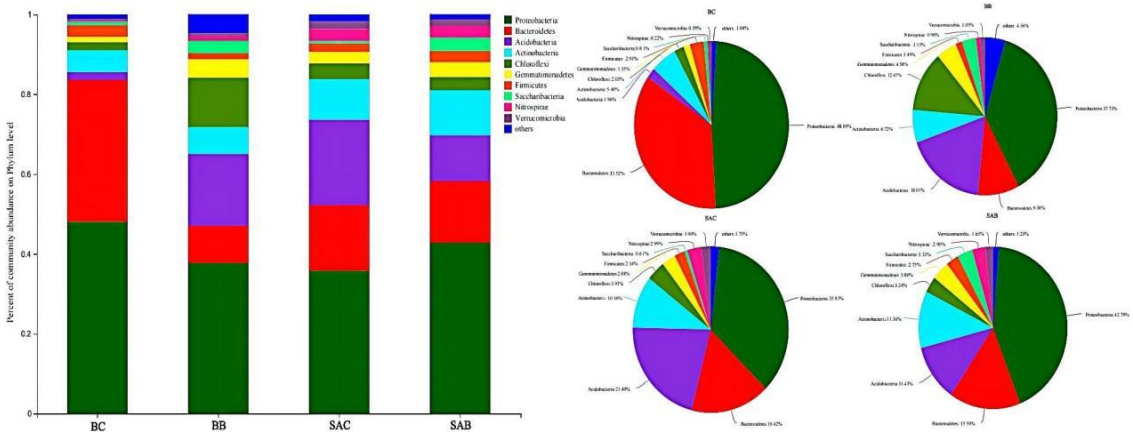

Figure 2. *Relative abundance of species at phylum level in all samples*

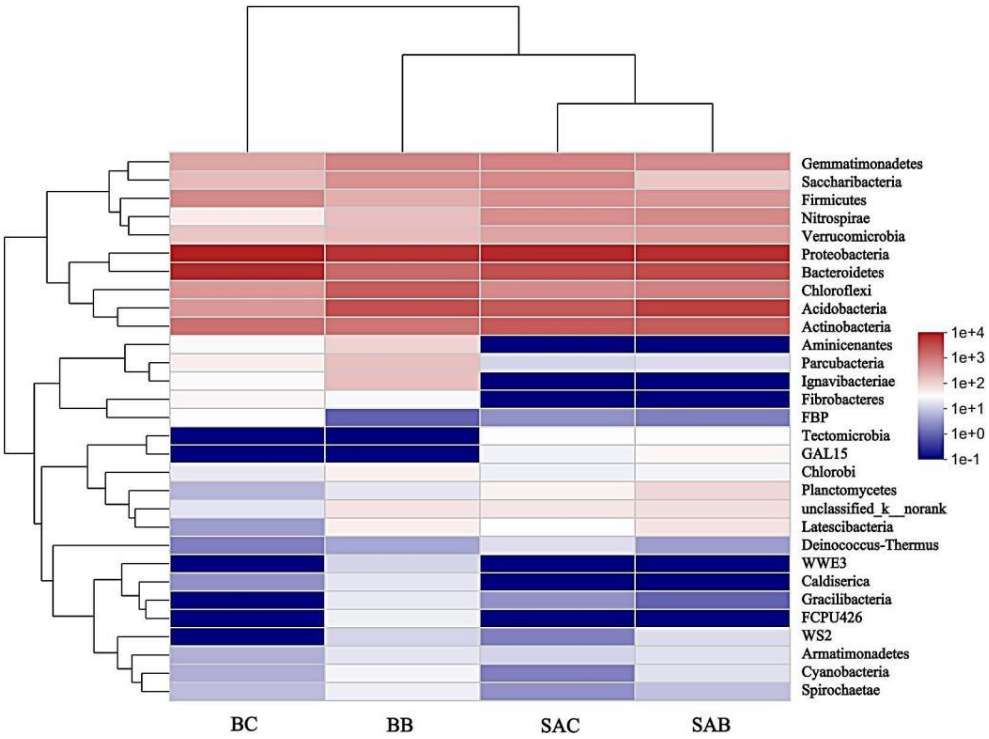

Figure 3*. Analysis of relative abundance of biochar of soil microbial community composition at the phylum level*

Effect of biochar on functional taxa of soil bacterial

As depicted in *Figure 5,* biochar application changed the abundance of functional microorganisms in the black and saline-alkali soil. While biochar application in the

http://www.aloki.hu ● ISSN 1589 1623 (Print) ● ISSN 1785 0037 (Online)
DOI: http://dx.doi.org/10.15666/aeer/2003_28012816

black soil increased the abundance of bacteria, such as sulfur_respiration, nitrogen_fixation, nitrite_oxidation, ammonia_oxidation, and nitrification. Compared with BC, the abundance of ammonia_oxidation and nitrification was increased by 77.03% and 76.19%, respectively. Biochar application in the saline-alkali soil increased the abundance of aromatic_compound_degradation, methanol_oxidation, methylotrophy, ammonia_oxidation, and nitrification. Compared with the saline-alkaline soil, biochar application in the black soil significantly changed the abundance of functional microorganisms.

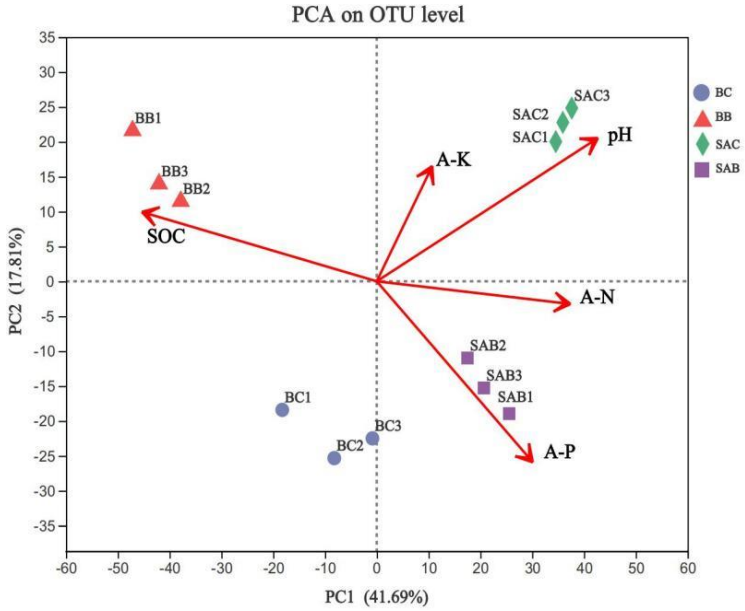

Figure 4. *PCA analysis of biochar on soybean rhizosphere soil*

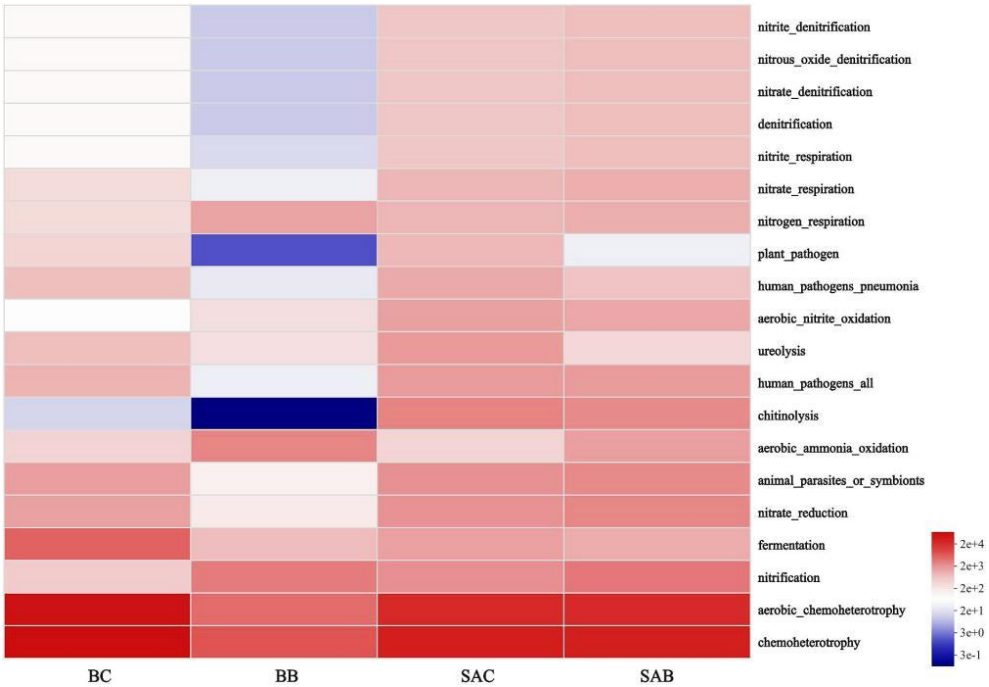

Figure 5. *Effect of biochar on functional taxa of soil bacterial*

http://www.aloki.hu ● ISSN 1589 1623 (Print) ● ISSN 1785 0037 (Online)
DOI: http://dx.doi.org/10.15666/aeer/2003_28012816

Discussion

Based on its physical characteristics and previous studies, biochar is characterized by porous structures and weak alkalinity, and has a strong ability to absorb water, store nutrients, and increase the soil organic carbon content (Panahi et al., 2020). The pores and surfaces of the biochar can also become a microenvironment suitable for soil microorganisms, which increases the number and activity of soil microorganisms and promotes the circulation of various elements in the soil (Palansooriya et al., 2019). Animal, plant, and microorganism residues are the main sources of soil organic matter, which are derived from a complex physical and chemical transformation processes of microorganisms and soil (Indoria et al., 2018). Organic carbon is an important soil component, despite the small proportion it takes in total soil weight, the quantity and quality of the soil organic carbon content is an important indicator of soil quality (Ondrasek et al., 2019). The results in this study showed that biochar can increase the accumulation of the soil organic carbon content, and the application of greater amounts of biochar had a significant effect on the organic carbon content. After the application of the biochar in the soil, the biochar has easily volatile substances and the oxidation of the surface functional group of biochar at the initial stage, but it was passivated with the prolonging retention of the biochar in soil after biochar application (El-Naggar et al., 2019). The interaction between biochar and soil produced a protective mechanism, which not only increased the oxidation stability of soil organic carbon but also promoted its accumulation in soil (Feng et al., 2021; Yang et al., 2019).

In modern agricultural management, successive chemical fertilizer application causes soil acidification and continuous loss of base ions, resulting in poor soil, thus affecting crop growth (Dumortier et al., 2020). In the presence of more base ions, such as potassium, sodium, calcium, and magnesium, the content of exchangeable hydrogen and aluminum ions in soil were reduced by the adsorption of biochar, so the soil pH value can be improved by the biochar (Leng et al., 2019). The soil pH was determined by the base ions, since the biochar has a higher number of base ions, it was considered to be a better modifier to improve soil than lime, but it had no significant effect on alkaline soil (Fan et al., 2018).

As a biocatalyst in the soil, the main function of soil enzymes is to promote the biochemical reaction and the physicochemical properties of soil, as well maintain ecological balance (Wołejko et al., 2020). The application of biochar is able to affect this activity (Jabborova et al., 2021). The soil enzymes are mainly derived from the cell secretions of animals, plant roots, and microorganisms in soil, and the activity of the soil enzymes can reflect the intensity and direction of various biochemical processes in soil (Awet et al., 2018). Two effects have been observed on aspects of biochar on the soil enzyme activity, which might be involved in the reaction between the biochar and target substrates (Gorovtsov et al., 2020). First, the adsorption of the biochar on the reaction substrate contributed to enzyme catalysis and therefore improved the soil enzyme activity (Ameur et al., 2018). Second, the adsorption of biochar on enzymes protected the binding sites of enzyme catalysis, thus preventing enzyme catalysis (Lopes et al., 2021). In this study revealed that biochar can increase the content of the related enzymes in the chernozem, and also significantly enhanced the contents of urease, catalase and phosphatase in soil, but had no significant effect on the activity of invertase. Urease, an important hydrolase involved in the circulation of soil nitrogen, functions to catalyze the hydrolysis of urea in soil, which characterizes the intensity of nitrogen supply in the soil (Monge et al., 2018). The increase of urease activity may be

http://www.aloki.hu ● ISSN 1589 1623 (Print) ● ISSN 1785 0037 (Online)
DOI: http://dx.doi.org/10.15666/aeer/2003_28012816

due to the increasing demand of soybeans on nitrogen, which thereby stimulate nitrogen fixation in rhizobia (Laroca et al., 2018). The increasing activity of hydrogen peroxide may be related to the improved soil environment after the application of the biochar, which provides good conditions for the growth and reproduction of microorganisms and is beneficial to their metabolism, thus improving the soil enzyme activity (Lehmann et al., 2011). The soil pH value increased significantly with the application of biochar, which indirectly led to an enhancement of invertase activity (Sheng and Zhu., 2018).

Previous studies have reported a significant change in the community composition and bacterial and archaeal diversity both in the Amazon black soil and biochar improved soil (Zhang et al., 2021). Compared with the unmodified soil, the bacterial diversity of soil increased by 25%, which was reflected at the level of genera, species, and families (Otsuka et al., 2008). The nitrogen-fixing bacteria, possessing nitrogen-fixing enzymes, are a special type of bacteria, which can convert molecular nitrogen in the atmosphere into nitrate through nitrification for easy absorption by the plants (Igiehon and Babalola, 2018). Biochar could provide a favorable niche for nitrogen fixation due to its low oxygen partial pressure and decreased oxygen concentration (Wu et al., 2020). Meanwhile, its low inorganic nitrogen content could also provide favorable conditions for the implantation of nitrogen-fixing bacteria on the surface of biochar, making it a dominant population (Zhou et al., 2016). In these studies, a total of 23047 sequences belonging to 27 bacterial phyla, including Proteobacteria, Bacteroidetes, Acidobacteria, Actinobacteria, Chloroflexi, Gemmatimonadetes, Firmicutes, Saccharibacteria, Nitrospirae, Verrucomicrobia, were detected in all the samples. While in this study, these bacteria were most dominant in the black and saline-alkali soil, and the primary microbial groups in the northern farmland soil (Yao et al., 2017; Sun et al., 2014).

According to the phylum, genus, and species-level classification of species difference analysis, Heatmap sequence analysis, and functional prediction analysis, biochar application could increase or inhibit the abundance of some microorganisms. It is mainly manifested by the following aspects: firstly, biochar application could improve the abundance of nitrifying bacteria in the black and saline-alkali soil. It could also improve soil aeration, reduce soil denitrification rate, and nitrite nitrogen production due to its porous nature (George et al., 2016). Secondly, soil nitrification is affected by several factors, such as soil type, aeration conditions, water content, temperature, soil pH, and substrate nitrogen concentration (Hu et al., 2021). Therefore, the addition of biochar to soil might change the living environment of nitrifying bacteria related to N_2O production by changing the soil properties, thereby promoting or inhibiting N_2O production through nitrification (Novak et al., 2016). Biochar could promote the abundance of Archaea (AOA). AOA, and nitrite-oxidizing bacteria, which are the primary synergists of soil nitrification (Wang et al., 2021a). In the soil nitrification process, the major completion stage includes the oxidation of ammonia to hydroxylamine under the action of ammonia monooxygenase produced by *amoA*, gene of AOA and ammonia-oxidizing bacteria (AOB), then further oxidation to NO_2^- under the action of hydroxylamine oxidoreductase, and finally, the catalysis of nitrite oxidoreductase by *nor* gene of nitrite-oxidizing bacteria oxidizing $NO_2^-$to NO_3^- (Beeckman et al., 2018). Evidence shows that the addition of biochar could increase the soil pH, which might exert a certain impact on the growth and reproduction of AOA and AOB, thus affecting nitrification (Li et al., 2021). As for the soil with biochar, the AOA diversity decreased, but the gene copy number significantly increased, while the

http://www.aloki.hu ● ISSN 1589 1623 (Print) ● ISSN 1785 0037 (Online)
DOI: http://dx.doi.org/10.15666/aeer/2003_28012816

diversity and gene copy number of AOB significantly increased (Cao et al., 2021). Furthermore, the porous surface of biochar could adsorb and store water and nutrients, providing excellent habitat conditions for soil microorganisms, especially bacteria, to improve the abundance of AOB, AOA, and other flora and accelerate the corresponding soil nitrification process (Wang et al., 2021b).

In this study, biochar application in the black and saline-alkali soil significantly inhibited the abundance of plant pathogenic. Soil-borne diseases are mostly caused by the pathogens living in the soil with plant residues and infect the plants from the root or stem under appropriate conditions (de Medeiros et al., 2021). The emerging global warming and strong promotion of protected land planting have increased the occurrence of soil-borne diseases in protected cultivation, resulting in huge economic losses (Bai et al., 2018). Although a lot of research has been carried out on the prevention and control of soil borne diseases, there is still a lack of cost-effective, efficient, wide adaptability, and practical technology that can be popularized in a large area (Elad et al., 2011). Recently, biochar as a new material integrating fertilizer, adsorbent, and modifier, with great potential and development prospects, has been widely adopted to prevent and control the soil-borne diseases (Ren et al., 2022). Accumulating studies have proved that biochar mainly affects the soil and plant root environment through the following mechanisms to inhibit the plant diseases occurrence: improving the physical and chemical properties of soil is conducive to plant growth but not conducive to the growth of pathogens (Gu et al., 2017); improve the available nutrients content in the soil, promote plant growth and improve disease resistance (Viger et al., 2015). Inhibit pathogenic bacterial growth through competition, heavy parasitism, and antibiotic secretion; direct inhibition of pathogens; induced plant disease resistance; strong adsorption of organic matters by biochar, and affecting the signal substances secreted by the plant roots attract pathogens and the infectious substances secreted by pathogens (Rasool et al., 2021). Overall, promoting the growth of beneficial microorganisms in the soil is one of the primary reasons for the control effect of biochar on plant pathogenic (Jaiswal et al., 2018). The 16S rRNA homology analysis results showed that most bacteria had more than 98% homology with *Pseudomonas*, *Bacillus*, *Rhizobium,* and *Bacillus brevis*, which promoted plant growth and had biological control function. Furthermore, the antibiotics producing *Pseudomonas fluorescens*, *Pseudomonas aeruginosa,* and *Pseudomonas Mendoza* were isolated and identified. It can be seen that the application of biochar in soil could promote the growth of various beneficial microorganisms and effectively inhibit the occurrence of plant diseases.

Conclusion

In this study, the application of biochar increased the content of soil organic carbon, pH value, available nitrogen, available kalium and available phosphorus under the concentration range of biochar. It also promoted the enzyme activity of rhizosphere soil in the black and saline-alkali of soybean farmland and increased the abundance of bacteria and microorganisms in the black and saline-alkali soil. Biochar affected the composition of the soil bacterial community in the black and saline-alkali soil, of which Proteus, Bacteroides, and Acidobacteria were the dominant bacteria. It also inhibited the relative abundance of bacteria, such as solibacterales, clostridiales, and rhodocyclales. Biochar application promoted the abundance of nitrification, AOA, and functional bacteria of plant pathogenic in the tested soybean rhizosphere soil, the abundance of

http://www.aloki.hu ● ISSN 1589 1623 (Print) ● ISSN 1785 0037 (Online)
DOI: http://dx.doi.org/10.15666/aeer/2003_28012816

functional genes related to nitrification, and the growth of various beneficial microorganisms, effectively inhibiting the plant diseases. The CCA at the OTU level showed that SAC and BB had a significant correlation with total phosphorus, organic carbon, and soil pH environmental factors, indicating that the change in soil characteristics might indirectly affect biochar application on soil bacterial community structure. In order to maximize the effective of biochar in the prevention and control of soil-borne diseases, it is necessary to comprehensively consider the preliminary treatment of biochar, supporting management measures in the field and collaborative technology. At present, there is a lack of research in this area, so it is also the focus of future research.

Acknowledgements. This article was supported by the Natural Science Foundation of Heilongjiang Province China (Grant No. LH2021D014).

Conflict of interests. The author confirms that this article content has no conflict of interests.

REFERENCES

[1] Ameur, D., Zehetner, F., Johnen, S., Jöchlinger, L., Pardeller, G., Wimmer, B., Keiblinger, K. M. (2018): Activated biochar alters activities of carbon and nitrogen acquiring soil enzymes. – Pedobiologia 69: 1-10.

[2] Awet, T. T., Kohl, Y., Meier, F., Straskraba, S., Grün, A. L., Ruf, T., Emmerling, C. (2018): Effects of polystyrene nanoparticles on the microbiota and functional diversity of enzymes in soil. – Environmental Sciences Europe 30(1): 1-10.

[3] Bai, Z. G., Caspari, T., Gonzalez, M. R., Batjes, N. H., Mäder, P., Bünemann, E. K., Goede, R. D., Brussaard, L., Xu, M. G., Ferreira, C. S. S., Reintam, E., Fan, H. Z., Mihelič, R., Glavan, M., Tóth, Z. (2018): Effects of agricultural management practices on soil quality: a review of long-term experiments for Europe and China. – Agriculture, Ecosystems & Environment 265: 1-7.

[4] Beeckman, F., Motte, H., Beeckman, T. (2018): Nitrification in agricultural soils: impact, actors and mitigation. – Current Opinion in Biotechnology 50: 166-173.

[5] Cao, H., Jia, M., Xun, M., Wang, X., Chen, K., Yang, H. (2021): Nitrogen transformation and microbial community structure varied in apple rhizosphere and rhizoplane soils under biochar amendment. – Journal of Soils and Sediments 21(2): 853-868.

[6] Cha, J. Y., Cha, Y., Oh, N. H. (2019): The effects of tree species on soil organic carbon content in South Korea. – Journal of Geophysical Research: Biogeosciences 124(3): 708-716.

[7] Chen, H. M., Ma, J. Y., Wang, X. J., Xu, P. P., Zhang, S., Zhao, Y. W. (2019): Effects of biochar and sludge on carbon storage of urban green roofs. – Forest 9(7): 413.

[8] de Medeiros, E. V., Lima, N. T., de Sousa Lima, J. R., Pinto, K. M. S., da Costa, D. P., Franco Junior, C. L., Hammecker, C. (2021): Biochar as a strategy to manage plant diseases caused by pathogens inhabiting the soil: a critical review. – Phytoparasitica 49(4): 713-726.

[9] Delang, C. O. (2018): The consequences of soil degradation in China: a review. – GeoScape 12(2): 92-103.

[10] Dominic, W., Amonette, J. E., Street-Perrott, F. A., Lehmann, J., Joseph, S. (2018): Sustainable biochar to mitigate global climate change. – Nature Communications 8: 1-9.

[11] Dumortier, J., Dokoohaki, H., Elobeid, A., Hayes, D. J., Laird, D., Miguez, F. E. (2020): Global land-use and carbon emission implications from biochar application to cropland in the United States. – Journal of Cleaner Production 258: 120684.

http://www.aloki.hu ● ISSN 1589 1623 (Print) ● ISSN 1785 0037 (Online)
DOI: http://dx.doi.org/10.15666/aeer/2003_28012816

[12] Elad, Y., Cytryn, E., Meller Harel, Y., Lew, B., Graber, E. R. (2011): The biochar effect: plant resistance to biotic stresses. – Phytopathologia Mediterranea 50: 335-349.
[13] El-Naggar, A., Lee, S. S., Rinklebe, J., Farooq, M., Song, H., Sarmah, A. K., Ok, Y. S. (2019): Biochar application to low fertility soils: a review of current status, and future prospects. – Geoderma 337: 536-554.
[14] Fan, Q., Cui, L., Quan, G., Wang, S., Sun, J., Han, X., Yan, J. (2018): Effects of wet oxidation process on biochar surface in acid and alkaline soil environments. – Materials 11(12): 2362.
[15] Feng, W., Yang, F., Cen, R., Liu, J., Qu, Z., Miao, Q., Chen, H. (2021): Effects of straw biochar application on soil temperature, available nitrogen and growth of corn. – Journal of Environmental Management 277: 111331.
[16] George, C., Kohler, J., Rillig, M. C. (2016): Biochars reduce infection rates of the root-lesion nematode *Pratylenchus penetrans* and associated biomass loss in carrot. – Soil Biology and Biochemistry 95: 11-18.
[17] Ghorbanzadeh, N., Mahsefat, M., Farhangi, M. B., Rad, M. K., Proietti, P. (2020): Short-term impacts of pomace application and Pseudomonas bacteria on soil available phosphorus. – Biocatalysis and Agricultural Biotechnology 28: 101742.
[18] Gorovtsov, A. V., Minkina, T. M., Mandzhieva, S. S., Perelomov, L. V., Soja, G., Zamulina, I. V., Yao, J. (2020): The mechanisms of biochar interactions with microorganisms in soil. – Environmental Geochemistry and Health 42(8): 2495-2518.
[19] Gu, Y., Hou, Y. G., Huang, D. P., Hao, Z. X., Wang, X. F., Wei, Z., Jousset, A., Tan, S. Y., Xu, D. B., Shen, Q. R., Xu, Y. C., Friman, V. P. (2017): Application of biochar reduces *Ralstonia solanacearum* infection via effects on pathogen chemotaxis, swarming motility, and root exudate adsorption. – Plant and Soil 415(1/2): 269-281.
[20] Gu, Z., Xie, Y., Gao, Y., Ren, X., Cheng, C., Wang, S. (2018): Quantitative assessment of soil productivity and predicted impacts of water erosion in the black soil region of northeastern China. – Science of the Total Environment 637: 706-716.
[21] He, T. H., Liu, D. Y., Yuan, J. J., Luo, J. F., Lindsey, S., Bolan, N., Ding, W. X. (2018): Effects of application of inhibitors and biochar to fertilizer on gaseous nitrogen emissions from an intensively managed wheat field. – Science of the Total Environment 1: 628-629.
[22] Hu, J., Zhao, Y., Yao, X., Wang, J., Zheng, P., Xi, C., Hu, B. (2021): Dominance of comammox Nitrospira in soil nitrification. – Science of the Total Environment 780: 146558.
[23] Hurisso, T. T., Moebius-Clune, D. J., Culman, S. W., Moebius-Clune, B. N., Thies, J. E., Van Es, H. M. (2018): Soil protein as a rapid soil health indicator of potentially available organic nitrogen. – Agricultural & Environmental Letters 3(1): 180006.
[24] Igiehon, N. O., Babalola, O. O. (2018): Rhizosphere microbiome modulators: contributions of nitrogen fixing bacteria towards sustainable agriculture. – International Journal of Environmental Research and Public Health 15(4): 574.
[25] Indoria, A. K., Sharma, K. L., Reddy, K. S., Srinivasarao, C., Srinivas, K., Balloli, S. S., Raju, N. S. (2018): Alternative sources of soil organic amendments for sustaining soil health and crop productivity in India–impacts, potential availability, constraints and future strategies. – Current Science 115(11): 2052-2062.
[26] Jabborova, D., Ma, H., Bellingrath-Kimura, S. D., Wirth, S. (2021): Impacts of biochar on basil (*Ocimum basilicum*) growth, root morphological traits, plant biochemical and physiological properties and soil enzymatic activities. – Scientia Horticulturae 290: 110518.
[27] Jaiswal, A. K., Frenkel, O., Tsechansky, L., Elad, Y., Graber, E. R. (2018): Immobilization and deactivation of pathogenic enzymes and toxic metabolites by biochar: a possible mechanism involved in soilborne disease suppression. – Soil Biology and Biochemistry 121: 59-66.

http://www.aloki.hu ● ISSN 1589 1623 (Print) ● ISSN 1785 0037 (Online)
DOI: http://dx.doi.org/10.15666/aeer/2003_28012816

[28] Jiao, X. Q., Mongol, N., Zhang, F. S. (2018): The transformation of agriculture in China: looking back and looking forward. – Journal of Integrative Agriculture 17(4): 755-764.
[29] Kaltas, M., Javidoglu, L. (2019): Comparison of enzyme production rate of extracted native bacteria from saline and alkaline soil. – Medbiotech Journal 3(3): 84-87.
[30] Laroca, J. V. D. S., Souza, J. M. A. D., Pires, G. C., Pires, G. J. C., Pacheco, L. P., Silva, F. D. D., Souza, E. D. D. (2018): Soil quality and soybean productivity in crop-livestock integrated system in no-tillage. – Pesquisa Agropecuária Brasileira 53: 1248-1258.
[31] Lehmann, J., Rillig, M. C., Thies, J., Masiello, C. A., Hockaday, W. C., Crowley, D. (2011): Biochar effects on soil biota - a review. – Soil Biology and Biochemistry 43(9): 1812-1836.
[32] Leng, L., Huang, H., Li, H., Li, J., Zhou, W. (2019): Biochar stability assessment methods: a review. – Science of the Total Environment 647: 210-222.
[33] Li, M., Zhang, J., Yang, X., Zhou, Y., Zhang, L., Yang, Y., Yan, Q. (2021): Responses of ammonia-oxidizing microorganisms to biochar and compost amendments of heavy metals-polluted soil. – Journal of Environmental Sciences 102: 263-272.
[34] Liu, Q., Tang, J., Liu, X., Song, B., Zhen, M., Ashbolt, N. J. (2019): Vertical response of microbial community and degrading genes to petroleum hydrocarbon contamination in saline alkaline soil. – Journal of Environmental Sciences 81: 80-92.
[35] Lopes, É. M. G., Reis, M. M., Frazão, L. A., da Mata Terra, L. E., Lopes, E. F., dos Santos, M. M., Fernandes, L. A. (2021): Biochar increases enzyme activity and total microbial quality of soil grown with sugarcane. – Environmental Technology & Innovation 21: 101270.
[36] Ma, D. D. (2018): New soybean variety Suinong 35 and its high yield cultivation techniques. – Agricultural Development & Equipments 4: 154 (in Chinese).
[37] Minkina, T. M., Mandzhieva, S. S., Burachevskaya, M. V., Bauer, T. V., Sushkova, S. N. (2018): Method of determining loosely bound compounds of heavy metals in the soil. – MethodsX 5: 217-226.
[38] Monge, E. C., Tuveng, T. R., Vaaje-Kolstad, G., Eijsink, V. G., Gardner, J. G. (2018): Systems analysis of the glycoside hydrolase family 18 enzymes from Cellvibrio japonicus characterizes essential chitin degradation functions. – Journal of Biological Chemistry 293(10): 3849-3859.
[39] Nannipieri, P., Trasar-Cepeda, C., Dick, R. P. (2018): Soil enzyme activity: a brief history and biochemistry as a basis for appropriate interpretations and meta-analysis. – Biology and Fertility of Soils 54(1): 11-19.
[40] Nkongolo, K. K., Narendrula-Kotha, R. (2020): Advances in monitoring soil microbial community dynamic and function. – Journal of Applied Genetics 61: 249-263.
[41] Novak, J. M., Ippolito, J. A., Lentz, R. D., Spokas, K. A., Bolster, C. H., Sistani, K., Trippe, K. M., Phillips, C. L., Johnson, M. G. (2016): Soil health, crop productivity, microbial transport, and mine spoil response to biochars. – BioEnergy Research 9(2): 454-464.
[42] Ondrasek, G., Begić, H. B., Zovko, M., Filipović, L., Meriño-Gergichevich, C., Savić, R., Rengel, Z. (2019): Biogeochemistry of soil organic matter in agroecosystems & environmental implications. – Science of The Total Environment 658: 1559-1573.
[43] Otsuka, S., Sudiana, I., Komori, A., Isobe, K., Deguchi, S., Nishiuama, M., Shimizu, H., Senoo, K. (2008): Community structure of soil bacteria in a tropical rainforest several years after fire. – Microbes and Environments 23: 49-56.
[44] Ou, Y., Rousseau, A. N., Wang, L. X., Yang, B. X. (2017): Spatio-temproal patterns of soil organic carbin pHin relation to environmental factors: a case study of the black soil region of northeastern China. – Agriculture Ecosystems & Environment 245: 22-31.
[45] Palansooriya, K. N., Wong, J. T. F., Hashimoto, Y., Huang, L., Rinklebe, J., Chang, S. X., Ok, Y. S. (2019): Response of microbial communities to biochar-amended soils: a critical review. – Biochar 1(1): 3-22.

http://www.aloki.hu ● ISSN 1589 1623 (Print) ● ISSN 1785 0037 (Online)
DOI: http://dx.doi.org/10.15666/aeer/2003_28012816

[46] Panahi, H. K. S., Dehhaghi, M., Ok, Y. S., Nizami, A. S., Khoshnevisan, B., Mussatto, S. I., Lam, S. S. (2020): A comprehensive review of engineered biochar: production, characteristics, and environmental applications. – Journal of Cleaner Production 270: 122462.
[47] Rasool, M., Akhter, A., Soja, G., Haider, M. S. (2021): Role of biochar, compost and plant growth promoting rhizobacteria in the management of tomato early blight disease. – Scientific reports 11(1): 1-16.
[48] Ren, L., Hao, B., Fang, W., Zhang, D., Cheng, H., Li, Q., Cao, A. (2022): Combination of modified biochar and polyurea microcapsules to co-encapsulate a fumigant via interface polymerization for controlled release and enhanced bioactivity. – Pest Management Science 78(1): 73-85.
[49] Sheng, Y., Zhu, L. (2018): Biochar alters microbial community and carbon sequestration potential across different soil pH. – Science of the Total Environment 622: 1391-1399.
[50] Sun, D. Q., Meng, J., Liang, H., Yang, E., Huang, Y. W., Chen, W. F., Jiang, L. L., Lan, Y., Zhang, W. M., Gao, J. P. (2014): Effect of volatile organic compounds absorbed to fresh biochar on survival of Bacillus mucilaginosus and structure of soil microbial communities. – Journal of Soils and Sediments 15: 271-281.
[51] Viger, M., Hancock, R. D., Miglietta, F., Taylor, G. (2015): More plant growth but less plant defence? First global gene expression data for plants grown in soil amended with biochar. – GCB Bioenergy 7(4): 658-672.
[52] Wang, J. L., Wang, S. Z. (2019): Preparation, modification and environmental application of biochar: a review. – Journal of Cleaner Production 227(1): 1002-1022.
[53] Wang, C., Chen, D., Shen, J., Yuan, Q., Fan, F., Wei, W., Wu, J. (2021a): Biochar alters soil microbial communities and potential functions 3–4 years after amendment in a double rice cropping system. – Agriculture, Ecosystems & Environment 311: 107291.
[54] Wang, G., Li, Q., Yuwen, C., Gong, K., Sheng, L., Li, Y., Chen, R. (2021b): Biochar triggers methanogenesis recovery of a severely acidified anaerobic digestion system via hydrogen-based syntrophic pathway inhibition. – International Journal of Hydrogen Energy 46(15): 9666-9677.
[55] Wołejko, E., Jabłońska-Trypuć, A., Wydro, U., Butarewicz, A., Łozowicka, B. (2020): Soil biological activity as an indicator of soil pollution with pesticides - a review. – Applied Soil Ecology 147: 103356.
[56] Wu, X., Sun, Y., Deng, L., Meng, Q., Jiang, X., Bello, A., Xu, X. (2020): Insight to key diazotrophic community during composting of dairy manure with biochar and its role in nitrogen transformation. – Waste Management 105: 190-197.
[57] Wu, G. Q., Li, H., Zhu, Y. H., Li, S. J. (2021): Comparative physiological response of sainfoin (Onobrtchis viciaefolia) seedings to alkaline and alkaline and saline-alkaline stress. – Journal of Animal & Plant Sciences 31(4): 1028-1035.
[58] Yang, X., Tsibart, A., Nam, H., Hur, J., El-Naggar, A., Tack, F. M., Ok, Y. S. (2019): Effect of gasification biochar application on soil quality: trace metal behavior, microbial community, and soil dissolved organic matter. – Journal of Hazardous Materials 365: 684-694.
[59] Yao, Q., Liu, J., Yu, Z., Li, Y., Jin, J., Liu, X., Wang, G. (2017): Changes of bacterial community compositions after three years of biochar application in a black soil of northeast China. – Applied Soil Ecology 113: 11-21.
[60] Yi, Y., Huang, Z., Lu, B., Xian, J., Tsang, E. P., Cheng, W., Fang, Z. (2020): Magnetic biochar for environmental remediation: a review. – Bioresource Technology 298: 122468.
[61] Yu, H., Liu, R., Hu, Y., Xu, B. (2017): Flavor profiles of soymilk processed with four different processing technologies and 26 soybean cultivars grown in China. – International Journal of Food Properties 20(sup3): S2887-S2898.
[62] Zhang, H., Wang, S., Zhang, J., Tian, C., Luo, S. (2021): Biochar application enhances microbial interactions in mega-aggregates of farmland black soil. – Soil and Tillage Research 213: 105145.

http://www.aloki.hu ● ISSN 1589 1623 (Print) ● ISSN 1785 0037 (Online)
DOI: http://dx.doi.org/10.15666/aeer/2003_28012816

[63] Zhou, J., Jiang, X., Zhou, B. K., Zhao, B. S., Ma, M. C., Guan, D. W., Li, J., Chen, S. F., Cao, F. M., Shen, D. L., Qin, J. (2016): Thirty-four years of nitrogen fertilization decreases fungal diversity and alters fungal community composition in black soil in northeast China. – Soil Biology and Biochemistry 95: 135-143.

http://www.aloki.hu ● ISSN 1589 1623 (Print) ● ISSN 1785 0037 (Online)
DOI: http://dx.doi.org/10.15666/aeer/2003_28012816

REMOVAL OF Pb AND As BY BACTERIA ISOLATED FROM SEDIMENTS OF LAS VÍRGENES DAM AND RÍO CONCHOS IN THE STATE OF CHIHUAHUA, MEXICO

SOTO-PADILLA, M. Y.[1*] – HERNÁNDEZ-PEÑA, C. C.[2] – BERNADAC-VILLEGAS, L. G.[1] – FLORES-TAVIZÓN, E.[1] – DOMÍNGUEZ-ACOSTA, M.[1] – VÁZQUEZ-GÁLVEZ, F. A.[1] – ALVARADO-SOTO, S.[1] – DE LOS SANTOS-VILLALOBOS, S.[3]

[1]*Instituto de Ingeniería y Tecnología, Universidad Autónoma de Ciudad Juárez, Chihuahua, México*

[2]*Instituto de Ciencias Biomédicas, Universidad Autónoma de Ciudad Juárez, Chihuahua, México*

[3]*Intituto Tecnológico de Sonora, Sonora, México*

[*]*Corresponding author*
e-mail: marisela.soto@uacj.mx; phone: +52-656-688-4846

(Received 14th Jan 2022; accepted 21st Mar 2022)

Abstract. Lead (Pb) and Arsenic (As) are elements that negatively affect all living organisms if present in the environment. These elements have been reported in the sediments of water supply basins in the State of Chihuahua, Mexico. The current study consisted of the isolation of bacteria and investigating their growth capacity and the potential removal of Pb and As. Thus, two Gram-positive bacteria resistant to Pb and two Gram-positive bacteria resistant to As were isolated. The phylogenetic analysis -based on the 16S rRNA gene- identified them as *Paenibacillus illinoisensis* (Pb114002), *Bacillus luti* (Pb214001), *Paenibacillus ginsengagri* (As115004), and *Bacillus freudenreichii* (As215002). *Paenibacillus illinoisensis* (Pb114002) showed a Pb removal percentage of 65.67% in the supernatant and *Bacillus luti* (Pb214001) displayed 6.57%. Regarding As, removal percentages in the supernatant shown were 11.96% by *Paenibacillus ginsengagri* (As115004) and 42.72% by *Bacillus freudenreichii* (As215002).
Keywords: *morphological characterization, 16S rRNA, heavy metal, metalloid, bioremediation*

Introduction

The Las Vírgenes dam belongs to the municipality of Rosales in the State of Chihuahua, located to the North-West of the municipalities of Meoqui and Delicias. This dam belongs to the sub-basin of the San Pedro River, which is located in the Municipality of Satevó, while the Río Conchos is located near the city of Ojinaga. Both are considered vital basins for the supply of hydric resources for the habitants who live near, as well as their use for economic activities in the region. However, some studies report the presence of heavy metal contamination at these sites (Holguín et al., 2006; Rubio et al., 2013), which affects water quality and consequently cause health and environmental problems. Among the contaminants present in the water, particularly those used for human consumption and food production, arsenic (As) occupies an important place due to the impact on health due to its intake, which has caused the spread of chronic regional endemic hydroarsenicism (HACRE), a chronic disease that can evolve into more serious pathologies such as different types of cancer, the maximum permissible limit of As recommended by World Health Organization (OMS) in drinking water is 10 µg/L (Medina-Pizzali et al., 2018; Olmos and Ridolfi, 2018). Likewise, lead is highly toxic and can accumulate in living organisms because it does not have a defined biological function

http://www.aloki.hu ● ISSN 1589 1623 (Print) ● ISSN 1785 0037 (Online)
DOI: http://dx.doi.org/10.15666/aeer/2003_28172829

and is regarded as biologically nonessential (Ali et al., 2019), but it has adverse effects on different essential biochemical processes, and it is toxic at even low levels of exposure (Rodríguez-Rey et al., 2016). Environments contaminated by heavy metals and metalloids tend to be ideal niches for other organisms which can develop in extreme conditions, these organisms are called extremophiles (Jorquera et al., 2019), as well as microorganisms that grow in high concentrations of metals, called metal resistant. Bacteria that are tolerant to heavy metals are capable of accumulating them intracellularly and the presence of metal-binding proteins internally in the cell is associated with the reduction of their toxicity (Suárez and Reyes, 2002). Thus, the use of metalophilic microorganisms is of great importance and scientific interest, in addition to the fact that they can be applied in environmental biotechnology processes for the removal of metals (Orji et al., 2021). The interaction between microorganisms and metals or metalloids has environmental importance, metalophilic bacteria can play a very important role in the biogeochemical cycle of heavy metals, as well as the remediation of contaminated environments by heavy metals or metalloids (Hu et al., 2021). Currently, environmental biotechnology is used to decontaminate or alleviate contamination, therefore, the objective of this study was to evaluate the potential of metalophilic bacteria in the removal of lead (Pb) and arsenic (As), isolated from sediments of bodies of water in the State of Chihuahua, Mexico.

Materials and methods

Microbial isolation and morphological characterization

The sediment sampling of the Las Vírgenes dam and the Conchos river was carried out at the coordinates 28°09'58.82" N 105°37'43.95" W and 29°32′41.59" N 104°28′35.66" W, respectively. The sediment samples were taken in the summer of 2018. Fifteen samples were collected in sterile 50 mL Falcon tubes, which were stored in a cooler at 4˚C and transported to the laboratory for analysis (Hernández-Peña et al., 2021). Subsequently, 10 g of sediment was weighed and incubated at 37°C for 21 days at 200 rpm in nutrient broth (DIFCO) supplemented with lead nitrate [$Pb(NO_3)_2$] or arsenic trioxide (As_2O_3) for a concentration of 10 mg/L of Pb or As. Samples of the culture medium were taken after 0, 3, 7, 14, and 21 days of incubation. The collected samples were cultured in Petri dishes with nutrient agar enriched with 10 mg/L of Pb or As, for which serial dilutions (10^6) were carried out. Morphologically different colonies were selected for isolation on Petri dishes containing the culture medium indicated above, by using Scottish stria. The scanning electron microscope (SEM) (Hitachi SU5000) was used to determine cell morphology; for this, bacteria cells with a growth time of 48 hours were collected, washed, fixed with 2% formaldehyde, and dried by dehydration by applying acetone and ethyl alcohol (Soto-Padilla et al., 2018).

Molecular identification of isolated bacteria

The DNA extraction of the isolated strains was carried out with the phenol-chloroform-isoamyl alcohol method (Guo et al., 1997). The 16S rRNA amplification, sequencing, and bioinformatic analysis were carried out as reported by Soto-Padilla et al. (2018). For the amplification protocol, the universal primer 27F (5'-AGAGTTTGATCMTGGCTCAG-3') and 1492R (5'TACGGYTACCTTGTTACGACTT-3') were used for fragments of 1500 bp, Master mix (PROMEGA) was used with a final volume of 50 µL, the purification was

http://www.aloki.hu ● ISSN 1589 1623 (Print) ● ISSN 1785 0037 (Online)
DOI: http://dx.doi.org/10.15666/aeer/2003_28172829

carried out using UltraClean® 15DNA Purification Kit. The sequencing was carried out by the National Laboratory of Genomics for Biodiversity (LANGEBIO) using the Sanger platform. The bioinformatic analysis of the sequences obtained from the bacterial strains was carried out by Finch TV, CLUSTALX 2.1, SEAVIEW, and MEGA 7.0 (Hernández-Peña et al., 2021). Phylogenetic trees were constructed using the Neighbor-joining method; and the Tamura-Nei model of distance analysis and 500 Bootstrap replications were assessed to support internal branches (Soto-Padilla et al., 2018).

Bacterial resistance to Pb or As

This test was carried out to evaluate the minimum inhibitory concentration (MIC), which the strains tolerate lead and arsenic, the test was carried out in Petri dishes with nutritive agar (DIFCO) enriched with 100, 200, 400, 600, 800, 1000, and 1200 mg of Pb/L or As/L. Petri dishes were prepared in triplicate for each concentration and bacterial strain; in addition, uninoculated control was used for all concentrations (Pellizzari et al., 2015). The Petri dishes were incubated at 37°C and growth was observed at 72 h.

Bacterial growth kinetics in presence of Pb or As

The culture medium (nutrient broth added with Pb or As at a concentration of 100 mg/L) was inoculated with 10% (v/v) of each isolated bacteria and incubated in Erlenmeyer flasks. The inoculated flasks were incubated on an orbital shaker (222DS-LABNET) at 37°C at 200 rpm. The experiments were carried out in triplicate. For the evaluation of bacterial growth, 3 mL aliquots of the culture medium were taken at intervals of 2 h. Bacterial growth was estimated by turbidimetry at a wavelength of 600 nm in the UV-Vis spectrophotometer (Lambda 2) (Thacker et al., 2007).

Pb or As removal kinetics

The removal of Pb or As was evaluated by taking 3 mL aliquots of the culture medium at 2 h intervals, the samples were centrifuged at 3000 rpm for 15 minutes. The concentration of Pb or As was determined using the atomic absorption (Perkin-Elmer, Canada) spectrometry method (Hernández-Garcia et al., 2008). All experiments were conducted in triplicate.

Results and discussion

Microbial isolation and morphological characterization

Four bacterial strains were isolated under the presence of Pb or As from the sampling sites located in the State of Chihuahua. Both Pb and As are elements that affect human health and also cause an imbalance in the trophic chain of ecosystems (Nava-Ruíz and Méndez-Armenta, 2011). Strains Pb114002 and Pb214001 were isolated from both sampling sites in the presence of Pb (10 mg/L), as well as strains As115004 and As215002 in the presence of As (10 mg/L). Strains Pb114002 and Pb214001 showed a difference in growth in circular and massive forms, respectively; in the same way, they differ in pigmentation, strain Pb114002 showed yellow colonies, and strain Pb214004 showed white colonies. Regarding the colonies of strains with the ability to grow under As, differences between strain As115004 (beige) and As215002 (white). Based on the microscopic morphology (*Figure 1*) using the scanning electron microscope (SEM), cells with the shape of a bacillus (Pb114002) and coccobacillus (Pb214001) were observed,

http://www.aloki.hu ● ISSN 1589 1623 (Print) ● ISSN 1785 0037 (Online)
DOI: http://dx.doi.org/10.15666/aeer/2003_28172829

which have an average size of 1.5 µm and 1.0 µm, respectively. The strains that grew in As showed a bacillary form, with an average size of 1.4 µm. For the Gram stain, the four strains are identified as Gram-positive bacteria. The presence of heavy metals and metalloids in sediments of reservoirs in the state of Chihuahua, Mexico has been reported (Hernández-Garcia et al., 2008). Pb concentrations ranged from 58 to 94 mg/Kg in sediments, exceeding the recommended limit of 50 mg/Kg; the metalloid As was presented in concentrations around 17 mg/Kg of sediment, coinciding with different studies that show the presence of these elements in the riparian zones of the Conchos River (Holguín et al., 2006; Hernández-Garcia et al., 2008). Various studies have been carried out regarding the isolation of bacteria resistant to Pb or As in different environmental sites, and detected a low number of bacterial isolates (Chatterjee et al., 2012; Pandey and Bhatt, 2015; Dey et al., 2016; Kalita and Joshi, 2017; Uqab et al., 2020), coinciding with our research which shows that there is not a high presence of microorganisms living to on the presence of Pb and As. The morphological characterization observed by the isolated bacterial strains is shown in *Figure 1*, it is observed that Gram-positive bacteria predominate in the form of short bacilli that range from 1 to 1.5 µm.

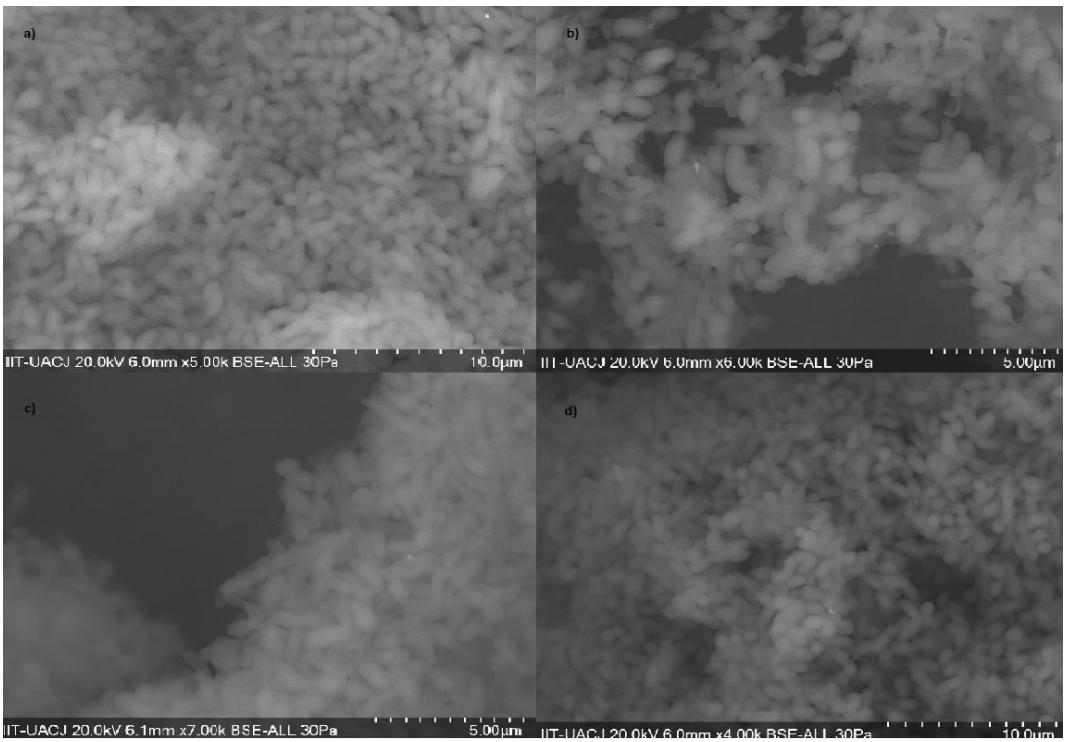

Figure 1. *A high-resolution image of bacterial colonies of the strain taken under a scanning electron microscope (SEM), a) Pb114002, b) Pb214001, c) As115004, d) As215002*

Molecular identification of isolated bacteria

Based on sequencing the 16S rRNA gene, the isolated bacteria strains tolerant to Pb (Pb114002 and Pb214001) were taxonomically affiliated to the species *Paenibacillus illinoisensis* (MW363241.1) and *Bacillus luti* (NR_157730.1), respectively (*Figures 2 and 3*). Bacterial strains tolerant to As (As115004 and As215002) were identified as belonging to the species *Paenibacillus ginsengagri* (MH491058.1) and *Bacillus*

http://www.aloki.hu ● ISSN 1589 1623 (Print) ● ISSN 1785 0037 (Online)
DOI: http://dx.doi.org/10.15666/aeer/2003_28172829

freudenreichii (KT291163.1), respectively. The analysis of the percentage of similarity showed values between 97.5% and 98.4% with the reference strains. Most of the reports of isolation and specie identification in soils, sediments, and waters with high concentrations of heavy metals and metalloids belong to the genera *Staphylococcus, Bacillus, Micrococcus, Achromobacter, Pseudomonas*, and *Klebsiella* (Carrillo-Pérez et al., 2004; Cervantes et al., 2006; Murthy et al., 2012; Oves et al., 2013; Dey et al., 2016; Kalita and Joshi, 2017; Uqab et al., 2020). Based on the phylogenetic analysis (16S rRNA) of these bacterial strains showed the presence of two genera, *Bacillus* and *Paenibacillus,* which correspond to two families Bacillaceae and Paenibacillaceae, these families belong to a Bacillales order and a Bacilli class. Research works related to the genus *Paenibacillus* have been reported from soil and water samples, but none of them in the presence of Pb or As. Mead et al. (2012) report that *Paenibacillus lautus* was isolated from Yellowstone National Park, and report that its presence in environments similar to our sampling site. Doukyu et al. (2003) report the isolation of *Paenibacillus illinoisensis* from soil samples in the Kanton area of Japan. Regarding the presence of the genus *Bacillus*, they have been identified in sites with both Pb and As (Murthy et al., 2012; Oves et al., 2013; Dey et al., 2016; Satyapal et al., 2016; Uqab et al., 2020), most of them from soils and sediments with contamination by heavy metals and metalloids, as the sampling sites of the present study.

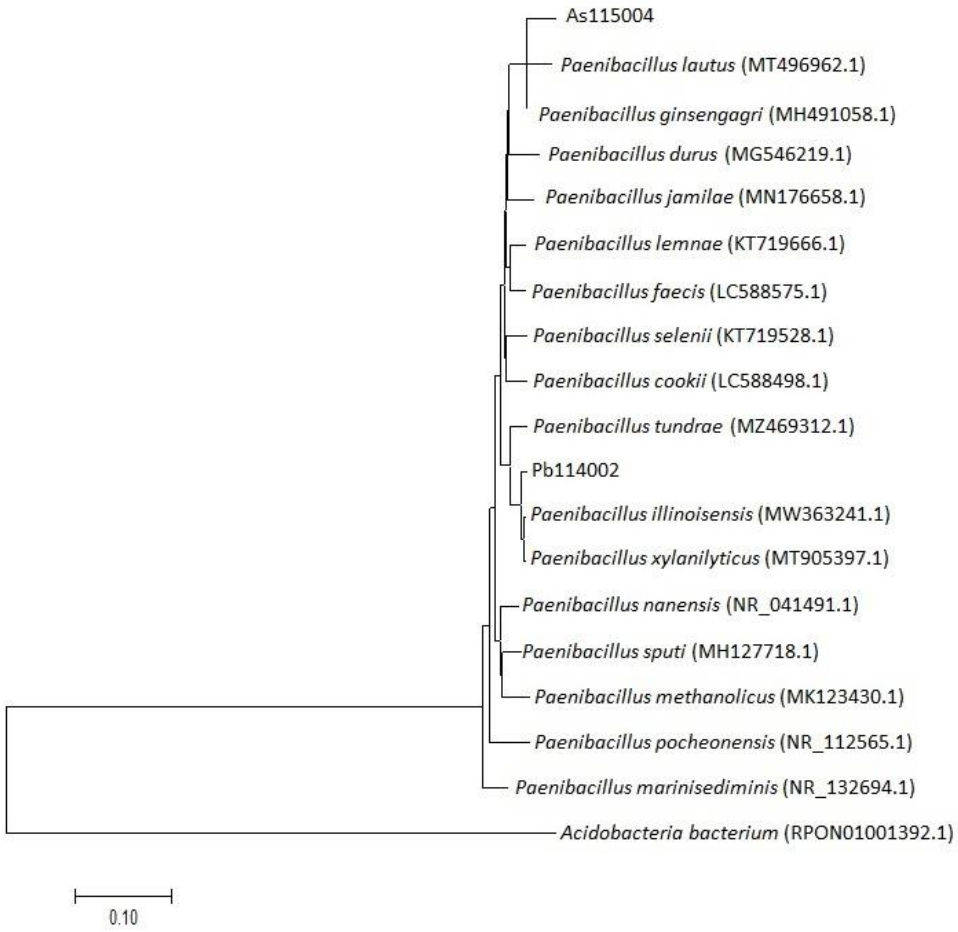

Figure 2. *Phylogenetic tree of the strains Pb114002 and As115004 with respect to the species of Paenibacillus conducted with the Neighbor Joining method, the accession number registered on the NCBI for the species utilized in the analysis is shown in parenthesis*

http://www.aloki.hu ● ISSN 1589 1623 (Print) ● ISSN 1785 0037 (Online)
DOI: http://dx.doi.org/10.15666/aeer/2003_28172829

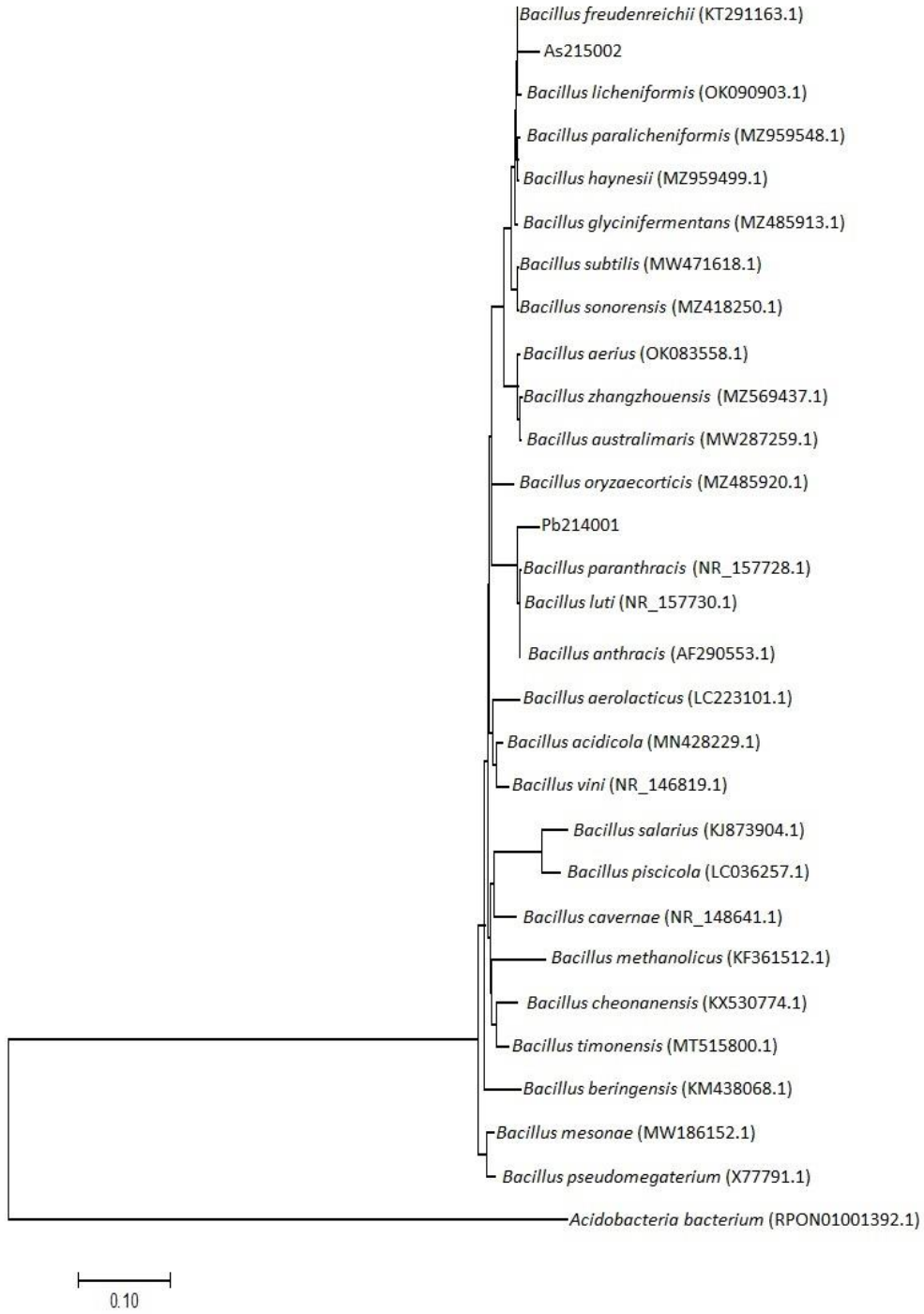

Figure 3. *Phylogenetic tree of the strains Pb214001 and As215002 concerning the species of Bacillus conducted with the Neighbor-Joining method, the accession number registered on the NCBI for the species utilized in the analysis is shown in parenthesis*

Bacterial resistance to Pb or As

The evaluation of the minimum inhibitory concentration (MIC) Pb or As of the identified bacterial strains is observed in *Table 1*. The strain *Paenibacillus illinoisensis* (Pb114002) showed resistance to 400 mg/L Pb and *Bacillus luti* (Pb214001) showed a

http://www.aloki.hu ● ISSN 1589 1623 (Print) ● ISSN 1785 0037 (Online)
DOI: http://dx.doi.org/10.15666/aeer/2003_28172829

MIC of 800 mg/L Pb. For the bacterial strains resistant to As, *Paenibacillus ginsengagri* (As115004) showed a MIC of 1000 mg/L As, and the strain *Bacillus freudenreichii* (As215002) showed a MIC of 400 mg/L As. Regarding the MIC for the studied strains, it can be observed that strains isolated in the presence of Pb coincide with the values shown by the bacterium of the genus *Paenibacillus* reported by Govarthanan et al. (2016), where a MIC of 400 mg/L was observed; regarding the MIC values for *Bacillus* strains in the presence of Pb have ranged between 125 to 1700 mg/L of Pb (Murthy et al., 2012; Oves et al., 2013; Uqab et al., 2020), the obtained value for the bacterial strain of this study was of 800 mg/L. Govarthanan et al. (2016) report the effect on the growth kinetics of bacteria of the genus *Paenibacillus* in the presence of As, showing a MIC of 400 mg/L, a value below the MIC obtained in our study for the strain of the genus *Paenibacillus* in the presence for this metalloid. The reports of the species of the genus *Bacillus* show MIC values between 550 and 750 mg/L (Pandey and Bhatt, 2015; Dey et al., 2016), without coinciding with the MIC values presented by the bacterial strain identified in this research, which presented a value of 400 mg/L.

Table 1. *The minimum inhibitory concentration of the bacterial isolated after 72 h of incubation*

Bacterial strain	Metal concentration (mg/L)						
	100	200	400	600	800	1000	1200
Paenibacillus illinoisensis	+	+	+	-	-	-	-
Bacillus luti	+	+	+	+	+	-	-
Paenibacillus ginsengagri	+	+	+	+	+	+	-
Bacillus freudenreichii	+	+	+	-	-	-	-

+ Microorganism growth, - Absence of microorganisms

Bacterial growth kinetics in presence of Pb or As

The average values of the triplicates of the microbial growth curve for the strains ANPb114002 and ANPb214001 at a concentration of 100 mg/L Pb is shown in *Figure 4*, and the average values of the microbial growth curve corresponding to the strains As115004 and As215002 is shown in *Figure 5*. The growth kinetics of the four strains analyzed showed an average adaptation time from 3 to 4 hours, the maximum absorbance value is presented at 12 hours of incubation. Jarosławiecka and Piotrowska-Seget (2014), attribute various mechanisms for the resistance of microorganisms to Pb that involve adsorption by extracellular polysaccharides, and regulation through protein expression. For their part, Pandey and Bhatt (2015) mention that the microbial capacity to grow in high concentrations of arsenic is favored by a variety of specific mechanisms that include cell accumulation, surface sorption, biotransformation, and precipitation by oxidation/reduction reaction. When performing the growth kinetic analysis in the presence of Pb and As we can see that the maximum absorbance value is shown at 12 hours of incubation. Govarthanan et al. (2016) report the growth kinetics for the bacterium *Paenibacillus* sp. as maximum absorbance values for both Pb and As in a time of 24 hours.

http://www.aloki.hu ● ISSN 1589 1623 (Print) ● ISSN 1785 0037 (Online)
DOI: http://dx.doi.org/10.15666/aeer/2003_28172829

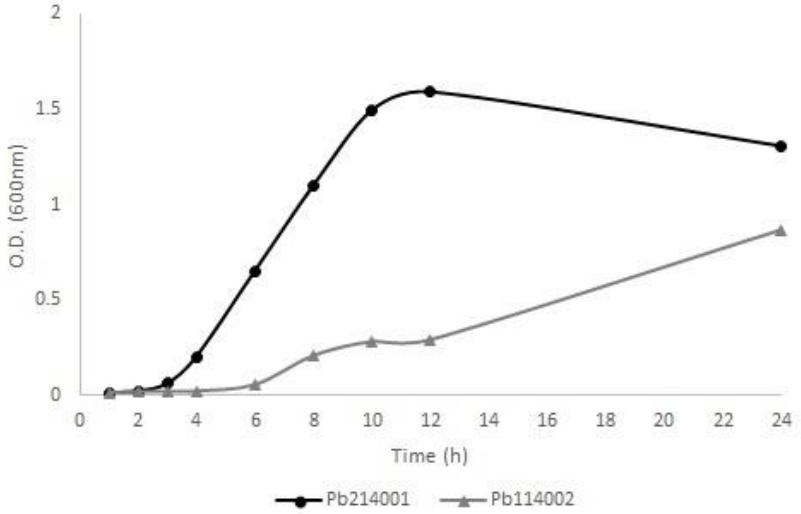

Figure 4. *Kinetic cellular growth of the strains Pb114002 and Pb214001*

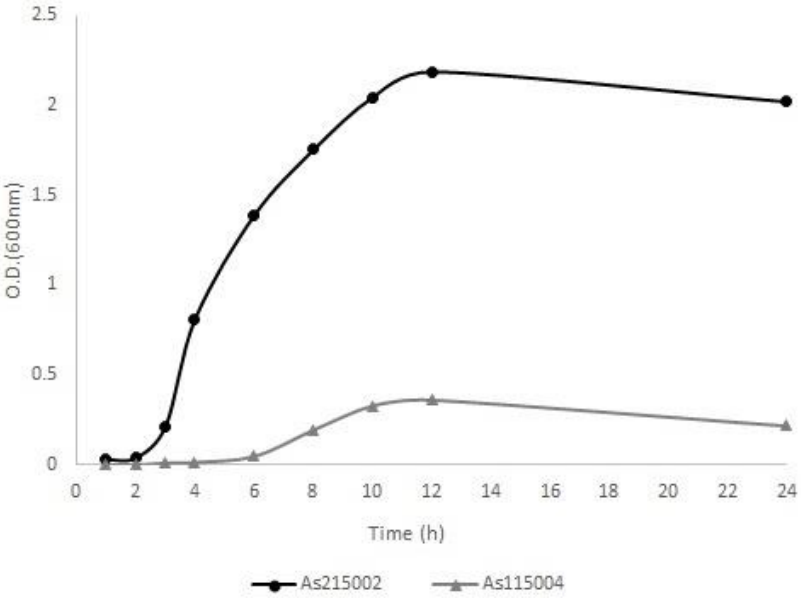

Figure 5. *Kinetic cellular growth of the strains As115004 and As215002*

Pb or As removal kinetics

The kinetics of removal of Pb (Pb114002 and Pb214001) showed that strains exposed to an initial concentration of this metal (100 mg/L) were able to remove 65.67% of Pb in a time of 24 hours (*Figure 6*). On the other hand, strains (As115004 and As215002) exposed to an initial concentration of 100 mg/L As showed removal of 42.72% in 24 hours (*Figure 7*). *Figures 6 and 7* show the average values of the triplicates. Thus, according to data obtained from the metal and metalloid removal kinetics, *Table 2* shows the estimated removal percentages for the *Paenibacillus* and *Bacillus* strains of the Las Vírgenes Dam and the Conchos River of the State of Chihuahua. Mexico.

http://www.aloki.hu ● ISSN 1589 1623 (Print) ● ISSN 1785 0037 (Online)
DOI: http://dx.doi.org/10.15666/aeer/2003_28172829

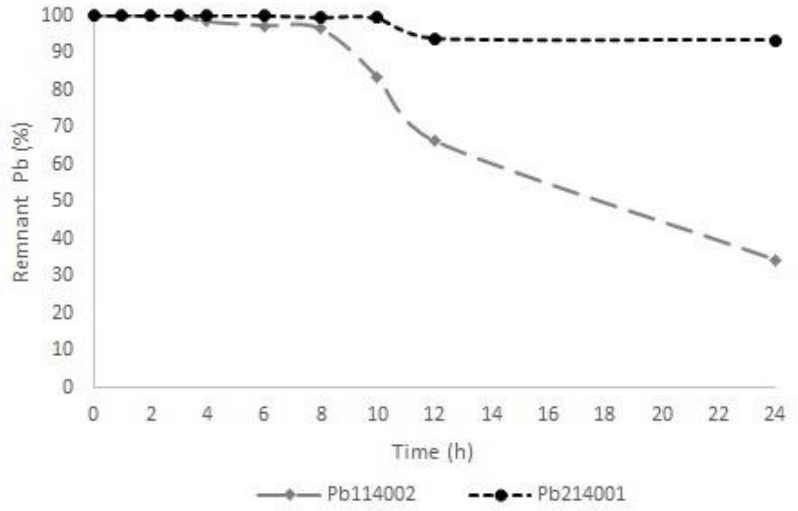

Figure 6. *Kinetics of the removal of Pb to 100 mg/L by the strains Pb114002 and Pb214001*

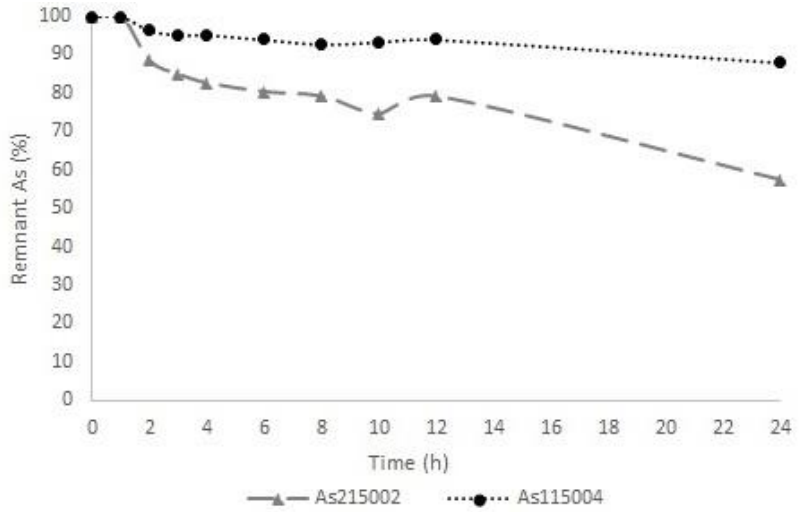

Figure 7. *Kinetics of the removal of As to 100 mg/L by the strains As115004 and As215002*

Table 2. *Removal of Pb and As from isolated bacteria*

Bacterial strain	Remotion (%)
Paenibacillus illinoisensis	65.67
Bacillus luti	6.57
Paenibacillus ginsengagri	11.96
Bacillus freudenreichii	42.72

Various microorganisms have been applied for the bioremediation of different heavy metals and metalloids, these microorganisms are identified within the group of otorhinophilic microorganisms classified as metalophiles due to their tolerance to heavy metal concentrations. A variety of mechanisms allow them to tolerate high concentrations of these compounds (Chien and Han, 2010; Oliart-Ros et al., 2016). In the bioremediation

http://www.aloki.hu ● ISSN 1589 1623 (Print) ● ISSN 1785 0037 (Online)
DOI: http://dx.doi.org/10.15666/aeer/2003_28172829

processes of Pb and As, various mechanisms such as biosorption, bioaccumulation, and biotransformation have been studied both by bacteria of the genus *Bacillus* and *Paenibacillus*. Chatterjee et al. (2012) mention that in bioremediation processes, microorganisms decrease the bioavailability of heavy metals in such a way that they provide an alternative to detoxify the pollutant in the environment, in the evaluation carried out shows a Pb removal of 81% at 72 h. Thus, Govarthanan et al. (2016) report removal of 40% at 48 h using a bacterium of the genus *Paenibacillus*. The bioadsorption process is characterized by non-specific binding from metal ions to polysaccharides and extracellular proteins (Satyapal et al., 2016), the Pb biosorption process was evaluated by Oves et al. (2013) demonstrating with their results the application of *Bacillus thuringiensis* in the biosorption process of different heavy metals. Similarly, Murthy et al. (2012) reported the biosorption of Pb using the bacterium *Bacillus cereus* with a reduction of the concentration in the medium of 90% in a time of 48 h. The bioaccumulation mechanism is the entry of heavy metals through bacterial membranes, including ion pumps, ion channels, carrier-mediated transport, endocytosis, and lipid permeation (Satyapal et al., 2016). Uqab et al. (2020) report the sequestration of 65% of Pb by the bacterium *Bacillus thuringiensis*, a study similar to the accumulation reported by Pandey and Bhatt (2015), but in their case, it is the accumulation of As by *Bacillus* sp. reporting values of 60%. Bacteria have been reported to have arsenic redox potential, as well as the production of genes and enzymes involved in the transformation of arsenic (Satyapal et al., 2016; Suhadolnik et al., 2017). Dey et al. (2016) report a 51.45% removal of As applied to a bacterium isolated from groundwater in India and belonging to the genus *Bacillus*. On the other hand, Govarthanan et al. (2016) report removal of around 30% at 24 h using the bacterium *Paenibacillus* sp. isolated from the roots of *Tridax procumbens*. The results obtained in our investigation regarding the removal of Pb and As, shown in table 2, exceed the values shown by *Paenibacillus* reported by Govarthanan et al. (2016) for removal of Pb by *Paenibacillus illinoisensis*, but not for removal As by *Paenibacillus ginsengagri*.

Conclusion

Based on the results of this research the presence of microorganisms with resistance to contaminating metals in the sediments sampled from water bodies was demonstrated. Similarly, the genus *Paenibacillus* and *Bacillus* were identified within these microorganisms. The research also showed that a noticeable remotion of metal occurred after 24 hours of bioremediation up to 50% in the case of Pb. Based on the promising results obtained in our work, further research needs to be developed to understand the biochemical and/or molecular mechanisms used by the strains to design bioproducts for Pb and As remediation *in situ*.

REFERENCES

[1] Ali, H., Khan, E., Ilahi, I. (2019): Environmental chemistry and ecotoxicology of hazardous heavy metals: environmental persistence, toxicity, and bioaccumulation. – Journal of chemistry 4: 1-14. https://doi.org/10.1155/2019/6730305.

[2] Carrillo-Pérez, E., Ruiz-Manríquez, A., Yeomans-Reina, H. (2004): Aislamiento, identificación y evaluación de un cultivo mixto de microorganismos con capacidad para

http://www.aloki.hu ● ISSN 1589 1623 (Print) ● ISSN 1785 0037 (Online)
DOI: http://dx.doi.org/10.15666/aeer/2003_28172829

degradar DDT. – Revista Internacional de Contaminación Ambiental 20: 69-75. https://www.redalyc.org/articulo.oa?id=37000203.

[3] Cervantes, C., Espino-Saldaña, A. E., Acevedo-Aguilar, F., León-Rodríguez, I. L., Rivera-Cano, M. E., Avila-Rodríguez, M., Wróbel-Kaczmarczyk, K., Wróbel-Zasada, K., Gutiérrez-Corona, J. F., Rodríguez-Zavala, J. S., Moreno-Sánchez, R. (2006): Interacciones microbianas con metales pesados. – Revista Latinoamericana de Microbiología 48: 203-210. https://www.medigraphic.com/pdfs/lamicro/mi-2006/mi062v.pdf?q=metales.

[4] Chatterjee, S., Mukherjee, A., Sarkar, A., Roy, P. (2012): Bioremediation of lead by lead-resistant microorganisms, isolated from industrial simple. – Advances in Bioscience and Biotechnology 3: 290-295. http://dx.doi.org/10.4236/abb.2012.33041.

[5] Chien, C. C., Han, C. T. (2010): Tellurite Resistance and Reduction by a *Paenibacillus* sp. Isolated from Heavy Metal-Contaminated Sediment. – Environmental Toxicology and Chemistry 28: 1627-1632. https://doi.org/10.1897/08-521.1.

[6] Dey, U., Chatterjee, S., Mondal, N. K. (2016): Isolation and characterization of arsenic-resistant bacteria and possible application in bioremediation. – Biotechnology Reports 10: 1-7. http://dx.doi.org/10.1016/j.btre.2016.02.002.

[7] Doukyu, N., Kuwahara, H., Aono, R. (2003): Isolation of *Paenibacillus illinoisensis* that produces cyclodextrin glucanotransferase resistant to organic solvents. – Bioscience, Biotechnology, and Biochemistry 67: 334-340. https://doi.org/10.1271/bbb.67.334.

[8] Govarthanan, M., Mythili, R., Selvankumar, T., Kamala-Kannan, S., Rajasekar, A., Chang, Y. C. (2016): Bioremediation of heavy metals using an endophytic bacterium *Paenibacillus* sp. RM isolated from the roots of Tridax procumbens. – Biotechnology 6: 1-7. https://doi.org/10.1007/s13205-016-0560-1.

[9] Guo, C., Sun, W., Harsh, J. B., Ogram, A. (1997): Hybridization Analysis of Microbial DNA from Fuel Oil–Contaminated and Noncontaminated Soil. – Microbial Ecology 34: 178-187. https://doi.org/10.1007/s002489900047.

[10] Hernández-Garcia, Y., Sosa-Cerecedo, M., Moreno, M., Alcalá, J., Puga, S. (2008): Evaluación de la contaminación por metales pesados y arsénico en sedimento en embalses del estado de Chihuahua, México. – Revista Latinoamericana de Recursos Naturales 4: 89-94. https://www.itson.mx/publicaciones/rlrn/Documents/v4-n2-7-evaluacion-de-la-contaminacion-por-metales-pesados.pdf.

[11] Hernández-Peña, C. C., Lares-Villa, F., Santos-Villalobos, S. D. L., Estrada-Alvarado, M. I., Cruz-Soto, A., Flores-Tavizón, E., Soto-Padilla, M. Y. (2021): Reduction in concentration of chromium (VI) by *Lysinibacillus macroides* isolated from sediments of the Chapala Lake, Mexico. – Anais da Academia Brasileira de Ciências 93: 1-11. https://doi.org/10.1590/0001-3765202120190144.

[12] Holguín, C., Rubio, A. H., Olave, M. E., Saucedo, R., Gutiérrez, M., Bautista, R. (2006): Calidad del agua del Río Conchos en la región de Ojinaga, Chihuahua: parámetros fisicoquímicos, metales y metaloides. – Universidad y Ciencia 22: 51-63. https://www.redalyc.org/articulo.oa?id=15402204.

[13] Hu, X., Wang, J., Lv, Y., Liu, X., Zhong, J., Cui, X., Zhang, M., Ma, D., Yan, X., Zhu, X. (2021): Effects of heavy metals/metalloids and soil properties on microbial communities in farmland in the vicinity of a metals smelter. – Frontiers in Microbiology 12: 1-13. https://doi.org/10.3389/fmicb.2021.707786.

[14] Jarosławiecka, A., Piotrowska-Seget, Z. (2014): Lead resistance in microorganisms. – Microbiology 60: 12-25. https://doi.org/10.1099/mic.0.070284-0.

[15] Jorquera, M. A., Graether, S. P., Maruyama, F. (2019): Editorial: Bioprospecting and Biotechnology of Extremophiles. – Frontiers in Bioengineering and Biotechnology 7: 204. https://doi.org/10.3389/fbioe.2019.00204.

[16] Kalita, D., Joshi, S. R. (2017): Study on bioremediation of Lead by exopolysaccharide producing metallophilic bacterium isolated from extreme hábitat. – Biotechnology Reports 16: 48-57. https://doi.org/10.1016/j.btre.2017.11.003.

http://www.aloki.hu ● ISSN 1589 1623 (Print) ● ISSN 1785 0037 (Online)
DOI: http://dx.doi.org/10.15666/aeer/2003_28172829

[17] Mead, D. A., Lucas, S., Copeland, A., Lapidus, A., Cheng, J. F., Bruce, D. C., Goodwin, L. A., Pitluck, S., Chertkov, O., Zhang, X., Detter, J. C., Han, C. S., Tapia, R., Land, M., Hauser, L. J., Chang, Y. J., Kyrpides, N. C., Ivanova, N. N., Ovchinnikova, G., Woyke, T. (2012): Complete genome sequence of *Paenibacillus* strain Y4. 12MC10, a novel *Paenibacillus lautus* strain isolated from Obsidian Hot Spring in Yellowstone National Park. – Standards in Genomic Sciences 6: 366-385. https://doi.org/10.4056/sigs.2605792.

[18] Medina-Pizzali, M., Robles, P., Mendoza, M., Torres, C. (2018): Ingesta de arsénico: el impacto en la alimentación y la salud humana. – Revista Peruana de Medicina Experimental y Salud Pública 35: 93-102. https://doi.org/10.17843/rpmesp.2018.351.3604.

[19] Murthy, S., Bali, G., Sarangi, S. K. (2012): Biosorption of lead by *Bacillus cereus* isolated from industrial effluents. – Biotechnology Journal International 2: 73-84. https://core.ac.uk/download/pdf/72804029.pdf.

[20] Nava-Ruíz, C., Méndez-Armenta, M. (2011): Efectos neurotóxicos de metales pesados (cadmio, plomo, arsénico y talio). – Archivos de neurociencias 16: 140-147. https://www.medigraphic.com/pdfs/arcneu/ane-2011/ane113f.pdf.

[21] Oliart-Ros, R. M., Manresa-Presas, Á., Sánchez-Otero, M. G. (2016): Utilización de microorganismos de ambientes extremos y sus productos en el desarrollo biotecnológico. – CienciaUAT 11: 79-90. https://www.redalyc.org/articulo.oa?id=441946945006.

[22] Olmos, V., Ridolfi, A. S. (2018): Hidroarsenicismo: mecanismos de acción asociados a la toxicidad del arsénico. – Acta Toxicológica Argentina 26: 32-44. http://www.scielo.org.ar/scielo.php?script=sci_arttext&pid=S1851-37432018000100004.

[23] Orji, O. U., Awoke, J. N., Aja, P. M., Aloke, C., Obasi, O. D., Alum, E. U., Udu-Ibiam, O. E., Oka, G. O. (2021): Halotolerant and metalotolerant bacteria strains with heavy metals biorestoration possibilities isolated from Uburu Salt Lake, Southeastern, Nigeria. – Heliyon 7: 1-8. https://doi.org/10.1016/j.heliyon.2021.e07512.

[24] Oves, M., Khan, M. S., Zaidi, A. (2013): Biosorption of heavy metals by *Bacillus thuringiensis* strain OSM29 originating from industrial effluent contaminated north Indian soil. – Saudi Journal of Biological Sciences 20: 121-129. https://doi.org/10.1016/j.sjbs.2012.11.006.

[25] Pandey, N., Bhatt, R. (2015): Arsenic resistance and accumulation by two bacteria isolated from a natural arsenic contaminated site. – Journal of Basic Microbiology 55: 1275-1286. http://dx.doi.org/10.1002/jobm.201400723.

[26] Pellizzari, E. E., Marinich, L. G., Flores, S. A., Giménez, C. M. (2015): Degradación de arsénico por *Pseudomonas aeruginosa* para bioremediaciónde agua. Estudio preliminar. – Avances en ciencias e ingeniería 6: 1-6. https://www.redalyc.org/articulo.oa?id=323635882001.

[27] Rodríguez-Rey, A., Cuéllar-Luna, L., Maldonado-Cantillo, G., Suardiaz-Espinosa, M. E. (2016): Efectos nocivos del plomo para la salud del hombre. – Revista Cubana de Investigaciones Biomédicas 35: 251-271. https://www.medigraphic.com/pdfs/revcubinvbio/cib-2016/cib163f.pdf.

[28] Rubio, A. H., Ochoa, R. J. M., Quintana, R. M., Saucedo, T. R., Ortiz, D., Rey, B. N. L., Espinoza, P. J. R. (2013): Development of a Water Quality Index (WQI) of an Artificial Aquatic Ecosystem in Mexico. – Journal of Environmental Protection 4: 1296-1306. https://doi.org/10.4236/jep.2013.411151.

[29] Satyapal, G. K., Rani, S., Kumar, M., Kumar, N. (2016): Potential role of arsenic resistant bacteria in bioremediation: current status and future prospects. – Journal of Microbial and Biochemical Technology 8: 256-258. http://dx.doi.org/10.4172/1948-5948.1000294.

[30] Soto-Padilla, M. Y., Gortares-Moroyoqui, P., Cira-Chavez, L. A., Estrada-Alvarado, M. I. (2018): Biochemical and molecular characterization of a native haloalkalophilic tolerant strain from the Texcoco Lake. – Polish Journal of Microbiology 67: 377-382. https://doi.org/10.21307/pjm-2018-047.

http://www.aloki.hu ● ISSN 1589 1623 (Print) ● ISSN 1785 0037 (Online)
DOI: http://dx.doi.org/10.15666/aeer/2003_28172829

[31] Suárez, P., Reyes, R. (2002): La incorporación de metales pesados en las bacterias y su importancia para el ambiente. – Interciencia 27: 160-164. https://www.redalyc.org/articulo.oa?id=33906702.

[32] Suhadolnik, M. L., Salgado, A. P., Scholte, L. L., Bleicher, L., Costa, P. S., Reis, M. P., Dias, M. F., Ávila, M. P., Barbosa, F. A. R., Chartone-Souza, E., Nascimento, A. M. (2017): Novel arsenic-transforming bacteria and the diversity of their arsenic-related genes and enzymes arising from arsenic-polluted freshwater sediment. – Scientific Reports 7: 1-17. https://doi.org/10.1038/s41598-017-11548-8.

[33] Thacker, U., Parikh, R., Shouche, Y., Madamwar, D. (2007): Reduction of chromate by cell-free extract of *Brucella* sp. Isolated from Cr(VI) contaminated sites. – Bioresource Technology 98: 1541-1547. https://doi.org/10.1016/j.biortech.2006.06.011.

[34] Uqab, B., Nazir, R., Ganai, B. A., Rahi, P., Rehman, S., Farooq, S., Dar, R., Parray, J. A., Al-Arjani, A. F., Tabassum, B., Abd_Allah, E. F. (2020): MALDI-TOF-MS and 16S rRNA characterization of lead tolerant metallophile bacteria isolated from saffron soils of Kashmir for their sequestration potential. – Saudi Journal of Biological Sciences 27: 2047-2053. https://doi.org/10.1016/j.sjbs.2020.04.021.

http://www.aloki.hu ● ISSN 1589 1623 (Print) ● ISSN 1785 0037 (Online)
DOI: http://dx.doi.org/10.15666/aeer/2003_28172829

Applied Ecology and Environmental Research

International Scientific Journal

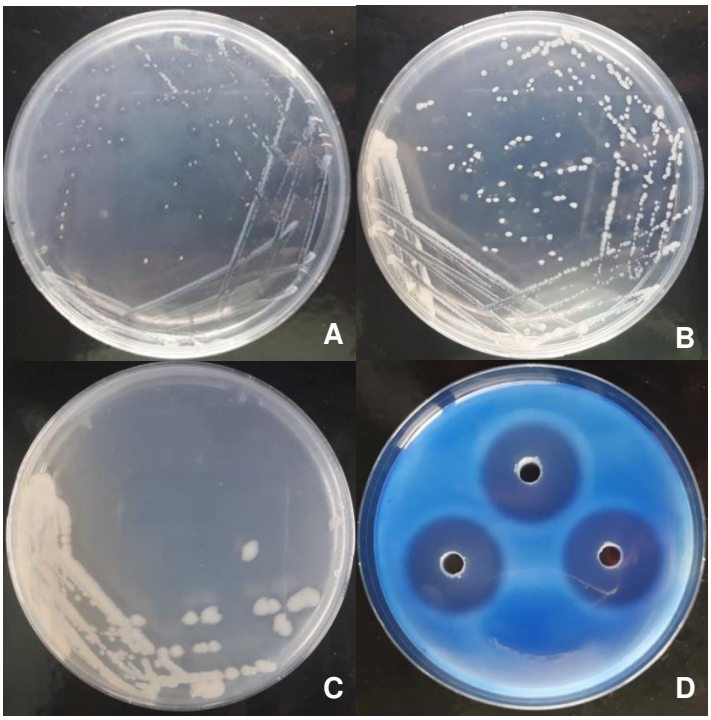

VOLUME 20 * NUMBER 3 * 2022

Published: May 31, 2022
http://www.aloki.hu
ISSN 1589 1623 / ISSN 1785 0037
DOI: http://dx.doi.org/10.15666/aeer